QD
1
S923

ARKIV FÖR KEMI

UTGIVET AV

KUNGL. SVENSKA VETENSKAPS-
AKADEMIEN

Band 8

Med 56 avhandlingar

ALMQVIST & WIKSELL / STOCKHOLM

1956

Häfte	1	innehållande	Nr	1—12	utkom	den	9	maj	1955
»	2	»	Nr	13—20	»	»	10	»	1955
»	3	»	Nr	21—26	»	»	11	»	1955
»	4	»	Nr	27—39	»	»	17	»	1955
»	5	»	Nr	40—50	»	»	9	jan.	1956
»	6	»	Nr	51—56	»	»	17	febr.	1956

ÅTTONDE BANDETS INNEHÅLL

Sid.

1. Drake, B., Contributions to the theory of gradient elution analysis . . . 1– 21
2. Gronowitz, S. and Rosenberg, A., Infra-red investigation of the conjugation of the isomeric thiophenecarboxylic acids and thiophenecarboxaldehydes . . . 23– 27
3. Halvarson, K. and Melander, L., Acid-induced hydrogen exchange in thiophene . . . 29– 32
4. Johansson, G., The kinetics of the polymorphic transformation of silver sulphate . . . 33– 48
5. Jorpes, E. and Mutt, V., On the strength of secretin . . . 49– 51
6. Myrbäck, K. and Willstaedt, E., Inhibition of yeast invertase (saccharase) by metal ions. I. The uranyl ion . . . 53– 59
7. von Euler, H. und Glaser, A., Zur Kenntnis alicyclischer Reduktone. I 61– 65
8. von Euler, H. und Hasselquist, H., Entstehung von aci-Reduktonen . 67– 72
9. Resegotti, L. und von Euler, H., Über die Katalase-Aktivität der Leber und Milz von Ascitestumor-Ratten während der Behandlung mit cytostatischen Substanzen . . . 73– 78
10. Matell, M., Stereochemical studies on plant growth regulators. X. Configuration of optically active α-phenoxy- and α-(2-naphthoxy)-*n*-valeric acid 79– 86
11. Gronowitz, S., 4-bromo-2-thiophenecarboxylic acid . . . 87– 88
12. Hedlund, I., Synthesis of (–)-2D, 5L- and (+)-2L, 5D-dimethyladipic acids by *bis*-degradation of (+)-3D, 6L- and (–)-3L, 6D-dimethylsuberic acids respectively . . . 89–100
13. Rydberg, J., Studies on the extraction of metal complexes. XII-A. The formation of composite, mononuclear complexes. Part A: Theoretical . 101–112
14. Rydberg, J., Studies on the extraction of metal complexes. XII-B. The formation of composite, mononuclear complexes. Part B: Studies on the Th- and U(VI)-acetylacetone-H_2O-organic solvent systems . . . 113–140
15. Boman, H. G., On the relation between phosphorolysis and glycolysis in human erythrocytes . . . 141–142
16. Rosenberg, A. and Schotte, L., Stereochemical studies on dicarboxylic acids. II. The formation of quasi-racemic compounds as determined by infrared absorption . . . 143–151
17. Johansson, G., The mechanism of the polymorphic transformation of mercuric iodide . . . 153–158
18. Drake, B., Chromatography combined with automatic recording of electrolytic conductivity. III. Developments and tests of the apparatus and of the method . . . 159–170
19. Drake, B., Chromatography combined with automatic recording of electrolytic conductivity. IV. Elution analysis of some amino acids, amines, and alkali metals on Dowex 50 in various solvents . . . 171–188
20. Drake, B., Chromatography combined with automatic recording of electrolytic conductivity. V. Model experiments on gradient elution analysis 189–196

Sid.

21. von Euler, H. und Hasselquist, H., Über Galaktose als Ausgangsmaterial für Reduktone und über die biologische Bildung der Ascorbinsäure 197–204
22. Brattsten, I., Continuous zone electrophoresis by crossed velocity fields in a supporting medium. The electric control of the fractionation process 205–226
23. Brattsten, I., Continuous zone electrophoresis by crossed velocity fields in a supporting medium. Fractionation of protein mixtures and description of the cuvette 227–244
24. Edstrand, M. and Blomqvist, G., The crystal structure of $NH_4Cl \cdot As_2O_3 \cdot \frac{1}{2} H_2O$ 245–256
25. Edstrand, M., On the structures of antimony (III) oxide halogenides. III. The crystal structure of $[Sb_8O_8(OH)_4]\,[(OH)_{2-x}(H_2O)_{1+x}]Cl_{2+x}$ 257–277
26. Edstrand, M., On the structures of antimony (III) oxide halogenides. IV. The crystal structure of $Sb_8O_{10}(OH)_2I_2$ and isomorphous bromide and chloride 279–298
27. Sjövall, J., New solvents for the separation of bile acids with paper chromatography. Bile acids and steroids. 30 299–301
28. Eriksson, S. and Sjövall, J., The absorption spectra of bile acids in sulfuric acid. Bile acids and steroids. 31 303–310
29. ——, The absorption spectra of conjugated bile acids in sulfuric acid. Bile acids and steroids. 32 311–315
30. Sjövall, J., Quantitative determination of bile acids on paper chromatograms. Bile acids and steroids. 33 317–324
31. Wideqvist, S., The time-variable in chemical kinetics 325–330
32. Norman, A., Preparation of conjugated bile acids using mixed carboxylic acid anhydrides. Bile acids and steroids. 34 331–342
33. Gronowitz, S. and Halvarson, K., The hydrogen isotope effect in the metalation of thiophene 343–345
34. Brattsten, I., Continuous zone electrophoresis by crossed velocity fields in a supporting medium. Analysis of protein fractions obtained from normal human serum 347–360
35. Melander, L., Some considerations on substitution reactions in the thiophene ring 361–366
36. Myrbäck, K. and Willstaedt, E., Studies on yeast invertase (saccharase). Localization of the enzyme in the cell and its liberation 367–374
37. von Euler, H. und Hasselquist, H., Oxydo-reduktive Funktionen der aci-Reduktone 375–380
38. Hasselquist, H., Isolierung von aci-Reduktonen und Derivaten derselben 381–386
39. Pettersson, K., Thermal analysis of systems of some optically active diarylpropionic acids 387–392
40. Myrbäck, K., Inhibition of yeast invertase (saccharase) by metal ions. II. Action of Ag^+, Cu^{++}, Cd^{++}, Zn^{++} ions and their complex formation with acetate ions 393–400
41. Serck–Hanssen, K., Optically active higher aliphatic hydroxy-compounds. II. The synthesis of (+)- and (–)-2-Tetracosanol 401–410
42. Bruun, H. H., Optical studies of compressed surface layers on an aqueous substrate. With 12 figures in the text 411–422
43. Liljeblad, R., Equilibrium pressure for different temperatures between graphite and diamond 423–432

Sid.

44. Fredga, A. and Sikström, Å., An investigation on caronic acid 433–440
45. Gronowitz, S., 3-Substituted thiophenes. A study in synthesis 441–448
46. Aleixandre, V. and Verduch, A. G., Some aspects on the stannic oxide–zinc oxide powder reaction 449–456
47. Schotte, L., γ-Butyrolactone. Some reactions involving ring fission . . . 457–461
48. Fredga, A., Studies on synthetic growth substances. VIII. The enanthiomorphs of α-(1-naphthyl)-propionic acid 463–468
49. Boström, H., Jorpes, E., Månsson, B., Rodén, L. and Vestermark, A., On the partial purification of a liver factor stimulating the sulphate exchange of chondroitin sulphuric acid 469–480
50. Giuliano, R., Turnover of plasma iron 481–485
51. Sandström, J., On carboxy-dithiocarbhydrazides and *N*-aminorhodanines 487–521
52. Sandström, J., On the formation of pyrazoles from thiohydrazides and α-halogencarbonyl compounds 523–544
53. Wideqvist, S., The calculation of rate constants for competitive, consecutive reactions 545–549
54. Schotte, L. and Rosenberg, A., Stereochemical studies on dicarboxylic acids. III. The infrared absorption of some α,α'disubstituted acids of different types 551–566
55. Gronowitz, S. and Larsson, S., Resolution and configuration of 3-thenylsuccinic acid 567–577
56. Schotte, L., Spectrochemical studies on disulphides. I. An Investigation of some linear and cyclic carboxylic substituted disulphides with special reference to the 1,2-dithiolane system 579–596

ARKIV FÖR KEMI Band 8 nr 1

Communicated 8 September 1954 by ARNE WESTGREN and ARNE FREDGA

Contributions to the theory of gradient elution analysis

By BIRGER DRAKE

With 16 figures in the text

In the chromatographic process known as gradient elution[1], a sample is moved through a sorbent[2] by means of a flowing solution in which the concentration of one or several gradient substances[3] is continuously varied (see, e.g., [1]). In spite of the good results obtained with this method, the available theories [1–3] seem to be rather limited. A general theory is not easily supplied, however, and the present paper should only be considered an attempt at formulating some basic concepts.

The general problem is suitably presented by a reference to Fig. 1. The middle part of this figure refers to the descending migration of the gradient substance and of two test substances through a vertical column, while the upper and lower parts indicate the composition of influent and effluent, respectively. The solvent is assumed to move (with a constant, low speed) corresponding to the slope of the dashed line. Each thin line represents a certain concentration of the gradient substance, and the thick lines represent the concentration maximum of the zones of the test substances.

A vertical line ("isochrone", cf. [4, 6]) through such a diagram indicates the position of the test substances in the column after the addition of a certain volume of the eluent—cf. the appearance of a one-dimensional paper chromatogram with coloured substances. A horizontal line ("isoplane") indicates the volumes that have been added when the test substances pass a certain cross-section of the column, e.g., its lower end.

Obviously, the migration of a test substance is governed by

1) the shape of the influent gradient,
2) the migration of this gradient through the column (with or without sorption; with or without developing a front), and
3) the dependence of the migration rate of the test substance on the concentration of the gradient substance and, in the case of non-linear isotherms, on the concentration of the test substance itself.

---

[1] Gradient elution analysis is in this paper called *gradient elution.*

[2] The words *sorbent, sorption, sorb,* etc., here signify all physical chemical processes that can be utilized as the basis for chromatography. Thus, adsorption, ion exchange and partition between two liquids are included together with precipitation, salting out, etc. The advantage of using such a broad definition is quite obvious when considering the frequent difficulty of deciding which process is applicable in a special case (cf. [4, 5]).

[3] A substance whose concentration in the eluent is continuously changed, is here called a *gradient substance.* For simplicity, the treatment has been limited to the case where only one gradient substance is used.

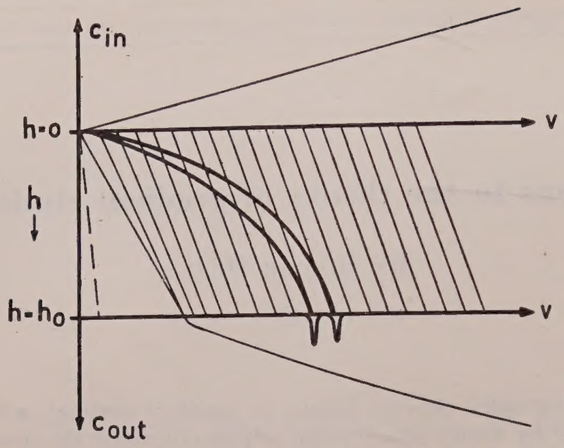

Fig. 1. Schematic diagram showing, *middle part*—the downwards migration of solutes through a vertical sorption column as a function of the added volume; *upper part*—concentration in the influent; *lower part*—concentration in the effluent.
- - - - solvent; ——— gradient substance; ▬▬ test substances.

These are the factors that will be considered here. In a complete treatment, consideration should also be paid, for instance, to the spreading of zones caused by non-equilibrium [7–10]. However, by the use of a column with a high number of "theoretical plates", the difference between the general solution and the special solution presented here can be made small.

When the test substances have linear isotherms, they will migrate independently, and the formulas reported below can be used for each component. For test substances with curved isotherms the circumstances are much more complicated. Because of the present lack of experimental data, however, an elaborate mathematical treatment would be rather useless, and no attempt has been made to derive the relevant formulas.

In the following mathematical and graphical treatment, the above-mentioned factors 1, 2 and 3 are first separately treated. Formulas obtained in this way are then combined and used to derive mathematical expressions for the migration curves in some special cases. For more complicated cases, in which the mathematical treatment was found inconvenient, graphical methods are devised. Finally, some problems of migration and separation efficiency are discussed.

Symbols, listed in the order in which they appear

c_{in} = concentration in which the gradient substance is added to the column
v = volume added to the column
c_{e}^0 = constant concentration of the gradient substance which is added to the first mixing chamber
c_1, c_2 = concentrations of the gradient substance in two mixing chambers
V_1, V_2 = volumes of liquid in the two mixing chambers
V_{tot} = $V_1 + V_2$
k = various parameters (see eqs. (4), (7), (32), (37))

R_F = rate of migration of a solute divided by the rate of migration (rate of flow) of the solvent (cf. [11])
$v_{0,\,s}$ = volume of the mobile phase of the column
h = height in the column, measured from the upper end, where the runs are started
h_0 = total height of the column
w = "corrected volume", corresponding to constant c_g-values (see Fig. 3 and eq. (5))
α = partition coefficient[1] for a solute $= m/c$ (e.g., mg/gm divided by mg/ml = ml/gm)
Q = proportion between stationary phase and mobile phase, measured in such a unit that $Q \times \alpha$ is the "mass distribution" of the solute between the two phases (i.e., the ratio of amounts in the stationary phase and in the mobile phase in a certain layer of the column). With the notations used by MARTIN and SYNGE [7], $Q = A_S/A_L$
c = concentration[2] in the mobile phase (e.g., mg/ml)
m = concentration[2] in the stationary phase (e.g., mg/gm or mg/ml). At equilibrium, the function $m = \mathrm{f}(c)$ is called the sorption isotherm
$\mathbf{H}$ $= h_0/v_{0,s}\,Q$ = height of column per unit amount of sorbent

subscript s signifies the solvent: h_s
subscript g signifies the gradient substance: h_g, α_g, $R_{F,g}$
subscript t signifies a test substance: h_t, α_t, $R_{F,t}$
subscript 0 signifies a value corresponding to the lower end of the column: h_0, $v_{0,s}$
superscript 0 signifies a starting value: V_1^0, V_2^0, c_1^0, c_2^0
superscript crit signifies a critical value: c_g^{crit}

Other symbols are universally adopted or are explained in the text.

The ultimate goal of the mathematical treatment can be formulated as the determination of a migration function $h_t = \mathrm{J}(v)$ for a set of values of V_1^0 (or V_{tot}^0), c_e^0, c_1^0, c_2^0, h_0, $v_{0,\,s}$, Q, α_g, and—for test substances with curved isotherms—c_t. Here, the variable v is considered independent and the variable h dependent, while all other variables are treated as parameters.

The shape of the influent gradient

Exponential [1, 12, 13] and linear [14] gradients are most often used, but the production of gradients having a (within limits) arbitrary shape has also been described [15–17].

In an Appendix (p. 16) it is shown that very simple arrangements are capable of giving a sufficiently great variety of gradient types. Consequently, the treatment has been limited to these cases. The calculations in the Appendix can be summarized in the following formulas, which give the influent concentration, c_{in}, of the gradient substance as a function of volume added to the column, v, and of the parameter values c_e^0, c_1^0, c_2^0, V_1^0, V_2^0 and V_{tot}^0.

$$c_{\text{in}} = c_e^0 - (c_e^0 - c_1^0)\,\mathrm{e}^{-\frac{v}{V_1^0}} \qquad (1)$$

---

[1] The word *partition coefficient* is here used for all sorption processes and not only for partition between two liquids.

[2] or any other property that can be similarly treated.

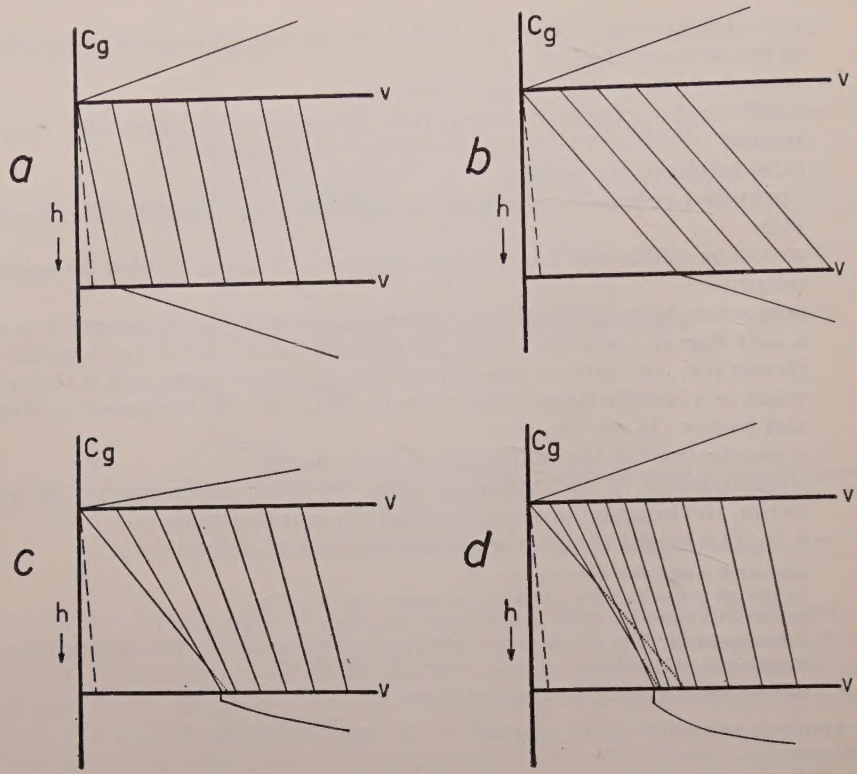

Fig. 2. The migration of a gradient substance through a sorption column.—a and b, with a linear isotherm, $R_{F,g} = 0.4$ and 0.1, respectively, and with linear influent gradients; c and d, with a LANGMUIR isotherm and with linear influent gradients of different steepness.

$$c_{\text{in}} = c_{\text{e}}^0 - \frac{V_1^0}{V_1^0 - V_2^0}(c_{\text{e}}^0 - c_1^0)\, e^{-\frac{v}{V_1^0}} - \left(\frac{c_{\text{e}}^0 V_2^0 - c_1^0 V_1^0}{V_1^0 - V_2^0} - c_2^0\right) e^{-\frac{v}{V_2^0}} \tag{2}$$

$$c_{\text{in}} = c_{\text{e}}^0 - (c_{\text{e}}^0 - c_1^0)\frac{v}{V_2^0}\, e^{-\frac{v}{V_2^0}} - (c_{\text{e}}^0 - c_2^0)\, e^{-\frac{v}{V_2^0}} \tag{3}$$

$$c_{\text{in}} = c_{\text{e}}^0 - (c_{\text{e}}^0 - c_2^0)\frac{v + V_2^0}{V_2^0}\, e^{-\frac{v}{V_2^0}} \tag{3 a}$$

$$c_{\text{in}} = c_{\text{e}}^0 - (c_{\text{e}}^0 - c_2^0)\left(1 - \frac{v}{V_{\text{tot}}^0}\right)^{1/k} \tag{4}$$

$$c_{\text{in}} = c_{\text{e}}^0 - (c_{\text{e}}^0 - c_2^0)\left(1 - \frac{v}{V_{\text{tot}}^0}\right) = c_2^0 + (c_{\text{e}}^0 - c_2^0)\frac{v}{V_{\text{tot}}^0}\,. \tag{4 a}$$

Eq. (1) corresponds to an exponential gradient and eq. (4a) to a linear gradient, while the other formulas give different shapes according to the values chosen for the

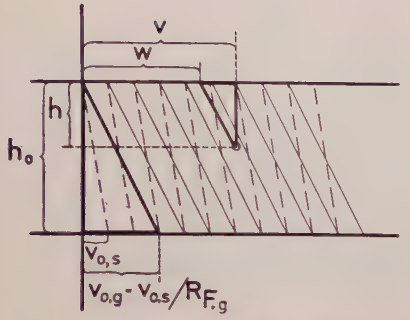

Fig. 3. The relation between the variables v and w, as referred to the encircled point.

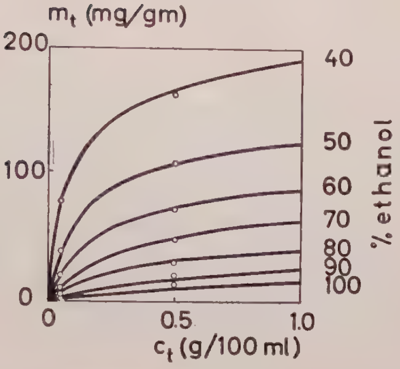

Fig. 4. Isotherms, $m_t = f(c_t)$, for the sorption of caprylic acid on charcoal in the presence of from 40 to 100 per cent ethanol. The smoothed sorption values for $c_t = 0.05\,\%$ and $c_t = 0.5\,\%$ according to eqs. (11) and (12) have been inserted as circles.

parameters. The appearance of some curves corresponding to these formulas is shown in the Appendix (Fig. 15). There, the formulas are also given in a simplified form for the case where $c_{in}^0 = 0$ (eq. (39)–(42a)).

The migration of the gradient substance

If α_g is independent of c_g, i.e., if *the sorption isotherm of the gradient substance is linear*, all concentrations will migrate with the same speed. Figs. 2 a and b illustrate this case for the two $R_{F,g}$-values 0.4 and 0.1. If $\alpha_g = 0$, i.e., if the gradient substance is not at all sorbed, the migration lines will of course coincide with the migration lines of the solvent.

In this case, all migration lines are parallel, and the variable v can preferably be exchanged for another, w, which is constant along these lines. By using the two triangles marked off in Fig. 3 (see also eq. (6)) one obtains

$$v \left[= w + \frac{v_{0,s}\,h}{h_0\, R_{F,g}} \right] = w + \frac{v_{0,s}\,h}{h_0}\,(1 + Q\,\alpha_g). \tag{5}$$

The function $c_g(w)$ that will be used below (cf. eq. (16)) is obtained, if v in eqs. (1)–(4a) is replaced by w.

If *the sorption isotherm of the gradient substance is curved*, the migration problem becomes much more difficult. An approximate solution can be obtained, however, by drawing an h/v-diagram with straight lines for a series of c_{in}-values. The slope, $\mathrm{d}h_g/\mathrm{d}v$, of the lines is calculated (cf. [7]) by the aid of the formula

$$\left[R_{F,g} = \left(\frac{\mathrm{d}h_g}{\mathrm{d}v}\right) : \left(\frac{\mathrm{d}h_s}{\mathrm{d}v}\right) = \right] \frac{\mathrm{d}h_g}{\mathrm{d}v} \cdot \frac{v_{0,s}}{h_0} = \frac{1}{1 + Q\,\alpha_g}. \tag{6}$$

Values of α_g are obtained directly from the assumed isotherm; e.g., for a LANGMUIR isotherm:

$$\alpha_g = \frac{f(c_g)}{c_g} = \frac{1}{c_g} \cdot \frac{k_g\, c_g}{1 + l_g\, c_g} = \frac{k_g}{1 + l_g\, c_g}\,. \tag{7}$$

In the two cases shown in Figs. 2 c and d, it is assumed that (i) the gradients are linear but of different steepness, (ii) a LANGMUIR isotherm with $k_g = 12$ and $l_g = 1$ is valid, and (iii) $Q = 2$. If it is also assumed that a front is formed where two migration lines cross, Figs. 2 c and d demonstrate the formation of a front, the shape of which is dependent on the experimental conditions. The last assumption is not perfectly correct. The results are, however, qualitatively consistent with observations made by HAGDAHL (private communication) during the development of the coupled filters described by him [10], and it seems justified to use this simplified picture of the process as a useful approximation.

The migration rate of a test substance as a function of the concentration of the gradient substance

For the concentration maximum of a zone of *a test substance with linear isotherms*, the following formula (cf. [11]) is valid

$$\left[R_{F,\mathrm{t}} = \left(\frac{\mathrm{d}\,h_\mathrm{t}}{\mathrm{d}\,v}\right) : \left(\frac{\mathrm{d}\,h_\mathrm{s}}{\mathrm{d}\,v}\right) = \right] \frac{\mathrm{d}\,h_\mathrm{t}}{\mathrm{d}\,v} \cdot \frac{v_{0,\mathrm{s}}}{h_0} = \frac{1}{1 + Q\,\alpha_\mathrm{t}} \tag{8}$$

where α_t is an empirically determinable function of c_g only.

When *a test substance has curved isotherms*, the migration rate is a function of both c_g and c_t. In such a case, $R_{F,t}$ has different values for different parts of the zone, and eq. (8) is valid only for infinitesimally small changes of v. However, α_t and $R_{F,t}$ can always—for a given value of c_t—be treated formally as functions of c_g only.

Available empirical data for the determination of $\alpha_t(c_g)$ and $\alpha_t(c_g, c_t)$ are scarce and often difficult to evaluate for this special purpose. To the end that this paper is not made purely theoretical, however, the following empirical formulas will be included in the treatment.

$$\alpha_t(c_g) = \frac{p - c_g}{c_g - q} \qquad (\text{for } q < c_g < p) \tag{9}$$

$$\alpha_t(c_g, c_t) = p \cdot 10^{-q' c_g} = p \cdot e^{-q c_g} \qquad (p = p(c_t);\ q = q(c_t)). \tag{10}$$

According to BOMAN (private communication; see also [18]), formula (9) is valid for the sorption of the prostatic phosphatase on Dowex 50. It should be observed that in this case $c_g = \mathrm{pH}$. For the small pH-range where this formula is valid, however, the pH-change can be made to parallel the addition of one buffer to another, so that c_g can formally be treated as a concentration. It is here assumed that the isotherms are linear.

Formula (10) can be shown to be approximately valid for the sorption of caprylic acid on charcoal in the presence of varying concentrations of ethanol (Fig. 4). For the c_t-values 0.05 % and 0.5 %, the sorption data (extracted from Fig. 3 in ref. [19]) are satisfactorily represented by the two expressions

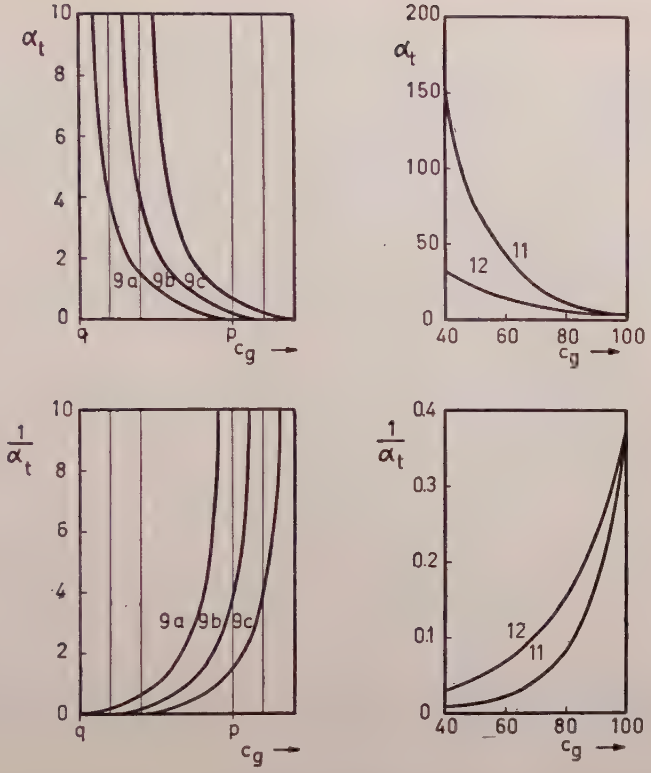

Fig. 5. Examples of possible relationships between the partition coefficient α_t (and its inverse value) and the concentration c_g of the gradient substance. The numbers in the diagrams correspond to the equations given in the text (*a*, *b* and *c* correspond to three different sets of p and q values, of which only the set for case 9*a* is shown).

$$\alpha_t(c_g) = 2500 \cdot 10^{-0.030\, c_g} = 2500 \cdot e^{-0.069\, c_g} \qquad (c_t = 0.05\ \%) \qquad (11)$$

$$\alpha_t(c_g) = 175 \cdot 10^{-0.018\, c_g} = 175 \cdot e^{-0.0415\, c_g} \qquad (c_t = 0.5\ \%). \qquad (12)$$

Fig. 5 shows the appearance of curves corresponding to formula (9) for three different sets of p and q values, and to formulas (11) and (12). Because the function $1/\alpha_t$ will be used later (eq. (18)), it has also been plotted.

Computation of migration curves for a test substance

A gradient substance with a linear isotherm. The first case considered is that in which *the test substance is sorbed with linear isotherms.* This case, which in practice is probably better treated by elution at a constant c_g-value (cf. [1]), is here included in the theoretical treatment as being an interesting and easily computed boundary case. Assuming that the migration of the concentration maximum of the zone is determined by eq. (8), the following expression is obtained for dv/dh_t

$$\frac{\mathrm{d}\,v}{\mathrm{d}\,h_t} = \frac{v_{0,s}}{h_0}\,(1 + Q\,\alpha_t). \tag{13}$$

Another expression for $\mathrm{d}v/\mathrm{d}h_t$ is obtained from formula (5) by differentiation for the case where $h = h_t$

$$\frac{\mathrm{d}\,v}{\mathrm{d}\,h_t} = \frac{\mathrm{d}\,w}{\mathrm{d}\,h_t} + \frac{v_{0,s}}{h_0}\,(1 + Q\,\alpha_g). \tag{14}$$

The combination of formulas (13) and (14) gives

$$\frac{\mathrm{d}\,w}{\mathrm{d}\,h_t} = \frac{v_{0,s}}{h_0}\,Q\,(\alpha_t - \alpha_g). \tag{15}$$

Because $c_g = c_g(w)$, α_t is a function of w, and the following expressions are obtained for the differential $\mathrm{d}h_t$ and its integral

$$\mathrm{d}\,h_t = \frac{h_0\,\mathrm{d}\,w}{v_{0,s}\,Q\,(\alpha_t\,[c_g\,(w)] - \alpha_g)}, \tag{16}$$

$$\Delta h_t = \frac{h_0}{v_{0,s}\,Q}\int_{w_1}^{w_2} \frac{\mathrm{d}\,w}{\alpha_t\,[c_g\,(w)] - \alpha_g}. \tag{17}$$

One special case is here immediately discernible: $\alpha_g = 0$, which implies that the gradient substance is not at all sorbed. The integral is then simplified to

$$\Delta\,h_t = \frac{h_0}{v_{0,s}\,Q}\int_{w_1}^{w_2} \frac{\mathrm{d}\,w}{\alpha_t\,[c_g\,(w)]}. \tag{18}$$

The possibility of solving these integrals depends on the complexity of the "double function" $\alpha_t[c_g(w)]$. Eqs. (19)–(22) show some rather simple solutions which have been obtained on the following assumptions: $h = 0$ for $v = 0$; for eq. (20), $1/k = 1/2$; for the first three cases, $c^0_{in} = \mathrm{q}$ and $c^0_e = \mathrm{p}$, i.e., c_g varies from q to p when w/V^0_1 and w/V^0_{tot} vary from 0 to ∞ and from 0 to 1, respectively. For simplicity, $h_0/v_{0,s}Q$ is replaced by $\mathbf{H}$.

Eqs. (1) and (9) $$h_t = -\mathbf{H}\left(\frac{w}{1+\alpha_g} + \frac{V^0_1}{\alpha_g\,(1+\alpha_g)}\log_e\left(1 + \alpha_g - \alpha_g\,e^{\frac{w}{V^0_1}}\right)\right) \tag{19}$$

Eqs. (4) and (9) $h_t =$

$$-\mathbf{H}\left(\frac{w}{1+\alpha_g} + \frac{2\left(\sqrt{1 - \frac{w}{V^0_{tot}}} - 1\right)V^0_{tot}}{(1+\alpha_g)^2} + \frac{2\,\alpha_g V^0_{tot}}{(1+\alpha_g)^3}\log_e\left[(1+\alpha_g)\sqrt{1 - \frac{w}{V^0_{tot}}} - \alpha_g\right]\right) \tag{20}$$

Eqs. (4 a) and (9) $$h_t = -\mathbf{H}\left(\frac{w}{1+\alpha_g} + \frac{V^0_{tot}\log_e\left[1 - (1+\alpha_g)\,\frac{w}{V^0_{tot}}\right]}{(1+\alpha_g)^2}\right) \tag{21}$$

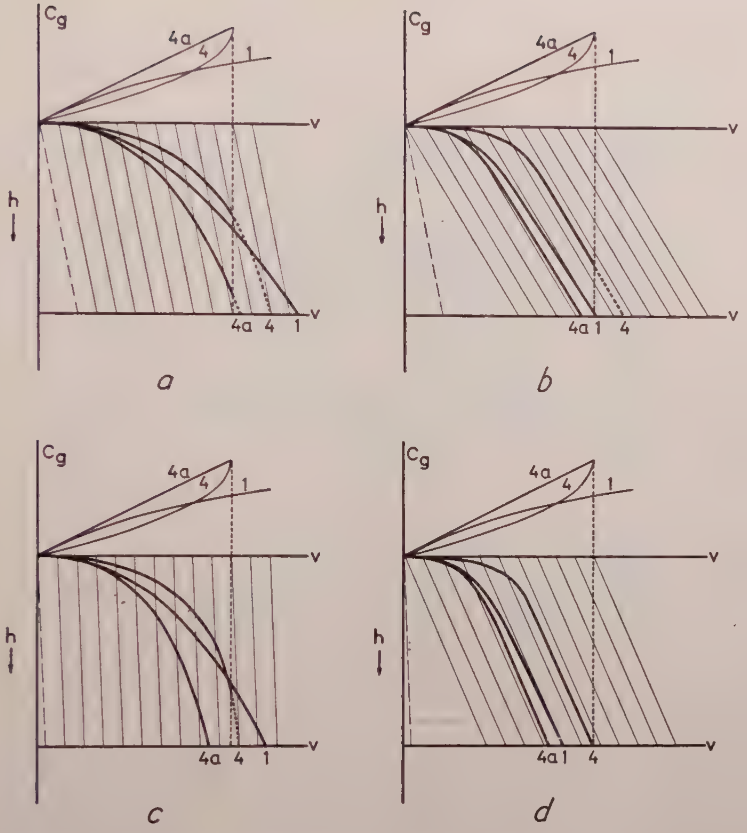

Fig. 6. Examples of migration curves—according to eqs. (19)–(21) and (19a)—for cases where the gradient is linear (4a), exponential (1) and concave (4).

a) $\alpha_g = 0, Q = 1$ b) $\alpha_g = 2, Q = 1$
c) $\alpha_g = 0, Q = 5$ d) $\alpha_g = 2, Q = 5$

Eqs. (4 a) and (10) $$h_t = -\mathbf{H}\left(\frac{w}{\alpha_g} + \frac{V^0_{\text{tot}}}{\mathrm{q}\,(c^0_e - c^0_2)\,\alpha_g}\log_e \frac{\mathrm{p}\cdot \mathrm{e}^{-\mathrm{q}\left[c^0_2 + (c^0_e - c^0_2)\frac{w}{V^0_{\text{tot}}}\right]} - \alpha_g}{\mathrm{p}\cdot \mathrm{e}^{-\mathrm{q}\,c^0_2} - \alpha_g}\right). \quad (22)$$

When $\alpha_g = 0$, this value can be introduced directly into formulas (20) and (21). For the other two cases, however, the integrals must be solved from the start with $\alpha_g = 0$. In that way, the following formulas are obtained

Eqs. (1) and (9); $\alpha_g = 0$ $$h_t = \mathbf{H}\left(V^0_1\,\mathrm{e}^{\frac{w}{V^0_1}} - w - V^0_1\right), \quad (19\text{ a})$$

Eqs. (4 a) and (10); $\alpha_g = 0$ $$h_t = \mathbf{H}\,\frac{\mathrm{e}^{\mathrm{q}\,c^0_2}\,V^0_{\text{tot}}}{\mathrm{p}\,\mathrm{q}\,(c^0_e - c^0_2)}\left(\mathrm{e}^{\mathrm{q}\,(c^0_e - c^0_2)\frac{w}{V^0_{\text{tot}}}} - 1\right). \quad (22\text{ a})$$

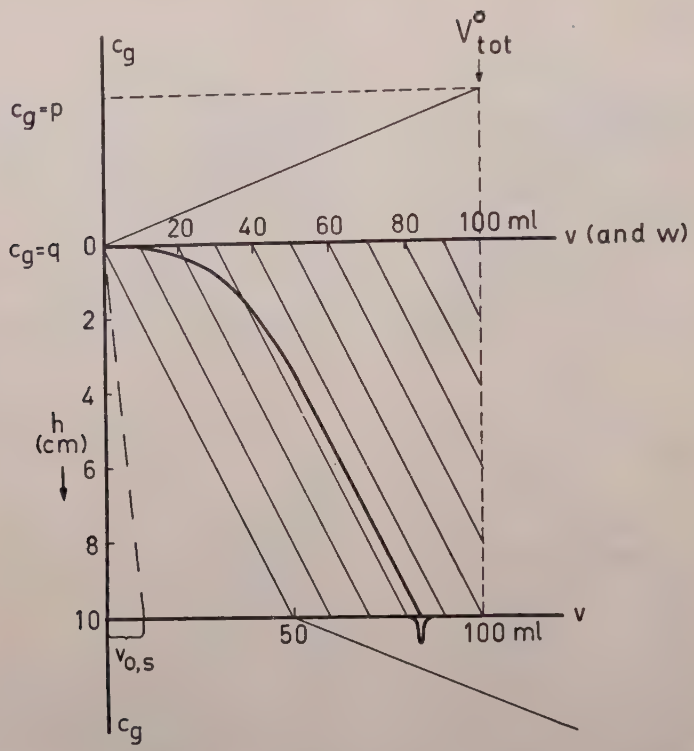

Fig. 7. The migration of a substance according to eq. (21) for the case where the parameters have the following values:

$\alpha_g = 2$ ml/gm
$Q = 2$ gm/ml
$v_{0,s} = 10$ ml
$V^0_{tot} = 100$ ml
$c^0_2 = q$ (= pH at start)
$c^0_e = p$ (≐ final pH)
$h_0 = 10$ cm (column diameter = approx. 10 mm)

When the integrals cannot or need not be solved, the graphical method described below may be used, or the area under the curve $\mathrm{d}h_t/\mathrm{d}w = \mathrm{f}(w)$ (see eq. (16)) may be measured.

When a function $h_t = \mathrm{F}(w)$ has been determined, the corresponding function $h_t = \mathrm{J}(v)$ can be formulated implicitly by using eq. (5)

$$v = w + \frac{v_{0,s} h_t}{h_0}(1 + Q\,\alpha_g) = \mathrm{G}(h_t) + \frac{v_{0,s} h_t}{h_0}(1 + Q\,\alpha_g). \qquad (23)$$

Here, $w = \mathrm{G}(h_t)$ signifies the inverse function of $h_t = \mathrm{F}(w)$. If $\mathrm{G}(h_t)$ can be expressed in explicit form, the curve for $h_t = \mathrm{J}(v)$ is obtained by plotting v as a function of h_t. If, however, this is not feasible, $\mathrm{J}(v)$ may be obtained instead by plotting h_t as a function of w in an h/v-diagram in which lines for constant values of w have been drawn (the latter method can be used to advantage also when $\mathrm{G}(h_t)$ can be expressed explicitly).

From the large number of possible combinations of parameter values, those represented in Fig. 6 have been arbitrarily chosen for the purpose of illustration. The

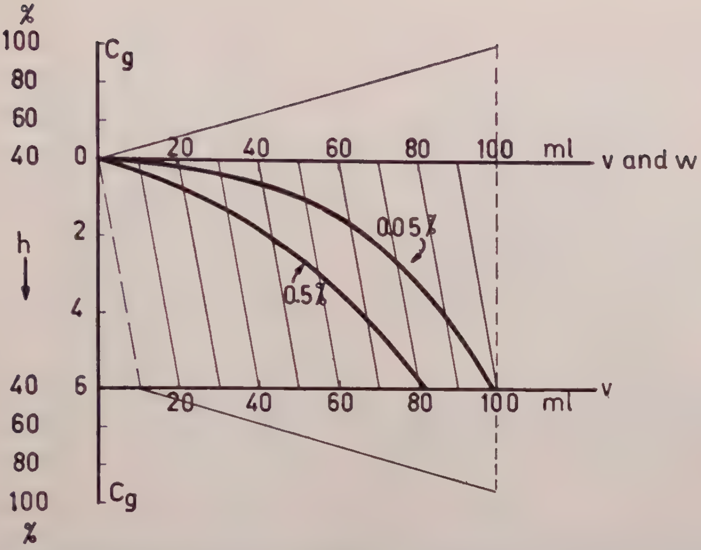

Fig. 8. Calculated migration—according to eq. (22 a)—of a test substance with LANGMUIR isotherm for the case where the gradient substance is not sorbed. The height, h, is plotted in **H** units

functions $h_t = F(w)$ have been computed according to formulas (19)–(21) and (19 a) and three curves for different gradient shapes have been plotted in each h/v-diagram by the aid of eq. (5). Two values each of α_g and of Q have been used, but it should be remembered that only one value of α_g is strictly applicable to the practical case which corresponds to formula (9). The actual value is at present unknown, but it probably lies between 1 and 3. In all cases, the columns are assumed to contain the same amount of sorbent, which implies that $v_{0,s}$ is inversely proportional to Q because $Q.v_{0,s}$ is the amount of sorbent in the column. In practice the variation of $v_{0,s}$, simultaneously keeping $Q.v_{0,s}$ constant, can be effected by mixing the sorbent with various amounts of some inert substance, and by appropriately increasing the tube diameter.

In order to increase the practical value of this paper, a diagram with coordinate scales and parameter values clearly indicated has also been prepared (Fig. 7). The diagram has been drawn on the assumptions that (i) $\alpha_g = 2$; $Q = 2$; (ii) a linear gradient is used, and (iii) the migration line corresponds to the α_t-curve marked 9 a in Fig. 5.

For *test substances with curved isotherms*, the migration formulas are much more complicated than those given above. Unfortunately, the formulas derived previously are not applicable here (see, e.g., TISELIUS [20] and CLAESSON [21] for frontal analysis, GLUECKAUF [8, 22] for elution of test substances with LANGMUIR isotherms, and MARTIN and SYNGE [7] for elution of test substances with linear isotherms). The reason is that the previous formulas refer to a constant composition of the solvent, and that gradient elution usually implies just the transition from curved to linear isotherms.

No attempt will be made here to solve the general problem, which involves complicated partial differential equations. Instead, an artifice is practised that permits an approximate treatment. On the isotherm valid for the initial value of c_g, one

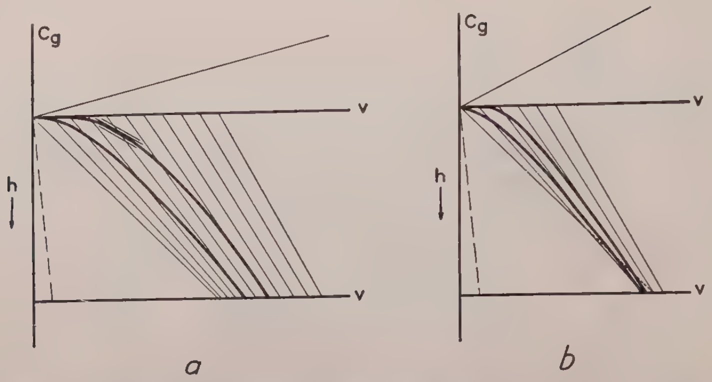

Fig. 9. Graphically determined migration curves—according to eq. (9)—of two test substances sorbed with linear isotherms for the case where a LANGMUIR isotherm—eq. (7)—is valid for the gradient substance. With the two steepnesses of the influent gradient, one run is successful and the other unsuccessful.

point is chosen somewhere above the most curved part (e.g., at $c_g = 0.5\ \%$), and another in a region near the origin where the isotherm is practically linear (e.g., at $c_g = 0.05\ \%$). If, for instance, eq. (22a) is applied to these two c_t-values, two curves are obtained, between which the test substance will migrate. Fig. 8 shows an example of a pair of curves, obtained on the assumption that the gradient is linear and that eqs. (11) and (12) are valid.

A gradient substance with a curved isotherm. In this case, formulas (14)–(18) cannot be used, because the successive concentrations of the gradient substance do not move with the same speed. Because no mathematical expression is available for this case, a simple method will instead be described for the visualization of the procedure.

A diagram (see Fig. 9) is constructed in the following way. The axes of an h/v-diagram are drawn, and the migration of the gradient substance is represented by straight lines as in Figs. 2c and d. A suitable part of each straight line is then crossed by several short lines whose slope signifies the rate of migration of the test substance at the actual c_g-value. Such construction lines are shown on one of the c_g-lines in Fig. 9a only. For the calculation of slope, eq. (8) can be used, if α_t is known as a function of c_g. Finally, the graphical solution is accomplished by drawing a curve in such a way that, whenever it crosses a c_g-line, it has the same slope as the corresponding construction lines.

Each one of the two hypothetical cases in Fig. 9 includes two test substances with linear isotherms. Eq. (7) is here applied instead of the unknown isotherm for the corresponding practical case.

Discussion on questions of migration and separation efficiency

From Fig. 6 it can be concluded that, with the assumptions made and with not too low α_g-values, the type of the gradient has only a small influence on the shape

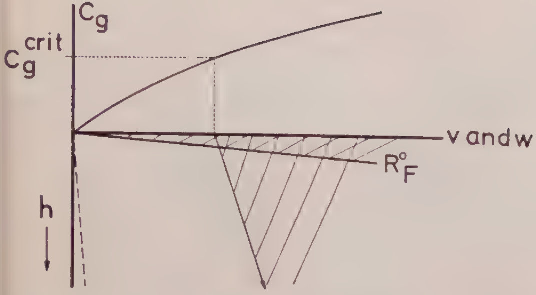

Fig. 10. Schematic diagram showing the region (not hatched) in which a migration line can exist, when there is a value, c_g^{crit}, for which $\alpha_t = \alpha_g$.

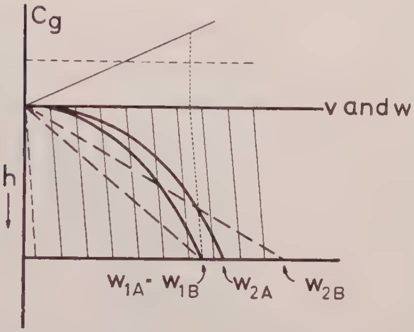

Fig. 11. Schematic diagram illustrating the relative zone-compressing effect of gradient elution (see the text).

of the migration curves. It should also be noted that when a concave gradient rises steeply towards the final value, the last part of the gradient is not utilized, because this part will never reach the lower end of the column (cf. dotted parts of the migration lines). Thus, a linear (or simple exponential) gradient should be capable of affording many separations which have hitherto been performed with more complicated types of gradients.

The peak effluent volume is determined by several factors, and it is therefore impossible to draw a final conclusion about sorption properties from a single experiment. However, two runs on columns identical but for their height are, together with a knowledge of $R_{F,g}$, sufficient to determine if a certain test substance migrates with the same speed as the gradient substance, i.e., if the c_g^{crit}-value has been reached. If such is the case (cf. Figs. 6b and d) for two test substances, a run with a longer column would not improve the separation, and the peak effluent volumes can be used as good characteristics of the substances in question; if it is not the case (cf. Figs. 6a and c), a comparison of two runs will still yield useful information on how to change the experimental conditions in order to improve the separation, etc.

When the test substances have curved isotherms, and when a small sample is applied to the column, each zone will spread rather rapidly, so that the maximal concentration decreases. This causes the front to move more slowly, and the zone will become narrower than shown in Fig. 8. In extreme cases, the maximal concentration may decrease to such an extent that it reaches the lowest, nearly straight part of an isotherm that is still curved in its upper part. After this has happened, the conditions are similar to those valid for test substances with linear isotherms. That such circumstances can occur in practical work is evident from the experimental data of ALM [23] and LAKSHMANAN and LIEBERMAN [17] who have reported effluent peak concentrations of the order of 0.01 %. Actually, it seems as if the use of such low concentrations had contributed effectively to these authors' successful separations.

A comparison of the two diagrams in Fig. 9 shows that a successful separation cannot be obtained when the substances to be separated migrate into a region where a front is being formed (this restriction was pointed out, but not illustrated, by ALM *et al.* [1]). In Fig. 9b there is a certain separation in the upper part of the column, but

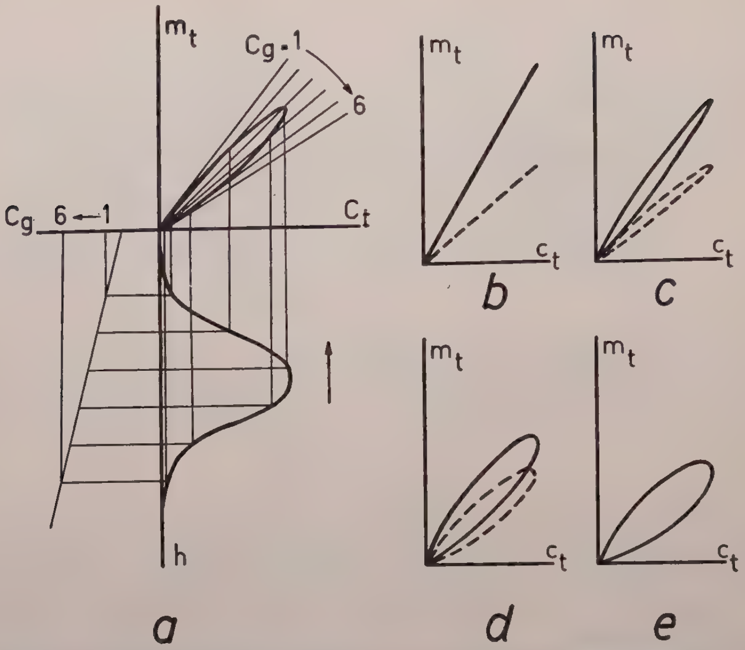

Fig. 12. Schematic diagram for "working-isotherms".—a, principle of construction; b–e, diagrams for two substances with linear isotherms and with no gradient, a flat, a moderate and a steep gradient, respectively.

in the lower part the zones are again brought close together. In such a case, a decrease of the column length or of the steepness of the gradient would give a better separation.

Each curve for which α_t reaches α_g at a finite w-value, can exist only in a region which has as its upper limit a line through the origin indicating the initial rate of migration, $R^0_{F,t}$, and a line indicating the critical c_g-value which makes $\alpha_t = \alpha_g$ (see Fig. 10). Good separations can be expected, when the test substances have different c_g^{crit}-values, especially when $R^0_{F,t}$ is very low. This seems to be the case for many proteins [24] whose sorption properties are often drastically changed within a small c_g-range.

If it is assumed that for two test substances, S_1 and S_2, the two "corrected migration rates" dh_{t_1}/dw and dh_{t_2}/dw are proportional for all c_g-values, these substances will migrate, e.g., as shown by the thick lines in Fig. 11. If, instead, the same test substances are assumed to be eluted at a constant c_g-value (represented by the horizontal dashed line in the upper part of the diagram) at which the isotherms for the two substances are linear, the migration lines will be straight. If it is also assumed that the second run is performed with a column of such size that the first substance, S_1, comes out at the same effluent volume as in the first case ($w_{1A} = w_{1B}$), the thick dashed lines in Fig. 11 are obtained. Evidently, the second substance, S_2, comes out much later in the last case (w_{2B} instead of w_{2A}), implying that gradient elution—as compared to usual elution—automatically causes the zones to approach each other, a process which hereafter will be referred to as a compression of zones.

In this connection, it should be noted that gradient elution is often resorted to,

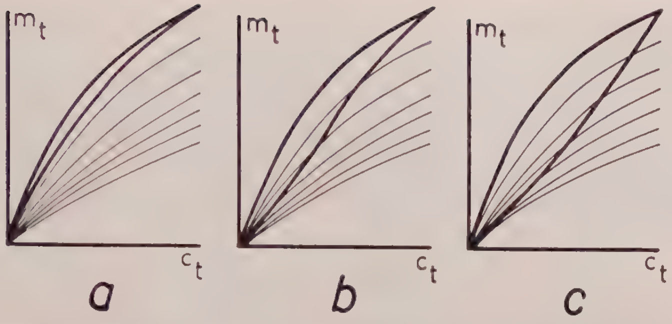

Fig. 13. Schematic diagram of "working-isotherms" for a substance with curved isotherms.—a, a flat, b, a moderate, and c, a steep gradient.

when it is desired to get a compression of zones. Examples of this are the cases where a mixture contains a number of substances covering quite a large α_t-range, or where a mixture contains substances whose sorption properties are insufficiently known. In usual elution, these cases demand such a low concentration of the eluting agent for the successful separation of the least sorbed substances that the substances with the strongest sorption will be eluted unreasonably slowly. Gradient elution seems to be of great help in such cases, but it should be borne in mind that there is always a risk of impaired separation by the application of this special type of elution.

A certain understanding of the relation between zone spreading and zone compression can be obtained by applying the concept of "working-isotherms" (see Fig. 12a). This word has been chosen to signify the locus for those combinations of concentration, c_t, and amount sorbed, m_t, which at a certain instant are co-existent in various parts of a zone. It should be noted that the zones are now assumed to occupy a finite length of the column.

Fig. 12a shows that a working-isotherm consists of a loop (these loops have been purposely exaggerated in Figs. 12 and 13), of which the upper arc corresponds to the front of the zone, while the lower one corresponds to its tail. For a substance with linear isotherms, this means that both the front and the tail will become sharpened, because a convex isotherm gives a front sharpening (and a tailing), while a concave isotherm gives a tail sharpening (but a diffuse front).

The schematical Figs. 12b–e show some fictitious working-isotherms for a pair of zones of two similar substances with linear isotherms, during elution with a solution of constant composition, and with gradients of different steepness. The diagrams show that the width of the loops increases, and that the difference between the working-isotherms decreases, when the steepness of the gradient is increased. This confirms the statement above that the zone-sharpening effect of gradient elution is accompanied by a relative compression of the zones.

When the isotherms of a test substance are curved, the working-isotherms have quite another appearance (see the schematical Fig. 13). Because of the front sharpening, all concentrations in the front are located within a narrow c_g-range. This means that the upper arc of the working-isotherm will practically coincide with the appropriate "gradient-free" isotherm. The shape of the lower arc will, however, depend on the steepness of the gradient. When this is made steeper, the lower arc becomes less curved, passes a stage where it is slightly S-shaped, and becomes finally—for very steep gradients—concave. It should be observed that this tail-sharpening effect can occur only when the gradient is rather steep.

When several zones of test substances with curved isotherms are present together, the problem becomes very complicated and cannot be treated within the scope of this paper. However, present knowledge clearly shows that, when using gradient elution, one always has to face the problem of choosing such experimental conditions that the desired zone sharpening is obtained together with an acceptably small zone compression.

APPENDIX

Equations for the shape of some simple gradients

A gradient is produced by continuously mixing two or more solutions in such a way that the concentration in the resulting solution of one or several substances steadily increases or, more seldom, decreases. The mixing is usually obtained by having one solution flow into another in a mixing chamber, but more than one mixing chamber may also be used.

For use in gradient elution, the gradient may be straight, concave, convex, or S-shaped. Below, it will be shown that all these shapes can be obtained by the use of one cylindrical solution container and one or two cylindrical mixing chambers, if all the vessels have a constant or proportionately varying liquid volume. Thus, only these cases will be considered in the following treatment.

For all mixing procedures, the following formula is valid: $\mathrm{d}\mathbf{M} = (\mathrm{d}\mathbf{M})_{\mathrm{in}} + (\mathrm{d}\mathbf{M})_{\mathrm{out}}$, where $\mathbf{M}\,(= V \cdot c)$ is the amount of the gradient substance in the mixing chamber. For the cases treated here, this fundamental formula may be written

$$c_{\mathrm{x}}\,\mathrm{d}V_{\mathrm{x}} + V_{\mathrm{x}}\,\mathrm{d}c_{\mathrm{x}} = c_{\mathrm{x}-1}\,\mathrm{d}v_{\mathrm{in}} + c_{\mathrm{x}}\,\mathrm{d}v_{\mathrm{out}} \qquad (24)$$

where x signifies the actual mixing chamber and x − 1 the preceding mixing chamber or the solution container, while v_{in} and v_{out} are the volumes coming into and going out from the mixing chamber.

Case 1. One mixing chamber with constant volume

It is assumed that $c_1 = c_1^0$ when $v = 0$, and that $V_1 = \text{const.} = V_1^0$ (see Fig. 14 left). Because $\mathrm{d}V_{\mathrm{x}} = \mathrm{d}V_1 = 0$, eq. (24) gives

$$V_1^0\,\mathrm{d}c_1 = (c_{\mathrm{e}}^0 - c_1)\,\mathrm{d}v \qquad (25)$$

which on integration gives

$$c_{\mathrm{in}} = c_1 = c_{\mathrm{e}}^0 - (c_{\mathrm{e}}^0 - c_1^0)\,\mathrm{e}^{-\frac{v}{V_1^0}}. \qquad (26)$$

Case 2. Two mixing chambers with constant, different volume

It is assumed that $c_1 = c_1^0$ and $c_2 = c_2^0$ when $v = 0$; $V_2 = V_2^0$; $V_1 = V_1^0 = V_2^0/k$ (see Fig. 14 middle). For the first mixing chamber (volume V_1^0), eq. (26) gives

$$c_1 = c_{\mathrm{e}}^0 - (c_{\mathrm{e}}^0 - c_1^0)\,\mathrm{e}^{-\frac{v}{V_1^0}}. \qquad (27)$$

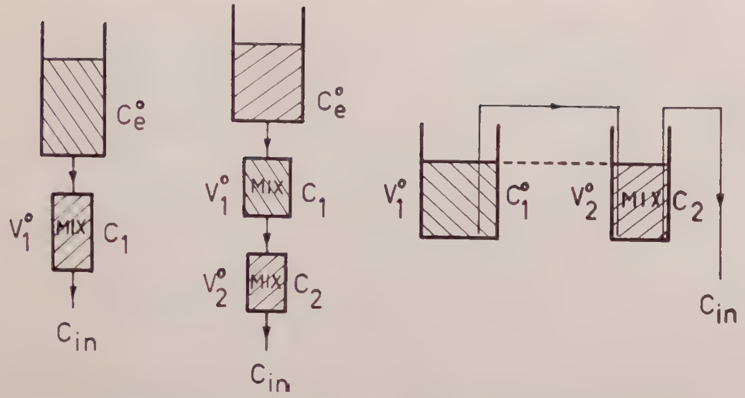

Fig. 14. Schematic drawing of some simple arrangements for the production of gradients.—*Left*, with one closed mixing chamber; *middle*, with two closed mixing chambers; *right*, with one open mixing chamber and one open solution container, in which the liquid surfaces are kept at the same level by means of a siphon.

For the second mixing chamber, the volume (V_2^0) is constant, i.e., $\mathrm{d}V_x = \mathrm{d}V_2 = 0$, but the influent concentration is variable, so that eq. (24) gives

$$V_2^0 \, \mathrm{d}c_2 = (c_1 - c_2)\, \mathrm{d}v. \tag{28}$$

Combined with eq. (27) this gives

$$\mathrm{d}c_2 = \frac{1}{V_2^0}\left(c_e^0 - (c_e^0 - c_1^0)\, \mathrm{e}^{-\frac{v}{V_1^0}} - c_2\right)\mathrm{d}v = \left(c_e^0 - (c_e^0 - c_1^0)\, \mathrm{e}^{-\frac{v}{V_1^0}}\right)\mathrm{d}\left(\frac{v}{V_2^0}\right) - c_2\, \mathrm{d}\left(\frac{v}{V_2^0}\right). \tag{29}$$

By multiplication with the integrating factor e^{v/V_2^0}, the differential equation

$$\mathrm{d}\left(c_2\, \mathrm{e}^{\frac{v}{V_2^0}}\right) = \mathrm{e}^{\frac{v}{V_2^0}}\left(c_e^0 - (c_e^0 - c_1^0)\, \mathrm{e}^{-\frac{v}{V_1^0}}\right)\mathrm{d}\left(\frac{v}{V_2^0}\right) \tag{30}$$

is obtained. On integration, this gives

$$c_{\mathrm{in}} = c_2 = c_e^0 - \frac{V_1^0}{V_1^0 - V_2^0}(c_e^0 - c_1^0)\, \mathrm{e}^{-\frac{v}{V_1^0}} - \left(\frac{c_e^0 V_2^0 - c_1^0 V_1^0}{V_1^0 - V_2^0} - c_2^0\right)\mathrm{e}^{-\frac{v}{V_2^0}} \tag{31}$$

or, if kV_1^0 is substituted for V_2^0

$$c_{\mathrm{in}} = c_e^0 - \frac{c_e^0 - c_1^0}{1-k}\, \mathrm{e}^{-\frac{v}{V_1^0}} - \frac{k\, c_e^0 - c_1^0 - (1-k)\, c_2^0}{1-k}\, \mathrm{e}^{-\frac{v}{k V_1^0}}. \tag{32}$$

Obviously, eqs. (31) and (32) are useless, if the two mixing chambers have the same volume, because in such a case $V_1^0 - V_2^0 = 1 - k = 0$. For this reason, the following calculation is also made.

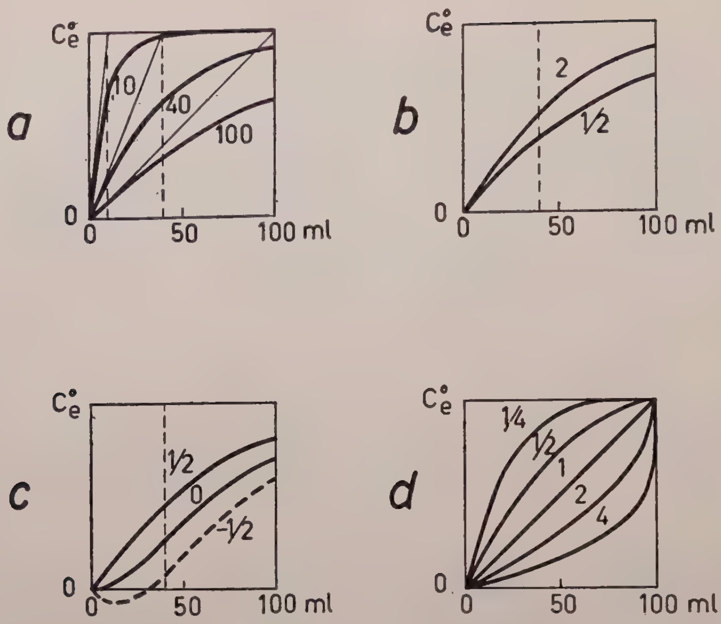

Fig. 15. Gradient shapes, $c_{\text{in}} = \mathrm{f}(v)$, according to a, eq. (39), with $V_1^0 = 10$, 40 and 100 ml (the thin lines show the slope of the curves at the start); b, eq. (40), with $V_2^0 = 40$ ml.; $c_1^0 = c_e^0/2$; $k = 2$ and 1/2; c, eqs. (41) and (41 a), with $V_2^0 = 40$ ml, $c_1^0 = c_e^0/2$, 0, $-c_e^0/2$; d, eqs. (42) and (42 a), with $V_{\text{tot}}^0 = 100$ ml, $k = 1/4$, 1/2, 1, 2 and 4. In all cases, $c_{\text{in}}^0 = 0$.

Case 3. Two mixing chambers with constant, equal volume

It is assumed that $c_1 = c_1^0$ and $c_2 = c_2^0$ when $v = 0$; $V_1 = V_2 = V_2^0$ (see Fig. 14 middle). By analogy with Case 2, the following formulas are obtained

$$\mathrm{d}\,c_2 = \left(c_e^0 - (c_e^0 - c_1^0)\,\mathrm{e}^{-\frac{v}{V_2^0}}\right)\mathrm{d}\left(\frac{v}{V_2^0}\right) - c_2\,\mathrm{d}\left(\frac{v}{V_2^0}\right) \tag{33}$$

$$\mathrm{d}\left(c_2\,\mathrm{e}^{\frac{v}{V_2^0}}\right) = \left(c_e^0\,\mathrm{e}^{\frac{v}{V_2^0}} - (c_e^0 - c_1^0)\right)\mathrm{d}\left(\frac{v}{V_2^0}\right) \tag{34}$$

$$c_{\text{in}} = c_2 = c_e^0 - (c_e^0 - c_1^0)\,\frac{v}{V_2^0}\,\mathrm{e}^{-\frac{v}{V_2^0}} - (c_e^0 - c_2^0)\,\mathrm{e}^{-\frac{v}{V_2^0}}. \tag{35}$$

The special case $c_1^0 = c_2^0$ gives

$$c_{\text{in}} = c_e^0 - (c_e^0 - c_2^0)\,\frac{v + V_2^0}{V_2^0}\,\mathrm{e}^{-\frac{v}{V_2^0}}. \tag{35 a}$$

Case 4. One mixing chamber and one solution container, the liquid volumes of which are variable but proportional

It is assumed that $c_1 = c_1^0 = c_e^0$; $c_2 = c_2^0$ when $v = 0$; $V_1 + V_2 = V_{\text{tot}}$; $V_2 = k\,V_1$ (see Fig. 14 right). According to the general eq. (24)

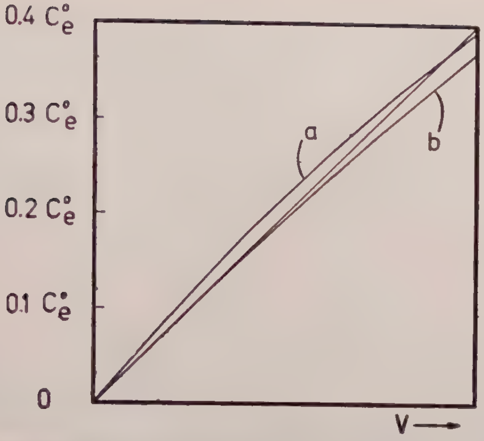

Fig. 16. Approximate linearity of the first 40 per cent of gradients according to *a*, eq. (39), and *b*, eq. (41 a) with $c_1^0 = c_e^0/2$.

$$V_2\,\mathrm{d}c_2 + c_2\,\mathrm{d}V_2 = -c_1\,\mathrm{d}V_1 + c_2\,\mathrm{d}V_{\mathrm{tot}} \tag{36}$$

which, because always $V_2 = kV_1$, can be transformed to

$$V_2\,\mathrm{d}c_2 = -(c_e^0 - c_2)\,\mathrm{d}V_1 = -(c_e^0 - c_2)\frac{\mathrm{d}V_2}{k}. \tag{37}$$

Integration gives

$$c_{in} = c_2 = c_e^0 - (c_e^0 - c_2^0)\left(1 - \frac{v}{V_{\mathrm{tot}}^0}\right)^{1/k}. \tag{38}$$

The special case $k = 1$ gives

$$c_{in} = c_e^0 - (c_e^0 - c_2^0)\left(1 - \frac{v}{V_{\mathrm{tot}}^0}\right) = c_2^0 + (c_e^0 - c_2^0)\frac{v}{V_{\mathrm{tot}}^0}. \tag{38 a}$$

General considerations

The formulas derived above can be presented in a simpler form, if W is substituted for v/V_1^0 and v/V_{tot}^0, and if c_{in}^0 is assumed to be zero. The following formulas are then obtained

Case 1 $(c_{in}^0 = c_1^0 = 0)$ $\quad c_{in} = c_e^0(1 - e^{-W})$ (39)

Case 2 $(c_{in}^0 = c_2^0 = 0)$ $\quad c_{in} = c_e^0 - \frac{c_e^0 - c_1^0}{1-k}e^{-W} - \frac{k\,c_e^0 - c_1^0}{1-k}e^{-\frac{W}{k}}$ (40)

Case 3 $(c_{in}^0 = c_2^0 = 0)$ $\quad c_{in} = c_e^0 - (c_e^0 + (c_e^0 - c_1^0)\,W)\,e^{-W}$ (41)

Case 3 a $(c_{in}^0 = c_1^0 = c_2^0 = 0)$ $\quad c_{in} = c_e^0(1 - (1 + W)\,e^{-W})$ (41 a)

Case 4 $(c_{in}^0 = c_2^0 = 0)$ $\quad c_{in} = c_e^0(1 - (1 - W)^{1/k})$ (42)

Case 4 a $(c_{in}^0 = c_2^0 = 0)$ $\quad c_{in} = c_e^0\,W.$ (42 a)

The shapes of some gradients corresponding to these formulas are shown in Fig. 15. When $c_{in}^0 \neq 0$, the application of the more general formulas gives other ordinate scales, but the shapes of the curves are not changed.

All formulas derived previously for gradient elution [1, 12, 13, 17] fit into some of the formulas given above (the production of gradients by the use of non-cylindrical solution containers and mixing chambers [15, 16] has not been considered here). The most general of the previous formulas is that given by LAKSHMANAN and LIEBERMAN [17]

$$c = c_0 - c_0 \left(\frac{a}{a + b\,t} \right)^{1/b} \tag{43}$$

which corresponds to eq. (42). The other formulas [1, 12, 13] correspond to eq. (39). In one case, a linear gradient [14], corresponding to eq. (42 a), has been used.

Usually, it is the first part of a gradient that is utilized, while the last part is often unused or even useless. Thus, the first part of the curves deserves special consideration. The slope of gradients—according to, e.g., Case 1, eq. (25) and Cases 2 and 3, eq. (28)—can be written

$$\frac{d\,c_{in}}{d\,v} = \frac{c_e^0 - c_1}{V_1^0} \quad \text{and} \quad \frac{d\,c_{in}}{d\,v} = \frac{c_1 - c_2}{V_2^0}. \tag{44 a and b}$$

For the initial conditions ($v = 0$), this gives

$$\left(\frac{d\,c_{in}}{d\,v} \right)_{v=0} = \frac{c_e^0 - c_1^0}{V_1^0} \quad \text{and} \quad \left(\frac{d\,c_{in}}{d\,v} \right)_{v=0} = \frac{c_1^0 - c_2^0}{V_2^0}. \tag{45 a and b}$$

For Case 1 above, formula (45 a) indicates a simple way of constructing the tangent of the gradient curve at $v = 0$ (cf. the thin lines in Fig. 15 a). For Case 2 above, formula (45 b) shows that the gradient has an initial slope of zero, if $c_2^0 = c_1^0$. This case has practical importance because it shows the possibility of producing a gradient that starts horizontally, as a prolongation of the base line. If $c_2^0 > c_1^0$, the gradient starts with a depression (see Fig. 15 c). At present, such a gradient seems to be useless in gradient elution.

It should be noted that a nearly linear gradient can be obtained, if the c_e^0-value is chosen much higher than the highest c_{in}-value desired. As an illustration of this, the first parts of two gradients—according to Case 1, eq. (39) and Case 3 a, eq. (41 a)—are compared, in Fig. 16, to a linear gradient.

Summary

Some basic concepts of the theory of gradient elution analysis have been formulated in order to illustrate the principles of the procedure and in order to facilitate the design of successful experiments.

Consideration has been paid to the shape of the influent gradient, to the migration of this gradient through the column, and to the strength of sorption of a test substance at different concentrations of the gradient substance and, for curved isotherms of the test substances, at different concentrations of the test substances themselves.

The migration of the peak concentration of narrow zones, when both the gradient substance and the test substances have linear isotherms, is expressed in mathematical

formulas. The case that the test substances have curved isotherms is treated in an approximative way. A graphical method is devised for the case that the gradient substance is sorbed with a curved isotherm.

From a discussion of migration and separation efficiency it is concluded that gradient elution may have obvious practical advantages over elution at a constant concentration of the eluting agent, but also that it cannot guarantee the improvement of the separation of a certain pair of substances. The reason for this is that the sharpening of zones by the action of the gradient must always be accompanied by a relative pushing together of the zones.

ACKNOWLEDGEMENT

The author is indebted to Professor Arne Tiselius and to his colleagues Hans Boman, Lennart Hagdahl and Jerker Porath for fruitful discussions and helpful suggestions. Mr. Göran Kjellberg, Stockholm, has kindly checked the mathematical treatment and offered valuable suggestions for its improvement, for which cordial thanks are expressed.

Institute of Biochemistry, University of Uppsala, Uppsala, Sweden.

REFERENCES

1. Alm, R. S., Williams, R. J. P., and Tiselius, A., *Acta Chem. Scand. 6,* 826 (1952).
2. Marshall, L. M., Donaldson, K. O., and Friedberg, F., *Anal. Chem. 24,* 773 (1952).
3. Mader, C., *Anal. Chem. 26,* 566 (1954).
4. Sillén, L. G., *Arkiv f. Kemi Min. Geol. 22 A,* No. 15 (1946).
5. *The van Nostrand Chemist's Dictionary,* New York, 1953.
6. Weyde, E., and Wicke, E., *Koll.-Z. 90,* 156 (1940).
7. Martin, A. J. P., and Synge, R. L. M., *Biochem. J. 35,* 1358 (1941).
8. Glueckauf, E., *J. Chem. Soc. 1947,* 1315.
9. Boyd, G. E., Myers Jr., L. S., and Adamson, A. W., *J. Am. Chem. Soc. 69,* 2849 (1947).
10. Hagdahl, L., *Acta Chem. Scand. 2,* 574 (1948).
11. Consden, R., Gordon, A. H., and Martin, A. J. P., *Biochem. J. 38,* 224 (1944).
12. Donaldson, K. O., Tulane, V. J., and Marshall, L. M., *Anal. Chem. 24,* 185 (1952).
13. Cherkin, A., Martinez, F. E., and Dunn, M. S., *J. Am. Chem. Soc. 75,* 1244 (1953).
14. Lindberg, B., and Wickberg, B., *Acta Chem. Scand. 7,* 140 (1953).
15. Desreux, V., *Rec. trav. chim. Pay-Bas 68,* 789 (1949).
16. Gross, J., and Martin, A. J. P., *Proc. Biochem. Soc. 51,* xxvii (1952); also private communication.
17. Lakshmanan, T. K., and Lieberman, S., *Arch. Biochem. Biophys. 45,* 235 (1953).
18. Boman, H. G., *Nature 173,* 447 (1954).
    —— To be published in *Biochem. Biophys. Acta.*
19. Williams, R. J. P., Hagdahl, L., and Tiselius, A., *Arkiv f. Kemi 7,* 1 (1954).
20. Tiselius, A., *Arkiv f. Kemi Min. Geol. 14 B,* No. 22, No. 32 (1940); *15 B,* No. 6, No. 18 (1941).
21. Claesson, S., *Arkiv f. Kemi Min. Geol. 20 A,* No. 3 (1945).
22. Glueckauf, E., *J. Chem. Soc. 1947,* 1308.
    —— *Proc. Royal Soc. 186 A,* 35 (1946).
23. Alm, R. S., *Acta Chem. Scand. 6,* 1186 (1952).
24. Tiselius, A., *Arkiv f. Kemi 7,* 443 (1954).

Tryckt den 9 mars 1955

Uppsala 1955. Almqvist & Wiksells Boktryckeri AB

ARKIV FÖR KEMI Band 8 nr 2

Communicated 10 November 1954 by Arne Fredga

Infra-red investigation of the conjugation of the isomeric thiophenecarboxylic acids and thiophenecarboxaldehydes

By Salo Gronowitz and Andreas Rosenberg

With 2 figures in the text

The effect of a −M-substituent (according to Ingold's terminology), such as −COOH or −CHO, in the 2-position of thiophene upon substitution is well established. Investigations of the dipole moment (1) indicate that the following resonance structures are of importance for 2-thiophenecarboxaldehyde:

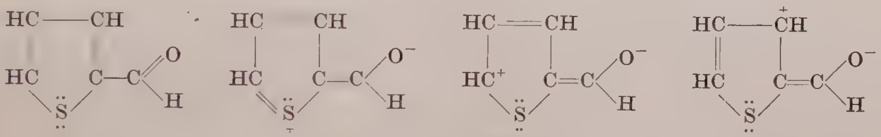

From these formulae it can be seen that a −M-substituent in the 2-position deactivates the whole nucleus against electrophilic substitution, but mostly in the 3- and 5-position (*ortho* and *para* position) quite in accordance with the conditions in benzene. On the other hand the sulphur atom activates the 5-position. Thus, depending on the relative strength of these effects monosubstitution is obtained predominantly in the 4- or 5-position. As the −CHO group has a stronger −M-effect than the −COOH group, due to inner conjugation in the latter, substitution is obtained almost exclusively in the 4-position, when nitrating 2-thiophenecarboxaldehyde (2) and predominantly in the 5-position on nitration of 2-thiophenecarboxylic acid (3). Disubstitution always results in 4- and 5-substituted compounds and trisubstitution cannot be obtained.

Very little is known about the directing influence of 3-substituted thiophenes of this type. It has been assumed by analogy with benzene chemistry that the 4- and 2-positions are deactivated by a −M-substituent. Campaigne and Bourgeois (4) recently investigated the bromination and chlorination of 3-thiophenecarboxylic acid obtaining monohalogenation in the 5-position and dihalogenation in the 5- and 2-positions. However, it was found by the present authors that through extensive bromination of 3-thiophenecarboxylic acid 2,4,5-tribromo-3-thiophenecarboxylic acid can be obtained. 2-Thiophenecarboxylic acid gives under the same conditions only 4,5-dibromo-2-thiophenecarboxylic acid (5). This seems to indicate that the 4-position is not selectively deactivated by a −M-substituent in the 3-position and that the conditions are not at all comparable with those in benzene. Also, investigations by Steinkopf *et al.* (6) on the dinitration and disulphonation of 2,5-dichlorothiophene, 2,5-dibromothiophene, 2,5-dimethylthiophene and 2-bromo-5-methylthiophene in the 3,4-positions show that a −M-substituent in the 3-position does not deactivate the 4-position. It has also been shown by STEINKOPF (7) that 3-nitrothiophene gives triacetoxymercury-3-nitrothiophene. Under the same conditions only a diacetoxymercury-2-nitrothiophene is obtained from 2-nitrothiophene. The explanation given by HARTOUGH (8) of these experimental facts seems somewhat unlikely.

In order to explain these experimental results the following resonance formulae are assumed by us to contribute to the structure of thiophenes containing a −M-substituent in the 3-position. (Illustrated for the aldehyde.)

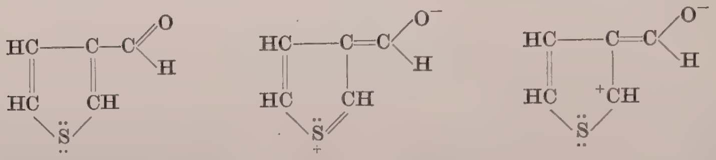

It should be noted that no structure can be constructed which has a positive charge on the carbon atom in the 4-positon without placing a decett around the sulphur. These formulae indicate that a −M-substituent by its mesomeric effect most strongly deactivates the 2-position, but that *both* the 4- and 5-positions are not deactivated to the same extent as the 2-position. The most reactive position is thus the 5-position which is activated by the sulphur atom and not influenced directly by the substituent. It is however difficult to decide whether the deactivating effect of the substituent on the 2-position is strong enough to counteract the activating effect of the sulphur atom on this position, thus rendering the 4-position more reactive than the 2-position. These formulae also explain the ease with which three substituents can be introduced in these compounds.

If we now consider the resonance formulae of thiophene compounds with a −M-substituent in the 2-position, we see that there are three resonance formulae where the carbon-carbon bond between the ring and the substituent is of double bond character. Considering the resonance possibilities for the 3-isomers only two forms with these conditions can be found. Thus it should be expected that if these formulae represent the real resonance states, the 2-substituted compounds should conjugate to a higher degree than the corresponding 3-isomers. The dissociation constants of 2- and 3-thiophenecarboxylic acids (9) also indicate that in the 2-isomer the carboxyl group is more effectively conjugated with the thiophene nucleus than in the 3-isomer. 2-Thiophenecarboxylic acid is a considerably stronger acid than 3-thiophenecarboxylic acid.

In order to confirm our views on the conjugation conditions in these compounds we decided to investigate the infra-red absorption spectra of the isomeric thiophenecarboxylic acids and of the aldehydes. It is generally accepted that conjugation results in a shift of the main C = C and C = O absorption bands towards lower frequencies (10, 11, 12). At the same time it is generally known that differences in substitution or physical state influence the position of the carbonyl band (10, 13). In order to avoid such complications the unsubstituted acids and aldehydes were examined in chloroform solution so that no other factors capable of affecting the frequency were present.

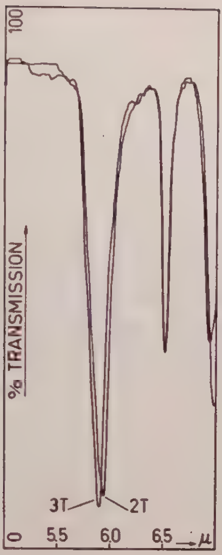

Fig. 1. 2T is 2-thiophenecarboxylic acid, 3T is 3-thiophenecarboxylic acid.

Fig. 1 shows the carbonyl bands of the isomeric thiophenecarboxylic acids. The complete absorption curves of these acids have been previously published by GRONOWITZ (14). 2-Thiophenecarboxylic acid shows the $C=O$ frequency at 1679 cm^{-1} and 3-thiophenecarboxylic acid at 1690 cm^{-1}. The shift observed is thus 11 cm^{-1}. Fig. 2 shows the IR absorption spectra of 2- and 3-thiophenecarboxaldehydes. The carbonyl frequency of the 2-isomer is at 1673 cm^{-1} and of the 3-isomer at 1691 cm^{-1}. The difference is thus 18 cm^{-1}. The difference in conjugation between 2- and 3-substituted thiophenes is influenced by the internal conjugation in the substituent. Thus it is clear that the difference between the thiophenecarboxaldehydes should be larger than between the corresponding acids. When compared with a shift of 30 cm^{-1} measured by RASMUSSEN *et al.* (10) for conjugation of aliphatic ketones, the results obtained by us show that the differences in conjugation between 2- and 3-substituted thiophenealdehydes and acids are of such an order that differences in substitution reactions are to be expected and supports the explanation proposed by us.

Experimental

2-Thiophenecarboxylic acid was prepared according to SCHLENK and OCHS (15). The acid was recrystallised several times from water. M.p 129–130°. *3-Thiophenecarboxylic* acid was prepared according to GRONOWITZ (14). M.p. 138–139°. *2-Thiophenecarboxaldehyde* was synthezised according to KING and NORD (16), and *3-thiophenecarboxaldehyde* via the reaction of 3-thienyllithium with N,N-dimethylformamide (17). The aldehydes were carefully distilled and the infra-red spectra immediately recorded.

2,4,5-Tribromo-3-thiophenecarboxylic acid. On 0.5 g 3-thiophenecarboxylic acid was poured an excess of bromine. The bromine was evaporated over night and the white residue recrystallised from toluene, giving 1.2 g (80 %) of 2,4,5-tribromo-3-thiophenecarboxylic acid. M.p. 203–205°.

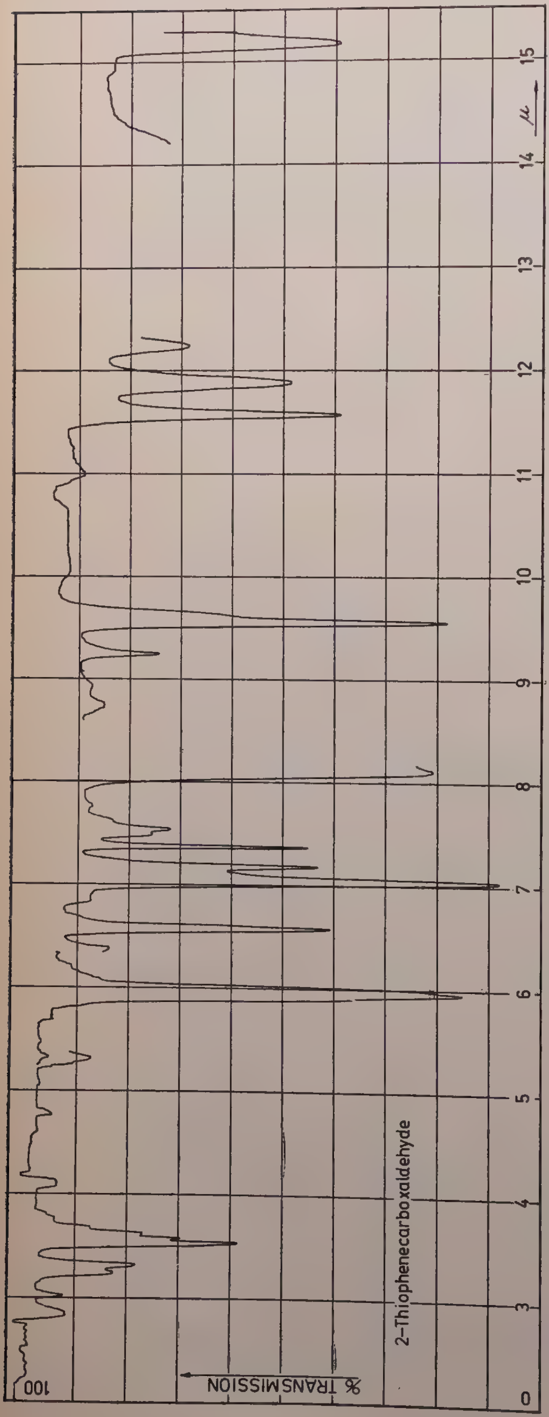
2-Thiophenecarboxaldehyde
% TRANSMISSION
100
0
3
4
5
6
7
8
9
10
11
12
13
14
15
μ

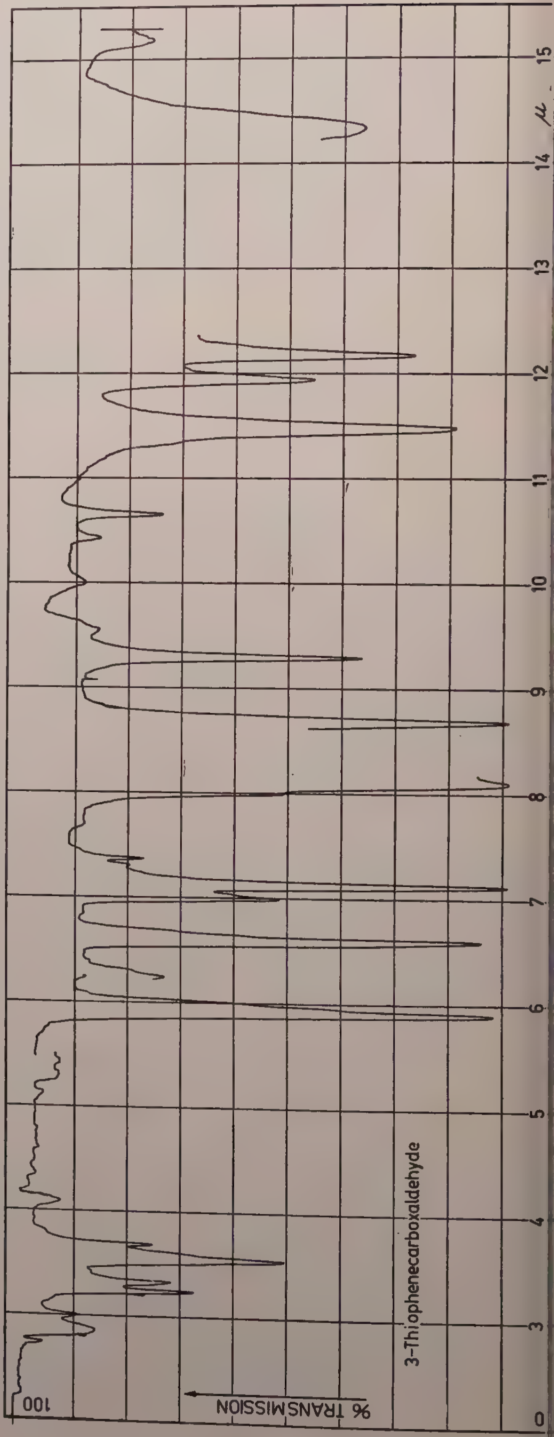
3-Thiophenecarboxaldehyde
% TRANSMISSION
100
0
3
4
5
6
7
8
9
10
11
12
13
14
15
μ

Anal. 159.20 mg: 9.01 ml 0.04802-N NaOH; — 13.12 mg: 5.56 ml 0.01956-N $Hg(NO_3)_2$;
$C_5HBr_3O_2S$ (364.9) calc. Equiv. wt. 364.9 Br 65.71 %
found » » 368.0 » 65.94 %

A Perkin Elmer mod 21 spectrophotometer equipped with NaCl prism was used for the infra-red measurements. The substances were examined as ca 2 % solutions in chloroform.

Summary

In order to explain the differences in the substitution reactions of 2- and 3-thiophenecarboxylic acids and 2- and 3-thiophenecarboxaldehydes the difference in conjugation between these compounds has been studied by IR absorption measurements. It has been found, that the 2-substituted compounds are more effectively conjugated than the corresponding 3-isomers.

The authors are indebted to Mr. R. Öhberg for the analyses and to Mr. S. Bergvall for taking the IR spectra.

Department of Organic Chemistry, Chemical Institute and Institute of Biochemistry, University of Uppsala, October 1954.

REFERENCES

1. Keswani, R., and Freiser, H., J. Am Chem. Soc. *71*, 1789 (1948).
2. Foye, W. C., Hefferren, J. J., and Feldmann E. G., J. Am. Chem. Soc. *76*, 1378 (1954).
3. Rinkes, I. J., Rec. trav. chim. *51*, 1134 (1932).
4. Campaigne, E., and Bourgeois, R. C., J. Am. Chem. Soc. *76*, 2445 (1954).
5. Bonz, R., Ber *18*, 2308 (1886).
6. Steinkopf, W., Jacob, H., and Penz, H., Ann. *512*, 136 (1934).
   Steinkopf, W., Poulsson, I., and Herdey, O., Ann. *536*, 128 (1938).
   Steinkopf, W., and Höpner, T., Ann. *501*, 174 (1933).
7. Steinkopf, W., Ann. *545*, 38 (1940).
8. Hartough, H. D., Thiophene and Its Derivatives. New York 1952, p. 223.
9. Steinkopf, W., Die Chemie des Thiophens. Dresden und Leipzig 1941, p. 85.
10. Rasmussen, R. S., Tunnicliff, D. D., and Brattain, R. R., J. Am. Chem. Soc. *71*, 1086 (1949).
11. Thompson, H. W., and Torkington, P., J. Chem. Soc. *1945*, 640.
12. Hunsberger, I. M., J. Am. Chem. Soc. *72*, 5626 (1950).
13. Hartwell, E. J., Richards, R. E., and Thompson, H. W., J. Chem. Soc. *1948*, 1436.
14. Gronowitz, S., Arkiv Kemi *7*, 361 (1954).
15. Schlenk, W., and Ochs, R., Ber *48*, 679 (1915).
16. King, W. J., and Nord, F. F. J. Org. Chem. *13*, 635 (1948).
17. Gronowitz, S., To be published.

Tryckt den 9 mars 1955

Uppsala 1955. Almqvist & Wiksells Boktryckeri AB

ARKIV FÖR KEMI Band 8 nr 3

Communicated 1 December 1954 by ARNE FREDGA

Acid-induced hydrogen exchange in thiophene

By KJELL HALVARSON and LARS MELANDER

With 2 figures in the text

As the acid-induced hydrogen exchange in aromatic compounds has been shown to follow the orientation rules of electrophilic substitution (1, 2) it could be anticipated that the hydrogen exchange in thiophene should be considerably more rapid in position 2 than in position 3 (cf. (3)). Measurements of the exchange rates should be of interest, since they will generally give a fairly accurate value even if the rates differ in order of magnitude, and the side-reactions are relatively unimportant under the conditions of the experiment, as compared to other kinds of substitution. SCHREINER (4) has used the exchangeability of the hydrogen atoms of thiophene for the preparation of more or less completely deuterated thiophenes by means of interaction with heavy sulphuric acid, but no measurements of the relative exchange rates of the two different positions were made.

The existing great difference in exchange rate between the two positions made it possible to use the exchange also as a method of preparation of tracer amounts of thiophene-2-t and -3-t. The former could be prepared in a short exchange procedure, during which only a small amount of the latter is formed. Under other conditions (stronger acid, longer exchange period, and higher temperature) exchange in all positions could be managed (4), and the isotopic hydrogen subsequently removed almost exclusively from position 2 by a proper choice of conditions.

When the tritium content of such a preparation is represented as a function of the time of exchange with a suitable acid, the shape of the curve will indicate the presence of the isomer. Thus the exchange may be used even as an analytical procedure.

Experimental

Tritium.—The tritium used originates from the Atomic Energy Research Establishment, Harwell.

Determination of tritium.—The combustion of thiophene was carried out according to two methods, both of which are considered satisfactory. According to one method, the compound is burned over copper oxide at 750°C in a stream of oxygen, the sulphur dioxide being retained in lead chromate at 430°C (5). According to the other, the compound is burned over Vinosit B at 650°C in a stream of oxygen.

The tritium in the water obtained from the combustion was determined with the same method and apparatus as described previously (6). The accuracy was ± 2 %. The corrections for the natural decay of tritium were made assuming its half-life to be 12.5 years.

Preparation of tracer amounts of thiophene-2-t.—10 ml of thiophene and 9 ml of 59.4 % sulphuric acid containing tritium were shaken vigorously for 80 minutes at

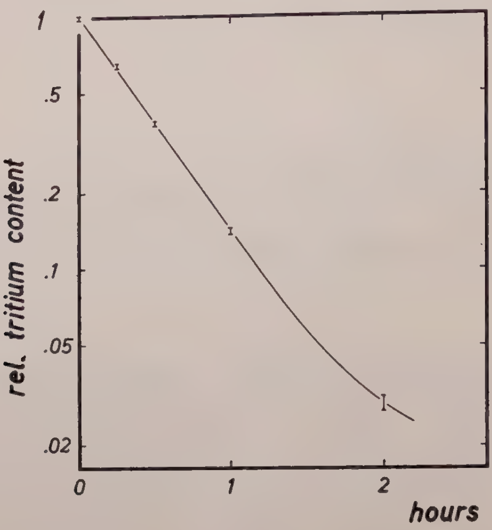

Fig. 1. Semilogarithmic plot of relative specific activity of thiophene-2-t as a function of time of exchange (2 ml of thiophene shaken with 20 ml of 59.4 % sulphuric acid at 25°C).

25°C. The thiophene was separated off, washed with water, dried with calcium chloride, and distilled. In connexion with the distillation inactive thiophene was added in a suitable amount to give a convenient specific activity.

3 ml of the preparation was shaken twice for 80 minutes with 20 ml portions of 59.4 % inactive sulphuric acid, washed, dried, and distilled. 2.2 % of the activity was left, corresponding to thiophene-3-t formed during the preparation.

Preparation of tracer amounts of thiophene-3-t.—10 ml of thiophene and 6 ml of 69 % sulphuric acid containing tritium were shaken vigorously for 26.5 hours at 40°C (4). The thiophene was separated off, washed with water, dried with calcium chloride, and distilled. During this purification inactive thiophene was added in an amount appropriate to give a convenient specific activity.

3 ml batches of the preparation were shaken with 20 ml of 53.7 % perchloric acid for 19.5 hours at 25°C. After separation, washing, and drying, two such batches of thiophene were combined and shaken once more with a similar batch of the same inactive acid. The thiophene was finally washed, dried, and distilled. (Perchloric acid was used in the preliminary experiments of this investigation. The operations described in this paragraph could of course have been carried out as well or even better with sulphuric acid, the latter giving less side-reactions.)

The results given below show that the preparation obtained is practically free of thiophene-2-t.

Exchange experiments.—2 ml of thiophene, containing tracer amounts of thiophene-2-t or -3-t, was shaken vigorously with 20 ml of 59.4 % inactive sulphuric acid for different periods of time at 25.0°C. The reaction was interrupted by means of the addition of crushed ice. The thiophene was separated off, washed with water, dried with calcium chloride, distilled, and burned as described above.

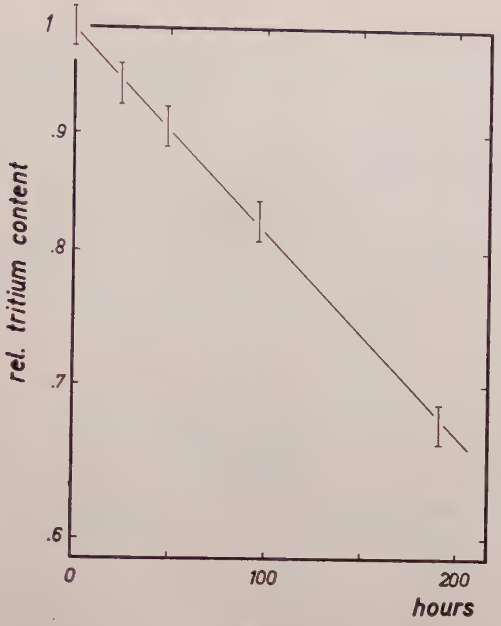

Fig. 2. Semilogarithmic plot of relative specific activity of thiophene-3-t as a function of time of exchange (2 ml of thiophene shaken with 20 ml of 59.4 % sulphuric acid at 25°C).

Results

The results obtained are represented in Figs. 1 and 2, where the final activity of the different thiophene samples has been plotted on a logarithmic scale (the activity of the initial material being used as unit) as a function of exchange time. The values obtained for thiophene-2-t were all corrected for the slight content of thiophene-3-t, the latter being assumed to remain constant during these relatively short periods of time.

The exchange rates are obtained from the initial slopes of the curves (7). The resulting ratio of the exchange rates of tritium in the position 2 and 3, respectively, of thiophene is 955 ± 140 (maximum error), measured in the direction from thiophene to acid.

Even after the longest period of reaction, about 8 days, no appreciable fraction of the thiophene disappeared, but the sample was slightly greenish, and a small amount of precipitate had formed, which never occurred during the shorter periods. The amount of side-reactions is believed to be unimportant in the interpretation of the present results, but, on the other hand, it does not seem advisable to continue the exchange until complete equilibrium is attained. Thus the curves shown give no information about the position of the isotope exchange equilibrium.

An exchange experiment with tritium initially being present in 53.7 % perchloric acid showed that the rapid exchange with the 2-position caused the tritium content to approach such a limiting value (at 25°C) that the heavy isotope might be supposed slightly to prefer the position in the acid to the 2-position in thiophene.

Some benzene might have contaminated the thiophene, but that would have had little influence on the result. Benzene is sulphonated considerably slower than thiophene and will undergo no chemical change, including hydrogen exchange, under the experimental conditions. If no separation in distillation occurs between the two, the benzene will play just the same role as the inactive thiophene, i.e. to be a diluent for the traces of thiophene-t actually observed.

Similar experiments with deuterium are planned for the investigation of the influence of hydrogen mass on the exchange rates.

Nobel Institute of Chemistry, Stockholm 50, Sweden.

REFERENCES

1. C. K. Ingold, Structure and Mechanism in Organic Chemistry, London 1953, pp. 303–4.
2. S. Olsson and L. Melander, Acta Chem. Scand. *8*, 523 (1954).
3. H. D. Hartough, Thiophene and Its Derivatives, New York 1952, p. 145, Table V-1.
4. H. Schreiner, Sitzungsber. Österr. Akad. Wiss., Abt. IIb, *160*, 702 (1951).
5. Houben-Weyl, Methoden der organischen Chemie, Band II, Stuttgart 1953, pp. 214–16.
6. L. Melander, Acta Chem. Scand. *2*, 440 (1948), Arkiv Kemi *2*, 211 (1950), pp. 257–60.
7. L. Melander, Arkiv Kemi *7*, 287 (1954).

Tryckt den 9 mars 1955

Uppsala 1955. Almqvist & Wiksells Boktryckeri AB

ARKIV FÖR KEMI Band 8 nr 4

Communicated 10 November 1954 by ARNE WESTGREN and J. ARVID HEDVALL

The kinetics of the polymorphic transformation of silver sulphate

By GEORG JOHANSSON

With 8 figures in the text

Introduction

The kinetics of the transition processes in solids, claim a certain interest, as an investigation of these problems might elucidate the influence a lattice transition has been proved to exert on the velocity of reactions occurring in the solid state (9). Silver sulphate is one of the substances that are particularly interesting in this connection, as it has been shown that it exhibits a pronounced increase of reactivity in the vicinity of the transition point (1).

On investigating the diffusion of silver ions in silver sulphate (2), the temperature function of the diffusion constant showed a discontinuity at 430°C, which is about 20°C higher than the value for the transition point of silver sulphate as given in the relevant literature (3). A more exact determination of the position of the transition point by means of differential thermal analysis (3) confirmed, however, that the correct value is 430°C, but that the high-temperature modification can be undercooled by about 20°C.

The present investigation was undertaken in order to elucidate the kinetics of transition. In particular, determinations of the nucleation frequency at different temperatures were performed; and it was then possible to draw certain conclusions about the importance of nucleation for the magnitude of the hysteresis range. Experiments were also made in order to measure the linear transition velocity in polycrystalline preparations, and an investigation of the influence of the size of the crystallites on this velocity has given information about the factor determining the transition velocity. The determinations were made by thermal methods, partly with an apparatus for differential thermal analysis, partly in a high-temperature thermostat.

Method of determination

The formation of nuclei and its dependence on temperature was investigated by determining the transition velocity in preparations containing a large number of silver sulphate crystals of a certain size; these crystals were isolated from each other by a suitable dilution medium. If the crystals are sufficiently small, the transformation of such a small crystal will take place very rapidly as soon as a nucleus has been formed, and the transition velocity for the whole sample will constitute a direct measure of the nucleation frequency. Various crystal sizes and different dilution

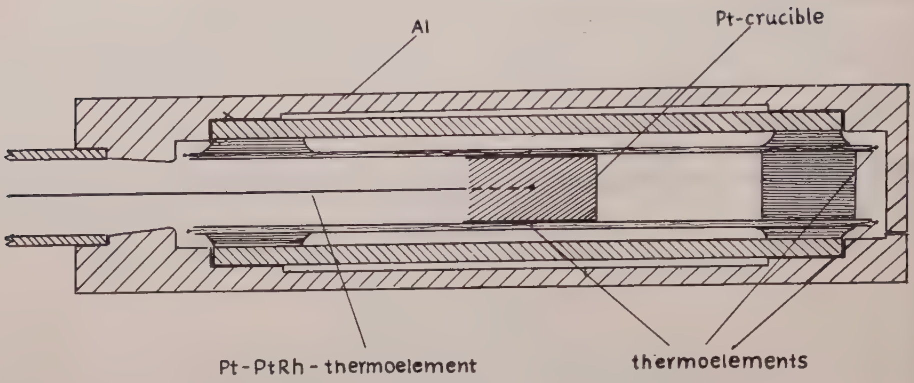

Fig. 1. The measuring tube for the high temperature thermostat.

media have been investigated, and the nucleation frequency has been measured in the apparatus for differential thermal analysis as a function of the temperature, and in the high-temperature thermostat as a function of the time at a constant temperature.[1]

The linear velocity was determined in the high-temperature thermostat. The preparation was placed in a cylindrical platinum crucible, and the velocity with which the transition progressed in the crucible was followed by observing the increase in temperature of the preparation.

Experimental equipment

The apparatus for differential thermal analysis was of the same type as described earlier by HEDVALL, LINDNER and HARTLER (3). The temperature of the nickel block was measured with a Pt-PtRh-element and a millivoltmeter. The difference in temperature between the sample and the comparison substance ($\alpha - Al_2O_3$) was measured with a "Pallaplat" thermocouple connected with the same galvanometer that was used with the thermostat described below. A reading of 1 mm on the galvanometer scale meant about 0.0015° C (at 400° C), when no extra resistance coil was introduced into the galvanometer circuit. The regulation of the increase and decrease of temperature in the furnace was done manually.

A thermostat of the same type as the one constructed by BORELIUS for investigating metal alloys (4) was used at the determinations at constant temperature. It consists of a cylindrical block of aluminum, weighing about 16 kg, insulated with asbestos paper and placed in a copper vessel containing water that can be boiled at constant pressure. In this way it is possible to keep constant the exterior temperature of the block, and consequently the loss of heat. The heating is done by means of stabilized alternating current, in this case from a Sorensen stabilator guaranteed to keep the desired voltage within ± 0.01 per cent. The measuring tube is placed in the middle of the aluminum block; it contains a number of thermocouples connected in series, by means of which it is possible to determine the temperature difference between the aluminum block and the preparation to be investigated. The measuring tube used in the present investigation is shown in Fig. 1. It consists of 29 pythagoras tubes (diameter 1 mm) joined together with porcelain paste, fashioned into a cylinder (diameter 10 mm), and fired at high temperature. In order to make the construction more robust, it was enclosed in a tube of pythagoras material. "Pallaplat" thermocouples (0.2 mm) connected in series are placed in the thin pythagoras tubes in such a way that every other junction is found in the middle, and consequently in close contact with the sample, and every other junction at the end of the tubes; they consequently assume the same temperature as the aluminum block. The leads to the thermocouples are drawn from the thermostat to a commutator free from disturbances from thermo-electric forces, and then to a sensitive mirror galvanometer. The disturbing thermo-electric forces originating in the leads can be compensated by means of the commutator. The galvanometer reading is directly proportional to the difference in temperature between the preparation and the thermostat, and it may be reduced by various resistance coils that may be introduced into the circuit. In order to eliminate exterior disturbances as far as possible the temperature in the room was kept constant by means of a heating arrangement regulated by a mercury relay and a contact thermometer.

---

[1] A similar method has been employed by TURNBULL (6) and by POUND and LAMER (7) for determining the nucleation frequency in supercooled liquids.

The preparation to be investigated was placed in a cylindrical crucible of 0.1 mm platinum sheet, which fitted exactly into the measuring tube. The preliminary heating was done in a separate furnace, from which the crucible could be directly transferred to the thermostat.

Calibration of the measuring tube to the high-temperature thermostat

In order to get a quantitative measure of the amount of heat evolved in the preparation, and consequently of the transition velocity, from the galvanometer reading, the apparatus must be calibrated by evolving a known quantity of heat in the preparation. This can be done by means of Peltier heat (5). This method presupposes, however, that the quantity of heat developed in this way is uniformly distributed throughout the preparation, and as it here is a question of substances with very low heat conductivity, it is possible that this condition is not fulfilled, with consequent errors in the results. In order to investigate the influence of this factor, determinations of the transition heat of silver sulphate were made in crucibles of varying height, and the results compared to each other. The results indicate that the low heat conductivity cannot cause any marked error in the calibration with Peltier heat, on condition that the crucible is not too high.

The measurements were performed in the following way: The platinum crucible was filled with silver sulphate, and a 0.5 mm Pt-PtRh thermocouple was introduced in such a manner that the junction was placed in the centre of the crucible. The preparation was heated in the preheating furnace to about 500°C and was then cautiously placed in the thermostat. When perfect thermal equilibrium had been attained after about 40 minutes, the transition was induced by moving a small porcelain cylinder into contact with the preparation; one edge of the cylinder had been coated with the low-temperature modification of silver sulphate (Fig. 1). The temperature of the thermostat was adjusted in such a manner that the time of transition was about five hours, the temperature increase of the preparation did not then exceed a couple of tenths of degrees centigrade. (Investigations proved, however, that the same results were obtained at the determinations with even considerably higher transition velocities.) The induction period was sufficiently extended to ensure that the transformation occurred all the time only at the boundary surface formed between the high-temperature and the low-temperature modification. The calibration took place immediately after the transition was concluded by passing a current through the thermocouple. By repeating the measurement after the current had been reversed it was possible to eliminate the Joule heat (5).

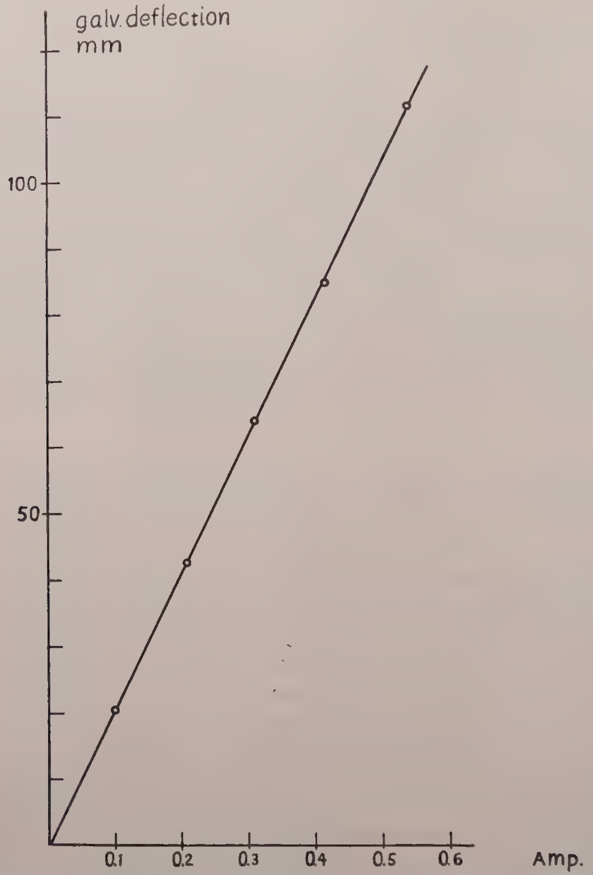

Fig. 2. Calibration diagram for a platinum crucible containing 3 g Ag_2SO_4.

Expressed in cal/sec. the Peltier heat liberated by a current of I amperes from the thermocouple is

$$P = \pm 0.239\ e\ T\ I;$$

where e is the thermo-electric force in volts per degree and T the absolute temperature.

If it is assumed that the galvanometer reading during the transition process is directly proportional to the effect developed in the preparation, i.e.

$$P = as,$$

where s is the galvanometer reading, the proportionality constant a can be calculated by means of the calibration (BORELIUS (5)).

Fig. 2 shows a calibration diagram, where the galvanometer reading is plotted as a function of the current strength through the thermocouple for a 20 mm high crucible. No noticeable deviation from a straight line could be observed even with a 40 mm high crucible. The proportionality constant was 1.18 microcalories per second per mm galvanometer reading for a 20 mm high crucible containing 3 g silver sulphate, when no extra resistance coil was introduced into the circuit.

In order to get a correct value of the quantity of heat developed at a certain moment, it is necessary, when there occur rapid changes in the galvanometer readings, also to take into consideration the effect that is used up for the temperature change of the preparation. The effect developed in the preparation can in this case be expressed by the following formula (cf. Borelius (5))

$$P = as + b\frac{ds}{dt};$$

where b can be determined by measuring the cooling velocity of the preparation.

The heat of transition was calculated by graphic integration of the transition diagrams (Fig. 8). The results for some crucibles of different heights will be seen from Table 1.

Table 1.

Silver sulphate		Heat of transition cal/g
Weight, g	Height, mm	
6.374	39	11.63
3.937	24	14.11
3.055	19	14.35
2.789	17	14.38

The heat of transition determined in this way differs considerably in the case of the highest crucible from that obtained for the smaller crucibles, while the largest difference between the latter amounts to less than 2 per cent. It appears, then, that calibration with Peltier heat should give correct results on condition that the height of the crucible does not exceed about 20 mm, and that consequently the liberated heat in these conditions is uniformly distributed in the preparation.

The formation of nuclei

Materials and methods.—The silver sulphate was pure laboratory salt (Baker's Analyzed); for some control tests it was further purified by recrystallization. After grinding in an agate mortar it was separated into suitable fractions by centrifuging. The results were controlled by microscopic examination, and the separation into fractions usually had to be repeated, as the small grains showed a tendency to adhere to larger grains and in that way be included in a larger-size fraction. The silver sulphate was as far as possible protected from light during this work. The fractions employed were as follows:

1. < 1.3 μ
2. 1.3–2.4 μ
3. 7–11 μ
4. 23–26 μ

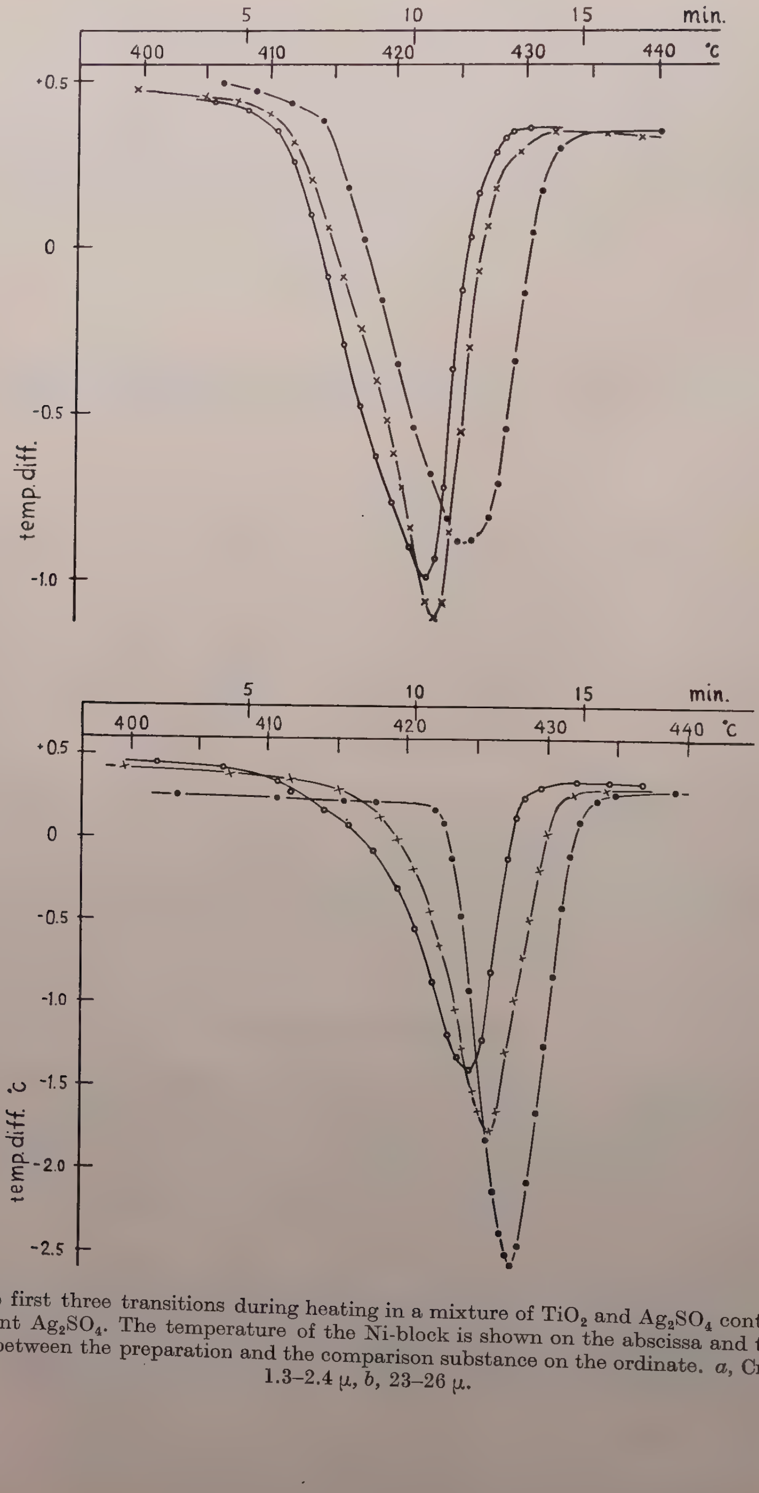

Fig. 3. The first three transitions during heating in a mixture of TiO_2 and Ag_2SO_4 containing 20 vol. per cent Ag_2SO_4. The temperature of the Ni-block is shown on the abscissa and the temp. difference between the preparation and the comparison substance on the ordinate. *a*, Crystal size 1.3–2.4 μ, *b*, 23–26 μ.

An examination of the fraction with the largest grain-size showed that the size of the crystals did not change even after several consecutive transformations. On measuring the linear velocity at experiments where the silver sulphate was compressed in the platinum crucible, it showed however, at an investigation subsequent to the transitions, that small pieces had been detached from the larger crystals; this process, however, did not occur to any larger extent.

The following media have been tried as dilution media:

Al_2O_3 (C. P. Baker's Analyzed) which was heated to 1200–1250° C for one to two hours (α-Al_2O_3).
TiO_2 (C. P. Baker's Analyzed) which was heated to 1000–1050° C for $2\,^1/_2$ hours (rutile).
ZrO_2 (Merck)
Graphite

The mixing of the silver sulphate and the dilution medium was performed as carefully as possible, and in such a way that the grain-size was not altered. The transition process was then studied by means of the apparatus for differential thermal analysis with alumina as comparison substance. The results are shown in Fig. 3–6 and Tables 3–4.

The necessary degree of dilution was determined by investigating how the maximum velocity of the transition from the high-temperature to the low-temperature modification was displaced as the degree of dilution was increased. A decrease from 20 to 10 volume per cent silver sulphate involved a lowering of the temperature for the maximum transition by about 5 to 10° C. Further dilution, however, did not cause any noticeable change. The crystals appear to be fully isolated from each other only in a mixture which contains merely about 10 volume per cent silver sulphate. In view of the small difference between 10 and 20 volume per cent some of the differential thermal analyses have been performed on 20 per cent mixtures, as the galvanometer deflection otherwise would have been too small in certain cases.

The transition from the low-temperature to the high-temperature modification.—It will be seen from Fig. 3 that on heating the course of the transition occurs in practically the same way in diluted as in pure silver sulphate. The position of the transition point seems to be slightly influenced by the grain-size, and is about 5° C. lower for the fraction 1–2 μ than for non-fractioned silver sulphate (Table 2). It is also evident that at repeated transformations of the same mixture, the transition point is displaced towards lower temperatures.

A comparison of the surfaces below the transition curves will also give an idea of a possible decomposition of the silver sulphate, and it appears that such a process to some extent does occur, at least on heating the preparation to temperatures above *c.* 500° C. Both the displacement of the transition point towards lower temperatures and the decomposition process seems to be more marked in using Al_2O_3 as admixture than in using TiO_2.

The transition from the high-temperature to the low-temperature modification.—It will be seen from Fig. 4 that the transition on cooling is highly dependent on the grain-size. The results are reproducible, however, and are not changed to any appreciable extent when the transition is repeated.

Tables 3–4 summarize the values obtained for the temperatures where the transition attains maximum velocity in the various cases. As may be seen from the diagrams the cooling velocity of the furnace was not constant, but its "natural" cooling was exploited, because the galvanometer was highly sensitive to small changes in potential on the furnace. An investigation proved, however, that the temperature of maximum transition was not affected even if the temperature curve was flattened by slowing up the cooling of the furnace at the start.

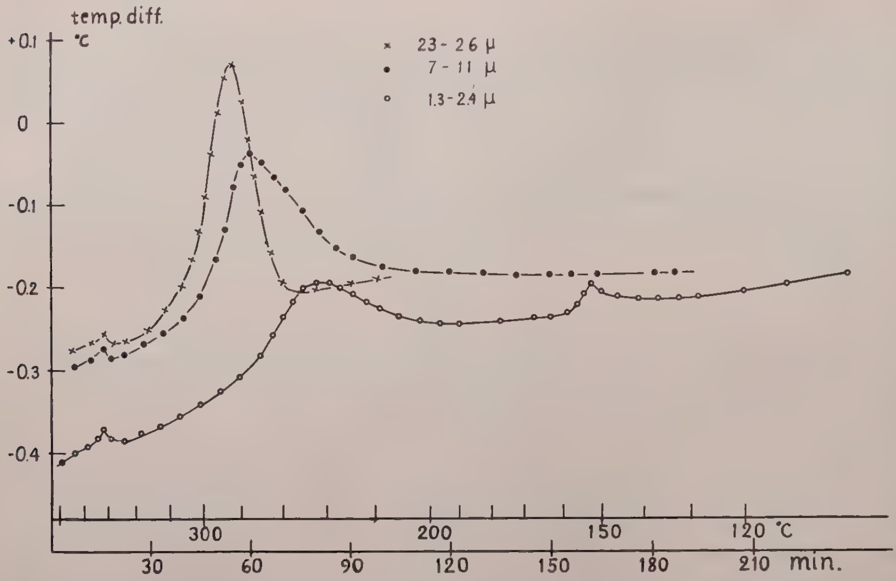

Fig. 4. The transition on cooling for some different crystal sizes. Dilution medium TiO_2. 20 vol. per cent Ag_2SO_4.

If the values referring to the different dilution media are compared, it will be found that in the case of the grain-sizes 23–26 µ and 7–11 µ the maximum transition occurs at the same temperatures (288 and 277° C respectively) for both the Al_2O_3 and the TiO_2 admixtures. For the smaller grain-sizes, however, the corresponding temperature values are not uniform. In the case of the grain-size 1.3–2.4 µ the values are, for Al_2O_3-Ag_2SO_4: 218°C; for TiO_2-Ag_2SO_4: 246°C; for ZrO_2-Ag_2SO_4: 263°C; and for graphite-Ag_2SO_4: 232°C (these temperatures refer to 20 per cent mixtures and are therefore, as mentioned previously, slightly too high).

The course of the nucleation will be entirely different, if the preparation is preheated to a temperature only just above the transition point before a cooling curve is plotted. This may be observed in Fig. 6 for Ag_2SO_4, grain-size 23–26 µ, admixed with Al_2O_3. The heating was here discontinued at 435°C, and the maximum transition velocity occurs already at 376°C, i.e. at a temperature 90°C higher than in other cases. This means that nuclei of the low-temperature modification exist even above the transition point. This phenomenon can hardly be caused by too low a transition velocity, rather it is a question of thermodynamically stable nuclei; this is proved by the fact that the nucleation process is not changed even if the preheating is extended over a considerable period.

Nucleation frequency at constant temperature

The transition velocity in mixtures with TiO_2 has also been investigated at constant temperatures. In this case the silver sulphate was 10 weight per cent, or about 7.5 volume per cent, of the mixture, and the crystals should therefore have been entirely isolated from each other at the transition. The determination was made in the

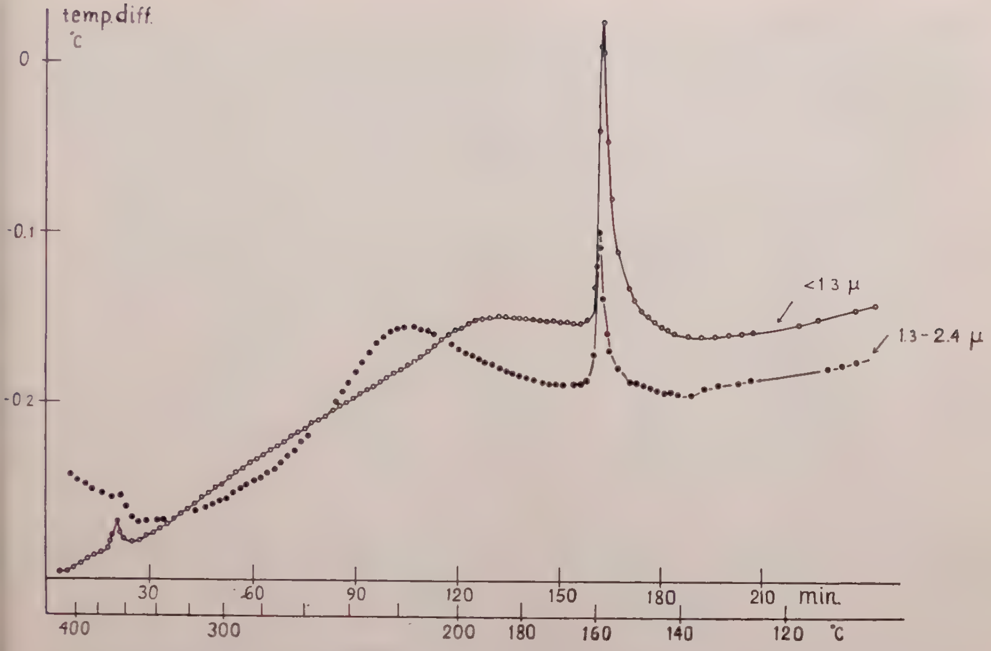

Fig. 5. The transition on cooling in Al_2O_3-Ag_2SO_4 mixtures. 20 vol. per cent Ag_2SO_4.

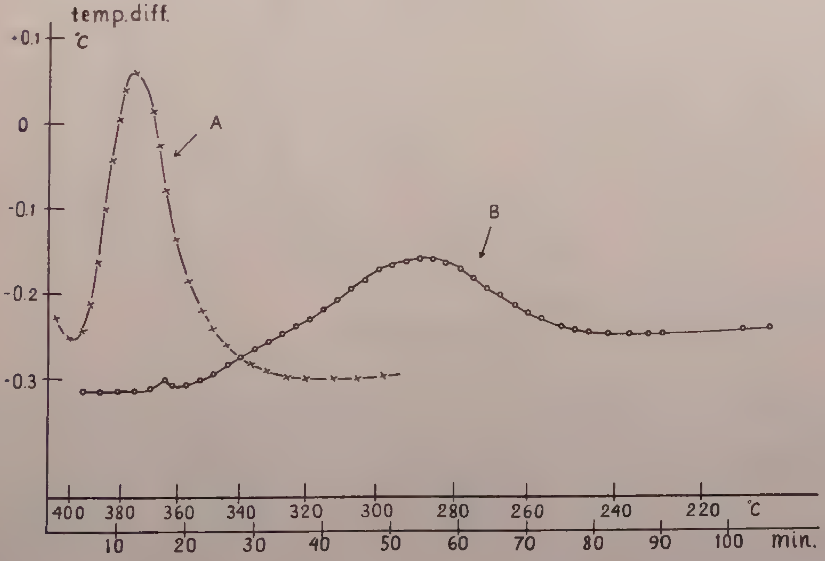

Fig. 6. The effect of the preheating on the course of the transition on cooling of Ag_2SO_4 diluted with Al_2O_3. 20 vol. per cent Ag_2SO_4. Crystal size 23–26 μ. *A*, Preheated to 430–7° during one hour. *B*, Preheated to 475°.

Table 2. The temperature of the nickel block at the start of the transition in undiluted silver sulphate. Heating velocity 2.3°C/min.; the heating discontinued at 490°C. Cooling velocity 3.3°C/min. A direct determination of the position of the transition point in non-fractioned silver sulphate by plotting a heating curve gives the value 428°C. The experimental error in the temperature values ±2°C.

Crystal size μ	On heating		On cooling	
	1st transition	2nd transition	1st transition	2nd transition
Non-fractioned	428	428	404	—
23–26	425	425	410	413
7–11	425	425	407	—
1.3–2.4	421	421	410	407
< 1.3	417	418	—	405

Table 3. The transition from the high-temperature to the low-temperature modification of silver sulphate diluted with alumina.

Crystal size μ	Volume per cent Ag_2SO_4	Number of previous transitions	Preheated to °C	Transition maximum °C
23–26	20	1	543	290
„	„	3	495	288
„	„	5	435	376
„	„	6	430–7[1]	374
„	„	7	475	287
7–10	20	0	483	280
„	„	1	485	277
1.3–2.4	20	0	484	218
„	„	1	482	219
1.3–2.4[2]	10	0	471	211
„	„	1	523	209–14
< 1.3	20	0	468	197

[1] Preheating extended to one hour.
[2] The silver sulphate purified by one recrystallization.

high-temperature thermostat and with the same arrangements as described earlier in connection with the determination of the heat of transition of silver sulphate. The platinum crucible with the mixture was preheated to a sufficiently high temperature (about 500°C) to ensure that there should not remain any nuclei of the low-temperature modification, and was then cautiously introduced into the thermostat. The cooling of the crucible to the determination temperature must as far as possible take place in the thermostat, as the transition process in the crystals might otherwise easily be started by impacts against the crucible when it was slid into the measuring tube.

Table 4. The transition from the high-temperature to the low-temperature modification of silver sulphate diluted with TiO_2.

Crystal size μ	Volume per cent Ag_2SO_4	Number of previous transitions	Preheated to °C	Transition maximum °C
23–26	20	0	483	287
,,	,,	1	542	286
7–11	20	0	485	276
,,	,,	1	492	276
7–11	10	0	496	264
,,	,,	1	485	262
7–11[1]	10	0	503	266
7–11	5	0	485	262
1.3–2.4	20	0	468	247
,,	,,	1	488	246
1.3–2.4[1]	10	0	470	241
< 1.3	10	0	468	214

[1] The silver sulphate purified by one recrystallization.

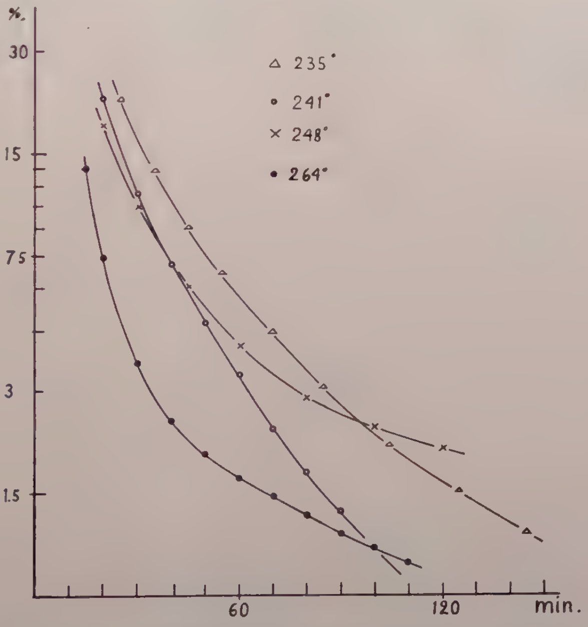

Fig. 7. The rates of transition, expressed as amount of Ag_2SO_4 transformed per hour, at some constant temperatures. Dilution medium TiO_2. 7.5 vol. per cent Ag_2SO_4. Crystal size 1.3–2.4 μ.

Fig. 7 shows the measurement results from investigations of mixtures of Ag_2SO_4 (grain-size 1.3–2.4 μ) with TiO_2. The velocity is very high at first, and seems then very slowly to approach zero. This course of the curves prevents extrapolation to the time zero, and it is therefore impossible to integrate the curves in order to determine the quantity of silver sulphate which has been transformed at a certain time. The slow approach towards zero of the transition velocity also involves difficulties in determining the zero reading of the galvanometer. The measurements were extended over so long a period that it was certain that the reading was constant, and by comparing it with the zero reading for the same mixture containing only the low-temperature modification of Ag_2SO_4, it was possible to determine the reading with reasonable accuracy.

The calibration was made by means of Peltier heat in the manner described previously and the heat of transformation was assumed to be the same as at 420°C.

Investigations of other grain-sizes and dilution media gave the same result.

Discussion of the results

On condition that the formation of nuclei is a homogeneous process and that all crystals are of the same size, the probability of transition should be the same for each crystal, and the course of transition can be described with the usual expression for radioactive decomposition:

$$-\frac{dN}{dt} = kN,$$

where N is the number of non-transformed crystals at the time t.

Or, after integration

$$N = N_0 \, e^{-kt}$$

where N_0 is the number of crystals at the start of transition ($t = 0$). If N or $-\dfrac{dN}{dt}$ is plotted as a function of time in a semi-logarithmical diagram, the result should in this case be a straight line.

But this simple formula will not suffice to describe the course of the transition if the formation of nuclei is a heterogeneous process, i.e. is dependent on impurities distributed either in the interior or along the surfaces of the crystals, and if the impurities possess different potentialities in their capacity of nuclei, or occur in varying numbers in the different crystals. The different values for the constant k for different types of nuclei must then be taken into consideration, for instance,

$$N = N_1 e^{-k_1 t} + N_2 e^{-k_2 t} + N_3 e^{-k_3 t} + \cdots$$

where N_1 (N_2, etc.) denotes the number of crystals where the transition is induced by nuclei with the constant k_1 (k_2, etc.). This course of the process can consequently not be described by a straight line in a semi-logarithmical diagram; the results may be difficult to interpret as in such a case there will probably also occur nuclei of several different types and in varying numbers within one and the same crystal.

The course of the curves in Fig. 7, as well as the fact that the transition velocity at a certain temperature seems to approach zero long before the whole amount of silver sulphate has been transformed, appears to indicate that it is here a question of heterogeneous formation of nuclei, and nuclei with entirely different activation energies. On account of the above-mentioned difficulties with regard to extrapolation it is neither possible to calculate the activation energy, nor possible to draw any conclusions whether the number of nuclei is proportional to the surface or the volume of the crystals.

The results from the differential thermal analyses appear also to be most easily explainable on the assumption of a heterogeneous formation of nuclei. The insignificant difference between the results obtained with the two larger grain-sizes and the absence of effect from the dilution medium in these cases seem to point that way. With decreasing grain-size the number of potential nuclei will become so small in most of the crystals, however, that the transition maximum is considerably displaced towards a lower temperature, and at the same time less active nuclei will have the opportunity to exert a certain effect, i.e. the dilution medium will attain a certain importance.

In order to investigate whether these assumed impurities might be removed from the silver sulphate, some of the experiments were repeated with a silver sulphate which had been purified by one recrystallization. However, no change could be observed in the course of the transition.

For all the dilution media there is a further maximum at 160° C on the transition curves for the two smallest grain-sizes; in contrast to the other one it is very sharply defined. It is difficult to explain the cause of this maximum. It can hardly be caused by impurities or decomposition products, firstly, because it does not occur in the case of the larger grain-sizes, and, secondly, does not occur when the preparation has been heated to only about 400° C before plotting the cooling curve, i.e. to a temperature immediately below the transition point. One explanation of the phenomenon might be that the silver sulphate, which on account of the small grain-size is still untransformed at this temperature, is transformed into another crystal modification than the one stable at this temperature; a more plausible explanation might be that the substance here enters the range of homogeneous formation of nuclei, i.e. that stable nuclei are spontaneously formed in the crystals. The activation energy of the homogeneous formation of nuclei should in that case be of such a magnitude that the velocity of formation increased extremely rapidly with the temperature within a very narrow temperature interval; this hypothesis agrees with the corresponding conditions in supercooled liquids (6, 7).

The linear velocity

The transition from the high-temperature to the low-temperature modification starts only after a certain period of induction at temperatures not too far removed from the transition point, and it is therefore, as mentioned previously, possible to let the silver sulphate attain perfect thermal equilibrium at determinations of the transition velocity in the high-temperature thermostat before the transition is induced, for instance, by touching the silver sulphate at one end of the crucible with a preparation of the low-temperature modification of silver sulphate. The experimental arrangements are shown in Fig. 1.

The curves in Fig. 8 show the courses of three consecutive transitions in the same preparation at 423° C. The height of the crucible was 17 mm, and ordinary silver sulphate was used without any preliminary fractioning. The velocity of the first transition is considerably less than that of the second transition, and attains not much more than half the value of the latter. The velocity then shows some increase at each of the following transitions; besides, the irregularities occurring at the process seem to grow more and more common. The result was the same even if the prepara-

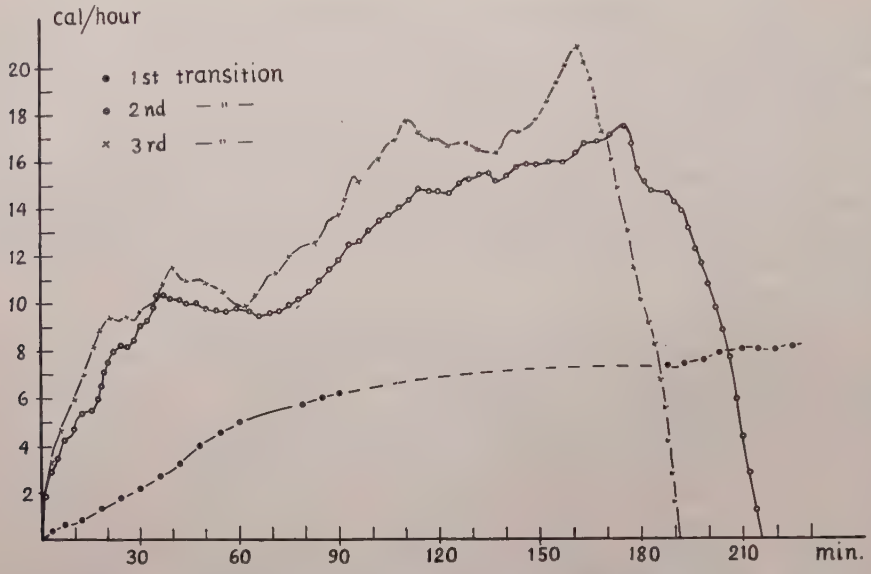

Fig. 8. The linear rate in non-fractioned Ag_2SO_4 at 423°C. The length of the crucible 17 mm.

tion had been subjected to a number of transitions in rapid succession before the determination in the thermostat.

The condition for inter-comparisons of velocities at consecutive determinations is, of course, a uniform progress of the transformation front on each occasion, i.e. as uniformly as possible from the end of the crucible where the transition was induced. To judge from the velocities it seems that the aforementioned condition is not always fulfilled, the boundary surface between the two phases to some extent changing its surface during the course of the transition. There is also the possibility that changes in the orientation of the individual crystals, caused by the transition, may effect an alteration of the velocity. The latter hypothesis, in particular, would explain the large difference in velocity between the first and the second transition.

It is difficult accurately to determine the dependence of the transition velocity on temperature in view of the lack of reproducibility of the velocity determinations at constant temperature. Several experiments indicated, however, that in the temperature range 420° to 425°C the velocity was approximately proportional to the supercooling.

At temperatures above 425°C it was no longer possible to induce the transition by bringing the preparation into contact with the low-temperature modification. Below 420°C, on the other hand, it could be induced merely by a light impact on the platinum crucible.

It is possible to envisage two distinct phenomena as determining the velocities at these transition measurements, first, the crystal transformation itself, and, second, the induction of the transition process in the individual crystals, i.e. the formation of nuclei at the contact between a crystal of the low-temperature modification and one of the high-temperature modification. In the first case the velocity of transition should be practically independent of crystal size, in the latter case the velocity should increase with the size. In order to explore these possibilities the transition velocities were compared at 421°C for some fractions of silver sulphate; the second and third transitions were used for the comparisons as they exhibited a reasonably satisfactory mutual agreement. The transition velocity proved to be considerably higher for a larger grain-size than for a smaller one, and the proportion between the measured velocities was approximately equal to the proportion between the mean diameters of the compared fractions. The velocity appears to be inversely proportional to the number of induction possibilities; and this seems to indicate that the crystal transition itself takes a rapid course, but that the process of nucleation is not easily accomplished at the boundary surface between a crystal pertaining to the low-temperature modification and one pertaining to the high-temperature modification.

Comparisons with transition processes in other substances

The formation of nuclei seems to play an important role for the transition velocity in silver sulphate, and it is therefore of a certain interest to investigate whether the conditions are similar at transitions in other substances. The magnitudes of the hysteresis ranges were therefore investigated, as well as the changes in the transition processes at dilution with an inert substance. The investigations covered, first, some substances resembling Ag_2SO_4, viz. Li_2SO_4, Na_2SO_4 and K_2SO_4 (the low-temperature modification of Na_2SO_4 and Ag_2SO_4 are isomorphous (8); the high-temperature modification of Ag_2SO_4 has not been investigated yet), and, secondly, sodium, potassium and cesium perchlorate, and also cesium chloride. The investigations comprised ordinary heating and cooling curves, and differential thermal analysis, both of the pure substances and of dilutions with alumina. No specific grain-size was used and to judge from the experiences with silver sulphate, the dilution was probably not quite sufficient completely to isolate the crystals from each other. The results may be summarized as follows:

Na_2SO_4 has a transition point at 240°C with a hysteresis interval of about 10°C. The dilution does not affect the transition from high-temperature to low-temperature modification.

Li_2SO_4 (transition point about 575°C). The hysteresis range is about 4°C. The dilution makes the transition from the high-temperature to the low-temperature modification less sharply defined, but seems otherwise to have no effect worth mentioning.

K_2SO_4 (transition point about 590°C). The hysteresis range is less than 1°C, and the dilution has no appreciable effect.

Perchlorates. The dilution does not appear noticeably to affect the transition from low-temperature to high-temperature modification. In the reverse direction, however, the transition is less sharply defined, and at the same time displaced towards a lower temperature. This effect is largest for $CsClO_4$ and smallest for $NaClO_4$. As might be expected the hysteresis interval also increases in the series sodium, potassium, cesium perchlorate. The difference in temperature for maximum transition velocity in pure and in diluted salt is about 5, 10 and 15°C for $NaClO_4$ (transition point 308°C), $KClO_4$ (transition point 300°C) and $CsClO_4$ (transition point 219°C) respectively. The greatest difficulties for the formation of nuclei therefore exist in the cesium perchlorate. If the preheating only slightly exceeds the transition point temperature, the transition will be more sharply defined in the diluted salt, and will occur at higher temperature.

CsCl (transition point 469°C). The hysteresis range is about 20°C, and the transition from the high-temperature to the low-temperature modification starts at about 20°C lower temperature for the diluted salt than for the pure one.

In no single one of the investigated substances is the transition affected by the dilution to the same extent as in silver sulphate. In the case of lithium, sodium and potassium sulphate there is practically no effect. In the case of the perchlorates, as also cesium chloride, the conditions are similar to those in silver sulphate, but the formation of nuclei appears to take place with greater facility.

Summary

Investigations were made of the nucleation frequency and the linear transition velocity at the transition from the high-temperature to the low-temperature modification of silver sulphate.

The formation of nuclei was studied by determining the transition velocity in preparations containing a large number of silver sulphate crystals of determined size; they were prevented from coming into contact with each other by adding a suitable dilution medium. The dependence of temperature, crystal size and thermal pre-treatment was investigated. The formation of nuclei proved to be a heterogeneous process.

The linear velocity was investigated in poly-crystalline preparations, and the factor determining the velocity seems to be the induction at crystal interfaces rather than the transition itself. It is not possible to induce the transition by contact with the low-temperature modification at temperatures above 425°C.

The transition point for the transformation from the low-temperature to the high-temperature modification tends to be displaced towards lower temperatures in the case of very small crystal sizes. The nucleation frequency is high at a transition in this direction, and dilution does not affect the course of the transition.

Qualitative investigations were made into the formation of nuclei at transitions of Li_2SO_4, Na_2SO_4, K_2SO_4, and of $NaClO_4$, $KClO_4$, $CsClO_4$ and CsCl, and the results compared to those obtained at the transitions in silver sulphate.

My thanks are due to Professor J. A. Hedvall for his interest in and encouragement of the work.

REFERENCES

1. J. A. Hedvall and J. Heuberger, Z. anorg. Chem. *135* (1924), 49.
2. G. Johansson and R. Lindner, Acta Chem. Scand. *4* (1950), 782.
3. J. A. Hedvall, R. Lindner, and N. Hartler, Acta Chem. Scand. *4* (1950), 1099.
4. G. Borelius, Réactions dans l'état solide. Paris 1948.
5. G. Borelius, J. Andersson and K. Gullberg, Ing. Vet. Akad. Handl. No. 169 (1943).
6. D. Turnbull, J. Chem. Physics *20* (1952), 411.
7. G. M. Pound and V. K. LaMer, J. Am. Chem. Soc. *74* (1952), 2323.
8. M. A. Bredig, J. Phys. Chem. *46* (1942), 747.
9. J. A. Hedvall, Reaktionsfähigkeit fester Stoffe. Leipzig 1938.

Tryckt den 9 mars 1955

Uppsala 1955. Almqvist & Wiksells Boktryckeri AB

ARKIV FÖR KEMI Band 8 nr 5

Read 1 December 1954

On the strength of secretin

By Erik Jorpes and Viktor Mutt

The statements found in the literature concerning the biological activity of secretin are very unclear, partly because of the different techniques applied in its assay and partly because of the lack of a commonly accepted secretin standard.

The early workers used dogs exclusively and measured the volume of the pancreatic juice as collected from a cannula inserted into the main pancreatic duct. As a threshold dose Ivy *et al.* (1) in 1930 designated the amount of secretin which in a 14–20 kg anesthetized dog caused a 10-drop (0.4 ml) increase in the rate of flow of the pancreatic juice within a 10-minute period, the normal basal flow usually being one drop every two minutes. Mellanby (2) who in 1928 used cats, likewise measured the volume of the juice secreted.

In 1928 Hammarsten *et al.* introduced the principle of titrating the bicarbonate secreted by the pancreas of an anesthetized cat under secretin stimulation. As a unit Wilander and Ågren (4) defined the amount of secretin, which in the cat produces 0.1 ml of 0.1 normal bicarbonate in 10 min. Hammarsten *et al.* (5) showed in 1937 that in man the amounts of bicarbonate and the volume of the juice secreted correspond directly to the injected dose of secretin at least with amounts of secretin not exceeding 15 cat units per kg body weight. Recently Werner and Mutt (6) found in man within a certain range a practically stoichiometric relationship between the dose of secretin injected intravenously and the amount of bicarbonate secreted by the pancreas. Thus the principle of titrating the bicarbonate can safely be applied, provided a reference substance of known strength is used in the assay.

As to the choice of the reference substance, the crystalline picrolonates, containing secretin, prepared by Hammarsten *et al.* (7) in 1933 and by Greengard and Ivy (8) in 1938 can hardly be recommended. When the latter authors repeated the crystallization procedure, elaborated by the Hammarsten group, they obtained a picrolonate with a quite different composition. They found slightly more than 80 per cent of picrolonic acid in the crystals, whereas Hammarsten *et al.* stated that this acid constituted only a very small part of them. Thus Ågren (9) in 1934 obtained 3.8 g of secretin chloride from 4.2 g of picrolonate. The picrolonates were consequently not identical. They have furthermore been shown not to be homogeneous. The preparation of Greengard and Ivy, considered by them to be a crystalline salt of the pure secretin, was shown by Greengard, Wolfrom and Ness (10) in 1947 to be an aniline-secretin-picrolonate or a pyridine-secretin-picrolonate complex, depending upon the solvent used, aniline or pyridine. In hot nitroethane the aniline- or pyridine picrolonate, identified from their X-ray diffraction pattern, went into solution leaving an insoluble amorphous secretin-picrolonate.

The picrolonates are not easily prepared (Hammarsten *et al.*, 5) and are furthermore, because of their insolubility in water, difficult to handle.

As to the biological activity of the picrolonates the Hammarsten preparation was assayed to about 250 cat units/mg (7, 9) and the Greengard-Ivy preparation to about 12.5 Ivy-dog threshold doses or 250 cat units/mg (8), which would correspond to about 1250 cat units/mg of the free secretin base of this preparation. Taking into account that picrolonic acid made up only an insignificant part of the former picrolonate and ⅘ of the latter, there is a great discrepancy in the results. Doubilet (11), who dissolved the crystalline picrolonate of Greengard and Ivy in propylene glycol, found in 1946 in 13 dogs an Ivy-dog threshold dose in 2.4 (0.66–5.7) γ of the secretin base per kg body weight, the picrolonic acid assumed to make up 80 per cent of the crystals. In a 10–15 kg dog, as used by Doubilet, the Ivy-dog threshold dose would be 0.024–0,036 mg corresponding to 40–28 doses per mg. This would make 800–560 cat units per mg of secretin base, or less than the 1250 cat units/mg reported by Greengard and Ivy in 1938.

In discussing the strength of secretin it is quite interesting to note that László Takacz in Budapest in 1928 reported on a secretin purified by means of ultrafiltration through a collodion membrane, of which he used 0.015–0.04 mg per kg or 1–2 mg per person for a secretin test in man.

Our first secretin standard was found to have a strength of 550 cat units per mg lyophilized substance. It was prepared as described by us in 1952. Of this 0.025 mg was found to be a convenient dose. It gave in 184 cats a mean value of 1.37 ± 0.03 ml of 0.1 N alkali in ten minutes after injection, the σ of an individual figure being 0.4 ml. Between 1.0 and 2.5 ml of 0.1 N alkali there was usually a good proportionality between the dose of secretin given and the volume of 0.1 N bicarbonate solution secreted.

The assay in the cat was for one of our later samples, having a strength of approximately 1000 cat units per mg of organic material, checked through an assay in man (Werner and Mutt, 6). A definite pancreatic response was obtained with 2.5 γ per kg of body weight. 15 cat units (0.015 mg) per kg were found to correspond approximately to the commonly used dose in the ordinary secretin test in man, i.e. one clinical unit (16 cat units) per kg (Dreiling, 15). This dose, or about 1 mg per person, gave in 10 healthy medical students during the course of one hour a secretion of 120–229 ml of 0.1 N bicarbonate solution or 113–192 ml of duodenal juice. The figures are of about the same order of magnitude as those obtained by previous authors in the secretin test in man. The strength of the secretin preparation used cannot be much below the assumed value of 1000 cat units per mg.

Attempts at further purification of the secretin gave samples having an activity of 1200 (13) and 1500 (14) cat units per mg of organic material. This proved, however, to be far from the final strength. If the isoelectric methanol procedure was applied to preparations from which the bulk of the inert protein had been removed by precipitation from aqueous solution with *n*-propanol, preparations could be obtained with an activity of 5000 to 7000 c.u. calculated per mg ash-free substance. The activity of these preparations could be adsorbed on stearic acid from a 0.1 mol. phosphate buffer, pH 7.1, leaving the bulk of the inert material including salts unadsorbed. After elution with 1 per cent acetic acid and lyophilization the substance had an activity of 22,000 to 25,000 c.u. per mg. The final purification of two batches of secretin gave the same results. One of them was assayed in 6 cats and the second in 2 cats.

The strength of these secretin preparations is lying on an unexpectedly high level. For a secretin test in man about 0.05 mg should be sufficient. In fact one milligram of this secretin, given in appropriate doses, should in man stimulate a secretion of about four liters of water and at least 34 grams of sodium bicarbonate. From this follows that all the secretin preparations hitherto reported in the literature must have been grossly impure.

Summary

A report is made on the strength of secretin preparations submitted to different purification procedures. The strongest preparations, purified by means of adsorption on stearic acid, showed an activity of 22,000 to 25,000 cat units per mg.

This investigation was aided by grants from the Knut and Alice Wallenberg Foundation, the Swedish Cancer Society and the Magnus Bergvall Foundation.

Chemistry Department II, Karolinska Institutet; the Insulin Laboratory of the Vitrum Company, Stockholm, Sweden.

REFERENCES

1. Ivy, A. C., Kloster, G., Drewyer, G. E., and Lueth, H. C., Am. J. Physiol. *95*, 35 (1930).
2. Mellanby, J., J. Physiol. *66*, 1 (1928).
3. Hammarsten, E., Wilander, O., and Ågren, G., Acta Med. Scand. *68*, 239 (1928).
4. Wilander, O. and Ågren, G., Bioch. Zeitschr. *250*, 489 (1932).
5. Hammarsten, E., Ågren, G., and Lagerlöf, H., Acta Med. Scand. *92*, 256 (1937).
6. Werner, B. and Mutt, V., Scand. J. Clin. Lab. Invest. *6*, 228 (1954).
7. Hammarsten, E., Hammarsten, H., Ågren, G., and Wilander, O., Bioch. Zeitschr. *264*, 275 (1933).
8. Greengard, H. and Ivy, A. C., Am J. Physiol. *124*, 427 (1938).
9. Ågren, G., Skand. Arch. Physiol. *70* (1934).
10. Greengard, H., Wolfrom, M. L., and Ness, R. K., Fed. Proc. *6*, 115 (1947).
11. Doubilet, H., Gastroenterology *7*, 108 (1946).
12. Takacz, L., Z. ges. exper. Med. *63*, 553 (1928).
13. Jorpes, E. and Mutt, V., Arkiv f. Kemi *6*, Nr 23, 273 (1953).
14. —— Nature *172*, 124 (1953).
15. Dreiling, D. A., New York State J. Med. *53*, 671 (1953).

Tryckt den 7 mars 1955

Uppsala 1955. Almqvist & Wiksells Boktryckeri AB

ARKIV FÖR KEMI Band 8 nr 6

Read 13 October 1954

Inhibition of yeast invertase (saccharase) by metal ions

I. The uranyl ion

By KARL MYRBÄCK and EBBA WILLSTAEDT

With 2 figures in the text

In an earlier investigation (1) it was shown that the inhibition of yeast invertase by several metal ions (Ag^+, Cu^{++}, Pb^{++}, Zn^{++}, Cd^{++}) depends in a characteristic manner on the pH of the enzyme-substrate-inhibitor system. If the relative activity (inversion velocity) in experiments with a certain inhibitor concentration is plotted against pH, an "inhibition-pH-curve" is obtained which is roughly parallel to the alkaline branch of the activity-pH-curve of the enzyme (examples in Fig. 2). It could be shown that these results can be explained on the basis of an extension of the theory originally proposed by HUDSON (2) and MICHAELIS (3) that the enzyme is an ampholyte and that only the electrically neutral enzyme molecules and not its positive or negative ions are enzymatically active. It was assumed (1, 4) that the enzyme is a weak acid with $K_A \sim 10^{-6.6}$; the dissociation curve of this acid was, according to MICHAELIS, supposed to be identical with the alkaline branch of the activity-pH-curve. This part of the curve is independent of the substrate concentration and, accordingly, the said acid group of the enzyme is not involved in the binding of the substrate. Nevertheless, this group is essential for the enzymatic action. Hydrolysis of the substrate takes place only when this group (in the enzyme-substrate compound) is undissociated, the undissociated group probably acting as a proton donor in the exchange reaction (4). Furthermore it was assumed that the enzyme molecule has a basic group with $K_B \sim 10^{-3}$ which is, on the whole, determining for the acid branch of the activity-pH-curve. (K_B is defined as follows: $K_B = [\mathrm{H}^+] \cdot [:\mathrm{N{-}EH}]/[\mathrm{H}\overset{+}{\mathrm{N}}\mathrm{{-}EH}]$, where :N–EH designates the uncharged enzyme molecule.) This basic group of the enzyme is essential for the binding of the substrate and is able to combine with the substrate only in its uncharged state (:N–EH) whereas the corresponding cation, $\mathrm{H}\overset{+}{\mathrm{N}}\mathrm{{-}EH}$, does not combine. Accordingly, in acid solution ($\mathrm{pH} < \sim 4$) there is a competition between substrate and H^+ ions for the basic, substrate-binding group of the enzyme, and the acid branch of the activity-pH-curve is dependent on the substrate concentration.

The inhibition of yeast invertase by the metal ions mentioned above is reversible and non-competitive (1) and depends on pH in exactly the manner which must be expected if the ions form slightly dissociated salts with the acid group of the enzyme molecule. The inhibition-pH-curves are determined by

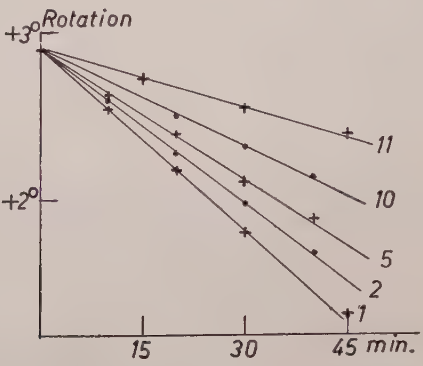

Fig. 1. Determination of relative reaction velocity from decrease of optical rotation.

$$\text{Relative activity} = \frac{1}{1 + \dfrac{K_A}{[H^+]}\left(1 + \dfrac{[M^+] - [EM]}{K_{met}}\right)}$$

where $[M^+]$ is the total metal ion concentration, [EM] the concentration of the metal salt of the enzyme, and K_{met} the dissociation constant of the salt. If [EM] is small compared to $[M^+]$, the formula is simplified to

$$\text{Relative activity} = \frac{1}{1 + \text{const} \cdot \dfrac{K_A}{[H^+]}}$$

indicating that the inhibition-pH-curves have the same form as the alkaline branch of the activity-pH-curve.

Divergences from this form may, of course, occur if the approximation applied above is not allowed or if other groups of the enzyme molecule than the acid group mentioned are involved. In the case of yeast invertase it is found that the inhibition-pH-curves of the Hg^{++} ion diverge from those of other metal ions tested, which may possibly indicate that Hg^{++} also reacts with basic groups of the enzyme.

The general interest in uranium compounds and their physiological actions has stimulated a number of investigations on their inhibiting action on certain enzymes. In most experiments the uranyl ion, UO_2^{++}, was used, generally in the form of uranyl acetate. From a survey by A. L. DOUNCE and TIEN HO LAN (5) it appears that the uranyl ion has, in general, a moderately strong inhibiting action on enzymes, but fairly large differences are observed between individual enzymes: some are only slightly inhibited, but at least two (thrombin and phosphorylase) rather severely. The degree of inhibition, and probably also the dependence of inhibition upon pH, varies strongly with the nature and concentration of the buffer used in the activity assay. This is easily explained since the uranyl ion is strongly complexed by most buffers used in enzyme experiments. (In certain cases even the substrate may be a complexing agent.) The complex uranyl ions obviously have no inhibiting action on enzymes. The authors state, as a general feature of the inhibition experiments with various enzymes, that the degree of inhibition by a certain amount of uranyl ion increases with increasing pH. i.e., is higher in acid solution than at neutrality.

The authors offer the following explanation: "This phenomenon can be explained at least partly by the fact that the precipitating action and hence probably the general aggregating tendency of U_6 on proteins generally increases as the pH approaches the isoelectric point of the protein, for proteins with the isoelectric point in the range 4 to 6. This phenomenon is also partly attributable to the fact that lowering of the pH often acts upon the buffer system (and sometimes the substrate) so as to increase the amount of uncomplexed uranyl ion in the solution". However, it does not seem self-evident that the inactivation, i.e., the formation of an enzyme-metal ion complex, should always be parallel to the "precipitating" or "aggregating" action on proteins of the ion in question. Since the effect of pH on the uranyl ion poisoning of various enzymes reported by DOUNCE and LAN is the reverse of that observed with yeast invertase and other metal ions, it seemed worth while to investigate the action of the uranyl ion on this enzyme.

It was found that, in the absence of buffer, yeast invertase is rather sensitive to uranyl acetate. At pH about 5 a concentration of 3×10^{-5} uranyl acetate caused an inhibition of about 50 %. Since the enzyme solution, though free from dialyzable impurities, may well have contained inactive substances capable of binding or complexing the uranyl ion, it is possible that the (unknown) pure enzyme may be still more strongly inhibited.

In the presence of a sodium acetate - acetic acid buffer the inactivation of the enzyme by the above-mentioned concentration of uranyl acetate was substantially abolished. For instance, in 0.05 N sodium acetate + 0.05 N acetic acid no inhibition was found with 10^{-4} or 10^{-3} M uranyl acetate. Obviously this is due to the complexing of the uranyl ion by sodium acetate, well known from physico-chemical investigations on the complexity of the uranyl ion (6).

Since complex formation was to be expected with all common buffer solutions, suitable in the pH-range 3–7, it was necessary to determine the dependence of the inactivation upon pH in experiments without buffer. pH was adjusted to the desired values by addition of very diluted HCl or NaOH, respectively, and pH was determined electrometrically in all assay mixtures. The accuracy of the pH determinations is probably not very great.

The activity-pH-curve of yeast invertase without inhibitor was found to be the same in the presence or the absence of acetate buffer (Table 1). It is well known from many investigations that the curve is also independent of the degree of purity of the enzyme preparation. Even the enzyme in the intact yeast cell shows the same curve, suggesting that the enzyme is situated on the outside of the cell membrane (7).

Experiments with two different concentrations of uranyl ion and with variation of pH were carried out (Table 2). The results are plotted in Fig. 2 from which it is evident that in the region of optimal activity of the enzyme the inactivation increases strongly with increasing pH. In Fig. 2 some experiments from an earlier investigation have been included for a comparison. It appears that the inhibition-pH-curves of the uranyl ion have the same general form as those of the other metal ions investigated: The inhibition curves are parallel to the alkaline branch of the activity-pH-curve of the enzyme, which is easily understood from the foregoing if the metal ions are supposed to form weakly dissociated salts with the acid group of the enzyme ($K_A \sim 10^{-6.6}$) whose dissociation curve is supposed to be the alkaline branch of the activity-pH-curve.

The inhibition of yeast invertase by uranyl ion is immediate. Incubation of enzyme and uranyl acetate for a reasonable period of time before the activity assay does

Table 1. Activity-pH-curve of yeast invertase.

Experiment No.	pH regulated by	pH	Decrease of rotation, 30 min.	Relative activity
1	HCl	2.49	0.78°	72
2	Acetate	3.00	0.92	84
3	Acetate	3.30	1.02	94
4	Acetate	4.43	1.08	99
5	—	4.53	1.09	100
6	Acetate	4.74	1.08	99
7	Acetate	5.37	1.04	95
8	NaOH	5.56	0.96	88
9	Acetate	5.98	0.84	77
10	NaOH	6.45	0.59	54
11	Acetate	6.80	0.35	32
12	NaOH	6.91	0.34	31

Table 2. Inhibition by uranyl acetate at different pH's.

$UO_2^{++} = 3 \times 10^{-5}$		$UO_2^{++} = 10^{-4}$	
pH	Relative activity	pH	Relative activity
3.45	98	3.42	87
3.88	99	3.65	89
4.48	78	4.20	67
4.80	66	4.99	19
5.20	40		
5.57	22		
6.15	15		
6.76	11		
6.82	11		

Table 3. Reversibility of the inactivation.

Reaction time min.	Optical rotation		
	Experiment *a*	Experiment *b*	Experiment *c*
0	3.02	3.02	3.02
15	2.89	2.56	2.54
30	2.68	2.08	2.06
50	2.44	1.50	1.52
Relative activity, %	40	100	100

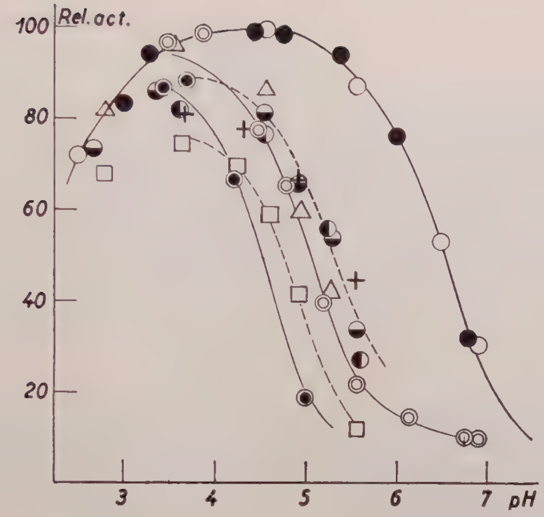

Fig. 2. Activity-pH-curve of yeast invertase.

● Acetate buffer, no inhibitor.
○ No buffer, no inhibitor.

Inhibition-pH-curves

◎ UO_2^{++}, 3×10^{-5} *M.*
◉ UO_2^{++}, 10^{-4} *M.*
☐ Ag^{+}, 2×10^{-6} *N.*
△ Cu^{++}, 6×10^{-3} *N.*
◐ Pb^{++}, 6×10^{-3} *N.*
◒ Zn^{++}, 6.8×10^{-3} *N.*
— + Cd^{++}, 9.1×10^{-3} *N.*

Table 4. Dependence on substrate concentration.

Saccharose %	Inhibition %
1	66
2	70
4	68
20	65

not increase the degree of inhibition. The inhibition is immediately and completely reversible (Table 3). It is non-competitive, i.e. independent of the substrate concentration (Table 4). This was found also for Ag^{+} and other metal ions (1) and the results agree with the fact that the alkaline branch of the activity-pH-curve is independent of the substrate concentration.

Thus in the case of yeast invertase, the uranyl ion behaves like most other metal ion inhibitors. Their action can be described as a salt formation with the acid group of the enzyme corresponding to the alkaline branch of the activity-pH-curve. Studies on the interaction between the uranyl ion and proteins or other substances (5) support the belief that carboxyl groups are preferentially involved in the binding of the metal ion. This is also in accord with the assumption of the binding by an acid group of the invertase molecule.

Experimental

Enzyme preparation.—2 kg baker's yeast was kneeded with 100 ml ethyl acetate until fluid. 100 ml toluene was added and the mixture was kept at about 20° for 20 hours. It was then diluted with about 10 l of water and centrifuged in a Sharpless supercentrifuge. The extract was discarded and the solids were suspended in a large volume of water and centrifuged. This washing was repeated once and finally the solids were suspended in 2 l of water + toluene. Most of the invertase was still present in the yeast remnants and did not pass into solution upon standing at room temperature for months. Obviously the proteolytic enzymes responsible for the solubilization of invertase on yeast autolysis, have been completely removed or destroyed during plasmolysis and washing.

To 200 ml suspension was added 1 g papain ("Papain powder", Biddle, Sawyer & Co.) and 0.2 g cysteine hydrochloride. After five days at 20° practically all invertase was dissolved. Solid ammonium sulfate was added to the mixture until complete saturation. The clear centrifugate which contains all enzyme was dialyzed in cellophane bags until free from salts.

Determination of inversion velocity.—Unless otherwise stated, 4.75 g saccharose was dissolved in water containing buffer or HCl or NaOH in amounts calculated to give the desired pH. In the inhibition experiments suitable amounts of a 10^{-2} or 10^{-3} M uranyl acetate solution were added. The volume was brought to 95 ml, the mixture was temperated at 30° and 5 ml enzyme solution was added. After suitable intervals 10 ml samples were pipetted into 10 ml N sodium carbonate solution whereby the enzyme action was stopped and the mutarotation immediately abolished. The rotation was measured in 2 dm tubes and was plotted against time as in Fig. 1. For degrees of hydrolysis less than about 40 % the curves are practically straight lines and the decrease of rotation at a certain reaction time may be taken as a measure of the inversion velocity.

Activity-pH-curve.—In a few experiments it was checked that the enzyme preparation used had the normal pH-curve with and without acetate buffer (Table 1). pH was measured in all reaction mixtures with the glass electrode. Some experiments are shown in Fig. 1, illustrating the straight line decrease of optical rotation. The relative activities (inversion velocities) are plotted against pH in Fig. 2. The agreement with previous determinations of the activity-pH-curve is very good.

Inhibition by uranyl acetate.—Preliminary experiments showed that, without addition of acetate buffer or other pH-regulating substances, the enzyme was strongly inhibited by 10^{-4} M and completely by 10^{-3} M uranyl acetate at pH 5. In acetate buffer (0.10 M acetic acid + 0.05 N NaOH; pH = 4.6) no inhibition was caused by 10^{-4} M or 10^{-3} M uranyl acetate, obviously because of the complex formation with sodium acetate. Thus it was necessary to carry out the experiments without addition of buffer. Small amounts of HCl or NaOH were added and the pH was measured after the determination of the reaction velocity.

In experiments without pH-regulating agents (pH = 5.2) a total concentration of 3.10^{-6} M uranyl acetate had no perceptible inhibiting action, but 3.10^{-5} M caused about 50 % inhibition. Using the inhibitor concentrations 3.10^{-5} M and 10^{-4} M respectively, experiments at different acidities were carried out and the relative inversion velocity was measured (Table 2).

Reversibility of the inactivation.—15 ml enzyme solution was mixed with 15 m

3.10^{-4} *M* uranyl acetate solution. After 5 minutes incubation 10 ml samples were added to the following reaction mixtures (30°):

a) 4.75 g saccharose in 90 ml water,

b) 4.75 g saccharose in 10 ml acetate buffer (as above) + 80 ml water.

The inversion velocity was determined in both solutions and in a control (experiment *c*) without uranyl acetate (Table 3). As seen from the table, the complexing agent (sodium acetate) reverses the inhibition immediately and completely.

Dependence on the substrate concentration.—Experiments were performed with 3.10^{-5} *M* uranyl acetate, pH = 5.3, and different substrate concentrations; controls without inhibitor (Table 4). The inhibition is independent of substrate concentration.

Summary

In absence of buffers yeast invertase is fairly strongly inhibited by the uranyl ion. Uranyl-complexing agents, e.g. acetate buffer, protect the enzyme effectively against uranyl poisoning. The inhibition of invertase by uranyl ion increases strongly with increasing pH in the region of optimum activity of the enzyme. This is explained by the assumption that the uranyl ion, like most other heavy metal ions, forms a salt with an acid group, possibly a carboxyl group, of the enzyme molecule. The inhibition is reversible and non-competitive.

Institute of Organic Chemistry and Biochemistry, University, Stockholm.

REFERENCES

1. Myrbäck, K., Hoppe Seylers Z. physiol. Chem. *158*, 160 (1926).
2. Hudson, C. S., J. Am. Chem. Soc. *32*, 1220 (1910).
3. Michaelis, L. and Davidsohn, H., Biochem. Z. *35*, 386 (1911); Michaelis, L. and Rothstein, M., Ibid. *110*, 217 (1920).
4. Myrbäck, K., Ann. Acad. Sci. Fennicae Ser. II A. Chem. (1955) In Press.
5. Dounce, A. L. and Tien Ho Lan, in Voegtlin, C. and Hodge, H. C., Pharmacology and Toxicology of Uranium Compounds, McGraw-Hill Book Co, New York 1949, p. 759.
6. Ahrland, S., Acta Chem. Scand. *5*, 199 (1951).
7. Thorsell, W. and Myrbäck, K., Arkiv Kemi *3*, 323 (1951); Wilkes, B. G. and Palmer, E. T., J. Gen. Phsysiol. *16*, 233 (1923); Rothstein, A. and Meier, R., Arch. Biochem. Biophys. *48*, 55 (1954).

Tryckt den 7 mars 1955

Uppsala 1955. Almqvist & Wiksells Boktryckeri AB

ARKIV FÖR KEMI Band 8 nr 7

Vorgelegt am 13. Oktober 1954

Zur Kenntnis alicyclischer Reduktone I

Von Hans von Euler und Armin Glaser

Mit 4 Figuren im Text

Endiolisierung der DL-epi-meso-Inosose und der Scyllo-meso-Inosose

Meso-Inosit, in Pflanzen und Tieren sehr verbreitet, ist bekanntlich, wie auch Biotin, ein Bestandteil des Bios und wird meist der B-Vitamin-Gruppe zugezählt. Jedenfalls wirkt Inosit als Wachstumsfaktor; in chemischer Hinsicht sind aber seine diesbezüglichen Funktionen noch ungeklärt.

Es ist eine im Arbeitsgebiet dieses Institutes über Reduktone liegende Aufgabe, die Beteiligung der entsprechenden *Inososen* an den Inositwirkungen in Tierorganen (Leber, Blut, Gehirn, auch Tumoren) besonders beim mikrobiologischen Stoffwechsel des Darmes festzustellen.

Die DL-epi-meso-Inosose wurde für unsere Versuche dargestellt nach Th. Posternak (Helv. 19, 1337; 1936) und über das Phenylhydrazon nach Posternak u. Carter gereinigt. Das so gewonnene Inosose-Präparat liess sich mit TR zu 95 % als Endiol titrieren. Es reduzierte TR in neutraler Lösung nicht, sondern erst nach vorhergehender kurzer Einwirkung von Alkali.

In neutraler, wässriger Lösung liegt Scyllo-meso-Inosose, deren oxydative Bildung durch *Azotobacter suboxydans* von A. J. Kluyver[1], Th. Posternak[2] sowie von E. Chargaff[3] studiert wurde, in Ketoform vor. Sie wurde von Heyns u. Paulsen[4] auch durch katalytische Oxydation erhalten. In alkalischer Lösung lässt sie sich zu etwa 95 % als Endiol titrieren. Enzymatische Oxydationen des Inosits durch Tiergewebe wurden von Das u. Guha[5] nachgewiesen. Siehe auch Needham (1926).

Demgemäss gehört diese Inosose, ebenso wie die DL-epi-meso-Inosose zu derjenigen Klasse der Reduktone, die wir als *aci-Reduktone* bezeichnen. Die Reversibilität des Endiol-Keto-Gleichgewichts kommt im allgemeinen, aber keineswegs ausschliesslich, denjenigen Reduktonen zu, deren Endiolgruppe einem Carbonyl benachbart ist; z. B. befähigt auch die Stellung neben der Gruppe C:NH das Endiol zur Reduktion in saurer Lösung.

Wie Heyns und Paulsen feststellten, entstehen bei der katalytischen Oxydation von meso-Inosit Substanzen, die Fehlingsche Lösung und ammoniakalische Silberlösung in der Kälte reduzieren, und zwar wurde gezeigt, dass auf 1 Mol Glucose

---

[1] A. J. Kluyver u. A. G. J. Boezardt, Rec. trav. chim. Pays-Bas *58*, 956; 1939.

[2] Th. Posternak, Helv. *25*, 748; 1942. — *29*, 1991; 1946.

[3] E. Chargaff et al., J. Biol. Chem. *165*, 381; 1946. — *174*, 173, 1948 u. *175*, 929; 1948.

[4] K. Heyns u. H. Paulsen, Chem. Ber. *86*, 833; 1953.

[5] N. B. Das u. B. C. Guha, Zs. physiol. Chem. *231*, 157; 1935.

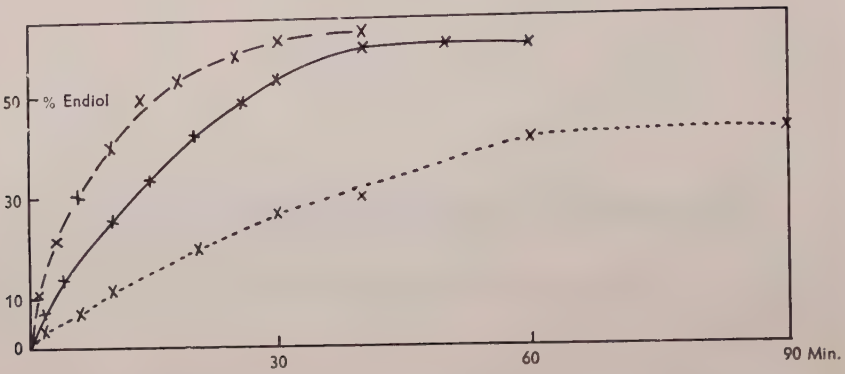

——— 0,4-*n* NaOH, ——— 0,2-*n* NaOH, ----- 0,1-*n* NaOH.

Fig. 1. Bildung des aci-Reduktons AG bei 20°.

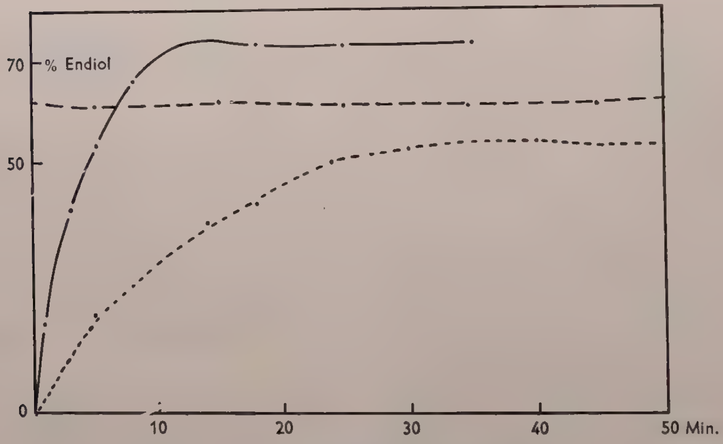

——— 0,4-*n* NaOH, ———— Stabilität des Endiols, ----- 0,1-*n* NaOH.

Fig. 2. Bildung des aci-Reduktons AG bei 30°.

etwa 2 Mole Cu_2O abgeschieden werden. Diese Reduktionsfähigkeit der Inosose kommt nur ihrer Endiolat-Form zu; die saure Lösung reduziert, wie erwähnt, nicht. Dagegen entsteht durch Einwirkung von 1-*n*. Alkali (20 Min. bei 30°) auf Inosose ein aci-Redukton, das also, wie die Reduktone I und II das Tillmans-Reagens (TR) in saurer Lösung reduziert und ca. 1 Endiolgruppe per Mol enthält.

Bildung eines aci-Reduktons durch Alkali-Behandlung der DL-epi-meso-Inosose

Wir geben hier zwei Versuchsreihen über den Einfluss der Alkali-Konzentration auf den zeitlichen Verlauf der aci-Redukton-Bildung; dieselben beziehen sich auf die Temperaturen ~20° und ~30°.

Bei denselben wurde die Inosose (variierend zwischen 50 und 60 mg) in 80–100 ml Wasser gelöst und unter Stickstoff mit einem abgemessenen Volumen einer 2-*n*. Natronlauge versetzt.

Von Zeit zu Zeit wurden der Reaktionslösung 10 ml entnommen, die man sofort unter Stickstoff in 0,5 ml Eisessig einfliessen liess und dann mit 0,01 *n*. TR-Lösung titrierte. Die Acidität dieser titrierten Lösung entsprach etwa pH = 5.

Die in den Fig. 1 und 2 zusammengestellten Titrationswerte beziehen sich also auf saure Lösungen und die Versuche zeigen, wieviel aci-Redukton (bzw. aci-Reduktone) sich unter der Einwirkung des Alkalis gebildet hat.

2 g Inosose wurden in 50 ml Wasser gelöst und bei 31° unter Stickstoff mit 25 ml 2-*n*. NaOH versetzt, wobei sich die Lösung braun färbt. Nach 10 Minuten wurde mit Essigsäure angesäuert. Zu der schwach essigsauren Lösung wurden 5 g Bleiacetat in 10 ml Wasser gegeben und auf pH 6,5 neutralisiert. Der entstandene Niederschlag wurde nach Absaugen mit Wasser, Aceton und Äther gewaschen.

Das fein pulverisierte Bleisalz wurde in 25 ml warmen Wassers aufgeschlämmt und mit H_2S zerlegt. Nach Absaugen des Bleisulfides wurde mit 5 ml Wasser gewaschen. Die Lösung wurde im Vacuum bei einer Badtemp. von 35° stark eingeengt. Über Nacht bildeten sich bei 6° Krystalle aus, die nach Waschen und Trocknen bei 114° zu sintern begannen, aber erst bei 151° vollständig unter Gasentwicklung schmolzen. Das nicht ganz einheitliche Rohprodukt zersetzt sich langsam bei Erwärmung. Es wurde 4mal aus Wasser umkrystallisiert, die Reinigung wurde papierchromatographisch verfolgt bis die Mutterlauge chromatographisch einheitlich war.

Papierchromatographie: Papier Munktell OB. Als Lösungsmittelgemisch diente Butanol/Eisessig/Wasser 4:1:1. Es wurde absteigend gearbeitet. Inosose zeigte einen Rf-Wert von 0,12–0,13.

Die Chromatographie des Pb-Salzes, mit H_2S zerlegt, zeigte eine Anzahl von Flecken Rf 0,19 (mittelstark); 0,37 stark; 0,58 schwach; 0,70 sehr schwach; 0,80 sehr schwach. Bei der Umkrystallisation verschwanden die Flecken in der Reihenfolge 0,70; 0,58; 0,80; 0,19; der Fleck 0,37 bleibt bestehen. Triose-Redukton (= Redukton I) zeigt einen Rf-Wert von 0,74. Um zu entscheiden, ob Redukton I gebildet worden ist, wurden andere Lösungsmittelgemische versucht.

	Pyridin / Amylalkohol / Wasser 14 / 14 / 12 aufsteigend	Butanol / Eisessig / Wasser 4 / 1 / 5 obere Phase absteigend
Inosose	0,34	0,24
Redukton I	0,75	0,76
Bei der Alkali-Behandlung entstanden Substanzen vom Rf	0,13; 0,19; 0,35; 0,45	0,12; 0,25; 0,44; 0,50

Die Entwicklung wurde mit ammoniakalischer Silberlösung, mit TTC in Alkali oder mit TR-Lösung durchgeführt. Im letzteren Fall erscheint die Inosose erst nach Besprühen mit Alkali, wenn das Pyridin restlos aus dem Papier entfernt ist.

Bei der Alkali-Behandlung der Inosose wird kein Triose-Redukton unter den eingehaltenen Bedingungen gefunden. Die mit TR entwickelten Chromatogramme zeigen aber, dass andere Reduktone gebildet wurden.

Analyse des aci-Reduktons AG

Für $C_6H_{10}O_6$	Gef.	C 40,45	H 5,81
	ber.	40,45	5,65

Titration mit Alkali. 23,9 mg Sbst. AG in 15 ml Wasser gelöst, mit 0,1 *n.* NaOH F = 1,065 gegen Phenolphtalein titriert, verbrauchen 1,212 ml Natronlauge. Daraus berechnet sich das Äquivalentgewicht

$$\frac{23{,}9}{1{,}212 \cdot 0{,}1065} = 185.$$

Titration mit TR-Lösung 5,1 mg Sbst. AG in 15 ml Wasser gelöst, + 1 Tropfen Eisessig. Die Titration mit 0,01 *n.* TR-Lös. unter Stickstoff ergab einen Verbrauch von 5,92 ml TR-Lös. Daraus berechnet sich[1] das Mol Gew.

$$\frac{5{,}1 \cdot 2}{0{,}00920 \cdot 5{,}92} = 187.$$

Wird die obige Lösung alkalisch gemacht, so tritt ein weiterer Verbrauch an TR auf, der wohl auf sekund. Endiolisierung oder auf teilweise Spaltung von AG zurückzuführen ist.

Die Bildung des aci-Reduktones AG aus Inosose lässt sich folgendermaassen formulieren:

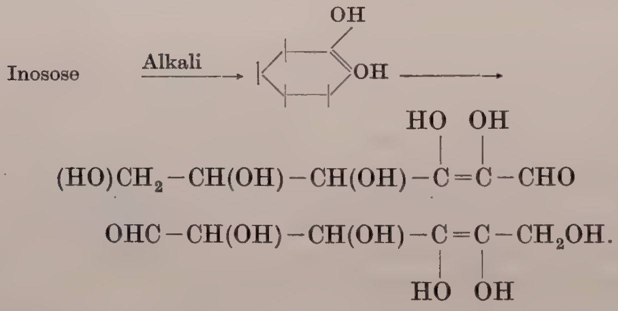

$$(HO)CH_2-CH(OH)-CH(OH)-\overset{HO}{\overset{|}{C}}=\overset{OH}{\overset{|}{C}}-CHO$$

oder

$$OHC-CH(OH)-CH(OH)-\underset{HO}{\underset{|}{C}}=\underset{OH}{\underset{|}{C}}-CH_2OH.$$

Dabei ist die Annahme gemacht, dass zwischen den C-Atomen 3 und 4 eine Spaltung eintritt. Vgl. EULER u. H. HASSELQUIST, Reduktone (Verlag Enke), S. 13. Aber auch die cyklische Form ist nicht ausgeschlossen.

Darstellung eines 2,4-Dinitrophenylhydrazons des aci-Reduktons AG

Versetzt man eine warme wässrige Lösung von aci-Redukton AG mit einer Lösung von 2,4-Dinitrophenylhydrazin in warmer verd. Salzsäure, so fällt ein rotes Phenylhydrazon aus; es wurde abgesaugt und mit Wasser gewaschen. Es beginnt bei 155° zu sintern, ist aber erst bei 175° unter Zersetzung geschmolzen. Für das 2,4-Dinitrophenylhydrazon der Inosose gibt POSTERNAK[2] 270° an.

Farbreaktion mit konc. Schwefelsäure erst blau, dann rotviolett, dann in schmutzig schwarz übergehend. Es liess sich deshalb nicht entscheiden, ob die Endiolgruppe noch unverändert vorliegt. Das Phenylhydrazon löst sich in Alkohol mit gelbroter Farbe, was eine Titration in saurer Lösung sehr erschwerte.

Das aci-Redukton AG reagiert mit Triphenyltetrazoniumchlorid in alkalischer Lösung in der Kälte. Papierchromatogramme, mit TTC entwickelt, zeigen dasselbe Bild wie ammoniakalische Silberlösung, aber die Empfindlichkeit ist geringer.

---

[1] Nach den Titrations-Ergebnissen wäre auch eine Formel $C_6H_{10}O_6 \cdot {}^1/_2\, H_2O$ möglich, indessen stimmen die gefundenen Analysenwerte nicht damit überein.

[2] TH. POSTERNAK, Helv. *19*, 1338; 1936.

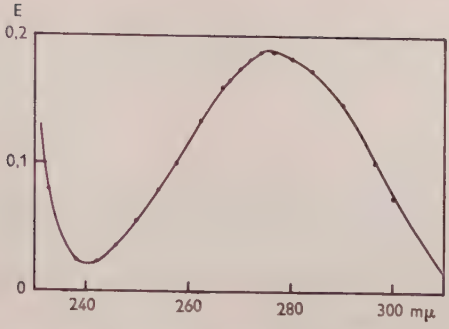

DL-epi-meso-Inosose in Wasser 6,51 · 10^{-3} Mol/l.

Fig. 3. Spektrum in wässriger Lösung: Schichtdicke 10 mm. Die Konzentration beträgt 11,6 mg in 10 ml, entsprechend 6, 51·10^{-3} Mol/Liter. Das Maximum liegt bei 275 mμ.

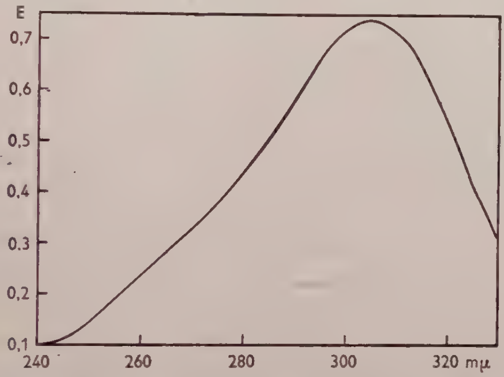

DL-epi-meso-Inosose in 0,1-*n* NaOH 2,07 · 10^{-4} Mol/l.

Fig. 4. Spektrum in 0,1-*n*. Natronlauge. Schichtdicke 10 mm. Die Konzentration beträgt 0,464 mg in 10 ml, entsprechend 2,07·10^{-4} Mol/Liter. Aus dem Lösungsmittel war der Sauerstoff durch Stickstoff ausgetrieben worden. Die Messung wurde 1/2 Stunde nach der Mischung vorgenommen. Das Maximum liegt bei 305 mμ.

UV-Messungen an DL-epi-meso-Inosose

Über das Spektrum der DL-epi-meso-Inosose liegen Ergebnisse von POSTERNAK[1] vor. HEYNS und PAULSEN fanden in guter Übereinstimmung mit POSTERNAK und mit CHARGAFF ein Maximum der Scyllo-meso-Inosose bei 281 mμ.

Unsere Messungen an DL-epi-meso-Inosose sind in den Fig. 3 und 4 zusammengestellt.

Die Verschiebung des Maximums durch 0,1 *n*. Alkali entspricht derjenigen, welche KARRER[2] für Ascorbinsäure angegeben hat.

Stockholm, Universität, Institut für organ.-chemische Forschung.

---

[1] TH. POSTERNAK, Helv. *29*, 1994; 1946.

[2] P. KARRER, H. SALOMON, R. MORF u. K. SCHÖPP, Biochem. Z. *258*, 4; 1932.

Tryckt den 7 mars 1955

Uppsala 1955. Almqvist & Wiksells Boktryckeri AB

ARKIV FÖR KEMI Band 8 nr 8

Vorgelegt am 24. November 1954

Entstehung von aci-Reduktonen[1]

Von Hans von Euler und Hans Hasselquist

Mit 2 Figuren im Text

Als zugehörig zu derjenigen Klasse der Reduktone, welche auch in saurer Lösung ihre Endiol-Struktur und demgemäss ihre hohe Reduktionsfähigkeit gegen Tillmans-Reagens u.a. beibehalten, wurde in vorhergehenden Mitteilungen[2] das Endiol II (aci-Redukton II) beschrieben. Es entsteht neben Triose-Redukton, das wir nunmehr als aci-Redukton I bezeichnen, bei der alkalischen Behandlung der Glucose[3] und anderer Zuckerarten[4], und wird in grösserer Ausbeute erhalten, wenn man bei der Erhitzung der Zuckerlösung die Temperatur 75–80° nicht überschreitet und nur etwa 2–3 Minuten mit 1-*n* Alkali erwärmt. Man fällt dann die Reduktone I und II als Pb-Salze, die fraktioniert und mit Schwefelsäure entbleit werden.

Aci-Reduktone entstehen aber auch auf anderem Wege, nämlich aus Dehydroascorbinsäure, und zwar wurde, wie S. 69 gezeigt wird, aci-Redukton III als ein Dioxytetron erkannt und mit einer von Micheel u. Haarhoff[5] dargestellten Substanz identifiziert.

Umsetzung des aci-Reduktons II mit *p*-Nitranilin

30 g des aci-Redukton-Pb-Salzes wurden in 300 ml Wasser aufgeschlämmt, mit Schwefelsäure entbleit, vom Bleisulfat abfiltriert und mit einer filtrierten Lösung von 6 g *p*-Nitranilin in 1000 ml Wasser + 5 ml konc. Schwefelsäure versetzt. Die nach eintägigem Stehen ausfallenden rotbraunen Flocken wurden abfiltriert, mit Wasser gewaschen und mit 50 ml Eisessig aufgekocht. Der ungelöste Anteil wurde dann warm abfiltriert und mit Eisessig gewaschen. Die braunroten Kristalle (Fraktion *A*) schmolzen bei 240° ohne Zersetzung. Aus dem Filtrat der Fraktion A erhielt man ausser weiteren Mengen dieser Fraktion bräunlich-gelbe Kristalle vom Schmpt 220°.

Die Fraktion *A* (im Ganzen 1,1 g) wurde mit Eisessig gereinigt und ergab nach Umkristallisieren kleine braune Nadeln vom Schmpt 245°. Dieselben sind schwerlöslich in allen üblichen organischen Lösungsmitteln. Das ameisensaure Salz kristallisiert in kleinen roten, flaumartigen Nadeln, die durch Wasser unter Rückbildung des Ausgangsmateriales leicht zerlegt werden. Mit Essigsäure gibt das aci-Redukton

---

[1] 37. Mitteilung über Reduktone.

[2] Euler u. H. Hasselquist, Virtanen-Festschrift, Finische Akad. d. Wissensch. 3 (1954). — Lieb. Ann. *588*, 205 (1954).

[3] Euler u. H. Hasselquist, Lieb. Ann. Chem. *588*, 205 (1954).

[4] Euler u. M. L. Stein, Dieses Arkiv; vorgelegt 13.X 1954.

[5] F. Micheel u. H. Haarhoff, Lieb. Ann. *545*, 28 (1940).

II Anilid — zum Unterschied vom *p*-Nitranilid des aci-Reduktons I, das ein gelbes Acetat liefert — *kein* Salz. Mit Alkali erhält man ein unlösliches, dunkelviolettes (vermutlich nitrolsaures) Salz, aus dem sich beim Ansäuren die ursprüngliche Substanz zurückbildet.

Bei Titration mit 0,01-*n* Tillmans-Reagens-Lös. ohne Zusatz von Alkali verbrauchten 2,3 mg Sbst. in ca. 10 ml Methanol 1,7 ml TR-Lösung.

$$E_{\text{gef.}} = \frac{2{,}3}{0{,}01 \cdot 1{,}7} = 135 \quad M_{\text{ber.}} = 270$$

Die aus Fraktion *B* erhaltenen Kristalle vom Schmpt 235° ergaben mit aci-Redukton I-Nitranilid keine Depression des Schmelzpunktes.

Das Pb-Salz des aci-Reduktons II, das dem chromatographischen Versuch zufolge nur wenig aci-Redukton I enthielt, muss bei der Umsetzung mit *p*-Nitranilin durch Spaltung etwa 50 % aci-Redukton I ergeben haben, da das Anilid des aci-Reduktons I in dieser Menge auftrat.

Die Einwirkung von Alkali bei 70–90°, durch welche aus Glucose die aci-Reduktone I und II entstehen, wurde wiederholt auch an anderen Zuckerarten untersucht, und es hat sich gezeigt, dass man auch aus diesen verschiedene Reduktone erhalten kann. Art und Menge dieser Endprodukte sind von der Temperatur und Dauer des Erhitzens abhängig und der chromatographische Test ergibt R_f-Werte, die je nach der Art und Anwendung des Entwicklers nicht unerheblich variieren können.

Im übrigen sei auf die Versuche von M. L. STEIN (l.c.) an Lactose, Glucosamin und Glucuronsäure verwiesen.

Durch die entsprechende Alkali-Behandlung der Ascorbinsäure konnten wir keine anderen Reduktone erhalten. Dieser Versuch gab jedoch Veranlassung zur Untersuchung der *Dehydro-ascorbinsäure*, auf welche sich die folgenden Ergebnisse beziehen.

Darstellung von aci-Redukton III aus Dehydro-ascorbinsäure

Die Dehydro-ascorbinsäure-Lösung, von der wir ausgingen, wurde folgendermassen dargestellt: 5,28 g Ascorbinsäure wurde in 30 ml Wasser gelöst und mit einer ätherischen Lösung von 3,3 g *p*-Chinon 10 Minuten geschüttelt, worauf das überschüssige Chinon durch dreimaliges Ausäthern der wässrigen Lösung entfernt wurde.

Die so bereitete Dehydro-ascorbinsäure-Lösung wurde mit dem gleichen Volumen einer 2-*n* Schwefelsäurelösung auf 90° gehalten, bis nach etwa 15 Minuten die Entwicklung von CO_2 aufhörte. Die erkaltete Reaktionslösung wurde mit Kochsalz gesättigt und zweimal mit Benzol extrahiert, wobei der Hauptteil der gebildeten Brenzschleimsäure in das Benzol überging.

Die mit Kochsalz gesättigte Lösung wurde nun zweimal mit Äthylacetat ausgeschüttelt. Die Äthylacetat-Schicht wurde mit wasserfreiem Natriumsulfat getrocknet und auf ein kleines Volumen eingeengt.

Aus der Äthylacetat-Lösung kristallisierte nun aci-Redukton III in fast reinem Zustand aus. Auch aus der Mutterlauge wurde noch etwas Redukton III gewonnen, wenn man zuerst durch Zusatz eines Überschusses von Äther verharzte Produkte ausfällte. Die davon abfiltrierte Lösung wurde nun zur Trocknen verdampft und mit wenig Äthylacetat versetzt, wodurch weiteres nahezu reines aci-Redukton gewonnen wurde.

Als recht konstante Gesamt-Ausbeute erhielten wir 130 ± 10 mg aci-Redukton III vom Schmpt 177–178°.

Aci-Redukton ist leicht löslich in Wasser, Äthylacetat, Aceton, Methanol, Äthanol und Butanol; ziemlich löslich in Äther, wenig löslich in Benzol und Chloroform; unlöslich in Petroleumäther.

Charakterisierung und Derivate des aci-Reduktons III

Aci-Redukton III entfärbt Tillmans-Reagens (TR) in saurer Lösung (pH 4) sofort. 6,8 mg Sbst. in 10 ml Wasser verbraucht 10,75 ml 0,0092-*n* TR-Lösung.

$$E_{\text{gef.}} = \frac{6{,}8}{0{,}0092 \cdot 10{,}75} = 69.$$

1,7 mg Sbst. verbrauchten 2,7 ml TR-Lösung

$$E_{\text{gef.}} = \frac{1{,}7}{0{,}0092 \cdot 2{,}7} = 69.$$

Bei der letzten Titration wurden unter Einleiten von Stickstoff 0,5 ml 2-*n* NaOH zugesetzt. Dabei ergab sich kein weiterer Verbrauch von TR. Im Gegensatz hierzu verbraucht Ascorbinsäure in alkalischer Lösung 2 Mole TR. Der Versuch zeigt, dass im aci-Redukton III keine Gruppe —CH—OH vorkommt, welche mit einer Ketogruppe des oxydierten erneut enolisiert werden kann.

Absorption in UV

24 mg in 1000 ml Wasser wurden im Beckmann-Apparat zur Feststellung des Absorptions-Maximums untersucht. Wie Figur 1 zeigt, wurde das Maximum bei 257,5 mμ gefunden.

Papier-Chromatographie

Alkali-Behandlung: 3 ml Dehydro-ascorbinsäure-Lösung wurden mit 4,5 ml 2-*n* Natronlauge unter Stickstoff 1 Minute auf 90° erwärmt, worauf die Reaktionslösung bis pH = 4 angesäuert wurde.

Lösung: Butanol-Eisessig-Wasser 4 : 1 : 1. Die Entwicklung durch Tillmans-Reagens an noch feuchtem Papier, also in stark saurer Lösung, ergab sofort 3 Stellen der Entfärbung, entsprechend den R_f-Werten 0,88, 0,32 und 0,18; ausserdem ein schwach ausgebildeter Flecken bei R_f 0,41 wie Fig. 2 zeigt.

Analyse, Schmelzpunkt und Reduktionsfähigkeit zeigten eine auffallende Ähnlichkeit unseres Reduktons mit dem von F. MICHEEL auf ganz anderem Wege dargestellten 3,4-Dioxy-5-methyltetron. Um die Frage nach der Identität der beiden Stoffe zu entscheiden, hat H. HASSELQUIST[1] das Tetron nach dem Verfahren von Micheel mit einer leichten Modifikation dargestellt. Mit diesem Produkt wurde dann festgestellt, dass dasselbe den Schmelzpunkt unseres aci-Reduktons III *nicht erniedrigt*.

Umsetzung des aci-Reduktons III mit Diazomethan

100 mg analysenreinen aci-Reduktons III wurden sukzessive mit einer ätherischen Lösung von Diazomethan versetzt, wobei kräftige Stickstoffentwicklung eintrat. Überschuss von Diazomethan veranlasste erfahrungsgemäss eine schlechte Ausbeute

---

[1] H. HASSELQUIST, Dieses Arkiv, im Druck.

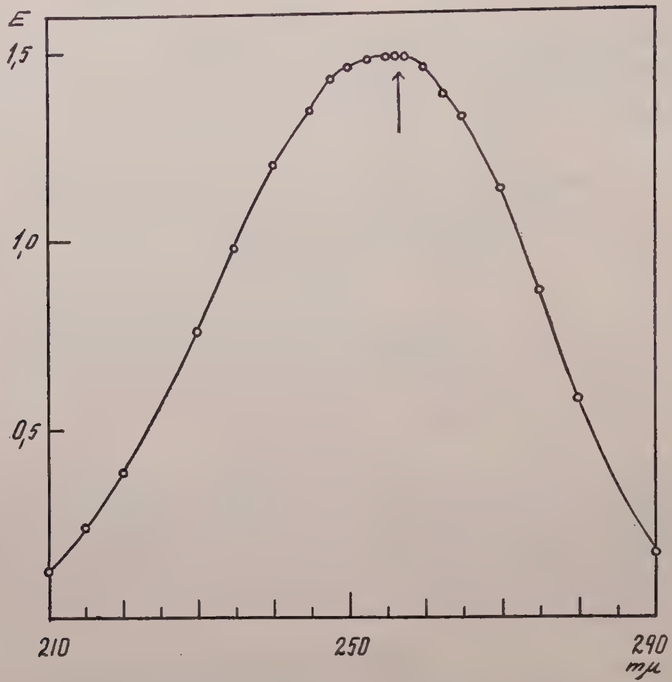

Fig. 1. aci-Redukton III. 24 mg/1000 ml Wasser.

an kristallisierter Substanz und wurde deshalb möglichst vermieden. Vermutlich entsteht andernfalls ein Diäther als nicht kristallisierendes Öl.

Nach Abschluss der Stickstoff-Entwicklung (etwa 2 Minuten) wurde das Reaktionsgemisch im Vacuum bei 30° eingedunstet. Der Rückstand, ein hellgelbes Öl, begann beim Reiben sofort in langen Nadeln zu kristallisieren. Durch Extraktion des Ganzen mit kaltem Petroleumäther ging der Hauptteil in Lösung, der Rest bestand aus einem gelben Öl. Beim Eindunsten der Petroleumäther-Lösung auf ein kleines Volumen erschienen farblose Nadeln mit wenigen kleinen Öltröpfchen. Schmelzpunkt: 86–88°. Nach wiederholter Umkristallisation in ganz wenig Benzol schmolzen die farblosen Prismen bei 116–116,5°. Ausbeute 18 mg.

Der entstandene Diazoäther ist leicht löslich in Chloroform, Äthylacetat, Äther, Aceton, Methanol, Äthylalkohol, ziemlich leicht löslich in Benzol, wenig löslich in Petroleum-Äther, schwerlöslich in Wasser.

Analyse:

Für $C_6H_8O_4$ berechnet:	C = 50,00 %	H = 5,60 %	CH_3O = 21,53 %
gefunden:	50,13 %	5,88 %	21,08 %

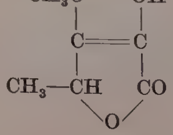

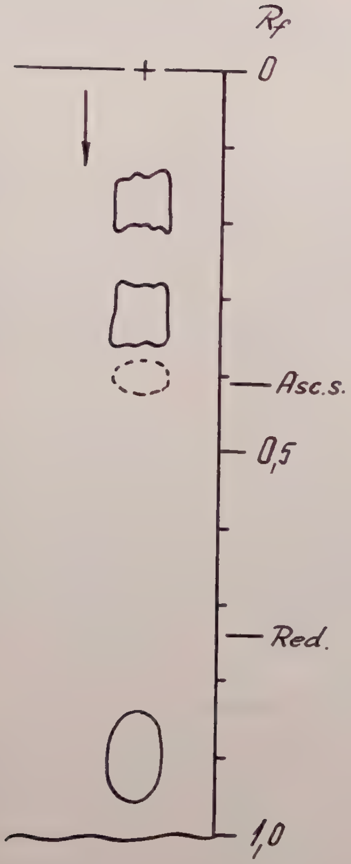

Fig. 2.

Umsetzung des aci-Reduktons III mit Phenylhydrazin

60 mg aci-Redukton III, in 10 ml Wasser gelöst, werden mit 250 mg Phenylhydrazin-Chlorhydrat + 500 mg NaAc + 5 ml Eisessig drei Stunden auf 90° erwärmt. Die Lösung färbt sich allmählich gelbrot und scheidet rote stabförmige Kristalle aus. Dieselben werden abfiltriert, gewaschen und getrocknet, und schmelzen bei 139–160° ohne Zersetzung. Die getrocknete Substanz wird in überschüssigem siedendem Petroleumäther gelöst. Nach dem Erkalten wird eine kleine Menge kleiner bräunlicher Stäbchen abfiltriert. Das Petroleumäther-Filtrat wird zur Trockne verdampft und die ausgeschiedenen roten Nadeln in der Wärme in möglichst wenig Eisessig gelöst. Es entstehen intensiv rote Nadeln vom Schmelzpunkt 184,5–185°. Ausbeute: 15 mg, die *Schmelze* ist *intensiv rot.*

Aus dem Eisessig-Filtrat schieden sich gelbrote Kristalle vom Schmelzpunkt 184,5–185° ab. Auch diese Schmelze ist *intensiv rot.* Ein Mischschmelzpunkt zeigt keine Depression. Beim Umkristallisieren der roten Nadeln aus Essigsäure wurden die gelbroten Nadeln unverändert mit dem Schmelzpunkt 184,5–185° wieder erhalten. Diese gelbroten Kristalle nahmen bei Zimmertemperatur einen immer stärker roten

Farbton an, *ohne dass eine Gewichtsveränderung eintrat.* Es scheint also eine innere Strukturveränderung im Molekül stattzufinden, die sich etwa folgendermassen formulieren lässt.

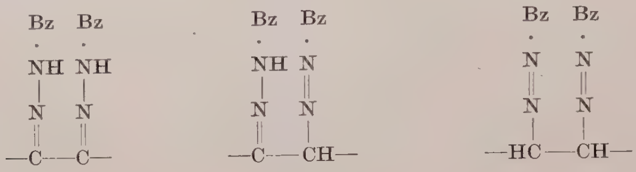

$$\begin{array}{cc} Bz & Bz \\ \cdot & \cdot \\ NH & NH \\ | & | \\ N & N \\ \| & \| \\ -C & -C- \end{array} \qquad \begin{array}{cc} Bz & Bz \\ \cdot & \cdot \\ NH & N \\ | & \| \\ N & N \\ \| & | \\ -C & -CH- \end{array} \qquad \begin{array}{cc} Bz & Bz \\ \cdot & \cdot \\ N & N \\ \| & \| \\ N & N \\ | & | \\ -HC & -CH- \end{array}$$

Im geschmolzenen Zustand existiert *nur die rote Form.* Die Substanz ist leichtlöslich in Benzol, Aceton, Chloroform. Löslich in Petroleumäther, in warmen Methanol und Eisessig, schwerlöslich in Wasser.

Analyse:

Für $C_{17}H_{16}O_2N_4$	berechnet:	C = 66,22 %	H = 5,23 %	N = 18,17 %
	gefunden:	66,52 %	5,23 %	17,97 %

Im Anschluss an unsere Versuche über die Bildung der Reduktone I und II beim Abbau der Glucose in mässig alkalischen Lösungen lag die Frage nahe, ob auch bei anderen Abbau-Wegen Reduktone als Zwischenprodukte entstehen. Der natürliche enzymatische Abbau einerseits in höheren Pflanzen, andererseits in Mikroorganismen, für welchen früher besonders die Wege über Dioxyaceton, Glycerinaldehyd und Glyoxal bzw. Methylglyoxal in Betracht gezogen wurden, wird in einer Arbeit von EULER und M. L. STEIN besprochen.

Wenn wir den oxydativen Abbau von Hexosen in den Bereich unserer Untersuchung zogen, so gingen wir dabei aus von Ergebnissen von KARRER und K. PFAEHLER[1], FLEURY und LANGE[2] sowie PERLIN[3] über die Oxydation von Glucose durch Perjodsäure, durch welche — wie bei der Einwirkung von Alkali auf Dehydroascorbinsäure — 1 C-Atom abgespalten wird.

Wir wollten uns zunächst Erfahrung darüber verschaffen, ob bei dem oxydativen Glucose-Abbau aci-Redukton I als Zwischenprodukt entsteht und wir haben zur Ausarbeitung einer Methodik das Verhalten von aci-Redukton I zu Dimedon geprüft aber noch kein einheitliches Produkt erhalten.

Herrn Ingenieur ERIK ERIKSSON danken wir für eifrige Hilfe bei der Ausführung der Versuche.

Stockholm, Universität, Institut för organ.-chemische Forschung.

---

[1] P. KARRER und K. PFAEHLER, Helv. *17,* 766 (1934).
[2] P. FLEURY und J. LANGE, J. Pharm. Chem. (8) *17,* 1 (1933).
[3] PERLIN, J. Am. Chem. Soc. *76,* 2595 (1954).

Tryckt den 12 mars 1955

Uppsala 1955. Almqvist & Wiksells Boktryckeri AB

ARKIV FÖR KEMI Band 8 nr 9

Vorgelegt am 24. November 1954

Über die Katalase-Aktivität der Leber und Milz von Ascitestumor-Ratten während der Behandlung mit cytostatischen Substanzen

Von Luigi Resegotti und Hans von Euler

Bei Untersuchungen des Stoffwechsels in Tumoren hat die katalatische Wirkung der Leber zeitig besondere Beachtung gefunden. Schon 1916 hat Brahn (1 a) als erster über die Erniedrigung des Gehaltes der Leber an Katalase berichtet; seine Befunde wurden dann bestätigt und erweitert von Colwell, Magot und in neuerer Zeit besonders von J. P. Greenstein (1 b). Von den bis jetzt in Betracht kommenden Enzymsystemen scheint die Katalase in normalen Ratten die grösste Konstanz zu zeigen; ihre Wirkung[1] ist in verschiedenen Teilen der Leber wenig verschieden und wenig abhängig von der Art der Tumoren; erheblich ist dagegen der Einfluss des Alters der Ratten (1 c).

Bei Ratten wurde die durch Tumoren erniedrigte Katalase-Wirkung der Leber beobachtet von Dounce und Skanewise (2) im Walker Carcinom 256, von Appleman, Skaninski und Stein (3) im Jensensarcom und im Fibrosarcom UCLA, von Klatt und Taylor (4) im spontanen Mamma-Carcinom DBA, und in anderen Tumoren. Euler und Heller (5) fanden diese Erniedrigung nach Fraktionierung durch Ultrazentrifugierung sowohl in den Mitochondrien als in der übrigen Fraktion. Die Katalase-Aktivität in der frischen Leber betrug k/Mitochondrion $1{,}46 \cdot 10^{-10}$ (5 b).

Für Lebern von Mäusen wurden entsprechende Resultate erhalten von Adams (6–7) mit den Sarcomen 37, 180 und 2146 und mit dem Carcinom 63; ferner von Greenfield und Meister (23) mit Mamma-Tumoren C3Hb, mit Walker-Sarcom und mit Fibrosarcom AXCMCA2 der Ratte. Zu erwähnen sind schliesslich neuere Untersuchungen, die japanische Forscher (8–10) an verschiedenem Material ausgeführt haben.

In der vorliegenden Arbeit wurde ein sich sehr schnell entwickelnder Tumor untersucht, nämlich das Yoshida Ascites Sarcom der Ratte. Weisse, 200–300 g schwere Ratten des norwegischen Albino-Stammes dieses Institutes wurden injiziert mit 0,3 ml Ascites der Yoshida Sarcom-Ratten (vgl. dieses Arkiv 7, nr 29; 1954). Bereits nach 3–4 Tagen zeigte sich die Entwicklung des Tumors durch das Auftreten des Ascites und durch die Vermehrung des Körpergewichtes. Am sechsten Tag stirbt im allgemeinen die Ratte, sofern sie nicht einer besonderen Behandlung unterworfen wurde.

Das uns zur Verfügung stehende Material haben wir in 6 Gruppen geteilt: Man kennt durch die Arbeiten von ADAMS den Einfluss des Geschlechts (12) und der Diät (13), besonders bezüglich Eisen, Kupfer und Mangan; deswegen wurden alle Tiere während der Versuche auf einer konstanten Diät gehalten, und man hat versucht, soweit möglich jeder Gruppe gleich viele Tiere jeden Geschlechts zuzuteilen.

---

[1] Wie früher wiederholt betont wurde (z. B. Euler u. Glaser, Dtsch. Med. Wochschr. *75*, 633; 1950), entnehmen wir unseren Messungen nicht den Enzym-*Gehalt* — das Enzym wird durch Aktivatoren und Inhibitoren beeinflusst — sondern die Enzym-*Wirkung*.

5 Ratten der Gruppe 1 wurden getötet, ohne eine vorhergehende Behandlung und den Mittelwert der normalen Katalase-Wirkung der Leber zu ermitteln.

Die 2. Gruppe umfasste nicht-tumortragende Tiere, welche eine mittlere Dosis von Colchicin erhalten hatten.

Die 3. Gruppe bestand aus Tieren, die eine mittlere Dosis von Tartrat des Methylesters der Trimethylcolchicinsäure erhielten. Wir bezeichnen dieses Salz mit der von LEITER und MITARB. (14) verwendeten Abkürzung NCI 1136.

Die 4. Gruppe umfasst die mit Ascites injizierten Ratten, welche keiner anderen Behandlung unterworfen waren.

Die Tiere der 5., mit Ascites injizierten Gruppe wurden mit verschiedenen Dosen von Colchicin behandelt.

Die Tiere der Gruppe 6 wurden behandelt mit verschiedenen Dosen des reinen Salzes NCI 1136. Sowohl Colchicin als auch das Salz NCI 1136 sind wasserlöslich; sie wurden intraperitoneal in 0,5%iger Lösung eingegeben. Die Injektionen wurden ausgeführt 3 Tage nach der Einführung des Tumors und die Tiere wurden nach weiteren 3 Tagen getötet.

Zur Verwendung kam reinstes kristallisiertes Colchicin der Fabriken *Sandoz*, Basel; das Präparat NCI 1136 wurde von der Firma *Farmitalia*, Milano, geliefert. Die Bestimmung der katalatischen Aktivität wurde ausgeführt durch die übliche Permanganat-Titration (15).

10 ml der homogenisierten Leber verdünnt 1:2500 mit Phosphat-Puffer von pH 6 wurden in Gegenwart von 100 ml einer Perhydrol-Lösung (0,5 ml in 1000 ml dest. Wasser) und von 40 ml Phosphat-Puffer gemischt. Die Titration wurde mit Kaliumpermanganat n/100 ausgeführt und die Proben, je 15 ml der zu untersuchenden Lösung, wurden im Augenblick der Mischung genommen, und dann nach 5, 10 und 15 Minuten. Die Ergebnisse der Messungen sind in der folgenden Tabelle ausgedrückt durch Kat. f. Reaktionskonstante k per g des frischen Organes.

Aus der Betrachtung der Tabelle ergeben sich einige interessante Tatsachen. Wie bei den anderen studierten Tumoren zeigen sich auch bei den Ascites-Tumoren die Katalase-Werte der Leber erniedrigt. In unseren Versuchen sind die Werte der Leber-Katalase um etwa 50 %, diejenigen der Milz-Katalase um etwa 70 % gegen die normalen erniedrigt.

Weder das Colchicin noch die normalen Tieren eingegebene Subst. NCI 1136 scheint die Katalase-Werte signifikativ zu beeinflussen. Die eingetretenen Variationen können sich auch in den normalen Tieren zeigen und beruhen teilweise auf der Tatsache, dass die 2. Gruppe unserer Tiere nur aus männlichen, die dritte Gruppe nur aus weiblichen Tieren bestand.

Die Katalase-Werte der Leber und Milz der mit Colchicin behandelten Ratten unterscheiden sich relativ wenig von den entsprechenden Werten der nicht behandelten Tiere. Die mit NCI 1136 injizierten Tiere haben normale katalatische Leberwerte, während die katalatischen Werte der Milz, wie auch später mitzuteilende Versuche gezeigt haben, wenig erniedrigt sind.

Wir haben auch die Gewichte der untersuchten Organe in Betracht gezogen. Mehrere Autoren haben eine Erhöhung des Lebergewichtes bei den Tumor-Ratten angenommen. ANNAN, MANGINELLI und ROTH (16) haben das Verhältnis berechnet,

Gruppe	Gewicht der Tiere	Gewicht der Leber	Kat./g Leber	Gesamt-Kat.	Kat./g des Tieres
Normale Tiere . . .	235	10,483	105,39	1104,703	4,7
Normale + Colchicin .	253	9,311	134,36	1251,015	4,9
Normale + NCI 1136 .	221	8,805	88,52	779,418	3,52
Ascites-Tiere	229	14,939	52,1	795,321	3,43
Ascites + Colchicin . .	246	14,24	46,40	660,736	2,68
Ascites + NCI 1136 .	252	14,569	95,27	1387,131	5,5

Gruppe	Gewicht der Tiere	Gewicht der Milz	Kat./g Milz	Gesamt-Kat.	Kat./g des Tieres
Normale Tiere . . .	235	1,88	15,242	28,654	0,1219
Normale + Colchicin .	253	1,12	18,146	20,377	0,0805
Normale + NCI 1136 .	221	—	—	—	—
Ascites-Tiere	229	1,26	6,95	8,757	0,0382
Ascites + Colchicin . .	246	0,97	6,737	6,575	0,0282
Ascites + NCI 1136 .	252	1,56	12,28	18,739	0,0743

zwischen dem Lebergewicht und dem Gewicht des gesamten Tieres und fanden bei den tumortragenden Tieren Werte, welche von 0,072 bis 0,031 von den normalen abwichen (Mittelwerte).

Das Lebergewicht hat sich bei unseren Versuchen als sehr konstant erwiesen sowohl bei den normalen als bei den Tumor-Tieren und im ganzen unabhängig von der Behandlung. Als Verhältnis zwischen dem Gewicht der Leber und dem des Tieres hat sich 0,040 bei den normalen und 0,059 bei den Ascites-Ratten ergeben.

Die Milz hat dagegen bemerkenswerte Variationen des Gewichtes gezeigt, welche verständlich werden wenn man eine grössere oder kleinere Anhäufung von Blut berücksichtigt, welche das Gewicht des ganzen Organes beeinflussen kann.

Es ist also nicht möglich, einen Einfluss des Tumors auf das Milzgewicht festzustellen.

Wir haben auch die Gesamt-Katalase der Leber und der Milz als absolute Gesamtwerte in Abhängigkeit vom Körpergewicht berechnet. Es hat sich gezeigt, dass die Gesamt-Katalase von Tumor nicht wesentlich beeinflusst wird, da die Erniedrigung per Gramm Substanz kompensiert wird von der Erhöhung des Lebergewichtes (4).

Auch in unseren Versuchen vermindert die Erhöhung des Gewichtes die Differenz zwischen der totalen Katalase der untersuchten Organe in tumortragenden und in Kontroll-Tieren. Immerhin bemerkt man in Bezug auf den Gesamtwert der Katalase eine erhebliche Verschiedenheit.

Auch in Bezug auf den Gesamtwert der Katalase verhalten sich die mit NCI 1136 behandelten Tiere wie die normalen.

Eine Erklärung dieses Phänomens stösst auf Schwierigkeiten. Die Frage, in welcher Weise ein noch unentwickelter Tumor die Leber-Katalase beeinflussen kann ist oft diskutiert worden. Wir wollen dabei nochmals hervorheben, dass es sich hierbei nicht um die Konzentration bzw. Menge an reinem Enzym, sondern um die *Aktivität* des ganzen *Enzymsystems* handelt, in die also die Wirkung von Aktivatoren und Inhibitoren eingeht.

Besonders bemerkenswert sind in dieser Hinsicht die Arbeiten von NAKAHARA und FUKUOKA (18–22), vgl. auch DAY *et al.* (23), welche in einer 1948 begonnenen Untersuchungsreihe die Erniedrigung der Katalase-Wirkung in Tumoren auf einen Hemmungsstoff zurückführen, den sie *Toxohormon* nennen. Dieser in den Homogenaten von Tumorlebern auftretende Stoff wurde von den japanischen Forschern aus den Homogenaten extrahiert und dialysiert und ruft nach Injektion in normale Mäuse eine Erniedrigung der Leberkatalase-Wirkung hervor. NAKAHARA und FUKUOKA konnten den Toxohormon-Gehalt von Tumorgewebe von Mäusen erheblich steigern durch Injektion von gewissen (*acht* verschiedenen) Aminosäuren; sie ziehen daraus den Schluss, dass diese Aminosäuren Komponenten des Toxohormons sind. Die dialysierbare Form des Toxohormons konnte aus einer nicht-dialysierbaren Form gewonnen werden.

An den Studien über das Toxohormon haben sich seit 1950 ADAMS, APPLEMAN, GREENFIELD u. MEISTER (26) sowie LUCKÉ, BERWICK und ZWECKER (24) beteiligt. Die letztgenannten Forscher haben eine Tumorratte mit einer normalen Ratte zur Parabiose vereinigt und konnten eine Erniedrigung des Leberkatalase-Wertes bei der normalen Ratte feststellen.

Da die Verbindung zwischen den Gefässen der beiden Tiere nur gering war — die Tiere hingen zusammen durch die Bauchwand ohne Verbindung der Bauchhöhle — so muss man annehmen, dass die in Rede stehende Substanz in mässiger Menge und nicht schnell eliminiert wurde.

Das Hormon wird als typisch für Tumoren betrachtet, weil die Implantation von schnell wachsenden, aber nicht neoplastischen Geweben, z. B. Stücken von Embryonen, die Katalase nicht verändert. Das Hormon erreicht wieder normale Werte 48 Stunden nach der chirurgischen Herausnahme der Tumoren.

Zu zeigen bleibt noch die Spezifität des Toxohormones, dass also das isolierte, oder wenigstens das aus Extrakten angereicherte und gereinigte Hormon nur die Katalase, nicht aber auch viele andere Enzyme beeinflusst.

Man könnte annehmen, dass NCI 1136 das Wachstum des Tumors blockiert und dass dieser Umstand unseren Befund erklärt. Indessen übt das Colchicin eine analoge Wirkung aus, und trotzdem bleibt die Katalase erniedrigt.

Andererseits werden normale Katalase-Werte bei Tieren gefunden, welche mit sehr kleinen Dosen von NCI 1136 behandelt waren und bei welchen die Autopsie reichlich Ascites mit einer seit vorhergehenden Tagen erhöhten Zahl von Tumorzellen per mm^3 ergeben hatte. Somit ist die versuchte sehr einfache Erklärung nicht sicher annehmbar. Wir haben deswegen eine direkte Wirkung der Substanz NCI 1136 auf die Katalase in Betracht gezogen. Wir haben daher Versuche angestellt, bei welchen wir in vitro Leberhomogenat einerseits von normalen, andererseits von Ascites-tumortragenden Ratten mit einer Lösung von NCI 1136 inkubierten. Die Katalase-Werte wurden nach 3stündiger und nach 24stündiger Inkubation gemessen und die Resultate waren identisch mit den in beiden Versuchsreihen angestellten Parallelversuchen.

Auch nach Injektion von Ascites, welcher im Kühlschrank 24 Stunden mit der gleichen Menge einer 0,5 %igen Lösung von NCI 1136 gemischt gestanden hatte, waren die Werte der Leberkatalase normal. Als reine Hypothese könnte man in Betracht ziehen, dass die Substanz NCI 1136 als Anti-toxohormon fungiert. Durch eine solche Hypothese könnte man vielleicht die subjektive Besserung erklären, die allerdings nicht immer mit einer objektiven Besserung parallel geht, wie man bei der klinischen Anwendung dieser Substanz beobachten kann (25).

Weitere Studien werden deshalb erforderlich sein, um diesen interessanten Punkt des Fragenkomplexes aufzuklären; gegenwärtig müssen wir uns darauf beschränken, unseren Befund mitzuteilen.

Zusammenfassung

Gegenstand der vorliegenden Untersuchung war die katalatische Aktivität der Leber und der Milz von Yoshida-Ascites-Tumoren tragenden Ratten, die mit Colchicin und mit dem D-Tartrat des Methylesters der Trimethyl-colchicinsäure (NCI 1136) behandelt waren.

Die Leber- und Milz-Katalase zeigte sich in Gegenwart des Ascites-Tumors erniedrigt. Die Eingabe von *Colchicin* hat dieses Ergebnis *nicht* geändert, während das NCI 1136 imstande zu sein scheint, die Katalase-Wirkung der Lebern der tumortragenden Ratten angenähert *auf den Normalwert zurückzuführen.*

Der Mechanismus der Erniedrigung der Leberkatalase-Wirkung durch Tumoren wird besprochen und einige Hypothesen werden erwähnt, um den Einfluss von der Substanz NCI 1136 zu erklären.

Riassunto

È stata studiata l'attività catalasica del fegato e della milza di ratti portatori di tumore ascite trattati con colchicina e col D-tartrato dell'estere metilico dell'acido trimetilcolchinico (NCI 1136).

La catalasi epatica e splenica si è dimostrata depressa della presenza del tumore. La somministrazione di colchicina non ha modificato il quadro, mentre l'NCI 1136 sembra capace di riportare ai valori normali la catalasi nel ratto portatore di tumore.

Viene discusso il meccanismo di depressione della catalasi epatica da parte dei tumori e si affacciano alcune ipotesi per spiegare l'azione dell'NCI 1136.

Stockholm, Universität, Vitamin-Institut.

LITERATUR

1 a. Brahn, B., Further researches on the enzymes in the liver of the cancerous. Sitzung der Kgl. Preuss. Akad. Wissensch. *20,* 478 (1916).

1 b. Greenstein, J. P. *et al.,* Relative activity of ... catalase ... in normal and cancerous hepatic tissues of the rat. J. Nat. Cancer Inst. *2,* 7 (1941).

2. Douce, A. L. u. Shanewise, R. P., Liver catalase of tumour bearing and leprous rats. Cancer Research *2,* 103 (1950).

3. Appleman, D., Skavinski, E. R. u. Stein, A. M., Catalase studies on normal and cancerous rat. Cancer Research *8,* 489 (1950).

4. Klatt, O. A. u. Taylor, A., The effect of tumour growth on liver catalase concentration. Cancer Research *10,* 764 (1951).

5 a. von Euler, H. u. Heller, L., Katalaseactivität in Leberfractionen normaler und sarkomtragender Ratten. Ztschr. Krebsforsch. *56,* 393 (1949).

5 b. von Euler, H., Actions of normal and sarcomatous sera on tumour cells. Pont. Acad. Sci. Ser. var. 7, 1949.

5 c. von Euler, B. u. v. Euler, H., Einflüsse von Wirkstoffen auf Lebensvorgänge normaler und sarkomtragender Ratten. Arkiv för Kemi 2, nr. 38, 1950.

6. Adams, D. H., The mechanism of the liver catalase depressing action of tumours in mice. Brit. J. Cancer *2,* 183 (1950).

7. Adams, D. H., Further observations on the liver catalase depressing of tumours. Brit. J. Cancer *1,* 115 (1951).

8. Yunoki, K., On the effects of Yoscida sarcoma on blood picture, blood and liver catalase activity in mice. Gann *43,* 81 (1952).
9. Mori, K. u. Momoki, S., Catalase studies on the liver of rats in the course of liver cancer production. Gann *43,* 85 (1952).
10. Iguchi, R., Study of catalase in cancer (especially stomach cancer). Gann *43,* 86 (1952).
11. von Euler, H., von Euler, B. u. Hasselquist, H., Untersuchungen am Yoshida-Ascites-Sarkom der Ratte. Arkiv f. Kemi 7, nr *29,* 19 (1954).
12. Adams, D. H., Mouse liver catalase. The antagonistic effect of tumour tissue upon the hormonal control mechanism. Brit. J. Cancer *4,* 409 (1951).
13. Adams, D. H., Effect on mouse liver catalase activity and blood haemoglobin level of a milk diet deficient in iron, copper and manganese. Biochem. J. *54,* 328 (1953).
14. Leiter, J., Hartwell, J. L., Ullyott, G. E. u. Schaer, M. J., Damage induced in sarcoma 37 with chemical agents. Derivatives of colchicine and isocolchicine. J. Nat. Canc. Inst. *13/5,* 1201 (1953).
15. von Euler, H. u. Josephson, K., Bezeichnung der Aktivität und Affinität von Enzymen. Ber. dtsch. chem. Ges. *56,* 1749 (1923).
16. Annan, E., Manginelli, A. u. Roth, A., Increased weight and mitotic activity in the liver of bearing rats and mice. Cancer Research *5,* 304 (1951).
17. Nakahara, W. u. Fukuoka, F., A toxic cancer tissue constituent as evidenced by its effects on liver catalase activity. Japan M. J. 1271, 1948.
18. Nakahara, W. u. Fukuoka, F., Toxhormone, a characteristic toxic substance produced by cancer tissues. Gann *40,* 45 (1949).
19. Nakahara, W. u. Fukuoka, F., Purification of toxohormone: A second study on toxohormone, a characteristic toxic substance produced by cancer tissues. Gann *41,* 47 (1950).
20. Fukuoka, F. u. Nakahara, W., Mode of action of toxohormone, a characteristic toxic substance produced by cancer tissues. Gann *42,* 55 (1951).
21. Fukuoka, F. u. Nakahara, W., Amino acids and toxohormone synthesis. A fifth study on toxohormone, a characteristic toxic substance produced by cancer tissue. Gann *44,* 1 (1953).
22. Nakahara, W. u. Fukuoka, F., Dialyzable form of toxohormone. A sixth study on toxohormone, a characteristic toxic substance produced by cancer tissue. Gann, *45,* 67 (1954).
23. Day, E. D., Gabrielson, F. C. u. Lipkind, J. B., Depressions in the activity of liver catalase in mice injected with homogenates of normal mouse spleen. J. Nat. Cancer Res. *15,* 239 (1954).
24. Lucké, B., Berwick u. Zwecker, J., Liver catalase activity in parabiotic rats with one partner tumour bearing. J. Nat. Canc. Inst. *13/3,* 681 (1952).
25. Paolino, W. u. Resegotti, L., Im Druck.
26. Greenfield, R. E. u. Meister, A., The effect of injections of tumor fractions on liver catalase activity of mice. J. Nat. Canc. Inst. *5,* 997 (1951).

Tryckt den 7 mars 1955

Uppsala 1955. Almqvist & Wiksells Boktryckeri AB

ARKIV FÖR KEMI Band 8 nr 10

Communicated 24 November 1954 by ARNE FREDGA and GUNNAR HÄGG

Stereochemical studies on plant growth regulators. X[1]

Configuration of optically active α-phenoxy- and α-(2-naphthoxy)-*n*-valeric acid

By MAGNUS MATELL

With 12 figures in the text

The optically active forms of α-phenoxy- and α-(2 naphthoxy)-propionic, -*n*-butyric and -*n*-caproic acids have been studied previously as plant growth regulators especially by ÅBERG (1). The lower homologues have been sterically connected with one another as well as with several other similar compounds (2), chiefly by means of the method of quasi-racemates (3). In an attempt to connect the caproic acids with the butyric acids this method gave no result. However, the corresponding valeric acids might be suitable intermediates as they would probably form quasi-racemates with the next lower homologues as well as with the higher ones. On the whole this assumption turned out to be correct. Besides this main purpose for the preparation of the optically active α-phenoxy- and α-(2-naphthoxy)-*n*-valeric acids it should be of some interest to investigate them in respect to plant growth regulating properties. Such data for two homologous series from the acetic acids up to the *n*-caproic acids would then be available.

The racemic forms of the acids to be resolved do not seem to have been described in the literature previously. However, several derivatives of α-phenoxy-*n*-valeric acid, e.g. chloride, amide, anilide, have been reported (4), though no data on the acid itself are given. The racemic forms were obtained in good yields by refluxing equimolecular quantities of the appropriate sodium phenolate and ethyl α-bromo-*n*-valerate in abs. ethanol followed by hydrolysis with aqueous sodium hydroxide. Both the acids were resolved using (+)- and (−)-β-phenyl*iso*propylamine which was found to give the best resolution of nine optically active bases tried.

The optical activity was measured in several solvents. From Tables 1 and 2 it is evident that the optical activity of the valeric acids is affected by the solvents in the same qualitative manner as the homologous acids. These data indicate that the compounds of Tables 1 and 2 which have the same direction of optical rotation also have the same configuration.

A more definite proof of the configurational relations was obtained by the quasi-racemate method. Preliminary experiments using the contact method (5) showed

---

[1] Part IX: Arkiv Kemi 7, 437 (1954).

Table 1. $[\alpha]_D^{25}$ for (−)-α-phenoxy-*n*-butyric acid [(−)-POB], (−)-α-phenoxy-*n*-valeric acid [(−)-POV] and (+)-α-phenoxy-*n*-caproic acid [(+)-POC].

Solvent	$[\alpha]_D^{25}$		
	(−)-POB	(−)-POV	(+)-POC
Acetone	−65.5°	−57.2°	+48.0°
Ethanol	−51.4°	−46.0°	+37.6°
Chloroform	−36.4°	−32.6°	+24.5°
Water (Na-salt) . . .	−20.6°	−20.5°	+16.2°
Benzene	− 5.2°	− 6.9°	+ 2.8°

Table 2. $[\alpha]_D^{25}$ for (−)-α-(2-naphthoxy) propionic acid [(−)-2 NOP], (+)-α-(2-naphthoxy)-*n*-valeric acid [(+)-2 NOV] and (+)-α-(2-naphthoxy)-*n*-caproic acid [(+)-2-NOC].

Solvent	$[\alpha]_D^{25}$		
	(−)-2 NOP	(+)-2 NOV	(+)-2 NOC
Acetone	−108.8°	+89.2°	+73.0°
Benzene	− 94.3°	+78.2°	+61.8°
Ethanol	− 93.3°	+73.6°	+58.6°
Water (Na-salt) . . .	− 73.4° [1]	+53.3°	+39.7°
Chloroform	− 62.1°	+49.4°	+37.5°

[1] NH_4-salt.

that (+)-α-phenoxy-*n*-valeric acid formed molecular compounds with (−)-α-phenoxy-*n*-butyric acid and (−)-α-phenoxy-*n*-caproic acid. (+)-α-(2-Naphthoxy)-*n*-valeric acid probably formed a molecular compound with (−)-α-(2-naphthoxy)-*n*-butyric acid but not with (+)- or (−)-α-(2-naphthoxy)-*n*-caproic acid.

To get further evidence for the quasi-racemic nature of these molecular compounds melting point diagrams were studied. In an earlier publication it has been shown that α-phenoxy- and α-(2-naphthoxy)-*n*-butyric acid are true racemates (6). From Figs. 1–4 it is seen that this is also the case with the homologous *n*-valeric and *n*-caproic acids. Among these six compounds the tendency to form racemic molecular compounds is greatest for the phenoxy acids. This is shown by the fairly well-pronounced middle parts of the curves. The 2-naphthoxy acids are very weak racemate formers, which is particularly prominent for the two higher homologues; in these cases the racemates melt considerably below their antipodes. This is probably the principal cause for the non-appearance of a quasi-racemic compound between these acids (Fig. 11).

Molecular compounds are formed between (+)-α-phenoxy-*n*-valeric acid and the (−)-forms of the homologous *n*-butyric acid (Fig. 5) and *n*-caproic acid (Fig. 7). These molecular compounds are evidently quasi-racemic as the acids with the same direction of optical rotation give no molecular compounds (Figs. 6 and 8). From this it can be concluded that the phenoxy acids with the same direction of optical rotation also have the same configuration. This conclusion is further supported by

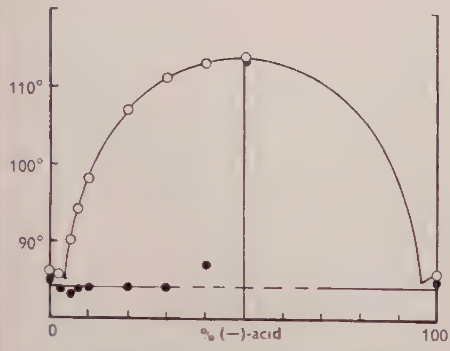

Fig. 1. (+)- and (−)-α-phenoxy-*n*-valeric acid.

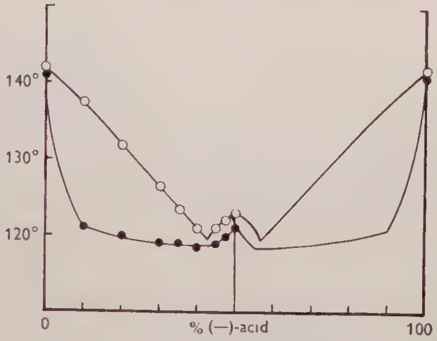

Fig. 2. (+)- and (−)-α-(2-naphthoxy)-*n*-valeric acid.

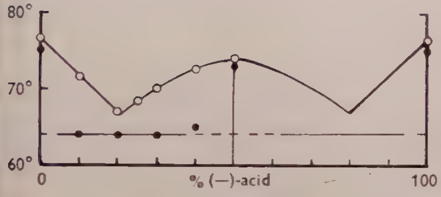

Fig. 3. (+)- and (−)-α-phenoxy-*n*-caproic acid.

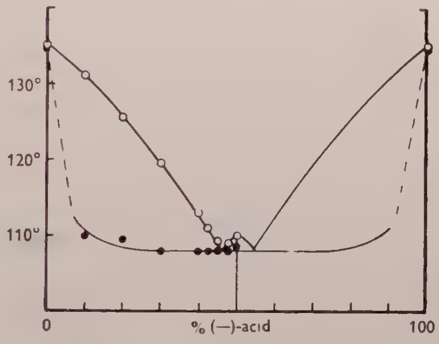

Fig. 4. (+)- and (−)-α-(2-naphthoxy)-*n*-caproic acid.

the isomorphism between the (+)-acids clearly shown by the shape of the thaw-melting point curves in Figs. 6 and 8.

(−)-α-(2-Naphthoxy)-*n*-valeric acid forms a molecular compound with (+)-α-(2-naphthoxy)-*n*-butyric acid (Fig. 9) while the acids with the same direction of optical rotation are isomorphic (Fig. 10). It can thus be unequivocally concluded that the acids with the same direction of optical rotation also have the same configuration. The very small extent of the middle part of the curve in Fig. 9 is probably due to the small racemate formation tendency of the components discussed above.

As seen from Fig. 12 (+)-α-(2-naphthoxy)-*n*-valeric acid and (+)-α-(2-naphthoxy)-*n*-caproic acid are isomorphic while the acids with opposite directions of rotation form a simple eutectic system (Fig. 11). Though no quasi-racemate is formed it is reasonable to conclude from the isomorphism that the acids with the same direction of optical rotation also have the same configuration.

It has been proved that (+)-α-phenoxy-*n*-butyric acid and (+)-α-(2-naphthoxy)-*n*-butyric acid have the same configuration as D-glyceric aldehyde (2). According to the results now presented the (+)-forms of the acids discussed here must also have the D-configuration.

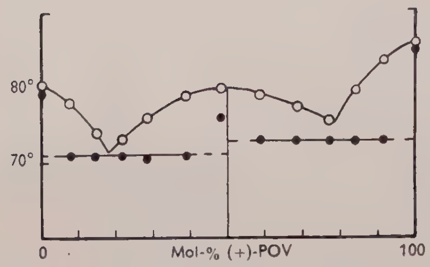

Fig. 5. (−)-α-Phenoxy-*n*-butyric acid [(−)-POB] and (+)-α-phenoxy-*n*-valeric acid [(+)-POV].

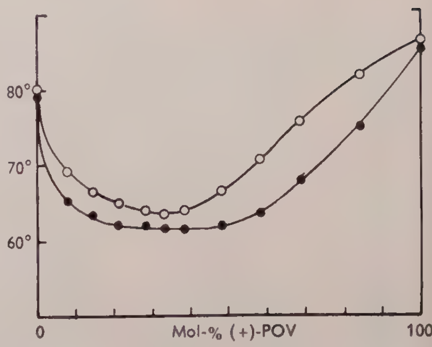

Fig. 6. (+)-α-Phenoxy-*n*-butyric acid [(+)-POB] and (+)-α-phenoxy-*n*-valeric acid [(+)-POV].

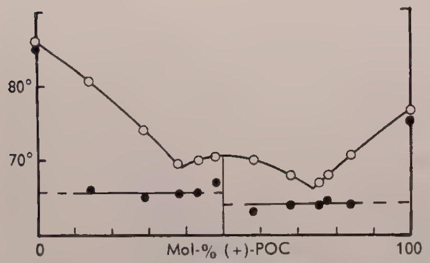

Fig. 7. (−)-α-Phenoxy-*n*-valeric acid [(−)-POV] and (+)-α-phenoxy-*n*-caproic acid [(+)-POC].

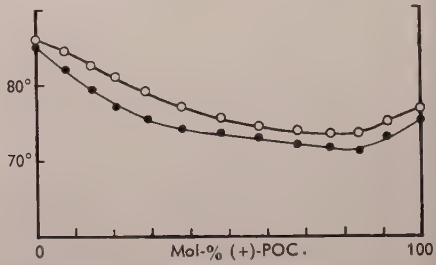

Fig. 8. (+)-α-Phenoxy-*n*-valeric acid [(+)-POV] and (+)-α-phenoxy-*n*-caproic acid [(+)-POC].

The plant growth regulating properties of the optically active α-phenoxy- and α-(2-naphthoxy)-*n*-valeric acids are being investigated by Dr. Börje Åberg. Preliminary experiments have shown that the biological activity of the *n*-valeric acids is intermediate to the homologous *n*-butyric and *n*-caproic acids. The (+)-forms have greater auxin activity than the (−)-forms and thus the acids now studied fit well into the series of stereochemical specific α-aryloxyalkylcarboxylic acids, the D-forms of which are more active as auxins than the L-forms.

Experimental

rac.-α-Phenoxy-n-valeric acid.—To a solution of sodium (3.45 g, 0.15 g-atom) in abs. ethanol (60 ml) were added phenol (14.1 g, 0.15 mole) and ethyl α-bromo-*n*-valerate (31.4 g, 0.15 mole). After refluxing for 4 hours 2-*N* sodium hydroxide (120 ml) was added and the solution refluxed for one hour. The alcohol was distilled off and the residue acidified with hydrochloric acid when an oil separated which soon solidified. The crude acid was taken up in ether and treated with 2-*N* sodium bicarbonate. The aqueous layer was acidified when a crystalline product was obtained. Yield 26.1 g (90 %). It was recrystallized from 85 % formic acid yielding 20.1 g acid with m.p. 113.5–114.0°.

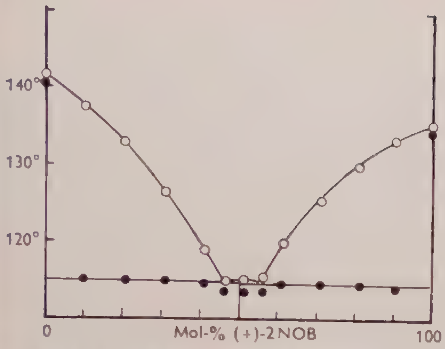

Fig. 9. (+)-α-(2-Naphthoxy)-*n*-butyric acid [(+)-2 NOB] and (−)-α-(2-naphthoxy)-*n*-valeric acid [(−)-2 NOV].

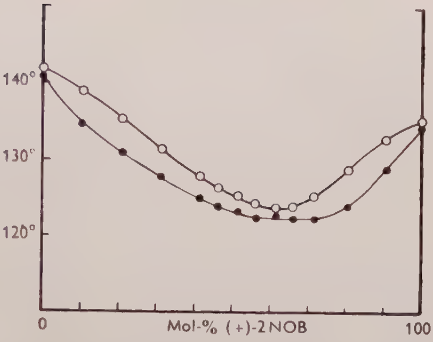

Fig. 10. (+)-α-(2-Naphthoxy)-*n*-butyric acid [(+)-2 NOB] and (+)-α-(2-naphthoxy)-*n*-valeric acid [(+)-2 NOV].

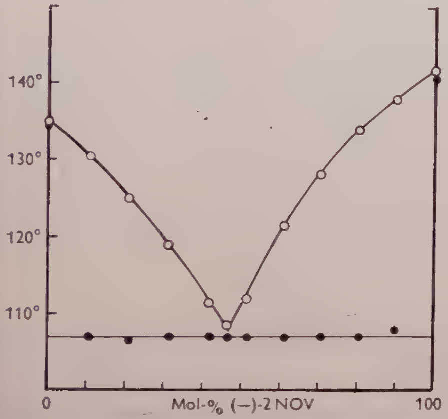

Fig. 11. (−)-α-(2-Naphthoxy)-*n*-valeric acid [(−)-2 NOV] and (+)-α-(2-Naphthoxy)-*n*-caproic acid [(+)-2 NOC].

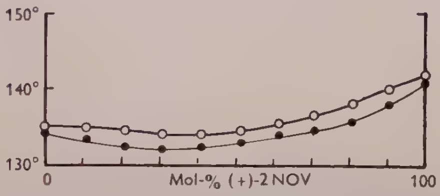

Fig. 12. (+)-α-(2-Naphthoxy)-*n*-valeric acid [(+)-2 NOV] and (+)-α-(2-Naphthoxy)-*n*-caproic acid [(+)-2 NOC].

78.14 mg acid: 8.33$_5$ ml 0.0484-*N* NaOH
$C_{11}H_{14}O_3$ calc. equiv. wt. 194.2
found ,, ,, 193.7

Rac.-α-(2-Naphthoxy)-n-valeric acid.—This acid was prepared in the same way as the phenoxy compound. Yield of crude acid 79 %, m.p. 117–121.5°. After recrystallization from 85 % formic acid and 60 % ethanol it melted at 121.0–122.8°.

89.70 mg acid: 7.94 ml 0.0464-*N* NaOH
$C_{15}H_{16}O_3$ calc. equiv. wt. 244.3
found ,, ,, 243.5

(+)- *and* (−)-*α-phenoxy-n-valeric acids.*—Most of the optically active bases tried for resolution gave noncrystallizing oils or salts from which only slightly active acids were obtained. Quinine gave some resolution but the best result was obtained with β-phenyl*iso*propylamine, the (−)-form of which gave a salt containing excess of the (+)-acid.

19.4 g (0.10 mole) α-phenoxy-*n*-valeric acid were dissolved in 100 ml 96 % ethanol. After adding 13.5 g (0.10 mole) (−)-β-phenyl*iso*propylamine, water (400 ml) was added and the solution left to crystallize for 6 hours. The salt was collected and recrystallized several times from 20 % ethanol. After each recrystallization $[\alpha]_D$ of the acid was determined, giving the following series: +8.6°, +33.2°, +41.6°, +44.8°, +45.8°, +45.9°, +45.2°. 6.45 g (20 %) pure (+)-acid-(−)-amine salt were collected. The acid was liberated from the salt and the crude acid (3.9 g) recrystallized from petroleum (b.p. 60–80°). 2.85 g pure (+)-acid were collected as small, colourless needles, m.p. 85.0–86.0°.

80.00 mg (+)-acid: 8.81$_5$ ml 0.0465-*N* NaOH
$C_{11}H_{14}O_3$ calc. equiv. wt. 194.2
found ,, ,, 195.2

0.2099 g dissolved in abs. *ethanol* to 20.06 ml: $2\alpha_D^{25} = +0.952°$, $[\alpha]_D^{25} = +45.5°$; $[M]_D^{25} = +88.4°$.

From the first two mother liquors 11.4 g acid with $[\alpha]_D = -23°$ were obtained. This acid and an equimolecular quantity of (+)-β-phenyl*iso*propylamine (7.9 g) were dissolved in 75 ml of hot 96 % ethanol. Water (300 ml) was added and the solution left to crystallize for 6 hours. The salt was recrystallized several times from 20 % ethanol. The resolution was followed by measuring the rotatory power of the acid of each fraction. The following series was obtained: −36.2°, −42.8°, −44.0°, −45.6°. 5.55 g (29 %) (−)-acid-(+)-amine salt were collected and from this salt were obtained 3.3 g of the crude (−)-acid. It was recrystallized from petroleum (b.p. 60–80°) yielding 2.4 g pure (−)-acid, m.p. 85.0–86.0°.

78.32 g (−)-acid: 8.62 ml 0.0465-*N* NaOH
$C_{11}H_{14}O_3$ calc. equiv. wt. 194.2
found ,, ,, 195.3

0.2053 g dissolved in abs. *ethanol* to 20.06 ml: $2\alpha_D^{25} = -0.942°$. $[\alpha]_D^{25} = -46.0°$; $[M]_D^{25} = -89.4°$.
0.2036 g dissolved in *acetone* to 20.06 ml: $2\alpha_D^{25} = -1.161°$. $[\alpha]_D^{25} = -57.2°$; $[M]_D^{25} = -111.1°$.
0.1971 g dissolved in *benzene* to 20.06 ml: $2\alpha_D^{25} = -0.135°$. $[\alpha]_D^{25} = -6.9°$; $[M]_D^{25} = -13.3°$.
0.2049 g dissolved in *chloroform* to 20.06 ml: $2\alpha_D^{25} = -0.665°$. $[\alpha]_D^{25} = -32.6°$; $[M]_D^{25} = -63.2°$.
0.1604 g neutralized with *aqueous NaOH* and made up to 20.06 ml: $\alpha_D^{25} = -0.164°$. $[\alpha]_D^{25} = -20.5°$; $[M]_D^{25} = -39.8°$.

(+)- and (−)-α-(2-naphthoxy)-n-valeric acids.—Preliminary experiments on resolution were carried out with 9 optically active bases. Of these only brucine and β-phenyl*iso*propylamine gave good resolution. Due to accidental lack of the (−)-form of the latter base brucine was first tried. The first recrystallization from 30 % ethanol gave a salt from which an acid with $[\alpha]_D = +25°$ (in ethanol) could be isolated. On further recrystallizations this value did not change. The rotatory power of the pure (+)-acid is +73.6° (in ethanol) and the salt should thus contain about 67 % of the (+)-acid and 33 % of the (−)-acid. A possible explanation is thus that the (+)-acid-brucine salt forms a molecular compound with the (−)-acid-brucine salt in the relation 2 : 1. Another explanation is that the salts are isomorphic, forming a phase system with a maximum at about 67 % in which case the relation 2 : 1 between (+)- and (−)-acid is a mere chance.

The acid regenerated from the brucine salt (10.9 g) and an equivalent quantity of (−)-β-phenyl*iso*propylamine (6.0 g) were dissolved in 360 ml of hot 70 % ethanol. After crystallization the salt was collected and recrystallized several times from 70–80 % ethanol. The rotatory power of the acids isolated from the salt fractions were: + 66.4°, + 72.2°, + 74.7° and + 74.2°. From the last fraction 4.6 g of the crude (+)-acid were collected, m.p. 140–141.2°. It was recrystallized from petroleum (b.p. 60–80°). It forms colourless, thread-like crystals with m.p. 140.8–141.7°.

62.90 g (+)-acid: 5.59$_5$ ml 0.0464-*N* NaOH
$C_{15}H_{16}O_3$ calc. equiv. wt. 244.3
found ,, ,, 242.2

0.1998 g dissolved in *ethanol* to 20.06 ml: $2\alpha_D^{25} = +1.467°$. $[\alpha]_D^{25} = +73.6°$; $[M]_D^{25} = +179.9°$.
0.1966 g dissolved in *acetone* to 20.06 ml: $2\alpha_D^{25} = +1.748°$. $[\alpha]_D^{25} = +89.2°$; $[M]_D^{25} = +217.8°$.
0.2117 g dissolved in *benzene* to 20.06 ml: $2\alpha_D^{25} = +1.650°$. $[\alpha]_D^{25} = +78.2°$; $[M]_D^{25} = +191.0°$.
0.1939 g dissolved in *chloroform* to 20.06 ml: $2\alpha_D^{25} = +0.954°$. $[\alpha]_D^{25} = +49.3°$; $[M]_D^{25} = +120.6°$.
0.1972 g neutralized with *aqueous NaOH* and made up to 20.06 ml: $2\alpha_D^{25} = +1.048°$. $[\alpha]_D^{25} = +53.3°$; $[M]_D^{25} = +130.2°$.

The acid from the first three mother liquours was dissolved with an equimolecular quantity of (+)-β-phenyl*iso*propylamine in hot 75 % ethanol. The salt which separated on standing was recrystallized several times from 75 % ethanol. The optical activity of the acid (in alcohol) increased in the following series: − 65.3°, − 71.9°, − 72.5°, − 72.5° and − 72.6°. 7.05 g of the pure (−)-acid-(+)-amine salt yielded 4.65 g (−)-acid. Recrystallization from 50 % ethanol yielded 4.1 g of the pure (−)-acid, m.p. 140.8–141.8°.

68.40 mg (−)-acid: 6.01$_5$ ml 0.0464-*N* NaOH
$C_{15}H_{16}O_3$ calc. equiv. wt. 244.3
found ,, ,, 245.0

0.2110 g dissolved in abs. *ethanol* to 20.06 ml: $2\alpha_D^{25} = -1.541°$. $[\alpha]_D^{25} = -73.3°$. $[M]_D^{25} = -178.9°$.

Melting point diagrams.—The samples were prepared by dissolving weighed quantities of the components in acetone. After evaporation, the residue was powdered and dried. All melting points were determined with a KOFLER hot stage microscope. The results are found in Figs. 1–12.

Summary

α-Phenoxy-*n*-valeric acid and α-(2-naphthoxy)-*n*-valeric acid have been synthesized. The racemic acids have been resolved into optical antipodes by means of β-phenyl*iso*propylamine. The racemic forms are true racemates, which is also the case with the homologous *n*-caproic acids. The configurations of the optically active α-phenoxy- and α-(2-naphthoxy)-*n*-valeric acids and the homologous *n*-caproic acids have been established by means of the method of quasi-racemates and by optical activity measurements in different solvents. The (+)-forms which have greater auxin activity than the (−)-forms belong to the D-glyceric aldehyde system.

The author is indebted to Mr. ANTS AAMISEPP for valuable assistance. Part of the expenses involved have been defrayed by a grant from the *Swedish Natural Science Research Council* which is gratefully acknowledged.

Laboratory of Organic Chemistry, Royal Agricultural College, Uppsala, November 1954.

REFERENCES

1. B. Åberg, Kgl. Lantbruks-Högsk. Ann. *20,* 241 (1953).
2. M. Matell, Ibid. *20,* 205 (1953).
3. A. Fredga, The Svedberg 1884 30.8 1944. Uppsala 1944, p. 261.
4. C. Hill, H. Schofield, A. Spriggs and M. Hill, J. Am. Chem. Soc. *73,* 1660 (1951).
5. L. Kofler and A. Kofler, Thermo-Mikro-Methoden. Innsbruck 1954, pp. 151, 237.
6. M. Matell, Arkiv Kemi *6,* 251 (1953).

Tryckt den 7 mars 1955

Uppsala 1955. Almqvist & Wiksells Boktryckeri AB

ARKIV FÖR KEMI Band 8 nr 11

Communicated 12 January 1955 by Arne Fredga

4-Bromo-2-thiophenecarboxylic acid

By Salo Gronowitz

In connection with work in progress on the resonance conditions in thiophenecarboxylic acids (1) the last of the six isomeric bromothiophenecarboxylic acids, 4-bromo-2-thiophenecarboxylic acid, has been synthesized. Steinkopf (2) tried unsuccessfully to synthesize this acid via the Grignard reaction of 2,4-dibromothiophene.

As Foye *et al.* (3) recently found that 2-thiophenecarboxaldehyde is exclusively nitrated in the 4-position when unprotected aldehyde is used, an obvious route to the 4-bromo-2-thiophenecarboxylic acid seemed to be the bromination of 2-thiophenecarboxaldehyde followed by oxidation of the bromoaldehyde. It was, however, found that besides smaller amounts of 5-bromo-2-thiophenecarboxylic acid formed through oxidation, the main product was 5-bromo-2-thiophenecarboxaldehyde. This is rather amazing as it is generally assumed that both bromination and nitration are electrophilic aromatic substitution reactions. The behaviour of 2-thiophenecarboxaldehyde upon bromination is quite similar to that of 1-naphtaldehyde (4).

It was, however, possible to obtain 4-bromo-2-thiophenecarboxylic acid through selective debromination of 4,5-dibromo-2-thiophenecarboxylic acid with *n*-butyllithium at low temperature.

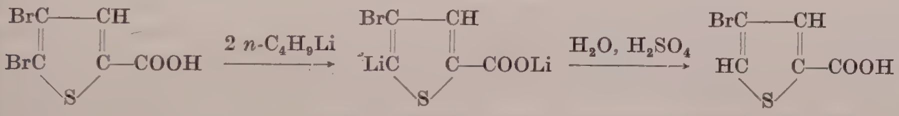

The acid could be recrystallised from water or ligroin (b.p. 80°–100°) as small white needles, m.p. 122°–123.5°. As could be expected it has the lowest melting point of the isomeric bromo-2-thiophenecarboxylic acids.

Experimental

All melting points are determined on the Kofler bank.

5-Bromo-2-thiophenecarboxaldehyde.—To 11.2 g (0.1 moles) 2-thiophenecarboxaldehyde in 15 ml of chloroform was added at once 16.0 g (0.1 moles) of bromine in 15 ml of chloroform. When the vigorous evolution of hydrogen bromide had subsided, the reaction mixture was refluxed for three hours. The mixture was cooled and extracted once with water, twice with dilute sodium carbonate and finally with water again and the organic layer was dried over magnesium sulphate. The aqueous layers were combined and acidified with hydrochloric acid in excess precipitating 0.6 g

(3 %) of 5-bromo-2-thiophenecarboxylic acid. After one recrystallisation from water the acid melted at 138°–141°. It gave no melting point depression with an authentic sample of 5-bromo-2-thiophenecarboxylic acid prepared through the Grignard reaction of 2,5-dibromothiophene. The dried organic layer was distilled through an efficient column giving 10.9 g (57 %) of 5-bromo-2-thiophenecarboxaldehyde, b.p. 105°–107°/11 mm Hg.

Semicarbazone m.p. 217°–218°, phenylhydrazone m.p. 111°–112°. GATTERMAN (5) gives the m.p. 200°–201° and 105° respectively.

Acid. M.p. 141°–142°. It gave no melting point depression with an authentic sample of 5-bromo-2-thiophenecarboxylic acid and had the same IR spectrum.

4-Bromo-2-thiophenecarboxylic acid.—11.5 g (0.040 moles) of 4,5-dibromo-2-thiophenecarboxylic acid (6) in 500 ml of absolute ether was placed in a four-necked flask fitted with a stirrer, dropping funnel, inlet tube for nitrogen and a calcium chloride tube. The flask was flushed with nitrogen and cooled in a Dry Ice-acetone mixture to −65°. With efficient stirring about 0.08 moles of *n*-butyllithium in 60 ml of ether was rapidly dropped into the solution which was stirred for an additional five minutes. The reaction mixture was poured into 300 ml of water. The aqueous phase was separated and acidified with dilute sulphuric acid. An oil separated which crystallised on standing in an ice-box. Yield 4.6 g (55 %) of crude acid. The acid was recrystallised first from ligroin (b.p. 80°–100°) and then from water giving 3.7 g of 4-bromo-2-thiophenecarboxylic acid, m.p. 122°–123.5°. The IR spectrum of the product shows that it is free from 5-bromo-2-thiophenecarboxylic acid.

Anal. 0.12913 g: 8.47 ml 0.07325 *N* NaOH; 0.02544 g: 6.32 ml 0.01956 *N* $Hg(NO_3)_2$.
$C_5H_3BrO_2S$ (207.1) calc. Equiv. wt. 207.1 Br 38.60 %
found Equiv. wt. 208.1 Br 38.84 %

Summary

It has been found that 2-thiophenecarboxaldehyde is brominated in the 5-position, although it is nitrated in the 4-position.

4-Bromo-2-thiophenecarboxylic acid has been synthesized through selective debromination of 4,5-dibromo-2-thiophenecarboxylic acid.

The author is indebted to Mr. R. ÖHBERG for the analyses and to Mr. S. BERGVALL for taking the IR spectra.

Department of Organic Chemistry, Chemical Institute, University of Uppsala, December 1954.

REFERENCES

1. GRONOWITZ, S., and ROSENBERG, A., Arkiv Kemi, *in print.*
2. STEINKOPF, W., JACOB, H., and PENZ, H., Ann. *512*, 136 (1934).
3. FOYE, W. C., HEFFERREN, J. J., and FELDMANN, E. E., J. Am. Chem. Soc. *76*, 1378 (1954).
4. RUGGLI, P., and PREUSS, R., Helv. Chim. Acta *24*, 1345 (1941).
5. GATTERMAN, L., Ann. *393*, 230 (1912).
6. HARTOUGH, H. D., Thiophene and Its Derivatives, New York 1952, p. 509.

Tryckt den 7 mars 1955

Uppsala 1955. Almqvist & Wiksells Boktryckeri AB

ARKIV FÖR KEMI Band 8 nr 12

Communicated 22 September 1954 by ARNE FREDGA and KARL MYRBÄCK

Synthesis of (−)-2D, 5L- and (+)-2L, 5D-dimethyladipic acids by *bis*-degradation of (+)-3D, 6L- and (−)-3L, 6D-dimethylsuberic acids respectively

By INGRID HEDLUND

With 3 figures in the text

Racemic 2,5-dimethyladipic acid has been resolved by NOYES and KYRIAKIDES (1), who obtained the dextrorotatory enantiomorph in an apparently pure state via the brucine salt. The optical rotation given is $[\alpha]_{D}^{28} = +31.3°$ (ethanol; *c*, 10). The compound began to soften at 103.5° and was completely melted at 105.5°. The levorotatory enantiomorph was not obtained in a pure state. The physical data reported are $[\alpha]_{D}^{28} = -23.4°$ (ethanol; *c*, 10) and melting range 85–103°, indicating the presence of about 12 % of the dextrorotatory form. The work of NOYES and KYRIAKIDES has recently been reproduced by BREWSTER (2), who reports for the dextrorotatory antipode m.p. 104.5–105.0° and a specific rotation of $[\alpha]_{D}^{27} = +30.75° \pm 0.22°$ (95 % ethanol; *c*, 4.52). No determination of the configuration of the optically active acids in relation to glyceraldehyde has been reported in the literature.

STÄLLBERG-STENHAGEN has synthesized a number of optically active methyl-substituted dibasic acids, which like 2,5-dimethyladipic acid possess two methylene groups in the middle of the chain (3–5). The acids were prepared by the KOLBE reaction from half-esters of optically active dibasic acids, and have therefore the active centres symmetrically placed with respect to the middle of the chain. It is found that all four acids shown in Chart 1 possess molecular rotations that are of the same sign but about twice as large as those of the corresponding monocarboxylic acids

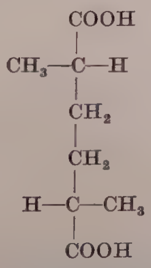

$$\begin{array}{c} \mathrm{COOH} \\ | \\ \mathrm{CH_3{-}C{-}H} \\ | \\ \mathrm{CH_2} \\ | \\ \mathrm{CH_2} \\ | \\ \mathrm{H{-}C{-}CH_3} \\ | \\ \mathrm{COOH} \end{array}$$

(+)-2L, 5D-dimethyladipic acid
$[M]_{D}^{28} = +54.5°$

I

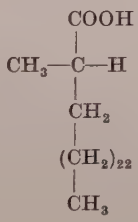

$$\begin{array}{c} \mathrm{COOH} \\ | \\ \mathrm{CH_3{-}C{-}H} \\ | \\ \mathrm{CH_2} \\ | \\ \mathrm{(CH_2)_{22}} \\ | \\ \mathrm{CH_3} \end{array}$$

(+)-2L-methylhexacosanoic acid
$[M]_{D}^{18} = +28°$ (7)

II

Chart 1^{1,2}

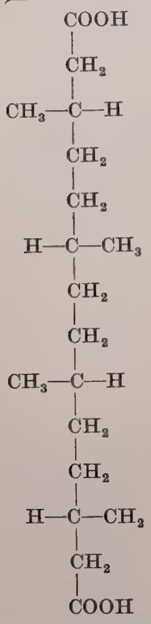

(−)-3L, 6D, 9L, 12D-tetramethyltetradecane-1,14-dioic acid
$[M]_D^{21} = -24°$ (4)

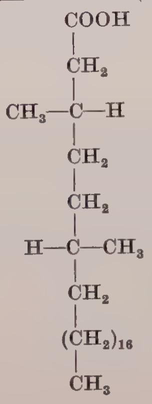

(−)-3L, 6D-dimethyltetracosanoic acid
$[M]_D^{21} = -15.6°$ (4)

3

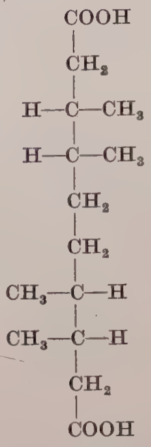

(+)-3, 4, 7, 8-tetramethylsebacic acid
$[M]_D^{25} = +57.3°$ (5)

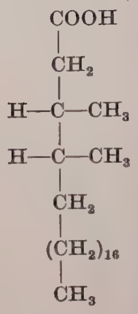

(+)-3, 4-dimethyldocosanoic acid
$[M]_D^{24} = +31.3°$ (5)

5

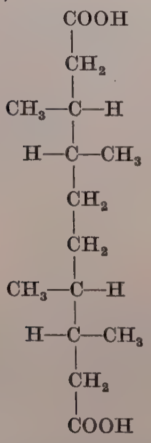

(+)-3, 4, 7, 8-tetramethylsebacic acid
$[M]_D^{25} = +32.9°$ (5)

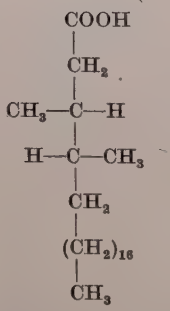

(+)-3, 4-dimethyldocosanoic acid
$[M]_D^{25} = +19.7°$ (5)

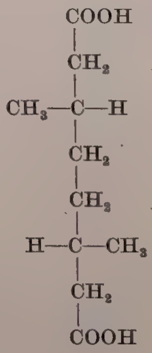

(−)-3L, 6D-dimethylsuberic acid
$[M]_D^{23} = -33.6°$ (3)

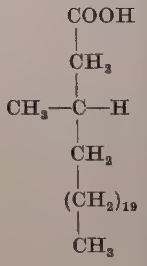

(−)-3L-methyltetracosanoic acid
$[M]_D^{25} = -13.2°$ (6)

obtained by replacing half of the dibasic acid molecule by a long *n*-alkyl group. The specific rotation reported for the dextrorotatory enantiomorph of 2,5-dimethyladipic acid corresponds to a molecular rotation $[M]_D^{28} = +54.5°$, i.e. nearly twice as large as the molecular rotation of (+)-2L-methylhexacosanoic acid (II), $[M]_D^{18} = +28°$ (7, 8). From these data it may be inferred that the dextrorotatory enantiomorph of 2,5-dimethyladipic acid is correctly named (+)-2L, 5D-dimethyladipic acid (I). A direct proof of the correctness of this conclusion has been obtained by synthesis of the antipodes of 2,5-dimethyladipic acid by *bis*-degradation of the two optically active 3,6-dimethylsuberic acids. The syntheses were performed in the manner outlined in Chart 2.

(+)-3D, 6L-Dimethylsuberic acid (III) (3) was converted into its silver salt (IV). The salt, which was obtained in practically quantitative yield, was subjected to degradation according to Hunsdiecker and Hunsdiecker (12). The isolation of the bromide (V) in a pure state was difficult owing to its ready decomposition with formation of hydrogen bromide even when the distillation was carried out at a low temperature. The best yield of distilled bromide was 37 % of the theoretical calculated on the silver salt (IV). Refluxing the bromide for 4–6 days with potassium acetate in a mixture of glacial acetic acid and butyl acetate (see Ställberg-Stenhagen (8)) gave the diacetate (VI). The b.p. was 93–95°, 0.5 mm, and the optical rotation $[\alpha]_D^{24} = +4.89°$, corresponding to a molecular rotation $[M]_D^{24} = +11.3°$. Hydrolysis of the diacetate gave (+)-2D, 5L-dimethyl-1, 6-dihydroxyhexane (VII), b.p. 148–150°, 17 mm, in a yield of 75 % of the theoretical. The optical rotation was $[\alpha]_D^{23} = +22.2°$ ($[M]_D^{23} = +32.5°$). Oxidation of the glycol with potassium permanganate in acetone solution was performed in a manner similar to that described by Ställberg-Stenhagen (8) for the oxidation of alcohols to monocarboxylic acids. It has been found previously (cf. Meyer (13), Ställberg-Stenhagen (14)), that oxidation of alcohols possessing a tertiary α-carbon atom with potassium permanganate to the corresponding α-methyl-substituted monocarboxylic acids readily gives α-hydroxy-acids as by-products. The present case, which involves the simultaneous oxidation of two alcoholic groups, leads to a complex reaction-product, the presence of hydroxylated material being indicated by a carbon content about 4 % lower than that calculated for the dicarboxylic acid (VIII). The isolation of the desired acid involved considerable loss of material. Repeated crystallizations from water, however, finally gave 56 mg of (−)-2D, 5L-dimethyladipic acid with m.p. 103.5–103.8° and $[\alpha]_D^{24} = -30.8° \pm 0.9°$ (in ethanol) ($[M]_D^{24} = -54°$). The value of the optical rotation is, within the experimental error, numerically equal to that reported for the antipode by Noyes and Kyriakides (1) and by Brewster (2). The small differences in melting-points are probably due to different techniques used in the determinations.

(+)-2L, 5D-Dimethyladipic acid was prepared in a similar manner from (−)-3L, 6D-dimethylsuberic acid. Undistilled bromide was used in the synthesis of the diacetate. The yield was 42 %, calculated on the (−)-3L, 6D-dimethylsuberic

---

Footnotes to Chart 1.

[1] The formulae are written according to Fischer's convention.

[2] The nomenclature is that employed by Ställberg-Stenhagen (9). See also Serck-Hanssen, Ställberg-Stenhagen, Stenhagen (10), and Klyne (11).

[3] The configuration of this pair of compounds in relation to glyceraldehyde has not yet been determined. That the dextrorotatory compounds have the same configurations follows from their synthesis, but the projections may actually belong to the levorotatory forms.

Chart 2[1]

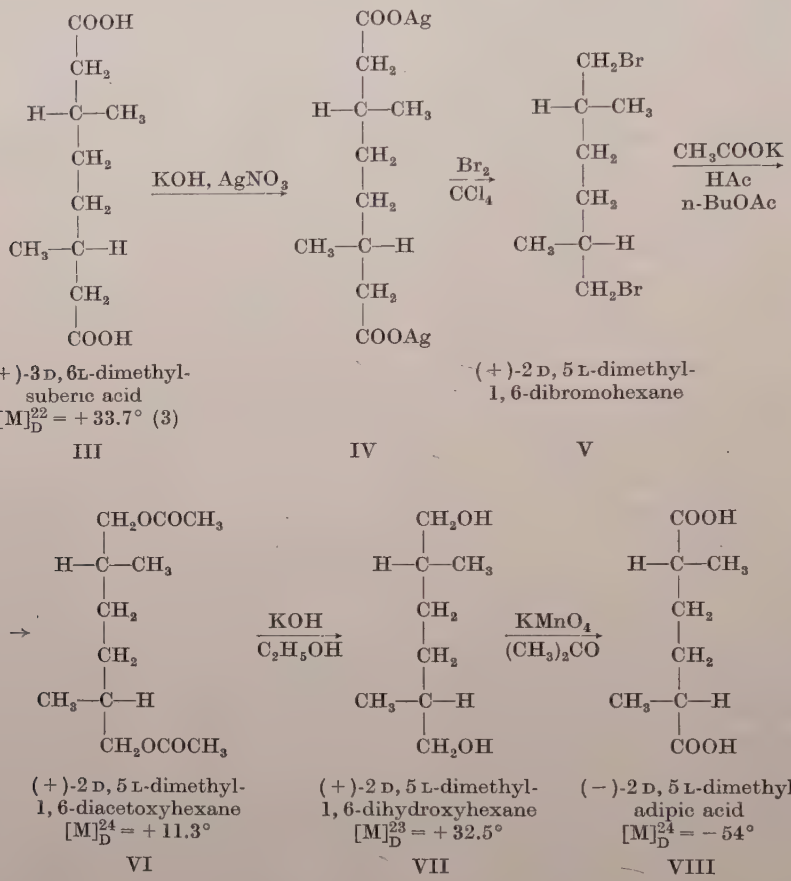

(+)-3D, 6L-dimethylsuberic acid $[M]_D^{22} = +33.7°$ (3)
III

IV

(+)-2D, 5L-dimethyl-1, 6-dibromohexane
V

(+)-2D, 5L-dimethyl-1, 6-diacetoxyhexane $[M]_D^{24} = +11.3°$
VI

(+)-2D, 5L-dimethyl-1, 6-dihydroxyhexane $[M]_D^{23} = +32.5°$
VII

(−)-2D, 5L-dimethyladipic acid $[M]_D^{24} = -54°$
VIII

acid used as initial material. The levorotatory glycol prepared by hydrolysis of the diacetate showed an optical rotation of $[\alpha]_D^{21} = -22.4°$ (homogeneous), i.e. equal to that of the antipode. Oxidation of the glycol gave (+)-2L, 5D-dimethyladipic acid with m.p. 103.2–103.8° and $[\alpha]_D^{24.5} = +30.6° \pm 0.6°$ (ethanol) in a yield of about 5 % of the theoretical.

In view of the low overall yield of the optically active 2,5-dimethyladipic acids in the present synthesis, a second synthetic route was contemplated, involving their preparation by the KOLBE reaction from the asymmetrical half-esters 1 and 2 of optically active methylsuccinic acid. The method has not been used, as it seems likely that the preparation in a pure state of the required half-esters 1 and 2 will present some difficulties. The separation of the two isomeric inactive methyl half-esters prepared from DL-methylsuccinic acid has only recently been accomplished by HANCOCK and LINSTEAD (15).

---

[1] See footnotes 1 and 2 to Chart 1.

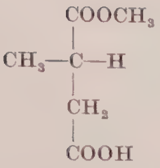

$$\begin{array}{c} COOCH_3 \\ | \\ CH_3—C—H \\ | \\ CH_2 \\ | \\ COOH \end{array}$$

1

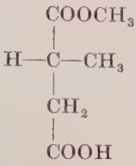

$$\begin{array}{c} COOCH_3 \\ | \\ H—C—CH_3 \\ | \\ CH_2 \\ | \\ COOH \end{array}$$

2

The melting-point of racemic 2,5-dimethyladipic acid prepared from the antipodes was found to be 74.5° (Kofler microscope). Zelinsky (17) and Brewster (2) give m.p. 74–76° and 75–76° respectively. The melting-point curve of the binary system of the antipodes was determined in the course of the present work. It does not with certainty exclude the formation of a racemic compound, but the X-ray powder diffraction patterns of the antipodes and of the racemic acid were practically identical in appearance. Powder diffraction patterns taken with a high-temperature X-ray camera (18) at temperatures near the melting points showed the same diffraction patterns as at room temperature. The infra-red absorption spectra of the antipodes and of the racemic form of 2,5-dimethyladipic acid in the solid state are identical within the experimental deviations (Fig. 1).

Fredga has employed the method of quasiracemates for the determination of configurational relationships between optically active compounds in a large number of cases (16). He has suggested that the behaviour of the binary systems of optically active 2,5-dimethyladipic acid and optically active dithiodilactic acid might be of interest in this connexion. Dithiodilactic acid may be thought of as being formally derived from 2,5-dimethyladipic acid by the replacement of —CH_2—CH_2— by —S—S— in the middle of the chain.

Specimens of the optically active dithiodilactic acids were kindly provided by Professor Fredga. As the specimens had been kept for some years they were recrystallized several times from benzene and from water. The melting-points of the (+)- and (−)-dithiodilactic acids used were 116.3–117.6° and 116.4–117.5° respectively.

It has been found that the optically active dithiodilactic acids have a very pronounced tendency to form a racemic compound (19), and in accordance with this it was found that the X-ray diffraction pattern of racemic dithiodilactic acid prepared from the antipodes was quite different from those of the active acids.

Fredga and his collaborators have found in a number of cases that quasiracemic compounds can be formed when in one of the components one methylene group has been replaced by one sulphur atom (19–21).

The replacement of —CH_2—CH_2— by —S—S—, however, probably involves a considerable change in the shape of the molecule. The bond lengths are changed, and the directions of the C-S bonds of the disulphide group tend to form an azimuthal angle probably different from that of the valency directions of the dimethylene group (cf. (22)). These differences may be large enough to prevent the formation of a quasiracemic compound. The melting-point curves of the binary systems of (+)- and (−)-dithiodilactic acid respectively and (−)-2D, 5L-dimethyladipic acid are reproduced in Figs. 2 and 3. It is evident that both systems show simple eutectic points.

As can be seen from Figs. 2 and 3, the left branch of the curve of (+)-dithiodilactic and (−)-dimethyladipic acid falls more sharply than the corresponding part of the

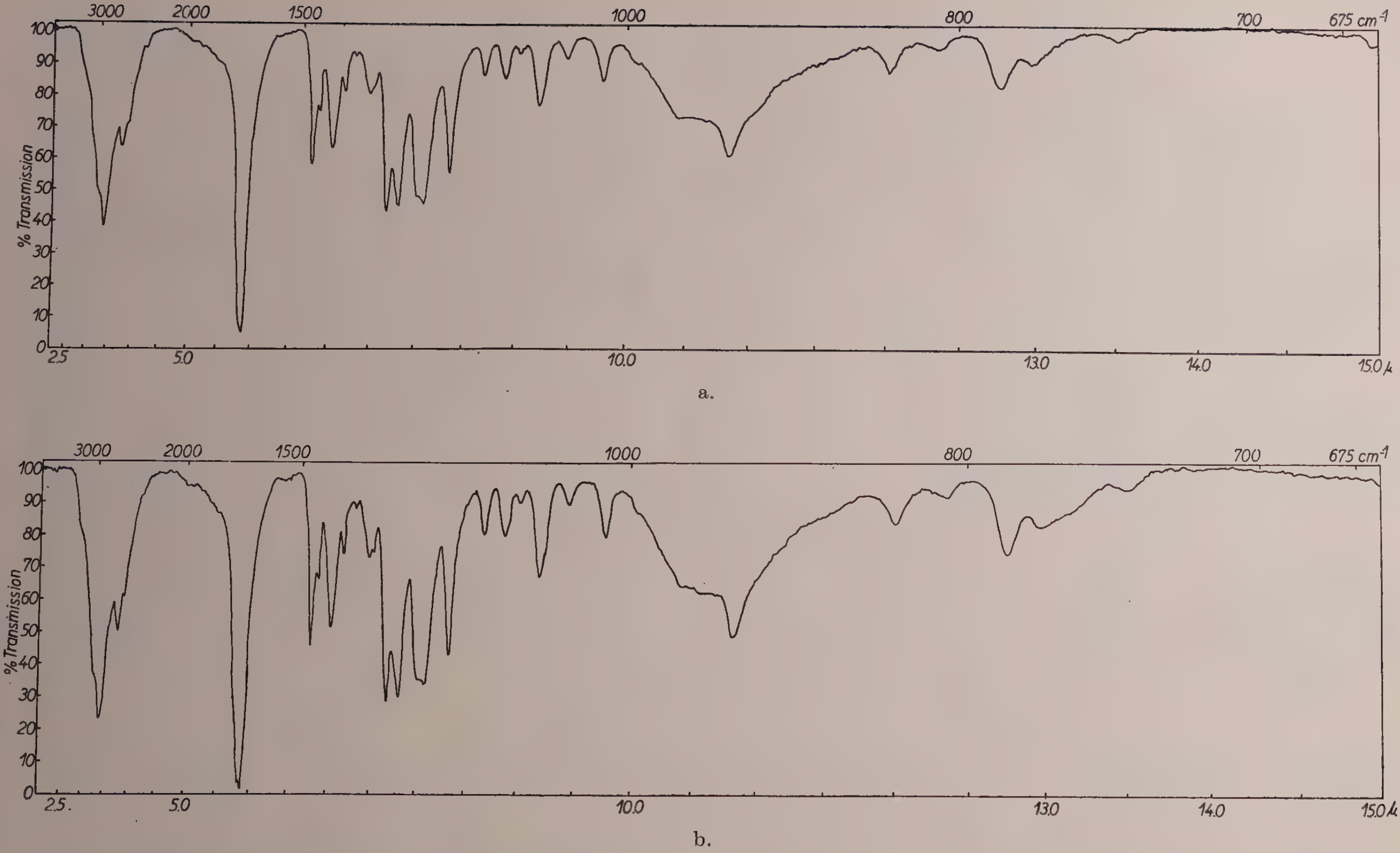

Fig. 1. Infra-red absorption spectra of 2,5-dimethyladipic acids in potassium bromide.—(*a*) (+)-2L, 5D-dimethyladipic acid, 0.9 mg in 250 mg of KBr. (*b*) Inactive 2,5-dimethyladipic acid prepared by evaporation of the solvent from a chloroform solution containing equal quantities of the antipodes (0.9 mg in 250 mg of KBr).

Chart 3

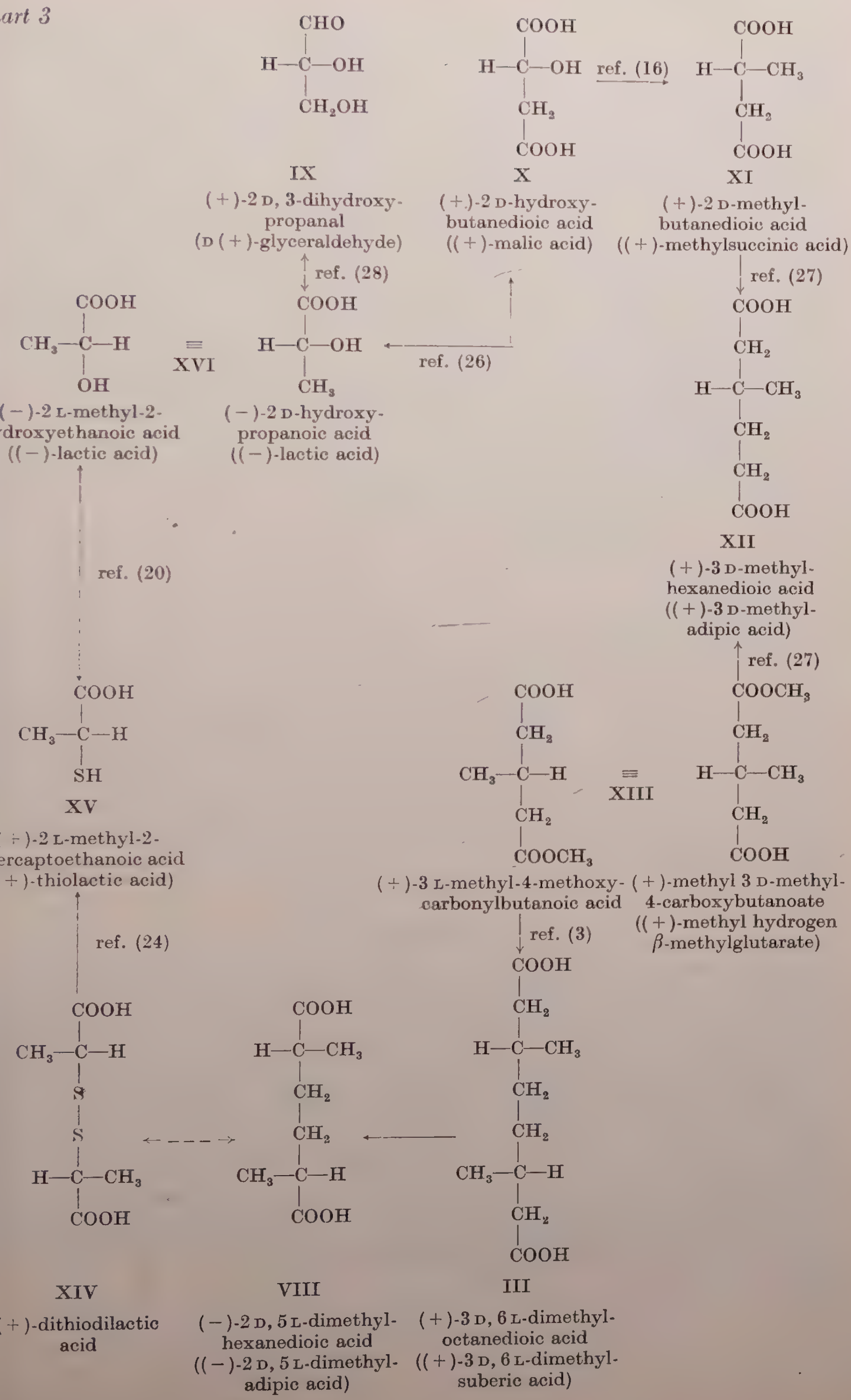

IX
(+)-2 D, 3-dihydroxypropanal
(D (+)-glyceraldehyde)

X
(+)-2 D-hydroxybutanedioic acid
((+)-malic acid)

XI
(+)-2 D-methylbutanedioic acid
((+)-methylsuccinic acid)

(−)-2 L-methyl-2-hydroxyethanoic acid
((−)-lactic acid)

XVI
(−)-2 D-hydroxypropanoic acid
((−)-lactic acid)

XII
(+)-3 D-methylhexanedioic acid
((+)-3 D-methyladipic acid)

(+)-3 L-methyl-4-methoxycarbonylbutanoic acid

XIII
(+)-methyl 3 D-methyl-4-carboxybutanoate
((+)-methyl hydrogen β-methylglutarate)

XV
(+)-2 L-methyl-2-mercaptoethanoic acid
((+)-thiolactic acid)

XIV
(+)-dithiodilactic acid

VIII
(−)-2 D, 5 L-dimethylhexanedioic acid
((−)-2 D, 5 L-dimethyladipic acid)

III
(+)-3 D, 6 L-dimethyloctanedioic acid
((+)-3 D, 6 L-dimethylsuberic acid)

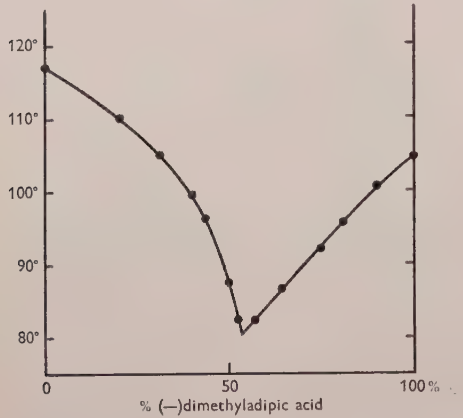

Fig. 2. (+)-Dithiodilactic acid and (−)-2D, 5L-dimethyladipic acid.

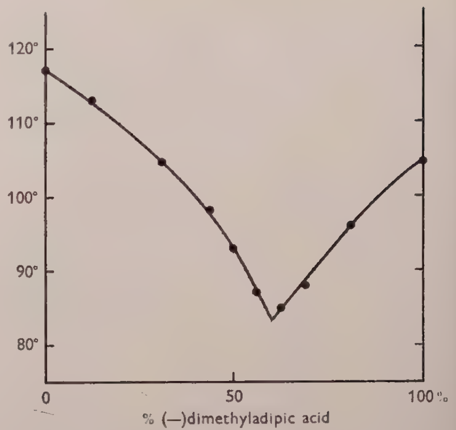

Fig. 3. (−)-Dithiodilactic acid and (−)-2D, 5L-dimethyladipic acid.

other curve. Fredga has found this to be the case on several occasions when the acids forming the system have opposite configurations (23). From this it may be concluded that the methyl groups in the dextrorotatory form of dithiodilactic acid have the positions shown in the Fischer projection formula (XIV) of Chart 3.

The configuration of (+)-3,6-dimethylsuberic acid (III) relative to D(+)-glyceraldehyde (IX) is known via (+)-malic acid (X), (+)-3D-methyladipic acid (XII) and (+)-methyl hydrogen β-methylglutarate (XIII). The corresponding Fischer projection formulae are shown in Chart 3. The present work gives the relative configuration of (−)-2,5-dimethyladipic acid (VIII). On the other hand Fredga has found that (−)-lactic acid (XVI) has the same configuration as (+)-thiolactic acid (XV) (20), which latter has been synthesized by Lovén ((24); see also Bernton, (25)) by cleavage of (+)-dithiodilactic acid. This acid thus has the configuration shown in formula (XIV) of Chart 3, viz. that of (+)-2L, 5D-dimethyladipic acid. The result tallies with the conclusion drawn above from the appearance of the melting-point diagrams.

Experimental[1, 2, 3]

(+)-2D, 5L-Dimethyl-1, 6-dibromohexane

(+)-3D, 6L-Dimethylsuberic acid (14.4 g, 0.07 mole, $[\alpha]_D^{23.5} = +16.9°$ (chloroform; *c*, 16.9; *l*, 1) was dissolved in 96 % ethanol (300 ml) and the warm solution poured

---

[1] The melting-points recorded in this paper were taken in capillary tubes (carefully cleaned and dried before use) using calibrated Anschütz thermometers completely immersed in a well-stirred bath of liquid paraffin. A low rate of heating (about 1 degree per minute) was used near the melting-point.

[2] The optical rotations were measured in a Schmidt & Haensch polarimeter of the triple-field Lippich type.

[3] The infra-red absorption curves were recorded on a double-beam spectrophotometer of the type described by Hornig, Hyde, and Adcock (29), built by Dr. Marcus Skogh of this Institute, the potassium bromide technique introduced by Stimson and O'Donnell (30) and Schiedt and Reinwein (31) being used. Disks of pure potassium bromide were placed in the reference beam.

into a warm solution of potassium hydroxide (9.5 g) in ethanol (300 ml). The hot clear solution was poured into a hot solution of silver nitrate (24.6 g) in ethanol (450 ml) under strong mechanical stirring. The reaction was carried out in subdued light. The reaction-mixture was allowed to stand overnight at room temperature in a dark place. The slightly brownish precipitate was filtered off by suction on a sintered glass funnel, removed from the filter, and washed in succession with hot water, 99,5 % ethanol, dry ether, and carbon tetrachloride (dried over phosphorus pentoxide). After drying overnight at a temperature of 50° the silver salt was pulverized in a mortar and further dried *in vacuo* at 100° for 48 hours. The yield of dry silver salt was 28.0 g, i.e. 94 % of the theoretical.

The finely-divided salt was suspended in dry carbon tetrachloride (125 ml), and dry bromine added drop by drop until the bromine colour persisted. The mixture was then refluxed for 30 minutes and allowed to cool. The silver bromide was filtered off and washed on the filter with warm carbon tetrachloride (100 ml). Ether was added to the filtrate, the solution washed with sodium carbonate solution and water, and the ether layer dried over sodium sulphate. The solvent was removed *in vacuo* at room temperature. There was a slight tendency to decomposition and formation of hydrogen bromide. The bromide was then distilled *in vacuo*. The distillation was difficult owing to formation of HBr. A considerable amount of a dark, viscous residue was left in the flask. The total yield of 6.7 g of the colourless distillate boiling at about 110°, 0.3 mm ($n_D^{22} = 1.499$) was 37 % of the theoretical.

(+)-2D, 5L-Dimethyl-1, 6-diacetoxyhexane

The bromide (6.7 g, 0.025 mole) was refluxed for 4 days with a solution of potassium acetate (35 g) in glacial acetic acid (70 ml) and butyl acetate (30 ml). Water was added, and the solution extracted with ether. The ether layer was washed with sodium carbonate solution and dried (sodium sulphate), the ether evaporated, and the residue distilled *in vacuo*. The yield of diacetate boiling at 93–95°, 0.5 mm, with $n_D^{22.5} = 1.4347$ and $d_4^{24} = 0.982$ was 3.09 g, i.e. 55 % of the theoretical.

Optical rotation: $\alpha_D^{24} = +0.96°$ (homogeneous; *l*, 0.2)
$[\alpha]_D^{24} = +4.89°$
$[M]_D^{24} = +11.3°$

Anal.:	Calcd. for $C_{12}H_{22}O_4$ (230.3)	C, 62.58; H, 9.63 %
	Found	C, 62.40; H, 9.42 %

(+)-2D, 5L-Dimethyl-1, 6-dihydroxyhexane

The diacetate (0.013 mole) just described was hydrolysed overnight with potassium hydroxide (6 g), 96 % ethanol (100 ml), and water (10 ml). The ethanol was evaporated, water added, and the solution extracted with ether in an apparatus for continuous extraction. The ether solution was dried (sodium sulphate) and the ether removed. The residue gave after distillation 1.48 g of dextrorotatory glycol, b.p. 148–150°, 17 mm, $n_D^{21} = 1.4582$, $d_4^{23} = 0.969$. The yield was 75 % of the theoretical.

Optical rotation: $\alpha_D^{23} = +4.31°$ (homogeneous: *l*, 0.2)
$[\alpha]_D^{23} = +22.2°$
$[M]_D^{23} = +32.5°$

Anal.:	Calcd. for $C_8H_{18}O_2$ (146.2)	C, 65.71, H, 12.41 %
	Found	C, 65.75, H, 12.33 %

(−)-2D,5L-Dimethyladipic acid

The glycol (1.0 g, 0.0068 mole) described above was dissolved in acetone (400 ml; the acetone was refluxed with potassium permanganate and distilled) containing 4 g of finely-divided potassium permanganate. The solution was kept at room temperature for 6 days. After acidification with sulphuric acid, perhydrol was added to remove excess permanganate and manganese dioxide. Some acetone was evaporated, a little water added, and the solution extracted with ether in an apparatus for continuous extraction. After drying the ether layer with sodium sulphate, the ether was removed. The residue, 2.7 g, was liquid. In order to remove water present benzene was added and distilled off again *in vacuo*. The still viscous residue weighing 1.5 g was further dried *in vacuo* over phosphorus pentoxide. It showed but a slight tendency to crystallize. Crystallization from ether - light petroleum was tried without success. Crystallization from water (see Noyes and Kyriakides (1)) was therefore attempted. The material did only partly dissolve in water. The clear aqueous solution was kept at room temperature for some days and the crystalline material formed filtered off. After drying, the crystals had m.p. 96–101° and showed an optical rotation of $[\alpha]_D^{24.5} = -27.8°$ (water; *c*, 4.8). After two crystallizations from water the m.p. was 103.6–104.0°. One further recrystallization finally gave 56 mg of (−)-2D,5L-dimethyladipic acid of m.p. 103.5–103.8°.

Optical rotation: $\alpha_D^{24} = -0.70° \pm 0.02°$ (99.5 % ethanol; *l*, 1; *c*, 2.27)
$[\alpha]_D^{24} = -30.8° \pm 0.9°$
$[M]_D^{24} = -54°$

Anal.: Calcd. for $C_8H_{14}O_4$ (174.2) C, 55.16, H, 8.10 %
Found C, 55.45, H, 8.08 %

(−)-2L,5D-Dimethyl-1,6-dihydroxyhexane

The silver salt of (−)-3L,6D-dimethylsuberic acid was prepared in the same manner as described for the antipode. The yield was nearly quantitative. Several bromination experiments were performed using the same procedure as for the antipode. Owing to decomposition and formation of HBr the yield of distilled bromide with $n_D^{21} = 1.499$ was only of the order of 10 % of the theoretical. The optical rotation was $\alpha_D^{23} = -0.30°$ (homogeneous; *l*, 0.2). Analysis gave Br, 56.65 %. Calculated for $C_8H_{16}Br_2$ (272.0) Br, 58.76 %. A higher-boiling fraction with $n_D^{22} = 1.479$ had an optical rotation of $\alpha_D^{23} = -4.18°$ (homogeneous; *l*, 0.5), and the bromine content was 33.45 %. This fraction evidently corresponds to 7-bromo-3L,6D-dimethylheptanoic acid. Calculated for $C_9H_{17}O_2$ Br (237.1): Br, 33.70 %. Considerable amounts of a dark undistillable material was left in the flask. Owing to the losses involved in the distillations, crude bromide was used for the preparation of the glycol. The crude bromide obtained from 30.5 g of silver salt was converted into the diacetate in the manner already described. The yield of product boiling at 81–84°, 0.1 mm, was 7.3 g, i.e. 43 % of the theoretical calculated from the (−)-3L,6D-dimethylsuberic acid. The optical rotation and the refractive index of the material, $\alpha_D^{20} = -3.98°$ (homogeneous; *l*, 1) and $n_D^{23.5} = 1.438$ respectively, indicated that it was not quite pure. No further attempts of purification were made at this stage. The diacetate was hydrolysed and extracted with ether in an apparatus for continuous extraction, the ether layer dried with sodium sulphate, and the ether removed. The following fractions were taken in the distillation of the residue.

Fraction 1. –104°, 0.5 mm; 0.02 g; $n_D^{26} = 1.4578$
2. 104–108.5°, 0.5; 0.17 ; $n_D^{26} = 1.4690$
3. 108.5–109°, 0.5; 1.19 ; $n_D^{26} = 1.4582$
4. 109–109.5°, 0.5; 1.11 ; $n_D^{26} = 1.4574$
5. 109.5–112°, 0.5–0.6; 0.85 ; $n_D^{26} = 1.4578$
6. 112°, 0.6; 0.14 ; $n_D^{26} = 1.4573$

The density of the combined fractions 4 and 5 was $d_4^{21} = 0.971$. Fraction 4 had an optical rotation of

$\alpha_D^{21} = -4.35°$ (homogeneous; l, 0.2)
$[\alpha]_D^{21} = -22.4°$
$[M]_D^{21} = -32.7°$

(+)-2L, 5D-Dimethyladipic acid

3.2 g (0.022 mole) of the combined fractions 3, 4, 5, and 6 were submitted to oxidation with the theoretical amount of potassium permanganate (7.8 g, finely powdered) in acetone (500 ml). After 3 days at room temperature most of the permanganate colour had disappeared. The material was worked up in the same manner as in the case for the antipode. Four crystallizations from water yielded 39 mg of (+)-2L, 5D-dimethyladipic acid in the form of white crystals melting at 103.2–103.8°.

Optical rotation: $\alpha_D^{24.5} = +0.99° \pm 0.02°$ (99.5 per cent ethanol; l, 1; c, 3.24)
$[\alpha]_D^{24.5} = +30.6° \pm 0.6°$
$[M]_D^{24.5} = +53°$

The mother liquids from the crystallizations were combined. A part of the water was removed and the solution kept in a refrigerator. After about one week the solution had deposited a beautiful single crystal weighing 40 mg. A further amount, 51 mg, of the acid was obtained from the mother liquids.

Thermal analysis

The melting-point curves were determined according to Kofler (32) using a "Heiztisch-Mikroskop RCH" from Optische Werke Reichert. The thermometer was calibrated against known compounds in the usual manner.

The binary mixtures of different composition were prepared as follows. About 10 mg of the enantiomorphs was weighed out on a microbalance, and each sample dissolved in about 0.5 ml of methyl ethyl ketone delivered from an "Agla" micrometer syringe. Methyl ethyl ketone was preferred to lower-boiling solvents such as acetone or ether in order to reduce errors due to evaporation of the solvent. Suitable volumes of the two solutions were pipetted out by means of the syringe, and mixed in small test tubes. The solvent was allowed to evaporate at room temperature. The residue was dissolved in a small amount of ether, and small drops allowed to evaporate on glass plates. The residue was carefully pulverized, and the beginning and the end of the melting determined in the Kofler microscope. The rate of heating was 1–2 degrees per minute. It has been pointed out by Matell (33) that the rate of heating (4 degrees per minute) used by Kofler and Kofler is rather too high.

Summary

(+)-2L,5D- and (−)-2D,5L-dimethyladipic acids have been synthesized by *bis*-degradation of the enantiomorphs of 3,6-dimethylsuberic acid.

The steric configuration of the 3,6-dimethylsuberic acids in relation to glyceraldehyde is known, and the configuration of the 2,5-dimethyladipic acids follows from the synthesis, which involves no rearrangement of the optically active centres.

The melting-point diagrams of the binary systems of (+)-dithiodilactic and (−)-2D,5L-dimethyladipic acids, and of (−) dithiodilactic and (−)-2D,5L-dimethyladipic acids, were determined. The diagrams give no evidence for the existence of a quasiracemic compound in any of the two systems.

ACKNOWLEDGEMENTS

The author is indebted to Professor Arne Fredga, Institute of Chemistry, University of Uppsala, for suggesting the present work, and for valuable discussions. The author is also indebted to Dr. Ingrid Fischmeister for the infra-red spectrograms, to Dr. Carl Lagercrantz for the loan of a Kofler hot-stage microscope, and to Mr. L. Ahlquist for technical advice. The analyses were carried out in the microanalytical laboratory of this Institute by Mr. L. Pettersson.

Department of Medical Biochemistry, Institute of Medical Chemistry, Uppsala, Sweden.

REFERENCES

1. Noyes, W. A. and Kyriakides, L. P., J. Amer. Chem. Soc. *32*, 1057 (1910).
2. Brewster, J. H., Ibid. *73*, 366 (1951).
3. Ställberg-Stenhagen, S., Arkiv för kemi *2*, 95 (1950).
4. —— Ibid. *2*, 431 (1950).
5. —— Ibid. *3*, 249 (1951).
6. —— Arkiv Kemi, Min. o. Geol. *26 A*, nr. 1 (1948).
7. —— Ibid. *23 A*, nr. 15 (1946).
8. —— Arkiv för kemi *1*, 153 (1949).
9. —— Ibid. *1*, 187 (1949).
10. Serck-Hanssen, K., Ställberg-Stenhagen, S., and Stenhagen, E., Ibid. *5*, 203 (1953).
11. Klyne, W., Chem. & Ind. 1022 (1951).
12. Hunsdiecker, H. and Hunsdiecker, Cl., Ber. *75*, 291 (1942).
13. Meyer, R., Ann. *219*, 234 (1883).
14. Ställberg-Stenhagen, S., Arkiv för kemi *3*, 267 (1951).
15. Hancock, J. E. H. and Linstead, R. P., J. Chem. Soc. *1953*, 3490.
16. Fredga, A., "The Svedberg 1884 30/8 1944", Uppsala 1944, p. 261.
17. Zelinsky, N., Ber. *24*, 3999 (1891).
18. Stenhagen, E., Acta Chem. Scand. *5*, 805 (1951).
19. Fredga, A., Arkiv Kemi, Min. o. Geol. *14 B*, nr 15 (1940).
20. —— Ibid. *14 B*, nr. 12 (1940).
21. —— Ibid. *15 B*, nr. 23 (1942).
22. Affleck, J. G. and Dougherty, G., J. Org. Chem. 15 (1950).
23. Fredga, A., Personal communication.
24. Lovén, J. M., J. pr. Ch. (2) *78*, 63 (1908).
25. Bernton, A., Dissertation, Uppsala (printed in Lund), 1932.
26. Freudenberg, K., Ber. *55*, 2027 (1914).
27. Ställberg-Stenhagen, S., Arkiv Kemi, Min. o. Geol. *25 A*, nr. 10 (1948).
28. Wolfrom, M. L., Lemieux, R. U., Olin, S. M., and Weisblat, D. J., J. Amer. Chem. Soc. *71*, 4057 (1949).
29. Hornig, D. F., Hyde, G. E., and Adcock, W. A., J. Opt. Soc. Amer. *40*, 497 (1950).
30. Stimson, M. M. and O'Donnell, M. J., J. Amer. Chem. Soc. *74*, 1805 (1952).
31. Schiedt, U. and Reinwein, H., Z. Naturforsch. *76*, 270 (1952).
32. Kofler, L., and Kofler, A., Mikro-Methoden, Innsbruck 1948.
33. Matell, M., Kungl. lantbrukshögskolans annaler *20*, 215 (1953).

Tryckt den 26 april 1955

Uppsala 1955. Almqvist & Wiksells Boktryckeri AB

ARKIV FÖR KEMI Band 8 nr 13

Communicated 13 October 1954 by ARNE WESTGREN and GUNNAR HÄGG

Studies on the extraction of metal complexes. XII-A

The formation of composite, mononuclear complexes. Part A: Theoretical

By JAN RYDBERG

With 3 figures in the text

Many variables are involved in the extraction of a metal from an aqueous solvent by means of an organic solvent. These variables are: the concentrations of the metal itself and of other cations in the solution, the concentrations of the different anions present, the organic solvent used, the temperature, etc. In many cases the distribution of the metal between the phases depends on these variables in a very complicated way.

Because the extraction of metals by organic solvents has become of great interest both in analytical and preparative chemistry, the conditions for such extractions have been much investigated in recent years [e.g. 1, 2]. Usually one variable has been studied at a time, and a reasonable explanation of the results has often been presented. The general picture of the more simple cases is that the metal ion M^{N+} reacts with the ligand A^- in the aqueous phase giving the complex MA_N, which is distributed between the two phases [e.g. 3, p. 451 ff.]. In some of these cases it has been possible to calculate formation constants for all of the complexes between the metal and the ligand (MA^{N-1}, MA_2^{N-2}, ..., MA_N, MA_{N+1}^{-1}, ...) [e.g. 4, 5]. Investigations of the influence of competing ligands, which may be denoted by B^-, on the distribution of M in the presence of A^- have made possible the calculation of the formation constants for the complexes MB_n^{N-n} (e.g. 6, 7). The number of solvent molecules bound to the metal complex has been studied in great detail for systems containing uranyl nitrate [e.g. 8, 9, 10].

Most comparisons of the distribution of a metal between water and different organic solvents have been made only in the presence of inorganic ligands like NO_3^- and Cl^- in aqueous solutions of high ionic strength [e.g. 11, 12]. The results have then usually been too complicated to encourage any theoretical analysis of the experimental data.

Analyses of solid samples have indicated the existence of very complicated compounds, containing—apart from the metal M—the radicals A and OH, and the uncharged molecules HA, H_2O and Org, where Org stands for the organic solvent molecule. Examples of this type of compounds are $Th(OH)_2CrO_4H_2O$ [13], UO_2Ox_2HOx (HOx = oxine) [14] and $Ni(CN)_2NH_3C_6H_6$ [15]. Compounds of the general type $M_mA_n(OH)_p(HA)_rOrg_s(H_2O)_t$ may therefore be formed, even if not all of the subscripts are greater than zero at the same time. Such complexes will in the following be called composite complexes, when they appear in solution, as distinguished from simple complexes with only one kind of ligand.

One may question if composite complexes necessarily exist in solution, even if they are found in solid samples. For example it has been shown that C_6H_6 in the $Ni(CN)_2NH_3C_6H_6$ compound, though it seems to be strongly bound, is only trapped in a cavity between sheets of $Ni(CN)_2NH_3$ molecules and bound to these molecules by weak van der Waals' forces. Thus no or only a few molecules of the type $Ni(CN)_2NH_3C_6H_6$ exist in solution. Evidence has also been given showing that a similar state of affairs exists for HOx in $ScOx_3HOx$ [16]. These phenomena with trapped molecules in solid samples are not unique. Definite conslusions about the composition of molecules in solution can therefore not be drawn only from analyses of solid samples. The definite proof of the structure of the dissolved molecule has to come from a direct investigation on the solution.

As far as is known to the present author no studies on the formation of composite complexes in solution have been made by means of extraction methods in which all variables concerned in the formation of the hypothetical complex $M_mA_n(OH)_p$ $(HA)_r(H_2O)_tOrg_s$ are considered. In the first part (XII-A) of this paper, a method is suggested for the determination of the composition of composite complexes and the calculation of their formation constants. In the second part (XII-B) of this paper (this journal, p. 113) the equations developed in the first part are used for the investigation of the Th- and U(VI)-acetylacetone-organic solvent-H_2O-systems.

1. The general distribution equation

It has been shown in a previous paper of this series [4] that the distribution ratio q of thorium between benzene and water in the presence of acetylacetone, here abbreviated to HAa, can be explained by the equation

$$q=\frac{\varkappa_4\cdot\lambda_4\cdot[\mathrm{Aa}^-]^4}{\sum\limits_{n=0}^{s}\varkappa_n\cdot[\mathrm{Aa}^-]^n}$$

where $\varkappa_n$ is the complexity product according to

$$\varkappa_n=[\mathrm{Th\,Aa}_n^{4-n}]\,[\mathrm{Th}^{+4}]^{-1}\,[\mathrm{Aa}^-]^{-n},$$

and λ_4 is the distribution constant of the unchanged complex, $ThAa_4$, between the two phases according to

$$\lambda_4=[\mathrm{ThAa}_4]_{\mathrm{org}}/[\mathrm{ThAa}_4]_{\mathrm{aq}}.$$

In the sum above, S is the maximum number of acetylacetonate groups which can be bound to each thorium atom.

Here and in the following, brackets mean concentration, the index "org" refers to the organic phase, and "aq" or no index refers to the aqueous phase.

For another combination of M and HA, more complicated complexes may be formed. Omitting the charges of the ions, these complexes can be written in the general form

$$M_mA_n(OH)_p(HA)_r(Org)_s(H_2O)_t.$$
(I)

The formation constant of this complex is defined by eq. (1):

$$\varkappa_{m,n,p,r,s,t} = \frac{[M_mA_n(OH)_p(HA)_r(Org)_s(H_2O)_t]}{[M]^m[A]^n[OH]^p[HA]^r[Org]^s[H_2O]^t}. \tag{1}$$

All variables in this equation are not independent of each other since we have the relations

$$[HA] \cdot k_a = [H][A], \tag{2}$$

$$[H_2O] \cdot k'_w = [H][OH]. \tag{3}$$

Using these equations one finds that

$$\begin{aligned}&[M]^m[A]^n[OH]^p[HA]^r[Org]^s[H_2O]^t \\ &\qquad = [M]^m[HA]^{n+r}[H]^{-n-p}[H_2O]^{p+t}[Org]^s \cdot k_a^n \cdot k'^p_w.\end{aligned} \tag{4}$$

If we introduce the quantities x, y and z, defined by

$$n+r=x \tag{5}$$

$$n+p=y \tag{6}$$

$$p+t=z \tag{7}$$

in the above relation, the formula of the composite complex will be

$$M_m(HA)_x(H)_{-y}(H_2O)_z(Org)_s.$$
(II)

It follows from eq. (4) that it will not be possible to distinguish between isomeric complexes. E.g. the complexes $MA_2(HA)(H_2O)(Org)$ and $MA(OH)(HA)_2(Org)$ of type I are both included in the complex $M(HA)_3(H)_{-2}(H_2O)(Org)$ of type II.

It is usually very difficult to determine the number of H_2O-molecules in a complex in aqueous solution, though this has been possible to do in some special cases [e.g. 17]. If the experiments are carried out at constant ionic strength, which means that H_2O is practically constant, the effect of the hydration may be included in the complexity constants, without need for special attention.

If the coordination number of the metal with respect to all ligands in the complex is known, the number z of H_2O molecules in the complex may be calculated from the difference between this coordination number and the number of coordinative positions around the metal in the complex occupied by ligands other than H_2O.

To begin with, we shall only concern ourselves with complexes of the type

$$M_m(HA)_x(H)_{-y}(Org)_s.$$

(III)

The new composite complexity product will be defined by

$$K_{m,\,x,\,y,\,s} = \frac{[M_m(HA)_x(H)_{-y}\,(Org)_s]}{[M]^m[HA]^x[H]^{-y}[Org]^s}. \tag{8}$$

The relation between K and $\varkappa$ will be

$$\varkappa_{m,\,n,\,p,\,r,\,s,\,t} \cdot k_a^n\, k_w^p = K_{m,\,x,\,y,\,z,\,s}. \tag{9}$$

According to equations (5) and (6), x means the total number of HA and A molecules and y the total number of A and OH molecules in the complex per metal atom.

The charge of a complex is $mN - y$; thus for an uncharged complex one must have $mN = y$. In the following *we shall assume that only uncharged species of M are dissolved in the organic solvent*—this will be true for most organic solvents and especially for those of low dipole moment. The general formula of the composite complex in the organic solvent will then be $M_m(HA)_x(H)_{-mN}(Org)_s$. The distribution of the metal between an organic and an aqueous phase should then follow

$$q = \frac{\sum\limits_{1}^{m}\sum\limits_{0}^{x}\sum\limits_{0}^{s} m \cdot K_{m,\,x,\,mN,\,s}\,\Lambda_{m,\,x,\,mN,\,s}\,[M]^m[HA]^x[H]^{-mN}[Org]^s}{\sum\limits_{1}^{m}\sum\limits_{0}^{x}\sum\limits_{0}^{y}\sum\limits_{0}^{s} m \cdot K_{m,\,x,\,y,\,s}[M]^m[HA]^x[H]^{-y}[Org]^s}. \tag{10}$$

$\Lambda_{m,\,x,\,mN,\,s}$ is the distribution constant of the complex $M_m(HA)_x(H)_{-mN}(Org)_s$ between the organic solvent and water.

To simplify the following discussion, *only mononuclear complexes will be considered*, i.e. $m = 1$. This will probably hold for most metal complexes at concentrations of the order of 10^{-3} moles/l or less, except when the metal is largely hydrolysed. If polynuclear complexes of M are formed, q will show a dependence on the metal concentration. The following equations are therefore valid only when q is found to be a function of [HA] and [H], but independent of $[M]_{tot}$.

2. The influence of organic solvents on the distribution curve

To obtain the constants including s in eq. (10), one may vary [Org] by the addition of a suitable third solvent. However, though this solvent may not react chemically with any part of the general composite complex, the activity coefficients in the system often vary to such an extent, that relatively little useful new information about the system will be obtained.

Let us instead consider the distribution ratios obtained for a certain metal M in two different solvent systems. The distribution ratio of M between the organic solvent Org′ and water is q', and that between Org″ and water q''. The complexity and distribution constants for $m = 1$ will be K'_{xys}, K''_{xys}, Λ'_{xNs} and Λ''_{yNs} respectively.

If the two distribution curves are compared *at the same* $[H]$ *and* $[HA]$ *in the aqueous phase*, the ratio between the two distribution factors q' and q'' will become

$$\frac{q'}{q''}=\frac{\sum\limits^{x}\sum\limits^{s} K'_{xNs}\cdot\Lambda'_{xNs}[\mathrm{HA}]^{x}[\mathrm{H}]^{-N}[\mathrm{Org}']^{s}\sum\limits^{x}\sum\limits^{y}\sum\limits^{s} K''_{xys}[\mathrm{HA}]^{x}[\mathrm{H}]^{-y}[\mathrm{Org}'']^{s}}{\sum\limits^{x}\sum\limits^{s} K''_{xNs}\cdot\Lambda''_{xNs}[\mathrm{HA}]^{x}[\mathrm{H}]^{-N}[\mathrm{Org}'']^{s}\sum\limits^{x}\sum\limits^{y}\sum\limits^{s} K'_{xys}[\mathrm{HA}]^{x}[\mathrm{H}]^{-y}[\mathrm{Org}']^{s}}. \tag{11}$$

In equilibrium experiments the aqueous phase will be saturated with the organic solvent, and vice versa. Since the solubility of the organic solvent in water is practically constant at constant ionic strength, *[Org′] and [Org″] will be constant.* In the following discussion, [Org′] and [Org″] can therefore be included in the K-values, where we thus put

$$K'_{xy}=\sum^{s} K'_{xys}[\mathrm{Org}']^{s}, \tag{12}$$

and use similar equations for K''_{xy}, $K'_{xN}\ \Lambda'_{xN}$ and $K''_{xN}\ \Lambda''_{xN}$.

This reduces eq. (11) to

$$\frac{q'}{q''}=\frac{\sum\limits^{x} K'_{xN}\Lambda'_{xN}[\mathrm{HA}]^{x}[\mathrm{H}]^{-N}\cdot\sum\limits^{x}\sum\limits^{y} K''_{xy}[\mathrm{HA}]^{x}[\mathrm{H}]^{-y}}{\sum\limits^{x} K''_{xN}\Lambda''_{xN}[\mathrm{HA}]^{x}[\mathrm{H}]^{-N}\cdot\sum\limits^{x}\sum\limits^{y} K'_{xy}[\mathrm{HA}]^{x}[\mathrm{H}]^{-y}}. \tag{13}$$

If complexes between the metal and the organic solvents Org′ and Org″ are formed, K'_{xy} must—except for a rare coincidence—be different from K''_{xy} (compare eq. 12). Further on, Λ'_{xN} will generally be different from Λ''_{xN}. The ratio q'/q'' will therefore be found to vary with [H] at constant [HA], or with [HA] at constant [H], if complexes are formed between the metal and one or both of the two organic solvents.

If no complex is formed between the metal and the organic solvent, s is equal to zero. Since the metal then only forms complexes with HA, A and OH, the complexity constants must be the same in the aqueous phases, i.e.

$$K'_{xy}=K''_{xy}. \tag{14}$$

If this condition is introduced in eq. (13), one obtains

$$\frac{q'}{q''}=\frac{\sum\limits^{x} K_{xN}\cdot\Lambda'_{xN}[\mathrm{HA}]^{x}}{\sum\limits^{x} K_{xN}\cdot\Lambda''_{xN}[\mathrm{HA}]^{x}}. \tag{15}$$

In this case the ratio q'/q'' is only a function of [HA] and independent of [H]. Experimentally this may be tested by plotting log q' and log q'' against log [H] at the same and constant [HA] in the aqueous phases. If log $\frac{q'}{q''}$ is found to be constant, this can then be taken as a proof that practically no complexes are formed between species containing M and the molecules Org′ or Org″.

In the special case when *one uncharged species with M dominates over all others in the organic solvents*, x has a single value. If we call this a, eq. (15) reduces to

$$\frac{q'}{q''}=\frac{\Lambda'_{aN}}{\Lambda''_{aN}}. \tag{16}$$

The ratio is then independent of both [H] and [HA] and the curves for log q' and log q'' will become parallel on plots either as a function of [H] at constant [HA], or as a function of [HA] at constant [H]. When this is found experimentally it may be taken as a proof that a complex of the formula $M(HA)_a(H)_{-N}$ dominates in both solvent combinations. This formula includes as usual a series of isomers of composition $MA_n(HA)_{a-n}(OH)_{N-n}$, where n can have any value between 0 and a or N.

3. Calculation of the composite complexity products K_{xy}

It will be assumed in this section that *only mononuclear complexes not containing organic solvent molecules* are formed, i.e. $m=1$ and $s=0$. It is always possible to test if this is the case (see previous sections) and if the following equations can thus be applied. The distribution of the metal between the two phases will then follow

$$q=\frac{\sum^{x} K_{x,N}\Lambda_{x,N}[HA]^{x}[H]^{-N}}{\sum^{x}\sum^{y} K_{x,y}[HA]^{x}[H]^{-y}}. \tag{17}$$

The distribution of the metal between the phases may vary with [H] and [HA] in several ways, depending on what types of complexes are formed, and several special cases may be distinguished. These cases will be treated in turn below. In favorable cases it should be possible to get at least approximate values for all constants in eq. (17).

Those who may not be familiar with "distribution curves" of the type $q=f([H])$ and $q=f([HA][H]^{-1})$, will in Figs. 1, 2 and 3 find some examples of distribution curves with the main features: a straight line with constant slope, which turns over into a horizontal line (plateau), where q is independent of [H] or $[HA][H]^{-1}$. In some cases the distribution curves will show, instead of a plateau, only a maximum and then decrease again, as is shown by the dotted lines in Fig. 1.

3 a. $q=f([HA][H]^{-1})$; complexes of type MA_n

It may be found that q varies both with [H] and [HA], but in such a way that it is constant for constant $[HA][H]^{-1}$ over the whole [H] and [HA] region investigated. This behavior is illustrated in Fig. 1. In Figure 1 a, log q is plotted against log $[HA][H]^{-1}$ or pA for different HA concentrations ($[HA'] > [HA''] > [HA''']$; log $[HA][H]^{-1} = pk_a - p$A. If q shall be a function of $[HA][H]^{-1}$ only, x must be equal to y or N, according to eq. (17), which then can be written

$$q=\frac{K_{NN}\Lambda_{NN}[HA]^{N}[H]^{-N}}{\sum^{x} K_{xx}[HA]^{x}[H]^{-x}}. \tag{18}$$

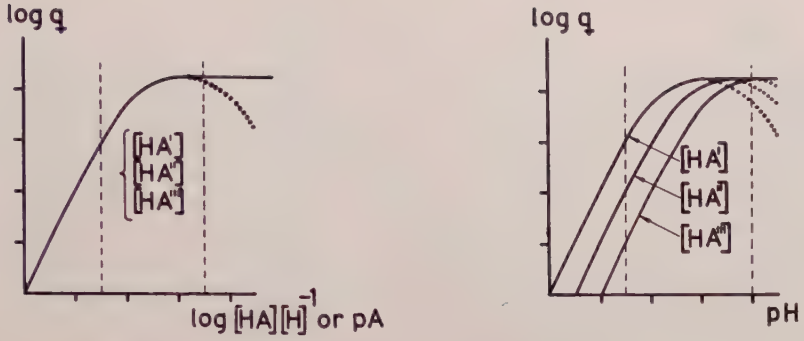

Fig. 1 a

Fig. 1 b

Fig. 1. The distribution q of a metal M between two phases as a function of (a) log $[\mathrm{HA}][\mathrm{H}]^{-1}$, ($b$) pH at different HA concentrations ($[\mathrm{HA}'] > [\mathrm{HA}''] > [\mathrm{HA}''']$), when positively (the dotted part for negatively) charged and uncharged MA_n-complexes are formed.

If we assume that when an HA and an OH group come together in the same complex, they immediately react to give A and H_2O, we can put $r = p = 0$ $(pH \ll pk_a)$. According to previous equations, eq. (18) can then be written

$$q = \frac{\varkappa_N \lambda_N [\mathrm{A}]^N}{\sum^{n} \varkappa_n [\mathrm{A}]^n}, \tag{19}$$

which is valid for the complex MA_n. It has been experimentally shown in several cases [4, 5] that the distribution of M between different solvents can be explained by this equation.

In Fig. 1 the left parts of the curves have a constant slope. It follows from eq. (18) that this is only possible if x is constant. The most common case is where $x = 0$, and the slope of the curve will then be equal to N, the charge of the uncomplexed metal ion. This is the maximum slope of the curve.

In the range where q is independent of $[\mathrm{HA}][\mathrm{H}]^{-1}$, it follows from eq. (18) that $x = N$. In this range the complex $\mathrm{M(HA)}_N\mathrm{(H)}_{-N}$ obviously dominates in both phases and q becomes equal to Λ_{NN}, the distribution constant of the uncharged complex. This range is demonstrated to the right of the second dashed vertical line in Figure 1 a.

When the distribution curve reaches a maximum, with or without exhibiting a plateau, and then decreases with increasing pH (the dotted parts in Fig. 1), it follows from eqs. (18) or (19) that the decrease can only be due to the fact that x or $n > N$, i.e. to the formation of negatively charged complexes. If a constant slope is found even on this side of the distribution curve, a stable negatively charged complex MA_S must exist. The slope of the line will then be $N - S$, which is also the charge of the complex MA_S.

There are many ways of evaluating the constants in an equation of the kind above [18]. The use of the "limit value method" of LEDEN [19] and "ligand number method" of BJERRUM [20] have been demonstrated for $n \leq N$ in a previous paper of this series [4]. They will therefore not be repeated here. Recently DYRSSEN and SILLÉN [21] have proposed a graphical two parameter method for calculating $\varkappa_n$ and λ_N from distribution curves. Their method is useful even if the curves do not exhibit

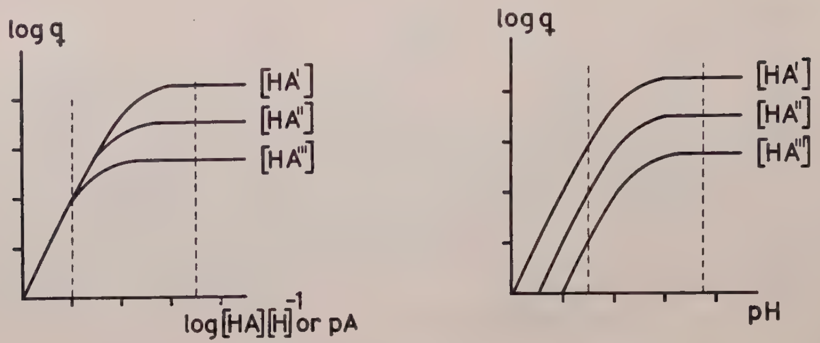

Fig. 2 a

Fig. 2 b

Fig. 2. The distribution q of a metal M between two phases as a function of (a) log [HA][H]$^{-1}$, (b) pH, at different HA concentrations ([HA′] > [HA″] > [HA‴]), when positively charged and uncharged $MA_n(OH)_p$-complexes are formed.

any plateau, but only a maximum, i.e. for the case where both positively and negatively charged complexes are formed in considerable amounts at the same time.

3 b. $q=f([HA][H]^{-1})$ at low pH, but not at high pH; complexes of type $MA_n(OH)_p$

Fig. 2 illustrates a case where $q=f([HA][H]^{-1})$ only in a pH-region where the metal hydrolysis is small. It has been concluded in the previous section that in this region $x=y$ and only complexes of type $M(HA)_x(H)_{-x}$ (or MA_n) should be formed. No additive compounds between MA_n and HA should then exist here, even at the highest HA concentration used, [HA′]. It is seen from equation (17) that the pH will not influence the formation of additive complexes with HA. It may therefore be concluded that such complexes can be neglected in the whole pH-region demonstrated in Fig. 2, i.e. we have $r=0$ in formula I. However, in the high pH-region, the hydrolysis of the metal is no longer depressed and deviations from the curve $q=f([HA][H]^{-1})$ may be found—in this pH-range $x \neq y$, and since $r=0$, p must differ from 0. Thus the type of complex formed should be $MA_n(OH)_p$, and one obtains

$$q=\frac{\sum\limits^{n}\varkappa_{n,\,N-n}\,\lambda_{n,\,N-n}\,[A]^n[OH]^{N-n}}{\sum\limits^{n}\sum\limits^{p}\varkappa_{np}\,[A]^n[OH]^p}. \tag{20}$$

According to this equation the complex $MA_n(OH)_{N-n}$ dominates both phases in the plateau region of Fig. 2, where [HA] = constant; n may have any value between 0 and N. However, the distribution constant of $M(OH)_N$, λ_{0N}, will in practically all cases be too low to be measured by the distribution method. If only $M(OH)_N$ was formed, q should be independent of [HA] and only vary with [H]. With ordinary organic solvents this case must be very rare and will not be further discussed here.

It has sometimes been found that it is difficult to decide from the experimental data if the case in Fig. 2 or that in Fig. 3 is valid. It is therefore advisable to

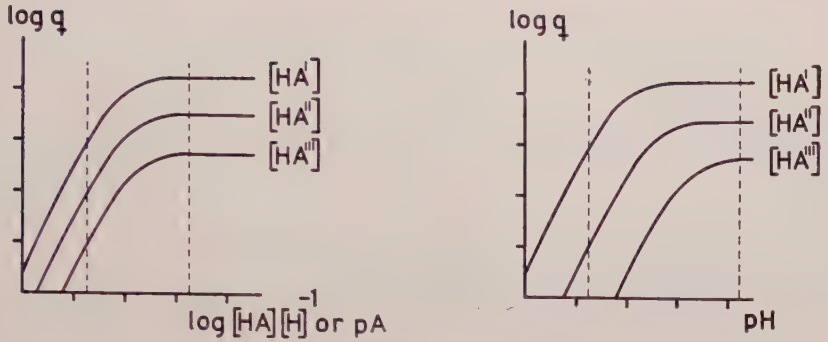

Fig. 3 a

Fig. 3 b

Fig. 3. The distribution q of a metal M between two phases as a function (a) of log $[HA][H]^{-1}$, (b) of pH, at different HA concentrations ($[HA'] > [HA''] > [HA''']$), when positively charged and uncharged $MA_n(OH)_p(HA)_r$-complexes are formed.

directly apply the equations for the general case, as soon as it has been established that not *only* complexes of the type MA_n are formed. The equations for the general case will be given in the next paragraph.

A and OH compete for the positions around M. An increase in [HA] without changing pH will increase [A] and therefore lessen the influence of the hydrolysis. In Fig. 2 the metal is least hydrolysed at the highest HA concentration, [HA']. If eq. (19) is found to be valid in a pH-region, where the hydrolysis of the metal is known to be considerable in the absence of HA, then the metal hydrolysis can probably be neglected up to pH $< pk_a$.

3 c. q varies with [HA] or [H] at constant $[HA] \cdot [H]^{-1}$; complexes of type $MA_n(OH)_p(HA)_r$

When it is found that q in no region is a function of $[HA][H]^{-1}$ alone, the conclusion may be drawn that complexes of the general type $MA_n(OH)_p(HA)_r$ are formed. Since it is not possible to distinguish by the distribution method between these complexes and $MA_{n+k}(OH)_{p-k}(HA)_{r-k}(H_2O)_k$, we shall only discuss the complex formula $M(HA)_x(H)_{-y}$, which includes all these isomers with varying k. In Fig. 3 the distribution curves are given for this general case.

For the calculation of the formation constants for this complex, we introduce a series of functions of [HA], f_λ and f_y, defined by

$$f_\lambda = \sum^{x} K_{xN} \Lambda_{xN} [HA]^x \tag{21}$$

and

$$f_y = \sum^{x} K_{xy} [HA]^x \tag{22}$$

in eq. (17), which can then be written

$$q = \frac{f_\lambda [H]^{-N}}{\sum^{y} f_y [H]^{-y}} = \frac{f_\lambda [H]^{-N}}{f_0 + f_1 [H]^{-1} + f_2 [H]^{-2} + f_3 [H]^{-3} + \cdots}. \tag{23}$$

To obtain f_y and f_λ we shall transform this eq. to

$$q^{-1}[\mathrm{H}]^{-N} = F_0 = f_0 \cdot f_\lambda^{-1} + f_1 f_\lambda^{-1} [\mathrm{H}]^{-1} + f_2 f_\lambda^{-1} [\mathrm{H}]^{-2} + \cdots, \tag{24}$$

which then is solved for $f_0 f_\lambda^{-1}$, $f_1 f_\lambda^{-1}$, etc. For each HA concentration a certain $f_y f_\lambda^{-1}$ value is obtained.

There are several methods of obtaining the coefficients of an equation like (24). Since the "limit method" of LEDEN [19] will exclusively be used in Part B of this paper, the different steps of this method will be indicated here for eq. (24).

For each curve in Fig. 3 b, i.e. for each HA concentration, a plot of F_0 against $[\mathrm{H}]^{-1}$ will yield a curve with a limiting value of $f_0 \cdot f_\lambda^{-1}$ and a limiting slope of $f_1 \cdot f_\lambda^{-1}$ when $[\mathrm{H}]^{-1}$ approaches zero:

$$\lim_{[\mathrm{H}]\to\infty} F_0 = f_0 \cdot f_\lambda^{-1} + (f_1 \cdot f_\lambda^{-1} [\mathrm{H}]^{-1} + \cdots). \tag{24 b}$$

With the $f_0 \cdot f_\lambda^{-1}$ value thus obtained, F_1 can be calculated according to eqs. (24 c) and (24 d).

$$F_1 = \frac{F_0 - f_0 \cdot f_\lambda^{-1}}{[\mathrm{H}]^{-1}} = f_1 f_\lambda^{-1} + f_2 f_\lambda^{-1} [\mathrm{H}]^{-1} + f_3 f_\lambda^{-1} [\mathrm{H}]^{-2} + \cdots \tag{24 c}$$

$$\lim_{[\mathrm{H}]\to\infty} F_1 = f_1 f_\lambda^{-1} + (f_2 f_\lambda [\mathrm{H}]^{-1} + \cdots). \tag{24 d}$$

From a plot of F_1 against $[\mathrm{H}]^{-1}$, $f_1 f_\lambda^{-1}$ and $f_2 f_\lambda^{-1}$ can be calculated from the intercept on the F_1-axis at $[\mathrm{H}]^{-1} = 0$ and the slope of the curve at this point. By successive formation of F_y-functions, all $f_y \cdot f_\lambda^{-1}$ values of the different HA concentrations can be obtained.

According to eq. (22),

$$f_0 = \sum^{x} K_{x0} [\mathrm{HA}]^x = K_{00} + K_{10} [\mathrm{HA}] + K_{20} [\mathrm{HA}]^2 + \cdots. \tag{25}$$

By definition (eq. 8), $K_{00} = 1$. The other terms with $x > 0$ in eq. (25) refer to additive complexes between the uncomplexed metal ion, M^{N+}, and one or several uncharged molecules of HA, i.e. the complexes of type $\mathrm{M(HA)}_x^{N+}$. If we a priori assume that the concentrations of all these complexes can be neglected compared with $[\mathrm{M}^{N+}]$, which probably often is the case, one gets $f_0 = 1$ and accordingly

$$\frac{f_0}{f_\lambda} = \frac{\Sigma K_{x0} [\mathrm{HA}]^x}{\Sigma K_{xN} \Lambda_{xN} [\mathrm{HA}]^x} \approx \frac{1}{f_\lambda}. \tag{26}$$

A certain f_λ value is obtained for each HA concentration. From the previously determined values of $f_y \cdot f_\lambda^{-1}$ at these HA concentrations and the assumption made in eq. (26), the different f_y values can be obtained as demonstrated e.g. for f_1 in eq. (27).

$$f_1 = \frac{f_1/f_\lambda}{f_0/f_\lambda} = \frac{f_1}{f_0} \approx f_1 = \Sigma K_{x1} [\mathrm{HA}]^x. \tag{27}$$

The f_λ- and the different f_y-functions are then solved for $K_{xN}\Lambda_{xN}$ and K_{xy}. With these values the distribution constants Λ_{xN} for the different uncharged complexes can be found. Examples of this method will be given in Part XII-B.

If considerable amounts of complexes of type $M(HA)_x^{N+}$ are formed, the approximation of f_0 in eq. (26) cannot be used. The exact solution of this equation (written in inverted form) is given by

$$\frac{f_\lambda}{f_0} = \Lambda_{0N}K_{0N} + (\Lambda_{1N}K_{1N} - \Lambda_{0N}K_{0N}\cdot K_{10})[\mathrm{HA}] + (\Lambda_{2N}K_{2N} - \Lambda_{1N}K_{1N}\cdot K_{10} + \\ + \Lambda_{0N}K_{0N}K_{10}^2 - \Lambda_{0N}K_{0N}K_{20})[\mathrm{HA}]^2 + \cdots + (\Lambda_{xN}K_{xN} - \\ - \sum_{i=0}^{i=x-1} C_i K_{x-i,\,0})[\mathrm{HA}]^x, \tag{28}$$

where C_i is the coefficient before the [HA]-term of the ith degree ($C_0 = \Lambda_{0N}K_{0N}$). With the method previously outlined, all constants in eq. (28) have been determined except for K_{x0}. However, all these constants include small systematic errors, if K_{x0} cannot be neglected.

The method of calculation given above has been developed for distribution experiments, where the total concentration of the ligand HA is much greater than the total metal concentration. This simplifies the measurements considerably, since [HA] will then be independent of [M]. However, if [HA] is of the same order as [M], it will vary depending on the degree of complex formation with M. If the amount of free HA can be measured, the amount of bound HA per central atom (the ligand number) can be calculated. The equations, which have to be derived to obtain K_{x0} from such measurements, will be similar to those given above. Since the derivation of these equations has been given elsewhere (e.g. [20]), it will not be given here. It should only be pointed out that the experimental difficulties to determine the concentration of free HA often are considerable.

Sometimes it may be possible to obtain approximate or maximum values of K_{x0} by other methods e.g. by spectrophotometric investigations of the effect of the addition of HA to highly acid solutions of M.

If the new values of K_{x0} are introduced in eq. (28), it can be solved more accurately for $\Lambda_{xN}K_{xN}$. With these values f_λ may be calculated, which may lead to new f_y values, and finally to new values for the constants K_{xy} and Λ_{xN}.

On the horizontal parts of Figs. 1 a–3 a, q is independent of pH. According to eq. (17), y must then be equal to N, which means that the aqueous phase contains very little of the charged species of M. In this pH-region we then find that on a plot of q against [HA]

$$\lim_{[\mathrm{HA}]\to\infty} q = \lim_{[\mathrm{HA}]\to\infty} \frac{\sum_{x=0}^{x=a} K_{xN}\Lambda_{xN}[\mathrm{HA}]^x[\mathrm{H}]^{-N}}{\sum_{x=0}^{x=a} K_{xN}[\mathrm{HA}]^x[\mathrm{H}]^{-N}} = \Lambda_{aN}, \tag{29}$$

where a is the maximum number of HA- and A-groups, which can be bound to M.

Summary

For the interpretation of the data obtained on the extraction of metal complexes to organic solvents from aqueous solutions of low and constant ionic strength, the following minimum number of variables has to be considered: the concentrations of the metal atom (M), main ligand (the base A^-), HA, OH^-, H_2O, organic solvent molecules (Org) and the temperature. This has been done in an attempt to determine the composition of the composite complexes of type $MA_n(OH)_p(HA)_r(Org)_s(H_2O)_t$ formed in a given system.

In this complex s and t can be determined only in special cases, and it is not possible to distinguish by equilibrium methods between isomers with the same values for $x = n + r$ and $y = n + p$. These isomers can be represented by the formula $M(HA)_x(H)_{-y}$.

It is shown that if the logarithm of the distribution of the metal between the organic solvent and water is plotted as a function of log $[HA][H]^{-1}$ for different HA concentrations, three different cases may be distinguished.

1) all curves coincide ($x = y$): this means that only complexes of type MA_n are formed, assuming that $[A] \gg [HA]$ [OH] (Figure 1 a);

2) the curves coincide at high values of log $[HA][H]^{-1}$, but not at low values ($x < y$): only complexes of type MA_n $(OH)_p$ are formed (Figure 2 a);

3) the curves never coincide ($x \gtrless y$): complexes of the general type $MA_n(OH)_p(HA)_r$ are formed (Fig. 3 a).

A general method to calculate formation constants for the complex $M(HA)_x(H)_{-y}$ from extraction data has been developed. It is also shown that from a comparison of the distribution ratios of the metal between water and several different organic solvents it is possible to determine if the metal forms a complex with the organic solvent molecules.

The author wishes to thank Professor L. G. SILLÉN for valuable advice and helpful criticism of this paper.

Research Institute of National Defence, Dept. 1, Sundbyberg 4, Sweden.

REFERENCES

1. H. M. IRWING, Quart. Rev. *5* (1951) 200.
2. R. E. TREYBAL, Ind. Eng. Chem. *45* (1953) 58.
3. A. E. MARTELL and M. CALVIN, Chemistry of Metal Chelate Compounds. New York 1952.
4. J. RYDBERG, Acta Chem. Scand. *4* (1950) 1503.
5. D. DYRSSEN, Svensk Kem. Tidskrift *65* (1953) 43.
6. R. E. CONNICK and W. H. MCVEY, J. Am. Chem. Soc. *71* (1949) 3182.
7. R. A. DAY and R. W. STOUGHTON, AECD-2756 (1949).
8. A. R. MATHIESON, J. Chem. Soc. *1949*, 5294.
9. L. I. KATZIN and J. C. SULLIVAN, J. Phys. Coll. Chem. *55* (1951) 346.
10. H. A. C. MCKAY *et al.*, Trans. Far. Soc. *47* (1951) 428, 437, 997, 1099, 1103.
11. R. BOCK and E. BOCK, Z. anorg. Chem. *263* (1950) 146.
12. L. YAFFE, Can. J. Res. *27 B* (1949) 638.
13. G. LUNDGREN and L. G. SILLÉN, Arkiv för Kemi *1* (1949) 277.
14. F. J. FRERE, J. Am. Chem. Soc. *55* (1933) 4362.
15. J. H. RAYNER and H. M. POWELL, J. Chem. Soc. *1952*, 319.
16. L. POKRAS, M. KILPATRICK, and P. M. BERNAYS, J. Am. Chem. Soc. *75* (1953) 1254.
17. J. P. HUNT and H. TAUBE, J. Chem. Phys. *18* (1950) 757.
18. J. C. SULLIVAN and C. J. HINDMAN, J. Am. Chem. Soc. *74* (1952) 6091.
19. I. LEDEN, Diss. Lund 1943.
20. J. BJERRUM, Diss. Copenhagen 1941.
21. D. Dyrssen and L. G. SILLÉN, Acta Chem. Scand. *7* (1953) 663.

Tryckt den 25 april 1955

Uppsala 1955. Almqvist & Wiksells Boktryckeri AB

ARKIV FÖR KEMI Band 8 nr 14

Communicated 13 October 1954 by ARNE WESTGREN and GUNNAR HÄGG

Studies on the extraction of metal complexes. XII-B

The formation of composite, mononuclear complexes. Part B: Studies on the Th- and U(VI)-acetylacetone-H_2O-organic solvent systems

By JAN RYDBERG

With 16 figures in the text

The theoretical possibilities of calculating complex formation constants for mononuclear complexes of the type $MA_n(OH)_p(HA)_r(Org)_s(H_2O)_t$ from distribution data have been discussed in Part A [22][1] of this paper. The applicability of the equations developed there has been tested here with the metals Th(IV) and U(VI). The equations can be used only if the acid HA gives complexes with the metal which are soluble in organic solvents (Org). Acetylacetone (HAa), which is a weak acid of $pk_a = 8.82$, gives such complexes with Th(IV) and U(VI).

Two restrictions were imposed on the equations for the calculation of formation constants in Part A: only mononuclear complexes were considered, and none of the ions were assumed to be soluble in the organic solvents. The first restriction usually limits the experiments to dilute solutions of the metal. It is somewhat difficult to verify that the second restriction is fulfilled in the experiments, but the use of solvents with low dipole moment will usually be adequate. As such solvents, benzene, chloroform and methyl isobutyl ketone (hexone) have been chosen.

Repeated use will be made throughout this paper of references and equations given in Part A.

EXPERIMENTAL

1. Procedure

Equal volumes of the organic and aqueous phases were shaken for 20 hours at 25°C. The aqueous phase was 0.1 *M* in ClO_4^- and contained $UO_2(ClO_4)_2$ or $Th(ClO_4)_4$. $HClO_4$ or NaOH was added to give a suitable pH. The acetylacetone (HAa) concentration in the organic phase was varied between 1.0 and 0.005 *M*. After equilibrium the phases were separated by centrifuging, and aliquots were taken out for either spectrophotometric, fluorophotometric or radiometric assay of the metal.

The uranium concentration in the aqueous phase at a distribution ratio $q > 0.1$ was determined with the method developed for these investigations by HÖK [23]:

---

[1] References 1–21 will be found in Part A [22].

After adjustment of pH, the aqueous phase was shaken twice with an 8-hydroxyquinoline (oxine) solution in chloroform. The uranyl oxinate in the two combined extracts was determined at 4250 Å with a Beckman DU Spectrophotometer. The concentration in the organic phase was calculated from the difference between the total uranium concentration and that found in the aqueous phase.

At low distribution ratios, $q < 0.1$, the uranium concentration of the organic phase was determined fluorophotometrically [24]. About 1 g of a mixture of 90 % NaF and 10 % Na_2CO_3 was fused in a Pt-dish, and a blank reading was taken on the fluorophotometer. Between 10 and 0.1 ml of the organic phase was then slowly evaporated on top of the fused mixture. The sample was then fused again and a new reading was taken. From the difference between these two readings the concentration of U in the organic phase could be found from the calibration curves. The fluorophotometer was constructed at *AB Atomenergi* [25].

No systematic differences could be found between the distribution ratios determined with the spectrophotometric and the fluorophotometric methods.

The Th concentration in each phase was determined radiometrically with the same method as described previously [26].

After equilibration, the pH of the aqueous phase was measured with a Radiometer pH-Meter, Type 3i, using glass- and saturated calomel electrodes. Since all other measurements here are made on concentrations, the readings of the pH-meter were calibrated against known hydrogen ion concentration in 0.1 *M* $NaClO_4$; in this paper pH is used as a symbol for $-\log[H]$, sometimes written *pc*H. Brackets will be used to indicate concentrations.

The concentration of HAa in the aqueous phase was calculated from the equation

$$[HAa]_{aq} = [HAa]_{org,\,init}(1 + k_a[H^+]^{-1} + k_d \cdot v_{org}/v_{aq})^{-1} \cdot v_{org,\,init}/v_{aq}\,,^{1} \qquad (30)^{2}$$

where the initial concentration of HAa in the organic phase (phase volume $v_{org,\,init}$) is $[HAa]_{org,\,init}$, when it is zero in the aqueous phase, i.e. $[HAa]_{aq,\,init} = 0$. If $v_{aq} = v_{org}$ in eq. (30) $[HAa]_{org,\,init}$ can be replaced by $[HAa]_{tot}$, the sum of the concentrations of HAa and Aa^- in both phases. In 0.1 *M* $NaClO_4$ the pk_a of acetylacetone has been found to be 8.82 at 25°C (27), while k_d is 5.95 for benzene–water (28), 5.9 for hexone–water, and 23.5 for chloroform–water [27].

When $v_{org} = v_{aq}$ and $v = v_{init}$, $[Aa^-]$ can be calculated from the equation

$$-\log[Aa^-] = pAa = pk_a + \log[H^+] - \log[HAa]_{tot} + \log(k_d + 1 + k_a[H^+]^{-1}). \quad (31)$$

The change of volume $(v - v_{init})$ due to mutual solubility of the solvents can be neglected for the systems benzene–water and chloroform–water. From KATZIN and SULLIVAN's [9] data on the hexone–water system DYRSSEN [5] has calculated that the mutual solubilities cause an increase in the volume of the aqueous phase of about 5 %, while the decrease in volume of the organic phase is approximately the same. If this is taken into account all *p*Aa-values for the hexone–water system should be about 0.02 *p*Aa-units higher. However this small change has been neglected here.

For the sake of simplicity the charges of the ions will often be omitted in the following.

---

[1] Equation (13) in paper II [4] of this series is not quite correct and should read as given above in eq. (30).

[2] Equations (1)–(29) will be found in Part A of this paper [22].

2. Chemicals

$NaClO_4$, which was used as a neutral salt for keeping constant ionic strength, was obtained by mixing equivalent amounts of NaOH and $HClO_4$ of analytical grade. An 0.1 *M* aqueous solution of this salt gave a pH of around 6.

The organic solvents benzene and chloroform were of analytical grade, while methyl isobutyl ketone (hexone) was of technical grade. Benzene and chloroform were shaken with water several times before use. Hexone was found to contain some acid impurities and was therefore first shaken with a NaOH solution, and then with water until a neutral pH was obtained in the water phase. The water used in the experiments was distilled once.

Acetylacetone of analytical grade was purified according to RYDBERG [28].

The metal perchlorates were prepared in the following manner: UO_3 of high purity, obtained from *AB Atomenergi*, was dissolved in a known excess of p.a. $HClO_4$ and diluted to make pH 1. No solid residue was left. $Th(ClO_4)_4$ solutions for radiometric work were prepared from a carrier-free $UX_1 + UX_2$ solution in $HClO_4$ [29] and p.a. $Th^{232}O_2$ dissolved in p.a. $HClO_4$.

RESULTS

3. Investigation of the concentration range for the formation of mononuclear complexes

3 a. The U(VI) complexes

If polynuclear complexes of a metal are formed in solutions investigated by the extraction method, the distribution ratio *q* should vary with the metal concentration at constant pH and ligand concentration (see eq. 10).

The distribution ratio *q* of U as a function of pH at three different metal concentrations is given in Fig. 4.[1] Two different acetylacetone concentrations have been used; the curves for different [U] should be compared only at the same $[HAa]_{aq}$. The total concentration of the uranium atoms in both phases will in the following be abbreviated to [U]; thus $[U]_{aq} + [U]_{org} = [U]$ for $v_{aq} = v_{org}$. It is seen that the curves for $[U] = 0.001$ (symbol □) and $[U] = 0.0001$ (symbol ■) coincide, while this is not the case for the pair $[U] = 0.010$ (symbol ●) and $[U] = 0.001$ (symbol ○) *M*.

When a complex is formed between U(VI) and acetylacetone, the free acetylacetone concentration in the solution will decrease. This decrease can be neglected as long as $[HAa]_{tot}$ is $\gg [U]$; in Fig. 4 $[HAa]_{tot}$ is ≥ 0.098 *M* for $[U] \leq 0.001$ *M*. However, for $[U] = 0.01$ *M* and $[HAa]_{tot} = 0.145$ *M* (●), a correction must be introduced for the decrease in $[HAa]_{tot}$ due to the complex formation with U. It will be shown later on that on the horizontal part of the curves in Fig. 4 approximately three acetylacetone groups are bound to each uranium atom. For $[U] = 0.0104$ *M*, the concentration of free HAa will then decrease from 0.145 *M* to 0.114 *M* ($[HAa]_{aq}$ decreases from 0.00590 to 0.00465 *M*). It is seen from Fig. 18 that at this corrected HAa concentration, one has to expect a distribution ratio of U corresponding to a log *q* value of 0.55. However, a value of 0.40 has been obtained in Fig. 4. This means that the increase in [U] from 0.001 to 0.01 *M* has decreased log q_{max} (the value of log *q* at the plateau) from 0.55 to 0.40.

---

[1] Fig. 1–3 are given in Part A of this paper.

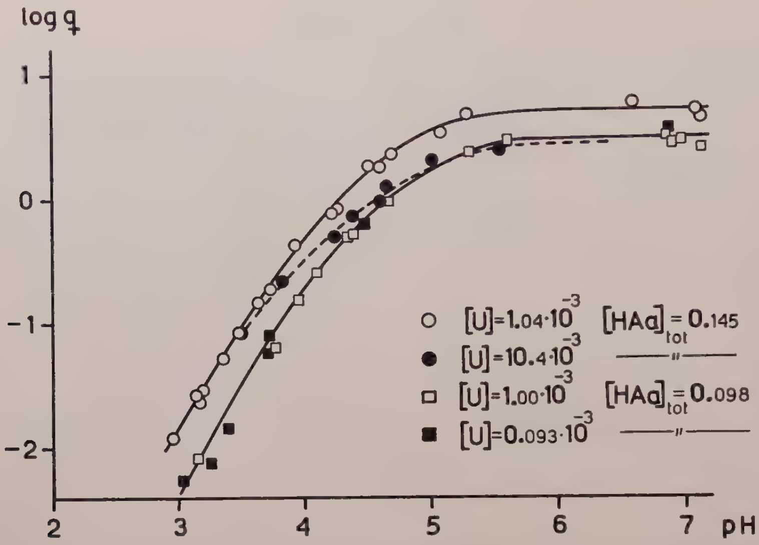

Fig. 4. The metal concentration dependence of the distribution q of U(VI) between $CHCl_3$ and H_2O in the presence of acetylacetone (HAa).

The decrease of log q, when [U] is increased from 0.001 M to 0.01 M ($[HAa]_{tot} = 0.145$) can be satisfactorily explained only by the assumption that polynuclear complexes are formed. Since log q does not change when [U] is decreased from 0.001 to 0.0001 M ($[HAa]_{tot} = 0.098$), one can conclude that the concentration of the polynuclear complexes of U(VI) can be neglected at $[U] \leq 0.001$ M at these HAa concentrations and pH.

In all the following experiments the U(VI) concentration has been around or below 0.001 M. Polynuclear complexes of U have therefore been neglected in the calculations.[1] In the equations applied on the U(VI) system, m has therefore been put equal to 1.

3 b. The Th(IV) complexes

The experiments with Th have been mostly carried out with tracer concentrations of the metal. In no case has the Th concentration been greater than 2.10^{-6} M. It has then been shown [4, 26] that a decrease of the Th concentration with several powers of ten does not influence the distribution ratio of q in the presence of an excess of acetylacetone. It may therefore be concluded that polynuclear complexes of thorium can be neglected in our acetylacetone solutions as long as $[Th] \leq 2.10^{-6}$ and $pH < 7$.

4. Investigation of the complex formation between the metals and the organic solvents

4 a. The U(VI)-H_2O-C_6H_6, -$CHCl_3$ and -$C_4H_9COCH_3$ systems

In the absence of acetylacetone it was found that no uranium could be extracted into $CHCl_3$ or $C_4H_9COCH_3$ (hexone) from aqueous solutions of pH 1–4.5 in 0.1 M

---

[1] See also footnote, p. 136.

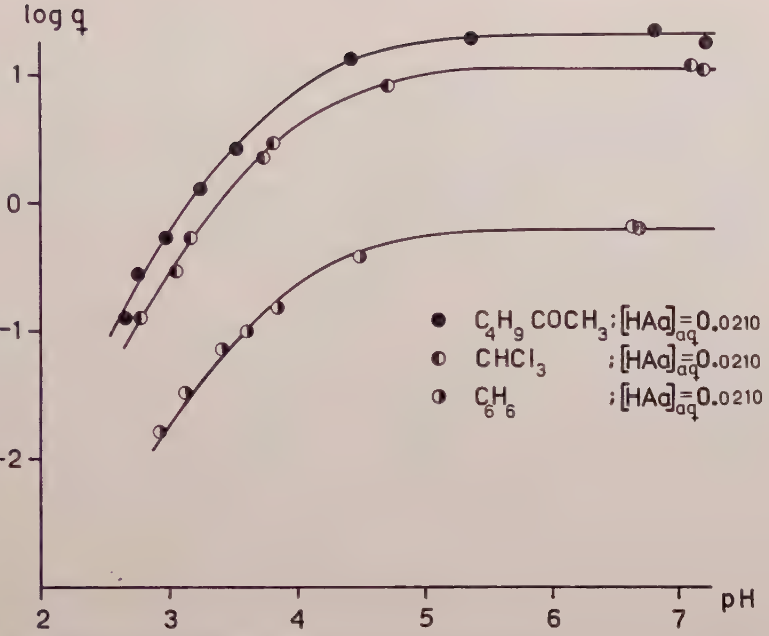

Fig. 5. The distribution q of U(VI) between H_2O and the organic solvents $C_4H_9COCH_3$, $CHCl_3$ and C_6H_6 as a function of pH at constant acetylacetone (HAa) concentration.

$NaClO_4$. From this it is concluded that the distribution ratio of U(VI) perchlorates between the organic and aqueous phases must be < 0.001.

The distribution ratio, q, for U(VI) in the solvent systems $CHCl_3$–H_2O, C_6H_6–H_2O and $C_4H_9COCH_3$–H_2O and in the presence of HAa was measured at different pH. The results are given in Fig. 5—all curves are for $[U] = 0.00104$ and $[HAa]_{aq} = 0.0210$ M. Since the distribution ratio of acetylacetone between $CHCl_3$ and H_2O is much greater ($k_d = 23.5$) than between C_6H_6 and H_2O ($k_d = 5.95$), and $C_4H_9COCH_3$ and H_2O ($k_d = 5.9$), the acetylacetone concentration in the organic phase will be much higher for the $CHCl_3$ system than for the two other systems. However, to make the curves for the different solvent systems comparable, only the aqueous phases must have the same acetylacetone concentration.

From the curves in Fig. 5 it is found that the vertical distance between the curves is constant—one obtains

$$q_{C_4H_9COCH_3}/q_{CHCl_3} = 1.8 \text{ and } q_{C_4H_9COCH_3}/q_{C_6H_6} = 33$$

at constant pH.

According to the paragraph on the influence of organic solvents on the distribution curves (Part A), the ratio of the distribution factors q' and q'' for two different solvent systems (H_2O–Org′ and H_2O–Org″) will be constant and independent of pH only if no complex is formed between the metal M and molecules of the organic solvent. From the experimental results given in Fig. 5 it can then be concluded that U(VI) does not seem to form any complexes with $C_4H_9COCH_3$, $CHCl_3$ or C_6H_6 in the aqueous acetylacetone solutions of pH < 7.

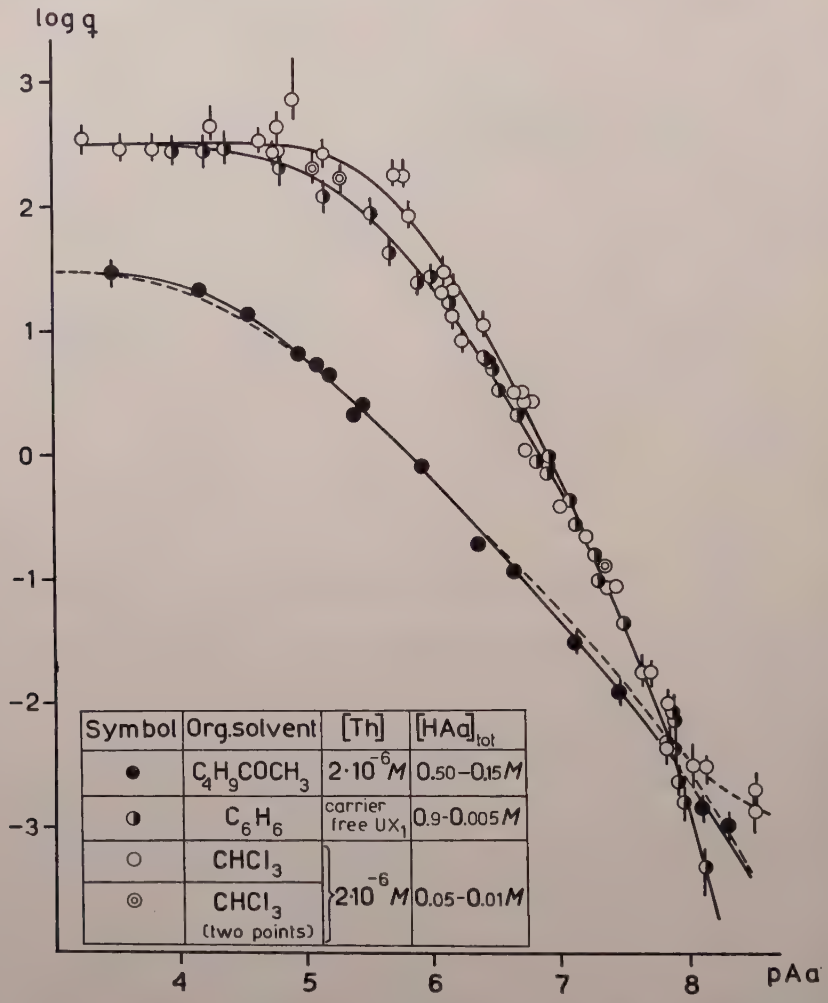

Fig. 6. The distribution q of Th between H_2O and the organic solvents $C_4H_9COCH_3$, $CHCl_3$ and C_6H_6 as a function of the acetylacetonate ion (Aa) concentration.

Although it has been shown that the uncharged U(VI)-acetylacetonate can form solid additive compounds with many different molecules, such as H_2O, C_5H_5N, etc. [30, 31], no compounds with $C_4H_9COCH_3$, $CHCl_3$ or C_6H_6 have been reported.

4 b. The Th(IV)-H_2O-C_6H_6, -$CHCl_3$ and -$C_4H_9COCH_3$ systems

In previous investigations on the thorium-acetylacetone system in the presence of C_6H_6 [4] and $CHCl_3$ [26], it has been found that the complexes formed between thorium and acetylacetone are of the general form MA_n. The distribution curves are then best compared at constant [Aa] (see eqs. 17–19).

In Fig. 6 the distribution ratios q are given as a function of pAa for the solvent systems $C_4H_9COCH_3$–H_2O, $CHCl_3$–H_2O and C_6H_6–H_2O. pAa has been calculated using eq. (31). It is seen that $q_{CHCl_3}/q_{C_6H_6}$ is approximately constant and equal to 1, when $pAa_{CHCl_3} = pAa_{C_6H_6}$. From this it can be concluded, according to Part A, that practically no complexes are formed between the thorium acetylacetonate molecules and the organic solvents $CHCl_3$ and C_6H_6. On the other hand MORGAN [32] concludes from an investigation of the infrared spectrum of thorium tetra-acetylacetonate in $CHCl_3$ that some kind of weak bond exists between the organic solvent molecules and the metal complex. However, this bond may be too weak in our aqueous solutions to manifest itself in the distribution experiments.

Since $[HAa]_{aq}$ and pH are almost the same in the $C_4H_9COCH_3$–H_2O and the C_6H_6–H_2O systems for identical pAa, there is no reason to believe that the complex formation between thorium and acetylacetone should be different in the two aqueous solutions. However, the ratio $q_{C_6H_6}/q_{C_4H_9COCH_3}$ varies considerably with pAa. This can be satisfactorily explained (see Part A) only by the assumption that a complex is formed between the thorium acetylacetonate and the hexone molecules.

5. Calculation of formation and distribution constants for the metal complexes

5 a. The U(VI) complexes

The distribution of U(VI) at a total concentration of ≤ 0.001 M between $CHCl_3$ and aqueous 0.1 M $NaClO_4$ has been studied at different pH and acetylacetone concentrations. The results are given in Fig. 7, where log q is plotted against pH. To facilitate a comparison with Figs. 3 a and b in Part A, log q is also given as a function of pAa in Fig. 8. pAa has been calculated from eq. (31) by introducing the appropriate constants:

$$pAa = 10.21 - pH - \log [HAa]_{tot}.$$

This equation is valid up to pH 7.5 as long as the volumes of the aqueous and chloroform phases are equal, and $[U]_{tot} \ll [HAa]_{tot}$.

If Figs. 7 and 8 are compared with Figs. 1, 2 and 3 (Part A), one easily sees that only the curves in Fig. 3 look similar to the experimental results of Figs. 7 and 8. Complexes of the general type $MA_n(OH)_p(HA)_r$ must therefore be considered. Since this complex is equivalent to $M(HA)_x(H)_{-y}$ and since polynuclear complexes and complexes with the organic solvents may be neglected, it should be possible to use the equations derived in Section 3 c of Part A to calculate the formation constants K_{xy}. From these K_{xy} values different complexity products $\varkappa_{npr}$ may be obtained. The same procedure as outlined in Part A will be followed here.

To simplify the calculations somewhat, the q values at pH 1.0, 1.6, 2.0, etc., up to pH 7.0, have been taken from the smooth curves, which have been drawn through the experimental points in Fig. 7. It is believed that this will increase the accuracy rather than decrease it. The curve through the experimental points in Fig. 7 can be drawn with a fairly good degree of accuracy, and will be a sort of mean value for the experimental points. The small deviations of the experimental points from this mean value will turn out as much larger deviations in the F_y functions, which are

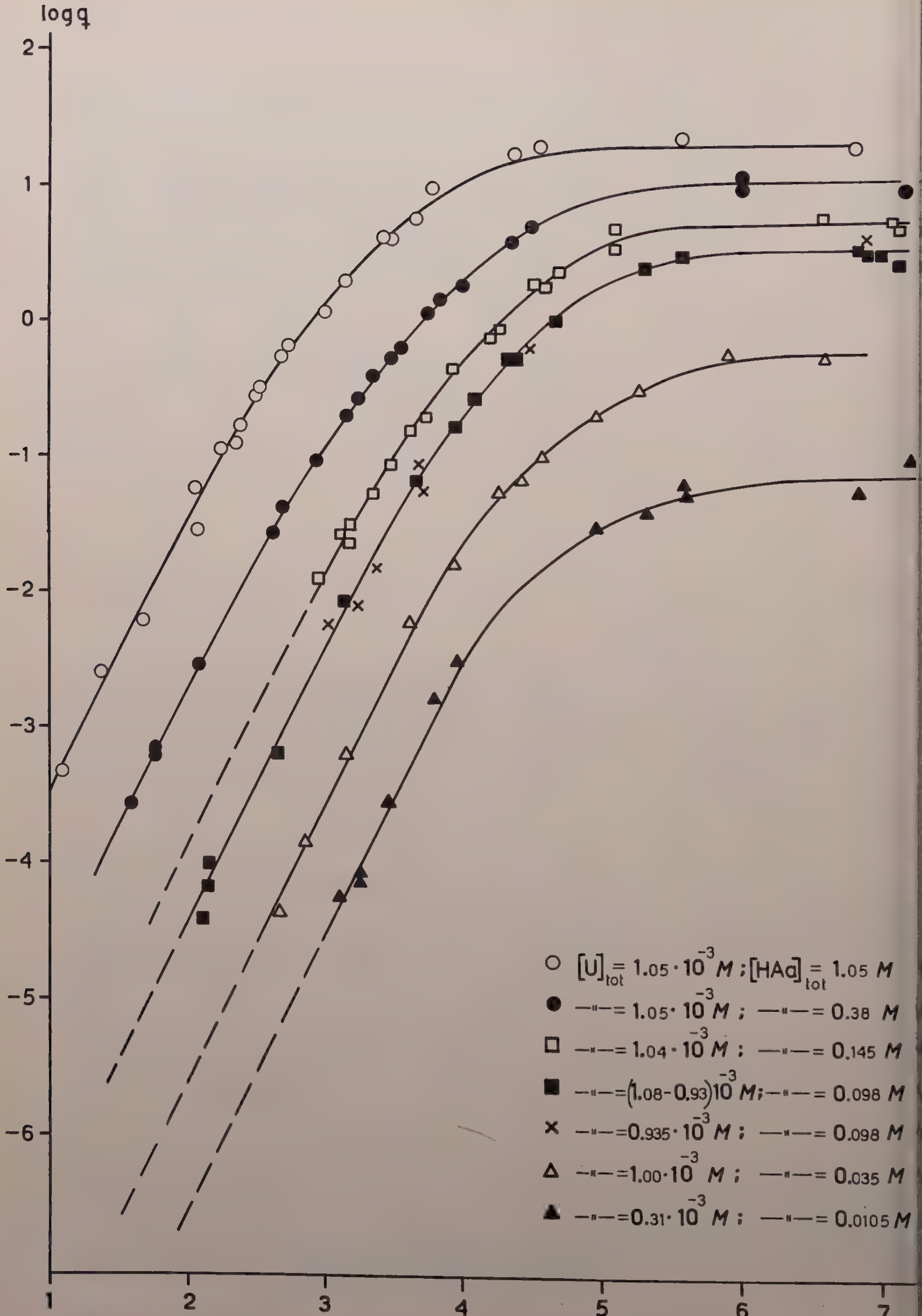

Fig. 7. The distribution q of U(VI) between $CHCl_3$ and H_2O as a function of pH at different acetylacetone (HAa) concentrations.

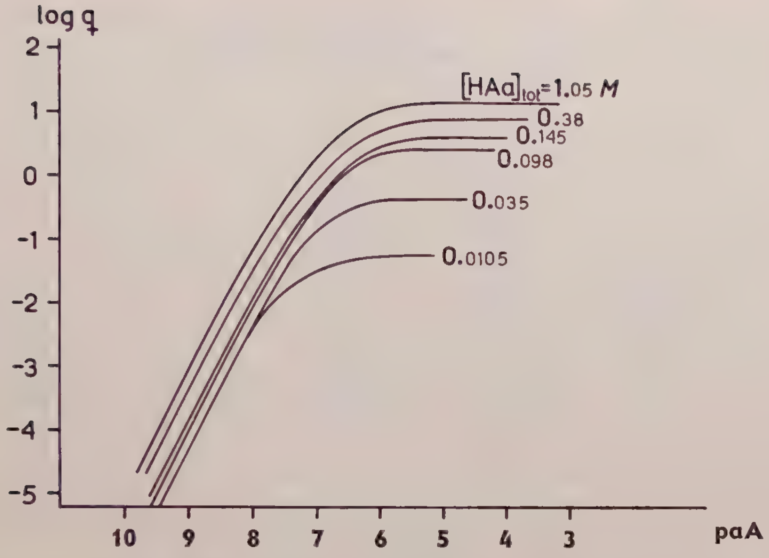

Fig. 8. The distribution q of U(VI) between $CHCl_3$ and H_2O as a function of the acetylacetonate ion (Aa) concentration.

used for the calculation of the $f_y \cdot f_\lambda^{-1}$ values. It will therefore be more difficult to draw lines through the F_y values if the experimental points are used than if values are taken from the smooth curves in Fig. 7.

The calculations of the different $f_y \cdot f_\lambda^{-1}$ functions, defined by eqs. (21) and (22), are made possible by using eqs. like (24).

In Tables 1–6, and Figs. 9–14, $f_y \cdot f_\lambda^{-1}$ has been calculated for the six different HAa concentrations. The $f_y f_\lambda^{-1}$ values thus obtained are collected in Table 7. If—to begin with—we neglect the complexes between UO_2^{2+} and HAa, i.e. put $f_0 = 1$, the different f_y values can easily be calculated using the $f_y f_\lambda^{-1}$ values in Table 7 (see eqs. 26–27). These results together with the f_λ values are also given in Table 7. With these f_y values the calculation of K_{xy} can be made.

Since $K_{00} = 1$ by definition and since it has been assumed that $f_0 = 1$, no calculation of K_{x0} can be made. The K_{x1} values are calculated from the f_1 values, and K_{x2} from the f_2 values, at different [HAa]. The G_x functions given in Tables 8 and 9 are formed in the same manner as shown above for the F functions $\left(G_0 = f_1;\ G_1 = \frac{G_0 - K_{0y}}{[\mathrm{HAa}]};\ \text{etc.}\right)$. The calculations are given in Tables 8–9 and Figs. 15–16.

From the G_1-curve in Fig. 16 one obtains $K_{12} \leq 0.1 \cdot 10^{-6}$ at $[\mathrm{HAa}]_{\mathrm{aq}} = 0$. The G_2 values in Table 9 are calculated on the assumption that $K_{12} = 0.1 \cdot 10^{-6}$. A straight line through these G_2 values gives $K_{22} = 0.3 \cdot 10^{-4}$ at $[\mathrm{HAa}] = 0$ and $K_{32} = 1.7 \cdot 10^{-3}$ from the slope.

If $K_{12} = 0$, the G_2' values in Table 9 are obtained. These values pass through a minimum around $[\mathrm{HAa}]_{\mathrm{aq}} = 0.004$. This behaviour with a minimum is quite anomalous. Though the accuracy is rather low, it is believed that the G_2 values are more correct than the G_2' values.

Table 1. Calculations for the determination of $f_y \cdot f_\lambda^{1}$, according to eq. (24), for $[\mathrm{HAa}]_{\mathrm{aq}} = 0.0428\ M$; see also Fig. 9.

pH	log q	q^{-1}	F_0	F_1	F_2
1.0	−3.50	$3.16\ 10^{3}$	$3.16\ 10^{5}$		
1.6	−2.30	$5.00\ 10^{2}$	$3.13\ 10^{5}$		
2.0	−1.50	$3.16\ 10^{1}$	$3.16\ 10^{5}$		
2.6	−0.45	2.82	$4.52\ 10^{5}$	$3.45\ 10^{2}$	
3.0	0.08	0.830	$8.30\ 10^{5}$	$5.16\ 10^{2}$	0.070
3.6	0.72	0.190	$3.04\ 10^{6}$	$6.83\ 10^{2}$	0.058
4.0	1.00	0.100	$1.00\ 10^{7}$	$9.7\ \ 10^{2}$	0.057
4.6	1.17	$6.75\ 10^{-2}$	$1.08\ 10^{8}$	$2.70\ 10^{3}$	0.056
5.0	1.21	$6.16\ 10^{-2}$	$6.16\ 10^{8}$	$6.16\ 10^{3}$	0.058
5.6	1.22	$6.03\ 10^{-2}$	$9.64\ 10^{9}$	$2.41\ 10^{4}$	0.059
6.0	1.22	$6.03\ 10^{-2}$	$6.03\ 10^{10}$	$6.03\ 10^{4}$	0.060
6.6	1.22	$6.03\ 10^{-2}$	$9.64\ 10^{11}$	$2.41\ 10^{5}$	0.060
7.0	1.22	$6.03\ 10^{-2}$	$6.03\ 10^{12}$	$6.03\ 10^{5}$	0.060

Table 2. Calculations for the determination of $f_y\, f_\lambda^{-1}$, according to eq. (24), for $[\mathrm{HAa}]_{\mathrm{aq}} = 0.0158\ M$; see also Fig. 10.

pH	log q	q^{-1}	F_0	F_1
1.6	−3.59	$3.89\ 10^{3}$	$6.22\ 10^{6}$	
2.0	−2.80	$6.30\ 10^{2}$	$6.30\ 10^{6}$	
2.6	−1.59	$3.89\ 10^{1}$	$6.22\ 10^{6}$	
3.0	−0.96	9.12	$9.12\ 10^{6}$	$2.86\ 10^{3}$
3.6	−0.15	1.41	$2.25\ 10^{7}$	$4.05\ 10^{3}$
4.0	0.26	0.55	$5.50\ 10^{7}$	$4.87\ 10^{3}$
4.6	0.70	0.20	$3.20\ 10^{8}$	$7.85\ 10^{3}$
5.0	0.85	$1.42\ 10^{-1}$	$1.42\ 10^{9}$	$1.42\ 10^{4}$
5.6	0.94	$1.15\ 10^{-1}$	$1.84\ 10^{10}$	$4.60\ 10^{4}$
6.0	0.96	$1.10\ 10^{-1}$	$1.10\ 10^{11}$	$1.10\ 10^{5}$
6.6	0.96	$1.10\ 10^{-1}$	$1.76\ 10^{12}$	$4.40\ 10^{5}$
7.0	0.96	$1.10\ 10^{-1}$	$1.10\ 10^{13}$	$1.10\ 10^{6}$

Table 3. Calculations for the determination of $f_y\, f_\lambda^{-1}$, according to eq. (24), for $[\mathrm{HAa}]_{\mathrm{aq}} = 0.00590\ M$; see also Fig. 11.

pH	log q	q^{-1}	F_0	F_1
1.6	−4.70	$5.02\ 10^{4}$	$8.05\ 10^{7}$	
2.0	−3.90	$7.95\ 10^{3}$	$7.95\ 10^{7}$	
2.6	−2.71	$5.14\ 10^{2}$	$8.24\ 10^{7}$	
3.0	−1.92	$8.32\ 10^{1}$	$8.32\ 10^{7}$	$0.20\ 10^{4}$
3.6	−0.88	7.60	$1.22\ 10^{8}$	$1.11\ 10^{4}$
4.0	−0.34	2.19	$2.19\ 10^{8}$	$1.38\ 10^{4}$
4.6	0.26	0.55	$8.30\ 10^{8}$	$1.87\ 10^{4}$
5.0	0.50	$3.16\ 10^{-1}$	$3.16\ 10^{9}$	$3.08\ 10^{4}$
5.6	0.63	$2.35\ 10^{-1}$	$3.76\ 10^{10}$	$9.40\ 10^{4}$
6.0	0.65	$2.24\ 10^{-1}$	$2.24\ 10^{11}$	$2.24\ 10^{5}$
6.6	0.65	$2.24\ 10^{-1}$	$3.58\ 10^{12}$	$8.95\ 10^{5}$
7.0	0.65	$2.24\ 10^{-1}$	$2.24\ 10^{13}$	$2.24\ 10^{6}$

Table 4. Calculations for the determination of $f_y\, f_\lambda^{1}$, according to eq. (24), for $[\mathrm{HAa}]_{\mathrm{aq}} = 0.00400\ M$; see also Fig. 12.

pH	log q	q^{-1}	F_0	F_1
2.0	–4.44	$2.75\ 10^{4}$	$2.75\ 10^{8}$	
2.6	–3.24	$1.74\ 10^{3}$	$2.78\ 10^{8}$	
3.0	–2.45	$2.82\ 10^{2}$	$2.82\ 10^{8}$	
3.6	–1.33	$2.14\ 10^{1}$	$3.42\ 10^{8}$	$2.10\ 10^{4}$
4.0	–0.73	5.37	$5.37\ 10^{8}$	$2.59\ 10^{4}$
4.6	–0.06	1.15	$1.84\ 10^{9}$	$3.90\ 10^{4}$
5.0	0.22	$6.03\ 10^{-1}$	$6.03\ 10^{9}$	$6.01\ 10^{4}$
5.6	0.41	$3.90\ 10^{-1}$	$6.25\ 10^{10}$	$1.56\ 10^{5}$
6.0	0.46	$3.47\ 10^{-1}$	$3.47\ 10^{11}$	$3.47\ 10^{5}$
6.6	0.46	$3.47\ 10^{-1}$	$5.55\ 10^{12}$	$1.39\ 10^{6}$
7.0	0.46	$3.47\ 10^{-1}$	$3.47\ 10^{13}$	$3.47\ 10^{6}$

Table 5. Calculation for the determination of $f_y\, f_\lambda^{-1}$, according to eq. (24), for $[\mathrm{HAa}]_{\mathrm{aq}} = 0.00143\ M$; see also Fig. 13.

pH	log q	q^{-1}	F_0	F_1
2.0	–5.58	$3.80\ 10^{5}$	$3.80\ 10^{9}$	
2.6	–4.37	$2.46\ 10^{4}$	$3.84\ 10^{9}$	
3.0	–3.58	$3.80\ 10^{3}$	$3.80\ 10^{9}$	
3.6	–2.38	$2.40\ 10^{2}$	$3.84\ 10^{9}$	
4.0	–1.64	$4.37\ 10^{1}$	$4.37\ 10^{9}$	
4.6	–1.00	10.0	$1.60\ 10^{10}$	$3.02\ 10^{5}$
5.0	–0.70	5.00	$5.00\ 10^{10}$	$4.61\ 10^{5}$
5.6	–0.41	2.57	$4.11\ 10^{11}$	$1.02\ 10^{6}$
6.0	–0.32	2.08	$2.08\ 10^{12}$	$2.08\ 10^{6}$
6.6	–0.29	1.95	$3.12\ 10^{13}$	$7.80\ 10^{6}$
7.0	–0.29	1.95	$1.95\ 10^{14}$	$1.95\ 10^{7}$

Table 6. Calculations for the determination of $f_y\, f_\lambda^{-1}$, according to eq. (24), for $[\mathrm{HAa}]_{\mathrm{aq}} = 0.00043\ M$; see also Fig. 14.

pH	log q	q^{-1}	F_0	F_1
2.0	–6.56	$3.62\ 10^{6}$	$3.62\ 10^{10}$	
2.6	–5.36	$2.29\ 10^{5}$	$3.66\ 10^{10}$	
3.0	–4.56	$3.62\ 10^{4}$	$3.62\ 10^{10}$	
3.6	–3.36	$2.29\ 10^{3}$	$3.66\ 10^{10}$	
4.0	–2.53	$3.38\ 10^{2}$	$3.38\ 10^{10}$	
4.6	–1.80	$6.30\ 10^{1}$	$1.01\ 10^{11}$	
5.0	–1.55	$3.55\ 10^{1}$	$3.55\ 10^{11}$	$3.19\ 10^{6}$
5.6	–1.32	$2.09\ 10^{1}$	$3.34\ 10^{12}$	$8.28\ 10^{6}$
6.0	–1.25	$1.78\ 10^{1}$	$1.78\ 10^{13}$	$1.78\ 10^{7}$
6.6	–1.21	$1.62\ 10^{1}$	$2.57\ 10^{14}$	$6.43\ 10^{7}$
7.0	–1.21	$1.62\ 10^{1}$	$1.62\ 10^{15}$	$1.62\ 10^{8}$

Table 7. Calculation of f_y from the $f_y \, f_\lambda^{-1}$ values determined in Fig. 9–14, assuming that $f_0 = 1$.

$[\mathrm{HAa}]_{\mathrm{aq}} 10^3$	$f_0 \, f_\lambda^{-1}$	$f_1 \, f_\lambda^{-1}$	$f_2 \, f_\lambda^{-1}$	f_λ	f_1	f_2
42.8	$3.14 \; 10^5$	$4.5 \; 10^2$	0.060	$3.18 \; 10^{-6}$	$1.43 \; 10^{-3}$	$1.91 \; 10^{-7}$
15.8	$6.30 \; 10^6$	$3.0 \; 10^3$	0.103	$1.59 \; 10^{-7}$	$4.76 \; 10^{-4}$	$1.64 \; 10^{-8}$
5.90	$8.14 \; 10^7$	$1.1 \; 10^4$	0.212	$1.23 \; 10^{-8}$	$1.35 \; 10^{-4}$	$2.60 \; 10^{-9}$
4.00	$2.78 \; 10^8$	$2.5 \; 10^4$	0.320	$3.60 \; 10^{-9}$	$0.90 \; 10^{-4}$	$1.15 \; 10^{-9}$
1.43	$3.81 \; 10^9$	$2.5 \; 10^5$	1.93	$2.62 \; 10^{-10}$	$0.66 \; 10^{-4}$	$0.51 \; 10^{-9}$
0.43	$3.64 \; 10^{10}$	$2.5 \; 10^6$	15.7	$2.75 \; 10^{-11}$	$0.69 \; 10^{-4}$	$0.43 \; 10^{-9}$

Table 8. The calculation of G_x from f_1 and [HAa] for the determination of K_{x1}; see also Fig. 15.

$[\mathrm{HAa}]_{\mathrm{aq}} 10^3$	$G_0 10^4$	$G_1 10^2$
42.8	14.3	3.2
15.8	4.76	2.6
5.90	1.35	1.3
4.00	0.90	0.8
1.43	0.66	—
0.43	0.69	—

Table 9. The calculation of G_x from f_2 and [HAa] for the determination of K_{x2}; see also Fig. 16.

$[\mathrm{HAa}]_{\mathrm{aq}} 10^3$	$G_0 \; 10^9$	$G_1 \; 10^6$	$G_2 \; 10^4$	$(G_2' \; 10^4)$
42.8	191	4.46	1.0	(1.04)
15.8	16.4	1.01	0.6	(0.64)
5.90	2.60	0.37	0.5	(0.62)
4.00	1.15	0.19	0.2	(0.48)
1.43	0.51	0.08	—	(0.70)
0.43	0.43		—	(1.6)

The K_{xy} values are collected in Table 10, where they also are given in exponential form with the experimental limits of error. Only six different HAa concentrations have been investigated, which means that no more than six points can be obtained on the curves in Fig. 15 and 16. For the calculation of G_1 and G_2 fewer points will be available. This implies that the accuracy in the calculations of the K_{xy}-values is not very great. In some instances the true constants may therefore be somewhat different from the values given here.

With decreasing pH, the curves in Figure 7 approach an asymptote of slope 2. The relation between q and [H] can then be given as $q = \text{const} \cdot [\mathrm{H}]^{-2}$. It is seen from eq. (23) that this slope must be equal to $-N$, where N is the charge of the uncomplexed metal ion. This agrees with the well-known fact that the U(VI) ion in acid solutions has the formula UO_2^{2+}.

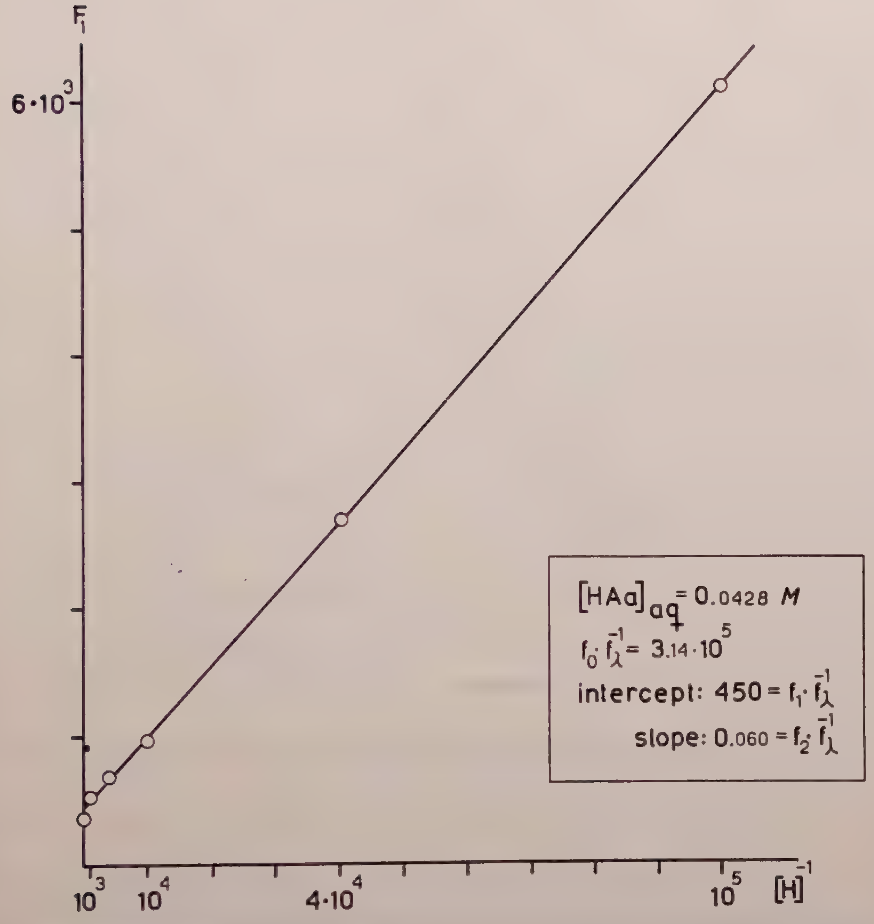

Fig. 9. The determination of $f_y\, f_\lambda^{-1}$ according to eq. (24) and Table 1 for $[\mathrm{HAa}]_{\mathrm{aq}} = 0.0428\ M$.

For the calculation of $K_{xN}\Lambda_{xN}$, where $N=2$, we use the f_λ values in Table 7, which were obtained on the assumption that $f_0=1$. Using the same limiting method as above, $K_{x2}\Lambda_{x2}$ is calculated in Table 11 and Fig. 17; the V_x^1 functions are formed like the F functions

$$\left(V_0' = f_\lambda \cdot f_0^{-1};\ V_1' = \frac{V_0' - K_{02}\Lambda_{02}}{[\mathrm{HAa}]};\ \text{etc.}\right).$$

The $K_{x2}\Lambda_{x2}$ values thus obtained are collected in Table 12.

Since a straight line is finally obtained in Fig. 17 no higher values of $K_{xN}\Lambda_{xN}$ than $K_{3N}\Lambda_{3N}$ can be obtained. This means that the only detectable complexes of uranium in the organic phase are those with $x=2$ and $x=3$, i.e. complexes containing 2 and 3 HAa- or Aa-groups.

With the $K_{x2}\Lambda_{x2}$ values and the previously determined values of K_{x2}, the distribution constants Λ_{x2} of the uncharged complexes can be calculated. This is done in Table 12, where the composition of the extracted complexes is also given.

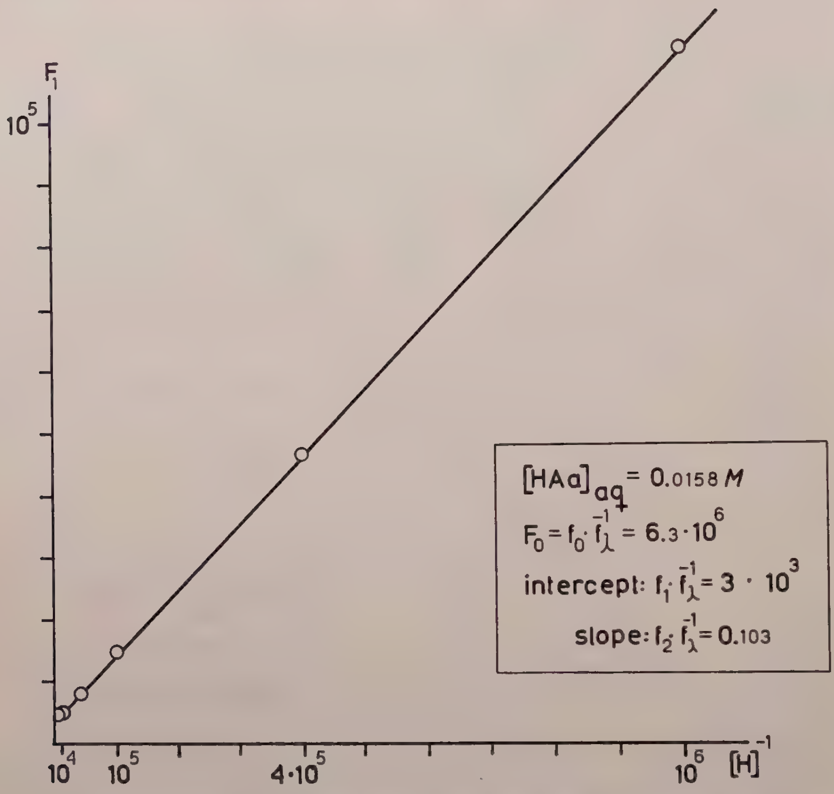

Fig. 10. The determination of $f_y f_\lambda^{-1}$ according to eq. (24) and Table 2 for $[HAa]_{aq} = 0.0158\ M$.

Table 10. The K_{xy} values obtained for the U(VI) complexes in aqueous solutions containing acetylacetone, on the assumption that $\sum^{x} K_{x0} [HAa]^x = 1$.

y / x	1	2
0	$0.6 \cdot 10^{-4}$ $10^{-4.2 \pm 0.1}$	$0.4 \cdot 10^{-9}$ $10^{-9.40 \pm 0.04}$
1	$1.0 \cdot 10^{-2}$ $10^{-2.0 \pm 0.1}$	$\leq 0.1 \cdot 10^{-6}$ $\leq 10^{-7.0}$
2	0.7 $10^{-0.15 \pm 0.1}$	$0.3 \cdot 10^{-4}$ $10^{-4.5 \pm 0.2}$
3	— —	$1.7 \cdot 10^{-3}$ $10^{-2.8 \pm 0.2}$

If the log q values for the horizontal part of the curves in Fig. 7 (log q_{max}) are plotted against log $[HAa]_{aq}$, which is done in Figure 18, the curves tend to go towards a maximum at high HAa concentrations. This maximum value must be equal to the distribution constant of the complex containing the maximum numbers of HAa-

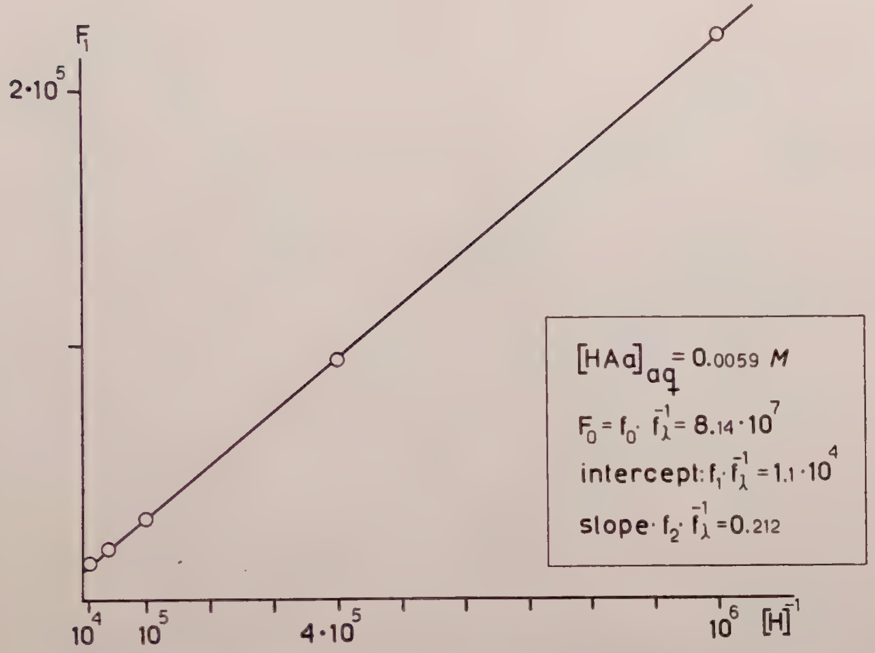

Fig. 11. The determination of $f_y\, f_\lambda^{-1}$ according to eq. (24) and Table 3 for $[HAa]_{aq} = 0.0059\ M$.

Table 11. The determination of $K_{x2}\Lambda_{x2}$ from the f_λ values in Table 7; see also Fig. 17.

$[HAa]_{aq}$	V'_0	V'_1	V'_2
0.0428	$3.18\ 10^{-6}$	$7.44\ 10^{-5}$	$1.74\ 10^{-3}$
0.0158	$1.59\ 10^{-7}$	$1.00\ 10^{-5}$	$0.63\ 10^{-3}$
0.00590	$1.23\ 10^{-8}$	$2.09\ 10^{-6}$	$3.54\ 10^{-4}$
0.00400	$3.60\ 10^{-9}$	$9.00\ 10^{-7}$	$2.25\ 10^{-4}$
0.00143	$2.62\ 10^{-10}$	$1.83\ 10^{-7}$	$1.28\ 10^{-4}$
0.000429	$2.75\ 10^{-11}$	$6.40\ 10^{-8}$	$1.50\ 10^{-4}$

and Aa-groups—this follows from eq. (29). This complex has previously been shown to be $M(HA)_3(H)_{-2}$. From the figure one gets $\log q_{\max} = 1.30 \pm 0.1$, or $q_{\max} = 20 \pm 5$. This value agrees well with that previously and independently determined, i.e. $\Lambda_{32} = 22$ in Table 12.

If the different values of K_{xy} and Λ_{x2}, which are collected in Tables 10 and 12, are introduced in eq. (28), one finds that these values should be correct as long as $K_{10} < 10$, $K_{20} < 10^6$ and $K_{30} < 10^9$. With these values the maximum fraction of the metal which can be complexed as $UO_2(HAa)_x^{2+}$ is easily calculated. One obtains a ratio $\sum_1^3 [UO_2(HAa)_x^{2+}]/[UO_2^{2+}] < 10^5$ at the highest HAa concentration used, i.e. at $[HAa]_{aq} = 0.0428\ M$. Since this value is independent of pH,

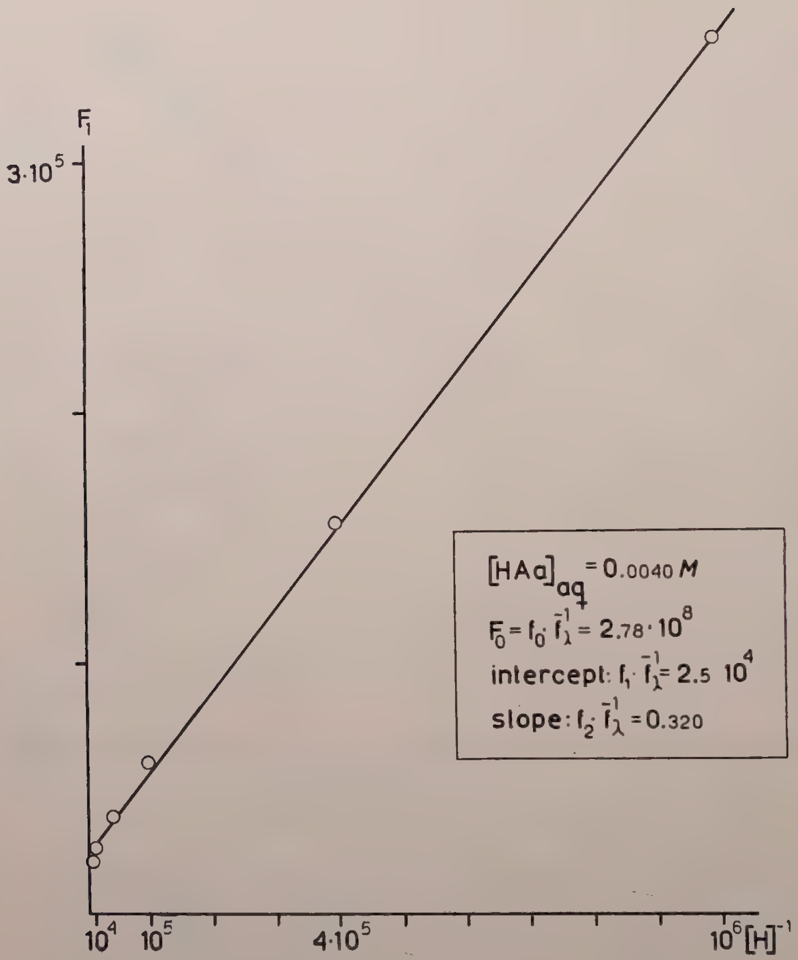

Fig. 12. The determination of $f_y f_\lambda^{-1}$ according to eq. (24) and Table 4 for $[HAa]_{aq} = 0.0040\ M$.

Table 12. Calculation of constants for the distribution of uncharged U(VI) complexes between $CHCl_3$ and H_2O.

x	$K_{x2}\ \Lambda_{x2}$	K_{x2}	Λ_{x2}	Composition of complexes
0	$\ll 10^{-11}$	$0.4 \cdot 10^{-9}$	$\ll 0.02$	$UO_2(H)_{-2}(H_2O)$?
1	$\ll 10^{-8}$	$\leq 0.1 \cdot 10^{-6}$	$\ll 0.1$	$UO_2(HAa)\ (H)_{-2}(H_2O)$?
2	$1.0\ 10^{-4}$	$0.3 \cdot 10^{-4}$	3.3	$UO_2(HAa)_2\ (H)_{-2}(H_2O)$?
3	$3.8\ 10^{-2}$	$1.7 \cdot 10^{-3}$	22	$UO_2(HAa)_3\ (H)_{-2}(H_2O)$?

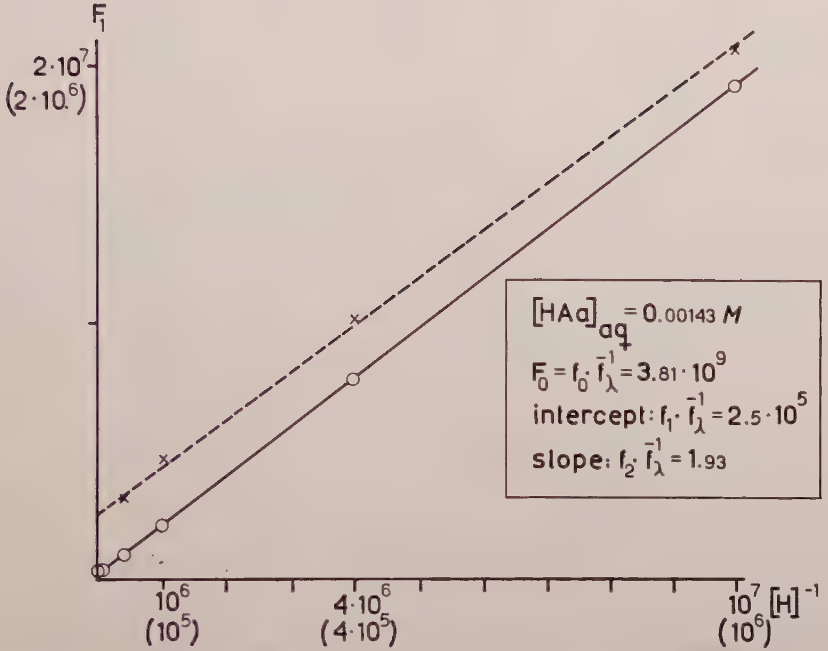

Fig. 13. The determination of $f_y \, f_\lambda^{-1}$ according to eq. (24) and Table 5 for $[HAa]_{aq} = 0.00143$ *M*.

it should be possible to test it at a pH, where complexes with OH^- and Aa^- can be neglected.

A spectrophotometric study of the change of the uranyl spectrum by the addition of HAa at pH = 0 was therefore undertaken. Fig. 19 shows three of the spectra obtained in 1.0 *M* $HClO_4$ at 25° C. Since the extinction of the uranyl-acetylacetone complexes is much greater than that of UO_2^{2+} and appears in the same wavelength region, the decrease in UO_2^{2+} due to complexing with HAa cannot be determined. However, since the general shape of the upper spectrum does not change very much with increasing concentration of HAa, it is felt that this spectrum is more probably due to the formation of complexes like UO_2Aa^+, UO_2Aa_2 or UO_2Aa_2HAa than to complexes like $UO_2(HAa)_x^{2+}$.

From the measurements of extinction at the uranyl peak of 4150 Å as a function of the acetylacetone concentration (Table 13), it can be seen that the UO_2^{2+} extinction, and consequently concentration, does not change to any great extent up to an HAa concentration of the order of 0.1 *M*. It can further be calculated from the constants

Table 13. The extinction coefficient *E* at 4150 Å of an 0.010 *M* UO_2^{2+} solution in 1.0 *M* $HClO_4$ as a function of the HAa concentration.

$[HAa]_{aq}$	0.000	0.050	0.099	0.30	0.53	0.98
E	0.076	0.075	0.078	0.092	0.109	0.156

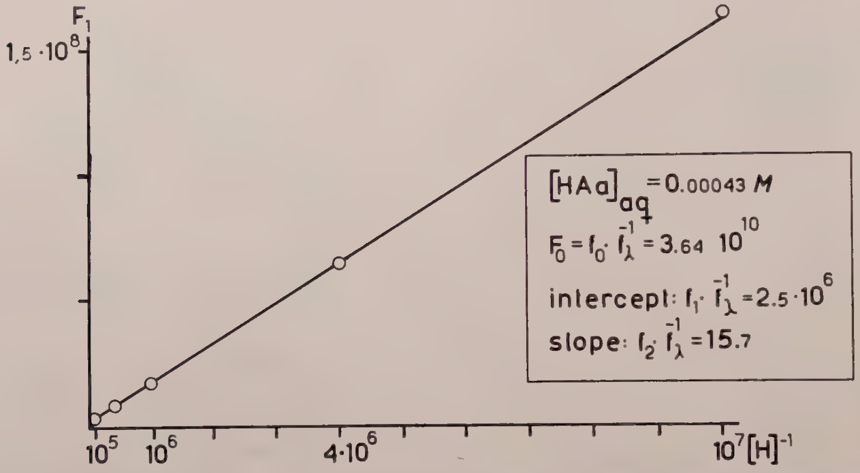

Fig. 14. The determination of $f_y\, f_\lambda^{-1}$ according to eq. (24) and Table 6 for $[HAa]_{aq} = 0.00043\ M$.

obtained in Table 10 that, at this pH and $[HAa]_{aq}$, less than 1 % of the singly charged and uncharged uranyl complexes is formed.

If one assumes that the molar extinction coefficients of the $UO_2(HAa)_x^{2+}$ complexes are different from that of UO_2^{2+}, one can then conclude that the ratio $\Sigma\,[UO_2(HAa)_x^{2+}]/[UO_2^{2+}]$ must be less than 0.1 at $[HAa]_{aq} \leq 0.1\ M$. The maximum values of K_{x0} will then be $K_{10} < 1$, $K_{20} < 10$ and $K_{30} < 100$.

The assumption that the concentrations of the $UO_2(HAa)_x^{2+}$ complexes could be neglected compared with that of $[UO_2^{2+}]$, which made it possible to put $f_0 = 1$, is thus found to be reasonable. One can therefore conclude that the K_{xy} and Λ_{xy} values given in Tables 10 and 12 do not contain any errors due to formation of $UO_2(HAa)_x^{2+}$-complexes.

5 b. The Th(IV) complexes

The formation constants for the complexes $ThAa^{+3}$, $ThAa_2^{2+}$, $ThAa_3^{+}$ and $ThAa_4$, as well as the distribution constants of the uncharged complex $ThAa_4$ between water and the organic solvents have been calculated in previous papers [4, 26].

It was pointed out in section 4 b that the difference between the hexone and chloroform or benzene curves in Fig. 6 could be explained by assuming that a thorium complex is formed with hexone molecules but not with chloroform or benzene molecules. The formation constants for these complexes can be calculated from the hexone curve in Fig. 6 by applying the method of graphical derivation (see paper [4], p. 1515). The following results are then obtained:

$$ThAa_2Hex_{s_1}^{2+} + Aa^- \rightleftharpoons ThAa_3Hex_{s_2}^{+} + (S_1 - S_2)\,Hex \quad k_3 = 10^{8.0 \pm 0.15}$$

$$ThAa_3Hex_{s_2}^{+} + Aa^- \rightleftharpoons ThAa_4Hex_{s_3} + (S_2 - S_3)\,Hex \quad k_4 = 10^{4.3 \pm 0.15}$$

$$(ThAa_4Hex_{s_3})_{aq} \rightleftharpoons (ThAa_4Hex_{s_3})_{org} \quad \lambda_4 = 10^{1.5 \pm 0.1}$$

S_1, S_2 and S_3 represent a certain number of hexone molecules. Using these constants the dashed curve in Fig. 6 is obtained.

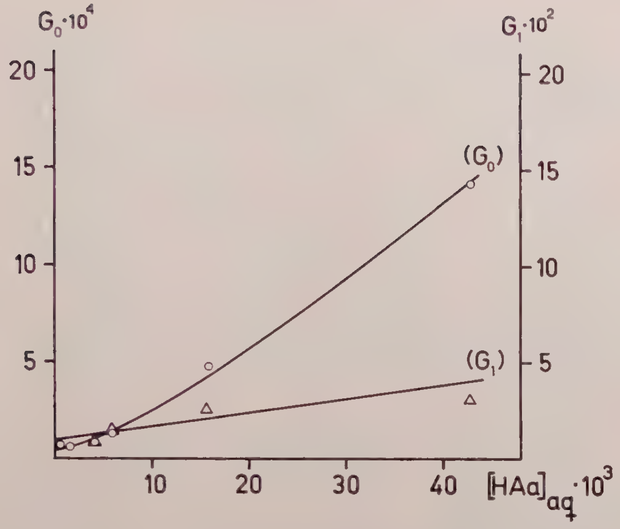

Fig. 15. The determination of K_{x1}; see also Table 8.

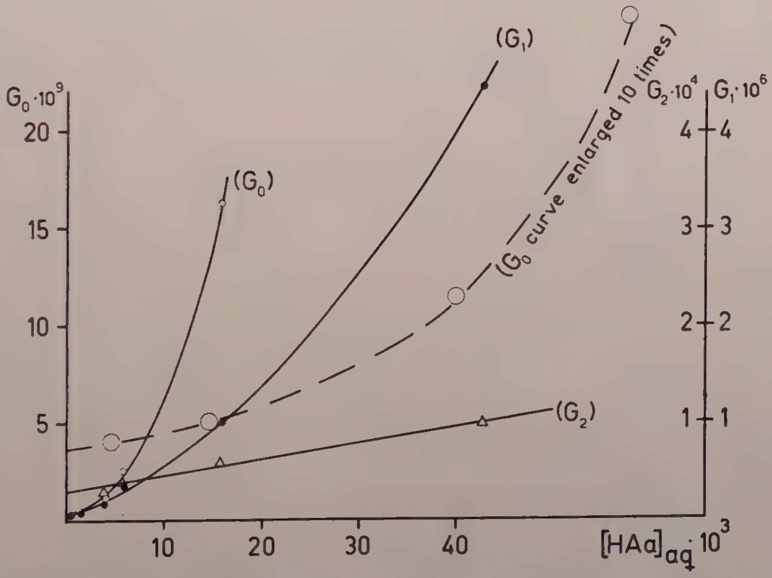

Fig. 16. The determination of K_{x2}; see also Table 9.

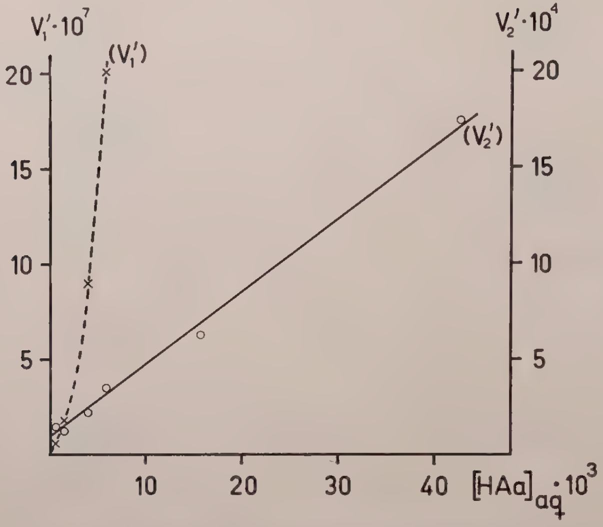

Fig. 17. The determination of $\Lambda_{x2} K_{x2}$; see Table 11.

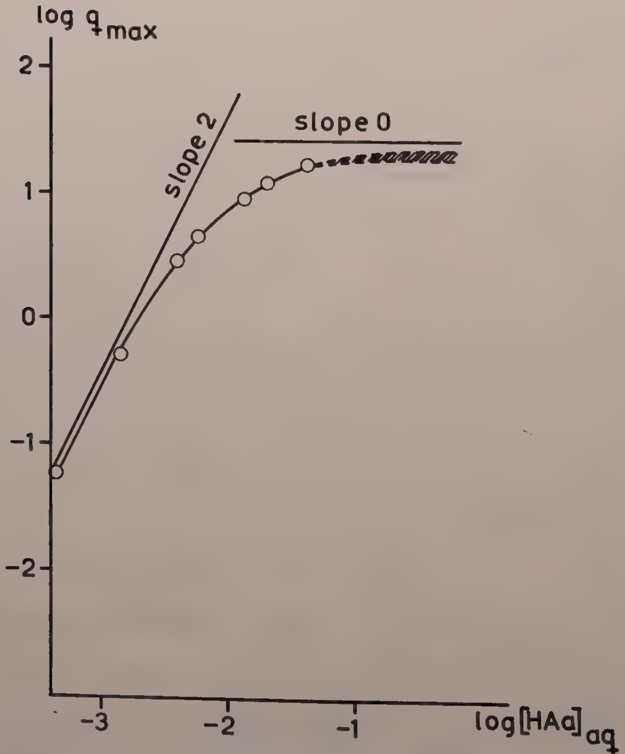

Fig. 18. The distribution q of U(VI) at pH 7 (q_{max}) as a function of the acetylacetone (HAa) concentration.

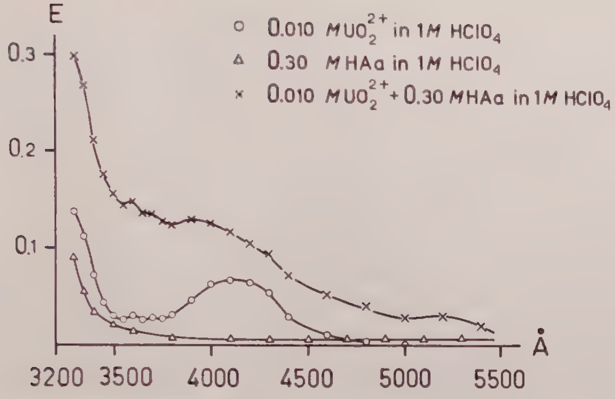

Fig. 19. Absorption spectra of UO_2^{2+}, acetylacetone (HAa), and mixtures of both in 1 M $HClO_4$ at 25° C.

6. Gravimetric analysis of some solid U(VI)-HAa complexes

Some information about the composition of the uncharged complexes in the solutions may be obtained from an analysis of solid U(VI)-acetylacetone complexes. Three different experiments were therefore carried out, in which uranium was precipitated by the addition of alkali to 0.1 M UO_2^{2+} solutions in 0.1 M HNO_3. In two of the experiments some acetylacetone had previously been added, while in one of the experiments a $CHCl_3$-phase was also present. The original compositions of the solutions are given in the left part of Table 14. This table also contains the results of the gravimetric analyses of the precipitates and supernatant solutions—each value is an average of two or more analyses.

It was believed that the precipitates of experiments "no. 2" and "no. 3" could be mixtures of several different complexes, one of them perhaps being uranyl hydrox-

le 14. Gravimetric analyses of U(VI) complexes precipitated under various conditions.

p. o.	Original composition of solutions				Composition after precipitation						
					Supernatant soln.		Analysis of solid substances				
	Phase	[HAa]	[U]	pH	[U]	pH	% U	% C	% H	Aa:U	Origin
	H_2O	0 M	0.1 M	1	0.00073 M	6.3	60	—	—	—	original precipitate
	H_2O	1.0 M	0.1 M	1	0.0055 M	6.6	43.7	29.2	3.76	2.65:1	original precipitate
							44.1	28.3	3.70	2.54:1	$CHCl_3$-soluble fraction (95 %)
	H_2O	0.041M	0.1 M	1	0.021 M	3.6	45.3	24.0	3.30	2.10:1	original precipitate
							47.4	24.9	3.43	2.08:1	$CHCl_3$-soluble fraction (76 %)
							58.4	1.0	1.36	0:1	$CHCl_3$-insoluble fraction (24%)
	$CHCl_3$	1.0 M	—		0.083 M		40.7	31.4	3.67	3.05:1	evaporated original $CHCl_3$-phase

ide. The precipitates were therefore shaken with $CHCl_3$, which should dissolve the uranyl acetylacetone complexes, but not the hydroxide.

In experiment "no. 3" only 76 % of the uranium dissolved. The analysis of the substance obtained on the evaporation[1] of this solution showed that approximately 2 acetylacetone groups were bound to each U-atom—the composition of this complex is closest to $UO_2Aa_2(H_2O)_2$ (theoretical composition: 47.2 % U, 23.8 % C, 3.59 % H), though it is not definitely proved that it is not $UO_2Aa_2H_2O$ (theoretical composition: 48.9 % U, 24.7 % C, 3.31 % H). The analysis of the residue, which was not soluble in the $CHCl_3$ solution, indicated that it was practically pure uranyl hydroxide.

The crystals obtained on the evaporation of the $CHCl_3$-phase in equilibrium with the aqueous phase of experiment "no. 3", were found to contain 3 acetylacetone groups per U atom. The composition of the solid substance corresponds either to $UO_2Aa_2HAaH_2O$ (theoretical composition: 40.6 % U, 30.7 % C, 4.13 % H) or UO_2Aa_2HAa (theoretical composition: 41.8 % U, 31.7 % C, 3.91 % H). Since the U analyses are believed to be more accurate than the C and H analyses, the former complex seems more probable. HAGER [31] has obtained a similar compound, $UO_2Aa_2HAaNH_3$, with an excess of acetylacetone and ammonia in a methyl alcohol solution.

In experiment "no. 2", the precipitate dissolved practically completely (95 %) in the $CHCl_3$ solution. The composition of the precipitate obtained on evaporation[1] of this $CHCl_3$ solution does not fit with the composition of any mononuclear U-HAa complex. It was therefore believed that it was a mixture of the two complexes $UO_2Aa_2(H_2O)_2$ and $UO_2Aa_2HAaH_2O$. BILTZ and CLINCH [30], and ABRAHAMSON and BROWN [33], have performed experiments similar to our experiment "no. 2" and obtained a precipitate of the composition 48.8 % U, 24.7 % C, and 3.0 % H. They ascribe this composition to the complex $UO_2Aa_2H_2O$. Since they do not give the exact conditions of their experiment, it is not possible to account for the discrepancy between their result and ours.

It seems probable that complexes with only two acetylacetone groups per U atom are formed with a deficit of acetylacetone while in large excess of HAa only complexes with three acetylacetone groups per U atom are formed. In the intermediate region considerable amounts of both are obtained.

DISCUSSION

7. The U(VI) complexes

7 a. Complexes in the organic phase

It has been shown in the previous sections that the U(VI)-species, which are extracted from the aqueous to the organic phase, are mainly UO_2Aa_2 and UO_2Aa_2HAa, perhaps containing some coordinated solvent molecules. The distribution constants of these complexes between $CHCl_3$ and water were found to be 3.3 and 22 respectively. From the results of the gravimetric analyses it was concluded that the complexes in the $CHCl_3$-phase were probably $UO_2Aa_2(H_2O)_2$ and $UO_2Aa_2HAaH_2O$, though the number of H_2O molecules bound to the complexes was a little uncertain.

Additive compounds between UO_2Aa_2 and uncharged molecules have previously been reported and all been found to be fairly easily soluble in solvents of low dipole moment [30–33]. HAGER [31] has prepared a number of compounds UO_2Aa_2HAaX in methyl alcohol solutions, where X is NH_3, CH_3NH_2 or $C_6H_5NH_2$. On the assumption that U(VI) has a coordination number of 7, he proposes the composition IV for the complex with $X = NH_3$.

---

[1] Some HAa was probably lost during evaporation.

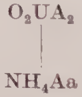

IV

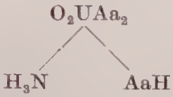

V

However, he also suggests V as a possible structure, in which U(VI) should have a coordination number of 8. X-ray crystallographic data show that the most common coordination number of U(VI) towards oxygen is 8, but sometimes a coordination number of 6 has also been found. According to MARTELL and CALVIN [3, p. 240] 8 is the common coordination number of the elements Mo, W and U. A number of recent investigations on solutions of uranyl complexes [8, 10, 34, 35] indicate that the uranyl ion has a coordination number of 6 relative to oxygen, which may correspond to a maximum coordination number of 8 for the metal atom in its hexavalent state. It seems reasonable to believe that all coordinative positions of an atom in solution are occupied as long as no steric hindrance occurs. Structure V therefore appears more probable than structure IV. This also agrees with our complex $UO_2Aa_2HAaH_2O$.

It is therefore believed that the U(VI) complexes in the $CHCl_3$-phase saturated with water are $UO_2Aa_2(H_2O)_2$ and $UO_2Aa_2HAaH_2O$. If the reaction in both the $CHCl_3$ and aqueous phases is

$$UO_2Aa_2(H_2O)_2 + HAa \rightleftharpoons UO_2Aa_2HAaH_2O + H_2O,$$

we can find that the equilibrium constant for this reaction in the organic phase is ~ 14, if $[H_2O]$ is put equal to 1 for both phases.

7 b. Complexes in the aqueous phase

According to eq. (9), each K_{xy} value corresponds to a certain $\varkappa_{npr}$ value. With the constants, k_a and k_w, we have

$$\varkappa_{npr} = K_{xy} \cdot 10^{+8.82\,n + 13.80\,p}.$$

It is seen from eq. (5) and (6) that several different combinations of n, p and r can be obtained for a certain combination of x and y.

From the dissociation constant of $10^{-8.8}$ for acetylacetone and the ionic product of $10^{-13.8}$ for water in 0.1 M $NaClO_4$ of 25°C, it follows that in an aqueous solution $[HAa][OH]/[Aa] = 10^{-5.0}$. It therefore seems improbable that OH and HAa will exist beside each other at the same time in a complex. If the complex $MA_n(OH)_p(HA)_r$ is once formed, OH and HAa will probably immediately react to give $MA_{n+r}(OH)_{p-r}(H_2O)_r$, if $p > r$. Though it is hard to prove, it seems reasonable to assume that the complexes with a minimum number of OH groups (minimum p value) will dominate over the other species with the same x and y values. This limits the possible combinations of n, p and r.

Table 15. Equilibrium constants[1] for the U(VI) complexes in 0.1 M $NaClO_4$ at 25°C.

Reaction	Equil. const.
$UO_2^{2+} + OH^- \rightleftarrows UO_2OH^+$	$10^{9.6}$
$UO^{2+} + 2OH^- \rightleftarrows UO_2(OH)_2$	$10^{18.2}$
$UO_2^{2+} + OH^- + Aa^- \rightleftarrows UO_2AaOH$	$\leq 10^{15.6}$
$UO_2^{2+} + Aa^- \rightleftarrows UO_2Aa^+$	$10^{6.8}$
$UO_2^{2+} + Aa^- + HAa \rightleftarrows UO_2AaHAa^+$	$10^{8.7}$
$UO_2^{2+} + 2Aa^- \rightleftarrows UO_2Aa_2$	$10^{13.1}$
$UO_2^{2+} + 2Aa^- + HAa \rightleftarrows UO_2Aa_2HAa$	$10^{14.8}$
$UO_2^{2+} + HAa \rightleftarrows UO_2HAa^{2+}$	< 1
$UO_2^{2+} + 2HAa \rightleftarrows UO_2(HAa)_2^{2+}$	< 10
$UO_2^{2+} + 3HAa \rightleftarrows UO_2(HAa)_3^{2+}$	< 100
$(UO_2Aa_2)_{aq} \rightleftarrows (UO_2Aa_2)_{CHCl_3}$	3.3
$(UO_2Aa_2HAa)_{aq} \rightleftarrows (UO_2Aa_2HAa)_{CHCl_3}$	22

The $\varkappa_{npr}$ values which have been calculated from the K_{xy} values of Table 12, are collected in Table 15. From these values and the relation

$$\varkappa_n = \prod_{i=0}^{i=n} k_i \qquad (32)$$

the different compexity constants k_i can be obtained.

It has been shown previously that no complex is formed between the metal and the organic solvents. We can therefore assume that the saturated complex contains t molecules of water. If the coordination number of the UO_2-group is 6, and we assume that Aa occupies two, and the other molecules or ions one coordinative position each around UO_2, it follows that $t = 6 - x - y$. Since complexity constants for a number of definite x and y values have been determined, the number of water molecules in these complexes can be obtained from this equation, if one definite coordination number really does exist for all uranium complexes.

One may think that the complex UO_2Aa_2HAa should rather be HUO_2Aa_3 which dissociates into H^+ and $UO_2Aa_3^-$. However, if this complex did exist, the curves in Fig. 7 should first increase to a maximum and then decrease with increasing pH; the curves would then resemble the dotted ones in Fig. 1 (Part A). Since this is not the case, negatively charged complexes of U(VI) cannot have been formed to any large extent in the solutions investigated here.

Only in the case of the U(VI) hydrolysis can a comparison be made with previously determined equilibrium constants. This hydrolysis has been studied by several authors and by different methods. LONGSWORTH [36] reports two constants which, recalculated to our complexity constant scale, give $\varkappa_{01} = 10^{10.7}$ and $\varkappa_{02} = 10^{20.4}$. From the polarographic measurements of HARRIS and KOLTHOFF [37], a value

---

[1] In a recent investigation (S. AHRLAND, S. HIETANEN and L. G. SILLÉN, Acta Chem. Scand. 8 (1954) 1907) a mechanism for the uranyl hydrolysis has been proposed, which does not include the formation of UO_2OH^+ and $UO_2(OH)_2$. This discrepancy will be analysed in a subsequent paper (XII, Part C, to be published in this journal).

$\varkappa_{01} = 10^{9.7}$ is obtained. AHRLAND [38] found mono- and dinuclear complexes; from his first mononuclear formation constant a $\varkappa_{01}$ value of $10^{9.3}$ can be calculated (1 M ionic strength). SUTTON [39] concludes that very little of the mononuclear complexes are formed, but gives formation constants for some polynuclear complexes. According to SILLÉN [40], from a recalculation of AHRLAND's data one may conclude that a primary dinuclear complex is formed, to which identical hydrolysed uranyl groups are added, thus building up very large polynuclear complexes.[1] In the investigations mentioned above the U(VI) concentration has usually been $> 10^{-3}$ M.

The agreement between AHRLAND's, and HARRIS and KOLTHOFF's, $\varkappa_{01}$ value and that obtained here ($10^{9.6}$) is very good, while the agreement with LONGSWORTH's results is reasonable. Since the original paper of LONGSWORTH could not be obtained, the reason for the difference cannot be indicated here.

In the investigation of the number of U atoms in each complex at the beginning of this paper, it could be concluded from the data of Fig. 4 that polynuclear complexes of U(VI) could be neglected for $[U] \leq 10^{-3}$ M and $[HAa]_{aq} \geq 0.0040$ M, and $pH \leq 7$, but not for $[U] > 10^{-3}$ M. From the result that the polynuclear complexes found at $[U] = 0.01$ M obviously prefer the aqueous phase rather than the $CHCl_3$ solution (q decreases with increasing [U]) and the fact that polynuclear complexes of U(VI) have only been reported in connection with its hydrolysis [41], the conclusion may be drawn that our polynuclear complexes at $[U] = 0.01$ M are probably hydrolysed uranium species. The question then arises why we do not find any polynuclear complexes at $[U] = 10^{-3}$ M, when both SUTTON and SILLÉN report polynuclear complexes at this concentration. There may be two explanations.

The concentration of free UO_2^{2+} ions decreases with increasing HAa concentration. Thus about 95 % of the uranium will be found to be UO_2^{2+} in an 0.001 M HAa solution of pH 3, while only about 10 % UO_2^{2+} will be found if the solution is 0.1 M in acetylacetone. Since the tendency to form polynuclear complexes decreases with decreasing UO_2^{2+} concentration, the concentration of polynuclear complexes will be found to be much lower in the presence of acetylacetone than in its absence. The acetylacetone in our solutions may thus lower the concentration of UO_2^{2+} to such a considerable degree that polynuclear complexes are undetectable.

With decreasing HAa concentration the hydrolysed fraction of U(VI) will increase and show a maximum for the last two curves in Fig. 7. The constants given in Table 15 for the formation of hydrolysed U(VI) species will therefore rely very much on these two curves. However, due to experimental difficulties no tests for polynuclearity have been made in this region. Thus it has not been proved that only mononuclear complexes are formed at these small values

Table 16. Equilibrium constants for Th(IV) acetylacetone complexes in 0.1 M $NaClO_4$ at 25°C in the presence of a methyl isobutyl ketone (Hex) phase.

Reaction	Equil. const.
$ThAa_2Hex_4^{2+} + Aa^- \rightleftarrows ThAa_3Hex_2^+ + 2Hex$	$k_3 = 10^{8.0}$
$ThAa_3Hex_2^+ + Aa^- \rightleftarrows ThAa_4 + 2Hex$	$k_4 = 10^{4.3}$
$(ThAa_4)_{aq} \rightleftarrows (ThAa_4)_{hexone}$	$\lambda_4 = 10^{1.5}$

---

[1] See footnote, p. 136.

of [HAa] and [H]. The constants given in Table 15 for complexes containing OH can therefore not be regarded as conclusive.[1] However, it seems remarkable that the same constants should be obtained for a fictive mononuclear hydrolysis process with different U(VI) concentrations and so different methods of investigation as spectrophotometric, potentiometric, polarographic and two-phase distribution.

8. The Th(IV) complexes

8 a. Complexes with hexone

There are a great number of facts indicating that Th has a coordination number of 8 (e.g. [42]). In a previous section the formation of $ThAa_nHex_s$ complexes have been reported. It seems reasonable to believe that each Aa-group occupies 2, and each Hex-group 1, coordination positions around Th. In the complex some water molecules may also be coordinated to saturate the coordination number of 8. We shall therefore write the complex $ThAa_nHex_s(H_2O)_t$, where we have $8 = 2n + s + t$.

The equilibrium constant for the reaction

$$ThAa_3(H_2O)_2^+ + Aa^- \rightleftharpoons ThAa_4 + 2\,H_2O$$

has been determined to be $10^{5.0\pm0.05}$ [26], where $[H_2O] = 1$. Since we have obtained here another constant for the reaction

$$ThAa_3(Hex)_{s_2}(H_2O)_t^+ + Aa^- \rightleftharpoons ThAa_4(Hex)_{s_3} + (S_2 - S_3)Hex + t\,H_2O,$$

$k_4 = 10^{4.3\pm0.15}$, the two reactions must involve different Th species. We can first conclude that $s_3 = 0$, since $ThAa_4$ is a saturated complex. It seems reasonable to believe that the complexes are symmetrical with respect to H_2O and Hex. From this it then follows that $s_2 = 2$ and $t = 0$ in the reaction formula above.

We can then write the other reaction in the hexone system

$$ThAa_2Hex_{s_1}(H_2O)_t^{2+} + Aa^- \rightleftharpoons ThAa_3Hex_2^+ + (S_1 - 2)\,Hex + t\,H_2O,$$

for which the equilibrium constant $k_3 = 10^{8.0\pm0.15}$ was obtained. In this case we have two possibilities; either $s_1 = 2$ and $t = 2$, or $s_1 = 4$ and $t = 0$. In the former case the work required to replace 2 molecules of H_2O by Aa^- in the coordination sphere should be almost the same as that for the reaction

$$ThAa_2(H_2O)_4^{2+} + Aa^- \rightleftharpoons ThAa_3(H_2O)_2^{2+} + 2\,H_2O,$$

for which an equilibrium constant of $10^{6.0}$ ($[H_2O] = 1$) has previously been obtained [26]. Since the equilibrium constant is much higher in the presence of hexone, we must conclude that $t = 0$ and $s_1 = 4$ in this reaction.

From this "method of exclusion" it then follows that the constants obtained should refer to the reactions given in Table 16.

---

[1] See footnote, p. 136.

8 b. The influence of the hydrolysis

From studies of the hydrolysis of thorium KRAUS and HOLMBERG [43] found that Th already polymerises at pH 3 in $5 \cdot 10^{-4}$ M solutions. LUNDGREN and SILLÉN [13] and LUNDGREN [44] have demonstrated that, in the solid compounds $Th(OH)_2$-CrO_4H_2O and $Th(OH)_2SO_4$, the crystals are built up of long chains with the composition $(Th(OH)_2)_n^{+2n}$. That the hydrolysed Th complexes in solution probably consist of long chains of composition $Th(OOHTh)_n$ is shown by HIETANEN [45].

From the theoretical part of this paper it follows that if polynuclear hydrolysed Th species are formed, the distribution curves should show a [Th] and pH dependence at constant pAa. The fact that neither of these dependences is found indicates that the hydrolysis of the metal can be neglected.

If one uses the constants obtained by HIETANEN for the polynuclear hydrolysis of thorium and makes the assumption that this hydrolysis mechanism also holds for our low Th concentrations, one will find that the experiments have been carried out very close to the "hydrolysis border"; a few percent of the metal has probably been hydrolysed. The use of KASPER'S [46] constants for a presumed mononuclear hydrolysis will lead to approximately the same result. It was found that the experimental points for the hexone curve fell somewhat below the curve when the HAa concentration was decreased to < 0.05 M. This is certainly caused by the hydrolysis of a considerable part of the metal at this low HAa concentration. However, in the experiments recorded in Fig. 6, the hydrolysed amount was so low that it could not be observed. The results, however, indicate that the thorium hydrolysis can be studied by the extraction method if the parameters are varied properly.

In a recent paper KRAUS and HOLMBERG [47] point out that their work and also HIETANEN'S [45] on the hydrolysis of Th is in complete disagreement with the conclusion, which has been formed both here and in a previous paper by the author [4], that the Th-hydrolysis can be neglected in our distribution experiments up to pH 6. Their statement appears to be based on a misinterpretation. Certainly the concentration of the hydrolysed species of thorium at pH $\approx$ 6 is much greater than the concentration of free Th^{4+}. However, in the papers [4, 26] it is only stated that

$$\sum^{m,p}[Th_m(OH)_p] \ll \sum^{n}[ThAa_n] \text{ at pH} \le 6,\ [HAa]_{aq} \ge 0.005\ M \text{ and } [Th] \le 2.10^{-6}\ M.$$

This means that *the concentration of hydrolysed Th can be neglected compared with the concentration of Th acetylacetone species.*

Summary

The distribution of U(VI) and Th between water and organic solvents (C_6H_6, $CHCl_3$, $C_4H_9COCH_3$) has been studied as a function of pH and acetylacetone (HAa) concentration. Formation constants have been calculated for the complexes UO_2Aa_n-$(OH)_p(HAa)_r$, where n and $p \le 2$ and $r \le 3$, and constants are given for the distribution of UO_2Aa_2 and UO_2Aa_2HAa between $CHCl_3$ and H_2O (Table 15).

$ThAa_n$ ($n = 2$ and 3) was found to give complexes with the solvent methyl isobutyl ketone ($C_4H_9COCH_3 = Hex$) and equilibrium constants for the reaction of $ThAa_2Hex_4^{2+}$ and $ThAa_3Hex_2^{+}$ with Aa^- are given (Table 16).

All experiments have been carried out in 0.1 M $NaClO_4$ at 25°C.

The author wishes to thank the head of FOA 1, Prof. G. LJUNGGREN, for his kind interest in this work, Prof. L. G. SILLÉN for many valuable suggestions, and Mrs. BRITTA RYDBERG for carrying out most of the experiments.

Research Institute of National Defence, Dept. 1, Sundbyberg 4, Sweden.

REFERENCES

(*References 1–21 will be found in Ref. 22*)

22. J. RYDBERG, Previous paper, this journal.
23. B. HÖK, Svensk Kem. Tidskr. *65* (1953) 106.
24. G. R. PRICE, R. J. FERRETTI, and S. SCHWARTZ, Anal. Chem. *25* (1953) 322.
25. R. SKJÖLDEBRAND, AB Atomenergi, Stockholm; Report November 1953.
26. J. Rydberg, Arkiv för Kemi *5* (1953) 413.
27. J. RYDBERG, Svensk Kem. Tidskr. *65* (1953) 37.
28. J. RYDBERG, Svensk Kem. Tidskr. *62* (1950) 179.
29. D. DYRSSEN, Svensk Kem. Tidskr. *62* (1950) 153.
30. W. BILTZ and J. A. CLINCH, Z. anorg. Chem. *40* (1904) 218.
31. K. HAGER, Z. anorg. Chem. *162* (1927) 82.
32. H. W. MORGAN, AECD-2659 (1949).
33. E. W. ABRAHAMSON and A. S. S. BROWN, J. Am. Chem. Soc. *72* (1950) 1424.
34. J. HALPERN, Can. J. Chem. *31* (1953) 705.
35. S. AHRLAND, Acta Chem. Scan. *7* (1953) 485.
36. LONGSWORTH *et al.*, MDDC 911.
37. W. E. HARRIS and I. M. KOLTHOFF, J. Am. Chem. Soc. *69* (1947) 446.
38. S. AHRLAND, Acta Chem. Scand. *3* (1949) 374.
39. J. SUTTON, J. Chem. Soc. *1949*, 5275.
40. L. G. SILLÉN, Symposium on Coordination Chemistry; Copenhagen 1953.
41. R. E. CONNICK, Symposium on Complex Ions and Polyelectrolytes, Ithaca, N.Y. 1951.
42. J. P. HUNT and H. TAUBE, J. Chem. Phys. *19* (602) 1951.
43. K. A. KRAUS and R. W. HOLMBERG, AEDC-2919 (1950).
44. G. LUNDGREN, Arkiv för Kemi *2* (1950) 535.
45. S. HIETANEN, Acta Chem. Scand. *8* (1954) 1626.
46. J. KASPER, Diss. Baltimore 1941.
47. K. A. KRAUS and R. W. HOLMBERG, J. Phys. Chem. *58* (1954) 325.

Tryckt den 26 april 1955

Uppsala 1955. Almqvist & Wiksells Boktryckeri AB

ARKIV FÖR KEMI Band 8 nr 15

Communicated 12 January 1955 by ARNE TISELIUS

On the relation between phosphorolysis and glycolysis in human erythrocytes

By HANS G. BOMAN

In a recent investigation FÅHRÆUS and BOMAN (1) studied temperature effects on the red cells. It was found that incubating the erythrocytes at 40–41° for 5 hours gave rise to large changes in cell volume and that this phenomenon was connected with the dephosphorylation, the glycolysis and the potassium content of the red cells. However, it was also found that the heating produced a lowering of the pH from 7.5 to 7.35 (figs. 10 and 20)[1] and that direct acidifying by CO_2 had a similar influence on the cells as heating. It is, therefore, evident that the pH of the blood is very important for the balance between different metabolic processes.

This is in agreement with older studies by MARTLAND (2) and by RAPOPORT and GUEST (3) showing that the red cells hydrolyse phosphoric esters at pH values below 7.35, but synthesise them above 7.35. From the results of FÅHRÆUS and BOMAN it can be seen that in all experiments where there is a strong phosphorylysis (figs. 7, 8, and 9) the pH has been decreased either by CO_2 or by heating.

Further, it has been shown by GUEST and RAPOPORT (4) that the main part of the organic phosphate of human blood is 2,3-diphosphoglyceric acid. Other important phosphoric esters present in the blood must be glucose-6-phosphate and all the other intermediary phosphorylised reaction products of glycolysis. All these compounds must be regarded as possible substrates for the acid phosphatases of the red cells.

According to the "Embden-Meyerhof" scheme the phosphorylation occurs through transfer of the terminal phosphate of ATP to glucose, a reaction which is catalysed by a phosphokinase.

On the basis of this knowledge it is possible to put forth the following relation between phosphorolysis and glycolysis in human erythrocytes *in vitro*:

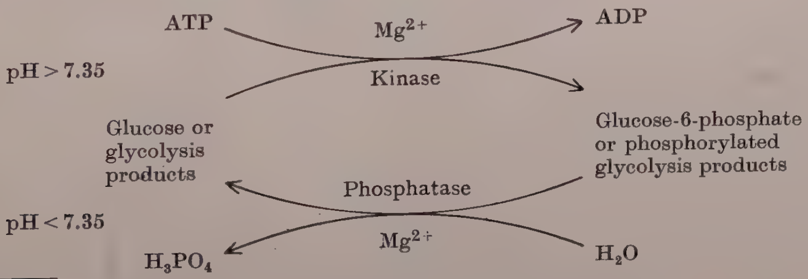
ATP
Mg2+
ADP
pH > 7.35
Kinase
Glucose or glycolysis products
Glucose-6-phosphate or phosphorylated glycolysis products
Phosphatase
pH < 7.35
Mg2+
H3PO4
H2O

---

[1] All numbers of figures here given refer to FÅHRÆUS and BOMAN (1).

The direction of the reaction in the above formula would be regulated by the pH of the blood and the pH optima for the different enzymes. However, the control mechanism, even *in vivo*, must at least be influenced by the following two factors:

The first one is the variation of the pH optimum with the substrate concentration. This has been found for several enzymes, among them alkaline phosphatases (cf. Ross *et al.* (5)). A similar relation would explain the differences in the pH optima found by ABUL-FADL and KING (6) and by TSUBOI and HUDSON (7) for the acid phosphatases of the red cells.

The second factor is the concentration of magnesium which is known to be an activator of both phosphokinases and acid phosphatases. Moreover SADASIVAN (8, 9) has demonstrated that also the pH optimum can be strongly influenced by small amounts, not only of magnesium, but of calcium and zinc ions. These metals are present in the blood and their concentrations are thus likely to influence the activities of the metal-ion-activated enzymes considered here.

In a steady state system with constant pH these factors may thus together regulate not only the proportions but also *the absolute concentrations* of the different reaction intermediates in the glycolytic scheme. This can be seen from the fact that if the substrate concentration is suddenly increased the enzyme will hydrolyse the substrate until that substrate concentration is reached at which the pH optimum is so distant from the constant (physiological) pH that the splitting by the phosphatase is balanced by the synthetic activity of the kinase.

Naturally, it is very difficult to prove a hypothesis like this. It is not yet possible to determine the concentration of the different natural substrates present in the blood and the pH optima for the enzymes in the complete system. However, the hypothesis may contribute to the understanding of some of the physical properties of the red cells as studied by FÅHRÆUS and BOMAN (1). It also offers an explanation of the role of the acid phosphatases of the erythrocytes and it does not seem to contradict our present information about the red cells.

I wish to thank Drs. O. SNELLMAN and B. MALMSTRÖM for stimulating discussions about this metabolic problem.

Institute of Biochemistry, University of Uppsala, Uppsala, Sweden.

REFERENCES

1. FÅHRÆUS, R., and BOMAN, H. G., Acta Soc. Med. Upsaliensis *59*, 317 (1954).
2. MARTLAND, M., Biochem. J. *19*, 117 (1925).
3. RAPOPORT, S., and GUEST, G. M., J. Biol. Chem. *129*, 781 (1939).
4. GUEST, G. M., and RAPOPORT, S., J. Biol. Chem. *123*, XLVII (1938).
5. ROSS, M. H., ELY, J. O., and ARCHER, J. G., J. Biol. Chem. *192*, 561 (1951).
6. ABUL-FADL, M. A. M., and KING, E. J., Biochem. J. *45*, 51 (1949).
7. TSUBOI, K. K., and HUDSON, P. B., Arch. Biochem. *43*, 339 (1953).
8. SADASIVAN, W., Arch. Biochem. *37*, 172 (1952).
9. ——, Nature *170*, 421 (1952).

Tryckt den 26 april 1955

Uppsala 1955. Almqvist & Wiksells Boktryckeri AB

ARKIV FÖR KEMI Band 8 nr 16

Communicated 1 December 1954 by ARNE TISELIUS and ARNE FREDGA

Stereochemical studies on dicarboxylic acids

II. The formation of quasi-racemic compounds as determined by infrared absorption

By ANDREAS ROSENBERG and LENNART SCHOTTE

With 8 figures in the text

In the problem of establishing the configurative relationships between different optically active substances the formation of quasi-racemic compounds plays an important role. A molecular compound formed from two optically active substances is considered as a quasi-racemic compound, if, and only if, each component forms a molecular compound only with one antipode of the other. In such a case it is of course obvious that the steric factors are of primary importance in the formation of the compounds. The quasi-racemate method has been thoroughly investigated and successfully applied to a number of steric problems by FREDGA and collaborators (1). The main factor is that the structural differences between the compounds investigated must not be too great, but also the tendency of the enantiomorphs to form a true racemic compound seems to be important. MATELL (2) has, however, found that the formation of quasi-racemates depends more on structural similarities than on tendencies to form true racemates.

Although X-ray diagrams often prove to be of value, the existence of the quasi-racemic compounds is usually demonstrated by means of melting point curves. These diagrams can be obtained according to RHEINBOLDT (3), but as this method is rather time-consuming, the application of the microscopical methods of KOFLER (4), as shown by MATELL (5), has proved very valuable. However, when the substances decompose during the melting process or racemize at higher temperatures, the use of the melting point method is difficult if not impossible. An investigation of the solubility properties and the optical activity in different solvents then often gives valuable information.

Work done previously on the infrared absorption of stereoisomeric compounds, amongst others by ELIEL and KOFRON (6) and the present authors (7 and 8), has shown that the differences observed are significant enough to distinguish between the active and racemic forms of the same substance. Thus it could be assumed that a study of the infrared absorption curves for different mixtures of optically active substances should give valuable evidence for the existence of quasi-racemic compounds. The tendency to form such compounds should appear as differences in the absorption curves obtained from two different equimolar mixtures of the pair of compounds examined, where one mixture consists of the (+)- and (−)-forms of the respective substances, the other of the two components having the same mode of rotation.

The first system investigated consisted of α,α′-dimethylglutaric acid (I), α-methylglutaric acid (II), methyl-thiodiglycolic acid (III), and thiodilactic acid (IV).

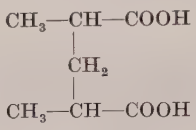

$$\begin{array}{l} CH_3{-}CH{-}COOH \\ \qquad | \\ \qquad CH_2 \\ \qquad | \\ CH_3{-}CH{-}COOH \end{array}$$

(I)

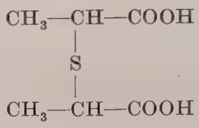

$$\begin{array}{l} CH_3{-}CH{-}COOH \\ \qquad | \\ \qquad S \\ \qquad | \\ CH_3{-}CH{-}COOH \end{array}$$

(IV)

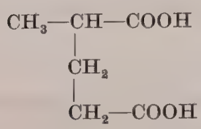

$$\begin{array}{l} CH_3{-}CH{-}COOH \\ \qquad | \\ \qquad CH_2 \\ \qquad | \\ \qquad CH_2{-}COOH \end{array}$$

(II)

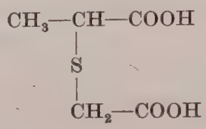

$$\begin{array}{l} CH_3{-}CH{-}COOH \\ \qquad | \\ \qquad S \\ \qquad | \\ \qquad CH_2{-}COOH \end{array}$$

(III)

It has been experimentally proved by FREDGA that equimolar amounts of optically active (I) and (II) (9) and (I) and (IV) (10), if crystallized together, form quasi-racemic compounds. A similar mixture of optically active (II) and (III) (9) shows no such tendency. The behaviour of (III) and (IV) from this point of view has not been investigated previously.

The mixtures were prepared by weighing equimolar amounts of the pure optically active substances, dissolving them in a suitable solvent and mixing the solutions. The solution thus obtained was dropped on finely pulverized potassium bromide, which was then dried *in vacuo* over phosphorus pentoxide and pressed to a transparent disc according to the method developed by SCHIEDT and REINWEIN (11). For each pair of substances to be examined two mixtures were prepared as outlined above.

Figures 1 and 2 represent respectively the spectra of (+)-α,α′-dimethylglutaric acid (I) mixed with (−)-α-methylglutaric acid (II) and (+)-α,α′-dimethylglutaric acid (I) mixed with (+)-α-methylglutaric acid (II). The spectrum of the mixture of the dextrorotatory compounds is an additive spectrum of the individual substances. This was verified by comparing this absorption curve with a spectrum obtained from a mechanical mixture of the same components in the dry state. If we now compare the infrared absorption curve of the mixture of (+)- and (−)-forms represented by Figure 1 with that in Figure 2 we see that, among other changes, a number of new absorption peaks are observed which were absent in the spectrum of the mixture of both the (+)-acids. These absorption peaks, e.g. at 7.51 μ, 9.65 μ, 11.95 μ and 12.35 μ, characteristic for the quasi-racemic compound, seem to be at frequencies found in the pure components although their positions are shifted in varying degrees as compared to their positions in the component state. A very interesting band is the broad absorption band commonly ascribed to the out of plane bendings of OH (12). For the pure optically active substances it is found at 10.70–10,75 μ. However, for the quasi-racemic compound it has been clearly shifted to 10.80 μ. The weak but well-defined absorption peak at 10.25 μ is further missing even at very high concentrations in the spectra of the separately examined components.

The additive absorption of the pure optically active substances found in the spectrum of the (+)-acid mixture between 8–8.25 μ is completely absent in that of the quasi-racemic compound. The general appearance of the spectra of mixtures from acids having the same mode of optical rotation is that of an impure substance.

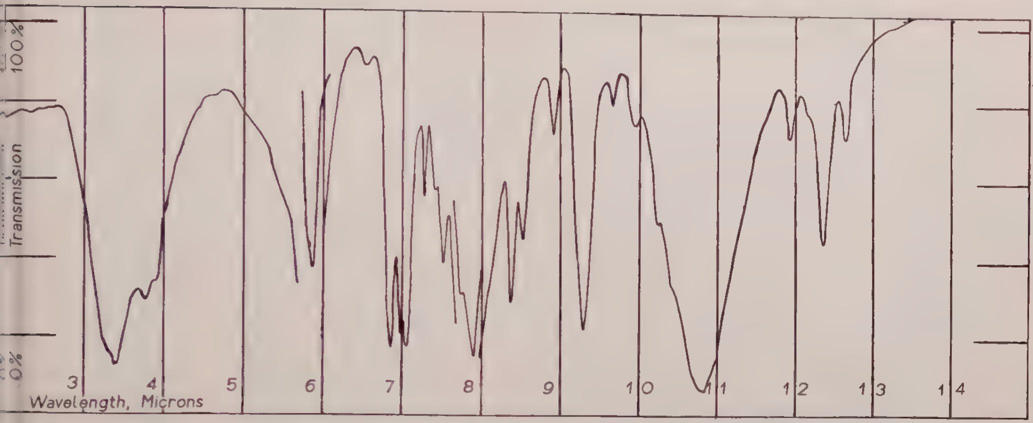

Fig. 1. (+)-α,α′-Dimethylglutaric acid and (−)-α-methylglutaric acid.

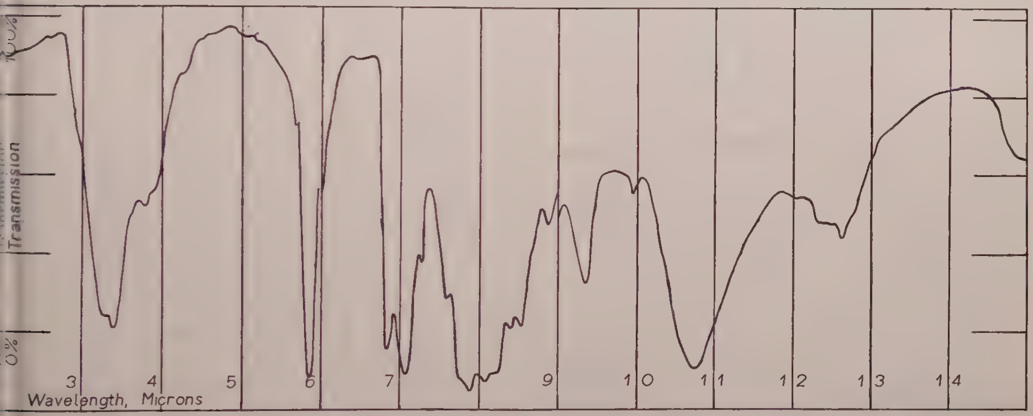

Fig. 2. (+)-α,α′-Dimethylglutaric acid and (+)-α-methylglutaric acid.

This phenomena of bad resolution is usually observed when substances investigated in the solid state contain impurities. The spectra of solutions are seldom influenced by foreign matter as long as these do not tend to form complexes or react chemically in the solvent used.

By examining the system α-methylglutaric acid (II) and methyl-thiodiglycolic acid (III), it was possible to study the behaviour of the infrared absorption curves of the two different mixtures of optically active acids when no quasi-racemic compound is formed. As shown by FREDGA the melting point curves obtained form mixtures of the optically active forms of methyl-thiodiglycolic acid (III) and α-methylglutaric acid (II) are very similar in shape and of the common eutectic type (9). It was thus impossible to draw any conclusions on the steric relationships of these acids. For our investigation the procedure outlined above was repeated. Figure 3 shows the spectrum of a mixture of the levorotatory forms of the two substances. When compared with Figure 4, representing the absorption of the mixture of the

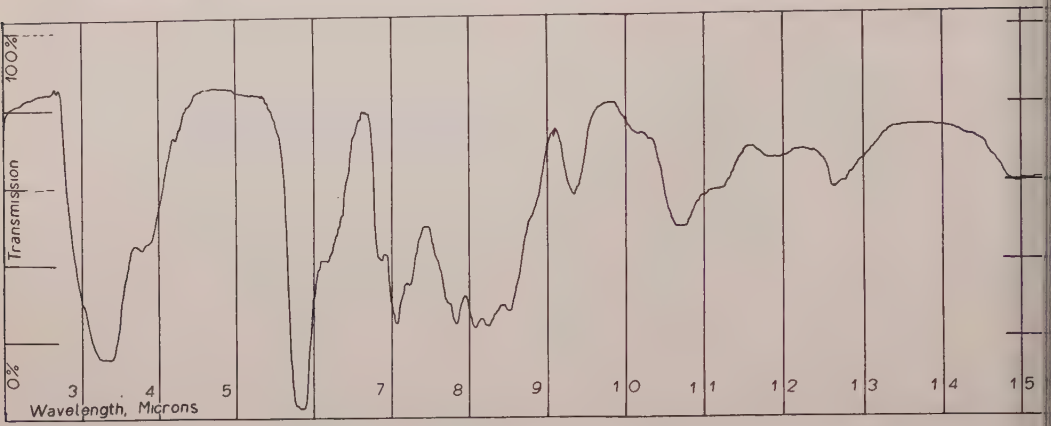

Fig. 3. (−)-Methyl-thiodiglycolic acid and (−)-α-methylglutaric acid.

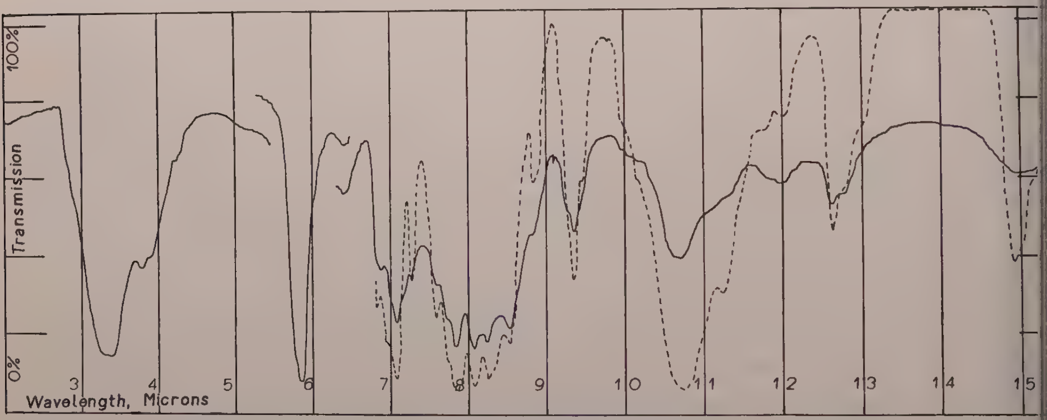

Fig. 4. (−)-Methyl-thiodiglycolic acid and (+)-α-methylglutaric acid. The dotted curve represents the *dry* mixture of the same acids.

acids with opposite modes of rotation, no differences in the positions of the bands can be detected, nor do any new bands appear. The dotted curve in Figure 4 represents the spectrum of a dry mixture containing (+)-(II) and (−)-(III), showing the additive absorption. It is thus quite obvious that the (+),(−)-mixture behaves exactly in the same manner as the (−),(−)-mixture forming no molecular compound.

The only difference observed between different preparations of both the mixtures was that the relative intensity of some absorption bands could be variable up to 2 or 3 % of transmission. As these differences were observed even between different preparations of the same type of mixture, they are probably due to difficulties in weighing, mixing and crystallizing such small amounts of material in exactly reproducible proportions.

The next pair of acids to be investigated was α,α′-dimethylglutaric acid (I) and thiodilactic acid (IV). Figure 5 represents part of the infrared spectra of both the

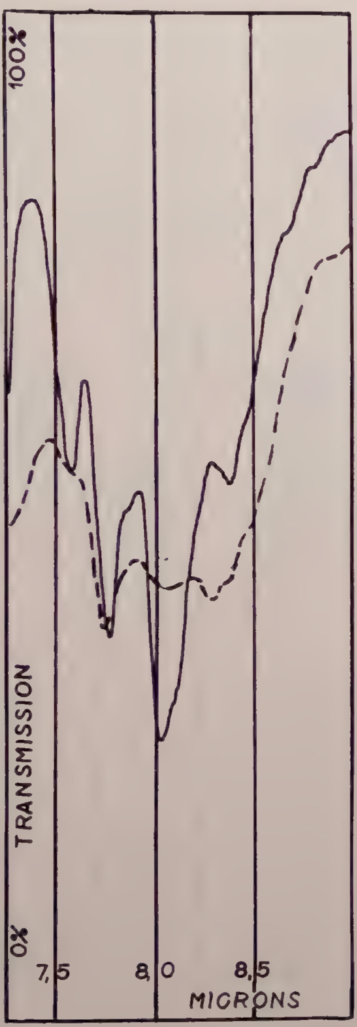

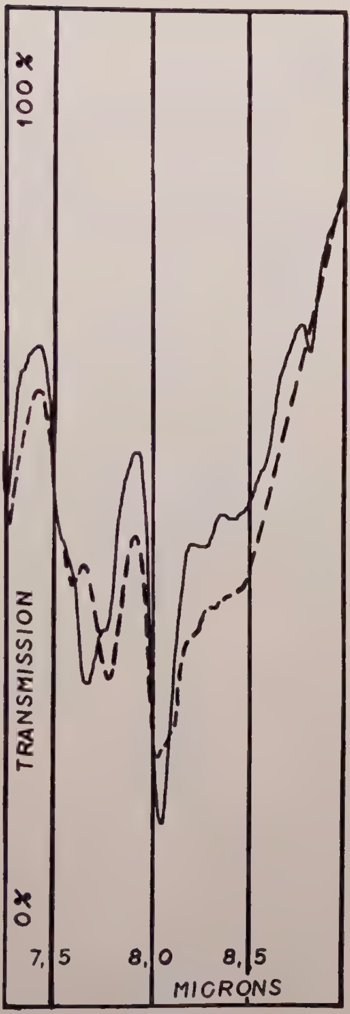

Fig. 5. (+)-α,α'-Dimethylglutaric acid and (+)-thiodilactic acid.
(+)-α,α'-Dimethylglutaric acid and (−)-thiodilactic acid (dotted curve).

Fig. 6. (−)-Methyl-thiodiglycolic acid and (+)-thiodilactic acid.
(−)-Methyl-thiodiglycolic acid and (−)-thiodilactic acid (dotted curve).

mixtures, recorded between 7.25 μ and 9 μ, which usually is a representative region. Differences exist, however, even at longer wavelengths. The differences observed support the previous result by Fredga (10), who demonstrated the existence of a quasi-racemic compound in this case by means of melting point curves.

Figure 6 shows the spectra of the different mixtures of optically active methylthiodiglycolic acid (III) and thiodilactic acid (IV). From the absorption curves between 7.25 μ and 9 μ it is clear that the differences in the positions of the absorption bands are distinct enough to justify the conclusion that the two acids with opposite modes of optical rotation form a quasi-racemic compound if crystallized

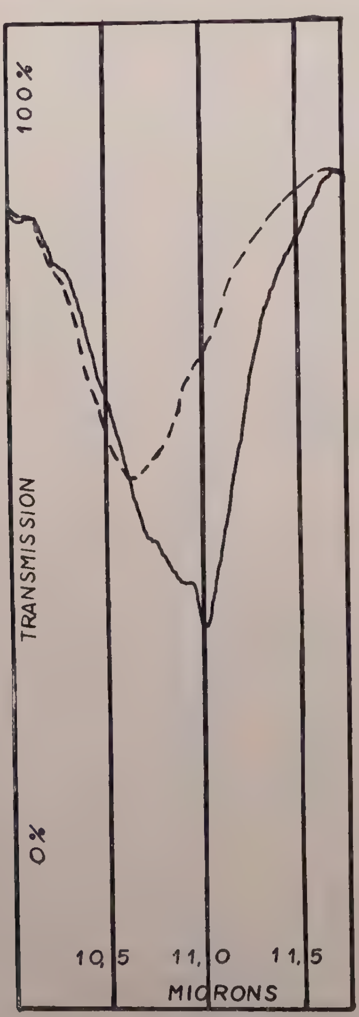

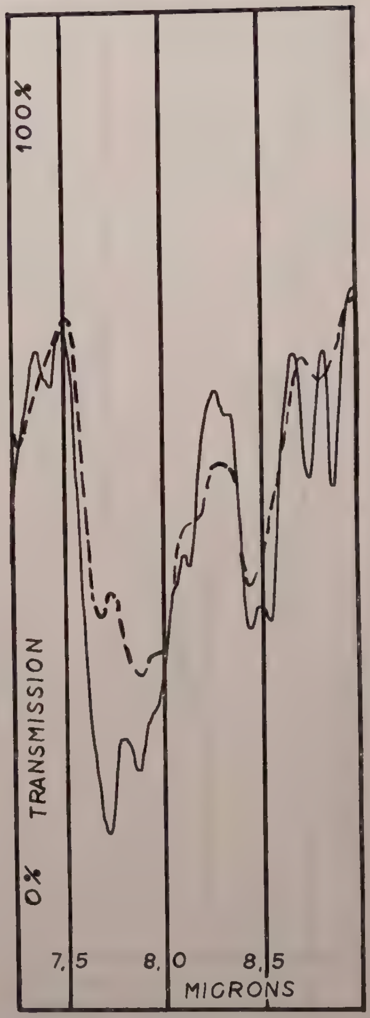

Fig. 7. (+)-Selenophane-2,5-dicarboxylic acid and (−)-thiophane-2,5-dicarboxylic acid. (+)-Selenophane-2,5-dicarboxylic acid and (+)-thiophane-2,5-dicarboxylic acid (dotted curve).

Fig. 8. (+)-Cyclotetramethylene-diselenide-3,6-dicarboxylic acid and (−)-1,2-dithiane-3,6-dicarboxylic acid.
(+)-Cyclotetramethylene-diselenide-3,6-dicarboxylic acid and (+)-1,2-dithiane-3,6-dicarboxylic acid (dotted curve).

together. The steric relationships between the two acids was previously indicated by the fact that the active forms with the same mode of optical rotation can be prepared from the same optically active thiolactic acid (10 and 13).

From the study of a system of four aliphatic dicarboxylic acids it is thus clearly demonstrated that by infrared methods an identification of any possible tendency to form molecular compounds of the quasi-racemic type is practicable. In order to find out if this effect is general for systems of different types, the investigation was also extended to some heterocyclic acids, the steric relationships of which were already established. Thus the optically active forms of thiophane-2,5-dicarboxylic acid (V) (tetrahydrothiophene-2,5-dicarboxylic acid), and selenophane-2,5-dicarboxylic acid (VI) (tetrahydroselenophene-2,5-dicarboxylic acid) were examined in mixtures in the same way as outlined above. The choice of these analogous compounds with sulphur and selenium as heteroatoms is especially well-grounded, since the possibility of obtaining quasi-racemic compounds for such systems has been investigated in several cases (1). The configuration determinations here usually do not present any difficulties.

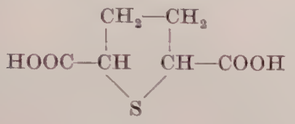

(V)

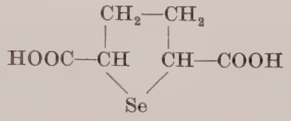

(VI)

Figure 7 shows a part of the infrared spectra of the two mixtures. The region between 10–11.75 μ was chosen, as the shift of the broad OH-band is extremely well-defined and easy to detect. The existence of a quasi-racemic compound in this system has previously been demonstrated by FREDGA (14) by means of melting point diagrams. It is obvious from the absorption curves that the infrared results support this statement.

The last system examined consisted of 1,2-dithiane-3,6-dicarboxylic acid (VII) and cyclotetramethylene-diselenide-3,6-dicarboxylic acid (VIII). It is of interest to mention here that according to investigations by FREDGA (15) valuable information about the steric relationships of the optically active six-membered cyclic dicarboxylic acids (VII) and (VIII) can be obtained by solubility determinations. We have here a case, where the substances melt with decomposition, thus making the use of melting point curves impossible. However, from a careful comparative study of solubility properties of the sulphur and selenium derivatives, FREDGA concluded that a quasi-racemic compound is formed between the respective acids with opposite modes of rotation. Our infrared examination of the system in question has also given evidence for the existence of a molecular compound.

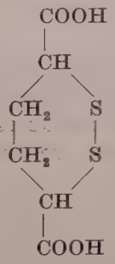

(VII)

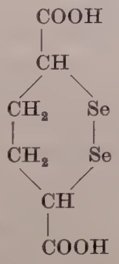

(VIII)

The absorption curves are given in Figure 8, from which it is evident that the differences are rather obvious. The two similar peaks between 8.5 μ and 9.0 μ in the spectrum of the (+)-acid mixture are not due to any interference phenomena, as they are identical for several preparations with different amounts of potassium bromide resulting in discs of varying thickness.

Table 1. Data of the dicarboxylic acids investigated.

Substance	Melting point	Reference
(+)-α,α′-Dimethylglutaric acid (I)	79°	(9)
(+)-α-Methylglutaric acid (II)	82°– 83°	(9)
(−)-α-Methylglutaric acid (II)	82°– 83°	(9)
(−)-Methyl-thiodiglycolic acid (III)	77°– 78°	(9)
(+)-Thiodilactic acid (IV)	117°	(10)
(−)-Thiodilactic acid (IV)	117°–118°	(10)
(+)-Thiophane-2,5-dicarboxylic acid (V)	180°	(14)
(−)-Thiophane-2,5-dicarboxylic acid (V)	179°–180°	(14)
(+)-Selenophane-2,5-dicarboxylic acid (VI)	173°–174°	(14)
(+)-1,2-Dithiane-3,6-dicarboxylic acid (VII)	255°[1]	(15)
(−)-1,2-Dithiane-3,6-dicarboxylic acid (VII)	255°[1]	(15)
(+)-Cyclotetramethylene-diselenide-3,6-dicarboxylic acid (VIII)	*c.* 205° (d)[1]	(15)

[1] Preheated apparatus.

The evidence now presented gives a fairly good picture of the possiblities of the infrared method. As can be seen from the absorption curves the main differences between the (+),(+)- and (+),(−)-mixtures usually occur in the region of 7 μ to 9 μ and at longer wavelengths. The main carbonyl stretching frequency which for the true racemic compounds is often shifted in position as compared with the optically active forms, is unchanged in all the systems studied. This indicates that the changes of intermolecular distances in the formation of quasi-racemic compounds often are less than in the formation of true racemic structures.

In practice, care must be exercised when comparing the spectra of different mixtures. Dry equimolar mixtures of the components have infrared absorption curves with sharp peaks all being well resolved, as the smallest particles in the potassium bromide solution are pure crystals of the components. But when the same amount of this mixture is first dissolved and then crystallized, the infrared spectrum looses much of its resolution and many details are lost entirely. It has already been pointed out that this effect is analogous to that of any impurity which hinders the formation of a regular crystal lattice. The samples should thus be treated in exactly the same manner in order to allow a direct comparison.

It seems to us that if used with proper caution this infrared method provides an extremely convenient way of rapidly determining any tendency to form molecular compounds of a quasi-racemic character. The examination is possible even when only very small amounts of optically active substances are available.

Experimental

A Perkin Elmer model 21 spectrophotometer equipped with sodium chloride prism was used for the infrared absorption measurements. The solid samples of the acids were examined as solid pressed potassium bromide plates according to the method described by Schiedt and Reinwein (11).

Summary

A method involving the use of infrared absorption measurements to determine the existence of molecular compounds of quasi-racemic nature is presented.

The method is based upon studies on systems of aliphatic and heterocyclic carboxylic acids.

The probable existence of a quasi-racemic compound between the optically active forms of methyl-thioglycolic acid and thiodilactic acid with opposite modes of rotation has been pointed out.

Acknowledgements

The authors want to express their sincere gratitude to Professor ARNE TISELIUS and Professor ARNE FREDGA for their stimulating interest. All the substances were kindly placed at our disposal by Professor FREDGA.

Thanks are also due to Mr. STIG BERGWALL for valuable help with the experimental work.

This investigation is a part of a program on infrared research, which is financially supported by grants from the ROYAL SWEDISH ACADEMY OF SCIENCES, THE STATE COUNCIL OF TECHNICAL RESEARCH and the ROCKEFELLER FOUNDATION.

Institute of Biochemistry and Laboratory of Organic Chemistry, Chemical Institute, University of Uppsala, November 1954.

REFERENCES

1. A. FREDGA, "The Svedberg 1884 30/8 1944", 261 (Uppsala 1944).
2. M. MATELL, Arkiv Kemi *5* (1952) nr. 3.
3. H. RHEINBOLDT, J. prakt. Chem. [2] *111*, 242 (1925).
4. L. and A. KOFLER, Mikro-Methoden, p. 115 (Innsbruck 1948).
5. M. MATELL, Mikrochem. mikrochim. Acta *38*, 532 (1951).
6. E. L. ELIEL and J. T. KOFRON, J. Am. Chem. Soc. *75*, 4585 (1953).
7. A. ROSENBERG and L. SCHOTTE, Acta Chem. Scand., *8*, 867 (1954).
8. L. SCHOTTE and A. ROSENBERG, Arkiv Kemi *7* (1954) nr. 51.
9. A. FREDGA, Arkiv Kemi, Mineral., Geol. *24 A* (1947) nr. 32.
10. A. FREDGA, Arkiv Kemi, Mineral., Geol. *14 B* (1940) nr. 12.
11. U. SCHIEDT and H. REINWEIN, Z. Naturforsch. *7 b*, 270 (1952).
12. D. HADZI and N. SHEPPARD, Proc. Roy. Soc. (London) *216*, 247 (1953).
13. A. FREDGA, Arkiv Kemi, Mineral., Geol. *17 A* (1943) nr. 17.
14. A. FREDGA, J. prakt. Chem. [2] *150*, 124 (1938).
15. A. FREDGA, Arkiv Kemi, Mineral., Geol. *12 A* (1938) nr. 27.

Tryckt den 26 april 1955

Uppsala 1955. Almqvist & Wiksells Boktryckeri AB

ARKIV FÖR KEMI Band 8 nr 17

Communicated 26 January 1955 by J. A. Hedvall

The mechanism of the polymorphic transformation of mercuric iodide

By Georg Johansson

With 3 figures in the text

Mercuric iodide has a transition point at 127°C. The yellow high-temperature modification, however, can exist even at room temperature and is only after a certain induction period transformed into the red modification. The transition process can easily be observed because of the distinct colour change, and in well-developed crystals of yellow HgI_2 it always occurs in the same manner, with the interface between the two modifications parallel to the crystal edges, which seems to indicate that the transformation may take place through a concerted movement of the atoms in the lattice. The present investigation intends to show that by making a comparison between the structures of the two modifications it is possible to arrive at certain conclusions regarding the probable course of the transition process, conclusions which agree with experimental data.

The crystal structures of the two modifications

Red mercuric iodide has a tetragonal structure with the space group D_{4h}^{15}–P4/nmc (1), and the lengths of the axes are:

$$a = 4.356\ \text{Å};\ c = 12.34\ \text{Å}.$$

The unit cell contains 2 HgI_2 in the following positions:

Hg: $0, 0, 0;\ \frac{1}{2}, \frac{1}{2}, \frac{1}{2};$
I: $0, \frac{1}{2}, u;\ \frac{1}{2}, 0, \bar{u};\ 0, \frac{1}{2}, u+\frac{1}{2};\ \frac{1}{2}, 0, \frac{1}{2}-u.\ (u = 0.14)$

This is a layer structure, and each mercury atom is tetrahedrally surrounded by four iodine atoms at a distance of 2.78 Å.

Yellow mercuric iodide is orthorhombic with the space group C_{2v}^{12}–Cmc2_1 and the axis lengths

$$a = 4.674\ \text{Å};\ b = 7.32\ \text{Å};\ c = 13.76\ \text{Å}.$$

The unit cell contains 4 HgI_2. According to Wyckoff (1) no satisfactory values have been obtained for the parameters in yellow mercuric iodide. Gorsky (2), however, found at a structural investigation parameter values that closely approach those in mercuric bromide, which is isomorphous with yellow mercuric iodide; these values will be employed in the following considerations:

$$\begin{aligned}&\text{Hg: } 0, u, 0;\ 0, \bar{u}, \tfrac{1}{2};\ \tfrac{1}{2}, \tfrac{1}{2}+u, 0;\ \tfrac{1}{2}, \tfrac{1}{2}-u, \tfrac{1}{2};\\ &\text{I (I): } 0, v, w;\ 0, \bar{v}, \tfrac{1}{2}+w;\ \tfrac{1}{2}, \tfrac{1}{2}+v, w;\ \tfrac{1}{2}, \tfrac{1}{2}-v, \tfrac{1}{2}+w;\\ &\text{I (II): } 0, v_2, \bar{w};\ 0, \bar{v}_2, \tfrac{1}{2}-w;\ \tfrac{1}{2}, \tfrac{1}{2}+v_2, \bar{w};\ \tfrac{1}{2}, \tfrac{1}{2}-v_2, \tfrac{1}{2}-w;\\ &\qquad u = 0.341;\ v = 0.597;\ v_2 = 0.085;\ w = 0.132.\end{aligned}$$

This, too, is a layer structure, but every mercury atom is octahedrally surrounded by six iodine atoms, two at a distance of 2.62 Å, and four at a distance of 3.46 Å.

The transition mechanism

If the change of structure is considered from the aspect of the change in the linkage of the mercury atom, the transition process may be analyzed on the basis of the following assumptions: (i) The four iodine atoms to which the mercury atom is linked in red HgI_2 are among those six iodine atoms to which it is linked in the high-temperature modification, and at the transition yellow→red HgI_2 the bonds are not broken with the two iodine atoms that are most strongly bound. (ii) The transition process may to some extent take place through a concerted movement of the atoms.

The first assumption should be the more probable from the purely energetic point of view. The second assumption is based on the experimental observations during transition processes.

The transition from yellow to red mercuric iodide

The number of possibilities for the change to tetrahedral coordination are reduced to four by the first of the above-mentioned conditions, and all these possible changes fall within the original layer. Fig. 1 shows a projection of the two structures on the *ab* plane in such an orientation to each other that the relationship between the two lattices is quite evident. The possible directions of displacement are then [1 0 0], [$\bar{1}$ 0 0], [0 1 0] and [0 $\bar{1}$ 0]. Investigation shows, however, that the two last-named directions cannot involve a transition to the low-temperature modification by any simple and concerted movement of the different atoms, and according to the premisses only the directions [1 0 0] and [$\bar{1}$ 0 0]; are therefore possible for the displacement.

It will be seen from Fig. 1 that the transition involves an increase of the distances between atoms along the direction of the *a* axis (about 32 per cent), and a decrease of the distances along the *b* axis (about 16 per cent). There must consequently exist a direction (between the above-mentioned ones) where the distance remains constant, and it turns out that along the diagonal in the unit cell of the yellow modification the distance between the mercury atoms is practically the same as that along any of the crystallographic axes in the red modification. The transition process may consequently progress in this direction without any deformation of the original crystal worth mentioning, and without any stresses accumulating during the course of the transition process. The course of the process may be seen in Fig. 2, where unit cells of the low-temperature modification are shown, and also the atom displacements necessary for the transition; these displacements consequently all take place in the same direction. If the change of structure continues in the other directions, there will evidently occur considerable stresses in the diagonal direction, stresses which will increase during the course of the transition. It may then be expected that the transformation takes a rapid course along one of the diagonal directions, while

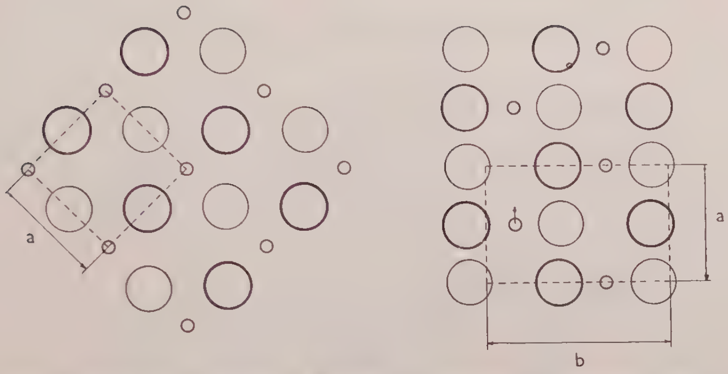

Fig. 1. Projection of the lattice of red and yellow HgI_2, respectively, in the *ab* plane. The positions of the mercury atoms (small circles) are on the same plane as the paper; the heavily marked iodine atoms occupy a plane above the paper surface, the other iodine atoms a plane below this surface.

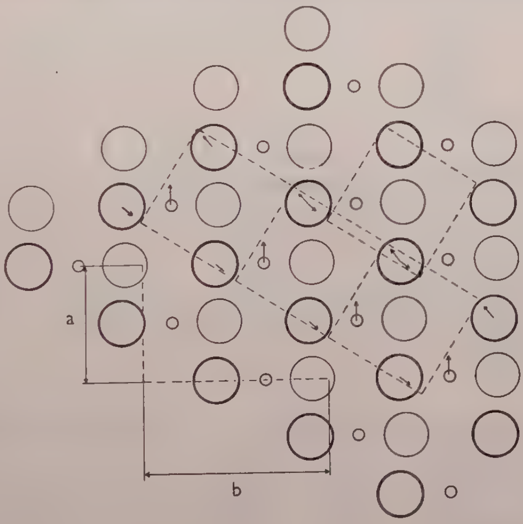

Fig. 2. The change from yellow to red mercuric iodide.

the continued transformation in the direction of the other diagonal makes considerably slower progress, and in such a way that the transformation front all the time is parallel to the first direction.

A closer examination of the atom positions in the relevant directions shows correspondence of the atom coordinates for the two modifications. This examination may be performed by rotating the coordinate system for the high-temperature modification until one axis coincides with one of the diagonal directions. After recalculating the coordinates to the axis lengths of the low-temperature modification and a displacement in parallel of the coordinate system, so that one of the iodine atoms in the tetrahedron denoted I obtains the same coordinates both in the high-temperature and in the low-temperature modification, the following coordinates are obtained for the atoms in the corresponding tetrahedra (cf. Fig. 2).

	High-temperature modification			Low-temperature modification		

I

Hg	0.27→ 0.50	0.64→ 0.50	0.51	½	½	½
I	0.50	0	0.36	½	0	0.36
	0.50	1.00	0.36	½	1	0.36
	0.04	0.27	0.65	0	½	0.64
	0.94	0.69	0.65	1	½	0.64

II

Hg	0.27→ 0.50	1.63→ 1.50	0.51	½	3/2	½
I	0.50	1.00	0.36	½	1	0.36
	0.50	2.00	0.36	½	2	0.36
	0.04	1.27	0.65	0	3/2	0.64
	0.94	1.69	0.65	1	3/2	0.64

III

Hg	0.27→ 0.50	2.63→ 2.49	0.51	½	5/2	½
I	0.50	2.00	0.36	½	2	0.36
	0.50	2.99	0.36	½	3	0.36
	0.04	2.27	0.65	0	5/2	0.64
	0.94	2.69	0.65	1	5/2	0.64

Two of the iodine atoms in a tetrahedron consequently occupy the same relative positions in both modifications, and the same is true of the mercury atoms after the change from 6-fold to 4-fold coordination. The other two iodine atoms are displaced in opposite directions, and to about the same extent in each tetrahedron (about 0.9 Å in the diagonal direction).

In the adjacent layer the following coordinates are obtained in one of the tetrahedra, on the assumption that the mercury atom is displaced in the same direction as in the previous layer:

	High-temperature modification			Low-temperature modification		
Hg	−0.02→ 0.21	1.18→ 1.05	−0.05	0	1	0
I	0.21	0.55	0.10	0	½	0.14
	0.21	1.54	0.10	0	3/2	0.14
	−0.25	0.82	−0.20	−½	1	−0.14
	0.65	1.24	−0.20	½	1	−0.14

The displacements in the diagonal direction are here the same as in the previous case, but the whole tetrahedron is further displaced in a direction at roughly right angle to the diagonal.

The transition from red to yellow mercuric iodide

The number of possibilities of transition from tetrahedral to octahedral coordination will be six in the given conditions, of which four can occur within the original layer, while the last two occur through displacement of the mercury atom along the direction of the *c* axis. The two last-named possibilities do not, however, appear to be able to cause a transition to the high-temperature modification through a concerted

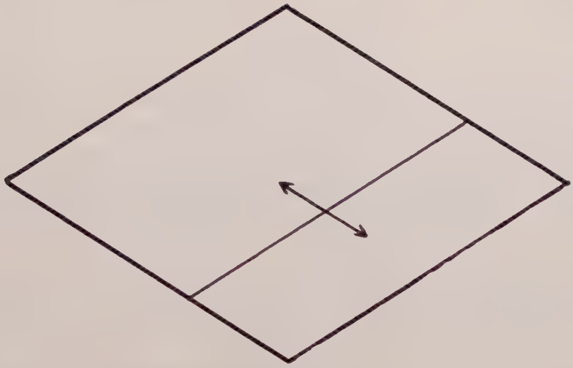

Fig. 3. The transition from yellow to red mercuric iodide.

movement of the atoms. In the case of the other possibilities the analysis will be analogous to that given previously (cf. Fig. 1). The interface should in this case be parallel to one of the axis directions.

Experimental investigations of the transition process

The transformation of yellow mercuric iodide crystals, formed by crystallization from a solution of HgI_2 in alcohol, has been described by COPPOCK (3), who observed the process with a microscope: "After about 15 minutes, nucleation usually occurs along the whole length of the crystal edge; the interface then advances rapidly across the crystal parallel to the opposite edge. Occasionally nucleation occurs as a thin strip in the interior of the crystal parallel to the edges; the interface then moves out towards the edges of the crystal with approximately the same linear rate in both directions. It appears that nucleation occurs along some weak axes in the crystal and immediately spreads along the whole length."

KOHLSCHÜTTER (4) has made a very thorough investigation of this transition. In the case of well-formed orthorhombic crystals of yellow mercuric iodide with edges parallel to the above-mentioned diagonal directions the transition started as a red hair-line, which suddenly expanded over the base surface parallel to the edges (Fig. 3). After a while it spread first on one side and then on the other, but all the time parallel to the edges. During this process the transition started in more deeply placed layers, and could in this way occur simultaneously in several layers, which, however, were always parallel to each other. During the transition the crystal split up along these surfaces (i.e. at right angles to the c axis), and the planes detached in this way proved to be of ever smaller dimensions the greater the magnification used for examination.

The theoretical conclusions advanced regarding the transition process at the change from the yellow to the red modification of mercuric iodide consequently show good agreement with the experimental observations. No such regularity of the phenomena has been observed, however, at the transition in the reverse direction. According to KOHLSCHÜTTER (4), the yellow colour suddenly spreads all over the crystal at the transition point, or else it appears in the form of separate nuclei, from which it then rapidly expands in all directions.

Summary

The transition mechanism at the change from the yellow to the red modification of mercuric iodide is discussed from the point of view of the structure of the two modifications, and the results are compared with the transition process as observed at experiments.

The author wishes to express his gratitude to Professor J. A. HEDVALL for his kind interest in this work.

Institutionen för silikatkemisk forskning, Jan. 20, 1955.

REFERENCES

1. R. W. G. WYCKOFF, Crystal Structures. Vol. I.
2. W. S. GORSKY, Phys. Z. Sowjetunion *5*, 367 (1934).
3. J. B. M. COPPOCK, Nature *133*, 570 (1934).
4. H. W. KOHLSCHÜTTER, Koll. Chem., Beihefte *24*, 319 (1927).

Tryckt den 19 april 1955

Uppsala 1955. Almqvist & Wiksells Boktryckeri AB

ARKIV FÖR KEMI Band 8 nr 18

Communicated 9 February 1955 by Arne Tiselius and Arne Fredga

Chromatography combined with automatic recording of electrolytic conductivity

III. Developments and tests of the apparatus and of the method

By Birger Drake

With 6 figures in the text

In the present paper, the continued work of the author on the use of conductivity recording as an aid in chromatography [1] will be described, and several factors will receive a more comprehensive treatment.

Chromatographic equipment

In some cases, the normal chromatographic equipment of this institute (cf., e.g., [2]) has been used, but in most cases modifications have been made which will be briefly described here.

Fig. 1 shows (right) a glass column whose funnel-shaped upper part is provided with a standard ground-glass joint (Quickfit, B 14). The hatched area in the conical part below the resin signifies a cotton wool plug, pressed down by means of a stainless steel rod with a flat end surface. In the same figure (left), a separatory funnel used as a solvent container and a special air inlet tube are shown. The latter serves the double function of converting the separatory funnel into a Mariotte flask and enclosing the solvent in a space where evaporation is prevented (the loop of the air inlet tube is charged with some drops of the same solvent). By the use of this device, the base line is generally beautifully horizontal, while previously it could sometimes happen that it drifted slowly (cf. the upper and lower diagrams in Fig. 10 of ref. [1]). The volume of the separatory funnel has usually been 100 ml, as in Fig. 1, but in longer runs volumes of 200 or 250 ml were used.

Perspex columns with screw couplings (similar to the metal "filters" described by Claesson [3]) have also been used. These columns were provided with a drop tip of the same dimensions as the tip of usual hypodermic syringes. In order to reduce volume lags (cf., e.g., [4]), this drop tip has in later experiments been inserted directly into the short rubber tube at the inlet end of the conductivity cell.

HETP values (cf., e.g., [5]) have been calculated for the two column sizes most frequently used, 2 × 200 mm and 4 × 440 mm, according to the approximative formula $r = 2\pi(H/h)$. Here, r is the number of theoretical plates in the column, H is the maximal concentration (height) of a certain peak, and h is the hypothetical

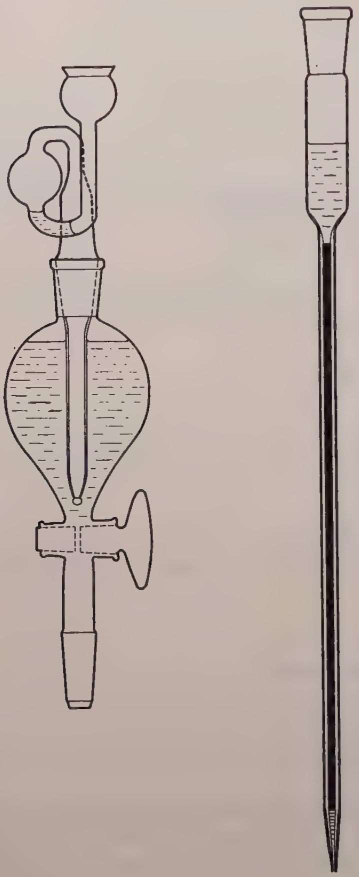

Fig. 1. Drawing of (right) a chromatographic tube, 2 × 200 mm, and (left) a separatory funnel with a special air inlet tube.

concentration (height) obtained when the total amount in that peak is divided by the volume from the start of the experiment to the emergence of that peak. When using recording on a strip chart, volumes and concentrations are most conveniently measured in centimeters, and the amount in the peaks im cm^2.

The following experimental data are typical.

1) 0.50 mg aspartic acid, run in 0.1 *N* HCl on Dowex 50 in a column with 2 mm diameter and 205 mm height: H = 6.9 cm and h = (30.6 cm^2/48.7 cm) = 0.63 cm. This gives r = 760.

2) 1.02 mg aspartic acid, run in 0.4 *N* HCl on Dowex 50 in a column with 4 mm diameter and 445 mm height: H = 3.25 cm and h = (9.9 cm^2/60.1 cm) = 0.165 cm. This gives r = 2300.

The absolute values of HETP are 0.26 and 0.19 mm, respectively, indicating that the separation efficiency of the larger column is superior to that of the smaller one, mainly because the larger column is more than twice as high as the smaller one.

Conductivity data of solvents used

For the convenience of the reader, relevant conductivity data of different solvents are reported here. The values should not be considered a contribution to our knowledge of physical chemical constants but only a guide for choosing a suitable value of the cell constant K for a special purpose.

In Table 1, a number of conductance values are given, together with the original experimental data and the corresponding resistance values for specified values of the cell constant. Usually, the author has worked in the region 500–15,000 ohms and the extension downwards to values around 5 ohms is made because DE VERDIER and SJÖBERG have reported the use of such low values [6]. For the extension upwards, there does not seem to be any defined limit.

Table 1. Comparison of resistances at various cell constants, and of conductances, for some solvents used by the author (temperature = 25°C). Italics signify actually measured values; other values are rounded.

Main substance	Added substance	Resistance at cell constant K =							Conductance ohm^{-1} cm^{-1}
		1	10	64.5	100	209	478	1 000	
0.02 *N* HCl		120	1 220	*7 850*	12 200			120 000	0.0082
0.1 *N* HCl		25	250	*1 630*	2 520			25 000	0.0395[1]
0.25 *N* HCl		10	110		1 070		*5 130*	11 000	0.093
0.3 *N* HCl		9	90		890	*1 860*		9 000	0.112
0.4 *N* HCl		7	70		680	*1 425*	*3 260*	7 000	0.147
1.0 *N* HCl		3	30		300		*1 450*	3 000	0.330
0.25 *N* HCl	30 % ethanol	20	205	*1 320*	2 050			21 000	0.049
0.4 *N* HCl	30 % ethanol	15	135	*880*	1 370			14 000	0.073
0.1 *N* HCl	0.1 % HCHO	25	255	*1 645*[2]	2 550			26 000	0.039
0.1 *N* HCl	0.3 % HCHO	25	255	*1 655*[2]	2 560			26 000	0.039
0.1 *N* HCl	1 % HCHO	25	265	*1 695*[2]	2 630			26 000	0.038
0.1 *N* HCl	3 % HCHO	30	280	*1 800*[2]	2 790			28 000	0.036
0.1 *N* HCl	10 % HAc	30	310	*2 000*	3 100			31 000	0.032
0.1 *N* HCl	50 % HAc	85	850	*5 500*	8 520			85 000	0.0117
0.85 % LiCl		60	585	*3 735*	5 800			58 000	0.0173
1 % NaCl		60	580	*3 740*	5 800			58 000	0.0172
1.5 % NaCl		40	400	*2 565*	3 980			40 000	0.0251
2 % NaCl		30	305	*1 970*	3 050			31 000	0.033
4 % NaCl		15	165	*1 070*	1 660			17 000	0.060
1 % NH_4Cl		45	440	*2 845*	4 420	*9 225*		44 000	0.0227
2 % NH_4Cl		25	230	*1 485*	2 300	*4 800*		23 000	0.043
1.25 % KCl		50	490	*3 165*	4 900			49 000	0.0204
1.25 % KCl	0.008 *N* HCl	45	430	*2 770*	4 300			43 000	0.0233
1.0 *M* KCl	0.1 *N* HCl	8	75		730		*3 475*	7 000	0.138
Phosphate buffer pH = 7.0; 0.1 *M*		90	905	*5 830*	9 040			90 000	0.0111

---

[1] This is a reference value that originally was the theoretical 0.0390 (cf. [1], [7]) but which has changed to this value during a couple of years.

[2] In these cases, the corresponding value for 0.1 *N* HCl vas 1 640 ohms.

The magnitude and influence of capacitance unbalances

All conductivity cells act as the combination of a resistance and a capacitance. The magnitude of the resistance is a function of the composition of the solution in the cell, while the magnitude of the capacitance is a function also of the nature of the surface of the electrodes, of the current density, etc. Because the circumstances are too complex to be successfully treated here in a theoretical way, a more practical treatment will be used.

The important questions in this connection are: how large is the capacitance unbalance in practice, and what is the influence of the capacitance unbalance on the sensitivity and on the accuracy of the recording of conductivity? These questions have been studied by comparing the observed capacitance changes for certain concentration changes with the experimentally determined sensitivity and accuracy of the electronic apparatus at specified values of capacitance unbalance.

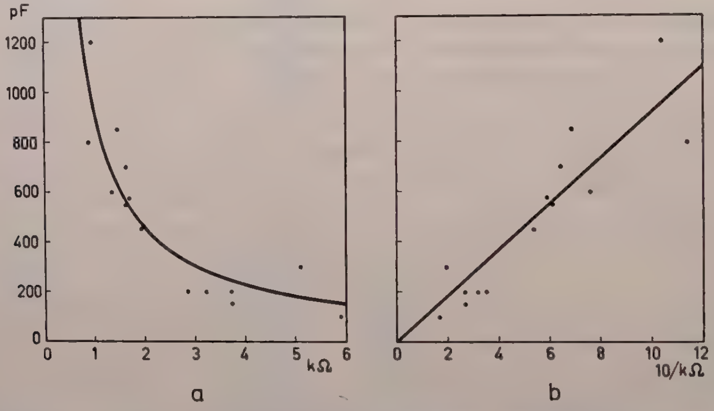

Fig. 2. Capacitance values as a function of cell resistance, measured in kilo-ohms (a), and of its inverse value (b).

Fig. 2 shows some values obtained for widely different solvents with a micro conductivity cell of cell constant $K = 64.5$. The capacitance values are plotted as a function of the cell resistance, and also as a function of the inverse value of the cell resistance. At balance, the voltage (V) across the cell has always been approximately the same (about 0.5 volts). This means that $1/R = I/V$ has been proportional to I (I = current in, e.g., milliamperes). For one and the same cell, the current density is proportional to the current, and hence to $1/R$. Thus, it can be inferred from Fig. 2 b that there is an approximate proportionality between the capacitance and the current density.

Fig. 2 a shows that at about 1630 ohms, which is the R value most common in this work, the capacitance change with a change of the cell resistance is $\Delta C/\Delta R = 0.4$ pF/ohm. Now, this value should be compared to the maximal resistance change that in practice is placed over the strip chart. In the present work, this value is 200 ohms, and the maximal capacitance unbalance will then be 80 pF. With other useful potentiometer ranges, e.g., 100, 50 or 25 ohms, the maximal capacitance unbalance will of course become proportionately smaller.

Table 2. The influence of capacitance unbalance on the magnitude of the inactive range of the balancing mechanism and on the deviation from the accurate value (the latter is indicated by full-faced letters).

Apparatus	Capacitance unbalance ΔC (pF)	Inactive range		Central value R_{centr}	ΔR_{centr}
		$R_{\min} - R_{\max}$	ΔR		
Earlier	0	2 028.29–2 028.44	0.15	**2 028.36**	—
	100	2 027.96–2 028.46	0.50	2 028.21	– 0.15
	500	2 026.15–2 028.6	2.45	2 027.38	– 0.98
New	0	1 805.0 –1 805.2	0.2	**1 805.1**	—
	100	1 804.7 –1 805.0	0.3	1 804.85	– 0.25

The values of capacitance unbalance reported above will get their proper meaning when they are compared to the sensitivity and accuracy of balancing. Here, the sensitivity is measured by the inverse value of the range within which the balancing arrangement is inactive, and the accuracy is measured by the inverse value of the deviation of the center of the inactive range from the accurate value at exact capacitance balance. When increasing the capacitance unbalance, both the sensitivity and the accuracy will decrease, as shown in Table 2. This phenomenon is observed to about the same degree with the earlier apparatus described in ref. [1] and with the new apparatus which will be described below. With the former apparatus, the relays were observed while the potentiometer motor was disconnected, but with the latter apparatus the motor had to be in operation continuously.

Taken together, the data in this section of the paper indicate that capacitance unbalances met with in practice are small enough to permit a satisfactorily sensitive and accurate recording of electrolytic conductivity.

Further development of earlier formulas

The formulas given in [1] for the estimation of the amount N_B of a substance B in a flowing solution

$$N_B = \int_{V_1}^{V_2} c_B \, dV = k_B \cdot k_t \int_{t_1}^{t_2} p_B \, dt \qquad (1)$$

are not very convenient in the form given. However, their use is greatly facilitated if the variables are expressed in units of length (e.g., in centimeters). This means that one has to determine, on the strip chart, two coefficients $k_{t,\,\mathrm{cm}} = \mathrm{hours/cm}$ and $k_{B,\,\mathrm{cm}} = \mathrm{ohms/cm}$.[1] The formula for the analysis of a flowing solution can then be written

$$N_B = k_{B,\,\mathrm{cm}} \cdot k_B \cdot k_{t,\,\mathrm{cm}} \cdot k_t \int_{(\mathrm{cm})_{t,1}}^{(\mathrm{cm})_{t,2}} (\mathrm{cm})_B \, d\,(\mathrm{cm})_t \qquad (2)$$

---

[1] The four notations $k_{B,\,\mathrm{cm}}$, k_B, $k_{t,\,\mathrm{cm}}$ and k_t correspond to k_2, k_1, k_3/k_4 and k_3, respectively, in the paper of DE VERDIER and SJÖBERG [6].

where $(\mathrm{cm})_\mathrm{B}$ signifies length between the curve and the interpolated base line on the strip chart in the ohms direction and $(\mathrm{cm})_t$ length in the time direction. However, the integral in eq. (2) is identical to the area of a certain peak on the strip chart, and this can easily be measured by the aid of a planimeter, calibrated in cm². Thus, formula (2) can be written

$$\mathbf{N}_\mathrm{B} = k_{\mathrm{B,\,cm}} \cdot k_\mathrm{B} \cdot k_{t,\,\mathrm{cm}} \cdot k_t \cdot \mathbf{A} \tag{3}$$

where **A** signifies the measured peak area.

In eq. (3), k_B has the dimension eq. cm^{-3} ohm^{-1} and it is, under specified conditions, identical to $\Delta c_\mathrm{A}/\Delta \mathrm{R}$ in eq. (11) in ref. [1]. Thus, eq. (3) can be written

$$\mathbf{N}_\mathrm{B} = -\frac{\varkappa^2\left(1+\dfrac{K_\mathrm{A}}{c_{\mathrm{H}^+}}\right)}{\mathrm{K}\mathbf{F}\,(u_{\mathrm{A}^+}-u_{\mathrm{H}^+})}\, k_{\mathrm{B,\,cm}} \cdot k_t \cdot k_{t,\,\mathrm{cm}} \cdot \mathbf{A} \tag{4}$$

or, if the relation $\mathrm{R}\times\varkappa=\mathrm{K}$ is applied,

$$\mathbf{N}_\mathrm{B} = -\frac{\mathrm{K}\left(1+\dfrac{K_\mathrm{A}}{c_{\mathrm{H}^+}}\right)}{\mathrm{R}^2\,\mathbf{F}\,(u_{\mathrm{A}^+}-u_{\mathrm{H}^+})} \cdot k_{\mathrm{B,\,cm}} \cdot k_t \cdot k_{t,\,\mathrm{cm}} \cdot \mathbf{A}. \tag{5}$$

In this formula, K, K_A, c_{H^+}, R, **F**, $k_{\mathrm{B,\,cm}}$, k_t, $k_{t,\,\mathrm{cm}}$ and **A** can easily be determined during each run or once and for all before the experiments, or they can be obtained from the literature. Unfortunately, the mobility values u_{A^+} are only occasionally to be found in the literature. However, the formula is derived merely to show what basic factors are important in determining the magnitude of response, and in practice it is always necessary to determine experimentally the exact k_B value for each substance in the chromatographic system used.

A correction formula for the lack of linearity of response

When the conductivity changes are small, it does not matter whether conductance or resistance is recorded, and the formulas derived above can be used to advantage. When the changes are greater, however, the recording of conductance is superior to the recording of resistance, because the conductance change but not the resistance change is a linear function of the amount of exchange of one ion for another (cf. formulas (8) and (11) in ref. [1]). For resistance recording, it can be shown that the following formula gives the correction that should be subtracted from the value obtained by planimetry of the peaks.

$$\%\ \text{error} = 100\left[\left(\frac{\Delta \mathrm{R}_\mathrm{max}}{\mathrm{R}_0}\right)\cdot\frac{1}{\sqrt{2}} - \left(\frac{\Delta \mathrm{R}_\mathrm{max}}{\mathrm{R}_0}\right)^2\cdot\frac{1}{\sqrt{3}} + \cdots - \cdots\right]. \tag{6}$$

Here, $\Delta \mathrm{R}_\mathrm{max}$ and R_0 are the peak height in ohms and the resistance of the pure solvent, respectively. This formula has been derived on the following assumptions:

1) formula (10) in ref. [1]

$$\frac{\mathrm{d\,R}}{\mathrm{d}\,c_{\mathrm{A}}} = -\frac{\mathrm{K\,F}\,(u_{\mathrm{A}^+} - u_{\mathrm{H}^+})}{\varkappa^2 \left(1 + \dfrac{K_{\mathrm{A}}}{c_{\mathrm{H}^+}}\right)} \tag{7}$$

is valid, and

2) the elution peak has the form of an error curve (cf. [5]), i.e., the following expression is valid

$$\Delta\,\mathrm{R} = \Delta\,\mathrm{R}_{\mathrm{max}} \cdot \mathrm{e}^{-q^2 (V - V_{\mathrm{max}})^2} \tag{8}$$

where q is a parameter and V_{max} is the volume at which $\Delta\,\mathrm{R} = \Delta\,\mathrm{R}_{\mathrm{max}}$.

Formula (6) can now be used to make a table of correction values (see Table 3). As an example of its application the following case may be quoted. At a total resistance of $\mathrm{R}_0 = 1640$ ohms, 0.30 mg aspartic acid gave a peak with the height $\Delta\,\mathrm{R}_{\mathrm{max}} = 16$ ohms. The correction is then 0.7 %, which lies within the range of experimental errors. In other cases, however, the correction may become so large that it must be taken into consideration. This was the case in the runs marked 46, 54 and 55 in Fig. 10 and Table 3 in the first paper of this series [1], when this correction was not yet in use. In those cases, the corrections were of the order of 3 % or lower. However, the values reported in that paper represented the weight fractions of aspartic acid in mixtures of aspartic and glutamic acid, so that the resulting correction would have been the difference between the corrections for the two amino acid peaks. Obviously, in such cases, no correction is necessary, if the two peaks are of almost the same height.

Table 3. Correction values in per cent, according to formula (6), to be subtracted from peak areas obtained by planimetry.

Relative change of resistance $\Delta\,\mathrm{R}_{\mathrm{max}}/\mathrm{R}_0$, in %	0	1	2	3	4	5	6	7	8	9	10
Correction, %	0	0.7	1.4	2.1	2.7	3.4	4.0	4.7	5.3	5.9	6.5

A device for direct recording of conductance

One way of avoiding the lack of linearity treated above would be to record conductance instead of resistance. In principle, this can be done (with a slightly more complicated apparatus) by using, for example, the proposed circuit shown in Fig. 3, right.

In resistance recording (Fig. 3, left), the following formula is valid for the output potentiometer circuit (the supply voltage is assumed to be taken from an 85A1 voltage stabilizing tube)

$$\mathrm{E}_{\mathrm{out}} = 85 \cdot \frac{\mathrm{x\,R_p}}{\mathrm{R_p} + \mathrm{R_1}}. \tag{9}$$

Because the potentiometer is driven synchronously with the balancing potentiometer, so that $\mathrm{x\,R_p}$ is proportional to $\Delta\,\mathrm{R}$, this can be written

$$\mathrm{E}_{\mathrm{out}} = \mathrm{const.} \times \Delta\,\mathrm{R}. \tag{10}$$

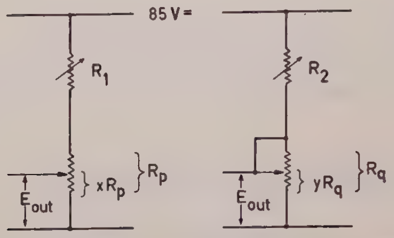

Fig. 3. Principal solution of the problem of conductance recording. Left, the output potentiometer circuit in the case of resistance recording; right, a suggested output potentiometer circuit for conductance recording.

In conductance recording, the rheostat R_1 is substituted by a decade resistance R_2, and the output line is short-circuited to the upper end of the output potentiometer. The formula then becomes

$$E_{out} = 85 \cdot \frac{y\,R_q}{R_2 + y\,R_q}. \tag{11}$$

If R_2 is so adjusted with respect to R_q that R_2/R_q = the quotient between the resistance of the decade resistance of the bridge and the total resistance of the added balancing potentiometer, formula (11) can be changed to

$$E_{out} = 85 \cdot \frac{\Delta R}{R_0 + \Delta R} = 85 \cdot \frac{R - R_0}{R} = 85 \cdot \frac{\frac{K}{\varkappa} - \frac{K}{\varkappa_0}}{\frac{K}{\varkappa}} = 85 \cdot \frac{\varkappa_0 - \varkappa}{\varkappa_0} = \text{const.} \times \Delta\varkappa. \tag{12}$$

Thus, in the former case (eq. (10)), the output voltage is proportional to ΔR, while in the latter case (eq. (12)) it is proportional to $\Delta\varkappa$.

A balancing mechanism without relays

The circuit of the apparatus described in [1], Fig. 4, includes one sensitive, polarized relay and two other relays. However, there seemed to be other suitable ways of obtaining the automatic balancing of the bridge. One of the principles considered was to feed the bridge with an AF signal modulated with 50 p/s frequency, and to use the rectified 50 p/s signal together with another 50 p/s signal taken directly from the mains for driving a balancing motor. A block diagram of a new curcuit for this purpose is shown in Fig. 4, and some details are shown in Fig. 5. The circuit parts not shown in detail here are of a simple, conventional design and in most cases similar to those shown in ref. [1], Fig. 4, or to the corresponding parts of the LKB Conductivity Bridge, type 3216.

A model apparatus has been constructed, in which oscillator, bridge, amplifiers, discriminator and balancing arrangement are all built into one single unit. In order to achieve a satisfactory operation, the bridge output transformer had to be turned around different axes until the noise became negligible. In the bridge amplifier, a twin-T section tuned to the AF frequency used (800 p/s) is inserted between the

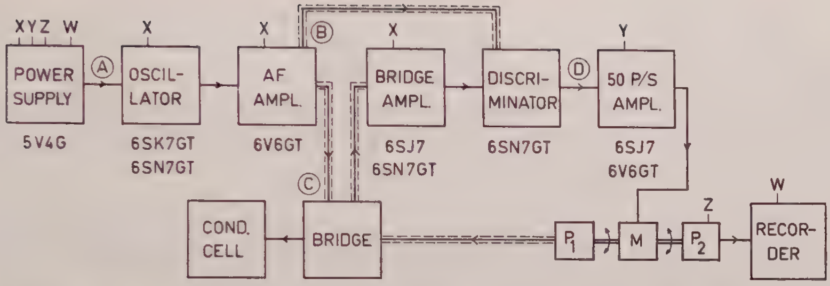
XYZ W
X
X
B
X
Y
POWER SUPPLY
A
OSCIL-LATOR
AF AMPL.
BRIDGE AMPL.
DISCRI-MINATOR
D
50 P/S AMPL.
5V4G
6SK7GT 6SN7GT
6V6GT
6SJ7 6SN7GT
6SN7GT
6SJ7 6V6GT
C
W
Z
COND. CELL
BRIDGE
P1
M
P2
RECOR-DER

Fig. 4. Block diagram of the new apparatus without relays. The encircled letters correspond to the same notations in Fig. 5; P_1 and P_2 are 10 revolutions potentiometers and M is a reversible motor. The letters X, Y, Z and W indicate supply of + 300 V, + 300 V, + 80 V stabilized, and 100 V A.C., respectively.

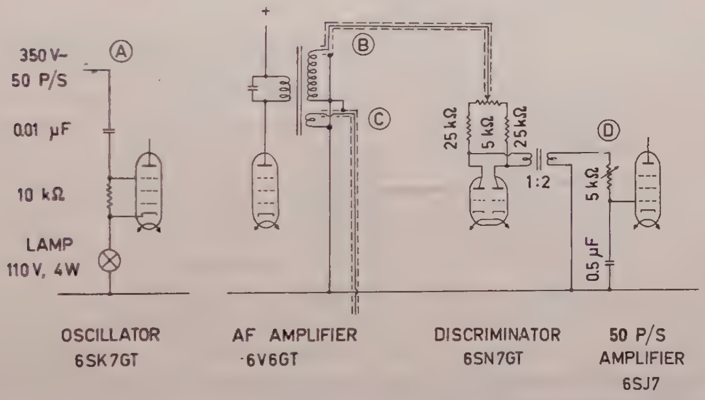
350 V~
50 P/S
A
0.01 µF
10 kΩ
LAMP
110 V, 4W
+
B
C
25 kΩ
5 kΩ
25 kΩ
D
1:2
5 kΩ
0.5 µF
OSCILLATOR
6SK7GT
AF AMPLIFIER
6V6GT
DISCRIMINATOR
6SN7GT
50 P/S
AMPLIFIER
6SJ7

Fig. 5. Some details of the circuit of the new apparatus. The encircled letters correspond to the same notations in Fig. 4.

6SJ7 tube and the first half of the 6SN7GT tube. In the same amplifier there are also facilities for adjusting the circuit to give the exact phase relationships for the proper rectification of a signal caused by resistance unbalance, while a capacitance unbalance is almost inactive. With the construction used here, potentiometer end-position switches cannot be used, and a friction coupling had to be inserted between the potentiometer motor and the two potentiometers.

The recorder used with this apparatus is a Micromax (Leeds & Northrup) 10 mV strip chart recorder, usually set for a paper speed of 1 inch per hour. The output circuit of the apparatus contains a drop coil of 500 (or 150) ohms, which is a rather high value for a recorder of this type (a Speedomax or a similar recorder would be preferable). However, with the output circuit used, the resistance of the drop coil cannot be decreased without introducing a deviation from the linear response.

The apparatus has been used during a couple of years, and after a necessary period of adjustments it has, in the hands of the author, been found reasonably satisfactory. The sensitivity is not less than that of the former apparatus (cf. data above in connection with the influence of capacity unbalance), and it has in some cases been as high as ± 0.5 to ± 1 ohm at 8000 ohms total resistance. Unfortunately, a slight drift of the phase relationships in various parts of this experimental model prevents the continuous utilization of this very high sensitivity.

When used as a measuring apparatus without recording, the correction to be applied is 0.07 % + 0.6 ohms. The accuracy of this correction is ± 0.4 ohms within the range 1000–10,000 ohms total resistance.

An adapter for the simultaneous recording with two conductivity cells

A self-recording conductivity bridge is quite expensive, and it is therefore desirable to be able to use it to record many simultaneous runs. However, there are some factors which prevent the immediate application of this principle. One of them is that a very fast recorder and a very fast balancing system are necessary, and this would make the whole arrangement more expensive than if the recording could be made more slowly. Another factor is that if the conductivity cells have widely different resistances and widely different capacitances, the recording with one single apparatus necessitates an adjustment of balancing resistor and balancing capacitor before each automatic balance adjustment.

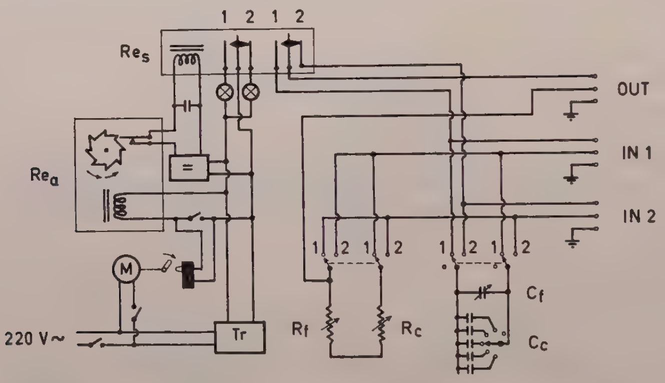

Fig. 6. Circuit diagram of an adapter for the simultaneous recording with two conductivity cells. *Tr* is an autotransformer for 20 V A.C.; *M* is a synchronous motor geared to, e.g., $^1/_3$ RPM and periodically closing a micro-switch; = is a rectifier for Re_s; Re_a is an alternating relay; Re_s is a switching relay; R_f and R_c are fine and coarse control of added resistance; C_f and C_c are fine and coarse control of added capacitance.

The possibility of constructing an adapter for two cells was mentioned in ref. [1], p. 411, and an example of a curve obtained with such an adapter was shown in that paper (Fig. 9). Here, the circuit of that adapter is shown in Fig. 6. The variable capacitor C_f has a capacitance between 50 and 600 pF, and the capacitors in C_c have the values 500, 1000, 1500, 2000 pF, etc. The ten resistors in R_f and the ten in R_c have the values 10 ohms and 100 ohms, respectively.

The adapter is convenient in use, but it has been found to introduce a small irregularity in the recording. The reason for this has not yet been clarified.

Miscellaneous

The regularity of the base line may be judged from the following data, pertaining to the earlier apparatus described in ref. [1].

In one case, a base line was drawn continuously during more than three days (strip chart width 28 cm, corresponding to 50 ohms). During this time, the recorded resistance decreased from 1645 ohms to 1642.5 ohms, i.e., a decrease of 0.05 % per day, while the short-period fluctuation amounted to less than 0.5 ohms, i.e., to less than 0.03 %. The flow velocity was held constant at 1.1 ml per hour. It should be mentioned that on many occasions irregularities occurred which were much larger than those reported here. However, the cause of these irregularities was often easily found, and the fault corrected.

In another case, the liquid flow was stopped suddenly during a recording of the base line after an elution analysis with 0.1 *M* potassium phosphate buffer, pH = 7.0, when the flow velocity had been 4.7 ml per hour. The resistance changed, during the first two hours after stopping, from 5823 to 5824 and then to 5820 ohms, where it first stayed practically constant and then rose slowly to 5821 ohms during the next ten hours. The maximal change is 4 ohms, i.e., about 0.07 %. This shows that the thermostating is effective at least up to flow velocities of a few milliliters per hour, and that polarization effects do not play an important role in spite of the fact that the electrode area is only about 4 mm^2.

One addition should be made to the description of the earlier apparatus for conductivity recording (cf. ref. [1]). It was found, after some time, that the balancing mechanism became liable to oscillate around the equilibrium value (so-called "hunting"). This could be avoided by moving the motor to a position adjacent to the two potentiometers, so that the long, and somewhat elastic, steel axle became unnecessary, and by changing the gearing from the motor to the potentiometers so that these were rotated ten revolutions in ten minutes, instead of in 50 seconds. In this way, the hunting was prevented, but the apparatus now balances very slowly, and a compromise between these two values would be better. Probably, a balancing in maximally 2 or 3 minutes would be feasible, and this period of time can without disadvantage be used in connection with most types of chromatography.

ACKNOWLEDGEMENTS

The author wishes to thank Professor ARNE TISELIUS for kind helpfulness and for all facilities put at his disposal. A large part of the expenses for apparatus construction has been defrayed by a grant to the Institute of Biochemistry from the Rockefeller and Wallenberg foundations, which is gratefully acknowledged.

Institute of Biochemistry, Uppsala University, Uppsala, Sweden.

REFERENCES

1. Drake, B., Arkiv f. Kemi *4*, 401 (1952).
2. Tiselius, A., Endeavour *11*, No. 41, Jan. 1952.
3. Claesson, S., Arkiv f. Kemi, Mineral. Geol. *23 A*, No. 1 (1946).
4. Drake, B., Anal. Chim. Acta *3*, 452 (1949).
5. Martin, A. J. P., and Synge, R. L. M., Biochem. J. *35*, 1358 (1941).
6. de Verdier, C.-H., and Sjöberg, C. I., Acta Chem. Scand. *8*, 1161 (1954).
7. Roth, W. A., and Scheel, K., Landolt-Börnstein, Physikalisch-chemische Tabellen, 1923–1936.

Tryckt den 19 april 1955

Uppsala 1955. Almqvist & Wiksells Boktryckeri AB

ARKIV FÖR KEMI Band 8 nr 19

Communicated 9 February 1955 by ARNE TISELIUS and ARNE FREDGA

Chromatography combined with automatic recording of electrolytic conductivity

IV. Elution analysis of some amino acids, amines, and alkali metals on Dowex 50 in various solvents

By BIRGER DRAKE

With 15 figures in the text

In previous papers of this series [1, 2], a method has been described for the analysis of the effluent from a chromatographic column by the use of automatic recording of electrolytic conductivity. In this paper, a number of experiments will be described that have been performed in order to study the possibilities of the method.

Because ion exchange systems seemed most promising (cf. Discussion in ref. [1]), such systems were tried first. Cation exchange, which is a more rapid and well defined process than anion exchange (cf., e.g., [3, 4]), was most frequently used, and only such experiments will be reported here. In order to facilitate a comparison between different runs, Dowex 50 was employed in all the experiments.

The groups of substances investigated have been amino acids and a peptide, glycylglycine (see also [1]), except the aromatic ones that may be sorbed to ion exchange resins by other forces than ion exchange (cf. [5]), hexosamines (see also [6]), other aliphatic amines, and the alkali metals lithium, sodium and potassium as well as ammonium which in all experiments described here can be regarded as an alkali metal.

The experiments reported here are selected out of a large number of theoretically possible cases, and are mainly intended to serve as a guide for other experiments in this field.

In the following, typical data will be presented under separate headings for the different chromatographic systems. After the short descriptions, comparisons will be made as regards the shape of the peaks, the position of the peaks (i.e., the elution volume), and the area of the peaks (i.e., the response sensitivity). Throughout the paper, the abbreviations for amino acids are the same as those used by BRAND and EDSALL [7]. For substances other than amino acids and alkali metals, the following abbreviations are used: GlyAm = glucosamine, GG = glycylglycine, and EtAm = ethanolamine.

General chromatographic data

The columns (cf. [2]) usually had the dimensions 2 × 200 mm or 4 × 400 mm (see also Table 3). The flow velocity was usually between 0.5 and 3 ml/hour. The adsorbent was Dowex 50, 200–400 mesh, 8 % cross-linkage, which had been washed (after treat-

Table 1. Amounts (in mg) of the amino acids most frequently used in different runs.

Figure	Asp	Glu	Ser	Thr	GG	HyPro	Gly	Ala	Val	Pro	Leu
1 A	0.20	0.14					0.21			0.60	
1 B			0.18	0.06			0.11	0.06	0.43		0.36
1 C	0.158						0.116		0.164		
2	0.27	0.73			0.30	0.47	1.01		0.67	0.80	1.25
3 A upper curve	0.108	0.097	0.0725								
3 A middle curve	0.39	0.35	0.265								
3 B	0.27	0.73			0.30	0.47	1.01		0.67	0.80	1.25
5 A	0.16						0.12		0.16		
5 B	0.29						0.22		0.31		
6 B							0.62	0.17			
12 A							0.525		0.20		0.63
12 B		0.53									
12 C						0.167				0.174	
12 D			0.35	0.36							

Table 2. Amount (in mg) of amines and alkali metals used in different runs.

Figure	GlyAmHCl	Urea	EtAm	LiCl	NaCl	AmCl	KCl
1 A	0.20						
1 C				0.184	0.184	0.148	
1 D				0.49	0.32	0.57	0.53
2, 3 B	0.77	0.40	0.45			0.70	
3 C				0.43	1.04	1.18	0.785
5 A				0.18	0.18	0.15	
5 C				0.42	0.42	0.33	
6 A				0.075	0.31		
6 C				0.295	0.31	0.85	
7					0.21	0.13	0.22
8 A				0.145		0.14	0.08
8 B				0.255		0.245	0.14
8 C				0.137		0.30	0.55
9				0.29	0.34		0.62
10 A						0.20	
10 B, C, D				0.11	0.23		
10 E				0.0092	0.0088		
11 A						0.475	
11 B						0.18	
11 C				0.095	0.20	0.18	
12 A	(0.1)						

ment with NaOH) with 1 *N* HCl and then with the solvent to be used. Before each run, the conductivity recorder was always used to control that the column was in equilibrium with the solvent.

Tables 1 and 2 show the amounts of various substances that were applied to the column in different runs.

Recording apparatus

In most of the experiments described here, the apparatus described in ref. [1] was used. This consisted of a LKB conductivity bridge, type 3216, and an adapter for recording on a Honeywell-Brown strip chart recorder, type Electronik, 2.5 mV (28 cm paper width). In some cases (see Figs. 9 and 12), the newer apparatus described in ref. [2] was used. This apparatus consisted of a special unit, comprising oscillator, bridge, amplifiers and a servo-mechanism, and a suitably connected Leeds & Northrup strip chart recorder, type Micromax, 10 mV (25 cm paper width).

In the experiments described in Figs. 2, 3 and 12 B, C and D, the cell constant was 478, in experiment 12 A it was 209, and in all other experiments it was 64.5.

The value of the bridge potentiometer resistance was 200 ohms (Figs. 1, 5 A and 14), 100 ohms (Fig. 12), 25 ohms (Fig. 3), or 50 ohms (all other figures). In some of the figures, the diagram height corresponds to a part of the strip chart width, only. In a number of diagrams, the base line has, fictitiously, been drawn as if it coincided with the volume axis.

Experiments with hydrochloric acid solutions: milligram quantities

Hydrochloric acid is the solvent most often used in the author's experiments. One reason for this choice is that the response of the conductivity recording is more sensitive in a moderately strong solution of a strong acid than in other solvents

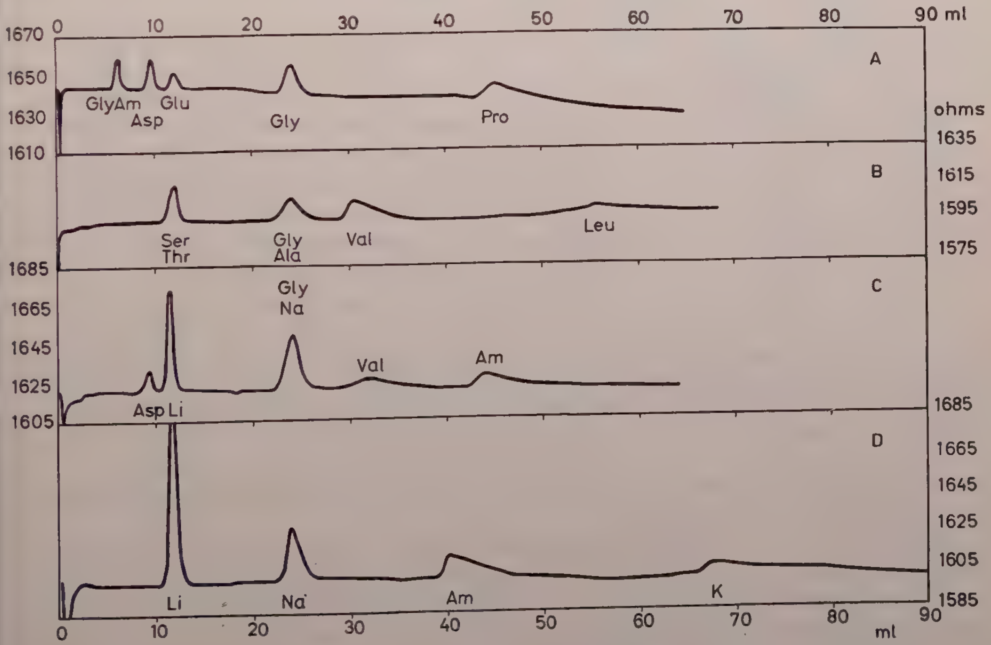

Fig. 1. Elution curves for runs in 0.1 *N* HCl on Dowex 50. The column dimensions and flow velocities were: A, 2 × 227 mm; 1.12 ml/hour; B, 2 × 200 mm; 1.60 ml/hour; C, 2 × 205 mm; 1.87 ml/hour; D, 2 × 200 mm; 1.56 ml/hour. For data on amounts of substances applied to the columns, see Tables 1 and 2.

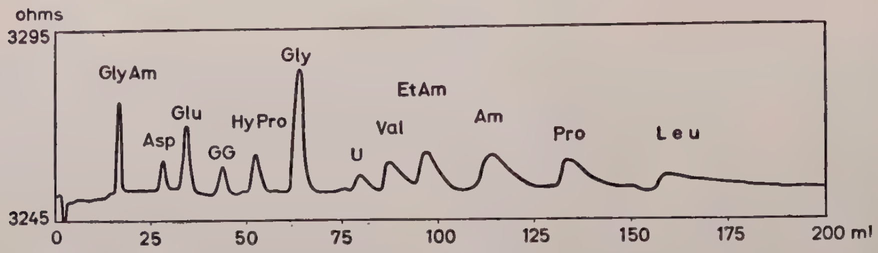

Fig. 2. Elution curve for a run in 0.4 N HCl on Dowex 50; 4 × 440 mm; 2.04 ml/hour (0–80 ml), and 1.93 ml/hour (after 80 ml). See Table 1.

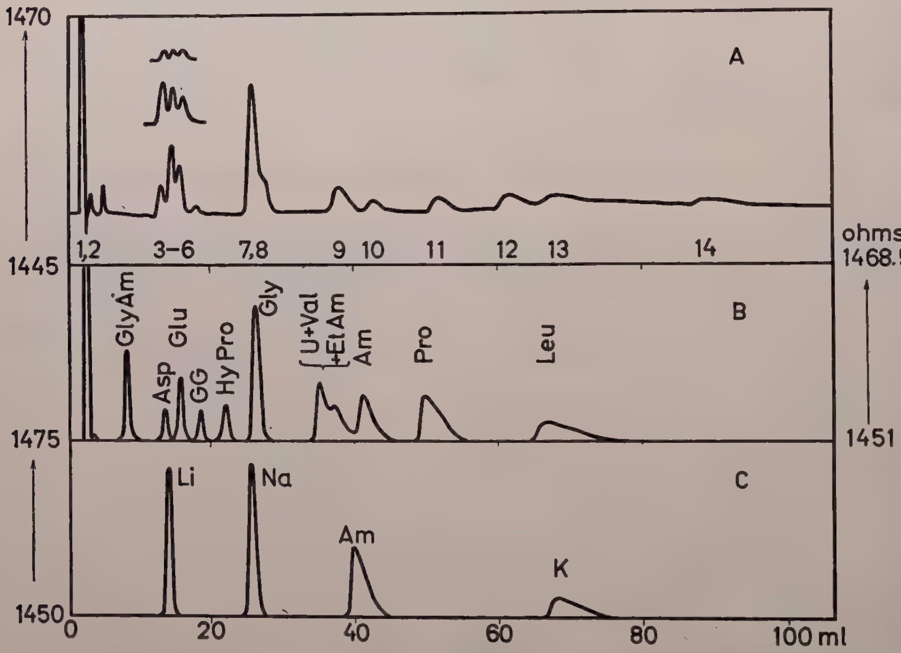

Fig. 3. Elution curves for runs in 1 N HCl on Dowex 50, all performed with the same column, 4 × 440 mm; A, 1.75 ml/hour; B, 1.92 ml/hour; C, 1.75 ml/hour. In diagram A, parts of the elution curves for two runs with different amounts of aspartic acid, serine and glutamic acid have been inserted above the whole curve for a run with 20 mg Aminosol. See the text and Tables 1 and 2.

(cf. [1], formulas (8) and (11)). Other reasons are that the solvent should be readily available and easily evaporated.

Usually, the concentrations of HCl have been 0.1, 0.25, 0.4 and 1.0 N. In one case (see next section), 0.02 N HCl has also been used, and in a few cases 0.3 N HCl was used. Unfortunately, with 1 N HCl the response sensitivity is rather low, and it can be deduced that at a concentration of 4 N HCl, the sensitivity is so small that a useful analysis becomes extremely difficult.

Figs. 1–3 show the elution curves for some typical runs with different concentrations of HCl. From Fig. 1 it is immediately seen that in 0.1 N HCl amino acids and alkali metals emerge from the column within about the same range. This means that amino acids cannot be analyzed by this method, if larger amounts of alkali metals are present. However, under suitable conditions it may be possible to analyze simultaneously some alkali metals and some amino acids (cf. Figs. 5 and 6). In such cases, an analysis of very different substances is afforded by one single method, i.e., the values for all substances are referred to one single property.

When Aminosol (a peptic digest of casein, used for amino acid therapy [8]) was analyzed (Fig. 3 A), some peaks were obtained at positions where peaks have not been observed under other circumstances. Probably, these peaks indicate zones of peptides (e.g., No. 1 and 2). Some other peaks are easily identified, e.g., No. 3, 4 and 5, which contain aspartic acid, serine (and threonine), and glutamic acid. The absence of hydroxyproline is confirmed (this amino acid would have emerged between the peaks No. 6 and 7).

In some runs in 0.4 *N* HCl, the elution curves of which are not shown here, it was found that hydroxylamine emerges very close to glycine, and methylamine very close to leucine, while ethylamine emerges later than methylamine. The peaks of the first substance were nearly symmetrical, while those of the two latter exhibited a pronounced tailing.

For a comparison of the curves in Figs. 1–3, see also below under the heading "Peak positions".

Experiments with hydrochloric acid solutions: microgram quantities of lithium and sodium

The usual range for the experiments described above is 0.1–1 mg. However, this range can be extended considerably downwards as, for example, in the analysis of lithium. The reasons for the higher sensitivity in this case are the low equivalent weight of this metal and the fact that it emerges first of all metals under the circumstances described here. In a usual run on a Dowex 50 column, 2 × 200 mm, in 0.1 *N* HCl, about 10 μg of lithium (corresponding to about 60 μg of lithium chloride) give a rather large peak, and even smaller quantities can easily be detected. This sensitivity can be increased further by using lower concentrations of hydrochloric acid. Below, some experiments performed in order to demonstrate this will be described.

Table 3. Experimental data for runs in 0.02 *N* HCl on columns packed with equal volumes of Dowex 50 and Celite.

No.	Column		Flow rate ml/hour	Amount (μg)		Peak area (cm^2)		k_B	
	mm × mm	ml		Li	Na	Li	Na	Li	Na
1	4 × 12.5	0.16	1.46	1.00	1.52	58.6	25.4	0.033	0.098
2	,,	,,	1.78	0.19		12.7		0.024	
3	3 × 83	0.59	2.00	0.27		15.7		0.022	
4	,,	,,	1.45	0.36		20.2		0.032	
5	,,	,,	2.7	0.81		29.5		0.026	
6	,,	,,	3.2	0.80	12.8	23.0	143.5	0.028	0.072
						Weighted mean		0.029	0.076

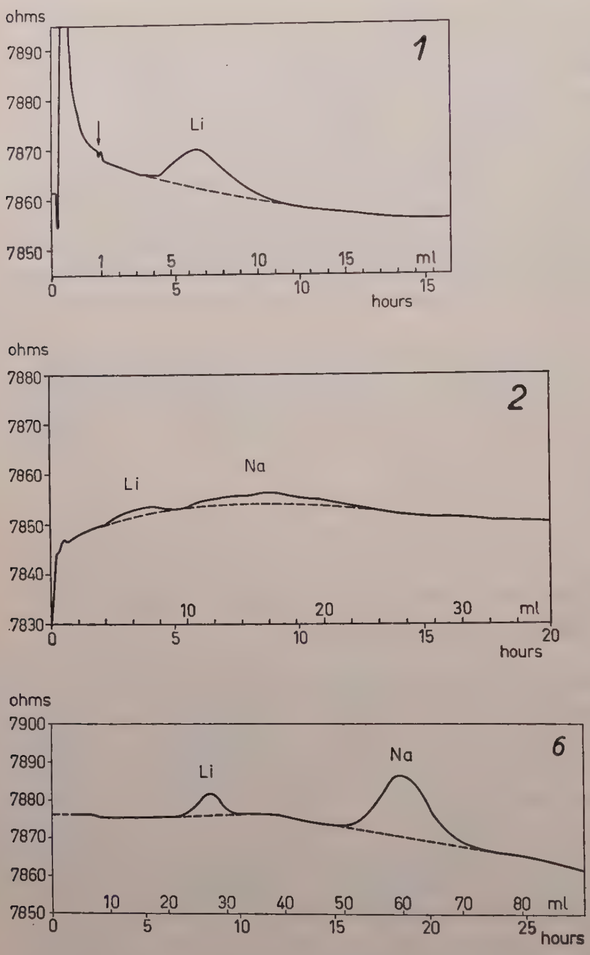

Fig. 4. Elution curves for runs in 0.02 N HCl on Dowex 50, mixed with an equal volume of Celite. For experimental data see Table 3.

0.004 N HCl was found inefficient as an eluting agent, but 0.02 N HCl was found suitable. First, a very small column with Dowex 50 was used: 4 × 12.5 mm, made of Perspex (see Table 3, run No. 1 and 2, and Fig. 4, upper and middle diagrams). Later, another Perspex column, 3 × 83 mm, was used with a mixture of equal volumes of Dowex 50 and Celite. In order to diminish evaporation from the upper surface of the liquid in the solvent container, a floating Perspex piston was used (cf. [9]). Data for the runs performed with this column are given in Table 3, and the curve for run No. 6 is also shown in Fig. 4, lower diagram.

In the runs with 0.02 N HCl, the total resistance (at a cell constant of 64.5) was 7900 ohms, and the strip chart width corresponded to a 50 ohms potentiometer in the bridge circuit. This means that the recorder range corresponded to only about 0.65 % of the total resistance.

In Table 3, the k_B values (cf. ref. [1]) have been reported. The spread of the values is rather high, about ± 20 %, but the absolute value of this spread is only 0.15 μg, which may be considered a reasonable value. One of the reasons for this low accuracy is that the raised sensitivity causes unavoidable irregularities of the base line which give large errors in the measurement of surface areas.

Since all metals other than the alkali metals are very strongly bound to a cation exchange resin of the type used here, it should be possible to determine very small amounts of lithium and sodium also in solutions containing much larger amounts of the heavier metals. Also, even large quantities of sodium should not disturb the analysis of lithium.

Experiments with hydrochloric acid solutions with various additions

Formaldehyde (0.1–1 %), ethanol[1] (30 %) and acetic acid (10 and 50 %) were added to HCl in order to determine their influence on the chromatographic behaviour. Of these substances, the first was believed to have an influence on the substances analyzed (cf. SCHRAMM and PRIMOSIGH [11]), while the two latter were believed to have an influence on the solvent.

The elution curves for some typical runs with mixtures of HCl and ethanol are shown in Figs. 5 and 6.

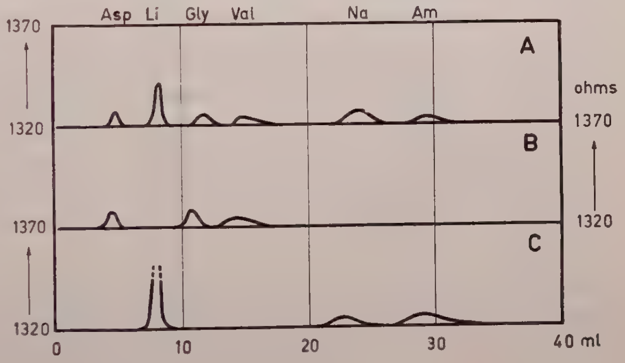

Fig. 5. Elution curves for runs in 0.25 N HCl containing 30 % ethanol on Dowex 50, all performed with the same column, 2 × 205 mm. A, 0.85 ml/hour; B, 0.58 ml/hour; C, 0.73 ml/hour. See Tables 1 and 2.

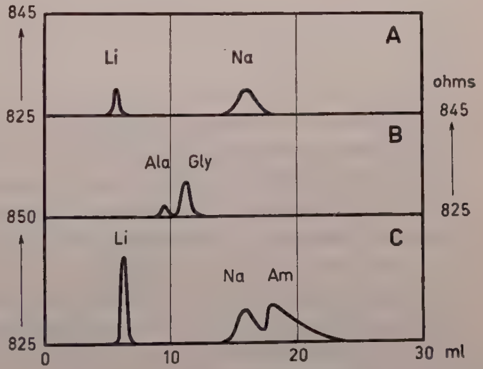

Fig. 6. Elution curves for runs in 0.4 N HCl containing 30 % ethanol on Dowex 50, all performed with the same column, 2.26 × 229 mm. A, 0.88 ml/hour; B, 0.88 ml/hour; C, 1.12 ml/hour. See Tables 1 and 2.

---

[1] The work on HCl solutions with ethanol was started before the appearance of the paper of HIRS, MOORE and STEIN [10] where they describe the use of 40 % ethanol as an addition to formate buffer for the separation of serine-threonine and of glycine-alanine, and after that publication the work was only partially pursued.

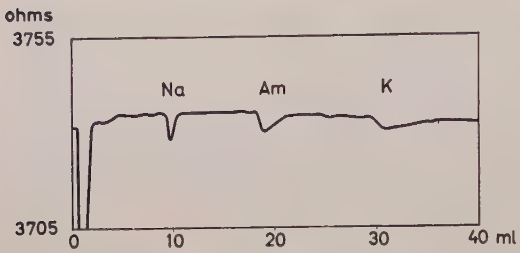

Fig. 7. Elution curve for a run in 0.85 % LiCl on Dowex 50. 2.06 × 205 mm; 0.52 ml/hour. See Table 2.

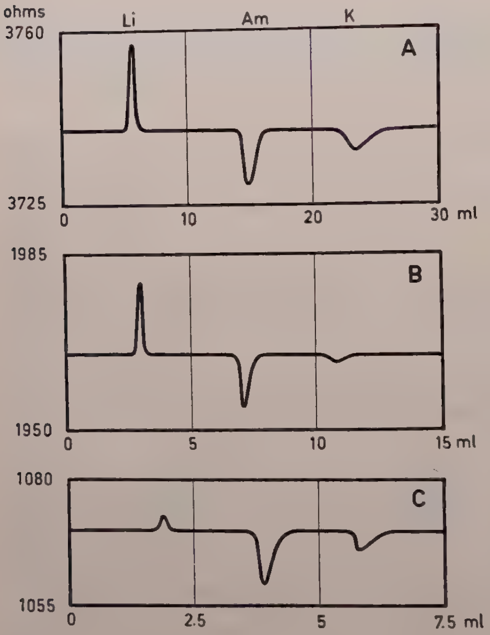

Fig. 8. Elution curves for runs in 1, 2 and 4 % NaCl on Dowex 50, all performed with the same column, 2.26 × 225 mm. A, 0.88 ml/hour; B, 0.52 ml/hour; C, 0.63 ml/hour (as regards the volume scales chosen, see below in the section on peak positions). See Table 2.

The curves for elution analyses in 0.1 N HCl with various additions of HCHO were so similar to corresponding runs without HCHO that they need not be published. A slight shift towards smaller elution volumes was observed, when the HCHO concentration was raised: 18, 17 and 16 ml, respectively, for aspartic acid, when the HCHO concentration was 0.1, 0.3 and 1.0 %, respectively.

It was found that formaldehyde has a destroying effect on Dowex 50. After the runs with amino acids in hydrochloric acid with various additions of formaldehyde, the ion exchange column was washed with pure HCl, and a new run was performed in a manner identical to that used before the experiments with formaldehyde. The peaks of aspartic acid and glutamic acid were then very drawn-out and correspondingly lower.

The addition of 10 % acetic acid to 0.1 N HCl depresses the conductance only a little and has no effect on the elution of, for example, serine and glycine. When

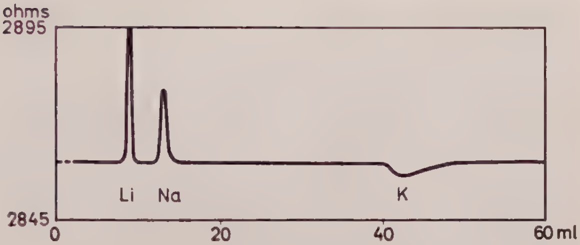

Fig. 9. Elution curve for a run in 1 % AmCl on Dowex 50, 2.66 × 205 mm, 1.18 ml/hour. See Table 2.

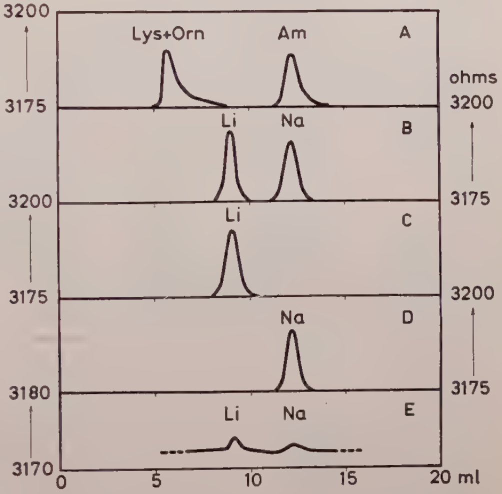

Fig. 10. Elution curves for runs in 1.25 % KCl on Dowex 50, all performed with the same column, 2.75 × 210 mm. A, 1.24 ml/hour (0–9 ml), and 0.95 ml/hour (after 9 ml); B, 1.55 ml/hour; C, 0.89 ml/hour; D, 1.64 ml/hour. In diagram A, lysine hydrochloride = 0.33 mg, and ornithine hydrochloride = 0.10 mg. For amounts of alkali metal chlorides, see Table 2.

50 % acetic acid is added, the capacitance of the cell decreases to about $^1/_3$ of the original value, and the base line becomes very unsteady. Also in this solvent, no effect on the elution of serine and glycine has been observed.

Experiments with alkali chloride solutions

Solutions of alkali chlorides have been investigated in order to determine the sensitivity that can be obtained with such solvents, and in order to establish the differences between hydrochloric acid and neutral chlorides. Also, it seemed of interest to investigate if there are specific properties of certain alkali metals in special cases.

Figs. 7–10 show the elution curves for some runs with various substances in the solvents mentioned. For comparisons of these curves, see below under the headings “peak shapes” and “peak positions”.

Experiments with acidified solutions of sodium and potassium chloride

When it was found that, as regards solvent properties, the alkali metal ions act in a way rather similar to that of hydrogen ions, it was deemed advisable to try alkali metal chloride solutions with an addition of enough acid to make the solution acid without adding so much that the hydrogen ions could compete with the alkali metal

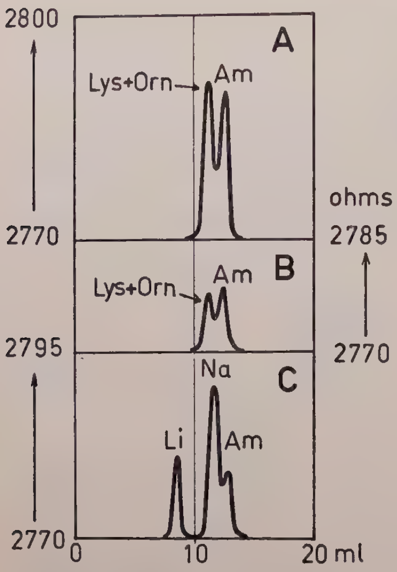

Fig. 11. Elution curves for runs in 1.25 % KCl with 0.008 N HCl on Dowex 50, both performed with the same column, 2.75 × 210 mm. A, 1.55 ml/hour; B, 1.58 ml/hour; A, 0.18 mg lysine hydrochloride and 0.20 mg ornithine hydrochloride; B, 0.068 mg lysine hydrochloride and 0.075 mg ornithine hydrochloride. For amounts of alkali metal chlorides, see Table 2.

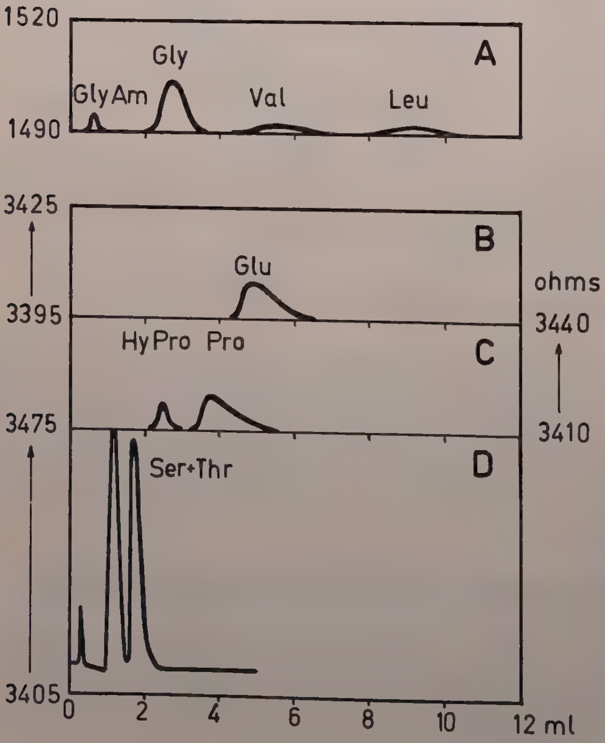

Fig. 12. Elution curves for runs in 0.1 N HCl with 1 M KCl on Dowex 50, all performed with the same column, 2.06 × 208 mm. A, 0.65 ml/hour; B, 0.66 ml/hour; C, 0.69 ml/hour; D, 0.37 ml/hour. In the experiment marked A, the cell constant was K = 209, while in the other experiments it was K = 478. See Table 1.

ions in the ion exchange reactions. A special importance of such a combined system is apparent when considering the fact that all the neutral amino acids occur as "zwitter" ions in neutral solutions, i.e., they migrate almost with the solvent in such solutions, while in acid solutions they behave as positively charged ions.

The solvents used were dilute solutions of sodium chloride or potassium chloride with the addition of a low concentration of HCl. Fig. 11 shows that the addition of as little as 0.008 *N* HCl to 1.25 % KCl gives a separation of Na and Am that is not observed without HCl (cf. Fig. 10). In runs with 1 % NaCl with 0.001 *N* HCl, similar effects have not been observed.

A solution containing 1 *M* KCl and 0.1 *N* HCl was also tried in order to study the chromatographic behaviour at a high ionic strength but at a lower hydrogen ion concentration than 1 *N* (see Fig. 12). There is a considerable change in the position of glutamic acid (and of aspartic acid), while the other amino acids have not changed their relative positions very much. In the lowest diagram in Fig. 12, the two first peaks represent the changes caused by HCl and KCl passing through the column.

Experiments with buffer solutions

Buffer solutions are used for the purpose of keeping the hydrogen ion concentration as constant as possible, and the conductance is to a large part caused by the hydrogen ions, at least at lower pH values. Thus, only very small changes of the conductivity values are to be expected in such cases. Some experiments have been performed, however, in order to see if there is some hope of using buffers in chromatography with conductivity recording.

The sodium citrate buffer used to advantage by Moore and Stein [12] was on two occasions found to give an astonishingly unsteady base line (see Fig. 13). This phenomenon has not been further investigated.

The phosphate buffer used by the same authors [12] was found serviceable. However, of several runs the one whose elution curve is shown in Fig. 14 was the most successful, and the other runs showed that this solvent cannot be regarded as ideal for this type of recording.

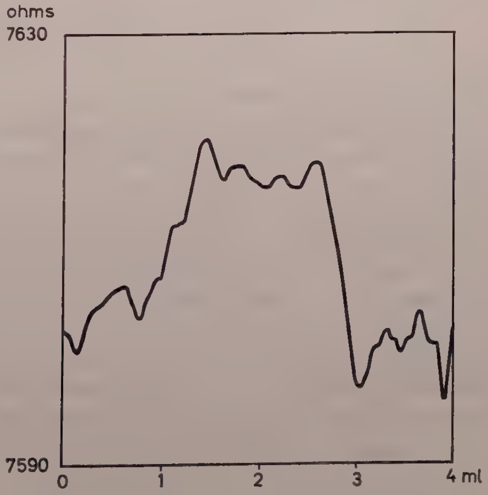

Fig. 13. Part of a recording of what was intended to be a base line with a 0.1 *M* sodium citrate buffer, pH = 3.42. 4 × 435 mm; about 3 ml/hour. See the text.

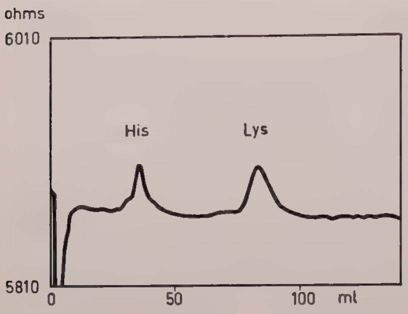

Fig. 14. Elution curve for a run in 0.1 *M* sodium phosphate buffer, pH = 7.0. 9 × 250 mm; 6.0 ml/hour. Histidine dihydrochloride = 0.72 mg, and lysine hydrochloride = 1.48 mg.

Comparison of elution curves: peak shapes

As is well known from the theory of chromatography, a linear sorption isotherm gives symmetrical peaks, while an isotherm convex upwards gives peaks with a "tail", and an isotherm concave upwards gives peaks of the reverse appearance, which will here be called peaks with a "neb".

The curves in this paper show that symmetrical peaks are typical for substances that are eluted with a high R_F value, while substances more slowly eluted emerge with tailing.

In a few runs with histidine in sodium chloride solutions, a remarkable "nebbing" has been observed. However, when these experiments were repeated a year later, no such "nebbing" was obtained, and the phenomenon could not be clarified. In some cases of overloading, a certain "nebbing" has also been observed.

Another property of the peaks is that they can deviate from the base line both upwards and downwards ("peaks" and "valleys"). This is in accordance with the theoretical formula (11) derived in an earlier paper [1]

$$\frac{\Delta \mathrm{R}}{\Delta c_{\mathrm{A}}} = -\frac{\mathrm{K\,F}\,(u_{\mathrm{A}^+} - u_{\mathrm{H}^+})}{\varkappa^2 \left(1 + \frac{K_{\mathrm{A}}}{c_{\mathrm{H}^+}}\right)} \tag{1}$$

that for a more general case could be written with u_{S^+} instead of u_{H^+} (u_{S^+} is the mobility of the positive ion of the solvent). For alkali metal ions, and other ions that do not have a dissociation at the pH used, the expression in parenthesis in the denominator can be omitted.

Evidently, if u_{S^+} is higher than u_{A^+} (which is the mobility value for the positive ion of the solute analyzed) the expression $\Delta \mathrm{R}/\Delta c_{\mathrm{A}}$ becomes positive, while the reverse is the case, if u_{S^+} is smaller than u_{A^+}. A good example of this phenomenon is given by Figs. 7–10, where the elution curves are given for three of the alkali metals in a solution of the fourth.

In cases where $u_{\mathrm{A}^+} = u_{\mathrm{S}^+}$, a zone of a substance A will not show up as a peak in the elution curve. Very often, this can be considered a great disadvantage of the method. However, there may be cases where such a concealing of a zone is desired.

Comparison of elution curves: peak positions

By peak position will here be meant the volume of effluent at which the maximal concentration of the peak emerges. The peak positions for a certain substance are obviously dependent on the properties and the amount of the sorbent, on the properties of the solvent, on the proportion between sorbent and solvent, etc. On the other hand, the relative peak positions for various substances in one and the same chromatographic system will depend on the specific properties of these substances.

A fact of general importance is that the peak positions vary with the concentration of electrolyte in the solvent. With HCl and NaCl solutions, for which solvents most data are available, the interesting fact has been observed that the elution volume of the peaks of many substances varies approximately inversely with the concentration of the electrolyte. This is shown, for example, by a comparison of the curves in Fig. 8 where the volume scales have been chosen so that the mentioned relationship is valid, if all peaks of the same substance occupy positions exactly above each other. In order to obtain a theoretical justification for this phenomenon, a calculation has been made, that will be reported in the next section.

As can be expected, the above-mentioned rule is not strictly valid. It has been observed both by the author and by many others, that a change of the concentration of the solvent has a different effect for different substances analyzed. This is clearly shown by a comparison of the elution curves for aspartic acid, serine, and glutamic acid in 0.1, 0.4 and 1.0 *N* HCl (see Figs. 1–3). In the last solvent, serine occupies a position between the two other amino acids, while at lower concentrations of HCl it emerges together with glutamic acid.

A remarkable change of peak position is obtained by the addition of, for example, 30–40 % ethanol to the solvent. This phenomenon was first described by Hirs, Moore and Stein [10] for the amino acid pairs alanine–glycine (cf. above, Fig. 6 B) and threonine–serine. In the experiments described here, it has been found that sodium shows a similar change of position, while the other alkali metals and ammonium do not change their position to any significant degree.

Quite a remarkable change of peak position is also obtained when 1 *M* KCl is added to 0.1 *N* HCl. In this case, the dicarboxylic amino acids are proportionately more strongly retained by the resin column than the neutral amino acids.

A theoretical formula for elution volumes in ion exchange chromatography of uni-uni-valent salts

For the derivation of a formula relating peak positions to physical chemical properties of the chromatographic system used, a linear isotherm, i.e., symmetrical peaks, are assumed. The following notations will be used (cf. Glueckauf [13]).

a_{MX}, a_{NX}, etc. = activity of the salt MX (NX, etc.) in the outside solution

$\bar{a}_{MX}$, $\bar{a}_{NX}$, etc. = activity of the salt MX (NX, etc.) in the resin phase

P = pressure (= energy change per unit volume)

v_{MX}, v_{NX}, etc. = effective solvated molar volume of the salt MX (NX, etc.)

[M], [N], etc. = equivalent concentration of the ion M^+ (N^+, etc.) in the outside solution

$[\overline{M}]$, $[\overline{N}]$, etc. = equivalent concentration of the ion M^+ (N^+, etc.) in the resin phase

γ_{MX}, γ_{NX}, etc. = mean activity coefficient of the salt MX (NX, etc.) in the outside solution

$\bar{\gamma}_{MX}$, $\bar{\gamma}_{NX}$, etc. = mean activity coefficient of the salt MX (NX, etc.) in the resin phase
R_F = migration rate of a chromatographic zone relative to the solvent (cf. [14])
A_S, A_L = cross-section area of the stationary phase and the mobile phase, respectively
V_S, V_M = total volumes of the stationary phase and the mobile phase, respectively
α = the partition coefficient of a solute between the resin phase and the outside solution
V_{tot} = the elution volume for a peak
V_{corr} = "corrected elution volume", i.e., $V_{tot} - V_M$.

By a strict application of thermodynamic formulas, GLUECKAUF has derived the following (slightly transformed) formula[1] for the equilibrium distribution of a uni-uni-valent electrolyte MX between an ion exchanger and the solvent [13]

$$\mathrm{R\,T}\ln\frac{a_{MX}}{\bar{a}_{MX}} = P\,v_{MX}. \tag{2}$$

By subtracting one such formula for a substance NX from the corresponding formula for MX, the following result is obtained

$$\mathrm{R\,T}\ln\frac{a_{MX}\,\bar{a}_{NX}}{\bar{a}_{MX}\,a_{NX}} = P\,(v_{MX} - v_{NX}). \tag{3}$$

Now, a_{MX}, etc., can be written $[M]\,\gamma_{MX}^2$, etc., and the formula takes the following form

$$\mathrm{R\,T}\ln\frac{[M]\,\gamma_{MX}^2\,[\bar{N}]\,\bar{\gamma}_{NX}^2}{[\bar{M}]\,\bar{\gamma}_{MX}^2\,[N]\,\gamma_{NX}^2} = P\,(v_{MX} - v_{NX}). \tag{4}$$

This formula clearly shows that the equilibrium is determined by activity coefficients, the swelling pressure of the resin, and the molar volumes of the substances exchanged for one another.

It can be shown [18] that the right hand side of formula (4) has only a small influence on the equilibrium. Thus, this term can be omitted and the rest of the formula rearranged. In such a way it is found that it can be written

$$\frac{[\bar{N}]}{[N]} = \frac{[\bar{M}]}{[M]}\cdot\frac{\bar{\gamma}_{MX}^2\,\gamma_{NX}^2}{\gamma_{MX}^2\,\bar{\gamma}_{NX}^2}. \tag{5}$$

Here, $[\bar{N}]/[N]$ is the quantity that is commonly called partition coefficient with the notation α.

According to MARTIN and SYNGE [14], the R_F value of a zone can be written

$$R_F = \frac{1}{1 + \alpha\,A_S/A_L}. \tag{6}$$

---

[1] Similar formulas were derived earlier by GREGOR *et al.* [15, 16] and, indeed, they may easily be derived from equations given by DONNAN in 1932 [17]. It seems as if the last-mentioned formulas would have been overlooked by the ion exchange investigators before GREGOR and GLUECKAUF.

A_S/A_L is here the quotient between the cross-section area of the stationary phase and that of the mobile phase, which (for cylindrical columns) is the same as the quotient between the total volume of the stationary phase and that of the moving phase $= V_S/V_M$.

Another expression for R_F is $R_F = V_M/V_{tot} = V_M/(V_M + V_{corr})$, which simply means that the R_F concept refers to effluent volumes instead of to lengths in the column. We can now write

$$R_F = \frac{1}{1+\alpha\, V_S/V_M} = \frac{1}{1+V_{corr}/V_M} \tag{7}$$

which shows that $\alpha \cdot V_S/V_M = V_{corr}/V_M$. This gives

$$V_{tot} = V_M + V_S\,\alpha. \tag{8}$$

Here, α can be replaced by $[\bar{N}]/[N]$ according to formula (5) so that the following final formula is obtained

$$V_{tot} = V_M + V_S \cdot \frac{[\bar{M}]}{[M]} \cdot \frac{\bar{\gamma}^2_{MX}\, \gamma^2_{NX}}{\gamma^2_{MX}\, \bar{\gamma}^2_{NX}}. \tag{9}$$

If volume changes can be neglected, V_S/V_M is a constant, and if the outside solution is dilute, $[\bar{M}]$ is constant and equal to the total capacity. For very small changes, all γ values will remain constant, and the corrected volume is then inversely proportional to the concentration [M] of the outside solution. The behaviour reported in the preceding section then has a theoretical foundation (actually, in Fig. 8, V_{tot} is used instead of V_{corr}, but this does not introduce any appreciable error, since V_M is only about 0.4 ml).

The theoretical formula furthermore demonstrates that for two different substances, N_1X and N_2X, the corrected elution volumes are proportional to the quotients between $\gamma^2_{N_1X}$ and $\gamma^2_{N_2X}$, which is easily found by making all other factors constant. This of course is a limiting case that pertains to the special condition that only very small amounts are applied to the column.

The last result—that peak positions are proportional to $\gamma^2_{N_1X}$—points to a method for determining quotients between resin-phase activities by chromatography.[1] One advantage of such an approach would be that several substances could readily be analyzed in the same run under exactly identical conditions. Also, no concentrations need be determined, since the peaks will emerge at the same position irrespectively of the amounts in the zones (as long as overload is prevented). Instead, elution volumes are measured, which is an easy (but not very exact) procedure. The method is similar to the determination of partition coefficients by partition chromatography [14], and with the derivation made above, it seems quite logical to compare the two processes.

Comparison of elution curves: peak areas

In previous papers [1, 2], theoretical formulas have been derived for the relation between amount of a substance in a chromatographic zone and the area of the peak recorded for that zone. Here, some data will be reported that have been obtained

---

[1] Previously, similar suggestions have been made by, among others, DU RIETZ [19] and SAMUELSON [20].

Table 4. Chromatographic data and analytical results for calibration runs with aspartic and glutamic acid in 0.1 *N* HCl.
(Upper left corners: Asp; lower right corners: Glu.)

No.	μg added	mg total	ml/hour	cm² corr.	μg found	100 minus % yield	μg A × 100 / μg A + μg B		
							exp.	calc.	Δ
1	566	0.57	1.295	101.5	545	−3.7			
2	566	0.57	1.27	101.4	550	−2.8			
3	340	0.91	1.21	79.7	349	+2.6	38.2	37.5	+0.7
	566		1.21	109.4	566	±0			
4	226	0.57	1.30	42.0	226	±0	39.3	40	−0.7
	339		1.29	63.4	349	+3.0			
5	226	0.57	1.29	42.2	226	±0	40.5	40	+0.5
	339		1.29	60.0	331	−2.4			
6	565	1.13	1.09	120.0	550	−2.7	49.2	50	−0.8
	565		1.10	119.5	568	+0.5			
7	424	0.85	1.13	92.4	437	+3.1	52.4	50	+2.4
	424		1.15	80.8	397	−6.4			
8	226	0.45	1.12	49.1	228	+0.9	50.2	50	+0.2
	226		1.13	46.5	226	±0			
9	113	0.23	1.12	24.3	113	±0	50.9	50	+0.9
	113		1.16	21.9	109	−3.5			
10	226	0.45	1.11	51.4	237	+4.9	52.0	50	+2.0
	226		1.11	46.2	219	−3.1			
11	113	0.23	1.08	26.1	117	+3.5	50.2	50	+0.2
	113		1.08	25.2	116	+2.7			
12	226	0.45	1.07	51.5	228	+0.9	50.7	50	+0.7
	226		1.09	47.6	222	−1.8			
13	453	0.68	1.28	85.0	451	−0.4	66.7	66.7	0
	226		1.29	40.6	225	−0.4			
14	453	0.68	1.30	85.9	463	+2.2	66.6	66.7	−0.1
	226		1.30	41.7	232	+2.7			
15	453	0.68	1.25	87.9	456	+0.7	66.9	66.7	+0.2
	226		1.25	42.7	226	±0			
16	566	0.71	1.26	109.4	571	+0.9	80.4	80	+0.4
	141		1.25	26.3	140	−0.7			

experimentally for aspartic and glutamic acid. The values obtained for other substances are not satisfactory from a statistical point of view, and they will not be reported in this paper. However, the data presented here are comprehensive enough to give an idea of the accuracy and usefulness of the method.

A series of calibration experiments was performed with various amounts and proportions of aspartic and glutamic acid on the same column. Both substances were first recrystallized from pure samples (Lemke and Eastman Kodak, respectively) and then carefully weighed and dissolved to give stock solutions in 0.1 *N* HCl. All runs were performed with this solvent on Dowex 50 in a glass column of the inner dimensions 2.65 × 205 mm. Experimental and analytical data for these runs have been collected in Table 4. In this table, the column "100 minus % yield" shows that about 75 % of the values are within ± 3 %, while two values are 5 and 6½ % in error. This is not comparable to the most refined and accurate methods in use at present, but in view of the difficulties of continuous recording of electrolytic conductivity during several days, the magnitude of error reported here can be considered reasonable.

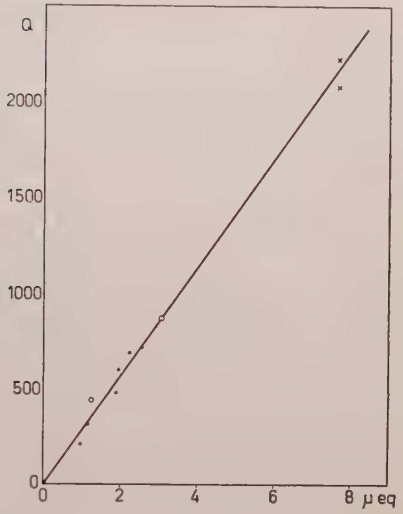

Fig. 15. Experimental Q values for aspartic acid, plotted against N_B (cf. formula (10)). ●, in 0.1 N HCl with a cell constant K = 64.5; ×, 0.4 N HCl with K = 209; ○, 0.4 N HCl with K = 478.

Another question is to what degree one can compare the peak areas obtained for a certain substance with different concentrations of the solvent electrolyte and with different values of the cell constant. According to formula (5) in the preceding paper [2], which can here suitably be rearranged to give

$$\mathrm{N_B} = -\frac{1}{\mathrm{F}\,\Delta u}\left(\frac{\mathrm{K}\left(1+\frac{K_\mathrm{A}}{c_{\mathrm{H}^+}}\right)}{\mathrm{R}^2}\cdot k_{\mathrm{B,\,cm}}\cdot k_\mathrm{t}\cdot k_{\mathrm{t,\,cm}}\cdot \mathbf{A}\right) = \frac{\mathrm{Q}}{\mathrm{F}\,\Delta u}, \tag{10}$$

such a comparison should be possible. In this formula, the letters signify the following quantities:

$\mathrm{N_B}$ = equivalents of the substance in the zone
F = one faraday = 96,494 coulombs eq^{-1}
Δu = the difference between the mobilities of the two exchanging ions
K = the cell constant of the conductivity cell
K_A = the dissociation constant of the carboxyl group of the amino acid
c_{H^+} = the hydrogen ion concentration
R = the resistance of the conductivity cell
$k_{\mathrm{B,\,cm}}$ = ohms per cm on the strip chart
k_t = the flow velocity in ml per hour
$k_{\mathrm{t,\,cm}}$ = hours per cm on the strip chart
A = the area of the peak in cm^2
Q = the expression within parenthesis in formula (10).

In Fig. 15, some data are given for aspartic acid, obtained on various occasions with a cell constant of 64.5 (0.1 N HCl), 209 (0.4 N HCl) and 478 (0.4 N HCl). The values have been collected from several runs which were not designed to give the highest possible accuracy as regards peak areas. However, it seems clear that there is a consistency in spite of the fact that there is a four-fold variation of the HCl concentration and a seven-fold variation of the value of the cell constant.

The straight line in Fig. 15 gives a value of Δu of 0.00284. Combined with the value 0.00320 for H^+ ions in HCl, the mobility value 0.00036 $cm^2\ sec^{-1}\ volt^{-1}$ is obtained for the aspartic acid ions. This value is of the right order of magnitude but, for obvious reasons, it cannot be expected to be absolutely correct.

ACKNOWLEDGEMENTS

The author wishes to thank Professor ARNE TISELIUS for kind interest in this work and for facilities put at his disposal. The author is also indebted to many of his colleagues at the Institute of Biochemistry, Uppsala, for helpful discussions on various problems of chromatography. A large part of the expenses for the equipment used in this work has been defrayed by grants to the Institute from the Rockefeller and Wallenberg foundations, which is gratefully acknowledged.

Institute of Biochemistry, Uppsala University, Uppsala, Sweden.

REFERENCES

1. DRAKE, B., Arkiv f. Kemi *4,* 401 (1952).
2. DRAKE, B., Arkiv f. Kemi *8,* 159 (1955).
3. KUNIN, R., and BARRY, R. E., Ind. Eng. Chem. *41,* 1269 (1949).
4. NACHOD, F. C., and WOOD, W., J. Am. Chem. Soc. *66,* 1380 (1944).
5. DAVIES, C. W., and THOMAS, G. G., J. Chem. Soc. *1951,* 2624.
6. DRAKE, B., and GARDELL, S., Arkiv f. Kemi *4,* 469 (1952).
7. BRAND, E., and EDSALL, J. T., Ann. Rev. Biochem. *16,* 223 (1947).
8. VRETLIND, A., Acta Physiol. Scand. *27,* 189 (1952).
9. CLAESSON, S., Arkiv f. Kemi, Mineral. Geol. *23 A,* No. 1 (1946).
10. HIRS, C. H. W., MOORE, S., and STEIN, W. H., J. Biol. Chem. *195,* 669 (1952).
11. SCHRAMM, G., and PRIMOSIGH, J., Ber. *77,* 417 (1944).
12. MOORE, S., and STEIN, W. H., J. Biol. Chem. *192,* 663 (1951).
13. GLUECKAUF, E., *Proc. Roy. Soc. 186 A,* 35 (1947).
14. MARTIN, A. J. P., and SYNGE, R. L. M., Biochem. J. *35,* 1358 (1941).
15. GREGOR, H. P., J. Am. Chem. Soc. *70,* 1293 (1948).
16. GREGOR, H. P., J. Am. Chem. Soc. *73,* 642 (1951).
17. DONNAN, F. G., and GUGGENHEIM, E. A., Z. physik. Chem. A *162,* 346 (1932).
    DONNAN, F. G., Z. physik. Chem. A *168,* 369 (1934).
18. KITCHENER, J. A., Ion Exchange and its Applications, p. 17, Soc. of Chem. Industry, London, 1954.
19. DU RIETZ, C., Diss., Tekn. Högskolan, Stockholm, 1938.
20. SAMUELSON, O., Diss., Tekn. Högskolan, Stockholm, 1944.

Tryckt den 20 april 1955

Uppsala 1955. Almqvist & Wiksells Boktryckeri AB

ARKIV FÖR KEMI Band 8 nr 20

Communicated 9 March 1955 by ARNE WESTGREN and ARNE FREDGA

Chromatography combined with automatic recording of electrolytic conductivity

V. Model experiments on gradient elution analysis

By BIRGER DRAKE

With 3 figures in the text

Earlier publications in this series [1–3] have described the analysis of, for example, amino acids by chromatography combined with a simultaneous recording of electrolytic conductivity. During the continued work, the idea turned up to apply the same method also to gradient elution analysis (cf., for example, [4]).

Before any experiments were performed, some calculations demonstrated that gradient elution can be considered a practical method which, however, should not be expected to guarantee a better separation of any pair of substances than elution at a suitable constant concentration. A more comprehensive treatment led to the formulation of a simple theory for special cases of gradient elution [5], which confirmed this statement. Consequently, the practical work was confined to some simple model experiments which will be described here.

Theoretical

In most cases, a useful gradient involves a change in the recorded property that is very much larger than the small changes caused by normal amounts of the substances analyzed. Also, the concentration range covered by the gradient is often too large to be successfully recorded with an apparatus of the accurate type described earlier in this series [1, 6]. Therefore, if automatic recording is to be applied directly to gradient elution analysis, a special treatment is usually necessary. In such cases, some form of compensation of the changes caused by the gradient must be introduced. Three such arrangements will be discussed here.

An obvious way is to extend the range of recording, for example, by introducing a contact arrangement that shifts the balancing resistance when the recorder reaches the edge of the strip chart.[1] This method, however, has some drawbacks, e.g., a more complicated electro-mechanical equipment, a curve cut into pieces, and an inconvenient change in cell capacitance during an experiment.

---

[1] An arrangement of this kind has recently been advertised by Minneapolis-Honeywell Brown Regulator Co., Philadelphia 44, Pa., U.S.A.

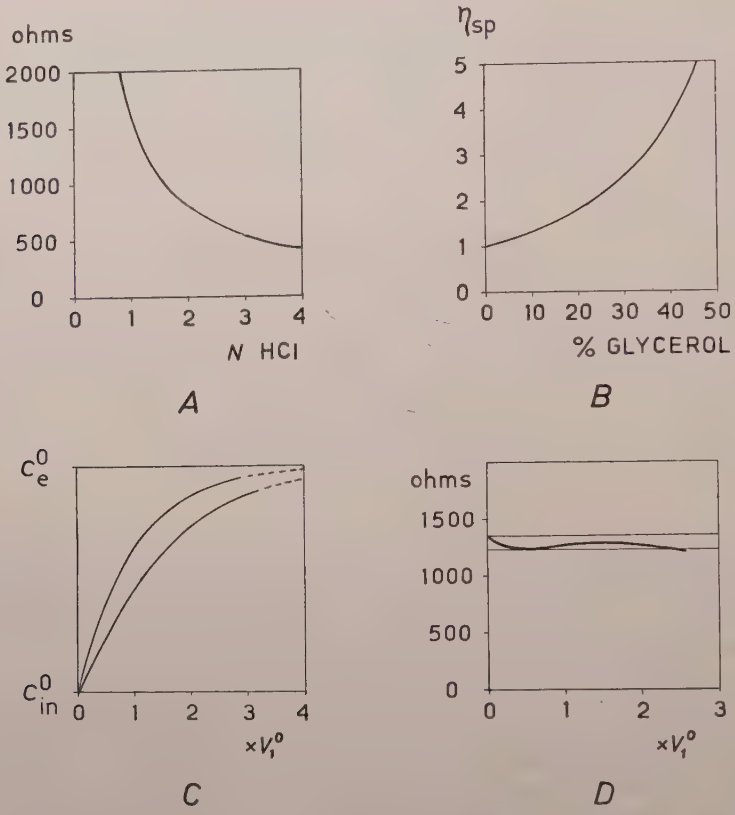

Fig. 1. Diagrams pertaining to the mixing of an HCl gradient and a glycerol gradient to give a combined gradient with nearly constant conductance. (a) resistance as a function of HCl concentration, (b) specific viscosity as a function of glycerol concentration, (c) suggested shape of the combined gradients, and (d) calculated resistance values at effluent volumes of 0–3 times the volume of one of the two equal mixing chambers.

Another approach would be to change, continuously and in a prescribed manner, the balancing resistance in the conductivity bridge. In such a case, a discontinuity in the recorded line is avoided, but the capacitance change would still be unbalanced. The apparatus may, of course, also be equipped with a synchronous arrangement for the continuous balancing of the cell capacitance, but this would make it rather too complex.

A third method, which has been adopted here, is to mix two gradients of which one is used because of its effect on the sorption properties of the substances analyzed, while the other is used only to correct the conductivity changes caused by the first. This can be afforded, for example, by combining one gradient of HCl with another gradient of glycerol, so that the increasing conductivity of the acid is counteracted by the increasing viscosity of the glycerol. Under proper conditions, the result will be that a base line is obtained which is more or less straight and which does not move outside the strip chart.

Suitable shapes of combined gradients. Since the conductivity of HCl is not exactly a linear function of the concentration and, especially, since the viscosity of glycerol is a definitely curved function of the concentration, the two gradients must have different shape. Fortunately, such gradients can easily be obtained in the same flowing solution by the use of two mixing chambers connected in series (cf. Cases 2 and 3 in [5], APPENDIX). As an example, the following preliminary calculation is reported. It is here assumed that literature data [7] can be used, and that WALDEN's rule (conductance × viscosity = constant) can be applied.

The resistance of different HCl solutions and the viscosity of different glycerol solutions are those shown in Fig. 1, a and b. It is obvious that a horizontal base line can be obtained only if the glycerol concentration is increased faster than the HCl concentration within the first part of the gradient. An acceptable balancing of these two factors would conceivably be obtained if the two gradients were, for example, those shown in Fig. 1 c, i.e., a simple exponential gradient for glycerol (cf. eq. (39) in [5])

$$c_{\mathrm{in}} = c_{\mathrm{e}}^{0}\,(1 - \mathrm{e}^{-W}) = 50\,(1 - \mathrm{e}^{-W})\ \% \tag{1}$$

and a more complex gradient for HCl (of a type corresponding to eq. (41) in [5])

$$c_{\mathrm{in}} - 0.12 = c_{\mathrm{e}}^{0} - (c_{\mathrm{e}}^{0} + (c_{\mathrm{e}}^{0} - c_{1}^{0})\,W)\,\mathrm{e}^{-W} = 0.44 - (0.44 + 0.22\,W)\,\mathrm{e}^{-W}. \tag{2}$$

W is here the quotient between the influent volume and the volume of one of the two mixing chambers.

In this case, the HCl concentration varies linearly with the influent volume in the first part of the gradient, which fact may be of value in practical cases (for theoretical purposes, a linear gradient is certainly advantageous, cf. below). The quantity that should be constant is $\mathrm{R} \times \eta_{\mathrm{sp}}$, where R is the resistance of a certain concentration of HCl without glycerol, and η_{sp} is the specific viscosity of a certain concentration of glycerol, assumed to be independent of the presence of HCl. Fig. 1 d shows that, under the conditions mentioned and with the concentrations given in Table 1, upper line, $\mathrm{R} \times \eta_{\mathrm{sp}}$ should be practically constant in the range 0.1–0.4 N HCl, the deviation from linearity being only some few percent.

Migration formulas. The formulas derived in ref. [5] for specified ideal cases cannot be employed here, because other relationships between HCl concentration and sorption strength were considered in that paper. Fortunately, however, the relationship for alkali metals is very simple (see [3]) and can suitably be written

$$\alpha_{\mathrm{t}} = \frac{\mathrm{P}}{c_{\mathrm{H}^{+}}} \tag{3}$$

where α_{t} = partition coefficient between the resin phase and the outside phase, P = a parameter, increasing with increasing sorption strength, and $c_{\mathrm{H}^{+}}$ = the HCl concentration.

For an ion exchange resin that can be considered saturated with H^{+}, there is a negligible additional sorption of such ions, i.e., $\alpha_{\mathrm{g}} = 0$ (α_{g} = partition coefficient of the "gradient substance", which in this case is HCl, between the resin phase and the outside phase). The formula for the length Δh_{t} travelled by the maximum concentration of a zone can then be written (cf. [5], formula (18))

$$\Delta h_t = \mathbf{H}\int_{w_1}^{w_2} \frac{\mathrm{d}w}{\alpha_t} = \frac{\mathbf{H}}{\mathrm{P}}\int_{w_1}^{w_2} c_{\mathrm{H}^+}\,\mathrm{d}w. \tag{4}$$

Here, **H** is the length of column containing a unit amount of the sorbent, and w is the effluent (more correctly the influent) volume.

In order to solve the integral in formula (4), c_{H^+} must be known as a function of w. For the first part of the gradient described above, the HCl concentration increases almost linearly, and the integral will get the simple form of a second order expression,

$$\Delta h_t = \frac{\mathbf{H}}{\mathrm{P}}\int_{w_1}^{w_2} (\alpha + 2\beta w)\,\mathrm{d}w = \frac{\mathbf{H}}{\mathrm{P}}\Big[\,\alpha w + \beta w^2\Big]_{w_1}^{w_2} \tag{5}$$

where α and β are two empirical parameters. For the complete gradient, a much more complicated expression is valid which will not be used in this paper. Therefore, the derivation of such a formula is not attempted here.

Formula (5) has been used for the calculation of theoretical values for the elution volumes of the four alkali metals employed as test substances. The result of that calculation is: Li, 4 ml; Na, 7 ml; Am, 10 $\frac{1}{2}$ ml; and K, 15 $\frac{1}{2}$ ml. This result was obtained on the assumptions that formulas (3) and (5) are valid, and that the chromatographic equipment was that described here. Also, it was assumed that the elution volumes in a constant HCl concentration of 0.1 *N* on the same column would be 5 $\frac{1}{2}$, 11, 19 $\frac{1}{2}$ and 33 ml (cf. [3]).

Experimental

Preliminary experiments. A simple trial-and-error procedure, including the measurement of some mixtures of HCl and glycerol, was followed. In this way, it was found that a conceivable arrangement for the production of an HCl-glycerol gradient with a practically constant conductance would be two mixing chambers of equal volume, coupled in series, and containing at the start the concentrations given in Table 1, upper line.

Table 1. Concentrations of HCl and of glycerol to be employed in order to obtain a combined gradient with nearly constant conductance.

	Substance	In the solution container	In the first mixing chamber	In the second mixing chamber
First attempt	HCl glycerol	0.56 *N* 55 %	0.34 *N* 55 %	0.12 *N* 0 %
Final choice	HCl glycerol	0.56 *N* 55 %	0.25 *N* 62.5 %	0.12 *N* 0 %

By running an empty gradient, it was found that a better combination of starting values would be that given in Table 1, lower line. Even in this case, the base line did not become perfectly straight but it stayed well within the permissible range.

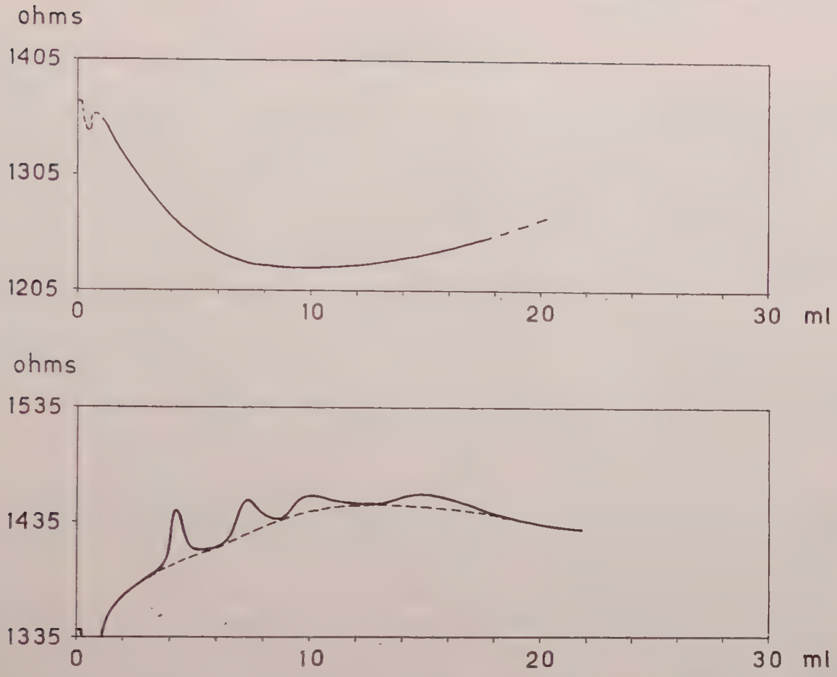

Fig. 2. Gradient elution curves. (a) an empty gradient, according to Table 1, upper line, and (b) an experiment with 0.25 mg LiCl, 0.53 mg NaCl, 0.48 mg AmCl, and 1.00 mg KCl, according to Table 1, lower line.

No further attempt was made to produce a more nearly linear base line, because this would have involved quite cumbersome trial-and-error work with successive adjustments of all the concentrations and perhaps also of the quotient between the volumes of the two mixing chambers.

Gradient production. The gradients were produced in the following way. Two chromatographic columns of Perspex with screw threads at the ends (cf. [3]) were used as mixing chambers. They were firmly connected by means of a capillary coupling piece, and capillary drop tip pieces were fastened to the free ends. By means of Polythene sleeving (about 3 mm outer diameter) and small pieces of rubber tubing, the two drop tips were connected to a motor-driven hypodermic syringe and to the chromatographic column, respectively. Before assembling, the two mixing chambers were filled with the appropriate solutions (see Table 1), and a glass bead was placed in each. The syringe was also filled with its appropriate solution.

When starting an experiment, the two connected mixing chambers were given an oscillating movement (6 RPM) around a horizontal axis through the capillary between them by the aid of a rotating excentric disk. In that way, the glass beads caused a thorough mixing of the contents of the two mixing chambers.[1]

---

[1] An advantage of this method of mixing over those described previously (see, e.g., [4, 8–11]) is that the same arrangement can be used for many runs simultaneously. Also, the mixing chambers and the mixing beads can be made of any material, since there is no magnetism involved in the mixing procedure.

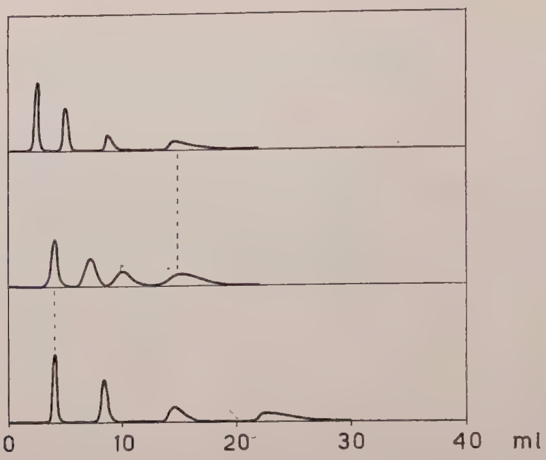

Fig. 3. Comparison between a gradient elution curve (cf. Fig. 2b) in the middle diagram and two hypothetical elution curves in 0.1 *N* HCl. The latter have been recalculated from experimental data [3] to give the same elution volume for K^+ and Li^+, respectively.

Chromatographic equipment. In all experiments described here, the sorbent was Dowex 50, 200–400 mesh, with 8 % cross-linkage, mixed with an equal volume of Celite that had been repeatedly sedimented in about 25 cm of distilled water between 5 and 15 minutes. At the start of the experiments, the sorbent had been washed with 0.12 *N* HCl.

The chromatographic column was made of Perspex and had the inner dimensions 3 × 83 mm. Drop tips were used at both ends, and the lower tip was connected directly to the inlet end of the conductivity cell (see [1], Fig. 3).

In all the model runs, lithium, sodium, ammonium and potassium chloride were employed as test substances.

Recording apparatus. The conductivity bridge and the adapter described in [1] were used together with a conductivity cell (cell constant K = 64.5) and a BROWN strip chart recorder. Normally, the balancing resistance was put at a value between 1200 and 1300 ohms, and a 200-ohms, 10-turn helical potentiometer was connected in series. Thus, the total resistance was about 1450 ohms, and the recording range was about 14 % of the total resistance.

Results

A few runs were performed with the equipment described above. Fig. 2 a shows the recorded curve for an empty gradient corresponding to the values in Table 1, upper line. Fig. 2 b shows a typical curve for a gradient elution experiment with the solutions given in Table 1, lower line. The four peaks represent from left to right: 0.25 mg LiCl, 0.53 mg NaCl, 0.48 mg AmCl, and 1.00 mg KCl.

According to the calculation of HCl concentrations in the effluent reported above, the elution volumes for the four peaks ($4\frac{1}{2}$, $7\frac{1}{2}$, $10\frac{1}{2}$ and 15 ml) correspond to the following HCl concentrations: 0.16, 0.20, 0.25, and 0.31 *N*. These values are satisfactorily similar to the corresponding values obtained in the calculation made above (4, 7, $10\frac{1}{2}$ and $15\frac{1}{2}$ ml).

Discussion

In the schematical Fig. 3, a comparison is made between gradient elution analysis and the usual type of elution at a constant concentration. The middle diagram corresponds to Fig. 2 b, while the other two diagrams correspond to hypothetical elution analyses at a constant concentration of HCl. The two latter curves have been drawn in such a way as to make either the potassium peak or the lithium peak coincide with the corresponding peak in the curve for the gradient elution experiment. Fig. 3 shows clearly that gradient elution, as expected, causes the zones to emerge closer together than in the usual type of elution.

Another important question is: To what extent can the diminished spreading of the zones counteract the fact that the zones are brought closer together? This question cannot be answered by the simple model experiments described here, and there is still no complete theoretical or practical solution of the problem of the relative efficiency of gradient elution analysis as compared to elution analysis at a suitable constant concentration.

As regards quantitative analysis by automatic recording of electrolytic conductivity, gradient elution is conceivably less accurate than elution at a constant concentration. One of the reasons for the lower accuracy is the fact that each zone emerges within a range of, for example, HCl concentrations. Thus, the magnitude of response is not the same for different parts of the same zone, and the peak area will consequently to some degree depend on the extent of zone spreading. However, if a number of experiments are performed under as nearly identical conditions as possible, it should be feasible to obtain empirical factors which can be employed for a reliable, but not extremely accurate, quantitative analysis of different substances.

Summary

It is shown that automatic recording of electrolytic conductivity may be used in following the concentration-volume curve for a number of zones in gradient elution analyses. This is achieved by the combination of two different gradients, for example, one of HCl and one of glycerol, so that the base line becomes nearly linear.

ACKNOWLEDGEMENTS

The author wishes to thank Professor Arne Tiselius for helpful criticism and for all facilities put at his disposal. Expenses connected with apparatus construction have been defrayed by grants to the Institute of Biochemistry from the Rockefeller and Wallenberg foundations, which is gratefully acknowledged.

REFERENCES

1. Drake, B., Arkiv f. Kemi *4*, 401 (1952).
2. Drake, B., and Gardell, S., Arkiv f. Kemi *4*, 469 (1952).
3. Drake, B., Arkiv f. Kemi *8*, 171 (1955).
4. Alm, R. S., Williams, R. J. P., and Tiselius, A., Acta Chem. Scand. *6*, 826 (1952).
5. Drake, B., Arkiv f. Kemi *8*, 1 (1955).
6. Drake, B., Arkiv f. Kemi *8*, 159 (1955).
7. Roth, W. A., and Scheel, K., Landolt-Börnstein, Physikalisch-chemische Tabellen, 1923–36.
8. Donaldson, K. O., Tulane, V. J., and Marshall, L. M., Anal. Chem. *24*, 185 (1952).
9. Cherkin, A., Martinez, F. E., and Dunn, M. S., J. Am. Chem. Soc. *75*, 1244 (1953).
10. Desreux, V., Rec. trav. chim. Pay-Bas *68*, 789 (1949).
11. Lakshmanan, T. K., and Liebermann, S., Arch. Biochem. Biophys. *45*, 235 (1953).

Tryckt den 20 april 1955

Uppsala 1955. Almqvist & Wiksells Boktryckeri AB

ARKIV FÖR KEMI Band 8 nr 21

Vorgelegt am 26. Januar 1955

Über Galaktose als Ausgangsmaterial für Reduktone und über die biologische Bildung der Ascorbinsäure

Von Hans von Euler und Hans Hasselquist

Mit 2 Figuren im Text

Nachweis von aci-Reduktonen aus Galaktose

Triose-Redukton entsteht nicht nur durch alkalische Behandlung der Glucose (Euler u. Martius, 1933) sondern auch mehrerer anderer Monosen und Biosen, und zwar findet man dieses aci-Redukton auch in alkalisch behandelten Lösungen von Fruktose, Mannose, Xylose, Ribose, Arabinose, Rhamnose, ferner Maltose und Laktose.

Aus Glucose und vermutlich auch aus anderen der genannten Zuckerarten, welche nach Lobry de Bruyn und Alberda van Ekenstein in alkalischer Lösung bis zur Erreichung eines Gleichgewichtes ineinander übergehen, entstehen neben Triose-Redukton auch aci-Redukton II, worüber bereits mehrfach berichtet wurde.[1]

Galaktose weicht in dieser Hinsicht von anderen Hexosen ab. Papierchromatographische Versuche haben uns zunächst gezeigt, dass aus Galaktose das Triose-Redukton unter den von uns eingehaltenen Bedingungen überhaupt nicht oder in minimalen Mengen entsteht.

1 g D-Galaktose wurde unter Stickstoff in 5 ml 2-*n*. NaOH gelöst, auf dem Wasserbad 3 Minuten auf 80° erhitzt und hierauf mit 4-*n*. HCl angesäuert. Die Reaktionsmischung wurde dann dreimal ausgeäthert. Die klar gelbe Ätherschicht wurde mit wasserfreiem Natriumsulfat getrocknet und im Vacuum bei 30° bis auf etwa 2 ml eingedunstet. Diese Lösung, die in *saurer* Lösung Tillmans-Reagenz kräftig reduziert, wurde nun zum Chromatogramm verwendet. Auch die mit Äther ausgeschüttelte wässrige Lösung enthielt Endiole, die TR in saurer Lösung reduzieren. Sie kamen darin in wesentlich geringerer Konzentration vor und konnten deshalb durch das Papierchromatogramm nicht reproduziert werden. Das stark reduzierende Pb-Salz konnte später aus dieser Lösung isoliert werden; es wird durch ein besonderes Chromatogramm beschrieben werden.

Papier: Munktells OB.

Lösung: 4 Tle *n*-Butanol, 1 Tl Eisessig, 1 Tl Wasser.

Entwickler: TR in alkoholischer Lösung (wurde sofort nach der Chromatographierung, während das Papier noch feucht war, verwendet, also in saurem Milieu).

Vergleichs-Substanzen: Triose-Redukton, 3,4-Dioxy-5-methyltetron.

---

[1] Euler und H. Hasselquist, Acad. Scient. Fennica, Virtanen-Festschrift 1955. — Lieb. Ann. Chem. 588, 205; 1954. — Dieses Arkiv Band 8, 1955, im Druck.

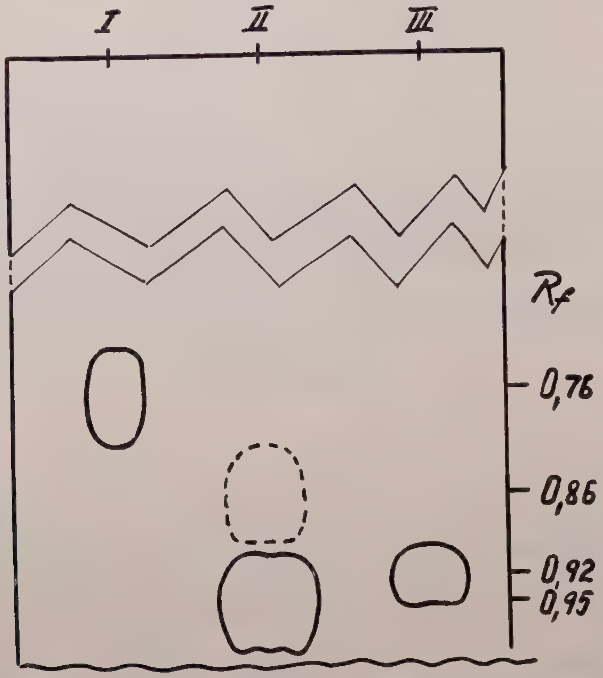

Fig. 1.

I. Aci-Redukton I.
II. Äther-Extr. d. Galaktose.
III. 3,4-Dioxy-5-methyl-tetron.

Aus dem Chromatogramm wird ersichtlich, dass die alkalisch behandelte Galaktose-Lösung eine Substanz vom $R_f = 0{,}95$ und eine zweite vom schwächer hervortretenden Flecken $R_f = 0{,}86$ enthält, die mit dem aci-Redukton I nicht identisch sein kann. Letzteres konnte aus Galaktose überhaupt nicht nachgewiesen werden, nicht einmal mit Hilfe von *p*-Nitranilin oder Benzidin, welche mit Triose-Redukton stark gefärbte Verbindungen liefern. Um zu untersuchen, ob die Substanz $R_f = 0.86$ mit Tetron identisch ist, wurde folgendes Chromatogramm II (mit folgender Mischung) hergestellt: 4 Tle *b*-Butanol, 1 Tl Eisessig, 5 Tle Wasser.

Diese Mischung wurde gut geschüttelt, worauf ihre Oberschicht zur Chromatographierung verwendet wurde.[1]

Vergleichs-Substanzen: Triose-Redukton, Reduktinsäure, Dioxymethyltetron, Ascorbinsäure, Dioxymaleinsäure.

Dem Chromatogramm II (Fig. 2) zufolge kann die aus der alkalibehandelten D-Galaktose (ätherlöslicher Teil) gewonnene Substanz $R_f = 0{,}96$ mit keiner der untersuchten Vergleichs-Substanzen identisch sein. Dagegen können wir noch nicht entscheiden, ob die aus Galaktose erhaltene Substanz $R_f = 0{,}89$ mit dem Tetron identisch ist, für das wir hier $R_f = 0{,}90$ finden. In einem späteren Versuch ergab der Fleck $R_f = 0{,}89$ mit *p*-Aminobenzoesäure eine schwach gelbe Farbe (ob dieselbe vom

---

[1] L. W. MAPSON u. S. M. PARTRIDGE, Nature 164, 479; 1949.

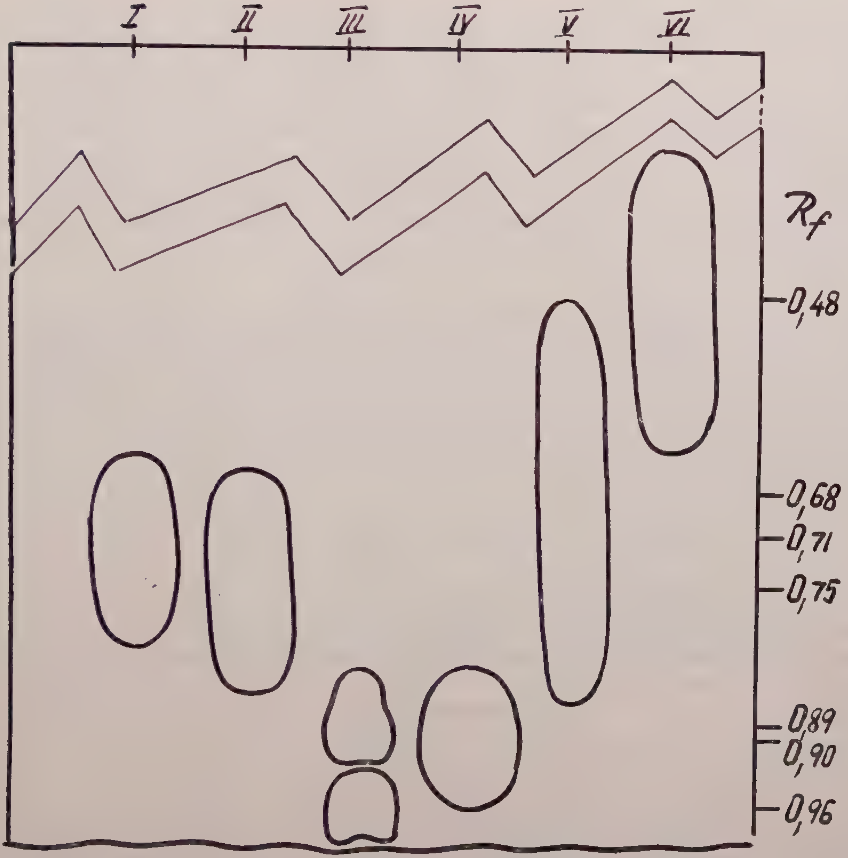

Fig. 2.

I. Aci-Redukton I.
II. Reduktinsäure.
III. Äther-Extr. Galaktose.
IV. 3,4-Dioxy-methyl-tetron.
V. Dioxy-maleinsäure.
VI. Ascorbinsäure.

Endiol oder etwa von einer Substanz herrührt, die gleich schnell wandert, liess sich noch nicht entscheiden), während das Tetron sich mit *p*-Aminobenzoesäure nicht zu einem farbigen Produkt vereinigt.

Reaktion der alkalisch behandelten Galaktose mit *p*-Aminobenzoesäure

Da das Endiol, das in der Ätherschicht der alkalisch behandelten D-Galaktose auftritt, nicht in kristallinischer Form isoliert werden kann (grosse Mengen einer anderen Substanz, die hygroskopisch ist, nicht als Endiol fungiert und sich in Äther löst, sind gleichzeitig anwesend), so wurde in folgender Weise versucht, ein Derivat mit unveränderter Endiol-Gruppe zu erhalten:

10 g D-Galaktose wurden unter Stickstoff in 50 ml 2-*n*. NaOH gelöst, bei 85° zwei Minuten auf dem Wasserbad erwärmt und dann mit 16 g $PbAc_2$ in 200 ml Wasser

versetzt, unter fortgesetztem Stickstoffstrom. Die hierbei entstehende Bleisalzfällung wurde mit Wasser gewaschen, wobei etwas Bleisalz mit brauner Farbe in Lösung ging.

Das in saurer Lösung stark TR-reduzierende Filtrat wurde mit Schwefelsäure auf pH 8 angesäuert, das gebildete Bleisulfat abfiltriert und mit *p*-Aminobenzoesäure, in 100 ml Wasser gelöst, versetzt. Die Lösung färbt sich allmählich intensiv gelb und scheidet nach etwa 1 Stunde gelbbraune glänzende Nadeln aus. Diese wurden nach 1 Tag abfiltriert, mit Wasser und dann mit Aceton gewaschen. Das Rohprodukt, 55 mg, schmolz bei 245° unter Zersetzung; durch Umkristallisieren aus Eisessig stieg der Schmpt. auf 249° (Sbst. 221).

Reduziert TR bei pH 5.

Die Sbst. 221 ist schwerlöslich in allen üblichen organischen Lösungsmitteln, ziemlich löslich in Eisessig und scheidet sich nicht daraus durch Zusatz von Wasser aus (zum Unterschied von der unmittelbar fallenden PAB-Verbindung des Reduktons). Löst sich leicht in Pyridin; bald nach der Lösung kristallisiert ein Salz in braunen Kristallen aus, das sich in warmem Wasser unter Rückbildung der ursprünglichen Substanz hydrolysiert.

Für $C_{19}H_{18}O_7N_2$	berechnet:	C = 59,06 %	H = 4,70 %	N = 7,25 %
	gefunden:	58,68 »	4,78 »	7,34 »

Titrierung der Substanz 221 mit TR in saurer Lösung:

8,7 mg der *p*-Aminobenzoesäure-Verbindung 221, in 3 ml warmen Eisessig gelöst und mit 15 ml Wasser verdünnt, wurden mit 0,01-*n*. TR bis zur bleibenden Rotfärbung titriert.

Verbrauch = 7,7 ml 0,01-*n*. TR

$$E_{\text{gef.}} = \frac{8{,}7}{0{,}01 \cdot 7{,}7} = 113.$$

Titrierung der D-Galaktose in alkalischer Lösung mit TR: 2,4 mg D-Galaktose in 15 ml Wasser wurden bei 80° unter Stickstoff mit 0,1 ml 2-*n*. NaOH versetzt (die Lösung war 0,013-*n*. bezüglich NaOH) und bei der gleichen Temperatur mit 0,01-*n*. TR titriert.

Bei dieser NaOH Konzentration ist TR bei 80° selbst stabil und liefert keine roten Spaltprodukte, was bei höheren NaOH Konzentrationen eintritt. Deswegen kann man unter obigen Bedingungen die Galaktose mit TR bis zu einem scharfen Übergangspunkt (schwache Blaufärbung) titrieren.

Verbrauch von TR bei der Titrierung in etwa 20 Min.: 3,3 ml.

Ein Mol D-Galaktose ($E = 90$), also 1 Endiol würden 2,67 ml 0,01-*n*. TR-Lösung verbrauchen. Der so festgestellte Verbrauch zeigt, dass ein Mol D-Galaktose 1,23 Mol Endiol entspricht.

Anthron-Versuch: In schwefelsäurer Lösung, 40 % bei 20°C Grünfärbung.

Alkali-Behandlung der D-Xylose bei 90°

Das von anderen untersuchten Hexosen abweichende Verhalten der Galaktose hat uns veranlasst, den Einfluss der Konfiguration auf die Alkali-Stabilität zu untersuchen und in diesem Zusammenhang zunächst die D-Xylose zu prüfen.

5 g D-Xylose, in 75 ml Wasser, wurden mit 3,5 g $PbAc_2$ versetzt und auf 90° erwärmt. Nach Zugabe von 2,25 g NaOH in 25 ml Wasser liess man die Mischung 4 Minuten bei 90° reagieren und neutralisierte dann mit Eisessig bis auf pH 7. Das dabei gebildete schwerlösliche, braune Bleisalz wurde abfiltriert und zuerst mit Wasser, dann mit Aceton gewaschen. Es wurde nach Trocknen bei 20° in etwa 50 ml Aceton aufgeschlämmt und mit H_2S solange behandelt, bis eine braunschwarze Fällung von Schwefelblei entstand. Vom PbS wurde abfiltriert und die nun stark gelbe Acetonlösung im Vacuum bei 30° auf ein kleines Volumen eingedunstet. Die daraus entstehende Kristallmasse wurde mit etwas Aceton gewaschen. Ausbeute 65 mg Substanz, von der ein kleiner Teil zur Herstellung eines Papierchromatogramms verwendet wurde.

Papier: Munktell OB. — Lösung: 4 Tle *n*-Butanol, 1 Tl Eisessig, 1 Tl Wasser.

Entwickler: TR gelöst in Alkohol (entwickelt bei noch feuchtem Papier, d. h. bei starker Acidität).

Vergleichs-Subst.: aci-Redukton I.

Das Chromatogramm zeigte deutlich, dass die aus Xylose bei 90° gebildete Substanz mit aci-Redukton I (Triose-Redukton) identisch ist. Das aus der alkalischen Xylose-Lösung erhaltene *p*-Nitranilid und das PAB-Salz waren ebenfalls identisch mit den entsprechenden Redukton I-Produkten.

Die Reaktion von TR mit Alkali-behandelter Xylose-Lösung ist in unserem Arbeitskreis mehrfach untersucht worden.

Nach EULER u. HASSELQUIST[1] wird in warmer (65°) alkalischer Lösung von D-Xylose so viel TR verbraucht, wie wenn aus *einem* Mol der Pentose *zwei* Endiol-Gruppen gebildet würden. Wir haben dabei in Betracht gezogen, dass dieser Vorgang ohne Spaltung des Pentosemoleküls eintritt, etwa unter Bildung eines Bis-endiols, welches dann bei der Oxydation durch TR zerfällt.

Nach Versuchen von M. L. STEIN[2] liefert D-Xylose bei der (nicht-oxydativen) alkalischen Behandlung etwa 40 % mehr Endiol als D-Glucose. Wie in dieser Arbeit hervorgehoben wird, hängt die Bildung des aci-Reduktons I aus Xylose stark von der Temperatur und Zeit der Erhitzung in der alkalischen Lösung ab. Demgemäss wurde bei 75° in 3–10 Minuten Triose-Redukton nur spurenweise erhalten, während andere Reduktone auftraten, u. zw. entstand nach Erwärmen unter 75° ein Haupt-Flecken R_f 0,36.

Alkalische Behandlung der D-Galaktose bei 90° in Gegenwart von Bleiacetat

Zum Vergleich mit obigem Versuch wurde D-Galaktose in analoger Weise mit Alkali und $PbAc_2$ behandelt. Das entstandene hellbraune Bleisalz wurde feinpulverisiert in Aceton aufgeschlämmt und H_2S in die Suspension eingeleitet. Nach Abfiltrieren des Bleisulfates wurde die hellgelbe Acetonlösung im Vacuum bei 30° eingedunstet. Als Rückstand verblieb ein hellgelbes Öl, das durch Reiben teilweise kristallisierte. Nach Zusatz von etwas Aceton konnten die Kristalle abfiltriert werden. Ausbeute an reiner Subst. 7 mg.

Davon wurde ein Teil zur Papierchromatographie verwendet (ausgeführt wie mit D-Xylose), unter Anwendung von Triose-Redukton als Vergleichs-Substanz. Dabei ergab sich keinerlei Unterschied bez. R_f, das zu 0,76 ermittelt wurde. Auch wurde das gleiche *p*-Nitranilid wie mit Redukton erhalten. Wie der Versuch zeigt, entsteht also aus D-Galaktose bei 90° in Gegenwart von $PbAc_2$ ebenfalls Triose-Redukton, allerding *in wesentlich geringerer Ausbeute* als aus Xylose und Glucose.

---

[1] EULER u. H. HASSELQUIST, Experientia 5, 81 (1949), Karrer-Festschrift.

[2] M. L. STEIN u. EULER, Dieses Arkiv 8, 1955, im Druck.

Verhalten der D-Galaktose und der D-Glucose in saurer Lösung bei 150°

Versuch I: 1 g D-Glucose + 10 ml 5 %ige Schwefelsäure-Lösung im zugeschmolzenen Bombenrohr.

Versuch II: 1 g D-Galaktose + 10 ml 5 %ige Schwefelsäure-Lösung im zugeschmolzenen Bombenrohr.

Die beiden Rohre wurden im Wärmeschrank bei 150° 45 Minuten erhitzt und kühlten sich über Nacht ab. In beiden Röhren schied sich annähernd die gleiche Menge einer schwarzen Humin-artigen Substanz aus. Beide Lösungen entfärbten TR in saurer Lösung und enthielten ein aci-Redukton.

1 ml jeder der beiden Lösungen wurde mit NaAc bis pH = 5,5 versetzt und mit 0,01-*n* TR titriert.

Verbrauch im Galaktoseversuch	1,70 ml.
» » Glucoseversuch	1,10 ml.

1 g Galaktose verbrauchte also nach der sauren Behandlung	17 ml.
1 g Glucose » » » » » »	11 ml.

Aus 1 g D-Galaktose würden sich also etwa 15 mg Substanz, berechnet auf Triose-Redukton, bilden, aus 1 g D-Glucose etwa 10 mg.

Versuche und Erwägungen über die biologische Bildung der Askorbinsäure

Während die Askorbinsäure durch mehrere wertvolle Methoden (T. REICHSTEIN u. a.) in grossem Masstab künstlich dargestellt wird, ist noch nichts darüber bekannt, auf welchen Wegen Pflanzen, Tiere und Mikroorganism dieses mannigfach wirksame[1] wichtige Vitamin erzeugen. In tierphysiologischen und pflanzenphysiologischen Versuchen wurde in den letzten Jahren dieses Problem angegriffen, wobei vorzugsweise Synthesen aus einfachen Bestandteilen des Stoffwechsels erwogen wurden. Unter den Mechanismen, die für die Synthese in Betracht gezogen wurden, ist keiner chemisch genügend präzisiert, um experimentell geprüft bzw. gestützt werden zu können. Am nächsten liegt in dieser Hinsicht die Annahme, dass der Aufbau der Askorbinsäure sich von demjenigen der einfachen Zuckerarten erst in den letzten Reaktions-Stadien unterscheidet, aber anfangs mit der Synthese der Monosen parallel geht. Die ersten Stadien des Zuckeraufbaues gehen bekanntlich vom Formaldehyd aus (O. LÖW; EMIL FISCHER, 1888), verlaufen über Glycolaldehyd[2] und umfassen ev. Brenztraubensäure und deren Aminierungsprodukte[3, 4]. Diese Aufbau-Vorgänge sind aber auch für die Hexosen so wenig im einzelnen erforscht, dass z. B. über die Unterschiede in der Synthese der Glucose und Galaktose nichts bekannt ist. Offenbar sind an diesen grundlegenden Synthesen zahlreiche noch nicht isolierte Enzyme (Isomerasen und Phosphorylasen) und als Wuchsstoffe fungierende Co-Enzyme beteiligt.

---

[1] EULER u. H. HASSELQUIST, Zs. physiol. Chem. 288, 4; 1951.

[2] EULER, Grundlagen und Ergebnisse der Pflanzenchemie 2. u. 3. Teil, Braunschweig 1909. — Ber. 39, 39; 1906.

[3] J. MAYER u. W. A. KREHL, Nutrition 35, 523; 1948.

[4] C. W. WOODRUFF u. W. J. DARBY, J. Biol. Chem. 172, 851; 1948.

Der Askorbinsäure-Gehalt der Tierorgane ist von so vielen Bestandteilen der Nahrung (Vitamin A, Pteroylglutaminsäure, Glutathion) abhängig, dass es sehr schwer ist, aus diesbezüglichen Konzentrations-Angaben Schlüsse auf die Askorbinsäure-bildenden Reaktionen zu ziehen.

Im Tierkörper kommen auch Umwandlungen von Hexosen in Betracht, GUHA, und GOSH[1] entnehmen ihren Ergebnissen, dass Manose als Vorstufe bzw. Katalysator einer starken Askorbinsäure-Bildung fungiert.

Als Ort der Askorbinsäure-Bildung im Tierkörper haben FR. G. HOPKINS (1934)[2] u.a. den Darm angegeben. Hier bleibt aber zu entscheiden, ob und in welchem Grad bei den verschiedenen Tierarten die Darmwand selbst oder die Bakterienflora des Darmes an der Askorbinsäure-Synthese mitwirkt.

Hält man an der Auffassung fest, dass die Askorbinsäure in Tier und Pflanze durch Abbau oder Umwandlung eines körpereigenen Substrates entsteht, so erhebt sich die Frage nach der Natur dieses Substrates. Glukose kommt in erster Linie in Betracht.

Über den Einfluss zugesetzter Stoffe auf Ratten besitzen wir keine anderen eigenen Beobachtungen als über eine Erhöhung der Askorbinsäure-Konzentration nach Eingabe von Karotin.[3] In diesem Zusammenhang wurde auch versucht, ein genaueres Bild über die Entstehung der Askorbinsäure im *keimenden Samen* zu gewinnen.

Gegenüber den Ansätzen zahlreicher Forscher, die Ascorbinsäure in Pflanzen von ihren Bau- und Nahrungs-Stoffen abzuleiten, schien uns die Annahme näher zu liegen, dass — wenigstens in einem grossen Teil der Fälle — die Ascorbinsäure im lebenden Organismus parallel mit den Kohlehydraten gebildet wird.

Unsere Problemstellung haben wir in letzter Zeit wieder aufgenommen im Zusammenhang mit dem Nachweis neuer Reduktone, die sich aus alkalisch behandelten Zuckerarten isolieren liessen.[5] Mit papierchromatographischen Methoden haben wir untersucht, ob sich in pflanzlichem, Askorbinsäure-reichem Material (junge Kohlblätter, keimende Erbsen, besonders Zitronensaft) neben der Askorbinsäure auch andere Reduktone finden, die eventuell als Zwischenprodukte der Askorbinsäure-Synthese angesehen werden könnten. In dem am besten untersuchten Material, dem Zitronensaft, hat sich aber ausser Askorbinsäure bisher kein anderes Redukton nachweisen lassen. In den Versuchen mit jungen Kohlblättern und keimenden Erbsen konnten einige manchmal erhaltene schwache Anzeichen von Reduktonen im papierchromatographischen Versuch nicht mit Sicherheit reproduziert werden.

Es würde zu weit führen, an dieser Stelle auf die vom botanisch-physiologischen Standpunkt aus angestellten interessanten Versuche von SMITH[6] und von BHARANI und Mitarb.[7] einzugehen.

---

[1] B. C. GUHA u. A. R. GHOSH, Nature 134, 739; 1934.

[2] FR. G. HOPKINS, Chem. & Ind. 53, 774; 1934; Biochem. J. 30, 1446; 1936.

[3] EULER u. E. KLUSSMANN, Arkiv f. Kemi 11 B Nr. 17, 1933.

[4] Z. KERTESZ, Biochem. J. 32, 621; 1938.

[5] EULER u. H. HASSELQUIST, dieses Arkiv 8, im Druck. 1955.

[6] F. G. SMITH, Plant Physiol. 27, 736; 1952.

[7] S. P. BHARANI, Y. S. SHAH u. A. SREENIVASA, Proc. India Acad. Science B 37, 33; 1953.

Viele Tatsachen deuten darauf hin, dass Ascorbinsäure im lebenden Organismus als Co-Enzym fungiert. Szent-Györgyi[1] hat angenommen, dass in grünen Blättern ein spezifisches Enzym vorkommt, welches Askorbinsäure reversibel oxydiert (diese Oxydation wird nach Hopkins und Morgan[2] durch Glutathion gehemmt). Ein besonderes oxydo-reduzierendes Ascorbinsäure-System fanden Euler und Günther[3] in den Augenlinsen, wo es das dort mangelnde Diaphorase-Cytochrom-System vertritt.[4]

Wie Cozymase (Co-Dehydrase I) und wie Flavin-adenin-mono- und di-nukleotide an verschiedene Apodehydrasen gebunden fungieren können, so dürfte auch die Askorbinsäure ihre Wirkungen in Verbindung mit verschiedenen Apo-Enzymen ausüben. Bis jetzt ist es aber nicht gelungen diese Verbindungen, die nach der Gleichung

$$K = \frac{\text{Co-Enzym} \times \text{Apo-Enzym}}{\text{Holo-Enzym}}$$

anscheinend weitgehend gespalten sind und wie die Riboflavinphosphorsäure des gelben Fermentes (H. Theorell) nur unter geeigneten Konzentrations- und Aciditäts-Bedingungen vereinigt werden können, zu isolieren.

Ob und in welchem Grade die aci-Reduktone überhaupt an Träger-Moleküle gebunden werden, sei es durch Vermittlung von PO_4 oder von Metallhydroxyden, müssen weitere Versuche zeigen.

Stockholm, Universität, Institut f. organ.-chem. Forschung.

---

[1] A. v. Szent-Györgyi, Zs. f. physiol. Chem. 254, 147; 1938.

[2] Fr. G. Hopkins u. E. J. Morgan, Biochem. J. 30, 1446; 1936. — Vgl. auch Z. Kertesz, Biochem. J. 32, 621; 1938.

[3] Euler u. G. Günther, Z. physiol. Chem. 256, 229; 1938.

[4] Euler, Sv. Kem. Tidskr. 45, 1933. — Arkiv f. Kemi etc. 11 B Nr. 18; 1933.

Tryckt den 23 april 1955

Uppsala 1955. Almqvist & Wiksells Boktryckeri AB

ARKIV FÖR KEMI Band 8 nr 22

Communicated 24 November 1954 by ARNE WESTGREN and GUNNAR HÄGG

Continuous zone electrophoresis by crossed velocity fields in a supporting medium

The electric control of the fractionation process

By INGER BRATTSTEN

With 12 figures in the text

In continuous fractionation by crossed electric and hydrodynamic flow fields, as described by SVENSSON and BRATTSTEN [1] and GRASSMANN and HANNIG [2], the efficiency of the process largely depends upon the control of all factors which cause remixing of the separating substances. Maximum efficiency requires that the net displacements remain constant during the operation, and one very important problem is how to avoid fluctuations from time to time of the net displacements.

For a substance i of mobility u_i the horizontal displacement at the level of outflow from the column is

$$E u_i t \text{ cm.}$$

E = field strength, volt cm^{-1};
u = electric mobility, cm^2 volt^{-1} sec^{-1};
t = time of transfer through the column, sec.

From the operational point of view it is more convenient to regard the displacement of a substance as a function of the component velocities in the vertical and horizontal directions, i.e. the hydrodynamic velocity, V_h, and the electric velocity, V_e. The former is inversely proportional to the time of transfer, t, and the latter equals $E u_i$. Hence

$$E u_i t = k \frac{V_{e,i}}{V_h} \tag{1}$$

k = a constant.

The equation states that the net displacement of a substance remains constant as long as the ratio of the component velocities does not vary.

If disturbing effects are present, they cannot in general be expected to exert a proportional influence on both component velocities. A non-proportional variation of the velocities will manifest itself as a change of the velocity ratio if its cause is a time-depending factor. If the disturbances do not change with time, the paths of the substance bands in the column may remain quite constant in time, in spite of the local velocity differences. Since all kinds of variations cause remixing to some extent by increasing the diffusion in the zones, it is evident that the control of the displacement process should be directed in the first place to regulate time-depending factors which influence the velocity ratio, but also to keep the component velocities as constant as possible in space and time.

This paper deals with the combined, continuous regulation of the component velocities and the simultaneous control of the temperature in the cell. The control of the heat transfer equilibrium is indicated as a means of maintaining constant velocities as well as a safeguard against dangerous rises in temperature.

The regulation of the component velocities and the bath temperature

The hydrodynamic velocity.—The transport of liquid through the cell is effected by means of a type of peristaltic pump, which gives a very uniform flow [3]. The pump apparatus is operated by a d.c. motor, and the volume velocity of the liquid is proportional to the speed of the motor. Since the speed of the motor depends upon the motor torque and the load, the hydrodynamic velocity is sensitive to changes in the operating voltage and temperature. Accurate regulation of the velocity requires that the motor is run on a constant current basis, but the fluctuations are generally moderate when instead a constant voltage source is used.

The electric velocity.—The regulation of the electric velocities of the separating substances is conditioned by the relationships:

$$V_{e,i} = E u_i = \frac{I u_i}{\varkappa} \tag{2}$$

$$\varkappa = F \Sigma c_i u_i \tag{3}$$

$$u_i = f(c_1, c_2, c_3, \ldots, T). \tag{4}$$

I = current density, amp cm^{-2};
$\varkappa$ = specific conductivity, $\mathrm{ohm}^{-1}\ \mathrm{cm}^{-1}$;
F = Faraday's constant, 96,500 coulomb $\mathrm{equivalent}^{-1}$;
c = ionic concentration, equivalent cm^{-3};
T = temperature, °C.

These equations show that the electric velocities are functions of the current, the ionic medium and the temperature. If steady-state conditions prevail in the separation column with regard to the chemical composition and the temperature, the electrical velocities are adequately controlled by regulation of the current supplied to the cell. If, further, the resistance in the circuit outside the separation zone is also constant, regulation of the supply voltage can be substituted for direct current control.

Both the chemical composition of the conducting medium and the cell temperature are intrinsically related to the electrical transport. Steady-state conditions with regard to the ion distribution in the cell have to be achieved by proper chemical composition of the liquids introduced [4]. The thermal equilibrium will be treated in this connection.

The regulation of the temperature.—The general relationships between the temperature and the electric velocity reveal in what practical cases temperature fluctuations influence this variable. According to equations (3) and (4) the mobility and hence the conductivity are functions of the temperature. The temperature coefficients of the mobilities are positive by about 2 per cent per degree, but the numerical values vary considerably with the nature of the ions. Although the temperature coefficients of the mobilities and the conductivity are rarely the same, it is customary to regard the ratio $u_i/\varkappa$ as constant within a limited temperature range [5]. When this is true the only variable left on the right side of equation (2) is the current. The general conclusion can be drawn that the regulation of the temperature is sufficiently accurate when the variations are within the limits where the ratio $u_i/\varkappa$ is approximately constant.

However, if the current is supplied from a constant voltage source, the temperature dependence of the velocities is never completely cancelled. The reason is that the resistance in the cell varies inversely as the conductivity, and by Ohm's law:

$$E = \frac{I}{\varkappa}. \tag{5}$$

Thus, to maintain the potential gradient constant when the conductivity changes, the current must receive proportional increments. If the voltage drop across the electric field is fixed to a constant value and the temperature changes, both the conductivity and the current will change. The result of the temperature fluctuations will be that the electric velocity increases with increasing temperature and decreases with decreasing temperature, even within the (narrow) range where the ratio $u/\varkappa$ remains constant. This variation of the electric velocity is absent by direct current control. Is the variation only slight, it can be compensated indirectly by regulation of the hydrodynamic velocity.

Maintenance of a constant temperature requires control of the heat exchange equilibrium. The heat produced by the electrophoretic current is removed from the cell by circulating water of 0°C in contact with the front and back walls. The temperature reaches a stable value when the rate of extraction of heat equals that of production. For a certain system the temperature rise in the cell under normal working conditions can be described by an equation of the form

$$\frac{I_2^2}{\varkappa_2} - \frac{I_1^2}{\varkappa_1} = C\,(T_2 - T_1) \tag{6}$$

$\frac{I^2}{\varkappa}$ = electric power, watt cm^{-3};

1, 2 = indices, referring to the steady states *1* and *2*, characterized by the currents I_1 and I_2, the conductivities $\varkappa_1$ and $\varkappa_2$, and the temperatures T_1 and T_2.

C = a constant.

In principle, regulation of the temperature is conceivable by adjustment of the electric power or/and the cooling capacity. In practice, maximum cooling is almost always preferable. Under these conditions all adjustments of the temperature have to take place by regulation of the electric power. This arrangement is the most suitable one also from the point of view that the electric reactions are instantaneous, whereas the time constant of the cooling system is of the order of magnitude of a few minutes. Since the fractionation column must have a thickness corresponding to the desired rate of the fractionation and the walls must be firm enough to withstand the mechanical strain, the steps of conduction always become rate-determining in the heat transfer.

If the stream of cooling water is sufficiently turbulent, very little can be gained by increasing further the volume velocity of the water. On the whole, no simple way of decreasing significantly the functional inertia in the process of heat extraction appears to be available at the present.

Unsteady thermal conditions in the cell may give rise to two apparently very dissimilar phenomena, namely (i) a slow fluctuation of the temperature which may or may not alter the net displacements (see p. 207); (ii) abrupt changes which in a few minutes are capable of increasing the temperature to the boiling point, thus interrupting the experiment and causing damage to the cuvette. It is evident that the apparatus can be safeguarded in the latter respect by including a suitable relay arrangement in the circuit. But it is not sufficient only to protect against damage; smooth operation requires continuous control, and it is also possible by this means to eliminate at an early stage disturbances which might otherwise develop to dangerous proportions.

Equation (6) is useful as a guide for coarse adjustments of the power to a selected temperature value. But this equation is only concerned with the steady-state conditions before and after a change and gives no information about the course of the reactions in the intermediate, unsteady phase. Yet, a method of regulation is directly concerned with the control of the unsteady state. By simple arguments it is possible to deduce the tendency in the electrochemical equilibrium shifts. Hence, a satisfactory control of the heat transfer can be based on observations of the behaviour of the system under those working conditions where regulation is needed.

In the first place, the course of the development in the transition intervals is related to the inertia in the process of heat extraction. A change in the rate of the heat production has to be balanced by a corresponding change in the rate of extraction of heat, but the temperature gradient, needed to effect this change, develops only slowly. When the electric variables and the temperature in the cell are plotted as functions of time, a lag of the temperature of some minutes is almost always observed in the curves (cf. Figs. 2, 8, and 9). Further, the development depends upon the magnitude of the changes and the temperature level in the cell. As long as the equilibrium temperature is low, the stable state is easily restored, even if the disturbances are great. With increasing temperature the inherent instability of the system increases, and the temperature exhibits a tendency slowly to drift to higher values. The development of the temperature curve after a power increase is different when the power is supplied from a constant voltage source and when a constant current is used. The two types of curves are shown in Figs. 1*a* and 2*a*. In the case of Fig. 1 a stabilised current was used and the increments amounted to 10–20 % of the total value. After each increase the temperature smoothly rose to a new value, where it remained constant. In the case of Fig. 2 the power was obtained from a constant voltage supply. Under these conditions the first part of the temperature curve has the form of a wave, which changes into an even part. The temperature of the maximum is always higher than that of the following steady state. A minimum below the equilibrium value is generally discernible even when the net rise of the temperature is only a few degrees. The corresponding curves for the voltage and the current, respectively, as functions of time are also shown, Figs. 1*b* and 2*a*. These experiments were performed with the usual electrophoresis cell under typical working conditions [4]. The temperature in the cell was measured with the aid of a thermocouple having a time constant of 5 seconds.

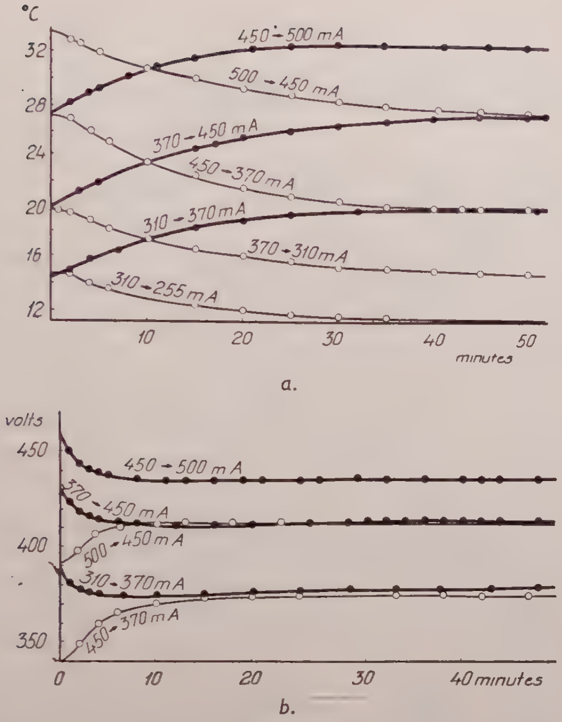

a.

b.

Fig. 1. *Effect of changes in the heat transfer equilibrium. Current stabilised.*—Cooling temperature: 0°C. Current reset at time 0 as indicated in the diagrams. *a*, The bath temperature as a function of time. *b*, The voltage drop as a function of time.

The observed temperature curves can easily be explained qualitatively. The initial increase of the power raises the production of heat. Since the process of extraction of heat lags behind that of production, surplus heat is stored up in the cell, and the temperature rises. This, in turn, automatically increases the mobilities and the conductivity. Depending upon whether the power is supplied from a constant voltage source or from a constant current source, the development follows different paths.

Supposing first that the power is supplied from a constant voltage source, the initial temperature rise will increase both the conductivity and the current (cf. p. 207), and a process of continuous equilibrium shifts starts, which gradually displaces the power, the temperature, the conductivity, and the current to higher values. As the temperature rises, also the rate of extraction of heat increases. By the interaction of these two processes, which are not in phase with one another, a state of more or less pronounced oscillations develops, which may give rise to a temperature curve like that of Fig. 2*a*. It is well conceivable that if the waves of heat are too high or come too closely, an upper limit will be reached, where spontaneous return to the steady state is no longer possible. If the temperature level in the cell is high enough, the state where slow temperature fluctuations ordinarily prevail may degenerate into instability, with a "heat collapse" of the perspex cuvette as one of the results. This course of the development is illustrated in Fig. 2*b*, although the experiment was broken before the dangerous temperature rise started.

If the power is instead supplied from a constant current source, the initial temperature rise will as before increase the mobilities and the conductivity, but the changes in this case primarily

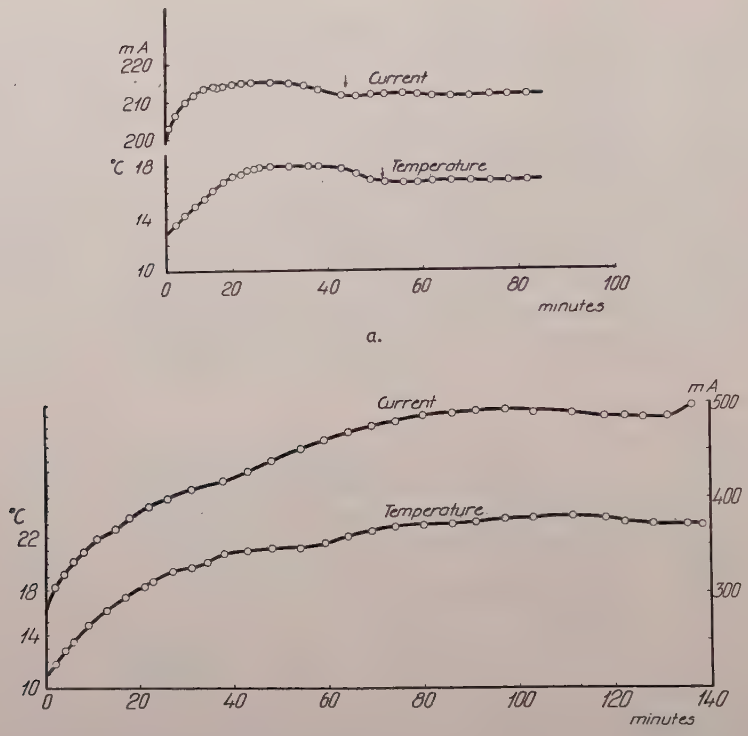

a.

b.

Fig. 2. *Effect of changes in the heat transfer equilibrium. Voltage stabilised.*—Cooling temperature: 3°C. *a*, The voltage increased from 350 to 420 volts at time 0. The arrows indicate the lag in time of the temperature function. *b*, The voltage increased from 300 to 460 volts at time 0.

contribute to a certain reduction of the power. Due to the mutual adjustments of the temperature, the conductivity, and the power, a kind of mechanism of autoregulation develops, which tends to reduce the amplitude of the changes. In Fig. 1 *b* a rapid voltage drop is recorded directly after the increase of the current. This indicates that a considerable reduction of the power takes place even before the rate of extraction of heat has reached its maximum value. Whether the current is increased or decreased, the smooth development of the steady state is favoured by the autoregulation of the power achieved when the current is controlled.

In the transitions represented by Figs. 1 and 2 a the changes of the cell resistance essentially corresponded to the temperature dependence of the conductivity; in that pictured in Fig. 2 b this effect was enhanced by the appearance of conductivity gradients in the separation zone of the cell.

The experimental facts show that regulation of the power is needed for control of the heat transfer equilibrium under the reported conditions and allow the conclusion that such regulation can be arranged by means of stabilisation of the bath current.

The regulation of the resultant velocity

The resultant velocity should be regulated by adjustments of the component velocities in such a manner that the net displacements are kept in the desired position in the column during the time of the operation.

The simplest means for regulation is to use the line voltage without further stabilisation, either directly (d.c.) or for feeding a transformer and rectifier (a.c.). Both component velocities are in this case subjected to the influence of variations in the supply voltage. Since the time of transfer is about 2–3 hours, random changes of the voltage of relatively short duration to a great extent are cancelled, especially if the source of the current is the same in both processes. However, a variety of factors are left uncontrolled, which may seriously interfere with the fractionation if circumstances are unfavourable. The role of the temperature factor has been pointed out, and further, the applied voltage includes the voltage drop in the electrode compartments, where steady-state conditions generally do not prevail. The conductivity variations in these parts of the circuit can be considerable and give rise to variations of the current as well. Although the accuracy achieved by this method may be sufficient for some purposes, the lack of reliability is always a drawback. The introduction of a device for better control of the velocities is clearly indicated.

The great practical importance of the thermoregulation achieved by continuous regulation of the electrophoretic bath current gives preference to this method over voltage control, although it involves the control of a relatively high power, and voltage control is generally more easily arranged. The latter method will suffice only in the special case that control of the heat transfer by continuous regulation of the power is not needed. The stabilisation of the bath current can be performed by feedback control with the aid of a thyratron or transductor system [6] and selenium dry plate rectifiers [7]. Other alternatives are also possible. A short account of these methods is given in the Appendix, p. 222.[1]

The hydrodynamic velocity should of course be regulated with the same accuracy as the electric velocity. The power consumption of the pump motor is small (maximum 50 watts), and the stabilisation of the current is no more difficult than that of the voltage. Independent control of the component velocities would require two separate units for stabilisation of the bath and motor currents. However, since special temperature regulation is needed only for the electrophoresis bath, accurate regulation of the resultant velocity can also be obtained if the pump motor is run from a constant voltage supply, and the speed of the motor used as the reference input in the control circuit of the regulator for the bath current. By this means the electric velocities can be continuously brought to follow the (small) variations of the hydrodynamic velocity, so that the velocity ratios are kept constant.[2]

Since stabilised a.c. voltage is available in the laboratories of the present Biochemical Institute, the last-mentioned method of regulation was adopted. The complete experimental arrangement includes the following parts: the electrophoresis apparatus, the pump apparatus, the regulating apparatus, and the power supply with transformers and rectifiers (see Fig. 11).

---

[1] In 1950, an equipment for current stabilisation for 500 watts output power was designed by Mr. BENGT HEDIN, the Gustaf Werner Institute for Nuclear Chemistry. The design contained a commercial current stabiliser, an electronic amplifier, a transductor amplifier, and two selenium rectifiers with transformers and filter circuits. Only the rectifiers could be procured, however.

[2] It has been pointed out to the author by Dr. D. L. MOULD, the Rowett Research Institute, Aberdeenshire, that maintenance of a constant speed of the pump motor by means of a feedback control circuit, as used in a cinema projector motor, would be an advantage for long duration separation.

For the pump apparatus the a.c. voltage from the central stabiliser is transformed by means of a *Variac* transformer (1–250 volts) and passed to a selenium rectifier. The d.c. terminals of the rectifier are connected to the motor. The speed of the motor is adjusted by regulation of the input voltage. The accuracy of the stabilisation is 1 %. The d.c. motor has an output power of 50 watts. The rotor and stator are connected in series. The speed can be varied within the range of 2000–4000 r.p.m. To the shaft of the motor is attached a tachometer generator of the type F.F.$^1/_2$, Evershed and Vignoles, Ltd., England. It generates approximately 28 volts per 1000 r.p.m. with a reported average deviation from linearity of 0.5 %.

For the electrophoresis apparatus the power is supplied from the a.c. mains. The bath circuit contains in series: a transductor regulator, a transformer, a rectifier unit, and the electrophoresis apparatus. The transformer is designed for 500 watts and has two secondary windings. The dual selenium bridge rectifiers each contain a filter circuit. They are designed for 550 watts, giving in series 0.5 A at 1100 volts, and in parallel 1 A at 550 volts. Of the output power, about 10 per cent is needed for the regulating apparatus.

In the regulating circuit the speed of the pump motor is translated into an e.m.f. by means of the tachometer generator attached to the shaft and a potential difference derived by passing the bath current through a resistance. The error signal is the difference between these two voltage drops. It is received by the control winding of the first-stage transductor. After amplification the impulse is transferred to the control winding of the second-stage transductor, where further amplification is actuated. The output a.c. voltage of this transductor is supplied to the transformer in the bath circuit. The regulator is designed for an output power of 500 watts; the time constant is approximately 0.5 sec., and the total power amplification 36,000 times, which gives an accuracy better than 1 %. The regulating equipment was delivered by Asea Ltd., Västerås, Sweden, in December 1952. It is described by its designer in the Appendix.

The accuracy

The accuracy of the regulating equipment is directly related to the power amplification in the transductor system. Since the constructional and running costs increase with the degree of amplification, a greater accuracy should not be chosen than really necessary.

With a time of transfer of 2–3 hours small random changes of short duration are relatively unimportant. If the disturbances extend over several hours, more accurate regulation is required. Such disturbances of the current may be due to fluctuations of the frequency, migration of small heat or conductivity gradients, or variation of the cooling conditions. Cooperation of several errors also increases the requirements of accuracy in the regulation. But it is relatively unimportant if the regulation is less accurate when the deviations are great, because the general validity of the fractionation process requires that such changes of any duration are excluded.

In the present cuvette a substance band can be displaced horizontally about 20 cm. The distance between each two outlet tubes is 0.5 cm. Therefore, an error in the current of 2.5 %, active during the time of transfer, will shift the band over to the next outlet tube, which would definitely be too much. It was concluded that an accuracy of 1 % in the elimination of errors in the current of 5 % and less should be sufficient.

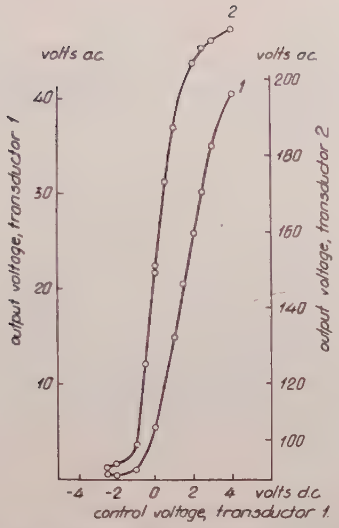

Fig. 3. *Static characteristics of transductors 1 and 2 (cf. Fig. 11).*—The output voltages of the two transductors have been plotted as functions of the control voltage of transductor *1* (*e* in Fig. 10 b).

Experimental part

The success of the electric process control rests upon two equally important conditions, namely satisfactory operation of the control device, and validity of the following assumptions employed:

1. The variation of the hydrodynamic velocity is proportional to that of the speed of the pump motor.
2. Within a limited temperature range the variation of the electric velocity is proportional to that of the bath current and independent of temperature fluctuations.
3. The net displacements remain constant in space and time when a constant ratio is maintained between the speed of the pump motor and the bath current.
4. A constant current device simultaneously controls the temperature in the cell.

The transductor regulator has been tested very thoroughly with regard to efficiency and regulating power; a few results will be reported here.—*The relation between the control voltage and the output voltages of the two transductors* was derived experimentally, see Fig. 3. Accurate regulation is obtained within the range where both curves are linear; that is, when the control voltage is between -0.5 and 1.5 volts. The control voltage is the difference between the generator voltage and the voltage drop across resistance R_1 in Fig. 11, which conducts the bath current. In order to get optimum conditions for the regulation, the bath current and the speed of the pump motor should be so balanced that the control voltage always remains within the range of -0.5 to 1.5 volts.

While the regulating equipment is working, the measurement of the momentaneous values of the variables is complicated by the fluctuations. For this reason the numerical material was collected by means of a *Speedomax* automatic recorder, type *G*, model *S*, Leeds & Northrup Co., U.S.A. Fig. 4 refers to an experiment where the generator voltage was stepwise adjusted to new values. The subsequent variation of the bath current was actuated by the regulator. The record

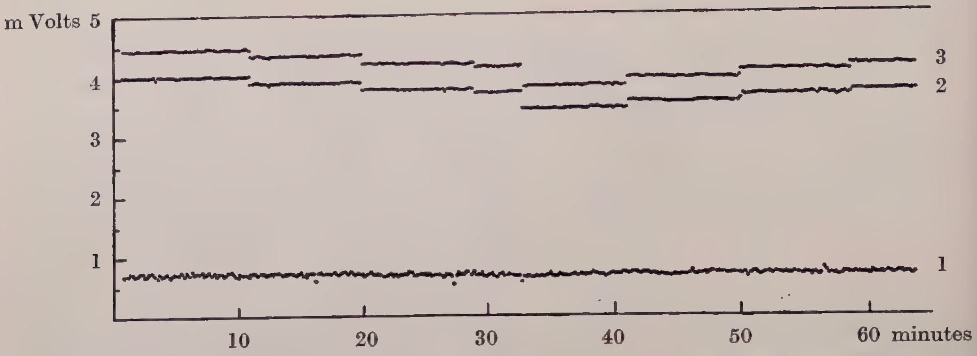

Fig. 4. Automatic records of the control voltage *e* (cf. Fig. 10 b), *1*; the bath current, *2*; and the generator voltage, *3*.

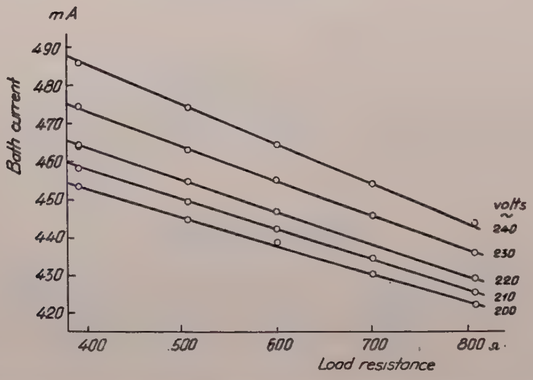

Fig. 5. *Test of the regulating power.*—The bath current as a function of the load resistance at some fixed values of the a.c. supply voltage. Generator voltage 65 volts.

shows that the systematic variation of the control voltage is strikingly small as compared to the swift, random fluctuations of this variable.

In the case of Fig. 5 a record of this type was used for deriving the effect of *variations of the input a.c. voltage* and *variations of the load resistance*. Both the transductor regulator and the pump motor were supplied from constant voltage sources. The resistance R_1 was not adjusted during the experiment. Instead of the cell a rheostat was used. The generator voltage was kept at 65 volts. With increasing load resistance the control voltage gradually dropped towards zero, implying that the lower limit of the range of regulation was approached. The diagram shows that the influence of a variable resistance is to a large part compensated; for example, at 660 ohms a variation of ± 5 % only gives a variation of the current of 1.1 %. The effect of a variable voltage supply is relatively more pronounced.

The influence of *varying the speed of the pump motor* was investigated similarly. The supply voltage was in this case kept constant at 220 volts, and three series of measurements were performed at load resistances of 500, 600, and 700 ohms. The plotting of the average values of the current and the generator voltage gave the three straight lines shown in Fig. 6, indicating that the adaptation of the current is practically complete in the range covered by the experiments.

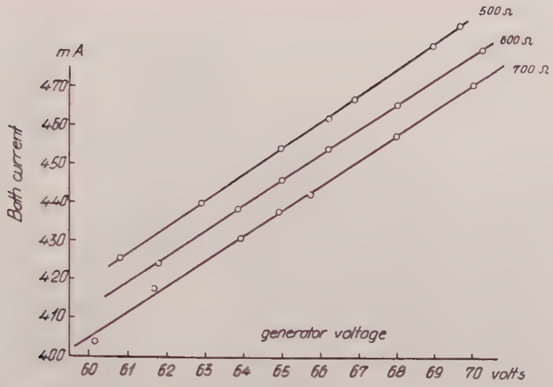

Fig. 6. *Test of the regulating power.*—The bath current as a function of the generator voltage at load resistances of 500, 600 and 700 ohms.

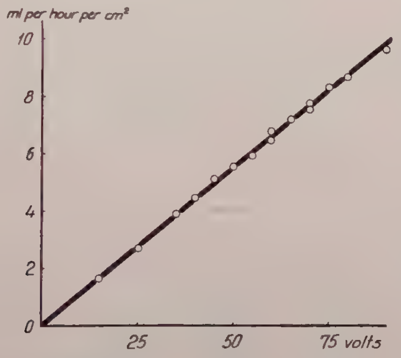

Fig. 7. *The relation between the hydrodynamic velocity and the pump speed.*—The volume velocity of the percolating liquid, in ml per hour per cm^2, as a function of the generator voltage.

The accuracy in extended runs was also tested. A typical experiment will be briefly reported. In a 24 hours' run the current was 600 mA., the generator voltage 72 volts, and the load resistance 496 ohms, with an estimated variation of less than 5 %. The bath current, the generator voltage, and the ratio between these variables were recorded by means of the *Speedomax* recorder. The readings on the paper strip were used for a statistical computation of the constancy of the ratio between the bath current and the generator voltage. The computed average was 1.024 ± 0.001, and the statistical standard deviation 0.0037.

The basic principles for the fractionation control, listed above, have also been tested experimentally.—*The relation between the volume velocity and the speed of the pump motor* was determined by measuring the volumes of the effluent liquid at various rates. The speed of the pump motor was recorded as the e.m.f. generated by the tachometer generator. The experimentally found linearity of this tool was at least as good as that reported, i.e. better than 0.5 %. In Fig. 7 the measured volume velocity (ml per hour per cm^2) was plotted against the generator voltage. A linear relationship was obtained, except at the highest velocities, where the increase of the load torque is perceptible (above 12 ml per hour per cm^2).

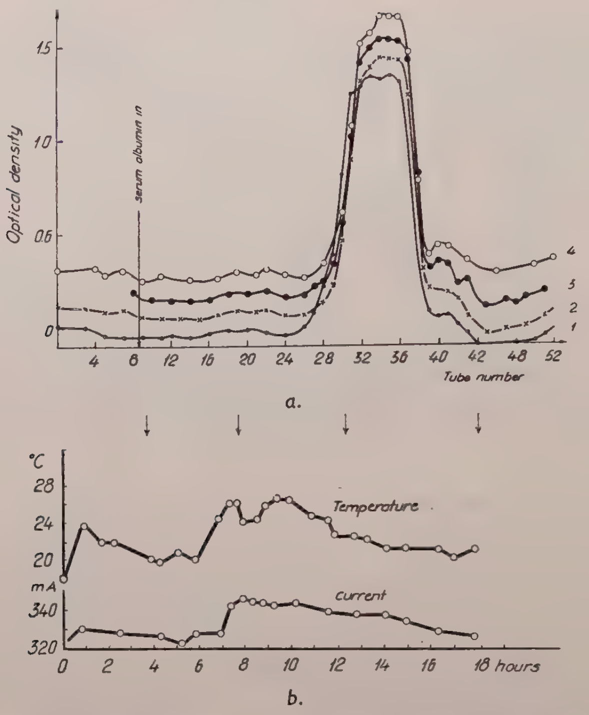

Fig. 8. *Electrophoresis of serum albumin.—a,* The optical density of the fractions as a function of the tube number. The curves 1–4 refer to samples taken as indicated in *b*. The optical density scale is valid for curve 1; for each following curve 0.1, 0.2, and 0.3 o.d. units, respectively, have to be subtracted from the readings in the diagram. *b*, The current and the temperature in the cell as functions of time.

The proportionality between the electric velocity and the bath current was investigated by electrophoresis of a solution of serum albumin (Armour, bovine) in phosphate buffer of the ionic strength 0.05 and pH = 7.6, see Fig. 8*a* and *b*. In this experiment the source of the power was the mains supply without stabilisation of current. The hydrodynamic velocity was instead regulated to follow the variations of the bath current (cf. p. 220). During the run, which lasted 18 hours, the process had to be watched, and when necessary the current was reduced by adjustments of the voltage across the bath electrodes. The variations of the current and the temperature are recorded in Fig. 8*b*. The average values of the variables were: volume velocity of the liquid, 7.7 ml per hour per cm^2; power applied, 200 watts; current, 335 mA; and temperature, 26°C. At four occasions (indicated in Fig. 8*b*) samples of the effluent fractions were analysed for protein in a Beckman spectrophotometer, model DU, at 280 mμ. Fig. 8*a* shows the curves obtained by plotting the optical density readings against the fraction numbers. In the diagram each curve is displaced 0.1 unit in the upward direction relative to the preceding one. In spite of the considerable variations in the working conditions the coincidence between the curves is good. The slight shift of the protein band in the first sample is undoubtedly due to the fact that stationary conditions had not by then developed in the column. Since the variations of the current were cancelled by the continuous adjustment of the pumping velocity, the conclusion is justified that the variation of the electric velocity of serum albumin was actually proportional to that of the bath current under the prevailing conditions.

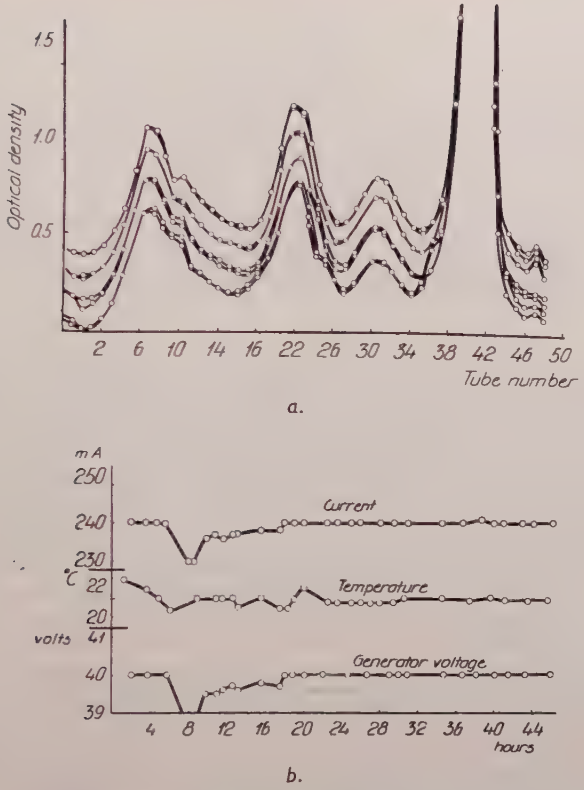

Fig. 9. *Fractionation of blood serum.*—*a*, The optical density of the fractions as a function of the tube number. Eight portions of fractions were collected. The optical density scale refers to the first two portions. For each following pair of curves 0.1, 0.2, and 0.3 o.d. units, respectively, have to be subtracted from the readings. *b*, The generator voltage, the current, and the temperature as functions of time.

The validity of the assumptions 3 and 4 (p. 213) has been confirmed in fractionation work during about two years. As an example, a recent fractionation of normal human blood serum will be described, see Fig. 9*a* and *b*. 150 ml of a serum solution containing 1.8 % of protein was injected during 46 hours. The electrolyte medium consisted of a veronal buffer of the ionic strength 0.03 and pH = 8.6. The volume velocity was 3.5 ml per hour per cm^2 and the power supplied 135 watts. The current was 240 mA and the temperature 21°C. The effluent liquid was collected in eight portions and the concentration distribution in each series of fractions determined spectrophotometrically at 284 mμ. The curves obtained are collected in Fig. 9*a*, each pair of curves being shifted upwards 0.1 units relative to the preceding one. Fig. 9*b* contains records of the generator voltage, the current and the temperature in the cell. Once or twice the generator voltage was adjusted to the selected value of 40.0 volts; with these exceptions the electrical process required no supervision but proceeded under approximately constant conditions during the whole run. Due to the general constancy in the process it was possible to correlate the slight fluctuations of the temperature to observed temporary changes in the cooling bath or electrode compartments.

Discussion

The test experiments reported here are typical and give evidence that the principles employed in the fractionation control are valid under the specified conditions.

Efficient control of the heat production requires that the variations of the bath current are eliminated sufficiently rapidly. In the experiment referring to Fig. 1 the transductor regulator was used, and the smooth transition from one steady state to another can be regarded as a proof that the time constant of the regulator is small enough.

In Fig. 5 is recorded the experimentally determined dependence of the bath current on the load resistance. Although the variation of the current is not completely cancelled, it can be deduced from the curves that a decrease of the load resistance will always result in a decrease of the power to the cell. This evidence is supported by the experimental finding that complete break in the circulation of the cooling water may well cause a temperature rise of some few degrees, but in particular a considerable decrease of the voltage across the electrodes. Even if this state is allowed to prevail for 1–2 hours, no sign of damage can be detected on the cuvette or the regulator. It is apparent that the current regulator serves the purpose of being a regulator of the power to the cell, safeguarding against autoinduced rises due to an initial increase of the conductivity.

However, the curves in Fig. 5 also show that an increase of the load resistance causes the power to increase. Therefore, the safeguarding action of the regulator is restricted to the case that the conductivity accidentally increases in the cell. If, for example, the feeder lines from the supply liquid were run dry, air would be pumped into the cuvette instead of the conducting liquid, and the resistance would increase. An accident of this kind could give rise to an increase in the heat production equally sudden and dangerous as those experienced when the current is not controlled and the conductivity rises. The principally important difference between these two cases is that only the former kind of accident can easily be avoided by proper supervision of the apparatus during the runs.

The regulating power of the transductor regulator is further impaired by changes of the pump speed which displace the control voltage outside the range of regulation (cf. Fig. 3 and the Appendix). The net displacements of the separating substances are obviously influenced by such changes, but it has been found that the equipment is not damaged even if the pump speed is reduced to zero, and also that the regulator retains most of its safeguarding power against decreases in the load resistance.

In conclusion, experience has shown that the transductor regulator provides general security against dangerous rises of the power. Safety can be further improved by the introduction of relays safeguarding the bath circuit against interruptions in the transfer of cooling water or electrolyte liquids. But provided the supervision of the experiments is satisfactory, especially with regard to the transfer of the liquids, such relays are hardly necessary in a laboratory scale apparatus.

Fig. 5 is interesting in that it gives some information about the systematic error in the current caused by a temperature change in the cell. The curves show that the variation of the bath current due to a change of the load resistance is reduced by the stabiliser by about 5 times. If the resistance varies inversely as the conductivity and the temperature coefficient is about 2 per cent per degree, a temperature rise will increase the bath current by hardly more than 0.4 per cent per degree under conditions equivalent to those in the experiment.

According to Fig. 5 the variations of the bath current caused by changes of the supply a.c. voltage are not negligible, especially when the voltage increases. Nevertheless, the accuracy of the regulation in extended runs is very good, as reported on p. 215. The results obtained show that the inherent stabilisation against voltage fluctuations is valid and makes possible direct feeding of the regulator from the a.c. mains supply (cf. p. 225). This is of course especially valuable when high powers are needed.

In fractionation experiments of long duration it is possible to keep both the displacements and the temperature practically constant by means of the transductor regulator. Fig. 9*b* shows that the constancy of the electric variables and the temperature is better in the later part of the experiment than in the former one. This is not fortuitous; during the first hours fluctuations occur and several adjustments are generally needed before steady conditions develop. On one occasion the apparatus was run continuously during a fortnight without any sign of deterioration being detected in the meantime. When the variation of the temperature is not greater than that recorded in Fig. 9*b*, the systematic error thereby introduced in the current is negligible.

Moreover, the present method of regulation also provides optimum conditions for obtaining sharp zone boundaries. By running the pump motor from a constant voltage supply and using the pump speed as the command in the feedback control circuit, both the hydrodynamic and electric velocities can be kept approximately constant. Under these conditions variations in time of the hydrostatic and electroosmotic pressures can be avoided and the spreading of the protein zones by temporary velocity gradients in the liquid reduced to a minimum. The blurring due to changes in the electroosmotic pressure-velocity equilibrium in the cell is particularly marked when the current is suddenly broken or applied. Therefore, if maximum sharpness of the boundaries is wanted all from the beginning of the fractionation, steady-state conditions should be allowed to develop in the column before the injection of the protein mixture is started.

Since very constant conditions can be maintained over long periods of time, it is now possible to run the fractionation process at a slow rate and extend the experiment until sufficient quantities of material have been collected. The serum fractionation referring to Fig. 9 was performed in this way. A total displacement of 20 cm was obtained by the application of 135 watts, but the yield per hour was only 63 mg of protein distributed over 40 fractions according to optical density curve. The agreement between these curves and the sharpness of the peaks (Fig. 9*a*) show that the relatively long time of transfer in the electric field, about 3.2 hours, did not introduce much disturbance due to time-depending effects. At the operating temperature, 21°C, the denaturation of the proteins is probably not great; the fractions were quite clear when they left the cuvette.

Prolonged experiments performed under stable conditions have also proven to be a practical method with regard to the attendance on the process. In addition to the automatic control, the electrical process requires only slight attention, but the electrophoresis apparatus—like any other machine—requires a general, fairly regular inspection when it is working. The functioning of the motors and other mechanical parts must be controlled, the supply liquids to the cell and electrode compartments renewed at intervals, and the fractions collected and analyzed. This work can easily be managed by one person, but in order to avoid fatigue in long runs or leaving the apparatus without control in the nights, the service is preferably arranged by alternation between two persons.

In equation (6), (p. 207), the value of the constant C depends, *inter alia*, upon the porosity of the capillary system and the conductivity of the flowing liquid. In general, the same power gives a greater temperature rise in a fine packing than in a coarse one, and greater the lower the conductivity of the buffer. For this reason the temperature curves obtained with systems of different chemical composition are not directly comparable. A systematic investigation of the steady-state temperature under various conditions has not been made, but the material collected allows the general conclusion that the cell can safely be operated at a higher temperature level when the current is continuously controlled than was possible when the adjustments had to be performed by hand. The safe temperature limit appears to vary considerably; in the case of Fig. 1 (veronal buffer of the ionic strength 0.05) the system showed no sign of instability at a cell temperature of 35°C and in other cases steady temperatures of 45°, or even higher, have been obtained. With a veronal buffer of the ionic strength 0.03 the safe limit is definitely lower, probably in the neighbourhood of 30–35°C. Above this range the stabilisation of the current is insufficient for impeding the drift towards higher temperatures.

With the present cuvette (4) the full capacity of the regulating equipment cannot be applied. If higher currents than 500 mA are to be used, more space is needed for the development of the concentration gradients adjacent to the electrodes. This limit corresponds to a maximum power of about 200 watts, but higher powers can be used without thermal disturbances. Yet it can be regarded as experimentally established that an apparatus of this size requires a type of fractionation control which includes control of the heat transfer by regulation of the power. Since a control without stabilisation of the current can more easily be arranged, this method had to be tried before the transductor regulator could be procured. A device for feedback control was introduced,[1] where the bath current, obtained by transforming and rectifying the power from the a.c. mains supply, was used as the reference for controlling the pump speed. The experiments referred to in Figs. 2 and 8 were performed by this method. It was found that sufficiently steady conditions could not be obtained in this way. Very careful supplementary control of the experiments was needed, which made the attendance work tiring and impaired the results in fractionation experiments.

---

[1] The principle of design of this equipment is similar to that of the transductor regulator (Fig. 10), although the roles of the bath current and pump speed are interchanged; the bath current is here the command and the pump speed the controlled variable. A control voltage is derived by passing the bath current through a resistance and subtracting the e.m.f. generated by the tachometer attached to the shaft of the pump motor. The control voltage is received by a two stage electronic amplifier, which gives a total amplification of 2250 times. The rectified output voltage of the amplifier is supplied to the stator winding of the pump motor. The rotor is run on a constant d.c. voltage. The motor is designed according to the requirement that the speed should be proportional to the stator voltage. By variation of this voltage the speed can be varied between 2150–3600 r.p.m., which gives a sufficiently wide range for the regulation. This apparatus was designed and constructed by Mr. PER SVEDBERG, Elektrolux Ltd., Stockholm.

As stated on p. 211, a method of regulation which does not involve control of the power is appropriate when the heat transfer is satisfactorily regulated by some other means. This condition is fulfilled when a cell of smaller capacity than the present one is used and the power applied accordingly lower. The cooling system itself is then capable of keeping the bath temperature practically constant. For example, an apparatus for continuous electrophoresis in a small scale has previously been developed in this laboratory [8]. No difficulties have been experienced in keeping a stable, low temperature in this cell. A continuous-working mechanical device is needed for the supply of liquid also in this apparatus, and the electronic device sketched in the footnote p. 220 can easily be attached to the circuit and used for control of the process. In this case the control obtained is quite satisfactory. When the power applied is sufficiently small, an electronic current stabiliser of any of the types now in use in analytical electrophoresis [9, 10, 11] can be used as well, although the combined control of the hydrodynamic and electric velocities appears to possess some advantages. A small size apparatus for continuous operation is very useful when only small quantities of material are available for fractionation.

However, the greater the capacity of the cell the more necessary becomes the control of the heat transfer by regulation of the power. All evidence hitherto gained indicates that continuous control of the bath current, combined with an appropriate relay arrangement; should be sufficient for this purpose, even if the power is raised beyond the laboratory scale. Since a transductor regulator can be designed according to widely different demands of output power and accuracy [12], a description of this tool has been appended to this article.

ACKNOWLEDGEMENTS

The author is very grateful to Professor ARNE TISELIUS for permission to carry out this work at the Institute of Biochemistry and for financial support from grants to the Institute (the Rockefeller Foundation, the Wallenberg Foundation, and the Swedish Natural Science Research Council).

I also wish to thank Dr. E. MORATH, Electrolux, Ltd., Stockholm, for the gift of a regulating equipment, including the pump motor and tachometer generator; Mr. E. HELSING, Asea, Ltd., Västerås, for his readiness to undertake the construction of the transductor regulator; and to acknowledge my indebtedness to the engineers, Mr. B. HEDIN, Mr. P. SVEDBERG, and Mr. L. LANNEFORS, who in successive steps of the investigation contributed with much useful information on the subject of regulation technique.

APPENDIX

Description of the regulating equipment

By Lennart Lannefors[1]

General.—Fractionation control by automatic regulation of the bath current requires an apparatus which will maintain a constant ratio between the bath current and the speed of the pump motor. Control of the bath current also implies control of the bath temperature.

The above control can be provided by means of a feedback control system [6] employing a transductor (magnetic amplifier) for the amplification. The principle of design is shown in Fig. 10*a* and the coupling is symbolized in the block diagram of Fig. 10*b*. The following notations are used:

c = the controlled current;
v = the speed of the pump motor;
r = the input reference voltage, proportional to the speed of the pump motor;
b = the voltage from the resistance R_1, proportional to the controlled current.
e = the actuating signal (the error), i.e. the difference between r and b;
m = the voltage applied to the bath electrodes;
R = the bath resistance;
g = the transductor amplification;
h = the proportionality factor between b and c (in Fig. 10, $h = R_1$);
a = the proportionality factor between r and v.

For a definite speed of the pump motor, v, it is desired to keep the bath current, c, constant. If, for example, the current c tends to increase, the voltage drop across the resistance R_1 increases, too. Since this voltage drop is referred to the reference voltage r, a difference voltage e is obtained, which actuates the transductor to decrease its output voltage in order to restore the current to its original value. The accuracy of this restoration increases in proportion to the amplification in the transductor.

The steady-state operation of the system can be described by the following simplified equations derived from the block diagram in Fig. 10*b*:

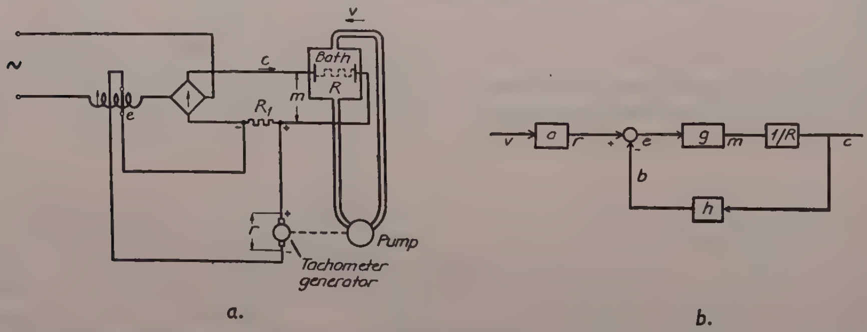

Fig. 10. *The feedback control system.*—*a*, Principle of design. *b*, Block diagram of the system.

---

[1] Allmänna Svenska Elektriska Aktiebolaget, Ludvika, Sweden; present adress: ESAB, Laxå, Sweden.

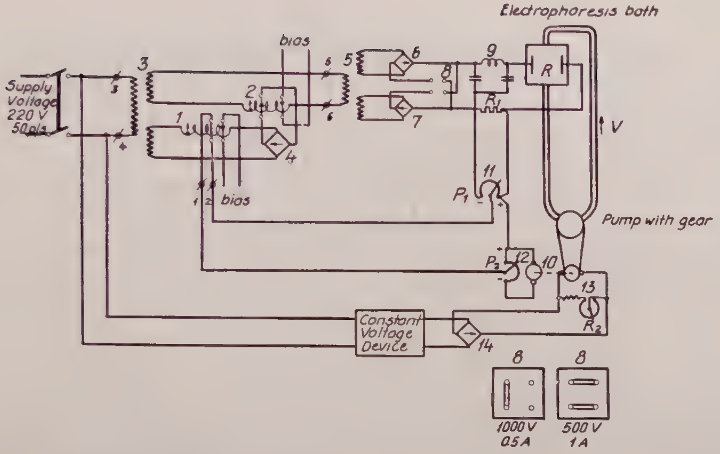
Electrophoresis bath
bios
3
5
6
9
R
Supply
Voltage
220 V
50 p/s
2
8
7
R_1
1
4
V
11
1
2
bios
P_1
Pump with gear
P_2
12
10
13
R_2
Constant
Voltage
Device
14
8
8
1000 V
0.5 A
500 V
1 A

Fig. 11. *Schematic diagram for the feedback control system.—1*, first-stage transductor; *2*, second-stage transductor; *3*, *5*, Transformers; *4*, *6*, *7*, *14*, Rectifiers; *8*, Terminals; *9*, Filter; *10*, Tachometer generator; *11*, *12*, *13*, Potentiometers.

$$m = ge \tag{1}$$

$$e = r - b \tag{2}$$

$$b = hc \tag{3}$$

$$r = av \tag{4}$$

$$c = \frac{1}{R} m. \tag{5}$$

Combining equations (1)–(5)

$$c = \frac{g \frac{1}{R} a}{1 + \frac{g h}{R}} \cdot v. \tag{6}$$

If now the gain g is made great,

$$\frac{g h}{R} \gg 1.$$

Then equation (6) can be written approximately as

$$c = \frac{a}{h} \cdot v \tag{7}$$

where a and h are constants. Equation (7) shows that the ratio between the bath current c and the speed of the pump motor v is constant and also that the current c is independent of the bath resistance R.

In this case a transductor [13] has been used for the amplification g. Other alternatives could be thyratrons [14], or some type of rotating amplifier [15]. Vacuum tubes are not recommended

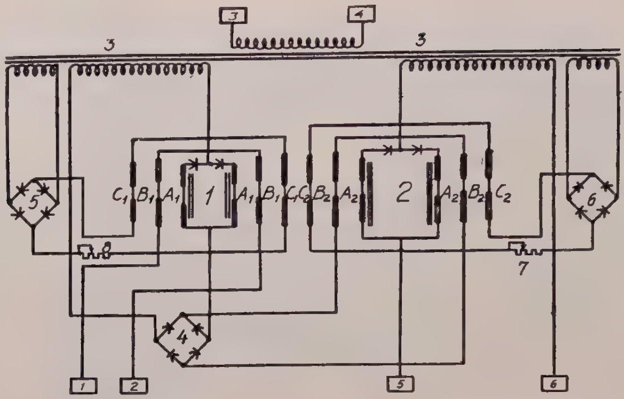

Fig. 12. *Coupling diagram of the two-stage transductor.*—*1*, Transductor *1* with power winding A_1A_1 and control windings B_1B_1 and C_1C_1. *2*, Transductor *2* with power winding A_2A_2 and control windings B_2B_2 and C_2C_2. *3*, Transformers. *4*, *5*, and *6*, Selenium rectifiers. *7*, *8*, Resistors.

for this application since the output power required of the amplifier is about 500 watts. Thyratrons can be used, but they require periodic inspection and replacement. The advantage of thyratrons of having practically no time lag is less significant in this case, since the process variations in the bath itself are of the order of a few minutes. Ordinary transductors and rotating amplifiers have a time constant of about 0.1–0.5 sec., which is quite sufficient for an application of this type. A transductor regulator is a static device with no moving parts requiring periodic maintenance; for this reason it is preferred to rotating amplifiers.

The regulating equipment.—The transductor regulator is illustrated diagramatically in Fig. 11. The gain g (cf. Fig. 10) is deviced from two transductors, *1* and *2*, coupled in cascade. The power amplification of the first transductor is about 3000 and that of the second one about 12. The cascaded coupling therefore gives a total power amplification of approximately 36,000 and makes possible control with only a very small power input. The d.c. output power from transductor *2* is transformed to a higher voltage by the transformer *5*, the output of which is rectified by the selenium rectifiers *6* and *7*. The bath electrodes are connected to the d.c. side of the rectifiers through the smoothing filter *9*.

As symbolized in the block diagram (Fig. 10*b*) and by equation (2) a term b, which is proportional to the bath current c, must be subtracted from the reference input r in order to obtain the error signal e. This signal actuates the two stage transductor amplifier to eliminate the error. This subtraction takes place in the circuit which consists of the potentiometers P_1 and P_2 and the control winding of transductor *1*. The voltage taken from the potentiometer P_1 corresponds to the factor b in the block diagram.

Equation (7) shows that the ratio of the speed of the pump motor to the bath current is dependent on the magnitude of the constants a and h. These constants can be altered by adjusting the potentiometers P_2 and P_1 respectively, thereby varying the bath current c with the speed v constant.

If the hydrodynamic velocity is also to be changed, the speed of the pump motor must be changed. This motor is supplied with a d.c. voltage which is obtained from a constant voltage a.c. device and rectified with the aid of a selenium rectifier. The motor speed is changed by varying the motor field with the resistor R_2.

As is shown in Fig. 11, the main rectifier is composed of two parts, *6* and *7*, which are supplied by a transformer having two secondary windings. The primary winding of this transformer is connected to the output terminals of transductor *2*. The rectifiers *6* and *7* can be coupled either in series or in parallel. With the series coupling one will obtain a maximum of 1000 volts and 0.5 A at the bath and with the parallel coupling 500 volts and 1 A. If only one fixed coupling were to be used, all of the regulator components would have to be designed for 1000 volts and 1 A, i.e. 1000 watts. With the arrangement shown in Fig. 11 these components need only be designed for 500 watts.

The transductor amplifier.—The two stage transductor amplifier is shown in some detail in Fig. 12. Each of the transductors consists of two separate cores with the a.c. windings (power windings) coupled in parallel. Both the transductors have auto-selfexcitation, i.e. selfexcitation obtained with the aid of the power winding [13]. This type of selfexcitation results in a very high degree of amplification, as is evidenced by the static characteristics of the two transductors, cf. Fig. 3.

Each transductor has two windings (BB and CC) in addition to the power windings (AA), see Fig. 12. The winding B_1B_1 is the control winding of transductor *1* and connected (by terminals 1 and 2), to the circuit containing the potentiometers P_1 and P_2 (see Fig. 11). The error voltage e (see Fig. 10) is applied to this winding. The winding C_1C_1 is used as a bias winding, i.e. for displacing the mean operating point on the static characteristic. Since the voltage proportional to the controlled variable (current c) is balanced against the reference voltage r, the operating point in the controlled circuit should be as near as possible to that point which requires no control current.

The output power of transductor *1* is rectified by rectifier *4* (Fig. 12) and applied to the control winding B_2B_2 of transductor *2*. The ampere turns, which are obtained from this control power, are compensated by the ampere turns of the bias winding C_2C_2. The bias winding C_2C_2 is fed from rectifier *6* and its ampere turns adjusted with the aid of resistance *7*. Both the transductors are supplied by the transformer *3* which is, in turn, connected to the line voltage (220 V, 50 p/s) at terminals 3, 4.

A significant advantage of this regulator is that it can be connected to the local a.c. supply without auxiliary apparatus for voltage stabilisation. This performance has been obtained by appropriate bias in the transductor *1*, which compensates the current variations in power windings A_1A_1 orginating from fluctations in the supply voltage.

The pump motor.—Since the ratio between the bath current and the pump speed is controlled by the regulator to be constant (see equation (7)), the accuracy of the constant voltage device for the pump motor need not be great. A constant voltage device for the small power of the pump motor can easily be built in [16].

Summary

Continuous fractionation control is indicated as a means of maintaining stationary conditions during the process with regard to the electric and hydrodynamic velocities and the heat transfer.

The net displacements of the separating substances, which should be controlled to be constant, depend upon the ratios of the electric and hydrodynamic velocities. Control of the heat transfer requires regulation of the power expended. Both the electric velocities and the power are satisfactorily controlled by stabilisation of the bath current. The hydrodynamic velocity varies proportionately with the pump speed.

A method of fractionation control has been deviced where the pump speed is the command in a feedback control system for regulation of the bath current. By this means a proportional variation of the electric and hydrodynamic velocities is ascertained. By operating the pump motor from a constant current source both

component velocities can be kept constant. Approximately constant working conditions in the above respects can also be maintained when the pump motor is supplied from a constant voltage source. This arrangement is used in the present laboratory. Fig. 9*a* and *b* illustrates a fractionation of blood serum which is representative of the method.

The actuation of the error signals from the control circuit takes place in a two stage transductor amplifier with a total power amplification of 36,000 times. The regulating equipment is described by its designer in the Appendix.

Institute of Biochemistry, University of Uppsala, Uppsala, Sweden.

REFERENCES

1. Svensson, H. and Brattsten, I., *Arkiv Kemi* 1 (1949) 401.
2. Grassman, W. and Hannig, K., *Z. angew. Chem.* 62 (1950) 170.
3. Brattsten, I., *Arkiv Kemi* 4 (1952) 503.
4. Brattsten, I., *Arkiv Kemi 8* (1955) 227.
5. Tiselius, A., *Biochem. J.*, 31 (1937) 1464.
6. Brown, G. and Cambell, P., *Principles of Servomechanisms.* John Wiley and Sons, New York 1948.
7. Aikman, O. S., *Machine Design* 23 (1951) 163.
8. Brattsten, I. and Nilsson, A., *Arkiv Kemi* 3 (1951) 337.
9. Carson, Jr., W. N., *Anal. Chem.* 22 (1950) 1565.
10. Spiro, M. and Parton, H. N., *Trans. Faraday Soc.* 48 (1952) 263.
11. *Type LKB 3021 Tiselius-Svensson Electrophoresis Apparatus. Instructions for Use.* Stockholm 1950, p. 25.
12. a Lamm, A. U., *The Transductor, with Special Reference to Transductor Control of Rectifiers.* (Diss.) Stockholm 1943.
    b Lamm, A. U., *Trans. Am. Inst. Elec. Engrs.* 66 (1947) 1078.
13. Hedström, S. E. and Borg, L. F., *Electronics* 21 (1948) 88.
14. Millman, J. and Seely, S., *Electronics.* McGraw-Hill Book Company, Inc. New York 1941, p. 330.
15. Lehmann, G., *Elec. Commun.* 30 (1953) 12.
16. Quimby, R., *Electronic Inds* (1948) 14.

Tryckt den 25 april 1955

Uppsala 1955. Almqvist & Wiksells Boktryckeri AB

ARKIV FÖR KEMI Band 8 nr 23

Communicated 10 November 1954 by A. Tiselius and H. Theorell

Continuous zone electrophoresis by crossed velocity fields in a supporting medium

Fractionation of protein mixtures and description of the cuvette

By Inger Brattsten

With 7 figures in the text

In continuous fractionation by zone electrophoresis stationary conditions should prevail in the flow field (1). In the present apparatus the hydrodynamic velocity is effected by a pumping device (2), which transports the liquid through the cell at an approximately constant rate. With the pump speed as the command a feedback system has been introduced for the control of the bath current (3). By these means it is possible to conduct the fractionation process under practically constant conditions, provided the chemical composition of the separation field remains constant in time.

The latter condition implies that the composition of the conducting medium must be chosen with due regard to the number of coulombs needed for the separation and the space conditions in the cell. It is evident that both the dimensions of the cuvette and the porosity of the supporting system influence the requirements on the liquid medium. Since the electric process control makes possible the use of low fractionation rates, relatively fine packings have to be used in order to suppress convection currents and diffusion. In the fractionation of serum proteins and similar substances satisfactory results have been obtained with any of the substances tested, e.g. glass powder (1), cellulose powder[1], starch (4).[2] The conducting systems described herein are adapted to these types of supporting media and the characteristics of the present cuvette. The resolution achieved and the rates of fractionation in some different cases are reported in the description of the fractionation experiments.

The cuvette

The design of the perspex cuvette is shown in Fig. 1 *a* and *b*. The separation cell itself is built as a closed unit, where the driving pressure is effected by the pump apparatus (2). The inner dimensions are: length 280 mm, height 300 mm, and thickness 10 mm. To the front and back walls of the trough are attached cooling mantles connected by rubber leads to a thermostated cold water bath. By means of a cir-

---

[1] The use of cellulose powder as the supporting medium was suggested to the author by Dr. Stanford Moore, The Rockefeller Institute, New York, in 1950.

[2] Some experiences of these substances as packing materials will be reported later; cf. also ref. 5.

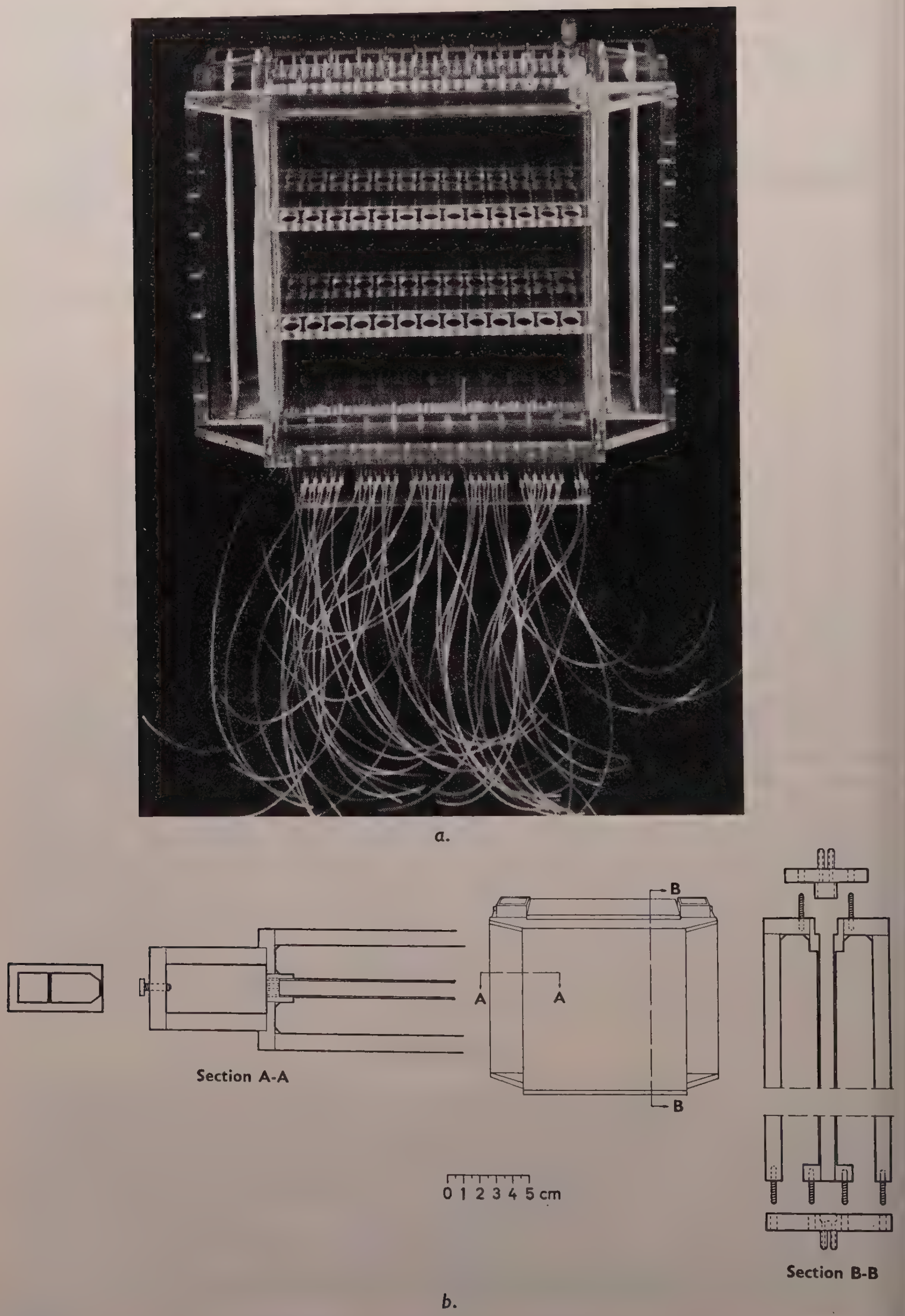
a.
B
A
A
B
Section A-A
0 1 2 3 4 5 cm
Section B-B
b.

Fig. 1. *The cuvette.*—*a.* Photograph of the cuvette.—*b.* Drawing, showing the design. The sections *A–A* and *B–B* are indicated in the full drawing. In section *A–A* the electrode compartment is drawn to the left of the cell; in section *B–B* the top and bottom plates are drawn above and below the centre part.

culation pump water from this bath is sucked through the cooling mantles of the cuvette at a rate varying between 5 and 10 l per minute. The top and bottom plates are also seen in Fig. 1. The top plate contains in all 28 inlet and the bottom plate 56 outlet nipples. These are connected by polythene tubing to the pump apparatus. Pads of pyrex wool prevent the packing material from entering the tubes.

To allow control of the temperature in the bath, the cuvette is equipped with a thermocouple projecting 60 mm above the bottom plate. The Cu-constantan wires are electrically insulated by a thin polythene cover. The second junction is kept at the temperature of the cooling bath, generally a few degrees above zero. By this device the temperature in the cell can be measured with a time lag of about 1 second.

The electrode vessels are built as separate units, clamped to the separation cell by screws in the end plates of the cuvette. The walls between the cell and the electrode vessels are perforated and enclose membranes of cellophane or parchment paper, which allow the transport of ions but prevent hydrodynamic flow disturbances from reaching the separation field. The electrode vessels are divided into two compartments each. The outer ones contain the electrodes immersed in free liquid. The electrodes consist of 1 mm platinum wire, wound round rectangular frames of plast-coated steel wire. The inner electrode compartments are separated from the free liquid by membranes and filled with a fairly coarse glass powder. The electrode liquid is supplied from two Mariotte flasks and withdrawn by pumping. The pump apparatus is similar, in principle, to that employed for the cell itself (2), but only contains one section and is operated by a small synchronous motor. The rates of flow of the electrode solutions are so regulated that pH remains unchanged in the compartments adjacent to the cell. After having passed the electrode compartments the liquids are mixed in equivalent portions and the resulting solution is refilled into the supply bottles with the aid of a circulation pump.

In the construction of a perspex cuvette two properties of the material give rise to difficulties, namely its low thermal conductivity and softness to mechanical strain. Good conditions for the heat transfer can only be obtained if the walls conducting the heat are thin, but mechanical strength requires thick walls. In the present design these demands have been observed by making the cell walls in contact with the cooling water 1 mm thick and transferring as far as possible the mechanical strain to the firm lateral walls and those of the cooling mantles. Since the thin perspex walls separating the electrophoresis bath from the cooling water are quite flexible, their main importance is for the electrical insulation; the mechanical strength and fixation of the form are obtained by the insertion of 4 mm thick brass gratings outside these walls and five thin bars across the packing inside the cell. The brass gratings are kept in position by perspex bars in the cooling mantles, see Fig. 1 *a*. The cuvette is mounted in an iron frame. The frame metal is insulated by a plast coating.

The necessity of insulating the bath from the ground requires that all joints of the cuvette are tight. Without special tools for the application of a uniform pressure at the cementing, complete and permanent insulation can be obtained by the use of a thick jelly of partially polymerized methyl methacrylate as the cement material and reinforcement of the joints by triangular lists in the corners, cf. Fig. 1 *b*.

The conducting system

The rates of migration of the substances to be separated are constant only if the electric field remains constant in space and time. This condition includes the requirements of constant conductivity and low concentrations of the protein ions relative to the salt content of the medium (5, 6). The difficulties of extracting the Joule heat generally makes necessary the achievement of a sufficiently strong electric field by a low conductivity rather than a strong current. Satisfactory results have nevertheless been obtained when protein mixtures are fractionated in media containing only the sodium salt of any of the common buffer acids in a concentration of 0.03–0.05-C.

If the same electrolyte solution is supplied to all parts of the system, the only foreign ions which may disturb the migration process are the hydrogen and hydroxyl ions produced at the electrodes. They are most easily removed by increasing the streaming velocity in the electrode compartments. Such a differentiation of the hydrodynamic velocity is possible when water transport between the electrode compartments and the separation zone is impeded by membranes in the end walls of the cell (8, 9, 10). However, those membranes which are sufficiently impermeable to the water particles in general also retard to some extent the ions conducting the bath current. Since the sodium and acetate ions apparently pass a parchment paper or cellophane membrane rather freely, the convention has been adopted always to supply a concentrated sodium acetate solution (0.4-C) to the electrode vessels and the anode part of the separation zone, i.e. essentially those parts of the electric field where the anions migrate into the membranes. On the cathode side, the acetate ion migrates towards the separation zone. If the conducting medium of this zone is not an acetate buffer, a moving boundary develops with the acetate ion as the following ion species. The migration of this boundary is restricted by supplying the medium electrolyte as a more concentrated solution to the field inside the cathode membrane than to the separation zone (cf. TISELIUS (11)). A system of this type is outlined in Fig. 2, *a* and *b*. Here the zones of concentrated solutions limiting the separation zone towards the electrode compartments constitute two reservoirs whence the acetate ion is transferred into the anode compartment and the veronal ion from the cathode to the anode side of the separation zone, respectively. The middle zone remains unchanged during the transfer if the reservoir of the veronal ion contains a certain surplus of this species.

The quantities of the ions transferred during the passage of the column can easily be estimated when the current, the time of transfer and the transport numbers are known, but for arranging the liquid system some additional factors must also be considered. The mobility differences and number of the components to be separated determine the distribution of the available space between the separation and end zones. The mutual balancing of the breadths and concentrations of the two end zones involves considerations of the density and solubility properties of the solutions and the mobilities of the anions. If the mobilities differ, either of the moving boundaries in the concentrated zones tends to become diffuse—"Whetham's rule" (12); (13). When the following ion at a boundary is faster than the leading one, the content of the latter in the concentrated zone must be increased above the theoretical value in order to limit the propagation of the faster ion. Further, the pH of the solutions generally requires adjustment by addition of suitable, small amounts of acetic acid or sodium hydroxide to the electrode liquid. The transference num-

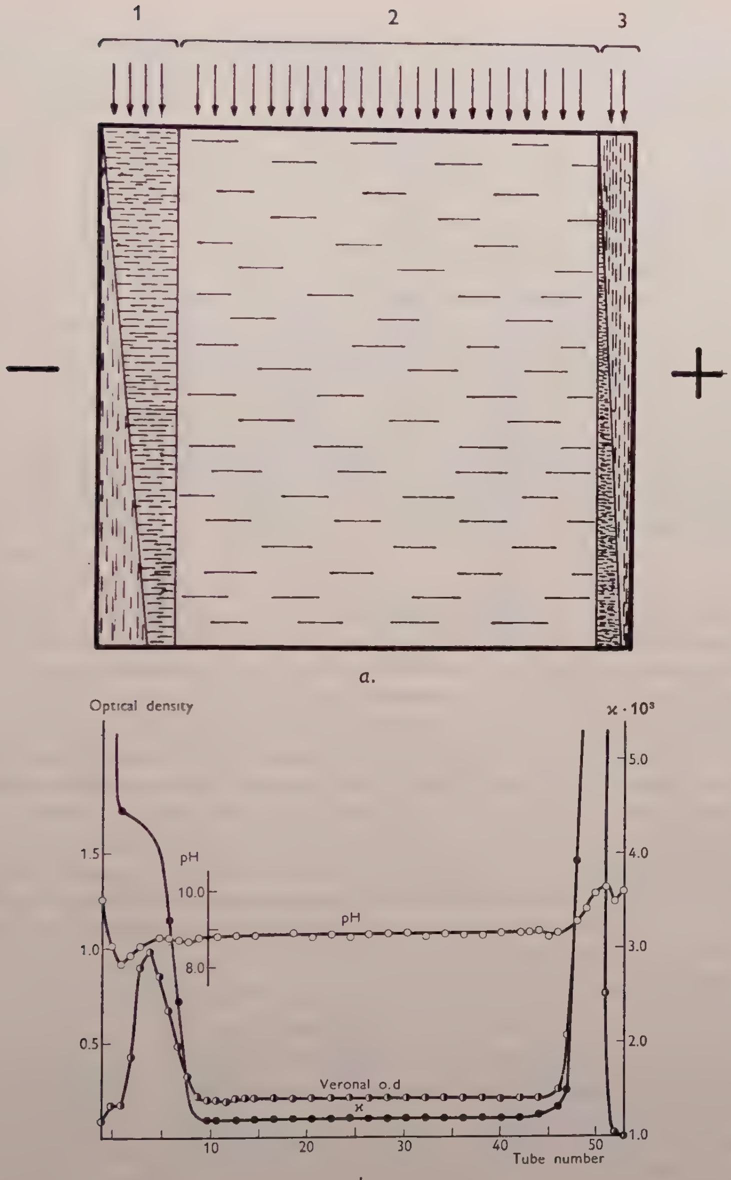

a.

b.

Fig. 2. *The conducting system.*—*a*. Schematic representation of the conducting system. The arrows indicate the supply of liquid by the inlet openings. Within the flow field the vertical lines illustrate the concentration boundaries between the dilute and concentrated buffer media, and the inclined lines the (moving) boundaries between the concentrated buffer and acetate solutions. The following solutions were injected: *1*, Concentrated veronal buffer, $\mu = 0.28$, pH = 8.8; *2*, Dilute veronal buffer, $\mu = 0.05$, pH = 8.8; *3*, Concentrated acetate solution, containing sodium acetate, 0.4-C and sodium hydroxide, 0.005-C. Bath current: 450 mA, rate of liquid flow: 7.0 ml hour^{-1} cm^{-2}, temperature: 21°C. Supporting system: glass powder.—*b*. Analysis of the fractions collected in a test experiment without supply of protein solution. The conductivity, pH, and optical density, at 284 mμ, of the fractions are recorded as functions of the tube number. The optical density is a function of the veronal concentration in the solution.

bers in the dilute and concentrated solutions of the medium electrolyte should be the same; if they differ, the concentration boundary acquires a mobility in the electric field. For example, if a phosphate buffer is used, an initial pH gradient across the concentration boundary may cause the origin of one or even two moving boundaries.

In experiments 1 and 3, described in the following section, constant rates of migration of the protein ions were obtained by arranging the liquid systems according to these principles.

However, a controlled variation of the protein velocities within the separation field sometimes is preferable to constant rates. In general, the electric velocities change at every boundary where the substances migrate into a new liquid medium. Therefore, a controlled variation can be obtained if solutions of suitably modified compositions are introduced into successive parts of the separation zone.

A certain differentiation of the protein mobilities is possible by the application of a pH gradient in the cell, but migration against a conductivity gradient is more expedient if greater effects are wanted. When an ion migrates into a zone of increased conductivity, it normally suffers a retardation proportional to the decreases of the field strength and its mobility. Therefore, the insertion of a horizontal conductivity gradient in the path of a protein band may have the effect of concentrating the substance to a zone considerably narrower than that injected. The conductivity gradient can be arranged by increasing stepwise the concentration in the solutions supplied to the separation zone. In experiment 2 (see p. 233) the fastest component was purified and enriched by fractionation in a liquid medium containing the same buffer solution in two different concentrations.

Inversed conditions, i.e. when an ion species migrates into a medium of lower conductivity, normally give rise to a certain dilution and broadening of the substance band. Nevertheless, under special conditions a system of this type has proven capable of enhancing the resolution of a mixture. In experiment 4 a small, continuous conductivity gradient was arranged by allowing a limited penetration of the acetate ion into the separation zone. In this field the conductivity increased vertically but decreased horizontally in the direction of the migration. The main effect was a retardation of the slow components relative to the fast ones, allowing improved resolution of the latter. The magnitude of a gradient of this kind can be controlled by means of the ion content of the veronal reservoir zone inside the cathode membrane.

In designing an electrolyte system for the fractionation of a certain mixture the approximate composition is computed from available data. As a guide for adjustments and a final check that the stationary conditions in the column are as expected, test runs are performed prior to the application of the protein mixture. The fractions collected in these runs are analysed with regard to pH, conductivity, and, possibly, some ion species. These data provide information necessary for the control of the electric field conditions, cf. Figs. 2 *b*, 3, 5 *a*, 6 *a*.

Separation experiments

1. Separation of serum proteins at pH = 4.5

The conducting system was obtained by injecting an acetate buffer of the ionic strength 0.025 and pH = 4.5 into the separation zone and a more concentrated

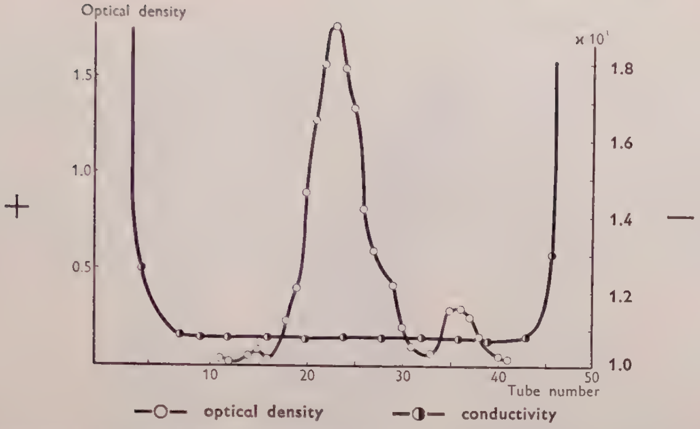

Fig. 3. *Electrophoresis of normal human serum in an acetate buffer of the ionic strength 0.025 and pH = 4.5,* cf. exp. 1.—The optical densities of the fractions at 280 mμ represent the protein distribution. The conductivity in the separation field has been recorded by plotting the conductivities of the fractions as a function of the tube number.

solution of the same buffer ($\mu = 0.4$) to the end zones of the field. Fig. 3 contains a record of the conductivity, showing that constant conditions prevailed in the separation zone. A current of 300 mA was applied and the volume velocity of the flowing liquid was 2.9 ml per hour per cm^2. The supporting medium consisted of glass powder. The temperature in the packing was 16.8°C. The protein mixture was injected by one inlet tube, corresponding to Nos. 18 and 19 in the diagram. It contained normal human serum, diluted to a protein concentration of about 2 per cent and dialyzed against the dilute acetate buffer. The protein content of the fractions was measured spectrophotometrically at 280 mμ.[1] The distribution curve is recorded in Fig. 3. At the pH of the medium the mobility of serum albumin is slight. A general resolution of the component proteins was not obtained, although the heterogeneity is apparent from the shape of the major peak. Only two components were clearly separated from the main portion of the protein.

2. Fractionation of the algae proteins phycoerythrin and phycocyanin with simultaneous concentration of the former

The processes of separation and concentration took place in a medium containing the ions Na^+, $H_2PO_4^-$, and HPO_4^{2-} and glass powder as the supporting substance. According to the measurements of TISELIUS (6) the mobility of phycoerythrin, at the prevailing pH of 7.6, is about twice a great as that of phycocyanin.

The experiment is most easily described with reference to Fig. 4 *a*. The following solutions were injected: (1) Concentrated phosphate buffer, pH = 7.6, $\mu = 0.25$ (4 tubes); (2) Dilute phosphate buffer, pH = 7.6, $\mu = 0.03$, (10 tubes); (3) A solution of phycoerythrin and phycocyanin, dialyzed against the dilute phosphate buffer[2]

---

[1] For all light absorption analyses a Beckman spectrophotometer, Model DU, was used.

[2] The protein mixture was extracted from the alga *Ceramium* by the method of KYLIN (14; cf. ref. 6, p. 48). In solutions containing either or both of the two coloured proteins the concentrations were estimated spectrophotometrically with the aid of the extinction coefficients given by LEMBERG (15).

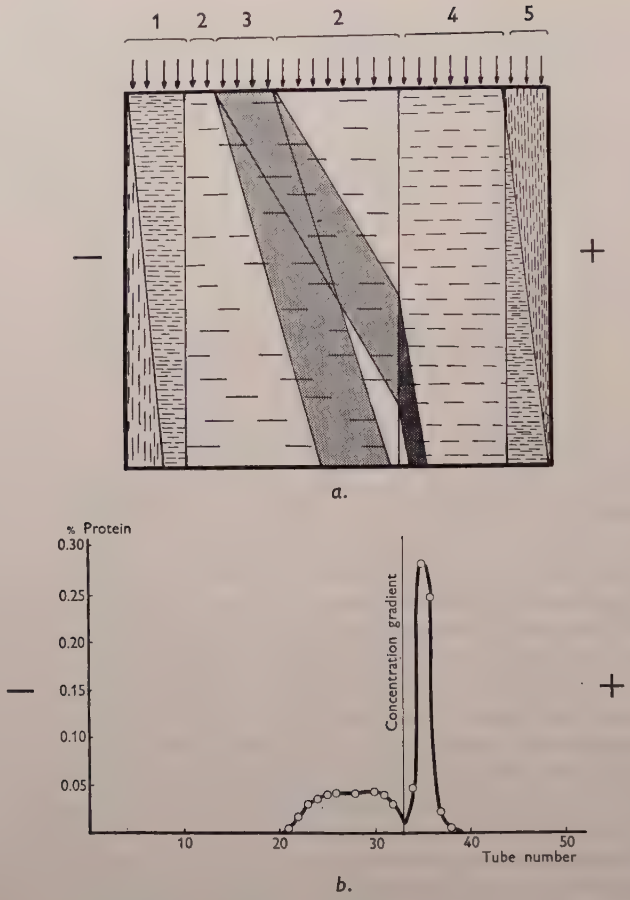

Fig. 4. *Separation of phycoerythrin and phycocyanin with simultaneous concentration of the former,* cf. exp. 2.—*a*. Schematic representation of the flow field. The protein zones are shaded. An explanation of the drawing and the compositions of the solutions injected are given in the text.—*b*. The distribution of the two proteins in the fractions. The optical density readings have been recalculated to give the protein content in per cent.

(4 tubes); (4) Concentrated phosphate buffer, pH = 7.6 and μ 0.15 (7 tubes); (5) Sodium acetate solution, 0.4-C (3 tubes). A current of 217 mA was applied, the rate of flow was 7.95 ml per hour per cm^2, and the temperature rise in the cell 13°C.

Fig. 4 *a* shows the presence of an electrically immobile concentration gradient in the conducting system, in addition to the four immobile and the two moving boundaries of the end zones. According to the drawing, the resolution of the component proteins (the shaded zones) was complete in the dilute medium. The concentration process started when the front of the faster component reached the vertical gradient, where its angle of inclination suddenly decreased in approximate proportion to the concentration ratio of the two adjacent phosphate solutions.

The development of the red phycoerythrin and blue phycocyanin zones could be followed visually. The changes in the breadth and direction of the phycoerythrin band at the concentration boundary gave direct information about the migration conditions in the column.

Spectrophotometric estimation of the protein contents of the injected solution and the fractions gave, for the former, 0.075 % of phycoerythrin and 0.05 % of phycocyanin; for the fractions, the concentrations recorded in the distribution curve, Fig. 4 *b*. If only the two main fractions of the phycoerythrin band were collected, each 31.5 ml of the protein mixture, injected during one hour, corresponded to a yield of 8 ml of (electrophoretically) pure phycoerythrin solution. Simultaneously the concentration was raised from 0.075 % in the mixture to 0.25 % in the pure solution.

3. Fractionations in veronal buffer (pH 8.4–8.6)

In a number of fractionations the conducting medium has consisted of a veronal buffer. The composition of a system of this type is outlined in Fig. 2 *a* and *b*. These diagrams show that an ionic strength of the medium of 0.05 gives a separation zone extending about 19 cm horizontally. By decreasing the ionic strength to 0.04 or 0.03 the fractionation can be accomplished at lower currents. Consequently, the reservoir zones limiting the separation field towards the electrode compartments can be reduced, and space is gained for the separation process. Fig. 5 *a* refers to a system containing in the middle part a veronal buffer of the ionic strength 0.03 and pH = 8.6. In this case the separation zone covers the field between the tubes 3 and 48, a distance of about 22 cm.

Three fractionations in this medium will be described. Starch was used as the supporting substance, and in each case the protein solution was injected by one inlet tube. Since the light absorption of the veronal ion is strong at 278–280 mμ but rapidly decreases at longer wavelengths, the optical densities of the fractions were determined at 284 mμ, where the serum proteins still retain most of their absorbing power. The protein distribution was derived by subtracting the optical density due to the electrolyte medium from these readings and plotting the resulting values against the tube number. The optical densities of samples collected prior to the appearance of protein in the effluent liquid were substituted for those due to the background electrolyte in the protein solutions.

a. Fractionation of normal human serum, Fig. 5 b.—The dialyzed serum solution, containing approximately 2 % of protein, was injected at a rate of 3.6 ml per hour. 230 mA were applied, and the bath temperature amounted to 24° C. 15 ml of whole serum was fractionated. The material collected was used for an investigation the homogeneity of the fractions. The components present in the fractions were identified by paper electrophoresis, ultracentrifugation, and some other chemical and physico-chemical means (16).

b. Fractionation of a pathological serum (allergic asthma), Fig. 5 c.—This serum had an exceptionally high reaginic titer.[1] 35 ml of whole serum was fractionated after dilution 4.2 times and dialysis. The current was 240 mA, the volume velocity of the flowing liquid 4 ml per hour per cm^2, and the bath temperature 25.5° C. The protein content of the fractions gave a distribution curve which strikingly deviated from that normally obtained, Fig. 5 *c*; cf. Fig. 5 *b*. An analysis by moving boundary

---

[1] Personal communication by Dr. H. COLLDAHL, St. Göran's Hospital, Stockholm, cf. also ref. 17.

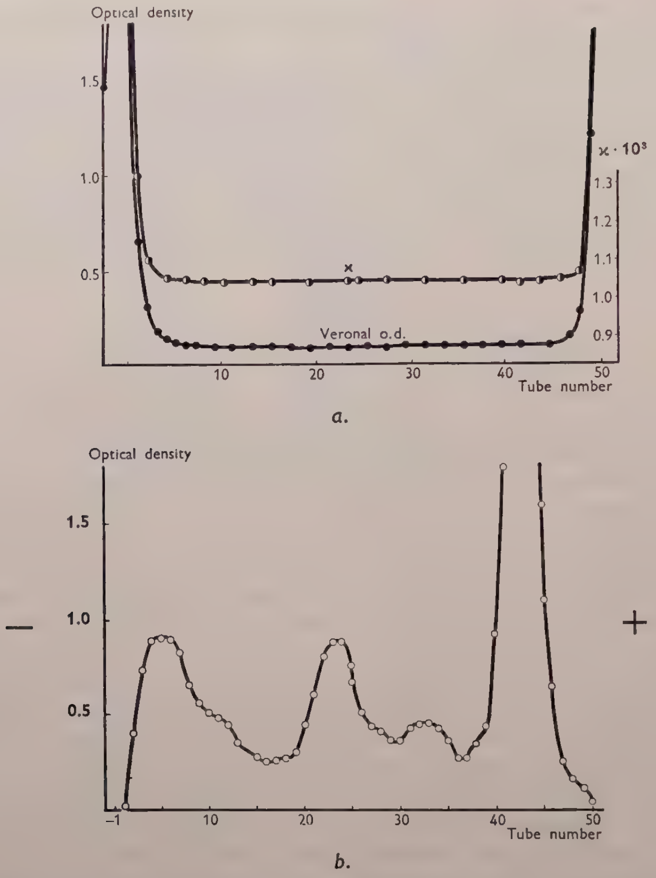

Fig. 5. *Fractionations in veronal buffer of the ionic strength 0.03 and pH = 8.6.*—*a*. Records of the conductivity and optical density, at 284 mμ, of the fractions in a test experiment without application of protein.—*b*. Fractionation of normal human serum, cf. exp. 3 *a*.—*c*. Fractionation of a pathological serum, cf. exp. 3 *b*.—*d*. Fractionation of cerebrospinal fluid, cf. exp. 3 *c*. In the diagrams *b*–*d* the distribution of the protein material in the fractions is represented by the optical density function.

electrophoresis confirmed the result that this serum contained the globulin components, especially the α-group, in abnormally high concentrations. In accordance with the high globulin content of the fractions the coloured zones were pronounced: pink (fractions Nos. 21, 22, 23), brownish-red (Nos. 25, 26, 27, 28), and yellow (Nos. 29, 30 and 37, 38, 39, 40). The fractions were used for an investigation of their reagin content (18).

c. Fractionation of normal human cerebrospinal fluid, Fig. 5 d.—About 1 l of spinal fluid was fractionated after concentration dialysis to a final volume of 50 ml. The protein concentration of this mixture was approximately 1 %. A current of 230 mA was applied, giving a temperature rise in the cell of 18°C. 3.6 ml of liquid was injected per hour per cm². The fractionation was performed with the aim of isolating the minor component migrating in front of the albumin peak (X-protein,

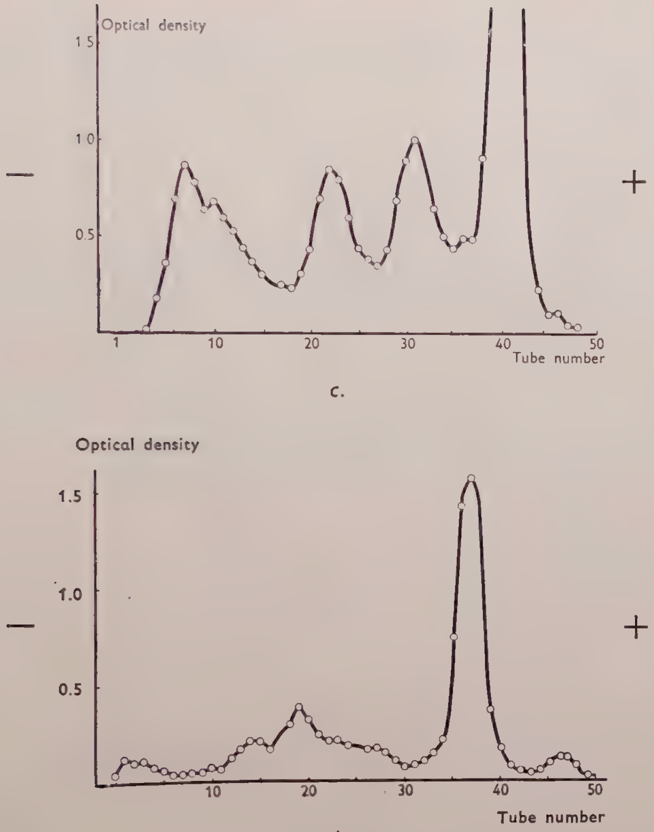

c.

d.

Vorfraktion), (19, 20). The preparation of the cerebrospinal fluid for the fractionation and the analysis of the isolated material were performed by ALY (21). In the optical density pattern, Fig. 5 *c*, the τ-component (22) is visible closely behind the β-globulin peak.

4. Fractionation of normal serum at pH 8.6 in a system containing a conductivity gradient

By decreasing further the veronal content in the concentrated end zone and, slightly, in the separation zone a conducting system was derived, which allowed fractionation, under controlled conditions, in the presence of a conductivity gradient. The records of the conductivity, pH, and increase in the veronal content at the bottom level of the cell, Fig. 6 *a*, gave evidence that the acetate ion was present in the dilute veronal buffer of the separation zone. In this field the electric migration velocities of the slow components of serum gradually decreased as the bottom level was approached. The fastest components migrated in the uniform field of the very dilute veronal buffer, where a relatively small current produced the

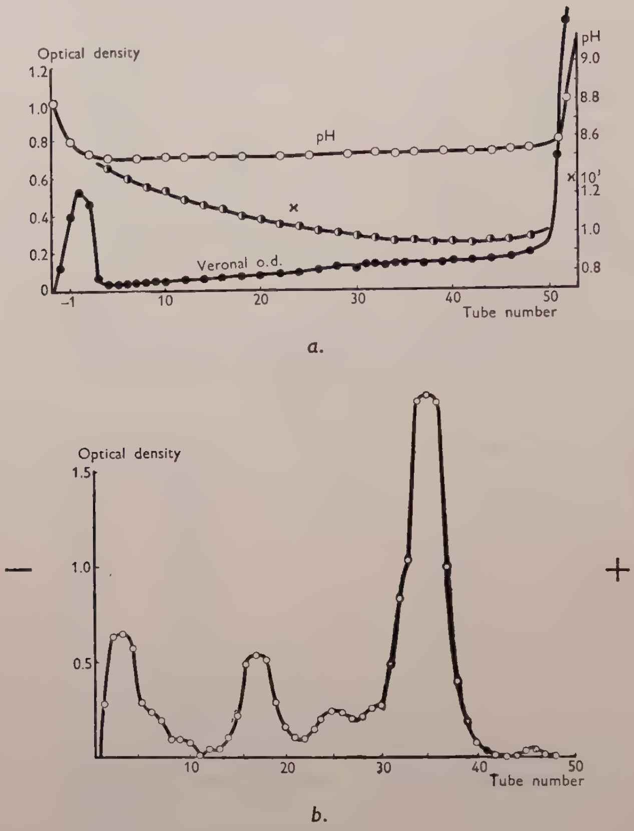

Fig. 6. *Fractionation of normal human serum in a veronal buffer containing a conductivity gradient,* cf. exp. 4.—*a*. Records of the optical density, at 284 mμ, the conductivity and pH of the fractions in a test experiment prior to the application of the protein solution.—*b*. The protein distribution in the fractions, as represented by the optical densities at 284 mμ.

velocities needed for separation of the component bands. Therefore, the serum pattern retracted into the separation zone, and free space was gained in front of the albumin band; cf. Fig. 5 *b*. These conditions favour the resolution of minor components having higher mobilities than the albumin.

Such components have been detected in certain pathological sera by boundary electrophoresis (23, 24). When normal sera are analyzed by the ordinary procedure, the fastest boundary in each limb of the U-tube generally belongs to the albumin component (25), but small amounts of faster components can also be resolved from the albumin boundaries in normal sera by prolonging the electrophoresis or reducing the buffering capacity of the medium (26, 27). Likewise, every serum fractionated by the procedure described herein has given an optical density pattern containing at least one small peak in front of the albumin zone. A similar result has been obtained by Grassmann and Hannig by electrophoresis in filter paper (28).

The fractionation depicted in Fig. 6*b* aimed at the isolation of the minute front component. The serum solution contained 1.5 % of protein, and was injected at a rate of 3.8 ml per hour. A current of 222 mA was applied, giving an operating temperature of 17°C in the bath.

Discussion

In the experiments reported the rate of fractionation and resolution of the protein components approximately correspond to the maximum capacity of the present cell. A higher, uniform resolution of all the serum protein components would require extension of the separation zone in the horizontal direction, i.e. increase of the cell size.

The resolving power of a reported system may be defined by the mobility difference between two components of a mixture, which leave the column as infinitely narrow zones separated by a distance of 1 cm horizontally. The maximum resolution which can be obtained in a certain fractionation experiment depends upon the mobility differences between the components to be separated, the initial zone breadth, the spreading of the zone boundaries during the migration, and the resolving power. When the electric mobilities of the protein ions are known, the resolving power of the system can be derived (1, 29). An experimental measure of the total spreading is obtained by comparing the final zone breadth with that of the injected mixture.

The translation of the experimental resolution into the mobility scale is suitably based on reference values obtained by the moving boundary method under ordinary working conditions. The electrophoresis of serum has been extensively studied at pH = 8.6 in media containing veronal buffers of varying ionic strengths (30, 25). According to the measurements of ARMSTRONG, BUDKA and MORRISON (25) the mobilities in a veronal buffer of the ionic strength 0.2 are, for serum albumin $-5.1 \cdot 10^{-5}$, and for γ-globulin $-1.2 \cdot 10^{-5}$ cm^2 volt^{-1}sec^{-1}; i.e., the mobility difference is $-3.9 \cdot 10^{-5}$ cm^2 volt^{-1} sec^{-1}. In fractionations equivalent to experiment 3*a* the centre of the albumin band is normally separated from that of the γ-globulin band by a distance of 18 cm. Provided the mutual ratios of the component mobilities are the same in the two media, this displacement difference corresponds to a resolving power of 0.22 mobility units per cm under the reported conditions. Since the fractionation is actually performed in a conducting medium of very low ionic strength, approximately 0.03, the mobilities of the protein ions are considerably higher in the fractionation column than in the reference medium and the conductivity lower—two factors of importance for the achievement of sufficiently high migration velocities without the application of a strong current.

The fractionation diagrams reproduced in Figs. 5 and 6 are all based on a single physico-chemical property of the solutions, the optical density. Because of the great heterogeneity of the serum proteins, these patterns hardly reveal the final zone breadths and degree of spreading of singular components. Only comprehensive analyses of each fraction may serve to identify the individual proteins present (cf. ref. 16).

In the present cuvette, flow disturbances due to variations of the hydrostatic pressure are effectively excluded by the combined methods of regulating the liquid transfer by the pump apparatus and closing the cell towards the electrode compartments by highly water-impermeable membranes. The electric process control also

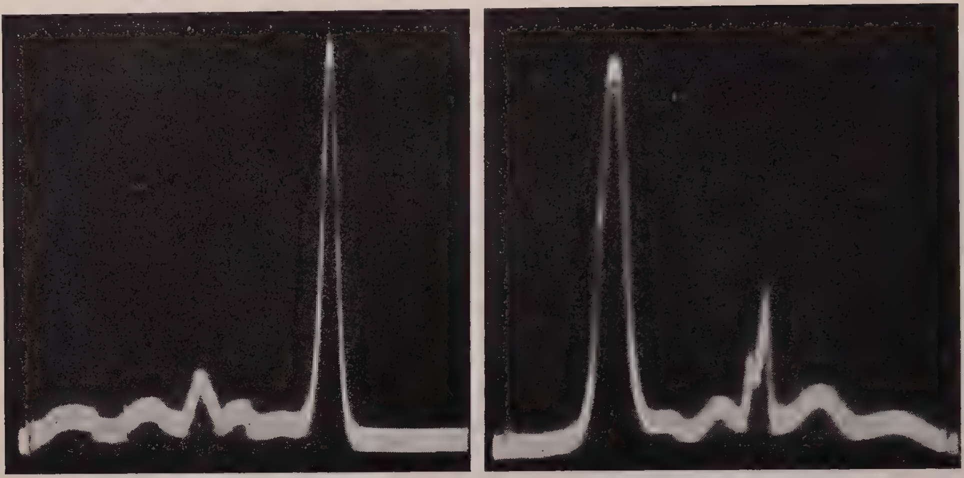

a.

b.

Fig. 7. *Electrophoresis analysis of normal human serum by the moving boundary method.*—The protein solution (2 %) was analyzed in a veronal buffer of the ionic strength 0.2 and pH = 8.6. *a.* Optical pattern of the ascending boundaries after the passage of 450 amp.sec., $\theta = 38\overset{\circ}{.}6$. *b.* Optical pattern of the descending boundaries after the passage of 500 amp.sec., $\theta = 45\overset{\circ}{.}3$.

insures against migration disturbances of various kinds. However, from the moving boundary electrophoresis it is a well-known fact that the protein charges, in a certain medium, influence the electric migration of these substances in approximate proportion to their contributions to the conductivity. When a fractionation is performed in so dilute a medium as a 0.03-C sodium veronal solution, the question arises whether "boundary anomalies" perceptibly contribute to the zone spreading during the transfer.

A moving boundary analysis of the serum fractionated as described in experiment 3 *a* gave the boundary diagrams shown in Fig. 7 *a* and *b*. The protein concentration in this experiment was 2 %, the ionic strength of the veronal buffer 0.2, and pH = 8.6. The non-conformity of the two patterns in Fig. 7 give evidence that the protein velocities changed at the boundaries also in this medium. At this pH the greatest velocity changes are always caused by the albumin ion. In the boundary electrophoresis the ascending, leading boundaries of the globulin zones all migrate within the albumin region, but the descending, rear boundaries lag behind the albumin zone. Hence a considerable conductivity gradient may develop in the U-tube, and the leading boundaries normally migrate faster than the trailing ones; the former are sharpened by the current, but the latter gradually become blurred. In the fractionation field principally similar effects are present, but the conditions are here more favourable because the mutual superposition of all the component zones is a transient state only. In several instances the conductivity of the serum fractions has been measured, but the variations were always slight, although greater in the albumin than the globulin range.

In spite of the fact that the protein distribution is registered by means of different physical properties of the proteins and different types of systems in the fractionation diagram, Fig. 5 *b*, and the moving boundary patterns, Fig. 7 *a* and *b*, a comparison of these records discloses some characteristic effects of the low ionic strength in the fractionation experiment. Contrary to the ordinary moving boundary pattern, a partial resolution of the γ-globulin peak into two has been recorded in every fractionation equivalent to experiment 3 *a*. Between the γ- and β-globulin peaks and within the β-globulin peak the differentiation of the pattern is definitely more pronounced, but the resolution is less good in the α-globulin group. The α-globulin zone is here partially superimposed by the rear albumin boundary. In front of the albumin zone we find the small peak corresponding to a component of still unknown composition (cf. p. 238).[1] The comparison indicates that the resolving action of the great field strength predominates over the charge effect in the region of the slow globulin components, whereas the latter is manifest in the decreased resolution at the rear of the albumin zone and easy separation of the faster trace component from the leading boundary. The conclusion that boundary anomalies contribute to the zone spreading essentially in the albumin range is supported by the experience that the resolution of the α-globulin from the albumin peak is more dependent on the total protein concentration than the differentiation of the slow components in the fractionation diagram. It should be noted that principally similar conditions, viz. the migration disturbances at albumin boundaries were used by HOCH (31, 32) for eliciting the rapid trace components of serum and cerebrospinal fluid in the boundary electrophoresis.

The isolation of these trace components, as described in the experiments 3 *c* and 4, provided some interesting problems. With a reported mobility difference of about 15 %, the separation of these components from the albumin zone should be easily performed. In the course of several fractionations of cerebrospinal fluid concentrates it was observed that decreasing the ionic strength improved the resolution of the front component, but contrary to expectation the leading albumin boundary never became very sharp. No conclusive proof could be derived whether this behaviour indicated some degree of heterogeneity within the albumin zone or had some other cause, nor could it be decided with certainty from the optical density records, whether one or more trace components were normally present in the fractionated material (cf. ref. 21). Only in a few sera, where some degree of denaturation was indicated by the turbidity, was the differentiation of the fast component into two or three peaks clearly established.

Whereas a uniform development of the serum pattern was pursued in the "normal" case of Fig. 5 *b*, the resolution of singular components can often be improved by a certain differentiation of the electric velocities in the flow field; for example, in the serum pattern a greater resolution of the γ-group can be obtained at a sacrifice in the resolution of the fast components. The differentiation of the velocities can generally be achieved by the application of a conductivity or pH gradient. Being based on mobility differentiation by complex formation (cf. ref. 33), the second method is related in principle to those recently applied by MOULD and SYNGE to the fractionation of hydrolysis products of amylose (34, 9) and by CONSDEN and STANIER and others to separations of sugars (35, 36, 37, 38, 39, 40). By similar means the limitation in space of the cuvette can be compensated to some extent. Since a small cuvette and the use of a low current considerably simplifies the management of the apparatus, the cuvette described in this report has been considered to be adequate in the present research. But it is evident that an increase of the electric current employed in the fractionation process offers great advantages with regard to the possibilities of solving new problems and increasing the yield. Therefore, a certain increase of the dimensions of the cell, notably its length, is indicated.

---

[1] In Fig. 5 *b* this peak is hidden by the veronal gradient of the concentrated end zone; see instead Figs. 5 *c* and 6.

The stronger the currents applied, the greater are the demands on control of the working conditions. In order to acertain the stationary state due attention must be given to the ion reactions occurring outside the separation zone. In the present apparatus the zones of concentrated electrolyte solutions present on both sides of the separation zone ensure very constant field conditions (cf. Fig. 9 *a* and *b* in ref. 3), but experience has shown that the equilibrium state is not always reached in a period equal to the time of transfer. In some instances minor fluctuations in the voltage drop, the temperature, and the displacements of the fastest components indicate a slight unsteadiness in the electric field, often prevailing over periods of 5–10 hours. It can be concluded that schematic representations like those of Fig. 2 *a* and 4 *a* generally involve simplifications of the conditions. Further, there is little doubt that the tendency to instability discussed in ref. 3 is to be associated with the changes of the direction and strength of the electric field caused by local variations of the ion content in the cell. The general stability improves when moving salt gradients are excluded as far as possible from the bath and the conductivity gradients across remaining, moving salt boundaries are reduced by the use of sufficiently high salt contents in the end zones of the cell.

These zones of concentrated solutions were originally introduced in order to simplify the ion transport through the membranes. At the current densities used, membranes of natural parchment, parchment paper or cellophane rapidly became destroyed by polarization effects in certain buffer solutions. These effects were especially strong in veronal buffers, but also in a concentrated phosphate buffer the use of a membrane of parchment paper on the anode side gave rise to gas production, a considerable heating, and pH changes. In solutions of the sodium salts of glycine or acetic acid no difficulties were encountered. However, even when the buffer anion of the separation zone does not cause polarization at the membranes a concentrated acetate buffer is generally suitable as the electrode liquid. This buffer substance has the advantages of being relatively cheap, highly soluble and possessing a low anionic mobility.

Summary

In continuous fractionation by crossed electric and hydrodynamic flow fields the substances to be fractionated are injected into the separation column as a mixed zone. During the passage of the electric field the component zones are resolved according to their electrical velocities. In order to maintain the displacements of the component zones constant during a fractionation experiment the process must be conducted under stationary conditions. This paper deals with the chemical composition of the conducting medium and fractionations of protein mixtures in some reported media. The present cuvette is also described.

If a uniform mobility distribution is wanted, a dilute buffer solution of uniform conductivity and an ionic strength of 0.05–0.03 is supplied to the separation field. Between this zone and the electrode compartments end zones of concentrated solutions are inserted in the flow field. The end zones contribute to the constancy of the system by simplifying the ion exchange with the electrode compartments and restricting the migration of foreign ions into the separation zone.

Using the albumin mobility of $-5.1 \cdot 10^{-1}$ cm^2 volt^{-1} sec^{-1} as the reference, a veronal system of the type described has an average resolving power of $0.22 \cdot 10^{-5}$ mobility units per cm at a rate of fractionation of approximately 1 ml of whole serum per hour. Fractionations in this medium of normal and pathological serum and cerebrospinal fluid are reported.

In the present experimental arrangement the rate and resolution are mainly restricted by the size of the cell (length 280 mm, height 300 mm, and thickness 10 mm). Increased resolution within a limited mobility range or concentration of certain components of a mixture can be obtained if the electric velocities are suitably biased by means of a conductivity gradient in the separation field.

I am very much indebted to Professor Arne Tiselius for the laboratory facilities put at my disposal and financial support from the grants to the Institute of Biochemistry (The Rockefeller Foundation, the Wallenberg Foundation, and the Swedish Natural Science Research Council).

Institute of Biochemistry, University of Uppsala, Uppsala.

REFERENCES

1. Svensson, H. and Brattsten, I., *Arkiv Kemi 1* (1949) 401.
2. Brattsten, I., *Arkiv Kemi 4* (1952) 503.
3. Brattsten, I., *Arkiv Kemi 8* (1955) 205.
4. Kunkel, H. G. and Slater, R. J., *Proc. Soc. Exper. Biol. Med. 80* (1952) 42.
5. Tiselius, A., and Flodin, P., *Advances in Protein Chem. 8* (1953) 461.
6. Tiselius, A., *Nova Acta Soc. Scient. Reg. Upsaliensis Ser. IV 7* No. 4 (1930).
7. Svensson, H., *Arkiv Kemi Mineral. Geol. 22 A* No. 10 (1946).
8. Grassmann, W. and Hannig, K., *Z. angew. Chem. 62* (1950) 170.
9. Mould, D. L. and Synge, R. L. M., *Biochem. J. 58* (1954) 585.
10. Bradish, C. J. and Smart, N. V., *Nature 174* (1954) 272.
11. Tiselius, A., *Svensk Kem. Tidskr. 50* (1938) 58.
12. Whetham, W. C. D., *Phil. Trans. Roy. Soc. London 184 A* (1893) 337.
13. Kohlrausch, F., *Ann. Physik Chem. 62* (1897) 209.
14. Kylin, H., *Z. physiol. Chem. 69* (1910) 169.
15. Lemberg, R., *Ann. Chem. 461* (1928) 46.
16. Brattsten, I., Arkiv Kemi *8* (1955) 346.
17. Juhlin-Dannfelt, C., Schnabel, M., and Wiholm, S., *Acta Allergol. 6* (1953) 1.
18. Brattsten, I., Colldahl, H., and Laurell, H., *Acta Allergol.* (1955).
19. Kabat, E. A., Moore, D. H., and Landow, H., *J. Clin. Invest. 21* (1942) 571.
20. Scheid, K. F. and Scheid, L., *Arch. Psychiat. Nervenkrankh. 117* (1944) 219, 641.
21. Aly, F. W., *Biochem. Z. 325* (1954) 505.
22. Bücher, T., Matzelt, D., and Pette D., *Klin. Wochschr. 30* (1952) 325.
23. Seibert, F. B. and Nelson, J. W., *J. Biol. Chem. 143* (1942) 29.
24. Seibert, F. B. and Nelson, J. W., *Am. Rev. Tuberc. 47* (1943) 66.
25. Armstrong, Jr, S. H., Budka, M. J. E., and Morrison, K. C., *J. Am. Chem. Soc. 69* (1947) 416.
26. Ligeti-Hoch, C. and Hoch, H, *Biochem. J. 43* (1948) 556.
27. Hoch, H. and Chanutin, A., *J. Biol. Chem. 200* (1953) 241.
28. Grassman, W. and Hannig, K., *Z. physiol. Chem. 292* (1953) 32.
29. Brattsten, I. and Nilsson, A., *Arkiv Kemi 3* (1951) 337.
30. Longsworth, L. G., *Chem. Revs. 30* (1942) 323.
31. Hoch, H., *Biochem. J. 46* (1950) 199.
32. Hoch, H. and Chanutin, A., *Proc. Soc. Exper. Biol. Med. 81* (1952) 628.
33. Longsworth, L. G. and McInnes, D. A., *J. Gen. Physiol. 25* (1942) 507.

34. Mould, D. L. and Synge, R. L. M., *Biochem. J. 50* (1951) xi.
35. Consden, R. and Stanier, W. M., *Nature 169* (1952) 783.
36. Jaenicke, L., *Naturwiss. 39* (1952) 1.
37. Michl, H., *Monatsh. Chem. 83* (1952) 737.
38. Micheel, F. and Van de Kamp, F.-P., *Angew. Chem. 64* (1952) 607.
39. Foster, A. B., *Chem. and Indust.* (1952) 1050.
40. Gross, D., *Nature 172* (1953) 908.

Tryckt den 25 april 1955

Uppsala 1955. Almqvist & Wiksells Boktryckeri AB

ARKIV FÖR KEMI Band 8 nr 24

Communicated 23 February 1955 by ARNE WESTGREN and GUNNAR HÄGG

The crystal structure of $NH_4Cl \cdot As_2O_3 \cdot \frac{1}{2}H_2O$

By MAJA EDSTRAND and GÖRAN BLOMQVIST

With 7 figures in the text

During the structure determinations of some antimony(III)oxide halogenides performed by one of us [1, 2, 3] it was found that antimony atoms have both a three and a four coordination. In $(NH_4)_2SbCl_5$ [4] we have found a five coordination of antimony and, in this reference, a review of coordination numbers found in different compounds containing trivalent antimony is given. It seemed then of interest to investigate the structures of some trivalent arsenic compounds, which might have some features in common with the antimony oxide halogenides. In GMELIN [5] some arsenic(III)oxide halogenides are described, which appear to be difficult to obtain in crystalline form when they do not contain water. In the volumes of GMELIN dealing with the alkali metals a number of compounds are described which can be written $MeX \cdot nAs_2O_3$, where MeX is an alkali or ammonium halogenide, and which also crystallize and apparently have hexagonal symmetry. These compounds seemed thus to be well suited for an X-ray structure determination. Hoping that the simplest formula would mean the simplest structure we started our investigation with the compounds with $n = 1$. (More than a year after these investigations were started we obtained a private communication from Professor A. E. VAN ARKEL of Leiden that he is working on the crystal structure of $KCl \cdot 2As_2O_3$.)

The question is now if arsenic is bonded only to the oxygen atoms with three bonds in the form of a trigonal pyramid as in the oxides As_2O_3 [6, 8, 9, 10] or if there are any additional bonds to the chlorine atoms. In the halogenides of trivalent arsenic there is the same three coordination (at least in the gas phase), see e.g. GMELIN [7].

Preparation and analysis

Compounds of the type $MeX \cdot nAs_2O_3$ with $n = 1$ and 2 have been prepared by RÜDORFF [11], who also discusses some results obtained by earlier investigators. He reports that it at first seemed as if some of these compounds contained water of constitution, but that the water content seemed to vary in different preparations, a fact which he explained as due to enclosure of mother liquor in the crystals. The compound $NH_4Cl \cdot As_2O_3$ has been prepared by RÜDORFF [11] and by BRAND and ROSENKRANZ [12] in the form of crystal crusts or crystalline precipitates, which seem to be free from water of constitution. SCHREINEMAKERS and DE BAAT [13] has obtained it as a phase in the ternary system $NH_4Cl—As_2O_3—H_2O$. We have repeated these previous methods, but the crystals were not of sufficient size for single crystal photographs. We therefore made some modifications of these methods specially by introducing hydrothermal methods and have made experiments at several temperatures and varied the conditions but we give here only the results of interest in this case. (1) 1 g As_2O_3 was dissolved in 20 ml 10 % NH_3 solution. Into a few ml of the resulting solution, varying amounts of 25 % HCl solution were poured, taking care that there was a surplus of acid. The solution was then sealed in a Pyrex tube and kept in an oven at about 120° C for 24 h. Of duplicate samples one was taken out to cool quickly in the air, while the other was allowed to cool slowly in the oven. It seems as though the crystallization takes part during cooling, and accordingly we obtained the best crystals on slow cooling. The crystals were sucked free from mother liquor, dried first between filter papers and then in a vacuum desiccator above sulfuric acid. (2) As_2O_3 and an equal amount by weight or more of NH_4Cl and some water were sealed in a Pyrex tube and treated in the same way as in method (1).

By the methods mentioned we obtained crystals which gave powder photographs which were very similar but not quite identical. We found from single crystal photographs that the crystals as a rule had superstructures which seemed to be a little different for different preparations although they apparently are based on the same principle. In one case we obtained crystals without superstructure in the form of hexagonal plates. They were prepared by method (1) by taking 1.5 ml of the solution of As_2O_3 in ammonia and 2.5 ml 25 % HCl, which, however, gave us only very small amounts of substance. Later on we tried to repeat this synthesis to obtain more substance for analysis. We did not succeed in this as we always obtained crystals with superstructure. It seemed, however, probable that a structure found for the crystals without superstructure, would be a building element in the superstructures. We shall try to solve this problem later on.

We made some analyses of the substances with superstructure, as it is likely that they have at least approximately the same proportions of As_2O_3 and NH_4Cl as the investigated crystals. The substance was first dissolved in a dilute solution of sodium hydroxide. For the arsenic determination the solution was acidified with hydrochloric acid and titrated with potassium bromate with naphthol blue-black as indicator [14]. For the determination of chlorine the solution was acidified with nitric acid and titrated by the Volhard method in the presence of nitrobenzene.

	Ammonium	Chlorine	Arsenic	Water
	%	%	%	%
Calc. for $NH_4Cl \cdot As_2O_3 \cdot \frac{1}{2}H_2O$	6.93	13.62	57.55	3.46
Calc. for $NH_4Cl \cdot As_2O_3$	7.18	14.11	59.61	
Found		13.89, 14.24, 13.95	56.70, 57.45, 57.7	

These values show that the superstructure substances contain NH_4Cl and As_2O_3 in the proportions 1:1, but they do not clearly indicate anything about the water content. As a water determination would require a large amount of substance, we could not perform it.

Unit cell and space group

Single crystals were selected and rotation and Weissenberg photographs were taken with Cu-radiation. We had the following series of Weissenberg photographs (double films): *hki*0, *hki*1, *hki*2, *hki*3, *hki*4, *h*0*il*, *h*1*il*, and *h*2*il*. Relative intensities of the reflections were estimated visually by comparison with an intensity scale obtained by exposing an interval of a zero layer line, containing a strong reflection, with different exposure times on a pack of four double films. They were then corrected for the Lorentz and polarization factors using the curves given by Kaan and Cole [15].

Table 1. Powder photograph of $NH_4Cl \cdot As_2O_3 \cdot \frac{1}{2}H_2O$. Cr$K\alpha$-radiation $\lambda = 2.2909$ Å. The horizontal line marks the boundary between the angular ranges of two different focusing cameras. Reflections coinciding with β-reflections are given in brackets. Notations: st = strong, m = medium, w = weak, v = very.

h k i l	$10^4 \sin^2\theta$ calc	$10^4 \sin^2\theta$ obs	*I* calc	*I* obs
$10\bar{1}2$	0962	0954	87	s−
0004	1322	1316	16	m
$10\bar{1}3$	1375	1373	461	vs
$11\bar{2}0$	1895	1895	553	s+
$10\bar{1}4$	1954	1954	39	w
$11\bar{2}1$	1977		0	
0005	2066	2071	37	s
$11\bar{2}2$	2225	2231	523	s+
$20\bar{2}0$	2535	2539	1	vw
$20\bar{2}1$	2618		4	
$11\bar{2}3$	2648	2646	94	vw
$10\bar{1}5$	2708	2712	156	vs
$20\bar{2}3$	2867	2867	53	m
0006	2987	2992	10	m
$11\bar{2}4$	3229	3230	312	s+
$20\bar{2}3$	3282	(3292)	87	(m)
$10\bar{1}6$	3621	3622	35	m
$20\bar{2}4$	3863	3863	212	m-
$11\bar{2}5$	3976	3978	324	s+
0007	4066	4063	52	s
$12\bar{3}0$	4436	4436	69	w
$12\bar{3}1$	4519	4520	35	w
$20\bar{2}5$	4610	4612	232	s
$10\bar{1}7$	4700	4700	108	s
$12\bar{3}2$	4768	4769	106	w
$11\bar{2}6$	4889		15	
$12\bar{3}3$	5183	5181	465	m+
0008	5311		2	
$20\bar{2}6$	5522	5519	63	vw
$30\bar{3}0$	5704	5703	356	m+
$12\bar{3}4$	5764		47	
$30\bar{3}1$	5787		2	
$10\bar{1}8$	5944		3	
$11\bar{2}7$	5967	5963	523	s
$30\bar{3}2$	6036	6031	350	m−
$30\bar{3}3$	6451	6436	63	vw
$12\bar{3}5$	6511	6505	231	w
$20\bar{2}7$	6601	6591	265	w+
0009	6721	6721	77	w

The crystals proved to be hexagonal with the c-axis perpendicular to the plane of the crystal plates. The cell dimensions were more accurately determined from powder photographs, cf. Table 1, as

$$a = 5.25_4 \text{ Å}, \quad c = 12.57_4 \text{ Å}, \quad V = 300.6_0 \text{ Å}^3$$

with an accuracy of about 0.2 %.

If 2 formula units are assumed per unit cell, the density would be $d_{\text{calc}} = 2.88$,

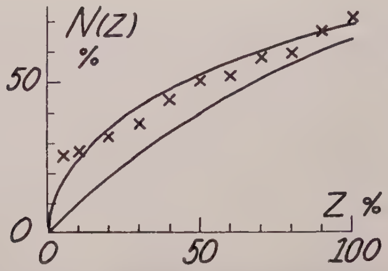

Fig. 1. Intensity statistics for $h0\bar{h}l$. x represents the experimental intensity distribution compared with the theoretical centric distribution (upper curve) and the theoretical acentric distribution (lower curve).

we found $d_{\text{obs}} = 2.73$, 2.73 for crystals with superstructure. (The density of the crystals was determined from the loss of weight in benzene.)

In the photographs there are no reflections, which are systematically absent. This is characteristic of the space group No. 177, $P622 - D_6^1$ [16]. We applied the method of intensity statistics [17, 18] to the $h0\bar{h}l$ zone to ascertain that the atoms (at least the heavy ones) are situated in a way which gives a symmetry centre to this projection (see Fig. 1), which the intensity distribution also seems to indicate. This makes it unnecessary to consider some of the lower space groups. (See also the recent paper by HARGREAVES: Some observations on the probability distribution of X-ray intensities [28].)

Patterson syntheses

In order to find the arsenic positions we calculated the Patterson projections $P(UVp)$, see Fig. 2, and $P(UpW)$, see Fig. 3. Considering the space group $P622$ the four arsenic atoms can be situated either in the fourfold position $4(h)$ or in a combination of a threefold and a onefold position, a combination of two twofold positions or a combination of a twofold position and two onefold positions. As can be seen from the figures, high maxima are only found at u or $v = 0, \frac{1}{3}, \frac{2}{3}, 1, \ldots$. This fact indicates that the four arsenic atoms cannot be situated in a combination of one- and threefold positions, as this requires vectors at u or $v = \frac{1}{2}$. It also excludes the combination $2(e) + 1(a) + 1(b)$, which only gives vectors at $u = v = 0$. The combinations $2(c) + 2(d)$, $2(c) + 1(a) + 1(b)$, and $2(d) + 1(a) + 1(b)$ give vectors with $w = \frac{1}{2}$, where no maximum has its centre in $P(UpW)$, and thus these combinations can be excluded. The remaining possibilities give the following vectors in the Patterson space $P(UVW)$:

I	within	$2(c)$ and $2(d)$ of weight 1		$\pm(\frac{1}{3}, \frac{2}{3}, 0)$
II	within	$2(e)$ of weight 1		$\pm(0, 0, 2z)$
III	between	$2(e)$ and $2(c)$ of weight 2		$\pm(\frac{1}{3}, \frac{2}{3}, \pm z)$
IV	between	$2(e)$ and $2(d)$ of weight 2		$\pm(\frac{1}{3}, \frac{2}{3}, \frac{1}{2} \pm z)$
V	within	$4(h)$ of weight 1	A	$\pm(\frac{1}{3}, \frac{2}{3}, \pm 2z)$
		of weight 2	B	$\pm(\frac{1}{3}, \frac{2}{3}, 0)$
			C	$\pm(0, 0, 2z)$

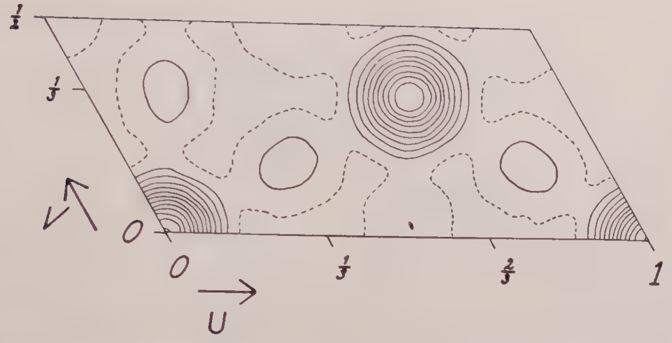

Fig. 2. $P(UVp)$. Contours at an interval of 100 arbitrary units. Negative values dotted.

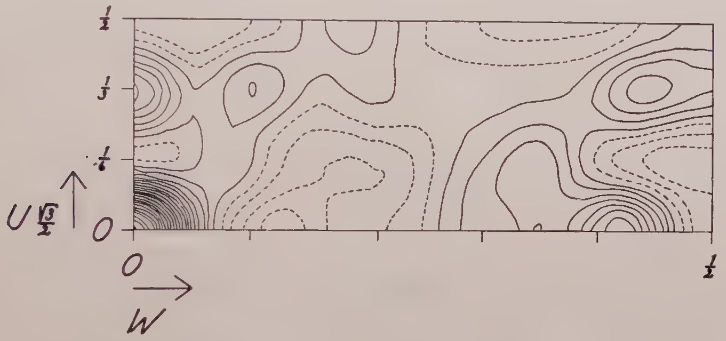

Fig. 3. $P(UpW)$. Contours at an interval of 50 arbitrary units. Negative values dotted.

To decide between these possibilities we use $P(UpW)$. The combinations $2(e)+2(c)$ and $2(e)+2(d)$ require that maxima of the type (uw) corresponding to the vectors III and IV have double the height of the maxima of the type $(u0)$ and $(0w)$ corresponding to the vectors I and II. Since the observed heights are contrary to this and the observed w-values of the peaks, which would correspond to the vectors II, III, and IV, are not in favour of these combinations, it is reasonable to exclude them.

We then have to consider only the position $4(h)$ and the corresponding vectors of group V, and find that the observed heights of the maxima are in good agreement with the weights of the vectors A, B, and C. The maximum at $u=0$ in $P(UpW)$ gives $w=2z=0.418$, 0.582 .... which gives $z=0.209$ or 0.291. As these two z-values only mean a translation of $\frac{1}{2}$ along the z-axis we chose $z=0.209$.

In order to locate the light atoms we tried the "Vector Convergence Method" [20], which had been successful in the case of $(NH_4)_2SbCl_5$ [4]. Starting with arsenic in $4(h)$ we obtained the xy-projection given in Fig. 4. There are indications of light atoms at x and $y=0$ and $\frac{1}{2}$. It seems probable that this corresponds to six oxygen atoms situated either in $6(i)$ or in $3(f)+3(g)$, specially as the length of the a-axis is approximately four times the radius of the oxygen ion, where $6(i)$ seems more probable than the other possibility. The xz-vector convergence diagram did not give an unambiguous indication of the positions of the light atoms. Therefore we found it better to use Fourier projections in this case.

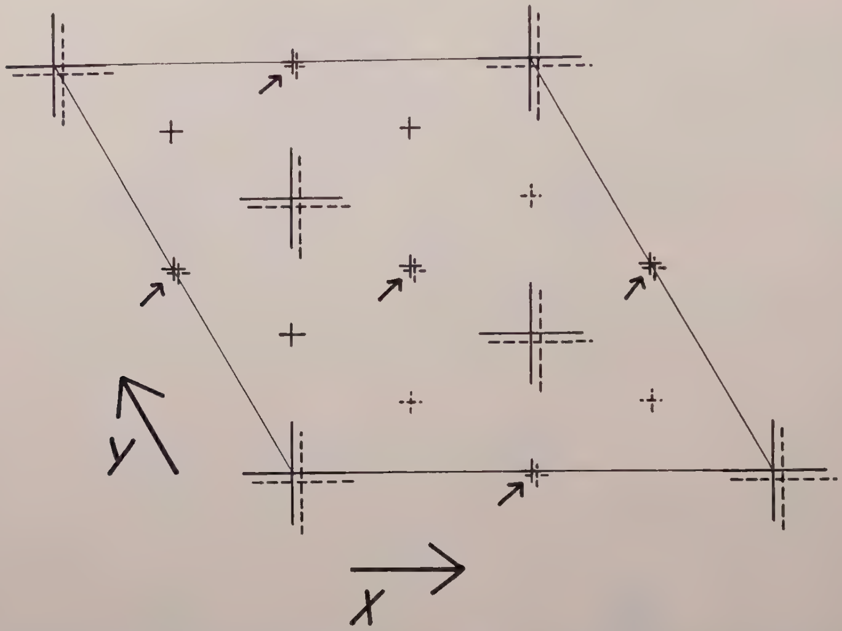

Fig. 4. The *xy*-vector convergence diagram. The crosses mark the centres of the Patterson peaks and their sizes indicate the height of the peaks. One set of Patterson maxima is marked with full lines and the other with dotted lines. The small arrows point at the finally accepted oxygen positions.

The ρ (*XpZ*)-projection

The Fourier syntheses have been calculated with $|F_{\text{obs}}| = \sqrt{\frac{I}{Lp}}$ where F is the structure factor, I is the estimated intensity, Lp are the combined Lorentz and polarization factors. In all syntheses the value of $F(000)$ has been omitted. Correction for absorption has not been applied. The maxima have been located by the interpolation table given by BOOTH [21].

For the first projection we determined the signs of the highest F-values entirely by assuming four arsenics in $4(h)$ $\frac{1}{3},\frac{2}{3},z$ with $z = 0.209$. We then found indications of six oxygens in $6(i)$ $\frac{1}{2},0,z$ with a z-parameter, which gave an arsenic surrounded by three oxygens at quite reasonable distances. There was also an indication of two chlorines in $2(e)$ $0,0,z$. At this stage we thought that the substance had the formula $NH_4Cl \cdot As_2O_3$ and thus we had to find the positions of two ammonium ions. Successive refinements gave some low maxima corresponding to the positions $2(d)$, $1(a)$, and $1(b)$. As an ammonium ion situated in $1(b)$ $0,0,\frac{1}{2}$ would give a distance NH_4^+–Cl^- of about 2.2 Å, which appears very short compared with the sum of the ionic radii of 3.24 kX [22], it did not seem very probable that two ammonium ions would be situated in $1(a) + 1(b)$. Thus we assumed that they are situated in $2(d)$ $\frac{1}{3},\frac{2}{3},\frac{1}{2}$, which gives reasonable NH_4^+–Cl^- distances although longer than the sum of the ionic radii.

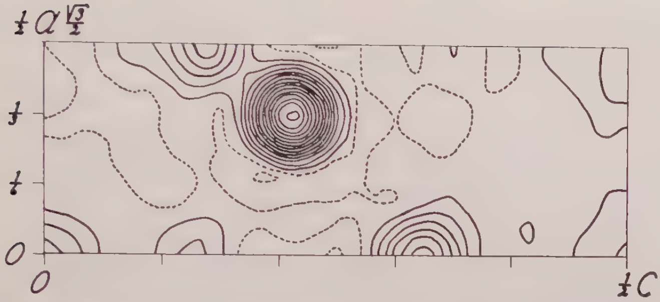

Fig. 5. ϱ (XpZ). Contours at an interval of 100 arbitrary units. Negative values dotted.

The final $\varrho(XpZ)$-projection is given in Fig. 5. There is still a low peak at the origin. The distance from the origin to the surrounding oxygen atoms is about 3.1 Å. This means that there is room for an atom at 0,0,0, or rather a molecule for the reason of electro-neutrality. As has been mentioned previously (p. 245), some compounds of the type $MeX \cdot nAs_2O_3$ have been reported to enclose mother liquor in the crystals, and that careful drying is necessary to remove all the water. This seems to suggest that, if the peak at the origin is a real maximum and not a false detail, it would correspond to a water molecule. We then arrived at the following set of parameters (for oxygen in 6(i) we obtain the projection of one atom at $x=0$ in $\varrho(XpZ)$ and of two atoms at $x=\frac{1}{2}$, and give therefore z as the weighted average):

		x	y	z
4 As	in 4(h)	$\frac{1}{3}$	$\frac{2}{3}$	0.211_9
6 O	in 6(i)	$\frac{1}{2}$	0	$\frac{1}{3}(0.126+2\cdot 0.137)=0.13_3$
2 Cl	in 2(e)	0	0	0.323
2 NH_4^+	in 2(d)	$\frac{1}{3}$	$\frac{2}{3}$	$\frac{1}{2}$
1 H_2O?	in 1(a)	0	0	0

It is a little difficult to state the accuracy of the parameters and the distances. However, the difference between the two oxygen z-parameters is 0.011, which is equivalent to 0.14 Å. Since the x- and y-parameters do not have variable values it is perhaps reasonable to assume that the As–O distances are accurate at least to within ± 0.15 Å, and that the accuracy of the As–Cl distances is a little better. The Cl–O distances can be expected to be the least accurate.

When calculating the F-values we found that they were considerably improved if we applied a temperature factor. We then assumed that the temperature factor B is the same for all atoms and for all directions within a Weissenberg photograph, and obtained the value of B by plotting $\log \frac{F_o}{F_c}$ against $\sin^2\theta$ omitting the weakest reflections. We found for $hki0$ $B=0.97\cdot 10^{-16}$ and for $h0\bar{h}l$ $B=3\cdot 10^{-16}$. The F-values were then calculated as

$$F_{\text{calc}} = \text{const}\; e^{-B\left(\frac{\sin\theta}{\lambda}\right)^2} [f_{As} A_{As} + f_{Cl} A_{Cl} + f_O (A_O + A_{H_2O}) + f_N A_{NH_4^+}]$$

where f_{As}, f_{Cl}, f_O, and f_N are the atomic scattering factors for arsenic, chlorine, oxygen, and nitrogen with due consideration being taken to their variation with θ [22].

Table 2. Observed and calculated F-values of $hki0$ for a Weissenberg photograph of $NH_4Cl \cdot As_2O_3 \cdot \frac{1}{2}H_2O$. Cu$K\alpha$-radiation.

$hki0$	F_c	F_o	$hki0$	F_c	F_o
$10\bar{1}0$	−42	46	$40\bar{4}0$	−1	
$11\bar{2}0$	123	128	$32\bar{5}0$	−17	15
$20\bar{2}0$	5	30	$41\bar{5}0$	61	63
$21\bar{3}0$	−29	36	$50\bar{5}0$	−15	12
$30\bar{3}0$	89	89	$33\bar{6}0$	53	50
$22\bar{4}0$	104	96	$42\bar{6}0$	−3	
$31\bar{4}0$	−20	27	$51\bar{6}0$	−13	13

Table 3. Calculated and observed F-values of $h0\bar{h}l$ for a Weissenberg photograph of $NH_4Cl \cdot As_2O_3 \cdot \frac{1}{2}H_2O$. Cu$K\alpha$-radiation.

l	$000l$		$10\bar{1}l$		$20\bar{2}l$		$30\bar{3}l$		$40\bar{4}l$		$50\bar{5}l$	
	F_c	F_o	F_c	F_o	F_c	F_o	F_c	F_o	F_c	F_o	F_c	F_o
0			−75	65	6	40	131	131	−1		−14	19
1			−41	46	12		7	18	0		−8	12
2	−196	111	60	70	42	63	−90	103	19	31	13	19
3	−147	133	135	146	53	45	−37	46	28	30	26	28
4	61	59	−38	35	−79	71	66	69	−34	37	−11	
5	90	92	−73	68	−80	100	63	85	−39	46	−20	23
6	44	50	33	32	40	52	11		20	17	9	15
7	−96	100	54	51	76	62	−77	74	35	36	14	15
8	−17	21	−8		18	19	−31	31	7			
9	100	111	−17	18	−7	14	54	58	−4			
10	58	66	−23	19	−29	26	44	55	−16	10		
11	−66	69	12		−7		−28	23				
12	−50	60	40	37	23	28	−24	28				
13	3		6									
14	40	52	−29	24								
15	25	22										
16	−13	11										

The values of the reliability factor $R = \frac{\sum \| F_o | - | F_c \|}{\sum | F_o |}$ are (only with observed reflections) (a) without H_2O for $hki0$ $R = 0.11$ and for $h0\bar{h}l$ $R = 0.20$, and (b) with H_2O for $hki0$ $R = 0.11$ and for $h0\bar{h}l$ $R = 0.16$ which is better than (a). Thus it seems justified to assume the existence of a water molecule in the position $1(a)$, which has been included in the ultimately calculated F-values. The calculated and observed F-values are given in Tables 2 (for $hki0$) and 3 (for $h0\bar{h}l$).

For the powder photographs the intensities have been calculated as $I_{\text{calc}} = pF^2_{\text{calc}}$ without the temperature factor being taken into account and with $p =$ number of cooperating planes, cf. Table 1. As can be expected for crystal plates the intensities are influenced by orientation effects.

From the tables and the R-values it is clear that the agreement between calculated and observed F-values and intensities is satisfactory except for the reflection $20\bar{2}0$ which is clearly observed although the calculated value is very low. The calculated

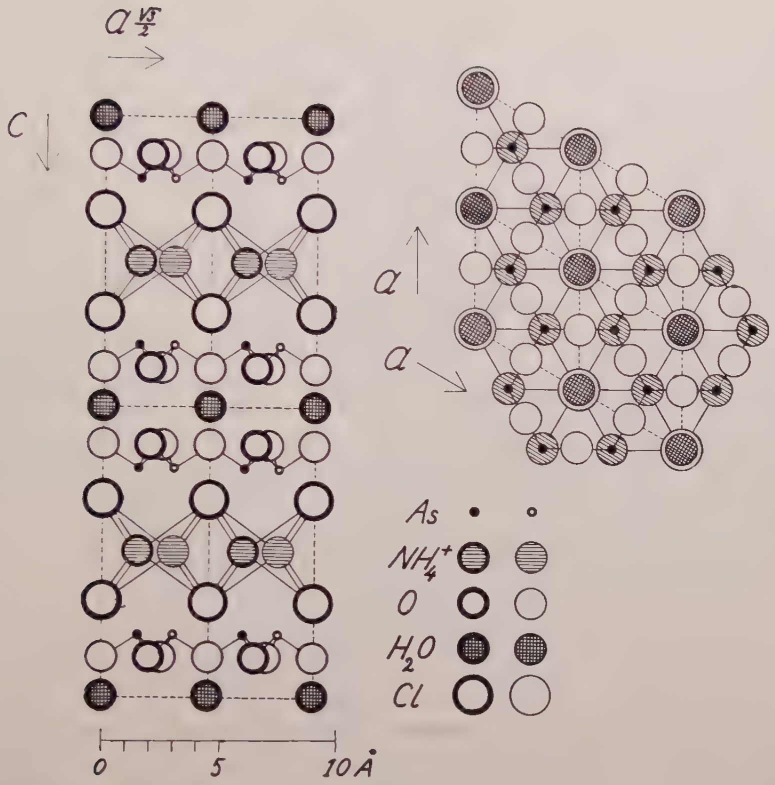

Fig. 6. Orthogonal projections of the structure of $NH_4Cl \cdot As_2O_3 \cdot \frac{1}{2} H_2O$. Both projections show at least four adjacent unit cells. Superimposed oxygen atoms are symmetrically displaced in the *ac*-projection.

$F(20\bar{2}0)$ cannot be altered by variation of the x- and y-parameters as these have fixed values with the assumed atomic positions. Since the agreement otherwise is good it seems probable that the structure is essentially right and that it is not necessary to consider a lower space group. However, we do not know very much about the real values of the atomic scattering factors in this compound and we have not taken the hydrogen atoms into account. There are As_2O_3 sheets in the structure (cf. below), quite likely with directed covalent bonds in the sheet. This might cause a deformation of the outer electron shell of these atoms, a fact which also would influence the atomic scattering factors. Such deformations are assumed to exist for the carbon atom in diamond, where the "forbidden" reflection 222 has been observed, see for instance discussions in The Crystalline State, Vol. I [23], II [24], and III [19]. In a layer structure the thermal motions of the atoms certainly are anisotropic, which might influence the intensities in different ways.

Discussion of the structure

Projections of the structure of $NH_4Cl \cdot As_2O_3 \cdot \frac{1}{2}H_2O$ are given in Figs. 6 and 7. They are orthogonally projected along the a- and c-axis. In all projections four adjacent unit cells are given so that the building principle of the structure will be

Table 4. Interatomic distances in $NH_4Cl \cdot As_2O_3 \cdot \frac{1}{2}H_2O$. – Å units.

As – 3 O (O – 2 As)	1.8_1
As – 3 Cl (Cl – 6 As)	3.3_4
As – NH_4	3.6_2
As – 3 As (NH_4^+ – 3 NH_4^+) . .	3.03
NH_4^+ – 6 Cl (Cl – 6 NH_4^+) . .	3.7_6
Cl – 6 O (O – 2 Cl).	3.5_5
Cl – Cl.	4.4_5
O – 4 O (in a sheet)	2.63
O – O (between two sheets). .	3.3_4
H_2O – 12 O (O – 2 H_2O) . . .	3.1_1

more obvious. The interatomic distances are given in Table 4 and the accuracy of the distances discussed on p. 251.

It is clear from Fig. 6 that we have a layer structure, which is in good agreement with the shape of the crystals, which form plates with the *c*-axis perpendicular to the plate. In the structure there are endless sheets of As_2O_3 (see Fig. 7). Arsenic is in close contact with three oxygen atoms with the distances As–O = 1.8_1 Å and with all arsenic atoms on one side of the oxygen sheet. The As–O distances are in good agreement with those reported from the oxides in the cubic As_2O_3 [8] 1.80 ± 0.05 kX and in the monoclinic modification Claudetite [9, 10] about 1.80 Å. In our structure the angles O–As–O are 93° and the angles As–O–As are 114°. The As–Cl distance is 3.3_4 Å, which is too long to indicate a covalent bond, since the As–Cl distance found by microwave methods in $AsCl_3$ is 2.161 ± 0.004 Å [25]. (The chloride ions are, however, in better contact with the oxygen atoms of the As_2O_3 sheet.) The observed three coordination of arsenic can be explained both with and without the assumption of a stereochemically active unshared electron pair [26]. If we in this case assume an unshared electron pair, then an ammonium ion is situated in its direction with a distance As–NH_4^+ of 3.6_2 Å.

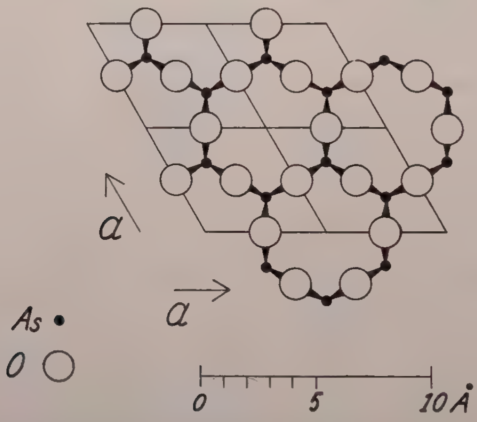

Fig. 7. Projection of an As_2O_3 sheet. The lines mark the boundaries of four unit cells.

The ammonium ions are surrounded by six chloride ions at the corners of a trigonal prism at the distances 3.7_6 Å, which is longer than the sum of the ionic radii

3.24 kX [22]. Thus there are layers of ammonium chloride in the structure. The chloride ions are surrounded by six ammonium ions on one side and by six arsenic atoms at long distances on the other side.

The As_2O_3 sheets are situated in pairs with the oxygen atoms turned towards each other. An oxygen atom in one layer is in contact with only one oxygen atom in the other layer at a distance of 3.3_4 Å. As can be seen in Fig. 7 there are large holes in the As_2O_3 sheet, which give a large hole in the structure at the origin. We have assumed a water molecule in this hole, by reasons mentioned above (p. 245, 251, and 252), and it would be surrounded by twelve oxygen atoms at a distance of 3.1_1 Å. Perhaps a water molecule in this position would tend to make the contacts between the two As_2O_3 sheets more stable.

It is obvious that most of the interatomic distances except those in the As_2O_3 sheet are longer than the sum of radii. Such features are, however, known for other layer structures as for instance the bismuth(III)oxide halogenides investigated by SILLÉN [27].

Summary

$NH_4Cl \cdot As_2O_3 \cdot \frac{1}{2} H_2O$ has been investigated by X-ray methods. It is hexagonal with $a = 5.25_4$ Å, $c = 12.57_4$ Å, $V = 300.6_0$ Å^3, $Z = 2$, and space group No. 177, $P622$–D_6^1. The atomic positions have been found from Patterson and electron density projections. The atomic coordinates are given on p. 251 and the interatomic distances in Table 4. Evidence of the water content has been found from the X-ray data, since there was not sufficient substance without superstructure available for a chemical analysis.

The structure is represented in Figs. 6 and 7. It seems to form a new structure type. The atoms are situated in sheets perpendicular to the c-axis. It contains an uncharged layer of As_2O_3 with all arsenic atoms on one side of the oxygen sheet. Arsenic has three coordination. The As_2O_3 layers are situated in pairs with the oxygens turned towards each other. Water is perhaps situated in holes in this double layer. Between these double layers there are layers of NH_4Cl.

The authors wish to thank Professor A. ÖLANDER for his encouraging interest and for valuable discussions. The investigation has been financially supported by *Statens Naturvetenskapliga Forskningsråd* (Swedish Natural Science Research Council).

University of Stockholm, Institute of Inorganic and Physical Chemistry, February, 1955.

REFERENCES

1. EDSTRAND, M., Acta Chem. Scand. *1* (1947) 178.
2. EDSTRAND, M., Arkiv Kemi *6* (1953) 89.
3. EDSTRAND, M., 3 a Arkiv Kemi *8* (1955) 257.
   3 b Arkiv Kemi *8* (1955) 279.
4. EDSTRAND, M., INGE, M., and INGRI, N., Acta Chem. Scand. *9* (1955) 122.
5. Gmelins Handbuch der anorganischen Chemie, 8th Ed., No. 17, Arsen, Weinheim 1952, p. 392, 403, and 414.
6. Ibid. p. 255–56.
7. Ibid. p. 361–62, 369–70, 393–94, and 407–08.
8. ALMIN, K. E. and WESTGREN, A., Arkiv Kemi, Mineral. Geol. *15 B* (1942) N:o 22.
9. BECKER, K. A., PLIETH, K., and STRANSKI, N., Z. anorg. u. allgem. Chem. *266* (1951) 293 and *269* (1952) 92.
10. FRUEH JR., A. J., Am. Mineralogist *36* (1951) 833.

11. Rüdorff, Fr., Ber. deut. chem. Ges. *19* (1886) 2668.
12. Brand, K. and Rosenkranz, E., Pharm. Zentralhalle *78* (1937) 685.
13. Schreinemakers, F. A. H. and de Baat, W. C., Verslag Gewone Vergader. Wis- en Natuurk. Afdeel. *24* (1915) 130.
14. Smith, G. F. and May, R. L., Ind. Eng. Chem. Anal. Ed. *13* (1941) 460.
15. Kaan, G. and Cole, W. F., Acta Cryst. *2* (1949) 42.
16. International Tables for X-Ray Crystallography, Vol. I, Birmingham 1952.
17. Howells, E. R., Phillips, D. C., and Rogers, D., Acta Cryst. *3* (1950) 210.
18. Lipson, H. and Cochran, W., The Determination of Crystal Structures, London 1953, p. 35–41.
19. Ibid., p. 306.
20. Beevers, C. A. and Robertson, J. H., Acta Cryst. *3* (1950) 164.
21. Booth, A. D., Fourier Technique in X-Ray Organic Structure Analysis, Cambridge 1948, p. 64.
22. Internationale Tabellen zur Bestimmung von Kristallstrukturen, Vol. II, Berlin 1935.
23. Bragg, W. L., The Crystalline State, Vol. I, A General Survey, London 1939, p. 55.
24. James, R. W., The Optical Principles of the Diffraction of X-Rays, London 1948, p. 321–22.
25. Kisliuk, P. and Townes, C. H., J. Chem. Phys. *18* (1950) 1109.
26. Pauling, L., The Nature of the Chemical Bond, 2nd Ed. Ithaca, New York 1944, p. 76–80, 110.
27. Sillén, L. G., X-Ray Studies on Oxides and Oxyhalides of Trivalent Bismuth. (Diss.) Stockholm 1940, p. 73–74.
28. Hargreaves, A., Acta Cryst. *8* (1955) 12.

Tryckt den 25 april 1955

Uppsala 1955. Almqvist & Wiksells Boktryckeri AB

ARKIV FÖR KEMI Band 8 nr 25

Communicated 9 March 1955 by Arne Westgren and Gunnar Hägg

On the structures of antimony (III) oxide halogenides. III

The crystal structure of $[Sb_8O_8(OH)_4]\,[(OH)_{2-x}(H_2O)_{1+x}]Cl_{2+x}$

By Maja Edstrand

With 13 figures in the text

In the first paper in this series concerning $Sb_4O_5Cl_2$ (ref. *1*), it was mentioned that on further hydrolysis of $SbCl_3$ crystal needles are formed, which according to Lea and Wood (*4*) are metastable with the formula, $Sb_4O_3(OH)_5Cl$. The author (*1*) mentioned that the preliminary results in the present investigation were not in accordance with this formula. This paper will give the results for the substance in question.

Preparation

Cooke (*5*) has described a product with the formula $Sb_8O_{11}Cl_2$, which he obtained in the form of small needles, when precipitated antimony oxide chloride, under a very large volume of water containing a small amount of tartaric acid, was exposed to sunlight during a summer. The crystals are described as rhombic prisms, probably monoclinic. Apparently only chlorine analyses have been performed. They might be identical with $[Sb_8O_8(OH)_4]\,[(OH)_{2-x}(H_2O)_{1+x}]Cl_{2+x}$ since their chlorine content falls within the range of the observed values for this substance, and the preparations have been performed in a similar way, or with another substance, which also has needle-shaped crystals and has the idealized formula $Sb_8O_{10}(OH)_2Cl_2$, of which an account will be given in the next paper in this series (*3*).

Lea and Wood (*4*) prepared the compound by diluting a solution of antimony(III)oxide in hydrochloric acid with water so as to bring the final chlorine concentration slightly below decinormal. The precipitate, at first apparently amorphous, was, after standing for several days, gradually transformed into needle-shaped crystals. They report that the analyses of the crystals from different preparations showed considerable variation with regard both to the antimony and chlorine present. This they explained as due to impurities in the preparations as could be verified from a careful microscopical examination. They thought it identical with Cooke's oxide chloride, but ascribed to it the formula $Sb_4O_3(OH)_5Cl = Sb_8O_{11}Cl_2 \cdot 5H_2O$. They considered it metastable.

Bloom and Buerger (*6*) might have prepared this compound during the investigation of the polymorphous forms of Sb_2O_3, when they found that the orthorhombic high temperature form was obtained by hydrolysis of $SbCl_3$ at room temperature. As far as the author is aware they have not published any results in connection with this compound.

Present investigation

For brevity $[Sb_8O_8(OH)_4][(OH)_{2-x}(H_2O)_{1+x}]Cl_{2+x}$ will be called the γ-phase. The preparations seemed to be somewhat influenced by chance, which would be in agreement with LEA and WOOD's (*4*) statement that this phase is metastable. In one series of experiments (1), solid $SbCl_3$ was mixed with various amounts of water and precipitation immediately occurred. The precipitate then crystallized after some time. In the other series (2), a fairly concentrated solution of $SbCl_3$ in hydrochloric acid was prepared in a volumetric flask. From this solution portions were pipetted, which were diluted with various amounts of water. It was supposed that the precipitate, initially formed, would be a little more homogenous in method (2) than in method (1).

In method (1) the γ-phase was obtained in the range where $SbCl_3$ and H_2O were mixed in the weight proportions 1:50 to 1:100. The crystallization was fairly rapid. After 15 days or less at room temperature, the crystals were filtered off, washed with ethanol and ether and dried. When mixtures in the proportions 1:60 and 1:80 were rotated in a water bath at 15°C for 6 days, the crystalline precipitate consisted of $Sb_4O_5Cl_2$, a fact which is in good accordance with the assumption that the γ-phase is metastable. When NaCl was added to the dilutions 1:100, $Sb_4O_5Cl_2$ was formed.

Method (2). 58.4 g $SbCl_3$ was dissolved in 60 ml concentrated HCl solution and diluted to 200 ml without any formation of a precipitate. Into 10 ml of this solution, various amounts of water in the range from 210 to 1000 ml were poured. In some experiments the crystallization took place in a thermostat at 15.5°C and in others in an open window in the sunshine during summer time (an influence from COOKE's (*5*) experiments). After 1 to 3 days the crystallization seemed to be complete. Even if the γ-phase could be obtained in the whole range, the crystals were sometimes contaminated with $Sb_4O_5Cl_2$ specially for the lower dilutions. There does not seem to be any evidence that sunlight is of any importance.

It has not yet been possible to obtain a bromide or iodide isomorphous with the γ-phase.

Analyses and discussion of the formula

For the determination of antimony the substance was dissolved in hydrochloric acid and titrated with potassium bromate. In some cases the titration was carried out at about 60°C with methyl red as indicator (*7*) and in others potentiometrically at room temperature (*8*).

For the determination of chloride the substance was decomposed by boiling with a concentrated sodium carbonate solution in a platinum dish. The filtrate was acidified with nitric acid and the chloride was precipitated as AgCl. The determination was in some cases made gravimetrically and in others as a potentiometric titration (*9*).

The total amount of water was determined according to HARTWIG-BENDIG's modification of the PENFIELD method by mixing the sample with $PbCrO_4$ (*10*).

The density of the crystals was determined from the loss of weight in benzene.

The results are given in Table 1. It is quite obvious that there is a variation in the chloride content, which follows the dilution. There is no clear variation in the antimony and water analyses, but their accuracy is also much less. The observed values are not in good agreement with LEA and WOOD's formula $Sb_4O_3(OH)_5Cl = Sb_8O_{11}Cl_2 \cdot 5\,H_2O$ (*4*), since all the chloride values found are too high and all the water values are too low. The water analyses are in much better agreement with the formula $Sb_8O_{11}Cl_2 \cdot 4\,H_2O$, but the chloride values are still too high.

Table 1. Some analytical data on the γ-phase. These samples appeared pure judging from powder photographs. Data from microscopical examination indicated under Remarks.

Sample no.	Preparation		Remarks	Analyses			Density	Dimensions of the small unit cell			
	Method	Dilution		Sb %	Cl %	H_2O %		a Å	b Å	c Å	V Å^3
27	(1)	1: 60	γ + small amounts of "amorphous" matter	74.9							
28	(1)	1: 70	same	74.1	6.22						
29	(1)	1: 80	γ + very small amounts of "amorphous" matter	75.0	6.17						
30	(1)	1: 90	same	75.8			4.18				
31	(1)	1: 100	γ + small amounts of "amorphous" matter	74.7			4.10				
96	(2)	10 + 270	γ + small amounts of $Sb_4O_5Cl_2$?			5.6					
101	(2)	10 + 270	same		6.37	5.3					
105	(2)	10 + 360	pure γ	74.6	6.00	5.9					
106	(2)	10 + 360	,, ,,	74.7							
110	(2)	10 + 505	,, ,,	74.4	5.83	5.7					
111	(2)	10 + 1000	γ + small amounts of "amorphous" matter		5.68	5.4		9.63_5	13.13_2	4.08_3	516.6_1
98	(2)	10 + 210	γ + small amounts of $Sb_4O_5Cl_2$?					9.63_5	13.13_6	4.08_8	517.4_0
										m.v.	517.0
			Calculated for A(0)	74.30	5.41	6.87	4.21				
			A(¼)	74.04	6.06	6.68	4.23				
			B(0) = C(0)	75.33	5.48	5.57	4.15				
			B(¼)	74.80	6.13	5.71	4.18				
			C(¼)	75.06	6.15	5.38	4.17				

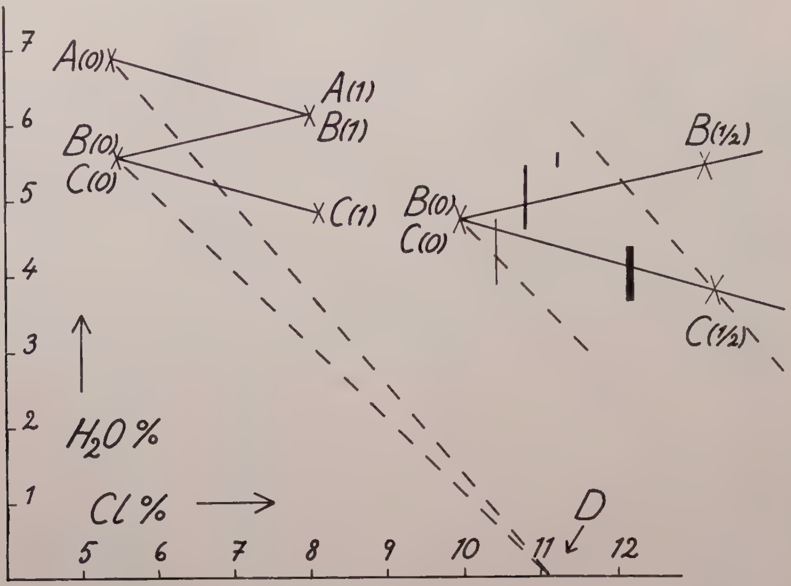

Fig. 1. $A(x) = [Sb_8O_8(OH)_4][(OH)_{2-x}(H_2O)_2]Cl_{2+x}$
$B(x) = [Sb_8O_8(OH)_4][(OH)_{2-x}(H_2O)_{1+x}]Cl_{2+x}$
$C(x) = [Sb_8O_8(OH)_4][(OH)_{2-x}H_2O]Cl_{2+x}$
D = $Sb_4O_5Cl_2$

An enlarged portion of the diagram is given to the right in the figure, where the long rectangles (almost lines) correspond to the observed values. The size of the rectangles indicate the variations in the analyses for each substance. For further explanations see text.

We can assume a variable composition. Chloride ions can be taken up by the γ-phase either by the exchange of one OH^- and one Cl^-, or just by an uptake of a Cl^-, which then must be accompanied by an uptake of a positive ion for instance a hydrogen ion to make the substance electrically neutral. To facilitate the discussion, chloride and water analyses for a substance are given as a rectangle in the diagram in Fig. 1. The lines correspond to some different ways of interpretation.

For the following discussion we must refer to the results from the structure determination. Assuming the formula $Sb_8O_{11}Cl_2 \cdot 5\,H_2O$, there are in all 16 oxygen atoms in the small unit cell. Of these, four corresponding to H_2O and OH^- are situated in a fourfold position in a channel in the structure. Even if there is a fair amount of room in this channel, it does not seem possible to take up a chloride ion in it without a considerable alteration of the length of the axes. From Table 1 it is obvious that there is scarcely any significant variation in the axes. From space considerations it does not appear quite improbable to exchange one of the OH^- in the channel to a Cl^-. This would be indicated by the formula $A(x) = [Sb_8O_8(OH)_4][(OH)_{2-x}(H_2O)_2]Cl_{2+x}$, whose composition follows the line A(0)–A(1) in Fig. 1.

If we assume the formula $Sb_8O_{11}Cl_2 \cdot 4\,H_2O$ there must be vacancies in the oxygen positions in the small unit cell. It seems reasonable to locate these vacancies in the channel. There can then be formed holes of sufficient size to accommodate a chloride ion. With reference to the conditions of preparation it appears likely that the negative charge is compensated by a hydrogen ion. In this case the total number of oxygen atoms would be constant, but the water content would vary a little. This mechanism could be explained by the formula $B(x) = [Sb_8O_8(OH)_4][(OH)_{2-x}(H_2O)_{1+x}]Cl_{2+x}$, whose composition follows the line B(0)-B(1) in Fig. 1. Of course it would also be possible in this case with an exchange of OH^- and Cl^-. This could be explained by the formula $C(x) = [Sb_8O_8(OH)_4][(OH)_{2-x}H_2O]Cl_{2+x}$, which gives a variable number of oxygens in the cell. Its composition follows the line C(0)–C(1) in Fig. 1. We have C(0) = B(0).

Another explanation of the variable analytical results would be that the substances are mixtures of a phase with a composition corresponding to A(0) or B(0) and $Sb_4O_5Cl_2$ indicated by the dotted lines A(0)–D and B(0)–D in Fig. 1. A more complicated case would be if they are mixtures of $A(x)$, $B(x)$ or $C(x)$ with $x \neq 0$ and $Sb_4O_5Cl_2$. The observed values would then fall on lines connecting a point on one of the lines $A(x)$, $B(x)$ or $C(x)$ with D. A mixture of A(0) and $Sb_4O_5Cl_2$ and the alternative $A(x)$ do not seem to fit the observed values. Thus $A(x)$ can be entirely excluded. A mixture of B(0) and $Sb_4O_5Cl_2$ is also not a good explanation. It seems as though $B(x)$ and $C(x)$ with $x \neq 0$ are the best interpretations. If we assume that the substances consist of pure γ-phase, which is a little questionable, it is very difficult to say which one of $B(x)$ and $C(x)$ is the best. But if we assume the substances to be a mixture of γ-phase and small amounts of $Sb_4O_5Cl_2$, it seems as if the alternative $B(x)$ would explain the observed values a little better. The γ-phase has therefore been assigned the formula $B(x)$, but we cannot entirely exclude the alternative $C(x)$.

Unit cell and space group

Single crystals were selected and set and rotation and Weissenberg photographs taken around all the three axes. The crystals proved to be orthorhombic with the *c*-axis coinciding with the needle-axis, which is about 4 Å. While the investigation was in progress, some extremely weak zones were discovered in new rotation photographs which indicated that the *c*-axis was four times longer than first thought. The dimensions of the small unit cell were more accurately determined from powder photographs. The dimensions (with an accuracy of about $\pm 0.05\,\%$) are given in Table 1 and the $\sin^2\theta$ in Table 2. The theoretical densities in Table 1 have been calculated with $Z = 1$ and with a mean value of the volume of 517.0 Å³.

Since the zones, which indicated the longer *c*-axis, are so weak that they are easily overlooked, it was supposed that the main features of the structure would be found from the small unit cell. Considering the small unit cell, the reflections with $h + k + l = 2n + 1$ are systematically absent in the photographs. This is characteristic of the space groups No. 71, $Immm - D_{2h}^{25}$, No. 44, $Imm2 - C_{2v}^{20}$, No. 24, $I2_12_12_1 - D_2^9$, and No. 23, $I222 - D_2^8$ (*11*).

The intensities of the reflections in the Weissenberg photographs have been estimated visually and corrected for the Lorentz polarisation factors given in Internationale Tabellen (*12*).

Table 2. Powder photograph of $[Sb_8O_8(OH)_4][(OH)_{2-x}(H_2O)_{1+x}]Cl_{2+x}$. Cr $K\alpha$-radiation, $\lambda = 2.2909$ Å. The horizontal line marks the boundary between the angular ranges of two different focusing cameras. Reflections systematically absent have been omitted. Reflections coinciding with β-reflections are given in brackets. Notations: st = strong, m = medium, w = weak, v = very.

h k l	$10^4 \sin^2\theta$ calc	$10^4 \sin^2\theta$ obs	*I* calc	*I* obs
1 3 0	0827	0824	17	w+
0 1 1	0867	0872	37	m
2 2 0	0873		19	
1 0 1	0933	0935	16	w
0 4 0	1218	(1216)	29	(st−)
1 2 1	1238		21	
3 1 0	1356	1356	39	st+
2 1 1	1436	1433	36	m
0 3 1	1476	1475	128	st
2 4 0	1786	(1783)	41	(m+)
3 3 0	1965	1965	138	st+
1 5 0	2045	2042	58	m−
2 3 1	2045		49	
3 0 1	2071	2071	110	m+
1 4 1	2151	2148	18	w
4 0 0	2275	(2268)	2	(w+)
3 2 1	2375	2374	3	vw
4 2 0	2579		0	
0 5 1	2694		1	
0 6 0	2740	(2735)	46	(m+)
4 1 1	3142		3	
0 0 2	3164	3165	90	w+
3 5 0	3182		0	
2 5 1	3263		0	
3 4 1	3289	(3298)	130	(m+)
2 6 0	3309		41	
1 1 2	3383	3377	16	vvw
0 2 2	3469	3466	19	vvw
4 4 0	3493		3	
5 1 0	3631	3643	32	m
1 6 1	3673		13	
2 0 2	3733	(3738)	39	(w−)
4 3 1	3751		1	
1 7 0	3872	3880	13	w−
1 3 2	3992	(3986)	23	(w−)
2 2 2	4038	(4044)	23	(vvvw)
5 3 0	4242	(4251)	67	(m+)
5 0 1	4346	4352	50	w+
0 4 2	4382		41	

Tab. 2 (cont.)

h k l	$10^4 \sin^2\theta$ calc	$10^4 \sin^2\theta$ obs	*I* calc	*I* obs
0 7 1	4520	(4517)	72	(w$^+$)
3 1 2	4520		52	
5 2 1	4650	4655	23	vvw
3 6 1	4811	4809	149	m$^-$
0 8 0	4871	(4870)	2	(vvvw)
2 4 2	4951	(4953)	55	(vvvw)
4 5 1	4969		5	
3 7 0	5009	5014	54	w$^-$
4 6 0	5015		0	
2 7 1	5089	5078	108	w$^-$
6 0 0	5119	5118	37	m$^-$
3 3 2	5129		191	
1 5 2	5209	(5218)	7	(vvvw)
6 2 0	5423		4	
4 0 2	5439		2	
2 8 0	5440		1	
5 5 0	5457	(5461)	8	(vw)
5 4 1	5564	5555	74	w
4 2 2	5744		0	
1 8 1	5804		0	
0 6 2	5904	(5894)	72	(vw)
6 1 1	5986	(5992)	31	(vw$^+$)
1 9 0	6307		3	
6 4 0	6336	6331	23	vvw
3 5 2	6347		0	
2 6 2	6473	(6454)	58	(vvw)
6 3 1	6595	6587	135	w$^+$
4 4 2	6657		5	
4 7 1	6795	(6764)	3	(vvw)
5 1 2	6795		49	
3 8 1	6942	(6932)	12	(vw)
0 9 1	6956		39	

Patterson syntheses

In order to find the positions of the eight antimony atoms and to try to rule out some of the possible space groups, the Patterson projections $P(UVp)$ (see Fig. 2), $P(pVW)$ (see Fig. 3) and $P(UpW)$ (see Fig. 4) were calculated. From Figs. 3 and 4 it is obvious that there are high maxima at only $w = 0$, $\frac{1}{2}$, and 1.

We consider first the highest space group *Immm*. The eight antimony atoms can be situated according to the following alternatives: in one eightfold position, in two fourfold positions, in one fourfold and two twofold positions, or in four twofold positions. The combination $2(a) + 2(b) + 2(c) + 2(d)$ does not give a reasonable ex-

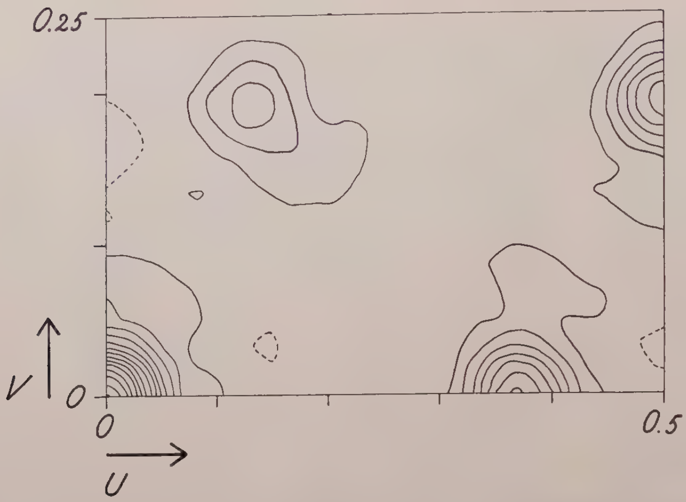

Fig. 2. $P(UVp)$. Contours at an interval of 30 arbitrary units. Negative values dotted.

planation to the observed peaks and would also give a distance Sb–Sb of about 2 Å, which is very improbable. Thus this combination can be excluded. Such a short Sb–Sb distance or even shorter would also be found for the positions 4(i), 4(j), 8(k), 8(l), and 8(m), which thus can be entirely excluded from discussion. All the three peaks in $P(UVp)$ at $u = 0.370$, $v = 0$; $u = \frac{1}{2}$, $v = 0.192$; and $u = 0.131$, $v = 0.191$ cannot be satisfactorily explained at the same time by the combinations 4(e) + 4(f) and 4(g) + 4(h) since they demand that u or $v = 0$, $\frac{1}{2}$ and 1. They are thus excluded. By the same reason all combinations involving one fourfold and two twofold positions can be excluded. The remaining possiblities give the following vectors in the Patterson projection $P(UVp)$:

I within 4(e) and 4(f) of weight 2	A	$\pm(2x, 0)$
	B	$\pm(\frac{1}{2} + 2x, \frac{1}{2})$
of weight 4	C	$\frac{1}{2}, \frac{1}{2}$
II within 4(g) and 4(h) of weight 2	A	$\pm(0, 2y)$
	B	$\pm(\frac{1}{2}, \frac{1}{2} + 2y)$
of weight 4	C	$\frac{1}{2}, \frac{1}{2}$
III between 4(e) and 4(g) or 4(h) of weight 4	A	$\pm(x_1, \pm y_2)$
	B	$\pm(\frac{1}{2} + x_1, \frac{1}{2} \pm y_2)$
IV between 4(f) and 4(g) or 4(h) of weight 4	A	$\pm(x_1, \frac{1}{2} \pm y_2)$
	B	$\pm(\frac{1}{2} + x_1, \pm y_2)$

The following vectors are given in the Patterson space $P(UVW)$:

V within 8(n) of weight 2	A	$\pm(2x, \pm 2y, 0)$
	B	$\pm(\frac{1}{2} + 2x, \frac{1}{2} \pm 2y, \frac{1}{2})$
of weight 4	C	$\pm(2x, 0, 0)$
	D	$\pm(\frac{1}{2} + 2x, \frac{1}{2}, \frac{1}{2})$
	E	$\pm(0, 2y, 0)$
	F	$\pm(\frac{1}{2}, \frac{1}{2} + 2y, \frac{1}{2})$
of weight 8	G	$\frac{1}{2}, \frac{1}{2}, \frac{1}{2}$

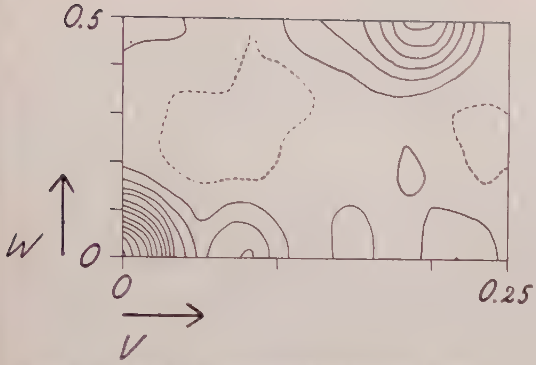

Fig. 3. $P(pVW)$. Contours at an interval of 100 arbitrary units. Negative values dotted.

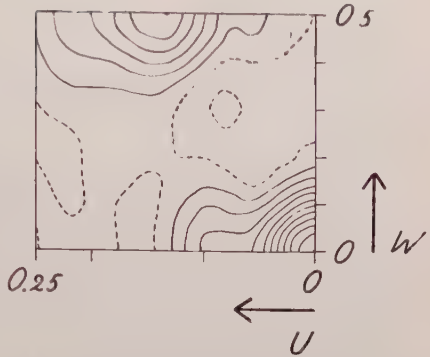

Fig. 4. $P(UpW)$. Contours at an interval of 15 arbitrary units. Negative values dotted.

We find that the combinations $4(e) + 4(g)$, $4(e) + 4(h)$, $4(f) + 4(g)$, and $4(f) + 4(h)$ require that peaks corresponding to the vectors III and IV have double the height of the peaks corresponding to the vectors I A, B and II A, B. Since the observed heights are contrary to this, it seems reasonable to exclude these combinations, specially as also the observed coordinates of the peaks do not favour such an explanation.

We then have to consider only the position $8(n)$ and the corresponding vectors of group V, and find that both the heights and coordinates of the maxima are in good agreement with what is required by these vectors. In $P(UVp)$ the maximum at $v = 0$ gives us $u = 2x = 0.3696$, 0.6304, which gives $x = 0.1848$, 0.3152, the maximum at $u = \frac{1}{2}$ gives us $v = \frac{1}{2} \pm 2y = 0.1923$, 0.8077, which gives $y = 0.1538$, 0.3462. In $P(pVW)$ the maximum at $w = \frac{1}{2}$ gives $v = \frac{1}{2} \pm 2y = 0.1914$, 0.8086, which gives $y = 0.1543$, 0.3457. In $P(UpW)$ the maximum at $w = \frac{1}{2}$ gives $u = \frac{1}{2} \pm 2x = 0.1393$, 0.8607, which gives $x = 0.1804$, 0.3197. However, it is easily found that we need only consider parameters within the limits $0 \leq x \leq \frac{1}{4}$ and $0 \leq y \leq \frac{1}{4}$. Therefore we assume that the eight antimony atoms are situated in $8(n)$ with $x = 0.183$, $y = 0.154$.

The space group *Imm*2. Choosing the c-axis as the polar axis the xy-projection becomes identical with *Immm*, and thus only the eightfold position $8(e)$ is possible. The antimony atoms are, however, in this case situated in the same relative positions as in *Immm* and it is therefore not necessary to consider *Imm*2 at this stage.

With the orientation *I*2*mm* the position $8(e)$ is not possible as this would require that all the high peaks in $P(UVp)$ are situated at $u = 0$, $\frac{1}{2}$, and 1. Combinations containing $4(c)$ are not possible since we would with Sb in this position obtain a Sb–Sb distance $= 2z \leq 2$ Å. Combinations involving four twofold positions are not possible because they require that all maxima in $P(UVp)$ are situated at $v = 0$, $\frac{1}{2}$, and 1.

The remaining possibilities give the following vectors in the Patterson space $P(UVW)$:

I within $2(a)$ and $2(b)$ of weight 2		$\frac{1}{2}, \frac{1}{2}, \frac{1}{2}$
II within $4(d)$ of weight 2	A	$\pm(0, 2y, 0)$
	B	$\pm(\frac{1}{2}, \frac{1}{2} + 2y, \frac{1}{2})$
of weight 4	C	$\frac{1}{2}, \frac{1}{2}, \frac{1}{2}$
III between two positions $4(d)$ of weight 2	A	$\pm(x_1 - x_2, \pm(y_1 \pm y_2), 0)$
	B	$\pm(\frac{1}{2} + x_1 - x_2, \frac{1}{2} \pm (y_1 \pm y_2), \frac{1}{2})$

IV between 4(*d*) and 2(*a*) of weight 2	A	$\pm(x_1 - x_2, \pm y_1, 0)$
	B	$\pm(\frac{1}{2} + x_1 - x_2, \frac{1}{2} \pm y_1, \frac{1}{2})$
V between 4(*d*) and 2(*b*) of weight 2	A	$\pm(x_1 - x_2, \frac{1}{2} \pm y_1, 0)$
	B	$\pm(\frac{1}{2} + x_1 - x_2, \pm y_1, \frac{1}{2})$

The combination of two positions 4(*d*) is not possible since the high peak at $v = 0$ in $P(UVp)$ can only be explained with some combinations of the following values of y_1 and y_2: 0, $\frac{1}{4}$, $\frac{1}{2}$. These y-values do not give vectors II B which are able to explain the high peak at $u = \frac{1}{2}$ in $P(UVp)$. An equivalent discussion excludes the combination of 4(*d*) with two twofold positions. Thus *I2mm* can be eliminated.

The orientation *Im2m* can be ruled out for reasons similar to those for *I2mm*.

The space group $I2_12_12_1$. Combinations of two fourfold positions of the same sort are not possible since they would require that all peaks in $P(UVp)$ are situated at u or $v = 0$, $\frac{1}{2}$, and 1. The combination 4(*a*) + 4(*b*) is not possible since it demands maxima in $P(pVW)$ and $P(UpW)$ at $w = \pm\frac{1}{4}$, which do not exist. The combinations 4(*a*) + 4(*c*) and 4(*b*) + 4(*c*) would demand maxima in $P(UVp)$ at u or $v = \pm\frac{1}{4}$, which do not exist. Thus all the fourfold positions can be excluded. The eightfold position 8(*d*) gives the following vectors in the Patterson space $P(UVW)$:

of weight 2	A	$\pm(2x, \frac{1}{2}, \frac{1}{2} \pm 2z)$
	B	$\pm(\frac{1}{2} + 2x, 0, \pm 2z)$
	C	$\pm(0, 2y, \frac{1}{2} \pm 2z)$
	D	$\pm(\frac{1}{2}, \frac{1}{2} + 2y, \pm 2z)$
	E	$\pm(2x, \frac{1}{2} \pm 2y, 0)$
	F	$\pm(\frac{1}{2} + 2x, \pm 2y, \frac{1}{2})$
of weight 8	G	$\frac{1}{2}, \frac{1}{2}, \frac{1}{2}$

From $P(UpW)$ we find that the vector C gives $w = \frac{1}{2} \pm 2z = 0, 1 \ldots$ which gives $z = \pm\frac{1}{4}$. From $P(pVW)$ we find that the vector B gives $w = \pm 2z = 0, 1 \ldots$ which gives $z = 0$ and $\frac{1}{2}$. Thus the two projections require different z-values for their interpretation and we can therefore exclude 8(*d*) and accordingly the whole space group from consideration.

The space group *I*222. A combination of 2(*a*) + 2(*b*) + 2(*c*) + 2(*d*) does not give a reasonable explanation of the observed peaks and would also give a too short Sb–Sb distance. The positions 4(*i*) and 4(*j*) can be entirely excluded since they correspond to a distance Sb–Sb ≤ 2 Å. Combinations of two fourfold positions of the same sort and also 4(*e*) + 4(*f*) and 4(*g*) + 4(*h*) are not possible since they would demand that all peaks in $P(UVp)$ are situated at u or $v = 0$, $\frac{1}{2}$ and 1. The combinations 4(*e*) + 4(*g*), 4(*e*) + 4(*h*), 4(*f*) + 4(*g*), and 4(*f*) + 4(*h*) give in the projection $P(UVp)$ exactly the same set of vectors as the corresponding positions in *Immm* and can thus be excluded for the same reasons. The eightfold position 8(*k*) gives the following vectors in the Patterson space $P(UVW)$:

of weight 2	A	$\pm(2x, \pm 2y, 0)$
	B	$\pm(\frac{1}{2} + 2x, \frac{1}{2} \pm 2y, \frac{1}{2})$
	C	$\pm(2x, 0, \pm 2z)$
	D	$\pm(\frac{1}{2} + 2x, \frac{1}{2}, \frac{1}{2} \pm 2z)$
	E	$\pm(0, 2y, \pm 2z)$
	F	$\pm(\frac{1}{2}, \frac{1}{2} + 2y, \frac{1}{2} \pm 2z)$
of weight 8	G	$\frac{1}{2}, \frac{1}{2}, \frac{1}{2}$

Comparing the vectors C and E with $P(pVW)$ and $P(UpW)$ we find that they give $w = \pm 2z = 0$ and 1 and thus $z = 0$ or $\frac{1}{2}$. With these z-values, $8(k)$ becomes identical with $8(n)$ in the space group *Immm.*

Since all the lower space groups, when they are possible, give antimony positions which are identical with those found for *Immm* with $8(n)$ cf. p. 265, we only consider this space group.

Fourier syntheses

Fourier syntheses have been used to refine the antimony parameters and to get an idea of the positions of the light atoms. The syntheses have been calculated with $|F_{\text{obs}}| = \sqrt{\frac{I}{Lp}}$ where F is the structure factor, I the estimated intensity and Lp are the combined Lorentz and polarization factors. In all syntheses the value of $F(000)$ has been omitted. Correction for absorption has not been applied. The maxima have been located using the interpolation table given by BOOTH (*13*).

For the first projections the signs of the highest F-values were determined using the approximate antimony parameters. From the first $\varrho(XYp)$, it was clear that two chlorine atoms are situated in one of the twofold positions $2(a)$ or $2(c)$. The other two electron density projections indicate $2(c)$ as the probable one, although the corresponding peaks are low. The cut $\varrho(XY0)$ has also been calculated and this clearly indicated two chlorines in $2(c)$ $\frac{1}{2},\frac{1}{2},0$. The final $\varrho(XYp)$-projection is given in Fig. 5, the final $\varrho(pYZ)$-projection in Fig. 6 and the final $\varrho(XpZ)$-projection in Fig. 7. There are some low maxima which might correspond to oxygen positions. The interpretation of such low peaks must be performed with some care since they might be false details corresponding to diffraction and absorption effects. With the parameters from $\varrho(pYZ)$ and $\varrho(XpZ)$ we have the following probable atomic positions in the space group *Immm*: 8 Sb in $8(n)$ with $x = 0.183_5$, $y = 0.152_9$, 2 Cl in $2(c)$, 8 O_1 in $8(n)$ with $x = 0.28_1$, $y = 0.30_2$, 4 O_2 in $4(g)$ with $y = 0.23_1$, and 4 (3) O_3 in $4(h)$ with $y = 0.43_0$.

The oxygen positions

Since the oxygen positions derived from the electron density projections might be a little doubtful, it is advisable also to ascertain these positions from space considerations and to add information obtainable from more detailed intensity discussions.

In the oxides the Sb–O distance is 2.0 kX (*14, 15*). Considering this and the fact that the c-axis, which coincides with the needle-axis, is about 4 Å in the γ-phase, it seems very probable that there is an oxygen atom situated almost exactly between two antimony atoms, which are 4 Å apart. In this way there could be formed endless –Sb–O–Sb-O-chains along the needle-axis. Judging from the formula of the γ-phase, this is possible with either oxygen atoms or hydroxyl groups in the chain. However, in the compounds $Sb_8O_{10}(OH)_2X_2$ (*3*), which also have a needle-axis of about 4 Å, there appear to be the same types of chains but in these compounds there are not sufficient hydroxyl groups to form a chain. This seems to favour the assumption that oxygen atoms and not hydroxyl groups form the chains in the γ-phase. The oxygen position O_1 found in the Fourier syntheses seems to be located in fairly good accordance with what can be expected from an oxygen atom in a Sb–O chain.

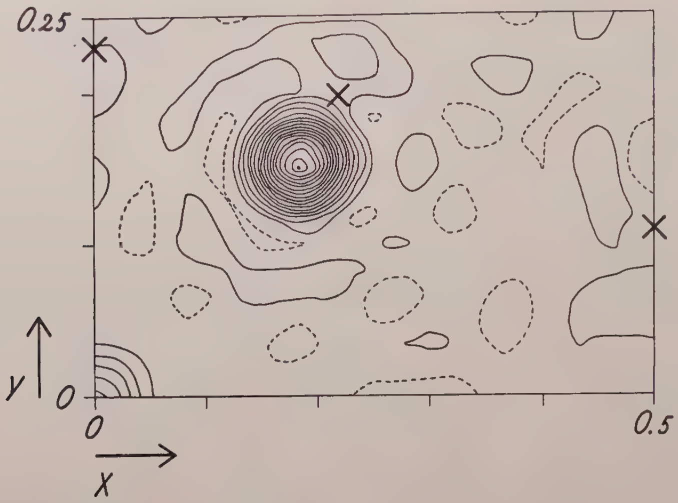

Fig. 5. $\varrho(XYp)$. Contours at an interval of 50 arbitrary units. Negative values dotted. The final oxygen positions are marked ×.

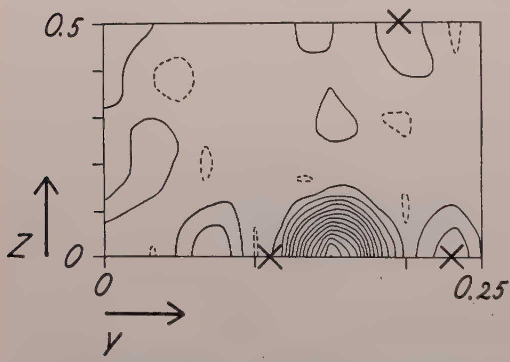

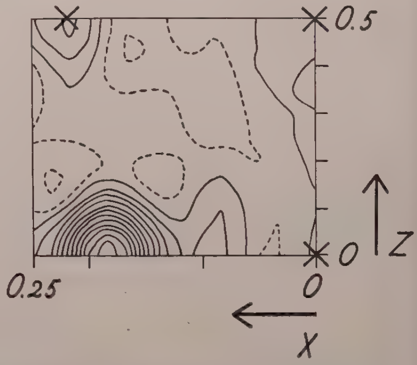

Fig. 6. $\varrho(pYZ)$. Contours at an interval of 100 arbitrary units. Negative values dotted. The final oxygen positions are marked ×.

Fig. 7. $\varrho(XpZ)$. Contours at an interval of 30 arbitrary units. Negative values dotted. The final oxygen positions are marked ×.

The sum of the ionic radii of oxygen and chlorine are with values from Internationale Tabellen (*12*):

O–Cl 3.13 kX (GOLDSCHMIDT), 3.21 kX (PAULING)
O–O 2.64 ,, ,, 2.80 ,, ,,

Spheres of appropriate radii, inside which no oxygen centres could occur, were imagined around the antimony and chlorine centres. Considering the short *c*-axis and the space group *Immm*, the atoms can only be situated in the mirror planes perpendicular to the *c*-axis. Therefore it is only necessary to make a cut at $z=0$. Within a distance of about 1.3 Å from a mirror plane no oxygens can be situated.

In the cut given in Fig. 8, the different places, where there is room for oxygen atoms, are indicated. It is possible with eightfold, fourfold, and twofold positions. Since there evidently is room for the oxygen O_1, which would be a constituent of the Sb–O chain, this position was taken into account with the parameters on p. 267. In Fig. 9 we can see the space which is left for the remaining seven or eight oxygens (during the structure determination it was for a long time thought that Lea and Wood's formula with sixteen oxygens in the cell was correct). These oxygens must correspond to OH^- and H_2O. Now we have only four- and twofold positions to consider. It seemed likely that some or all of these oxygens would be in contact with the antimony atoms. The twofold positions correspond to $2(b)$ and $2(d)$. Oxygens in these positions would not be in contact with any of the other atoms and, if both were occupied, these oxygens would have a distance between them of about 2 Å. These facts make it reasonable to exclude the twofold positions entirely. The fourfold positions, which give contacts or near contacts with antimony atoms, are indicated as I and II. Since an oxygen at I comes in better contact with two antimony atoms without being squeezed by the chlorine than an oxygen at II, it appears reasonable to locate four hydroxyl groups at I in $4(g)$ with the y-parameter from $\varrho(pYZ)$.

In Fig. 10, the space which remains for the three oxygens, which must correspond to both OH^- and H_2O, is indicated. They can be located in the fourfold positions indicated as II and III in a channel in the structure. At first, II seemed preferable to III because this position would bring the oxygens almost in contact with two antimony atoms. There is however no peak in $\varrho(XYp)$ (Fig. 5) corresponding to II, whereas there are peaks both in $\varrho(XYp)$ and $\varrho(pYZ)$ (Fig. 6) which approximately agree with III. As mentioned before such low peaks can be false details. Therefore three dimensional Fourier syntheses were calculated and attempts made to substract the antimony peak and perhaps also some of the diffraction effects from $\varrho(XYp)$. From these calculations nothing appeared that made II preferable to III. It was instead on the contrary.

At this stage a very careful calculation of $F(hk0)$ was performed with a temperature factor $B = 1.16 \cdot 10^{-16}$, which had been obtained by plotting $\log \frac{F_o}{F_c}$ against $\sin^2\theta$. When these calculations were performed, the author had only a fairly weak $hk0$ Weissenberg photograph. The reliability factor

$$R = \frac{\Sigma \big| |F_o| - |F_c| \big|}{\Sigma |F_o|}$$

was calculated for some different alternatives always omitting the non-observed reflections.

With Sb in $8(n)$ $x = 0.185$, $y = 0.153$

(1) O_1 in $8(n)$ $x = 0.278$, $y = 0.324$ and O_2 in $4(g)$ $y = 0.225$
(a) without O_3 $R = 0.145$
(b) with O_3 in $4(h)$ $y = 0.400$ $R = 0.144$; $y = 0.432$ $R = 0.140$
(c) with O_3 in $4(e)$ $x = 0.248$ $R = 0.173$

(2) O_1 in $8(n)$ $x = 0.310$, $y = 0.324$ and O_2 in $4(g)$ $y = 0.219$
(a) without O_3 $R = 0.153$
(b) with O_3 in $4(h)$ $y = 0.400$ $R = 0.134$; $y = 0.432$ $R = 0.145$
(c) with O_3 in $4(e)$ $x = 0.248$ $R = 0.162$

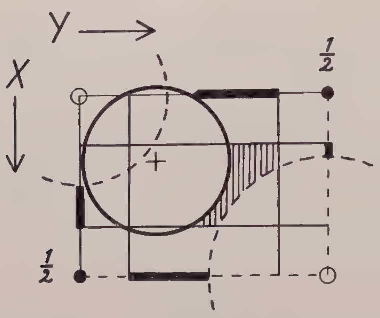

Fig. 8. Cut at $z = 0$ for the localization of the oxygen atoms. + centre of Sb, thick circle = forbidden area around Sb. ○ projections of centre of Cl, dotted circle = forbidden area around Cl. The possible oxygen positions are: hatched area = eightfold position, broad black lines = fourfold positions and black points = twofold positions.

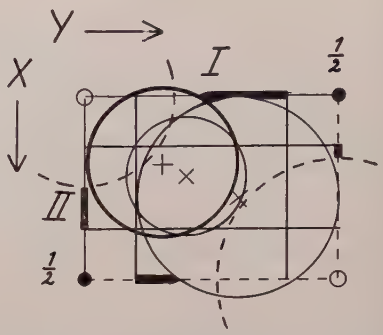

Fig. 9. Cut at $z = 0$ for the localization of oxygen atoms. The oxygens O_1 are now included. + centre of Sb, thick circle = forbidden area around Sb. ○ projections of centre of Cl, dotted circle = forbidden area around Cl. × projections of centre of O, thin circle = forbidden area around O. The possible oxygen positions are: broad black lines = fourfold positions and black points = twofold positions.

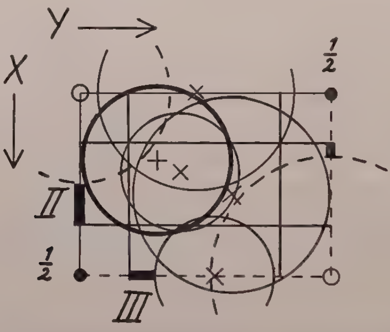

Fig. 10. Cut at $z = 0$ for the localization of oxygen atoms. The oxygens O_1 and O_2 are now included. + centre of Sb, thick circle = forbidden area round Sb. ○ projections of centre of Cl, dotted circle = forbidden area around Cl. × projections of centre of O, thin circle = forbidden area around O. The possible oxygen positions are: broad black lines = fourfold positions and black points = twofold positions.

It is obvious that 4 O_3 in 4(*e*), which corresponds to the alternative II, is favoured neither by the *R*-values nor by the Fourier syntheses. It thus appeared that III is more likely than the other alternatives for O_3. We find however that with the *y*-parameter for O_3 given on p. 267 the distance from one O_3 to its mirror image would be 1.84 Å, which is much too short for an O–O distance. It therefore seemed better to determine this parameter from space considerations. The nearest neigbours to O_3 are the oxygens O_2. This seemed at first a little peculiar but, considering that O_2 corresponds to hydroxyl groups and O_3 corresponds to both hydroxyl groups and water, we find that all the contacts between nearest neighbours of O_2 and O_3 can be formed by hydrogen or hydroxyl bonds, since there are just sufficient number of hydrogen atoms for this. Thus all the O_3 atoms will be structurally equivalent.

Assuming all distances for nearest neighbours of O_3 and O_2 equal we find O_3 in $4(h)$ with $y=0.390$.

It does not seem as if the coordinations of the atoms would be improved by assuming a lower space group for the small unit cell. Some of the irregularities in the number of atoms can probably cause the extremely weak zones, which increase the needle-axis fourfold. Some hints about the interpretation of these weak zones will be given in the next section. It did not seem worth-while to give an exact explanation of them. We then have the following atomic coordinates in the space group *Immm* for $[Sb_8O_8(OH)_4][(OH)_{2-x}(H_2O)_{1+x}]Cl_{2+x}$

		x	y	z
8 Sb	in $8(n)$	0.183_5	0.152_9	0
2 Cl	in $2(c)$	$\frac{1}{2}$	$\frac{1}{2}$	0
8 O_1	in $8(n)$	0.28_1	0.30_2	0
4 O_2 (OH)	in $4(g)$	0	0.23_1	0
3 O_3 (OH, H_2O)	in $4(h)$	0	0.39_0	$\frac{1}{2}$

By comparing the different Fourier projections the accuracy of the parameters can be estimated to be approximately $\pm 0.001 = \pm 0.01$ Å for Sb and $\pm 0.02 = \pm 0.3$ Å for O. It is probable that the Sb–O distances are accurate to within about ± 0.3 Å.

F-values were then calculated using

$$F_{\text{calc}} = \text{const}\left[f_{\text{Sb}} A_{\text{Sb}} + f_{\text{Cl}} A_{\text{Cl}} + f_{\text{O}} \sum_{1}^{3} A_{\text{O}_i}\right]$$

where f_{Sb}, f_{Cl}, and f_{O} are the atomic scattering factors of antimony, chlorine, and oxygen with due consideration being taken to their variation with θ (*12*). No temperature factor has been included. The calculated and observed F-values are given in Tables 3 (for $hk0$) and 4 (for $0kl$). With non-observed reflections omitted, the reliability factor R is, for $hk0$, 0.13 and, for $0kl$, 0.23 (when the reflections most strongly affected by absorption depending on the needle-shape are omitted 0.19).

For the powder photographs, the intensities have been calculated as $I_{\text{calc}} = pF^2_{\text{calc}}$ with p = number of cooperating planes, cf. Table 2. As can be expected for crystal needles, the intensities are influenced by orientation effects.

Discussion of the structure

Projections of the structure are given in Fig. 11 and the interatomic distances in Table 5. The accuracy of the distances is discussed above. As has been mentioned before there are –Sb–O–Sb–O-chains along the needle-axis of the crystal with a distance Sb–O of 2.1_5 Å. Two chains are situated together with antimony in one chain in contact with oxygen in the neighbouring chain at a distance of 2.1_7 Å and thus form a double chain. These double chains are joined by hydroxyl groups with a distance Sb–OH of 2.0_4 Å forming sheets, in a way which is best seen in Fig. 12. These sheets have the composition $[Sb_8O_8(OH)_4^{4+}]_\infty$. There is no close contact between antimony and chlorine corresponding to a covalent bond, since the distance Sb–Cl is 3.37 Å, which is much longer than the distance in $SbCl_3$ in the gas phase recently determined by KISLIUK (*16*) to be 2.325 ± 0.005 Å by microwave methods. Long Sb–Cl distances are, however, found in other antimony(III)oxide chlorides.

Table 3. Calculated and observed F-values of $hk0$ for a Weissenberg photograph of $[Sb_8O_8(OH)_4][(OH)_{2-x}(H_2O)_{1+x}]Cl_{2+x}$. Cu $K\alpha$-radiation.

k	$0k0$		$1k0$		$2k0$		$3k0$		$4k0$		$5k0$		$6k0$		$7k0$		$8k0$		$9k0$		$10k0$		$11k0$	
	F_c	F_o	F_c	F_o	F_c	F_o	F_c	F_o	F_c	F_o	F_c	F_o	F_c	F_o	F_c	F_o	F_c	F_o	F_c	F_o	F_c	F_o	F_c	F_o
0					–39	46			10	13			45	40			–34	37			25	19		
1			20	21			–32	42			29	32			– 5				– 9				20	16
2	–31	33			23	34			– 1				–10	8			15	14			– 6			
3			–21	29			61	66			–42	49			15	17			21	17			–29	28
4	–39	44			33	37			9	10			–25	25			33	32			–11	9		
5			12	16			0				15	15			1				6				4	
6	50	50			–33	31			– 2				30	30			–32	28			17	11		
7			18	23			–38	36			33	35			– 4				–20	12			32	21
8	9	8			5				2				12				– 2							
9			– 9	9			33	35			–21	20			8				18	11				
10	–35	39			28	30			10				–28	24			37	32						
11			– 6				15	17			–12	10			3									
12	20	20			– 9	10			– 1				18	12			–15	15						
13			20	17			–28	28			34	32												
14	25	26			–14	13			0				18	15										
15			– 1				9	7																
16	–28	28			21	22																		

Table 4. Calculated and observed F-values of $0kl$ for a Weissenberg photograph of $[Sb_8O_8(OH)_4]\,[(OH)_{2-x}(H_2O)_{1+x}]Cl_{2+x}$. Cu$K\alpha$-radiation.

k	$0\,k\,0$		$0\,k\,1$		$0\,k\,2$		$0\,k\,3$		$0\,k\,4$		$0\,k\,5$	
	F_c	F_o	F_c	F_o	F_c	F_o	F_c	F_o	F_c	F_o	F_c	F_o
0					133	151			88	69		
1			60	90			43	48			31	9
2	–58	38			– 42	60			–27	17		
3			–113	118			–81	88			–62	24
4	–75	86			– 62	74			–46	33		
5			– 12				– 7					
6	98	127			81	70			63	32		
7			84	66			64	42				
8	19	22			17				14			
9			– 61	77			–51	39				
10	–67	93			– 60	63			–52	42		
11			– 43	46			–37	23				
12	38	52			36	35						
13			72	82			63	64				
14	47	61			45	52						
15			– 31	30								
16	–53	59										

Table 5. Interatomic distances in $[Sb_8O_8(OH)_4]\,[(OH)_{2-x}(H_2O)_{1+x}]Cl_{2+x}$. Å units. The numerals 2 × and 4 × before a distance means that it occurs twice or four times. (H) after a distance indicates a probable hydrogen bond.

Sb–4 O	$2 \times 2.1_5$ (in the chain direction), 2.0_4, 2.1_7
Sb–2 Cl (Cl–8 Sb)	3.3_7
O_1–3 Sb	$2 \times 2.1_5$, 2.1_7
O_2–2 Sb	2.0_4
Cl–8 O	$4 \times 3.3_5$, $4 \times 3.6_6$
O_1–Cl	3.3_5
O_2–2 Cl	3.6_6
O_1–7 O	2.5_3, 2.8_6, $2 \times 2.9_7$, 3.2_9, $2 \times 3.5_8$
O_2–8 O	$2 \times 2.8_6$, $2 \times 2.9_2$ (H), $4 \times 2.9_7$
O_3–9 O	2.8_9 (H), $2 \times 2.9_2$ (H), $2 \times 3.2_9$, $4 \times 3.5_8$
Sb–6 Sb	2 × 3.51, 3.54, 4.02, 2 × 4.08

All antimony atoms are surrounded by four oxygens in a type of coordination found earlier for some, but not all, antimony atoms in $Sb_4O_5Cl_2$ (*1*) and SbOCl (*2*) and also for all antimony atoms in $Sb_8O_{10}(OH)_2X_2$ (*3*). In $[Sb_8O_8(OH)_4][(OH)_{2-x}(H_2O)_{1+x}]Cl_{2+x}$ all of the oxygens, which are involved in this four coordination, have been located by electron density projections. The coordination is clearly seen in

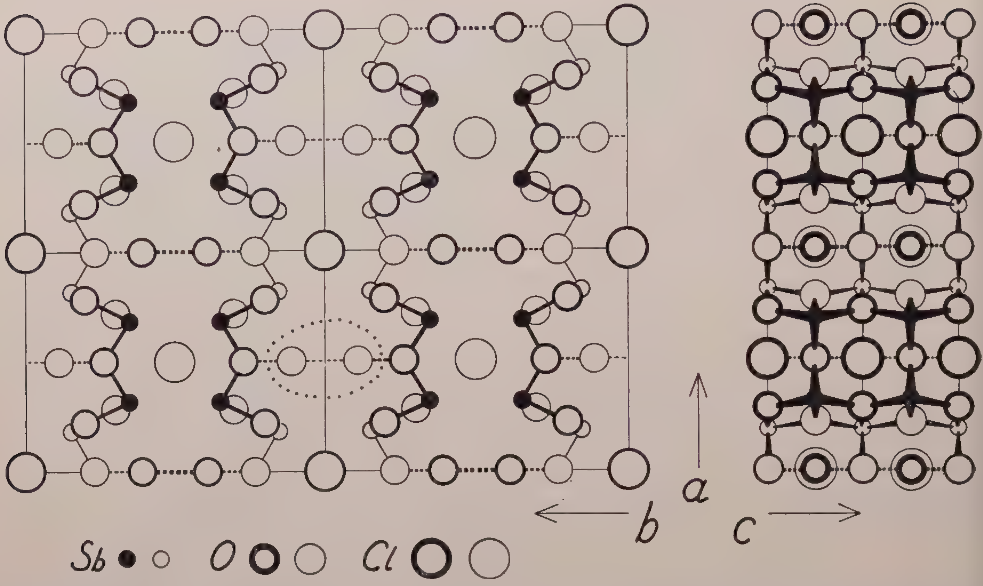

Fig. 11. Projections of the structure of $[Sb_8O_8(OH)_4][(OH)_{2-x}(H_2O)_{1+x}]Cl_{2+x}$. Both projections show four adjacent unit cells. Dotted lines indicate probable hydrogen bonds. The dotted curve encloses two of the oxygens O_3.

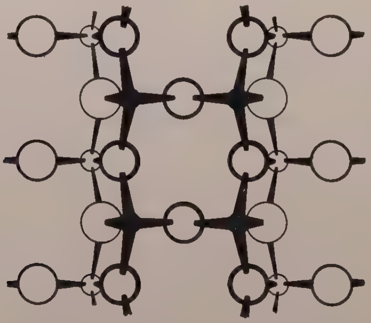

Fig. 12. Sb–O chains joined by OH to form a $[Sb_8O_8(OH)_4^{4+}]_\infty$ sheet. The small circles indicate Sb and the large ones O. The four coordination is obvious.

Fig. 12. Perhaps this coordination can be described as a deformed $TeCl_4$ configuration, which is approximately a deformed trigonal bipyramid with an equatorial corner unoccupied and, according to PAULING (*17*), with a stereochemically active unshared electron pair directed towards it. STEVENSON and SCHOMAKER (*18*) have found this configuration by an electron diffraction study of gaseous $TeCl_4$. A similar configuration has been found for the $IO_2F_2^-$ ion in KIO_2F_2 by HELMHOLZ and ROGERS (*19*) and for diphenylselenium dibromide (*20*) and dichloride (*21*) by MCCULLOUGH and HAMBURGER. According to DIATKINA (*22*) the $TeCl_4$ structure can be accounted for without hybridization with the unshared electron pair.

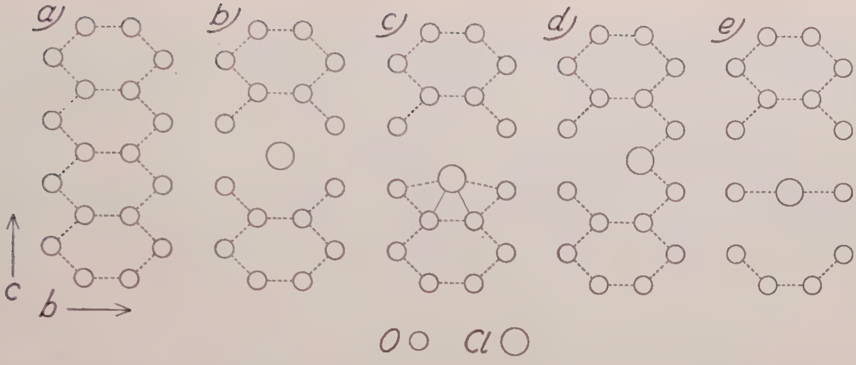

Fig. 13. System of probable hydrogen bonds, which are indicated by dotted lines. Four units along the *c*-axis are given. For further explanations see text.

In the present structure we have the following angles in the four-coordination. The two "diagonal" O–Sb–O angles are 143°, 85° and the other four O–Sb–O angles are two of 72° and two of 90°.

The chlorines are surrounded by eight antimony atoms at the distances 3.37 Å. If a chlorine had been situated in $2(a)$ it would have been surrounded by four antimony atoms at a distance of about 2.7 Å. The X-ray data are, however, not in favour of this. Assuming a stereochemically active unshared electron pair for antimony, it does not seem unreasonable that this electron pair would have a repulsing effect on the negative chloride ion, thus making the Sb–Cl distance long. The chlorines are in better contact with oxygen atoms.

As mentioned on p. 269 the oxygens O_3 are situated in a channel in the structure and correspond to both OH^- and H_2O. The O_3 atoms can be assumed to form hydrogen or hydroxyl bonds with each other and the O_2 atoms, in a way which makes all the O_3 atoms structurally equivalent. These O–O distances are 2.9 Å, which is however a little long for such bonds, cf. a discussion by WELLS (*23*). The accuracy of these distances is, however, not very large. The system of hydrogen bonds is represented in Fig. 13. (a) corresponds to LEA and WOOD's formula, which is identical with A(0). In this case all the positions O_3 would be filled. As it has been indicated in the discussion of the formula where the alternative $B(x)$ has been preferred, there must be vacancies in the O_3 positions, whose number are constant. If two adjacent O_3 are removed there will be formed a hole of sufficient size to accomodate a chloride ion. Actually this hole is so large that a chloride ion situated in the centre of it is scarcely in contact with any other atoms, since the distance to its nearest neighbour, an O_2 atom, is 4.0_8 Å. This corresponds to (b) in Fig. 13. Contacts with neighbouring atoms can, however, be formed if the chloride ion is situated in an unsymmetrical manner in the hole, where it might be partly bound by hydrogen bonds. Two alternatives of this sort are given by (c) and (d) in Fig. 13. The alternative (e) corresponds to the removal of four adjacent O_3 atoms at the same time. The distance $Cl–O_2$ would in this case be about 3.5 Å, perhaps involving hydrogen bonds. It seems, however, that the probability for the removal of four adjacent O_3 would be less than that for removing only two O_3 atoms at the same time. The formation of holes in the channels in the structure and the inclusion of chloride ions in some of the holes will probably account for the very weak zones, which increase the needle-axis fourfold, since the holes might be arranged in a regular way.

The fact that there are Sb–O chains in this structure may perhaps be an explanation of the circumstance that, on further hydrolysis of $SbCl_3$, orthorhombic Sb_2O_3 in chain form is obtained, although this is the high temperature modification (*6*). The chains in these two compounds are, however, not identical.

This work was almost finished about five years ago. However, the uncertainty of the formula and the coordination of antimony made it seem advisable to investigate some other compounds of trivalent antimony before any definite conclusions were drawn.

Summary

The probably metastable $[Sb_8O_8(OH)_4][(OH)_{2-x}(H_2O)_{1+x}]Cl_{2+x}$ has been investigated by X-ray methods. This formula is based on chemical analyses combined with structural evidence and seems to be the most probable one of several discussed. It is orthorhombic, the cell dimensions are given in Table 1. The *c*-axis (needle-axis) is increased fourfold due to extremely weak zones. The small unit cell contains one formula unit, with the space group No. 71, $Immm - D_{2h}^{25}$ as the most probable one. The atomic positions have been found from Patterson and electron density projections. The oxygen positions have been checked from space considerations. The atomic coordinates are given on p. 271 and the interatomic distances in Table 5.

The structure is represented in Figs. 11, 12 and 13. Along the needle-axis there are Sb–O chains which are coupled together forming endless sheets of the composition $[Sb_8O_8(OH)_4^{4+}]_\infty$. All Sb–Cl distances are much longer than the covalent bond length. In channels in the structure there are OH^- and H_2O, which presumably form hydrogen or hydroxyl bonds with each other and the OH groups of the sheet. There are vacancies in the oxygen positions in these channels and in this way holes are formed of sufficient size to accomodate extra chloride ions.

Antimony is surrounded by four oxygens situated at four of the corners of a deformed trigonal bipyramid with one of the equatorial corners unoccupied, perhaps with an unshared electron pair directed towards it. It is similar to the four-coordinations found for some of the antimony atoms in $Sb_4O_5Cl_2$ (*1*) and SbOCl (*2*). This resembles the $TeCl_4$ (*18*) configuration.

The author wishes to thank Professor A. ÖLANDER for his encouraging interest and for valuable discussions. Thanks are also due to Mr. G. BLOMQVIST for drawing some of the figures. The investigation has been financially supported by *Statens Naturvetenskapliga Forksningsråd* (Swedish Natural Science Research Council).

University of Stockholm, Institute of Inorganic and Physical Chemistry, February 1955.

REFERENCES

1. EDSTRAND, M., Acta Chem. Scand. *1*, 178 (1947) (= Part I).
2. EDSTRAND, M., Arkiv Kemi *6*, 89 (1953) (= Part II).
3. EDSTRAND, M., Arkiv Kemi *8*, 279 (1955) (= Part IV).
4. LEA, C. and WOOD, J. K., J. Chem. Soc. *125*, 137 (1924).
5. COOKE, J. P., Proc. Am. Acad. Arts Sci. *13*, 111 (1877).

6. Bloom, M. C. and Buerger, M. J., Z. Krist. *96*, 369 (1937).
7. Kolthoff, I. M., Die Massanalyse, Berlin 1928, p. 443.
8. Kolthoff, I. M. and Furman, N. H., Potentiometric Titrations, 2nd Ed., New York 1947, p. 303.
9. Ibid. p. 147.
10. Hartwig-Bendig, M., Z. angew. Mineral. *3*, 213 (1941).
11. International Tables for X-Ray Crystallography, Vol. I, Birmingham 1952.
12. Internationale Tabellen zur Bestimmung von Kristallstrukturen, Vol. II, Berlin 1935.
13. Booth, A. D., Fourier Technique in X-Ray Organic Structure Analysis, Cambridge 1948, p. 64.
14. Almin, K. E. and Westgren, A., Arkiv Kemi, Mineral. Geol. *15 B*, N:o 22 (1942).
15. Buerger, M. J. and Hendricks, S. B., Z. Krist. *98*, 1 (1938).
16. Kisliuk P., J. Chem. Phys. *22*, 86 (1954).
17. Pauling, L., The Nature of the Chemical Bond, 2nd Ed., Ithaca, New York 1944, p. 111.
18. Stevenson, D. P. and Schomaker, V., J. Am. Chem. Soc. *62*, 1267 (1940).
19. Helmholz, L. and Rogers, M. T., J. Am. Chem. Soc. *62*, 1537 (1940).
20. McCullough, J. D. and Hamburger, G., J. Am. Chem. Soc. *63*, 803 (1941).
21. McCullough, J. D. and Hamburger, G., J. Am. Chem. Soc. *64*, 508 (1942).
22. Diatkina, M., Acta Physicochim. U.R.S.S. *20*, 407 (1945).
23. Wells, A.F., Structural Inorganic Chemistry, 2nd Ed., Oxford 1950, p. 235–258, 413–415.

Tryckt den 25 april 1955

Uppsala 1955. Almqvist & Wiksells Boktryckeri AB

ARKIV FÖR KEMI Band 8 nr 26

Communicated 9 March 1955 by ARNE WESTGREN and GUNNAR HÄGG

On the structures of antimony (III) oxide halogenides. IV

The crystal structure of $Sb_8O_{10}(OH)_2I_2$ and isomorphous bromide and chloride

By MAJA EDSTRAND

With 13 figures in the text

In connection with the structure determination of the needle-shaped crystals of $[Sb_8O_8(OH)_4][(OH)_{2-x}(H_2O)_{1+x}]Cl_{2+x}$ (ref. *3*) it seemed of interest to investigate the needle-shaped crystals of $Sb_8O_{10}(OH)_2X_2$ where X = I, Br, and Cl, specially since they have a needle-axis of about the same length as the first substance.

Preparation

For the structure determination of $Sb_4O_5Cl_2$ and $Sb_4O_5Br_2$ the best crystals were obtained by hydrothermal syntheses (*1*). The only other antimony (III) oxide halogenides known, obtained by hydrolysis of SbX_3, which are not microcrystalline are SbOCl (*2*) and $[Sb_8O_8(OH)_4][(OH)_{2-x}(H_2O)_{1+x}]Cl_{2+x}$ (*3*). It appeared probable that some other products of hydrolysis might be obtained as crystals of sufficient size for single crystal X-ray photographs, by preparation at elevated temperatures.

Some preliminary hydrothermal syntheses were performed with $SbBr_3$ and SbI_3 as starting materials in sealed thick-walled Pyrex or Supremax tubes with an inner diameter of 3–11 mm at temperatures of 180° to 320°C. As expected, crystallization occurred in many cases which was particularly remarkable for the iodides since the products of hydrolysis at room temperature are only microcrystalline. In several cases the crystallization must have taken place in the vapour phase, since there were long crystal needles hanging from the walls above the surface of the liquid. It is not easy to say if there might have been a temperature gradient in the oven favouring the crystallization out of the vapour phase. Some crystal needles of $Sb_8O_{10}(OH)_2Br_2$ were obtained in this way.

Since it was evident that high temperatures had a very favourable influence on the speed of crystallization, it appeared of interest to study the hydrolysis at even higher temperatures. The glass tubes are, however, corroded fairly quickly by water at high temperatures and there seemed therefore to be some risk that matter from the glass might enter into the antimony compounds. For this reason gold tubes were used as reaction vessels. Three tubes equipped with lids and with an inner volume of about 23 ml were of pure gold, and one tube (also with lid) with an inner volume of about 30 ml was of 23 carat gold. After filling, the gold tubes were sealed in Pyrex tubes which then were placed inside an autoclave with a little water outside the Pyrex tube to make the vapour pressures on both sides of the Pyrex walls approximately equal. The autoclaves were manufactured by the American Instrument Company. Three were made of the steel, 18-8 Stainless 316, and one of the steel, 13 Chrome Stainless 410. The vessels were provided with a threaded opening in the head and another in the bottom. These openings were sealed by means of silver gaskets and screws.

Since hydrochloric, hydrobromic or hydroiodic acid would be evolved during the reactions and since these acids when wet can be expected to be highly corrosive, according to information from the manufacturer, to the metals of the autoclaves, it did not seem advisable to allow them to come into contact with the interior of the vessels.

It can be mentioned that the outer surfaces of the Pyrex tubes were white and very rough after an exposure to water for about 12 h at 350°C. The internal side where the vapours were acid was, however, not corroded to any appreciable extent.

Unfortunately it was not possible to quench the products. When the hot autoclave was plunged into water, the vapour pressure outside the Pyrex tube fell much quicker than that inside with the result that the tube exploded. Therefore the autoclaves were just left to cool at room temperature, which took about two or three hours. There always seemed to be some distillation of substance from the gold tubes out into the Pyrex tubes. The reproducibility of the results is a little uncertain, since a synthesis performed in a manner apparently identical with a previous one did not always give the same result. The surfaces of the gold tubes were markedly changed during the experiments and gold crystals sometimes contaminated the products. In these cases it is very difficult to judge if the crystallization has taken place in the liquid phase or the vapour phase inside the gold tubes. Syntheses have been performed with a systematic variation of the proportions of SbX_3 and H_2O. Here, however, only the results of interest in connection with $Sb_8O_{10}(OH)_2X_2$ are given.

$Sb_8O_{10}(OH)_2I_2$ has been obtained inside the gold tubes when mixtures in the weight proportions 1:24 and 1:48 have been kept at 310–315°C for 3–7 days. The crystals were washed with acetone and ether and dried.

$Sb_8O_{10}(OH)_2Br_2$ has been obtained as needles above the liquid surface in Pyrex tubes when $SbBr_3$ and H_2O in the weight proportions 1:20 and 1:30 have been kept at about 185°C for 20 days and at about 280°C for 8 days. The crystals were washed with ethanol and ether and dried. It has been obtained inside the gold tubes when mixtures in the weight proportions 1:24 to 1:60 have been kept at 310–315°C for 5 days. The crystals, which were not always pure phase, were washed with acetone and ether and dried. It may also have been obtained in microcrystalline form by hydrolysis at room temperature when $SbBr_3$ and H_2O have been mixed in the weight proportions 1:30 to 1:200.

$Sb_8O_{10}(OH)_2Cl_2$ has been obtained inside the gold tubes, when mixtures of $SbCl_3$ and H_2O in the weight proportions 1:40 to 1:160 have been kept at 305–310°C for five days. Another phase has also been obtained in this range. The crystals were washed with ethanol and ether and dried.

Analyses and density determination

On account of the limited volumes of the gold tubes only small amounts of substance were obtained. Before analysis, the substances were separated from small quantities of impurities under a microscope. The total amount of purified substance varied between 25 and 115 mg. Because of this, the density was first determined, using the total amount of substance, from the loss of weight in benzene. The benzene was then allowed to evaporate at room temperature from the crystals, which, when they seemed to be dry, were weighed at intervals of one day until their weight was constant. The dry crystals were then used for the analyses.

Samples weighing from 3 to 14 mg were used for the analyses. Duplicate analyses were always performed since this seemed to give better information concerning the accuracy of the analyses

Table 1. Analyses and densities for $Sb_8O_{10}(OH)_2X_2$.

Substance	Sb %	X %	H_2O %	d	Total amount of substance in mg
SbOJ A 8 a	67.76, 68.06	17.94, 18.55		5.54	82
SbOJ A 12 a	69.58, 67.71	18.12, 18.69		5.69	41
obs. m.v.	68.28	18.33		5.62	
$Sb_8O_{11}I_2$ calc	69.38	18.08		5.66	
$Sb_8O_{10}(OH)_2I_2$ calc	68.51	17.85	1.27	5.74	
SbOBr 52 a	74.38, 74.64	11.67, 12.61		5.68	65
SbOBr A 4 a	72.23, 73.33	12.46, 12.81		5.53	114
SbOBr A 8 a	72.42, 72.44	12.51, 12.80		5.50	41
obs. m.v.	73.24	12.48		5.57	
$Sb_8O_{11}Br_2$ calc	74.36	12.20		5.65	
$Sb_8O_{10}(OH)_2Br_2$ calc	73.35	12.04	1.36	5.72	
SbOCl A 7 a	77.42, 77.92	5.71, 6.11		5.22	28
SbOCl A 8 a	77.27, 79.44	5.58, 6.04		5.09	25
obs. m.v.	78.01	5.86		5.16	
$Sb_8O_{11}Cl_2$ calc	79.78	5.81		5.37	
$Sb_8O_{10}(OH)_2Cl_2$ calc	78.62	5.72	1.45	5.45	

than a single analysis of a larger sample. The weighings were performed on an air-damped semimicro balance.

For the halogen analyses, the samples were boiled with a solution containing 0.2–0.5 g sodium carbonate in a platinum dish. After filtration the halogenide was titrated by the Volhard method, in the case of chloride in the presence of nitrobenzene. 0.01-M solutions were used in the titrations and the solution in the titration vessel was cooled with ice to diminish the solubility of the silver halogenides.

For the antimony analyses, the samples were dissolved in hydrochloric acid and titrated with 0.01-N potassium bromate solution with naphthol blue-black as indicator (*4*). In the case of the iodides, the iodide ion had to be removed before the titration, since it would otherwise interfere. Approximately the calculated amount of potassium bromate necessary to oxidize the iodide ion to free iodine was added, and the iodine evaporated by heating. Then a little more bromate was added and the procedure repeated until all iodine had evaporated. Then sodium sulfite was added to reduce any oxidized antimony, the excess of sulfur dioxide evaporated and then the titration performed in the usual way.

Since a water determination would require much substance it could not be performed.

The results are given in Table 1 together with the theoretical values for $Sb_8O_{11}X_2$ and $Sb_8O_{10}(OH)_2X_2$. It appeared at first probable that these compounds would correspond to COOKE's oxide chloride $Sb_8O_{11}Cl_2$ (*5*). The way in which COOKE prepared it seems, however, to suggest that it is identical with $[Sb_8O_8(OH)_4][(OH)_{2-x}(H_2O)_{1+x}]Cl_{2+x}$ (*3*). The analyses alone do not decide between the two alternatives of the formula. The structure determination seems to favour the idealized formula $Sb_8O_{10}(OH)_2X_2$. The structure seems to be a little too compact to allow extra halogenide ions to be taken up.

As far as the author is aware the compounds $Sb_8O_{10}(OH)_2X_2$ have not been described in the literature before, in any case not the iodide and the bromide.

Unit cell and space group

The crystals have a very pronounced needle-shape, which made it very difficult to find the orientation of the axes in a plane perpendicular to the needle-axis. Thus rotation and Weissenberg photographs were taken only around the needle axis (b-axis) with Cu-radiation for all the three oxide halogenides. All the three substances have a b-axis of about 4 Å, which is increased fourfold due to extremely weak zones. Since the chloride gave much weaker photographs, the weak zones could not be observed in this case. Referring to the short b-axis, we have the following set of Weissenberg photographs (in some cases double films): $h0l$, $h1l$, and $h2l$. The reflections in the Weissenberg photographs are often broad. For the iodide and the bromide, Weissenberg photographs were taken of some of the very weak zones using a Mueller tube and very long exposure times. Only the weak zones which are neighbours to strong zones are observed, thus referred to the long b-axis the zones $2 + 4n$ are absent. It was found that the crystals of the chloride were always twinned.

Referred to the small unit cell the crystals are monoclinic. The cell dimensions were determined from the rotation and the Weissenberg photographs. Using $\lambda_{\mathrm{Cu}K\alpha_1} = 1.54051$ Å, where the α_1 and α_2 reflections were separated, and $\lambda_{\mathrm{Cu}K\alpha} = \frac{1}{3}(2\lambda_{\alpha_1} + \lambda_{\alpha_2}) = 1.54176$ Å, where these reflections were not separated, the following values were found:

	$Sb_8O_{10}(OH)_2I_2$	$Sb_8O_{10}(OH)_2Br_2$	$Sb_8O_{10}(OH)_2Cl_2$
a	19.3_1 Å	19.1_2 Å	19.0_3 Å
b	4.1_4 Å	4.0_8 Å	4.0_8 Å
c	10.9_3 Å	10.5_1 Å	10.3_5 Å
β	109.6°	110.0°	110.0°
V	823.2 Å^3	770.4 Å^3	755.1 Å^3

The observed densities indicate two formula units in the unit cell, cf. Table 1.

The intensities were estimated visually and then corrected for the Lorentz and polarization factors using the curves given by KAAN and COLE (*6*).

In the Weissenberg photographs, all reflections with $h + k = 2n + 1$ are systematically absent, which is characteristic of the space groups No. 12, $C2/m - C_{2h}^3$, No. 8, $Cm - C_s^3$, and No. 5, $C2 - C_2^3$ (*7*). To try to decide between these three space groups, the method of intensity statistics (*8, 9*) was applied to the $h0l$ zones of $Sb_8O_{10}(OH)_2I_2$, cf. Fig. 1, and of $Sb_8O_{10}(OH)_2Br_2$, cf. Fig. 2. The intensity distribution seems to

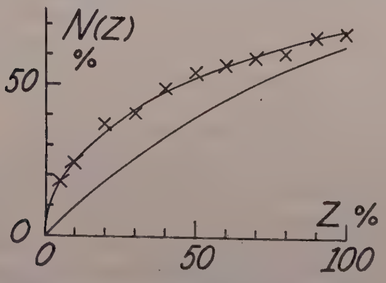

Fig. 1. Intensity statistics for $h0l$ of $Sb_8O_{10}(OH)_2I_2$. × represents the experimental intensity distribution compared with the theoretical centric distribution (upper curve) and the theoretical acentric distribution (lower curve).

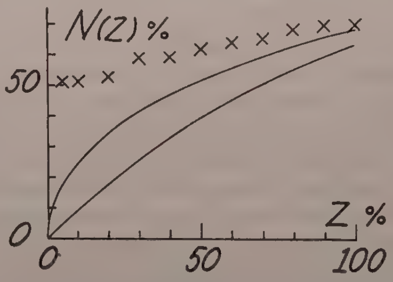

Fig. 2. Intensity statistics for $h0l$ of $Sb_8O_{10}(OH)_2Br_2$. × represents the experimental intensity distribution compared with the theoretical centric distribution (upper curve) and the theoretical acentric distribution (lower curve).

indicate symmetry centres in both cases. It thus seems reasonable to exclude the space group Cm. Since the b-axis of the small cell is only 4 Å, it appears probable that the atoms are situated in or near planes which are 2 Å apart. On account of this, the structure determination was started with the space group $C2/m$.

A complete structure determination has not been carried out for the chloride, since the crystals were twinned in a way which made the $h0l$ and $h0\bar{l}$ reflections coincide when $h = 8$ and 16. Parameters derived from such photographs cannot be very accurate. The photographs (and also Patterson projection) had so many similarities with those of the bromide that there can be no doubt that the substances are isomorphous.

Patterson syntheses and vector convergence diagrams

There are 16 antimony atoms and 4 halogen atoms in the small unit cell. To try to find their positions, the Patterson projection $P(UpW)$ was calculated for the iodide, cf. Fig. 3, and for the bromide, cf. Fig. 4. Considering the space group $C2/m$, the eightfold position $8(j)$ and the fourfold positions $4(h)$, $4(g)$, $4(f)$ and $4(e)$ can be excluded since they would give a distance between atoms of the same sort ≤ 2 Å. It seemed probable that the majority of the atoms would be situated in the fourfold position $4(i)$. With positions of this kind we have the following vectors in the Patterson projection $P(UpW)$:

of weight 2	A	$\pm(2x_i, 2z_i)$	
	B	$\pm(\frac{1}{2}+2x_i, 2z_i)$	
of weight 4	C	$\pm(x_i - x_j, z_i - z_j)$	$i \neq j$
	D	$\pm(x_i + x_j, z_i + z_j)$	
	E	$\pm(\frac{1}{2}+x_i - x_j, z_i - z_j)$	
	F	$\pm(\frac{1}{2}+x_i + x_j, z_i + z_j)$	
	G	$\frac{1}{2}, 0$	

From the appearance of the Patterson projections, it is obvious that many peaks coincide or almost coincide. In this case maxima corresponding to the vectors A and B would give a key to the structure. Since their weight is only two, false details might easily be mistaken for such maxima. By a comparison of the two projections we find that there are two low peaks marked as I and II which are found in both projections. It seemed therefore probable that they would correspond to Sb–Sb vectors of the type A or B. The best way to try to find out how the heavy atoms are situated relatively to each other seemed to be by applying the "Vector Convergence Method" described by BEEVERS and ROBERTSON (*10*). With the assumption that the peak I corresponds to a vector B, x- and z-parameters have been derived for one heavy atom and the xz-vector convergence diagrams, which are given in Fig. 5 for the iodide and in Fig. 6 for the bromide, have been constructed. By a comparison between the two diagrams it appeared probable that the hatched areas would correspond to positions of heavy atoms. Since these positions accounted for the peak II, it was not necessary to use this peak for an alternate vector convergence diagram.

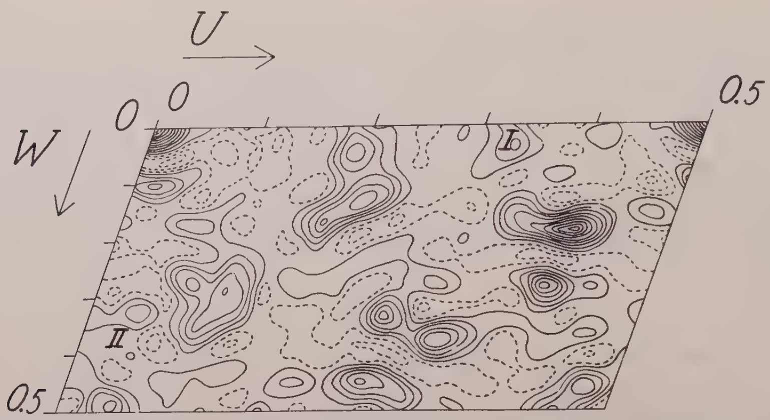

Fig. 3. $P(UpW)$ of $Sb_8O_{10}(OH)_2I_2$. Contours at an interval of 100 arbitrary units. Negative values dotted.

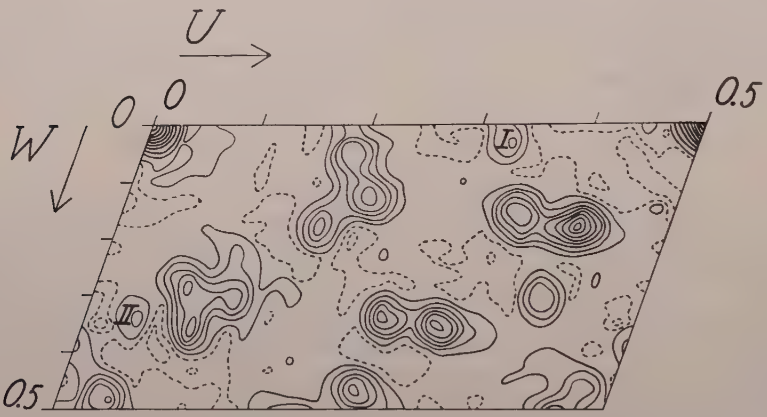

Fig. 4. $P(UpW)$ of $Sb_8O_{10}(OH)_2Br_2$. Contours at an interval of 100 arbitrary units. Negative values dotted.

Fourier syntheses

The approximate parameters obtained from the vector convergence diagrams have been refined by Fourier syntheses. The syntheses have been calculated with $|F_{\mathrm{obs}}| = \sqrt{\frac{I}{Lp}}$, where F is the structure factor, I the estimated intensity and Lp are the combined Lorentz and polarization factors. In all syntheses the value of $F(000)$ has been omitted. Correction for absorption has not been applied. The maxima have been located using the interpolation table given by BOOTH (*11*).

The refinement proceeded in the usual way. Already in the first projection of the bromide, it was evident which one of the atomic positions corresponded to the halogen position. The final $\varrho(XpZ)$-projections are given for the iodide in Fig. 7 and for the

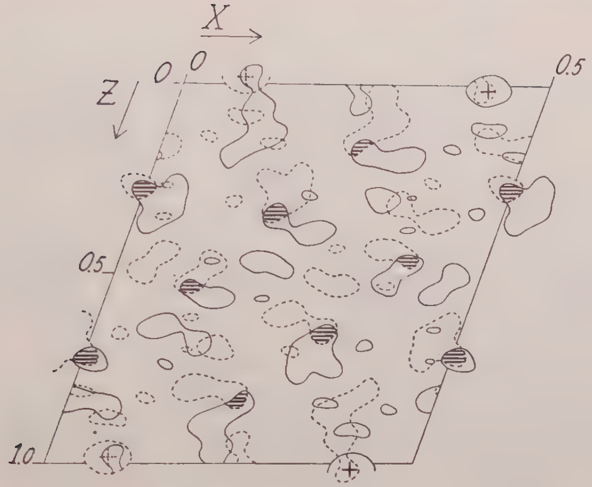

Fig. 5. The xz-vector convergence diagram of $Sb_8O_{10}(OH)_2I_2$. The centres of the atomic positions derived from the peak I in $P(UpW)$ are marked with crosses. Only the positive 100 contour in $P(UpW)$ has been drawn. One set of Patterson maxima is marked with full lines and the other with dotted lines. The hatched areas indicate convergence to positions of heavy atoms.

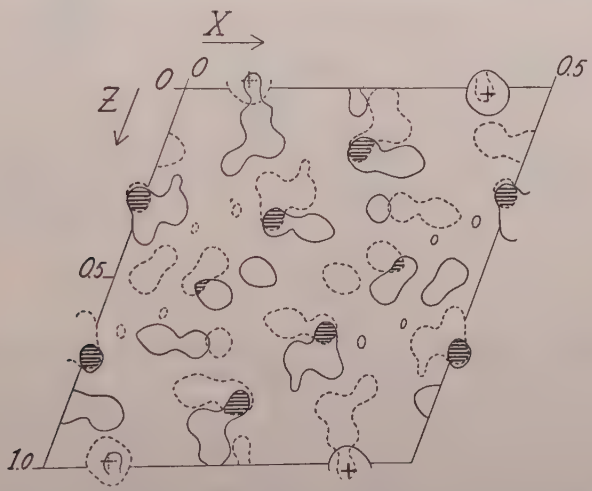

Fig. 6. The xz-vector convergence diagram of $Sb_8O_{10}(OH)_2Br_2$. The centres of the atomic positions derived from the peak I in $P(UpW)$ are marked with crosses. Only the positive 100 contour in $P(UpW)$ has been drawn. One set of Patterson maxima is marked with full lines and the other with dotted lines. The hatched areas indicate convergence to positions of heavy atoms.

bromide in Fig. 8. From a comparison of the two projections it is obvious which peak corresponds to the halogen. From a comparison between calculated and observed $F(h10)$ values, it was easily found which of the atoms are situated in $y = 0$ and which ones in $y = \frac{1}{2}$. From these considerations we arrived at the following coordinates for the heavy atoms, all situated in 4(i), and chosen so that $y = 0$.

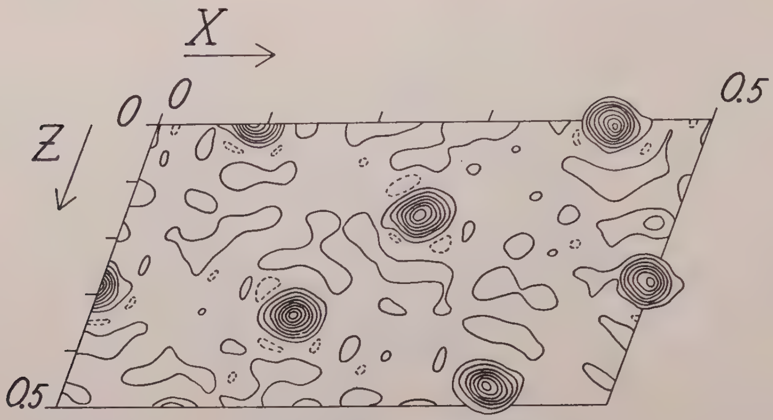

Fig. 7. $\varrho(XpZ)$ of $Sb_8O_{10}(OH)_2I_2$. Contours at an interval of 400 arbitrary units. Negative values dotted.

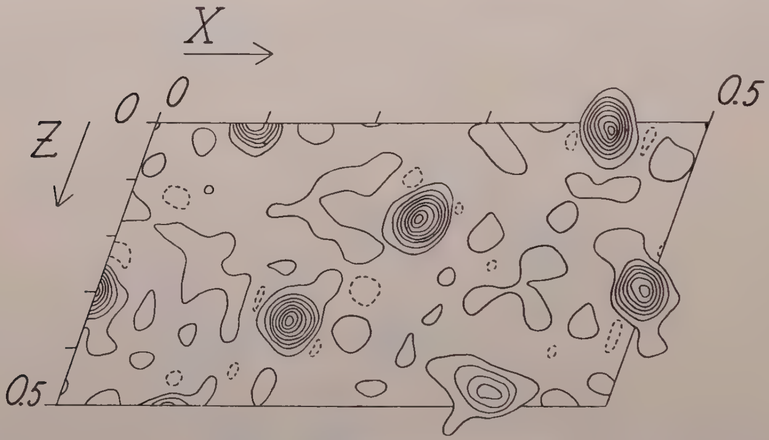

Fig. 8. $\varrho(XpZ)$ of $Sb_8O_{10}(OH)_2Br_2$. Contours at an interval of 200 arbitrary units. Negative values dotted.

	$Sb_8O_{10}(OH)_2I_2$		$Sb_8O_{10}(OH)_2Br_2$	
	x	z	x	z
Sb_1	0.268_5	0.164_5	0.270_5	0.168_8
Sb_2	0.495_8	0.283_3	0.495_5	0.296_2
Sb_3	0.085_8	0.991_0	0.086_8	0.987_0
Sb_4	0.314_7	0.661_8	0.314_7	0.650_5
X	0.114_7	0.534_5	0.110_2	0.523_7

It is a little difficult to make any statements about the accuracy of the parameters.

It can be mentioned that before these direct methods were used and when only a Patterson projection of the bromide with not very well resolved peaks was available, a sort of trial and error Fourier method was adopted, since this Patterson projection

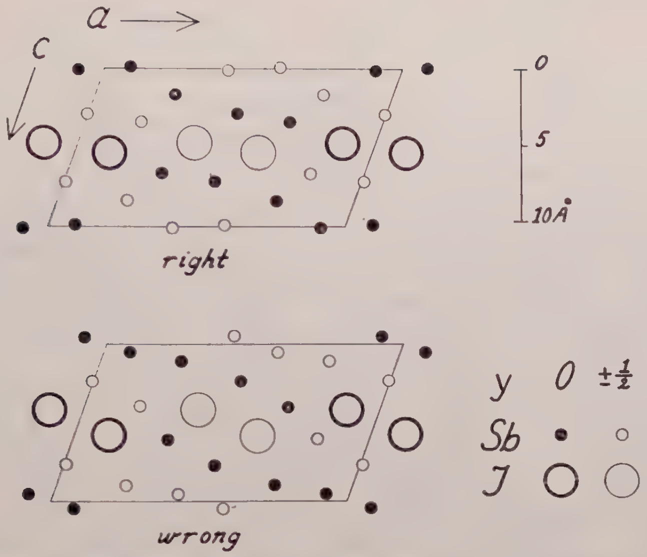

Fig. 9. $Sb_8O_{10}(OH)_2I_2$. Comparison between the projections of the positions of the heavy atoms in the finally accepted structure and in the wrong structure.

did not seem to permit an interpretation. This gave peaks in the Fourier projection, which apparently corresponded to plausible antimony positions. When a photograph of the iodide was obtained, Fourier projections were directly calculated and indicated the same antimony positions. It seemed a little peculiar that peaks, which might correspond to halogen positions, were very low specially in the case of the iodide. The atomic positions explained the high peaks in the Patterson projections quite satisfactorily, but did not account for some of the low peaks e.g. those marked as I and II. When the reliability factor

$$R = \frac{\Sigma \left| |F_o| - |F_c| \right|}{\Sigma |F_o|}$$

was calculated for the iodide it was found to be about 0.45, which seemed very dubious, specially since there were considerable amounts of false details in the Fourier projections. With the atomic positions found from the vector convergence diagram and refined by one Fourier projection, the R-value for the iodide was 0.24, which thus was a considerable improvement. This made the new alternative seem much more probable. Only considering the heavy atoms, the right and wrong structures have many features in common which can be seen in Fig. 9. It is thus obvious that Fourier methods must be handled with some care. Similar remarks have been made for instance by LUZZATI in connection with the structure determination of $HNO_3 \cdot 3H_2O$ (*12*).

The oxygen positions

It did not seem likely that the low peaks in the electron density projections would give any reliable indications of the oxygen positions. Therefore they have been located from space considerations.

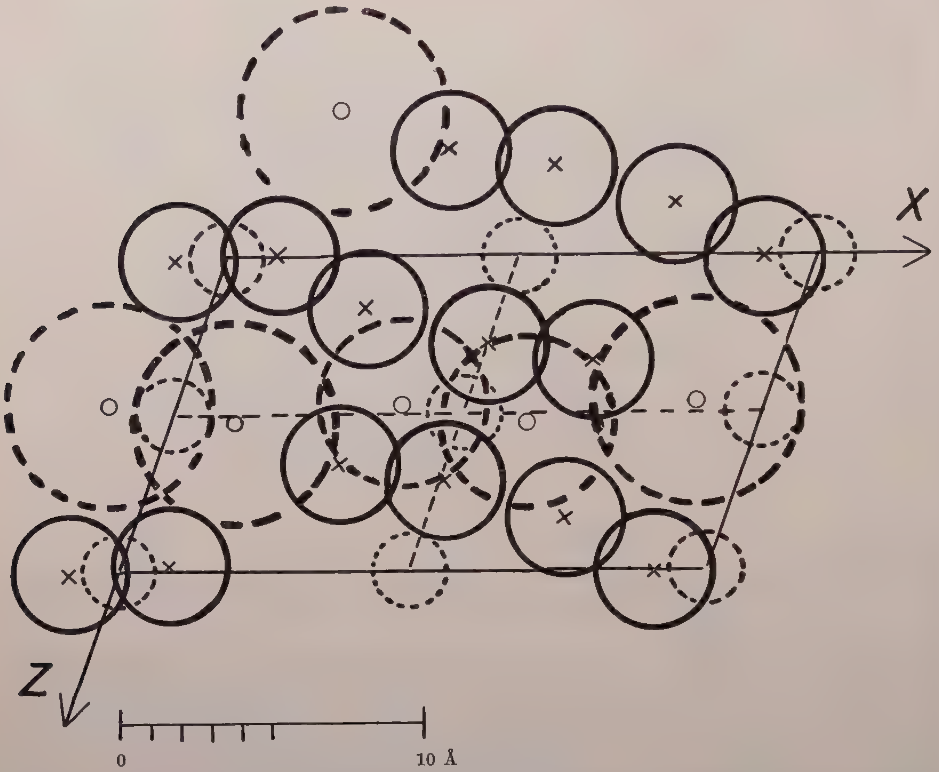

Fig. 10. Cut at $y = 0$ for the localization of the oxygen atoms. × centre of Sb, thick circle = forbidden area around Sb. ○ projection of centre of I, thick dotted circle = forbidden area around I. Thin dotted circle = forbidden area around symmetry centre.

In the needle-shaped crystals of $[Sb_8O_8(OH)_4][(OH)_{2-x}(H_2O)_{1+x}]Cl_{2+x}$ with a needle-axis of about 4 Å, it has been found that there are Sb–O chains along this axis (*3*). This fact strongly suggests that there are similar chains in $Sb_8O_{10}(OH)_2X_2$, since the needle-axis has approximately the same length.

In the oxides, the Sb–O distance is 2.0 kX (*13, 14*). The sum of the ionic radii of oxygen and iodine or bromine are with values from Internationale Tabellen (*15*):

O–I	3.52 kX	(Goldschmidt),	3.56 kX	(Pauling)	
O–Br	3.28 „	„	3.35	„	„
O–O	2.62 „	„	2.80	„	„

In this discussion only the details from the iodide will be given. Spheres of appropriate radii, inside which no oxygen centres could occur, were imagined around the antimony and iodine centres. Considering the space group $C2/m$ and the short *b*-axis, the atoms can only be situated in the mirror planes perpendicular to this axis with a distance between these planes of about 2 Å. Therefore it is only necessary to make a cut at $y = 0$.

In the cut given in Fig. 10 the areas are marked which are forbidden by antimony, iodine and the fact that an oxygen atom must not come too close to its centrosymmetrically situated oxygen neighbour. There is obviously a considerable space

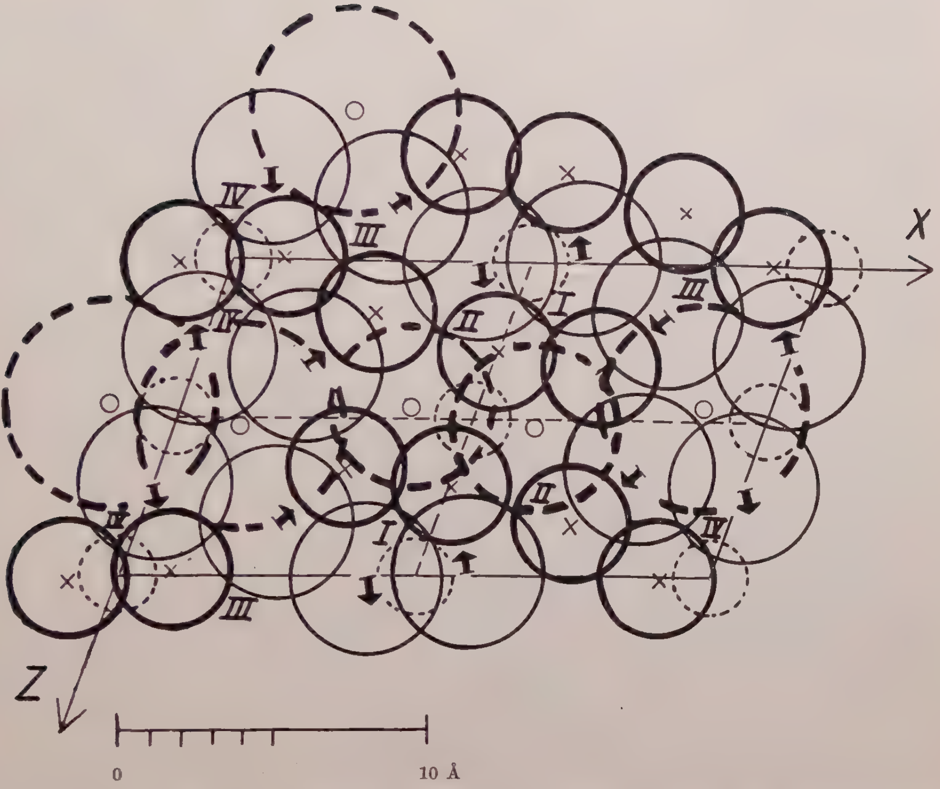

Fig. 11. Cut at $y = 0$ for the localization of the oxygen atoms. × centre of Sb, thick circle = forbidden area around Sb. ○ projection of centre of I, thick dotted circle = forbidden area around I. Thin dotted circle = forbidden area around symmetry centre. Thin circle = forbidden area around O. The small arrows indicate the direction in which an oxygen in one chain has to be moved to come in closer contact with antimony in a neighbouring chain. Possible oxygen positions at I, II, III, and IV.

for oxygen atoms. As mentioned above there are reasons to suggest Sb–O chains along the needle-axis. As a starting point we assume that an oxygen atom in a Sb–O chain is situated exactly between two antimony atoms in straight line with them, although a Sb–O–Sb angle of 180° is not very favourable. In Fig. 11 those positions are marked where there now is room or nearly room for additional oxygen atoms. Ruling out positions which would give an oxygen atom in contact with only one antimony, we have possible positions at I, II, III, and IV. It appears at first a little difficult to decide between these positions for the remaining oxygen atoms. When the structure determination was started we thought that the formula was $Sb_8O_{11}X_2$ in analogy with Cooke's formula $Sb_8O_{11}Cl_2$ (*5*). This meant that there would be, besides the sixteen oxygens in the chains, still six oxygens to locate presumably in one twofold and one fourfold position. It is a striking fact that with the space group $C2/m$ there scarcely seems to be any room in the twofold positions. From Fig. 10 it is obvious that oxygen in $2(a)$ $0, 0, 0$ would be squeezed between two antimony atoms, and oxygen in $2(b)$ $0, \frac{1}{2}, 0$ would not come into contact with any antimony atoms at all.

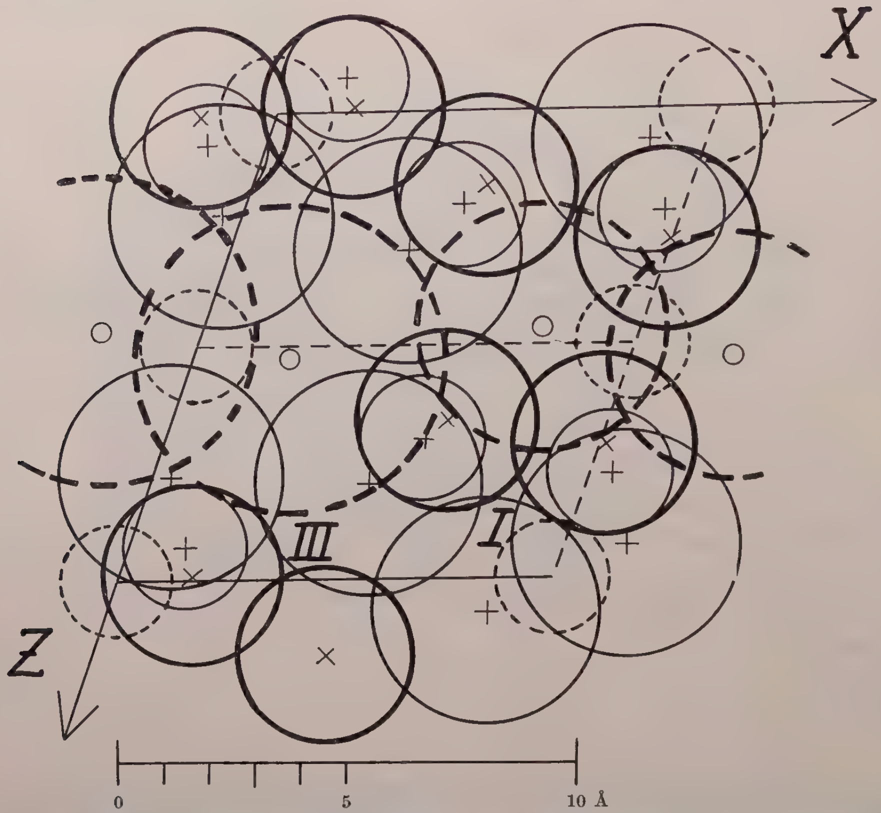

Fig. 12. Cut at $y = 0$ for the localization of the oxygen atoms. The chain oxygen atoms have been included with their final positions. × centre of Sb, thick circle = forbidden area around Sb. ○ projection of centre of I, thick dotted circle = forbidden area around I. Thin dotted circle = forbidden area around symmetry centre. + projection of centre of O, thin circle = forbidden area around O. Possible oxygen positions at I and III.

If we assume perfectly straight Sb-O chains we find that the distance from one oxygen to an antimony atom in the nearest Sb–O chain is 2.8–2.9 Å for all the four different chains. This is exactly the same distance as we would obtain in $[Sb_8O_8(OH)_4][(OH)_{2-x}(H_2O)_{1+x}]Cl_{2+x}$ if we made the same assumption of straight chains. In the latter structure we have found from electron density projections that the oxygens in the chain are moved out from the straight line so that they come approximately in contact with antimony atoms in the neighbouring chain, an oxygen atom in a chain thus being almost equidistant to three antimony atoms. It seems reasonable to assume that the Sb–O chains in the structure under investigation have close similarities with these chains. In Fig. 11 the small arrows point in the direction the oxygen atoms have to be moved to come into closer contact with antimony atoms in neighbouring chains.

We make the assumption that an oxygen atom in a chain is situated approximately equidistant to its three nearest antimony neighbours, and we assume also that this is the minimum distance. With these new oxygen positions we make a cut at $y = 0$ to locate the remaining oxygen atoms, see Fig. 12. It is obvious that the only places, where there is room for other oxygen atoms, are those indicated as I and III, since they would be considerably squeezed by other atoms if other positions were assumed. I and III correspond, however, to two fourfold positions and with the formula $Sb_8O_{11}I_2$ we have only six oxygens left. Considering the space group $C2/m$ there is, however, clearly no room in any of the twofold positions. We might assume the lower space group $C2$ but still with the Sb–O chains according to $C2/m$. Then the twofold position $2(a)$ $0, y, 0$ appears at first likely, but oxygen here comes either in too close contact with the antimony atoms Sb_3 or the oxygen atoms O_3 (it seems convenient to have the same index for antimony and oxygen belonging to the same Sb–O chain).

By calculating the Sb–I distances we find that they are all very long, the shortest being 3.5_7 Å. Since the Sb–I distance found in SbI_3 in the gas phase by electron diffraction methods is 2.75 ± 0.02 kX (*16*) or 2.70 kX (*17*), it does not appear probable that there are any covalent bonds between antimony atoms and iodine atoms. There is thus no special reason for any antimony atom to have an oxygen coordination different from that of the other antimony atoms. We find now that with eight oxygen atoms situated in the two fourfold positions marked as I and III, all the antimony atoms are surrounded by four oxygen atoms in the same type of four-coordination as has been found in $[Sb_8O_8(OH)_4][(OH)_{2-x}(H_2O)_{1+x}]Cl_{2+x}$ (*3*). For the reason of electro-neutrality either some of the oxygens must correspond to hydroxyl groups or some of the antimony atoms must be pentavalent. Some tests for pentavalent antimony were made with diphenylamine, but they were negative. Thus it appeared more likely to assume hydroxyl groups, corresponding to the formula $Sb_8O_{10}(OH)_2I_2$. Another possibility would be that there are vacancies in the oxygen positions corresponding to the formula $Sb_8O_{11}I_2$. However, a closer inspection of the structure seems to favour the formula $Sb_8O_{10}(OH)_2I_2$, which will be discussed in the next section. We arrive then at the following set of probable oxygen positions:

	$Sb_8O_{10}(OH)_2I_2$		$Sb_8O_{10}(OH)_2Br_2$	
	x	z	x	z
O_1	0.25_1	0.79_7	0.25_0	0.79_0
O_2	0.02_2	0.77_8	0.02_3	0.76_9
O_3	0.43_3	0.07_0	0.43_1	0.07_6
O_4	0.20_5	0.29_8	0.20_6	0.30_7
O_5 (OH) . .	0.19_0	0.98_6	0.19_1	0.98_5
O_6	0.41_9	0.78_7	0.42_0	0.77_7

It is impossible to make any statements concerning the accuracy of the oxygen parameters.

F-values were then calculated as

$$\text{for the iodide } F_{\text{calc}} = \text{const}\left[\sum_1^4 A_{\text{Sb}_i} + \frac{f_{\text{I}}}{f_{\text{Sb}}} A_{\text{I}} + \frac{f_{\text{O}}}{f_{\text{Sb}}} \sum_1^6 A_{\text{O}_i}\right]$$

$$\text{for the bromide } F_{\text{calc}} = \text{const}\left[f_{\text{Sb}} \sum_1^4 A_{\text{Sb}_i} + f_{\text{Br}} A_{\text{Br}} + f_{\text{O}} \sum_1^6 A_{\text{O}_i}\right]$$

where f_{Sb}, f_{I}, f_{Br}, and f_{O} are the atomic scattering factors of antimony, iodine, bromine, and oxygen with due consideration being taken to their variation with θ (*15*). The calculated and observed F-values are given for $h0l$ of $Sb_8O_{10}(OH)_2I_2$ in Table 2, for

Table 2. Calculated and observed F-values of $h0l$ for a Weissenberg photograph of $Sb_8O_{10}(OH)_2I_2$. Cu$K\alpha$-radiation.

h	$h00$		$h01$		$h02$		$h03$		$h04$		$h05$		$h06$		$h07$		$h08$		$h09$		$h010$		$h011$		$h012$		$h013$	
	F_c	F_o	F_c	F_o	F_c	F_o	F_c	F_o	F_c	F_o	F_c	F_o	F_c	F_o	F_c	F_o	F_c	F_o	F_c	F_o	F_c	F_o	F_c	F_o	F_c	F_o	F_c	F_o
22	51	71	49	50	−20																							
20	−14	13	13	12	−68	39	26	25	32																			
18	13	14	−23	13	10		−54	46	−27	20	−30	23	−49															
16	37	20	−54	45	−43	37	1		46	25	−41	23	19		−45													
14	−8		70	65	−10	14	3		32	20	−36	30	−13	21	62	70	51	45										
12	38	33	11		−28	18	42	33	12	14	78	60	−5		20	12	9	10	4									
10	58	81	29	42	−4		44	41	14	13	−43	34	−9		65	56	−13	12	35	34	−19							
8	20	18	−30	28	−25	25	−76	79	44	39	−14	13	−16	20	−3		−22	23	−84	92	10	13	38					
6	−14	17	−40	58	−10	9	22	20	−19	16	−67	72	−11	23	−37	40	36	37	−33	30	−12	20	−33	24	−22			
4	12	12	35	52	−100	133	4		14		−8	16	−6		44	47	−46	55	−46	54	28	13	−2		25	22		
2	−3		−4		24	21	45	39	21	25	25	18	−59	82	47	52	29	39	26	20	15	19	58	58	−53	57	18	
0			2		−4		17	16	35	37	−2		65	86	35	47	−5		11	14	−7		56	69	19	33	31	20
−2			5		−4		3		75	64	−57	64	−20	18	0	12	12	13	−33	34	66	83	−18	13	−43	44	−14	8
4			−2	6	−38	46	−12	13	−53	53	−10	9	−5		2		8	18	−76	98	−17	20	−5		−8	20	−42	45
6			−37	52	−86	142	53	64	−6	9	−38	35	−48	35	10		−64	77	13	14	−1		−3		−31	34	−50	67
8			−10	12	1	9	−33	30	5	10	−27	33	−22	26	70	59	−3		−28	31	−11		22	24	−48	62	69	74
10			−62	78	15	20	44	47	63	57	−1		43	47	−15	13	34	27	5		43	40	61	71	0		22	
12			63	68	−10		44	51	32	32	−45	54	36	34	53	45	24	20	−15		45	48	−43	37	25	25	17	25
14			−7	13	−34	29	29	13	2		35	30	−36	31	22	20	−31	24	−44	31	32	27	36	30	−36	44	−29	24
16			−33	34	−12	14	33	31	−51	46	−56	53	−23	14	17		−34	28	11	14	−59	42	−7	12	−56	65	−15	
18			−54	31	−43	34	−44	37	31	20	−60	44	4	14	7	14	−63	44	−56	33	25	20	10		−33	50		
20			−29	22	30	32	21	23	1	14	−40	19	1		0		64	37	−26	16	40	37	2		−25			
22			20	15	−52	27	65	49	1	16	14		60	52	45	30	−22	14	5	9	39	56	18					
24			19		16	20	56	50	28	24	2	11	−38	32	74	54	−12											

Table 3. Calculated and observed *F*-values of *h0l* for a Weissenberg photograph of $Sb_8O_{10}(OH)_2Br_2$. Cu$K\alpha$-radiation.

h	*h*00		*h*01		*h*02		*h*03		*h*04		*h*05		*h*06		*h*07		*h*08		*h*09		*h*010		*h*011		*h*012		*h*013	
	F_c	F_o	F_c	F_o	F_c	F_o	F_c	F_o	F_c	F_o	F_c	F_o	F_c	F_o	F_c	F_o	F_c	F_o	F_c	F_o	F_c	F_o	F_c	F_o	F_c	F_o	F_c	F_o
22	28	38	17	5																								
20	-2		1		-22	10	11	10																				
18	5		-9		1		-29	37	-9		-19																	
16	11		-25	45	-27	24	14	14	12		-16		4															
14	0		40	47	-10		6		10		-16	16	0		40	40	1											
12	30	29	-3		-7		20	17	16	17	34	35	-4		10		1		4									
10	43	52	20	34	0		26	34	4		-32	32	14		21	19	-3		9									
8	7		-16	12	-28	28	-40	40	27	30	-13		-8		-2		-24	21	-36	33	23	10						
6	-10		-31	31	-7		21	14	-28	27	-34	43	-13	10	-8		11		-15		-6		-12					
4	18	12	20	21	-79	57	8		10		-9	11	8		21		-37	39	-3		11		4					
2	-3		-5		28	28	33	38	23	20	3		-25	28	33	32	14		12		22	13	10		-23	10		
0			6		-8	9	24	22	20	18	3		50	55	9		0		0		6		19	15	8			
-2			5		-11	14	15	19	47	56	-46	54	-11		4		-11		-3		30	22	-29	13	-15		-6	
4			-11	12	-27	32	-16	19	-44	54	-6		-5		7		-12		-37	42	-4		-5		-17	8	4	
6			-39	36	-64	54	43	46	-8	9	-33	38	-15	13	-5		-35	42	16		-1		-2		-19		-13	
8			4		-1		-16	14	3		-24	36	4		44	47	-8		-9		10		-5		-4		40	35
10			-42	39	12		39	42	34	35	9		26	29	-5		16	14	4		32	22	22	13	-4		4	
12			33	41	-1		34	40	12		-31	37	29	29	25	31	0		6		9		-26	9	14	8	9	
14			-9	13	-17	13	8		4		10		-15	10	8		-31	22	-17		20	16	0		-22	16	4	
16			-19	28	-7		20	17	-36	42	-30	45	-8		-3	10	-13	10	3		-24	18	-10		-27	20	3	
18			-22		-27	39	-16	14	6		-27	32	13	10	2		-39	40	-10		16	13	-6	7	3			
20			-19	20	22	21	13	25	2		-13		2	13	8		23	17	-1		27	20	-6					
22			6		-14		27	34	-2		7		39	47	12	7	-8		8	12	10							
24			8		4		26	13	13	16	-5		-9		22	19	-13		18									

Table 4. Calculated and observed F-values of hll for a Weissenberg photograph of $Sb_8O_{10}(OH)_2Br_2$. Cu$K\alpha$-radiation.

h	$h,1,0$		$h,1,1$		$h,1,2$		$h,1,3$		$h,1,4$		$h,1,5$		$h,1,6$		$h,1,7$		$h,1,8$		$h,1,9$		$h,1,10$		$h,1,11$		$h,1,12$	
	F_c	F_o	F_c	F_o	F_c	F_o	F_c	F_o	F_c	F_o	F_c	F_o	F_c	F_o	F_c	F_o	F_c	F_o	F_c	F_o	F_c	F_o	F_c	F_o	F_c	F_o
21	−22	17	13		37	29																				
19	10		−34	37	−10		−15		−24																	
17	−44	48	−6		14		−23		−6		−28	31														
15	−14		−10		13		−25	33	−19		36	36	13		−13											
13	−22	26	16		17	20	42	42	−8		18		10		−5		14									
11	3		38	47	30	22	−18		6		35	37	14	19	23	17	−5		7							
9	−7	10	−39	39	43	51	−2		−5		14		−14		−48	41	18	12	5		−15					
7	−10		13		−13		−42	41	−28	30	−24	13	15	20	−29	24	−8		−9		−31	31				
5	−80	82	−13		−5		−31	31	−5		27	12	−39	27	−27	24	−3		2		14		−6			
3	−5		18	15	17	14	−2		−57	63	32	33	8		0		27	20	25	14	−37	35	20			
1	−5		18		17	12	−2		50	49	38	36	22	20	1		−4		40	44	17		16		24	10
−1			16		90	99	−24	23	5		18	24	−3		1		53	53	−12		−14		−9		2	
3			−15	11	−27	25	−9		−10		23	16	12	15	−58	64	−5		−4		−26	14	−2		21	
5			32	29	−4		−18	20	−16	20	−17	16	−57	59	3		−5		3		−27	20	−37	28	−4	
7			−25	26	−5		−50	54	−35	39	55	62	−20	19	−30	32	2		−10		−28	24	40	23	3	
9			5		27	28	14		20	17	−14	11	10		−10		30	27	46	40	−8		−1		25	25
11			39	51	35	39	−45	46	29	29	40	52	20		16		29	34	−22		20		17		33	24
13			−4		22	25	29	36	−10		24	31	−18		−29	24	35	37	17		−20	19	5		−2	
15			37	39	−24		−25	35	−17		1		−6		13		−23	24	−8		−39	40	−6		16	
17			−31	37	10		−30	44	4		12		−54	63	−28	48	6		−9		−15		5		−30	
19			2		7		−24	14	−16	14	−6		22		−16	18	25	17	−6		−42	31	9			
21			21	24	2		−5		42	46	19	37	−5		−1		11		11		31					
23			33	25	32	38	0		−18		32	42	−6		17		37									

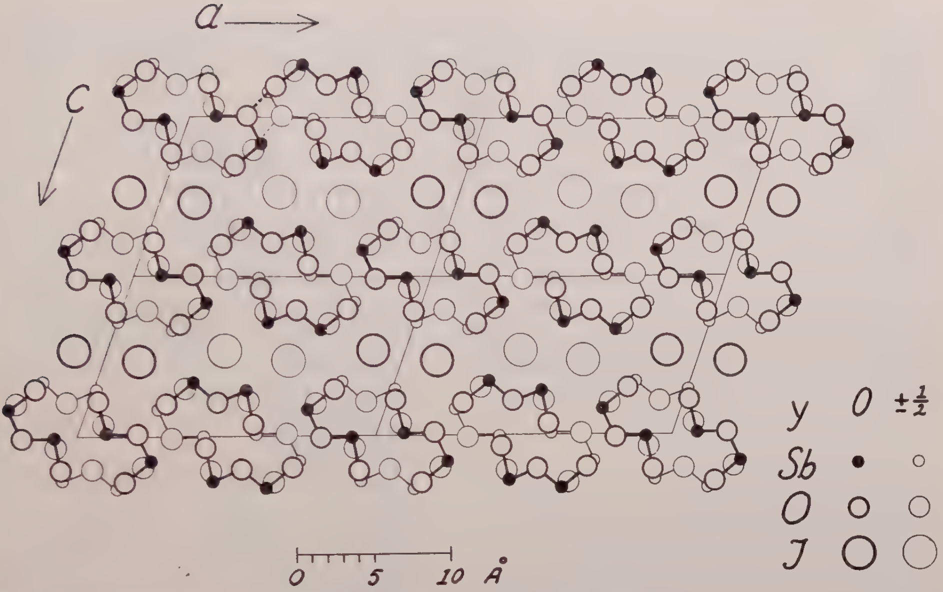

Fig. 13. Projection of the structure of $Sb_8O_{10}(OH)_2I_2$. Four adjacent unit cells are given. Sb–O contacts are marked as full lines. Probable hydrogen bonds are indicated by dotted lines, but only at one place.

$Sb_8O_{10}(OH)_2Br_2$ *h0l* in Table 3, and *h1l* in Table 4. When only observed reflections have been included, we have the following reliability factors for *h0l* of the iodide: $R = 0.22$ with the oxygens included and $R = 0.24$ without the oxygens, for *h0l* of the bromide: $R = 0.21$ with the oxygens included and $R = 0.23$ without the oxygens, and for *h1l* of the bromide: $R = 0.16$ with the oxygens included and $R = 0.18$ without the oxygens. It is thus obvious that the oxygens improve the *R*-values and this fact seems to indicate that the assumed oxygen positions are probable. When the oxygens had been located in the wrong structure they did not improve the *R*-values. These facts appear to indicate the proposed structure as being reasonable.

Discussion of the structure

A projection along the needle-axis of the structure of $Sb_8O_{10}(OH)_2I_2$ is given in Fig. 13. Interatomic distances are given for both the iodide and bromide in Table 5. In the following, only the iodide is discussed in detail since the corresponding distances for the bromide are easily found in Table 5. As has been mentioned before, there are –Sb–O–Sb–O– chains along the needle-axis. All of the antimony atoms are involved in the formation of such chains. The Sb–O distance is 2.1_7 Å within all the different chains. The chains are grouped together in pairs so that antimony in one chain is in contact with oxygen in the neighbouring chain at a distance varying between 2.2_0 and 2.2_4 Å. These double chains are joined by oxygens or hydroxyl groups with Sb–O distances varying between 2.0_2 and 2.0_4 Å forming flat "cylinders" consisting of four double chains, in this respect being thus similar to $[Sb_8O_8(OH)_4][(OH)_{2-x}(H_2O)_{1+x}]Cl_{2+x}$ although there are sheets and not "cylinders" in the latter structure. As has been mentioned on p. 291, all the Sb–I distances are much longer than the corresponding covalent bond length.

Table 5. Interatomic distances in $Sb_8O_{10}(OH)_2X_2$. Å units. The numerical $2\times$ before a distance means that it occurs twice. (H) after a distance indicates a probable hydrogen bond.

	$Sb_8O_{10}(OH)_2I_2$	$Sb_8O_{10}(OH)_2Br_2$
$Sb_1-4\,O$	$2\times 2.1_7$ (in Sb–O chain), 2.0_3, 2.2_0	$2\times 2.1_5$ (in Sb–O chain), 2.0_1, 2.2_1
$Sb_1-2\,X$	3.9_0	3.8_4
$Sb_2-4\,O$	$2\times 2.1_7$ (in Sb–O chain), 2.0_4, 2.2_4	$2\times 2.1_4$ (in Sb–O chain), 2.0_1, 2.2_2
$Sb_2-4\,X$	$2\times 3.5_9$, $2\times 3.9_6$	$2\times 3.3_3$, $2\times 3.8_0$
$Sb_3-4\,O$	$2\times 2.1_7$ (in Sb–O chain), 2.0_3, 2.2_4	$2\times 2.1_4$ (in Sb–O chain), 2.0_0, 2.2_0
$Sb_4-4\,O$	$2\times 2.1_7$ (in Sb–O chain), 2.0_2, 2.2_2	$2\times 2.1_5$ (in Sb–O chain), 2.0_0, 2.2_2
$Sb_4-3\,X$	$2\times 3.5_7$, 3.6_4	$2\times 3.3_7$, 3.6_7
$O_1\ -3\,Sb$	$2\times 2.1_7$, 2.2_2	$2\times 2.1_5$, 2.2_2
$O_2\ -3\,Sb$	$2\times 2.1_7$, 2.2_4	$2\times 2.1_4$, 2.2_0
$O_3\ -3\,Sb$	$2\times 2.1_7$, 2.2_4	$2\times 2.1_4$, 2.2_2
$O_4\ -3\,Sb$	$2\times 2.1_7$, 2.2_0	$2\times 2.1_5$, 2.2_1
$O_5\ -2\,Sb$	2.0_3, 2.0_3	2.0_0, 2.0_1
$O_6\ -2\,Sb$	2.0_2, 2.0_4	2.0_0, 2.0_1
$X\ -9\,Sb$	$2\times 3.5_7$, $2\times 3.5_9$, 3.6_4, $2\times 3.9_0$, $2\times 3.9_6$	$2\times 3.3_7$, $2\times 3.3_3$, 3.6_7, $2\times 3.8_4$, $2\times 3.8_0$
$X\ -8\,O$	3.1_8, 3.5_5, 3.5_7, 3.6_7, $2\times 3.9_3$, $2\times 3.9_4$	3.1_4, 3.2_5, 3.3_7, 3.5_2, $2\times 3.9_3$, $2\times 3.6_4$
$O_1\ -X$	3.1_8	3.1_4
$O_2\ -2\,X$	3.5_5, 3.6_7	3.2_5, 3.5_2
$O_4\ -3\,X$	3.5_7, $2\times 3.9_3$	3.3_7, $2\times 3.9_3$
$O_6\ -2\,X$	3.9_4	3.6_4
$O_1\ -6\,O$	$2\times 2.5_9$, 2.7_0(H), $2\times 3.0_6$, 3.2_8	$2\times 2.5_5$, 2.6_6(H), $2\times 3.0_3$, 3.3_0
$O_2\ -5\,O$	$2\times 2.6_1$, $2\times 2.8_9$, 3.2_8	$2\times 2.5_7$, $2\times 2.8_6$, 3.2_4
$O_3\ -7\,O$	$2\times 2.6_1$, 2.7_6, 3.0_1, $2\times 3.0_5$, 3.4_2	$2\times 2.5_7$, 2.7_4, 3.0_8, $2\times 3.0_0$, 3.5_2
$O_4\ -5\,O$	$2\times 2.5_9$, $2\times 3.0_6$, 3.3_2	$2\times 2.5_5$, $2\times 3.0_5$, 3.3_0
$O_5\ -9\,O$	2.7_0(H), $2\times 3.0_5$, $2\times 3.0_5$, $2\times 3.0_6$, 3.2_8, 3.3_2	2.6_6(H), $2\times 2.9_8$, $2\times 3.0_0$, $2\times 3.0_3$, 3.2_4, 3.3_0
$O_6\ -7\,O$	2.7_6, $2\times 2.8_9$, 3.0_1, $2\times 3.0_6$, 3.2_8	2.7_4, $2\times 2.8_6$, 3.0_8, $2\times 3.0_5$, 3.3_0
$X\ -3\,X$	$2\times 4.1_4$, 4.2_4	$2\times 4.0_8$, 4.0_7
$Sb_1-10\,Sb$	3.4_0, $2\times 3.5_4$, $2\times 4.0_0$, 4.1_4, $2\times 4.1_4$, $2\times 4.2_7$	3.3_8, $2\times 3.5_4$, $2\times 3.9_3$, 4.0_4, $2\times 4.0_8$, $2\times 4.1_7$
$Sb_2-6\,Sb$	3.5_0, $2\times 3.5_5$, 4.1_4, $2\times 4.1_4$	3.4_8, $2\times 3.5_1$, 4.0_4, $2\times 4.0_8$
$Sb_3-10\,Sb$	3.3_9, 3.4_0, $2\times 3.5_5$, $2\times 4.1_4$, $2\times 4.1_8$, $2\times 4.2_7$	3.4_2, 3.3_8, $2\times 3.5_1$, $2\times 4.0_8$, $2\times 4.1_6$, $2\times 4.1_7$
$Sb_4-9\,Sb$	3.5_0, $2\times 3.5_4$, $2\times 4.1_4$, $2\times 4.1_4$, $2\times 4.1_8$	3.4_8, $2\times 3.5_4$, $2\times 3.8_6$, $2\times 4.0_8$, $2\times 4.1_6$

All antimony atoms are surrounded by four oxygen atoms in a coordination earlier found for some, but not all, antimony atoms in $Sb_4O_5Cl_2$ (*1*) and SbOCl (*2*), and for all antimony atoms in $[Sb_8O_8(OH)_4][(OH)_{2-x}(H_2O)_{1+x}]Cl_{2+x}$ (*3*). In the last paper this coordination is discussed in detail specially with consideration to the similarities with the $TeCl_4$ structure (*18*) and the probability of a stereochemically active unshared electron pair. A stereochemically active unshared electron pair might have a repulsing effect on the negative halogenide ions, thus making the Sb–X distances long.

In the present structure we have the following O–Sb_i–O angles

	"diagonal" angles		remaining four angles	
Sb_1	145°	103°	two of 73°	two of 93°
Sb_2	145°	80°	,, ,, 73°	,, ,, 87°
Sb_3	145°	100°	,, ,, 73°	,, ,, 93°
Sb_4	145°	101°	,, ,, 73°	,, ,, 94°

As has been mentioned on p. 281, the chemical analyses do not decide between the two formula $Sb_8O_{11}X_2$ and $Sb_8O_{10}(OH)_2X_2$. However, when inspecting the proposed structure carefully, we find that the closest contact between atoms belonging to two different "cylinders" is between the oxygen atoms O_1 and O_5 with a distance of 2.7_0 Å. The shortest Sb–O contact in this direction is 2.9_2 Å between Sb_1 and O_5. This seems to suggest that we have a hydroxyl group in O_5 and that there is a hydrogen or hydroxyl bond between O_5 and O_1, since the distance is of the same magnitude as of other observed hydrogen bonds, see e.g. WELLS (*19*). In this way the "cylinders" would be joined to form sheets of the composition $[Sb_8O_{10}(OH)_2^{2+}]_\infty$ with sheets of iodide ions between them.

The iodide ions are surrounded by nine antimony atoms at distances varying between 3.5_7 and 3.9_6 Å. The iodide ions are, however, in close contact with eight oxygen atoms at distances varying between 3.1_8 and 3.9_4 Å, in fairly good agreement with the sum of ionic radii of about 3.5 Å, since only one is shorter than 3.5 Å. The short I–O distance is not very serious, since the large halogenide ions are easily deformed.

As mentioned before the needle-axis of about 4 Å in $Sb_8O_{10}(OH)_2X_2$ is increased fourfold due to extremely weak zones. This phenomenon of a needle-axis increased fourfold also occurs in $[Sb_8O_8(OH)_4][(OH)_{2-x}(H_2O)_{1+x}]\,Cl_{2+x}$ (*3*), where it is supposed to be caused by vacancies in one of the oxygen positions and by inclusion of extra chloride ions in holes in the structure. In $Sb_8O_{10}(OH)_2X_2$ the observed halogen percentages are a little higher than the calculated. There do not, however, seem to be any holes in this structure of a sufficient size for inclusion of extra halogenide ions. The weak zones might be due either to vacancies in some of the atomic positions or to the fact that the atoms may not be situated in mirror planes as we have assumed but may be moved a little out of them, the space group being thus other than $C2/m$.

If we assume vacancies in the atomic positions it appears at first probable that they might exist in the oxygen positions and the composition be close to the formula $Sb_8O_{11}X_2$. An inspection of the Weissenberg photographs of the weak zones shows that the intensities in these photographs do not fall off appreciably with θ, as it seems likely that they would do if they were due only to oxygen atoms. The antimony percentages observed are all a little lower than the calculated ones. This might be an indication of vacancies in the antimony positions. The accuracy of the analyses is, however, not so good that it permits very precise conclusions. We can just guess that the heavy atoms are involved in the formation of the weak zones in some way. On account of the complexity of the structure it seems to be too laborious to try to find an exact interpretation of the weak zones.

In connection with these structures with a needle-axis of about 4 Å, a mineral Sb_3O_4Cl reported a few years ago by FORNASERI (*20*) seems to be of interest since it exists in the form of needle-shaped crystals and has a needle-axis of 3.97 Å. The structure of it has, however, not yet been determined, since the Weissenberg photographs were reported to be difficult to interpret.

Summary

Compounds with the idealized formula $Sb_8O_{10}(OH)_2X_2$ with X = I, Br or Cl have been prepared by hydrothermal syntheses and been investigated by X-ray methods. They are monoclinic, the cell dimensions are given on p. 282. The *b*-axis (needle-axis) is increased fourfold due to extremely weak zones. The small unit cell contains two

formula units, with the space group No. 12, $C2/m - C^3_{2h}$ as the most probable one. The positions of the heavy atoms have been found from Patterson projections and vector convergence diagrams. Their parameters have been refined by electron density projections. The oxygen atoms have been located from space considerations. The coordinates of the heavy atoms are given on p. 286 and of the oxygen atoms on p. 291. The interatomic distances are given in Table 5.

The structure is represented in Fig. 13. Along the needle-axis there are Sb–O chains which are coupled together forming flat "cylinders" consisting of four double chains. Contacts between the "cylinders" are probably formed by hydrogen or hydroxyl bonds thus giving endless sheets of the composition $[Sb_8O_{10}(OH)_2^{2+}]_\infty$. Between these sheets there are sheets of halogenide ions. All Sb–X distances are much longer than the covalent bond length.

All the antimony atoms have the same type of four coordination, where one antimony atom is surrounded by four oxygen atoms at four of the corners of a deformed trigonal bipyramid with one of the equatorial corners unoccupied, perhaps with an unshared electron pair directed towards it. It is similar to the four-coordinations found for some of the antimony atoms in $Sb_4O_5Cl_2$ (*1*) and SbOCl (*2*) and for all antimony atoms in $[Sb_8O_8(OH)_4][(OH)_{2-x}(H_2O)_{1+x}]Cl_{2+x}$ (*3*). This resembles the $TeCl_4$ configuration (*18*).

The author wishes to thank Professor A. Ölander for his encouraging interest and for many very valuable discussions. Thanks are also due to Mr. G. Blomqvist for drawing some of the figures. The investigation has been financially supported by *Statens Naturvetenskapliga Forskningsråd* (Swedish Natural Science Research Council).

University of Stockholm, Institute of Inorganic and Physical Chemistry, March 1955.

REFERENCES

1. Edstrand, M., Acta Chem. Scand. *1*, 178 (1947) (= Part I).
2. Edstrand, M., Arkiv Kemi *6*, 89 (1953) (= Part II).
3. Edstrand, M., Arkiv Kemi 257 (1955) (= Part III).
4. Smith, G. F. and May, R. L., Ind. Eng. Chem. Anal. Ed. *13*, 460 (1941).
5. Cooke, J. P., Proc. Am. Acad. Arts Sci. *13*, 111 (1877).
6. Kaan, G. and Cole, W. F., Acta Cryst. *2*, 42 (1949).
7. International Tables for X-ray Crystallography, Vol. I, Birmingham 1952.
8. Howells, E.R., Phillips, D. C., and Rogers, D., Acta Cryst. *3*, 210 (1950).
9. Lipson, H. and Cochran, W., The Determination of Crystal Structures, London 1953, p. 35–41.
10. Beevers, C. A. and Robertson, J. H., Acta Cryst. *3*, 164 (1950).
11. Booth, A. D., Fourier Technique in X-Ray Organic Structure Analysis, Cambridge 1948, p. 64.
12. Luzzati, V., Acta Cryst. *6*, 156 (1953).
13. Almin, K. E. and Westgren, A., Arkiv Kemi, Mineral. Geol. *15 B*, N:o 22 (1942).
14. Buerger, M. J. and Hendricks, S. B., Z. Krist. *98*, 1 (1938).
15. Internationale Tabellen zur Bestimmung von Kristallstrukturen, Vol. II, Berlin 1935.
16. Gregg, A. H., Hampson, G. C., Jenkins, G. I., Jones, P. L. F., and Sutton, L. E., Trans. Faraday Soc. *33*, 852 (1937).
17. Hassel, O. and Sandbo, A., Z. physik. Chem. *B 41*, 75 (1938).
18. Stevenson, D. P. and Schomaker, V., J. Am. Chem. Soc. *62*, 1267 (1940).
19. Wells, A. F., Structural Inorganic Chemistry, 2nd Ed., Oxford 1950, p. 238.
20. Fornaseri, M., Atti accad. naz. Lincei, Rend., Classe sci. fis., mat. e nat. *3*, 365 (1947).

Tryckt den 25 april 1955

Uppsala 1955. Almqvist & Wiksells Boktryckeri AB

ARKIV FÖR KEMI Band 8 nr 27

Communicated 9 March 1955 by KARL MYRBÄCK and HUGO THEORELL

New solvents for the separation of bile acids with paper chromatography

Bile acids and steroids 30

By JAN SJÖVALL

In an investigation concerning the quantitative determination of bile acids after their separation by paper chromatography according to SJÖVALL (1, 2) it was found that the isopropyl ether used in the moving phase interfered with the sulfuric acid·spectra used for the quantitative determination (3, 4). It was therefore necessary to find another solvent which could be used for the separations. This paper reports the successful use of amyl acetate : heptane or ethylene chloride : heptane as moving phases in paper chromatography of bile acids. After proper purification ethylene chloride did not affect the reactions used for quantitative determination (5).

Experimental

For details see SJÖVALL (1, 2).

All solvents were redistilled. Equal parts of the phases were equilibrated before use.

Whatman 3 MM filter paper was used. It was found that if the papers were equilibrated with the two phases in the atmosphere of the chromatographic chamber for 12 hours before development the treatment of the papers with acetic acid could be omitted.

The chromatograms were run in a constant temperature room at 23° C.

Results

A. Amyl acetate: heptane as moving phase

Table 1 shows the behaviour of different bile acids in ascending chromatography in solvent media containing as moving phase amyl acetate and heptane in different proportions and as stationary phase 70 % acetic acid. It must, however, be emphasized that the R_F values are subject to fairly large variations. They are given in this table only to make possible a quick choice of suitable systems for a desired separation. Reference acids always have to be run parallel with an unknown sample.

The free and conjugated desoxycholic and chenodesoxycholic acids do not separate in ascending chromatography. The two free acids are separated with descending chromatography for 30 hours with amyl acetate : heptane 90 : 10 as

Table 1. R_F values of bile acids in ascending chromatography using amylacetate : heptane as moving phase. Stationary phase 70 per cent acetic acid.

Amyl-acetate : heptane	Acids*									
	TC	TCD	TD	GC	GCD	GD	C	HD	CD	D
10 : 90	0	0	0	0	0	0	0	0.01	0.07	0.09
20 : 80	0	0	0	0	0	0.01	0.02	0.07	0.17	0.21
30 : 70	0	0	0	0	0.01	0.02	0.06	0.16	0.29	0.33
40 : 60	0	0	0	0.01	0.05	0.07	0.16	0.31	0.46	0.50
50 : 50	0	0	0	0.03	0.13	0.17	0.28	0.44	0.58	0.58
60 : 40	0	0	0	0.12	0.32	0.34	0.43	0.60	0.66	0.66
70 : 30	0.01		0.04	0.31	0.52	0.55	0.59			0.75
80 : 20	0.06		0.16	0.51	0.68	0.68	0.79			0.80
85 : 15	0.18	0.29	0.32							

* TC = taurocholic acid
TCD = taurochenodesoxycholic acid
TD = taurodesoxycholic acid
GC = glycocholic acid
GCD = glycochenodesoxycholic acid
GD = glycodesoxycholic acid
C = cholic acid
HD = hyodesoxycholic acid
CD = chenodesoxycholic acid
D = desoxycholic acid

moving phase. Their glycine conjugates are separated after 36 hours descending chromatography with amyl acetate : heptane 40 : 60 as moving phase. 70 % acetic acid is used as stationary phase in both cases.

The advantage of using amyl acetate in the moving phase lies mostly in the separation of bile acids conjugated with taurine. The spots are very well-defined and a complete separation of taurochenodesoxycholic and taurodesoxycholic acids can be achieved after 46 hours descending chromatography using amyl acetate : heptane 80 : 20 as moving phase. The stationary phase is 70 % acetic acid.

B. Use of ethylene chloride in the moving phase

70 % acetic acid has been used as stationary phase throughout.

Properly purified ethylene chloride does not contain compounds which interfere with the sulfuric acid reaction used for quantitative determinations of bile acids (5). Except for this quality it does not offer any advantages over isopropyl ether as far as the qualitative separation of free and glycine conjugated bile acids is concerned. For a desired separation ethylene chloride can be used in the moving phase in the same proportion to heptane as that earlier described for isopropyl ether (2). Desoxycholic and chenodesoxycholic acids are separated by descending chromatography for 30 hours using ethylene chloride : heptane 20 : 80 as moving phase and their glycine conjugates are separated after 32 hours of descending chromatography with ethylene chloride : heptane 50 : 50 as moving phase.

Using mixtures of ethylene chloride and *n*-butanol as moving phase taurine conjugated acids can be separated. With these phases too, more well-defined spots are obtained than with the butanol system earlier described (2). Taurolithocholic, taurodesoxycholic and taurocholic acids can be separated with ascending chromatography using ethylene chloride : butanol 90 : 10 — 80 : 20 as moving phase. Taurodesoxycholic and taurochenodesoxycholic acids are separated after 48 hours descending chromatography using ethylene chloride: butanol 95 : 5 as moving phase although some streaking of the spots is observed.

Summary

Some new solvent media for the separation of free and conjugated bile acids with paper chromatography have been described. A system consisting of ethylene chloride : heptane : acetic acid is especially suitable when the separation is combined with quantitative determination of the bile acids with sulfuric acid.

For the first time it has been possible to separate taurochenodesoxycholic and taurodesoxycholic acids.

Thanks are due to Dr. John Sjöquist for valuable suggestions and discussions during the course of this work.

This work has been supported by a grant from the Medical Faculty of the University of Lund.

Department of Physiological Chemistry, University of Lund, Lund, Sweden.

REFERENCES

1. Sjövall, J., Acta Chem. Scand. *6*, 1552 (1952).
2. Sjövall, J., Acta Chem. Scand. *8*, 339 (1954).
3. Eriksson, S. and Sjövall, J., Arkiv Kemi *8*, 303 (1955).
4. Eriksson, S. and Sjövall, J., Arkiv Kemi *8*, 311 (1955).
5. Sjövall, J., Arkiv Kemi *8*, 317 (1955).

Tryckt den 26 april 1955

Uppsala 1955. Almqvist & Wiksells Boktryckeri AB

ARKIV FÖR KEMI Band 8 nr 28

Communicated 9 March 1955 by KARL MYRBÄCK and HUGO THEORELL

The absorption spectra of bile acids in sulfuric acid

Bile acids and steroids. 31

By STEN ERIKSSON and JAN SJÖVALL

With 4 figures in the text

During an investigation of the bile acid composition of bile using paper chromatography it was found desirable to have a simple and rapid method for the quantitative determination of bile acids on the chromatograms. The absorption of steroids in sulfuric acid have proved to be of great value in the studies of steroid hormones with paper chromatography (1, 2, 3) and it was decided to try similar methods in the bile acid field.

The spectra of bile acids in sulfuric acid of different concentration have earlier been studied by BANDOW (4). The fluorescence of bile acids (mainly cholic acid) in concentrated sulfuric acid has been known for a long time and attempts have been done to isolate the fluorescent substances formed (5, 6). Methods for the determination of bile acids have been based on the fluorescence reaction (7).

KIER (8) has developed a method for the determination of cholic and desoxycholic acids in mixtures based on the fact that these acids give slightly different absorption spectra in 65 per cent sulfuric acid. The method has been improved by MOSBACH *et al.* (9) who found that heating 15 minutes at 60°C gave completely different spectra for cholic and desoxycholic acid in 65 per cent sulfuric acid.

This paper reports a more detailed study of the absorption spectra of different bile acids in sulfuric acid of different concentrations under various heating conditions. It is conveniently divided into three sections: A. Absorption spectra of bile acids in concentrated sulfuric acid; B. Absorption spectra of bile acids in 65 per cent sulfuric acid under different heating conditions; C. Quantitative applications.

A. Absorption spectra of bile acids in concentrated sulfuric acid

Experimental

The sulfuric acid used was "Merck p.a." 95–97 per cent, *d* 1.84. The spectra from 220 to 600 mμ were determined in a Beckman model DU spectrophotometer. Silica cells 3 × 10 ± 0.01 mm with a volume of 0.8 ml were used. With proper adjustment of the cell holder allowing the light beam to pass through the centre of the cell and with a slit width of 0.4 mm it was not necessary to use a diaphragm.

0.3 ml of an alcohol solution containing approximately 100 μg bile acid per ml was pipetted into pyrex tubes 16 × 95 mm which could be closed with a cap having an outlet tubing bent downwards. The alcohol was evaporated in an oven at 100°C for about 4 hours; the cap prevented dust particles from contaminating the sample. The tubes were allowed to cool to room temperature after which 1 ml sulfuric acid was added. After 2 hours at room temperature the spectra were measured.

Purity of compounds. Cholic, desoxycholic, chenodesoxycholic and hyodesoxycholic acids were purified as described in section B. The other compounds were kindly supplied by Prof. S. BERGSTRÖM. They had been synthesized according to standard methods and showed the melting points reported in the literature.

Results

In Table 1 are recorded the maxima and minima for the different bile acids tested. The figures within brackets give the extinction coefficient at the corresponding wavelength. To simplify the tabulation each characteristic absorption band is represented by a single wave length rather than by a range if such exists.

It is seen that bile acids, having neither hydroxyl or acetoxy group nor any double bond, do not give any marked maxima at concentrations tested (Nos. 12, 15, 19 and 27). The fairly strong maximum of cholanic acid at 313 mμ reported by BERNSTEIN and LENHARD (2) seems to have been due to impurities in their cholanic acid.

Acids with one hydroxyl group (Nos. 23 and 25) give a low maximum around 316 mμ ($E_{1\,\mathrm{cm}}^{1\%} \sim 100$). Addition of keto groups usually increase the optical density (Nos. 11, 14, 18, 21). 3 α-hydroxy-12-keto-cholanic acid in addition has a strong maximum ($E_{1\,\mathrm{cm}}^{1\%}$ 225) at 390 mμ which is not present in the 3 α-hydroxy-7-keto-cholanic acid.

Introduction of a double bond (Nos. 24, 26) also increases the optical density and the spectrum bears more resemblance to that of a dihydroxy acid. This is more obvious in the 65 % sulfuric acid (see section B).

The dihydroxy acids (Nos. 13, 16, 20) have a higher maximum ($E_{1\,\mathrm{cm}}^{1\%} \sim 300$) than the monohydroxy acids. Fig. 1 shows the spectrum of desoxycholic acid (No. 16). The spectrum of apocholic acid (No. 17), a dihydroxy acid with a 8–14 double bond, is closely similar to that of trihydroxy acids.

The trihydroxy acids (Nos. 1, 6 and 7) and trihydroxycoprostane (No. 8) all have similar spectra with a characteristic strong maximum at 389–390 mμ. The spectrum of cholic acid (No. 1) is shown in Fig. 2.

It may be further noted that methyl esters have the same spectra as free acids while the spectrum of triacetoxy cholic acid (No. 5) deviates clearly from that of cholic acid.

Some concentration studies on the common bile acids have been done (Nos. 1, 13, 16, 20). These acids all follow Beer's law within the concentration range studied (< 30 μg per ml). Concentrated sulfuric acid thus can be used for quantitative measurements but as it is very sensitive to dust particles we have preferred to use 65 per cent sulfuric acid in quantitative work.

B. Absorption spectra of bile acids in 65 per cent sulfuric acid

Experimental

The sulfuric acid was prepared in the following way. To 30 ml redistilled water in a 100 ml volumetric flask 67 ml 97 per cent sulfuric acid was added. After cooling the volume was made up to 100 ml with redistilled water.

Table 1.

(For explanations see text.)

No.	Compound	Concentrated sulfuric acid 2 hours 20° C				65% sulfuric acid 15 min. 60° C			
		Max. mμ ($E^{1\%}_{1\,\mathrm{cm}}$)		Min. mμ ($E^{1\%}_{1\,\mathrm{cm}}$)		Max. mμ ($E^{1\%}_{1\,\mathrm{cm}}$)		Min. mμ ($E^{1\%}_{1\,\mathrm{cm}}$)	
1	3α,7α,12α-trihydroxy-cholanic acid	305 (132) 478 (63)	389 (661)	256 (69) 438 (44)	335 (107)	320 (357)	389 (48)	250 (65)	350 (20)
2	3α,7α,12α-trihydroxy-cholanic acid methyl ester	302 (98) 480 (60)	389 (705)	253 (43) 436 (36)	331 (71)	320 (394)	388 (56)	250 (71)	350 (24)
3	3α,7α-diacetoxy-12α-hydroxy-cholanic acid	316 (208) 500 (78)	390 (224)	253 (55) 460 (54)	342 (75)	320 (284) 488 (81)	387 (79)	246 (56) 438 (52)	352 (28)
4	3α,7α-diacetoxy-12α-hydroxy-cholanic acid methyl ester	317 (199) 505 (78)	390 (232)	255 (52) 460 (62)	344 (78)	318 (281) 488 (74)	390 (77)	248 (53) 440 (50)	350 (26)
5	3α,7α,12α-triacetoxy-cholanic acid	310 (192)		252 (56)		275 (74) 385 (402)	326 (79)	248 (40) 333 (77)	293 (49)
6	3α,7α,12α-trihydroxy-norcholanic acid	304 (95) 480 (58)	389 (458)	254 (42) 442 (43)	334 (77)	317 (222)	389 (129)	255 (54)	345 (34)
7	3α,7α,12α-trihydroxy-bisnorcholanic acid	306 (136) 443 (112)	390 (490)	260 (64) 437 (110)	333 (107)	320 (300)	388 (172)	255 (81)	345 (57)
8	3α,7α,12α-trihydroxy coprostane	322 (177) 484 (126)	390 (334)	257 (67) 439 (93)	347 (153)	320 (350)	391 (48)	250 (67)	355 (21)
9	3α,7α-dihydroxy-12-keto-cholanic acid	280 (154) 480 (46)	391 (221)	251 (91) 442 (35)	315 (74)	280 (203) 480 (58)	388 (45)	235 (78) 411 (18)	341 (35)
10	3α,12α-dihydroxy-7-keto-cholanic acid methyl ester	302 (201)	390 (100)	245 (90)	347 (58)	320 (250)	389 (33)	250 (28)	358 (17)
11	3α-hydroxy-7,12-diketocholanic acid	293 (207)		255 (82)		—		—	
12	3,7,12-triketo-cholanic acid	—		—		—		—	
13	3α,7α-dihydroxy-cholanic acid	310 (261)		250 (55)		272 (99)	380 (580)	242 (46)	297 (45)
14	3α-hydroxy-7-keto-cholanic acid	301 (161)		240 (69)		—		—	
15	3,7-diketo-cholanic acid	—		—		—		—	
16	3α,12a-dihydroxy-cholanic acid	312 (268)		245 (74)		275 (103)	385 (453)	250 (68)	300 (60)
17	3a,12α-dihydroxy-Δ^{8-14}-cholenic acid	303 (122) 478 (61)	390 (676)	254 (56) 435 (40)	334 (92)	320 (388)	389 (78)	248 (74)	350 (32)
18	3α-hydroxy-12-keto-cholanic acid	317 (177)	390 (225)	264 (70)	346 (85)	302 (170)		—	
19	3,12-diketo-cholanic acid	—		—		—		—	
20	3α,6a-dihydroxy-cholanic acid	305 (308)		246 (59)		276 (84)	380 (390)	246 (32)	295 (74)
21	11-hydroxy-12-keto-cholanic acid	323 (207)		248 (45)		—		—	
22	Δ^{9-11}-12-keto-cholenic acid	305 (268)	394 (38)	240 (90)	362 (19)	297 (220)		—	
23	3α-hydroxy-cholanic acid	316 (90)		250 (26)		—		—	
24	3β-hydroxy-Δ^{5-6}-cholenic acid	307 (304)		250 (64)		276 (89)	382 (482)	250 (43)	296 (71)
25	12α-hydroxy-cholanic acid methyl ester	317 (110)		246 (26)		—		—	
26	12α-hydroxy-Δ^{3-4}-cholenic acid methyl ester	304 (207)	380 (99)	252 (134)	360 (94)	282 (125)	381 (136)	250 (105)	337 (59)
27	Cholanic acid	—		—		—		—	

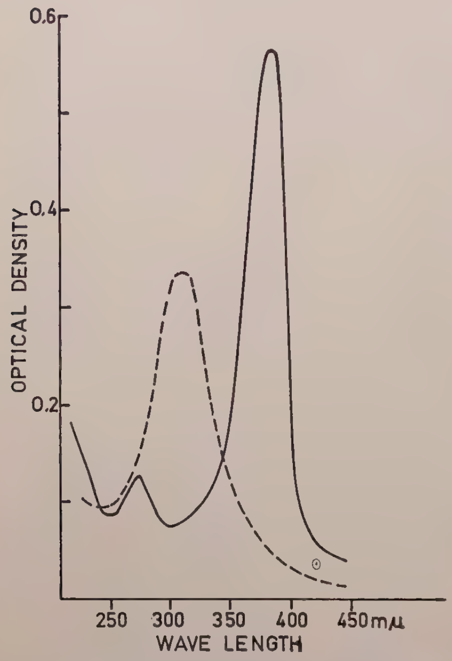

Fig. 1. Spectra of 12.5 γ desoxycholic acid in 1 ml concentrated sulfuric acid after 2 hours at room temperature (----------) and in 1 ml 65 % sulfuric acid after heating for 15 minutes at 60°C (———).

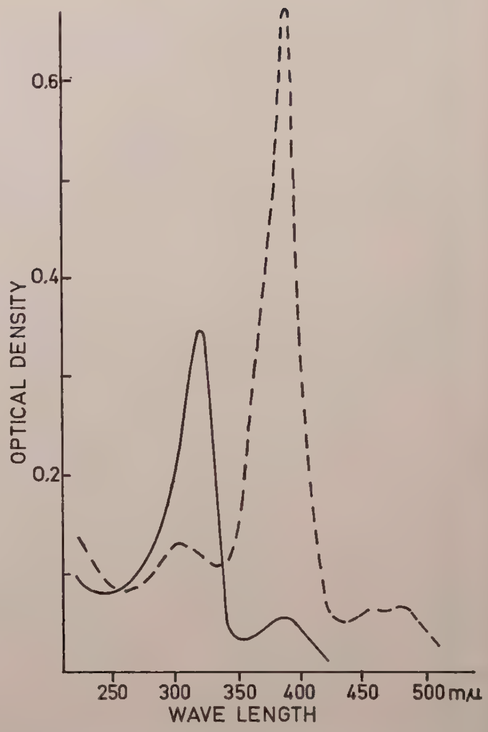

Fig. 2. Spectra of 10 γ cholic acid in 1 ml concentrated sulfuric acid after 2 hours at room temperature (----------) and in 1 ml 65 % sulfuric acid after heating for 15 minutes at 60°C (———).

The bile acids were pipetted and evaporated as described in section A. After adding 1 ml of the sulfuric acid the tubes were heated 15 minutes at 60 ± 1°C in a water bath and were then cooled in tap water and allowed to stand for 15 minutes at room temperature before the measurements.

Purity of compounds (see also section A). The acids used for the time studies and the quantitative work (section C) were purified until they only showed one spot on paper chromatograms (10). In some instances they had to be purified by reversed phase chromatography (11, 12). They were recrystallized until having the constant melting point reported in literature and finally dried at 0.1 mm for 20 hours over P_2O_5 at 70°C.

Results

In Table 1 there are given the maxima and minima for the spectra of the different compounds. The spectra differ much from those obtained in concentrated sulfuric acid. One hydroxyl group only does not give any maximum in a saturated bile acid and the addition of keto groups (Nos. 11, 14, 18, 21) causes the appearance of a maximum only in one case (No. 18). Acids with two hydroxyl groups have a typical strong maximum at 380–390 mμ (Nos. 13, 16 and 20; Fig. 1). Their spectra are similar

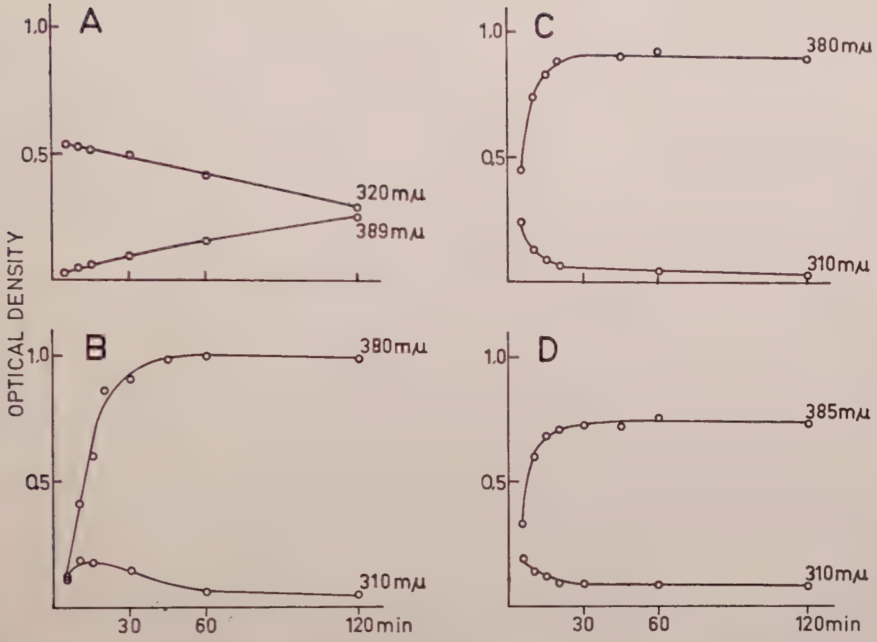

Fig. 3. Effect of heating at 60°C on the optical densities at the main maxima of cholic (A), hyodesoxycholic (B), chenodesoxycholic (C) and desoxycholic (D) acids in 65% sulfuric acid. 15 γ of each acid was dissolved in 1 ml of the sulfuric acid.

to those of the monohydroxy-monounsaturated acids (Nos. 24 and 26). Apocholic acid (No. 17) and the trihydroxy compounds (Nos. 1, 2, 6, 7 and 8) all have similar spectra with the main maximum at 320 mμ (Fig. 2).

Time studies. The spectra of bile acids change with the time of heating at 60°C. MOSBACH *et al.* (9) used this fact for a differential determination of mixtures of cholic and desoxycholic acids. After 15 minutes cholic acid has its main maximum at 320 mμ whereas desoxycholic acid exhibits a strong maximum at 385 mμ. Fig. 3 shows the optical density at the characteristic maxima of some common bile acids after different time of heating at 60°C. The optical density at 320 mμ of cholic acid gradually decreases and at the same time the extinction at 389 mμ increases. As it is not possible to increase the molar extinction by prolonged heating the quantitative measurements were carried out after 15 minutes at 60°. The dihydroxy acids studied, hyodesoxycholic, chenodesoxycholic and desoxycholic acid (Nos. 20, 13 and 16), however, show higher optical densities at their main maxima after incubation for a longer time and a plateau value is obtained after about 45 minutes. In quantitative measurements of these acids we have chosen 60 minutes at 60°C as a suitable heating time.

C. Application of the absorption spectra to quantitative determinations

Since this investigation was done partly in order to develop a method for the quantitative determination of individual bile acids after separation by paper chromato-

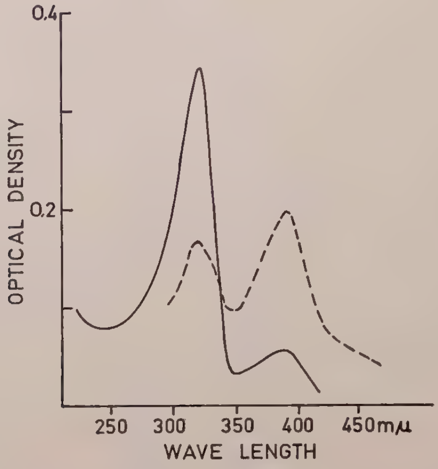

Fig. 4. Spectra of 10 γ cholic acid with (---------) and without (———) the addition of 8 γ ferric chloride in 1 ml 65 % sulfuric acid after heating for 15 minutes at 60° C.

graphy, we wanted to study the reproducibility of quantitative measurements. As mentioned in section A we have preferred the use of 65 per cent sulfuric acid for this purpose.

Experimetal

Standard solutions containing 1 mg purified (see section B) bile acid per ml ethanol were used. 20 μl were transferred with a constriction pipette into the test tubes and dried as described in section A. 1 ml 65 per cent sulfuric acid was added. The tubes were thoroughly shaken to ensure complete dissolution of the bile acid. Cholic acid samples were heated for 15 minutes and the dihydroxy acids for 60 minutes at 60°C. After cooling the tubes were allowed to stand for 15 minutes at room temperature. The cholic acid was measured at 320 mμ, hyodesoxycholic and chenodesoxycholic acid at 385 mμ. The optical densities remained constant for at least one hour after cooling.

Results

The four acids tested all follow Beer's law within the concentration ranges studied ($<$ 30 μg per ml 65 % sulfuric acid).

It was found impossible to avoid variations in the optical density values from day to day. However, differences within duplicates were found to be quite small (Table 2). Thus, when unknown amounts of an acid are to be determined, measurement of a standard always has to be carried out simultaneously.

It was observed that the use of glass-distilled water for the preparation of 65 per cent sulfuric acid was essential. Small amounts of iron completely change the spectrum of cholic acid. Fig. 4 shows the normal spectrum of cholic acid in 65 per cent sulfuric acid after 15 minutes at 60°C and the spectrum obtained under the same conditions when the sulfuric acid contained approximately 3 μg of iron (as ferric chloride) per ml. In the presence of iron the sample turns strongly yellow during the heating process. Normally only a very faint yellow-green colouration can be observed. Table 3 shows the effect of different amounts of ferric ions on the recovery of cholic acid using the

Table 2. Difference (*d*) within duplicate values.

Acid	Mean difference, %	*i*[1] %	Range %	*N*[2]
Cholic	0.80	1.24	4.06	30
Hyodesoxycholic	1.30	1.75	4,05	16
Chenodesoxycholic	0.87	1.11	2.60	15
Desoxycholic	0.97	1.32	3.37	17

[1] Standar error of individual differences within duplicates $\sqrt{\frac{\Sigma d^2}{N}}$.

[2] N = number of sets of duplicates.

Table 3. Effect of added ferric chloride on quantitative determination of cholic acid. All figures represent the average of two determinations. The recovery is calculated from the optical density at 320 mμ of the cholic acid in the absence of ferric chloride.

Cholic acid added, γ	Fe^{3+} added γ	Optical density at 320 mμ	Optical density at 389 mμ	% cholic acid recovered
10	0	0.340	0.040	
10	1	0.290	0.120	85.4
10	2	0.250	0.150	73.6
10	3	0.200	0.185	58.8

Table 4. Effect of added ferric chloride on quantitative determination of cholate according to IRWIN *et al.* (13). All figures represent the average of two determinations. The recovery is calculated from the figures obtained for cholic acid in the absence of ferric chloride.

Cholic acid added, γ	Fe^{3+} added γ	Optical density at 620 mμ	% cholic acid recovered
200	0	0.480	
200	20	0.430	89.7
200	40	0.410	85.5
200	60	0.375	78.2

standard procedure for the determinations. It is seen that with increasing amounts of iron the recovery is gradually lowered. It was to be expected that the same would be true for determinations of cholic acid according to IRWIN, JOHNSTON and KOPALA (13) and such determinations were carried out (Table 4).

IRWIN *et al.* (13) have observed that the use of ethyl ether containing peroxides for the extraction of bile acids interferes with the quantitative determination of cholate. The same was observed to be true for isopropyl ether and this solvent therefore could not be used in the moving phase when bile acids should be determined after separation by paper chromatography (14). Peroxides were removed from the isopropyl ether by shaking with a solution of ferrous sulphate in 50 per cent sulfuric acid. After drying over $CaCl_2$ the isopropyl ether was distilled and its effect on the absorption spectrum of cholic acid in 65 per cent sulfuric acid was tested at various intervals after the distillation. 0.1 ml isopropyl ether was evaporated together with 20 μl of the cholic acid solution (see Experimental). Cholic acid was determined in the usual way in 65 per cent sulfuric acid. When the newly distilled isopropyl ether had been added all cholic acid added was recovered. Adding isopropyl ether 1, 2 and 6 days after its distillation the recoveries of cholic acid were 95, 75 and 54 per cent, respectively (the isopropyl ether was stored in the dark).

SUMMARY

1. The absorption spectra (220–600 mμ) of some unconjugated bile acids in concentrated sulfuric acid at room temperature and in 65 per cent sulfuric acid after heating 15 minutes at 60°C have been determined.
2. Saturated bile acids with three hydroxyl groups (3 α, 7 α, 12 α) have a characteristic maximum at 389 mμ in concentrated sulfuric acid. In 65 per cent sulfuric acid the main maximum appears at about 320 mμ.
3. Saturated dihydroxy-acids in concentrated sulfuric acid have their main maximum between 305 and 312 mμ. After heating in 65 per cent sulfuric acid a characteristic maximum is found at 380–385 mμ.
4. The influence of heating time on the spectra of some common bile acids in 65 per cent sulfuric acid has been studied.
5. Concentration studies of the common bile acids have been done and the standard error of the difference within duplicates has been determined.
6. The effect of iron and ether peroxides on the absorption spectra has been investigated.

This work is part of an investigation supported by grants from the Medical Faculty of the University of Lund.

Department of Physiological Chemistry, University of Lund, Sweden.

REFERENCES

1. Zaffaroni, A., Recent Progress in Hormone Research *8*, 51 (1953).
2. Bernstein, S. and Lenhard, R. H., J. Org. Chem. *18*, 1146 (1952).
3. Axelrod, L. R., J. Biol. Chem. *205*, 173 (1953).
4. Bandow, F., Biochem. Z. *301*, 37 (1939).
5. Pregl. F., Hoppe-Seylers Z. physiol. Chem. *45*, 166 (1905).
6. Jenke, M. and Bandow, F., Hoppe-Seylers Z. physiol. Chem. *249*, 16 (1937).
7. Minibeck, H., Biochem. Z. *297*, 29 (1938).
8. Kier, L. C., J. Lab. Clin. Med. *40*, 755 (1952).
9. Mosbach, E. H., Kalinsky, H. J., Halpern, E., and Kendall, F. E., Arch. Biochem. Biophys. *51*, 402 (1954).
10. Sjövall, J., Acta Chem. Scand. *8*, 339 (1954).
11. Bergström, S. and Sjövall, J., Acta Chem. Scand. *5*, 1267 (1951).
12. Sjövall, J., Acta Physiol. Scand. *29*, 232 (1953).
13. Irwin, J. L., Johnston, C. G., and Kopala, J., J. Biol. Chem. *153*, 439 (1944).
14. Sjövall, J., Arkiv Kemi *8*, 317 (1955).

Tryckt den 26 april 1955

Uppsala 1955. Almqvist & Wiksells Boktryckeri AB

ARKIV FÖR KEMI Band 8 nr 29

Communicated 9 March 1955 by KARL MYRBÄCK and HUGO THEORELL

The absorption spectra of conjugated bile acids in sulfuric acid

Bile acids and steroids. 32

By STEN ERIKSSON and JAN SJÖVALL

With 2 figures in the text

In a previous paper (1) where the pertinent literature was quoted we have reported the absorption spectra of some free bile acids in 96 and 65 per cent sulfuric acid. In bile, however, the bile acids are found mainly as conjugates with glycine and taurine. It was thus desirable to investigate the absorption spectra of the common conjugated bile acids in sulfuric acid of various concentrations.

A. Absorption spectra of conjugated bile acids in concentrated sulfuric acid

Experimental. For details see Eriksson and Sjövall (1). 20 μl of an alcohol solution containing 1 mg bile acid or its sodium salt per ml were transferred with a constriction pipette into the pyrex tubes. The alcohol was evaporated in an oven at 100°C for about 4 hours and after cooling to room temperature, 1 ml sulfuric acid was added. After 2 hours at room temperature the spectra were measured.

Purity of compounds. The conjugated acids used were kindly put at our disposal by Dr. NORMAN. Analytical values of these acids can be found in his paper (2) on the synthesis of conjugated bile acids.

Results

The maxima and minima for the different compounds tested are recorded in Table 1. The figures within brackets give the extinction coefficients ($E_{1\,\mathrm{cm}}^{1\,\%}$) at the corresponding wavelength. No definite differences between the absorption spectra of the free and their corresponding conjugated bile acids can be observed. The conjugates of cholanic acid show a diffuse maximum around 315 mμ, which is not present when the cholanic acid is unconjugated. The conjugates of chenodesoxycholic acid exhibit two additional maxima at 388 and 450 mμ not found with the free acid.

B. Absorption spectra of conjugated bile acids in 65 per cent sulfuric acid

The 65 per cent sulfuric acid was prepared as previously described (1). The bile acid samples were prepared as in section A.

Table 1. Absorption spectra of conjuga

Compound	Concentrated sulf		
	Max. mμ ($E^{1\%}_{1\,\mathrm{cm}}$)		
Glycocholic acid	303 (96)	389 (637)	479 (62)
Taurocholic acid(-Na)	303 (81)	389 (546)	480 (54)
Glycodesoxycholic acid	313 (206)		
Taurodesoxycholic acid(-Na)	315 (174)		
Glycochenodesoxycholic acid(-Na)	308 (180)	388 (69)	446 (30)
Taurochenodesoxycholic acid(-Na)	308 (150)	384 (87)	450 (30)
Glycolithocholic acid	315 (95)		
Taurolithocholic acid	312 (95)		
Glycocholanic acid	315 (32)		
Taurocholanic acid(-Na)	315 (22)		

Table 1 shows the spectra obtained after heating for 15 minutes at 60°C. The conjugates of cholanic acid do not show the small maximum obtained at 315 mμ in concentrated sulfuric acid. The conjugates of the dihydroxy acids studied show quite different spectra compared with those of the free dihydroxy acids. The conjugates of chenodesoxycholic acid exhibit their main absorption at 305 mμ whereas free chenodesoxycholic acid has its main maximum at 380 mμ. The two small maxima

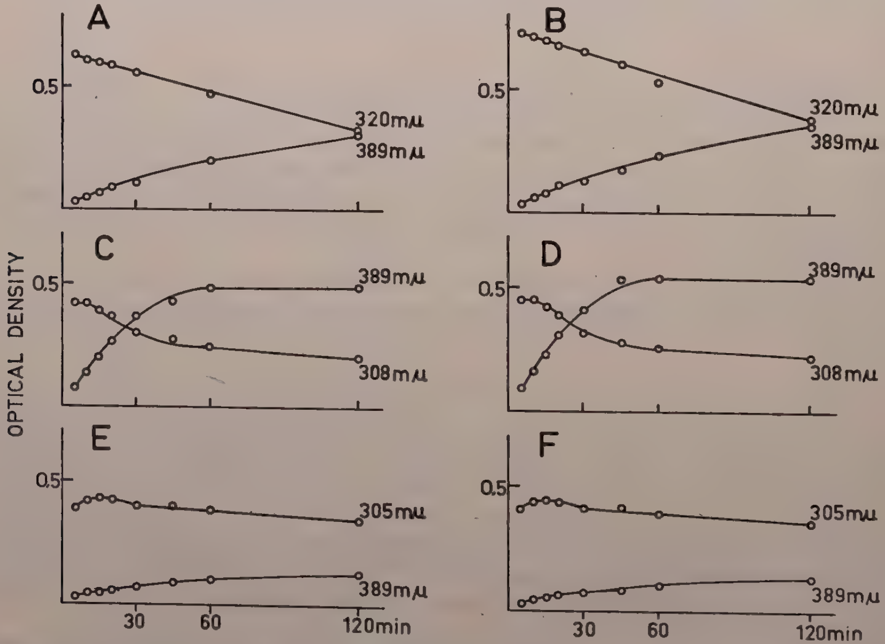

Fig. 1. Effect of heating at 60°C on the optical densities at the main maxima of conjugated bile acids in 65 per cent sulfuric acid. A. Sodium taurocholate; B. Glycocholic acid; C. Sodium taurodesoxycholate; D. Glycodesoxycholic acid; E. Sodium taurochenodesoxycholate; F. Sodium glycochenodesoxycholate. 20 γ of each compound was dissolved in 1 ml of the sulfuric acid.

e acids (for explanations see text).

d, 2 hours 20° C			65 % sulfuric acid, 15 min. 60° C			
Min. mμ ($E_{1\,\mathrm{cm}}^{1\%}$)			Max. mμ ($E_{1\,\mathrm{cm}}^{1\%}$)		Min. mμ ($E_{1\,\mathrm{cm}}^{1\%}$)	
255 (37)	332 (72)	433 (36)	320 (355)	389 (34)	252 (62)	354 (10)
255 (39)	333 (61)	436 (29)	320 (300)	389 (43)	254 (50)	352 (10)
252 (62)			308 (195)	389 (155)	255 (54)	350 (85)
252 (60)			308 (185)	389 (140)	255 (49)	350 (74)
250 (41)	381 (64)	428 (28)	305 (220)		252 (28)	
252 (43)	380 (81)	430 (27)	305 (209)		256 (43)	
250 (25)			315 (23)		245 (7)	
250 (19)			319 (48)		250 (17)	
250 (7)			—		—	
250 (13)			—		—	

around 390 and 450 mμ found in concentrated sulfuric acid are not present when the conjugates of chenodesoxycholic acid are heated in 65 per cent sulfuric acid. The conjugates of desoxycholic acid exhibit their principal maximum at 308 mμ (385 mμ for the free desoxycholic acid) and give an additional maximum at 389 mμ not found in concentrated sulfuric acid. In 65 per cent sulfuric acid the conjugates of cholic acid havê the same maxima as the free cholic acid.

C. Time studies

The spectra of the free bile acids change with the time of heating in 65 per cent sulfuric acid at 60°C. The same holds true for the conjugated bile acids. Fig. 1 shows the optical density at the characteristic maxima of some conjugated bile acids after different time of heating at 60°C. The optical density at 320 mμ of the conjugated cholic acids decreases and at the same time the extinction at 389 mμ increases. As it is not possible to increase the molar extinction by prolonged heating the quantitative measurements (section D) of conjugated cholic acids were performed after 15 minutes at 60°C. The conjugates of desoxycholic acid on heating get higher optical densities at 389 mμ and a plateau value is reached after about 60 minutes. The optical density at 305 mμ of the conjugated chenodesoxycholic acids decreases very slowly. Time studies were also performed with 70, 80 and 96 per cent sulfuric acids. The acids studied were glyco- and taurodesoxycholic acid and glycochenodesoxycholic acid. They were heated for 15, 30 and 60 minutes at 60° or 80°C.

Heating at 60°C in 70 per cent sulfuric acid did not increase the optical density at 389 mμ of the conjugated desoxycholic acids as it did in the 65 per cent sulfuric acid. After heating at 80°C the main maximum, however, was found at 389 mμ. Glycochenodesoxycholic acid behaved approximately as in 65 per cent sulfuric acid.

In 80 per cent sulfuric acid the conjugated desoxycholic acids have their main maxima at 308 mμ. The optical density at 389 mμ increases only very slowly even during prolonged heating at 60 and 80°C. The main maximum of glycochenodesoxycholic acid still remains at 305 mμ during heating but the molar extinction is slightly elevated as compared with that in 65 per cent sulfuric acid. Heating at 60 and 80°C in 96 per cent sulfuric acid does not cause any significant changes in the spectra of conjugated desoxycholic acids as compared with those obtained at

Table 2. Difference (*d*) within duplicates values.

Compound	Mean difference %	i^1 %	Range %	N^2
Glycocholic acid	0.51	0.66	1.44	11
Taurocholic acid(-Na)	0.82	1.03	2.14	12
Glycodesoxycholic acid	1.85	2.25	4.12	11
Taurodesoxycholic acid(-Na)	2.02	2.33	4.15	11
Glycochenodesoxycholic acid(-Na)	1.03	1.18	2.54	11
Taurochenodesoxycholic acid(-Na)	1.28	1.60	3.54	10

[1] Standard error of individual differences within duplicates $\sqrt{\frac{\Sigma d^2}{N}}$.

[2] N = number of sets of duplicates.

room temperature. Only a slight increase in optical densities can be observed. There is a definite increase in molar extinction of glycochenodesoxycholic acid at 308 mμ when heated in concentrated sulfuric acid at 60 and 80°C.

D. Applications of the absorption spectra to quantitative determinations

Experimental. Samples were prepared as described in section A. 65 % sulfuric acid was used throughout. In some cases the molar extinction could be increased by using more concentrated sulfuric acid (see above) but it was observed that the variations within duplicates at the same time was increased. Glycocholic, taurocholic, glycochenodesoxycholic and taurochenodesoxycholic acids were heated for 15 minutes at 60°C. Glycodesoxycholic and taurodesoxycholic acids were heated for 60 minutes at 60°C. After the heating procedure the samples were cooled and allowed to stand at room temperature for 15 minutes before the measurements.

Conjugates of cholic acid were measured at 320 mμ, conjugates of desoxycholic acid at 389 mμ, and conjugates of chenodesoxycholic acid at 305 mμ. Optical densities remained constant for at least 1 hour. As found with the free bile acids it was impossible to avoid differences in molar extinction from day to day. However, differences

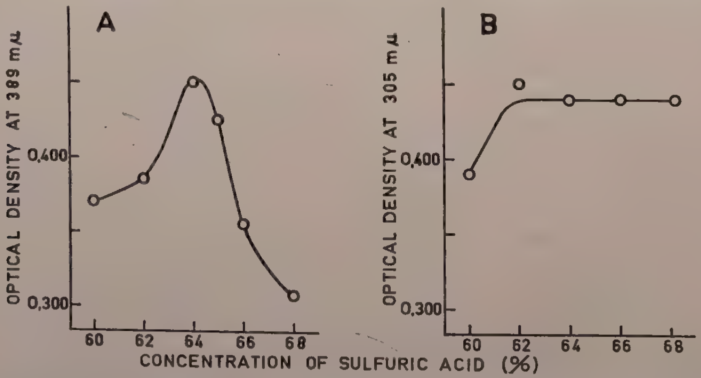

Fig. 2. Influence of the concentration of the sulfuric acid on the optical density. A. 17.5 γ sodium taurodesoxycholate in 1 ml sulfuric acid. Heated 60 minutes at 60°C. Measured at 389 mμ; B. 20.9 γ sodium taurochenodesoxycholate in 1 ml sulfuric acid. Heated 15 minutes at 60°C. Measured at 305 mμ.

within duplicates were quite small as seen in Table 2. The only exception to the above stated are the conjugated desoxycholic acids which show larger variations within duplicates. This might possibly be due to the sensitivity for small variations in the concentration of the sulfuric acid. Fig. 2 shows the effect of these variations upon the optical density at 389 mμ of taurodesoxycholic acid and at 305 mμ for taurochenodesoxycholic acid. The optical density at 305 mμ for the conjugated chenodesoxycholic acids stays quite constant in 62–68 per cent sulfuric acid.

SUMMARY

1. The absorption spectra (200–600 mμ) of the common conjugated bile acids in concentrated sulfuric acid at room temperature and in 65 per cent sulfuric acid after heating for 15 minutes at 60°C have been determined.

2. Under these conditions there is no significant difference between the spectra of glycine- and taurine-conjugated acids.

3. Significant differences in absorption spectra between conjugated and free dihydroxy acids have been noted.

4. The influence of heating time at 60 and 80°C on the spectra of the conjugated acids in 65, 70, 80 and 96 per cent sulfuric acid has been studied.

5. Concentration studies of the common conjugated bile acids have been done and the standard error of the difference within duplicates has been determined.

Department of Physiological Chemistry, University of Lund, Lund, Sweden.

REFERENCES

1. Eriksson, S. and Sjövall, J., Arkiv Kemi *8*, 303 (1955).
2. Norman, A., Arkiv Kemi (1955). *8*, 331 (1955).

Tryckt den 26 april 1955

Uppsala 1955. Almqvist & Wiksells Boktryckeri AB

ARKIV FÖR KEMI Band 8 nr 30

Communicated 9 March 1955 by KARL MYRBÄCK and HUGO THEORELL

Quantitative determination of bile acids on paper chromatograms

Bile acids and steroids. 33

By JAN SJÖVALL

With 2 figures in the text

Various methods for the determination of bile acids have been developed during the last thirty years. Until recently, most methods were based on the Pettenkofer reaction and therefore reflected the concentration of cholic acid only (for example see 1, 2, 3, 4, 5). Some investigators have estimated conjugated bile acids as the difference between amino nitrogen before and after hydrolysis of the bile (6). Sulphur determinations have also been carried out to determine the amount of taurine-conjugated bile acids. Polarimetric methods (7), and methods based on the ability of bile acids to lower surface tension and hemolyze red blood cells (8) have been described. Many workers have determined cholic acid by its fluorescense in concentrated sulfuric acid (9, 10). Methods claimed to be specific for desoxycholic acid have involved the use of benzaldehyde or salicylaldehyde together with dilute sulfuric acid (11, 12). The colour reaction of chenodesoxycholic acid with *p*-dimethylaminobenzaldehyde in 75 % sulfuric acid has been studied (13) and recently a method for the determination of chenodesoxycholic acid in bile has appeared (14).

These methods have for the most part been limited to the determination of only one bile acid, or of the total sum of bile acids, or of fractions composed of different amounts of various bile acids. Attempts have been made to achieve a differential determination of two or more bile acids in mixtures. By combining several of the methods described, DOUBILET (15) could determine glycine and taurine conjugated acids, cholic acid and total bile acids. MURAKAMI (16) separated free and conjugated bile acids with an extraction procedure and then determined cholic and desoxycholic acids using vanillin and phosphoric acid. Other methods for the simultaneous determination of cholic and desoxycholic acids have involved the use of vanillin and phosphoric acid (17, 18) or 65 % sulfuric acid (19, 20). WOOTTON (21) has developed a method for the quantitative estimation of free bile acids in mixtures using a combination of adsorption chromatography and infrared analysis. This method as well as counter-current distribution procedures (22) and column partition chromatography (23, 24, 25, 26) permits the quantitative determination of bile acids in complex mixtures. WIGGINS (27) has combined counter-current distribution with Wootton's method and been able to determine various conjugated bile acids. These more comprehensive methods are time-consuming and not quite suitable for routine analyses.

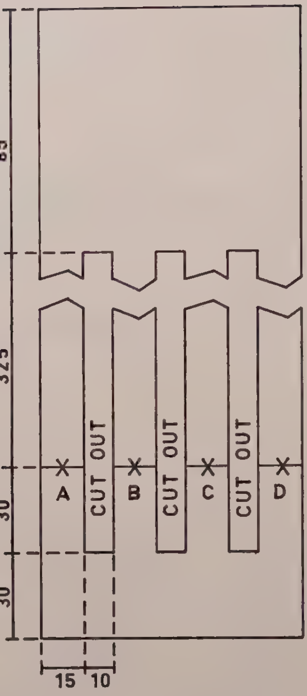

Fig. 1. Preparation of paper. All dimensions are given in millimeters. A: Blank strip; B and C: Strips to be eluted for quantitative determination; D: Strip to be sprayed for the localization of the acids.

Several methods for the qualitative separation of bile acids by paper chromatography have appeared lately (for references see 28). The purpose of this investigation was to attempt to refine the paper chromatographic method of Sjövall (28) for quantitative work. Similar methods for the quantitative determination of steroid hormones after paper chromatographic separation have been published lately (see for example Zaffaroni (29), Axelrod (30), Bush (31) and Rubin *et al.* (32)).

Experimental

Details of the paper chromatography have been published earlier (28, 33).

Solvents:

Glass distilled water.

Ethanol, 96 %, redistilled.

Acetic acid, 97–99 %, redistilled.

Ethylene chloride having no light absorption at 270 mμ when compared with water. Purified by shaking with concentrated sulfuric acid, washed with water, dried over K_2CO_3 and distilled.

n-Heptane redistilled.

n-Butanol redistilled.

Preparation of paper. Whatman 3MM filter paper was cut in strips, 9 cm wide and 46.5 cm long. These strips were cut as shown in Fig. 1 so that four separate strips each 1.5 cm wide and all held together by intact paper at both ends were obtained. The starting line for ascending chromatography was drawn with a pencil 6 cm from the lower end of the paper (Fig. 1). When the papers had been cut they were washed in an ordinary tank for descending chromatography. Three sheets (with the starting line downwards) were hung on each side of the trough at the top of the tank.

The washing solvents were placed in the trough in the following sequence: 450 ml ethanol; 300 ml 10 % acetic acid/water (v/v); 450 ml ethanol; 100 ml ethylene chloride : acetic acid 90 : 10 and finally 450 ml ethanol. With this procedure (completed in about three days) most of the "dirt" in the paper was removed and no substances interfering with the quantitative determinations remained. After having been washed the papers were dried at 100°C.

Preparation and development of the chromatograms. The solutions for quantitative determinations contained approximately 1 μg of the bile acid or its sodium salt in 1 μl of alcohol. For purity of the acids see previous communications (34, 35). The solution was applied along the starting line of three of the strips (B, C, D, Fig. 1) with a 20 μl constriction pipette. One strip (A, fig. 1) served as a blank. To get the band as narrow as possible a continuous stream of hot air was blown on the starting line from underneath during the application. The air was heated by letting it go through a wide glass tubing heated with a Bunsen flame. It must not be heated by contact with hot iron or copper wires or tubing because of the influence of these metals on the quantitative determinations.

Ascending chromatograms were run with the phases previously described (33). For the chromatography of free and glycine conjugated bile acids the moving phase was ethylene chloride : heptane 60 : 40 or 70 : 30, saturated with an equal volume of the stationary phase, 70 % acetic acid/water (v/v). Ethylene chloride : butanol 90 : 10 or 80 : 20 equilibrated with 70 % acetic acid, was used as the moving phase for the separation of the taurine conjugated bile acids. The papers were hung in the tanks as earlier described (28) and were allowed to equilibrate in the atmosphere of the moving and stationary phases for at least 8 hours. However, no filter paper strips were placed around the walls of the tank in order to diminish the risk of bringing "dirt" into the moving phase. The tanks were only covered with a ground glass plate, no silicone or other grease was used.

After the equilibration period, the chromatogram was run until the solvent front reached the upper end of the strips. This required between 5 and 10 hours depending on the amount of ethylene chloride in the moving phase.

Elution and determination of the separated acids. After chromatography the papers were removed from the tank and allowed to hang at room temperature for ½–1 hour. Strip D (Fig. 1) was cut out and the spots were revealed by spraying with a solution of phosphomolybdic acid (10 % in ethanol) followed by drying at 100°C. The strip was stapled back in its original position beside the chromatogram which had been mounted with adhesive tape on a glass plate. The zones on strip A, B and C corresponding to the spots on strip D (Fig. 1) were cut out and eluted in the apparatus schematically shown in Fig. 2. In our laboratory an apparatus 1 meter long which permits the simultaneous elution of 19 filter paper pieces in about one hour has been used. One end of the strip which had been cut out was clamped between two microscopic slides 3 mm thick as shown in Fig. 2. Ethanol was delivered onto the upper ends of the slides at an approximate rate of 6 ml per hour from a glass tubing that had been drawn out to a capillary. 4 ml ethanol was used for the elution of each filter paper piece. The eluate was collected in pyrex test tubes which had been washed in chromic acid overnight. Because of the evaporation of ethanol from the filter paper pieces the eluate usually had a volume of about 2 ml. The ethanol was evaporated by placing the test tubes in an oven at 100°C for 4–6 hours. During the elution of the filter paper pieces 20 μl of a standard solution of the bile acid to be determined containing 1 μg per μl had been pipetted into two test tubes. These standards were dried in the oven at the same time as the eluates from the chromatograms. During the evaporation process the test tubes were protected from being contaminated with dust by a covering glass plate supported about one cm above the test tubes. When dry, the test tubes were taken out and allowed to cool down to room temperature. The acids were now ready for the identification by means of their spectra in sulfuric acid and for the quantitative determination. These techniques have been described in previous papers (34, 35) and only a short description of the quantitative determination will be given here.

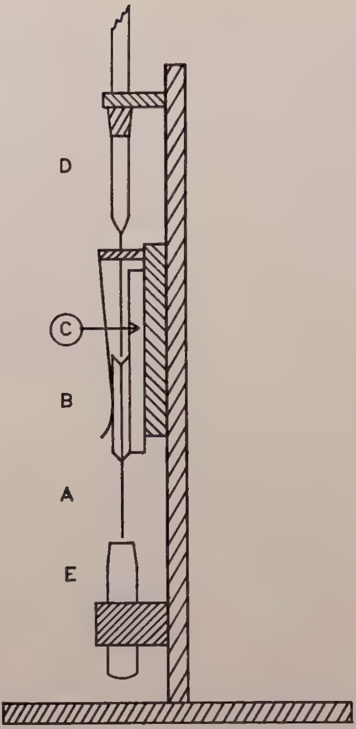

Fig. 2. Schematic side view of the apparatus for elution of bile acids from filter paper strips. The strip A containing the bile acid is clamped between two microscopic slides B which are pressed together with a spring against a glass plate C. Alcohol is delivered through a capillary from the glass tubing D. The eluate is collected in a test tube E.

1 or 2 ml (depending on the optical density to be expected) 65 % sulfuric acid was accurately pipetted into the test tubes containing the eluted acids and the eluate of the corresponding filter paper blank. The two standards and a blank were treated in the same way. The tubes containing the eluates from the chromatogram were thoroughly shaken in a shaking apparatus for 5 minutes to insure a complete dissolution of the bile acid. The samples and the standards were then heated at 60°C in a water bath for the appropriate time. Free and conjugated cholic acids and conjugated chenodesoxycholic acids were heated for 15 minutes; free and conjugated desoxycholic acids, chenodesoxycholic acid and hyodesoxycholic acid were heated for 60 minutes. After the heating period the test tubes were cooled in tap water and allowed to stand for 15 minutes at room temperature. The optical density was measured in a Beckman spectrophotometer model DU using silica cells 0.3 × 10 mm. Free and conjugated cholic acids were measured at 320 mμ; chenodesoxycholic and hyodesoxycholic acids at 380 mμ; conjugated chenodesoxycholic acids at 305 mμ; desoxycholic acid at 385 mμ and conjugated desoxycholic acids at 389 mμ.

Results

Only synthetic bile acids, singly or in mixtures, have been determined thus far. Table 1 lists the quantitative recovery of pure bile acids after paper chromatography under the conditions described. The mean recovery is practically quantitative and the variations within the different runs are small. The values listed have been obtained after chromatography of between 10 and 20 μg. The lower limit for the determinations is determined by the extinction coefficients of the bile acids in the sulfuric

Table 1. Recovery of pure bile acids after paper chromatography.

Acid[1]	Number of trials	Amount	Mean recovery per cent	Range
GC	8	19.2	99.1	97.3–101.0
TC	10	20.5	98.1	96.7–100.0
C	20	17.5	98.5	95.9–101.1
GD	6	17.7	98.3	97.0– 98.9
TD	9	16.7	99.1	96.6–102.1
D	6	20.8	99.7	98.6–100.5
GCD	6	18.4	100.3	98.8–102.5
TCD	6	18.8	100.0	98.6–102.5
CD	10	19.0	100.5	96.5–102.3
HD	16	9.8	98.6	96.8–100.0

[1] C = cholic acid
D = desoxycholic acid
CD = chenodesoxycholic acid
HD = hyodesoxycholic acid
Prefix G = glyco-
Prefix T = tauro-

Table 2. Recovery of bile acids after chromatography of mixtures.

Acids[1]	Number of trials	Amount	Recovery per cent
C		17.5	98.4; 98.4
+	2		
D		18.5	102.7; 100.3
GC		19.2	100.7; 102.1
+	2		
GCD		18.4	101.3; 100.8
GD		17.7	102.5; 102.2
+	2		
D		18.5	96.7; 96.7
GCD		18.4	98.3; 99.7
+	2		
CD		19.0	98.7; 98.7

[1] See Table 1.

acid. Using 1 ml of sulfuric acid, the optical density of the different acids at their characteristic maxima lies between 0.023 (conjugated chenodesoxycholic acids) and 0.065 (hyodesoxycholic acid) for 1 μg bile acid with the method described. The upper limit for the determinations is determined by the capacity of the filter paper and the solvent systems. This capacity has not been determined, but 80 μg of an acid can easily be run without streaking. The volume of the sulfuric acid has to be increased, of course, in order to keep the optical density within the measurable range of the spectrophotometer. Thus any amount of bile acid between 2 and 80 μg can be determined with fairly good accuracy.

Table 2 shows the recovery of bile acids in some separations of mixtures. The application of the method to descending chromatography to make possible the differential determination of free and conjugated desoxycholic and chenodesoxycholic acids is being investigated.

Discussion

Since the development of this method has involved extensive studies of factors influencing the quantitative recovery of bile acids after paper chromatography it might be appropriate to discuss some of the steps described under Experimental.

Washing of the papers. The problem of "dirt" in the filter paper has been recognized by many investigators working with quantitative paper chromatography. The spectrum of cholic acid in 65 % sulfuric acid after heating is altered if the acid is eluted from a chromatogram developed on unwashed paper. The extinction coefficient at 320 mμ is lowered and the main maximum is found at 389 mμ. A similar spectrum is found after the addition of ferric chloride as described in a previous communication (34). When the washing procedure described is used, no changes in the spectra of pure bile acids in 65 % and 96 % sulfuric acid can be observed after chromatography. The spectra are measured against a blank for a corresponding filter paper piece. The filter paper blank prepared as described gives an optical density of 0.005 to 0.020 at 320 mμ when heated in 1 ml 65 % sulfuric acid.

Solvent systems for the chromatography. At the beginning of this investigation the solvent systems originally described (28) were used. Preliminary results have been reported (36) but it was found that for some acids the recoveries were variable. The effect of the solvents in the moving phase on the quantitative determination of the bile acids was tested. The influence of isopropyl ether on the recovery of cholic acid has been reported (34). Freshly distilled, peroxide free isopropyl ether did not influence the recovery but even after one day 0.1 ml isopropyl ether, when evaporated with 10 μg cholic acid before the determination in 65 % sulfuric acid, reduced the value considerably. At the same time the spectrum changed in approximately the same way as it did in the presence of filter paper "dirt" or ferric chloride. It was found, however, that when 0.1 ml isopropyl ether:heptane 75:25 (as moving phase equilibrated with 70 % acetic acid) was evaporated together with 10 μg cholic acid before the determination in 65 % sulfuric acid, the recovery was not reduced to the same extent as with isopropyl ether alone even after storing the isopropyl ether:heptane for a week. Approximately 90–95 per cent of the cholic acid was recovered. The heptane used has no effect on the determinations of cholic acid, possibly the acetic acid destroys peroxides which can interfere with the sulfuric acid chromogens.

Ethylene chloride, after purification as described, was found not to influence the quantitative determinations of bile acids with the technique used, and suitable systems for the separation of the bile acids with paper chromatography were worked out (33). The use of amyl acetate:heptane as moving phase (33) was found to be especially suitable for the separation of taurine conjugated bile acids, but it has not yet been possible to obtain an amyl acetate pure enough to be without influence on the quantitative determinations. The ethylene chloride:butanol phase (33) used in this work does not influence the quantitative determinations.

Elution of the acids after chromatography. In the ascending chromatography a bile acid always travels exactly the same distance on the three strips of the filter paper, and therefore the procedure for cutting out the spots was found sufficiently accurate.

The efficiency of the elution process was tested and it was found that 2 ml ethanol eluted 97 per cent of the bile acid. Elution with 4 ml of ethanol gave a quantitative recovery of the bile acid.

4–6 hours at 100°C was found to be a suitable time for the evaporation of the ethanol in the eluate. There was no detectable destruction by heat, the recovery was the same after 16 hours at 100°C as after 4 hours.

Quantitative determination. The quantitative determination of pure bile acids has been discussed in previous papers (34, 35). Because of the small amount of "dirt" (giving light absorption in sulfuric acid) that is still left in the papers after the washing procedure, filter paper blanks always have to be run parallel with the bile acid samples. It has been found that the bile acids are more difficult to dissolve in 65 % sulfuric acid when they have been eluted from the chromatograms than when they are pipetted directly into test tubes. This is probably due to the remaining traces of "dirt" eluted from the filter paper. If the chromatographic tanks are sealed with silicone grease this difficulty in dissolving the bile acids is still more pronounced. Therefore no grease is used for the sealing of the tanks and the test tubes are thoroughly shaken for 5 minutes when the sulfuric acid has been added. When 96 % sulfuric acid is used the bile acids dissolve without difficulty.

If the above-mentioned directions are carefully followed, the method described can be used for the quantitative determination of synthetic bile acid mixtures. The application to biological materials is under investigation.

SUMMARY

A method is described for the quantitative determination of mixtures of free and conjugated bile acids. The bile acids are separated by paper chromatography and after elution are spectrophotometrically determined in 65 % sulfuric acid. The recoveries are quantitative and the variations between different determinations are small.

The author wishes to thank Prof. S. Bergström for his continuous interest in this work and for many valuable discussions. Thanks are also due to Dr. A. Norman for generous gifts of conjugated bile acids.

This work is part of an investigation supported by grants from the Medical Faculty of the University of Lund.

Department of Physiological Chemistry, University of Lund, Lund, Sweden.

REFERENCES

1. Aldrich, M. and Bledsoe, M. S., J. Biol. Chem. *77*, 519 (1928).
2. Gregory, R. and Pascoe, T. A., J. Biol. Chem. *83*, 35 (1929).
3. Reinhold, J. G. and Wilson, D. W., J. Biol. Chem. *96*, 637 (1932).
4. Josephson, B., Biochem. J. (London) *29*, 1519 (1935).
5. Irvin, J. L., Johnston, C. G., and Kopala, J., J. Biol. Chem. *153*, 439 (1944).
6. Foster, M. G. and Hooper, C. W., J. Biol. Chem. *38*, 355 (1919).
7. Josephson, B. and Jungner, G., Biochem. J. (London) *30*, 1953 (1936).
8. Lichtman, S., J. Biol. Chem. *107*, 717 (1934).
9. Jenke, M. and Bandow, F., Hoppe-Seyler's Z. physiol. Chem. *249*, 16 (1937).
10. Minibeck, H., Biochem. Z. *297*, 29 (1938).
11. Kaziro, K. and Shimada, T., Hoppe Seyler's Z. physiol, Chem. *254*, 57 (1938).
12. Szalkowski, C. R. and Mader, W. J., Anal. Chem. *24*, 1602 (1952).
13. Saba, G., J. Biochem. (Japan) *31*, 43 (1940).

14. Isaksson, B., Acta Chem. Scand. *8*, 889 (1954).
15. Doubilet, H., J. Biol. Chem. *114*, 289 (1936).
16. Murakami, E., J. Biochem. (Japan) *39*, 17 (1952).
17. Abe, Y., J. Biochem. (Japan) *26*, 323 (1937).
18. Pratt, E. L. and Corbitt, H. B., Anal. Chem. *24*, 1665 (1952).
19. Kier, L. C., J. Lab. Clin. Med. *40*, 755 (1952).
20. Mosbach, E. H., Kalinsky, H. J., Halpern, E., and Kendall, F. E., Arch. Biochem. Biophys. *51*, 402 (1954).
21. Wootton, I. D. P., Biochem. J. (London) *53*, 85 (1953).
22. Ahrens, E. H. Jr. and Craig, L. C., J. Biol. Chem. *195*, 763 (1952).
23. Bergström, S. and Sjövall, J., Acta Chem. Scand. *5*, 1267 (1951).
24. Sjövall, J., Acta Physiol. Scand. *29*, 232 (1953).
25. Norman, A., Acta Chem. Scand. *7*, 1413 (1953).
26. Mosbach, E. H., Zomzely, C., and Kendall, F. E., Arch. Biochem. Biophys. *48*, 95 (1954).
27. Wiggins, H. S., Biochem. J. (London) *56*, xxxix (1954).
28. Sjövall, J., Acta Chem. Scand. *8*, 339 (1954).
29. Zaffaroni, A., Rec. Progr. Horm. Res. *8*, 51 (1953).
30. Axelrod, L., Rec. Progr. Horm. Res. *9*, 69 (1954).
31. Bush, I. E., Rec. Progr. Horm. Res. *9*, 321 (1954).
32. Rubin, B. L., Dorfman, R. J., and Pincus, G., Rec. Progr. Horm. Res. *9*, 213 (1954).
33. Sjövall, J., Arkiv Kemi *8*, 299 (1955).
34. Eriksson, S. and Sjövall, J., Arkiv Kemi *8*, 303 (1955).
35. Eriksson, S. and Sjövall, J., Arkiv Kemi *8*, 311 (1955).
36. Eriksson, S. and Sjövall, J., Acta Chem. Scand. *8*, 1099 (1954).

Tryckt den 26 april 1955

Uppsala 1955. Almqvist & Wiksells Boktryckeri AB

ARKIV FÖR KEMI Band 8 nr 31

Communicated 9 February 1955 by ARNE FREDGA

The time-variable in chemical kinetics

By SIGVARD WIDEQVIST

The possibility of changing the time-variable seems to have been used very little in the treatment of problems in reaction kinetics.

For a simple second-order reaction

$$\begin{array}{cccc} \mathrm{A} + & \mathrm{B} \rightarrow & \mathrm{C} + & \mathrm{D} \\ a-x & b-x & x & x \end{array}$$

the extent of the reaction is related to the time by the differential equation

$$dx/dt = k(a-x)(b-x). \tag{1}$$

Eq. (1) can easily be converted into the differential equation for a first-order reaction by putting

$$(b-x)\,dt = d\theta. \tag{2}$$

Then we get

$$dx/d\theta = k(a-x). \tag{3}$$

On integration we obtain

$$k = \frac{1}{\theta} \ln \frac{a}{a-x} \tag{4}$$

where

$$\theta = \int_0^t (b-x)\,dt. \tag{5}$$

The magnitude of the velocity constant k is not altered by this operation. The new time variable, θ, is easily determined as the area between the curve $b-x=f(t)$ and the t-axis.

In the same manner, the differential equation for a first-order reaction

$$dx/dt = k(a-x) \tag{6}$$

can be converted into the differential equation for a zero-order reaction. Substitution of $d\theta$ for $(a-x)\,dt$ thus gives

$$dx/d\theta = k. \tag{7}$$

On integration we obtain

$$k = x/\theta. \tag{8}$$

The formal transformation of a first-order reaction into a zero-order reaction will be illustrated by the alkaline hydrolysis of ethyl phenylcyanoacetate. This ester easily dissolves in aqueous alkali with the formation of enolate. In the solution a rapid hydrolysis of the ester group takes place. If the alkali is saturated with the ester, the hydrolysis follows the first-order kinetics.

The measurements were performed at 25.0° C. Samples were taken with a 10 ml pipette and allowed to flow into excess dilute hydrochloric acid. The excess acid was determined by titration with standardized sodium hydroxide. The results are recorded in Table 1. For comparison, the velocity constant k was calculated as a first-order constant from the integrated form of eq. (6) and as a zero-order constant according to eq. (8). The quantity θ was calculated by graphical integration.

Table 1. The hydrolysis of ethyl phenylcyanoacetate by sodium hydroxide at 25.0° C.

$t_{\text{min.}}$	$a-x$	θ	$k_{\text{Eq. (6)}}$	$k_{\text{Eq. (8)}}$
0	0.1881			
10	.1679	1.781	0.01134	0.01135
20	.1493	3.366	1154	1153
30	.1336	4.781	1141	1140
40	.1180	6.039	1165	1161
50	.1061	7.160	1145	1145
60	.0952	8.166	1134	1148
70	.0851	9.068	1132	1136
		Mean value	0.01144	0.01145

The method of reducing the reaction order by changing the time-variable, although of little importance in the case of simple second-order reactions, is very advantageous in the treatment of competitive consecutive second-order reactions:

$$\begin{array}{ccccccc} A & + & B & \rightarrow & C & + & D \\ a-x & & b-x-y & & x-y & & x+y \end{array}$$

$$\begin{array}{ccccccc} C & + & B & \rightarrow & E & + & D \\ x-y & & b-x-y & & y & & x+y. \end{array}$$

It was thus shown by the present author [1] and independently by FRENCH [2] that the nonintegrateable differential equation system

$$dx/dt = k_1(a-x)(b-x-y) \tag{9}$$

$$dy/dt = k_2(x-y)(b-x-y) \tag{10}$$

can be converted into the easily integrated equation system

$$d\,x/d\,\theta = k_1\,(a-x) \tag{11}$$

$$d\,y/d\,\theta = k_2\,(x-y) \tag{12}$$

by putting $(b-x-y)\,d\,t = d\,\theta$.

From the integrated form of eq. (11) and (12) it is fairly easy to calculate the velocity constants k_1 and k_2.

The velocity constants k_1 and k_2 can also be directly calculated from eq. (9) and (10) by using the "time-ratio method" of FROST and SCHWEMER. For details the reader is referred to the original paper by FROST and SCHWEMER [3] and to a brief survey by FROST and PEARSON [4]. It is, however, necessary to give some information in order to facilitate the understanding of the method.

FROST and SCHWEMER defined $\varkappa = k_2/k_1$. Further they introduced $\tau = k_1\,a\,t$. Thus

$$k_1 = \tau/at. \tag{13}$$

The extent ot the reaction was defined as $z/2\,a$, where $z = x+y$. The quantity $1/\varkappa$ was tabulated as a function of the time-ratios for 60/20, 60/30, 60/40, 60/50, 50/20, and 50/30 per cent reaction. It is thus possible to get $\varkappa$ from the experimental curve $2\,a - z = f\,(t)$. In another table τ was recorded as a function of $1/\varkappa$ for 20, 30, 40, 50, and 60 per cent reaction. From τ the relation (13) gives k_I. Finally one finds k_2 as $k_1\,\varkappa$.

However, the tables calculated by FROST and SCHWEMER are valid only for the case where the initial concentrations of the reacting substances are exactly equivalent, i.e. $b = 2\,a$. As mentioned by FROST and SCHWEMER, there where in fact no measurements available in the literature which could be used to test the time-ratio method. Either the initial conditions did not correspond to those considered by FROST and SCHWEMER, namely equivalent concentrations, or the extent of the reaction was not sufficiently great. Therefore the authors were forced to make their own measurements on the hydrolysis of alkyl esters of dicarboxylic acids by alkali at equivalent concentrations.

The time-ratio method is undoubtedly the most rapid method of calculating the velocity constants for two competitive, consecutive, second-order reactions from one single run of measurements. It would therefore be a pity, if the use of the method should be limited to the rather uncommon case, where the reacting substances are present in equivalent concentrations.

However, it can be shown that the tabulated functions of FROST and SCHWEMER can be used to calculate k_1 and k_2 for any second-order two-stage reaction, irrespective of the initial concentrations, by applying the method of changing the time-variable. The only restriction is that $b > a$, or, preferably, $\geq 2\,a$, for it is self-evident that the extent of the raction becomes too slight, if b is too small in comparison with a.

We regard again the differential equation system

$$d\,x/d\,t = k_1\,(a-x)\,(b-z) \tag{9}$$

$$d\,y/d\,t = k_2\,(x-y)\,(b-z) \tag{10}$$

where $z = x+y$. By multiplication with $\dfrac{2\,a-z}{2\,a-z} \equiv 1$ we obtain

$$d\,x/d\,t = k_1\,(a-x)\,(2\,a-z)\,\frac{b-z}{2\,a-z} \tag{14}$$

$$d\,y/d\,t = k_2\,(x-y)\,(2\,a-z)\,\frac{b-z}{2\,a-z} \tag{15}$$

and by putting

$$\frac{b-z}{2\,a-z}\,d\,t = d\,\theta \tag{16}$$

we obtain the equation system

$$d\,x/d\,\theta = k_1\,(a-x)\,(2\,a-z) \tag{17}$$

$$d\,y/d\,\theta = k_2\,(x-y)\,(2\,a-z) \tag{18}$$

which is valid for two competitive, consecutive, second-order reactions with equivalent initial concentrations for the reacting substances. Now we have the new time-variable

$$\theta = \int_0^t \frac{b-z}{2\,a-z}\,d\,t \tag{19}$$

which is the area between the curve $\frac{b-z}{2\,a-z} = f\,(t)$ and the t-axis.

The method of changing the time-variable will be illustrated by the measurements on the alkaline hydrolysis of diethyl succinate performed by KNOBLAUCH [5]. The measurements were performed at 25° C. The initial concentrations of ester and alkali were $a = 2.331 \cdot 10^{-3}$ and $b = 7.814 \cdot 10^{-3}$, respectively. Thus we have $2\,a = 4.662 \cdot 10^{-3}$ and

Table 2. The hydrolysis of diethyl succinate by alkali in aqueous solution at 25°C. (From the measurements of KNOBLAUCH [5].)

$t_{\text{min.}}$	$(b-z)\cdot 10^3$	$(2\,a-z)\cdot 10^3$	$\frac{b-z}{2\,a-z}$	$\theta_{\text{min.}}$
0	7.814	4.662	1.676	0
8	6.545	3.393	1.929	14.42
10	6.390	3.236	1.973	18.32
12	6.227	3.075	2.025	22.32
14	6.064	2.912	2.082	26.43
16	5.910	2.758	2.143	30.65
18	5.851	2.699	2.168	34.96
20	5.748	2.596	2.214	39.35
29	5.466	2.314	2.362	59.94
31	5.396	2.244	2.405	64.70
39	5.183	2.031	2.552	84.53
47	4.968	1.816	2.736	105.68

$$\theta = \int_0^t \frac{b-z}{2a-z}\,dt = \int_0^t \frac{7.814\cdot 10^{-3} - z}{4.662\cdot 10^{-3} - z}\,dt. \tag{19 a}$$

The values of θ are recorded in Table 2. The values of $2a-z$ were plotted against θ. From a smoth curve drawn through the points the times for 20 % up to 60 % reaction were read. The value for 50 % reaction seemed, however, to be less accurate and was thus discarded. From the θ ratios the corresponding values of $1/\varkappa$ were found by interpolation in the $1/\varkappa$-table of FROST and SCHWEMER, and then after taking the average the value of τ and k_1 were determined using the τ-table of FROST and SCHWEMER. Table 3 shows the results of the calculations.

Table 3. Calculation of rate constants.

% Rx	$\theta_{\text{min.}}$	Percentages compared	θ ratio	$1/\varkappa$
20	9.47	60/20	10.444	8.081
30	17.11	60/30	5.785	8.452
40	30.00	60/40	3.298	8.208
60	98.95			

Average $1/\varkappa = 8.25$.

% Rx	τ	k_1	k_2
20	0.2759	12.49	1.514
30	0.5097	12.78	1.549
40	0.8815	12.61	1.528
60	2.913	12.65	1.534

Average $k_1 = 12.63$; $k_2 = 1.531$.

Under the assumption that $y=0$ at the beginning of the reaction and that $x=a$ at the end of the reaction, KNOBLAUCH tried to calculate the velocity constants by use of the ordinary equations for a single-step second-order reaction. The following values were obtained.

$t_{\text{min.}}$	8	10	12
k_1	13.88	13.55	13.90

$t_{\text{min.}}$	375	417	486	535
k_2	1.423	1.343	1.296	1.788

Summary

A method for solving problems in reaction kinetics by changing the time-variable has been suggested. The use of the method is illustrated by examples.

Laboratory of Organic Chemistry, University of Uppsala.

REFERENCES

1. Wideqvist, Acta Chem. Scand. *4*, 1216 (1950).
2. French, J. Am. Chem. Soc. *72*, 4806 (1950).
3. Frost and Schwemer, J. Am. Chem. Soc. *74*, 1268 (1952).
4. Frost and Pearson, Kinetics and Mechanism, New York 1953, p. 168.
5. Knoblauch, Z. physik. Chem. *26*, 96 (1898).

Tryckt den 26 april 1955

Uppsala 1955. Almqvist & Wiksells Boktryckeri AB

ARKIV FÖR KEMI Band 8 nr 32

Communicated 9 March 1955 by Karl Myrbäck and Hugo Theorell

Preparation of conjugated bile acids using mixed carboxylic acid anhydrides

Bile acids and steroids. 34

By Arne Norman

Conjugated bile acids are best prepared by synthetic methods from the purified free bile acids and taurine or glycine because the isolation from bile is a troublesome and uncertain procedure. Bondi and Müller (1) described the first syntheses of conjugated bile acids. They converted cholic acid through the ester and hydrazide into the azide, which was then coupled with glycine or taurine in an alkaline medium. The corresponding conjugates of desoxycholic acid were synthesized by this method by Wieland (2). Another route for the synthesis of conjugated bile acids was reported by Cortese and Bauman (3, 4) who formylated the bile acids to protect the hydroxyl groups and then coupled the chlorides of the acids directly with glycine or taurine in the presence of alkali. Cortese's experimental improvements (5) in the Bondi-Müller method rendered this more convenient than his own Schotten-Bauman procedure. Cortese and Bauman's procedure for the formylation of bile acids has been found to give non-crystallizable syrups which were considered to be mixtures of partially formylated derivates. Stacey and Webb (6) obtained a better yield by direct formylation of sodium salt of the bile acid and used this modification in the synthesis of conjugated bile acids according to Cortese and Bauman. This method was found unsuitable for the synthesis of conjugated keto bile acids by coupling of the free keto acid (Gautier and Quy 7) (cf. 32). Instead, the conjugate of the corresponding hydroxy acid was synthesized and this was then oxidized to the keto form.

The above-mentioned methods involve several reaction steps and the over-all yields calculated on the bile acid are usually less than 50 per cent. They are therefore unsuitable for the synthesis of conjugates on a small scale. A suitable method for this purpose has recently been reported by Bergström and Norman (8). They applied the peptide synthesis method with carbonic-carboxylic acid anhydrides developed independently by Wieland and Bernhard, Boissonnas and Vaughan et al. (9–12) to the synthesis of conjugated bile acids.

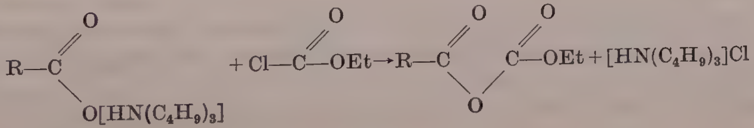

$$R{-}C(=O){-}O[HN(C_4H_9)_3] + Cl{-}C(=O){-}OEt \rightarrow R{-}C(=O){-}O{-}C(=O){-}OEt + [HN(C_4H_9)_3]Cl$$

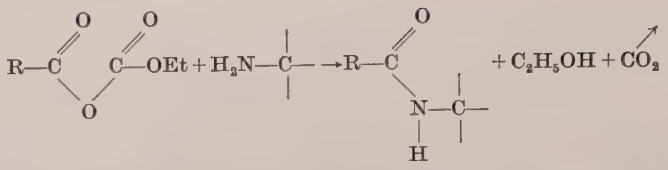

In the present investigation, this method has been developed further. The preparation of the glycine and taurine conjugates of cholic, desoxycholic, chenodesoxycholic, lithocholic and cholanic acid is described. Synthesis of conjugated keto bile acids was found possible and a description of the preparation of glyco- and taurodehydrocholic acids is given. The method has been used for the synthesis of 24-^{14}C labelled conjugated bile acids on a micro scale.

Experimental

Purification of the conjugated bile acids was in some cases effected by reversed phase partition chromatography on hydrophobic supercel (21, 22, 15). The phase systems are the same as those used by Norman (15). The purity of the synthetic bile acids was checked by the paper-chromatographic method of Sjövall (23, 24).

All m.ps. were determined using an aluminium-block apparatus and are corrected.

The optical rotations were determined in a Schmidt-Haentsch polarimeter readable to 0.01° with a 2-dm micro-tube of about 1 ml capacity or a 4-dm tube of about 30 ml capacity.

All yields are corrected for moisture content.

Equivalent weights were determined by micro titration. The microanalyses given in Table 1 were performed at the Microchemical Laboratory, Department of Chemistry, University of Copenhagen. Before analysis, the bile acids were dried at 130° for five hours and at 10 mm Hg pressure over P_2O_5.

Samples of bile acids:

It is necessary to have carefully purified bile acids. Even small amounts of impurities might make crystallization of the conjugated acid impossible.

Cholic acid. Commercial preparations were found to contain a small percentage of a dihydroxy bile acid. After one crystallization from 70 per cent ethanol (cf. 7), no bile acid other than the cholic acid was detected on paper chromatograms. M.p. 198–199°. (Lit.: m.p. 199–200° (7)).

Desoxycholic acid was prepared according to Reichstein and Sorkin (13) by saponification the corresponding methyl ester diacetate, which is obtained from commercial preparations of desoxycholic acid. M.p. 175–177°. (Lit.: m.p. 176–177° (13).)

Chenodesoxycholic acid was prepared by K. Pääbo essentially according to the procedure of Haslewood *et al.* (14). The material obtained was purified by chromatography on kiselguhr columns with phase system F (15). Crystallization from ethyl acetate-light petroleum gave a product with m.p. 142–143°.

Lithocholic acid was prepared from desoxycholic acid according to Bergström and Haslewood (16). The yield was improved by addition of hydrazine hydrate in the Kishner-Wolff treatment. The products of the hydrolysis were acidified and distributed between equal volumes of 70 per cent ethanol and light petroleum, which removed any cholanic acid. The residue from the aqueous phase was crystallized from acetic acid-water. M.p. 182–183°. Repeated recrystallization did not alter the melting point. (Lit.: m.p. 184–185° (16).)

Cholanic acid was prepared according to Borsche and Halwass (17) from triketocholanic acid

Table 1.

Substance	Formula	Equivalent weight		Analyses							
				% C		% H		% N		% S	
		Calc.	Found	Calc.	Found	Calc.	Found	Calc.	Found	Calc.	Found
lycocholic acid	$C_{26}H_{43}O_6N$	465.6	469	67.06	66.87	9.31	9.47	3.01	2.91		
a-glycocholate	$C_{26}H_{42}O_6NNa$	487.6						2.87	2.93		
a-taurocholate	$C_{26}H_{44}O_7NSNa$	537.7		58.08	57.10	8.25	8.31	2.61	2.63	5.96	5.66
lycodesoxycholic acid	$C_{26}H_{43}O_5N$	449.6	447	69.45	69.50	9.64	9.85	3.12	3.03		
a-glycodesoxycholate	$C_{26}H_{42}O_5NNa$	471.6						2.97	2.95		
a-taurodesoxycholate	$C_{26}H_{44}O_6NSNa$	521.7		59.86	59.43	8.50	8.48	2.69	2.75	6.15	5.95
a-glycochenodesoxycholate	$C_{26}H_{42}O_5NNa$	471.6		66.21	65.90	8.98	8.91	2.97	2.99		
a-taurochenodesoxycholate	$C_{26}H_{44}O_6NSNa$	521.7		59.86	59.37	8.50	8.43	2.69	2.61	6.15	6.00
lycolithocholic acid	$C_{26}H_{43}O_4N$	433.6	431	72.01	71.95	10.00	10.10	3.23	3.12		
a-glycolithocholate	$C_{26}H_{42}O_4NNa$	455.6						3.07	2.99		
aurolithocholic acid	$C_{26}H_{45}O_5NS$	483.7	486	64.56	64.37	9.38	9.44	2.90	2.83	6.63	6.45
a-taurolithocholate	$C_{26}H_{44}O_5NSNa$	505.7						2.77	2.70	6.34	6.08
lycocholanic acid	$C_{26}H_{43}O_3N$	417.6	417	74.77	74.93	10.38	10.42	3.35	3.26		
a-glycocholanate	$C_{26}H_{42}O_3NNa$	439.6						3.19	3.35		
aurocholanic acid	$C_{26}H_{45}O_4NS$	467.7	463	66.77	66.65	9.70	9.55	3.00	3.14	6.86	6.96
a-taurocholanate	$C_{26}H_{44}O_4NSNa$	489.7						2.86	2.71	6.55	6.47
lycodehydrocholic acid	$C_{26}H_{37}O_6N$	459.6	458	67.95	67.80	8.12	7.97	3.05	3.07		
aurodehydrocholic acid	$C_{26}H_{39}O_7NS$	509.6	512	61.27	60.95	7.71	7.59	2.75	2.63	6.29	6.55

via Kishner-Wolff treatment of the semicarbazone. The cholanic acid was extracted after the hydrolysis with light petroleum and crystallized from acetic acid. M.p. 164–165°. (Lit.: m.p. 161° (17).)

Triketocholanic acid was obtained by oxidation of cholic acid with chromic acid (18). M.p. 237–239°. (Lit.: m.p. 237° (34).)

24-^{14}C-labelled bile acids were those prepared by Bergström, Rottenberg and Voltz (19).

Reagents:

Tri-n-butylamine, redistilled over BaO. *Ethylchlorocarbonate,* redistilled. *Dioxan* was purified and redistilled over sodium (20). B.p. 101–102°. *Glycine* and *taurine* were recrystallized commercial products. (Anal. Calc. for taurine: N 11.20; S 25.62. Found: N 11.10; S 25.62. Calc. for glycine: N 18.66. Found: N 18.65.)

Description of syntheses

Sodium taurocholate. 53.1 g (130 mmoles) of cholic acid and 30.7 ml (130 mmoles) of tri-*n*-butylamine were dissolved in 150 ml dioxan with slight warming. The solution was cooled to +10° and 13.4 ml (130 mmoles) of ethylchlorocarbonate were added. After 15 minutes at +10°, a solution of 17.9 g taurine (143 mmoles) in 143 ml of *N* NaOH was added and the mixture rapidly stirred. Precautions must be taken owing to the rapid and vigorous evolution of CO_2. After about fifteen minutes when the gas evolution had subsided, sodium hydroxide was added to give pH 8–9 (phenolphthalein). The solution was then evaporated *in vacuo* to a syrup and dissolved in 400 ml of boiling ethanol. After cooling to room temperature, the solution was filtered. Ethyl acetate was added to the filtrate to incipient cloudiness, and the solution left to stand overnight at 0°. The crystals were filtered and washed with ether, air dried, and dissolved in 600 ml of 90 per cent ethanol, after which ether was added to incipient cloudiness. When crystallization had begun, the mixture was placed in the ice-box. After 24 hours, the crystals were thoroughly washed on a Büchner funnel with ethanol-ether 1:1, followed by ether, and air dried; yield 60.4 g (79 per cent). Melting point 225–235°. Two recrystallizations from ethanol-ethyl acetate and 90 per cent ethanol-ether did not alter the m.p.

When the sodium taurocholate failed to crystallize from the reaction mixture, it was first salted out with sodium chloride as described by HAMMARSTEN (18) and then crystallized from 90 per cent ethanol-ether.

Glycocholic acid. The synthesis and purification have been described earlier (8). One synthesis starting from 150 mmoles yielded 69 per cent glycocholic acid, m.p. 165–168°, unaltered by recrystallization from the same solvents (ethanol-ethyl acetate). 1 g of this sample was dissolved in 5 ml of hot ethanol and diluted with 95 ml boiling water, and stored at 0° overnight. M.p. 132–134°. A sample dried at 70° for 5 hours over P_2O_5 at 0.1 mm Hg gave the same m.p. Another crystalline modification ("*paraglycocholic acid*") was obtained according to the directions of CORTESE and BAUMAN (3). The glycocholic acid was refluxed for 5 hours in water, filtered hot and washed with boiling water. M.p. 190–195°.

Sodium glycocholate. 1 g of the free acid was dissolved in 50 ml ethanol and neutralized with sodium ethoxide (phenolphthalein). After adding 5 ml of water and enough ether to cause incipient cloudiness, the mixture was stored overnight at 0° and filtered; yield 95 per cent.

Sodium taurodesoxycholate. 34.14 g (87 mmoles) of desoxycholic acid and 20.5 ml (87 mmoles) of tri-*n*-butylamine in 175 ml dioxan were treated with 8.3 ml (87 mmoles) of ethylchlorocarbonate and 11.98 g of taurine as described above. One hour after the addition of taurine, sodium hydroxide was added until the solution was neutral to phenolphthalein. The solution was transferred to a large dish and evaporated on a water bath. The remaining gum was dissolved in 600 ml of boiling ethanol. Undissolved material was filtered off and the filtrate evaporated until crystallization occurred. After standing overnight in an ice-box, the crystals were filtered off and thoroughly washed with small volumes of ice-cold ethanol, followed by ethanol-ether 1:1 and ether, and air dried. Yield 32.25 g (66 per cent). M.p. 169–174°. Recrystallization from ethanol raised the m.p. to 171–175°. Further recrystallization from 90 per cent ethanol-ether did not alter the m.p.

Glycodesoxycholic acid. A solution of 0.984 g (2.5 mmoles) of desoxycholic acid and 0.59 ml (2.5 mmoles) of tri-*n*-butylamine in 5 ml of dioxan was cooled to 8° and 0.238 ml (2.5 mmoles) of ethylchlorocarbonate added. After 15 minutes at this temperature, 0.206 g (2.75 mmoles) of glycine in 2.75 ml of *N* sodium hydroxide was added, and after the gas evolution had subsided, the reaction mixture was evaporated to dryness *in vacuo*. The residue was dissolved in about 20 ml of water and acidified to pH 1 with hydrochloric acid. The precipitate was washed with water until free of HCl. The crude product was crystallized from a few ml of hot ethanol by adding water to incipient cloudiness, and stored at 0° overnight. Yield 928 mg (76 per cent). M.p. 180–182°. Two recrystallizations from ethanol-water raised the m.p. to 187–188°. Further recrystallization from ethanol-ethyl acetate did not alter the m.p.

Sodium glycodesoxycholate. The salt was prepared as described under sodium glycocholate and crystallized from 90 per cent ethanol-ether. Yield 94 per cent.

The glycine and taurine conjugates of chenodesoxycholic, lithocholic, cholanic and dehydrocholic acid were synthesized as described for the cholic and desoxycholic acid derivatives. In the following, therefore, only a description is given of the purification of the reaction products by crystallization and in some cases by column chromatography. The sodium salts were crystallized from ethanol or 90 per cent ethanol-ether (see Table 2).

Sodium glycochenodesoxycholate. After evaporation of the reaction mixture and dissolving in water, acidification with hydrochloric acid gave a sticky precipitate which was washed with water

Table 2.

Substance	Crystallized from	Melting point, °C		Moisture determination	
		Present investigation	Literature	Present investigation	Literature
lycocholic acid	EtOH–EtoAc	165–168		< 1 %	
(normal form)	5 % EtOH–H_2O	132–134	about 130 (3); 133–152 (1)	5.85 %	5.75 %[1]
(para form)		190–195	192–195 (3); 193–195 (28)	< 1 %	
a-glycocholate	90 % EtOH–Et_2O	230–240	—	8.3–10.9 %	
a-taurocholate	90 % EtOH–Et_2O	225–235	225–235 (29)	4.2–12.3 %	2–250 % (29)
lycodesoxycholic acid	EtOH–H_2O	187–188	180–187 (4); 184 (7); 187–188 (2)	3.75–3.96 %[2]	4.4–3.5 % (2); 4.32 % (4)
	EtOH–EtoAc	186–188	—	< 1 %	
a-glycodesoxycholate	90 % EtOH–Et_2O	245–250	—	4.3–12.2 %	—
a-taurodesoxycholate	90 % EtOH–Et_2O	171–175	160–175 (29)	7.2–9.1 %	2–250 % (29)
a-glycochenodesoxycholate	EtOH–Et_2O	160–170	—	4.2–8.5 %	
a-taurochenodesoxycholate	EtOH–EtoAc	165–175	—	4.8–9.3 %	
lycolithocholic acid	EtOH–H_2O	181–182	—	2.9–3.5 %	
	EtoAc	212–214	—	< 1 %	
aurolithocholic acid	EtOH–H_2O	212–213	—		
	EtOH–EtoAc	212–213	—	3.5–6.1 %	
a-glycolithocholate	90 % EtOH–Et_2O	210–220	—	2.8–5.6 %	
a-taurolithocholate	90 % EtOH–Et_2O	220–230	—	4.1–9.0 %	
lycocholanic acid	EtOH–H_2O	204–206	—	< 0.1 %	
	heptane	204–206	—	< 0.1 %	
aurocholanic acid	EtOH	241–243	—	< 0.1 %	
a-glycocholanate	90 % EtOH–Et_2O	230–240	—	4.1–6.5 %	
a-taurocholanate	90 % EtOH–Et_2O	220–240	—	4.6–8.4 %	
lycodehydrocholic acid	EtOH–H_2O	240–242	248 (7) 244–246 (32)	< 0.1 %	2 H_2O (7)
aurodehydrocholic acid	EtOH–EtoAc	237–238	—	< 1 %	

[1] Calc. 5.49 % for 1.5 H_2O (3); 2 H_2O (7).
[2] Calc. 3.85 % for 1 H_2O.

until free of hydrochloric acid. It was found impossible to crystallize the free acid or its sodium salt and the acid was therefore purified by chromatography. 800 mg of the crude acid were chromatographed on a 45 g hydrophobic Supercel column with phase system C. The glycochenodesoxycholic acid was eluted at 1000–1300 ml effluent from the free chenodesoxycholic acid that remained in the stationary phase. The fractions containing the glycochenodesoxycholic acid were evaporated to dryness *in vacuo*. The free acid could not be crystallized (cf. 35). The residue was therefore dissolved in a few ml of ethanol and neutralized with sodium ethoxide. The sodium salt crystallized on adding ether to incipient cloudiness. Filtration after standing overnight in the ice-box.

Sodium taurochenodesoxycholate. Since taurochenodesoxycholic acid is very soluble in water, it cannot be separated by precipitation with hydrochloric acid from an aqueous solution. The concentrated reaction mixture was dissolved in *N* sodium hydroxide and the tributylamine extracted with two portions of ether. The taurochenodesoxycholic acid was then extracted from the acidified aqueous solution with butanol. The tributylamine salt cannot be separated from the taurine conjugate by butanol extraction. Even an extraction from a solution 3 *N* in hydrochloric acid gave the taurine conjugate partly as the butylamine salt. Ether extraction from an alkaline solution, however, effected a complete separation of these two components.

Table 3. Optical rotations for free and conjugated bile acids (all positive). All determinations were made in a 2 dm micro-tube, except for the free acids and salts of cholic and desoxycholic acids and their conjugates that were measured in a 4 dm tube.

Substance	Solvent	Present investigation, $[\alpha]_D^{23}$; $[M]_D^{23}$			Literature
		c = 1	c = 2.5	c = 5	
Cholic acid	ethanol	35.4 ± 1.0 *145 ± 4*	35.0 ± 0.8 *143 ± 3*		$[\alpha]_D^{20} = 35.07$ (c = 0.432 – 1.440, ethanol) (27); $[\alpha]_D^{20} = 35 \pm 0.5$ (c = 1.06, 70 % ethanol (7).
Glycocholic acid	ethanol	30.6 ± 0.6 *143 ± 3*	30.5 ± 0.3 *142 ± 2*	30.4 ± 0.4 *142 ± 2*	$[\alpha]_D^{20} = 33.5$; 32.5; 32.3 (c = 1; 2.5; 5, ethanol) (27); $[\alpha]_D^{18.5} = 32.0$ (c = 4.9, ethanol) (7); $[\alpha]_D^{23} = 32.5$ (c = 7.5, 95 % ethanol) (3); $[\alpha]_D^{17} = 30.5$ (c = 1.576, ethanol) (6).
Na-cholate	water	32.5 ± 1.2 *140 ± 5*	28.5 ± 0.6 *123 ± 2*	27.4 ± 0.4 *118 ± 2*	$[\alpha]_D^{20} = 31.0$; 29.5; 28.85 (c = 1; 2.5; 5, water) (27).
Na-taurocholate	water	25.2 ± 1.0 *136 ± 5*	24.0 ± 0.4 *129 ± 2*	21.7 ± 0.3 *117 ± 2*	$[\alpha]_D^{20} = 22.6$; 22.1; 21.65 (c = 1.25; 2.5; 5 water) (27); $[\alpha]_D^{23} = 23.6$ (c = 2.5, water) (5).
Na-glycocholate	water	29.2 ± 1.0 *142 ± 5*	26.5 ± 0.6 *129 ± 3*	24.0 ± 0.2 *117 ± 1*	$[\alpha]_D^{20} = 32.0$; 27, 8; 26.35 (c = 1; 2.5; 5, water) (27); $[\alpha]_D^{24} = 32.0$; 27.6 (c = 1; 2.5, water) (5).
Desoxycholic acid	ethanol	54.0 ± 0.4 *212 ± 2*	53.6 ± 0.4 *210 ± 2*		$[\alpha]_D^{20} = 57.02$ (c = 2.03, ethanol) (30); $[\alpha]_D^{20} = 55.56$ (c = 0.5 – 5, ethanol) (27); $[\alpha]_D^{17.5} = 52.8 \pm 2$ (c = 1.515, ethanol) (13).
Glycodesoxycholic acid	ethanol	45.9 ± 0.8 *206 ± 4*	46.4 ± 0.5 *209 ± 2*	46.2 ± 0.5 *209 ± 2*	$[\alpha]_D = 48.7$ (c = 2.389, ethanol) (2); $[\alpha]_D = 48.0$ (c = 4.71, 95 % ethanol) (4); $[\alpha]_D^{17} = 48.6$ (c = 2.042, ethanol) (7).
Na-desoxycholate	water	46.30 ± 1.0 *192 ± 4*	43.1 ± 0.4 *179 ± 2*	42.3 ± 0.3 *175 ± 2*	$[\alpha]_D^{20} = 47.5$; 45.7; 45.4; (c = 1; 2.5; 5, water) (27).
Na-glycodesoxycholate	water	41.2 ± 1.0 *194 ± 5*	38.5 ± 0.5 *182 ± 2*	37.8 ± 0.4 *178 ± 2*	$[\alpha]_D^{21} = 44.9$; 39.6 (c = 1.03; 2.53, water) (5).
Na-taurodesoxycholate	water	37.0 ± 0.8	34.4 ± 0.4	33.7 ± 0.3	$[\alpha]_D^{21} = 33.8$ (c = 2.4, water) (5).

Na-chenodesoxycholate	water	12.5 ± 1.5 *52 ± 6*	9.9 ± 0.6 *41 ± 3*	8,5 ± 0.4 *35 ± 2*	
Na-glycochenodesoxycholate	water	9.2 ± 1.5 *43 ± 7*	8.5 ± 0.6 *40 ± 3*	7.2 ± 0.5 *34 ± 2*	
Na-taurochenodesoxycholate	water	9.0 ± 1.2 *47 ± 6*	8.0 ± 0.6 *42 ± 3*	7.0 ± 0.5 *37 ± 3*	
Lithocholic acid	ethanol	35.0 ± 0.8 *132 ± 3*	34.4 ± 0.5 *130 ± 2*		$[\alpha]_D^{21} = 36.0$ (c = 0.56, ethanol) (16); $[\alpha]_D = 35.2$ (c = 1.5, ethanol) (31); $[\alpha]_D = 35$ (c = 1.17, ethanol) (26).
Glycolithocholic acid	ethanol	30.6 ± 1.5 *133 ± 6*	29.9 ± 0.2 *130 ± 1*		
Taurolithocholic acid	ethanol	27.2 ± 0.8 *132 ± 4*			
Cholanic acid	ethanol	27.8 ± 0.8 *100 ± 3*	28.8 ± 1 *104 ± 4*		$[\alpha]_D^{20} = 21.50$ (c = 3.895, ethanol) (33).
Glycocholanic acid	ethanol	23.6 ± 0.5 *99 ± 2*			
Taurocholanic acid	ethanol	21.3 ± 1.0 *100 ± 5*			
Dehydrocholic acid	90 % ethanol	26.2 ± 0.6 *105 ± 3*			$[\alpha]_D = 26$–27 (0.942, ethanol) (34).
Glycodehydrocholic acid	90 % ethanol	23.4 ± 0.5 *107 ± 2*			$[\alpha]_D^{18} = 26.73$ (c = 1.051, 85 % ethanol) (7).
Taurodehydrocholic acid	90 % ethanol	20.5 ± 0.6 *105 ± 3*			

It was impossible to crystallize the free acid or its sodium salt and therefore the acid was subjected to chromatography for purification. One gram of a butanol extract was run through a 70 g hydrophobic Supercel column (phase system D). The fractions containing the taurochenodesoxycholic acid were evaporated *in vacuo,* dissolved in 50 ml ethanol and neutralized with Na-ethoxide. The sodium salt was crystallized after addition of ethyl acetate (about 50 ml). After storing in the ice-box overnight, the solution was filtered and the crystals thoroughly washed with ether. Yield 400 mg. Further material was obtained from the mother liquid by crystallization from a smaller volume.

Glycolithocholic acid. When the residue from the evaporated reaction mixture was dissolved in hot distilled water and acidified to pH 1, a flocculent precipitate appeared. This was filtered off and thoroughly washed with water. After drying, it was taken up in a minimum amount of hot ethanol and ethyl acetate was added to incipient cloudiness. Yield 66 per cent. M.p. 212–214°. Further recrystallization did not alter the melting point. After crystallization of the same sample from ethanol and water, the m.p. 180–181° was obtained and this was found to remain constant after further crystallization from the same solvents. When crystallized from ethanol-ethyl acetate, the higher m.p. was again obtained.

Taurolithocholic acid. The taurolithocholic acid was precipitated from an acidified aqueous solution and crystallized from ethanol and ethyl acetate (cf. 8). Yield 84 per cent. M.p. 208–211°. One more crystallization raised the m.p. to 212–213° (unaltered by further recrystallization).

Glycocholanic acid. Glycocholanic acid precipitated as a gelatinous mass after acidification with hydrochloric acid and was therefore extracted with ethyl acetate. The residue was dissolved in heptane and the solvent evaporated until crystallization occurred. Yield 68 per cent. M.p. 204–206° (constant on further crystallization from heptane).

Taurocholanic acid. An amount of hydrochloric acid equivalent to the amount of bile acid was added to the concentrated reaction mixture. After dissolving in ethanol and filtering, the sodium salt was precipitated by neutralization with Na-ethoxide. In this way the tributylamine was removed. The sodium salt was dissolved in water and the free acid precipitated by acidification. When a gelatinous mass was obtained, it was extracted with butanol. The residue in the combined butanol phases was distributed between equal volumes of 70 per cent ethanol and light petroleum by a three stage counter-current extraction. The cholanic acid enters the petroleum phase and was thus separated from the taurine conjugate which remained in the ethanol phase. The residue from the combined ethanol phases was dissolved in the minimum amount hot ethanol. The ethanol was evaporated until crystallization occurred. Filtration after standing overnight in the icebox. Yield 79 per cent. M.p. 241–243°. Further crystallization from ethanol gave a product with the same m.p.

Glycodehydrocholic acid. Glycodehydrocholic acid, precipitated from an acidified water solution, crystallized from dilute acetic acid, m.p. 236–239°. Yield 69 per cent. Recrystallization from ethanol-water gave the melting point 240–242° unaltered after further crystallization.

Taurodehydrocholic acid. The reaction mixture was evaporated, dissolved in N NaOH and extracted with ether. Acidification of the aqueous solution to pH 1 did not precipitate the free acid, which was therefore extracted with butanol. The free acid was dissolved in a minimum amount of hot ethanol and ethyl acetate added to incipient cloudiness. M.p. 237–238°, unaltered after further recrystallization. Yield 72 per cent.

Synthesis of labelled bile acids on a micro scale

The reaction conditions are essentially the same as described above. When working with ^{14}C-labelled bile acids on a small scale it is necessary to purify the products by

Table 4. Synthesis of conjugated 24-^{14}C-labelled bile acids.

Substance	Mmole of free bile acid	Mmole of tri-*n*-butylamine	Mmole of ethyl-chlorocarbonate	Mmole of glycine-taurine	Yield in per cent
Taurocholic acid	0.5	0.5	0.5	0.55	87
,, ,, ...	0.25	0.25	0.316	0.375	93
,, ,, ...	0.06	0.06	0.12	0.12	29
Glycocholic acid	0.5	0.5	0.5	0.55	87
Taurochenodesoxycholic acid	0.12	0.12	0.15	0.18	88
Taurodesoxycholic acid . . .	0.25	0.25	0.25	0.275	84
,, ,, . . .	0.06	0.06	0.06	0.066	51
,, ,, . . .	0.06	0.06	0.06	0.09	53
,, ,, . . .	0.06	0.06	0.075	0.09	65
Glycodesoxycholic acid . . .	0.025	0.025	0.025	0.275	57
,, ,, . . .	0.075	0.075	0.094	0.113	82

chromatography. After chromatographic separation of the reaction mixture, it was possible to get quantitative and qualitative information about the reaction products. In the syntheses, therefore, some modifications of the reaction conditions were made and their influence of the yield was studied.

Glycocholic acid-24-^{14}C. A solution of 204.3 mg of cholic acid-24-^{14}C (0.5 mmoles) and 0.12 ml 0.5 mmoles) of tri-*n*-butylamine in 2 ml dioxan was cooled to +8° and 0.048 ml (0.5 mmoles) of ethylchlorocarbonate added with a micropipette. After 15 min. at this temperature, 0.55 mole of glycine in 0.55 ml *N* NaOH was added. To investigate if the time after the addition of the aminoacid had any influence on the yield, one-third of the reaction mixture was evaporated after 15 min. when the gas evolution had subsided, dissolved in water, acidified to pH 1 and extracted with ether. The same procedure was applied to the second one-third after 1 hour and to the rest after 24 hours. The different ether extracts were run on 13.5 g kiselguhr columns with phase system C. All the labelled material was recovered in two bands: the first contained glycocholic acid and the second free cholic acid. The yield of glycocholic acid was: after 15 min., 87 per cent; 1 hour, 86 per cent; 24 hours, 87 per cent.

Taurodesoxycholic acid-24-^{14}C. 98.1 mg of desoxycholic acid-24-^{14}C (0.24 mmole) and 0.059 ml of tri-*n*-butylamine in 1 ml of dioxan at +8° were treated with 0.0238 ml of ethylchlorocarbonate. After 15 minutes, 34.3 mg of taurine in 2.75 ml of *N*/10 sodium hydroxide were added and the mixture left overnight. The reaction mixture was evaporated, dissolved in *N* sodium hydroxide and extracted twice with ether. After acidification to pH 1, the free acid was extracted with butanol. The residue from the butanol phase was chromatographed with phase system D. The eluted labelled material was found in one peak at the position of the taurodesoxycholic acid. The labelled material remaining in the stationary phase was rechromatographed with solvent system F and proved to be unchanged desoxycholic acid.

Taurocholic acid-24-^{14}C, taurochenodesoxycholic acid-24-^{14}C, taurolithocholic acid-24-^{14}C. For reaction conditions and yields, see Table 4. It was found necessary to remove the tributylamine by ether extraction from an alkaline water solution before the butanol extraction of the free taurine conjugate. Chromatographic purification was performed with solvent system D.

Glycodesoxycholic acid-24-^{14}C. Chromatographically purified with solvent system C. The glycine conjugate was eluted at 100–130 ml (4.5 g column), while the free bile acid stayed in the column.

Discussion

The method of synthesis

The method employing mixed carbonic-carboxylic anhydrides in the synthesis of peptide bonds, independently described by WIELAND and BERNHARD, BOISSONNAS and VAUGHAN (9–12), differs somewhat in the reaction conditions used. For the synthesis of conjugated bile acids, the conditions proposed by BOISSONNAS are the most suitable as they give the highest yield for reaction in aqueous medium. Dioxane is the best solvent for the tri-*n*-butylamine salts of the bile acids. Furthermore, since the taurine ester is unstable, the coupling reaction has to be performed with the Na-salt of taurine in an aqueous medium. For the synthesis of glycine conjugates of the less substituted bile acids, the reaction can be carried out in chloroform using ethyl glycinate. The yields are as good as in the aqueous medium.

Syntheses of ^{14}C-labelled conjugated bile acids and chromatographic separation favoured the study of the reaction conditions and the following results were obtained. Great precaution must be taken to exclude moisture from the reaction mixture in the first step (careful drying of the solvents and the bile acid is necessary) to avoid decomposition of the anhydride. The yield was found to be somewhat higher with an excess of chlorocarbonate (25 per cent). No byproducts of the bile acids were formed. Further excess (50 and 100 per cent), however, markedly lowered the yield. The reaction was complete within 15 minutes after the addition of the conjugate to the anhydride. Excess of glycine or taurine has no influence. The yield was found to be between 80 and 90 per cent for quantities of about 0.2–0.5 mmole. On a micro scale, the yield was smaller, but in all cases above 50 per cent. The yield of the crystallized product in large scale synthesis varied between 60 and 80 per cent.

Compared with earlier reported methods, the use of mixed carbonic-carboxylic anhydrides for syntheses of conjugated bile acids offers great advantages. The reaction can be done in one stage without purification of the products of the different steps and the reaction leads to products with high initial purity and complete lack of by-product formation. No interference with the hydroxyl or keto groups occurs. Yields are excellent also from syntheses on a micro scale.

Thermal investigation

The melting points of the conjugated bile acids are rather unsharp compared with the corresponding free bile acids (cf. Table 2). The melting points for the sodium salts are difficult to determine and hence in Table 2 only the temperature range in which melting occurs is given. Several authors (28) describe two crystalline modifications of glycocholic acid: a normal form (m.p. about 130°) crystallized from aqueous ethanol and a "para-form" (m.p. 190–195°) that is obtained when the former is boiled in water. Similar results were obtained with our material. Besides these two modifications a third was obtained after crystallization from ethanol-ethyl acetate (m.p. 165–168°) with the same optical rotation obtained for the normal and the "para-form". Glycolithocholic acid also was found to exist in two different crystalline modifications. X-ray investigations are needed to clarify these questions of polymorphism.

Polarimetric determination

The determinations of the optical activity were made in the same solvent and with the same concentrations for the free and conjugated bile acids in order to permit comparison of the molecular rotation. The results are given in Table 3. About the same molecular rotation was found for the glycine and taurine conjugates and the corresponding free bile acid, thus indicating that the conjugation does not contribute to the optical activity. The optical activity of the sodium salts was influenced by the concentration and the optical activity decreased with increasing concentration. This is in agreement with the findings of JOSEFSSON (27) and is probably caused by micelle formation by the sodium salts in aqueous solution.

Moisture determination

Drying at 70°, for 5 hours at 0.1 mm Hg was found necessary to obtain a constant weight for the conjugated bile acids. The sodium salts require a higher temperature (100°), but contrary to CORTESE's findings, drying at 130° *in vacuo* did not give further weight decreases in any of the cases. Only for the glycocholic and glycodesoxycholic acid was a constant moisture content observed. With the other samples, varying results were obtained, and hence in Table 2 only the maximum and minimum values for the moisture contents of different air-dried crystal fractions are given.

SUMMARY

The glycine and taurine conjugates of cholic, desoxycholic, chenodesoxycholic, lithocholic, cholanic and dehydrocholic acid have been synthesized using mixed carbonic-carboxylic acid anhydrides in the coupling reaction. The free acids and the sodium salts have been characterized. The method has also been used to synthesize conjugated bile acids on a micro scale.

This work has been supported by a grant from the Medical Faculty, University of Lund, and by "Knut och Alice Wallenbergs Stiftelse".

Department of Physiological Chemistry, University of Lund, Lund, Sweden.

REFERENCES

1. BONDI, S. and MÜLLER, E., Hoppe-Seyler's Z. physiol. Chem. *47*, 499 (1906).
2. WIELAND, H., Hoppe-Seyler's Z. physiol. Chem. *106*, 181 (1919).
3. CORTESE, F. and BAUMAN, L., J. Am. Chem. Soc. *57*, 1393 (1935).
4. CORTESE, F. and BAUMAN, L., J. Biol. Chem. *113*, 779 (1936).
5. CORTESE, F., J. Am. Chem. Soc. *59*, 2532 (1937).
6. STACEY, M. and WEBB, M., Proc. Roy. Soc. B, *134*, 523 (1947).
7. GAUTIER, B. and QUY, N. H., Ann. Pharm. Franc. *5*, 556 (1947).
8. BERGSTRÖM, S. and NORMAN, A., Acta Chem. Scand. *7*, 1126 (1953).
9. WIELAND, T. and BERNHARD, H., Ann. *572*, 190 (1951).
10. BOISSONNAS, R. A., Helv. Chim. Acta *34*, 874 (1951).
11. VAUGHAN, J. R. JR. and OSATO, R. L., J. Am. Chem. Soc. *74*, 676 (1952).

12. Vaughan, J. R. Jr. and Osato, R. L., J. Am. Chem. Soc. *73*, 5553 (1951).
13. Reichstein, T. and Sorkin, M., Helv. Chim. Acta *25*, 797 (1942).
14. Andersson, I. G., Haslewood, G. A. D., Wiggins, H. S., and Wootton, I. D. P., Nature, Lond., *169*, 621 (1952).
15. Norman, A., Acta Chem. Scand. *7*, 1413 (1953).
16. Bergström, S. and Haslewood, G. A. D., J. Chem. Soc. *1939*, 540.
17. Borsche, W. and Halwass, F., Ber. *55*, 3324 (1922).
18. Hammarsten, O., Ber. *14*, 71 (1881).
19. Bergström, S., Rottenberg, M., and Voltz, J., Acta Chem. Scand. *7*, 481 (1953).
20. Pestemer, M., Angew. Chem. *63*, 118 (1951).
21. Bergström, S. and Sjövall, J., Acta Chem. Scand. *5*, 1267 (1951).
22. Sjövall, J., Acta Physiol. Scand. *29*, 232 (1953).
23. Sjövall, J., Acta Chem. Scand. *8*, 339 (1954).
24. Sjövall, J., Arkiv f. Kemi, *8*, 317 (1955).
25. Hammarsten, O., Hoppe-Seyler's Z. physiol. Chem. *43*, 127 (1904).
26. Barton, D. H. R., and Brooks, C. J. W., J. Chem. Soc. 1949, 2596.
27. Josefsson, B., Biochem. J. (London) *29*, 1484 (1935).
28. Letsche, E., Hoppe-Seyler's Z. physiol. Chem. *60*, 462 (1909).
29. Cortese, F. and Bashour, J. T., J. Biol. Chem. *119*, 177 (1937).
30. Wieland, H. and Sorge, H., Hoppe-Seyler's Z. physiol. Chem. *97*, 1 (1916).
31. Ruzicka, L. and Goldberg, M. W., Helv. Chim. Acta *18*, 668 (1935).
32. Takeda, K., Otsuka H., and Tanaka, K., J. Pharm. Soc., Japan *72*, 1212 (1952).
33. Wieland, H. and Boersch, E., Hoppe-Seyler's Z. physiol. Chem. *106*, 193 (1919).
34. Schenck, M., Hoppe-Seyler's Z. physiol. Chem. *69*, 383 (1910).
35. Yomasaki, S., Okayama Med. J. *56*, 287 (1944).

Tryckt den 23 april 1955

Uppsala 1955. Almqvist & Wiksells Boktryckeri AB

ARKIV FÖR KEMI Band 8 nr 33

Communicated 23 February 1955 by ARNE FREDGA

The hydrogen isotope effect in the metalation of thiophene

By SALO GRONOWITZ and KJELL HALVARSON

There are still different opinions on the mechanism of the metalation reaction and GILMAN (1) has recently given a survey of this reaction.

MORTON (2) stresses the importance of the metallic cation and pictures the mechanism as an electrophilic attack of the cation on the carbon atom, the removal of the proton being of secondary importance. There is no doubt that this mechanism is valid for the mercuration of aromatic compounds under certain conditions (3).

It has, however, been found by one of us (S. G. (4)) that the directing and activating influence of substituents in the 3-position of thiophene on metalation with organolithium compounds is in accordance only with nucleophilic properties of the organolithium compound. This indicates that the important and rate determining step of the metalation with organolithium compounds is a nucleophilic attack on hydrogen by the carbanion of the metalating agent.

In order to gain more information about the mechanism of this reaction we have studied the influence of the mass of the hydrogen on the reaction velocity using the tritium method of MELANDER (5). We have investigated the competitive metalation of thiophene and tracer amounts of thiophene-2-t (6). MELANDER (7) has pointed out that the most favourable conditions for experiments with competition within the same molecule is to have only two positions available and to make the conversion as quantitative as possible. Thus thiophene is very well suited for investigation by this method as the metalation with n-butyllithium proceeds smoothly and can safely be assumed to be quantitative.

It was found that the isotopic rate ratio k_T/k_H was 0.17 or less, i.e. protium is replaced at least six times faster than tritium in the metalation of thiophene with n-butyllithium. This shows that the mechanism of metalation is different from that of aromatic nitration and bromination, where no isotope effect has been found (5). The observed isotope effect does not in itself eliminate the possibility of electrophilic substitution. MELANDER (5) has pointed out that an isotope effect is to be expected if the electrophilic reaction is of normal S_E2 type or if the elimination of hydrogen after the electrophilic attack is rate-determining as has been found for sulphonation (8). The directing effect of 3-substituted thiophenes (4) and also of 2-substituted naphtalenes (9), however, make an electrophilic mechanism improbable. The isotope effect obtained is in accordance with nucleophilic activity of the metalating agent and shows that the elimination of hydrogen is the rate determining step. The magnitude of the isotopic rate ratio is that to be expected and is of the same order as that obtained by MELANDER (10) for the reduction of diazonium salts. Metalation of thiophene-3-t shows that no hydrogen exchange occurs in the 3-position during the reaction, as the whole activity, within the experimental error, was retained in the 2-thiophenecarboxylic acid.

Similar conclusions have been drawn by BRYCE-SMITH (11) for the mechanism of the metalation of aromatic hydrocarbons by alkylsodium and -potassium compounds. Using deuterium technique he has found an isotope effect in the metalation of benzene and toluene by ethylpotassium (12). The initial coordination, which greatly facilitates the metalation of thiophene (4), is of course not possible for the metalation of alkylbenzenes.

Experimental

Tritium. The tritium used originates from the Atomic Energy Research Establishment, Harwell, England.

Preparation of tracer amounts of thiophene-2-t and -3-t. Thiophene was shaken with sulphuric acid containing tritium. The preparations were carried out in about the same manner as described previously (6).

Determination of tritium. The combustion of thiophene and 2-thiophenecarboxylic acid was carried out in a stream of oxygen over Vinosit B followed by a plug of silver wool (8 cm) and copper oxide wire (4 cm). The temperature of the main part of Vinosit B was 650°–670° C and of the silver plus copper oxide part 480°–500° C. In ordinary gravimetric analysis (semi-micro) sulphur and halogens are retained by Vinosit B but in this case a fairly large amount of silver wool was used since otherwise the Geiger-Müller tube seemed to be poisoned after a few measurements. The tritium in the water obtained from the combustion was determined with the same method and apparatus as described previously by MELANDER (13).

Metalation of thiophene. All the reactions were carried out in the usual Grignard apparatus in a nitrogen atmosphere.

Exp. 1.—To a solution of 9.2 g (0.11 moles) of thiophene-2-t in 100 ml of absolute ether was added in a slow stream 0.11 moles of *n*-butyllithium in 150 ml of ether. The reaction mixture was refluxed for half an hour and was then poured on a slurry of Dry Ice and ether. When the temperature had reached 0°C the reaction mixture was hydrolysed with 125 ml of water. The aqueous phase, which was weakly alkaline, was separated and acidified in the cold with 5 % sulphuric acid against congo red. Under these conditions no acid induced hydrogen exchange occurs. The aqueous phase was at once extracted several times with ether and the ether evaporated leaving 12.2 g (87 %) of 2-thiophenecarboxylic acid. The acid was recrystallised twice from water and decolourised with charcoal. M.p. 128.5°–129.7°.

Exp. 2.—5.95 g (0.071 moles) of thiophene-2-t was metalated with only 0.037 moles on *n*-butyllithium giving 4.41 g (49 %) acid.

Exp. 3.—6.12 g (0.0725 moles) of thiophene-3-t was metalated with 0.075 moles of *n*-butyllithium giving 8.82 g (95 %) acid.

Table 1.

Exp.	Starting material	Yield, %	Fraction of tritium retained
1	thiophene-2-t	> 87	0.89 ± 0.03
2	,,	> 49	0.57 ± 0.02
3	thiophene-3-t	> 95	0.97 ± 0.04

The isotopic rate ratio was calculated according to MELANDER (14). In order to calculate k_T/k_H it is necessary to know the amount of reaction. It is assumed that the metalation of thiophene with *n*-butyllithium is quantitative when equivalent amounts are used. The yield of 2-thiophenecarboxylic acid was in one case 95 % and in another 87 %. The losses may be accounted for through hydrolysis of 2-thienyllithium during the carbonation and through ketone formation. Calculated on the assumption of a quantitative yield in the metalation an upper limit of k_T/k_H equal to 0.17 is obtained. The result in experiment 2 is in complete agreement with this value. The accuracy in the determination of the yield does not allow a determination of the lower limit. Since k_T/k_H is necessarily larger than zero the lower limit of the fraction of tritium retained in the product, equal to 0.86, requires the yield of 2-thienyllithium to be at least 97 % in experiment 1 (14). The data are collected in Table 1.

Summary

A rather large isotope effect has been observed for the metalation of thiophene containing tracer amounts of thiophene-2-t with *n*-butyllithium. The isotope effect is in accordance with nucleophilic acitivity of the metalating agent.

The authors wish to express their thanks to Professor ARNE FREDGA and Docent LARS MELANDER for valuable discussions.

Department of Organic Chemistry, Chemical Institute, University of Uppsala, and Nobel Institute of Chemistry, Stockholm 50, February 1955.

REFERENCES

1. GILMAN, H., and MORTON, J. W., Organic Reactions VIII, 258 (1954).
2. MORTON, A. A., J. Am. Chem. Soc. *69*, 969 (1947).
3. KLAPPROTH, W. J., and WESTHEIMER, F. H., J. Am. Chem. Soc. *72*, 4461 (1950).
4. GRONOWITZ, S., Arkiv Kemi *7*, 361 (1954).
5. MELANDER, L., Arkiv Kemi *2*, 211 (1950).
6. HALVARSON, K., and MELANDER, L., Arkiv Kemi *8*, 29 (1955).
7. MELANDER, L., Arkiv Kemi *2*, 211 (1950), p. 253.
8. BERGLUND-LARSSON, U., and MELANDER, L., Arkiv Kemi *6*, 219 (1953).
9. SUNTHANKAR, S. V., and GILMAN, H., J. Org. Chem. *16*, 8 (1951).
10. MELANDER, L., Arkiv Kemi *3*, 525 (1951).
11. BRYCE-SMITH, D., J. Chem. Soc. *1954*, 1079.
12. BRYCE-SMITH, D., GOLD, V., and SATCHELL, D. P. N., J. Chem. Soc. *1954*, 2743.
13. MELANDER, L., Acta Chem. Scand. *2*, 440 (1948).
    —— Arkiv Kemi *2*, 211 (1950), pp. 257–260.
14. —— ibidem, p. 251, Fig. 9:1.

Tryckt den 23 april 1955

Uppsala 1955. Almqvist & Wiksells Boktryckeri AB

ARKIV FÖR KEMI Band 8 nr 34

Communicated 13 April 1955 by ARNE WESTGREN and ARNE TISELIUS

Continuous zone electrophoresis by crossed velocity fields in a supporting medium

Analysis of protein fractions obtained from normal human serum

By INGER BRATTSTEN

With 5 figures in the text

In a recent paper some fractionations of serum by continuous electrophoresis at pH 8.6 have been described (1). The optical density records of the protein distribution in the fractions give information about the average resolving power under the reported conditions, but they hardly reveal the separation of singular protein constituents and the degree of purity of the fractionated material. In order to obtain a more complete picture of the fractionation conditions these measurements have been supplemented by analyses of representative fractions by nitrogen, ultraviolet absorption and conductivity determinations and heterogeneity tests by electrophoresis and ultracentrifugation.

Experimental

Material and methods

The serum investigated has been obtained from one healthy individual, donor in the blood bank of the University Clinic, Uppsala. The blood samples were collected under fasting conditions and the serum obtained fractionated within the next few days. Six preparations were performed during a period of six months.

The details of the fractionation technique have been reported in ref. 1. To obtain comparable results, the experimental conditions were the same in all the preparations, i.e. the separation took place in a veronal buffer of ionic strength 0.03 and pH 8.6. The cell temperature was 18°C. During the time of transfer through the column, 3.9 hours, a current of 230 mA effected a total separation of the protein constituents of 24 cm, which corresponds to a distribution into 48 fractions. Prior to the fractionation the serum was diluted to a protein concentration of 1.5 % and dialyzed against the dilute veronal buffer. When necessary the fractions were concentrated for the analyses by ultrafiltration or pervapouration in cellophane bags. When the latter method was used, the veronal ions were first removed by dialysis. The solutions used for the sedimentation and nitrogen analyses were equilibrated by dialysis against a phosphate buffer of ionic strength 0.05 and pH = 6.83. All the protein solutions were handled under aseptic conditions as far as possible and stored at 4°C.

Total nitrogen was determined by Kjeldahl analyses according to the micromodification of MARKHAM (2). The refractive index increment was recorded by means of a Bellingham-Stanley refractometer (accuracy: $5 \cdot 10^{-6}$), the optical density by a Beckman spectrophotometer, Model DU, and the conductivity by a L.K.B. resistance bridge according to SHEDLOVSKY (3) (accuracy: better than 2‰). In all measurements the equilibrium buffer was used as the blank.

Electrophoretic analyses were performed by the moving boundary method in a L.K.B. apparatus according to TISELIUS-SVENSSON (4) or by paper electrophoresis according to the method of WIELAND and FISCHER (5). In the moving boundary analyses a veronal buffer of ionic strength 0.1 or 0.2 was used and for the paper electrophoresis Michaelis' buffer of ionic strength 0.08 and pH = 8.8. The protein spots on the paper strips were stained with Amidoschwarz 10 B Bayer in a methanol-acetic acid solution as described by GRASSMAN, HANNIG and KNEDEL (6).

The sedimentation analyses were carried out with the aid of the oil turbine ultracentrifuge of the Institute of Physical Chemistry as described by SVEDBERG and PEDERSEN (7, 8).

Results

The fractionation diagram.—Optical density measurements at 284 mμ have been adopted as a simple method of recording the protein distribution in the series of fractions collected in a preparation experiment. To allow a correction for the absorption of the veronal ion in the buffer medium, a series of buffer fractions, which have passed the flow field under stable conditions, is always collected. In the subsequent series of protein fractions the absorption of the proteins is derived by subtracting from the optical density readings for each fraction the density of the same fraction in the pure buffer series.

In Fig. 1 *a* the optical density of a series of protein fractions has been recorded as a function of the tube number. In order to remove the veronal ion, the same solutions were then dialyzed against a phosphate buffer of ionic strength 0.05 and pH 6.83 without significant volume changes. The dialysis was continued until a blank containing only veronal buffer was free from nitrogen by Kjeldahl analysis. The ultraviolet absorption of the solutions so obtained was again measured at 284 mμ. These readings are recorded in Fig. 1 *b*, and Fig. 1 *c* shows the nitrogen content of the same solutions. The nitrogen values are based on single Kjeldahl analyses, hence accidental errors have not been cancelled. In general, an accuracy better than 2 % is obtained in series measurements of this kind.

Routine conductivity analyses are used as a sensitive method for detecting foreign salt ions in the separation field (1). By proper adjustments of the ratio between the electric current and the liquid flow rate a constant conductivity can be obtained in the buffer solution emerging from the separation zone. Under these conditions it is generally found that the conductivity of the solution having passed the flow field is consistently slightly lower than that of the injected solution. On several occasions the conducitivity has also been measured during the fractionation, i.e. on the serum fractions. These measurements record the conductivity changes caused by the presence of the protein in the electric field. A record of this type is shown in Fig. 1 *d*. The conductivities of the fractions containing pure buffer showed a fluctuation amounting to about 1 per cent of the mean value, $1.02 \cdot 10^{-3}$ ohm^{-1} cm^{-1}.

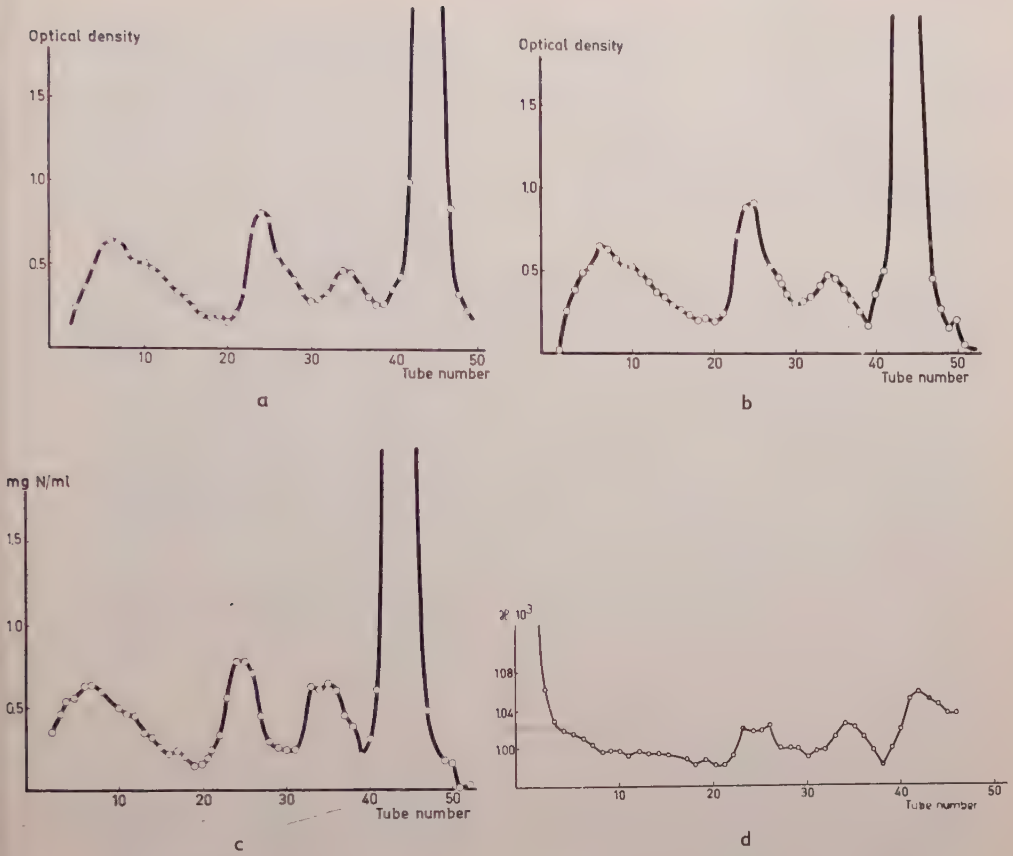

Fig. 1. *The fractionation diagram.* — *a.* The optical density at 284 mμ in the presence of veronal buffer of the ionic strength 0.03 and pH = 8.5. *b.* The optical density of the same fractions after removal of the veronal ion by dialysis against a phosphate buffer of the ionic strength 0.05 and pH 6.83. *c.* The nitrogen content of the fractions after the dialysis. *d.* The conductivity of the fractions, recorded in the presence of the veronal ion.

Each lot of serum obtained from the blood bank was analyzed by moving boundary electrophoresis at the ionic strength 0.2. The optical patterns from a typical analysis has been reproduced in ref. 1, p. 240. The relative concentrations of the components were estimated by computation of the ratios between the areas in both patterns. The mobility computations were also based on data from both limbs. The observed variations between the different lots of serum were never great. In comparison with the values obtained by ARMSTRONG, BUDKA and MORRISON under similar conditions (9), the γ-globulin content was always high and that of the α-globulins low, but the range of the normal variations of these components was not surpassed. In Table 1 are listed average values of the relative concentrations of the components and their mobilities.

Analysis of singular fractions.—The ultraviolet absorption of the fractions Nos. 6 (γ-globulin), 24 (β-globulin), 34 (α-globulin), and 45 (albumin) was studied in more

Table 1. Analyses by moving boundary electrophoresis of the serum investigated.

	γ-globulin	β-globulin	α_2-globulin	α_1-globulin	albumin
Relative concentration, % . .	14.0	13.9	7.3	4.1	60.4
Mobility, $-\mu \cdot 10^5$	1.0	2.3	3.0	3.9	5.0

detail after removal of the veronal ion by dialysis and nitrogen determination by Kjeldahl analyses. Although pH was controlled to be constant and a linear relationship prevailed between the optical density and the nitrogen values in the range of the measurements (below the optical density 0.9), the conversion factor was found to vary considerably from preparation to preparation. Within the same preparation the agreement was good, excepting some β-globulin solutions, the optical density of which slowly increased on standing for some days without any noticeable trace of turbidity. However, the shape of the extinction curves was in all instances well reproducible. In the diagram, Fig. 2, the extinction values at 280 mμ are averages from four preparations; the accuracy of the globulin curves is believed to lie within 10 %, that of the albumin curve within 1–2 %.

For the sedimentation and electrophoretic analyses the fractions Nos. 1–25, 28, 34, 35, 41 and 45 were transferred to phosphate buffer by dialysis and concentrated to a protein content of 0.5–1 %. The concentration procedure generally caused a slight turbidity of the β- and, occasionally, the α-globulin solutions. Water-clear concentrates were always obtained from the γ-globulin and albumin solutions. If necessary, the α-globulin concentrates could easily be cleared by centrifugation, but it was generally impossible to remove a certain opalescence from the concentrated β-globulin solutions by this means. The latter solutions had a distinct brownish-salmon colour, the albumin solutions were light yellow; both the γ- and α-globulin solutions were always colourless.

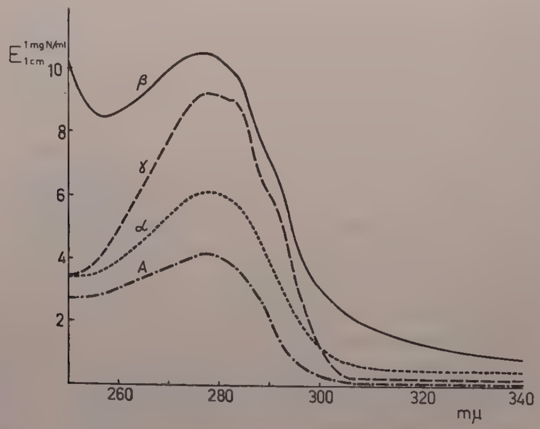

Fig. 2. *The absorption spectra* given by the fractions 6 (γ-globulin), 24 (β-globulin), 34 (α-globulin), and 45 (albumin). The extinction coefficients have been computed on the basis of the nitrogen content of the fractions.

Fig. 3. *Electrophoresis on filter paper* (Whatman No. 1). — *a*. Simultaneous migration of the fractions 6, 24, 34, and 45 and a sample of whole serum. *b*. Simultaneous migration of the γ-globulin fractions 2, 3 (pooled); 5, 6 (pooled); 8; 10; 12; 14; 16; 18, 19, 20 (pooled). On the paper strip to the left in the figure a reference spot of albumin is also present.

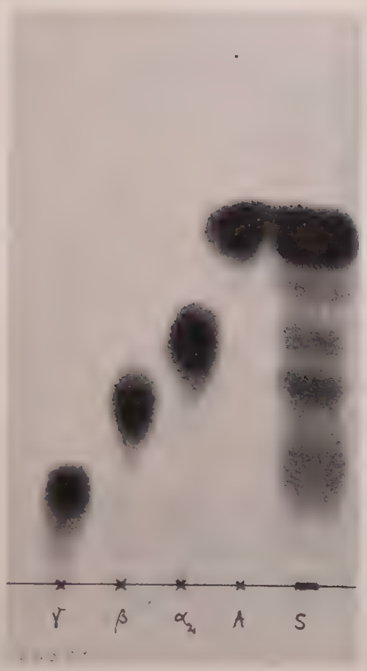

a

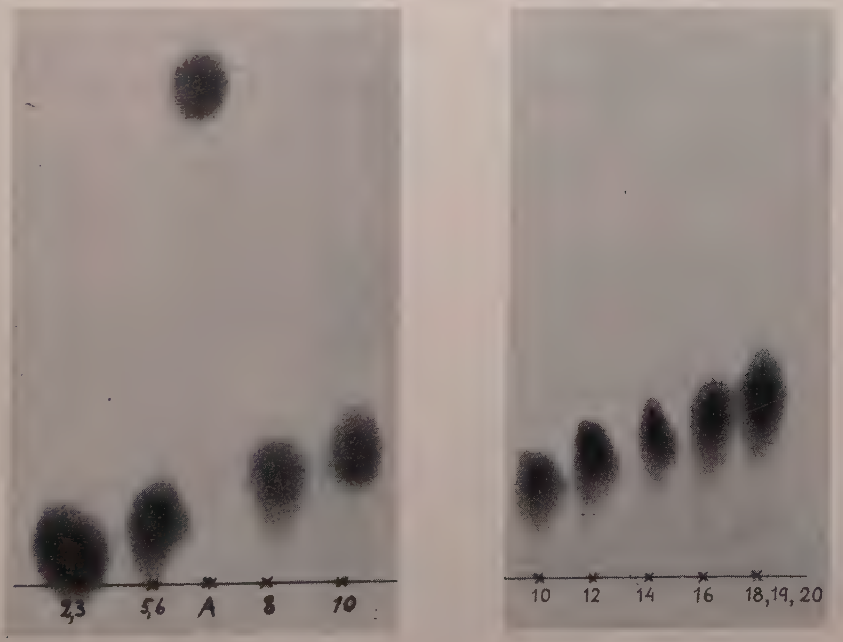

b

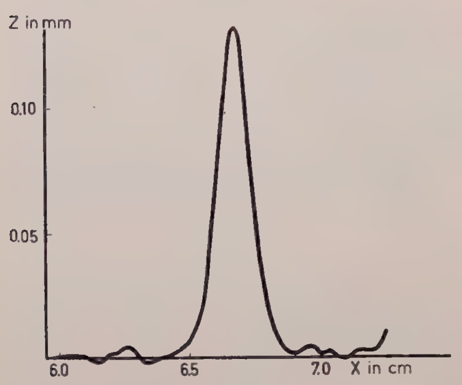

γ-globulin

a

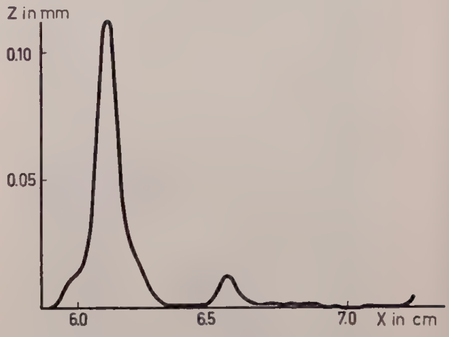

b

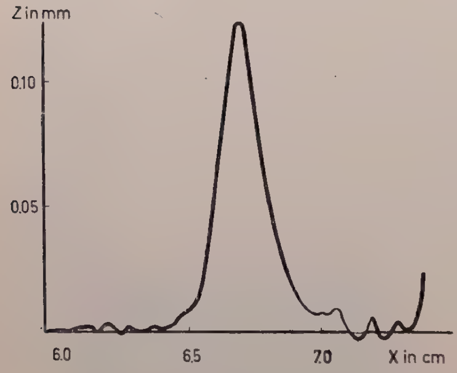

β-globulin

c

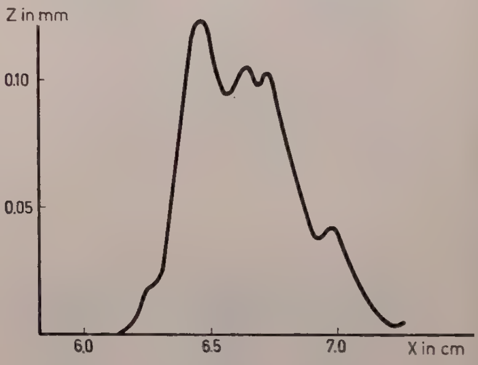

d

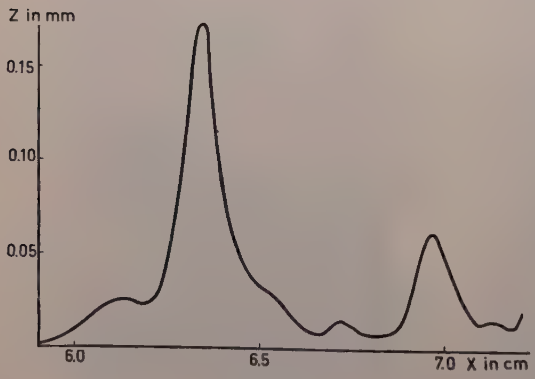

α-globulin

e

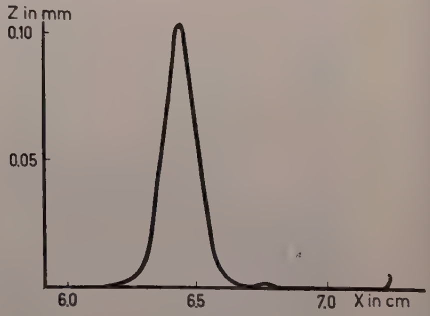

albumin

f

Table 2. Results of the sedimentation analyses.

Fraction No.	Concentration $\Delta n \cdot 10^5$	s_{20} (relative concentration of components given in parentheses)
6	63	6.5 (100 %)
10	51	6.5 (100 %)
12	137	6.6 (93 %), 18.2 (7 %)
14	160	6.2 (83 %), 17.5 (17 %)
16	119	4.4 (10 %), 6.6 (80 %), 18.5 (10 %)
18, 19, 20	180	~4 (9 %), 6.5 (71 %), 19.0 (11 %)
22	180	5.0 (32 %), 6.0 (68 %)
24	71	5.0 (100 %)
28	84	4.7 (40 %), 5.8 (18 %), 6.4 (28 %), ~ 12 (13 %)
34	201	3.2 (9 %), 7.0 (62 %), 12.6 (5.3 %), 15.9 (24 %)
41	152	3.86 (100 %)
45	155	3.85 (100 %)

Fig. 3 shows some results of the analyses by paper electrophoresis. In Fig. 3 *a* the fractions corresponding to the principal maxima in the fractionation curve (Fig. 1 *a*) have been analyzed together with a sample of whole serum. In the case of Fig. 3 *b* the γ-globulin fractions and those intermediate between the γ- and β-globulin groups in the fractionation diagram were simultaneously submitted to electrophoresis in order to demonstrate the mobility differences of the proteins present. Fractions representative of the four main components have also been investigated by the moving boundary method. In each instance the optical pattern showed a single moving boundary, but the α-globulin boundaries became more diffuse during the migration than those obtained with the other components. Systematic heterogeneity studies by means of the reversible boundary spreading (10) have not been made.

In the sedimentation experiments the rotor speed generally was 1000 r.p.s. and the cell temperature ranged between 25 and 30°C.[1] When direct observations of the

---

[1] The cell temperature was derived from the thermocouple readings according to an empirical formula given by PEDERSEN March 1955. The experiments were carried out February–June 1954. The new calibration values give appreciably lower sedimentation constants than those previously computed.

Fig. 4. *Sedimentation diagram* obtained with fractions representative of the various electrophoretic groups. Rotor speed: 1000 r.p.s. — Concentrations as given in Table 2.

Figure, part	Fraction No.	Scale distance cm	Time after attainment of full speed, minutes
a	6	4.0	60
b	18, 19, 20	1.0	20
c	24	4.0	80
d	28	8.0	65
e	34	4.0	30
f	45	1.0	75

The minor irregularities at the baseline, especially pronounced in the β-globulin diagram (*c*), are believed to be due to convections, imperfections in the cell, etc.

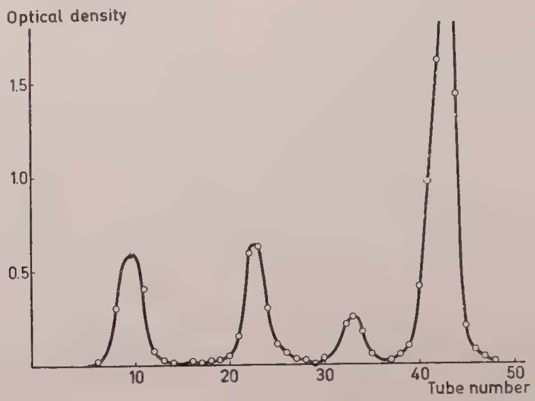

Fig. 5. *Separation of a mixture of fractions Nos. 11, 24, 34 and 45.* Optical density record at 284 mμ.

scale displacements indicated the presence of a component of high sedimentation rate in the sample ($s_{20} \sim 18$–20 S), the experiment was repeated at a lower field strength; usually 600 r.p.s. was chosen. In the computations of the sedimentation constants the partial specific volume has been put equal to 0.739. The experimental data have been collected in Table 2. Fig. 4 shows the sedimentation diagrams obtained for each of the fractions Nos. 6, 24, 34, and 45, which represent the maxima in the albumin and the three globulin groups; Nos. 18, 19, 20 (pooled), intermediate between the γ- and β-globulin groups; and No. 28, in front of the β-globulin maximum (cf. Fig. 1 *a*). The scale diagrams showing the sedimentation of the γ- and β-globulins and the albumin each contain only one, fairly symmetrical peak. In the α-globulin diagram at least four components can be distinguished, and the unsymmetrical spreading of the intermediate, major peak is apparent. It should be noted that a component with s_{20} in the range of 18 S was present in this solution and also in the fractions 12–20 (cf. Fig. 4 *b*), whereas a similar constituent could not be detected in the three different fractions here analyzed which belonged to the β-globulin group Nos. 22, 24, and 28 (cf. Fig. 4 *c* and *d* and Table 2). The fractions 12–20 were only analyzed once; with these exceptions the results are based on several sedimentation analyses of equivalent fractions from different preparations.

The validity of the fractionation process was also submitted to a direct test by separation of a mixture of single fractions, one from each of the main electrophoretic groups. Aliquots of the fractions Nos. 9, 24, 34 and 43 were mixed, concentrated by pervapouration, dialyzed against the veronal buffer of ionic strength 0.03, and reinjected into the separation field. The result of this fractionation is shown in Fig. 5. Kjeldahl analysis of the centre fraction in the albumin zone gave a nitrogen content of 0.48 mg per ml, i.e. a protein concentration of about 0.3 %.

Discussion

The last-mentioned experiment shows the behaviour of some selected protein fractions in the flow field. According to Fig. 5, the pooled fractions Nos. 9, 24, 34 and 43 were again resolved into four distinct zones separated by free interspaces. A comparison with Fig. 1 *a* shows that the mutual sites of the four zones remained unchanged. The experiment allows the conclusion that each of the four fractions comprised proteins belonging to a limited mobility range only and that the intermediate components did not perceptibly influence the migration conditions in the serum fractionation. A similar result was obtained by paper electrophoresis experiments, see Fig. 4 *a*. In the latter record the displacements of the singular spots agree well with those belonging to the whole serum pattern, thus allowing the characterization of the globulin fractions as α_2-, β-, and γ-globulins, respectively. The electrophoretic identity of the fractionated protein material was further established by mobility studies by moving boundary electrophoresis.

In the continuous-flow test experiment the four protein zones emerged from a mixed zone of 11 mm initial breadth. Hence the migration through the column was accompanied by a zone broadening of the order of 100 %, see Fig. 5. A broadening of this magnitude is to be regarded as normal under the selected working conditions. In each case the spreading is partly due to heterogeneity of the protein sample with regard to its electric mobility and partly to be ascribed to disturbances inherent in the flow field. The difficulties in obtaining pure protein preparations for test experiments always renders uncertain any estimation of the heterogeneity of the components by means of the fractionation records. In the present case the protein samples used in the repeated run were obtained by fractionating whole serum into 48 portions of gradually increasing mobility, but the unavoidable deviations from constancy in the flow field widens the mobility range covered by each fraction.

The test fractions were selected from the principal maxima in the distribution curve because such maxima often indicate the predominance of singular components. However, the protein mixture present in blood serum is now known to contain a large number of components (11, 12). The precise fractionation methods elaborated at Harvard Medical School in Boston have made possible the isolation and characterization of several serum constituents within each of the main electrophoretic groups (e. g. 13, 14, 15, 16). Studies of γ-globulin by the method of electrophoresis-convection (17, 18) and lipoprotein by flotation experiments in the ultracentrifuge (19, 20) have revealed the existence of series of proteins, the members of which differ only slightly with regard to their electric mobility and flotation rate, respectively. The complexity of the serum proteins is further evidenced by investigations by other methods, e.g. salt precipitation (21, 22, 23), refined moving boundary techniques (24, 25; 10), diffusion (26, 27), and gel diffusion (28). Therefore, even if the maxima in the fractionation diagram—as obtained by the procedure reported herein—are due to certain major constituents of the protein mixture in serum, it is rather to be expected that each or most of the fractions obtained should contain a heterogeneous protein material.

Some information in this respect was obtained by the sedimentation experiments. With the exception of the fractions representing the maximum in the β-globulin group, the γ-globulins, and the albumins all the fractions investigated were clearly heterogeneous in the ultracentrifuge, in particular the globulin fractions in front of the maximum in the β-globulin group. In two instances the resolution was apparently less in the sedimentation experiments than in electrophoresis. Fraction No. 41, which in the ultracentrifuge only gave a single, fairly symmetrical boundary, could be resolved into one albumin and one α_1-globulin component by paper electrophoresis. Similarly, the γ-globulin fractions investigated showed hardly any significant differences in the ultracentrifuge, but their mobility differences could easily be demonstrated by paper electrophoresis, cf. Fig. 3 *b*.

The sedimentation analyses are too few and incomplete to allow accurate computations of the sedimentation constants. If Pedersen's equations for the concentration dependence of the sedimentation constants of albumin and γ-globulin (29) are used for a recalculation of the experimental s_{20}-values to zero concentration of protein, 4.3_2 S and 6.7_5 S are obtained, respectively. These values are averages from each three sedimentation experiments which agreed to within 0.4 %. The constants are in satisfactory agreement with those given by Charlwood for albumin (26) and by Cann *et al.* for γ-globulin (30), although higher than those obtained in previous measurements at this institute by a factor corresponding to the new temperature correction (cf. p. 353, the footnote).

Without making any definite statements as to the identity of the components observed in the present sedimentation studies, the results may be correlated with those obtained by Cohn and his coworkers by means of ethanol fractionation procedures.

In γ-globulin preparations Oncley, Scatchard and Brown found 75–85 % of a substance sedimenting with a constant of about 7.2 S; the remaining material, which was reported to be somewhat heterogeneous, had a mean sedimentation constant of about 10 S (13). Deutsch *et al.* found 70 % of light material with s_{20} equal to 7 and 9 S and 30 % of a heavy component having a sedimentation constant of 18 S (16). The latter constituent was confined to the γ_1-portion of the fractions investigated, which were prepared from pooled plasma. By means of the electrophoresis-convection technique Cann *et al.* have been able to prepare a γ-globulin from individual sera which contained 99 % of the 6 S-component (30). They suggested that a high yield of heavy material in the γ-globulin preparations, as obtained by Deutsch and coworkers, may be related to the fractionation method or the use of pooled plasma as the starting material. In the present sedimentation analyses both the γ-globulin maxima in the distribution curve (Fig. 1 *a*) were found to contain proteins having a sedimentation constant of 6.7 S exclusively, see Table 2 and Fig. 4 *a*. The fractions 12–20 in Fig. 1 *a*, intermediate between the γ- and β-globulin maxima and approximately corresponding to the γ_1-component defined by Deutsch and coworkers, contained as main constituent a protein defined by a sedimentation constant in the range of 6.2–6.6 S at the experimental concentrations. In addition, as much as 15–20 % of a component with $s_{20} \sim 18$ S was present; in some instances a bump at the rear edge of the main peak in the scale diagram indicated the presence of light material, presumably with a sedimentation constant of about 4 S, cf. Fig. 4 *b*.

Contrary to the simplicity of the sedimentation pattern obtained from the fraction corresponding to the β-globulin maximum, Fig. 4 *c*, the faster β- and the α_2-globulin fractions revealed a considerable complexity in the ultracentrifuge, Fig. 4 *d* and *e*. By the ethanol precipitation methods several individual β- and α-globulins have been isolated and characterized by physico-chemical methods. Summaries of these findings have been tabulated by Cohn *et al.* (14), Oncley (11), and Hughes (12). The following serum components have been assigned definite sedimentation constants:

β_2-Globulins	7 S
β_1-Protein	5 S
β_1-Metal combining protein	5.0 S
β_1-Lipoprotein	7 S
β_1-Lipid-poor euglobulins	7 S 20 S
α_2-Protein	2.9 S
α_2-Glycoprotein	9 S
α_2-Mucoprotein	9 S
α_1-Acid glycoprotein	3.5 S
α_1-Lipoproteins	5 S

A comparison of the findings listed in Table 2 with the results obtained by COHN and his coworkers indicates a general, qualitative agreement as to the sequence of the protein constituents in electrophoresis and the ultracentrifuge. However, the substances which migrated in front of the β-globulins according to the fractionation diagram in Fig. 1 *a* were found to contain a relatively high concentration of a component defined by a sedimentation constant $\sim$ 11 S. Sedimentation constants of a similar order of magnitude have only been reported for certain of the γ-globulins (10 S), hence it is not easy to correlate the present finding with any previous ones. Further, COHN *et al.* ascribe the sedimentation constant 20 S to a protein migrating as a β_1-globulin, but in the present investigation a component having a comparable sedimentation rate was instead found among the α_2-globulins.

In agreement with the findings listed above, the β-globulin fractions contained components with sedimentation constants in the range of 7 S, but the centre fraction only showed a single, fairly symmetrical peak (cf. Fig. 4 *c*), the migration of which was characterized by the sedimentation constant 5.0 S. Qualitative analyses showed that this fraction was rich in lipids and a determination of the partial specific volume gave the value 0.822; hence it probably contained one or several lipoproteins in high relative concentrations. The reddish colour of the solution suggests the presence of the metal combining protein described by SHADE and CAROLINE (31). It is significant that the observed sedimentation constant, 5.0 S, was higher than that to be expected for the metal combining protein and lower than those of the lipid-poor euglobulins and the β_1-lipoprotein isolated by ONCLEY, GURD and MELIN (32). These proteins are reported to be major constituents of the electrophoretic β_1-globulin group. The facts suggest that the fraction analyzed was a mixture of several different proteins, which sedimented together in the ultracentrifuge.

Among the α_2-globulins a glycoprotein and a mucoprotein have been distinguished, both of which are characterized by the s_{20}- value 9 S. By part at least, these substances may account for the intermediate, major peak in the scale diagram given by fraction 35, which is reproduced in Fig. 4 *e*. Whether any of the substances defined as α_1-globulins were also present in this fraction and contributed to the complexity of the sedimentation diagram cannot be decided. In paper electrophoresis the migration of the α-globulin fraction No. 35, relative to that of the components of whole serum, never indicated any contamination of α_1-globulins. By an equivalent procedure α_2-globulin from two other sera—one normal and one pathological—has also been prepared and analyzed in the ultracentrifuge. In both instances the scale diagrams agreed qualitatively with that shown in Fig. 4 *e*.

The extinction curves given in Fig. 2 hence refer to serum fractions which by all evidence are to be regarded as mixtures of several proteins—even in the case of the albumin solution, the yellow colour of which indicates the presence of a bilirubin-albumin complex. By the fractionation procedure the components of extreme mobilities have been removed from the intermediate fractions in each group, which were used for the density measurements. For this reason the extinction curves do not strictly apply to the electrophoretic components in the conventional sense but rather to a (partially) purified mixture of the major constituents of each group. The extinction coefficient of the albumin preparation is in good agreement with that reported by RIDEAL and ROBERTS for bovine serum albumin at pH 6 (33). In the case of the three other preparations no directly comparable values exist in the literature. The ultraviolet absorption spectrum has been studied by LERNER and BARNUM (34) and LÖFFLER, WUNDERLY and WUHRMANN (35). However, following the recommendation of HOLIDAY (36) these measurements have been carried out at pH 2 and 10 in order to allow discrimination between the contributions of the tryptophane and tyrosine residues to the absorption. At these pH values γ-globulin was found to possess the highest specific extinction coefficient. LÖFFLER *et al.* have determined the ultraviolet absorption properties of a β-globulin preparation from a case of β-myeloma. At pH 2 and 10 the extinction coefficient was lower than that of γ-globulin, but at pH 5.2, the experimentally determined isoelectric point of their preparation, the β-globulin coefficient was the highest. The choice of pH in the present investigation, 6.81, may account in part for the finding that the specific extinction coefficient of the faintly brownish β-globulin preparation was greater than that of the γ-globulin preparation. When the optical density was instead recorded at 750 mμ by means of the phenolic group reagent according to LOWRY *et al.* (37) the mutual relation between the extinction coefficients was found to be: $E_{\text{albumin}} = 1$; $E_{\alpha\text{-globulin}} = 1.1$; $E_{\beta\text{-globulin}} = 1.3$; $E_{\gamma\text{-globulin}} = 1.6$ (relative values).

The spectrophotometric studies on protein fractions representing the four electrophoretic groups mainly served the practical purpose of providing a convenient method for routine analyses, which does not cause denaturation of the proteins present. In an ordinary serum fractionation 15–30 ml of whole serum is generally applied, and the effluent fractions are collected in portions of about 10 ml. Hence a considerable number of samples remain to be examined during or immediately after the preparation. The strong absorption of the veronal ion at 280 mμ makes impossible optical density measurements at this wavelength when the ionic strength of the veronal buffer is in the range of 0.03 and higher, but the specific absorption rapidly decreases when the wavelength is increased[1]. Methods based on protein staining have also been tried, e.g. the modification of the Folin-Ciocalteu method described by LOWRY *et al.* (37), but they were found more time-consuming and less accurate. For example, the latter method involves several volume measurements and the deviations from Beer's law impair the results, unless the protein concentration is kept within a limited low range. Direct measurements of the optical density at 284 mμ has the advantage that the protein concentrations usually applied (2 % and lower in the injected solution) give globulin concentrations which fall within the suitable optical density range, i.e. 0.8–0.9 and lower. For the control of the fractionation process and rapid estimates of the concentrations involved it is unimportant that the much higher concentrations within the albumin apex cannot be recorded directly by this means.

In the fractionation diagram, the optical density readings in the case of Fig. 1 *a* refer to pH = 8.5–8.6 and a medium of veronal buffer and those in the case of Fig. 1 *b* to pH = 6.81 and a medium which does not absorb in the ultraviolet region. The transfer to the latter medium involves slight shifts of the extinction coefficients according to their pH-dependence and cancels errors in the veronal blanks due to changes in the veronal concentration at the protein boundaries The conductivity record shown in Fig. 1 *d* gives evidence of significant changes in this property, which are partly due to the concentration variations of the veronal ion. With regard to the absorption at 284 mμ the absolute magnitude of the changes are nevertheless unimportant and can be estimated to correspond to a concentration change of the veronal ion of less than $2 \cdot 10^{-3}$ equivalents per liter. A corresponding change in the optical density would be of the order of 0.01. Accordingly, as shown in

---

[1] The optical density relative to water of a 0.03–C sodium veronal solution is 0.79 at 280 mμ and 0.26 at 284 mμ.

Figs. 1 *a* and *b*, the differences between the two records are very slight, thus indicating that direct readings of the optical density of the fractions at 284 mμ in the veronal buffer can be used for a concentration determination by translation into nitrogen values.

The conductivity record shown in Fig. 1 d is tentative. As demonstrated by SVENSSON (38), the conductivity variations at the protein boundaries give important information about the migration conditions, and it is to be expected that systematic measurements of the conductivity of protein fractions will explain certain typical features in the fractionation diagram and help to deduce optimum conditions in separations of various kinds.

Summary

By continuous zone electrophoresis at pH 8.6 a serum solution containing 1.5 % of protein has been fractionated into 48 portions. In order to test the validity of the fractionation process and obtain an orientation with regard to the distribution of the protein constituents the fractions have been analyzed by some current physico-chemical methods.

By paper electrophoresis it can be shown that material from the principal maxima of the distribution curve migrate as singular spots at rates characteristic of the γ-, β-, α-globulins and albumin, respectively. When successive fractions of the γ-group are simultaneously submitted to electrophoresis on the paper, the line connecting the centres of the spots gradually becomes inclined, thus indicating the mobility differences of the protein constituents.

In the ultracentrifuge the fractions corresponding to the maxima in the γ- and β-globulin groups and the albumin fractions show homogeneous migration. The α_2-globulin fractions investigated contained at least four components. The fractions intermediate between the γ- and β-globulin groups contained as a main constituent a globulin of the sedimentation constant 6.2–6.6 S at the experimental concentrations. A component of high sedimentation rate, s_{20} about 19 S, was present in these fractions and in the α-globulin group. For albumin the sedimentation constant 4.3 S and for γ-globulin 6.7 S were computed.

The protein distribution in the fractions can be derived by measurements of the optical density at 284 mμ and translated into nitrogen values by means of experimentally determined extinction curves, valid for the main fractions of the four electrophoretic groups.

ACKNOWLEDGEMENTS

Indebtedness is expressed to Professor ARNE TISELIUS for laboratory facilities put at my disposal and financial support from grants to the Institute of Biochemistry (from the Swedish Natural Science Research Council, the Wallenberg Foundation, and the Rockefeller Foundation).

I also wish to express my gratitude to Professor CARL DRUCKER for performing two specific volume determinations; to Dr. K. O. PEDERSEN for advice in connection with the sedimentation experiments; and to Mr. EVALD HELLMAN and Miss ANNA-LISA NORLING, who carried out the computations and contributed with critical discussions of the results.

Miss KARIN SÖDERBLOM gave a very valuable assistance in the preparation work, which is gratefully acknowledged.

REFERENCES

1. Brattsten, I., *Arkiv Kemi 8* (1955) 227.
2. Markham, R., *Biochem. J. 36* (1942) 790.
3. Shedlovsky, T., *J. Am. Chem. Soc. 52* (1930) 1793.
4. *Type LKB 3021 Tiselius-Svensson Electrophoresis Apparatus. Instructions for Use.* Stockholm 1950.
5. Wieland, Th. and Fischer, E., *Naturwiss. 35* (1948) 29.
6. Grassmann, W., Hannig, K., and Knedel, M., *Dtsch. med. Wschr. 76* (1951) 333.
7. Svedberg, T. and Pedersen, K. O., *The Ultracentrifuge.* Oxford 1940.
8. Pedersen, K. O., *in* Institut international de chimie Solvay, ed., *Les Protéines, Rapports et Discussions.* Bruxelles 1953, p. 19.
9. Armstrong, Jr., S. H., Budka, M. J. E., and Morrison, K. C., *J. Am. Chem. Soc. 69* (1947) 416.
10. Alberty, R. A., *J. Am. Chem. Soc. 70* (1948) 1675.
11. Oncley, J. L., *in* Robert Gould Research Foundation, ed., *Symposia on Nutrition. Plasma Proteins, Volume II.* Cincinnati 1950, p. 3.
12. Hughes, W. L., *in* Neurath, H. and Bailey, K., *The Proteins, Volume II, Part B*, p. 663.
13. Oncley, J. L., Scatchard, G., and Brown, A., *J. Phys. Coll. Chem. 51* (1947) 184.
14. Cohn, E. J., Gurd, F. R. N., Surgenor, D. M., Barnes, B. A., Brown, R. K., Derouaux, G., Gillespie, J. M., Kahnt, F. W., Lever, W. F., Liu, C. H., Mittelman, D., Mouton, R. F., Schmid, K., and Uroma, E., *J. Am. Chem. Soc. 72* (1950) 465.
15. Hughes, W. L., Jr., *J. Am. Chem. Soc. 69* (1947) 1836.
16. Deutsch, H. F., Alberty, R. A., and Gosting, L. J., *J. Biol. Chem. 165* (1946) 21.
17. Cann, J. R., Brown, R. A., Kirkwood, J. G., and Hink, J. H., *J. Biol. Chem. 185* (1950) 663.
18. Cann, J. R., Campbell, D. H., Brown, R. A., and Kirkwood, J. G., *J. Am. Chem. Soc. 73* (1951) 4611.
19. Gofman, J. W., Lindgren, F. T., and Elliott, H. A., *J. Biol. Chem. 179* (1949) 973.
20. Jones, H. B., Gofman, J. W., Lindgren, F. T., Lyon, T. P., Graham, D. M., Strisover, B., and Nichols, A. V., *Am. J. Med. 11* (1951) 358.
21. Hewitt, L. F., *Biochem. J. 30* (1936) 2229; *31* (1937) 360.
22. Kekwick, R. A., *Biochem. J. 32* (1938) 552.
23. Derrien, Y., *Svensk Kem. Tidskrift 59* (1947) 139.
24. Hoch, H., *Biochem. J. 46* (1950) 199.
25. Hoch, H. and Morris, C. J. O. R., *Nature 156* (1945) 234.
26. Charlwood, P. A., *Biochem. J. 51* (1952) 113; *52* (1952) 279; *56* (1954) 259.
27. Charlwood, P. A., *J. Phys. Chem. 57* (1953) 125.
28. Oudin, J., *Soc. chim. biol. 29* (1947) 140.
29. Pedersen, K. O., *Ultracentrifugal Studies on Serum and Serum Fractions.* Diss. Uppsala 1945.
30. Cann, J. R., Brown, R. A., Singer, S. J., Shumaker, J. B., and Kirkwood, J. G., *Science 114* (1951) 30.
31. Shade, A. L. and Caroline, L., *Science 104* (1946) 340.
32. Oncley, J. L., Gurd, F. R. N., and Melin, M., *J. Am. Chem. Soc. 72* (1950) 458.
33. Rideal, E. K. and Roberts, R., *Proc. Roy. Soc. London Ser. A 205* (1951) 391.
34. Lerner, A. B. and Barnum, C. P., *Arch. Biochem. 10* (1946) 417; *11* (1946) 505.
35. Löffler, W., Wunderly, Ch., and Wuhrmann, F., *Schweiz. Med. Wschr. 79* (1949) 595.
36. Holiday, E. R., *Biochem. J. 30* (1936) 1795.
37. Lowry, O. H., Rosebrough, N. J., Farr, A. L., and Randall, R. J., *J. Biol. Chem. 193* (1951) 265.
38. Svensson, H., *J. Am. Chem. Soc. 72* (1950) 1974.

Tryckt den 6 maj 1955

Uppsala 1955. Almqvist & Wiksells Boktryckeri AB

ARKIV FÖR KEMI Band 8 nr 35

Communicated 23 February 1955 by ARNE FREDGA

Some considerations on substitution reactions in the thiophene ring

By LARS MELANDER

With 1 figure in the text

The most satisfactory theory of the electronic structure of the thiophene nucleus seems at present to be that introduced by LONGUET-HIGGINS (1). According to this theory, the sulphur atom supplies two electron orbitals of pd^2 hybridization type to the π-electron system. Their geometrical shape makes them a very good substitute for the two p orbitals of two adjacent carbon atoms in a benzene ring, so that the sulphur atom, then, could truly be said to replace the fragment —CH=CH— of the ordinary benzene molecule, without, as we know, too much change in the physical and chemical properties.

The electronegativity scale of PAULING (2) assigns the same value to sulphur and carbon, and LONGUET-HIGGINS presents more evidence making it highly probable that the coulomb integrals of the sulphur orbitals (and also the resonance and overlap integrals between the two) should be approximately equal to those of the carbon orbitals concerned. This implies that there will be no difference in net electrical charge between the different atoms of thiophene, just as in the case of benzene. There is, however, a slight difference in geometry between the two molecules, and the main difference in chemical behaviour is believed to arise from a difference in the interaction between neighbouring carbon and sulphur orbitals as compared to that between a pair of carbon orbitals. By means of the method of molecular orbitals (LCAO) and making use of the known resonance (or better: "delocalization") energies of thiophene and benzene, LONGUET-HIGGINS was able to show that the resonance and overlap integrals between neighbouring carbon and sulphur orbitals are about 80 % of the corresponding integrals with pure carbon orbitals involved. For pairs of neighbouring carbon orbitals, as well as for the pair of sulphur orbitals in thiophene, these integrals were assumed to have the same value as between neighbouring carbons in benzene.

DE HEER (3) has extended these calculations, and on the same assumptions has calculated magnitudes such as free valencies and self-polarizabilities of the carbon atoms. Owing to the initially equal charge density, these magnitudes will determine the response of the molecule in the early stages of chemical attacks of different kinds, the self-polarizability being related to INGOLD's "electromeric" effect. As could be anticipated from the picture of thiophene as an intermediate between benzene and butadiene, position 2 is more susceptible than position 3 to different kinds of attack.

Some work going on (e.g. (4, 5)) made it of interest to know the energy of the hypothetical substitution intermediates, analogous to the quinonoid intermediate in the electrophilic substitution of benzene and its derivatives (6). The calculation of the π-electron energy of these structures with four localized bonds at one of the carbon atoms corresponds exactly to WHELAND's calculation (7) for benzene and some of its derivatives and allied substances. This model is related to the activated complex in substitution reactions, and in the case of nitration of benzene derivatives it is a real intermediate of some stability, in which case the true activated complex of the entire reaction is already past before the intermediate is reached. In such cases calculations of the present kind will be a valuable complement to such as those carried out by DE HEER, because they could be said to approach the activated complex from the opposite direction.

The symbols used in the following agree as well as possible with those used by LONGUET-HIGGINS and by WHELAND, the difference between these papers, however, being appreciable. In the following, α denotes the coulomb integral for both kinds of atoms, γ the resonance integral and S the overlap integral for neighbouring atoms of the same kind, and $x\gamma$ and xS are the same magnitudes for unlike neighbours. As usual it is assumed that the resonance and overlap integrals are proportional to one another. The parameter x is retained in the equations, so the results will not be limited to the most probable value, $x = 0.8$.

If E denotes the energy, and

$$\frac{\alpha - E}{\gamma - SE} = -k,$$

the secular equations could be written

for attack in position 2:

$$\begin{vmatrix} -k & 1 & 0 & 0 & 0 \\ 1 & -k & x & 0 & 0 \\ 0 & x & -k & 1 & 0 \\ 0 & 0 & 1 & -k & 1 \\ 0 & 0 & 0 & 1 & -k \end{vmatrix} = 0;$$

for attack in position 3:

$$\begin{vmatrix} -k & 1 & 0 & 0 & x \\ 1 & -k & x & 0 & 0 \\ 0 & x & -k & 1 & 0 \\ 0 & 0 & 1 & -k & 0 \\ x & 0 & 0 & 0 & -k \end{vmatrix} = 0;$$

with the respective roots

$$\begin{array}{ll} k = \sqrt{2+x^2} & \qquad k = \sqrt{1+x+x^2} \\ \phantom{k = {}}1 & \qquad \phantom{k = {}}\sqrt{1-x+x^2} \\ \phantom{k = {}}0 & \qquad \phantom{k = {}}0 \\ \phantom{k = {}}-1 & \qquad \phantom{k = {}}-\sqrt{1-x+x^2} \\ \phantom{k = {}}-\sqrt{2+x^2} & \qquad \phantom{k = {}}-\sqrt{1+x+x^2} \end{array}$$

The resonance part of the energy, E–α, may be obtained from the relation

$$E - \alpha = \frac{k(\gamma - S\alpha)}{1+kS} = \frac{k}{1+kS}\beta,$$

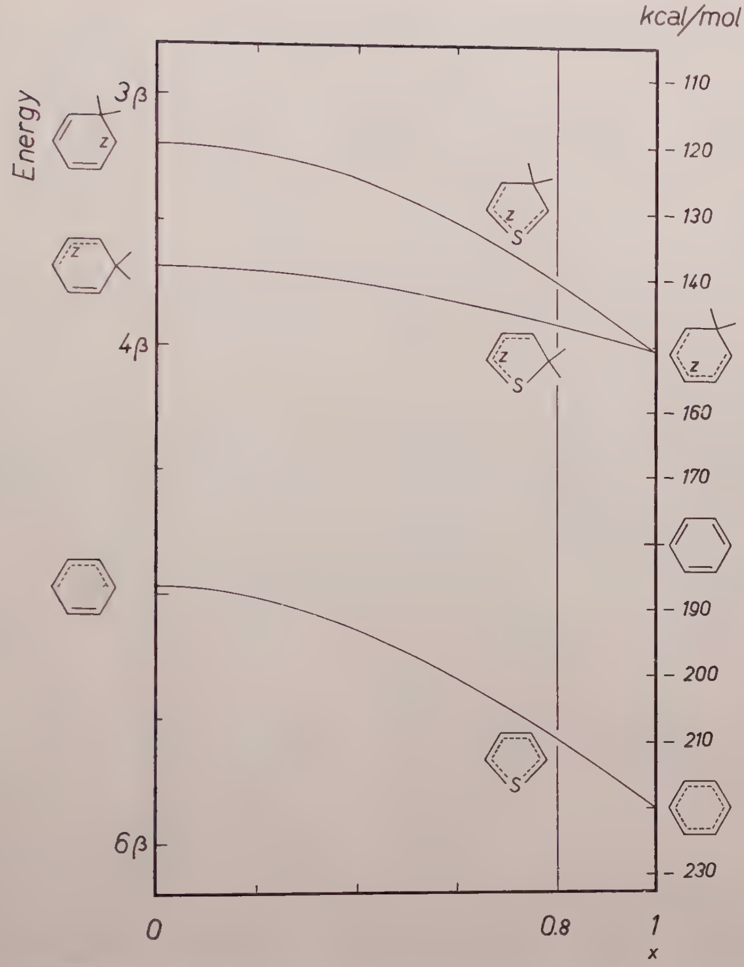

Fig. 1. Resonance part of energy of benzene, thiophene, some related substitution intermediates, and allied structures. x measures the extent of interaction between sulphur and carbon orbitals. For explanations, see the text.

where $\beta = \gamma - S\alpha$ is used as the unit of energy, -37.5 kcal/mol, following exactly the same energy calibration as LONGUET-HIGGINS, and S could be put equal to $\frac{1}{4}$. The sign of k has also been chosen in conformity with the same paper, and the roots above have been arranged in such an order as to give descending stability to the energy levels. Since the third roots are equal to zero the resonance energy of the system will be the same irrespective of whether 4, 5, or 6 π-electrons are involved, i.e. the conclusions drawn as to the relative stability of the intermediates hold irrespective of whether the substitution reaction is electrophilic, homolytic, or nucleophilic, respectively.

Fig. 1 shows the resonance part of the energies of the two intermediates, as well as that of the initial molecule (1), for the complete range $x = 0$ to $x = 1$. In the molecular formulae, full-drawn lines indicate localized bonds, and dashed lines indicate delocalization. The sign z indicates a positive, zero, or negative charge, corresponding to whether the attack has been electrophilic, homolytic, or nucleophilic. The best value of x is considered by LONGUET-HIGGINS to be 0.8, because that gives delocalization energies of thiophene and benzene relative to the cyclohexatriene structure in the ratio 3:4, respectively.

If all other kinds of energy involved are assumed to be equal, it is evident from the figure that the hypothetical intermediate in the substitution of thiophene in position 2 is energetically more accessible than in the case of benzene, where it has been shown to play an important role. Thus there seems to be no reason of this kind why the substitution reactions should not proceed via this path in thiophene, and the difference is able to explain a higher reaction rate in the position 2 in thiophene than in benzene. As to the position 3, the energy of the intermediate relative to the initial molecule is very closely the same as in the case if benzene, and the difference between the two positions in thiophene, about 6 kcal/mol if $x = 0.8$, also explains the difference in reactivity satisfactorily. Other things being equal, a difference of 4.1 kcal/mol in the activation energy is sufficient to give a rate ratio of about 1000 at room temperature, as found for the hydrogen excange (4). In support of these conclusions, it should be pointed out that the calculations of DE HEER, dealing with the very earliest stage of the attack, give rise to the same qualitative results.

The question arises as to why nitrothiophene cannot be prepared by the ordinary methods used in the benzene series, but fairly easily by means of benzoyl or acetyl nitrate. According to GOLD, HUGHES and INGOLD (8), dinitrogen pentoxide is the attacking entity under the latter conditions, not nitronium ion as for instance in mixed nitric and sulphuric acids. It should be remembered that the sulphur atom in thiophene carries a lone electron pair, not taking part in the π-electron system. The C–S–C angle as given by SCHOMAKER and PAULING (9) is $91 \pm 4°$, and hence no extensive hybridization towards sp^2 can have taken place in the unperturbed molecule. Thus the orbital of the lone electron pair is mainly of the s type and has probably fairly weak directional properties, which, however, could probably be increased towards sp^2 simultaneously with an increase of the angle on the approach of an electrophilic entity. It does not seem quite improbable that a nitronium ion will predominantly attack the sulphur atom. Owing to the charge brought by the ion and the strong electron-demanding properties (inductive as well as mesomeric) of the nitro group, the partial butadiene character of the molecule might be strengthened, with polymerization as a consequence. There is probably some analogy between this and what happens to the pyrrole molecule when it is forced to accept a proton, a process, however, which in a straightforward manner localizes two of the electrons of the aromatic sextet as a σ N—H bond.[1]

The strongly acidic properties of ordinary nitration media could be thought to cause the sulphur atom to accept a proton, but other than bringing a charge, the hydrogen introduced has none of the mentioned properties of the nitro group. Sulphonation might be carried out in fairly concentrated sulphuric acid. Exchange experiments (4) have shown, moreover, that protons may attack the molecule at carbon under conditions which cause no appreciable destruction. In extremely strong acids things might be different, but the nitronium ion is believed, in any case, to be more destructive than the proton to the aromatic system.

---

[1] The writer takes this opportunity to thank Professor ARNE FREDGA, who pointed out this analogy during an interesting discussion.

Since sulphonation is possible under ordinary conditions, the attacking species in this type of reaction cannot exert the same influence as the nitronium ion. The difference might have several reasons, for instance the higher electronegativity of nitrogen, or the possibility of a neutral attacking entity in sulphonation.

As to the mechanism of attack of the dinitrogen pentoxide, Gold, Hughes, Ingold and Williams (10) consider it in aprotic solvents a single-stage bimolecular process, in which one part of the molecule accepts the proton and another donates the nitro group.

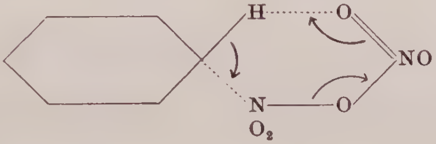

With such a mechanism the free nitronium ion will hardly occur in the solution, and the media used have also a relatively low acidity. Thus none of the two cations which could be believed to be responsible for the side-reactions of thiophene is present to any appreciable extent under the conditions which have been found favourable to the nitration of thiophene. Certainly they will not be present in concentrations comparable to those of ordinary nitration media.

Nobel Institute of Chemistry, Stockholm 50, Sweden.

REFERENCES

1. H. C. Longuet-Higgins, Trans. Faraday Soc. *45*, 173 (1949).
2. L. Pauling, The Nature of the Chemical Bond, Ithaca, N.Y., 1945, Table 11-2.
3. J. de Heer, J. Am. Chem. Soc. *76*, 4802 (1954).
4. K. Halvarson and L. Melander, Arkiv Kemi *8*, 29 (1955).
5. S. Gronowitz and K. Halvarson, Arkiv Kemi, in print.
6. L. Melander, Arkiv Kemi *2*, 211 (1950).
7. G. W. Wheland, J. Am. Chem. Soc. *64*, 900 (1942).
8. V. Gold, E. D. Hughes and C. K. Ingold, J. Chem. Soc. (London) *1950*, 2467.
9. V. Schomaker and L. Pauling, J. Am. Chem. Soc. *61*, 1769 (1939).
10. V. Gold, E. D. Hughes, C. K. Ingold, and G. H. Williams, J. Chem. Soc. (London) *1950*, 2452.

Tryckt den 6 maj 1955

Uppsala 1955. Almqvist & Wiksells Boktryckeri AB

ARKIV FÖR KEMI Band 8 nr 36

Read 23 February 1955

Studies on yeast invertase (saccharase)

Localization of the enzyme in the cell and its liberation

By Karl Myrbäck and Ebba Willstaedt

With 1 figure in the text

In the course of various investigations on yeast saccharase evidence has accumulated that the enzyme is localized on the outside of the cell membrane or, in any case, in a region of the cell where the pH is (practically) equal to that of the surrounding medium, in contrast to the cytoplasmatic region where regulating mechanisms enable the cell to retain its pH in narrow limits rather independently of the pH of the medium. This is already evident from the fact, demonstrated by Willstätter (1), that the saccharase of the living yeast cell has precisely the same activity-pH-curve as the free, soluble enzyme.

The enzyme system of the alcoholic fermentation ("zymase") behaves quite differently. The activity-pH-curve of the fermentation by living yeast has a very broad optimum from about $pH = 3$ to about $pH = 8$, whereas the pH-curve of the enzyme system after destruction of the cell membrane (in the case of brewery bottom yeast simply by drying) has a very narrow optimum between pH 6.0 and 6.5 (2). It must be concluded that the "zymase" system is localized in the cytoplasma or anyway inside the cell membrane. The broad pH-optimum of the living cell is only apparent; the pH at the site of the enzyme system may well be in the neighborhood of 6 when the pH of the surrounding medium is 3.

The localization of the yeast saccharase outside the cell membrane has also been demonstrated by inhibition experiments with uranyl salts (3). The inhibition was reversed by inorganic phosphate in the medium of a concentration considerably lower than the intracellular concentration of inorganic phosphate.

Yeast saccharase is a rather stable enzyme, even in relatively acid solution (e.g. $pH = 3$). However, it is rapidly inactivated at $pH < 2$. The zymase system, i.e. one or more of the enzymes taking part in the alcoholic fermentation reaction sequence, with their pH-optimum in less acid solution ($pH = 6$–6.5) than saccharase, has a considerably lower stability in acid solution. It will be shown in the following that treatment of fresh baker's yeast with diluted hydrochloric acid destroys saccharase much more rapidly than it does the fermentation enzyme system. This can only mean that the yeast saccharase is exposed to the acid reaction of the medium whereas the fermentation enzyme system is not.

The yeast saccharase is very firmly bound to the cell membrane, at least in certain types of yeast. In a previous communication (4) experiments were reported on the liberation of the saccharase of baker's yeast from the cell remnants after plasmolysis of the cells. It was found that, of several enzymes tested, only papain (and probably other proteinases of the papain type) is able to liberate saccharase and it was concluded that the enzyme of the cells is bound to insoluble proteins. However, the insoluble enzyme-protein compound has the same catalytic activity as the free soluble enzyme. The situation may therefore also be expressed in the following way: The native enzyme in the living cell is an insoluble protein; by the action of papain this protein is broken down in such a way that one part of the original molecule, still possessing the full enzymatic activity, is rendered water-soluble. As far as our experience goes, this soluble protein is stable against further attack by the proteinase. New experiments on the liberation of soluble saccharase will be presented here.

By plasmolysis of baker's yeast with ethyl acetate, thorough washing of the cell remnants and treatment with papain, very active saccharase solutions could be obtained. The enzyme in these solutions is soluble in saturated ammonium sulphate solution; impurities could therefore be removed by saturation of the suspension after the papain treatment with solid ammonium sulphate and filtration. Salts and low-molecular impurities could be removed by dialysis without loss of enzyme. Since these enzyme solutions were prepared in an unusual way it seemed of interest to determine their action as to the formation of higher oligosaccharides during the hydrolysis of saccharose. BACON and EDELMAN (5) found an intermediate formation of several oligosaccharides during hydrolysis of saccharose and inulin. They considered that the same enzyme is responsible for both hydrolytic and transferring activities. ARONOFF (6) could not verify this statement, but later on ARONOFF and BACON (7) found it highly improbable that the formation of oligosaccharides is caused by a separate enzyme, different from saccharase. In the meantime several authors have found a "transglycosylase" activity in various saccharase preparations and also in other carbohydrase preparations, hitherto regarded as purely hydrolytic. Since yeast saccharase is not known in the pure state, the possibility cannot be quite excluded that the formation of oligosaccharides is caused by a contaminating "transglycosylase". However, the possibility seems remote and, in any case, our yeast saccharase preparations gave the same formation of oligosaccharides as that found by others.

Localization of saccharase in the yeast cell

The destroying action of diluted hydrochloric acid on saccharase and on the fermentation enzyme system was determined. The following experiments were carried out:

a) 5 g fresh baker's yeast was suspended in 50 ml 0.1 *N* hydrochloric acid.

b) 5 g yeast in 50 ml 1 per cent phosphate buffer, pH = 6.

Both suspensions were stored at 20° for 18 hours. They were centrifuged, the yeast was washed twice with water and resuspended in 50 ml 1 per cent phosphate buffer, pH = 6.

Determination of saccharase activity. 4.75 g saccharose, 10 ml acetate buffer, pH = 4.5, 89 ml water, 1 ml yeast suspension, toluene, 30°. 10 ml samples were mixed with 10 ml *N* sodium carbonate solution and filtered. Optical rotation α was determined in 2 dm tubes (Table 1). It appears that about 99 per cent of the saccharase had been destroyed by the treatment with hydrochloric acid.

Fermentation experiments. 2 ml yeast suspension, 0.1 g sugar. The evolution of

Table 1. Destruction of saccharase by hydrochloric acid.

No acid treatment		Treated with 0.1 *N* acid	
Time	α	Time	α
0	3.00°	0	2.95°
1 min.	2.83	85 min.	2.85
5 ,,	1.92	3.5 h	2.32
10 ,,	1.13	5.5 ,,	2.04
15 ,,	0.54	22 ,,	0.04
Decrease in rotation/min.	0.22°	Decrease in rotation/min.	0.003°

Table 2. Determination of fermentation.

Yeast	Sugar	ml CO_2 after a fermentation time of										
		$^1/_4$	$^1/_2$	1	1.5	2.5	3	4	5	6	7	23 h
No acid treatment	Saccharose	2.9	6.0	12.0	16.5	22.0	22.1					
	Glucose	3.0	5.9	12.0	16.3	20.9	21.0					
	Maltose	0.7	1.3	6.5	11.2	19.8	20.4					
Acid-treated	Saccharose	1.2	2.4	4.7	6.5	10.5	12.5	16.0	18.8			
	Glucose	1.2	2.5	4.7	6.5	10.5	12.4	16.0	18.6			
	Maltose	0.2	0.3	0.4	0.5	1.4	2.2	3.5	5.2	8.5	13.0	19.5

carbon dioxide at 30° was measured (Table 2). It is evident from tables 1 and 2 that, whereas the saccharase had been almost completely destroyed by the acid treatment, the rate of fermentation of glucose and saccharose after the said treatment was still about 50 per cent of the rate before the treatment. Thus the fermentation enzymes, though in themselves less stable in acid solution than saccharase, have been much less damaged by the treatment with hydrochloric acid. The only explanation is that the fermentation enzyme system, in contrast to the saccharase, has never been exposed to the full acidity of the surrounding medium.

It may be pointed out in passing that these experiments furnish direct proof that the hydrolysis of saccharose by saccharase is not a prerequisite for the saccharose fermentation, at least not with this yeast. It can be concluded that the saccharose phosphorylase (or similar enzyme) responsible for the initial attack on saccharose has not been seriously damaged during the acid treatment, obviously because it is localized, like the other components of the fermentation enzyme system, in the interior of the cell.

It is evident from Table 2 that the fermentation of maltose has been more damaged than that of glucose and saccharose. The fermentation curves in Fig. 1 show that the effect of the acid treatment on maltose fermentation is virtually an extension of the "lag phase". This lag phase in maltose fermentation (evident also in curve c, Fig. 1) is characteristic of the baker's yeast used (8) and has been tentatively explained as caused by an adaptation, i.e. the formation or activation of an enzyme involved in

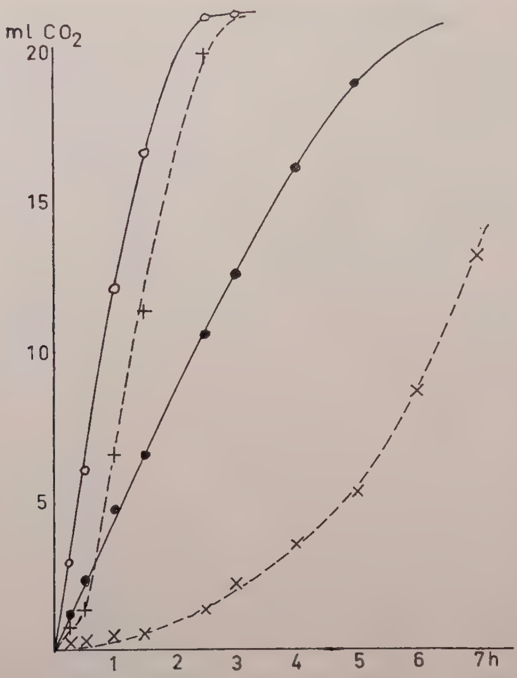

Fig. 1. a) ○———○ Yeast and glucose (saccharose). b) ●———● HCl-treated yeast and glucose (saccharose). c) +– – – –+ Yeast and maltose. d) ×– – – –× HCl-treated yeast and maltose.

the primary attack on the maltose molecule. The enzyme system responsible for the adaptation has obviously been more seriously damaged than the fermentation enzyme system itself.

Liberation of saccharase from insoluble complex

Fresh baker's yeast was kneeded with about 10 per cent ethyl acetate until a fluid state was reached. The mixture was shaken with about 10 per cent toluene and left overnight at 20°. It was then diluted with a large volume of water, centrifuged and washed. The residue was resuspended in water and toluene was added. The mixture was stored at room temperature; no spontaneous liberation of saccharase took place for several months.

The saccharase activity of suspension and filtrates was determined as described above; two experiments in Table 3. If α is plotted versus time a curve is obtained which initially is a straight line. The decrease in rotation per minute and ml suspension or filtrate, respectively, is a measure of the enzyme activity. E.g., the activity of one ml suspension (Table 3) in this arbitrary unit is $0.90/2 \times 5 = 0.090$, that of one ml filtrate 0.015. The activity values of the filtrates are less reproducible than those of the suspension, owing to the difficulty of obtaining filtrates completely free from supended material.

Influence of pH on liberation of saccharase. The liberation of saccharase at different pH's (without addition of protease) was investigated. It was found that storage of

Table 3. Saccharase activity of suspension and filtrate.

Suspension		Filtrate	
Reaction time, min.	α	Reaction time, min.	α
0	3.00°	0	3.00°
1	2.56	5	2.61
2	2.10	10	2.25
5	1.05	20	1.52
10	−0.08	30	1.00
20	−0.77	60	0.07

Table 4. Liberation of saccharase.

Treatment	Activity	
	Suspension	Filtrate
Water, pH = 5	0.090	0.015
Acetic acid, pH = 3, + 2°, 20 hours	0	0
,, ,, , pH = 4, + 2°, 20 ,, ...	0.091	0.015
NaOH, pH = 7,5, + 2°, 20 h	0.090	0.012
,, pH = 8.5, + 2°, 20 h	0.097	0.018
20 % guanidine.HCl, pH = 4.5, + 2°, 20 h	0.075	0.018
20 % ,, ,, pH = 7.7, + 2°, 20 h	0.062	0
1 % trypsin, pH = 8, 20°, 5 h	0.086	0.012
1 % ,, , pH = 8, 20°, 10 h	0.094	0.020
1 % ,, , pH = 8, 20°, 100 h	0.094	0.017
1 % papain, pH = 5, 20°, 70 h		0.030
1 % papain + 0.5 % cystein, pH = 5, 20°, 70 h		0.060
1 % ,, + 0.5 % ,, , pH = 5, 20°, 100 h		0.063
1 % ,, + 0.5 % ,, , pH = 5, 20°, 200 h	0.090	0.089

the suspension at + 2° and pH = 4 or 7.5 or 8.5 did not release any enzyme (Table 4). At pH = 3 all enzyme was destroyed.

Treatment with guanidine hydrochloride. The effect of guanidine hydrochloride on the liberation was investigated at pH 4.5 and 7.7, respectively. Treatment with a 20 per cent solution of the salt at + 2° for 20 hours had no effect (Table 4).

Treatment with pancreatin. Previous experiments have shown no or only a very slight action of pancreatin on the liberation af saccharase (4). New experiments (Table 4) gave the same result. The activity of the pancreatin preparation towards 4 per cent gelatin solution at pH = 8 was determined: A number of samples were prepared containing 10 ml gelatin solution and 5 ml 2 per cent solution of pancreatin. The samples were titrated after suitable times with 0.1 *N* NaOH in the presence of 10 ml 35 per cent formaldehyde (Table 5). The influence of the very active protease preparation upon the liberation of saccharase was determined: 10 ml yeast suspension as above, 0.1 g pancreatin, sodium carbonate to pH = 8. No action could be observed (Table 4). The pancreatin preparation was rich in trypsin and amylase and had a strong lipase action on olive oil. It is thus concluded that none of these enzymes has any action on the liberation of saccharase. It may appear a little astonishing that trypsin has no action while papain actively liberates saccharase.

Table 5. Hydrolysis of gelatin by pancreatin.

Time	ml 0.1 *N* NaOH
0	4.7
35 min.	8.4
90 ,,	10.4
5 hours	13.5
22 ,,	15.0
129 ,,	19.5

Table 6. Saccharase in heated yeast.

Temperature °C	Relative activity in	
	Yeast suspension	Filtrate
55	100	~2
60	—	~2
66	~ 0	~2

Treatment with papain. 10 ml suspension, 0.1 g papain powder, pH = 5. As in our earlier experiments papain was found to liberate saccharase. The action was strongly stimulated by cystein (Table 4).

The best way of recovering the saccharase from the slimy, papain-treated suspensions, was to saturate them with solid ammonium sulphate. All saccharase was found in the filtrates which could be dialyzed in cellophane bags without loss of enzyme.

Effect of heat-treatment of yeast. 5 g samples of fresh baker's yeast (25 per cent dry weight) were heated at different temperatures for 30 min. Water was added to 50 ml and a portion of the suspension was filtered. The saccharase activity of suspension and filtrate was determined (Table 6). It appears that no liberation of saccharase can be achieved by the heating of the yeast. The heated yeast samples were also quite inactive in fermentation experiments.

Effect of freezing on liberation of saccharase. Yeast samples were frozen in a mixture of solid CO_2 and acetone. Saccharase determinations in filtrates from the thawed material has a saccharase activity less than 2 per cent of that of the solid yeast remnants.

Effect of plasmolysis with solid NaCl. It is known that plasmolysis with NaCl of fresh baker's yeast (the same as that used here) yields an extract very rich in yeast phosphatase (9). The saccharase content of such plasmolysates (50 g yeast, 25 per cent dry weight, and 10 g NaCl) indicated that no liberation of the bound enzyme has taken place during plasmolysis. About 3 per cent of the yeast substance had passed into solution.

Transferase action of saccharase preparation

The experiments were carried out in a 40 per cent saccharose solution. The course of the hydrolysis in this solution was first compared with that of a normal inversion experiment:

Experiment 1. 4.75 g saccharose, 10 ml acetate buffer, pH = 4.5, 85 ml water, 5 ml saccharase solution, 30°. 10 ml samples + 10 ml *N* sodium carbonate solution. Rotation α in 2 dm tubes (Table 7).

Table 7. Saccharase activity in 4.75 and 40 percent saccharose solution.

5 ml enzyme solution in 100 ml 4.75 per cent saccharose		5 ml enzyme solution in 10 ml 40 per cent saccharose	
Reaction time	α	Reaction time	α
0	3.00	0	5.00
1.5 min.	2.96	10 min.	4.63 4.67
5.5 ,,	2.82	30 ,,	3.85 4.02
10.5 ,,	2.67	60 ,,	2.90 3.05
20.5 ,,	2.38	120 ,,	1.51 1.49
50 % hydrolysis after	105 min.	50 % hydrolysis after	110 min.

Table 8. Chromatogram spots.

Time min.	R_{Fr} values						
	1 Fructose	0.74 Glucose	0.44 Saccharose	0.32	0.21	0.16	0.13 Raffinose
10	+ +	+ +	+ + + +	+	?	+	(+)
30	+ + +	+ + +	+ + +	+	+ ?	+	(+)
60	+ + +	+ + +	+ + +	+	+	+	(+)
120	+ + + +	+ + + +	+ +	+ +	+	+ +	(+)

Experiment 2. 4 g saccharose, 1 ml acetate buffer, 1.4 ml water, 5 ml saccharase solution, 30°. 2 ml samples + 8 ml water + 10 ml *N* sodium carbonate, 2 dm tubes (Table 7). This table shows that the reaction rate is practically the same in both experiments.

From experiment 2 samples were removed and examined paper-chromatographically. 0.5 ml samples were mixed with 1.5 ml hot water and kept at 100° for a few minutes to stop the enzyme action. Suitable volumes were put on paper and irrigated with the usual ethyl acetate-acetic acid-water mixture. Descending technique; temperature 22°; time usually 42 hours. The treatment of the chromatograms has been described earlier (10). The position of the spots are given in the following as R_{Fr} values (= distance travelled by the spot, when the distance travelled by the fructose spot is put = 1). Table 8 gives a survey of the spots observed in experiment 2 after various reaction times. Glucose, fructose, saccharose and raffinose were put on as references. Two oligosaccharides with $R_{Fr} = 0.32$ and 0.16, respectively, were present already in the first sample after 10 minutes. The amounts of these oligosaccharides increased with reaction time and a third (weaker) spot with $R_{Fr} =$ 0.21 appeared.

Experiment 3 was identical with experiment 2 but on a fourfold scale. Samples for chromatography were taken every hour up to 18 hours and then after 25 and 52 hours. Polarimetric determinations showed that 90 per cent hydrolysis was reached after ca. 7 hours. In all chromatograms except the two last (25 and 52 hours) the same spots were observed as mentioned in table 7. The chromatograms for 25 and 52 hours contained only two spots, fructose and glucose. The newly-formed oligosaccharides were obviously hydrolyzed but at a comparatively slow rate.

Experiment 4 was performed at pH 2.6 but otherwise as experiments 2 and 3. The reaction rate was only slightly lower than in these experiments. The same spots appeared on the chromatograms.

The three spots on the chromatograms between the saccharose and the raffinose spots are probably identical with the three spots, originally observed by BACON and EDELMAN (5). By a refined paper-chromatographic technique and by paper electrophoresis further oligosaccharides have been shown to be present (11).

SUMMARY

Evidence has been presented supporting the conclusion, arrived at in previous investigations, that the saccharase of baker's yeast is localized on the outside of the yeast cell membrane and, therefore, exposed to the pH of the surrounding medium. The saccharase of baker's yeast can be completely destroyed without impairing the ability of the yeast to ferment saccharose.

The saccharase of baker's yeast is very firmly bound to the solid remnants of the cell membrane which resist plasmolysis and short autolysis of the cells. No other means to liberate the bound enzyme has been found than papain, activated by cystein. Trypsin has no action in this respect. The soluble saccharase is stable against papain. Plasmolysis of the cells with NaCl does not liberate saccharase.

Saccharase extracted from the washed solids after plasmolysis of the cells, shows the same transferring activity as other saccharase preparations. Three oligosaccharides with lower R_F values than saccharose were found.

Institute for Organic Chemistry and Biochemistry, University, Stockholm.

REFERENCES

1. WILLSTÄTTER, R. and RACKE, F., Ann. *425*, 1 (1921).
2. MYRBÄCK, K., Hoppe-Seylers Z. physiol. Chem. *139*, 30 (1924).
3. DEMIS, D. J., ROTHSTEIN, A., and MEIER, R., Arch. Biochem. Biophys. *48*, 55 (1954).
4. THORSELL, W. and MYRBÄCK, K., Arkiv Kemi *3*, 323 (1951).
5. BACON, J. S. D. and EDELMAN, J., Arch. Biochem. Biophys. *28*, 467 (1950).
6. ARONOFF, S., Ibid. *34*, 484 (1951).
7. ARONOFF, S. and BACON, J. S. D., Ibid. *41*, 476 (1952).
8. MYRBÄCK, K. and RENVALL, S., Arkiv Kemi, Mineral. Geol. *23 A*, No. 6 (1946).
9. SCHÖNBERG, K. and SPERBER, E., Svensk Kem. Tidskr. *57*, 117 (1945).
10. MYRBÄCK, K. and WILLSTAEDT, E., Arkiv Kemi *6*, 417 (1953).
11. WHITE, L. M. and SECOR, G. E., Arch. Biochem. Biophys. *36*, 491 (1952); GROSS, D., Nature *173*, 486 (1954); BACON, J. S. D., Biochem. J. (London) *57*, 320 (1954).

Tryckt den 6 maj 1955

Uppsala 1955. Almqvist & Wiksells Boktryckeri AB

ARKIV FÖR KEMI Band 8 nr 37

Vorgelegt am 23. Februar 1955

Oxydo-reduktive Funktionen der aci-Reduktone

Von Hans von Euler und Hans Hasselquist

Mit 3 Figuren im Text

Unter den verschiedenen Wirkungen der Ascorbinsäure in vitro, welche auch in der lebenden Zelle eine wesentliche Rolle spielen[1], ist eine der auffallendsten die Erniedrigung der Viscosität von Lösungen gewisser hochmolekularer Stoffe, besonders der Pectine[2]. Trotz zahlreicher Untersuchungen, unter denen hier nur diejenigen von Henglein[3], Kertesz[4] und Deuel[5] erwähnt seien, sind die chemischen Vorgänge, die diesen Viscositätsänderungen zugrunde liegen — sie werden in Gegenwart von Sauerstoff schon durch rel. kleine Menge von Reduktonen hervorgerufen — noch nicht quantitativ aufgeklärt, weder hinsichtlich der Ascorbinsäure noch hinsichtlich des Pectins oder anderer makromolekularer Stoffe wie Mucine oder Hyaluronsäure, in welche ebenfalls Uronsäuren eingehen und welche einer Oxydation unterliegen können.[6]

In einer vorhergehenden Mitteilung von H. v. Euler und M. L. Stein[7] wurde in Bestätigung der obenerwähnten früheren Arbeiten angegeben, dass die Viscositätsbeeinflussung durch Ascorbinsäure usw. bei Zusatz von Wasserstoffperoxyd ausserordentlich stark erhöht wird. Ferner wurde mitgeteilt, dass keineswegs allen Reduktonen, sondern nur den aci-Reduktonen der besprochene Viscositätseffekt eigen ist, sowie dass die Dehydro-ascorbinsäure, in welcher die Endiol-Gruppe durch eine Diketo-Gruppe ersetzt ist, die Viscosität des untersuchten Pektins nur unbedeutend erniedrigt.

Wir haben nun diese Versuche an einem besser definierten Pektin-Präparat wieder aufgenommen, zunächst um das Versuchsmaterial bez. der aci-Reduktone zu ergänzen und diese hinsichtlich ihrer Viscositäts-erniedrigenden Wirkung zu vergleichen und um später zu untersuchen, ob die gleiche Reihenfolge der Wirksamkeit auftritt, wenn diese aci-Reduktone an anderen Oxydo-reduktionen teilnehmen.

---

[1] Euler u. H. Hasselquist, Zs. physiol. Chem. 288, 4; 1951.

[2] Zur Nomenklatur der Pectinstoffe siehe F. A. Henglein, Makromol. Chem. 1, 70; 1947.

[3] F. A. Henglein u. G. Schneider, Ber. dtsch. chem. Ges. 69, 309; 1936. F. A. Henglein u. B. Vollmert, Makromol. Chem. 2, 77; 1948. — F. A. Henglein u. J. Krohn, Makromol. Chem. 4, 308; 1950. — F. A. Henglein, Moderne Methoden d. Pflanzenanalyse II, 226; 1955.

[4] Z. J. Kertesz, The Pectic Substances, New York, Intern. Publ., 1951.

[5] H. Deuel, J. Solms u. H. Altermatt, Viertelj.Schr. Naturf. Ges. Zürich 98, 49; 1953. — H. Deuel, Helv. Chim. Acta 26, 2002; 1943. — H. Deuel u. G. Huber, Helv. Chim Acta 33, 10; 1950.

[6] Neben den chemischen Veränderungen des Pectins und der aci-Reduktone muss auch die an den Kolloid-Teilchen durch Elektrolyte eintretende Dehydratation sowie ihre Formveränderung in Betracht gezogen werden.

[7] Euler u. M. L. Stein, Makromol. Chem. 15, 60; 1955.

Material und Methodik

Das Pektin[1] wurde zu den folgenden Untersuchungen aus Zitronenschalen dargestellt unter Modifizierung der Vorschrift von G. SCHNEIDER u. H. BOCK.

Aus den Schalen von 5 unreifen Zitronen wurde das weisse Fleisch fein zerschnitten und dann in 1,5 Liter Wasser 45 Minuten unter Einleiten von Stickstoff gekocht. Nach Filtration durch einen Büchnertrichter mit Kieselgur wurde eine klare, hellgelbe Lösung erhalten, die im Vakuum bei 40° auf ca 150 ml eingedunstet wurde. Hieraus wurde das Pektin mit dem gleichen Volumen 96 %igen Alkohols gefällt und ohne Anwendung von Filtrierpapier und ohne Absaugen in einem Büchnertrichter abfiltriert. Das Pektin wurde nun wieder in etwa 100 ml Wasser gelöst und wieder mit Alkohol gefällt. Dieses Verfahren wurde dann nochmals wiederholt. Hierauf liess man das Pektin an der Luft trocknen, befreite es dadurch von Alkohol, löste es wieder in Wasser und filtrierte nochmals durch Kieselgur.

Für die Überlassung der Reduktinsäure sind wir Herrn Prof. Dr. T. REICHSTEIN sehr zu Dank verpflichtet. Die Ascorbinsäure verdanken wir den Chemischen Fabriken KABI A.B., Stockholm. Die übrigen Reduktone sind hochgereinigte Präparate, deren Herstellung wir in früheren Mitteilungen beschrieben haben.

Die *Viscositätsmessungen* wurden in Ostwaldschen Viscosimetern ausgeführt, die sich in einem auf 30° gehaltenen Thermostaten befanden.

Die Reduktone wurden in äquimolekularen Lösungen verwendet. Als Puffer benützten wir eine Mischung von Dinatriumphosphat und Zitrat; die Puffersalze waren in der zu messenden Redukton-Lösungen 0,1 m. Enthielt die Lösung ein Fe^{II}-Salz, so wurde mit NaAc gepuffert. Die Lösungen wurden stets auf $pH = 7$ gehalten.

Die Grösse der Viscositätserniedrigung durch Reduktone ist, wie bekannt, sehr stark von der Acidität (pH) der Lösung abhängig, und zwar nimmt der Effekt mit steigender Alkalinität zu.

In der Regel wird die Viscosität einer Lösung durch η angegeben. Um η aus unseren Angaben berechnen zu können, haben wir die Durchlaufszeiten des Lösungsmittels und die specif. Gewichte unserer Lösungen bestimmt.

DEUEL berechnet aus seinen Messungen die Zähigkeitszahl

$$Z = \frac{\eta - \eta_0}{\eta_0 \cdot m}$$

Zu einfachen Vergleichen genügt die Angabe der direkt beobachteten Durchlaufszeit D und der zeitlichen Abnahme derselben, ΔD. Die Durchlaufszeit ist keine einfache Funktion der Pektin-Konzentration, da die Viscosität einer Pektinlösung ausser von der Acidität noch von dem Molekulargewicht, der Molekülform, der Hydratation des Pektins und von der Gegenwart anderer Lösungskomponenten abhängt.

Versuche

Mit unserem gereinigten Pektin-Präparat haben wir zunächst die Angaben von KERTESZ, DEUEL, HENGLEIN sowie M. L. STEIN bestätigt, dass die Viscosität des Pektins durch Ascorbinsäure allein bzw. durch H_2O_2 allein nur sehr langsam und in geringem Grad, durch beide zusammen aber sehr schnell und stark erniedrigt wird.

---

[1] Pektin ist nach dem Nomenklatur-Vorschlag von HENGLEIN, dem wir folgen, methylierte Polygalakturonsäure. Durch hydrolytische Entmethylierung entsteht daraus Pektinsäure (pectinic acid). Siehe z.B. Z. KERTESZ, The Pectic Substances. New York Interscience Publ. 1951. — DEUEL u. Mitarb., Naturforsch. Ges. Zürich 98, 63 1953.

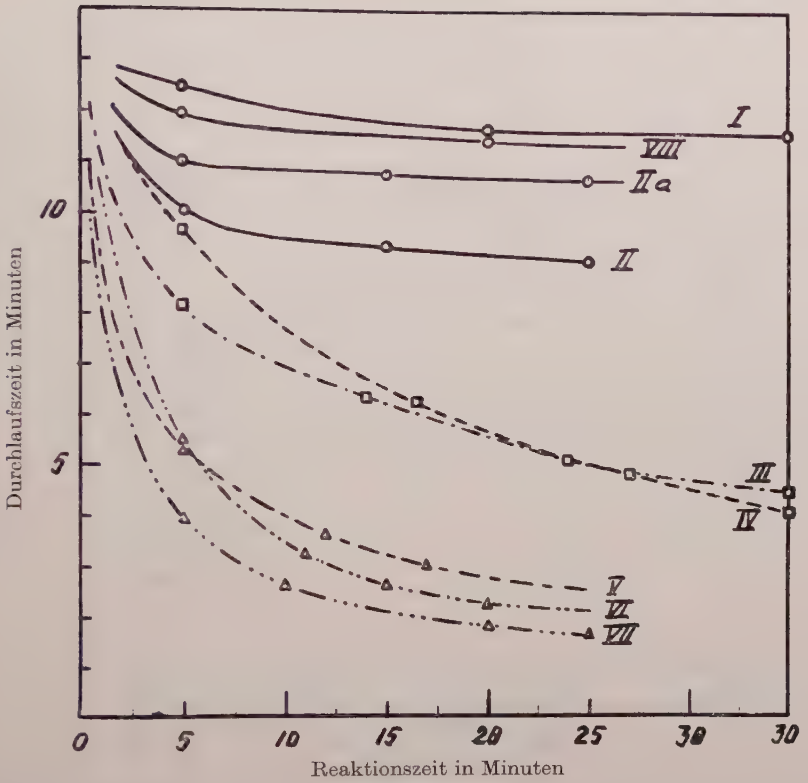

Fig. 1.

I. 2,8 mg Pektin / ml 0,1-m Na_2HPO_4-Zitrat-Pufferlös.
II. 2,8 mg Pektin + 0,17 mg H_2O_2 / ml 0,1-m Pufferlös.
II a. 2,8 mg Pektin + 0,17 mg H_2O_2 (0,02 mol / ml B_1).
III. 2,8 mg Pektin + 0,17 mg H_2O_2 + 0,37 mg Dioxy-maleinsäure / ml 0,1-m Pufferlös.
IV. 2,8 mg Pektin + 0,17 mg H_2O_2 + 0,22 mg aci-Redukton I / ml 0,1-m Pufferlös.
V. 2,8 mg Pektin + 0,17 mg H_2O_2 + 0,285 mg Reduktinsäure / ml 0,1 m Pufferlös.
VI. 2,8 mg Pektin + 0,17 mg H_2O_2 + 0,44 mg Ascorbinsäure / ml Pufferlös.
VII. 2,8 mg Pektin + 0,17 mg H_2O_2 + 0,325 mg 3,4-Dioxy-5-methyl-Tetron/ml Pufferlös.
VIII. 2,8 mg Pektin + Dehydro-askorbinsäure (0,0025 Mol / Liter).

Die Konz. sämtlicher Reduktone betrug 0,0025 Mol / Liter.

Wir geben unsere diesbezüglichen Versuche nur auszugsweise an.
Alle Versuchslösungen waren 0,1 mol. bez. des Na_2HPO_4-Zitrat-Puffers.
Alle Versuchslösungen enthielten 6,8 mg Pektin/ml Pufferlösung.

Versuch a. Die Lösungen enthielten H_2O_2-Mengen zwischen 5 mg und 0,63 mg/ml.

5 mg H_2O_2/ml. Durchlaufszeit *D*. Beginn 5′30″. Nach 1 St. 4′27″ Δ*D* 1′03″
0,65 mg H_2O_2/ml. Durchlaufszeit *D*. Beginn 5′30″. Nach 1 St. 4′46″ Δ*D* 0′44″

Versuchsreihe b. Die Lösungen enthielten Ascorbinsäuremengen zwischen 5 mg und 0,625 mg/ml.

5 mg Ascorbins./ml. Durchlaufseit *D*. Beginn 6′20″. Nach 16 St. 1′26″ Δ*D* 4′33″
0,625 mg Ascorbins./ml. Durchlaufszeit *D*. Beginn 6′20″. Nach 16 St. 2′36″ Δ*D* 3′44″

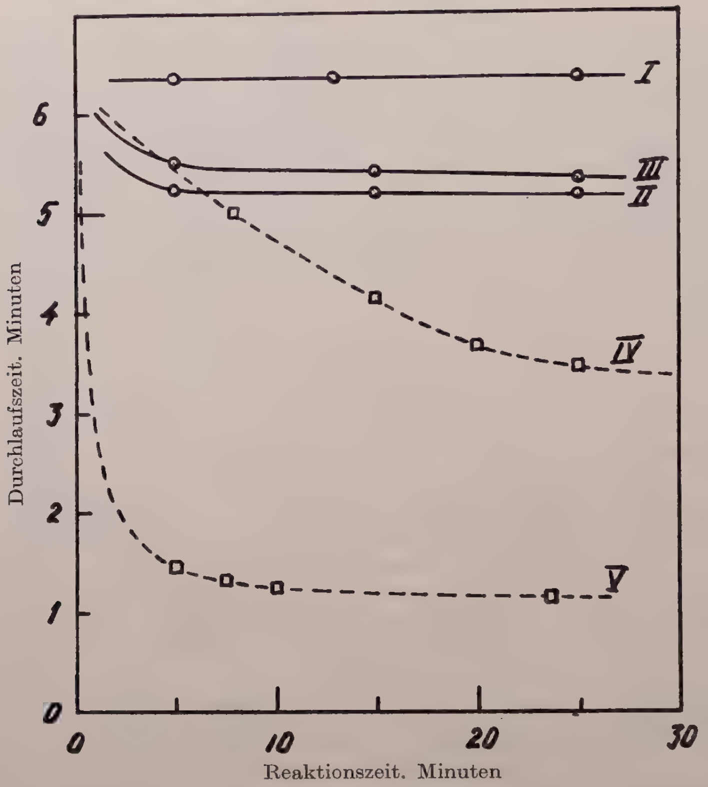

Fig. 2. Einwirkung von Hydroxylamin und von Fe^{II}-Salzen auf die Viscosität der Pektinsäure-Lösungen.

I. 2,8 mg Pektin / ml 0,1 mol. HAc-NaAc-Puffer.
II. 2,8 mg Pektin / ml + 0,11 mg NH_2OH / ml 0,1 mol Puffer-Lös.
III. 2,8 mg Pektin + 0,11 mg NH_2OH + 0,17 mg H_2O_2 / ml Puffer-Lös.
IV. 2,8 mg Pektin + 0,17 mg H_2O_2 + 0,70 mg $FeSO_4$ / ml Puffer-Lös.
V. 2,8 mg Pektin + 0,17 mg H_2O_2 + 0,70 mg $FeSO_4$ + 0,22 mg aci-Redukton I / ml Puffer-Lös.

Messungen bei 30° und pH 6,2 Acetatpuffer. H_2O_2-Konzentration: 0,005 Mol per Liter. Konzentrationen des Hydroxylamins, des $FeSO_4$ und des aci-Reduktons I = 0,0025 Mol per Liter Reaktionslösung.

Diese wie unsere übrigen Versuchsreihen zeigten, dass die Viscositäts-Effekte sich nur sehr wenig mit den Konzentrationen der Perhydroxyds bzw. der Ascorbinsäure änderten. Analoge Versuche wurden mit Triose-Redukton sowie mit dem Aci-Redukton III (Dioxy-Tetron) angestellt. Auch hier zeigte sich nur eine sehr geringe Variation des Viscositätseffektes mit der Konzentration der beiden Reduktone.

Viel deutlichere Einwirkungen auf die Viscosität des Pektins werden in Systemen erhalten, in welchen Reduktone und Hydroperoxyd mit oder ohne Zusatz von Fe^{II}-Ionen kombiniert sind. Wir haben den Vergleich zwischen den verschiedenen Reduktonen in solchen Systemen angestellt.

Wir haben die Ergebnisse in Fig. 1 zusammengestellt.

Besonders interessant ist der Einfluss der Ferro-Ionen auf die untersuchte Viscositätserniedrigung, wie er aus der Figur 2 hervorgeht.

Hydroxylamin hat, wie die Kurven II und III zeigen, unter den angegebenen Versuchsbedingungen keinen Einfluss auf die Viscosität des Pektins.

Unter den biologisch wichtigen Reaktionen, welche durch Ascorbinsäure in Gegenwart von H_2O_2 katalysiert werden, mögen hier hervorgehoben werden: die Überführung des Hämoglobins in Gallenfarbstoffe[1] sowie die Oxydation des Phenylalanins und des Tyrosins[2].

Besonders bemerkenswert ist die Sauerstoff-Übertragung durch Ascorbinsäure (frei oder als Co-Enzym an ein Prolin gebunden) in solchen Geweben, welche arm sind am Cytochrom-Diaphorase-System, wie Glaskörper, Kammerwasser und Linse des normalen Auges sowie gewisse Organe canceröser Individuen.

Die Kurven IV und V zeigen, wie stark die — vermutlich katalytische — Wirkung von Ionen zweiwertigen Eisens in Gegenwart von Hydroperoxyd und besonders in Gegenwart von Hydroperoxyd und aci-Redukton I ist.

Was die vorstehenden Ergebnisse[3] für das Studium der Reduktone besonders wertvoll macht ist der Umstand, dass die beobachteten Viscositätsänderungen auf einen oxydativen Abbau des Pektins zurückzuführen sind und dass es sich also hier um Oxydationskatalysen handelt, worauf schon die Ergebnisse früherer Autoren hindeuten.

Zur weiteren Aufklärung der Rolle der Reduktone haben wir noch die folgenden Versuche unternommen.

Verbrauch der Ascorbinsäure in Gegenwart von Pektin und Hydroperoxyd

10 ml Pektinlösung (7,2 mg Trockensubstanz/ml) wurden mit 5 ml Ascorbinsäurelösung (2,5 mg/ml) und 5 ml H_2O_2-Lös. (2,5 mg/ml) versetzt. Die beiden letzteren Lösungen waren 0,2 mol. bez. Na_2HPO_4-Zitratpuffer. Somit betrug die Endkonzentration Pektin 3,6 mg + 0,625 mg Ascorbinsäure (0,0035 mol) +0,625 mg H_2O_2 per ml 0,1 m Puffer.

Während der Reaktion dieser Mischung bei 30°, pH 7, wurden von Zeit zu Zeit je 2 ml Lösung entnommen und mit 0,007-*n* TR-Lösung titriert. Kurve II, Figur 3.

Der entsprechende Versuch mit den gleichen Konzentrationen, aber ohne H_2O_2 ist in Kurve I dargestellt.

Als Nullprobe eines ev. Verbrauches von TR mit H_2O_2 werden Titrationen mit den gleichen Konzentrationen wie im ersten Versuch angestellt, aber *ohne Zusatz von Ascorbinsäure. Dabei ergab sich indessen kein Verbrauch von TR.*

Die Kurven zeigen, dass Ascorbinsäure in Abwesenheit von H_2O_2 nicht in praktisch messbaren Mengen verbraucht wird. Kurve I. (Frühere Versuche zeigten, dass die Viscosität des Pektins durch Ascorbinsäure allein nicht merkbar verändert wird.) (Vgl. S. 377.)

Kurve II zeigt, dass die Ascorbinsäure in Gegenwart von H_2O_2 schnell (50 % in 13 Minuten) verbraucht wird. Dabei sinkt die Viscosität des Pektins stark.

---

[1] R. LEMBERG, u. J. W. LEGGE, Ann. Rev. Biochem. 19, 431; 1950. — C. H. GRAY, The Bile Pigments. Methuen & Co., London 1953.

[2] Vrgl. hierzu B. N. LA DU u. D. M. GREENBERG, Science 117, 111; 1953. — D. M. GREENBERG, Chemical Pathway of Metabolism. II. Acad. Press Publ. 1954. — K. G. RIENITS, J. Biol. Chem. 182, 11 1950. — H. A. PAINTER and S. S. ZILVA, Biochem. J. 46, 542; 1950.

[3] Wir haben im Anschluss an obige Messungen auch die Viscosität von Ascites-Flüssigkeit, gewonnen aus Yoshida-Ascites-Tumorratten untersucht, um den Einfluss auf das im Ascites vorhandene Mucin kennenzulernen.

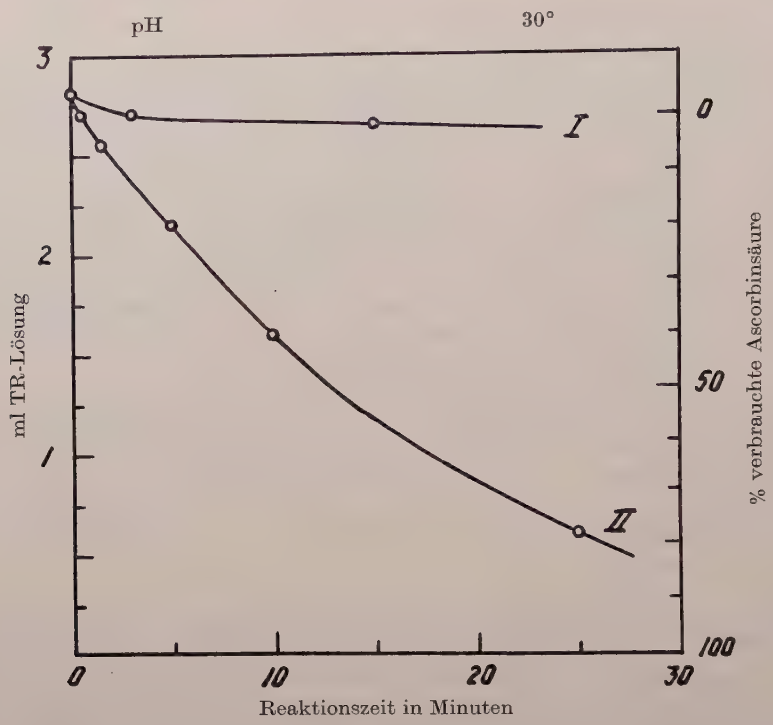

Fig. 3.

Es wurde untersucht, ob die im letztgenannten Versuch verbrauchte Ascorbinsäure die Bildung von Dehydro-ascorbinsäure veranlasst; dabei wurde in folgender Weise verfahren: Nach Einleiten von Stickstoff wurde die Lösung mit NaOH alkalisch gemacht und dann mit TR versetzt (die Dehydroascorbinsäure verbraucht in alkalischer Lösung die entsprechende Menge TR). Es wurde konstatiert, dass hier *kein Verbrauch von TR eintrat; somit ist hier bei der Oxydation von Ascorbinsäure keine Dehydroascorbinsäure entstanden.*

Frl. GUNHILD EDVARDSON danken wir für eifrige Mitarbeit bei den Viscositäts-Messungen.

Stockholm, Universität, Institut für organ.-chem. Forschung.

Tryckt den 7 maj 1955.

Uppsala 1955. Almqvist & Wiksells Boktryckeri AB

ARKIV FÖR KEMI Band 8 nr 38

Mitgeteilt am 24. November 1954 durch Hans von Euler

Isolierung von aci-Reduktonen und Derivaten derselben[1]

Von Hans Hasselquist

Mit 1 Figur im Text

In einer früheren Mitteilung über Reduktonanile[2] wurde ein Mono-benzoyl-redukton (dargestellt aus Redukton I nach Euler und Hasselquist[3]) beschrieben. Zur endgültigen Aufklärung seiner Struktur wurde dasselbe mit Mono-methylanilin umgesetzt. Dabei hat sich die so erhaltene Substanz identisch erwiesen mit der von Cocker[4] aus Monomethyl-anil-redukton-Na-Salz und Benzoylchlorid dargestellten (Schema S. 382). Dieser Versuch zeigt, dass der Benzoylrest im Monobenzoylredukton am C-Atom 2 sitzt.

In Zusammenhang mit dem Redukton-Na-Salz wurde auch untersucht, unter welchen Bedingungen Redukton I-Salze mit Schwermetallen entstehen.

Da die Dehydro-ascorbinsäure in saurer Lösung zu Dioxy-methyltetron (aci-Redukton III) gespalten wird, wurde versucht auch die anscheinend neuen Endiole zu isolieren, welche aus Dehydro-ascorbinsäure in *alkalischer Lösung* entstehen. Das Extinktions-Maximum jedes der beiden Endiole konnte erst gemessen werden, nachdem es gelungen war dieselben im Papierchromatogramm zu trennen und dieselben dann aus dem Papier zu extrahieren (siehe Versuch).

Die beiden aci-Reduktone zeigten die Extinktions-Maxima 260,0 mμ und 262,5 mμ.

Umsetzung von Mono-benzoylredukton I mit Mono-methylanilin

500 mg Mono-benzoylredukton (dargestellt nach Euler und Hasselquist, dieses Arkiv Band 3 nr 18 S. 140, 1951) wurden mit 10 ml Eisessig und 280 mg Mono-methylanilin bei Zimmertemperatur stehen gelassen und gingen unter Gelbfärbung in Lösung. Die Mischung wurde dann mit Wasser versetzt bis eine schwache Opaleszenz eintrat, und stand dann noch sechs Tage im Kälteschrank. Nach 4 Tagen fielen kleine gelbe Kristalle aus.

Durch Umkristallisieren aus wenig Äthylacetat erhielt man gelbe Prismen vom Schmpkt 151,5–152°.

Die Substanz war identisch mit dem von Cocker, O'Meara, Schwarz und Stuart aus Mono-methylanil-redukton-Na-Salz mit Benzoylchlorid (siehe Schema) dargestellten Anil. Dieser Versuch lässt vermuten, dass der Benzoyl-Rest im Mono-benzoyl-redukton am C-Atom 2 sitzt.

---

[1] 38. Mitteilung über Reduktone.

[2] H. Hasselquist, Arkiv f. Kemi Band 6 nr *37*, 1953, S. 381.

[3] H. von Euler und H. Hasselquist, Arkiv f. Kemi Band 3 nr 18, 1951, S. 140.

[4] W. Cocker, R. A. Q. O'Meara, J. C. P. Schwarz und E. R. Stuart, J. Chem. Soc. London 1950, 2052.

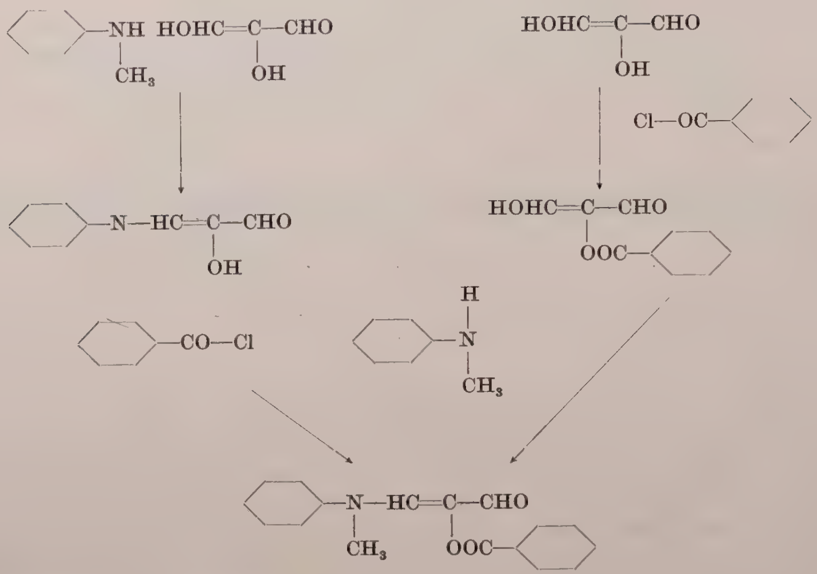

Cobalt-Salz des aci-Reduktons I

Durch Zusatz von Cobaltnitrat und gesättigter Natriumacetat-Lösung zur wässrigen Lösung des Reduktons I fiel nach einigen Minuten das Cobaltsalz des Reduktons als schwach rosa gefärbtes Pulver aus. Es wurde abgesaugt und mit Wasser, Aceton und schliesslich mit Äther gewaschen und im trocknen Zustand analysiert.

Analyse:

Für $C_3H_4O_4Co$ Berechnet: $C = 22{,}04\ \%$; $H = 2{,}47\ \%$; $CoO = 45{,}98\ \%$;
Gefunden: $21{,}95\ \%$ $2{,}78\ \%$ $47{,}63\ \%$.

Die Analyse zeigt, dass ein Ringschluss am Co-Sauerstoff nicht wahrscheinlich ist da die Hydrolyse an der OH-Gruppe am Kohlenstoff-Atom 2 gering zu sein scheint (eine Isolierung eines di-Na oder di-K Salzes des Reduktons gelang nicht, vielmehr konnte nur ein Mono-Salz in fester Form isoliert werden. Daraus folgt für das analysierte Salz die untenstehende offene Struktur.

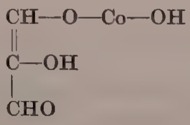

$$\begin{array}{l} \mathrm{CH{-}O{-}Co{-}OH} \\ \| \\ \mathrm{C{-}OH} \\ | \\ \mathrm{CHO} \end{array}$$

Barium-Salz des aci-Reduktons I

Bei der in gleicher Weise wie beim Cobalt-Salz ausgeführten Darstellung fiel das Barium-Salz in Form farbloser gut ausgebildeter Prismen aus, die nach mehrstündigem Stehen bei 20° aufs neue in Lösung gingen. Das Salz wurde nicht analysiert.

Bleisalz des aci-Reduktons I

Auf Grund der Analyse des Cobalt-Salzes wird man dem Blei-Salz die gleiche Struktur zuschreiben. Das Titrations-Äquivalent mit Tillmans-Reagenz ergab einen Wert, der zwischen einer Ringformel und einer offenen Formel lag. Letzterer Wert ist als der wahrscheinlichere anzunehmen.

Das Blei-Salz wurde dargestellt durch Mischung einer filtrierten wässrigen Lösung des Reduktons I und einer filtrierten Wasser-Lösung von $PbAc_2$ wobei eine gelblichweisse Fällung des Blei-Salzes erhalten wurde. Dieselbe wurde gewaschen und getrocknet.

Eingewogen: 44,4 mg $E_{\text{gef.}} = 151$
Eingewogen: 10,6 mg $E_{\text{gef.}} = 152$.

Messung der Extinktions-Maxima der aci-Reduktone IV ($R_f = 0{,}18$) und V ($R_f = 0{,}32$)

0,82 g Dehydro-ascorbinsäure, in 5 ml Wasser gelöst, wurde mit 2 g NaAc versetzt und auf dem Wasserbad auf 65° erwärmt. Nach Abschluss der CO_2-Entwicklung wurde die auf pH 6 angesäuerte Lösung chromatographiert. Anstatt Flecken wurde ein etwa 10 mm breites Band von 250 mm Länge als Ausgangslinie gesetzt.

Flüssigkeit: 4 Tle *n*-Butanol Papier: Munktell OB
1 Tl Eisessig
1 Tl Wasser

Sobald das Chromatogramm die Höhe von wenigstens 250 mm erreicht hat wurde das Papier bei 20° getrocknet, hierauf in 3 schmale Streifen zerschnitten, je einer an den beiden Seiten und einer in der Mitte des Chromatogrammes. Dieselben wurden mit einer alkoholischen Lösung von Tillmans-Reagenz entwickelt. Dabei konnte die Lage der aci-Reduktone im Chromatogramm bestimmt und jedes der beiden noch nicht entwickelten Chromatogramme einzeln ausgeschnitten werden.

Die betr. Papierstreifen, welche die Reduktone enthielten, wurden nun in sehr kleine Streifen zerschnitten und jeder mit 7 ml Wasser extrahiert und filtriert. Diese Lösungen wurden direkt zu den Extinktionsmessungen verwendet.

Man erhält eine geeignete Konzentration, wenn die Lösung mit $R_f = 0{,}18$ im Verhältnis 1 : 6 und die Lösung mit $R_f = 0{,}32$ im Verhältnis 1 : 3 verdünnt wird.

Versuche zur Isolierung der aci-Reduktone mit $R_f = 0{,}18$ und 0,32 aus der Alkali-behandelten Dehydro-ascorbinsäure

I. Behandlung in schwach-alkalischer Lösung

1,74 g Dehydro-ascorbinsäure, gelöst in 10 ml Wasser, wurden mit 4 g NaAc auf dem Wasserbad auf 65° erhitzt, wobei eine starke CO_2-Entwicklung eintrat. Dieselbe liess man bei Zimmertemperatur zum Abschluss kommen und versetzte die Lösung mit 3,8 ml konz. HCl und trocknete im Exsikkator über KOH. Nach Abdunsten des Wassers blieb ein gelbbraunes Öl zusammen mit Kochsalz-Kristallen zurück. Auf Zusatz von Aceton ging das Öl in Lösung. Ein Papierchromatographischer Versuch zeigte, dass die Aceton-Lösung den grössten Teil des Reduktons mit $R_f = 32$ enthielt. Die Aceton-Lösung wurde im Vacuum vollständig eingedunstet und das gelbbraune Öl war nun fast ganz vom Kochsalz befreit.

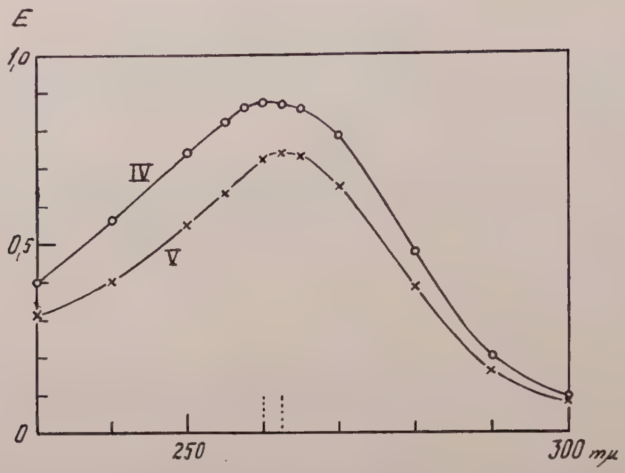

Fig. 1. Zusammenstellung der Extinktions-Maxima der aci-Reduktone

aci-Redukton	Maximum, mμ	pH
Ascorbinsäure	245,0	—
III (3,4-dioxy-5-methyltetron) . . .	257,5	5,5
IV (R_f = 0,18)	260,0	5,5
V (R_f = 0,32)	262,5	5,5
I	277,5	6,5
II	277,5	6,5

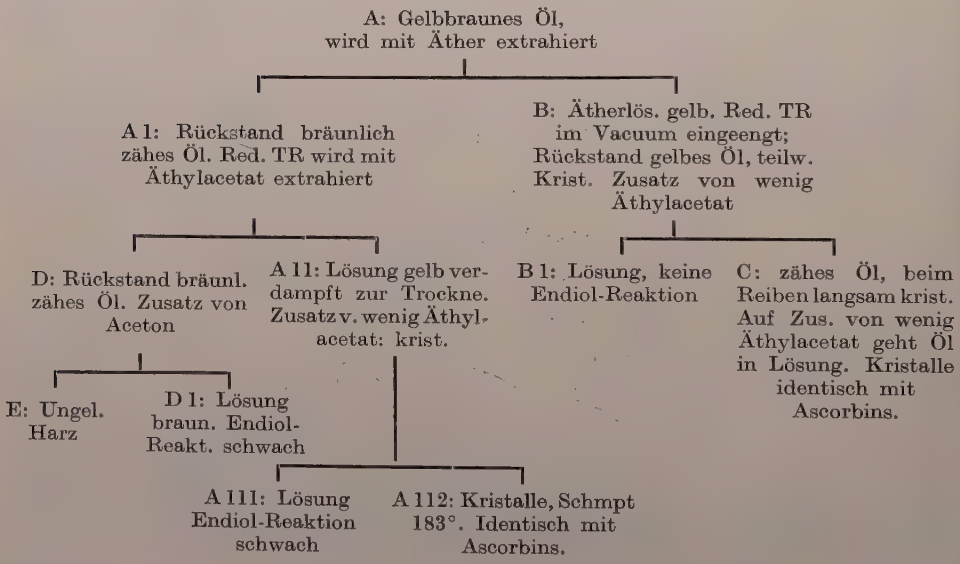

A: Gelbbraunes Öl, wird mit Äther extrahiert

A 1: Rückstand bräunlich zähes Öl. Red. TR wird mit Äthylacetat extrahiert

B: Ätherlös. gelb. Red. TR im Vacuum eingeengt; Rückstand gelbes Öl, teilw. Krist. Zusatz von wenig Äthylacetat

D: Rückstand bräunl. zähes Öl. Zusatz von Aceton

A 11: Lösung gelb verdampft zur Trockne. Zusatz v. wenig Äthylacetat: krist.

B 1: Lösung, keine Endiol-Reaktion

C: zähes Öl, beim Reiben langsam krist. Auf Zus. von wenig Äthylacetat geht Öl in Lösung. Kristalle identisch mit Ascorbins.

E: Ungel. Harz

D 1: Lösung braun. Endiol-Reakt. schwach

A 111: Lösung Endiol-Reaktion schwach

A 112: Kristalle, Schmpt 183°. Identisch mit Ascorbins.

Das Redukton mit $R_f = 0{,}32$ verschwand während der Fraktionierung. Möglicherweise hat dieses Redukton Ascorbinsäure zurückgebildet, die im Beginn der Fraktionierung nicht nachweisbar war (vgl. dieses Arkiv 7 nr 16, 1954).

II. Behandlung der Dehydro-ascorbinsäure in stärker alkalischer Lösung

1,74 g Dehydro-ascorbinsäure in 10 ml Wasser gelöst werden im Stickstoff-Strom mit 10 ml 2-*n* NaOH versetzt. Die Acidität war im Anfang pH = 10. Nach einer Minute langem Erhitzen auf dem Wasserbad fiel pH bis auf 7,5 und die Lösung wurde mit Essigsäure bis pH 7,0 versetzt. Die stark braun gefärbte Reaktions-Mischung wurde im Exsikkator über Kali eingedunstet; der Rückstand, ein braunes zähes Öl, wurde mit Methanol extrahiert. Diese Lösung zeigte keine Endiol-Reaktion.

Der Rückstand, nun ein festes hellbraunes Pulver, wurde durch Papier-Chromatographie untersucht und zeigte, dass ein Redukton mit $R_f = 0{,}18$ anwesend war. (Bei der Behandlung der Hydro-ascorbinsäure-Lösung mit Natriumacetat konnte ein Redukton mit $R_f = 0{,}32$ nachgewiesen werden; siehe S. 383.)

Das Redukton vom $R_f = 0{,}32$ war in Spuren anwesend und Ascorbinsäure wurde überhaupt nicht gefunden. Das hellbraune Pulver wurde in 10 ml Wasser gelöst und tropfenweise mit einer gesättigten Bariumacetat-Lösung versetzt, solange eine Fällung entstand. Hierauf wurde das Ganze filtriert, die Barium-Fällung mit Wasser nochmals gewaschen. Diese Barium-Fällung, und zwar eine grosse Menge, enthielt kein Endiol sondern nur grosse Mengen der Barium-Salze der Nebenprodukte der Reaktion, unter anderem Ba-oxalat. Das wässrige Filtrat, das nun eine schwach braune Farbe angenommen hatte, enthielt das Redukton mit $R_f = 0{,}18$. Die wässrige Lösung wurde aufs neue im Exsikkator bis auf ein geringes Volumen eingeengt. Durch Fällung mit Methanol entstand ein helles Pulver, welches das Endiol enthielt. Dieses Pulver erwies sich als hygroskopisch und ging an der Luft in eine dunkelbraune harte Masse über, welche immer noch die Endiol-Reaktion zeigte.

Darstellung des DL-3,4-dioxy-5-methyltetron nach MICHEEL[1] und HAARHOFF mit Redukton III aus Dehydro-ascorbinsäure identifiziert

I. Mono-chloressigsäure-benzoylester nach SEUBERT[2]. — 11 ml Benzylalkohol und 9,5 g Mono-chloressigsäure 15 Minuten von HCl-Gas durchströmt lassen zwei Schichten entstehen. Die Ester-Schicht wird im Scheidetrichter abgeschieden mit Wasser gewaschen, mit dem gleichen Volumen Benzol versetzt, getrocknet und im Vacuum destilliert. $\mathrm{Kp}_{30} = 152°$.

II. Benzoyl-glycolsäure-benzoylester. — 12 g des Mono-chloressigsäure-benzoylesters werden mit 10 g Natriumbenzoat + 1 g Natriumjodid + 60 ml Aceton im Rückfluss zwei Tage gekocht, nach Abfiltrieren des ungelösten Kochsalzes wird die Aceton-Lösung im Vacuum zur Trockne verdampft. Aus dem rückständigen Öl entstehende Kristalle werden aus Petroleum-Äther umkristallisiert und ergaben eine Ausbeute von 15 g in Form glänzender Blättchen vom Schmpkt 59–60°.

III. Darstellung des Benzoyl-milchsäure-äthylesters (FREUDENBERG, Ber. 57, 1552 (1924)). — 10 g Milchsäure-Äthylester + 9,9 ml Benzoylchlorid werden tropfenweise mit 7 ml Pyridin versetzt und reagieren unter starker Wärmeentwicklung. Nach 30 Minuten kristallisiert das Pyridinhydrochlorid aus. Nach Zusatz von überschüssigem Wasser ging das Pyridinhydrochlorid in der Wasserphase in Lösung. Die Esterphase wird zweimal mit Wasser gewaschen und im Vacuum destilliert. $Kp_{30} = 195°C$.

---

[1] F. MICHEEL u. H. HAARHOFF, Lieb. Ann. 545, 28 (1940).

[2] SEUBERT, Ber. 21, 282, 1888.

IV. Darstellung des Tetrons (Isolierung leicht modifiziert). — 10 g Benzoylglycolsäure-benzylester (II) und 8,3 g Benzoyl-milchsäure-äthylester (III) werden in 100 ml getrocknetem Benzol gelöst und unter strömendem N_2 mit 3,62 g Kalium vorsichtig auf 95° erwärmt. Wenn nach zwei Stunden alles Kalium in Lösung gegangen ist, werden 100 ml abs. Alkohol zugesetzt und wiederum drei Stunden gekocht, hierauf mit Eis gekühlt und eine berechnete Menge 2-*n* Schwefelsäure-Lösung zugesetzt. Im Scheidetrichter werden Benzol- und Alkohol-Wasser-Schicht getrennt, erstere mit Benzol ausgeschüttelt, wobei der nicht umgesetzte Ester in Lösung geht. Die das Tetron enthaltende Wasser-Schicht wird mit Äthylacetat dreimal ausgeschüttelt. Diese Lösung wird getrocknet und im Vacuum stark eingeengt. Das rückständige farblose Öl wird mit wenig Äther extrahiert und dieser im Vacuum verdampft. Hierbei entstehen farblose Kristalle des Tetrons, das in einer kleinen Menge Äthylacetat aufgeschlemmt und abfiltriert wird. Schmpkt = 176–177°.

Die Mischung dieses Produkts mit unserem aci-Redukton III aus Dehydro-ascorbinsäure ergab keine Depression.

Auch ein Chromatogramm zeigte die Identität des Tetrons mit unserem aci-Redukton III.

Stockholm, Universität, Institut för organ.-chemische Forschung.

Tryckt den 7 maj 1955

Uppsala 1955. Almqvist & Wiksells Boktryckeri AB

ARKIV FÖR KEMI Band 8 nr 39

Communicated 9 March 1955 by ARNE FREDGA

Thermal analysis of systems of some optically active diarylpropionic acids

By KURT PETTERSSON

With 8 figures in the text

Some years ago FREDGA proposed that a study of similarly constituted phenyl- and thienyl-substituted compounds should throw some light on the problem of aromaticity and the theory of optical activity (1). It was of interest, therefore, to study the diarylpropionic acids of the formulae (I)–(IV).

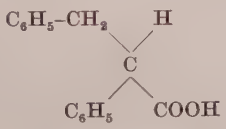

(I) α-Phenylhydro-cinnamic acid

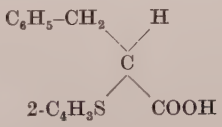

(II) α-(2-thienyl)-hydrocinnamic acid

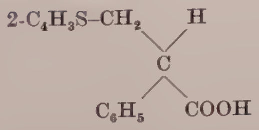

(III) 2-Thenylphenyl-acetic acid

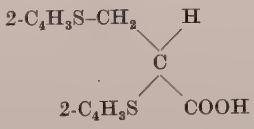

(IV) 2-Thenyl-2-thienyl-acetic acid

The acids were synthesized and resolved into optical antipodes and thermal analyses of eight of the sixteen possible two-component systems of the optically active acids were performed (2, 3). The results in these papers may be summarised as follows:

a) (+)- and (−)-(I) form a true racemate and show a pronounced tendency for racemate formation. The diagram is rather complex with three modifications of the inactive acid (3).

(+)- and (−)-(II) form a true racemate and show a moderate tendency for racemate formation (2).

(+)- and (−)-(III) form a true racemate and have a low tendency for racemate formation (2).

(+)- and (−)-(IV) form a solid solution with a melting-point maximum (pseudo-racemate) (3).

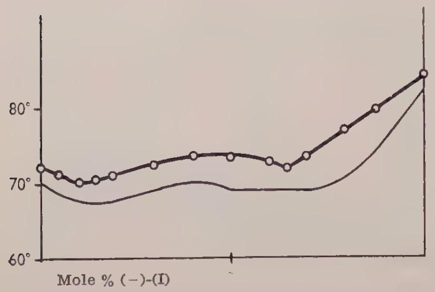

Fig. 1. (+)-(I) and (+)-(II).

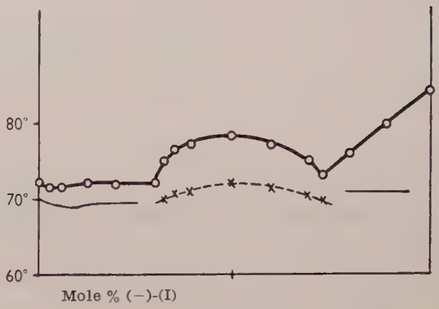

Fig. 2. (−)-(I) and (+)-(II).

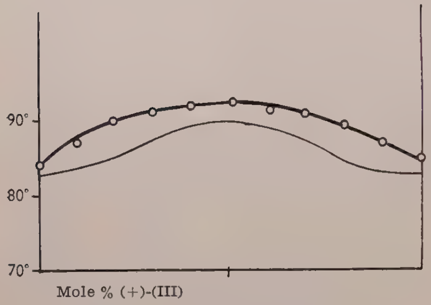

Fig. 3. (+)-(I) and (+)-(III).

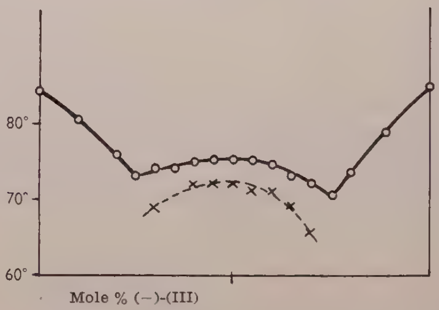

Fig. 4. (+)-(I) and (−)-(III).

b) The two diagrams obtained from the acids (I) and (IV) are of the usual eutectic type with an extended solubility of (IV) in (I) (3). The corresponding diagrams with the acids (II) and (III) are also of the eutectic type (2). In the diagrams mentioned in this paragraph there seems to be no quasi-racemate present.

The present paper deals with the remaining eight diagrams of the enantiomorphs of the acids (I)–(IV). Fig. 1 shows the diagram of the acids (I) and (II) with opposite direction of rotation. In the range between 0 % and about 60 % of (I) this diagram belongs to the rather rare type, consisting of a solid solution exhibiting a minimum at about 10 % as well as a maximum at about 50 %. This result is confirmed by a careful study of a contact preparation. The rest of the diagram is of the eutectic type with a moderate solubility of (II) in (I). For the question of configuration it is important to point out that the maximum at 50 % is to be considered as a pseudo-racemate and not as a molecular compound of the quasi-racemate type.

It has long been known that optically inactive α-phenylhydrocinnamic (benzylphenylacetic) acid is at least trimorphic (4). It is therefore interesting to note that the intermediary compounds formed with the optically active (I) and the oppositely rotating antipodes of (II) and (III) are also polymorphic (Figs. 2 and 4). At low concentrations of (−)-(I), the acids (+)-(II) and (−)-(I) form a solid solution with a minimum and, possibly, a maximum. At 50 % there is a dimorphic

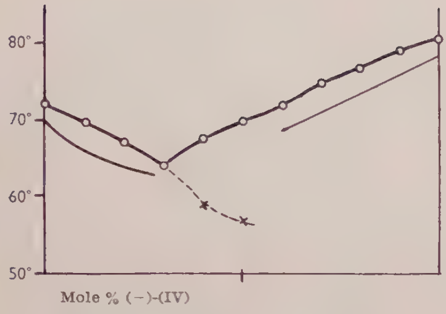

Fig. 5. (−)-(II) and (−)-(IV).

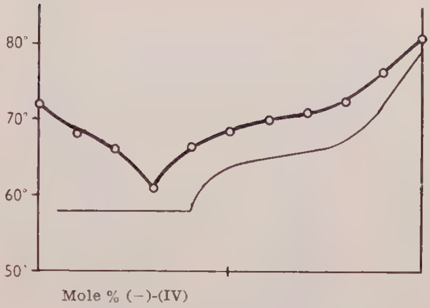

Fig. 6. (+)-(II) and (−)-(IV).

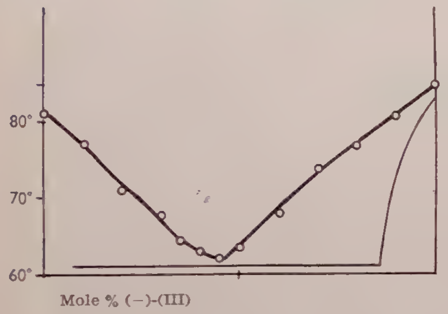

Fig. 7. (−)-(III) and (−)-(IV).

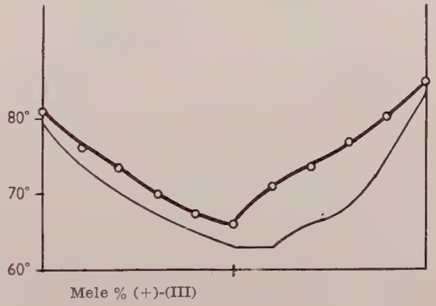

Fig. 8. (+)-(III) and (−)-(IV).

compound and at about 70 % of (−)-(I) a eutectic. A contact preparation clearly indicates that the lower branch of the curve in the centre of the diagram is to be distinctly kept apart from the left-hand one. Thus, there is a fundamental difference between diagrams 1 and 2, and the conclusion must be drawn that the intermediary compound in Fig. 2 is a quasi-racemate.

The enantiomorphs of the acids (I) and (III) with the same direction of rotation form a solid solution, extending through the whole diagram and with a melting-point maximum at 50 % (pseudo-racemate) (Fig. 3). The enantiomorphs with opposite direction of rotation form a dimorphic molecular compound which evidently must be a quasi-racemate (Fig. 4). It is noteworthy that in the region between 30 % and 60 % of (−)-(III) in Fig. 4 the lower melting points were obtained even after storage for more than two years. However, when melted at the lower melting points there remained traces of a solid residue which grew when the sample was allowed to crystallise and melt repeatedly at this temperature. During this process no racemisation occurs (2). The solid obtained in this manner melted at the higher melting points.

From Figs. 1–4 it appears that the enantiomorphs of the acid (I) form quasi-racemates with the oppositely rotating acids (II) and (III). It follows, then, that all of the three acids with the same direction of rotation have the same configuration. Unfortunately this could not be verified with the quasi-racemate method applied to the acids (II) and (III) (2).

Optically inactive (IV) is very likely a pseudo-racemate (3). Hence, the ability

Table 1. (+)-(I) and (+)-(II).

Mole % (+)-(I)	Melting point
0	71° –72°
4	68° –71°
10	67.5°–70°
14	67° –70.5°
19	67.5°–71°
30	69° –72.5°
40	70° –73.5°
50	69.5°–73°
59	69° –73°
65	69° –72.5°
70	69° –73.5°
79	70.5°–77°
87	73° –79°
100	82.5°–84°

Table 2. (–)-(I) and (+)-(II).

Mole % (–)-(I)	Melting point		
0	71°	–72°	
2.5	69.5°	–71.5°	
5	68.5°	–71.5°	
13	69°	–72°	
20	69°	–72°	
30	69°	–72°	
33		–75°	70°
35		–76.5°	70.5°
39		–77°	71°
49		–78°	72°
60		–77°	71.5°
70		–75°	70.5°
73		–73°	70°
80	71°	–76°	
89	71°	–79.5°	
100	82.5°	–84°	

Table 3. (+)-(I) and (+)-(III).

Mole % (+)-(III)	Melting point
0	82.5°–84°
10	84° –87°
20	85° –90°
30	87.5°–91°
40	89° –92°
51	89.5°–92.5°
61	88.5°–91.5°
70	87.5°–91°
80	84° –89.5°
90	83° –87°
100	83° –85°

Table 4. (+)-(I) and (–)-(III).

Mole % (–)-(III)	Melting point		
0	82.5°	–84°	
10	74°	–80.5°	
21	71°	–76°	
25	66°	–73°	
30		–74°	69°
36		–74°	
40		–75°	72°
45		–75.5°	72°
50		–75.5°	72°
56		–75.5°	71°
60		–74.5°	71°
65		–73°	69°
70		–72°	66°
76		–71°	
80	68°	–73.5°	
90	68°	–79°	
100	83°	–85°	

of the enantiomorphs to form racemates (true molecular compounds) must be questioned. No indications of quasi-racemate formation could be found either between (I) and (IV) (3), (II) and (IV), or (III) and (IV) (Figs. 5–8). There are, however, in all of the diagrams mentioned broad regions of solid solubility, but no information of the configuration of (IV) could be obtained with this method. The dashed branch of the curve in Fig. 5 seems to indicate a second modification of (–)-(IV), but verification of this by other means has not been possible.

The ability of a pair of enantiomorphs to form a racemate is indicated by the height of the part of the melting-point curve constituting the molecular compound.

Table 5. (–)-(II) and (–)-(IV).

Mole % (–)-(VI)	Melting point
0	71° –72°
10	66° –69.5°
20	63.5°–67°
30	62.5°–64°
40	–67.5° 59°
50	–70° 57°
60	69° –72°
70	71.5°–75°
80	74° –77°
90	76° –79.5°
100	79° –81°

Table 6. (+)-(II) and (–)-(IV).

Mole % (–)-(IV)	Melting point
0	71°–72°
10	58°–68°
20	58°–66°
30	58°–61°
40	58°–66.5°
50	64°–68.5°
60	65°–70°
70	66°–71°
80	67°–72.5°
90	72°–76.5°
100	79°–81°

Table 7. (–)-(III) and (–)-(IV).

Mole % (–)-(III)	Melting point
0	79° –81°
10	62° –77°
20	62° –71°
30	62° –68°
35	62° –64.5°
40	61.5°–63°
45	61° –62°
50	61° –63.5°
60	62° –68°
70	62° –74°
80	62° –77°
90	74° –81°
100	83° –85°

Table 8. (+)-(III) and (–)-(IV).

Mole % (+)-(III)	Melting point
0	79°–81°
10	74°–76°
20	70°–73.5°
30	67°–70°
40	65°–67.5°
50	63°–66°
60	63°–71°
70	66°–73.5°
80	68°–77°
90	75°–80.5°
100	83°–85°

This ability then decreases from (I) to (III) and is probably absent in (IV). It is noteworthy that the quasi-racemates in Figs. 2 and 3 follow the same order and that no quasi-racemate with (IV) could be found. This seems to indicate that the 2-thienyl group has a definitely lower tendency for quasi-racemate formation than has the phenyl group. The data are, however, too limited to allow this to be taken as a general conclusion. Because of the peculiar behaviour of optically inactive (IV) as a pseudo-racemate, the influence of structural differences cannot be elucidated. It seems probable, that a double replacement of a phenyl group for a 2-thienyl group (as between (I) and (IV) and between (II) and (III)) greatly reduces the possibility of quasi-racemate formation.

The quasi-racemate method has failed to give information about the configuration of (IV) as compared to the other three acids, but the optical activities, measured in representative solvents, offer a good foundation for the conclusion that the enantiomorphs of all four acids with the same direction of rotation have also the same configuration. Attempts to correlate the acids with D-glyceraldehyde are in progress.

Experimental

Samples for melting-point determinations: Weighed amounts of the optically active acids (total weight 10 mg) were dissolved in a few drops of acetone ("AnalaR" standards for laboratory chemicals). The solvent was removed and the residue carefully powdered and dried in a desiccator. The melting points were determined in a Kofler hot-stage microscope.

Summary

Eight of the sixteen possible two-component systems between the enantiomorphs of α-phenylhydrocinnamic acid (I), α-(2-thienyl)-hydrocinnamic acid (II), 2-thenylphenylacetic acid (III) and 2-thenyl-2-thienylacetic acid (IV) have been thermally analysed in a Kofler hot-stage microscope. From the occurrence of quasi-racemates it has been concluded that the acids (I)–(III) with the same direction of rotation have the same configuration. Among the compounds under discussion the 2-thiophene compounds have a markedly lower tendency for racemate formation than the phenyl analogs.

The author wishes to express his thanks to Professor ARNE FREDGA for valuable discussions and to Miss GUDRUN WILLDECK for preparing some of the melting-point samples. Thanks are also due to Messrs. PHARMACIA LTD., who kindly placed their Kofler microscope at the author's disposal.

Part of the expenses have been defrayed by a grant from the Nobel Fund of the Royal Swedish Academy of Science (*Kemiska prisgruppens särskilda fond*).

REFERENCES

1. FREDGA, A. and PALM, O., Arkiv Kemi, Mineral. Geol. *26 A*, nr 26 (1949).
2. PETTERSSON, K., Arkiv Kemi *7*, 279 (1954).
3. PETTERSSON, K., Arkiv Kemi *7*, 339 (1954).
4. v. MILLER, W. and ROHDE, G., Ber. *28*, 818 (1895).

Tryckt den 7 maj 1955

Uppsala 1955. Almqvist & Wiksells Boktryckeri AB

ARKIV FÖR KEMI Band 8 nr 40

Read 23 February 1955

Inhibition of yeast invertase (saccharase) by metal ions

II. Action of Ag^+, Cu^{++}, Cd^{++}, Zn^{++} ions and their complex formation with acetate ions

By Karl Myrbäck

With 1 figure in the text

The inhibition of many enzymes with heavy metal ions is reversible, e.g. by addition of hydrogen sulphide, and is regarded as being due to the formation of more or less dissociated, enzymatically inactive metal salts of the enzymes. In the case of yeast saccharase it could be shown (1) that the inactivation of the enzyme by several metal ions (Ag^+, Cu^{++}, Cd^{++}, Zn^{++}, Pb^{++}) is strongly dependent on the pH of the reaction mixtures. The inhibition-pH-curves obtained for constant metal ion concentration and variation of pH were found to be roughly parallel to the alkaline branch of the activity-pH-curve of the enzyme, indicating that the formation of the metal salt involves an acid group of the enzyme molecule, essential for the enzymatic activity. The experimental results are in agreement with the theory originally proposed by Hudson (2) and Michaelis (3) that yeast saccharase is an ampholyte and, particularly, that the alkaline branch of the activity-pH-curve is the dissociation curve of an acid group with $K_A \sim 10^{-6.6}$, the group which is believed to react with the metal ions. The idea that the uncharged state of this group, i.e. the presence of the proton, is required for the enzymatic activity, is also in agreement with the views expressed by Koshland (4) on the mechanism of hydrolase action (5). The metal ion inactivation of yeast saccharase is completely reversible and non-competitive which is in agreement with the fact that the alkaline branch of the activity-pH-curve of saccharase is independent of the substrate concentration (1).

If, in an experiment at the hydrogen ion concentration $[H^+]$, the metal ion concentration is called $[M^+]$ and the concentration of the enzyme metal salt is [EM], then the dissociation constant of the metal salt is

$$K_{\text{Met}} = 10^{-6.6} \cdot \frac{([M^+]-[ME])}{[H^+]} \quad \frac{[HE]}{[ME]} \tag{1}$$

where [HE] is the concentration of the active enzyme molecules, i.e. proportional to the reaction velocity actually found, v_{Met}. If the reaction velocity in an experiment at the same pH without metal ion is v_0, then [ME] is proportional to $v_0 - v_{\text{Met}}$. If the total metal ion concentration $[M^+]$ is not extremely small [ME] is negligible compared to $[M^+]$ and the formula simplifies to

$$K_{\mathrm{Met}} = 10^{-6.6} \cdot \frac{[\mathrm{M}^{+}] \cdot v_{\mathrm{Met}}}{[\mathrm{H}^{+}] \cdot (v_0 - v_{\mathrm{Met}})} \cdot \qquad (2)$$

Since $[\mathrm{M}^+]$ generally must be much greater than the enzyme concentration and consequently much greater than [ME] the calculation of K_{Met} appears to be extremely simple. However, that is so only if $[\mathrm{M}^+]$, i.e. the concentration of the metal ion, is either practically equal to the concentration directly derived from the amount of added metal salt, or can be calculated therefrom in some way. It seems that in many instances "inhibition constants" or enzyme-inhibitor dissociation constants have been calculated without regard to the fact that in experiments of this kind the actual concentration of free metal ion $[\mathrm{M}^+]$ may be very far from the value directly derived from the amount of added metal salt. Even disregarding the fact that metal-binding impurities in enzyme preparations may tend to lower the $[\mathrm{M}^+]$ value, it must be emphasized that many of the usual buffer mixtures used in enzyme experiments may have a profound influence on $[\mathrm{M}^+]$. An example was given in an earlier paper (6): In buffer-free solution uranyl salts cause a strong inhibition of yeast saccharase whereas a 100-fold amount of uranyl salt has no action at all if tested in an acetate buffer of normal type and concentration. This phenomenon is obviously due to the formation of uranyl-acetate complexes without any inhibiting action on the enzyme.

Since most of the metal ions of interest in connexion with enzyme work are more or less strongly complexed by usual buffer substances, substrates etc., it is not always so very easy to obtain a tolerably accurate value of the inhibiting power of the metal ion. It is often impossible or difficult to find an otherwise suitable buffer which does not form complexes with the metal ion in question. It is a matter of course that buffers and other substances must be avoided which are known to give *insoluble* compounds with the metal ion; experiments on the inhibition of saccharase or other enzymes by the Ag^+ ion in a solution containing Cl^- ions are of course meaningless. But it may well be that the use of buffers etc. which do not precipitate silver ions nevertheless lead to erroneous results if soluble silver complexes are formed. From experiments recorded in the following it appears, e.g., that even the use of such a harmless buffer as sodium acetate–acetic acid may lead to absurd results concerning the metal inhibition of saccharase if the complex formation between metal ion and acetate ions is disregarded. Similar conditions exist in the case of other enzymes, and the possible errors may be even greater with most other buffers than acetate–acetic acid.

Experimental

Enzyme preparation. The preparation of the yeast saccharase solution used in the following experiments has been described earlier (6). The activity of the solution was *If* = 20 (concerning definition of *If*, cf. Ref. 1), dry weight 1.6 mg/ml. As usual considerable amounts of polysaccharide were present; determination with the anthrone reagent showed a carbohydrate content ~ 80 per cent. The enzyme solution was freed from low-molecular impurities by thorough dialysis.

Acetate buffers. A number of buffer solutions were prepared by mixing a solution of sodium acetate (2 *N*) with varying amounts of acetic acid. pH of the mixtures was determined using the glass electrode. The pH of every individual assay mixture was furthermore determined. The concentrations of buffer mentioned in the following are the concentrations of the acetate ion. The free acetic acid is known to have little or no influence on the complexing action of the acetate ion.

Table 1. Inactivation of various yeast saccharase preparations by Ag^+ ions.

pH	Ag^+ added	Relative activity		
		$If = 20$	$If = 200$	$If = 17$
4.5	—	100	100	100
4.5	10^{-5} *N*	38	36	30
5.4	—	92	92	93
5.4	5×10^{-7}	62	70	76
5.4	10^{-6}	24	40	50
5.4	3×10^{-6}	11	13	12
5.4	10^{-5}	8	< 5	< 5
5.9	—	80	80	82
5.9	5×10^{-7}	63	52	55
5.9	10^{-6}	26	18	22

Assay. 4.75 g saccharose was dissolved in 95 ml water containing the desired amount of buffer. The mixture was temperated at 30° and 5 ml saccharase solution was added. 10 ml samples were taken after suitable reaction times and mixed with 10 ml *N* sodium carbonate solution whereby the reaction was stopped and the mutarotation of the reaction products immediately abolished. The rotation was determined in 2 dm tubes (sodium light). If the rotation is plotted versus reaction time a practically straight line is obtained for at least the first 30 per cent of the reaction. The decrease of rotation per minute can therefore be regarded as a correct expression for the initial reaction rate.

All values of relative activity of the enzyme are expressed as per cent of the activity without inhibitor at the pH optimum (pH = 4.5).

Results

a) *Inhibition by the Ag^+ ion*

It must be expected that, in impure enzyme solutions, Ag-binding contaminants lower the concentration of Ag^+ and simulate a too low sensitivity of the enzyme towards the inhibitor. This has been found to be the case with very impure yeast saccharase solutions, e.g. raw yeast autolysates (7). However, it seems that after a rather superficial purification of yeast saccharase the inhibition by Ag^+ at a certain pH is almost independent of the degree of purity of the enzyme preparation (1). Obviously this does not necessarily mean that the enzyme is the only component of the preparations which is able to combine with silver ions. Since the chief contaminants of most saccharase preparations are polysaccharides it may be that the Ag-binding substances in the preparations are much the same irrespective of the activity per dry weight. Nevertheless it seems remarkable that the degree of purity of the enzyme preparations plays such a small role for the inactivation by Ag^+ ions. The preparation used in the following experiments had been purified in quite another way than those investigated earlier and should be expected to contain different contaminants.

In table 1 determinations of the inhibition of this saccharase preparation ($If = 20$) are compared with corresponding figures from earlier investigations ($If = 200$, cf. Ref. 1; $If = 17$, cf. Ref. 7). Strictly speaking the figures are not exactly comparable as the concentration of sodium acetate buffer varied a little in the different series. However, since $[Ac^-]$ varied only between 0.04 and 0.08 and the Ag-complexing

Table 2. Action of silver ion in sodium acetate buffer of varying concentration.

Ag^+ added	Acetate N	Relative activity	
		found	corr.
—	0.0038	74	74
—	0.038	73	74
—	0.38	65	74
10^{-6} N	0.0038	20	20
10^{-6} N	0.038	24	25
10^{-6} N	0.38	39	45

power of acetate is rather weak (see below), the errors introduced by the varying acetate concentrations are quite small, and thus it appears from Table 1 that the sensitivity of the three saccharase solutions with widely different activity is practically the same.

The influence of acetate concentration on the inhibition was studied in a series of experiments at pH = 5.96 (Table 2). Since a strong solution of sodium acetate itself causes a slight decrease of the enzymatic activity, a correction for this has to be introduced. (The inhibiting action of sodium acetate varies strongly with pH; the inhibition-pH-curve is parallel to the alkaline branch of the activity-pH-curve of the enzyme (7).) It is seen from Table 2 that the inhibiting action of 10^{-6} N $AgNO_3$ diminishes with increasing concentration of sodium acetate. As will be shown here the explanation is that part of the Ag^+ ions are complexed by the acetate ions.

Fig. 1 shows the dependence of the relative activity upon Ag^+ concentration at pH = 5.96 and 0.0038 N sodium acetate (activity without Ag^+ at pH optimum put = 100). The curve shows that a relative activity of 45 (Table 2) corresponds to an Ag^+ concentration of ca. 4×10^{-7}. Since the added amount of $AgNO_3$ corresponded to 10^{-6} N it is concluded that in 0.38 N sodium acetate about 40 per cent of the Ag ion is free, i.e. not present in acetate complexes.

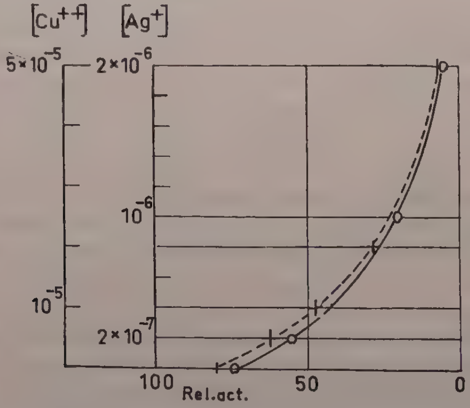

Fig. 1. Dependence of saccharase activity upon metal ion concentration.
+----------+ Cu^{++}: ○——○ Ag^+

Table 3. Concentration of free metal ion in acetate buffers.

Acetate N	Relative concentration of free metal ion				
	Ag^+		Cu^{++}		Cd^{++}
	LEDEN (8)	MACDOUGAL & PETERSEN (9)	FRONAEUS (10)	PEDERSEN (11)	LEDEN (8)
0.0038	99.7	98.1	84.5	67	92.9
0.038	91.7	82.7	28.7	21	49.5
0.38	47.5	27.7	0.7	< 1	1.7

The complex formation between Ag^+ and acetate ions has been determined by LEDEN (8). At 25° in 3 M perchlorate the following complexity constants were found: $\beta_1 = 2.36$ l/mole; $\beta_2 = 1.47$ (l/mole)^2; $\beta_3 = 0.33$ (l/mole)^3. From these values the concentration of free Ag^+ ion at the acetate concentrations of our experiments have been calculated (Table 3). The values are perhaps not directly applicable to our experiments which were performed at a much lower ionic strength. Nevertheless the agreement between the relative concentration of free Ag^+ ion in 0.38 N sodium acetate calculated from Leden's values (47.5 per cent) and our value (ca. 40 per cent) is satisfactory.

The complexing action of acetate on the Ag^+ ion has been studied also by MAC DOUGAL and PETERSON (9) in experiments, perhaps somewhat more comparable to ours. The authors find the following values for the two first complexity constants: $\beta_1 = 5.38$ l/mole; $\beta_2 = 4.35$ (l/mole)^2. The relative concentrations of free Ag^+ ion, calculated from these values are found in Table 3. The agreement between the value for 0.38 N acetate (27.2 per cent) and our value (ca. 40 per cent) is less satisfactory. On the other hand our values can obviously only be regarded as approximate. In any case it seems quite clear that the "protecting" action of sodium acetate upon saccharase against silver poisoning is caused by the formation of silver-acetate complexes.

b) Inhibition by the Cu^{++} ion

The inhibition of saccharase by cupric ions was studied earlier (1) in acetate buffer. Compared to Ag^+ the cupric ion was found to have a comparatively weak action. The apparent dissociation constant of the saccharase-Cu salt was found to be $K_{Cu} = 2.6 \times 10^{-4}$($K_{Ag} = 10^{\;7.4}$, calculated in the same way). Since the cupric ion has been shown to be strongly complexed by acetate ions it can be concluded that the actual copper ion concentration in the inhibition experiments was considerably lower than calculated from the amount of added copper salt and, consequently, that the value of K_{Cu} must be lower than the above value. A series of new experiments at pH = 5.96 are recorded in Table 4. It is seen from this table that a Cu^{++} concentration which causes practically complete inactivation of the enzyme in 0.0038 N acetate has only a very slight action in 0.38 N acetate. Since the relative activity depends on Cu^{++} concentration as shown in Fig. 1 it should be concluded that the relative amount of free Cu^{++} ion in 0.038 N acetate is about 20 per cent and in 0.38 per cent acetate less than 5 per cent.

The complexing of the Cu^{++} ion by acetate has been determined by FRONÆUS (10). The following constants were found in 1 M perchlorate: $\beta_1 = 47$ l/mole; $\beta_2 =$

Table 4. Inhibition of saccharase by Cu^{++}.

Cu^{++} added	Acetate *N*	Relative activity	
		found	corr.
—	0.0038	80	80
—	0.38	72	80
5×10^{-5}	0.0038	6	6
5×10^{-5}	0.038	40	42
5×10^{-5}	0.38	68	76

Table 5. Inhibition of saccharase by Cd^{++}.

Cd^{++} added	Acetate *N*	Relative activity	
		found	corr.
—	0.0038	85	85
—	0.38	76	85
1.1×10^{-4}	—	14	14
1.1×10^{-4}	0.038	33	35
1.1×10^{-4}	0.38	65	78

450 (l/mole)^2; $\beta_3 = 1150$ (l/mole)^3; $\beta_4 = 750$ (l/mole)^4. From these values the relative concentrations of Cu^{++} in our acetate buffers have been calculated (Table 3). For a 0.038 *N* acetate buffer we have estimated the relative value of [Cu^{++}] to be about 20 per cent while the calculation from Frohnæus' values gives 28.7 per cent. Considering the moderate accuracy of our value the agreement is satisfactory, and it is quite clear that determination of the inhibiting power of the Cu^{++} ion in acetate buffer, even of relatively low concentration, may lead to erroneous values due to the strong complexing action of the acetate ions.

PEDERSEN (11) has determined the complex formation in solutions of sodium acetate containing a small amount of cupric nitrate. A few values for the relative Cu^{++} ion concentration in acetate buffers, calculated from Pedersen's determinations, are included in Table 3. The agreement between these values and ours is satisfactory.

c) *Inhibition by the Cd^{++} ion*

In earlier determinations of the inhibitory action of the Cd^{++} ion on saccharase in acetate buffer (1) it was found that the inhibitory power of this ion is comparable to that of the Cu^{++} ion ($K_{Cd} = 5.7 \times 10^{-5}$). Since the Cd^{++} ion is complexed by acetate it could be expected that the inhibitory action would be considerably greater than calculated from the experiments. New determinations in Table 5; pH = 5.75. Acetate appears to have a strong "protecting" action.

From the inhibition curve it can be calculated that the relative concentration of free Cd^{++} in 0.38 *N* acetate is less than 4 per cent of the added cadmium salt concentration.

Table 6. Inhibition of saccharase by Zn^{++}.

Zn^{++} added	Acetate	Relative activity	
		found	corr.
	0.0038	80	80
—	0.38	72	80
3.5×10^{-4}	0.0038	44	44
3.5×10^{-4}	0.038	60	62
3.5×10^{-4}	0.38	66	74

LEDEN (8) has determined the complex formation between the Cd^{++} ion and acetate ions (in 3 M perchlorate). The complexity constants were found to be: $\beta_1 = 20$ l/mole; $\beta_2 = 190$ (l/mole)^2; $\beta_3 = 260$ (l/mole)^3; $\beta_4 = 100$ (l/mole)^4. The relative concentrations of free Cd^{++} ion in our acetate buffers has been calculated from these figures (Table 3). Since in 0.38 N acetate only about 2 per cent of the Cd is present as free Cd^{++} ion this agrees reasonably well with the figure derived from the saccharase inhibition experiments.

d) Inhibition by the Zn^{++} ion

Earlier experiments in acetate buffer (1) had shown about the same inhibitory power of the Zn^{++} ion as that of Cu^{++} or Cd^{++}. New experiments at different acetate concentrations have been carried out (Table 6); pH = 5.90. From these experiments it can be concluded that in 0.38 N acetate less than 20 per cent of the metal is present as free Zn^{++} ions.

SUMMARY

The inhibition of yeast saccharase by certain metal ions in sodium acetate buffers has been determined. Sodium acetate has a more or less pronounced "protecting" action against the metal inhibition. This is due to the formation of acetate complexes of the metal ions. Only the free metal ions, Ag^{+}, Cu^{++} etc. are active as inhibitors, i.e. they form slightly dissociated salts with the acid group of the saccharase molecule responsible for the alkaline branch of the activity-pH-curve of the enzyme. The acetate complexes of the metal ions do not combine with the enzyme and thus have no inhibitory action.

The inhibition experiments allow a rough calculation of the relative concentrations of the free metal ions, i.e. the degree of complex formation with the acetate ions. The figures obtained in this way are in good agreement with the (obviously more accurate) values obtained by other authors on the basis of emf titrations.

The possibility of complex formation between inhibitors and buffer ions must be considered in all experiments on enzyme inhibition. Even moderate concentrations of buffers, otherwise regarded as quite harmless, may profoundly alter the concentration of the inhibiting ion.

Approximate values of the dissociation constants of the enzyme metal salts may be calculated according to formula (2): $K_{\text{Ag}} = 9 \times 10^{-8}$; $K_{\text{Cu}} = 10^{-6}$; $K_{\text{Cd}} = 3 \times 10^{-6}$; $K_{\text{Zn}} = 8 \times 10^{-5}$.

The experimental part of this investigation has been carried out by Mrs. EBBA WILLSTAEDT whose assistance is gratefully acknowledged.

Institute for Organic Chemistry and Biochemistry, University, Stockholm.

REFERENCES

1. MYRBÄCK, K., Hoppe Seylers Z. physiol. Chem. *158*, 160 (1926).
2. HUDSON, C. S., J. Am. Chem. Soc. *32*, 1220 (1910).
3. MICHAELIS, L. and DAVIDSOHN, H., Biochem Z. *35*, 386 (1911); MICHAELIS, L. and ROTHSTEIN. M., Ibid. *110*, 217 (1920).
4. KOSHLAND, JR. D. E., Biol. Revs. *28*, 416 (1953); KOSHLAND, JR. and STEIN, S. S., J. Biol. Chem. *208*, 139 (1945).
5. MYRBÄCK, K., Ann. Acad. Sci. Fennicae., Ser. A. II. *No. 60*, 226 (1955).
6. MYRBÄCK, K. and WILLSTAEDT, E., Arkiv Kemi *7* (1955). In press.
7. MYRBÄCK, K., Arkiv Kemi, Mineral. Geol. *8*, No. 29 (1923).
8. LEDEN, I., Svensk Kem. Tidskr. *58*, 129 (1946).
9. MACDOUGAL, F. H. and PETERSON, S., J. Phys. & Colloid Chem. *51*, 1346 (1947).
10. FRONÆUS, S., Komplexsystemen hos kopper, Thesis, Lund 1948.
11. PEDERSEN, K. J., Kgl. Danske Videnskab. Selskab, Mat.-Fys. Medd. *22*, No. 12 (1945).

Tryckt den 2 juni 1955

Uppsala 1955. Almqvist & Wiksells Boktryckeri AB

ARKIV FÖR KEMI Band 8 nr 41

Communicated 1 December 1954 by ARNE FREDGA and GUNNAR HÄGG

Optically active higher aliphatic hydroxy-compounds

II. The synthesis of (+)- and (−)-2-Tetracosanol

By KLAUS SERCK-HANSSEN

The synthesis of (+)- and (−)-2-eicosanol was described in Part I (1). The essential steps were the resolution of β-acetoxybutyric acid and the lengthening of the carbon chain of the antipodes by anodic coupling with stearic acid.

By using other carboxylic acids, RCOOH, in the place of stearic acid, a great variety of optically active hydroxy-compounds of the general formula $CH_3CHOHCH_2R$ may be prepared. The main restrictions to the generality of the method are the inability of some carboxylic acids to undergo normal anodic coupling (2, 3), and technical difficulties during the electrolysis or the separation of the desired compound from the reaction mixture.

The normal 2-hydroxyalkanes from C_4 to C_{13} were resolved by PICKARD and KENYON (4, 5) through alkaloid salts of acid esters of the alcohols. This very fruitful method (6) failed however when applied to the homologous alcohols with 15 and 17 carbon atoms (7, 8). The present method is an alternative to resolution methods.

The 2-tetracosanols described in this communication were needed for monolayer studies. As outlined in Chart I, they were synthesized in the same way as the 2-eicosanols (1) by using behenic acid instead of stearic acid in the KOLBE electrosynthesis. By slightly modifying the resolution procedure, the antipodes of β-acetoxybutyric acid were obtained in higher yields than given in (1).

Table 1 gives the physical constants determined for racemic and optically active 2-tetracosanols and the corresponding acetates and acid phthalates.

Melting points and crystal spacings

All the compounds are polymorphic. So were the 2-eicosanols and corresponding derivatives described in (1). Except for the acetates, the melting points of corresponding antipodes are practically identical. The dextrorotatory acetate is considered to be purer than the antipode, because it crystallizes better. The fact that its low melting point is the same as for the racemic form supports this view. The coincidence of the lowest melting points for racemic and optically active forms was observed in the 2-eicosanols and their acetates and acid phthalates (1). The same phenomenon is observed again in the 2-tetracosanols but not in their acid phthalates. The lowest melting points of the latter are therefore given with reservation, especially as they are somewhat diffuse.

Table 1. Thermal, X-ray, and optical rotation data for 2-tetracosanols and derivatives.[1]

2-Tetracosanols					Acid phthalates			Acetates		
Racemic		+		−	+	−	Racemic	+	−	Racemic
M.p. °C	Long spacing	M.p. °C	Long spacing	M.p. °C	M.p. °C	M.p. °C	M.p. °C	M.p. °C	M.p. °C	M.p. °C
70.9–71.1 (70.5) 62.7–62.9	55.0 Å 29.2 Å	71.8–72.0 70.8–71.0 62.8–63.0	31.1 Å 40.4 Å 29.2 Å	71.6–71.8 70.8–71.0 62.9–63.1	69.0–69.4 66.1–66.4 (47.2–48.3)	69.0–69.5 66.0–66.3 (47.4–48.3)	71.3–71.5 46.3–46.9	47.6–47.8 42.6–42.8	(46.6–46.8) 42.3–42.5	44.7–44.9 42.6–42.8

	λ in Å	$c = 3.85,\ l = 2$		$c = 7.94,\ l = 2$		$c = 5.00,\ l = 1$		$c = 1.70,\ l = 1$	
		$[M]_{\lambda}^{23}$	$[\alpha]_{\lambda}^{23}$	$[\alpha]_{\lambda}^{22}$	$[M]_{\lambda}^{22}$	$[M]_{\lambda}^{21}$	$[\alpha]_{\lambda}^{21}$	$[\alpha]_{\lambda}^{24}$	$[M]_{\lambda}^{24}$
Optical rotations in chloroform	5893	11° ± 1	3.2° ± 0.3	2.9° ± 0.1	10.3° ± 0.4	122° ± 1	24.2° ± 0.4	23.5° ± 1.2	118° ± 6
	5461	13 ,,	3.6 ,,	3.5 ,,	12.5 ,,				
	4358	19 ,,	5.5 ,,	5.6 ,,	19.9 ,,				
	4047	22 ,,	6.3 ,,	6.2 ,,	21.9 ,,				
	3650	27 ,,	7.7 ,,	7.6 ,,	27.1 ,,				

Position and visually estimated form and intensity of strong $h\,k\,l$ reflections ("side spacings") from 2-tetracosanols

Racemic	M.p. 71°
	,, 63°
Optically active	,, 72°
	,, 71°
	,, 63°

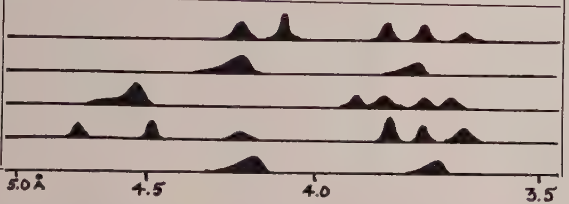

---

[1] The melting points recorded in this paper were determined in carefully cleaned capillary tubes using calibrated ANSCHÜTZ thermometers completely immersed in a well-stirred bath of liquid paraffin. A very low rate of heating was used near the melting point. Crystal spacings were measured by means of nickel-filtered Cu K$_\alpha$ radiation. The diffraction patterns were recorded on a flat film at a distance of 100 mm.

The optical rotations recorded in this table were measured with a photoelectric, ultraviolet polarimeter of the BRUHAT-GUINIER type (cf. Revue d'Optique *12*, 396 (1933)).

The polymorphism of the 2-tetracosanols is confirmed by the X-ray analysis. The low-melting forms have identical long spacings of 29.2 Å. As the 2-tetracosanol molecule has about the same length, this probably means that the molecules stand perpendicular to the layer plane. That the structures are similar is also indicated by nearly identical short spacings (4.19 and 3.75 Å for racemic, 4.16 and 3.71 Å for optically active 2-tetracosanol).

The high-melting modification of racemic 2-tetracosanol has the same melting point (71°) as the intermediate-melting form of the antipodes. Furthermore the two forms have at least four low order *hkl* reflections in common, with visually the same relative intensities between three of them (at 3.82, 3.74, and 3.65 Å). The intensity of the fourth common reflection (at 4.21–4.22 Å) is different for the two forms, and different in relation to the three other reflections. The long spacings are markedly different (55.0 and 40.4 Å). The intensities of the reflections alternate in both cases. The molecules of both forms are probably orientated with their chains inclined to the layer plane.

From the curve connecting melting points of racemic, normal 2-hydroxyalkanes from C_{14} to C_{20} (9), an extrapolated melting point of 71° is found for racemic 2-tetracosanol.

The somewhat diffuse intermediate melting point (70.5°) of the racemic alcohol may indicate the existence of a third modification, but it has so far not been possible to confirm this by X-ray analysis.

The high-melting modification of the antipodes (m.p. 72°) has a long spacing (31.1 Å) slightly longer than the length of the 2-tetracosanol molecule. Two of the short spacings (3.83 and 3.74 Å) are also found in the racemic and optically active forms melting at 71°.

Optical rotations

The differences in the optical rotations of corresponding antipodes lie within the limits of experimental error. Like 2-eicosanol (1) 2-tetracosanol shows simple dispersion. The molecular rotation in dilute chloroform solution is slightly lower for 2-tetracosanol (11° at 5893 Å) than for 2-eicosanol (11–13° (1, 10)), 2-octadecanol (15° (10)), and 2-octanol (12° (5)). For light of shorter wavelengths the difference between the molecular rotation of 2-tetracosanol and 2-eicosanol (1) becomes more pronounced.

The molecular rotations of the acid phthalates of the normal alcohols from 2-octanol to 2-tridecanol are close to 120° in 5 % chloroform solution (4, 5). This seems to be an upper limit for the homologous series, as the acid phthalates of both 2-eicosanol (1, 10) and 2-tetracosanol show a rotation of the same magnitude.

Configuration

The configuration of the optically active 2-tetracosanols relative to glyceraldehyde is determined by the configuration of the antipodes of β-acetoxybutyric acid, from which they are synthesized (Chart I) without the possibility of racemisation or WALDEN inversion (11). The configuration of the latter was established (1) by the

Chart I. Scheme of synthesis with data on yields.

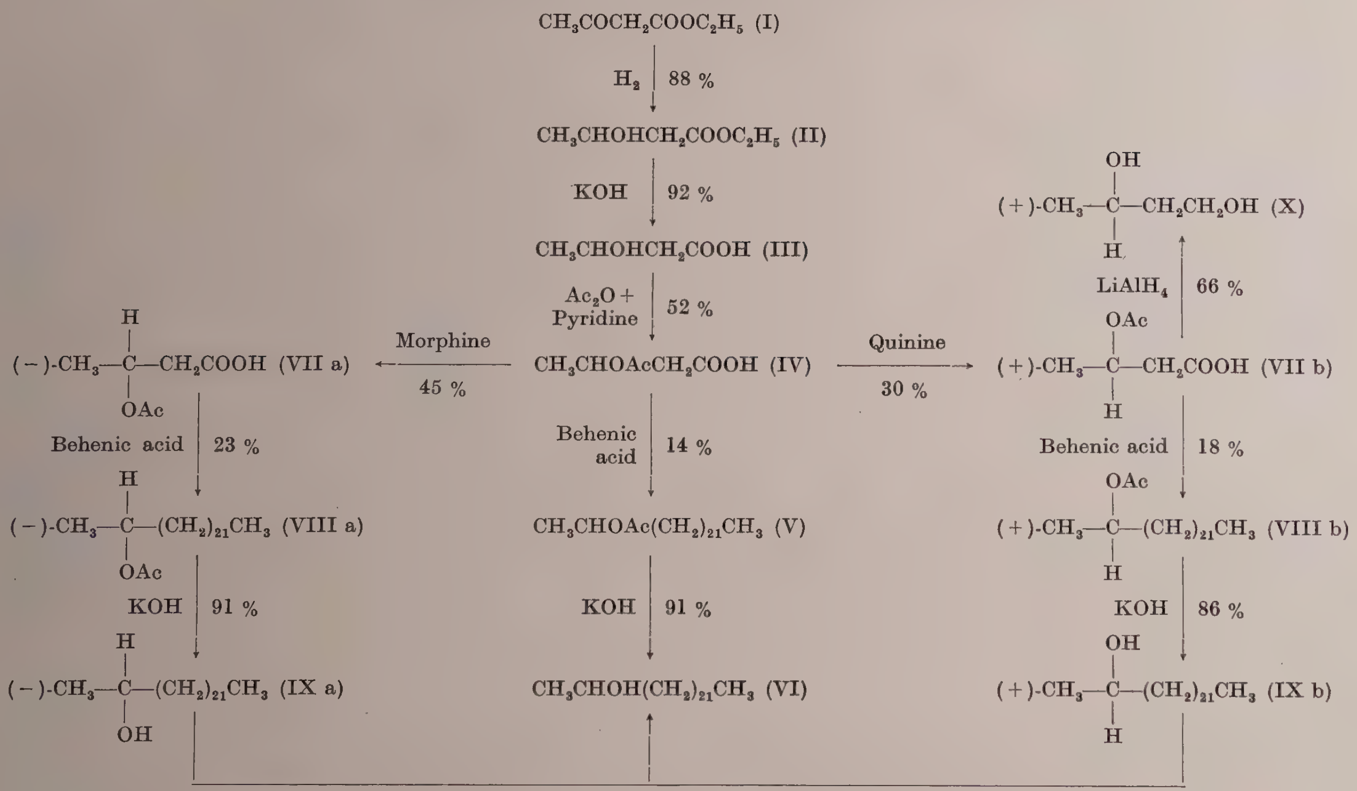
$CH_3COCH_2COOC_2H_5$ (I)
H_2 88 %
$CH_3CHOHCH_2COOC_2H_5$ (II)
KOH 92 %
$CH_3CHOHCH_2COOH$ (III)
Ac_2O + Pyridine 52 %
$CH_3CHOAcCH_2COOH$ (IV)
Morphine 45 %
Quinine 30 %
(−)-CH_3—C—CH_2COOH (VII a)
H
OAc
Behenic acid 23 %
(−)-CH_3—C—$(CH_2)_{21}CH_3$ (VIII a)
H
OAc
KOH 91 %
(−)-CH_3—C—$(CH_2)_{21}CH_3$ (IX a)
H
OH
Behenic acid 14 %
$CH_3CHOAc(CH_2)_{21}CH_3$ (V)
KOH 91 %
$CH_3CHOH(CH_2)_{21}CH_3$ (VI)
(+)-CH_3—C—CH_2CH_2OH (X)
OH
H
LiAlH$_4$ 66 %
(+)-CH_3—C—CH_2COOH (VII b)
OAc
H
Behenic acid 18 %
(+)-CH_3—C—$(CH_2)_{21}CH_3$ (VIII b)
OAc
H
KOH 86 %
(+)-CH_3—C—$(CH_2)_{21}CH_3$ (IX b)
OH
H

All the yields given in this chart are in % of the theoretical amount.

The formulae for the antipodes are FISCHER projections turned 90°.

conversion of (−)-β-acetoxybutyric acid to the ZnCa-salt of the configuratively known (12) (−)-β-hydroxybutyric acid, or (−)-3D-hydroxybutanoic acid, when named according to the rule (1, 14) that a substituent is labelled D when it falls on the right side in a FISCHER projection formula (13) with carbon atom no. 1 at the top. Correspondingly the systematic name for the levorotatory acetoxy acid is (−)-3D-acetoxybutanoic acid, and for the levorotatory tetracosanol synthesized from it, (−)-23D-hydroxytetracosane, or preferably (−)-2L-hydroxytetracosane, as this corresponds to the usual numbering.

That β-acetoxybutyric acid has the same configuration as β-hydroxybutyric acid rotating sodium light in the same direction, has now been confirmed by reduction of the former with $LiAlH_4$ to 1,3-butanediol of the same sign of rotation. This diol has earlier (15) been obtained from β-hydroxybutyric acid rotating in the same direction.

The reduction with $LiAlH_4$, known to proceed without racemization or WALDEN inversion (16), was performed on approximately 94 % optically pure (+)-β-acetoxybutyric acid. From the rotation of the resulting diol it follows that the specific rotation of the optically pure antipodes of 1,3-butanediol should be close to 28° *in substantia* and in chloroform (5 % solution) and close to 27° in ethanol (5 % solution). The highest reported values are 10–11° *in substantia* (17, 18) and 19° in ethanol (4 % and 10 % solution) (19, 20), but the samples were not claimed to be optically pure. The bisphenylurethanes recrystallized from alcohol had however practically the same specific rotations and melting points as the present preparation. These values ($[\alpha]_D^{20}$ 54° (ethanol, $c = 5$), m.p. 128°) therefore seem to be those of the optically pure antipodes of 1,3-bisphenylcarbamoyloxybutane, which apparently are less soluble in alcohol than the racemic form.

Experimental part[1]

Ethyl β-hydroxybutyrate (II), β-hydroxybutyric acid (III), and racemic β-acetoxybutyric acid (IV) were prepared as described in detail in Part I (1).

(−)-3D-Acetoxybutanoic acid (VII a)

The resolution of racemic acid was carried out essentially as described previously (1). The use of a more dilute solution made recrystallization of the alkaloid salt unnecessary:

132 g of morphine was dissolved in a solution of 73 g (0.5 mole) of β-acetoxybutyric acid in 225 ml of water at 70°. 450 ml of acetone was added after filtration,

---

[1] The electrolyses were run with 5 platinum electrodes (60 × 50 × 0.1 mm) mounted 3 mm apart in a bakelite frame.

The light petroleum used had a boiling range of 40–60°.

Boiling points are uncorrected.

Yields are given in % of the theoretical amount.

The melting points, which are corrected, were determined as described in footnote 1, Table 1.

The optical rotations recorded in this part were measured with a SCHMIDT & HAENSCH polarimeter of the triple-field LIPPICH type.

the dark brown solution cooled to −20°, and crystallization speeded up by stirring and scratching. The salt isolated by filtration and washed with acetone at room temperature weighed 83 g and consisted of white plates melting at 124°. It was dissolved in water, the morphine precipitated with ammonia water, and the filtrate acidified and extracted 5 times with ether. The half ester from the washed (H_2O) and dried (Na_2SO_4) extract was kept 15 hours *in vacuo* over concentrated sulphuric acid. Weight 16–17 g (*ca.* 45 % yield); n_D^{20} 1.429, α_D^{24} −2.86° (*in substantia*, $l = 1$).

(+)-3L-Acetoxybutanoic acid (VII b)

The procedure was the same as described in (1), except that partly resolved dextrorotatory acid (37 g, α_D^{23} +1.5° *in substantia*) from the mother liquor of the crystallization of the morphine salt was used instead of inactive acid. Three to four recrystallizations of the quinine salt gave about 44 g of optically pure salt or 10–12 g of (+)-*β*-acetoxybutyric acid (*ca.* 30 % yield); n_D^{23} 1.428, α_D^{23} +2.78° (*in substantia*, $l = 1$).

(+)-2D-Hydroxytetracosane (IX b)
(+)-2D-Tetracosanol

A solution of 0.1 g (4 milliatoms) of sodium in 40 ml of methanol was added to a solution of 5.82 g (0.04 mole) of (+)-*β*-acetoxybutyric acid and 13.6 g (0.04 mole) of behenic acid (m.p. 79.6–79.8°; purified as described for stearic acid in (1)) in 360 ml of warm methanol, and the electrolysis run for 6 hours at 100–150 volts without external cooling. The average current was approximately 1.5 amperes. 400 ml of water was then added, the precipitate filtered off, and both phases extracted 5 times with light petroleum. The combined extracts were washed with 2N ammonia water followed by water, and the residue from the dried (Na_2SO_4) extract distilled at 0.5 torr in a Claisen flask. 3.6 g (23 % yield) of crude acetate was collected between 184° and 193°. Attempts to purify the acetate by crystallization from light petroleum at −20° gave a dextrorotatory product ($[\alpha]_D^{23}$ +1.1° (chloroform, $c = 17$, $l = 1$)) with diffuse melting point. The impurity was probably mainly free alcohol, as the crude acetate on hydrolysis gave sharp-melting (+)-*2-tetracosanol* in high yield: a solution of 1.6 g of acetate in 100 ml of a 5 % methanolic solution of KOH containing 5 % of water and 15 % of benzene was refluxed for 1 hour. On cooling 1.3 g (91 % yield) of elongated plates with m.p. 71.8–72.0° crystallized from the alkaline solution. Recrystallization from light petroleum gave a second crystalline form melting at 70.8–71.0°. On melting and cooling, both forms gave a third modification melting at 62.8–63.0°. The two lower-melting forms gave the higher-melting one when their melts were kept at about 68°. The high-melting form crystallized more rapidly from the melt of the low-melting than from the melt of the intermediate-melting modification. Crystal spacings and optical rotations are given in Table 1.

	% C	% H
Found by analysis	81.6	14.2
Calculated for $C_{24}H_{50}O$ (354.6)	81.28	14.21

(+)-2D-Acetoxytetracosane
(+)-2D-Tetracosyl acetate (VIII b)

A solution of 0.35 g (1 millimole) of (+)-2-tetracosanol in 1 ml (10 millimoles) of acetic anhydride was refluxed for 4 hours. After 35 ml of ether had been added, crystallization was allowed to take place at −25°, giving 0.35 g (89 % yield) of *2-tetracosyl acetate* as transparent plates with m.p. 47.6–47.8°. By cooling the melt a second crystalline modification with m.p. 42.6–42.8° was obtained. Recrystallization from light petroleum at −25° did not change the melting points.

	% C	% H
Found by analysis	78.8	13.3
Calculated for $C_{26}H_{52}O_2$ (396.7)	78.72	13.21

(+)-2D-Tetracosyl hydrogen phthalate
Acid phthalate of (+)-2D-tetracosanol

180 mg (0.5 millimole) of (+)-2-tetracosanol, 74 mg (0.5 millimole) of phthalic anhydride, and 0.1 ml (1 millimole) of dry pyridine were mixed and kept at 115° for 20 hours. After cooling, the solid reaction mixture was dissolved in 5 ml of acetone and 50 ml of a half-saturated solution of sodium carbonate added slowly while shaking. After 3 hours any unesterified alcohol was extracted with light petroleum, the mixture acidified, and the *acid phthalate* taken up in chloroform. The crude phthalate (0.22 g, 86 % yield) from the washed (H_2O) and dried (Na_2SO_4) extract was crystallized from light petroleum at room temperature, giving spherulitic aggregates with constant m.p. 66.1–66.4°. A second crystalline form with m.p. 69.0–69.4° was obtained by slow cooling of the melt, whereas rapid cooling gave a third modification with m.p. 47.2–48.3°. The optical rotation is given in Table 1.

	% C	% H
Found by analysis	76.2	10.8
Calculated for $C_{32}H_{54}O_4$ (502.8)	76.44	10.83

(−)-2D-*tetracosanol* (IXa) and the corresponding *acetate* and *acid phthalate* were prepared in the same way as the antipodes by starting from (−)-β-acetoxybutyric acid (VIIa). Physical constants are given in Table 1.

Analyses	% C	% H
(−)-2-Tetracosanol	81.6	14.3
$C_{24}H_{50}O$ (354.6)	81.28	14.21
Acetate	78.8	13.1
$C_{26}H_{52}O_2$ (396.7)	78.72	13.21
Acid phthalate	76.2	10.7
$C_{32}H_{54}O_4$ (502.8)	76.44	10.83

(±)-2-Hydroxytetracosane (VI)

Racemic 2-tetracosanol was prepared from equal parts of the antipodes, and from racemic β-acetoxybutyric acid. Crystallized from light petroleum both samples melted at 70.9–71.1°. Rapid cooling of the melts gave a second modification with m.p. 62.7–62.9°. When the melts were kept at about 68° they crystallized slowly, and on heating remelted somewhat diffusely at about 70.5°. Crystal spacings are given in Table 1.

	% C	% H
Found by analysis	81.5	14.3
Calculated for $C_{24}H_{50}O$ (354.6)	81.28	14.21

(±)-2-Acetoxytetracosane (V)

Racemic 2-tetracosyl acetate was prepared in the same way as the optically active derivatives. Recrystallization from ether at −25° gave transparent plates with the constant melting point 44.7-44.9°. Cooling of the melt gave a second crystalline form with m.p. 42.6–42.8°.

	% C	% H
Found by analysis	78.9	13.3
Calculated for $C_{26}H_{52}O_2$ (396.7)	78.72	13.21

(±)-2-Tetracosyl hydrogen phthalate

The acid phthalate of racemic 2-tetracosanol was prepared in the same way as the optically active derivatives. The needle-formed crystals had the constant m.p. 71.3–71.5°. Cooling of the melt gave a second modification with m.p. 46.3–46.9°.

	% C	% H
Found by analysis	76.7	10.9
Calculated for $C_{32}H_{52}O_4$ (502.8)	76.44	10.83

(+)-1,3L-Dihydroxybutane (X)
(+)-1,3L-Butanediol

6.6 g (0.045 mole) of dextrorotatory β-acetoxybutyric acid (α_D^{21} +2.60° (*in substantia* $l = 1$), i.e. approximately 94 % optically pure) dissolved in 150 ml of dry ether, was added slowly (15 minutes) while stirring to a suspension of 5 g of $LiAlH_4$ in 150 ml of dry ether. After refluxing for 30 minutes, excess hydride was decomposed with ethyl acetate, the mixture acidified with dilute sulphuric acid, and the glycol extracted by shaking (6 times) with ethyl acetate. The extract was washed once with a small volume of saturated sodium carbonate solution, and the crude glycol (3.6 g) from the dried (Na_2SO_4) extract distilled in a Claisen flask at 9 torr. After a small forerun, about 2.7 g (66 % yield) of glycol was collected between 97° and 100°; n_D^{23} 1.4390, d_4^{23} 1.000. The constants agree closely with reported values (21). The corresponding molecular refraction R_D 23.70 is the same as the value calculated from VOGEL's bond refractions (22).

Optical rotations: $[\alpha]_D^{23}$ +26.64° ± 0.04 (*in substantia*, $l = 0.5$)
$[\alpha]_D^{23}$ +25.6° ± 0.4 (absolute alcohol, $c = 5$, $l = 1$)
$[\alpha]_D^{22}$ +26.4° ± 0.4 (chloroform, $c = 5$, $l = 1$)

The optically pure antipodes of 1,3-butanediol should thus have a specific rotation of 28° *in substantia* and in chloroform (5 % solution) and of 27° in ethanol (5 % solution).

(+)-1,3L-Bisphenylcarbamoyloxybutane

Bisphenylurethane of (+)-1,3L-butanediol

0.36 g (4 millimoles) of dextrorotatory 1,3-butanediol from the preceding experiment was heated for 1 hour at 100° with 1.07 g (9 millimoles) of phenyl isocyanate. The reaction product was dissolved in chloroform, an equal volume of light petroleum added, and crystallization allowed to take place at −20°, giving 1.18 g (90 % yield) of the *N*-phenylcarbamate. After 1 to 2 recrystallizations from alcohol at 0°, the product had m.p. 127.5–127.8° and the specific optical rotation $[\alpha]_D^{20}$ +54.2° (ethanol, $c = 5$, $l = 1$), unchanged on further crystallization. The constants agree closely with the highest reported values (17, 19, 20).

Summary

Optically pure dextro- and levorotatory 2-tetracosanol was synthesized via the acetates by anodic lengthening of the carbon chain of dextro- and levorotatory β-acetoxybutyric acid by means of behenic acid. Racemic 2-tetracosanol was prepared from the antipodes, and by using racemic instead of optically active β-acetoxybutyric acid in the KOLBE electrosynthesis.

The configuration of the optically active β-acetoxybutyric acids has been confirmed by reduction to the configurationally known 1,3-butanediol of the same sign of rotation.

ACKNOWLEDGEMENTS

The author is indebted to *Norges almenvitenskapelige forskningsråd* for a scholarship, and to the late Miss A. RENMAN and to Mr. L. PETTERSSON of the Microanalytical Laboratory of this institute for the analyses. The work was supported by grants from *Statens Medicinska Forskningsråd* to Prof. E. STENHAGEN.

Department of Medical Biochemistry, Institute of Medical Chemistry, University of Uppsala, Sweden.

REFERENCES

1. Serck-Hanssen, K., Ställberg-Stenhagen, S., and Stenhagen, E., Arkiv Kemi *5*, 203 (1953).
2. Weedon, B. C. L., Quart. Revs. *6*, 380 (1952).
3. Swann, S. in Weissberger, A., Technic of Organic Chemistry. New York 1948, Vol. II, p. 143.
4. Pickard, R. H. and Kenyon, J., J. Chem. Soc. *99*, 45 (1911).
5. —— *ibid. 105*, 830 (1914).
6. Ingersoll, A. W. in Adams, R. *et al.*, Organic Reactions. New York 1944, Vol. II, p. 376.
7. Pickard, R. H. and Kenyon, J., J. Chem. Soc. *101*, 620 (1912).
8. —— Proc. Chem. Soc. *27*, 312 (1911).
9. Breusch, F. L., Chem. Ber. *86*, 669 (1953).
10. Pangborn, M. C. and Anderson, R. J., J. Am. Chem. Soc. *58*, 10 (1936).
11. Cf. Linstead, R. P., Lunt, J. C., and Weedon, B. C. L., J. Chem. Soc. *1950*, 3333.
12. Levene, P. A. and Haller, H. L., J. Biol. Chem. *81*, 425, 703 (1929).
13. Fischer, E., Chem. Ber. *24*, 2683 (1891).
14. Klyne, W., Chemistry & Industry *1951*, 1022.
15. Levene, P. A. and Haller, H. L., J. Biol. Chem. *69*, 165 (1926).
16. Cf. Noyce, D. S. and Denney, D. B., J. Am. Chem. Soc. *72*, 5743 (1950).
17. Levene, P. A., Walti, A., and Haller, H. L., J. Biol. Chem. *71*, 465 (1926).
18. Neuberg, C. and Kerb, E., Biochem. Z. *92*, 96 (1918).
19. Levene, P. A. and Walti, A., J. Biol. Chem. *94*, 361 (1931).
20. Levene, P. A. and Haller, H. L., *ibid. 69*, 569 (1926).
21. Clendenning, K. A., MacDonald, F. J. ,and Wright, D. E., Can. J. Research *28B*, 608 (1950).
22. Vogel, A. I. *et al.*, J. Chem. Soc. *1952*, 514, 531.

Tryckt den 16 juni 1955

Uppsala 1955. Almqvist & Wiksells Boktryckeri AB

ARKIV FÖR KEMI Band 8 nr 42

Communicated 23 February 1955 by Arne Westgren and Gunnar Hägg

Optical studies of compressed surface layers on an aqueous substrate

By Henrik H. Bruun

With 12 figures in the text

In 1930, Zocher and Stiebel (1) introduced an ultramicroscopic technique for the study of monolayers by which they established the existence of inhomogeneities in the form of a "Punktstruktur" in extremely thin surface layers produced by compression of monomolecular layers on aqueous substrates. The inhomogeneities were evident as bright points of equal size situated more or less close to each other. Depending on the type of substance and the experimental conditions, these points varied both in appearance and spacing. They concluded that these points are characteristic features of compressed monolayers. The points were assumed to be drops of separated monolayer substance, possibly minute crystals, in the case of higher saturated fatty acids.

With a few compounds (palmitic and erucic acid), the surface layer substance exhibits a regular network with hexagonal or circular optically dark openings. In one case ("Holzöl"), in addition to the points, extended spots were observed which were oriented perpendicular to the direction of the compressing force. In contrast to the point structure, the layers with a net structure and those in which the spots were seen were very difficult to reproduce experimentally.

When the layers with point structure were subjected to compression, separation of granulates, folding, coalescing of the points and sometimes also recrystallization occurred.

The microscope system employed by Zocher and Stiebel comprised a microscope directed vertically against the liquid surface and attached to one edge of a brass trough and a cardioid condenser passing through the bottom of the trough by which the light rays were focussed on the liquid surface. The method has later been improved and used in monolayer studies to check the spreading of monolayer substance on the liquid surface and to observe the collapse of the surface films (2–8), as well as to study the solubilities of liquid compounds in monolayers (9–13). Also light projected form above has been employed in the microscopic studies of surface layers; an illuminator fitted with a ring condenser (Leitz Ultropak) has been used (14).

The present paper describes an ultramicroscopic study of the phenomena that take place when a monolayer supported on the liquid substrate is compressed to a small area at room temperature (20–23°). In parallel with these observations, the areas taken up by the surface layer and in some cases also the surface pressures have been measured with a surface balance. Some of the details of the observed structures have also been photographed.

The purpose of the study has been to obtain more knowledge about the phenomena that occur when surface layers are compressed under controlled conditions. It was expected that by using light projected from above, information could also be obtained about the topography of the surface. The work is a continuation of earlier studies (15–17) planned to elucidate the problem of the formation and structure of di- and multi-molecular layers on liquid substrates. This problem has been now and then discussed (18–20) but relatively little has been done to extend our knowledge of the phenomena involved although they may be important from the theoretical, biological and technical viewpoints.

Experimental

The microscope was attached to a Leitz crossbeam table on which it could be moved in a vertical position above the trough. An eye-piece giving a tenfold magnification, a Leitz Ultropak illuminator and an objective giving a 50-fold magnification (in a few cases 22 × and 11 ×) were employed. The photographs were taken with a Leica camera fastened to the microscope by an intermediate attachment (Leitz "Mikas"). The photographs reproduced were taken with an exposure time of 10–15 seconds and show an approximately 500-fold magnification. The voltage of the illuminator lamp, normally 8 volts, was temporarily increased to 20 volts for the exposures.

The surface balance was of the WILHELMY-DERVICHIAN type, as improved by ANDERSSON-GROTH, STÄLLBERG-STENHAGEN and STENHAGEN (21–22). It was an automatic-recording instrument and compressed the monolayer symmetrically by means of two barriers moving from the ends to the centre of the trough. The rate of compression was about 5 cm per minute, the compression being increased in steps when the microscope observations were made.

The compounds studied were spread from a solution in benzene or light petroleum ether (b.p. 60–80°) (concentration $\sim 2 \times 10^{18}$ molecules per ml). The substrate was dilute hydrochloric acid (0.001 *M*). The monolayer of aluminium monoisodextropimarate was obtained by spreading isodextropimaric acid on a substrate containing 0.001 mole of $KAl(SO_4)_2$ per litre and adjusted to pH 4.10 by adding dilute sodium hydroxide (23, 24).

Of the compounds studied, behenic acid (m.p. 79.7–79.9° (25)), (–)-α-methyl-α-ethyleicosanoic acid (m.p. 54.4–54.7° (26)) and ethyl α-bromobehenate (45–48°)[1] had been prepared at the Institute of Medical Chemistry of Uppsala University, isodextropimaric acid (m.p. 163–165° (corr.)) was obtained from Dr. C. G. HARRIS of the Hercules Powder Co., Wilmington, U.S.A., dextropimaric acid (m.p. 212–214° (corr.)) from Dr. O. JEGER of the Eidg. Techn. Hochschule in Zürich, and cholesterol was obtained from Prof. S. BERGSTRÖM at Lund University. (For surface balance data

---

[1] The specimen probably contained small amounts of ethyl behenate as an impurity.

Microphotographs of surface layers under different degrees of compression on an aqueous substrate. Magnification 500 ×. The light has been projected on the surface layer from above with a Leitz Ultropak Illuminator.

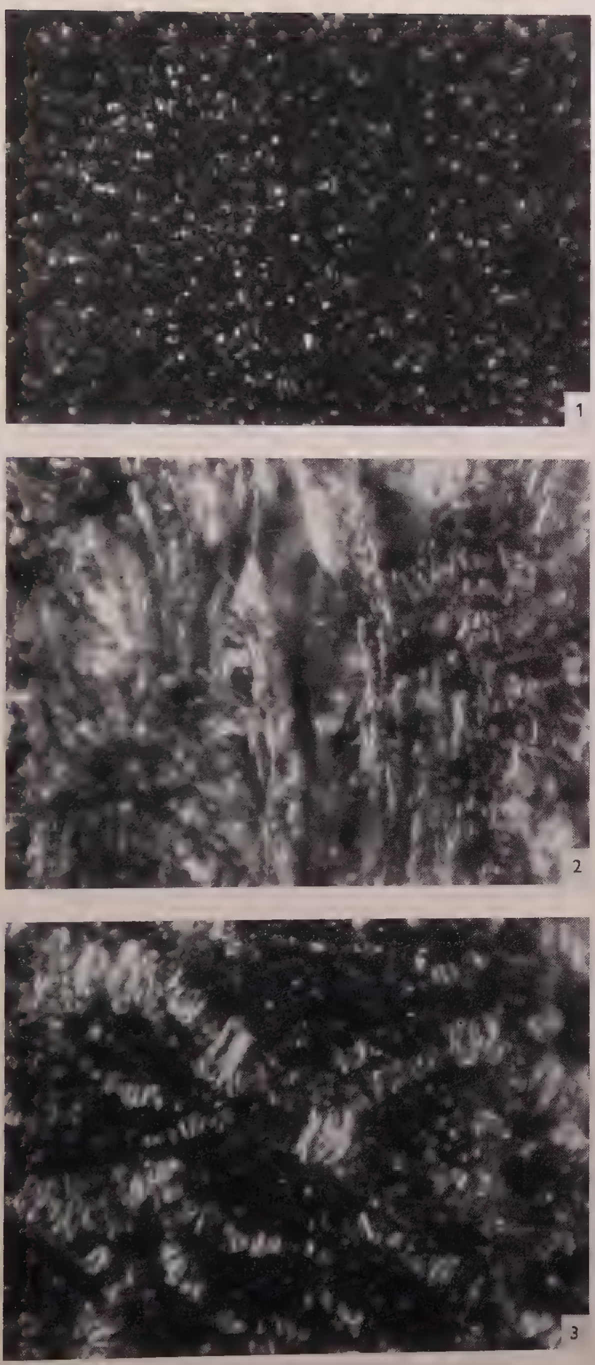

Figs. 1–3. Behenic acid.

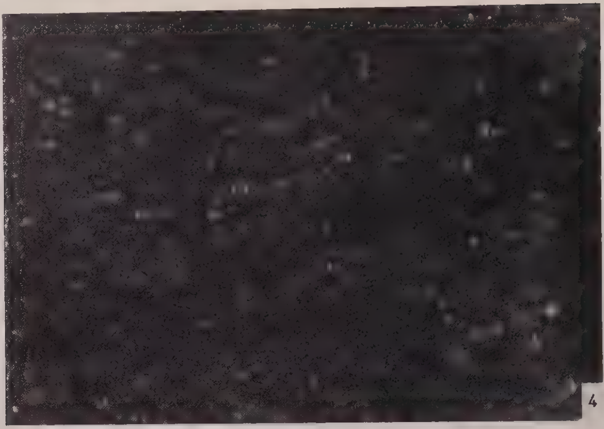

4

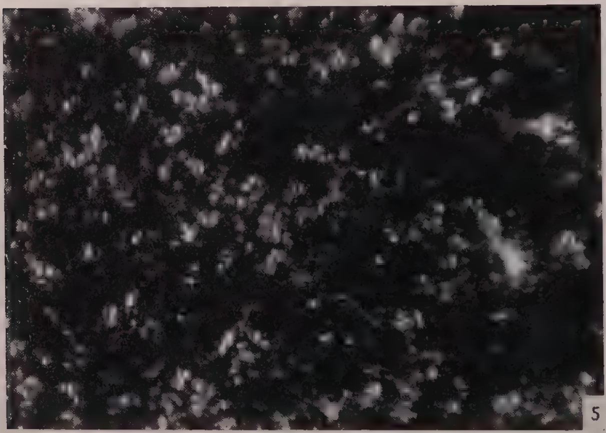

5

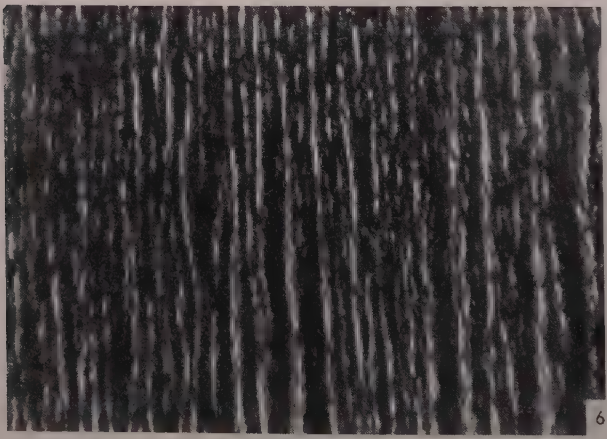

6

Figs. 4–6. (–)-α-Methyl-α-ethyleicosanoic acid.

Figs. 7–9. Isodextropimaric acid.

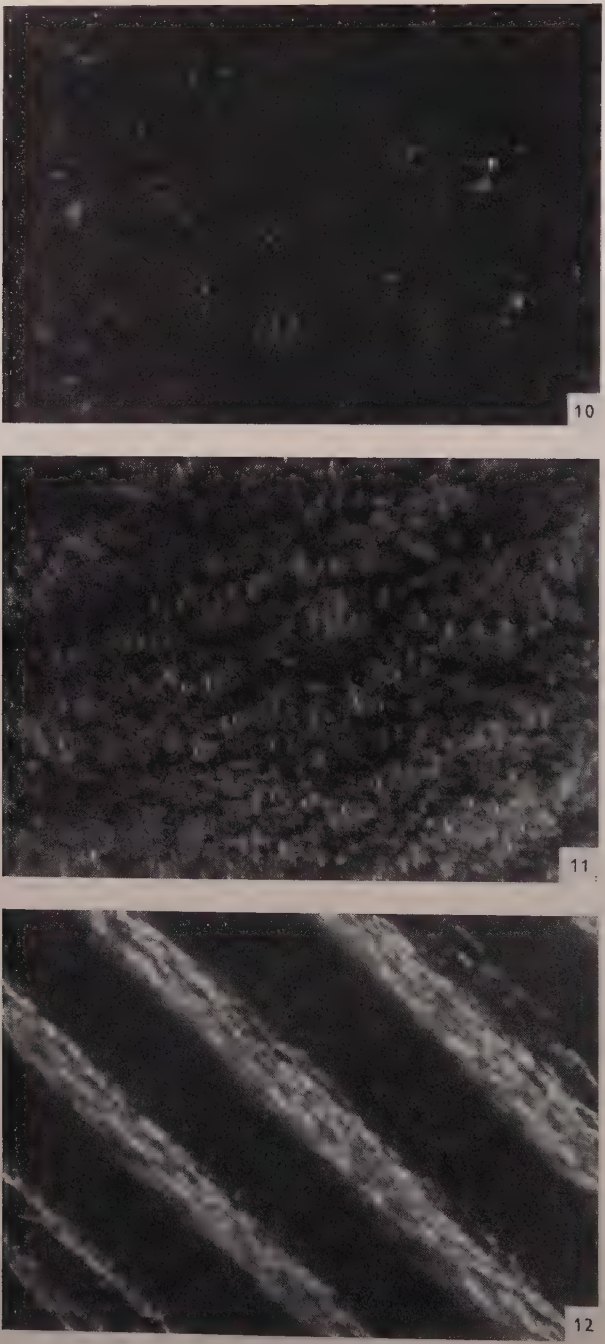

Figs. 10–12. Cholesterol.

previously obtained for the same samples and which this writer used for their characterization, see the following publications: behenic acid (22), (–)-α-methyl-α-ethyleicosanoic acid (26), pimaric acids (28, 15, 16, 23, 29)).

Microscopic observations

The following is a short description of the appearance of the surface layers under different degrees of compression. The degrees of compression are given in terms of fractions of the collapse area A_K[1] which, as long as the area requirement of the molecules corresponds to the collapse area and no aggregation of molecules takes place (the molecules are assumed to float like wooden blocks in the water surface), permits a calculation of the degree of compression in terms of the number of layers of molecules.

Behenic acid	($A_K = 19.3$ sq. Å/molecule (22))
0.30 A_K	Points forming irregular lines. — After dilatation and compression: a lattice of points and spots (*Fig. 1*). (Surface pressure: about 65 dynes/cm.)
0.04[2] A_K	Plate-like crystals, mainly in irregular bands. Isolated points and spots between the bands (*Fig. 2*). — After dilatation and compression: a lattice of points, spots and plate-like crystals.
0.03 A_K	Superposition of floes and coalescing of points, spots and crystal plates.
0.02 A_K	Extended parallel folds in which aggregates of crystals of varied appearance are seen. After dilatation: some of the folds have disappeared; their former places are occupied by crystal aggregates (*Fig. 3*).
(–)-α-Methyl-α-ethyleicosanoic acid	($A_K = 42.4$ sq. Å/molecule (27))
0.45 A_K	Point lattice. (Surface pressure: about 60 dynes/cm.)
0.2 A_K	Point and spots in a lattice (*Fig. 4*).
0.1 A_K	Dense lattice of points and spots. Some of the latter are observed to be upright crystalline plates (*Fig. 5*).
0.08 A_K	Dense array of platelets resembling bark.
0.05 A_K	Parallel folds (*Fig. 6*). — After dilatation: Large and small, freely moving floes of layer substance.
Ethyl α-bromobehenate	($A_K = 22$ sq. Å/molecule (27))
0.10 A_K	A linear fold with isolated small points. (Surface pressure 25 dynes/cm.)
0.07 A_K	As in the preceding, but with a larger number of folds.
0.03 A_K	Wide bands containing numerous enclosed (air?) bubbles that have resulted from fold formation.
Isodextropimaric acid	($A_K = 42.6$ sq. Å/molecule (28,23))
0.30 A_K	A lattice of points and spots. (Surface pressure about 40 dynes/cm.) In a study of the reproducibility of the area value, the following fractions of A_K were obtained: 0.29, 0.32, 0.29, and 0.30.

---

[1] For the exact meaning of A_K, see the definition of the point K_1 in the author's thesis, Acta Acad. Aboensis, Math. et Phys. *19*, No. 3 (1954), p. 21.

[2] The surface layer has been renewed after dilatation-compression treatment.

0.2 A_K	As in the preceding, but with a larger number of points and spots. — After dilatation and compression: as in the preceding, but large crystalline platelets are seen.
0.1 A_K	Numerous crystalline platelets oriented perpendicular to the direction of the compressing force (*Fig. 7*). — After dilatation and compression: very large crystalline plates (*Fig. 8*).
0.08 A_K	Clusters of crystalline plates.
0.05 A_K	Fold formation. — After dilatation: Floes are observed which do not move relative to each other. More or less distinct folds are noted in these (*Fig. 9*).
Dextropimaric acid	($A_K = 43.6$ sq. Å/molecule (23))
0.13 A_K	Isolated small points. (Surface pressure about 50 dynes/cm.) — After dilatation and compression: Point lattice.
0.08 A_K	Lattice of points and spots.
0.05 A_K	As in the preceding, but with numerous crystalline platelets.
0.01 A_K	Extensive fold formation.
Cholesterol	(A_K 36 sq. Å/molecule (27))
0.64 A_K	Lattice of points. (Surface pressure about 40 dynes/cm.)
0.3 A_K	Lattice of points and spots (*Fig. 10*).
0.2 A_K	Crystalline platelets, spots and points in dense array, the platelets mainly oriented perpendicular to the direction of compression (*Fig. 11*).
0.1 A_K	Dense bark-like array.
0.08 A_K	Large folds (*Fig. 12*[1]).
Aluminium monoisodextropimarate	($A_K = 40.3$ sq. Å/molecule (23))
0.1 A_K	Reflecting bands formed by folded layers with only a few bright points in the bands. (Surface pressure about 60 dynes/cm.)
0.06 A_K	As in the preceding, but with a larger number of points.
0.01 A_K	As in the preceding.

Survey of microscopic observations

In the case of behenic acid, (—)-α-methyl-α-ethyleicosanoic acid, isodextropimaric acid, dextropimaric acid and cholesterol, two relatively well differentiated stages are observed on compression. The first stage (Stage I) involves the development of inhomogenities and their compression into a dense array. The second stage (Stage II) involves coalescing of the inhomogenities to a carpet, production of conglomerates and granulates of varied appearance and gradual formation of parallel folds.

For (−)-α-methyl-α-ethyleicosanoic acid, isodextropimaric acid and cholesterol and under certain conditions (dilatation followed by compression) also for behenic and dextropimaric acids, the details of Stage I are similar:

a.—Inhomogeneities in the form of bright points and spots suddenly appear over the whole surface (Figs. 1, 4, and 10).

b.—The points and spots increase in number, some of them become larger on compression and form crystalline platelets which are vertically situated in the surface and largely oriented perpendicular to the direction of the compressing force (Fig. 5).

---

[1] The direction of the compressing force traverses this photograph diagonally perpendicular to the folds, in the other photographs parallel to the long edges.

c.—The inhomogeneities form a dense array without changing their appearance to any greater degree (Figs. 7 and 11).

The inhomogenities appear to form a more or less regular lattice. The "openings" in this lattice vary in size and are often circular in form. The lattice is clearly seen in Stages I a and I b and less distinctly when the layer is compressed further (Stage I c).

In the case of the compounds investigated, the point lattice is easily reproduced. It has always appeared after dilatation and compression, after renewal of the layer, and also when the layer has been compressed after it has lain on the substrate for a longer period.

When the surface layer is subjected to repeated dilatation and compression, more points appear in the lattice. The crystals also increase in size simultaneously, particularly in the case of isodextropimaric acid (Fig. 8). When the compression is discontinued, the crystal platelets decrease in size and also the number of points diminishes. The crystal platelets gradually move downwards, without, however, losing their vertical orientation, and suddenly disappear.

The first points generally appear for different substances at different degrees of compression, with areas between 0.64 A_K and 0.10 A_K. This particular degree of compression is readily reproduced in the case of isodextropimaric acid.

The features of Stage II vary considerably and are not as readily reproduced as those of Stage I. Fold formation in the case of behenic acid has followed the superposition of floes. With (−)-α-methyl-α-ethyleicosanoic acid and cholesterol, a bark-like surface develops. In the case of isodextropimaric acid, the surface is very uneven. The folds have been wide for behenic acid and cholesterol (Fig. 12) and rather narrow for (−)-α-methyl-α-ethyleicosanoic acid (Fig. 6).

The features of Stage II for isodextropimaric acid and cholesterol have varied with the rate of compression; variations have also been noted in different regions of the layer. In the latter respect, the distance from the barrier has been an influencing factor.

Differences have also been observed when the layers compressed into folds have been subjected to dilatation. In the case of isodextropimaric acid and partly also for behenic acid, the folds have again leveled out and the layer has partly reverted to the structures of Stages I c and I b (Figs. 9 and 3). The layers of cholesterol and dextropimaric break up and form immobile floes. The floes formed in this way from (−)-α-methyl-α-ethyleicosanoic acid layers move freely over the aqueous surface.

Stage II has developed for the various compounds at very different degrees of compression.

The two stages have not been clearly differentiated in the case of the ethyl α-bromobehenate and the aluminium monoisodextropimarate layers. With layers of the latter the first inhomogeneities observed involve formation of folds and only a few isolated points are simultaneously observed. For ethyl α-bromobehenate, the number of points has been relatively larger and fold formation has been limited. Floe formation has followed compression in the latter case and the superposition of the floes has resulted in wide bands (in which bubbles have been occluded). Aggregates of crystals have also been observed in the bands. All these observations have become evident at relatively high degrees of compression.

Conclusions

The points in Stage I undoubtedly correspond to the points in the point structure found by ZOCHER and STIEBEL to be characteristic of surface layers of a large number of compounds. The points are similar both in the mode of formation, appearance and stability, and in their behaviour on dilatation and compression. The present observations made with substances of markedly different molecular structure thus indicate that such inhomogeneities are general characteristics of surface layers formed by compression of insoluble monomolecular layers on aqueous substrates.

It is observed that a large portion of the point-like inhomogeneities increase in size on further compression of the layer and have been found to form crystal platelets vertically situated in the surface layer, and frequently oriented perpendicular to the direction of the compression. These platelets and points form a more or less regular lattice-like structure. ZOCHER and STIEBEL have observed inhomogeneities of similar type in a layer formed by one of their substances (Holzöl). In contrast to the present observations, however, these spots appeared irregularly and were difficult to reproduce, perhaps owing to a metal ion effect attributable to the brass trough they employed.

The observations indicate that the upright platelets and the spots from which they are formed, and evidently also the point-like inhomogeneities, are composed of crystals[1], but on the basis of the microscope observations it is not possible to obtain information about the structure of the layer between these particles. With the aid of the data on the degrees of compression when the first points are observed, it is, however, possible to conclude that in this region the surface layer contains very little of the compound in question; the surface layer is probably composed of only one monomolecular layer of the substance. In the case of cholesterol, the inhomogeneities were first observed when the degree of compression corresponded to an area of about 0.6 A_K. If it is assumed that the area requirement of the molecules is the same during the compression as when collapse occurs, viz. the collapse area A_K (see p. 417), the value 0.6 A_K implies that immediately before the point-like inhomogeneities appear, the surface layer has a thickness of only ten-sixths of the length of the molecule, i.e. a layer two molecules thick in which one third of the second molecular layer has not yet been filled. After the formation of points has occurred, the region of the layer between the points must necessarily be poorer in substance, since during this formation every visible point must have resulted from the aggregation of several thousands of molecules, as is shown by a simple calculation which takes into account the magnification of the microscope employed in the study. After the points have developed, the substance has thus been unable to form more than one complete layer one molecule thick in the region between the points.

In the case of other substances giving point lattices the inhomogeneities were first observed at compression values $= 0.3\ A_K$. This implies that before the formation of the points, the surface layer can be calculated to consist of three complete layers of molecules at the most. After the formation of the point lattice, the surface layer between the points must consequently be less than three molecules thick.

This distribution of substance in various regions of the lattice according to which a large number of molecules are concentrated in a few sites, while only one, or in some cases perhaps a few layers of molecules cover the remaining surface, is also characteristic for the system which develops on the surface in the reverse way, i.e. by a spontaneous spreading that takes place when an excess of insoluble crystalline (or liquid) substance comes into contact with a liquid surface (for a review, see e.g. (30)). This distribution is in both cases undoubtedly influenced by the presence of the liquid surface.

---

[1] Compression of monolayers of liquid compounds leads to the formation of lens-shaped drops as shown by the studies of ZOCHER and STIEBEL (1) and HARKINS *et al.* (9–13).

Although a lattice containing crystals was formed by isodextropimaric acid, such was not the case for the aluminium soap of isodextropimaric acid. The absence of this type of system with the latter is evidently due to the fact that the latter substance probably does not exist in crystalline form (for the properties of dibasic aluminium monorosinate, see (31) and (32)).

Large differences are shown by the layers compressed to small areas (Stage II), which are also evident in the results of ZOCHER and STIEBEL. This is not unexpected when we note that in contrast to the transformations involved in Stage I, the transformations at this stage occur in a tridimensional system composed almost solely of packed surface substance and separated from the aqueous surface and which is undergoing a process of crystallization characteristic of the substance in question.

SUMMARY

Microscope observations have been made of the phenomena that occur when insoluble monomolecular layers are compressed to small areas on an aqueous substrate. The layers have been illuminated by light projected from above. Photographs of various phases that develop on compression are reproduced in Figs. 1–12.

Compression of the surface layer first leads to the formation of a lattice of bright points, which grow larger on further compression and are found to consist of crystalline platelets situated upright in the surface and largely oriented perpendicular to the direction of the compressing force.

On the basis of surface balance data, it has been concluded that the surface layer between the points of the lattice is very poor in layer-forming substance and consists of one or only a few layers of molecules.

ACKNOWLEDGEMENTS

This study has been conducted at the Institute of Medical Chemistry of the University of Uppsala. I wish to express my sincere thanks to Professor E. STENHAGEN for suggesting the subject and for inviting me to Uppsala to carry out the work. I am also indebted to Mrs. K. NILSSON and Mr. L. AHLQUIST for their assistance with the surface balance measurements and photography.

My visit to Sweden has been made possible by a grant from the Committee for the Advancement of Natural Sciences appointed by the Finnish Government.

Institute of Medical Chemistry, University of Uppsala, Sweden.

Institute of Physical Chemistry, Åbo Akademi, Finland.

REFERENCES

1. Zocher, H. and Stiebel, F., Z. physikal. Chem. *147*, 401 (1930).
2. Adam, N. K., Trans. Far. Soc. *29*, 90 (1932).
3. Adam, N. K., Danielli, J. F., Haslewood, G. A. D., and Marrian, G. F., Biochem. J. *26*, 1233 (1932).
4. Hughes, A. H. and Rideal, E., Proc. Roy. Soc. (London) *A 137*, 62 (1932).
5. Adam, N. K. and Miller, J. G. F., Proc. Roy. Soc. (London) *A 142*, 401 (1933).
6. Danielli, J. F., Marrian, G. F., and Haslewood, G. A. D., Biochem. J. *27*, 311 (1933).
7. Danielli, J. F. and Adam, N. K., Biochem. J. *28*, 1583 (1934).
8. Adam, N. K., Askew, F. A., and Danielli, J. F., Biochem. J. *29*, 1786 (1935).
9. Fowkes, F. M., Myers, R. J., and Harkins, W. D., J. Am. Chem. Soc. *59*, 593 (1937).
10. Florence, R. T. and Harkins, W. D., J. Chem. Phys. *6*, 847 (1938).
11. —— Ibid. *6*, 856 (1938).
12. —— Nature *142*, 913 (1938).
13. Harkins, W. D. and Alexander, J., Colloid Chemistry, New York (1944), Vol. *5*, p. 64.
14. Ställberg, S. and Stenhagen, E., J. Biol. Chem. *143*, 171 (1942).
15. Bruun, H. H., Acta Chem. Scand. *6*, 798 (1952).
16. —— Ibid. *6*, 953 (1952).
17. —— Ibid. *6*, 955 (1952).
18. Lyon, C. G. and Rideal, E., Proc. Roy. Soc. (London) *A 124*, 349 (1929).
19. Zocher, H. and Stiebel, F., Z. physikal. Chem. *147*, 421 (1930).

19 b. Schulman, J. H. and Rideal, E. K., Proc. Roy. Soc. (London) *A 130*, 284 (1931).

20. Adam, N. K. and Miller, J. G. F., Proc. Roy. Soc. (London) *A 142*, 405 (1933).
21. Andersson-Groth, K. J. I., Ställberg-Stenhagen, S., and Stenhagen, E., *in* The Svedberg 1884 30/8 1944, Uppsala (1944), p. 11.
22. Ställberg-Stenhagen, S. and Stenhagen, E., Nature *156*, 239 (1945).
23. Bruun, H. H., Dissertation, Acta Acad. Aboensis, Math. et Phys. *19*, No. 3 (1954).
24. Ekwall, P. and Bruun, H. H., Acta Chem. Scand. *9*, 412, 424 (1955).
25. Stenhagen, E. and von Sydow, E., Arkiv för Kemi *6*, 309 (1953).
26. Ställberg-Stenhagen, S., Arkiv för Kemi *3*, 273 (1951).
27. Stenhagen, E., From measurements with recording Wilhelmy balance.
28. Bruun, H. H., Acta Chem. Scand. *6*, 494 (1952).
29. —— Finska Kem. Samf. Medd. *63*, 22 (1954).
30. Adam, N. K., The Physics and Chemistry of Surfaces, London (1949), p. 102.
31. Ekwall, P. and Bruun, H. H., Paper and Timber *B 32*, 194 (1950).
32. Back, E. and Steenberg, B., Sv. Papperstidn. *54*, 510 (1951).

Tryckt den 16 juni 1955

Uppsala 1955. Almqvist & Wiksells Boktryckeri AB

ARKIV FÖR KEMI Band 8 nr 43

Read 27 April 1955

Equilibrium pressure for different temperatures between graphite and diamond

By Ragnar Liljeblad

With 4 figures in the text

ASEA has for several years been working on the problem of making synthetical diamonds. In connection with this work the author has made the following calculation of the equilibrium pressure for different temperatures between graphite and diamond.

Theoretical deductions

According to the first principle of thermodynamics we have

$$dQ = dU + p\,dV \tag{1}$$

where Q is the heat transmitted to the body, U is the inner energy, p the specific pressure and V the volume. Consequently, $p\,dV$ is the work done by the pressure p.

If the process is reversible, that is if the system is very near equilibrium, we may write

$$dS = \frac{dQ}{T} \tag{2}$$

where T is the absolute temperature. Thus equ. (1) may be written

$$T\,dS = dU + p\,dV. \tag{3}$$

If p and T are constants we may write

$$d(U - TS + pV) = 0. \tag{4}$$

Thus at equilibrium the so-called Gibb's potential $U - TS + pV$ is a minimum. We give the symbols of the graphite indices 1 and of diamond indices 2. An index p means that the value of the quantity is valid at the equilibrium pressure p. At normal pressure p_0, generally one atmosphere we use the symbols U_1, U_2, S_1 and so forth without any further indices. According to equ. (4) the change of potential near equilibrium will be zero in moving from one phase to the other.

Thus

$$(U_{1p}-U_{2p})-T(S_{1p}-S_{2p})+p(V_{1p}-V_{2p})=0. \qquad (5)$$

But we have

$$p(V_{1p}-V_{2p})=p[(V_1-\Delta V_1)-(V_2-\Delta V_2)]=p(V_1-V_2)-p\Delta V_1+p\Delta V_2. \qquad (6)$$

In reversible compression of a body by the amount ΔV by increasing the pressure from p_0 to p, a work $\mu(p-p_0)\Delta V$ will be transferred to the body. (μ is a factor that by linear change of the volume with pressure is equal to $^1/_2$, but in reality generally somewhat smaller.)

This work is used partly to increase the inner energy, partly it will be transformed to heat that disappears, whereby the entropy is diminished by a corresponding quantity divided by T. For each phase may be written

$$U_p-TS_p=U-TS+\mu(p-p_0)\Delta V. \qquad (7)$$

Fom equ. (5), (6), and (7) we get

$$(U_1-U_2)-T(S_1-S_2)+\mu(p-p_0)\Delta V_1-\mu(p-p_0)\Delta V_2+$$
$$+p(V_1-V_2)-p\Delta V_1+p\Delta V_2=0. \qquad (8)$$

This equation may be transformed to

$$U_1+p_0V_1-(U_2+p_0V_2)-T(S_1-S_2)+(p-p_0)(V_1-V_2)=$$
$$=[(1-\mu)p+\mu p_0][\Delta V_1-\Delta V_2). \qquad (9)$$

However, the heat release Q_{12} at constant pressure p_0 and the temperature T is by transition from phase 1 to phase 2:

$$Q_{12}=U_1-U_2+p_0(V_1-V_2)=U_1+p_0V_1-(U_2+p_0V_2). \qquad (10)$$

From equ. (9) and (10) we get

$$Q_{12}-T(S_1-S_2)+(p-p_0)(V_1-V_2)-[(1-\mu)p+\mu p_0](\Delta V_1-\Delta V_2)=0. \qquad (11)$$

The heat release may in some cases be got directly. When such is not the case it may be had as the difference between the combustion heats for the two phases. Those are generally given at one atm. pressure and 25° C temperature. It is convenient to calculate with one mole of the substance. As may be seen from equ. (10), if the heat release is known at 25° C and the pressure p_0, we may have it at a temperature T and the same pressure by increasing its value at 25° C by

$$\int_{298}^{T}(C_1-C_2)\,dT$$

where C_1 and C_2 are the molar heats of the two phases at the constant pressure p_0.

$S_1 - S_2$ for one mole may be calculated from

$$S_1 - S_2 = \int_0^T \frac{C_1 - C_2}{T} \, dT.$$

The value of the entropy at absolute zero is, according to Nernst, zero and the integral may consequently be figured out if C_1 and C_2 are known for all temperatures between 0 and T. For graphite and diamond the entropies are given in the literature at one atmosphere and 25° C.

Equ. (11) may therefore be used for numerical calculations of the pressure that corresponds to equilibrium between the two phases at a certain temperature T. The equation may sometimes be simplified. At low values of p the compression may be overlooked for solid and fluid substances.

Thus the equation gets the form

$$Q_{12} - T(S_1 - S_2) + (p - p_0)(v_1 - v_2) = 0 \tag{12}$$

where v is the symbol for the mole volume.

More important is the case when the pressure is very high. Then p_0 may be overlooked as compared to p and we may write

$$Q_{12} - T(S_1 - S_2) + p\,[v_1 - v_2 - (1 - \mu)(\Delta v_1 - \Delta v_2)] = 0. \tag{13}$$

Numerical calculations

Heat content at 298° K and 1 atm. (ref. 1)

At 25° C and 1 atm. graphite to CO_2 393,355 ± 46 joule/mole

„ „ „ 1 „ diamond to CO_2 395,254 ± 115 joule/mole

The difference at 25° C or 298° K

$$Q_{12}^{298} = -1899 \pm 161 \text{ joule/mole}$$

A more recent and probably more exact value that will be used is

$$Q_{12}^{298} = -1896 \pm 124 \text{ joule/mole}$$

Entropy at 298° K and 1 atm. (ref. 1)

Graphite $S_1^{298} = 5.712 \pm 0.100$ joule/°C · mole

Diamond $S_2^{298} = 2.448 \pm 0.040$ joule/°C · mole

$$S_1^{298} - S_2^{298} = 3.264 \pm 0.140 \text{ joule/°C} \cdot \text{mole}$$

Equilibrium equation at 298° K

$$-1896-298\cdot 3.264+p\cdot 10^{-6}\,[(5.33-3.41)-0.5\cdot 5.33\cdot 0.037]=0$$

$$p=\frac{2870}{1.82}\cdot 10^{6}=1580\cdot 10^{6}\ \mathrm{N/m^2}=16{,}000\ \mathrm{kp/cm^2}.$$

Heat content at 1298° K and 1 atm.

$$Q_{12}=Q_{12}^{298}+\int_{298}^{1298}(C_1-C_2)\,dT.$$

For graphite we have in calories between 298 and 1300° K

$$C_1=-1.265+14.008\cdot 10^{-3}\cdot T-103.31\cdot 10^{-7}\cdot T^2+2.751\cdot 10^{-9}\,T^3 \quad \text{(ref. 2)}$$

and for diamond between 298 and 1300° K

$$C_2=2.162+3.059\cdot 10^{-3}\cdot T-1.303\cdot 10^{5}\cdot\frac{1}{T^2} \quad \text{(ref. 3)}.$$

The difference

$$C_1-C_2=-3.427+10.949\cdot 10^{-3}\cdot T-103.31\cdot 10^{-7}\cdot T^2+ +2.751\cdot 10^{-9}\cdot T^3+1.303\cdot 10^{5}\cdot\frac{1}{T^2}.$$

Thus

$$\int_{298}^{1298}(C_1-C_2)\,dT=155\ \text{cal.,}\quad \text{or}\quad =649.5\ \text{joule.}$$

$$Q_{12}=-1896+650=-1246\ \text{joule.}$$

Entropy difference at 1298° K and 1 atm.

$$(S_1-S_2)=3.264+4.19\cdot\int_{298}^{1298}\frac{(C_1-C_2}{T}\,dT$$

$$=3.264+1.408=4.672\ \text{joule/°C}\cdot\text{mole.}$$

Equilibrium equation at 1298° K

$$-1246-1298\cdot 4.672+p\cdot 10^{-6}\,[5.47-3.47-0.6\cdot 5.47\cdot 0.07]=0$$

$$p=\frac{7.316}{1.77}\cdot 10^{6}=4130\cdot 10^{6}\ \mathrm{N/m^2}$$

or

$$p=42{,}200\ \mathrm{kp/cm^2}.$$

Heat content at 2300° K

At a temperature above 1300° K the specific heats C_1 and C_2 at normal pressure are not known from the literature. However, generally the specific heats of solid bodies at constant volume and not too low temperatures are about 3 R in accordance with the equipartition principle, though for some substances as graphite and diamond the specific heats not only at lower temperatures but also at room temperature are considerably lower. Some of the degrees of freedom are so to say frozen in. But very seldom one finds solid substances with a specific heat above 3 R or 6 cal/mole. The formulas give values of C_1 and C_2 in the neighbourhood of $T = 1300°$ K near to 6 cal/mole. Consequently the author makes the assumption that the values of the specific heats at constant volume of graphite and diamond above 1300° K go asymptotically to 6.

Generally the specific heats of solid substances at constant pressure are regarded equal to the values at constant volume. However, this is not true at all for a substance such as diamond with a very low compressibility and a relatively high coefficient of thermal expansion. Even for graphite the difference between the specific heats at constant volume and constant pressure must not be neglected.

Generally we have

$$C_p - C_v = \frac{\alpha^2 v T}{\beta}$$

where α is the coefficient of thermal expansion, β the coefficient of compression and v the mole volume.

For graphite we have at 2300° K according to the diagrams, Figs. 1 and 2,

$$\alpha = 2.7 \cdot 10^{-5}\ 1/°\mathrm{C}$$

$$\beta = 2.3 \cdot 10^{-11}\ \mathrm{m}^2/\mathrm{N}$$

$$v = 5.62 \cdot 10^{-6}\ \mathrm{m}^3/\mathrm{mole}$$

$$(C_p - C_v)_1 = 0.41\ \mathrm{joule}/°\mathrm{C} \cdot \mathrm{mole} = 0.1\ \mathrm{cal}/°\mathrm{C} \cdot \mathrm{mole}$$

For diamond we have

$$\alpha = 3.6 \cdot 10^{-5}\ 1/°\mathrm{C}.$$

According to BRIDGMAN the compressibility of diamond is 15 to 20 times smaller than that of graphite. We write

$$\beta = \frac{2.3 \cdot 10^{-11}}{18} = 1.28 \cdot 10^{-12}\ \mathrm{m}^2/\mathrm{N}$$

$$v = 3.57 \cdot 10^{-5}\ \mathrm{m}^3/\mathrm{mole}$$

Thus

$$(C_p - C_v)_2 = 8.40\ \mathrm{joule}/°\mathrm{C} \cdot \mathrm{mole}$$

$$= 2.0\ \mathrm{Cal}/°\mathrm{C}\ \mathrm{mole}$$

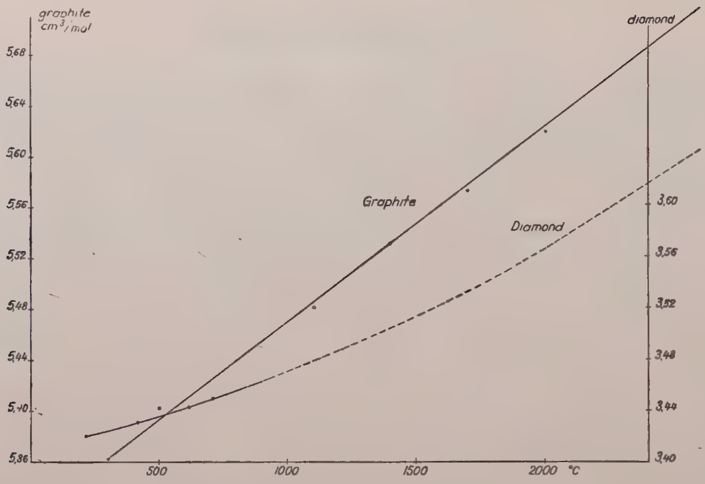

Fig. 1. Mole volume graphite–diamond.

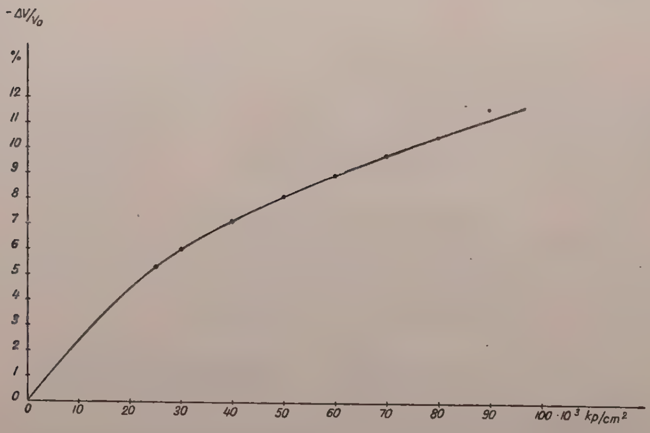

Fig. 2. Compression of Ceylongraphite (BRIDGMAN, P. Am. Acad. 76, 55, 1948).

With these values of $C_p - C_v$ the curves of C_1 and C_2 may be drawn up between 1300° K and 2300° K according to the diagram in Fig. 3.

We get by graphical integration

$$\int_{1298}^{2300} (C_1 - C_2)\, dT = -1335 \text{ Cal/mole} = -5600 \text{ joule/mole}$$

and

$$Q_{12} = -1246 - 5600 = -6846 \text{ joule/mole}$$

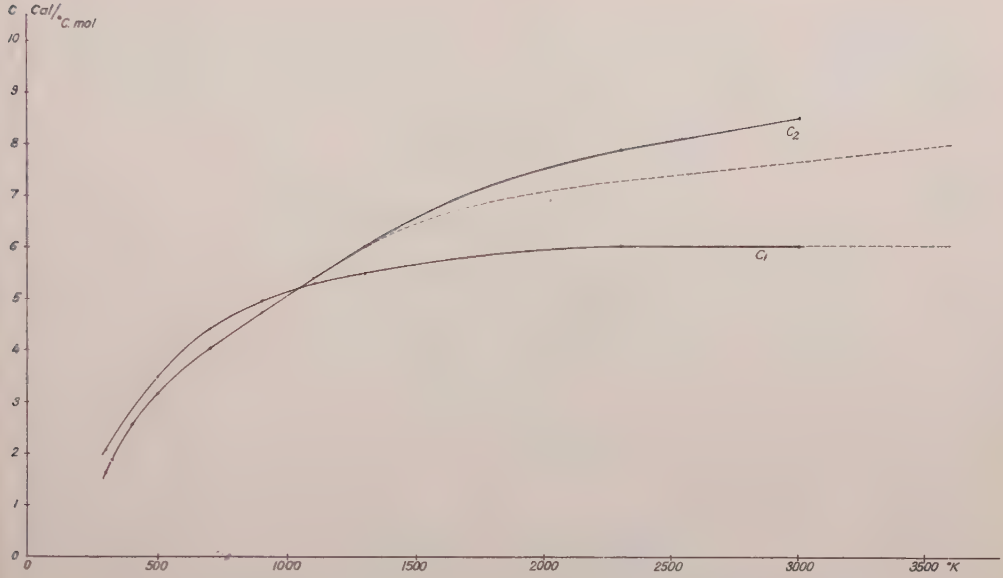

Fig. 3. Molar Specific heats at atmospheric pressure of graphite and diamond.

Entropy at 2300° K

$$(S_1 - S_2) = 4.672 + 4.19 \int_{1298}^{2300} \frac{C_1 - C_2}{T} \, dT$$

$$= 4.672 - 4.19 \cdot 0.727$$

$$= 1.63 \text{ joule}/{}^\circ\text{C} \cdot \text{mole}$$

Equilibrium equation at 2300° K

$$-6846 - 2300 \cdot 1.63 + p \cdot 10^{-6} [5.62 - 3.57 - 0.65 \cdot 5.62 \cdot 0.09] = 0$$

$$p = \frac{10{,}596}{1.72} \cdot 10^6 = 6125 \cdot 10^6 \text{ N/m}^2$$

$$= 62{,}500 \text{ kp/cm}^2.$$

Heat content at 3000° K

According to diagram 1 and 2 we have at 3000° K

$$(C_p - C_v)_1 = 0.12 \text{ Cal}/{}^\circ\text{C} \cdot \text{mole}$$

$$(C_p - C_v)_2 = 2.65 \text{ Cal}/{}^\circ\text{C} \cdot \text{mole}$$

The curves for C_1 and C_2 are drawn in accordance with this between 2300° K and 3000° K.

By graphical integration we get

$$\int_{2300}^{3000} (C_1 - C_2)\, dT = -6580 \text{ joule}$$

and

$$Q_{12} = -6846 - 6580 = -13{,}426 \text{ joule.}$$

Entropy at 3000° K

$$(S_1 - S_2) = 1.63 + 4.19 \int_{2300}^{3000} \frac{C_1 - C_2}{T}\, dT$$

$$= 1.63 - 4.19 \cdot 0.593$$

$$= -0.85.$$

Equilibrium equation at 3000° K

$$-13{,}426 + 3000 \cdot 0{,}85 + p \cdot 10^{-6}\,[5.73 - 3.66 - 0.65 \cdot 5.73 \cdot 0.09] = 0$$

$$p = \frac{10{,}936}{1.73} \cdot 10^6 = 6320 \cdot 10^6 \text{ N/m}^2$$

$$= 64{,}400 \text{ kp/cm}^2.$$

Heat content at 2600° K

$$\int_{2300}^{2600} (C_1 - C_2)\, dT = -2670 \text{ joule}$$

$$Q_{12} = -6846 - 2570 = -9416.$$

Entropy at 2600° K

$$S_1 - S_2 = 1.63 + 4.19 \int_{2300}^{2600} \frac{C_1 - C_2}{T}\, dT$$

$$= 1.63 - 4.19 \cdot 0.251$$

$$= +0.58.$$

Equilibrium equation at 2600° K

$$-9416 - 2600 \cdot 0.58 + p \cdot 10^{-6}\,[5.67 - 3.61 - 0.65 \cdot 5.67 \cdot 0.09] = 0$$

$$p = \frac{10{,}926}{1.73} \cdot 10^6 = 6320 \cdot 10^6 \text{ N/m}^2$$

$$= 64{,}400 \text{ kp/cm}^2.$$

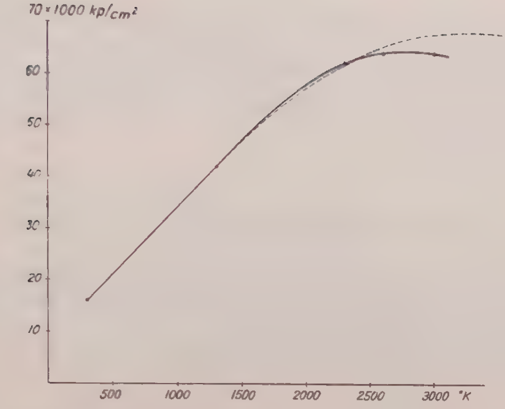

Fig. 4. Equilibrium pressure graphite–diamond.

The curve of the equilibrium pressure p as a function of T is given in the diagram, Fig. 4.

It may at first seem improbable that the equilibrium pressure has a maximum for a certain temperature. But one must remember that above 1050° K $C_2 > C_1$. Consequently the increase in $Q_{12} = \int (C_1 - C_2)\, dT$ above this temperature is negative. This tends to increase the pressure. But even the increase in the entropy difference $S_1 - S_2 = \int \frac{(C_1 - C_2)}{T}\, dT$ is negative. However, in the equilibrium equation $T\,(S_1 - S_2)$ is inserted with opposite sign and tends to diminish the pressure. Now the numerical value of $\int_{T_1}^{T_2} (C_1 - C_2)\, dT$ is obviously smaller than the numerical value of $T_2 \cdot \int_{T_1}^{T_2} \frac{C_1 - C_2}{T}\, dT$. Consequently the higher the temperature, the more the entropy will gain on the heat content, the pressure increase with temperature will diminish and the pressure will come to a maximum and begin to fall with the temperature. It is to be observed that the factor before p in the equation is approximately independent of temperature and pressure.

The curves of C_1 and C_2 above 1300° K are figured with the aid of certain physical constants. However, they are probably not far from reality. The calculated curves fit well with the empirical. The curve for diamond could hardly be drawn noticeably lower above 1300° K if it has to fit in with the empirical part of the curve. And this is based on careful measurements. It could possibly be drawn higher, for instance as a nearly straight line in the same direction as the empirical curve at 1300° K. This would mean that the compressibility of diamond would be even less than anticipated or the thermal expansion higher, or possibly that diamond shows anomalies even at high temperatures and has a $C_v > 6$ above about 1300° K. However, the result would only be that the maximum value of the equilibrium pressure would diminish to about 62,000 kp/cm² at about 2500° K. As another alternative the assumption is made that $C_p - C_v$

for diamond is less than calculated. C_2 is drawn in the diagram, Fig. 3, according to the dotted curve or as low as seems to be reasonably possible if it shall fit in with the empirical part of the curve. The consequences are shown by the dotted curve in the diagram, Fig. 4. The maximum equilibrium pressure will increase to 68500 kp/cm^2 at 3300 °K.

REFERENCES

1. F. D. Rossini and R. S. Jessup, Heat and free energy of formation of carbon dioxide, and of the transition between graphite and diamond. National Bureau of Standards, Research paper RP 1141, October 1938.
2. Spencer, Industrial Engineering Chemistry, Vol. 40, page 2150, 1948.
3. Kelly, Bulletin 371 U.S. Bureau of Mines 1934.

Tryckt den 16 juni 1955

Uppsala 1955. Almqvist & Wiksells Boktryckeri AB

ARKIV FÖR KEMI Band 8 nr 44

Read 13 April 1955

An investigation on caronic acid

By Arne Fredga and Åke Sikström

With 4 figures in the text

Optically active caronic acid has, in some cases, been obtained by oxidative degradation of natural products. The racemic acid has been resolved by Owen and Simonsen (1) using (+)- and (−)-nor-ψ-ephedrine; they found $[\alpha]_{5461} = +34.8°$ and $-34.5°$ respectively in ethanol solution. By ozonisation of (+)-*trans*-chrysanthemum acid, Staudinger and Ruzicka (2) obtained caronic acid having $[\alpha]_D^{19} = -33.3°$ (in absolute methanol). This is the highest value reported for acid from natural products, but owing to the difference in solvent and wave-length it is not directly comparable to the data of Owen and Simonsen (1).

The purpose of the present investigation was to determine the maximum activity for the acid under different conditions and to study the melting point diagram of the antipodes. The importance of this diagram for the identification of acid of lower activity obtained from natural products has already been pointed out by Gibson and Simonsen (3). It was also our intention to establish, if possible, the steric relation between caronic acid and terebic acid; the latter acid has already by one of us been related to the glyceraldehyde system (4) which is now known to represent the absolute configuration. In the meantime, this problem was solved by Crombie and Harper (5), who could convert (+)-chrysanthemum acid to (−)-terebic acid without disturbance of the asymetric center. The absolute configuration of (−)-caronic acid was thereby established.

As nor-ψ-ephedrine is not readily accessible, we tested different commercial alkaloids. The pure antipodes of caronic acid were easily obtained by the aid of (−)-ephedrine and quinine.

The rotatory power varies considerably with the solvent. It should be specially mentioned that the activity in absolute ethanol is about 8 % higher than in ordinary 96 % alcohol. The value found by us in the latter solvent is in good agreement with the data found by Owen and Simonsen "in alcohol" (1). In absolute methanol we found somewhat higher activity than Staudinger and Ruzicka (2), but as their value cannot be very accurate, the difference is probably not beyond the limits of error.

The melting points of racemic and active acid are nearly identical, 215° and 214.5° (corrected). The melting point diagram reveals the existence of a true racemic compound and two eutectic points at about 20 and 80 % of one antipode. The eutectic temperature lies at about 201° (Fig. 1).

The infrared absorption curves for active, racemic and *meso*-(*cis*)-acid in the crystalline state are given in Figs. 2–4. The spectra of the stereo-isomerides show

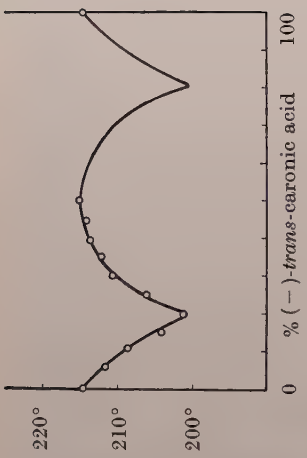

Fig. 1. Melting point diagram of the system (+)- and (−)-*trans*-caronic acid.

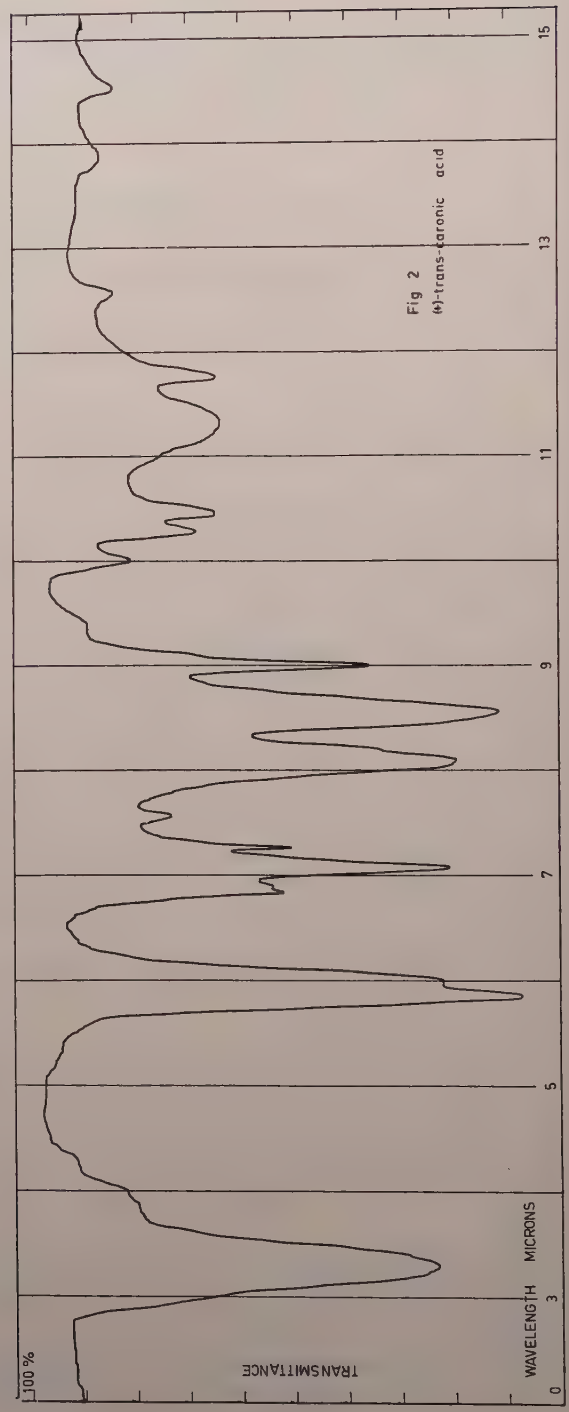

Fig 2
(+)-trans-caronic acid

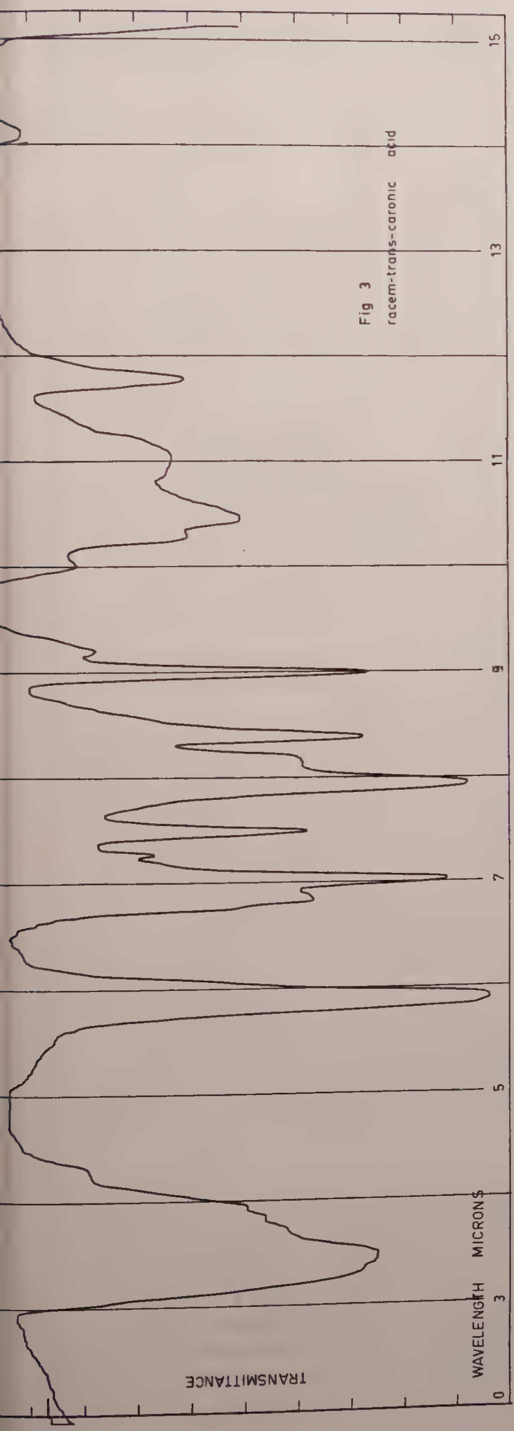

Fig 3
racem-trans-caronic acid

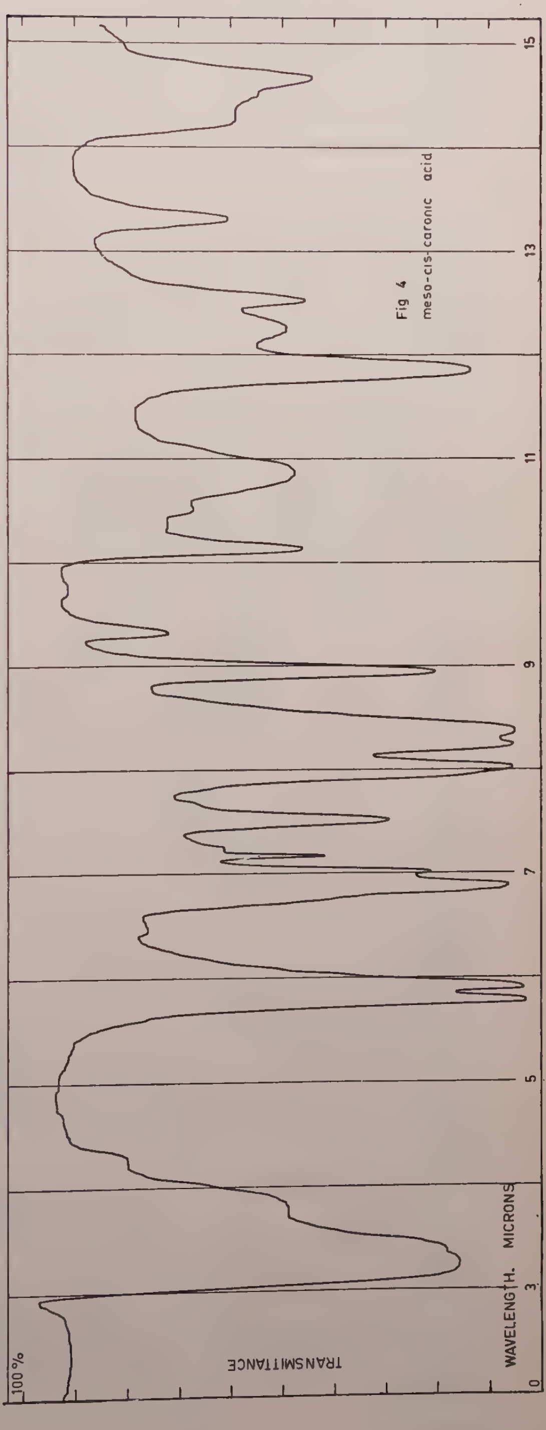

Fig 4
meso-cis-caronic acid

several obvious differences which will be discussed in detail elsewhere. Especially significant is the shape of the carboxyl band at about 5.8 μ; active and racemic acid have one strong band while that of the *meso*-acid is split up into two. A similar effect was reported by SCHOTTE and ROSENBERG for other pairs of cyclic racemic and *meso*-compounds (6).

Experimental

Preparation of racem-trans-*caronic acid.*—$\beta\beta$-Dimethylglutaric acid (obtained by oxidation of dimedone) was converted to anhydride and brominated. The crude product was treated with ethanol and the bromoester heated with potassium hydroxide in methanol solution. The different steps have been described by several authors (7–11), but the directions given are often brief and the yields rather small. In our experience, the following slightly modified procedure gives quite satisfactory results.

Dimedone (40 g) and potassium hydroxide (26 g) are dissolved in 250 ml water, the solution is refluxed for at least 5 minutes and cooled in ice water.

Bromine (160 g) is added to a mixture of ice and water (2000 g) in a 3 l beaker, and 50- % solution of sodium hydroxide is added with vigorous stirring till the colour of free bromine has disappeared; the solution is then pale yellow. A slight excess of sodium hydroxide is finally added.

The cool dimedone solution is then added dropwise to the hypobromite solution with efficient stirring in the course of about 25 minutes. The temperature is maintained at 0° by using an ice-salt bath. The reaction is completed when no precipitate is obtained if a sample of the solution is acidified with hydrochloric acid; if necessary some more sodium hydroxide and bromine are added. The excess of hypobromite is then destroyed by sodium sulphite, the solution is acidified with hydrochloric acid in excess and evaporated to about one third of its volume. It is then extracted with ether, the ether evaporated and the residue recrystallised from benzene. The yield of $\beta\beta$-dimethylglutaric acid is about 95 %.

In a 250 ml three-necked round-bottom flask fitted with thermometer, reflux condenser and dropping funnel are placed 89.9 g $\beta\beta$-dimethylglutaric acid and 90 ml thionyl chloride. Reaction starts with evolution of sulphur dioxide and hydrogen chloride. When the reaction slows down, the mixture is heated with reflux to 100° as long as gas is evolved. The excess of thionyl chloride is then distilled off under reduced pressure and bromine (90 g) is gradually added through the dropping funnel. The temperature is maintained at about 75° (radiator lamp) and the rate of the addition is so regulated that only minute amounts of bromine escape through the condenser (about 7 hours). Finally the solution is heated to 100° until the bromine colour has disappeared. It is then cooled and poured with stirring into 350 ml of absolute ethanol. The solution is heated to boiling for a short time and can be left to stand overnight.

About 200 ml of the ethanol are then distilled off and the still hot remaining solution is carefully added to 400 ml of a boiling 6-N methanol solution of potassium hydroxide. After refluxing for one hour, the alcohols are distilled of with gradual addition of water. At last the aqueous solution is cooled and acidified with sulphuric acid in excess. The caronic acid is extracted with ether. On evaporation of the ether solution about 39 g of crude acid are obtained. It is treated with norite and recrystallised from water yielding about 35 g of practically pure *trans*-caronic acid (39 % of the theory).

meso-(cis)-Caronic acid was prepared according to PERKIN and THORPE (10).

Preliminary experiments on resolution.—The common optically active bases were tested; as the acid is dibasic, two series of salts could be expected. The data are given in Tables 1 and 2; the best results were obtained if acid and base were brought together in the mole ratio 1:1. The rotatory power of the acid obtained from the salts was measured in ethanol.

Table 1.

Acid/base = 1 : 1

Base	Solvent	$[\alpha]_D^{25}$
(−)-Ephedrine	acetone	−15.1°
Strychnine	methanol	+26.5°
Brucine	methanol	+ 3.2°
Quinine	methanol	+27.1°

Quinidine, cinchonidine, α-phenyl-ethylamine and β-phenyl-*iso*propylamine gave no crystalline salts.

Table 2.

Acid/base = 1 : 2

Base	Solvent	$[\alpha]_D^{25}$
(−)-Ephedrine	acetone	− 9.7°
Strychnine	methanol	+14.8°
Brucine	methanol	+ 2.9°
Quinine	methanol	+ 1.6°

Quinidine and cinchonidine gave no crystalline salts.

The final resolution was carried out using (−)-ephedrine and quinine. 30.0 g (0.19 mole) *racem-trans*-Caronic acid and 35 g (0.19 mole) (−)-ephedrine were dissolved separately in 275 ml acetone +10 ml water, the two solutions were heated and mixed. After standing for some time at room temperature, the solution was left in a refrigerator for 48 hours. The salt obtained (32 g) was recrystallised several times from 96- % ethanol. The course of the resolution was tested on samples from the different crystallisations, from which the acid was liberated and examined in absolute ethanol (Table 3).

Table 3.

Crystallisation	1	2	3	4			7	8
ml solvent	570	160	150	110			61	47
g salt obtained	32.0	21.3	15.0	12.4			6.4	5.0
$[\alpha]_{5461}^{25}$	−23.6°	−35.3°	−35.7°	−37.5°			−37.4°	−37.6°

The mother liquor from the first crystallisation of the ephedrine salt was evaporated to dryness and the caronic acid liberated. 17.2 g having $[\alpha]_{5461}^{25} = +14.1^\circ$ (absolute ethanol) were obtained. This acid (0.109 mole) was dissolved with 35.3 g (0.109 mole) of quinine in 215 ml of boiling 96 % ethanol. The salt obtained after 48 hours in a refrigerator was recrystallised from the same solvent. As the salt was very sparingly soluble, it was dissolved by refluxing with a large volume of alcohol (given in brackets in the table) after which the solution was evaporated to a smaller volume and left to crystallise. The course of the resolution was tested as described above (Table 4).

Table 4.

Crystallisation	1	2	3			6
ml solvent	215	(600) 250	(510) 200			(450) 120
g salt obtained	31.3	24.9	21.5			13.3
$[\alpha]_{5461}^{25}$	$+35.7^\circ$	—	$+37.7^\circ$			$+37.7^\circ$

As the active acids were isolated with the aid of different alkaloids and the maximum activity remained constant during three or four recrystallisations af the salts, there can hardly be any doubt that they represent the pure enanthiomorphs. The alkaloid salts were not analysed, but the yields of liberated acid indicate that they contained acid and base in the ratio 1:1.

(−)-trans-*Caronic acid.*—The (−)-ephedrine salt (5.0 g) was decomposed with dilute sulphuric acid and the caronic acid was isolated by extraction with ether. After evaporation of the ether, the residue was recrystallised from water. The yield of pure acid was 1.5 g. It forms prisms or needles with m.p. 214.5° (corr.).

0.1213 g acid: 15.20 ml 0.1006-*N* NaOH.
$C_7H_{10}O_4$ (158.15) Equiv. wt. calc. 79.1, found 79.3.
0.4592 g acid dissolved in *absolute ethanol* to 10.00 ml: $2\,\alpha_{5461}^{25} = -3.44^\circ$. $[\alpha]_{5461}^{25} = -37.5^\circ$; $[M]_{5461}^{25} = -59.2^\circ$.

(+)-trans-*Caronic acid.*—The quinine salt (13.3 g) was decomposed as described above and the caronic acid recrystallised from water. The yield of pure acids was 4.1 g. In melting point and general appearance it was quite similar to the (−)-acid.

0.1164 g acid: 14.61 ml 0.1006-*N* NaOH.
$C_7H_{10}O_4$ (158.15) Equiv. wt. calc. 79.1, found 79.2.

The activity data are given in Table 5.

Table 5.

g = gram acid 10.00 ml solution

	g	$2\,\alpha_D^{25}$	$[\alpha]_D^{25}$	$[M]_D^{25}$	$2\,\alpha_{5461}^{25}$	$[\alpha]_{5461}^{25}$	$[M]_{5461}^{25}$
Ethanol (abs.)	0.3520	$+2.23^\circ$	$+31.7^\circ$	$+50.1^\circ$	$+2.65^\circ$	$+37.6^\circ$	$+59.5^\circ$
Ethanol (96 %)	0.3878	$+2.27^\circ$	$+29.3^\circ$	$+46.3^\circ$	$+2.68^\circ$	$+34.6^\circ$	$+54.6^\circ$
Methanol	0.3022	$+2.15^\circ$	$+35.6^\circ$	$+56.3^\circ$	$+2.55^\circ$	$+42.2^\circ$	$+66.7^\circ$
Acetone	0.3678	$+2.55^\circ$	$+34.7^\circ$	$+54.8^\circ$	$+3.03^\circ$	$+41.2^\circ$	$+65.1^\circ$
Dioxan	0.2762	$+1.52^\circ$	$+27.5^\circ$	$+43.5^\circ$	$+1.79^\circ$	$+32.4^\circ$	$+51.2^\circ$
Water	0.1551	$+0.58^\circ$	$+18.7^\circ$	$+29.7^\circ$	$+0.70^\circ$	$+22.6^\circ$	$+35.7^\circ$

Melting point diagram.—Weighed quantities of racemic and (+)-*trans*-caronic acid were mixed and dissolved in pure acetone, the acetone evaporated and the residue pulverised and dried over phosphorous pentoxide. The melting points were determined in an electrically heated apparatus (Phillips), calibrated with suitable test substances. The Kofler "Heiztisch-Mikroskop" technique could not be used owing to the rapid sublimation of the acid in the vicinity of the melting point. The determination in capillary tubes met with no difficulties; the same values were obtained in open and sealed tubes. The results are given in Fig. 1 and Table 6.

Table 6.

% (−)-acid	m.p.	% (−)-acid	m.p.
0.0	214.5°	30.1	210.5°
5.5	211.5°	34.9	212.0°
10.6	208.5°	39.1	213.5°
15.2	204.0°	44.8	214.0°
19.9	201.1°	50.0	215.0°
24.9	206.0°		

Infrared absorption spectra.—A Perkin-Elmer model 21 spectrophotometer equipped with sodium chloride prism was used. The solid samples of the acid were examined as pressed potassium bromide plates according to the method described by SCHIEDT and REINWEIN (12).

Solubility measurements.—Samples of the acids were shaken with water in a thermostat at 25°. Samples of the solutions were taken after 48 hours and titrated. The *meso*-(*cis*)acid was titrated as monobasic according to JONES and SOPER (13).

(+)-*trans*-Caronic acid: 9.98 ml saturated solution: 39.10 ml 0.0973-*N* NaOH. Solubility at 25°: 0.1906 mole/l = 30.1 g/l.

racem-*trans*-Caronic acid: 9.98 ml saturated solution: 22.19 ml 0.0973-*N* NaOH. Solubility at 25°: 0.1082 mole/l = 17.1 g/l.

meso-(*cis*)-Caronic acid. 4.64 ml saturated solution: 9.77 ml 0.1079-*N* NaOH (methyl red). Solubility at 25° 0.226 mole/l = 35.9 g/l.

Summary

racem-*trans*-Caronic acid has been resolved by a new procedure using (−)-ephedrine and quinine. The maximum activity found was $[\alpha]_{5461}^{25} = +37.7°$ and $-37.5°$ (in absolute ethanol). The rotatory power was measured at $\lambda = 5893$ ÅE and 5461 ÅE in different solvents. The melting point diagram of the antipodes shows the existence of a true racemic compound. Infrared spectra of active, racemic and *meso*-(*cis*)-acid are given.

The authors are indebted to Mr. A. ROSENBERG for valuable assistance and expert advice in connection with the infrared work. A grant from the *Nobel Fund of the Royal Academy of Sciences* (*Kemiska prisgruppens särskilda fond*) is gratefully acknowledged.

Laboratory of Organic Chemistry, Chemical Institute, University of Uppsala, March 1955.

REFERENCES

1. Owen, J. and Simonsen, J. L., J. Chem. Soc. *1933*, 1223.
2. Staudinger, H. and Ruzicka, L., Helv. Chim. Acta *7*, 201 (1924).
3. Gibson, C. S. and Simonsen, J. L., J. Chem. Soc. *1929*, 305.
4. Fredga, A., Svensk Papperstidn. *50*, Nr. 11B, 91 (1947).
5. Crombie, L. and Harper, S. H., J. Chem. Soc. *1954*, 470.
6. Schotte, L. and Rosenberg, A. To be published.
7. Walker, J. and Wood, J. K., J. Chem. Soc. *89*, 599 (1906).
8. Komppa, G., Ber *32*, 1423 (1899).
9. —— Ann. *368*, 135 (1909).
10. Perkin, W. H. and Thorpe, J. F., J. Chem. Soc. *75*, 48 (1899).
11. Ingold, C. K., J. Chem. Soc. *121*, 2676 (1922).
12. Schiedt, U. and Reinwein, H., Z. Naturforsch. *7 b*, 270 (1952).
13. Jones, I. and Soper, F. G., J. Chem. Soc. *1936*, 133.

Tryckt den 12 september 1955

Uppsala 1955. Almqvist & Wiksells Boktryckeri AB

ARKIV FÖR KEMI Band 8 nr 45

Communicated 27 April 1955 by ARNE FREDGA

3-Substituted thiophenes

A study in synthesis

By SALO GRONOWITZ

During the last six years a growing interest has arisen in 3-substituted thiophenes. Such compounds with pharmacological properties have been prepared especially by CAMPAIGNE and collaborators (1), and their activity compared with corresponding 2-substituted thiophene derivatives and benzene analogs.

In connection with an investigation of the aromatic character of 3-substituted thiophene compounds and especially differences between 2- and 3-substituted derivatives (2) and with an investigation of the optical activity of certain 3-substituted thiophene compounds (3), it has been of importance to work out new and convenient methods for the synthesis of such compounds and to make them more readily available. This is also of great preparative interest as it is possible to prepare otherwise difficultly available aliphatic compounds through desulphuration of thiophene compounds with Raney-nickel (4, 5, 6). Starting from 3-substituted thiophenes it is possible to synthesise aliphatic compounds with branched carbon chains.

CAMPAIGNE and his collaborators have exclusively prepared their 3-substituted derivatives through the side-chain bromination of 3-methylthiophene through N-bromosuccinimide with benzoylperoxide as a catalyst, a method which was discovered by them (7). The disadvantages of this method have earlier been discussed by the present author (8), who also has worked out a modification which gives more reproducible yields.

A more convenient variation of this method is to use instead of 3-methylthiophene, 2-bromo-3-methylthiophene, which is obtained in good yield in the bromination of 3-methylthiophene with N-bromosuccinimide using no catalyst. It may also be produced as a by-product in the bromination with catalyst. This compound can, as CAMPAIGNE (9) has found, be brominated in the side-chain with high yield and 2-bromo-3-thenylbromide is much more stable and less lachrymatory than 3-thenylbromide. It can be used as a starting material for 3-substituted thiophenes.

The present author has prepared 2-bromo-3-thenylsuccinic acid in an analogous way as earlier described for 3-thenylsuccinic acid (8). The bromine atom in this compound has been removed easily, conveniently and almost quantitatively by treatment with 5 % sodium amalgam in sodium carbonate solution. Halogen atoms may also conveniently be removed from the thiophene nucleus through catalytic dehalogenation with hydrogen over Pd catalyst (10) or in suitable cases with aluminium amalgam (11) in alcohol and ether or via the Grignard compound (12). *n*-Butyllithium is especially suitable for selective dehalogenation of an α-halogen, as the reaction can be carried out at such a low temperature that certain groups which otherwise react with organo-metal compounds do not interfere (13).

A route which seems quite appealing for the synthesis of 3-substituted thiophenes is to direct substitution into the 3-position by blocking the α-positions with easily removable groups. It is thus possible to acylate 2,5-dichlorothiophene in the 3-position (14). BLANCHETTE and BROWN (15) used this route for the preparation of 3-thiophenecarboxylic acid after having failed to brominate 3-methylthiophene in the side-chain after the method of CAMPAIGNE. They converted 2,5-dichloro-3-acetylthiophene via the haloform reaction to 2,5-dichloro-3-thiophenecarboxylic acid and then removed the chlorine with hydrogen over palladium catalyst. CAMPAIGNE and BOURGEOIS have recently found that lithium aluminium hydride eliminates halogen from the thiophene nucleus (16). It should thus be possible to convert 2,5-dichloro-3-acetylthiophene in one step to 1-(3-thienyl)-ethanol, which is a useful starting material for certain 3-substituted thiophenes. This compound may of course also be prepared through the reaction of 3-thienyllithium with acetaldehyde and has recently been synthesised through the reaction of 3-thiophenemagnesium bromide and acetaldehyde (17).

It is not suitable to block the α-positions with bromine, since, under the conditions of the FRIEDEL-CRAFTS reaction, acylation partially takes place in the α-position with replacement of bromine (18).

Attempts have earlier been made to prepare the useful chloromethyl compounds by means of chloromethylation of 2,5-dibromo- and 2,5-dichlorothiophene. CLARC *et al.* (19) have reported that they obtained 11 % of the chloromethyl derivative of 2,5-dichlorothiophene, and that 2,5-dibromothiophene did not react under the same conditions as used for thiophene. In his book *Thiophene and its Derivatives* HARTOUGH (20), however, mentions as an unpublished result that he and NORRIS have been able to chloromethylate the above-mentioned halothiophenes with 50 % yield using aqueous formaldehyde and hydrochloric acid at 60°. A similar statement appears in a recent patent by NORRIS (21). The present author, however, in spite of repeated experiments, has not been able to reach their yields. Even when the time of reaction was prolonged to 24 hours, most of the halothiophenes were recovered unchanged and the yield of the chloromethyl derivative was 10 to 15 %. The statement of HARTOUGH (20) that the reactivity of 2,5-dibromo- and 2,5-dichlorothiophene is comparable with that of mesitylene seems in any case to be an overestimation of the reactivity of the first-mentioned compounds.

HALVARSSON and MELANDER (22) have found that in hydrogen-exchange, which is an electrophilic substitution, the 2-position of thiophene is about 1000 times as reactive as the 3-position. Further VAVON *et al.* (23) found in their kinetic investigation of the chloromethylation with chloromethyl methyl ether in acetic acid, that halogen substitution decreases the reaction velocity very strongly. Thus mesitylene reacts 600 times faster than benzene, but chloromesitylene only two times faster than benzene. From these approximate calculations it may be inferred that 2,5-dichlorothiophene should be chloromethylated about 300,000 times slower than thiophene. As LAUER (24) has found that benzene is brominated about 20,000 times slower than thiophene the conclusion may be reached that 2,5-dichlorothiophene is chloromethylated at the most as rapidly as benzene. In an experiment under the same conditions under which VAVON *et al.* (23) had obtained 80 % of chloromethyl mesitylene, only traces of 2,5-dibromochloromethylthiophene were obtained and the rest of the 2,5-dibromothiophene was recovered unchanged.

Another complication in the chloromethylation of 2,5-dibromothiophene seems to be that chloromethylation also occurs to some extent in the 2-position with elimination of the bromine as in the acylation of 2,5-dibromothiophene. In an experiment in which the crude chloromethylated product was reacted with sodium ethyl ethane-1.1.2-tricarboxylate and the ester saponified and decarboxylated and the so obtained bromo-substituted thenylsuccinic acid dehalogenated a mixture of 2- and 3-thenylsuccinic acid was obtained, which could be identified by its melting point and by its infra-red spectrum which showed the absorption bands of both 2- and 3-thenylsuccinic acid. The infra-red spectrum of the 2,5-dibromothiophene used showed it to be essentially free from 2,3-dibromothiophene.

It was however possible to chloromethylate 2,5-dichlorothiophene under the conditions used by SOMMELET (25) for the chloromethylation of benzene. 2,5-Dichlorothiophene could be chloromethylated in good yield with chloromethyl methyl ether in carbon disulphide solution using stannic chloride as a catalyst. No unchanged 2,5-dichlorothiophene was recovered. A small higher boiling fraction was obtained, which probably is a mixture of the dichloromethylated product and the dithienylmethane derivative. The reaction is most probably of the FRIEDEL-CRAFTS type. The primarily formed 2,5-dichlorothenylether is cleaved by hydrogen chloride to 2,5-dichloro-3-thenylchloride and methanol. Probably 2,5-dichlorothiophene may also be chloromethylated according to the method of BLANC (26).

2,5-Dichloro-3-thenylchloride was converted in the usual manner to 2,5-dichloro-3-thenylsuccinic acid via a modified malonic ester synthesis with ethyl ethane-1.1.2-tricarboxylate. It could be converted to 3-thenylsuccinic acid by treatment with 5 % sodium amalgam.

It is possible to convert 2,5-dichloro-3-thenylchloride into 2,5-dichloro-3-thiophenecarboxaldehyde which also is a very useful intermediate. CAMPAIGNE *et al.* (27) obtained this aldehyde in 59 % yield by the SOMMELET reaction of 2,5-dichloro-3-thenylbromide, which they synthesised by chlorinating 3-methylthiophene to 2,5-dichloro-3-methylthiophene and brominating it in the side-chain with N-bromosuccinimide.

By blocking the reactive α-positions, thiophene compounds are stabilised and their tendency to polymerization diminished, making it thus possible to carry out reactions under more vigorous conditions (strongly acid medium) than with the corresponding unblocked 3-substituted thiophenes.

A third more direct route to 3-substituted thiophenes, which has been worked out by the present author, goes over 3-thienyllithium which is obtained through halogen-lithium interconversion between 3-bromothiophene and *n*-butyllithium (28) at low temperature. 3-Bromothiophene is easily available via the Grignard reaction of 2,3,5-tribromothiophene (29). Previously 3-thiophenecarboxylic acid has been synthesised from 3-thienyllithium and carbon dioxide. Now also 3-thiophenecarboxaldehyde has been obtained through the reaction of 3-thienyllithium with N,N-dimethylformamide and 2-(3-thienyl)-ethanol through the reaction with ethylene oxide. 3-Thiophenecarboxaldehyde has earlier been prepared by CAMPAIGNE and LESUER (7) through the SOMMELET reaction with 3-thenylbromide.

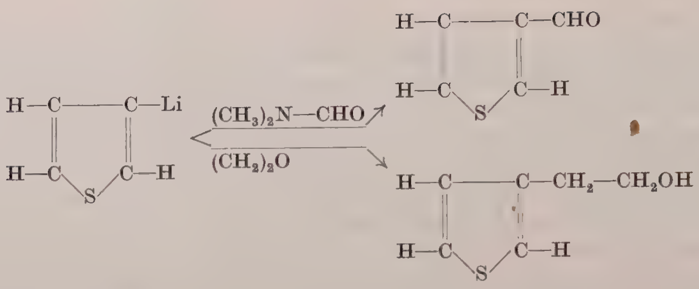

3-Thiophenecarboxaldehyde was condensed with ethyl malonate to ethyl 3-thenalmalonate which with 2 moles of potassium cyanide gives 2-(3-thienyl)-2-cyanopropionic acid, which was hydrolysed by boiling with water to 3-thienylsuccinic acid.

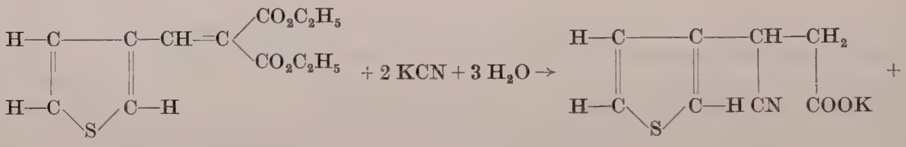

$+ KHCO_3 + 2\ C_2H_5OH + HCN.$

This acid is of interest in connection with the study of optically active 3-substituted derivatives of thiophene.

This method is especially useful for the preparation of 3-substituted derivatives containing an easily reducible group, which will not be stable under the conditions of dehalogenation.

Experimental

2-Bromo-3-thenylbromide.—This compound was, with some slight modifications, prepared according to the method of CAMPAIGNE and LESUER (9). To a refluxing solution of 44 g (0.25 moles) 2-bromo-3-methylthiophene and 0.5 g of benzoylperoxide in 175 ml of carbon tetrachloride a mixture of 44 g (0.25 moles) of N-bromosuccinicimide, purified according to CHAPMAN and WILLIAMS (30) and 0.5 g of benzoylperoxide was added through a short wide-bore condenser in small portions as rapidly as the vigorously refluxing solution allowed. After refluxing for three hours, the reaction mixture was cooled and filtered. The carbon tetrachloride was removed *in vacuo* and the residue fractionated, yielding 45 g (71 %) of 2-bromo-3-thenylbromide b.p. 88°–90° (4 mm Hg), which is much more stable than 3-thenylbromide and less lachrymatory.

Ethyl 1.(2-bromo-3-thenyl)ethane-1.1.2-tricarboxylate.—In a tree-necked flask fitted with a stirrer a dropping funnel and a reflux condenser with a calcium chloride tube, 4.1 g (0.18 moles) of sodium was dissolved in 175 ml of absolute ethanol and 44 g (0.18 moles) of ethyl ethane-1.1.2-tricarboxylate (31) was added. 45 g (0.18 moles) of 2-bromo-3-thenylbromide was added dropwise with stirring and after refluxing for four hours the mixture was neutral. The greater part of the alcohol was distilled off and the reaction product washed with water. The ester was extracted with ether, dried and fractionated *in vacuo*. The fraction boiling between 195°–202° (4 mm Hg) was taken as ethyl 1.(2-bromo-3-thenyl)ethane-1.1.2-tricarboxylate. The yield was 61 g (82 %).

2-Bromo-3-thenylsuccinic acid.—61 g (0.145 moles) of the ester was saponified by refluxing with 45 g (0.8 moles) of potassium hydroxide in a mixture of 350 ml of alcohol and 50 ml of water under nitrogen atmosphere to avoid darkening of the solution. The alcohol was distilled off and water added. After acidification with hydrochloric acid in excess the 1.(2-bromo-3-thenyl)ethane-1.1.2-tricarboxylic acid was extracted with ether and the ether evaporated yielding 47 g (96 %) of the acid. It decomposes under carbon dioxide evolution when heated above 140° and was not further investigated. It was converted to 2-bromo-3-thenylsuccinic acid by heating it in an oil-bath at 145° until the evolution of carbon dioxide had ceased. The acid was recrystallised several times from water. Yield 40 g (98 %) m.p. 127°–128°.

Anal. 0.06290 g: 8.90 ml 0.04802-*N* NaOH; — 0.02495 g: 4.40 ml 0.01956-*N* $Hg(NO_3)_2$.

$C_9H_9BrO_4S$ (293.1) calc. Equiv. wt. 146.5 Br 27.28
found ,, ,, 147.1 ,, 27.57

3-Thenylsuccinic acid.—4.9 g of 2-bromo-3-thenylsuccinic acid was dissolved in 50 ml Nsodium carbonate solution and treated with 5 % sodium amalgam for 24 hours at room temperature. The solution was decanted and the mercury washed with sodium carbonate solution. The solution was acidified with hydrochloric acid precipitating 3.0 g (84 %) of 3-thenylsuccinic acid. The acid was recrystallised once from water m.p. 136°. It was in every respect identical with an autentic sample of 3-thenylsuccinic acid (8).

2,5-Dichloro-3-thenylchloride.—26 g (0.17 moles) of 2,5-dichlorothiophene and 16 g (0.20 moles) of chloromethyl methyl ether were dissolved in 50 ml of carbon disulphide and cooled in an ice-salt mixture. 15 g (0.06 moles) of stannic chloride was added dropwise. The ice bath was removed after one hour and the mixture, in which two liquid phases had separated, was allowed to stand at room temperature for two hours and was then poured on ice water. The organic phase was separated and extracted several times with water. It was then dried, the carbon disulphide distilled off and the residue fractionated *in vacuo* yielding 19 g (55 %) of 2,5-dichloro-3-thenylchloride b.p. 107°–110° (14 mm Hg). A higher boiling residue amounting to six grams was not further examined.

2,5-Dichloro-3-thenylsuccinic acid.—The malonic ester synthesis using 1.14 g (0.050 moles) of sodium 12.3 g (0.050 moles) of ethyl ethane-1.1.2-tricarboxylate and 10.0 g (0.050 moles) of 2,5-dichloro-3-thenylchloride was carried out as described above. The reaction mixture was then hydrolysed with 16 g (0.29 moles) of potassium hydroxide without isolation of the ester. After acidification with hydrochloric acid in excess the 1.(2,5-dichloro-3-thenyl)ethane-1.1.2-tricarboxylic acid was extracted with ether. After removing the ether the acid was decarboxylised by refluxing with 50 ml of water. On cooling 11 g (78 %) of 2,5-dichloro-3-thenylsuccinic acid deposited as an oil, which crystallised on standing. The acid was recrystallised several times from a mixture of petrol and ethyl acetate from which it crystallises in white needles. M.p. 105°–106°.

Anal. 0.09068 g: 8.65 ml 0.07336-*N* NaOH; — 0.02733 g: 9.85 ml 0.01956-*N* $Hg(NO_3)_2$.

$C_9H_8Cl_2O_4S$ (283.1) calc. Equiv. wt. 141.5 Cl 25.05
found ,, ,, 142.9 ,, 25.00

3-Thenylsuccinic acid.—2.2 g of 2,5-dichloro-3-thenylsuccinic acid was treated with 5 % sodium amalgam in the same way as described above for 2-bromo-3-thenylsuccinic acid. The procedure had to be repeated twice in order to remove the halogen completely. Yield 1.3 g (78 %) m.p. 133°–135°. It gave no melting point depression with an authentic sample of 3-thenylsuccinic acid.

3-Thiophenecarboxaldehyde.—To a solution of 0.40 moles of *n*-butyllithium in 250 ml of ether cooled to −70° in a Dry Ice-acetone mixture and in a nitrogen atmosphere, 56 g (0.35 moles) of 3-bromothiophene in 100 ml of absolute ether, also cooled to −70°, was added in a slow stream under vigorous stirring. The mixture was stirred for an additional five minutes and rapidly transferred under nitrogen to a dropping funnel and in a slow stream added to a stirred solution of 40 g (0.6 moles) of N,N-dimethylformamide in 200 ml of absolute ether. It was allowed to stand overnight and then poured on ice water. The ethereal layer was extracted twice with dilute hydrochloric acid, with dilute bicarbonate solution and with water, dried and fractionated yielding 27 g (70 %) of 3-thiophenecarboxaldehyde b.p. 86°–87° (20 mm Hg). *2,4-dinitrophenylhydrazone* m.p. 235°–237°, *phenylhydrazone* m.p. 137°–138° *acid* m.p. 138°–139°. The melting points in the literature are 236°–237° (7), 138° (32) and 138°–139° respectively.

Its infra-red spectrum which has been published earlier (2) is free from the caracteristic absorption maxima of 2-thiophenecarboxaldehyde.

2-(3-Thienyl)-ethanol.—A solution of 3-thienyllithium at −70° prepared as above from 0.35 moles of *n*-butyllithium in 230 ml of ether and 51.5 g (0.32 moles) of 3-bromothiophene in 100 ml of absolute ether was rapidly transferred to a dropping funnel and rapidly added to a stirred solution of 20 g (0.5 moles) of ethylene oxide in 50 ml of absolute ether. The solution was allowed to stand for four hours and was then refluxed for two hours and decomposed by pouring on dilute hydrochloric acid. The ether phase was separated, washed with water, dried and fractionated yielding 11.2 g (28 %) of 2-(3-thienyl)-ethanol. B.p. 110°–111° (14 mm Hg).

Phenylurethane M.p. 75.5°–76.5°.

Anal. 0.03105 g: 0.07149 g CO_2 and 0.01484 g H_2O; 0,01800: 0.007184 g H_2SO_4.

$C_{13}H_{13}O_2SN$ (247.3) calc. C 63.13 H 5.30 S 12.97
found ,, 62.83 ,, 5.34 ,, 13.06

Ethyl 3-thenalmalonate.—26.5 g (0.24 moles) of 3-thiophenecarboxaldehyde, 38.9 g (0.24 moles) of ethyl malonate, 3.5 ml of piperidine, 0.7 g of benzoic acid and 140 ml of benzene were boiled in a flask fitted with a water separator connected to a reflux condenser. Heating was continued for six hours when the formation of water had ceased. After cooling, the residue in the flask was washed with water with dilute hydrochloric acid and finally with a saturated solution of sodium bicarbonate. The organic mixture was dried, the benzene removed by distillation and the residue fractionated *in vacuo*, yielding 46 g (77 %) of ethyl 3-thenalmalonate b.p. 148°–150° (3 mm Hg).

3-Thienylsuccinic acid.—To the hot stirred solution of 18.0 g (0.07 moles) of ethyl 3-thenalmalonate in 300 ml of 95 % alcohol in a nitrogen atmosphere is added 9.3 g (0.14 moles) of potassium cyanide dissolved in 30 ml of water. After a few minutes potassium bicarbonate began to separate and the mixture was refluxed for five hours. The solution was filtered and the precipitate washed with ethanol. The ethanol was removed by distillation during which some water was added from time to time to prevent evaporation to dryness. When all the ethanol was removed the residue was made slightly acid with hydrochloric acid and refluxed for one and a half hour with decolourising charcoal added. After filtering and cooling, 11.7 g (83 %) of 3-thienylsuccinic acid separated. The acid crystallises from water in white plates. M.p. 172°–173.5°.

Anal. 0.06941 g: 9.41 ml 0.07325-*N* NaOH; — 0.02941 g: 0.01425 g H_2SO_4.

$C_8H_8O_4S$ (200.2)	calc.	Equiv. wt.	100.1	S	16.01
	found	,, ,,	100.6	,,	15.83

Summary

Three different routes have been used for the synthesis of 3-substituted thiophenes:

1) The side-chain bromination of 3-methylthiophene and 2-bromo-3-methylthiophene.

2) The chloromethylation of 2,5-dichlorothiophene.

3) The halogen-lithium interconversion between 3-bromothiophene and *n*-butyllithium.

I wish to express my sincere gratitude to Professor ARNE FREDGA, who has introduced me to the fascinating field of thiophene chemistry, for his kind interest in my work and for many stimulating discussions. I am also indebted to Mr. R. ÖHBERG for the analyses and to Mr. S. BERGVALL for taking the IR spectra referred to in the discussion.

Department of Organic Chemistry, Chemical Institute, University of Uppsala, April 1955.

REFERENCES

1. CAMPAIGNE, E. and MONROE, P. A., J. Am. Chem. Soc. *76,* 2447 (1954).
2. GRONOWITZ, S. and ROSENBERG, A., Arkiv Kemi *8,* 23 (1955).
3. GRONOWITZ, S. and LARSSON, S., Arkiv Kemi (in print).
4. HANSEN, S., Acta Chem. Scand. *8,* 695 (1954).
5. BADGER, G. M., RODDA, H. J., and SASSE, W. H. F., J. Chem. Soc. *1954,* 41.
6. SY, M., BUU-HOI, N. P., and DAT-XUONG, N., Compt. rend, *239,* 1224 (1954).
   BUU-HOI, N. P., SY, M., and DAT-XUONG, N., Compt. rend. *240,* 785 (1955).
7. CAMPAIGNE, E. and LESUER, W. M., J. Am. Chem. Soc. *70,* 1555 (1948).
8. GRONOWITZ, S., Arkiv Kemi *6,* 283 (1953).
9. CAMPAIGNE, E. and LESUER, W. M., J. Am. Chem. Soc. *71,* 333 (1949).
10. MOZINGO, R. *et al.*, J. Am. Chem. Soc. *67,* 2092 (1945).
11. RINKES, I. J., Rec. trav. chim. *55,* 991 (1936).
12. STEINKOPF, W., JACOB, J., and PENZ, H., Ann. *512,* 136 (1934).
13. GRONOWITZ, S., Arkiv Kemi *8,* 87 (1955).
14. BACHMAN, G. B. and HEISEY, L. V., J. Am. Chem. Soc. *70,* 2378 (1948).
15. BLANCHETTE, J. A., and BROWN, E. V., J. Am. Chem. Soc. *73,* 2779 (1951).
16. CAMPAIGNE, E. and BOURGEOIS, R. C., J. Am. Chem. Soc. *76,* 2445 (1954).
17. TROYANOWSKY, C., Bull. soc. chim. France *1955,* 424.
18. GATTERMAN, L. and RÖMER, M., Ber. *19,* 688 (1886).
19. CLARC, J. H. *et al.*, J. Org. Chem. *14,* 216 (1949).
20. HARTOUGH, H. D., Thiophene and its Derivatives. New York 1952, p. 188.
21. NORRIS, H. D., U.S. 2,623049. C.A. *47,* 9365 (1953).
22. HALVARSON, K. and MELANDER, L., Arkiv Kemi *8,* 29 (1955).
23. VAVON, G., BOLLE, J., and CALIN, J., Bull. soc. chim. France *1939,* 1025.
24. LAUER, K., Ber. *69,* 2618 (1936).
25. SOMMELET, M., Compt. rend. *157,* 1443 (1913).
26. BLANC, G., Bull. soc. chim. France [4] *33,* 313 (1923).

27. Campaigne, E. *et al.*, J. Am. Chem. Soc. *75*, 988 (1953).
28. Gronowitz, S., Arkiv Kemi *7*, 361 (1954).
29. Gronowitz, S., Arkiv Kemi *7*, 267 (1954).
30. Chapman, N. B. and Williams, J. F. A., J. Chem. Soc. 1952, 1044.
31. Bischoff, C. A., Ann. *38* (1882).
32. Steinkopf, W. and Schmitt, H. F., Ann. *533*, 264 (1938).

Tryckt den 12 september 1955

Uppsala 1955. Almqvist & Wiksells Boktryckeri AB

ARKIV FÖR KEMI Band 8 nr 46

Communicated 1 June 1955 by ARNE WESTGREN and J. ARVID HEDVALL

Some aspects on the stannic oxide–zinc oxide powder reaction

By V. ALEIXANDRE and A. G. VERDUCH

With 7 figures in the text

As far as we know not much work has been done in order to elucidate the formation mechanism and properties of zinc orto-stannate, the main investigations performed on this compound being those concerning its structure and cationic distribution among the interstices provided by the cubic arrangement of its oxygen ions.

The zinc orto-stannate has a spinel structure of the type $M^{4+}\ M_2^{2+}\ O_4^{2-}$, and its cubic unit cell, of 8.667 Å (1) contains eight molecular groups, the composition being therefore: 8 Sn^{4+}, 16 Zn^{2+}, 16 O^{2-}.

The recent studies of VERWEY and HEILMANN (2) have thrown much light on the structure of zinc orto-stannate since they have been able to classify this compound as belonging to the "inverse" type of spinel structure. They have suggested the formula $Zn_8\ (Sn_8\ Zn_8)\ O_{32}$, in which a difference is made between cations occupying either the tetrahedral positions or the octahedral ones. The strong ability of Zn^{2+} ions to form four equivalent tetrahedral bonds (3) makes the eight available tetrahedral spaces to be occupied by the corresponding Zn^{2+} ions, the remaining ones, together with the eight stannic ions, being located in the available octahedral positions.

The purpose of this paper has been to determine the formation rate of the zinc orto-stannate at different temperatures as well as to elucidate the main direction of the matter transfer during the reaction.

Experimental

Taking into consideration the important role played by the physical purity of the original components in a solid state reaction, we decided to prepare by ourselves both the zinc oxide and the stannic oxide, in order to secure the reproducibility of the results.

The *zinc oxide* was prepared by heating $Zn(C_2H_3O_2)_2 \cdot 2\ H_2O$ (Merck, analytical reagent) at 300°C, during 24 hours, in air atmosphere. After this thermal treatment, the product was carefully ground and then reheated for another 24 hours at the same temperature. The second heating permitted a complete combustion of the remaining carbon particles.

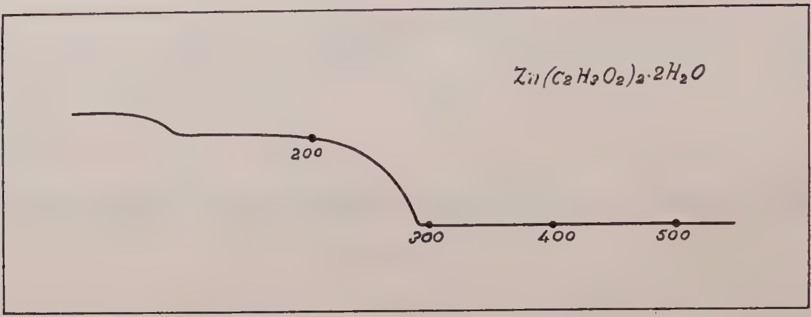

Fig. 1. — Decomposition of zinc acetate.

The choice of the lowest heating temperature was made according to the thermoponderogram of zinc acetate (Fig. 1).

By this method of preparation it was possible to obtain samples of zinc oxide very finely sized and showing a very high specific surface.

Samples of zinc oxide prepared by NATTA and CORRADINI (4) using a similar method showed an average size of particles of $2.5 \times 10^{-2}\ \mu$.

Though it is a very well known process, we tried to show once more the recrystallization of zinc oxide, using "indigo carmin" as an adsorbate. The raw zinc oxide (heated at 300°C) adsorbs 11.24 mg/g of this dye, while the same oxide heated to 800°C only adsorbs 0.62 mg/g. In both cases a solution of 200 mg/liter was used.

The *stannic oxide* was prepared by heating stannous oxide at 1100°C, during 15 hours, in air atmosphere, the stannous oxide being previously prepared from stannous chloride by ordinary chemical methods.

By microscopic analysis it was possible to ascribe to the SnO_2 particles an average radius of about 10 μ. That means a surface of 4.3×10^2 cm² g⁻¹, if spherical particles are considered.

From the great differences of particle size between both oxides ($\bar{r}_{SnO_2} \simeq 10\ \mu$; $\bar{r}_{ZnO} \simeq 1.3 \times 10^{-2}\ \mu$) it can be assumed, at a first approximation, that the large stannic oxide particles were completely surrounded by the small particles of zinc oxide, the original reaction interface being therefore that of the stannic oxide (4.3×10^2 cm² g⁻¹).

Using a powder mixture of both oxides (molar ratio SnO_2/ZnO equal to 1:2) pellets of 12 mm diameter and 3–4 mm thickness, were pressed, the only binder added before pressing being a small amount of distilled water (about 5 %).

After the pellets were dried at 110°C, we could start with the experiments.

The pellets were heated at constant temperature for increasing periods, the largest one being 70 hours approximately. In all cases the pellets were rapidly cooled from the heating temperature to room temperature.

By chemical and roentgenographic methods it was possible to demonstrate that both the formed zinc orto-stannate and the remaining stannic oxide were practically insoluble in an acid solution of 3 ml HNO_3 ($d = 1.33$) in 100 ml distilled water, whilst the ZnO (even heated at 1200°C) was rapidly dissolved in such a solution. These differences of solubility gave us an easy method to follow the yield of the reaction.

From the reaction yield, derived from gravimetric determinations, and the original reaction surface it can easily be calculated the reaction yield referred to as $SnZn_2O_4$

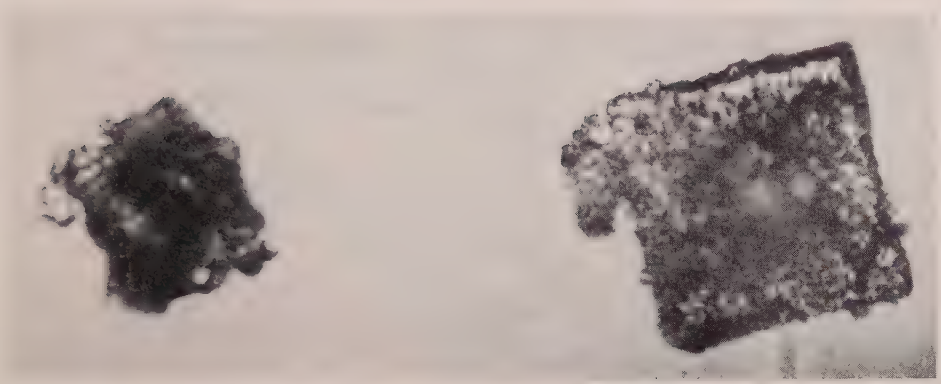

Fig. 2.

mol.cm^{-2}. This calculation is at least valid for the early stages of the reaction, in which the original reaction surface remains practically unchanged. In Fig. 3 the reaction yield is plotted against heating time for different constant temperatures.

Besides the reaction yield measurements we have also tried to show the volume expansion of the reacting mixture as a function of time at constant temperature.

A second series of experiments includes the measurement of the apparent specific weight as a function of temperature at a constant time of heating. Both series of experiments have been carried out using a mercury volumeter, previously described by the authors (5).

In order to obtain a sample of pure zinc orto-stannate the following method was developed: A thoroughly ground mixture of the reactants, SnO_2 and ZnO, in a molar ratio of 1:2.5, was kept to a temperature of 1190°C for 40 hours and then slowly cooled to the room temperature at an approximate rate of 5 degrees per hour. The remainder ZnO was dissolved using the above-mentioned acid solution. After the product was carefully washed with distilled water it was allowed to dry in an oven at 110°C.

The microscopic study of the zinc orto-stannate formed by this method shows a great majority of imperfect crystals as could be expected from a process of solid state reaction. But besides, owing to the large period of growth and slow rate of cooling, some of the crystals have freely grown and show a large size and a rather good cubic habit, as can be seen in Fig. 2.

The zinc orto-stannate thus obtained has a pycnometric density of 6.24, while the crystallographic density calculated on the basis of a unit cell of 8.667 Å (1) has a value of 6.36.

The X-ray examination of the reaction product clearly shows that the only new compound formed in the reaction is the zinc orto-stannate.

The diagram of the reaction product at 995°C (69 hours of heating) corresponds to a mixture of $SnZn_2O_4$, SnO_2 and ZnO. After extraction with dilute nitric acid the X-ray examination only shows the presence of $SnZn_2O_4$ and SnO_2.

Discussion

Before we started with our systematic studies of the reaction yield as a function of temperature, we had the opportunity to demonstrate that the reaction rate at temperatures below 900°C is extremely low and therefore is not worth while to in-

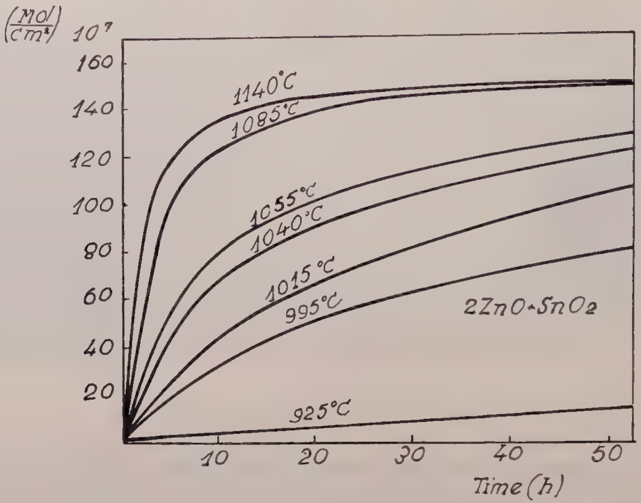

Fig. 3. — The formation rate of zinc orto-stannate by solid state reaction.

vestigate. On the other hand, the velocity of reaction at 1140°C is as high as to give reaction yields over 90 % in a few hours. Therefore we chose both these temperatures as the limits of our experiments.

The experiment at 925°C gives a yield graphic very close to a straight line (see Fig. 3).

The curvature of the isotherms increases as the temperature raises. In each curve two almost linear parts can be distinguished; the first one having a more pronounced slope than the second one. This means that the reaction progresses at first very rapid, the speed being lowered after a few hours of reaction.

In the first stage of the reaction the grains of stannic oxide and zinc oxide are in mutual contact. After a layer of stannate has been built up between the original grains, the diffusion of the mobile ions through this layer starts to play a role. The rate of the reaction depends at this stage on the rate of diffusion through the newly formed compound.

For the calculation of the activation energy of the reaction we have only taken into consideration the first process, in which the thickness of the zinc orto-stannate layer is still negligible.

On the assumption that the initial part of the isotherms is representative for the velocity of reaction, we have calculated from them the reaction velocity constants for each temperature.

The experimental values of the function $\log k = f\,(1/T)$ can be represented by a straight line, from which a value of 74,700 cal/mol. for the activation energy of the process can be calculated. The preexponential coefficient of the Arrhenius equation is 6.6×10^2 mol.cm^{-2} sec^{-1}.

By means of radiotracer methods, LINDNER (6) has found a value of 74,000 cal/mol. for the activation energy of the self-diffusion of Zn^{2+} ions through ZnO.

This similarity between the activation energy of the reaction and that of the self-diffusion of Zn^{2+} ions through ZnO can probably be due to the fact that the reaction is mainly governed by the self-diffusion of Zn^{2+} ions.

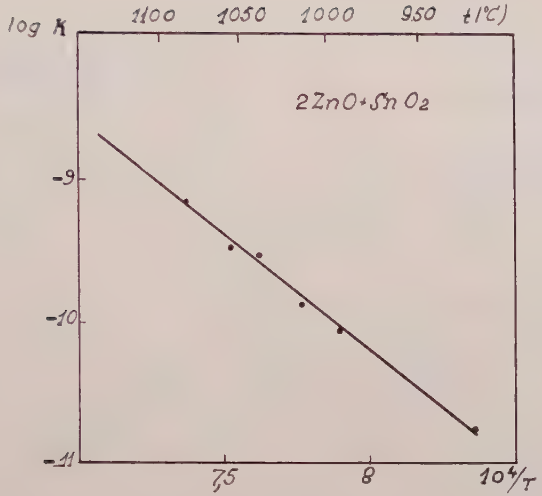

Fig. 4.

Using the method described by PLUMAT (7), HYSLOP and MCLEOD (8) studied the acidity and basicity of a number of oxides, silicates and spinels, with a view to explain some solid state reactions of ceramic interest.

The typical acid oxides (B_2O_3, SiO_2, etc.) show very high negative values, while the basic compounds show positive ones. From this scale can easily be seen that the SnO_2 (−2.73) is a little more acid than the ZnO (−2.01).

HYSLOP and MCLEOD carried out a comprehensive digest of those solid state reactions in which the direction of diffusion is known, and they concluded that the basic oxides have a tendency to diffuse through the acid ones. As examples of this behaviour they mention the following:

$\overrightarrow{\mathrm{CaO}} - \mathrm{SiO_2}$	(9)	$\overrightarrow{\mathrm{Na_2O}} - \mathrm{Al_2O_3} \cdot 2\,\mathrm{SiO_2}$	(10)
$\overrightarrow{\mathrm{PbO}} - \mathrm{SiO_2}$	(10)	$\overrightarrow{\mathrm{Cr_2O_3}} - \mathrm{ZnO}$	(11)
$\overrightarrow{\mathrm{ZnO}} - \mathrm{Al_2O_3}$	(10)	$\overrightarrow{\mathrm{Fe_2O_3}} - \mathrm{ZnO}$	(12)

in which the oxide carrying an arrow represents the mobile oxide that diffuses through the reaction product.

From this behaviour we are also inclined to suppose that in our system the ZnO mainly diffuses through the zinc orto-stannate layer built up between the grains of the reactants.

$$\mathrm{ZnO}\ \overset{\longrightarrow}{|}\ \mathrm{SnZn_2O_4}\ \big|\ \mathrm{SnO_2}$$

FEISER (13) relates the vapour pressure of zinc oxide to the absolute temperature by means of the equation

$$\log p_{mm} = -\frac{27,534}{T} + 16.594.$$

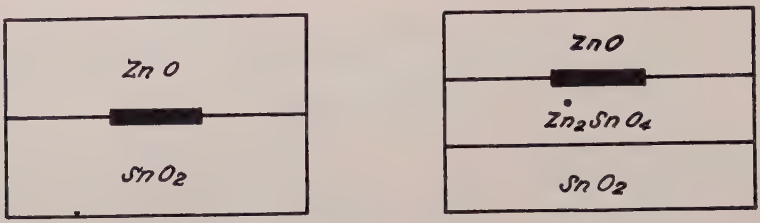

Fig. 5.

The same author gives for the stannic oxide:

$$\log p_{mm} = -\frac{28{,}338}{T} + 16.238.$$

The vapour pressures calculated for the temperature range in which we have developed our experiments are:

$$\begin{array}{lll} ZnO & p_{900^\circ} = 1.3 \times 10^{-7}\ \text{mm}; & p_{1150^\circ} = 1.8 \times 10^{-3}\ \text{mm} \\ SnO_2 & p_{900^\circ} = 1.2 \times 10^{-8}\ \text{mm}; & p_{1150^\circ} = 2.1 \times 10^{-4}\ \text{mm}. \end{array}$$

As can be seen, the vapour pressure of ZnO in this range of temperature is about ten times greater than that of SnO_2.

From these differences of vapour pressure between ZnO and SnO_2 it could also be expected that the zinc oxide played an important role in determining the reaction rate.

In addition to the above considerations on the mechanism of the zinc orto-stannate formation, we have tried to find an experimental support in order to clear up in a definitive way the direction of the fundamental flow of migration that causes the reaction to progress.

The method used has been that of the metallic mark. Between a pellet of ZnO and another one of SnO_2 a very thin foil of gold was placed. Both pellets, held together between two small plates of platinum, were heated at 1000°C for 70 hours. After this treatment a careful microscopic observation of the boundary was made. It could be shown that the small gold particles were located, after the reaction, between the zinc oxide surface and the newly formed layer of zinc orto-stannate, this being a proof of a matter transfer from the ZnO pellet to the SnO_2 one.

The measurements of apparent specific weight of the pellets (molar ratio SnO_2/ZnO equal to 1:2) have shown a clear expansion of the mixture during the heating process. In Fig. 6 can be seen the variation of apparent specific weight as a function of time for two different temperatures. In the same figure the corresponding yield curves for these temperatures have been represented, in order to see at a glance the existent correlation between the expansion of the pellets and the reaction yield.

A question arises now: Is the measured expansion a direct consequence of the changes in real specific weight during the reaction, or is it simply due to the appearance of a new texture? The calculation of the function $\delta = f(\alpha)$ has thrown some light on this problem. δ being the real specific weight of the mixture and α the yield of the reaction, the resulting equation is as follows:

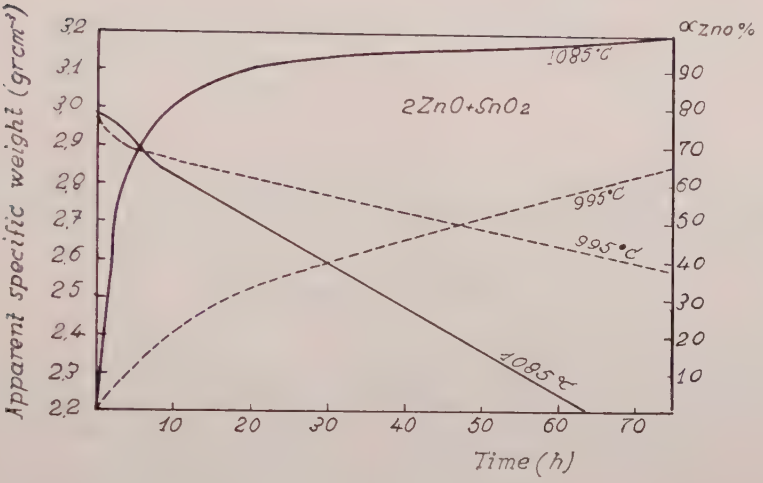

Fig. 6.

$$\delta = 0.06\,\alpha + 6.18.$$

The values used for this calculation have been the following:

$$\delta_{SnO_2} = 6.95 \quad (14); \qquad \delta_{ZnO} = 5.61 \quad (15); \qquad \delta_{SnZn_2O_4} = 6.24 \quad (\text{exp.})$$

If the only factors affecting the process would be the characteristic changes of volume of the solid phases, a slight shrinkage of the pellets should be expected. As the experiments show a clear expansion, together with a significant change in porosity, we have to admit the appearance of a more open texture during the reaction.

The mechanism of building up such a texture does not seem to be simple, though in our opinion a more favoured unilateral diffusion could be partially responsible of the expansion.

In Fig. 7 the changes of volume as a function of temperature (constant heating time 2 hours) are shown.

Three characteristic processes can be distinguished: Until 600°C a very slight expansion is the only effect observed, and this is probably due to the gaseous phase occluded. From this temperature a sharp shrinkage appears as a consequence of the recrystallization of zinc oxide. Over 1000°C the velocity of reaction is high enough to cause the new open texture, this effect being more significant than the shrinkage due to the recrystallization of the zinc oxide.

Summary

The chief purpose of this work was the determination of the rate of reaction between ZnO and SnO_2 and its variation as a function of temperature.

By the experimental curves of the reaction rate we obtained the function log $k = f\,(1/T)$ which allowed us to calculate a value of 74,700 cal/mol for the activation energy of the reaction.

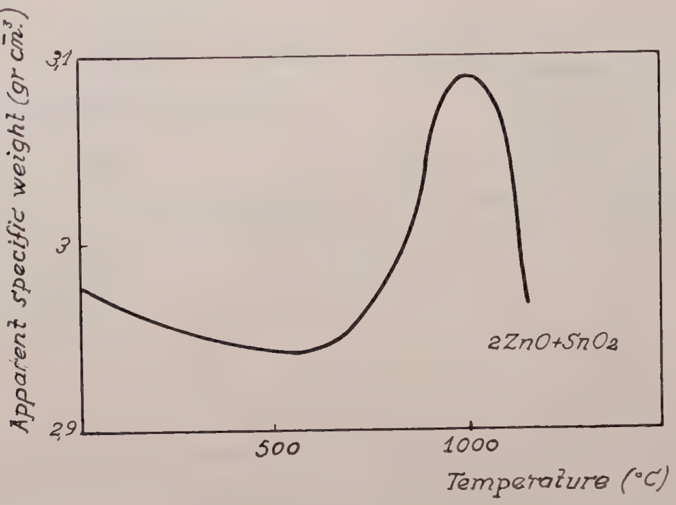

Fig. 7.

Our experiments proved that the matter transfer for the reaction is carried out by diffusion of the ZnO through the formed zinc orto-stannate.

By measurements of specific weight it was shown that the reacting mixture expands during the reaction. A more open texture is evolved by this process.

ACKNOWLEDGEMENT

The authors are greatly indebted to Dr. J. García Vicente for the development of the X-ray study involved in this paper.

Besides we want to acknowledge the collaboration with the Swedish Institute for Silicate Research and its director, Prof. J. A. Hedvall.

Instituto de Edafología y Fisiología Vegetal, Madrid.

REFERENCES

1. Taylor, N. W., Z. phys. Chem. *B29*, 247 (1930).
2. Verwey, E. J. W. and Heilmann, E. L., J. Chem. Physics *15*, 174 (1947).
3. Kimball, G. E., J. Chem. Phys. *8*, 188 (1940).
4. Natta, G. and Corradini, P., Proc. Int. Symp. Reactivity of Solids, Gothenburg, *1*, 273 (1954).
5. Aleixandre, V. and Verduch, A. G., Anal. Edaf. *10*, 327 (1951).
6. Lindner, R., Acta Chem. Scand. *6*, 457 (1952).
7. Plumat, M., Silicates Industr. *14*, 125 (1949).
8. Hyslop, J. F. and McLeod, M., Trans. Brit. Ceram. Soc. *50*, 265 (1951).
9. Jander, W. and Hoffmann, E., Z. anorg. Chem. *218*, 211 (1934).
10. Jagitsch, R., Nature, London, *164*, 497 (1949).
11. Hüttig, G. F., Disc. Faraday Soc., No. *8*, 215 (1950).
12. Hopkins, D. W., J. Electrochem. Soc. *96*, 195 (1949).
13. Feiser, J., Metall u. Erz *26*, 209 (1929).
14. Handbook of Chemistry and Physics, 30th Edition, 1947.
15. Esch, W., Gummi u. Asbest *4*, 233 (1951).

Tryckt den 12 september 1955

Uppsala 1955. Almqvist & Wiksells Boktryckeri AB

ARKIV FÖR KEMI Band 8 nr 47

Communicated 25 May 1955 by ARNE FREDGA

γ-Butyrolactone. Some reactions involving ring fission

By LENNART SCHOTTE

Some stereochemical observations on the reactions between the diastereomers of α,α'-dibromoglutaric acid and sodium disulphide (1) or potassium thiolacetate have led to the assumption that the substitution may proceed through a cyclic (2) or even a γ-lactone intermediate. It was therefore of interest to investigate the behaviour of γ-butyrolactone in reaction with some sulphur compounds. The substituents in the γ-lactone ring are certainly of importance for further reactions but model experiments on γ-butyrolactone itself should allow some general conclusions to be drawn.

There are only a few examples in the literature of reactions between sulphur compounds and γ-butyrolactone. In 1950 PLIENINGER (3) reports that the action of sodium methyl mercaptide on γ-butyrolactone under certain conditions yields the sodium salt of γ-methylmercapto-butyric acid. Further investigations of the same kind are described in (4) and (5). The last reference is a patent description from Badische Anilin & Soda Fabrik. A later patent (6) concerns the treatment of γ-butyrolactone with sodium sulphide in aqueous solution under pressure; γ,γ'-thiodibutyric acid is thus obtained in good yield. It should be noted that the reactions mentioned involve ring cleavage with alkyl–oxygen bond fission. Acid hydrolysis of γ-butyrolactone (7) or action of sodium alkoxides (8), on the other hand, cause acyl–oxygen bond cleavage analogous to the effect of ester hydrolysis in general.

The reactions of β-lactones, especially β-propiolactone, have been extensively studied (9). Different inorganic salts yield salts of β-substituted propionic acids and it is of special interest for this paper to notice the different rate of reaction for the sodium chloride and sodium hydrogen sulphide attack upon the lactone. In competition exclusive reaction with the sulphur compound is observed. Thiourea and β-propiolactone give nearly quantitative yield of β-*iso*thioureido-propionic acid. In all these reactions the lactone ring is opened at the oxygen–methylene carbon bond but with alcohols β-propiolactone forms two products depending on the catalyst present. Without catalyst or with acid catalysis the ring is opened as above, whereas with base catalysts the alcohol attack leads to a hydracrylate ester, i.e. cleavage of the oxygen–carbonylcarbon linkage. These results can be compared to the hydrolysis of β-lactones, where the reaction mechanism is different for water hydrolysis on the one hand and for alkaline and acid hydrolysis on the other hand. Using INGOLD's terminology (10) the water hydrolysis is of B_{AL^2} type involving alkyl–oxygen bond fission. It is not clearly understood why this mechanism B_{AL^2} is only recorded for β-lactones but it is probably best interpreted in terms of ring-strain.

The present author has investigated the action of sodium or potassium thiolacetate upon γ-butyrolactone under different conditions. It has been found that a reaction occurs to a certain extent according to the formula (I)

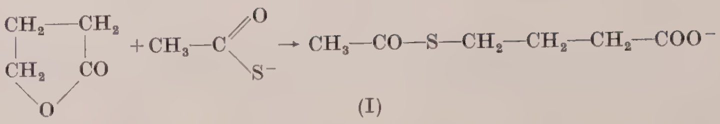

(I)

The best results are obtained in aqueous solution but it should be pointed out that the reaction is much slower than for *β*-lactones. This is of course in good accordance with the different stability of five- and four-membered rings (see experimental part). The amount of *γ*-acetylmercapto-butyric acid formed is determined after fractional distillation *in vacuo*. The acid has been characterized after hydrolysis and oxidation with iodine to *γ*,*γ*′-dithiodibutyric acid. The disulphide thus obtained was compared with an authentic sample (11). The observed yield of *γ*-acetylmercapto-butyric acid is a little too low as a slight hydrolysis of the acetyl group cannot be avoided under the conditions employed. For comparison it is important to note that alkali acetates treated in the same way do not react with *γ*-butyrolactone. Of course the objection could be raised that the *γ*-butyrolactone recovered is formed to some extent, during the distillation, from the corresponding *γ*-hydroxy acid which might be liberated on hydrolysis of the acetylated compound. It should, however, then be remembered that thiolesters undergo hydrolysis more rapidly than corresponding acetates (12).

Analogous observations concerning the reactivity have been made in reactions of *γ*-butyrolactone with thiourea. While *β*-propiolactone reacts already at room temperature in aqueous solution no effect is found even after refluxing thiourea in water together with *γ*-butyrolactone. An opening of the *γ*-lactone ring with alkyl–oxygen bond fission can, however, be effected if hydrobromic acid is added. A rather good yield of *iso*thiourea derivative is thus obtained, determined after characterization of the product as *γ*-mercaptobutyric acid and the related disulphide. The catalytic effect of hydrobromic acid is not necessarily due to a complete intermediate formation of *γ*-bromobutyric acid, which then should react easily with thiourea. This conclusion seems justified from experiments with various amounts of acid. The marked effect of protons upon the rate of ring opening is further demonstrated by the fact that the reaction can be performed also in the presence of sulphuric acid. The author is well aware of Kofod's interpretation (13) of the mechanism for the reaction between thiourea and alcohols in the presence of hydrogen halides. Although that reaction is very similar to the one studied here, it is believed that the addition of a proton to the oxygen atom in the lactone ring will considerably facilitate interaction to yield the *iso*thiourea derivative. Thiourea is then supposed to react in its ionic resonance form. The reaction is important as it implies that mercapto derivatives can be prepared quite generally not only from alcohols but also from lactones without intermediate isolation of a halogeno compound. The reaction has been performed previously in some very special cases (14; for reactions between alcohols and thiourea, see also 15).

No reaction is found between sodium disulphide and *γ*-butyrolactone in aqueous solution at room temperature. Due to the instability of disulphides upon treatment in an alkaline medium (16) a prolonged action under special conditions seems of no value. α-Chloro- and α-bromo-*γ*-butyrolactone give with sodium disulphide and sodium sulphide the expected α,α′-dithiodi-*γ*,*γ*′-butyrolactone and α,α′-thiodi-*γ*,*γ*′-butyrolactone respectively without complications. These reactions have been previously described for the chloro derivative (17).

From the theoretical point of view these reactions with *γ*-butyrolactone are interesting as different modes of ring fission can be studied. The attack of thiolacetate anion leads to an opening of the alkyl–oxygen bond; the most interesting thing to note is, however, the different reactivity of acetates and thiolacetates. The sulphur derivative reacts much more rapidly which surely can be combined with the often observed fact that SH^- is far more reactive than OH^- in replacement reactions of different types. It should further be noted that free thiolacetic acid differs considerably in reactivity from its anion. This is to be expected from the general behaviour of charged and uncharged molecules in the reactions under consideration.

In comparing the action of mercaptides and alkoxides on γ-butyrolactone the different character of sulphur and oxygen in electromeric displacements is clearly demonstrated. Alkoxides cause ring cleavage at the acyl carbon–oxygen bond whereas mercaptides give alkyl carbon–oxygen bond fission. The total amount of open-chain derivatives is higher for the sulphur compounds. The two possibilities for interaction with the γ-lactone can be illustrated in terms of the transition states (II) and (III),

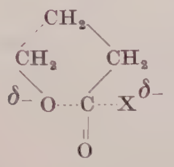

(II)

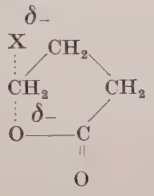

(III)

where X^- is the reacting nucleophilic reagent. In general it can be assumed that both acyl and alkyl attack occurs simultaneously but that in the case of alkoxides the acyl reaction is by far the more rapid one and is thus the only one observed. A reaction according to formula (II) is the only one that allows resonance between the reagent and the carbonyl group and should thus be appreciably favoured compared to (III), if X is able to conjugate. Now, oxygen conjugates better than sulphur and so when $X = RO^-$ a ring opening between acyl carbon and oxygen is to be expected. If, on the other hand, $X = RS^-$ an attack in either position can possibly be realised, and as seen from the experimental results, alkyl carbon–oxygen bond fission is preferred.

In the above-mentioned work of PLIENINGER (3) it is stated that sodium methyl mercaptide and γ-butyrolactone react in toluene solution to give an addition product which on heating yields γ-methylmercapto-butyric acid. A formula is proposed for the addition product and the reaction with ring opening is assumed to involve rearrangement. This seems unlikely to the author and as no facts are given to support the formula presented, it should be justified to formulate the compound simply as $C_4H_6O_2$, CH_3SNa. Under similar conditions analogous observations can be made in the reaction between sodium thiolacetate and γ-butyrolactone. In this manner the results are connected with the mechanism discussed above.

Experimental

γ-Acetylmercapto-butyric acid.—15.2 g (0.2 mole) of thiolacetic acid was neutralized with 8.0 g (0.2 mole) of sodium hydroxide in 40 ml of water. 17.2 g (0.2 mole) of γ-butyrolactone was added and the mixture refluxed with occasional shaking for 90 minutes. After standing for one hour at room temperature the reaction mixture, made weakly alkaline, was extracted repeatedly with ether. 9.0 g (52 %) of unchanged γ-butyrolactone, b.p. 82°/12 mm, was recovered. The aqueous solution was acidified with dilute sulphuric acid and extracted again with ether. After evaporation of the solvent γ-acetylmercapto-butyric acid was fractionated *in vacuo*. Yield 8.0 g (25 %) with b.p. 157°–159°/11 mm. No difference is found when the potassium salt of thiolacetic acid is used instead of the sodium salt.

The acetylmercapto derivative (8.0 g) was dissolved for hydrolysis in a solution of 8 g NaOH in 50 ml of water and kept overnight at room temperature. The thiol obtained was directly oxidized with iodine to the corresponding disulphide which separated as flaky crystals upon acidification with sulphuric acid. The disulphide acid was recrystallized twice from water; m.p. 109°–110° and yield 4.9 g (83 %). Mixed m.p. with an authentic sample: 109°.

Varied conditions for the treatment gave the following results:

(*a*) The reaction mixture was allowed to stand at room temperature for 24 hours. Most of the γ-butyrolactone was recovered unchanged (77 %).

(*b*) The mixture was refluxed for 1 hour. 11 g (65 %) of the lactone was isolated together with 3.5 g (11 %) of γ-acetylmercapto-butyric acid, b.p. 159°–160°/12 mm.

(*c*) Refluxing for 150 minutes yielded 8.5 g (50 %) of γ-butyrolactone unchanged and 7.5 g (23 %) of γ-acetylmercapto-butyric acid.

(*d*) The reaction mixture was refluxed for 6 hours and then kept at room temperature for another 20 hours. 8.0 g (25 %) of γ-acetylmercapto-butyric acid was isolated.

As separate experiments showed hydrolysis of the acetylated γ-mercaptobutyric acid to occur to a slight extent also in a neutral medium, the reaction time was not increased further. The action on the γ-lactone is nevertheless illustrated.

(*e*) 17.2 g (0.2 mole) of γ-butyrolactone was reacted with sodium thiolacetate prepared from 15.2 g (0.2 mole) of thiolacetic acid and 4.6 g (0.2 g at.) of sodium dissolved in 100 ml of absolute alcohol. The mixture was refluxed for 150 minutes. 1.6 g (5 %) of γ-acetylmercapto-butyric acid was isolated in addition to 11 g (65 %) of the unchanged γ-lactone.

(*f*) 0.2 mole of sodium thiolacetate was prepared as in (*e*) (except that 75 ml of alcohol was used) and precipitated completely from the alcoholic solution by the addition of ether. The sodium salt was heated together with 17.2 g (0.2 mole) of γ-butyrolactone in 100 ml of toluene for 3 hours at 50° with mechanical stirring. An addition product partly separated and the total amount remaining after evaporation of the solvent was divided in two parts. One of these was dissolved in water; from the acidified solution thiolacetic acid and γ-butyrolactone were recovered. The other part was heated for 30 minutes at 165° and then treated as above. 3.5 g (22 %) of γ-acetylmercapto-butyric acid was thus isolated.

(*g*) 17.2 g (0.2 mole) of γ-butyrolactone was added to a solution of 15.2 g (0.2 mole) of thiolacetic acid in 25 ml of water. The mixture was refluxed for 150 minutes and yielded upon isolation mostly unchanged γ-lactone (83 %) and no sulphide derivative.

(*h*) the same reagents as in (*g*) were mixed but without solvent. The solution was kept for 24 hours at room temperature; all the γ-butyrolactone was recovered.

Reactions of γ-butyrolactone with thiourea.—17.2 g (0.2 mole) of γ-butyrolactone, 15.2 g (0.2 mole) of thiourea and 40 g (0.24 mole) of hydrobromic acid (48 % in water) was refluxed with mechanical stirring for 12 hours. The reaction product was made strongly alkaline with a solution of 25 g of sodium hydroxide in 90 ml of water. The intermediate *iso*thiourea derivative was then hydrolyzed by refluxing for 2 hours. The alkaline solution was extracted with ether, the aqueous part acidified with sulphuric acid and extracted again. Upon evaporation of the solvent a product remained which on distillation (rapid) yielded 15.8 g (66 %) of γ-mercaptobutyric acid, b.p. 128–129°/11 mm. A solid disulphide residue remained. Recrystallized from water this acid showed m.p. 108°–110°. The total yield was about 70 %. The γ-mercaptobutyric acid isolated was characterized as the related disulphide. It was found that no appreciable deviations from this description occurred when smaller amounts of hydrobromic acid were used.

However, when the reaction was repeated with water added to the reagents instead of hydrobromic acid no yield of γ-mercaptobutyric acid could be observed. Only traces of mercaptan were qualitatively detectable. Treatment in the presence of dilute sulphuric acid (5 ml of concentrated acid in 50 ml of water), on the other hand, gave 3.1 g (13 %) of the mercapto acid under otherwise analogous conditions.

Summary

The reaction of γ-butyrolactone with salts of thiolacetic acid and thiourea respectively has been investigated. An opening of the ring system can be effected.

The different modes of attack of mercaptides and alkoxides on the γ-lactone ring have been discussed from a theoretical point of view.

ACKNOWLEDGEMENTS

The author wants to express his gratitude to Professor ARNE FREDGA for valuable discussions. He is also indebted to Mrs. KERSTIN CLAESON for help with the experimental work.

A grant from the *Swedish Natural Science Research Council* is gratefully acknowledged.

Laboratory of Organic Chemistry, Chemical Institute, University of Uppsala, May 1955.

REFERENCES

1. L. SCHOTTE, Acta Chem. Scand. *8*, 130 (1954).
2. M. J. S. DEWAR, The Electronic Theory of Organic Chemistry, p. 78 (Oxford 1949).
3. H. PLIENINGER, Chem. Ber. *83*, 265 (1950).
4. H. TANI and K. FUDO, Mem. Inst. Sci. Ind. Research, Osaka Univ. *6*, 100 (1948); C. A. *45*, 10198 c (1951).
5. H. WENDERLEIN and E. RAGER, Ger. Patent 840, 996 (1952); C. A. *47*, 1729 h (1953).
6. W. REPPE, H. FRIEDERICH, and H. LAIB, Ger. Patent 893, 501 (1953); C. A. *48*, 12791 d (1954).
7. F. A. LONG and L. FRIEDMAN, J. Am. Chem. Soc. *72*, 3692 (1950).
8. E. Y. SPENCER and G. F. WRIGHT, J. Am. Chem. Soc. *63*, 1281 (1941).
9. T. L. GRESHAM, J. E. JANSEN, F. W. SHAVER *et al.*, J. Am. Chem. Soc. *70*, 998–1006 (1948).
10. C. K. INGOLD, Structure and Mechanism in Organic Chemistry, p. 766 (London 1953).
11. B. HOLMBERG and E. SCHJÅNBERG, Arkiv Kemi *14 A* (1940) nr 7.
12. P. N. RYLANDER and D. S. TARBELL, J. Am. Chem. Soc. *72*, 3021 (1950).
13. H. KOFOD, Acta Chem. Scand. *7*, 1302 (1953).
14. L. J. REED *et al.*, J. Am. Chem. Soc. *75*, 1273 (1953).
15. R. L. FRANK and P. V. SMITH, J. Am. Chem. Soc. *68*, 2103 (1946).
16. A. SCHÖBERL and M. WIESNER, Ann. *507*, 111 (1933).
17. H. KRZIKALLA and A. TARTTER, Ger. Patent 801, 992 (1951); C. A. *45*, 5179 f (1951).

Tryckt den 12 september 1955

Uppsala 1955. Almqvist & Wiksells Boktryckeri AB

ARKIV FÖR KEMI Band 8 nr 48

Read 1 June 1955

Studies on synthetic growth substances

VIII. The enanthiomorphs of α-(1-naphthyl)-propionic acid

By Arne Fredga

With 1 figure in the text

A great number of optically active aryloxy-alkylcarboxylic acids have been tested as to their growth-regulating activity. In most cases, a significant difference between the enanthiomorphs was reported, and as far as the configurations have been determined, the enanthiomorph related to the D-hydroxy acid is more active (1). Similar effects have been found for optically active bicyclic acids like 1.2.3.4-tetrahydro-1-naphthoic acid (2) and hydrocoumarilic acid (3), but in these cases the configuration of the more active form is still unknown. As 1-naphthyl-acetic acid, representing a third type of compound, is known to possess strong auxin activity and has been extensivly investigated, it would be of great interest to study the corresponding propionic acid, which can be resolved into optically active forms.

The racemic acid was first prepared by Tiffeneau and Daudel by oxidation of the corresponding aldehyde, obtained from 1-propenyl-naphthalene by a "Tiffeneau rearrangement" (4). It was later obtained by Blicke and Feldkamp by methylation of diethyl 1-naphthylmalonate and subsequent hydrolysis and decarboxylation (5). They give the m.p. 148–149°; for racemic acid prepared from the pure antipodes the present author found 149–149.5°.

The acid is most conveniently prepared by methylation of ethyl 1-naphthyl-cyanoacetate and subsequent hydrolysis and decarboxylation according to a general procedure described by Wideqvist (6):

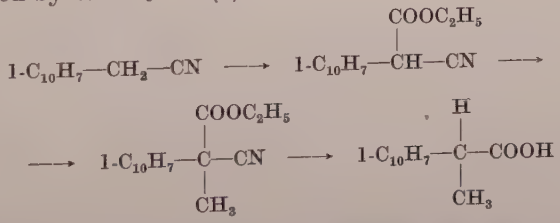

$$1\text{-}C_{10}H_7\text{—}CH_2\text{—}CN \longrightarrow 1\text{-}C_{10}H_7\text{—}\overset{\overset{\displaystyle COOC_2H_5}{|}}{C}H\text{—}CN \longrightarrow$$

$$\longrightarrow 1\text{-}C_{10}H_7\text{—}\underset{\underset{\displaystyle CH_3}{|}}{\overset{\overset{\displaystyle COOC_2H_5}{|}}{C}}\text{—}CN \longrightarrow 1\text{-}C_{10}H_7\text{—}\underset{\underset{\displaystyle CH_3}{|}}{\overset{\overset{\displaystyle H}{|}}{C}}\text{—}COOH$$

The present author, in collaboration with Mrs. G. Bergman, has also tried to prepare the acid by side-chain bromination of 1-ethyl-naphthalene and treatment of the bromo compound with cuprous cyanide. A nitrile was obtained in rather good yield, but the acid obtained on hydrolysis had the m.p. 157–158°. It was not identical either with α-(1-naphthyl)-propionic acid or with the corresponding β-propionic acid described by Mayer and Sieglitz (7).

Table 1. $[M]_D^{25}$ for α-(1-naphthyl)-propionic acid (I) and hydratropic acid (II).

Solvent	$[M]_D^{25}$	
	I	II
Benzene	361.5°	138.8°
2.2.4-Trimethylpentane	342.4°	—
Acetic acid	304.8°	131.1°
Acetone	292.1°	143.3°
Chloroform	268.2°	113.1°
Ethanol	240.9°	118.8°
Water (ion)	69.9°	8.7°

The resolution of the racemic acid could be performed with brucine and cinchonidine. It is essential to crystallise the brucine salt from pure methanol, even moderate amounts of water being very deleterious for the resolution. The m.p. of the active acid is 69–69.5°, that is 80° lower than that of the racemic compound. This is perhaps the greatest difference between an optically active compound and the corresponding racemate ever noticed.

The activity data of α-(1-naphthyl)-propionic acid and the corresponding phenyl compound, hydratropic acid, are given in Table 1. A certain parallelism is found, indicating that the acids with the same direction of rotation are sterically related. This assumption is corroborated by the formation of a quasi-racemic compound between (−)-α-(1-naphthyl)-propionic acid and (+)-hydratropic acid; the melting point diagram shows a very pronounced maximum at 50 mole-% (Fig. 1). Considering the difference in structure and physical properties between the acids (the m.p. of active and racemic hydratropic acid is 31° and 16.5° respectively), the formation of a quasi-racemic compound is in this case rather unexpected. Its existence must in some way be connected with the remarkable stability of the racemate of the 1-naphthyl compound.

There is very strong evidence that the *dextrorotatory* hydratropic acid has the configuration I (8, 9, 10, 11). The (+)-α-(1-naphthyl)-propionic acid is consequently represented by stereoformula II.

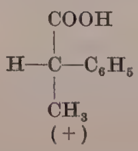

$$\begin{array}{ccc} & \mathrm{COOH} & \\ & | & \\ \mathrm{H}- & \mathrm{C} & -\mathrm{C_6H_5} \\ & | & \\ & \mathrm{CH_3} & \\ & (+) & \end{array}$$

(I)

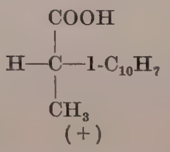

$$\begin{array}{ccc} & \mathrm{COOH} & \\ & | & \\ \mathrm{H}- & \mathrm{C} & -1\text{-}\mathrm{C_{10}H_7} \\ & | & \\ & \mathrm{CH_3} & \\ & (+) & \end{array}$$

(II)

If the 1-naphthyl group is regarded as a substituent to the aliphatic carbon chain, this acid must be assigned to the D-series.

As previously reported, the hydratropic acid has a rather weak auxin activity, the (+)-acid being about 100 times more active than the (−)-form in the *S-test* (flax-root growth inhibition test) (11). The growth-regulating activity of the α-(1-naphthyl)-propionic acid is being investigated by several scientists and the preliminary results seem to be of considerable interest. The activity in the *pea test* is a rather weak one without pronounced difference between the (+)- and (−)-forms

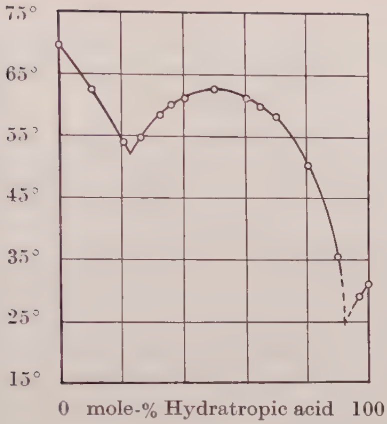

Fig. 1. (—)-α-(1-Naphthyl)-propionic acid and (+)-Hydratropic acid.

(12). In the *S-test*, the activity is rather strong (comparable to that of the 1-naphthylacetic acid), but also here there is no essential difference between the enanthiomorphs. In combination with anti-auxins, however, significant differences between (+)- and (−)-form were found (13). In the *Avena straight growth test*, the (+)-form shows a very high activity while the (−)-form is clearly less active (12, 13).

Experimental

***racem*-α-(1-Naphthyl)-propionic acid** was prepared according to the description given by WIDEQVIST for the butyric acid derivative (6). The hydrolysis of the nitrile proceeds rather slowly; if the reaction is not complete, considerable amounts of the amide are obtained. As it is insoluble in dilute alkali, it is easily separated from the acid.

The free acid was recrystallised several times, alternately from benzene and formic acid. M.p. 148–149°.

0.3399 g acid: 17.02 ml 0.0999-*N* NaOH. 20.62 mg acid: 59.00 mg CO_2 and 11.17 mg H_2O.

$C_{13}H_{12}O_2$ (200.23)	Found	equiv. wt. 200.0	C 78.02	H 6.08
	calc.	equiv. wt. 200.2	C 77.98	H 6.04

Resolution of the racemic acid. Preliminary experiments were carried out with different alkaloids and solvents. Brucine gives in pure methanol a strongly dextrorotatory acid but in dilute methanol only poor resolution. Also the quinine salt gives a good excess of (+)-acid. The (−)-acid can be isolated using the cinchonidine salt in dilute acetone or methanol. Cinchonine and quinidine give levorotatory acid of low activity, optically active benzedrine (β-phenyl-*iso*-propylamine) acid of the same direction of rotation as the base but poor resolution. Strychnine and α-phenylethylamine gave no crystalline salts.

40 g (0.2 mole) of racemic acid were dissolved with 0.2 mole of brucine in 350 ml of hot methanol. The salt was filtered off after 24 hours and recrystallised several times from pure methanol. The progress of the resolution was tested on small samples from each crystallisation, from which the acid was liberated and examined in absolute ethanol:

Crystallisation	1	2	3	4	5	6
ml methanol	350	240	220	200	180	165
g salt obtained	68.9	58.9	54.4	50.6	47.8	45.1
$[\alpha]_D$ of the acid	+ 80.5°	+ 106.5°	+ 116.5°	+ 118.5°	+ 119.5°	+ 119.5°

The mother liquor from the first crystallisation was evaporated to dryness at room temperature and the acid liberated; 17.0 g having $[\alpha]_D = -103°$ (absolute ethanol) were obtained. This acid (0.085 mole) was dissolved with 25 g (0.085 mole) of cinchonidine in 400 ml of boiling acetone and 300 ml of hot water were added. The salt obtained on standing was recrystallised from dilute acetone; as it is rather sparingly soluble, it is convenient to dissolve it in a small amount (*c.* 20 ml) of hot methanol, after which the acetone and the water are added. It is possible that a more favourable combination of solvents can be found on systematic investigation. The progress of the resolution was followed as described above:

Crystallisation	1	2	3	4	5	6	7
ml acetone	400	250	180	140	140	140	140
ml water	300	250	180	140	140	140	140
g salt obtained	38.4	34.9	32.5	30.5	28.9	27.6	25.9
$[\alpha]_D$ of the acid	− 111.5°	− 116°	− 117°	− 118.5°	− 119°	− 119·5°	− 119.5°

(+)-α-(1-Naphthyl)-propionic acid. The acid was liberated from the brucine salt with dilute sulphuric acid and extracted with ether. 44.2 g salt yielded 13.8 g of crude acid. After three recrystallisations from ligroin (b.p. 85–110°) there remained 10.5 g. The acid forms aggregates of small prisms or four-sided plates with m.p. 69–69.5°.

0.3153 g acid: 15.77 ml 0.0999-*N* NaOH.

$C_{13}H_{12}O_2$ Equiv. wt. calc. 200.2 found 200.1

0.2076 g dissolved in absolute *ethanol* to 10.00 ml: $2\alpha_D^{25} = +4.995°$. $[\alpha]_D^{25} = +120.3°$; $[M]_D^{25} = +240.9°$. — 0.2046 g dissolved in *acetone* to 10.00 ml: $2\alpha_D^{25} = +5.97°$. $[\alpha]_D^{25} = +145.9°$; $[M]_D^{25} = +292.1°$. — 0.2138 g dissolved in glacial *acetic acid* to 10.00 ml: $2\alpha_D^{25} = +6.51°$. $[\alpha]_D^{25} = +152.2°$; $[M]_D^{25} = +304.8°$. — 0.2025 g dissolved in *chloroform* to 10.00 ml: $2\alpha_D^{25} = +5.425°$: $[\alpha]_D^{25} = +133.9°$; $[M]_D^{25} = +268.2°$. — 0.2053 g dissolved in *benzene* to 9.99 ml: $2\alpha_D^{25} = +7.42°$. $[\alpha]_D^{25} = +180.5°$; $[M]_D^{25} = +361.5°$. — 0.2083 g dissolved in *2.2.4-trimethylpentane* to 10.00 ml: $2\alpha_D^{25} = +7.125°$. $[\alpha]_D^{25} = +171.0°$; $[M]_D^{25} = +342.4°$. — 0.2164 g *neutralised with aqueous NaOH* and made up with *water* to 10.00 ml: $2\alpha_D^{25} = +1.49°$. $[\alpha]_D^{25} = +34.4°$; $[M]_D^{25} = +69.9°$.

The *brucine salt* obtained in the course of the resolution forms short-prismatic crystals containing crystal solvent. It was not analysed.

(−)-α-(1-Naphthyl)-propionic acid. The acid was liberated from the cinchonidine salt with dilute sulphuric acid and extracted with ether. 25.9 g salt yielded 9.8 g of crude acid; after three recrystallisations from ligroin there remained 7.2 g with m.p. 69–69.5°.

0.3052 g acid: 17.48 ml 0.0999-*N* NaOH.

$C_{13}H_{12}O_2$ Equiv. wt. calc. 200.2 found 200.5

0.2021 g acid dissolved in absolute *ethanol* to 10.00 ml: $2\alpha_D^{25} = -4.855°$. $[\alpha]_D^{25} = -120.1°$; $[M]_D^{25} = -240.5°$.

Table 2. (−)-α-(1-Naphthyl)-propionic acid and (+)-hydratropic acid.

mole-% hydratropic acid	m.p.	mole-% hydratropic acid	m.p.
0.0	69.5°	60.3	61.1°
10.2	62.4°	65.0	59.8°
20.5	53.9°	70.1	58.2°
26.0	54.7°	80.3	50.3°
32.4	58.3°	90.0	35.5°
36.0	60.0°	97.0	28.9°
40.4	61.1°	100.0	31.0°
50.0	62.6°		

The *cinchonidine salt* obtained in the course of the resolution forms elongated prisms containing crystal solvent. It was not analysed.

Equivalent amounts of (+)- and (−)-acid were dissolved together in a little benzene and the racemic acid separating on cooling was recrystallised once from the same solvent. It had the m.p. 149–149.5°.

The melting point diagram was determined by RHEINBOLDT's method (14) using an apparatus described by FRIEDRICHS (15). As one of the eutectic points lies near room temperature, the crystallisation, pulverisation and filling into capillary tubes of the samples containing more than 50 mole-% of hydratropic acid had to take place in a cold-room (−14°C). The data for the system (−)-α-(1-naphthyl)-propionic acid–(+)-hydratropic acid are given in Fig. 1 and Table 2. The melting point curve for the system containing acids with the *same* direction of rotation was not examined in detail, but preliminary experiments indicate that the diagram is of the common eutectic type. The study of this diagram is rendered difficult by the low eutectic temperature and the viscosity of the melt.

Summary

The α-(1-naphthyl)-propionic acid has been resolved into the optically active forms using brucine and cinchonidine. The rotatory power found was $[\alpha]_D^{25} = +120.3°$ and −120.1° respectively (in absolute ethanol). The levorotatory acid gives with (+)-hydratropic acid a quasi-racemic compound, indicating that the acids with opposite directions of rotation have also opposite configurations.

Preliminary experiments on the auxin effect of the enanthiomorphs are reported.

ACKNOWLEDGEMENTS

The author is greatly indebted to Professor H. VELDSTRA, Amsterdam, and Dr. BÖRJE ÅBERG, Royal Agricultural College, Uppsala, for kindly reporting their preliminary results on the growth-regulating activity. Thanks are also due to Mr. R. ÖHBERG for preparing the 1-naphthyl-acetonitrile used as starting material and to Mr. B. SJÖBERG for analyses.

Laboratory of Organic Chemistry, Chemical Institute, University of Uppsala, May 1955.

REFERENCES

1. MATELL, M., Stereochemical studies on plant growth substances, Diss., Uppsala 1953. Also in Kgl. Lantbruks-Högsk. Ann. *20*, 205 (1953). Further references there.
2. VELDSTRA, H., and VAN DE WESTERINGH, C., Rec. trav. chim. *70*, 1113 (1951).
3. FREDGA, A., and VÁZQUEZ DE CASTRO Y SARMIENTO, C., Arkiv Kemi, *7*, 387 (1954).
4. TIFFENEAU, M., and DAUDEL, Compt. rendus *147*, 678 (1908).
5. BLICKE, F. F., and FELDKAMP, R. F., J. Am. Chem. Soc. *66*, 1087 (1944).
6. WIDEQVIST, S., Arkiv Kemi, Mineral., Geol. 24 B N:r 14 (1947).
7. MAYER, F., and SIEGLITZ, A., Ber. *55*, 1844 (1922).
8. ARCUS, C. L., and KENYON, J., J. Chem. Soc. *1939*, 916.
9. CAMPBELL, A., and KENYON, J., J. Chem. Soc. *1946*, 25.
10. MISLOW, K., and HEFFLER, M., J. Am. Chem. Soc. *74*, 3668 (1952).
11. FREDGA, A., Arkiv Kemi *7*, 241 (1954).
12. VELDSTRA, H., Private communication.
13. ÅBERG, B., Private communication.
14. RHEINBOLDT, H., J. prakt. Chem. [2] *111*, 242 (1925).
15. FRIEDRICHS, F., Z. angew. Chem. *34*, 61 (1921).

Tryckt den 14 september 1955

Uppsala 1955. Almqvist & Wiksells Boktryckeri AB

ARKIV FÖR KEMI Band 8 nr 49

Read 13 April 1955

On the partial purification of a liver factor stimulating the sulphate exchange of chondroitin sulphuric acid

By Harry Boström, Erik Jorpes, Bengt Månsson, Lennart Rodén and Anders Vestermark

With 5 figures in the text

During recent years, increasing interest has become focused on problems concerning the metabolism of the mucopolysaccharides. Efforts to elucidate the biosynthesis of their most important components, glucuronic acid and hexosamine, have been intensified (1). In addition, *in vivo* experiments have been made on various species of animals with a view to studying the rate of metabolism of the mucopolysaccharides, as well as the factors influencing it. The latter type of investigation has earlier been confined to problems dealing with the sulphate fixation in mesenchymal tissues and the sulphate exchange of sulpho-mucopolysaccharides. Such investigations have been made by several groups of workers, and surveys of the results have been published recently (2, 3).

During the past year, metabolic studies on the animal mucopolysaccharides have also been performed with the use of C^{14}-labelled compounds, such as carboxyl-labelled acetate and C^{14}-labelled glucose. Recent reports (1, 4) on the findings with respect to the rate of the carbon exchange in the chondroitin sulphuric acid seem to be in good agreement with earlier results based on experiments with S^{35}-labelled compounds (5, 6). Another matter of great interest is the fact that hyaluronic acid, according to the results obtained with C^{14}-labelled acetate, appears to have a rate of exchange several times more rapid than that of the sulpho-mucopolysaccharides (1, 4).

As far as the sulphate exchange of sulpho-mucopolysaccharides is concerned, it has also been possible to make *in vitro* studies of this reaction in the case of chondroitin sulphuric acid (2, 3), e.g. in surviving slices of cartilage incubated in Krebs-Ringer-bicarbonate solution containing S^{35}-labelled sulphate. Particular attention was paid to the possibilities of inhibiting this reaction by means of various enzyme inhibitors (7) and different drugs, such as cortisone (8, 9, 10) and salicylic acid (11). In addition, an analysis has recently been made of the relation between the sulphate exchange *in vitro* and the oxygen consumption (12).

The sulphate incorporation in chondroitin sulphuric acid *in vitro* can be stimulated by the addition of various compounds to the incubation solution. Thus, it has earlier been shown that the presence of glucose (3) stimulates the uptake of sulphate *in vitro*. Similar findings have been reported by other workers with respect to glucose and α-ketoglutaric acid (12, 10). A stimulation of the process of an entirely different order of magnitude than that obtained with these compounds can, however, be produced by the addition of small quantities of liver extract to the incubation solution, as described in a preliminary report (13). This observation was considered to indicate the presence in the liver of a factor stimulating the sulphate exchange in chondroitin sulphuric acid. A report is given in the present paper of the attempts made to isolate this active principle in the liver. An account is also given of preliminary results indicating that a similar active principle, possibly identical to the factor in the liver, is present in the serum of various species of animals.

Experimental

Reagents

1. Krebs-Ringer-bicarbonate solution.[1]
2. Krebs-Ringer-phosphate solution.[1]
3. (a) *Hypertonic Krebs-Ringer-bicarbonate solution* and
   (b) *Hypertonic Krebs-Ringer-phosphate solution* of such a composition that when 1 part of distilled water was added to 4 parts of (a) and (b), respectively, reagents 1 and 2, respectively, were obtained.
4. (a) *S^{35}-labelled Krebs-Ringer-bicarbonate solution* and
   (b) *S^{35}-labelled Krebs-Ringer-phosphate solution.* To 100 ml of reagents 1 and 2, respectively, was added 1 mC of carrier-free S^{35}-labelled sodium sulphate.[2] The solutions were stored at 0°C.
5. 2 per cent monoiodoacetic acid.
6. (a) Oxygen and
   (b) Oxygen–carbon-dioxide mixture: 93.5 per cent oxygen and 6.5 per cent carbon dioxide.
7. Ninhydrin reagent: 0.2 per cent ninhydrin in *n*-butanol.
8. Ethanol–water: 80 per cent ethanol in water.
9. *sec*-butanol–90 per cent formic acid–water: 75 + 15 + 10 parts, respectively.

Standardization technique

In the earlier investigations (13) on the stimulation of the sulphate exchange in chondroitin sulphuric acid *in vitro* produced by liver extract, the following procedure was used. Surviving slices of costal cartilage from a newly-killed calf were incubated in Krebs-Ringer-bicarbonate solution containing S^{35}-labelled sulphate. The chondroitin sulphuric acid was isolated from each sample, and the radioactivity of its sulphate group was determined after acid hydrolysis and precipitation as $BaSO_4$. This method (method I) has been described in an earlier paper (7).

In the attempts to purify the active principle in the liver, and to follow the physiological activity at the different stages of preparation, this technique proved to be too time-consuming. It was therefore simplified (method II).

---

[1] Prepared according to the directions given in W. W. UMBREIT, R. H. BURRIS, and J. F. STAUFFER, *Manometric Techniques*, Burgess Publishing Co., Minneapolis 15, Minn., 1947.

[2] Obtained from The Radiochemical Centre, Amersham, England.

Costal cartilage from 2–3 newly-killed suckling calves was freed from muscles and perichondrium, and sliced to a thickness of 0.6–0.7 mm in a modified slicing machine for cooked meat. The slices were received in a vessel containing Krebs-Ringer-bicarbonate solution. Circular pieces, about 7 mm in diameter, were then punched out of the slices, using a stainless tubular punch.

Into each of 30 Erlenmeyer flasks was poured 4 ml of a modified hypertonic Krebs-Ringer-bicarbonate solution (reagent 3 a); its composition was such that it became isotonic after the addition of 1 ml of distilled water to each flask. The flasks were divided into 6 groups with 5 flasks in each. 1 ml of distilled water was added to each of 4 flasks in the first group (positive controls). 1 ml of 2 per cent monoiodoacetic acid was added to the remaining flask in this group (negative control). In the remaining 5 groups, one preparation was standardized in each group. 0.2, 0.4, 0.6, 0.8 and 1.0 ml, respectively, of the same preparation was added to each of the five flasks in each group. The concentration ranged from 200 μg to 20 mg of dry substance per ml, according to the strength of the preparation. When the sample had been pipetted into the flask, water was added to make a final volume of 5 ml. Five or six circular slices of cartilage, prepared as described above, were added to each of the 30 flasks.

The flasks were then placed in a water bath at 37°C. During the course of the experiment the samples were aerated with the oxygen-carbon-dioxide mixture (reagent 6 b), and the flasks were rocked mechanically to and fro in the bath. After 1 hour, 1 ml of S^{35}-labelled Krebs-Ringer-bicarbonate solution (reagent 4 a) was added to each flask. After a further 2 hours, incubation was interrupted by the addition of 1 ml of 2 per cent monoiodoacetic acid (reagent 5) and the flasks were once more rocked mechanically for about 2 minutes. The slices of cartilage were then washed and dried as follows. The incubation solution was drawn off, after which the slices were washed three times with 50 ml of tap water each time. To each flask, 50 ml of saturated Na_2SO_4 solution were added, and the flasks with the slices of cartilage were kept overnight in an incubator at 40°C. The saturated Na_2SO_4 was then sucked off and the slices washed twice with tap water. This was followed by treatment in an incubator at 40°C for 1 hour with 50 ml of distilled water. The water was sucked off, and the slices of cartilage were dried with two 25-ml portions of absolute alcohol and one portion of ether.

Determination of the radioactivity in the slices of cartilage.—Four of the dry, circular slices of cartilage (their thickness after drying corresponding approximately to infinite thickness) were taken from each flask and placed in a specially constructed metal plate. It was provided with 4 circular holes; their diameter was such that the dry, somewhat elastic slices of cartilage could be pressed into them. The radioactivity of the different samples was then measured with a Geiger-Müller counter. A sufficiently large number of impulses were counted to ensure that the statistical measuring error did not exceed ± 2 per cent. The value for the negative control which, after careful washing, is equivalent to the background of the Geiger-Müller apparatus, was subtracted from the measuring values obtained. The mean value for the positive controls was then computed. The effect of the stimulating factor was thereafter obtained by expressing the radioactivity in the samples incubated in the presence of the different concentrations of the factor as a percentage of the mean value of the radioactivity in the positive controls.

The activity in the homogenate of various tissues was determined with the standardization method described (method II). For the determination of the activity in the serum of various animals, the method was modified as follows. Four ml of reagent 1 instead of reagent 3 were added to each flask from the start. The different sera were then added to the sample, either undiluted or after dilution with 1–3 parts of reagent 1, depending on the approximate physiologic activity in the respective serum. The final dilution to 5 ml was made with reagent 1 instead of with water.

The homogenization of tissues and organs was performed as follows. Small pieces with a total weight of 5–6 g (wet weight) were suspended in 2 parts of distilled water and homogenized in a microhomogenizer of the blender type[1] at maximal speed for three 30-second periods. The temperature of the homogenate was not allowed to exceed 20°C. The homogenate was then chilled to 0°C and was used after a few hours.

In order to facilitate comparisons between the results of standardization obtained in different experiments, it was found desirable to fix a unit for the activity studied. As a preliminary unit was chosen the quantity of an active substance that, in the standardization technique described, increased the sulphate exchange in chondroitin sulphuric acid by 100 per cent. The term S.E.S. unit (sulphate exchange stimulating unit) is suggested for this unit. On practical grounds, the abbreviations S.E.S. activity and S.E.S. factor are used analogously in the following.

Preliminary fractionation of the liver homogenate

1. Fresh liver from newly-killed suckling calves was homogenized, and 25 ml of the homogenate were centrifuged at 4000 *g* for 20 minutes. The precipitate, fraction A (low-speed precipitate), was collected, and the clear solution was once more centrifuged for 20 minutes at high speed (25,000 *g*). This gave two further fractions: fraction B (high-speed precipitate) and fraction C (high-speed supernatant).

2. 25 ml of liver homogenate were dialyzed in a cellophane bag against 500 ml of distilled water for a few hours at room temperature. The outer fluid was evaporated to 20 ml and was then divided into two equally large portions, one of which was heated to 100°C in a water bath.

The S.E.S. activity in the different fractions obtained under 1 (fractions A, B and C) and under 2 (inner fluid, outer fluid and boiled outer fluid) was determined.

Preparation of the "crude" S.E.S. factor

Three kg of fresh liver from suckling calves were cut into slices about 0.5 cm thick; they were extracted at room temperature with two 1.5-liter fractions of distilled water for 30 minutes, with sporadic manual stirring. The water extract was passed through a large Büchner funnel without filter paper. It was then heated rapidly in a steam bath to about 90°C after which the extract was cooled to 0°C and filtered through a linen bag. To each liter of the clear, reddish extract obtained in this way, 40 ml of a 20 per cent mercuric acetate solution were added with stirring. The solution was placed in the cold-room (0°C) for 3 hours. Centrifugation was then performed in a refrigerated centrifuge at 0°C and 3000 *g*. The precipitate was discarded. 80 ml of a 20 per cent mercuric acetate solution were added to each liter of the clear solution. After 3 hours in the cold-room at 0°C centrifugation followed. The supernatant was discarded and the precipitate was washed once with about 100 ml of distilled water. The washed precipitate was suspended in 25 ml of water, and was decomposed at 0°C by aeration for 1 hour with hydrogen sulphide. The solution was left at 0°C overnight, filtered, and the excess of hydrogen sulphide removed by aeration with air for 30 minutes. The solution was evaporated *in vacuo* at 10–20°C to a thin syrup. The active extract was stored in the frozen state at −15°C.

---

[1] From Edmund Bühler, Tübingen.

Purification by electrophoresis

At various stages in the purification process, the active fractions were submitted to both analytic and preparative paper electrophoresis.

For the *analytic paper electrophoresis*, an apparatus for horizontal paper electrophoresis and Munktell's electrophoresis paper were used. The potential gradient in the paper was approximately 6 V cm^{-1}. Electrophoresis was performed in 0.1 *M* acetate, phosphate or borate buffer, at a pH ranging from 4.6–9.2, for 4 hours. After completion of electrophoresis, the different parts of the paper were eluted with water and tested biologically. In some cases the substance was applied to the paper as a band. After the experiment, the paper was cut lengthwise; one half was then treated with the ninhydrin reagent (reagent 7) and the other half was tested biologically in different fractions.

Preparative vertical electrophoresis according to GRASSMANN and HANNIG (14), DURRUM (15) and BRATTSTEN and NILSSON (16) was also performed. In these experiments, a higher potential gradient (15–30 V cm^{-1}) was generally used, and both 0.3 *M* HAc (pH 2.7) and a 0.1 *M* phosphate buffer (pH 7.4) were tested as buffer substances. The apparatus separated each sample into 14 fractions, which were tested biologically according to method II.

Purification by paper chromatography

In a series of experiments, two-dimensional descending paper chromatography (Munktell's paper OB 50 × 50) was performed, with ethanol-water (reagent 8) as the first solvent and butanol-formic acid-water (reagent 9) as the second solvent, in the following way.

Two papers were loaded with 5–10 S.E.S. units of the "crude" factor or of the most active fraction obtained by preparative electrophoresis, as described. Both papers were allowed to run simultaneously for 8 hours in direction 1, after which they were dried in a drying chamber at 60°C for 5 minutes. The papers were then allowed to run for 18–20 hours in direction 2, after which they were dried for 5 minutes in a drying chamber at 60°C and then *in vacuo* for 1 hour at 60°C. After drying, both papers were examined under an ultraviolet lamp[1] and the dark and light spots seen in this light were marked on the chromatograms. One of the papers was developed by spraying with the ninhydrin reagent (reagent 7) and heating of the paper for 15 minutes in the drying chamber.

Small squares 3 × 3 cm were cut from the other paper, a 0.5 cm wide strip of paper being left between each square. The squares were attached to the edge of a filter paper with cellophane tape, and the filter paper was then moistened with water. After the water had flowed into the outermost edge of each square, a 0.5 cm wide strip was cut from each of them and was tested biologically according to method II. The network remaining in paper 2 after the squares had been cut out was developed with the ninhydrin reagent, as described.

---

[1] Mineralight, Mod. No. V 41, Amps. 0.25, Ultra-Violet Prod. Inc., South Pasadena, Calif.

Effect of the S.E.S. factor on the oxygen consumption in the slices of cartilage

Warburg's direct method (17) was used for studies of the oxygen consumption in the slices of cartilage. 25 circular slices of cartilage (corresponding to 130–140 mg dry weight), prepared from costal cartilage of suckling calves as described, were suspended in Krebs-Ringer-phosphate solution (reagent 2) in each of 12 Warburg flasks. To 4 of the flasks 0.2 ml of 1 per cent monoiodoacetic acid was added, to another 4 flasks 0.2 ml of distilled water, and to the remaining 4 flasks 300 µg (1 S.E.S. unit) of a crude preparation of the S.E.S. factor dissolved in 0.2 ml of distilled water. After the flasks had been aerated with oxygen and equilibrated at 37°C in a water bath, the oxygen consumption was measured for 1 hour. The sulphate incorporation in Krebs-Ringer-phosphate solution under similar conditions was determined in parallel experiments.

Results

S.E.S. activity in various organs in the rat

Fig. 1 shows the S.E.S. activity in different quantities of homogenate of various tissues and organs from the rat. It is seen that such activity was found not only in the liver, as reported earlier (13), but also in certain other organs. The highest S.E.S. activity was recorded in the liver (0.18 S.E.S. units/mg of dry substance) and the brain (0.21 S.E.S. units/mg of dry substance), but the content was also high in the skeletal muscle (0.12 S.E.S. units/mg of dry substance) and the heart (0.07 S.E.S. units/mg of dry substance). Very low activity was found in the lung, whereas no such activity was present in the spleen, kidney and small intestine. The two last-mentioned tissue homogenates caused, on the contrary, an inhibition of the reaction.

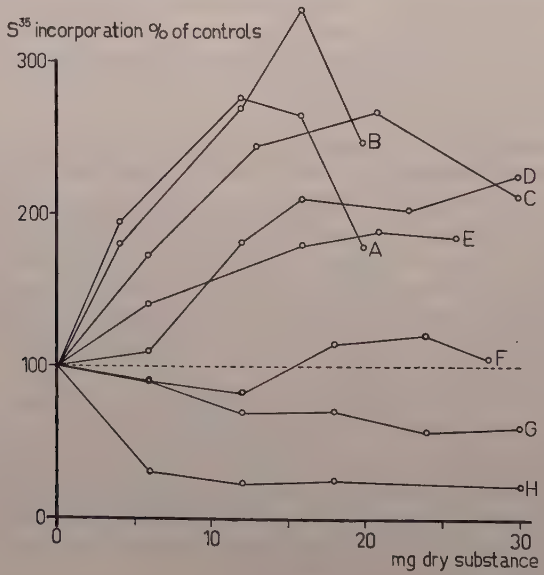

Fig. 1. S.E.S. activity in the homogenate of different organs from the rat. A, brain; B, liver; C, muscle; D, heart; E, lung; F, spleen; G, kidney; H, small intestine.

Table 1. S.E.S. activity in the liver homogenate and serum from various species of animals.

Species	Experiment	No. of S.E.S. units per ml serum	No. of S.E.S. units in liver homogenate per mg dry substance
Man: male 31 yrs.	1	9	—
,, 34 ,,	2	9	—
,, 32 ,,	3	8	—
Pigeon	1	16	—
	2	20	0.37
	3	24	—
Rabbit	1	9	—
	2	11	0.37
	3	15	—
Rat	1	10	0.17
	2	14	0.19
Guinea-pig	1	9	0.18
Sheep	1	5	0.09
Pig	1	4	0.11
Cow	1	4	0.04
	2	2	Only 60 % stimulation with 12 mg dry substance
Horse	1	2	Only 50 % stimulation with 18 mg dry substance

S.E.S. activity in serum and liver homogenates from various species of animals

It may be inferred from Table 1 that some S.E.S. activity was found in the serum and liver from various species of animals. The highest stimulation by the serum was obtained with serum from the pigeon (20 units/ml) and the lowest with serum from cattle (4 units/ml). Human serum resulted in moderate stimulation of the sulphate uptake.

Of the liver homogenates tested, pigeon liver showed the highest degree of stimulation and cattle liver the lowest S.E.S. activity. No tests were made with human liver homogenate. Table 1 shows that the S.E.S. activity in the serum and liver varied in the different species, but that some correlation seems to exist between the S.E.S. activity in the serum and liver of the same species of animal.

Fractionation of liver homogenate from the calf

1. Amongst the above-mentioned fractions A (low-speed precipitate), B (high-speed precipitate) and C (high-speed supernatant), only fraction C was found to contain S.E.S. activity.

2. On dialysis of the liver homogenate, all the S.E.S. activity was found in the outer fluid, whereas the inner fluid was completely inactive. No decrease in the activity in the outer fluid was noted when it was boiled and subsequently cooled.

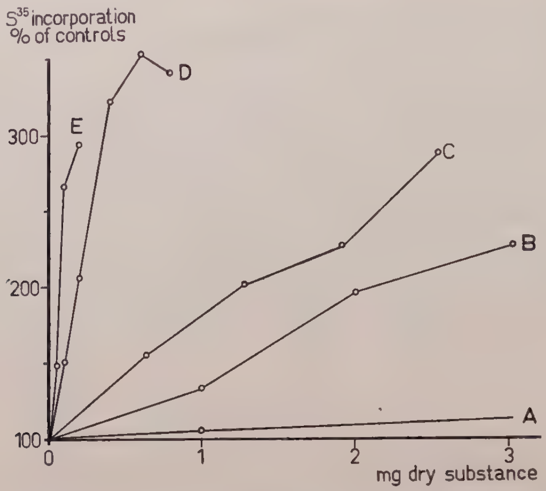

Fig. 2. Purification of the S.E.S. factor from homogenate of calf liver. A, homogenate; B, water extract; C, boiled extract; D, "crude" S.E.S. factor (see text); E, electrophoretically purified fraction.

"Crude" S.E.S. factor

The rising degree of purity in the different stages of purification of the "crude" S.E.S. factor is illustrated in Fig. 2, curves B–E. It is evident from the shape and course of the curves that increasing quantities of the S.E.S. factor (in mg of dry substance) produce an increasing degree of stimulation of sulphate incorporation (per cent of controls) according to a linear course, until maximal stimulation is reached at 270–450 per cent. Thereafter, the curves exhibit a falling or irregular tendency. The value for maximal stimulation caused by the same extract varied somewhat in the individual experiments, whereas the first rising part of the curve was relatively constant and easily reproducible in different standardization tests. As may be inferred from the figure, successive purification of the preparation results in an increasingly steep slope of the rising, linear part of the curve. If the S.E.S. activity is expressed in units, it is found that the liver homogenate contained a biological activity of 0.07 S.E.S. units/mg of dry substance, whereas the corresponding figure for the "crude" factor was 5 units/mg. Thus, a purification corresponding to about 70 times can be obtained in this way.

Paper electrophoresis of the S.E.S. factor

It is seen from Fig. 3 that, on analytic horizontal paper electrophoresis under the conditions stated, the S.E.S. activity was present at the site of application in a ninhydrin-positive area of the paper. This also applied in preparative electrophoresis according to GRASSMANN at pH 7.4. At a lower pH, the S.E.S. activity seemed, on the contrary, to migrate towards the cathode. Thus, in the latter case, the S.E.S. activity was found in the 4 fractions closest to the cathode, whereas the remaining 10 fractions were biologically inactive. The four active fractions exhibited a positive reaction to ninhydrin. On evaporation *in vacuo* with subsequent drying over NaOH in a desic-

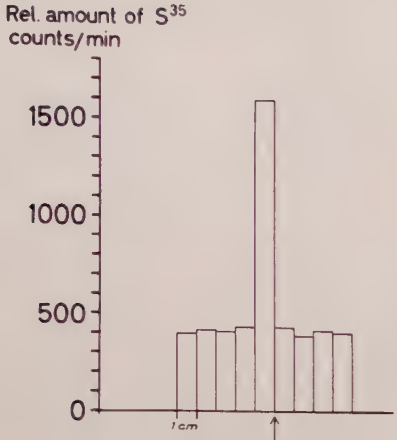

Fig. 3.

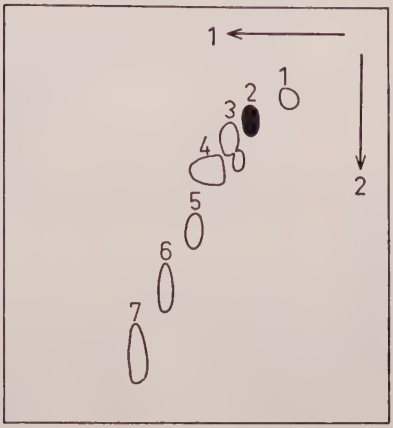

Fig. 4.

Fig. 3. Electrophoretic behaviour of "crude" factor in 0.1 *M* phosphate buffer at pH 7.4. The arrow denotes the site of application, and each column represents the activity in a 1 cm strip from the electrophoresis paper.

Fig. 4. Two-dimensional paper chromatography of an electrophoretically purified fraction of the S.E.S. factor. *1*, ethanol–water (reagent 8); *2*, butanol–formic-acid–water (reagent 9). Paper developed with ninhydrin (reagent 7). The S.E.S.-active spot is black.

cator, the two most active fractions were recovered as a white non-hygroscopic powder, whereas the content of the other fractions was strongly hygroscopic. The result of biological testing of the most active fraction obtained in a typical experiment is recorded in Fig. 2. Curve E shows that purification of the "crude" factor from 5 S.E.S. units/mg of dry substance to 14 units/mg of dry substance, i.e., about 3 times further purification, was obtained in this way.

Paper chromatography on the S.E.S. factor

Two-dimensional paper chromatography was performed both on the "crude" factor and on the most active electrophoretic fraction. In the former case, at least 10 ninhydrin-positive spots were obtained, and a number of dark and light spots were visible in ultraviolet light. In the latter case, 7 ninhydrin-positive spots were found, but no definitely ultraviolet-absorbing spots could be discerned. In both cases, the biological activity could be demonstrated in an area of the paper corresponding to a certain ninhydrin-positive spot. This is illustrated in Fig. 4, which shows a typical paper chromatogram of an electrophoretically purified fraction of the S.E.S. factor. Biological testing showed that the S.E.S. activity was localized to the ninhydrin-positive spot 2 on the chromatogram.

S.E.S. activity of certain known co-factors and substrates

Parallel to the attempts to isolate the S.E.S. factor, a large number of experiments were made with a view to ascertaining whether this factor is identical to any known co-factor, or to any particular substrate or combination of substrates. In these experiments, quantities of the relevant substances ranging from 10 μg to 10 mg

Table 2. Effect of various coenzymes and substrates on the sulphate incorporation in chondroitin sulphuric acid *in vitro.*

Substance	Standardization method used	Concentration mg/sample	Maximal S^{35} incorporation Controls = 100
DPN	I K.R.B.[1]	10.0	103
DPN	II ,,	1.0	142
TPN	,, ,,	0.3	120
Nicotinic acid amide	,, ,,	0.2	129
Glucose	,, ,,	10.0	123
Glutamic acid	,, ,,	8.8	106
α-ketoglutaric acid	,, ,,	4.4	115
Sodium succinate	,, ,,	11.9	105
Glucose	,, K.R.P [2]	5.4	143
Glutamic acid	,, ,,	4.4	116
α-ketoglutaric acid	,, ,,	3.5	130
Sodium succinate	,, ,,	1.4	140

[1] Suspending medium: reagent 1.
[2] Suspending medium: reagent 2.

were added to the incubation solution on standardization. The effect on the sulphate incorporation was then determined according to method I or II.

It is seen from Table 2 that certain other substances tested biologically produced some stimulation of the sulphate exchange in chondroitin sulphuric acid.

In addition to the substances listed in Table 2, different concentrations of the following substances were tested: ACTH, alanine, arginine, aspartic acid, coenzyme A, creatine, creatinine, cysteine, cystine, ethanolamine, flavin mononucleotide, folic acid, galactose, glucose-1-phosphate, glucuronolactone, glycine, glycocyamine, growth hormone, heparin, histidine, hydroxyproline, inositol, isoleucine, lactoflavin, leucine, leucylglycylglycine, lysine, mannose, methionine, norleucine, norvaline, ornithine, pantothenic acid, phenylalanine, phenylglycine, proline, pyridoxal HCl, rhamnose, ribose, serine, taurine, threonine, tryptophan, tyrosine, urea, valine, vitamin B_{12}, xylose.

No substance has, however, hitherto been found that has a degree of S.E.S. activity approaching that demonstrated in the "crude" S.E.S. factor.

Effect of the S.E.S. factor on the oxygen consumption in the cartilage slices

Fig. 5 shows the results of two parallel experiments, in which the oxygen consumption and the sulphate incorporation in the slices of cartilage were studied in Krebs-Ringer-bicarbonate solution. They were performed under standard conditions (curves A and A_1), in the presence of 1 S.E.S. unit of the "crude" factor (curves B and B_1) and in the presence of monoiodoacetic acid (curves C and C_1). It may be inferred from the figure that both the sulphate incorporation and the oxygen consumption in the slices of cartilage were inhibited by monoiodoacetic acid, whereas the sulphate uptake was stimulated by the S.E.S. factor, with no corresponding stimulation of respiration.

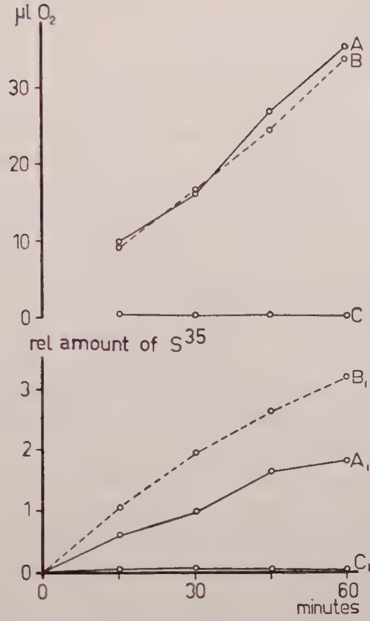

Fig. 5. Oxygen consumption (A, B, C) and sulphate incorporation (A_1, B_1, C_1) of costal cartilage from calves under standard conditions (A, A_1), in the presence of the S.E.S. factor (B, B_1) and in the presence of monoiodoacetic acid (C, C_1).

Discussion and summary

In earlier investigations on the sulphate exchange of chondroitin sulphuric acid (7), the S^{35} incorporation was determined after isolation of this compound from slices of cartilage incubated in the presence of S^{35}-labelled sulphate. In the present study, the S^{35} incorporation was determined directly in intact slices of cartilage, previously submitted to a special washing and drying procedure, by which contaminating inorganic sulphate was completely removed.

Small quantities of homogenate from organs and serum of different species of animals were found to be capable of stimulating the sulphate exchange *in vitro* of chondroitin sulphuric acid. This activity, which is ascribed to a sulphate exchange stimulating factor (S.E.S. factor), varied in intensity in different organs from the same species. On the other hand, it was shown that the strength of the S.E.S. activity in the organs and in the serum showed a species specificity in different species of animals. Finally, a comparison was made between the S.E.S. activity in the liver homogenate and in the serum of some species of animals. It was then found that those animals having a high S.E.S. activity in the liver also exhibited a high S.E.S. activity in the serum.

In preliminary experiments the S.E.S. activity of the liver had been found in a thermostable, dialyzable fraction of the liver homogenate (11).

In the present investigation, the S.E.S. factor of the liver was purified by fractional precipitation with mercuric acetate of a boiled extract of calf liver, followed by preparative paper electrophoresis. Two-dimensional paper chromatography then showed in the strongest preparation 7 ninhydrin-positive spots; one of them coincided with the localization of the S.E.S. activity.

In order to ascertain whether this compound is identical with any known cofactor or substrate, a large number of different substances, including available amino acids, were tested biologically. None of the substances tested exhibited an S.E.S. activity comparable to that obtained in the purified liver factor.

It is of particular interest to speculate on the relation between the factor in question and a number of other factors recently studied by other groups of workers, e.g., the UDP glucuronic acid recently isolated from rabbit liver by Storey and Dutton (18) and the active sulphate demonstrated by Bernstein and McGilvery (19). Little is known of the latter substance. The UDP glucuronic acid differs from the S.E.S. factor in that it has a strong ultraviolet absorption, whereas this was lacking in the S.E.S.-active spot on the paper chromatogram.

The Warburg tests performed in the present investigation seemed to show that the stimulation of the sulphate exchange in chondroitin sulphuric acid demonstrated is not correlated to a corresponding increase in oxygen consumption in the cartilage slices.

Note added in proof.—Further work has shown that the liver factor is probably identical to glutamine (Boström, H., Rodén, L., and Vestermark, A., Nature 1955 (in the press)).

This investigation was aided by grants from the Swedish State Medical Research Council, King Gustav's 80th Birthday Fund, the Swedish Rheumatic Association, the Swedish Cancer Society, and the Vitrum Company, Stockholm.

Chemistry Department II, Karolinska Institutet, Stockholm, Sweden.

REFERENCES

1. Dorfman, A., *in* Asboe-Hansen, G., Connective Tissue in Health and Disease. Munksgaard, Copenhagen, 1954, p. 81.
2. Boström, H., Arkiv f. Kemi *6*, 43 (1953).
3. Boström, H. and Jorpes, E., Experientia *10*, 392 (1954).
4. Schiller, S., Mathews, M. B., Goldfaber, L., Ludowieg, J., and Dorfman, A., J. Biol. Chem. *212*, 531 (1955).
5. Boström, H., J. Biol. Chem. *196*, 477 (1952).
6. Boström, H. and Gardell, S., Acta Chem. Scand. *7*, 216 (1953).
7. Boström, H. and Månsson, B., Arkiv f. Kemi *6*, 23 (1953).
8. Layton, L. L., Proc. Soc. Exp. Biol. and Med. *76*, 596 (1951).
9. Boström, H. and Odeblad, E., Arkiv f. Kemi *6*, 39 (1953).
10. Clark, I. and Umbreit, W. W., Proc. Soc. Exp. Biol. and Med. *86*, 558 (1954).
11. Boström, H. and Månsson, B., J. Pharm. Pharmacol. *7*, 185 (1955).
12. Boyd, E. S. and Neuman, W. F., Arch. Biochem. and Biophys. *51*, 475 (1954).
13. Boström, H. and Månsson, B., Acta Chem. Scand. *7*, 1014 (1953).
14. Grassmann, W. and Hannig, K., Naturwissenschaften *37*, 397 (1950).
15. Durrum, E. L., J. Am. Chem. Soc. *73*, 4875 (1951).
16. Brattsten, I. and Nilsson, A., Arkiv f. Kemi *3*, 337 (1951).
17. Umbreit, W. W., Burris, R. H., and Stauffer, J. F., Manometric Techniques and Tissue Metabolism. Burgess Publishing Co., Minneapolis, Minn., 1947.
18. Storey, I. D. E. and Dutton, G. J., Biochem. J. *59*, 279 (1955).
19. Bernstein, S. and McGilvery, R. W., J. Biol. Chem. *199*, 745 (1952).

Tryckt den 3 november 1955

Uppsala 1955. Almqvist & Wiksells Boktryckeri AB

ARKIV FÖR KEMI Band 8 nr 50

Communicated 27 April 1955 by GEORGE DE HEVESY and KARL MYRBÄCK

Turnover of plasma iron

By R. GIULIANO

With 5 figures in the text

It was known from clinical experience for many years that much or most of intravenously injected iron soon leaves the plasma. The highest serum iron values obtained after peroral iron tolerance tests in healthy people was about 300 μg per cent (1) and about the same values were obtained when ionized iron salts were injected intravenously. The subjects showed signs of intoxication if the intravenous iron injection was continued after this limit was reached (2). This observation induced HOLMBERG and LAURELL (3) to put forward the view that plasma is only capable of forming a complex binding of iron up to a certain limit corresponding to about 300 μg per cent iron. They were able to show that the iron in the plasma-iron-protein complex of physiological pH does not react with $\alpha\alpha_1$-dipyridyl (a strong complex former for ferrous iron) in spite of the presence of sodium dithionite. After addition of ferrous salts to serum the added iron is bound, up to a certain concentration denoted as saturation limit, in non-dipyridyl-reacting form. All iron added in excess over the saturation limits reacts, however, with dipyridyl. The physiological iron was found by LAURELL (9) to circulate bound to the β_1-globulin fraction making out 7 per cent of the total plasma protein. The iron-binding capacity of the rabbit plasma amounts to about 300 μg %. The binding capacity of plasma β_1-globulin or transferrin of the rabbit is about the same as that of the human and is far of being fully utilized. The iron content of the rabbit's plasma mostly varies between 130 and 230 μg %. only. The fasting mean serum iron content of rabbits as stated by Vahlquist (4) is 182 γ %, while NEANDER and VAHLQUIST (5) state 230 γ %.

The extent and rate of disappearance of intravenously injected iron ammonium citrate from the circulation of the rabbit was investigated by the last-mentioned authors (5). The present writer studied the rate of disappearance of injected labelled iron sodium citrate, this technique permitting not alone to determine the rate of disappearance of injected excess iron but also that of the rate of replacement of iron bound to β_1-globulin.

Experimental

Rabbits weighing 2 to 2.5 kg were injected into the vena jugularis with 2 to 560 μg of Fe^{59}-labelled iron as $FeCl_3$ of about 1 μcurie activity dissolved in 0.2 ml of physiological sodium citrate solution, and samples of 0.5 to 1.0 ml of blood were secured at intervals from the carotid. In other experiments a donor rabbit was injected with 2 to 6 μg of iron dissolved in sodium citrate. Blood was secured from this animal after the lapse of 1 hour or more and 6 ml of its heparinized plasma

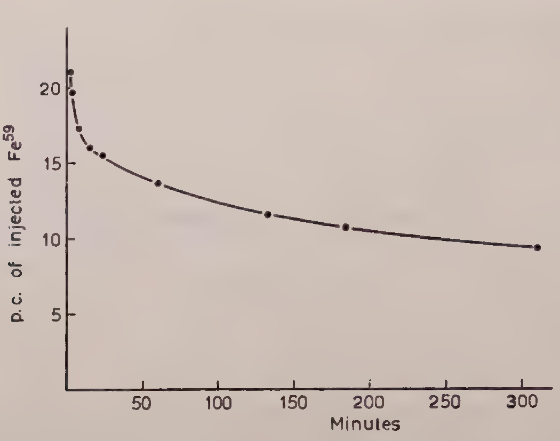

Fig. 1. Rate of disappearance of Fe^{59} from the plasma following injection of 560 microgram labelled iron as citrate.

injected into the vena jugularis of a sister rabbit. Urethane (1.5 g per kg body weight) was administered previous to injection into the vena jugularis.

The weight of the fresh and also of the dry plasma samples was determined. The radioactivity of dry plasma samples weighing 30 to 60 mg was then compared. The activity of a known aliquot of the donor plasma was determined in dry state as well, the specimen measured having the same weight as the secured dry plasma samples. Some of the acceptor rabbits were exposed two days previous to injection to a dose of 800 r of X-rays (165 kV, filter 1 mm Al, intensity 80 r/min.).

Results and discussion

The rate of disappearance from the serum of rabbits of 0.5–2.0 mg iron intravenously injected as ammonium citrate was, as already mentioned, investigated by NEANDER and VAHLQUIST by determining the iron content of serum samples secured at intervals. In the present investigation labelled iron was injected; by measuring the activity of plasma samples secured in the course of several hours not only could the rate of disappearance of the injected, not transferrin-bound iron be determined, but also the rate of disappearance of the transferrin-bound iron atoms present at the start of the experiment, which are replaced by non-radioactive iron atoms flowing mainly from the extracellular space and the reticulo-endothelial system into the plasma.

As seen from Fig. 1 after the lapse of 1.1 min. a mere 25 % of the injected 560 μg of labelled iron is present in the circulation. The plasma volume of the rabbit was 80 ml, its binding capacity for iron, about 300 μg %, being half utilized only.

NEANDER and VAHLQUIST observed already during the time of injection a disappearance of 70 to 80 % of iron from the serum. The injection took 2–4 min. in their experiments, and 20 sec. in ours; thus, our results hardly differ.

From the injected iron in our experiments 3.5 % was excreted through the kidneys and only 0.03 % was located in the bile.

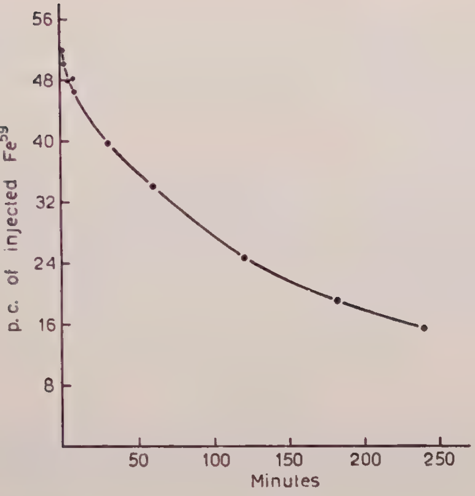

Fig. 2. Rate of disappearance of Fe^{59} from the plasma following injection of 2 microgram of iron as citrate.

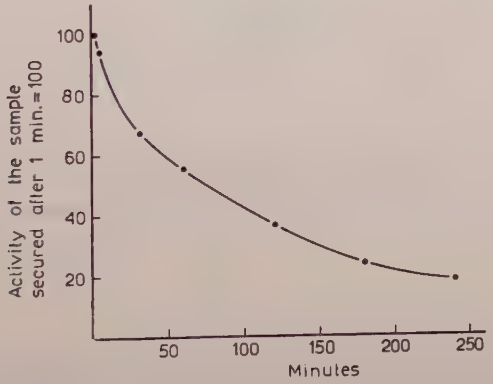

Fig. 3. Rate of disappearance of Fe^{59} from the plasma after injection of labelled iron transferrin containing plasma of a donor.

Fig. 2 shows the result of our experiment in which 2 µg of labelled iron were injected only. After the lapse of 1.1 min. 48 % of the injected iron left the circulation. As the transferrin content of plasma could in these experiments bind much more than 2 µg of iron, a large part of the injected iron must have left the circulation so rapidly that it had no opportunity to combine with transferrin. After further 4–5 min. the disappearance rate of labelled iron is about the same as that of the β_1-globulin bound transferrin iron, its half-value amounting to about 2 hours. In these experiments the mean value of injected iron excreted through the kidneys amounted to 0.05 %, 0.03 % being located in the bile.

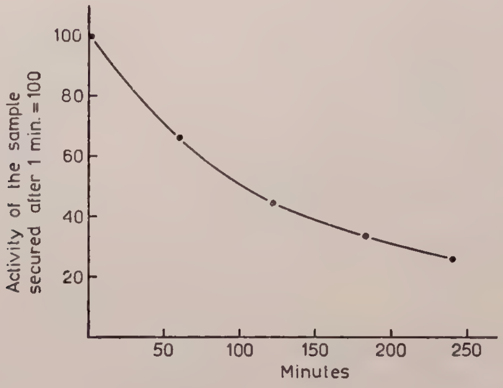

Fig. 4. Rate of disappearance of Fe^{59} from the plasma after injection of 1 microgram labelled iron transferrin containing plasma of a donor.

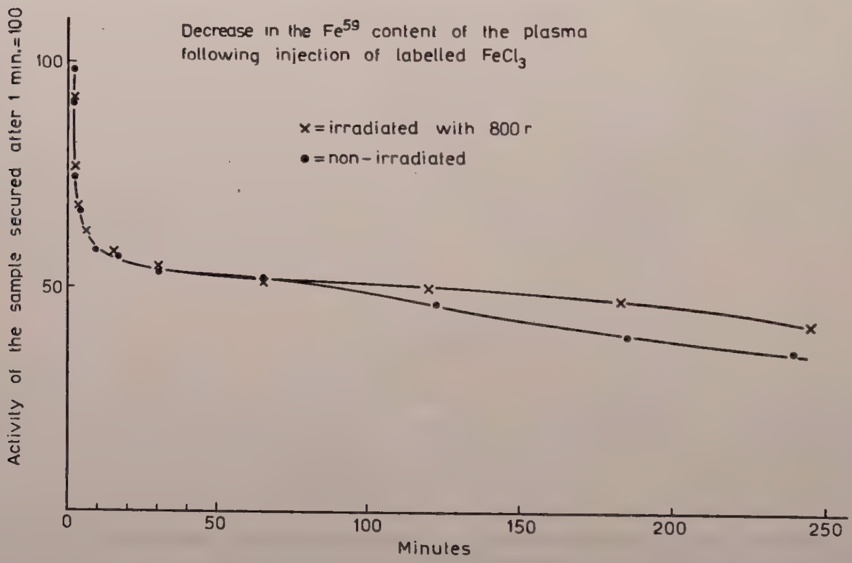

Fig. 5. Effect of exposure of the rabbit on the rate of disappearance of intravenously injected 560 microgram labelled iron from the plasma.

When injecting labelled plasma of a donor to which labelled iron was administered one hour or earlier, thus plasma containing transferrin iron only, this iron disappears from the plasma as seen from Figs. 3 and 4 with a half-value time of 2 hr.

About half of the iron which leaves the plasma is utilized in hemoglobin formation while the other half takes its way into the liver and other organs. Exposure to X-rays interferes with hemoglobin formation and correspondingly, as first shown by HENNESSY and HUFF (6), less Fe^{59} is incorporated into hemoglobin of the exposed animal. Due to this interference the iron atoms spend a longer time in the plasma of the irradiated rabbit; its transferrin-Fe^{59} content is higher than that of the controls, as shown in this laboratory (7, 8). As non-transferrin iron can be expected not to be utilized, or, more correctly, not directly utilized, in hemoglobin formation, the rate of disappearance of injected citrate iron is not to be expected to be influenced by exposure to X-rays.

Fig. 5 demonstrates the result of the effect of irradiation with 800 r two days previous to injection on the rate of disappearance of 560 μg iron injected as sodium citrate. Only in a later phase of the experiment in which the plasma contains transferrin iron only is the rate of disappearance of Fe^{59} slowed down in the exposed rabbit. In these experiments in the course of the first minute 80 % of the injected iron left the circulation while in the above-mentioned experiment (Fig. 1) the corresponding figure was 75 %.

Summary

From 560 μg labelled iron injected intravenously as sodium citrate, the injection taking 20 sec., 70 to 80 % left the circulation after the lapse of 1 minute. An almost identical result was obtained by NEANDER and VAHLQUIST injecting 0.5–2.0 mg iron and determining the iron content of the plasma by chemical analysis.

Making use of radio-iron as an indicator beside the rate of disappearance of the injected non-transferrin iron, the rate of replacement of transferrin iron atoms by extravascular ones can be determined as well. The half-lifetime of the transferrin iron atoms in the plasma of the rabbit is found to be about two hours.

Exposure of the rabbit to a dose of 800 r of X-rays does not influence the rate of disappearance of non-transferrin iron from the plasma in contrast to that of transferrin iron which is slowed down.

The author wishes to express his appreciation to Prof. GEORGE DE HEVESY for his help and encouragement in the conduct of this investigation, to Dr. ARNE FORSSBERG for irradiating the rabbits, and to Miss JUTTA SCHLIACK for assistance.

Institute of Organic Chemistry and Biochemistry, University of Stockholm.

REFERENCES

1. C. MOORE, W. ARROWSMITH, J. WELCH, and V. MINNICH, J. Clin. Invest. *18*, 553 (1939).
2. J. WALDENSTRÖM, Om järn och järnterapi. A.B. Ferrosan, Malmö 1944, p. 55.
3. C. G. HOLMBERG and C. B. LAURELL, Acta physiol. Scand. *10*, 307 (1945).
4. B. VAHLQUIST, Das Serumeisen. Diss. Acta pæd. 1941, *28*, Suppl. 5.
5. G. NEANDER and B. VAHLQUIST, Acta Physiol. Scand. *17*, 110 (1949).
6. T. J. HENNESSY and R. L. HUFF, Proc. Soc. Exptl. Biol. Med. *73*, 436 (1950).
7. G. HEVESY and G. DAL SANTO, Acta physiol. Scand. *32*, 339 (1954).
8. R. BONNICHSEN and G. HEVESY, Acta Chem. Scand. in print.
9. C. B. LAURELL, Acta physiol. Scand. *40*, 1 (1947).

Tryckt den 3 november 1955

Uppsala 1955. Almqvist & Wiksells Boktryckeri AB

ARKIV FÖR KEMI Band 8 nr 51

Communicated 13 October 1954 by ARNE FREDGA and BROR HOLMBERG

On carboxy-dithiocarbhydrazides and *N*-aminorhodanines

By JAN SANDSTRÖM

1. Introduction and survey

As a part of an investigation of different dithiocarbhydrazides, $RS \cdot CS \cdot NHNH_2$, attempts have been made to prepare a number of such compounds and derivatives thereof with one or two carboxy groups in the radical R.

The most simple compound of this class, S-carboxy-dithiocarbhydrazide (I), could not be prepared, nor could any of its derivatives. When ethyl chlorocarbonate was made to react with ammonium dithiocarbazinate, the only recognizable solid products were N,N'-bis-carbethoxyhydrazine (II) and ammonium chloride.

When the radical R contains a carboxy group in the α-position, the dithiocarbhydrazides (III) are stable only as salts. If the salt solutions are acidified, the primarily formed hydrazides immediately lose water and give cyclic anhydrides (X).

Thus potassium dithiocarbazinate and sodium monochloroacetate reacted in aqueous solution to give the salt of carboxymethyldithiocarbhydrazide (III a). When this solution was acidified, an anhydride was formed, which could be obtained in two forms, showing dimorphism and melting at 91°–92° and 100°–101° respectively.

$(HOCO \cdot S \cdot CS \cdot NHNH_2)$
I

$C_2H_5O \cdot CO \cdot NHNH \cdot CO \cdot OC_2H_5$
II

$(HOCOCHR \cdot S \cdot CS \cdot NHNH_2)$
III: a, $R = H$
b, $R = CH_3$
c, $R = C_6H_5$
d, $R = CH_2COOH$

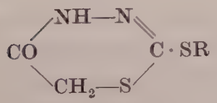

IV: a, $R = C_2H_5$
b, $R = CH_2COOH$
c, $R = CH_2CH_2COOH$

The reaction mixture from ammonium dithiocarbazinate and sodium monochloroacetate gave several reactions typical for dithiocarbhydrazides. It could be made to react with haloid esters giving derivatives of 1,3,4-thiadiazine. With ethyl bromide, 2-ethylthio-1,3,4,4H-thiadiazin-5(6)-one (IV a) (1) was obtained, with sodium monochloroacetate the corresponding carboxymethylthio derivative (IV b), m.p. 160°–160.5°, and with sodium β-bromopropionate the β-carboxyethylthio derivative (IV c), m.p. 164°–165°.

With thioesters 1,3,4-thiadiazoles were obtained. With dicarboxymethyl trithiocarbonate in excess of alkali the 2-carboxymethylthio-5-mercapto-1,3,4-thiadiazole (Va) already described by Bose (2) was obtained. This product was also obtained in good yield when two moles of dicarboxymethyl trithiocarbonate was dissolved in excess of alkali and made to react with one mole of hydrazine hydrate. In both reactions the bis-carboxymethyldithiocarbhydrazide (VI) may have been an intermediate compound, from which (Va) was formed by splitting off thioglycollic acid. However, analogous to bis-ethyldithiocarbhydrazide (1), (VI) could also be expected to split off hydrogen sulphide to form 2,5-bis-carboxymethylthio-1,3,4-thiadiazole (VIIa). No (VIIa) could be found in the reactions described, but it could easily be prepared from (Va) and sodium monochloroacetate and had m.p. 169°–170°.

The reaction between carboxymethyldithiocarbhydrazide salt solution and diethyl trithiocarbonate in exess of alkali gave a mixture of (Va) and 2-ethylthio-5-mercapto-1,3,4-thiadiazole (Vb), described in (1). No 2-carboxymethylthio-5-ethylthio-1,3,4-thiadiazole (VIIb) could be isolated, but this compound could easily be prepared from (Va) and ethyl bromide and from (Vb) and sodium monochloroacetate. It had m.p. 103°–104°.

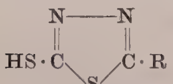

(HOCOCH$_2$S·CS·NHNH·CS·SCH$_2$COOH)
VI

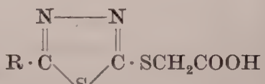

V: a, R = SCH$_2$COOH
b, R = SC$_2$H$_5$
c, R = OC$_2$H$_5$
d, R = C$_6$H$_5$

VII: a, R = HOCOCH$_2$S
b, R = C$_2$H$_5$S
c, R = C$_2$H$_5$O
d, R = C$_6$H$_5$

When the carboxymethyldithiocarbhydrazide salt solution was made to react with ethylxanthogenacetic acid, thioglycollic acid was split off and 2-ethoxy-5-mercapto-1,3,4-thiadiazole (Vc), m.p. 128°–128.5°, was formed. No 2-carboxymethylthio-5-ethoxy-1,3,4-thiadiazole (VIIc) could be isolated, but it was easily prepared from (Vc) and sodium monochloroacetate and had m.p. 85°–86°. The thiadiazole (Vc) was also prepared from potassium dithiocarbazinate and ethylxanthogenacetic acid.

Finally, with carboxymethyl dithiobenzoate the carboxymethyldithiocarbhydrazide salt solution gave a mixture of the already (1) described 2-phenyl-5-mercapto-1,3,4-thiadiazole (Vd) and 2-carboxymethylthio-5-phenyl-1,3,4-thiadiazole (VIId).

When solutions of carboxymethyldithiocarbhydrazide salt were made to react with formaldehyde or acetaldehyde and then acidified, no definable compounds could be obtained. With acetone the anhydride of carboxymethyldithiocarbhydrazide was obtained together with sticky products, and with levulinic acid an unstable acid was obtained. On slight heating it decomposed and gave the anhydride of carboxymethyldithiocarbhydrazide together with levulinic acid, and it was therefore not further investigated. With benzaldehyde and acetophenone stable hydrazones were obtained with m.p. 167°–168° and 159.5°–160° respectively. They could not be made to split off water to form cyclic anhydrides. The benzaldehyde carboxymethyldithiocarbhydrazone (VIII a) with hydrazine hydrate gave the previously (1) described monobenzaldehyde thiocarbhydrazone. With ethyl bromide in alkaline solution the benzaldehyde S′-ethyl-S″-carboxymethyl-*iso*dithiocarbhydrazone, m.p. 126°–127°, was obtained. This product was found to be identical with the one which was obtained (1) from benzaldehyde ethyldithiocarbhydrazone and sodium monochloroacetate, though it was to be expected, from the experiences of BUSCH (3–8), that the two products would show stereoisomerism. With sodium monochloroacetate (VIIIa) gave benzaldehyde S′, S″-bis-carboxymethyl-*iso*dithiocarbhydrazone (IX), melting from 148° to 208°. The wide melting range was due to a decomposition with the formation of benzaldehyde and a compound with m.p. 260°–261°, the composition of which showed a scanty agreement with the formula $C_{21}H_{18}O_5N_4S_3$. However, this product could not be purified, and it was therefore not further investigated.

$HOCOCHRS \cdot CS \cdot NHN : CH \cdot C_6H_5$

VIII: a, $R = H$
b, $R = CH_3$
c, $R = C_6H_5$
d, $R = CH_2COOH$

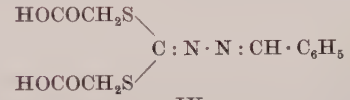

$$\begin{matrix} HOCOCH_2S \\ HOCOCH_2S \end{matrix} \!\!> C : N \cdot N : CH \cdot C_6H_5$$

IX

When solutions of carboxymethyldithiocarbhydrazide salt were added to mutarotated solutions of *l*-arabinose, *d*-glucose or *d*-mannose, considerable changes in the optical rotation of the solutions occurred, which may indicate the formation of hydrazides, but when the solutions were acidified, the anhydride of carboxymethyldithiocarbhydrazide separated, and from the solutions the free monosaccharides could be isolated as thiobenzhydrazides (9). As the desired hydrazides were not obtained, no experimental details have been given.

The anhydride of the carboxymethyldithiocarbhydrazide has been subjected to a separate investigation. It has previously been described by ANDREASCH (10), who obtained it from hydrazinium dithiocarbazinate and ethyl monochloroacetate and found m.p. 92°, and by HOLMBERG (11), who obtained it from the sodium salt of dicarboxymethyl trithiocarbonate and hydrazine hydrate and also reports m.p. 92°. These two authors formulate the compound as *N*-aminorhodanine or 3-aminothiazol-4(5)-one-2(3)-thione (Xa), and the results of the present investigation are in complete agreement with this formulation. The anhydride has also been described by BOSE (2), who obtained it from potassium dithiocarbazinate and ethyl monochloroacetate and reports m.p. 92°. However, he formulates the product as 1,3,4,4H-thiadiazin-5(6)-one-2-yl disulphide but, when his preparation was repeated by the author, a compound was obtained which was identical with the anhydride from potassium dithiocarbazinate and sodium monochloroacetate. Recently, the anhydride has been described by MATHES (12), who obtained it from ammonium dithiocarbazinate and monochloroacetic acid and reports m.p. 90°–91°. He formulates the product as 2-mercapto-1,3,4,4H-thiadiazin-5(6)-one (XI), isomeric with *N*-aminorhodanine, but he gives no proof to support his formulation. Besides, in his survey of the previously described mercaptothiadiazines, he erroneously includes the compounds obtained by BUSCH (13, 14) in reactions between ethylene bromide and potassium phenyldithiocarbazinate and related dithiocarbazinates. MATHES has not observed that BUSCH, in a later work (15), abandoned the mercaptothiadiazine formula (XII) and proved that the compounds are 1,3-dithiacyclopentan-2-one phenylhydrazone and related hydrazones (XIII).

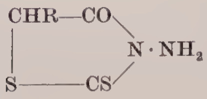

X: a, R = H
b, $R = CH_3$
c, $R = C_6H_5$
d, $R = CH_2COOH$

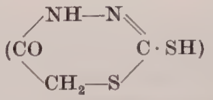

XI

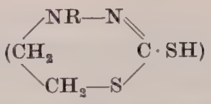

XII

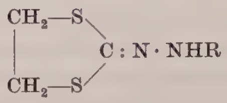

XIII

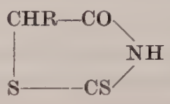

XIV: a–d as in X.

The correctness of formula (X) was proved by the reaction between the anhydride and nitrous acid. In this reaction the anhydride exchanged one amino group for hydrogen and gave the unsubstituted rhodanine (XIV a). This reaction is observed with several other heterocyclic compounds with amino groups attached to nitrogen in the heterocyclic ring (16–18). The presence of an amino group in the anhydride was further demonstrated by the fact that it gave Schiff bases (XV) with aromatic aldehydes and cinnamic aldehyde. The Schiff base with benzaldehyde had m.p. 137°–138°, with vanillin 186°–189° and with cinnamic aldehyde 145°–146°. All attempts to obtain Schiff bases with ketones and with aliphatic aldehydes, also monosaccharides, were in vain.

The 3-aminorhodanine contains an active methylene group, which can be made to condense with aromatic aldehydes, with cinnamic aldehyde, with acetone and with laevulic acid to compounds of type (XVI).

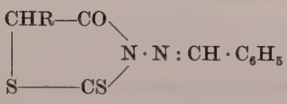

XV: a–d as in X

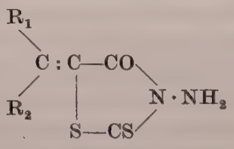

XVI

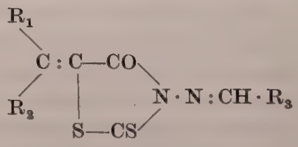

XVII

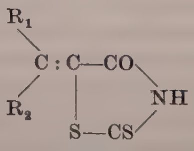

XVIII

With the aldehydes the condensations were effected by refluxing the components with fused sodium acetate in glacial acetic acid. For the ketones a solution of ammonium chloride in aqueous ammonia was found to be the best condensing agent (19).

The 3-amino-5-benzylidene-rhodanine had m.p. 199°–200° and gave Schiff bases (XVII) with benzaldehyde of m.p. 172°–173°, with vanillin of m.p. 210°–211° and with cinnamic aldehyde of m.p. 188°–189°. The 3-amino-5-vanillylidene-rhodanine had m.p. 206°–207° and gave Schiff bases with benzaldehyde of m.p. 204°–205°, with vanillin of m.p. 234°–236° and with cinnamic aldehyde of m.p. 201°–202°.

The 3-amino-5-cinnamylidene-rhodanine had m.p. 229.5°–230° and gave Schiff bases with benzaldehyde of m.p. 170°–171°, with vanillin of m.p. 199°–201° and with cinnamic aldehyde of m.p. 198°–204. The 3-amino-5-*iso*propylidene-rhodanine had m.p. 148°–149° and gave a Schiff base with benzaldehyde of m.p. 104°–105°. Finally, the 3-amino-5-[4′-carboxy-butylid-2′-ene]-rhodanine was unstable and could be obtained only as its ammonium salt with m.p. 159°–159.5°, and it was therefore not further investigated.

The 3-amino-5-benzylidene-rhodanine and the 3-amino-5-*iso*propylidene-rhodanine were degraded by nitrous acid to the corresponding, previously known rhodanine derivatives (XVIII), (28) and (31), which may serve as a further proof of their constitution. In the same reaction the 3-amino-5-vanillylidene-rhodanine gave 5-[5′-nitrovanillylidene]-rhodanine, m.p. 266°–267°, identical with the product from 5-nitro-vanillin and rhodanine. From 3-amino-5-cinnamylidene-rhodanine and nitrous acid no definable compound could be obtained.

When sodium *d,l*-α-bromopropionate was made to react with potassium dithiocarbazinate in water and the solution was acidified, 3-amino-5-methyl-rhodanine (X b), m.p. 65.5°–66°, was obtained. This compound was degraded by nitrous acid to the previously known 5-methylrhodanine (XIV b) (32). The Schiff base with benzaldehyde (XV b) could not be made to crystallize, but with veratraldehyde a crystalline compound was obtained with m.p. 139°–140°. When the reaction mixture from potassium α-bromopropionate and potassium dithiocarbazinate after some hours was made to react with benzaldehyde in ethanol, the dihydrate of the monopotassium salt of benzaldehyde α-carboxyethyldithiocarbhydrazone was obtained with m.p. 198°–199°. When a solution of this salt was acidified, the corresponding acid (VIII b) was obtained, m.p. 147°–147.5°.

When sodium *d,l*-α-chlorophenylacetate was made to react with potassium dithiocarbazinate in water, the solution after some hours deposited a small amount of 3-amino-5-phenyl-rhodanine (X c) with m.p. 121°–121.5°. The filtrate on acidification gave a further amount of the same compound. With nitrous acid (X c) gave the previously known 5-phenyl-rhodanine (XIV c) (33). This rhodanine could also be obtained by splitting off water from α-carboxybenzyl dithiocarbamate, prepared from ammonium dithiocarbamate and sodium *d,l*-α-chlorophenylacetate. This method is analogous to the method of Holmberg (20) for the preparation of rhodanine with carboxymethyl dithiocarbamate as intermediate compound.

With benzaldehyde the 3-amino-5-phenyl-rhodanine gave a Schiff base (XV c) with m.p. 156.5°–157°.

When the reaction mixture from potassium α-chlorophenylacetate and potassium dithiocarbazinate, after separating the first formed 3-amino-5-phenyl-rhodanine, was made to react with benzaldehyde in ethanol, the monopotassium salt of benzaldehyde α-carboxybenzyldithiocarbhydrazone was obtained, m.p. 159°–159.5°. When a solution of this salt was acidified, the corresponding acid (VIII c) was obtained, m.p. 175°–176°.

When ammonium dithiocarbazinate was made to react with sodium β-bromopropionate and the mixture was acidified after one day, the β-carboxyethyldithiocarbhydrazide (XIX) was obtained, m.p. 113.5°–114.5°. This product has recently been described by Mathes (21), who obtained it from ammonium dithiocarbazinate and β-propiolactone and reports m.p. 109°–111°. This hydrazide could not be made to split off water and cyclizate as distinct from the β-carboxyethyl dithiocarbamates, which give propiorhodanines (22).

When the β-carboxyethyldithiocarbhydrazide was dissolved in two equivalents of aqueous alkali and made to react with sodium monochloroacetate, after acidification, the 2-[β-carboxyethylthio]-1,3,4,4H-thiadiazin-5(6)-one (IV c) was obtained, identical with the product from carboxymethyldithiocarbhydrazide salt and sodium β-bromopropionate.

When an acid solution of the β-carboxyethyldithiocarbhydrazide was oxidized with iron (III) chloride, the 2,5-bis-[β-carboxyethylthio]-1,3,4-thiadiazole (XX a) was obtained, m.p. 144°–145°.

With carboxymethyldithiobenzoate the β-carboxyethyldithiocarbhydrazide gave 2-phenyl-5-mercapto-1,3,4-thiadiazole (V d) (1) and 2-[β-carboxyethylthio]-5-phenyl-1,3,4-thiadiazole (XX b), m.p. 112°–113°. The latter product was obtained in poor yield, but it could readily be prepared from 2-mercapto-5-phenyl-1,3,4-thiadiazole and sodium β-bromopropionate.

With acetaldehyde the β-carboxyethyldithiocarbhydrazide gave a crystalline hydrazone, m.p. 129°–129.5°, and with benzaldehyde a hydrazone with m.p. 160°–160.5°. When this hydrazone was oxidized with iodine, a disulphide was obtained, m.p. 161.5°–162.5°. When the hydrazone was oxidized with iron (III) chloride, the disulphide was obtained together with 2-[β-carboxyethylthio]-5-phenyl-1,3,4-thiadiazole (XX b).

When a solution of the benzaldehyde β-carboxyethyldithiocarbhydrazone in two equivalents of aqueous alkali was made to react with sodium monochloroacetate, and the mixture was acidified after one day, the benzaldehyde S′-carboxymethyl-S″-[β-carboxyethyl]-*iso*dithiocarbhydrazone (XXI) was obtained, m.p. 134°–135°. According to Busch (3–8) a stereoisomeric hydrazone might be obtained from benzaldehyde carboxymethyldithiocarbhydrazone and sodium β-bromopropionate. However, when this product was prepared, it was found to be identical with the compound just described.

The acetone β-carboxyethyldithiocarbhydrazone had m.p. 137°–138° and the pyruvic acid β-carboxyethyldithiocarbhydrazone had m.p. 159.5°–160°.

$HOCOCH_2CH_2S \cdot CS \cdot NHNH_2$

XIX

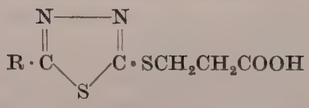

XX: a, $R = HOCOCH_2CH_2S$
b, $R = C_6H_5$

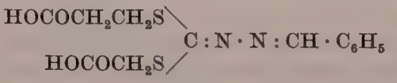

$$\begin{matrix} HOCOCH_2CH_2S\diagdown & \\ & C:N \cdot N:CH \cdot C_6H_5 \\ HOCOCH_2S\diagup & \end{matrix}$$

XXI

With *l*-arabinose the β-carboxyethyldithiocarbhydrazide gave a crystalline *l*-arabinose β-carboxyethyldithiocarbhydrazide hemihydrate, m.p. 121°–122°. The rotation of a pyridine solution of the hydrazide hemihydrate slowly increased, but the solution gradually darkened so that no end point of the rotation could be obtained After 18 hours $[\alpha]_D^{20}$ was $+21.6°$ (calculated on anhydrous substance). When this hydrazide was oxidized with iron (III) chloride, no crystalline product could be obtained. With *d*-glucose the β-carboxyethyldithiocarbhydrazide gave *d*-glucose β-carboxyethyldithiocarbhydrazide, m.p. 115°–120°, $[\alpha]_D^{20} = +26.8°$ and $[M]_D^{20} =$

+ 91.4° (in pyridine). When this hydrazide was oxidized with iron(III)chloride, the 2,5-bis-[β-carboxyethylthio]-1,3,4-thiadiazole (XXa) was obtained.

Kallenberg, in his investigation of the stereochemistry of dithiocarbamates and rhodanines (23), found that the hydrogen atoms in the 5-position of the rhodanines were so mobile, that no stereoisomerism due to asymmetry in this position could be found.

In order to find out if the hydrogen atoms in the 5-position of the 3-amino-rhodanines were mobile enough to cause an equally rapid inversion, the reaction between ammonium dithiocarbazinate and sodium *l*-bromosuccinate was studied.

The rotation of the mixture first increased and passed through a maximum after three hours and then slowly decreased and became constant after six days. When the solution was acidified after that time, only sticky decomposition products could be obtained. If the mixture was acidified after three hours, the 3-amino-5-carboxymethyl-rhodanine (Xd) monohydrate was obtained, m.p. 81°–82°. The product was inactive and identical with the anhydride obtained from ammonium dithiocarbazinate and sodium *d,l*-bromosuccinate. If benzaldehyde in ethanol was added to the reaction mixture from *l*-bromosuccinate and dithiocarbazinate after three hours and the mixture was acidified on the following day, the benzaldehyde α,β-dicarboxyethyldithiocarbhydrazone (VIIId) was obtained, m.p. 165°–165.5°, $[\alpha]_D^{20} = +9.16°$ and $[M]_D^{20} = +28.6°$ (in absolute ethanol). Thus, the disappearing of the optical acitivity is due to the ring closure, which is in good agreement with Kallenberg's results. From inactive material a benzaldehyde α,β-dicarboxyethyldithiocarbhydrazone was obtained with m.p. 169.5°–170°.

The correctness of structure (Xd) was demonstrated by the reaction with nitrous acid, whereby 5-carboxymethyl-rhodanine (XIVd) was obtained, m.p. 160°–161°, identical with the product from ammonium dithiocarbamate and sodium *d,l*-bromosuccinate. With benzaldehyde the 3-amino-5-carboxymethyl-rhodanine gave a Schiff base (XVd) with m.p. 189°–190°.

When the reactions, now described for bromosuccinic acid, were tried with *l*-bromosuccinamic acid, no crystalline products could be obtained.

2. Experimental

A. *The reaction between ammonium dithiocarbazinate and ethyl chlorocarbonate*

When solid ammonium dithiocarbazinate, 2.5 g, was ground with 2.5 g of ethyl chlorocarbonate in 15 ml of ether, the remperature rose and the mixture stiffened to a porridge of colourless crystals. On the following day the product was sucked off, washed with ether and recrystallized from 10 ml of water. From 2.8 g of crude product 0.9 g of colourless, rodshaped prisms were obtained, m.p. 133°–134°, according to analyses consisting of N,N'-bis-carbethoxyhydrazine (II).

For $C_6H_{12}O_4N_2$ (176.18)

calc.:	C 40.9	H 6.87	N 15.90 %,
found:	C 40.9*[1]	H 6.92*[1]	N 15.90 %.

---

[1] The analyses marked with an asterisk have been performed at the Analytical Department, University of Lund, and the rest by the author.

This compound was first described by CURTIUS and HEIDENREICH (24), who report m.p. 130°.

When the ethereal filtrate from the crude product was evaporated, only a small amount of sticky material was obtained. The water solution contained a considerable amount of ammonium chloride.

B. *Carboxymethyldithiocarbhydrazide and aminorhodanine*

a) *3-Aminorhodanine*

A solution of sodium monochloroacetate was prepared from 9.5 g of monochloroacetic acid and 10 g of sodium carbonate in 25 ml of water and made just alkaline to phenolphthalein with 7.5 ml of *N*-NaOH. In this solution 15 g of potassium dithiocarbazinate[1] was dissolved. After some minutes the temperature rose to about 40°, and when the solution had been cooled to room temperature it was diluted to 50 ml. If the reaction had been complete, this solution would have been a 2 *M* solution of carboxymethyldithiocarbhydrazide salt. However, if the solution was acidified at various times after its preparation, varying yields of aminorhodanine were obtained. The best yield, 75 %, was obtained if the solution was acidified after three hours, but then the liberation of a small amount of carbon disulphide indicated that the primary reaction was not completed. If the acidification was performed later, both yield and purity of the aminorhodanine decreased. After more than one day no crystalline product was obtained. As will be described later (p. 499), the salt solution with benzaldehyde gives a small amount of 3-amino-5-benzylidene-rhodanine together with benzalazine and benzaldehyde carboxymethyldithiocarbhydrazone (VIIIa). Therefore it seems probable that the carboxymethyldithiocarbhydrazide salt to a small extent had cyclizated to aminorhodanine.

The carboxymethyldithiocarbhydrazide salt solutions mentioned in the following descriptions of experiments were used about three hours after their preparation.

When 10 ml of a 2 *M* carboxymethyldithiocarbhydrazide salt solution was acidified after three hours with 10 ml of 2 *N*-HCl, the mixture deposited 2.3 g of pale yellow needles with m.p. 88°–89°. The product was recrystallized from 25 ml of ethanol and gave 1.8 g of pale yellow needles with m.p. 91°–92°.

For $C_3H_4ON_2S_2$ (148.20) (X a)

calc.:	C 24.3	H 2.72	N 18.90	S 43.3 %
found.:	C 24.4	H 2.72	N 18.91	S 43.1 %.

When the preparation was repeated after some time, a crude product was obtained with m.p. 99°–100° in the same yield. After recrystallization from ethanol the m.p. was 100°–101°.

found: C 24.4	H 2.76	N 18.90	S 43.2 %.

If a supersaturated solution of the low-melting form in ethanol was seeded with the high-melting, the resulting product was high-melting, but at first the reverse transformation could not be effected. However, when the high-melting form was dissolved in boiling ethanol in a laboratory, where no aminorhodanine had been prepared, and the solution was seeded with the low-melting form, the resulting product was low-melting.

---

[1] Prepared according to BUSCH (7).

b) *Reactions between carboxymethyldithiocarbhydrazide and haloid esters*

When a solution of 2.2 g of *ethyl bromide* in 40 ml of ethanol and 10 ml of 2 *N*-NaOH was added to 10 ml of the carboxymethyldithiocarbhydrazide salt solution just described, a homogeneous mixture was obtained. On the following day it was acidified with 5 ml of 5 *N*-HCl and separated 1.2 g of colourless, somewhat oily flakes of m.p. 120°–125°. The product was recrystallized from 5 ml of ethanol and gave 0.8 g of colourless, naphthaline-like flakes of m.p. 132°–132.5° alone and also on admixture with 2-ethylthio-1,3,4,4H-thiadiazin-5(6)-one (IV a) (1).

For $C_5H_8ON_2S_2$ (176.25) calc.: N 15.90, found: N 15.98 %.

A solution of 9.5 g of *monochloroacetic acid* and 10 g of sodium carbonate in 15 ml of water was made just alkaline to phenolphthalein with 5.5 ml of *N*-NaOH and then added to a mixture of 50 ml of 2 *M* carboxymethyldithiocarbhydrazide salt solution and 20 ml of 5 *N*-NaOH. On the following day the resulting clear mixture was acidified with 40 ml of 5 *N*-HCl. The mixture became cloudy and began to separate colourless prisms, and by the following day 6.8 g (about 30 % yield) of m.p. 154°–156° had been obtained. When 5 g of this product were recrystallized from 20 ml of ethanol, 3.1 g of colourless, irregular prisms were obtained, m.p. 158°–159°. A further recrystallization from 10 ml of ethanol gave 2.4 g of colourless prisms, m.p. 160°–160.5°, according to analyses consisting of 2-carboxymethylthio-1,3,4,4H-thiadiazin-5(6)-one (IV b).

For $C_5H_6O_3N_2S_2$ (206.24)

calc.:	C 29.1	H 2.93	N 13.58	S 31.1 %,	equiv.w.:	206.2,
found:	C 29.1	H 2.95	N 13.64	S 30.9* %,	„ „ :	206.8.

A solution of 6.1 g of *β-bromopropionic acid* and 2.1 g of sodium carbonate in 10 ml of water and 2.2 ml of *N*-NaOH (phenolphthalein) was added to a mixture of 20 ml of 2 *M* carboxymethyldithiocarbhydrazide salt solution and 8 ml of 5 *N*-NaOH. A clear mixture was obtained, which on the following day was acidified with 10 ml of concentrated hydrochloric acid. The mixture first remained clear but after some hours it began to separate colourless, irregular prisms, until the following day 2.1 g (24 % yield) with m.p. 160°–161° had formed. This product was recrystallized twice from 10 and 8 ml of ethanol and gave 1.4 g of colourless, rodshaped prisms, m.p. 164°–165° (product 1).

The same compound could be obtained from the β-carboxyethyldithiocarbhydrazide described later (p. 511) and sodium monochloroacetate. A solution of 1.4 g of monochloroacetic acid in 15.2 ml of *N*-NaOH (phenolphthalein) was added to a solution of 1.8 g of β-carboxyethyldithiocarbhydrazide in 20 ml of *N*-NaOH. When, on the following day, the clear mixture was acidified with 5 ml of 5 *N*-HCl, colourless, irregular prisms slowly began to separate, and on the following day 0.9 g was collected (41 % yield), m.p. 163°–164°. The product was recrystallized from 5 ml of ethanol and gave 0.8 g of colourless, rodshaped prisms (product 2) of m.p. 164°–165° alone and also on admixture with product 1. According to analyses the two products were 2-[β-carboxyethylthio]-1,3,4,4H-thiadiazin-5(6)-one (IV c).

For $C_6H_8O_3N_2S_2$ (220.26)

calc.:	C 32.7	H 3.66	N 12.72	S 29.1 %,	equiv.w.:	220.3,
found:	C 32.5[1]	H 3.54[1]	N 12.71[2]	S 29.1*[2] %,	„ „ :	220.0[2],

---

[1] Product 1.

[2] Product 2.

c) *Reactions between carboxymethyldithiocarbhydrazide and thioesters*

A solution of 4.6 g of *dicarboxymethyl trithiocarbonate* in 30 ml of 2 *N*-NaOH (50 % excess) was added to 10 ml of a 2 *M* carboxymethyldithiocarbhydrazide salt solution. On the following day the clear, yellow mixture was acidified with 20 ml of 5 *N*-HCl and 2.6 g (62% yield) of pale yellow prisms separated, m.p. 165°–166°. The product was recrystallized twice from 20 ml of water and gave 2.0 g of colourless flakes, m.p. 168°–169° (product 1).

A solution of 45.2 g of dicarboxymethyl trithiocarbonate in 25 ml of ethanol and 100 ml of 6 *N*-NaOH was cooled with ice, and 6.0 ml of 85 % aqueous hydrazine hydrate was added. The yellow colour soon faded, and on the following day the clear mixture was acidified with 125 ml of 5 *N*-HCl. Colourless flakes began to separate, and on the following day 17.8 g (85% yield) were obtained with m.p. 167°–169°. When 5 g of this product were recrystallized from 20 ml of water, 4.6 g of colourless flakes were obtained (product 2) with m.p. 168°–169° alone and also on admixture with product 1. According to analyses the products were 2-carboxymethylthio-5-mercapto-1,3,4-thiadiazole (Va).

For $C_4H_4O_2N_2S_3$ (208.27)

calc.:	C 23.1	H 1.94	N 13.45	S 46.2 %,	equiv.w.:	104.1 (alkali)	
found:	C 23.2[2]	H 1.98[2]	N 13.41[1]	S 46.0[1] %,	,, ,, :	104.2[1],	104.3[2]

calc.: equiv.w.: 208.3 (iodine),
found: ,, ,,: 203.0[1], 203.4[2].

This thiadiazole has previously been described by Bose (2), who obtained it from potassium dithiocarbazinate and monochloroacetic acid and reports m.p. 164°.

When a solution of 1.0 g of monochloroacetic acid in 10.5 ml of *N*-NaOH (phenolphthalein) was added to a solution of 2.1 g of carboxymethylthio-mercapto-thiadiazole in 20.2 ml of *N*-NaOH (phenolphthalein), a clear, colourless mixture was obtained. On the following day it was acidified with 5 ml of 5 *N*-HCl. The mixture stiffened to a porridge of long, colourless, rodshaped prisms, 2.1 g of m.p. 167°–168°. When 1.9 g of this product were recrystallized from 20 ml of water, 1.6 g of long, colourless, rodshaped prisms were obtained with m.p. 169°–170°, according to analyses consisting of 2,5-bis-carboxymethylthio-1,3,4-thiadiazole (VIIa).

For $C_6H_6O_4N_2S_3$ (266.31)

calc.:	C 27.1	H 2.27	N 10.52	S 36.1 %,	equiv.w.:	133.2,
found:	C 27.1	H 2.24	N 10.50	S 36.1 %,	,, ,,:	133.1.

A solution of 6.7 g of *diethyl trithiocarbonate* in 100 ml of ethanol was added dropwise with stirring to a mixture of 20 ml of 2 *M* carboxymethyldithiocarbhydrazide salt solution and 20 ml of 3 *N*-NaOH. On the following day the clear, yellow mixture, which smelt strongly of ethanethiol, had separated a small amount of colourless crystals. When 20 ml of water was added to the mixture, the crystals dissolved, and the mixture became turbid. It was evaporated to about 50 ml in a stream of air, and 0.3 g of a yellow oil separated and was taken up in ether. Acidification of the water solution with 25 ml of 5 *N*-HCl caused the separation of 5.0 g of a colourless crystal mass, m.p. 110°–120°. The product was treated with 20 ml of hot benzene and filtered hot from 1.6 g of colourless, irregular prisms, m.p. 150°–160° after sintering.

---

[1] Product 1. [2] Product 2.

This product was recrystallized twice from 15 and 10 ml of water and gave 1.0 g of colourless flakes, m.p. 167.5°–169° alone and also on admixture with 2-carboxymethylthio-5-mercapto-1,3,4-thiadiazole. The product showed equiv.w.: 104.7 (alkali) and 202.0 (iodine), calculated 104.1 and 208.3 respectively.

After cooling, the benzene solution separated 2.8 g of colourless prisms, m.p. 123°–125°. This product was recrystallized from 20 ml of benzene and gave 2.3 g of colourless prisms, m.p. 126°–127° alone and also on admixture with 2-ethylthio-5-mercapto-1,3,4-thiadiazole (V b), (1). The product showed the equiv.w.: 179.0 (alkali) and 175.0 (iodine), calculated 178.3.

When a solution of 1.1 g of ethyl bromide in 40 ml of ethanol was added to a solution of 2.1 g of carboxymethylthio-mercapto-thiadiazole (V a) in 20.2 ml of *N*-NaOH (phenolphthalein), a clear mixture was obtained, and on the following day a small amount of colourless crystals had separated. When 40 ml of water was added, the crystals dissolved, and the mixture was acidified with 10 ml of 2 *N*-HCl. On the following day 1.2 g of colourless, somewhat sticky flakes had separated, m.p. 100°–102°. The product was recrystallized from 5 ml of benzene and gave 1.1 g of colourless, thin, rodshaped prisms, m.p. 103°–104°. A further recrystallization from benzene did not change the m.p. (product 1).

A solution of 1.2 g (about 25 % excess) of monochloroacetic acid in 12.7 ml of *N*-NaOH (phenolphthalein) was added to a solution of 1.8 g of 2-ethylthio-5-mercapto-1,3,4-thiadiazole in 10.1 ml of *N*-NaOH (phenolphthalein). When the clear, colourless mixture was acidified on the following day, it became turbid, and an oil separated, which rapidly solidified to a colourless crystal mass, weighing 2.2 g and with m.p. 99°–100°. The product was recrystallized from 10 ml of benzene and gave 2.0 g of colourless, thin, rodshaped prisms, m.p. 103°–104° (product 2) alone and also on admixture with product 1. According to analyses the acid was 2-carboxymethylthio-5-ethylthio-1,3,4-thiadiazole (VII b).

For $C_6H_8O_2N_2S_3$ (236.32)

calc.: C 30.5	H 3.41	N 11.86	S 40.7 %,	equiv.w.:	236.3,
found: C 30.4[1]	H 3.39[1]	N 11.94[2]	S 40.7[2] %,	,, ,,:	236.7[1], 236.9[2].

While the reactions of carboxymethyldithiocarbhydrazide with dicarboxymethyl trithiocarbonate and with diethyl trithiocarbonate necessitated an excess of alkali, this was not the case with ethylxanthogenacetic acid and with carboxymethyl dithiobenzoate.

A solution of 7.2 g of *ethylxanthogenacetic acid* in 40.5 ml of *N*-NaOH was added to 20 ml of a 2 *M* carboxymethyldithiocarbhydrazide salt solution. A clear, colourless mixture was obtained, which soon began to smell of hydrogen sulphide and on the following day had deposited 3.2 g of colourless, somewhat sticky, rodshaped prisms, m.p. 115°–118°. The product was recrystallized from 20 ml of 50 % aqueous ethanol and gave 2.1 g of colourless, rodshaped prisms, m.p. 128°–128.5°. A further recrystallization did not change the m.p. According to analyses the product was 2-ethoxy-5-mercapto-1,3,4-thiadiazole (V c).

For $C_4H_6ON_2S_2$ (162.23)

calc.: C 29.6	H 3.73	N 17.27	S 39.5 %,	equiv.w.:	162.2,
found: C 29.4	H 3.62	N 17.31	S 39.7* %,	,, ,,:	162.6 (alkali) 159.4 (iodine).

---

[1] Product 1. [2] Product 2.

The filtrate from the crude product was acidified with 20 ml of 5 *N*-HCl and deposited a yellow oil, which solidified to 1.9 g of a somewhat sticky, yellow, crystalline mass, m.p. 140°–145° (decomp.). This product was recrystallized from 7.5 ml of 30 % aqueous ethanol and from a mixture of 5 ml of glacial acetic acid and 5 ml of benzene and gave 0.8 g of yellow flakes, m.p. 171°–172° (decomp.). According to analyses the product was dicarboxymethyl trithiocarbonate, probably formed by decomposition of ethylxanthogenacetate.[1]

For $C_5H_6O_4S_3$ (226.28)
calc.: C 26.5 H 2.67 %, equiv.w.: 113.1,
found: C 26.8 H 2.88 %, ,, ,,: 110.9.

The ethoxy-mercapto-thiadiazole (V c) could also be obtained by the reaction between ethylxanthogenacetate and potassium dithiocarbazinate. Solid potassium dithiocarbazinate, 3.0 g, was added to a solution of 3.6 g of ethylxanthogenacetic acid in 20.2 ml of *N*-NaOH (phenolphthalein). A clear, colourless mixture was obtained, which smelt strongly of hydrogen sulphide. On the following day 0.8 g of colourless, rodshaped prisms had separated, m.p. 126°–127°. The filtrate was acidified with 8 ml of 5 *N*-HCl and deposited a further 1.2 g of colourless prisms, m.p. 117°–125°. This product was recrystallized from 8 ml of benzene and gave 0.8 g of colourless, rodshaped prisms, m.p. 125°–126°. This product was combined with that first obtained and recrystallized from 10 ml of benzene. The result was 1.4 g of colourless, rodshaped prisms, m.p. 128°–128.5° alone and also on admixture with the ethoxy-mercaptothiadiazole described above.

A solution of 1.2 g of monochloroacetic acid in 12.5 ml of *N*-NaOH (phenolphthalein) was added to a solution of 1.6 g of the ethoxy-mercapto-thiadiazole in 10.2 ml of *N*-NaOH (phenolphthalein). A clear mixture was obtained, which on the following day was acidified with 6 ml of 5 *N*-HCl and deposited 1.7 g of colourless, rodshaped prisms, m.p. 85°–86°. The product was recrystallized from 5 ml of benzene and gave 1.6 g of colourless, rodshaped prisms with unchanged m.p. According to analyses the product was 2-carboxymethylthio-5-ethoxy-1,3,4-thiadiazole (VII c).

For $C_6H_8O_3N_2S_2$ (220.26)
calc.: C 32.7 H 3.66 N 12.72 S 29.1 %, equiv.w.: 220.3,
found: C 32.7 H 3.56 N 12.72 S 29.1* %, ,, ,,: 220.7.

A solution of 4.2 g of *carboxymethyl dithiobenzoate* in 20 ml of *N*-NaOH was added to 10 ml of a 2 *M* carboxymethyldithiocarbhydrazide salt solution. A clear, deep red solution was obtained, the colour of which soon faded to yellow. On the following day the mixture smelt strongly of hydrogen sulphide, and 3.0 g of a brown-yellow crystal powder had separated, m.p. 190°–200° (after sintering). The filtrate was acidified with 20 ml of 2 *N*-HCl and deposited 0.6 g of a reddish crystal mass, m.p. 155°–170° (after sintering). The two products were combined and ground with 20 ml of *N*-NaOH, which left undissolved 0.4 g of a grey-yellow crystal powder, m.p. 138°–141°. It was recrystallized from 5 ml of ethanol and gave 0.3 g of pale yellow flakes, m.p. 141°–142° alone and also on admixture with pure 2,5-diphenylthiadiazole. This compound was probably formed from carboxymethyl dithiobenzoate and hydrazine hydrate formed either by decomposition of potassium dithiocarbazinate or of carboxymethyldithiocarbhydrazide salt (26).

---

[1] Compare HOLMBERG (25).

Preliminary experiments had shown that the alkaline filtrate from the diphenylthiadiazole contained the salts of 2-phenyl-5-mercapto-1,3,4-thiadiazole (Vd) and 2-carboxymethylthio-5-phenyl-1,3,4-thiadiazole (VIId). As the two compounds have nearly the same solubilities in the ordinary solvents, they had to be separated by oxidizing the thiol to the corresponding disulphide, which is insoluble in aqueous alkali.

N-HCl was added by drops to the alkaline solution, until it was just turbid, when 4.9 ml of HCl had been added. The mixture then consumed 11.3 ml of 1.01 *N*-I (in aqueous KI-solution) to produce a sharp end point against starch. During the titration a brown-yellow crystal powder separated, 2.1 g of m.p. 136°–140°. The product was recrystallized from 30 ml of benzene and gave 1.7 g of colourless, rod-shaped prisms, m.p. 158°–159° alone and also on admixture with pure bis-[5-phenyl-1,3,4,-thiadiazol-2-yl] disulphide. This compound has not been described before. It was obtained when a 0.7 g of solution of iodine in 5 ml of ethanol was added to a solution of 1.0 g of 2-mercapto-5-phenyl-1,3,4-thiadiazole (1) in 5 ml of *N*-NaOH. The iodine colour disappeared at once, and the mixture deposited 0.9 g of pale yellow crystal powder, m.p. 136°–139°. It was recrystallized from 15 ml of benzene and gave 0.7 g of colourless, rodshaped prisms, m.p. 159°–160°. According to analyses it consisted of the disulphide mentioned above.

For $C_{16}H_{10}N_4S_4$ (386.51)

calc.:	C 49.7	H 2.60	N 14.50	S 33.2 %,
found:	C 49.8	H 2.69	N 14.53	S 33.3* %.

The filtrate from the first obtained disulphide was acidified with 3 ml of 2 *N*-HCl and deposited 0.9 g of grey-yellow, irregular prisms, m.p. 183°-184°. The product was recrystallized from 7 ml of ethanol and gave 0.7 g of grey-yellow, irregular prisms, m.p. 186°–187° alone and also on admixture with pure 2-carboxymethylthio-5-phenyl-1,3,4-thiadiazole (VIId), (1).

For $C_{10}H_8O_2N_2S_2$ (252.30) found equiv.w.: 253.0.

d) *Reactions between carboxymethyldithiocarbhydrazide and aldehydes*

A solution of 4.4 g of *benzaldehyde* in 20 ml of ethanol was added to 20 ml of a 2 *M* carboxymethyldithiocarbhydrazide salt solution. A clear, yellow mixture was obtained, which after some hours became turbid, and on the following day 1.6 g of a yellow crystalline mass had separated, melting from about 90° to about 170°. It was extracted three times with 5 ml of boiling benzene, and the benzene solutions were evaporated and gave 1.2 g of a yellow crystal mass. This was extracted with 5 ml of cold benzene, which was evaporated and gave 1.0 g of a yellow crystal mass. This was recrystallized from 3 ml of ethanol and gave 0.8 g of yellow, rodshaped prisms, m.p. 89°–91° alone and 90°–92° on admixture with pure benzalazine. The residue from the extractions with hot benzene was combined with the residue from the extraction with cold benzene and recrystallized from 8 ml of glacial acetic acid. The result was 0.3 g of yellow, rodshaped prisms, m.p. 198°–199° alone and also on admixture with the pure 3-amino-5-benzylidene-rhodanine described below.

The filtrate from the first product was acidified with 8 ml of 5 *N*-HCl and deposited 7.4 g of a pale yellow crystal mass, m.p. 155°–157°. This product was recrystallized twice from 20 and 15 ml of ethanol and gave 4.6 g of pale yellow, rodshaped prisms, m.p. 167°–168° (decomp.) in an open tube and 146°–149° in a closed one. According to analyses the product was benzaldehyde carboxymethyldithiocarbhydrazone (VIII a) with one mole of ethanol of crystallization.

For $C_{10}H_{10}O_2N_2S_2$, C_2H_6O (300.39)
calc.: C 48.0 H 5.37 N 9.33 S 21.4 %, equiv.w.: 150.2,
found: C 48.1 H 5.38 N 9.31 S 21.3 %, „ „: 158[1].

When 1.5 g of this product was recrystallized from 5 ml of glacial acetic acid, 0.7 g of pale yellow, rodshaped prisms were obtained, m.p. 167°–168° (decomp.) in an open tube as well as in a closed one.

For $C_{10}H_{10}O_2N_2S_2$ (254.32)
calc.: C 47.2 H 3.96 %,
found: C 47.4 H 3.97 %.

When this hydrazone was refluxed with ethanolic hydrochloric acid or with glacial acetic acid for a quarter of an hour, only sticky products were obtained instead of the expected anhydride.

When 100 % *hydrazine hydrate*, 0.6 ml (20 % excess), was added to a solution of 3.0 g of the hydrazone (with crystal ethanol) in 10 ml of ethanol and 10 ml of *N*-NaOH, a clear, yellow mixture was obtained. The yellow colour soon faded, and pale yellow, rodshaped prisms began to separate. After a week the yield was 1.3 g with m.p. 181°–182° (decomp.). The product was extracted with 10 ml of boiling ethanol, and the residue, 1.2 g, showed m.p. 185°–186° (decomp.). According to analysis the product was monobenzaldehyde thiocarbhydrazone, which has previously (1) been obtained from benzaldehyde ethyldithiocarbhydrazone and hydrazine hydrate and then showed m.p. 182.5°–183.5° (decomp., crude product).

For $C_8H_{10}N_4S$ (194.25) calc.: N 28.9, found: N 28.7 %.

A solution of 1.2 g of *ethyl bromide* in 15 ml of ethanol was added to a solution of 3.0 g of the hydrazone (VIII a) in 20 ml of *N*-NaOH. On the following day the clear, yellow mixture was acidified and deposited an oil. On scratching, this solidified to a pale yellow crystal mass, 2.8 g with m.p. 94°–95°. The product was recrystallized from 5 ml of ethanol and gave 2.4 g of pale yellow, flat, rodshaped prisms, m.p. 125°–126°. A further recrystallization from 5 ml of ethanol gave 2.2 g of prisms, m.p. 126°–127° alone and also on admixture with pure benzaldehyde S′-ethyl-S″-carboxymethyl-*iso*dithiocarbhydrazone from benzaldehyde ethyldithiocarbhydrazone and sodium monochloroacetate (1). When the experiment was repeated, the crude product, 2.8 g, showed m.p. 124°–126°. The low melting point of the crude product in the first experiment is probably due to dimorphism.

For $C_{12}H_{14}O_2N_2S_2$ (282.37)
calc.: N 9.92 %, equiv.w.: 282.4,
found: C 9.96 %, „ „: 282.4.

Monochloroacetic acid, 1.5 g (60 % excess), was dissolved in 15.9 ml of *N*-NaOH (phenolphthalein) and added to a solution of 3.0 g of the hydrazone in 20 ml of *N*-NaOH. On the following day the clear, yellow mixture was acidified and separated an oil, which solidified on scratching and gave 3.0 g of pale yellow crystal mass, melting from 148° to about 210° (decomp.). This product was very sensitive to heat and was precipitated as an oil from solvent mixtures, but it could conveniently be purified with the aid of its dipotassium salt. This was obtained when 3.1 g of the crude acid was dissolved in 5 ml of absolute ethanol and 15 ml of 1.7 *N*-KOH in absolute ethanol was added. The mixture was turbid and separated colourless flakes, the amount of which was further increased on the addition of 20 ml of ether. On the following day 3.8 g of flakes had separated, which on heating lost ethanol and then melted at 244°–246° (decomp.). The product was dissolved in 150 ml of hot ethanol, and after cooling 75 ml of ether was added. On the following day 3.4 g of colourless flakes had separated, m.p. 246°–246.5° (decomp., after giving off ethanol).

---

[1] Extremely blunt end point against phenolphthalein.

For $C_{12}H_{10}O_4N_2S_2K_2$, 0.5 C_2H_6O (411.56)
calc.: K 19.00 loss of weight 5.60 %,
found: K 19.02 „ „ „ 5.63 % (at 120°).

A solution of 2.1 g of the salt in 10 ml of water was acidified and deposited 1.5 g of pale yellow, rodshaped prisms, which melted from 148° to 200° (decomp.). According to analyses the product was benzaldehyde S′,S″-bis-carboxymethyl-*iso*dithiocarbhydrazone (IX).

For $C_{12}H_{12}O_4N_2S_2$ (312.36)

calc.: C 46.1	H 3.87	N 8.97	S 20.5 %,	equiv.w.:	156.2,
found: C 46.2	H 3.96	N 8.96	S 20.5* %,	„ „:	156.4.

In order to try to find out the reason for the wide melting range, 3.0 g of the acid was kept at 155° for five minutes. No evolution of gas was observed, but the sticky mixture smelt strongly of benzaldehyde. Some small drops on the sides of the flask were taken up in ethanol, and a drop of hydrazine hydrate was added. A yellow, crystalline precipitate was obtained, which had m.p. 92°–93° alone and also on admixture with pure benzalazine.

The remaining sticky mass was treated with 5 ml of boiling ethanol, and, on cooling, the mixture deposited 0.6 g of brown-yellow, rodshaped prisms, m.p. 260°–261 (decomp.). The product was very slightly soluble in the ordinary solvents. It could be dissolved in pyridine and in ethanolic sodium hydroxide and be precipitated with acetic acid, but the products always showed lower melting points. The crude product was analysed, and from the result the formula $C_{21}H_{18}O_5N_4S_3$ (502.62) can be calculated, though the agreement is not very satisfactory.

calc.: C 50.2	H 3.61	N 11.15	S 19.15 %,
found: C 50.7*	H 3.45*	N 10.82	S 18.75* %.

As the product could not be purified, no further attempts were made to establish its constitution.

When attempts were made to oxidize the benzaldehyde carboxymethyldithiocarbhydrazone with iron (III) chloride or with iodine, no definable products could be obtained.

e) *Reactions between carboxymethyldithiocarbhydrazide and ketones*

When a solution of 2.4 g of *acetophenone* in 10 ml of ethanol was added to 10 ml of a 2 *M* carboxymethyldithiocarbhydrazide salt solution, a clear, yellow mixture was obtained. On the following day 0.7 g of yellow flakes had separated, m.p. 121°–122°.

The product was recrystallized from 7 ml of ethanol and gave 0.6 g of yellow flakes, m.p. 123°–124°, containing 11.82 % of nitrogen. Acetophenone ketazine has m.p. 124° and contains 11.85 of nitrogen.

The filtrate from the first precipitate was acidified and deposited 3.0 g of pale yellow crystal powder, m.p. 153°–155°. This was recrystallized twice from 30 and 20 ml of ethanol and gave 1.6 g of pale yellow flakes, m.p. 159.5°–160° (decomp., rapid heating). According to analyses the product was acetophenone carboxymethyldithiocarbhydrazone.

For $C_{11}H_{12}O_2N_2S_2$ (268.35)
calc.: C 49.2 H 4.51 N 10.44 S 23.9 %, equiv.w.: 134.2,
found: C 49.1 H 4.49 N 10.47 S 24.0* %, „ „: 138[1].

f) *The reaction between aminorhodanine and nitrous acid*

3-Aminorhodanine, 7.4 g, was ground in a cooled mortar with 50 ml of ice-cold 2 *N*-HCl, and an ice-cold solution of 7 g of sodium nitrite in 30 ml of water was added by drops. A vigorous evolution of a colourless gas occurred, and when the reaction had ceased, 6.2 g of colourless crystal powder was collected. The product, m.p. 166°–168°, was recrystallized from 50 ml of 40 % aqueous ethanol and gave 4.6 g of colourless, irregular prisms, m.p. 168°–169° alone and also on admixture with pure rhodanine (XIV a). For this product NENCKI (27) reports m.p. 168°–170°.

For $C_3H_3ONS_2$ (133.18) calc.: N 10.52 %, found: N 10.42 %.

g) *The reactions between aminorhodanine and aldehydes*

When *benzaldehyde*, 2.2 g, was added to a solution of 3.0 g of aminorhodanine in 30 ml of hot ethanol, a clear, yellow solution was obtained. After two days it slowly began to deposit yellow flakes, and after a further two days a total of 3.8 g was obtained with m.p. 136°–137°. If a few drops of concentrated hydrochloric acid were added to the reaction mixture, the separation of crystals started almost immediately. The yield was the same, and this was also the case when the reaction was undertaken in 20 ml of hot glacial acetic acid. The product from the first preparation was recrystallized from 100 ml of ethanol and gave 2.8 g of flat, yellow, rodshaped prisms, m.p. 137°–138°. A further recrystallization from ethanol did not change the m.p. According to analyses the product was 3-benzylidenamino-rhodanine (XV a).

For $C_{10}H_8ON_2S_2$ (236.30)
calc.: C 50.8 H 3.41 N 11.86 S 27.1 %,
found: C 50.7 H 3.39 N 11.86 S 27.1 %.

When benzaldehyde and aminorhodanine were condensed with fused sodium acetate in glacial acetic acid, the isomeric 3-amino-5-benzylidene-rhodanine was obtained. Benzaldehyde, 2.2 g, was refluxed with 3.0 g of aminorhodanine and 4 g of fused sodium acetate in 30 ml of glacial acetic acid for one hour. On cooling, the mixture solidified to a cake of yellow, irregular prisms, 3.0 g with m.p. 195°–198°. The product was recrystallized from 70 ml of glacial acetic acid and gave 2.8 g of yellow, rodshaped prisms, m.p. 199°–200°.

Found: C 50.8 H 3.35 N 11.92 S 27.1 %.

---

[1] Blunt end point against phenolphthalein.

When 3-benzylidenamino-rhodanine was refluxed with fused sodium acetate in glacial acetic acid, it was transformed into 3-amino-5-benzylidene-rhodanine. A solution of 2.4 g of the former compound and 2 g of fused sodium acetate in 10 ml of hot glacial acetic acid was refluxed for one hour. On cooling, the mixture deposited 1.7 g of brown, irregular prisms, m.p. 186°–192° after sintering. The product was recrystallized from 50 ml of toluene and from 30 ml of glacial acetic acid and gave 1.0 g of yellow, rodshaped prisms, m.p. 198°–199° alone and 199°–200° on admixture with 3-amino-5-benzylidene-rhodanine.

The constitution of this compound was established by its reaction with nitrous acid. 3-Amino-5-benzylidene-rhodanine, 0.6 g, was ground with 10 ml of glacial acetic acid, and 1.5 g of solid sodium nitrite was added in portions. When the evolution of gas had ceased, the mixture was poured into 50 ml of water which caused the separation of a yellow crystal mass. The precipitate was sucked off and ground with 5 ml of *N*-NaOH. The alkaline solution was filtered from a small amount of unreacted starting material and then acidified. The precipitate, 0.5 g of yellow crystal powder, m.p. 198°–203°, was recrystallized from 10 ml of glacial acetic acid and gave 0.3 g of yellow, rodshaped prisms, m.p. 208°–209° alone and also on admixture with authentic 5-benzylidene-rhodanine.[1]

For $C_{10}H_7ONS_2$ (221.29)

calc.:	N 6.33 %,	equiv.w.: 221.3,
found:	N 6.33 %,	„ „: 220.1.

When an attempt was made to make the reaction more complete by heating the mixture to boiling, 0.3 g of yellow prisms were obtained, m.p. 236°-238°. The product was recrystallized from 10 ml of ethanol and gave 0.2 g of yellow prisms, m.p. 241°–243°. According to analyses the product was 5-benzylidene-thiazole-2(3),4(5)-dione. For this compound ANDREASCH (29) reports m.p. 242°.

For $C_{10}H_7O_2NS$ (205.23)

calc.:	C 58.5	H 3.44	N 6.83 %,
found:	C 58.0*	H 3.60*	N 6.97 %.

Finally the 3-benzylidenamino-5-benzylidene-rhodanine was prepared in the following way. A solution of 3 g (calc. 2.2 g) of benzaldehyde, 3 g of fused sodium acetate and 1.5 g of aminorhodanine in 15 ml of hot glacial acetic acid was refluxed for one hour. On cooling, the mixture deposited 2.8 g of yellow, rodshaped prisms, m.p. 171°–172°. The product was recrystallized from a mixture of 40 ml of benzene and 60 ml of absolute ethanol and gave 2.3 g of yellow hairs, m.p. 172°–173°. A further recrystallization from the same solvent mixture did not change the m.p.

For $C_{17}H_{12}ON_2S_2$ (324.41)

calc.:	C 62.9	H 3.73	N 8.64	S 19.8 %,
found:	C 63.0	H 3.72	N 8.63	S 19.8 %.

When this compound was left in contact with the mother liquor for two days, the hairs were transformed into eight-sided plates with the same m.p. When supersaturated solutions of the compound were seeded with either the hairs or plates, the precipitate had the same crystal form as the seedling.

---

[1] For this compound NENCKI (28) reports m.p. 200°, but when benzaldehyde and rhodanine were condensed with fused sodium acetate in glacial acetic acid or with ammonia and ammonium chloride, a product with m.p. 208°–209° was obtained in good yield.

The 3-benzylidenamino-5-benzylidene-rhodanine could also be prepared in the following way. Benzaldehyde, 1.1 g, was added to a solution of 1.0 g of 3-amino-5-benzylidene-rhodanine in 30 ml of hot glacial acetic acid. On cooling, the solution deposited 1.3 g of yellow hairs, m.p. 170°–171°. The product was recrystallized from a mixture of 15 ml of benzene and 30 ml of absolute ethanol and gave 1.2 g of yellow hairs. m.p. 172°–173° alone and also on admixture with the 3-benzylidenamino-5-benzylidene-rhodanine described above.

When 1 ml of concentrated hydrochloric acid was added to a solution of 1.5 g of *vanillin* and 1.5 g of aminorhodanine in 20 ml of hot ethanol, the mixture soon began to deposit crystals. On the following day 1.9 g of pale yellow, rodshaped prisms had separated, m.p. 180°–183°. The product was slightly soluble in hot ethanol and in hot benzene but could be recrystallized from a mixture of 25 ml of absolute ethanol and 25 ml of benzene. The yield was 1.3 g of yellow, rodshaped prisms, m.p. 186°–189° (after sintering and darkening from 170°). According to analyses the product was 3-vanillylidenamino-rhodanine.

For $C_{11}H_{10}O_3N_2S_2$ (282.33)

calc.:	C 46.8	H 3.57	N 9.92	S 22.7 %,
found:	C 46.7	H 3.57	N 9.94	S 22.7 %.

A solution of 3.0 g of aminorhodanine, 3.0 g of vanillin and 4 g of fused sodium acetate in 20 ml of hot glacial acetic acid was refluxed for one hour. On cooling, the mixture deposited 4.6 g of brickred, irregular prisms, m.p. 201°–204°. From this product 2.3 g were recrystallized twice from 70 ml of glacial acetic acid and gave 1.6 g of brickred, long plates, m.p. 206°–207°. According to analyses the product was 3-amino-5-vanillylidene-rhodanine.

Found:	C 46.9	H 3.60	N 9.90	S 22.7 %.

A suspension of 1.4 g of 3-amino-5-vanillylidene-rhodanine in 50 ml of glacial acetic acid was ground in a mortar, and 5.0 g of sodium nitrite was added in portions. When the evolution of gas had ceased, the mixture was poured into 200 ml of water. The undissolved material, 1.5 g of brown-yellow powder, m.p. 259°–260 (decomp.), was recrystallized twice from 250 ml of glacial acetic acid and gave 1.0 g of brown-yellow plates, m.p. 266°–267° (decomp.).

For $C_{11}H_8O_5N_2S_2$ (312.31)

calc.:	C 42.3	H 2.58	N 8.97	S 20.5 %,
found:	C 42.5*	H 2.74*	N 8.93	S 20.3 %.

This formula corresponds to the exchange of one amino group for hydrogen and one hydrogen atom for a nitro group. Since vanillin is nitrated in the 5-position by dinitrogen trioxide (30), it seems rather probable that the product described above is 5-[5′-nitrovanillylidene]-rhodanine. This compound could be obtained in the following way. A solution of 1.4 g of rhodanine, 2.0 g of 5-nitrovanilline[1] and 2 g of fused sodium acetate in 40 ml of hot glacial acetic acid was refluxed for half an hour. After cooling, the mixture deposited 1.7 g of grey-brown flakes, m.p. 259°–260° (decomp.). The product was recrystallized from 320 ml of glacial acetic acid and gave 1.3 g of grey-brown plates of the same shape as those described above. The m.p. was 266°–267° (decomp.).

Found:	C 42.3*	H 2.67*	N 8.96*	S 20.3* %.

---

[1] Prepared according to SIMONSEN and RAU (30).

The two products were recrystallized several times from glacial acetic acid without change in the m.p., but the difference in colour could not be removed. This difference may be due to some small impurity, which could not be removed by recrystallization. The identity of the two products was demonstrated by their solubilities in glacial acetic acid. In boiling glacial acetic acid the solubility was 0.4 g per 100 ml for both products. At room temperature the solubilities were 0.024 g and 0.020 g per 100 ml respectively. When 0.1 g of each product was mixed and treated with boiling glacial acetic acid, it was necessary to add 50 ml of the solvent for complete dissolution and not about 25 ml, which would have been the case if the two products had been different. On cooling, the mixture deposited 0.188 g of brown-yellow plates, m.p. 266°–267° (decomp.).

A solution of 1.5 g of aminorhodanine, 3.0 g of vanilline and 2.0 g of fused sodium acetate in 10 ml of hot glacial acetic acid was refluxed for one hour. On cooling, the mixture deposited 3.8 g of red-yellow, irregular prisms, m.p. 222°–225° (after sintering). When the product was recrystallized from 160 ml of glacial acetic acid, 1.0 g of brown-yellow granules were obtained, m.p. 234°–236°. A further recrystallization from glacial acetic acid did not change the m.p. On working up the mother liquor from the first recrystallization only tarry products were obtained. According to analyses the purified product was 3-vanillylidenamino-5-vanillylidene-rhodanine.

For $C_{19}H_{16}O_5N_2S_2$ (416.46)
calc.: C 54.8 H 3.87 N 6.73 S 15.40 %,
found: C 55.1 H 3.91 N 6.70 S 15.43 %.

Vanillin, 0.7 g, and 3-amino-5-vanillylidene-rhodanine, 0.7 g, were dissolved in 25 ml of hot glacial acetic acid. On cooling, the mixture deposited 0.8 g of brown-yellow, irregular prisms, m.p. 231°–233° alone and 232°–234° on admixture with the product described above. On attempts to recrystallize the product from glacial acetic acid or toluene only lower-melting products were obtained.

When 1 ml of concentrated hydrochloric acid was added to a solution of 1.4 g of *cinnamic aldehyde* and 1.5 g of aminorhodanine in 25 ml of hot ethanol, the mixture soon began to deposit crystals. On the following day 2.1 g of aggregates of yellow needles, m.p. 139°–140°, had separated. The product was recrystallized from a mixture of 10 ml of benzene and 25 ml of absolute ethanol and gave 1.6 g of pale yellow flakes, m.p. 145°–146°. According to analyses the product was 3-cinnamylidenamino-rhodanine.

For $C_{12}H_{10}ON_2S_2$ (262.34)
calc.: C 54.9 H 3.84 N 10.68 S 24.4 %,
found: C 55.1 H 3.82 N 10.71 S 24.3 %.

A solution of 6.0 g of aminorhodanine, 5.4 g of cinnamic aldehyde and 8 g of fused sodium acetate in 40 ml of hot glacial acetic acid was refluxed for one hour. On cooling, the mixture deposited 7.7 g of red-yellow, irregular prisms, m.p. 198°–202°. The product was recrystallized from a mixture of 110 ml of glacial acetic acid and 110 ml of toluene and gave 3.2 g of brown-red flakes, m.p. 229.5°–230°. A further recrystallization from 200 ml of the same solvent mixture gave 3.0 g of flakes with the same m.p. From the mother liquor of the first recrystallization only tarry products could be isolated. According to analyses the purified product was 3-amino-5-cinnamylidene-rhodanine.

Found: C 55.1 H 3.90 N 10.65 S 24.3 %.

A solution of 1.5 g of aminorhodanine, 3.0 g of cinnamic aldehyde and 2.0 g of fused sodium acetate in 10 ml of hot glacial acetic acid was refluxed for one hour. On cooling, the mixture deposited 2.8 g of red-brown flakes, m.p. 192°–194°. The product was recrystallized twice from 50 and 40 ml of toluene and gave 1.7 g of brown-yellow, glistening flakes, m.p. 198°–204°. According to analyses the product was 3-cinnamylidenamino-5-cinnamylidene-rhodanine.

For $C_{21}H_{16}ON_2S_2$ (376.48)
calc.: C 67.0 H 4.28 N 7.44 S 17.03 %,
found: C 67.0 H 4.32 N 7.42 S 17.10 %.

Cinnamic aldehyde, 0.5 g, was added to a solution of 0.7 g of 3-amino-5-cinnamylidene-rhodanine in 50 ml of hot glacial acetic acid. On the following day the mixture had deposited 0.8 g of brown-yellow flakes, m.p. 189°–193°, which were recrystallized twice from 15 ml of toluene and gave 0.6 g of brown-yellow flakes, m.p. 197°–203° alone and also on admixture with the 3-cinnamylidenamino-5-cinnamylidene-rhodanine described above.

Vanillin, 0.5 g, was added to a solution of 0.6 g of 3-amino-5-benzylidene-rhodanine in 20 ml of hot glacial acetic acid. On cooling, the mixture deposited 0.8 g of long, yellow, rodshaped prisms, m.p. 198°–211° (after sintering). The product was recrystallized from 20 ml of xylene and from 10 ml of glacial acetic acid and gave 0.4 g of yellow flakes, m.p. 210°–211°, according to analyses consisting of 3-vanillylidenamino-5-benzylidene-rhodanine.

For $C_{18}H_{14}O_3N_2S_2$ (370.43)
calc.: C 58.4 H 3.81 N 7.56 S 17.31 %,
found: C 58.2 H 3.83 N 7.58 S 17.38 %.

The isomeric 3-benzylidenamino-5-vanillylidene-rhodanine was obtained, when 0.5 ml of benzaldehyde was added to a solution of 0.7 g of 3-amino-5-vanillylidene-rhodanine in 25 ml of hot glacial acetic acid. The crude product was 0.8 g of brown-yellow, rodshaped prisms, m.p. 201°–203°. It was recrystallized from 25 ml of toluene and gave 0.7 g of yellow, felted hairs, m.p. 204°–205° alone and 175°–182° (after sintering) on admixture with the isomeric compound described above.

Found: C 58.5 H 3.85 N 7.54 S 17.23 %.

Cinnamic aldehyde, 0.5 ml, was added to a solution of 0.6 g of 3-amino-5-benzylidene-rhodanine in 20 ml of hot glacial acetic acid. On cooling, the mixture deposited 0.8 g of yellow hairs, m.p. 186°–187° (after sintering). The product was recrystallized from 10 ml of toluene and gave 0.6 g of yellow, felted hairs, m.p. 188°–189°. According to analyses the product was 3-cinnamylidenamino-5-benzylidene-rhodanine.

For $C_{19}H_{14}ON_2S_2$ (350.44)
calc.: C 65.1 H 4.03 N 7.99 S 18.30 %,
found: C 65.2 H 4.04 N 8.00 S 18.36 %.

The isomeric 3-benzylidenamino-5-cinnamylidene-rhodanine was obtained, when 0.5 ml of benzaldehyde was added to a solution of 0.7 g of 3-amino-5-cinnamylidene-rhodanine in 50 ml of hot glacial acetic acid. The crude product, 0.6 g of red-brown, glistening flakes with m.p. 165°–167°, was recrystallized from 5 ml of toluene and gave 0.5 g of yellow-brown flakes, m.p. 170°–171° alone and 155°–160° (after sintering) on admixture with the isomeric compound described above.

Found: C 65.2 H 4.05 N 7.97 S 18.23 %.

Cinnamic aldehyde, 0.5 ml, was added to a solution of 0.7 g of 3-amino-5-vanillylidene-rhodanine in 25 ml of hot glacial acetic acid. On cooling, 0.8 g of yellow-brown flakes separated, m.p. 198°–200. The product was recrystallized from 35 ml of glacial acetic acid and gave 0.6 g of yellow-brown flakes, m.p. 201°–202°. According to analyses the product was 3-cinnamylidenamino-5-vanillylidene-rhodanine.

For $C_{20}H_{16}O_3N_2S_2$ (396.47)

calc.:	C 60.6	H 4.07	N 7.07	S 16.17 %,
found:	C 60.4	H 4.07	N 7.11	S 16.14 %.

The isomeric 3-vanillylidenamino-5-cinnamylidene-rhodanine was obtained, when 0.6 g of vanilline was added to a solution of 0.7 g of 3-amino-5-cinnamylidene-rhodanine in 50 ml of hot glacial acetic acid. The crude product, 0.8 g of red, glistening, rodshaped prisms with m.p. 198°–200°, was recrystallized from 25 ml of glacial acetic acid and gave 0.5 g of red, rodshaped prisms, m.p. 199°–201° in an open tube and 190°–193° in a closed one. According to analyses the product was 3-vanillylidenamino-5-cinnamylidene-rhodanine with one mole of glacial acetic acid of crystallization.

For $C_{20}H_{16}O_3N_2S_2$, $C_2H_4O_2$ (456.52)

calc.:	C 57.9	H 4.42	N 6.14	S 14.05 %,
found:	C 58.2	H 4.43	N 6.12	S 14.05 %.

When 0.7 g of the crude product was recrystallized from 15 ml of toluene it lost the glacial acetic acid of crystallisation and separated as 0.5 g of brown-yellow flakes, m.p. 198°–200° in an open tube as well as in a closed one. On admixture with the isomeric compound the m.p. was 180°–190° (after sintering).

Found: C 60.6 H 4.10 N 7.13 S 16.10 %.

h) *The reactions between aminorhodanine and ketones*

A solution of 0.6 g of ammonium chloride and 1 ml of *acetone* in a mixture of 1 ml of concentrated aqueous ammonia and 2 ml of water was added to a solution of 1.5 g of aminorhodanine in 20 ml of hot ethanol. A clear, red solution was obtained, which on the following day had deposited 0.5 g of yellow, rodshaped prisms, m.p. 148°–149°, not changed by recrystallization from ethanol. According to analyses the product was 3-amino-5-*iso*propylidene-rhodanine.

For $C_6H_8ON_2S_2$ (188.26)

calc.:	C 38.3	H 4.28	N 14.88	S 34.1 %,
found:	C 38.4	H 4.28	N 14.89	S 34.1 %.

A suspension of 1.9 g of 3-amino-5-*iso*propylidene-rhodanine in 20 ml of glacial acetic acid was ground in mortar, and a solution of 1.0 g of sodium nitrite in 5 ml of water was added dropwise. When the evolution of gas had ceased, the undissolved material was collected. It was 1.6 g of yellow crystal powder, m.p. 197°–199°. The product was recrystallized from 10 ml of glacial acetic acid and gave 1.2 g of yellow, rodshaped prisms, m.p. 198°–199°. According to analyses the product was 5-*iso*-propylidene-rhodanine.

For $C_6H_7ONS_2$ (173.25)   calc.: N 8.09,   found: N 8.12 %.

This compound has previously been described by BROWN *et al.* (31), who obtained it from acetone and rhodanine with ammonia and ammonium chloride and report m.p. 196°–197°. When their preparation was repeated, a product was obtained with m.p. 198°–199°, not depressed by the product described above.

Benzaldehyde, 1.1 g, was added to a solution of 1.9 g of 3-amino-5-*iso*propylidene-rhodanine in 20 ml of hot glacial acetic acid. On the following day the mixture had deposited 2.1 g of yellow flakes, m.p. 103°–104°. The product was recrystallized from 20 ml of ethanol and gave 2.0 g of yellow, oblique plates, m.p. 104°–105°, according to analyses consisting of 3-benzylidenamino-5-*iso*propylidene-rhodanine.

For $C_{13}H_{12}ON_2S_2$ (276.37)

calc.:	C 56.5	H 4.38	H 10.14	S 23.2 %,
found:	C 56.3	H 4.38	N 10.12	S 23.2 %.

A solution of 2.4 g of ammonium chloride in 3 ml of concentrated aqueous ammonia and 5 ml of water was added to a solution of 3.0 g of aminorhodanine in 40 ml of hot ethanol. A red solution was obtained, which on the addition of a solution of 2.3 g of *levulinic acid* in 5 ml of ethanol turned yellow and deposited a small amount of brown crystal powder. On the addition of 30 ml of ether the mixture became turbid, and on the following day it had deposited 5.1 g of brown-yellow crystal powder, m.p. 154°–155° (decomp.). From this product 0.5 g was dissolved in 3 ml of hot water, the solution was cooled with ice, and a mixture of 15 ml of ethanol and 30 ml of ether was added. On the following day 0.3 g of brown-yellow, flat needles had separated, m.p. 159°–159.5° (decomp.). According to analyses the product was the ammonium salt of 3-amino-5-[4′-carboxy-butylid-2′-ene]-rhodanine.

For $C_{18}H_{13}O_3N_3S_2$ (263.32)   calc.: N 15.96 %,   found: N 15.98 %.

This salt was dissolved in water, and the solution was acidified. A sticky product separated, which solidified to a partly crystalline mass melting between 125° and 135°. All attempts to purify this product gave only sticky products which could not be made to crystallize.

When *acetophenone*, aminorhodanine and fused sodium acetate were refluxed with glacial acetic acid, only tarry products were obtained. The same occurred when attempts were made to condense acetophenone and aminorhodanine with the aid of ammonia and ammonium chloride.

C. *α-Carboxyethyldithiocarbhydrazide and 3-amino-5-methyl-rhodanine*

When 7.5 g of solid potassium dithiocarbazinate was added to a solution of 7.8 g of *d,l-α-bromopropionic acid* in 16.8 ml of 3 *N*-NaOH (phenolphthalein), a clear mixture was obtained. This was acidified after three hours and deposited a green-yellow oil, which solidified after a week and gave 7.6 g of colourless crystals, m.p. 62°–64°. The product was recrystallized from 25 ml of ethanol and gave 6.1 g of long, colourless, irregular prisms, m.p. 65.5°–66°, according to analyses consisting of 3-amino-5-methyl-rhodanine (X b).

For $C_4H_6ON_2S_2$ (162.23)
calc.: C 29.6 H 3.73 N 17.27 S 39.5 %,
found: C 29.5 H 3.72 N 17.28 S 39.4 %.

Solid *sodium nitrite*, 1.5 g, was added in portions with grinding to a suspension of 0.7 g of 3-amino-5-methyl-rhodanine in 10 ml of 2 *N*-HCl. The resulting clear solution soon began to deposit crystals, and by the following day 0.6 g of colourless, irregular prisms, m.p. 124°–125°, had formed. The product was recrystallized from 3 ml of benzene and gave 0.5 g of colourless, irregular prisms, m.p. 125°–126°, according to analyses consisting of 5-methyl-rhodanine (XIV b).

For $C_4H_5ONS_2$ (147.21)
calc.: N 9.52 %, equiv.w.: 147.2,
found: N 9.48 %, „ „: 146.0.

This compound has previously been described by BERLINERBLAU (32), who reports m.p. 123°.

Veratraldehyde, 1.0 g, was added to a solution of 0.8 g of 3-amino-5-methyl-rhodanine in 10 ml of ethanol. The mixture remained clear and colourless until the following day, when 1 ml of concentrated hydrochloric acid was added. The mixture became yellow and deposited and oil, which slowly solidified to 0.9 g of a pale yellow crystal mass, m.p. 138°–139°. The product was dissolved in 3 ml of hot benzene, and 10 ml of hot absolute ethanol was added. On cooling, the solution deposited 0.8 g of pale yellow, rodshaped prisms, m.p. 139°–140°. A further purification in the same way did not change the m.p. According to analyses the product was 3-veratrylidenamino-5-methyl-rhodanine.

For $C_{13}H_{14}O_3N_2S_2$ (310.38)
calc.: C 50.3 H 4.55 N 9.03 S 20.7 %,
found: C 50.3* H 4.60* N 9.01 S 20.5* %.

Solid potassium dithiocarbazinate, 3.0 g, was added to a solution of 3.1 g of *d,l*-α-bromopropionic acid in 20.3 ml of *N*-KOH (phenolphthalein). After two hours 2.2 g of *benzaldehyde* in 20 ml of ethanol was added to the clear solution. The mixture soon became turbid, and on the following day pale yellow, rodshaped prisms had separated. The product was sucked off, washed with benzene to remove some benzalazine, and with absolute ethanol and ether. The yield was 4.5 g with m.p. 198°–199° (decomp., after giving off water). According to analyses the product was a dihydrate of the monopotassium salt of benzaldehyde α-carboxyethyldithiocarbhydrazone.

For $C_{11}H_{11}O_2N_2S_2K, 2H_2O$ (342.47)
calc.: K 11.42 H_2O 10.52 %,
found: K 11.49 H_2O 10.59 % (in vacuum over phosphorus pentoxide).

A clear solution of 3.4 g of this salt in 40 ml of 50 % aqueous ethanol was acidified with 5 ml of 5 *N*-HCl in 5 ml of ethanol and deposited 2.1 g of pale yellow, irregular prisms, m.p. 138°–139°. The product was recrystallized three times from 60 % aqueous ethanol and gave 1.1 g of pale yellow, irregular prisms, m.p. 147°–147.5°, according to analyses consisting of benzaldehyde α-carboxyethyldithiocarbhydrazone (VIII b).

For $C_{11}H_{12}O_2N_2S_2$ (268.35)
calc.: C 49.2 H 4.51 N 10.44 S 23.9 %, equiv.w.: 134,
found: C 49.4* H 4.62* N 10.47 S 23.9* %, „ „: 143[1].

---

[1] Blunt end point with phenolphthalein.

D. *α-Carboxybenzyldithiocarbhydrazide and 3-amino-5-phenyl-rhodanine*

Solid potassium dithiocarbazinate, 3.0 g, was added to a solution of 4.4 g of *d,l-α-chlorophenylacetic acid* in 21.0 ml of *N*-NaOH (phenolphthalein). After five minutes the mixture began to deposit pale yellow needles. After two hours 0.4 g had separated, m.p. 120°–121°. The filtrate was acidified and deposited an oil, which rapidly solidified to 2.5 g of a pale yellow crystal mass, m.p. 115°–118°. It was recrystallized, together with the product first obtained, twice from 50 and 40 ml of ethanol and gave 2.0 g of pale yellow, rodshaped prisms, m.p. 121°–121.5°. According to analyses the product was 3-amino-5-phenyl-rhodanine (Xc).

$C_9H_8ON_2S_2$ (224.29)
calc.: C 48.2 H 3.59 N 12.49 S 28.6 %,
found: C 48.2 H 3.62 N 12.52 S 28.6 %.

Solid sodium nitrite, 1.4 g, was added in portions with grinding to a suspension of 1.1 g of 3-amino-5-phenyl-rhodanine in 10 ml of ethanol and 5 ml of 5 N-HCl. When the evolution of gas had ceased, the undissolved material was collected. It was 0.9 g of pale yellow crystal powder, m.p. 181°–183°, and it was recrystallized from 10 ml of ethanol. The yield was 0.5 g of pale yellow, irregular prisms, m.p. 182°–183°, according to analyses consisting of 5-phenylrhodanine (XIVc).

For $C_9H_7ONS_2$ (209.28)
calc.: C 51.7 H 3.37 N 6.69 S 30.6 %,
found: C 51.5* H 3.33* N 6.71 S 30.4* %.

This compound has previously been described by WHEELER and JOHNSON (33), who obtained it from diethyl α-phenyl-α-thiocyanato-malonate and thioacetic acid and subsequent treatment of the resulting dithiocarbamate with alkali. They report m.p. 178°–179°. The 5-phenylrhodanine could be prepared in the following way also. Solid ammonium dithiocarbamate, 3.0 g, was added to a solution of 4.4 g of *d,l*-α-chlorophenylacetic acid in 20.2 ml of *N*-NaOH (phenolphthalein). On the following day the yellow, clear mixture was acidified with 5 ml of 5 *N*-HCl and deposited 4.2 g of pale yellow, irregular prisms. From this product 4.0 g was dissolved in 10 ml of acetone, and 30 ml of chloroform was carefully added to the filtered solution. The mixture then deposited 2.6 g of pale yellow, oblique plates, which on heating in open as well as in closed tubes lost water and melted at 182°–183°. According to analyses the product was α-carboxybenzyl dithiocarbamate.

For $C_9H_9O_2NS_2$ (227.29)
calc.: C 47.6 H 3.99 N 6.16 S 28.2 %, equiv.w.: 227.3,
found: C 47.3* H 3.89* N 6.18 S 28.2* %, ,, ,,: 227.1.

When 1.8 g of the acid was refluxed with 10 ml of ethanol for 30 minutes, and the solution was allowed to cool, 1.4 g of pale yellow, thick, rectangular plates separated, m.p. 182°–183° alone and also on admixture with the 5-phenyl-rhodanine described above.

Found: N 6.69 %, equiv.w.: 208.0.

Benzaldehyde, 0.6 g, and 1.1 g of 3-amino-5-phenyl-rhodanine were dissolved in 10 ml of hot glacial acetic acid. On cooling, the mixture separated 1.5 g of yellow plates, m.p. 154°–156°. The product was recrystallized from 15 ml of glacial acetic acid and gave 1.3 g of yellow, thick, oblique plates, m.p. 156.5°–157°, according to analyses consisting of 3-benzylidenamino-5-phenyl-rhodanine (XV c).

For $C_{16}H_{12}ON_2S_2$ (312.40)
calc.: C 61.5 H 3.87 N 8.97 S 20.5 %,
found: C 61.3 H 3.70 N 8.95 S 20.7 %.

Solid potassium dithiocarbazinate, 3.0 g, was added to a solution of 4.4 g of *d,l*-α-chlorophenylacetic acid in 20.8 ml of *N*-KOH (phenolphthalein). After two hours the separated 3-amino-5-phenyl-rhodanine was sucked off, and a solution of 2.2 g of benzaldehyde in 20 ml of ethanol was added to the filtrate. The mixture remained clear, but after some hours it began to deposit crystals. On the following day 5.6 g of green-yellow flakes had separated, m.p. 149°–150° (decomp.). From this product 2.9 g were recrystallized from 40 ml of water and gave 2.1 g of pale yellow, flat, rodshaped prisms, m.p. 159°–159.5° (decomp.). According to analyses the product was the monopotassium salt of benzaldehyde α-carboxybenzyldithiocarbhydrazone.

For $C_{16}H_{13}O_2N_2S_2K$ (368.50) calc.: K 10.61, found: K 10.54 %.

A solution of 1.0 g of this salt in 40 ml of 50 % aqueous ethanol was acidified with 2 ml of 5 *N*-HCl in 2 ml of ethanol. On the following day 0.8 g of pale yellow, rodshaped prisms had separated, m.p. 170°–171° (decomp.). The product was recrystallized from 10 ml of ethanol and gave 0.5 g of pale yellow, rodshaped prisms, m.p. 175°–176° (decomp.). According to analyses the product was benzaldehyde α-carboxybenzyldithiocarbhydrazone (VIII c).

For $C_{16}H_{14}O_2N_2S_2$ (330.41)
calc.: C 58.2 H 4.27 N 8.48 S 19.41 %, equiv.w.: 165,
found: C 57.9* H 4.40* N 8.50 S 19.44* %, ,, ,,: 168[1].

When this hydrazone was refluxed with glacial acetic acid for half an hour, a small amount of 3-benzylidene-5-phenyl-rhodanine was formed, but this need not necessarily mean that the hydrazone has cyclizated as such. A possible explanation is also that the hydrazone has split off benzaldehyde, cyclizated and combined with benzaldehyde again.

E. *β-Carboxyethyldithiocarbhydrazide and its hydrazones*

a) *The preparation of β-carboxyethyldithiocarbhydrazide*

β-Bromopropionic acid, 15.3 g, was neutralized with a solution of 5.5 g of sodium carbonate in 20 ml of water and 5.5 ml of *N*-NaOH (phenolphthalein), and 13 g of solid ammonium dithiocarbazinate was added. The temperature rose to about 40°. On the following day the mixture was cooled to − 15° and acidified with 10 ml of 10 *N*-HCl. A sticky oil separated, which presently solidified to 13.3 g of a colourless crystal mass with m.p. 104°–106°. This product had a rather slight power of crystallization, which made the purification tedious. A solution of 5 g of the product in 20 ml of 50 % aqueous ethanol was freely evaporated to half the volume, when 3.6 g of colourless, irregular prisms, m.p. 110°–111°, had separated. This product was recrystallized once from 10 ml of water and twice from 15 ml of ethyl acetate and gave 1.4 g of colourless, irregular prisms, m.p. 113.5°–114.5°.

---

[1] Blunt end point with phenolphthalein.

For $C_4H_8O_2N_2S_2$ (180.24)

calc.:	C 26.7	H 4.47	N 15.54	S 35.6 %,	equiv.w.:	90.1,
found:	C 26.7	H 4.48	N 15.58	S 35.4 %,	,, ,,:	93.4[1].

The hydrazide is easily soluble in dilute acids, but no crystalline sulphate, hydrochloride, picrate or S-benzyl*iso*thiuronium salt of this hydrazide could be obtained.

b) *Oxidation of β-carboxyethyldithiocarbhydrazide*

When 20 ml of a 2 *M*-$FeCl_3$ solution was added to a solution of 3.6 g of β-carboxyethyldithiocarbhydrazide in 20 ml of *N*-HCl, a dark mixture was obtained with a slight evolution of a gas which contained hydrogen sulphide. On the following day the mixture had deposited a sticky, yellow-brown mass. This was separated and ground with 20 ml of *N*-NaOH and Norite. The mixture was filtered, and the filtrate was acidified with 10 ml of 2 *N*-HCl and deposited 1.0 g of grey-brown flakes with m.p. 136°–138°. This product was recrystallized twice from 25 and 20 ml of ethyl acetate and gave 0.5 g of pale yellow flakes, m.p. 144°–145°, according to analyses consisting of 2,5-bis-[β-carboxyethylthio]-1,3,4-thiadiazole (XXa).

For $C_8H_{10}O_4N_2S_3$ (294.36)

calc.:	C 32.6	H 3.42	N 9.52	S 32.7 %,	equiv.w.:	147.2,
found:	C 32.8	H 3.38	N 9.48	S 32.8 %,	,, ,,:	148.0.

When this oxidation was repeated with the hydrazide dissolved in ethanol, no definable product could be obtained.

c) *The reaction between β-carboxyethyldithiocarbhydrazide and carboxymethyl dithiobenzoate*

Carboxymethyl dithiobenzoate, 4.2 g, was dissolved in 20 ml of *N*-NaOH and added to a solution of 3.6 g of β-carboxyethyldithiocarbhydrazide in 20 ml of ethanol. The clear, red solution soon began to smell of hydrogen sulphide, and on the following day 1.6 g of pale yellow crystal powder had separated, m.p. 207°–209°. This product was recrystallized from 15 ml of ethanol and gave 1.1 g of pale yellow, irregular prisms, m.p. 213°–215° alone and 214°–215° on admixture with pure 2-phenyl-5-mercapto-1,3,4-thiadiazole (Vd).

For $C_8H_6N_2S_2$ (194.26) calc.:	equiv.w.:	194.3,
found:	,, ,,:	195.0 (alkali), 188.0 (iodine).

The filtrate from the crude product was acidified and deposited a dark red oil, which slowly solidified to an oily crystal mass. This was sucked off, when a considerable amount of red oil went into the filtrate. The remaining 2.2 g of red, sticky mass were dissolved in 5 ml of hot ethyl acetate. On cooling, 0.5 g of colourless, irregular prisms separated, m.p. 112°–113° and equiv.w.: 265.5. This product ought to be 2-[β-carboxyethylthio]-5-phenyl-1,3,4-thiadiazole (XXb), which compound could be obtained in better yield in the following way. A solution of 3.1 g of β-bromopropionic acid in

---

[1] Blunt end point against phenolphthalein.

20.4 ml of *N*-NaOH (phenolphthalein) was added to a solution of 4 g of 2-phenyl-5-mercapto-1,3,4-thiadiazole (V d) in 20.5 ml of *N*-NaOH (phenolphthalein). On the following day the clear mixture was acidified and separated an oil, which soon solidified to 5 g of a colourless crystal mass with m.p. 108°–110°. The product was recrystallized from 20 ml of ethyl acetate and gave 3.6 g of colourless, rodshaped prisms, m.p. 112°–113° alone and also on admixture with the product described above.

For $C_{11}H_{10}O_2N_2S_2$ (266.33)

calc.:	C 49.6	H 3.78	N 10.52	S 24.1 %,	equiv.w.:	266.3,
found:	C 49.7	H 3.84	N 10.50	S 24.1 %,	,, ,,:	265.6

d) *Aldehyde β-carboxyethyldithiocarbhydrazones*

β-Carboxyethyldithiocarbhydrazide, 1.8 g, was dissolved in 10 ml of ethanol, and 5 ml of a 10 % aqueous *acetaldehyde* solution was added. On the following day 0.3 g of colourless, irregular prisms had separated, m.p. 128°–129°. The filtrate was freely evaporated to 7 ml volume, when 1.1 g of pale yellow crystal mass had separated, m.p. 122°–124°. This product was recrystallized from 5 ml of ethyl acetate and gave 0.8 g of colourless, irregular prisms, m.p. 128°–129°. The two products were combined and recrystallized from 6 ml of ethyl acetate. The yield was 0.7 g of colourless, irregular prisms, m.p. 129°–129.5°, according to analyses consisting of acetaldehyde β-carboxyethyldithiocarbhydrazone.

For $C_5H_{10}O_2N_2S_2$ (206.28)

calc.:	C 34.9	H 4.89	N 13.58	S 31.1 %,	equiv.w.:	103,
found:	C 35.1	H 4.91	N 13.50	S 31.0 %,	,, ,,:	108[1].

A solution of 1.1 g of *benzaldehyde* in 10 ml of ethanol was added to a solution of 1.8 g of β-carboxyethyldithiocarbhydrazide in 10 ml of ethanol. On the following day the clear, yellow solution was carefully precipitated with 100 ml of water and deposited 2.4 g of pale yellow, irregular prisms with m.p. about 134°–142°. When the experiment was repeated with the hydrazide dissolved in the equivalent amount of *N*-HCl or *N*-NaOH, about the same yields were obtained, in the latter case after acidification. The combined products, 7.3 g, were dissolved in 10 ml of hot glacial acetic acid, and 30 ml of hot benzene was added. On cooling, the solution deposited 6.3 g of pale yellow, oblique prisms, m.p. 139°–145°. From this product 2.1 g were dissolved in 10 ml of *N*-NaOH, and a layer of benzene separated on the top of the liquid. When the benzene had evaporated, the solution was acidified and deposited 1.9 g of pale yellow, irregular prisms, m.p. 157°–158°. The rest of the recrystallized product, 4.2 g, was dissolved in 6 ml of hot glacial acetic acid, and 20 ml of hot benzene were added. Before any crystals had separated, the solution was seeded with the benzene-free product of m.p. 157°–158° and then deposited 3.4 g of pale yellow, oblique prisms, m.p. 160°–160.5°. Further recrystallization did not change the m.p. According to analyses the product was benzaldehyde β-carboxyethyldithiocarbhydrazone.

For $C_{11}H_{12}O_2N_2S_2$ (268.35)

calc.:	C 49.2	H 4.51	N 10.44	S 23.9 %,	equiv.w.:	134,
found:	C 49.5	H 4.54	N 10.51	S 23.9 %,	,, ,,:	145[1].

---

[1] Blunt end point against phenolphthalein.

From this product 2.7 g were dissolved in 5 ml of hot glacial acetic acid, and 15 ml of hot benzene were added. On cooling, the solution deposited 2.2 g of pale yellow, flat, oblique prisms, m.p. 139°–145° in an open tube and 135°–136° in a closed one.

For $C_{11}H_{12}O_2N_2S_2$, 0.4 C_6H_6 (299.58)

calc.:	C 53.7	H 4.85	N 9.35	S 21.4	C_6H_6 10.81 %,	equiv.w.:	150,
found:	C 53.6	H 4.79	N 9.38	S 21.4	C_6H_6 10.63[1] %,	,, ,,:	159[2].

A solution of 0.7 g of iodine in 10 ml of ethanol was added to a solution of 1.4 g of benzaldehyde β-carboxyethyldithiocarbhydrazone in 10 ml of *N*-NaOH and 25 ml of ethanol. The mixture soon began to deposit crystals, and on the following day 1.6 g of pale yellow, flat, rodshaped prisms had separated, m.p. about 210°–215° (decomp.). To judge from the sodium content the product might be an impure disodium salt of benzaldehyde β-carboxyethyl*iso*dithiocarbhydrazone disulphide.

For $C_{22}H_{20}O_4N_4S_4Na_2$ (578.64) calc.: Na 7.9, found: Na 6.6 %.

From this salt 1.4 g were dissolved in 10 ml of hot water, and the solution on acidification deposited 0.8 g of a pale yellow crystal mass with m.p. 156°–158° (decomp.). The product was recrystallized from 15 ml of ethanol and gave 0.7 g of pale yellow needles with m.p. 161.5°–162.5° (decomp.), (prod. 1).

When the experiment was repeated with the hydrazone dissolved in 5 ml of *N*-NaOH and 10 ml of ethanol, no sodium salt was obtained but 1.2 g of pale yellow needles with m.p. 157°–158° (decomp.). This product was recrystallized from 20 ml of ethanol and gave 1.0 g of pale yellow needles with m.p. 161.5°–162.5° (decomp.), (prod. 2).

According to analyses the two products consisted of benzaldehyde β-carboxyethyl*iso*dithiocarbhydrazone disulphide.

For $C_{22}H_{22}O_4N_4S_4$ (534.67)

calc.:	C 49.4	H 4.15	N 10.48	S 24.0 %,	equiv.w.:	267.3,
found:	C 49.5[3]	H 4.13[3]	N 10.45[4]	S 23.9[4] %,	,, ,,:	267.5[4].

When the hydrazone was dissolved in ethanol and oxidized with iodine, no definable product was obtained.

When 20 ml of a 2 *M*-$FeCl_3$ solution was added to a solution of 2.7 g of benzaldehyde β-carboxyethyldithiocarbhydrazone in 100 ml of ethanol, a clear, brown solution was obtained, which on the following day was freely evaporated to a sticky crystalline mass. This was shaken in a separating funnel with 25 ml of water and 25 ml of ether. The ethereal solution was extracted with 20 ml of *N*-NaOH and was then freely evaporated. Only a small, sticky residue was obtained. The alkaline solution was acidified and deposited a yellow oil, which presently solidified to 1.5 g of a crystal mass, melting from about 95° to 120°. The product was dissolved in 5 ml of hot ethyl acetate. On cooling, 0.26 g of pale yellow needles and 0.07 g of coarse prisms separated. The first mentioned product had m.p. 112°–113° alone and also on admixture with pure 2-[β-carboxyethylthio]-5-phenyl-1,3,4-thiadiazole (XX b).

For $C_{11}H_{10}O_2N_2S_2$ (266.33)

calc.:	C 49.6	H 3.78 %,	equiv.w.:	266.3,
found:	C 49.5	H 3.88 %,	,, ,,:	265.0.

---

[1] Loss of weight at 80°.

[2] Blunt end point against phenolphthalein.

[3] Prod. 1.

[4] Prod. 2

The coarse prisms showed m.p. 150°–152° alone and 153°–155° on admixture with the disulphide described above. The product was recrystallized from 1 ml of ethanol and gave 0.04 g of pale yellow needles, m.p. 160°–161° (decomp.).

When the benzaldehyde β-carboxyethyldithiocarbhydrazone was made to react with ethyl bromide in alkaline solution, no crystalline product was obtained.

When a solution of 1.4 g of monochloroacetic acid in 14.7 ml of *N*-NaOH (phenolphthalein) was added to a solution of 2.7 g of benzaldehyde β-carboxyethyldithiocarbhydrazone in 20 ml of *N*-NaOH, a clear mixture was obtained, which on the following day was acidified and then deposited an oil, which slowly solidified to 3.1 g of a pale yellow crystal mass, m.p. 129°–130°. This product was very sensitive to heat and was precipitated as an oil from solvent mixtures, but it could conveniently be purified over its dipotassium salt. From the crude acid 6.1 g were dissolved in 25 ml of absolute ethanol, and 25 ml of 2 *N*-KOH in absolute ethanol were added. On the following day 7.0 g of colourless nedles had separated, m.p. 250°–260° (decomp.). This product was dissolved in 200 ml of hot 90 % aqueous ethanol, and the solution was cooled with ice. On the addition of 100 ml of ether 4.5 g of colourless needles separated, m.p. 262°–263° (decomp., after giving off ethanol). According to analyses the product was benzaldehyde S′-carboxymethyl-S″-[β-carboxyethyl]-*iso*dithiocarbhydrazone dipotassium salt with half a mole of ethanol of crystallization.

For $C_{13}H_{12}O_4N_2S_2K_2$, 0.5 C_2H_6O (425.59)

calc.:	K 18.37	C_2H_6O	5.41 %,
found:	K 18.22	C_2H_6O	5.43 % in vacuum over phosphorus pentoxide at 140°.

When a solution of 2.1 g of this salt in 10 ml of water was acidified, 1.5 g of pale yellow, flat, rodshaped prisms separated, m.p. 134°–135°. This compound, which had equiv.w.: 163.4, calc.: 163.2 for benzaldehyde S′-carboxymethyl-S″-[β-carboxyethyl]-*iso*dithiocarbhydrazone (XXI), could also be obtained in the following way. A solution of 2.3 g of β-bromopropionic acid in 15.0 ml of *N*-NaOH (phenolphthalein) was added to a solution of 3.0 g of the previously (p. 499) described benzaldehyde carboxymethyldithiocarbhydrazone (with ethanol of crystallization) in 20 ml of *N*-NaOH. On the following day the clear mixture was acidified and deposited an oil, which slowly solidified to 3.1 g of a pale yellow crystal mass with m.p. 129°–130° alone and also on admixture with with the crude product from the experiment above. This product also gave a dipotassium salt with m.p. 262°–263°, and when a solution of this salt was acidified, the same acid was obtained as described above, m.p. and mixed m.p. 134°–135°.

For $C_{13}H_{14}O_4N_2S_2$ (326.38)

calc.:	C 47.8	H 4.32	N 8.58	S 19.65 %,	equiv.w.:	163.2,
found:	C 47.7	H 4.26	N 8.61	S 19.72 %,	,, ,,:	163.5.

e) *Ketone β-carboxyethyldithiocarbhydrazones*

A solution of 1 ml of *acetone* in 10 ml of water was added to a solution of 1.8 g of β-carboxyethyldithiocarbhydrazide in 10 ml of *N*-NaOH. On the following day the clear, colourless mixture was acidified with 5 ml of 2 *N*-HCl and deposited 1.8 g of pale yellow, irregular prisms, m.p. 133°–135°. The product was recrystallized from 5 ml of glacial acetic acid and gave 0.7 g of colourless, irregular prisms, m.p. 137°–138° (prod. 1).

A solution of 1 ml of acetone in 10 ml of water was added to a solution of 1.8 g of β-carboxyethyldithiocarbhydrazide in 10 ml of *N*-HCl. The mixture became turbid and deposited an oil, which presently solidified to 1.8 g of a crystal mass, m.p. 120°–130°. The product was recrystallized from 5 ml of glacial acetic acid and gave 0.7 g of colourless, irregular prisms (prod. 2), m.p. 137°–138° alone and also on admixture with prod. 1. According to analyses both products were acetone β-carboxyethyldithiocarbhydrazone.

For $C_7H_{12}O_2N_2S_2$ (220.31)

calc.:	C 38.2	H 5.49	N 12.72	S 29.1 %,	equiv.w.:	110,
found:	C 38.5[1]	H 5.45[1]	N 12.68[2]	S 29.0[2] %,	,, ,,:	111[1,3].

A solution of 0.9 g of *pyruvic acid* in 5 ml of water was added to a solution of 1.8 g of β-carboxyethyldithiocarbhydrazide in 10 ml of *N*-NaOH. On the following day the clear, yellow mixture was acidified with 10 ml of *N*-HCl and deposited 1.8 g of pale yellow flakes, m.p. 148°–150° (decomp.). The product was recrystallized from 15 ml of 30 % aqueous ethanol and gave 0.8 g of pale yellow flakes, m.p. 159.5°–160° (decomp., prod. 1). When the experiment was repeated with the hydrazide dissolved in 10 ml of *N*-HCl, the mixture became turbid and soon solidified to a porridge of pale yellow flakes, 2.0 g with m.p. 147°–150° (decomp.). The product was recrystallized in the same way as prod. 1 and gave 0.9 g of pale yellow flakes (prod. 2), m.p. 159°–160 (decomp.). According to analyses both products consisted of pyruvic acid β-carboxyethyldithiocarbhydrazone.

For $C_7H_{10}O_4N_2S_2$ (250.29)

calc.:	C 33.6	H 4.03	N 11.10	S 25.6 %,	equiv.w.:	83,
found:	C 33.8[1]	H 4.06[1]	N 11.13[2]	S 25.5[2] %,	,, ,,:	86[2,3].

f) *Monosaccharide β-carboxyethyldithiocarbhydrazides*

A solution of 1.5 g of *l-arabinose* in 10 ml of water was added after one day to a solution of 1.9 g of β-carboxyethyldithiocarbhydrazide in 10 ml of ethanol. The clear, colourless mixture then showed the following rotations in a one-decimeter tube:

t:	2.5	5	10	15	20	25	30	45
α_D^{20}:	+6.42°	+5.75°	+4.52°	+3.52°	+2.77°	+2.17°	+1.67°	+0.65°
t:	60	90	180	360	minutes.			
α_D^{20}:	+0.06°	−0.33°	−0.55°	−0.55°				

The mixture was freely evaporated to a volume of about 10 ml, and the separated colourless, irregular prisms were sucked off and air dried. The yield was 2.1 g with m.p. 121°–122° (decomp.). All attempts to recrystallize this product were in vain, but according to analyses it was a rather pure *l*-arabinose β-carboxyethyldithiocarbhydrazide hemihydrate.

For $C_9H_{16}O_6N_2S_2$, 0.5 H_2O (321.36)

calc.:	C 33.6	H 5.33	N 8.72	S 19.95 %,
found:	C 33.6	H 5.28	N 8.76	S 19.84 %.

---

[1] Prod. 1. [2] Prod. 2. [3] Blunt end point against phenolphthalein.

When the product was dried in vacuum over phosphorus pentoxide, it lost water extremely slowly with simultaneous decomposition. A solution of 0.4949 g of the substance in pyridine, adjusted to a total volume of 9.99 ml, showed the following specific rotations:

t:	4	8	60	1080	2520	minutes after the addition of pyridine.
$[\alpha]_D^{20}$:	+5.6°	+7.1°	+7.5°	+9.8°	+21.6°	

An increasing darkening of the solution made further readings impossible. $[\alpha]_D^{20}$ is calculated for the anhydrous hydrazide.

When the hydrazide in hydrochloric acid solution was made to react with *l*-arabinose, no crystalline product was obtained.

A solution of 1.8 g of *d-glucose* in 10 ml of water was added after one day to a solution of 1.9 g of β-carboxyethyldithiocarbhydrazide in 10 ml of ethanol. The clear, colourless mixture then showed the following rotations in a one-decimeter tube:

t:	3	5	10	15	20	30	45	60
α_D^{20}:	+4.27°	+4.26°	+4.17°	+4.12°	+3.99°	+3.84°	+3.56°	+3.33°
t:	90	150	240	360	730	1370	1740	minutes.
α_D^{20}:	+2.88°	+2.24°	+1.65°	+1.17°	+0.51°	+0.19°	+0.18°	

On free evaporation the mixture yielded a mass of colourless needles. The product was ground with 5 ml of water, sucked off and washed with 5 ml of water. The product was dried in the air for two days and then weighed 3.6 g. However, it still contained water. After drying in vacuum over phosphorus pentoxide it weighed 3.0 g and melted between 108° and 120°. This product was not hygroscopic. It could not be recrystallized, and because of the wide melting range no analyses were performed. A solution of 0.5718 g of the product in pyridine was adjusted to a total volume of 9.99 ml and then showed immediately, after one hour and on the following day, $\alpha_D^{20} = +1.49^\circ$ in a one-decimeter tube, $[\alpha]_D^{20} = +26.1^\circ$ and $[M]_D^{20} = +89.3^\circ$.

A solution of 1.8 g of *d*-glucose in 10 ml of water was added after one day to a solution of 1.9 g of β-carboxyethyldithiocarbhydrazide in 10 ml of *N*-HCl. The clear, colourless mixture then showed the following rotations in a one-decimeter tube:

t:	2	5	10	15	25	40	60	85
α_D^{20}:	+4.24°	+3.93°	+3.55°	+3.21°	+2.73°	+2.19°	+1.69°	+1.35°
t:	120	180	minutes.					
α_D^{20}:	+1.10°	+0.97°						

After 270 minutes the mixture had crystallized, and when the main portion of the solution was seeded with the crystals, 1.8 g of colourless needles were obtained in all (after drying in vacuum over phosphorus pentoxide) with m.p. 115°–120°. According to analyses the product was rather pure *d*-glucose β-carboxyethyldithiocarbhydrazide.

For $C_{10}H_{18}O_7N_2S_2$ (342.38)

calc.:	C 35.1	H 5.30	N 8.18	S 18.73 %,
found:	C 35.0	H 5.31	N 8.19	S 18.79 %.

A solution of 0.5189 g of this product in pyridine was adjusted to a total volume of 9.99 ml and then showed immediately, after one hour and on the following day, $\alpha_D^{20} = +1.39^\circ$ in a one-decimeter tube, $[\alpha]_D^{20} = +26.8^\circ$ and $[M]_D^{20} = +91.4^\circ$.

The foregoing experiment was repeated in double quantities, and after four hours the mixture had not begun to deposit crystals. Then 40 ml of an *M*-$FeCl_3$ solution was added. A dark brown mixture resulted with a weak evolution of gas. On the following day dark green, sticky masses were sucked off and dissolved in 30 ml of *N*-NaOH. The dark solution was treated with Norite and filtered. On acidification the filtrate was turbid and deposited 0.9 g of pale brown flakes, m.p. 141°–143°. The product was recrystallized from 20 ml of ethyl acetate and gave 0.5 g of pale yellow flakes, m.p. 144°–145°, according to analyses consisting of the already (p. 512) described 2,5-bis-[β-carboxyethylthio]-1,3,4-thiadiazole (XX a). A mixed m.p. showed no depression.

For $C_8H_{10}O_4N_2S_3$ (294.36)

calc.:	C 32.6	H 3.42	N 9.52	S 32.7 %,	equiv.w.:	147.2,
found:	C 32.6	H 3.40	N 9.41	S 32.4 %,	,, ,,:	147.4.

F. *α, β-Dicarboxyethyldithiocarbhydrazide and 3-amino-5-carboxymethyl-rhodanine*

Solid ammonium dithiocarbazinate, 1.3 g, dissolved rapidly in a solution of 2.0 g of *l-bromosuccinic acid*[1] in 20.3 ml of *N*-NaOH (phenolphthalein), and then the solution showed the following rotations in a one-decimeter tube:

t:	3	4	5	6	8	10	13	18
α_D^{20}:	−2.65°	−2.25°	−1.95°	−1.55°	−1.07°	−0.60°	−0.07°	+0.62°
t:	25	35	50	80	180	250	360	500
α_D^{20}:	+1.30°	+1.94°	+2.56°	+3.22°	+3.75°	+3.75°	+3.50°	+3.15°
t:	820	1320	3000	5960	9025	11,520	minutes.	
α_D^{20}:	+2.43°	+1.75°	+1.00°	+0.66°	+0.56°	+0.55°		

The *l*-bromosuccinate solution showed $\alpha_D^{20} = -3.78°$ before the addition of ammonium dithiocarbazinate.

When the reaction mixture was acidified with 5 ml of 5 *N*-HCl after 11,520 minutes, a clear, colourless solution was obtained, which on free evaporation gave only sticky products.

When a similar solution was acidified after 180 minutes, the mixture soon became turbid and began to separate crystals. On the following day 1.5 g of colourless, irregular prisms had separated, m.p. 79°–80°. The filtrate showed $\alpha_D^{20} = -0.14°$. The crystalline product was recrystallized twice from 10 ml of 25 % aqueous ethanol and gave 1.0 g of colourless, rodshaped prisms, m.p. 81°–82° in an open as well as in a closed tube. According to analyses the product was 3-amino-5-carboxymethyl-rhodanine (Xd) monohydrate.

For $C_5H_6O_3N_2S_2$, H_2O (224.25)

calc.:	C 26.8	H 3.60	N 12.49	S 28.6 %,
found:	C 26.7	H 3.62	N 12.55	S 28.5 %.

In attempts to titrate the product with 0.1 *N*-NaOH against phenolphthalein no reasonable end point could be obtained. In vacuum over phosphorus pentoxide the product lost a part of its water of crystallization. After two weeks the weight was constant, when about two thirds of the calculated loss of weight had occurred. When the product was dried att 100° and 0.5 mm over phosphorus pentoxide, the loss of weight was found to be 8.06 %, calc.: 8.03 %, but the resulting green-yellow glass could not be made to crystallize. It was then dissolved in hot water. On cooling, the starting material with m.p. 81°–82° was obtained.

---

[1] Prepared according to KALLENBERG (23).

The product was found to be optically inactive, and when the experiment was repeated with *d,l*-bromosuccinic acid, the same product was obtained with the same yield.

Solid *sodium nitrite*, 0.7 g, was added in portions with grinding to a cooled suspension of 1.3 g of 3-amino-5-carboxymethyl-rhodanine monohydrate in 5 ml of 2 *N*-HCl. When the evolution of gas had ceased, the undissolved material was collected. It was 0.9 g of colourless crystal powder, m.p. 159°–160°. The product was recrystallized from 8 ml of water and gave 0.5 g of colourless, irregular prisms, m.p. 160°–161°, according to analyses consisting of 5-carboxymethyl-rhodanine (XIV d).

For $C_5H_5O_3NS_2$ (191.22)

calc.:	C 31.4	H 2.64	N 7.33	S 33.5 %,	equiv.w.: 95.6,
found:	C 31.5*	H 2.73*	N 7.34	S 33.3* %,	,, ,,: 95.3.

This compound does not seem to have been described before. It could also be prepared in the following way. Solid ammonium dithiocarbamate, 1.5 g, was added to a solution of 2.0 g of *d,l*-bromosuccinic acid in 20.2 ml of *N*-NaOH (phenolphthalein). On the following day the clear mixture was acidified with 5 ml of 5 *N*-HCl and deposited 1.1 g of colourless, irregular prisms, m.p. 159°–160°. The product was recrystallized from 10 ml of water and gave 0.7 g of colourless, irregular prisms, m.p. 160°–161° alone and also on admixture with the 5-carboxymethyl-rhodanine described above.

Found: N 7.36 %, equiv.w.: 95.4.

A solution of 1.1 g of *benzaldehyde* in 5 ml of ethanol was added to a solution of 2.2 g of 3-amino-5-carboxymethyl-rhodanine monohydrate in 10 ml of ethanol. A clear, yellow mixture was obtained, which on the following day had deposited 2.6 g of pale yellow, irregular prisms, m.p. 189°–190°. The product was recrystallized from 25 ml of ethanol and gave 2.2 g of pale yellow, rodshaped prisms with the same m.p. According to analyses the product was 3-benzylidenamino-5-carboxymethyl-rhodanine (XV d).

For $C_{12}H_{10}O_3N_2S_2$ (294.34)

calc.:	C 49.0	H 3.42	N 9.52	S 21.8 %, equiv.w.: 294.3,
found:	C 48.9	H 3.40	N 9.55	S 21.8 %, ,, ,,: 294.7[1].

Solid ammonium dithiocarbazinate, 2.5 g, was added to a solution of 4.0 g of *l*-bromosuccinic acid in 41.0 ml of *N*-NaOH (phenolphthalein). After three hours a solution of 2.2 g of benzaldehyde in 40 ml of ethanol was added. On the following day the opalescent solution was evaporated to about 50 ml volume. A small amount of yellow, crystalline product was separated, and the filtrate was acidified with 10 ml of 5 *N*-HCl. The mixture slowly began to deposit crystals. On the following day 4.9 g of pale yellow, irregular prisms with m.p. 156°–157° (decomp.) had formed.

---

[1] The colour of an ethanolic solution of the compound sharply changed from yellow to red when an excess of alkali was added. This made it impossible but also unneccesary to use an indicator.

The product was recrystallized from a mixture of 60 ml of ethyl acetate and 100 ml of ligroin (b.p. 80°–100°) and then from half the amount of the same solvent mixture and gave 1.7 g of pale yellow, rodshaped prisms, m.p. 165°–165.5° (decomp.). According to analyses the product was benzaldehyde α,β-dicarboxyethyldithiocarbhydrazone (VIII d).

For $C_{12}H_{12}O_4N_2S_2$ (312.36)

calc.:	C 46.1	H 3.87	N 8.97	S 20.5 %,	equiv.w.:	104,
found:	C 46.3	H 3.96	N 8.96	S 20.4 %,	,, ,,:	111[1].

A solution of 0.7643 g of this product in absolute ethanol, adjusted to a total volume of 9.99 ml, showed $\alpha_D^{20} = +0.70°$ in a one-decimeter tube, $[\alpha]_D^{20} = +9.16°$ and $[M]_D^{20} = +28.6°$. When one ml of concentrated hydrochloric acid was added to 5 ml of this solution, no loss of its optical activity occurred during one week, which would have been the case if the compound had lost water and cyclizated.

When the experiment was repeated with *d,l*-bromosuccinic acid, an inactive benzaldehyde $\alpha.\beta$-dicarboxyethyldithiocarbhydrazone was obtained as pale yellow, flat, oblique plates with m.p. 169.5°–170° (decomp.). The yield was nearly the same as in the preparation of the active compound.

Found: C 46.3 H 3.88 %, equiv.w.: 113.[1]

This work was started at the Nobel Institute of the Royal Academy of Sciences, Department of Organic Chemistry, Stockholm, Sweden, and completed at the Department of Organic Chemistry, University of Lund, Lund, Sweden. I wish to express my thanks to Professor Bror Holmberg for his kind help and advice during the work and to Professor Erik Larsson for putting the facilities in Lund at my disposal. I am also indebted to *Kungliga Fysiografiska Sällskapet* for a grant.

REFERENCES

1. Sandström, J., Arkiv Kemi *4*, 297 (1952).
2. Bose, P. K., Quart. J. Indian Chem. Soc. *3*, 148 (1926), C. *1926*, II, 1651.
3. Busch, M., Ber. *34*, 1119 (1901).
4. Busch, M. and Krapf, H., J. pr. Chem. [2] *84*, 293 (1911).
5. Busch, M., Ber. *45*, 73 (1912).
6. Busch, M. and Cornelius, W., J. pr. Chem. [2] *93*, 32 (1916).
7. Busch, M. and Starke, M., J. pr. Chem. [2] *93*, 49 (1916).
8. Busch, M. and Biehler, F., J. pr. Chem. [2] *93*, 343 (1916).
9. Holmberg, B., Arkiv Kemi *4*, 33 (1952).
10. Andreasch, R., Monatsh. *29*, 399 (1908).
11. Holmberg, B., J. pr. Chem. [2] *81*, 464 (1910).
12. Mathes, R. A., J. Org. Chem. *17*, 877 (1952).
13. Busch, M., Ber. *27*, 2507 (1894).
14. Busch, M., J. pr. Chem. [2] *60*, 25 (1899).
15. Busch, M, and Lingenbrink, E., J. pr. Chem. [2] *61*, 336 (1900).
16. Curtius, Th. *et al.*, Ber. *40*, 836 (1907).
17. Hoggarth, E., J. Chem. Soc. *1952*, 4811.
18. Sandström, J., Arkiv Kemi *7*, 249 (1954).
19. Girard, M., Ann. Chim. *16*, 333 (1941).
20. Holmberg, B., J. pr. Chem. [2] *79*, 265 (1909).
21. Mathes, R. A., U.S. Pat. 2,623,059 Dec. 23, 1952; C.A. *47*, 9352h (1953).
22. Holmberg, B., Ber. *47*, 159 (1914).
23. Kallenberg, S., Diss. Lund 1919.
24. Curtius, Th. and Heidenreich, K., J. pr. Chem. [2] *52*, 476 (1895).

---

[1] Blunt end point against phenolphthalein.

25. Holmberg, B., J. pr. Chem. [2] *71*, 272 (1905).
26. Holmberg, B., Arkiv Kemi, Mineral. Geol. *17 A*, n:r 23, 9 (1944).
27. Nencki, M., J. pr. Chem. [2] *16*, 1 (1877).
28. Nencki, M., Ber. *17*, 2277 (1884).
29. Andreasch, R., Monatsh. *10*, 75 (1889).
30. Simonsen, J. L. and Rau, M. G., J. Chem. Soc. *113*, 24 (118).
31. Brown, F. C. *et al.*, J. Org. Chem. *15*, 174 (1950).
32. Berlinerblau, J., Ber. *19*, 124 (1886).
33. Wheeler, H. L. and Johnson, T. B., J. Amer. Chem. Soc. *24*, 680 (1902).

Tryckt den 14 november 1955

Uppsala 1955. Almqvist & Wiksells Boktryckeri AB

ARKIV FÖR KEMI Band 8 nr 52

Communicated 12 January by Arne Fredga and Bror Holmberg

On the formation of pyrazoles from thiohydrazides and α-halogencarbonyl compounds

By Jan Sandström

1. Introduction and survey

Bose (1) has investigated the reactions between 1-phenyldithiocarbhydrazides (I) and phenacylbromides and found that 1-phenyl-S′-phenacyl-S″-alkyl-*iso*dithiocarbhydrazides (II) were first formed, which could then be cyclised to 2-alkylthio-4-phenyl-5-aryl-1,3,4,4H-thiadiazines (III).

$RS \cdot CS \cdot NH \cdot NH \cdot C_6H_5$

I

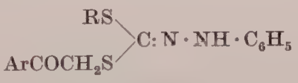

$$\begin{matrix} RS \\ ArCOCH_2S \end{matrix} \rangle C{:}\,N \cdot NH \cdot C_6H_5$$

II

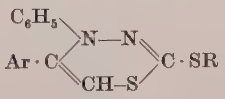

III

Similar compounds, with hydrogen instead of phenyl in the 1- and 4-positions respectively, could be expected from the reactions between 1-unsubstituted dithiocarbhydrazides and α-halogencarbonyl compounds. However, when chloroacetaldehyde, chloroacetone and 2-chlorocyclohexanone were made to react with methyl- or benzyldithiocarbhydrazide (2) in neutral or alkaline solution, only tarry products were obtained. When benzyldithiocarbhydrazide in alkaline solution was made to react with phenacyl bromide, a crystalline product was obtained, m.p. 98°–99°, which was found to be 2-benzylthio-5-phenyl-1,3,4,4H-thiadiazine (IVa). This compound was also obtained when benzyl chloride was added to an alkaline solution of 2-mercapto-5-phenyl-1,3,4,4H-thiadiazine (IVb), (3). It is rather sensitive to heat and in solution it decomposes within a few hours at room temperature.

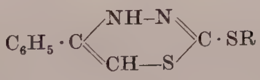

IV; *a*, $R = CH_2C_6H_5$, *b*, $R = H$

When dithiocarbhydrazides in neutral or alkaline solutions were made to react with ethyl α-chloroacetoacetate, a rather unexpected type of reaction took place. The reaction products were found to be sulphur and ethyl 3-alkylthio-5-methylpyrazole-4-carboxylates according to formula (*A*).

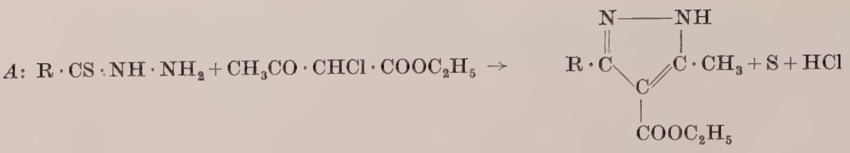

V

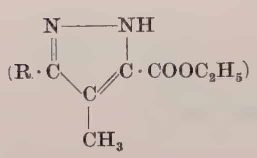

VI

a, $R = CH_3S$
b, $R = C_2H_5S$
c, $R = C_6H_5CH_2S$
d, $R = HOCOCH_2S$
e, $R = HOCOCH_2CH_2S$
f, $R = C_6H_5$
g, $R = C_2H_5O$

The sulphur was not always liberated in free state but was sometimes contained in a sticky, slightly soluble mass with a high content of sulphur. From this mass a small amount of pure sulphur could be extracted with boiling toluene. The pyrazole esters were obtained in good yields. The same reaction occurred with ethyl α-bromoacetoacetate, but the yields were in general much inferior.

This reaction does not definitely exclude the possibility that the products are ethyl 3-alkylthio-4-methyl-pyrazole-5-carboxylates (VI). However, when ethyl acetoacetate was made to react with methyl- and benzyldithiocarbhydrazide, the corresponding dithiocarbhydrazones (VII) were obtained in the crystalline state, m.p. 59°–60° and 69.5°–70° respectively. When ethanolic solutions of these hydrazones were treated with two equivalents of iodine or pyridinium tribromide, sticky masses with high contents of sulphur first separated, and from the filtrates, on the addition of water, the ethyl 3-methylthio- and 3-benzylthio-5-methyl-pyrazole-4-carboxylates were obtained. The reaction (*B*) proves, irrespective of the more subtle reaction mechanism, that the order of substitutents is that given in formula (V).

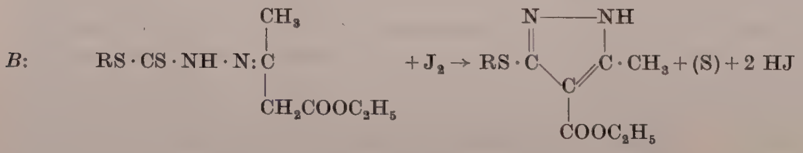

VII; *a*, $R = CH_3$, *b*, $R = CH_2C_6H_5$ V, *a* and *c*

It seems rather probable that the reactions (*A*) and (*B*) proceed with ethyl 2-alkylthio-5-methyl-1,3,4,4H-thiadiazine-6-carboxylates (VIII) as intermediates, for if the ethyl 2-mercapto-5-methyl-1,3,4,4H-thiadiazine-6-carboxylate (IX), (3) was made to react with benzyl chloride in the presence of one equivalent of sodium hydroxide in aqueous ethanolic solution, the pyrazole (V*c*) was obtained in good yield together with free sulphur (*c*). In the same way the mercaptothiadiazine (IX) reacted with sodium monochloroacetate in alkaline solution to give an almost quantitative yield of sulphur and the sodium salt of ethyl 3-carboxymethylthio-5-methyl-pyrazole-4-carboxylate (V*d*). This pyrazole was not formed in the reaction between ethyl α-chloroacetoacetate and a carboxymethyldithiocarbhydrazide salt solution (4).

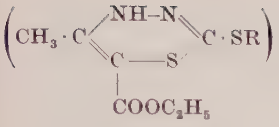

VIII

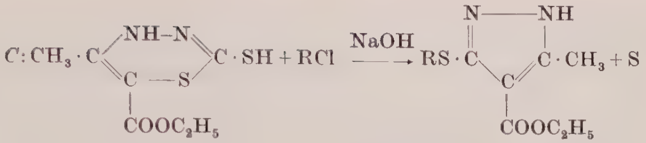

IX

The pyrazole esters (V) were hydrolysed to the corresponding carboxylic acids (X), and these in turn, on heating, lost carbon dioxide and gave, with one exception, the 3-alkylthio-5-methyl-pyrazoles (XI). All except one of these were liquid, and they were characterized as picrates.

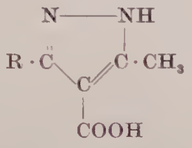

X; *a–f* as in V

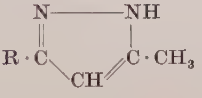

XI; *a–f* as in V

The following ethyl 3-alkylthio-5-methyl-pyrazole-4-carboxylate derivatives have been prepared: The 3-methylthio ester, (V*a*), m.p. 128°–129°; hydrochloride, m.p. 169°–171°; carboxylic acid (X*a*), m.p. 252.5°–253°; and picrate of (XIa), m.p. 164°–165°. The 3-ethylthio ester (V*b*) has m.p. 90°–91°, its hydrochloride has m.p. 143°–146°, the carboxylic acid (X*b*) has m.p. 203°–203.5°, and the picrate of (XI*b*) has m.p. 132°–133°. The ester (V*b*), the acid (X*b*) and the liquid pyrazole (XI*b*) have been described in a previous paper (5) as resulting from the reaction between the liquid ethyl acetoacetate ethyldithiocarbhydrazone and iodine. The 3-benzylthio ester (V*c*) has m.p. 126.5°–127°, the hydrochloride m.p. 158°–162°, the carboxylic acid (X*c*) m.p. 244°–245°, and the picrate of (XI*c*) m.p. 144.5°–145.5°.

The ethyl 3-carboxymethylthio-5-methyl-pyrazole-4-carboxylate (V*d*) has m.p. 182°–183°, and the corresponding carboxylic acid (X*d*) has m.p. 222°–223°. When this was heated above its melting point, it lost carbon dioxide, but the resulting product was a neutral tarry mass, from which aqueous sodium hydroxide could extract only a small amount of unchanged starting material.

β-Carboxyethyldithiocarbhydrazide (4, 6) and ethyl α-chloroacetoacetate reacted to give ethyl 3-[*β*-carboxyethylthio]-5-methyl-pyrazole-4-carboxylate (V*e*), m.p. 167°–168°. The carboxylic acid (X*e*) has m.p. 213°–214°, and the corresponding pyrazole (XI*e*) has m.p. 134°–135°.

However, the reaction is not restricted to the thiohydrazides hitherto mentioned. With 1-phenyl-methyldithiocarbhydrazide (I, R = CH_3), (7) ethyl α-chloroacetoacetate gave ethyl 1-phenyl-3-methylthio-5-methyl-pyrazole-4-carboxylate (XII), m.p. 109°–109.5°. It was hydrolysed to the corresponding carboxylic acid, m.p. 215°–216°. On heating above its melting point, this acid lost carbon dioxide and gave 1-phenyl-3-methylthio-5-methyl-pyrazole. It was liquid and was characterized by oxidation with hydrogen peroxide to the corresponding sulphone, m.p. 107°–108°. Both compounds have previously been described by MICHAELIS (8).

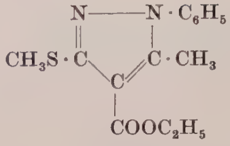

XII

Thiobenzhydrazide (9) and ethyl α-chloroacetoacetate gave the liquid ethyl 3-phenyl-5-methyl-pyrazole-4-carboxylate (V*f*), hydrochloride m.p. 155°–160°. The ester was hydrolysed to the corresponding carboxylic acid (X*f*), m.p. 262°–262.5°, and the acid was decarboxylated to the well-known (10, 11) 3-phenyl-5-methyl-pyrazole (XI*f*), m.p. 128°–128.5°, hydrochloride m.p. 205°–212° and picrate m.p. 160°–161°. The ester (V*f*) has been prepared by SJOLLEMA (10) from ethyl α-benzoyl-acetoacetate and hydrazine hydrate, but he gives no data for the compound. DE and DUTT (12) also claim to have prepared the ester (V*f*) from ethyl α-benzoyl-acetoacetate and thiosemicarbazide, but as they report m.p. 232° for the ester and give a nitrogen analysis as the only proof of structure, the report must be regarded as questionable. The carboxylic acid (X*f*), the pyrazole (XI*f*), its hydrochloride and picrate have been prepared by SJOLLEMA (10). For the acid he reports m.p. 260°–265°, for the phenyl-methyl-pyrazole m.p. 128° and for its hydrochloride m.p. 205°. He reports no m.p. for the picrate, but it has been described by POSNER (11), who reports m.p. 158–159°.

The ethylxanthogenhydrazide (13) and ethyl α-chloroacetoacetate gave a rather low yield of pure sulphur and ethyl 3-ethoxy-5-methyl-pyrazole-4-carboxylate (V*g*), m.p. 96°–97°, hydrochloride m.p. 161°–162°. On hydrolysis the corresponding carboxylic acid could not be isolated but mixtures of oily and water-soluble neutral products, the nature of which has not yet been established.

As distinct from the thiohydrazides hitherto mentioned, thiosemicarbazide does not give a pyrazole derivative in the reaction with ethyl α-chloroacetoacetate but the hydrochloride of a base $C_7H_{11}O_2N_3S$. The hydrochloride has m.p. 190°–191° and the base 184°–185°. According to a private communication from Professor HANS BEYER in Greifswald, this reaction has recently been subjected to a thorough investigation at his department, and therefore no attempts have been made to establish the constitution of the compound mentioned above.

When benzyldithiocarbhydrazide reacted with ethyl α-chloro-α-formylacetate (XIII), ethyl 3-benzylthio-pyrazole-4-carboxylate (XIV) was formed, m.p. 118°–119°. It was hydrolysed to the corresponding carboxylic acid, m.p. 260°–261°, and this acid was decarboxylated to the liquid 3-benzylthio-pyrazole, picrate m.p. 110°–111°.

$HCO \cdot CHCl \cdot COOC_2H_5$

XIII

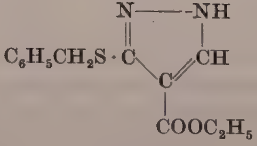

XIV

The different ethyl pyrazole-4-carboxylates now described are generally rather difficult to hydrolyse. A semiquantitative comparison shows that the 3-phenyl-5-methyl-pyrazole ester reacts most slowly with ethanolic potassium hydroxide. The 3-methylthio-, 3-ethylthio-, 3-benzylthio- and 3-ethoxy-5-methyl-pyrazole esters all show the same, somewhat higher rate. The introduction of a phenyl group in the 1-position or of a carboxy group in the 3-alkylthio group produces a considerable acceleration of the rate, and so does the exchange of the 5-methyl group for hydrogen. The last effect was to be expected for purely steric reasons.

It seems as if the carbethoxy group in the 6-position is responsible for the instability of the intermediate 1,3,4-thiadiazines. In order to see if other α-halogencarbonyl compounds with an electron-attracting group in the β-position of the carbonyl group would also have the same effect, 3-chloro-acetylacetone was made to react with benzyldithiocarbhydrazide. The resulting products were sulphur and 3-benzylthio-4-acetyl-5-methyl-pyrazole (XV), m.p. 169°–170°, 2,4-dinitrophenylhydrazone m.p. 227°–228°. When 1-phenyl-methyldithiocarbhydrazide (I, R = CH_3) reacted with 3-chloroacetylacetone, sulphur was formed together with 1-phenyl-3-methylthio-4-acetyl-5-methyl-pyrazole (XVI), m.p. 152°–153°, 2,4-dinitrophenylhydrazone m.p. 219°–220°. In the same reaction with thiobenzhydrazide no definable compound could be obtained.

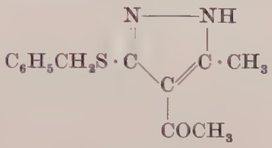
XV

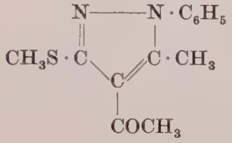
XVI

The ethyl 3-ethylthio-5-methyl-pyrazole-4-carboxylate (V*b*) has previously (5) been formulated as ethyl 3-methyl-5-ethylthio-*iso*pyrazole-4-carboxylate (XVII).

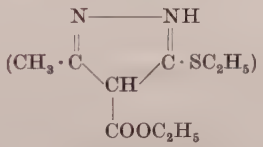
XVII

This formulation was made in order to keep the same order of bonds in the pyrazole as in the ethyl acetoacetate ethyldithiocarbhydrazone. However, attempts to prepare real 4-*iso*pyrazole derivatives from ethyl α-methylacetoacetate methyldithiocarbhydrazone (XVIII*a*), m.p. 63°–64°, and iodine or from methyldithiocarbhydrazide and ethyl α-chloro-α-methylacetoacetate have been in vain. In the first reaction no definable product was obtained, and in the second the first product was ethyl α-chloro-α-methylacetoacetate methyldithiocarbhydrazone (XVIII*b*), m.p. 59°–60°. In alkaline solution this hydrazone was cyclised in low yield to ethyl 2-methylthio-5,6-dimethyl-1,3,4-6H-thiadiazine-6-carboxylate (XIX), melting between 100° and 120°. It could not be obtained in a pure state.

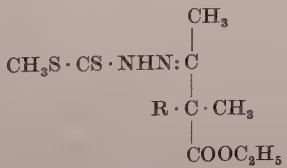
XVIII

a, R = H *b*, R = Cl

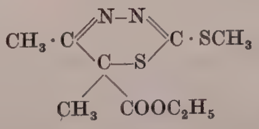
XIX

All pyrazoles now described except those with a phenyl group in the 1-position and, of course, those with free carboxyl groups give white precipitates with a solution of silver nitrate in ethanolic ammonia. This reaction is significant for pyrazoles with a free imino group, as was already found by Buchner (14). The silver salt of ethyl 3-methylthio-5-methyl-pyrazole-4-carboxylate (V*a*) was isolated for analysis. It was found to contain one atom of silver per molecule of pyrazole and showed m.p. 227°–228°. It is very slightly soluble in water, somewhat more in ethanol and is considerably soluble in toluene. It is obviously an internal complex.

Dvoretsky and Richter (15) have found that pyrazoles with a free imino group react with formaldehyde to give 1- or 2-hydroxymethyl derivatives with extreme ease. This was also found to be the case with the two pyrazoles selected for this reaction. The ethyl 1- or 2-hydroxymethyl-3-methylthio-5-methyl-pyrazole-4-carboxylate (XX*a*) has m.p. 133°–135°. When heated with ammoniacal silver solution, it splits off formaldehyde and gives the silver salt of the parent compound. The ethyl 1- or 2-hydroxymethyl-3-phenyl-5-methylpyrazole-4-carboxylate (XX*b*) has m.p. 110°–112°.

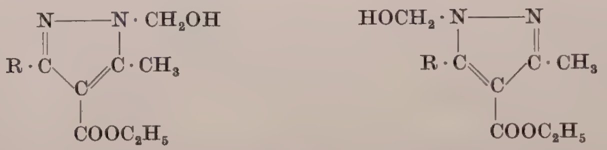

XX

a, R = CH_3S; *b*, R = C_6H_5

These results make it rather probable that the pyrazoles obtained in these reactions have the normal constitution with the "extra" hydrogen atom in the 1- or 2-position.

2. Experimental

A. 2-Benzylthio-5-phenyl-1,3,4,4H-thiadiazine

A solution of 4.0 g of phenacyl bromide in 50 ml of ethanol was added with stirring and cooling to a solution of 4.0 g of benzyldithiocarbhydrazide in 50 ml of ethanol and 20 ml of *N*-NaOH. The clear, yellow solution soon began to deposit pale yellow flakes. After one hour the product, 5.3 g with m.p. 93°–95°, was collected. It was dissolved in 100 ml of hot ethanol and the solution was immediately cooled with ice. The yield was 2.7 g of pale yellow plates, m.p. 98°–99°, according to analyses consisting of 2-benzylthio-5-phenyl-1,3,4,4H-thiadiazine (IV*a*).

For $C_{16}H_{14}N_2S_2$ (298.41)
calc.: C 64.4 H 4.73 N 9.39 S 21.5 %,
found: C 64.5*[1] H 4.82* N 9.42 S 21.5* %.

When the hot ethanolic solution of this compound was allowed to cool slowly, the resulting product was brown and its melting point was considerably lower.

---

[1] The analyses marked with an asterisk have been performed by Miss M. Westerdahl at the Analytical Department, University of Lund, and the rest by the author.

The thiadiazine was also prepared in the following way. A solution of 0.7 g of benzyl chloride in 10 ml of ethanol was added to a solution of 1.0 g of 2-mercapto-5-phenyl-1,3,4,4H-thiadiazine (IV*b*) in 5 ml of *N*-NaOH. The mixture immediately became turbid and began to deposit crystals. After one hour 0.9 g of pale yellow flakes was collected, m.p. 93°–94°. The product was recrystallized from 15 ml of ethanol as above and gave 0.5 g of pale yellow plates, m.p. 98°–99° alone and also on admixture with the thiadiazine described above.

Found: N 9.50* S 21.3 %.

B. Ethyl pyrazole-4-carboxylates

a. *Ethyl acetoacetate methyldithiocarbhydrazone and ethyl 3-methylthio-5-methyl-pyrazole-4-carboxylate*

A solution of 6.5 g of ethyl acetoacetate in 25 ml of ethanol was added to a solution of 6.3 g of methyldithiocarbhydrazide in 25 ml of ethanol. On the following day the clear, colourless mixture was poured into 300 ml of water. An oil separated, which on scratching solidified to 11 g of a colourless crystal mass, m.p. 57°–58°. The product was recrystallized from a mixture of 50 ml of chloroform and 100 ml of petroleum ether (b.p. 40°–60°) and gave 8.2 g of colourless, rod-shaped prisms, m.p. 59°–60°. According to analyses the product was ethyl acetoacetate methyldithiocarbhydrazone (VII*a*).

For $C_8H_{14}O_2N_2S_2$ (234.33)
calc.: C 41.0 H 6.02 N 11.96 S 27.4 %,
found: C 41.0 H 6.03 N 11.96 S 27.5 %.

A solution of 2.6 g of iodine in 40 ml of ethanol was added to a solution of 2.4 g of the hydrazone described above in 30 ml of ethanol. A clear, brown solution was obtained, which soon became turbid and on the following day had deposited 0.5 g of a red-yellow, amorphous mass, melting between 90° and 100°. The product contained 52 % of sulphur, and no definable compound could be extracted from it. The filtrate was precipitated with 400 ml of water and gave 1.1 g of brown flakes, m.p. 122°–125°. The product was recrystallized from 5 ml of benzene and gave 0.7 g of yellow flakes, m.p. 128°–129°.

When the experiment was repeated in the same amount of ethanol with the iodine replaced by 3.6 g of pyridinium tribromide, 1.0 g of the amorphous mass was obtained, and from the filtrate 0.7 g of yellow flakes, m.p. 124°–126°, was precipitated with water. The product was recrystallized from 4 ml of benzene and gave 0.6 g of yellow flakes, m.p. 128°–129°.

A solution of 2.1 g of ethyl α-bromoacetoacetate[1] in 10 ml of ethanol was added to a solution of 1.3 g of methyldithiocarbhydrazide in 10 ml of ethanol. The resulting clear, yellow mixture soon turned red and became turbid. On the following day a small amount of a red, sticky mass had separated, and the filtrate with 100 ml of water deposited 1.1 g of a sticky crystal mass. This was recrystallized from 5 ml of benzene and gave 0.3 g of pale yellow flakes, m.p. 125°–126° alone and 126°–127° on admixture with the products described above.

---

[1] Prepared according to BRÜHL (16).

A solution of 3.3 g of ethyl α-chloroacetoacetate[1] in 10 ml of ethanol was added to a solution of 2.5 g of methyldithiocarbhydrazide in 10 ml of ethanol. The clear, yellow solution soon turned red and after some hours it became turbid. On the following day 0.5 g of a red-yellow, sticky mass had separated, and the filtrate with 100 ml of water gave 3.5 g of a yellow crystal mass, m.p. 126°–127°.

The products melting between 125° and 129°, 5.1 g, were collected and recrystallized from 20 ml of benzene. The result was 3.9 g of colourless flakes, m.p. 128°–129°, according to analyses consisting of ethyl 3-methylthio-5-methyl-pyrazole-4-carboxylate (V*a*).

For $C_8H_{12}O_2N_2S$ (200.26)
calc.: C 48.0 H 6.04 N 13.99 S 16.01 %,
found: C 48.0 H 6.05 N 13.97 S 16.03 %.

When 2.5 g of methyldithiocarbhydrazide and 3.3 g of ethyl α-chloroacetoacetate were made to react in 15 ml of benzene, the mixture soon stiffened to a porridge of colourless hairs, which were sucked off and washed with carbon disulphide to remove a yellow impurity. The yield was 4.0 g with m.p. 169°–171° (after some sintering). According to analyses the product was the hydrochloride of the pyrazole (V*a*).

For $C_8H_{12}O_2N_2S$, HCl (236.71)
calc.: Cl 14.98 %, equiv. w: 236.7
found: Cl 14.95 %, equiv. w: 237.0.

Formalin, 1.5 ml, was added to a solution of 2.0 g of ethyl 3-methylthio-5-methyl-pyrazole-4-carboxylate in 10 ml of ethanol. After about twenty minutes the clear mixture began to deposit crystals, and on the following day 2.0 g of colourless, irregular prisms had separated, m.p. 133°–135° (after some sintering). The product was recrystallized from 10 ml of ethanol and gave 1.1 g of colourless, rod-shaped prisms with unchanged m.p. According to analyses the product was ethyl 1- or 2-hydroxymethyl-3-methylthio-5-methyl-pyrazole-4-carboxylate (XX*a*).

For $C_9H_{14}O_3N_2S$ (230.28)
calc.: C 46.9 H 6.13 N 12.17 S 13.92 %,
found: C 47.2* H 6.18* N 12.27* S 14.02* %.

A solution of 1.7 g of silver nitrate in 2 ml of water was mixed with 6 ml of 5 *N* ethanolic ammonia and diluted with ethanol to a total volume of 10.0 ml. From this solution 2 ml was added to a solution of 0.40 g of ethyl 3-methylthio-5-methyl-pyrazole-4-carboxylate in 4 ml of ethanol. A precipitate of colourless, rod-shaped prisms was immediately formed, which weighed 0.58 g and had m.p. 227°–228°. According to analysis it was the mono-silver salt of the pyrazole (V*a*).

For $C_8H_{11}O_2N_2SAg$ (306.12) calc.: Ag 35.1 %,
found: Ag 35.1 %.

When 2 ml of the silver solution was added to a solution of 0.46 g of the hydroxymethylpyrazole ester (XX*a*) in 5 ml of ethanol, the mixture became turbid and slowly separated a white precipitate. The mixture was heated on the water bath for half an hour, and then the precipitate was collected. The yield was 0.56 g of colourless, rod-shaped prisms, m.p. and mixed m.p. 227°–228°. The product contained 35.2 % of silver.

---

[1] Prepared according to ALLIHN (17).

A solution of 3.0 g of the pyrazole (V*a*) in 30 ml of *N*-NaOH and 30 ml of ethanol was refluxed for 6 hours, and then the ethanol was distilled off. An undissolved oily mass was taken up in 25 ml of ether, and the alkaline solution was acidified with 15 ml of 2 *N*-HCl. A colourless crystal powder separated with a simultaneous evolution of carbon dioxide. The yield was 1.0 g with m.p. 247°–247.5° (decomp.). The product was dissolved in 6 ml of *N*-NaOH and 15 ml of ethanol and then precipitated with 5 ml of 2 *N*-HCl in 5 ml of ethanol. The yield was 0.8 g of a colourless crystal powder with m.p. 252.5°–253° (decomp.), according to analyses consisting of 3-methylthio-5-methyl-pyrazole-4-carboxylic acid (X*a*).

For $C_6H_8O_2N_2S$ (172.20)
calc.: C 41.8 H 4.68 N 16.27 S 18.62 %, equiv. w.: 172.2
found: C 41.8 H 4.61 N 16.22 S 18.58 %, equiv. w.: 173.4

The ethereal extract from the alkaline solution was evaporated and gave a residue of 1.2 g of oil with crystals. It was treated with 3 ml of benzene and filtered from 0.3 g of unchanged starting material, m.p. 127°–128° alone and also on admixture with the pure pyrazole (V*a*).

The benzene solution was added to a solution of 1.5 g of picric acid in 30 ml of ethanol. On the following day the mixture had deposited 0.9 g of yellow, rod-shaped prisms, m.p. 164°–165°.

The acid (X*a*), 0.3 g, was kept at 260° until the evolution of carbon dioxide had ceased. The remaining brown oil, 0.2 g, was dissolved in 2 ml of ethanol and the solution was added to a solution of 0.4 g of picric acid in 10 ml of ethanol. On the following day 0.4 g of yellow, rod-shaped prisms had separated, m.p. 164°–165° alone and also on admixture with the picrate described above. The two compounds were combined, 1.3 g, and were recrystallized from 8 ml of ethanol, giving 1.1 g of yellow, rod-shaped prisms with unchanged m.p., according to analyses consisting of the picrate of 3-methylthio-5-methyl-pyrazole (XI*a*).

For $C_5H_8N_2S$, $C_6H_3O_7N_3$ (357.30)
calc.: C 37.0 H 3.10 N 19.60 S 8.97 %, equiv. w.: 357,
found: C 36.8 H 3.04 N 19.57 S 8.99 %, equiv. w.: 356.

b. Ethyl 3-ethylthio-5-methyl-pyrazole-4-carboxylate

A solution of 3.3 g of ethyl α-chloroacetoacetate in 10 ml of ethanol was added to a solution of 2.7 g of ethyldithiocarbhydrazide (5) in 10 ml of ethanol. The clear, yellow solution soon turned red, and after some minutes the temperature rose to about 70°. The solution was cooled under the tap, and within an hour it became turbid. On the following day 0.8 g of a yellow, amorphous mass had separated, containing about 70 % of sulphur, and when the filtrate was evaporated to dryness a residue of 4.7 g of yellow hairs was obtained, m.p. 143°–146° (after some sintering). From this product 4.5 g was recrystallized from 25 ml of benzene, giving 2.5 g of colourless hairs with unchanged m.p. According to analyses the product was the hydrochloride of ethyl 3-ethylthio-5-methyl-pyrazole-4-carboxylate (V*c*).

For $C_9H_{14}O_2N_2S$, HCl (250.74)
calc.: Cl 14.14 %, equiv. w.: 250.7
found: Cl 14.15 %, equiv. w.: 252.0.

When a solution of 1.3 g of the hydrochloride in 5 ml of ethanol was poured into 50 ml of water, an oil was obtained, which soon solidified to 1.1 g of a colourless crystal mass, m.p. 90°–91° alone and also on admixture with the pure pyrazole (V*b*) (5).

The picrate of the previously (5) described 3-ethylthio-5-methyl-pyrazole (XI*b*) was prepared in the following way. A solution of 0.4 g of the pyrazole in 5 ml of ethanol was added to a solution of 0.6 g of picric acid in 5 ml of ethanol. On the following day the mixture had deposited 0.7 g of yellow, rod-shaped prisms, m.p. 130°–131°. The product was recrystallized from 4 ml of ethanol and gave 0.6 g of yellow, rod-shaped prisms, m.p. 132°–133°.

For $C_6H_{10}N_2S$, $C_6H_3O_7N_3$ (371.32)
calc.: C 38.8 H 3.53 N 18.86 S 8.63 %, equiv. w.: 371,
found: C 38.7* H 3.49* N 19.00* S 8.50* %, equiv. w.: 376.

c. *Ethyl acetoacetate benzyldithiocarbhydrazone and ethyl 3-benzylthio-5-methyl-pyrazole-4-carboxylate*

A solution of 6.5 g of ethyl acetoacetate in 30 ml of ethanol was added to a solution of 10 g of benzyldithiocarbhydrazide in 50 ml of *N*-NaOH and 50 ml of ethanol. On the following day the clear, yellow solution was acidified with 25 ml of 2 *N*-HCl and deposited an oil, which presently solidified to 15.0 g of a yellow-brown crystal mass, m.p. 66°–67° (after some sintering). From this product 3.1 g was recrystallized from a mixture of 10 ml of benzene and 30 ml of ligroin (b.p. 80°–100°) and gave 1.7 g of colourless flakes, m.p. 69.5°–70°, according to analyses consisting of ethyl acetoacetate benzyldithiocarbhydrazone (VII*b*).

For $C_{14}H_{18}O_2N_2S_2$ (310.42)
calc.: C 54.2 H 5.84 N 9.03 S 20.7 %,
found: C 54.0 H 5.85 N 9.00 S 20.6 %.

A solution of 5.2 g of iodine in 75 ml of ethanol was added to a solution of 6.2 g of the hydrazone (VII*b*) in 125 ml of ethanol. On the following day 1.5 g of a yellow, amorphous mass had separated, melting between 60° and 110°. It contained about 40 % of sulphur. When 750 ml of water was added to the filtrate, 4.9 g of yellow-brown flakes separated, m.p. 121°–123°. The product was recrystallized twice from 40 and 20 ml of benzene and gave 3.3 g of colourless flakes, m.p. 126°–127°.

A solution of 3.6 g of pyridinium tribromide in 40 ml of ethanol was added to a solution of 3.1 g of the hydrazone (VII*b*) in 50 ml of ethanol. A turbid mixture resulted, which on the following day had deposited 1.9 g of a yellow, amorphous mass, melting between 60°–115° and containing 38 % of sulphur. The filtrate was precipitated with 500 ml of water and deposited 1.0 g of yellow flakes, m.p. 118°–121° (after sintering). The product was recrystallized from 5 ml of benzene and gave 0.8 g of colourless flakes, m.p. 126°–127°.

The products with m.p. 126°–127° were collected, 4.1 g, and were recrystallized from 25 ml of benzene. The yield was 3.7 g of colourless flakes, m.p. 126.5°–127°.

According to analyses the product was ethyl 3-benzylthio-5-methyl-pyrazole-4-carboxylate (V*c*).

For $C_{14}H_{16}O_2N_2S$ (276.35)
calc.: C 60.8 H 5.84 N 10.14 S 11.60 %,
found: C 61.0 H 5.81 N 10.09 S 11.58 %.

A solution of 2.1 g of ethyl α-bromoacetoacetate in 10 ml of ethanol was added to a solution of 2.0 g of benzyldithiocarbhydrazide in 20 ml of ethanol. The temperature rose to about 40°, and the resulting clear, brown solution soon became turbid. On the following day 0.6 g of a sticky, yellow mass had separated, and the filtrate was precipitated with water to deposit an oil, which on seeding with the pyrazole (V*c*) solidified to a yellow crystal mass, 2.4 g with m.p. 122°–123°. The product was recrystallized from 15 ml of benzene and gave 2.0 g of colourless flakes, m.p. 126°–127° alone and also on admixture with the pyrazole (V*c*). It contained 11.55 % of sulphur.

The same yield was obtained when the bromo ester was replaced by ethyl α-chloroacetoacetate. If this reaction was performed in benzene solution, the hydrochloride of the pyrazole (V*c*) was obtained. Ethyl α-chloroacetoacetate, 1.7 g, was added to a solution of 2.0 g of benzyldithiocarbhydrazide in 30 ml of hot benzene. After some hours the mixture began to deposit crystals, and on the following day 2.0 g of colourless hairs had separated, m.p. 158°–162° (after some sintering). The product had to be washed with carbon disulphide to remove a yellow impurity.

For $C_{14}H_{16}O_2N_2S$, HCl (312.81)
calc.: Cl 11.33 %, equiv. w.: 312.8
found: Cl 11.40 %, equiv. w.: 311.4.

When the hydrochloride was dissolved in ethanol and the solution was poured into much water, the pyrazole (V*c*) was obtained in a quantitative yield.

A solution of 1.7 g of ethyl α-chloroacetoacetate in 5 ml of ethanol was added to a solution of 2.0 g of benzyldithiocarbhydrazide in 30 ml of 0.33 *N* ethanolic ammonia. The clear, yellow mixture soon turned red and became turbid, and on the following day 0.3 g of pale yellow, rod-shaped prisms had separated, m.p. 118°–119° alone and also on admixture with pure sulphur. From the filtrate 2.5 g of yellow flakes, m.p. 118°–121°, was precipitated with 100 ml of water. The product was recrystallized twice from 15 and 10 ml of benzene and gave 1.5 g of colourless flakes, m.p. 126.5°–127° alone and also on admixture with the pyrazole (V*c*). The product contained 11.57* % of sulphur.

Ethanolic *N*-NaOH, 5 ml, was added to a solution of 0.7 g of benzyl chloride and 1.1 g of ethyl 2-mercapto-5-methyl-1,3,4,4H-thiadiazine-6-carboxylate (IX), (3) in 10 ml of ethanol. The mixture immediately turned red, and after a quarter of an hour it became turbid and began to deposit crystals. On the following day 0.11 g of pale yellow, rod-shaped prisms had separated, m.p. 119°–120° alone and also on admixture with pure sulphur. The filtrate was evaporated to dryness, and the sticky residue was recrystallized twice from 4 ml of toluene. The yield was 0.9 g of colourless flakes, m.p. 126°–127° alone and also on admixture with ethyl 3-benzylthio-5-methyl-pyrazole-4-carboxylate (V*c*).

For $C_{14}H_{16}O_2N_2S$ (276.34)
calc.: N 10.14 S 11.60 %,
found: N 10.10 S 11.53* %.

A hydrolysis experiment was performed in the following way. A solution of 5.5 g of the ester in 30 ml of ethanol and 30 ml of *N*-NaOH was refluxed for 6 hours. Then the ethanol was distilled off, and after cooling some separated oil was taken up in 30 ml of ether. The alkaline solution was acidified and deposited a white crystal powder under a considerable evolution of carbon dioxide. The product, 3.2 g, m.p. 242°–243° (decomp.), was very slightly soluble in all common solvents. It was dissolved in 20 ml of *N*-NaOH, 50 ml of ethanol was added and the solution was acidified with 5 ml of 5 *N*-HCl in 25 ml of ethanol. The mixture then deposited 2.8 g of a colourless crystal powder, m.p. 244°–245° (decomp.). According to analyses the product was 3-benzylthio-5-methyl-pyrazole-4-carboxylic acid (X*c*).

For $C_{12}H_{12}O_2N_2S$ (248.30)
calc.: C 58.0 H 4.87 N 11.28 S 12.91 %, equiv. w.: 248.3,
found: C 57.8 H 4.90 N 11.28 S 12.86 %, equiv. w.: 247.9.

The ether extract from the alkaline solution was evaporated and gave 0.8 g of a colourless oil as a residue. The oil did not crystallize when seeded with the starting material, and it was dissolved in 5 ml of ethanol, and a solution of 0.7 g of picric acid in 20 ml of ethanol was added. On scratching, the solution began to deposit yellow flakes, and on the following day 0.9 g had separated, m.p. 144°–145°. The product was recrystallized from 5 ml of ethanol and gave 0.7 g of yellow flakes, m.p. 144.5°–145.5° (prod. 1).

The acid (X*c*), 1.9 g, was kept at 250° until the evolution of carbon dioxide had ceased. The remaining brown oil, 1.7 g, was dissolved in 5 ml of ethanol, and a solution of 2.0 g of picric acid in 50 ml of ethanol was added. On the following day 3.4 g of yellow flakes had separated, m.p. 144°–145° alone and also on admixture with prod. 1. The new product was recrystallized from 20 ml of ethanol and gave 2.8 g of yellow flakes, m.p. 145°–145.5° (prod. 2). According to analyses both products consist of the picrate of 3-benzylthio-5-methyl-pyrazole (XI*c*).

For $C_{11}H_{12}N_2S$, $C_6H_3O_7N_3$ (433.39)
calc.: C 47.1 H 3.49 N 16.16 S 7.40 %, equiv. w.: 433,
found: C 47.2[1] H 3.48[1] N 16.19[2] S 7.41[2] %, equiv. w.: 431[1].

[1] Prod. 1. [2] Prod. 2.

d. Ethyl 3-carboxymethylthio-5-methyl-pyrazole-4-carboxylate

Monochloroacetic acid, 2.8 g, was neutralized against phenolphthalein with 30.1 ml of *N*-NaOH and added to a solution of 4.4 g of ethyl 2-mercapto-5-methyl-1,3, 4,4H-thiadiazine-6-carboxylate (IX), (3) in 20 ml of ethanol. On the addition of 20 ml of *N*-NaOH the mixture turned dark red, and within a few minutes it became turbid and began to deposit a pale yellow crystal powder. On the following day 0.60 g of this had formed, m.p. 119°–120° alone and also on admixture with pure sulphur. The pale yellow filtrate was acidified with 6 ml of 5 *N*-HCl and deposited 4.5 g of colourless, rectangular plates, m.p. 179°–180°. The product was most conveniently purified by aid of its potassium salt. The acid, 3.7 g, was dissolved in 25 ml of ethanol, 25 ml of ether was added and then 30 ml of 0.5 *N* ethanolic KOH. The mixture immediately solidified to a cake of colourless, rod-shaped prisms, 4.2 g of m.p. 214°–216° (decomp.). This product was recrystallized from 50 ml of ethanol and gave 3.4 g of colourless, rod-shaped prisms, m.p. 217°–218° (decomp.). According to analyses the salt contained one molecule of ethanol of crystallization.

For $C_9H_{11}O_4N_2SK$, C_2H_6O (328.43)
calc.: K 11.90 C_2H_6O 14.03 %,
found: K 12.00 C_2H_6O 13.98[1] %.

[1] Loss of weight at 140°.

From this salt 2.9 g was dissolved in 20 ml of hot 50 % aqueous ethanol and 2 ml of 5 *N*-HCl was added. On cooling, the mixture deposited 1.9 g of colourless, rectangular plates, m.p. 182°–183°. According to analyses the product was ethyl 3-carboxymethylthio-5-methyl-pyrazole-4-carboxylate (V*d*).

For $C_9H_{12}O_4N_2S$ (244.27)

calc.:	C 44.3	H 4.95	N 11.47	S 13.12 %,	equiv. w.: 244.3,
found:	C 44.3*	H 4.94*	N 11.50	S 13.05* %,	equiv. w.: 244.8.

From this product 1.2 g was dissolved in 12 ml of *N*-NaOH, and the solution was heated in a water bath for four hours. When the solution was acidified with 5 ml of 2 *N*-HCl, it deposited 0.8 g of a colourless crystal powder, m.p. 215°–216° (decomp.). This acid was recrystallized from 70 ml of water and gave 0.6 g of long, colourless plates, m.p. 222°–223° (decomp.). According to analyses it was 3-carboxymethylthio-5-methyl-pyrazole-4-carboxylic acid (X*d*).

For $C_7H_8O_4N_2S$ (216.21)

calc.:	C 38.9	H 3.73	N 12.96	S 14.83 %,	equiv. w.: 108.1,
found:	C 38.6	H 3.78	N 12.99	S 14.84* %,	equiv. w.: 108.5.

From this acid 0.22 g was kept at 220° until the evolution of carbon dioxide had ceased. After cooling, the tarry, brown residue was rubbed with 5 ml og 0.5 *N*-NaOH, but most of it remained undissolved. The alkaline filtrate was acidified with 3 ml of *N*-HCl and deposited 0.03 g of a grey crystal powder, m.p. 205°–210° (decomp.), equiv. w. 120. It obviously consisted of unchanged starting material.

e. *Ethyl 3-[β-carboxyethylthio]-5-methyl-pyrazole-4-carboxylate*

A solution of 5.0 g of ethyl α-chloroacetoacetate in 15 ml of ethanol was added to a solution of 5.7 g of β-carboxyethyldithiocarbhydrazide (4, 6) in 30 ml of ethanol. The clear, yellow solution soon turned red, and after some hours it became turbid. On the following day 1.3 g of a red-yellow, amorphous mass had separated, containing about 70 % of sulphur. It was extracted with 10 ml of boiling toluene and filtered from a sticky residue. On cooling, the toluene solution deposited 0.3 g of yellow, irregular prisms, m.p. 114°–116°. The product was recrystallized from 5 ml of benzene and gave 0.2 g of long, yellow prisms, m.p. 119°–120° alone and also on admixture with pure sulphur.

The filtrate from the amorphous mass was poured into 150 ml of 0.5 *N*-NaOH. A small amount of sticky material was filtered off, and the filtrate was acidified with 15 ml of 5 *N*-HCl. The result was 6.4 g of colourless, felted hairs, m.p. 165°–166°. The product was recrystallized from 30 ml of absolute ethanol and gave 5.5 g of colourless, felted hairs, m.p. 167°–168°, according to analyses consisting of ethyl 3-[β-carboxyethylthio]-5-methyl-pyrazole-4-carboxylate (V*e*).

For $C_{10}H_{14}O_4N_2S$ (258.29)
calc.: C 46.5 H 5.46 N 10.85 S 12.41 %, e quiv. w.: 258.3,
found: C 46.6* H 5.63* N 10.92 S 12.27* %, equiv. w.: 257.8.

For the hydrolysis experiments described later it was desirable to prepare the potassium salt of this acid. A solution of 1.3 g of the acid in 10 ml of ethanol and 25 ml of ether was mixed with 10 ml of 0.5 *N* ethanolic KOH. The mixture immediately stiffened to a mass of colourless flakes, 1.5 g with m.p. 212°–214° (decomp.), which was recrystallized from 20 ml of ethanol and gave 1.3 g of colourless, glistening plates, m.p. 215°–216° (decomp.).

For $C_{10}H_{13}O_4N_2SK$ (296.38) calc.: K 13.19 %,
found: K 13.16 %.

A solution of 2.6 g of the pyrazole ester (V*e*) in 30 ml of *N*-NaOH was heated in a water bath for four hours. After cooling, the clear solution was acidified with 15 ml of 3 *N*-HCl and deposited 1.5 g of a colourless crystal powder, m.p. 204°–205° (decomp.). The acid was dissolved in 10 ml of *N*-NaOH and 30 ml of ethanol, and then 2 ml of 5 *N*-HCl in 10 ml of ethanol was added. The yield was 1.0 g of colourless, rod-shaped prisms, m.p. 213°–214° (decomp.), according to analyses consisting of 3-[β-carboxyethylthio]-5-methyl-pyrazole-4-carboxylic acid (X*e*).

For $C_8H_{10}O_4N_2S$ (230.24)
calc.: C 41.7 H 4.38 N 12.17 S 13.92 %, equiv. w.: 115.1,
found: C 41.5* H 4.46* N 12.20 S 13.99* %, equiv. w.: 114.0.

When 0.5 g of this acid was kept at 220° until the evolution of carbon dioxide had ceased, a colourless oil was obtained, which, on cooling and scratching, solidified to a somewhat sticky crystal mass. This was dissolved in 2.5 ml of *N*-NaOH and 3 ml of ethanol, and 2.5 ml of *N*-HCl was added. The yield was 0.2 g of colourless, rod-shaped prisms, m.p. 134°–135°, according to analyses consisting of 3-[β-carboxyethylthio]-5-methyl-pyrazole (XI*e*).

For $C_7H_{10}O_2N_2S$ (186.23)
calc.: C 45.1 H 5.41 N 15.04 S 17.22 %, equiv. w.: 186.2,
found: C 45.2* H 5.56* N 15.08 S 17.07* %. equiv. w.: 185.2.

f. Ethyl 1-phenyl-3-methylthio-5-methyl-pyrazole-4-carboxylate

A solution of 1.7 g of ethyl α-chloroacetoacetate in 5 ml of ethanol was added to a solution of 2.0 g of 1-phenyl-methyldithiocarbhydrazide (I), (7) in 30 ml of 0.33 *N* ethanolic ammonia. The clear, yellow solution soon turned red, and after some hours a precipitate was formed. When this had settled, it was collected and found to consist of 0.15 g of ammonium chloride. On the following day the mixture had separated 0.3 g of long, yellow prisms, m.p. 116°–118° alone and 118°–119° on admixture with pure sulphur. The filtrate was evaporated to about 15 ml volume, when 1.7 g of yellow prisms had separated, m.p. 107°–109°. The product was recrystallized from 10 ml of ethanol and gave 1.4 g of pale yellow, oblique plates, m.p. 109°–109.5°. According to analyses the product was ethyl 1-phenyl-3-methylthio-5-methyl-pyrazole-4-carboxylate (XII).

For $C_{14}H_{16}O_2N_2S$ (276.35)
calc.: C 60.8 H 5.84 N 10.14 S 11.60 %,
found: C 60.3* H 5.82* N 10.17 S 11.75* %.

A solution of 2.8 g of the pyrazole (XII) in 50 ml of 0.4 *N* ethanolic KOH was refluxed for eight hours. On cooling, the solution deposited 3.0 g of colourless flakes, m.p. 301°–303°.

For $C_{12}H_{11}O_2N_2SK$, 0.2 C_2H_6O (295.61)
calc.: K 13.23 C_2H_6O 3.12 %,
found: K 13.15 C_2H_6O 2.92[1] %.

[1] Loss of weight at 120°.

A solution of 2.6 g of the potassium salt in 20 ml of lukewarm water was acidified with 2 ml of 5 *N*-HCl in 20 ml of ethanol. The mixture then deposited 1.9 g of colourless, needle-shaped prisms, m.p. 214°–216° (decomp.), which on recrystallization from 30 ml of ethanol afforded 1.4 g of colourles needles, m.p. 215°–216° (decomp.). According to analyses the product was 1-phenyl-3-methylthio-5-methyl-pyrazole-4-carboxylic acid.

For $C_{12}H_{12}O_2N_2S$ (248.30)
calc.: C 58.0 H 4.87 N 11.28 S 12.91 %, equiv. w.: 248.3,
found: C 58.1* H 4.97* N 11.23 S 12.82* %, equiv. w.: 246.6.

A 0.6 g sample of this acid was kept at 230° until the evolution of carbon dioxide had ceased. The remaining brown oil was taken up in 10 ml of ether, and the ether solution was extracted with 5 ml of 0.5 *N*-NaOH. On acidification with 1.5 ml of 2 *N*-HCl the alkaline extract deposited 0.2 g of a white crystal powder, m.p. 214°–215° (decomp.), equiv. w.: 250, obviously consisting of unchanged starting material. The ether solution was evaporated, and 0.3 g of a brown oil was obtained as a residue. This was dissolved in 2 ml of glacial acetic acid, and 0.5 ml of 30 % hydrogen peroxide was added. The solution remained unchanged for two days, and when the solvent was evaporated on a water bath, a brown oil was obtained as a residue. This oil was dissolved in 2 ml of ethanol, and on the addition of 3 ml of water an oil was precipitated, which slowly solidified to 0.2 g of a brown crystal mass, m.p. 103°–105°. This product was recrystallized from 25 ml of ligroin (b.p. 80°–100°) and afforded 0.15 g of colourless, pointed, rod-shaped prisms, m.p. 107°–108°. According to analyses the product was 1-phenyl-3-methylsulphonyl-5-methyl-pyrazole.

For $C_{11}H_{12}O_2N_2S$ (236.29)
calc.: C 55.9 H 5.12 N 11.86 S 13.57 %,
found: C 56.2* H 5.01* N 11.86* S 13.86* %.

For this sulphone MICHAELIS (8) reports m.p. 105°.

g. Ethyl 3-phenyl-5-methyl-pyrazole-4-carboxylate

A solution of 8.2 g of ethyl α-chloroacetoacetate in 20 ml of ethanol was added to a solution of 7.6 g of thiobenzhydrazide (9) in 50 ml of ethanol and 50 ml of *N*-NaOH. The mixture soon became red and turbid, and on the following day a red oil had separated. A further amount of oil was precipitated on the addition of 200 ml of water.

The mixture was extracted with 150 ml of ether, and an undissolved residue of 1.3 g of yellow, irregular prisms was collected, m.p. 116°–118°. This product was recrystallized from 13 ml of toluene and gave 0.9 g of yellow, oblique prisms, m.p. 119°–120° alone and also on admixture with pure sulphur. A sulphur analysis gave 100 % of sulphur.

The ether solution was evaporated and gave 10.5 g of a pale yellow, highly viscous oil. This was dissolved in 30 ml of absolute ethanol and 30 ml of ether, and 10 ml of 8 *N* ethanolic hydrochloric acid was added. The mixture immediately began to deposit crystals, and by the following day 9.0 g of colourless plates had formed, m.p. 155°–160°. According to analyses the product was the hydrochloride of ethyl 3-phenyl-5-methyl-pyrazole-4-carboxylate (V*f*).

For $C_{13}H_{14}O_2N_2$, HCl (266.72)
calc.: Cl 13.29 %, equiv. w.: 266.7,
found: Cl 13.26 %, equiv. w.: 268.0.

This hydrochloride, 5.4 g, was dissolved in 10 ml of ethanol, and 100 ml of water was added. A colourless, highly viscous oil separated, which could not be made to crystallize. It was then taken up in 50 ml of ether, the ether solution was dried with anhydrous sodium sulphate and the ether was distilled off on a water bath. The residue was distilled in vacuum, and between 145° and 150° at 0.5 mm 3.6 g of a colourless, highly viscous oil was obtained, according to analyses consisting of ethyl 3-phenyl-5-methyl-pyrazole-4-carboxylate (V*f*).

For $C_{13}H_{14}O_2N_2$ (230.26)
calc.: C 67.8 H 6.13 N 12.17 %,
found: C 67.6* H 6.31* N 12.34* %.

From this pyrazole 1.5 g was dissolved in 10 ml of ethanol, and 1 ml of formalin was added. The mixture remained clear until the following day, when it was poured into 30 ml of water. An oil separated, which soon solidified to 1.5 g of a colourless crystal mass, m.p. 106°–110° (after some sintering). The product was recrystallized from 10 ml of toluene and gave 1.1 g of colourless, rhombic plates and prisms, m.p. 110°–112°. According to analyses the product was ethyl 1- or 2-hydroxymethyl-3-phenyl-5-methyl-pyrazole-4-carboxylate (XX*b*).

For $C_{14}H_{16}O_3N_2$ (260.29)
calc.: C 64.6 H 6.20 N 10.76 %,
found: C 64.8* H 6.36* N 10.72 %.

A solution of 1.2 g of the pyrazole ester (V*f*) in 15 ml of 0.5 *N* ethanolic KOH was refluxed for 40 hours. Then 10 ml of water was added, the ethanol was distilled off and the separated oil was taken up in 10 ml of ether. The aqueous solution was acidified with 2 ml of 5 *N*-HCl and deposited 0.4 g of a colourless crystal powder, m.p. 255°–258° (decomp.). The product was dissolved in 3 ml of *N*-NaOH and 5 ml of ethanol, and the solution was heated to boiling. On the addition of 2 ml of 2 *N*-HCl in 2 ml of ethanol the mixture began to deposit colourless, rod-shaped prisms. On the following day the yield was 0.2 g with m.p. 262°–262.5° (decomp.). Determination of the equivalent weight showed that the product was 3-phenyl-5-methyl-pyrazole-4-carboxylic acid (X*f*).

For $C_{11}H_{10}O_2N_2$ (202.21) calc.: equiv. w.: 202.2,
found: equiv. w.: 203.0.

A 0.1 g sample of this acid was kept at 270° until the evolution of carbon dioxide had ceased. On cooling, the liquid residue solidified to a somewhat sticky crystal mass. This was dissolved in 1 ml of ethanol and precipitated with 1 ml of water as 0.06 g of colourless, felted hairs, m.p. 128°–128.5°. This product was also obtained when an attempt was made to obtain a better yield of the acid (X*f*) by using a large excess of KOH. A solution of 2.3 g of the pyrazole ester (V*f*) in 50 ml of 2 *N* ethanolic KOH was refluxed for 48 hours. The solution was then poured into 150 ml of water, which caused 1.6 g of colourless, felted hairs to separate, m.p. 126°–127°. The product was recrystallized from 45 ml of 50 % aqueous ethanol and gave 1.4 g of colourless, felted hairs, m.p. 128°–128.5° alone and also on admixture with the product described above. According to analysis the two products consist of 3-phenyl-5-methyl-pyrazole (XI*f*).

For $C_{10}H_{10}N_2$ (158.20) calc.: N 17.71 %,
found: N 17.77 %.

A 0.3 g sample of this pyrazole was dissolved in 5 ml of ethanol, and 5 ml of 8 *N* ethanolic hydrochloric acid was added, which caused 0.2 g of colourless, facetted prisms to separate, according to analyses consisting of the hydrochloride of the pyrazole (XI*f*).

For $C_{10}H_{10}N_2$, HCl (194.66)
calc.: Cl 18.21 %, equiv. w.: 194.7,
found: Cl 18.14 %, equiv. w.: 195.8.

A solution of 0.5 g of picric acid in 3 ml of methanol was added to a solution of 0.3 g of phenyl-methyl-pyrazole in 2 ml of methanol. On the following day the mixture had deposited 0.5 g of yellow, irregular prisms, m.p. 160°–161°.

For $C_{10}H_{10}N_2$, $C_6H_3O_7N_3$ (387.30)
calc.: N 18.08 %, equiv. w: 387,
found: N 18.03 %, equiv. w.: 393.

h. Ethyl 3-ethoxy-5-methyl-pyrazole-4-carboxylate

Ethylxanthogenacetic acid, 19 g, was dissolved in 50 ml of 2 *N*-NaOH, and 5 ml of hydrazine hydrate was added. The solution was turbid and deposited an oil, which on the following day was taken up in 50 ml of ether. The water solution was extracted with a further 50 ml of ether, and the ether solutions were combined and dried with anhydrous sodium sulphate. The ether solution is assumed to contain 0.1 mole of ethylxanthogenhydrazide (13). A solution of 16.5 g of ethyl α-chloroacetoacetate in 30 ml of ethanol was added. The colourless mixture soon turned yellow, and on the following day it had solidified to a cake of 8.0 g of colourless hairs and a small amount of yellow prisms. The filtrate on the addition of 10 ml of 5 *N* ethanolic hydrochloric acid separated a further 3.0 g of colourless hairs. The two products were combined and dissolved in 50 ml of hot absolute ethanol. A residue of pale yellow prisms, 0.4 g, was filtered from the solution. These had a m.p. of 118°–119°, undepressed on admixture with pure sulphur. To the ethanolic solution a mixture of 20 ml of 5 *N* ethanolic hydrochloric acid and 100 ml of ether was added, and 9.5 g of colourless, felted hairs separated, m.p. 161°–162°. According to analyses it was the hydrochloride of ethyl 3-ethoxy-5-methyl-pyrazole-4-carboxylate (V*g*) with one mole of ethanol of crystallization.

For $C_9H_{14}O_3N_2$, HCl, C_2H_6O (280.75)
calc.: Cl 12.63 C_2H_6O 16.41 %, equiv. w.: 280.8,
found: Cl 12.58 C_2H_6O 16.30[1] %, equiv. w.: 279.8.

[1] Loss of weight at 120°.

A portion of this salt, 2.8 g, was dissolved in 5 ml of hot ethanol, and 25 ml of hot water was added. On cooling, 2.0 g of colourless, large, pointed prisms separated, melting between 60° and 80°. According to analyses it was the monohydrate of the pyrazole (V*g*).

For $C_9H_{14}O_3N_2$, H_2O (216.24)
calc.: C 50.0 H 7.46 H_2O 8.33 %,
found: C 49.8* H 7.51* H_2O 8.26[1].

[1] Loss of weight in vacuum over phosphorus pentoxide.

The water-free substance had m.p. 96°–97°. If a supersaturated solution of the hydrate in aqueous ethanol was seeded with the anhydrous pyrazole, the latter separated out.

For $C_9H_{14}O_3N_2$ (198.22)
calc.: C 54.5 H 7.12 N 14.13 %,
found: C 54.4* H 7.26* N 14.17 %.

When attempts were made to hydrolyse this pyrazole ester with aqueous or ethanolic alkali, oils and sometimes water-soluble, semisolid products were obtained, which were neutral to phenolphthalein. It may be a matter of interest to establish their constitution, but it was found to be too time-consuming to be incorporated into the present investigation.

i. Ethyl 3-benzylthio-pyrazole-4-carboxylate

A solution of 2.8 g of ethyl α-chloro-α-formylacetate (XIII), (18) in 10 ml of ethanol was added to a solution of 4.0 g of benzyldithiocarbhydrazide in 30 ml of ethanol. A clear, yellow mixture was obtained, which soon became red and turbid. On the following day 0.8 g of a red, sticky mass had separated, containing 74 % of sulphur. The filtrate was poured into 400 ml of water and deposited 4.8 g of pale yellow, felted hairs, m.p. 100°–105°. The product was recrystallized twice from 25 ml of toluene and gave 3.4 g of colourless flakes, m.p. 118°–119°. According to analyses the product was ethyl 3-benzylthio-pyrazole-4-carboxylate (XIV).

For $C_{13}H_{14}O_2N_2S$ (262.32)
calc.: C 59.5 H 5.38 N 10.68 S 12.22 %,
found: C 59.7* H 5.43* N 10.58* S 12.14* %.

A solution of 1.3 g of this ester in 20 ml of 0.5 *N* ethanolic KOH was refluxed for five hours, when 10 ml of water was added and the ethanol was distilled off. On acidification the mixture deposited 0.8 g of a colourless crystal powder, m.p. 257°–259° (decomp.). The acid was dissolved in 5 ml of N-NaOH, filtered and heated to boiling with 5 ml of ethanol. On the addition of 1 ml of 5 N-HCl in 2 ml of ethanol the mixture deposited 0.7 g of colourless, rectangular plates, m.p. 260°–261° (decomp.) According to analyses the product was 3-benzylthio-pyrazole-4-carboxylic acid.

For $C_{11}H_{10}0_2N_2S$ (234.27)
calc.: C 56.4 H 4.30 N 11.96 S 13.68 %, equiv. w.: 234.3,
found: C 56.4* H 4.46* N 11.99 S 13.59* %, equiv. w.: 233.9.

A portion of this acid, 0.4 g, was kept at 270° until the evolution of gas had ceased. The remaining brown oil could not be made to crystallize. It was then taken up in 5 ml of ether and the solution was extracted with 3 ml of N-NaOH. The ether solution was then added to a solution of 0.4 g of picric acid in 4 ml of methanol. The solution was heated on a water bath until the ether had evaporated. On cooling, the mixture deposited 0.4 g of yellow plates, m.p. 109°–110°. The product was recrystallized from 3 ml of ethanol and gave 0.3 g of yellow plates, m.p. 110°–111°. According to analyses the product was the picrate of 3-benzylthio-pyrazole.

For $C_{10}H_{10}N_2S$, $C_6H_3O_7N_3$ (419.36)
calc.: C 45.8 H 3.12 N 16.70 S 7.64 %, equiv. w.: 419,
found: C 45.7* H 3.20* N 16.62 S 7.60* %, equiv. w.: 423.

k. Comparative hydrolysis experiments with ethyl pyrazole-4-carboxylates

In order to obtain an idea of the influence of the substituents on the rate of hydrolysis of the different pyrazole esters now described, they were subjected to hydrolysis under identical conditions, and the degree of hydrolysis was then used as a measure of the rate of hydrolysis. Two millimoles of each ester was refluxed for two hours with 10.0 ml of 0.5 N ethanolic KOH, and then 10.0 ml of 0.5 N-HCl was added. The degree of hydrolysis was determined by back-titrating with 0.1 N-NaOH against phenolphthalein, after applying a correction from a blank. The following results were obtained.

Ethyl pyrazole-4-carboxylate	Degree of hydrolysis %
3-phenyl-5-methyl-	4
3-methylthio-5-methyl-	7
3-ethylthio-5-methyl-	7
3-benzylthio-5-methyl-	7
3-ethoxy-5-methyl-	7
3-benzylthio-	57
3-carboxymethylthio-5-methyl-[1]	72
3-[β-carboxyethylthio]-5-methyl-[1]	78
1-phenyl-3-methylthio-5-methyl-	90

---

[1] As potassium salt.

C. 4-Acetyl-pyrazoles

a. 3-Benzylthio-4-acetyl-5-methyl-pyrazole

A solution of 1.7 g of 3-chloroacetylacetone (19) in 5 ml of ethanol was added to a solution of 2.0 g of benzyldithiocarbhydrazide in 10 ml of *N* ethanolic ammonia. The temperature rose to about 50°, and the mixture immediately turned red and began to deposit ammonium chloride. This was filtered off, and after some hours the mixture became turbid. On the following day 1.8 g of a yellow-brown, sticky crystal mass had separated, melting between 145° and 155°. The product was extracted with 40 ml of boiling ethanol and left an undissolved residue of 0.1 g of a yellow crystal powder, m.p. 118°–119° alone and 119°–120° on admixture with pure sulphur. The ethanol solution was evaporated to dryness and the residue was recrystallized twice from 15 ml of toluene. The yield was 0.8 g of pale yellow, rod-shaped prisms, m.p. 169°–170°. According to analyses the product was 3-benzylthio-4-acetyl-5-methyl-pyrazole (XV).

For $C_{13}H_{14}ON_2S$ (246.32)
calc.: C 63.4 H 5.73 N 11.37 S 13.02 %,
found: C 63.5* H 5.78* N 11.34 S 13.11* %.

A solution of 0.25 g of this pyrazole in 10 ml of ethanol was added to a solution of 0.20 g of 2,4-dinitrophenylhydrazine in 3 ml of 10 *N* ethanolic hydrochloric acid and 5 ml of water. A clear, red solution was obtained, which rapidly stiffened to a porridge of red needles. The yield was 0.40 g with m.p. 227°–228°. The product was recrystallized from 70 ml of toluene and gave 0.28 g of red flakes with unchanged m.p. According to analyses the product was 3-benzylthio-4-acetyl-5-methyl-pyrazole 2,4-dinitrophenylhydrazone.

For $C_{19}H_{18}O_4N_6S$ (426.44)
calc.: C 53.5 H 4.25 N 19.71 S 7.52 %,
found: C 53.8* H 4.43* N 19.65 S 7.38* %.

b. 1-Phenyl-3-methylthio-4-acetyl-5-methyl-pyrazole

A solution of 1.7 g of 3-chloroacetylacetone in 5 ml of ethanol was added to a solution of 2.0 g of 1-phenyl-methyldithiocarbhydrazide (I), (7) in 10 ml of *N* ethanolic ammonia. The temperature rose to about 50°, and the mixture immediately turned red and deposited a small amount of ammonium chloride. After some hours the filtered solution was turbid and yellow, and on the following day 2.5 g of a red-yellow crystal powder had separated, m.p. 144°–150° (after sintering). The product was extracted with 35 ml of boiling ethanol, and 0.1 g of a yellow crystal powder remained undissolved, m.p. 117°–119° alone and 118°–119° on admixture with pure sulphur. On cooling, the ethanolic solution deposited 2.0 g of pale yellow, rod-shaped prisms, m.p. 147°–150° (after sintering). This product was recrystallized from 10 ml of toluene and gave 1.6 g of colourless, long plates, m.p. 152°–153°. A further recrystallization from toluene did not change the m.p. According to analyses the product was 1-phenyl-3-methylthio-4-acetyl-5-methyl-pyrazole (XVI).

For $C_{13}H_{14}ON_2S$ (246.32)
calc.: C 63.4 H 5.73 N 11.37 S 13.02 %,
found: C 63.4* H 5.68* N 11.42 S 12.97* %.

A solution of 0.25 g of this pyrazole in 10 ml of ethanol was added to a solution of 0.20 g of 2,4-dinitrophenylhydrazine in 3 ml of 10 *N* ethanolic hydrochloric acid and 5 ml of water. A clear, red solution resulted, which after some minutes stiffened to a porridge of red needles. The yield was 0.38 g with m.p. 219°–220°. The product was recrystallized from 60 ml of toluene and gave 0.38 g of dark-red, irregular prisms of unchanged m.p. According to analyses it was 1-phenyl-3-methylthio-4-acetyl-5-methyl-pyrazole 2,4-dinitrophenylhydrazone with 0.6 mole of toluene of crystallization.

For $C_{19}H_{18}O_4N_6S$, 0.6 C_7H_8 (481.72)
calc.: C 57.8 H 4.77 N 17.45 S 6.66 C_7H_8 11.48 %,
found: C 58.2* H 5.00* N 17.51 S 6.58* C_7H_8 11.52[1] %.

[1] Loss of weight at 200°.

D. Experiments with ethyl α-methylacetoacetate and ethyl α-chloro-α-methylacetoacetate

A solution of 1.5 g of ethyl α-methylacetoacetate in 3 ml of ethanol was added to a solution of 1.3 g of methyldithiocarbhydrazide in 5 ml of ethanol. On the following day the clear, colourless mixture was poured into 50 ml of water, which caused a colourless oil to separate. On cooling and scratching it solidified to 2.3 g of a colourless crystal mass, m.p. 58°–60°. The product was dissolved in 10 ml of ethanol, the solution was cooled with ice and 10 ml of water was added with simultaneous seeding with the crude product. The yield was 1.7 g of colourless, rod-shaped prisms, m.p. 61°–62°. This product was recrystallized from a mixture of 3 ml of chloroform and 15 ml of carbon tetrachloride and afforded 1.4 g of colourless, rod-shaped prisms, m.p. 63°–64°. According to analyses the product was ethyl α-methylacetoacetate methyldithiocarbhydrazone (XVIII*a*).

For $C_9H_{16}O_2N_2S_2$ (248.36)
calc.: C 43.5 H 6.49 N 11.28 S 25.8 %,
found: C 43.6* H 6.41* N 11.21 S 25.9* %.

A solution of 5.2 g of iodine (0.04 g-equiv.) in 50 ml of ethanol was added to a solution of 5.0 g (0.02 moles) of the hydrazone (XVIII*a*) in 50 ml of ethanol. A clear, brown solution resulted, which remained unchanged for a week. Then the ethanol was evaporated, and a dark-brown, viscous oil was obtained as residue. This could not be made to crystallize, and no definable product could be extracted from it.

A solution of 1.8 g of ethyl α-chloro-α-methylacetoacetate (20) in 5 ml of ethanol was added to a solution of 1.3 g of methyldithiocarbhydrazide in 5 ml of ethanol. On the following day the clear, pale yellow solution was poured into 100 ml of water, which caused a colourless oil to separate. A sample of this oil was treated with concentrated hydrochloric acid and passed over into a crystal mass. On seeding with this, the main product solidified to 2.5 g of a pale yellow, crystalline mass, m.p. 58°–60°. From this product 0.8 g was dissolved in 5 ml of ethanol, and the solution was cooled with ice. The addition of 1 ml of water caused 0.5 g of pale yellow, rod-shaped prisms to separate, m.p. 59°–60°. According to analyses the product was ethyl α-chloro-α-methylacetoacetate methyldithiocarbhydrazone (XVIII*b*).

For $C_9H_{15}O_2N_2S_2Cl$ (282.81)
calc.: C 38.2 H 5.35 N 9.91 S 22.7 Cl 12.54 %,
found: C 38.1* H 5.52* N 9.96 S 22.9* Cl 12.62 %.

When this reaction was performed with the methyldithiocarbhydrazide dissolved in 10 ml of *N*-NaOH, only sticky products were obtained.

Attempts were made to cyclise the hydrazone (XVIII*b*) with alkali. *N*-NaOH, 10 ml, was added to a solution of 2.8 g of the hydrazone in 10 ml of ethanol. The mixture became red and turbid, and 1.8 g of a pale yellow, sticky mass separated. This could not be made to crystallize. It was dissolved in 25 ml of hot toluene and was filtered from a small amount of sticky material. On cooling, no precipitate was formed, but the addition of 100 ml of petroleum ether (b.p. 40°–60°) caused 0.7 g of a pale yellow crystal powder to separate. It melted between 100° and 120°. A further purification in the same way gave 0.4 g of a pale yellow crystal powder with the same melting range. According to analyses the product consisted of impure ethyl 2-methylthio-5,6-dimethyl-1,3,4,6H-thiadiazine-6-carboxylate (XIX).

For $C_9H_{14}O_2N_2S_2$ (246.34)
calc.: C 43.9 H 5.73 N 11.37 S 26.0 %,
found: C 42.9* H 5.66* N 11.29* S 26.5* %.

This work was started at the Nobel Institute of the Royal Academy of Sciences, Department of Organic Chemistry, in Stockholm and completed at the Department of Organic Chemistry, University of Lund, Lund, Sweden. I wish to express my thanks to Professor Bror Holmberg for his kind help and advice during this work and to Professor Erik Larsson for putting the facilities in Lund at my disposal. I am also indebted to *Doktor P. Håkanssons Stiftelse* for a generous grant.

REFERENCES

1. Bose, P. K., Quart. J. Indian Chem. Soc. *3*, 197 (1926). C. *1927* I, 608.
2. Busch, M. and Starke, M., J. pr. Chem. [2] *93*, 59 (1916).
3. Mathes, R. A., J. Org. Chem. *17*, 877 (1952).
4. Sandström, J., Arkiv Kemi. In press.
5. Sandström, J., Arkiv Kemi *4*, 297 (1952).
6. Mathes, R. A., U.S. Pat. 2,623,059. C. A. *47*, 9352h (1953).
7. Busch, M., Ber. *28*, 2646 (1895).
8. Michaelis, A., Ann. *338*, 298 (1904).
9. Holmberg, B., Arkiv Kemi, Mineral., Geol. *17A*, n:o 23 (1944).
10. Sjollema, B., Ann. *279*, 248 (1894).
11. Posner, Th., Ber. *34*, 3973 (1901).
12. De, S. C. and Dutt, D. N., J. Indian. Chem. Soc. *7*, 473 (1930).
13. Jensen, K. A., Z. anorg. und allgem. Chem. *221*, 15 (1934);
    Wangel, J., Arkiv Kemi *1*, 431 (1949).
14. Buchner, E., Ber. *22*, 2165 (1889).
15. Dvoretsky, I. and Richter, G. H., J. Org. Chem. *15*, 1285 (1950).
16. Brühl, J. W., Ber. *36*, 1722 (1903).
17. Allihn, F., Ber. *11*, 567 (1878).
18. Wislicenus, W., Ber. *43*, 3528 (1910).
19. Combes, A., C. r. *111*, 272 (1899).
20. Schmidt, J. and Aeckerle, E., Ann. *398*, 253 (1913).

Tryckt den 5 december 1955

Uppsala 1955. Almqvist & Wiksells Boktryckeri AB

ARKIV FÖR KEMI Band 8 nr 53

Communicated 25 May 1955 by ARNE FREDGA

The calculation of rate constants for competitive, consecutive reactions

By SIGVARD WIDEQVIST

The problem of calculating the velocity constants for a series of two competitive, consecutive reactions from one single run of measurements has not previously been the subject of a thorough statistical treatment.

Assume that we have the following sequence of second-order reactions:

$$\underset{a-x}{\mathrm{A}} + \underset{b-x-y}{\mathrm{B}} \xrightarrow{k_1} \underset{x-y}{\mathrm{C}} + \underset{x+y}{\mathrm{D}}$$

$$\underset{x-y}{\mathrm{C}} + \underset{b-x-y}{\mathrm{B}} \xrightarrow{k_2} \underset{y}{\mathrm{E}} + \underset{x+y}{\mathrm{D}}$$

Let a be the initial concentration of A and b that of B. At time t we have:

$a-x$ = conc. of A,
$b-x-y$ = conc. of B,
$x-y$ = conc. of the intermediate product C,
$x+y$ = conc. of the by-product D,
y = conc. of the final product E.

Put $x+y=z$. If k_1 and k_2 are the velocity constants for the first and the second reaction, respectively, we get the differential equations

$$dx/dt=k_1(a-x)(b-z), \tag{1}$$

$$dy/dt=k_2(x-y)(b-z). \tag{2}$$

The system of differential equations (1, 2) cannot be integrated. However, as pointed out by the present author [1], it is possible to make a formal reduction of the reaction order: On putting $(b-z)\,dt=d\vartheta$ we get

$$dx/d\vartheta=k_1(a-x), \tag{1 a}$$

$$dy/d\vartheta=k_2(x-y). \tag{2 a}$$

The equation system (1 a, 2 a) which is valid for a first-order reaction is easily integrated. On integration we obtain

$$z=a\left[2-\frac{k_1}{k_1-k_2}e^{-k_2\vartheta}-\frac{k_1-2\,k_2}{k_1-k_2}e^{-k_1\vartheta}\right] \tag{3}$$

where $\vartheta = \int_0^t (b-z)\,dt$. The velocity constant k_2 can be determined by a separate experiment. In spite of that, k_1 cannot be explicitly expressed because of the transcendent part $e^{-k_1\vartheta}$. As previously reported by the author, $e^{-k_1\vartheta}$ may be easily eliminated. Consider the function $z = f(\vartheta)$. The area between the curve and the ϑ-axis is

$$A = \int_0^\vartheta f(\vartheta)\,d\vartheta = \int_0^\vartheta z\,d\vartheta. \tag{4}$$

On combining eq. (3) and (4) and integrating we get

$$A = a\left[2\vartheta + \frac{k_1}{k_2(k_1-k_2)}\,e^{-k_2\vartheta} + \frac{k_1-2k_2}{k_1(k_1-k_2)}\,e^{-k_1\vartheta} - \frac{2k_2+k_1}{k_1 k_2}\right]. \tag{5}$$

On eliminating $e^{-k_1\vartheta}$ between eq. (3) and (5) we get

$$k_1 = \frac{z}{2a\vartheta - A - \dfrac{a}{k_2}(1-e^{-k_2\vartheta})}. \tag{6}$$

A necessary condition for the usefulness of eq. (6) is that the velocity constant k_2 can be separately determined. This is in fact often the case. Sometimes, however, it may be desirable to determine both k_1 and k_2 from one single run of measurements. This is necessary when the intermediate product formed in the first reaction cannot be isolated. For that case a very interesting method of calculation has recently been developed by FROST and SCHWEMER [2]. This method is based on the assumptions that the reactions are of the second order and that the reacting substances are initially present in equivalent amounts.

It is, however, possible to calculate both k_1 and k_2 from eq. (6). From eq. (6) we get

$$A = 2a\vartheta - \frac{a}{k_2}(1-e^{-k_2\vartheta}) - \frac{z}{k_1}. \tag{6 a}$$

Consider the function

$$A = F(\vartheta).$$

The area between the curve and the ϑ-axis is

$$B = \int_0^\vartheta F(\vartheta)\,d\vartheta = \int_0^\vartheta A\,d\vartheta = \iint_0^\vartheta z\,d\vartheta^2. \tag{7}$$

Combining eq. (6 a) and (7) we get

$$B = \int_0^\vartheta \left[2a\vartheta - \frac{a}{k_2}(1-e^{-k_2\vartheta}) - \frac{z}{k_1}\right] d\vartheta. \tag{8}$$

On integration we obtain

$$B = a\vartheta^2 - a\vartheta/k_2 - A/k_1 + a(1 - e^{-k_2\vartheta})/k_2^2. \tag{9}$$

On eliminating $e^{k_2\vartheta}$ between eq. (6 a) and (9) we get after simplification:

$$z = k_1 k_2 (a\vartheta^2 - B) + k_1 (a\vartheta - A) - k_2 A. \tag{10}$$

When k_2 is known we get

$$k_1 = \frac{z + k_2 A}{k_2 (a\vartheta^2 - B) + a\vartheta - A} \tag{10 a}$$

which is a more handy expression than eq. (6). It should be noted that no restrictions are associated with the application of eq. (10) concerning the concentrations of the reactants. Eq. (10) is furthermore valid for both first- and second-order reactions. In a first-order reaction the variable ϑ is identical with time; in a second-order reaction ϑ is the area between the curve $(b - z) = f(t)$ and t-axis, when t is the time. A, B, and ϑ may be evaluated by means of graphical integration, or by the use of Simpson's formula or the trapetzoid formula.

When a series of measurements is available, we may calculate k_1 and k_2 from eq. (10) by means of the method of least squares or the method of averages. It should, however, be mentioned, that it is often impossible to treat eq. (10) as if it had three linear coefficients k_1, k_2, and $k_3 \equiv k_1 k_2$. In this case the system is supplied with an additional degree of freedom with the result that unlikely values of k_1 and k_2 are obtained, and k_3 becomes inconsistent with the product $k_1 k_2$.

The calculation of k_1 and k_2 from eq. (10) is most conveniently performed in the following way:

Put $(a\vartheta - A)/z = p$, $A/z = q$, and $(a\vartheta^2 - B)/z = r$. Then we get on substituting in eq. (10)

$$k_1 p - k_2 q + k_1 k_2 r = 1. \tag{11}$$

Eq. (11) is treated by the method of least squares. Thus we have

$$F = \Sigma (k_1 p - k_2 q + k_1 k_2 r - 1)^2, \tag{12}$$

$$\partial F/\partial k_1 = 2\,\Sigma\,[(k_1 p - k_2 q + k_1 k_2 r - 1)\,(k_2 r + p)], \tag{13}$$

$$\partial F/\partial k_2 = 2\,\Sigma\,[(k_1 p - k_2 q + k_1 k_2 r - 1)\,(k_1 r - q)]. \tag{14}$$

On putting $\partial F/\partial k_1$ and $\partial F/\partial k_2 = 0$ we get

$$k_1 = \frac{\Sigma p + k_2 (\Sigma pq + \Sigma r) + k_2^2 \Sigma qr}{\Sigma p^2 + 2 k_2 \Sigma pr + k_2^2 \Sigma r^2} \tag{15}$$

and

$$k_2 = \frac{\Sigma q - k_1 (\Sigma pq + \Sigma r) + k_1^2 \Sigma pr}{2 k_1 \Sigma qr - k_1^2 \Sigma r^2 - \Sigma q^2} \tag{16}$$

If we know an approximate value of k_2 we can obtain a value of k_1 from eq. (15). By means of this value we can get a new and better value of k_2 from eq. (16) and so on, until constant values of k_1 and k_2 are obtained. The first approximate values of k_1 and k_2 are obtained directly from eq. (11) by means of the method of averages: Regard a series of equations

$$k_1 p_i - k_2 q_i + k_1 k_2 r_i = 1 \tag{11 a}$$

where $i = 1, 2, 3, \ldots 2n$. On adding the first n equations in one group and the last n equations in another group we get

$$k_1 \sum_1^n p_i - k_2 \sum_1^n q_i + k_1 k_2 \sum_1^n r_i = n, \tag{11 b}$$

$$k_1 \sum_{n+1}^{2n} p_i - k_2 \sum_{n+1}^{2n} q_i + k_1 k_2 \sum_{n+1}^{2n} r_i = n. \tag{11 c}$$

That the solution of the equation system (11 b, 11 c) does not give the definitive velocity constants is apparent, as different grouping of the data will lead to different resulting values k_1 and k_2. From eq. (15) and (16) we obtain a unique solution. There is, however, no use in solving this system directly, as an elimination of k_1 or k_2 would lead to very cumbersome expressions of the fourth degree.

The theoretical results obtained above were tested against the data of FROST and SCHWEMER [2] for the alkaline saponification of diethyl adipate in dioxane-water-potassium chloride solution at 25°. The results are shown in Table 1. A, B, and ϑ were calculated by means of the trapetzoid formula.

From the data in Table 1 the approximate valocity constants $k_1 = 0.08502$ and $k_2 = 0.03013$ are obtained by means of the equations (11 b) and (11 c).

Table 1. The saponification of diethyl adipate with sodium hydroxide. [Ester] $= a = 0.00498$; [Alkali] $= b = 0.00996$. (From the data of FROST and SCHWEMER [2].)

$t_{\text{sec.}}$	z	ϑ	A	B	k_1
165	0.00065	1.59	0.000517	0.000410	0.08569
370	.00132	3.43	.002329	.003028	8459
510	.00174	4.61	.004150	.006851	8550
628	.00205	5.56	.005954	.01166	8553
757	.00236	6.56	.008159	.01872	8559
965	.00277	8.10	.01211	.03430	8451
1180	.00320	9.60	.01658	.05581	8515
1357	.00348	10.77	.02050	.07754	8482
1671	.00397	12.73	.02779	.1248	8543
2062	.00443	14.98	.03725	.1980	8511
2468	.00486	17.14	.04727	.2892	8532
3077	.00540	20.08	.06236	.4505	8578
3664	.00576	22.65	.07671	.6293	8543
4466	.00620	25.84	.09580	.9046	8547
5271	.00656	28.73	.1142	1.2072	8558

Eq. (15) and (16) then gives the final velocity constants $k_1 = 0.08534$ and $k_2 = 0.03047$. FROST and SCHWEMER obtained the values $k_1 = 0.0856$ and $k_2 = 0.0305$. Column six in Table 1 indicates the k_1 values which are obtained from eq. (10 a) with the assumption that $k_2 = 0.03047$.

Summary

A method for the calculation of the velocity constants for a series of two competitive, consecutive reactions is described.

The method is not as rapid as the "time-ratio method" of FROST and SCHWEMER, but it has some advantages: (i) The method is valid for both first- and second-order reactions; (ii) it is not necessary that the reacting substances are present in stoichiometracally equivalent amounts; (iii) it is possible to make a statistical treatment of all the experimental material.

Laboratory of Organic Chemistry, University of Uppsala.

REFERENCES

1. WIDEQVIST, Acta chem. Scand. *4*, 1216 (1950).
2. FROST and SCHWEMER, J. Am. Chem. Soc. *74*, 1268 (1952).

Tryckt den 5 december 1955

Uppsala 1955. Almqvist & Wiksells Boktryckeri AB

ARKIV FÖR KEMI Band 8 nr 54

Communicated 13 April 1955 by Arne Tiselius and Arne Fredga

Stereochemical studies on dicarboxylic acids

III. The infrared absorption of some α,α′-disubstituted acids of different types

By Lennart Schotte and Andreas Rosenberg

With 10 figures in the text

In earlier publications we examined the infrared absorption curves of certain substituted dicarboxylic acids (1 and 2) and presented a new method of determining the formation of quasiracemic compounds by infrared measurements (3). As the infrared approach to stereochemical problems in general and diastereomers in particular seemed promising, this investigation is supposed to give further material for an expansion of the basis on which discussion can be carried on and conclusions drawn. In addition to the previously investigated α,α′-dimethylsubstituted dibasic acids the analogous chloro, bromo and ethyl derivatives of succinic acid, the diastereomers of α,α′-diethylglutaric acid and α,α′-dibromoadipic acid have been examined. The two forms of α,α′-dibromoglutaric acid have been prepared and examined also, but as the evidence for the assignment of the meso configuration to the high-melting isomer seems questionable, the discussion of these diastereomers will be given later by one of us (L. S.). In addition to the already mentioned dicarboxylic acids we have also investigated the infrared absorption spectra of the diastereomers of dithiodilactic acid, from which information can be obtained not only about the behaviour of the carbonyl frequency but also about that of the carbon–sulphur and sulphur–sulphur bond.

The halogeno substituted substances have been examined as Nujol mulls between 2 and 15 μ with sodium chloride prism. The region 15–25 μ has been recorded for most of the acids in question with potassium bromide prism, but as the assignment of the bands here is uncertain the spectra in this wavelength interval will not be published. The absorption maxima are, however, given in respective tables. The halogen compounds are studied as emulsions and not as potassium bromide plates in order to exclude the possibility of interaction between the substances to be examined and the phase material. Figs. 1 and 2 show the infrared absorption curves of the meso and racemic forms of α,α′-dichlorosuccinic acid. If we compare the two absorption spectra it can be seen that the curve obtained for the meso isomer shows a less elaborate structure. This is most clearly seen if the vibrations connected to the absorption peaks of the carboxylic groups are considered. First of all, the carbonyl stretching frequency found for the meso form at 5.84 μ has clearly split to two peaks at 5.70 μ and 5.83 μ respectively in the racemic isomer. The curve of the meso form

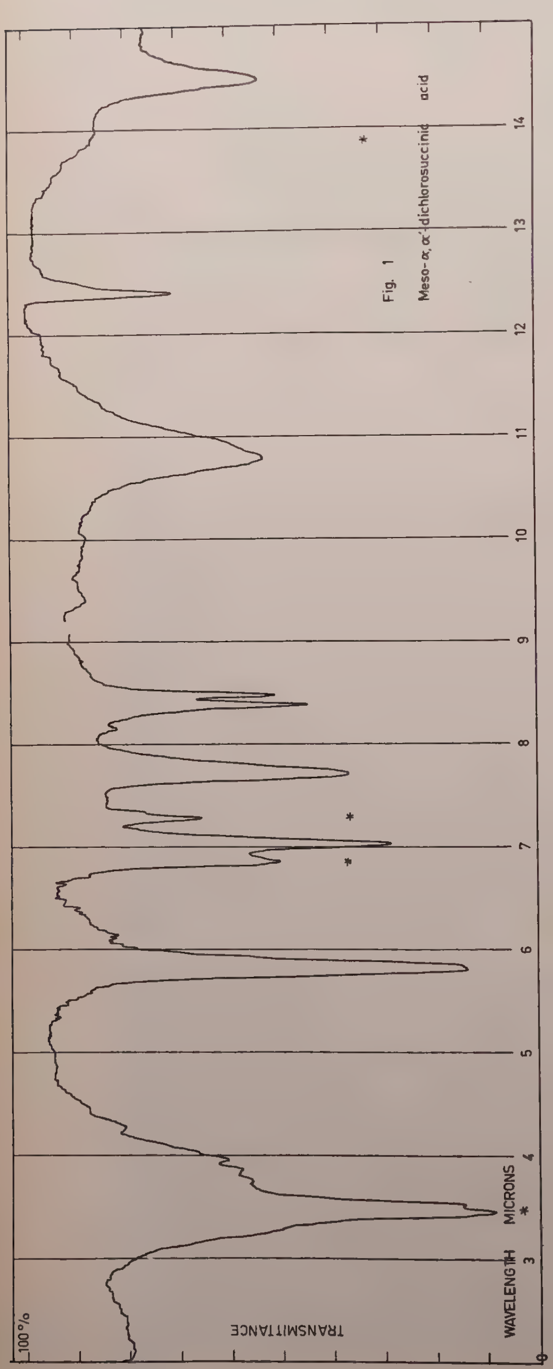

Fig. 1

Meso-α,α'-dichlorosuccinic acid

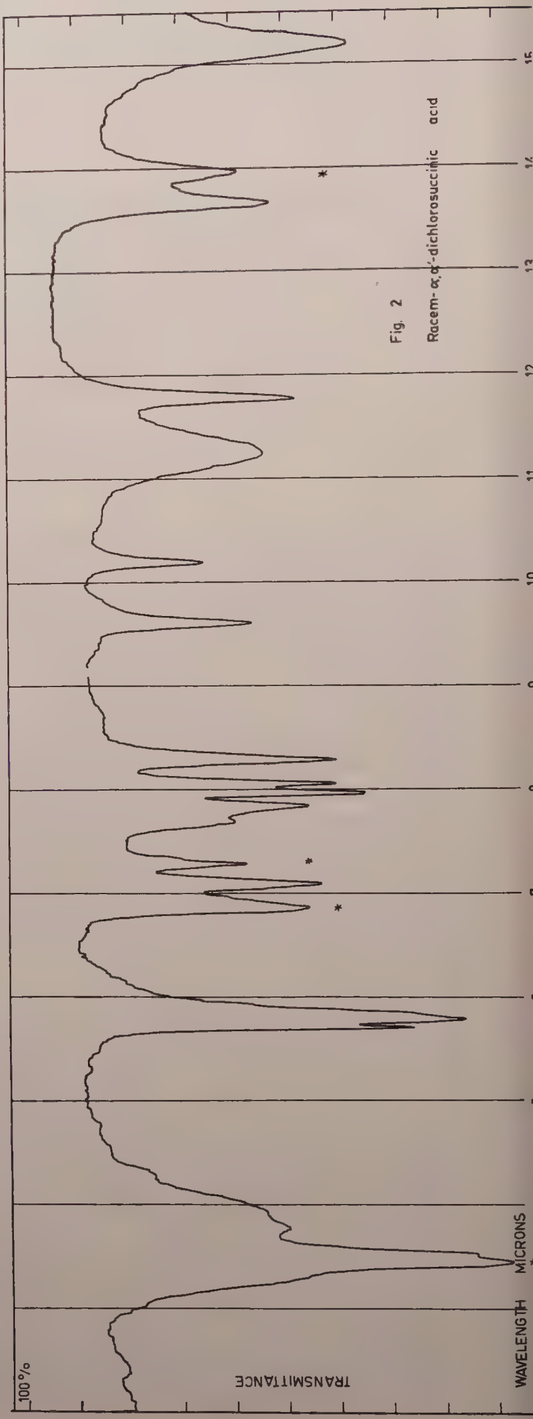

Fig. 2

Racem-α,α'-dichlorosuccinic acid

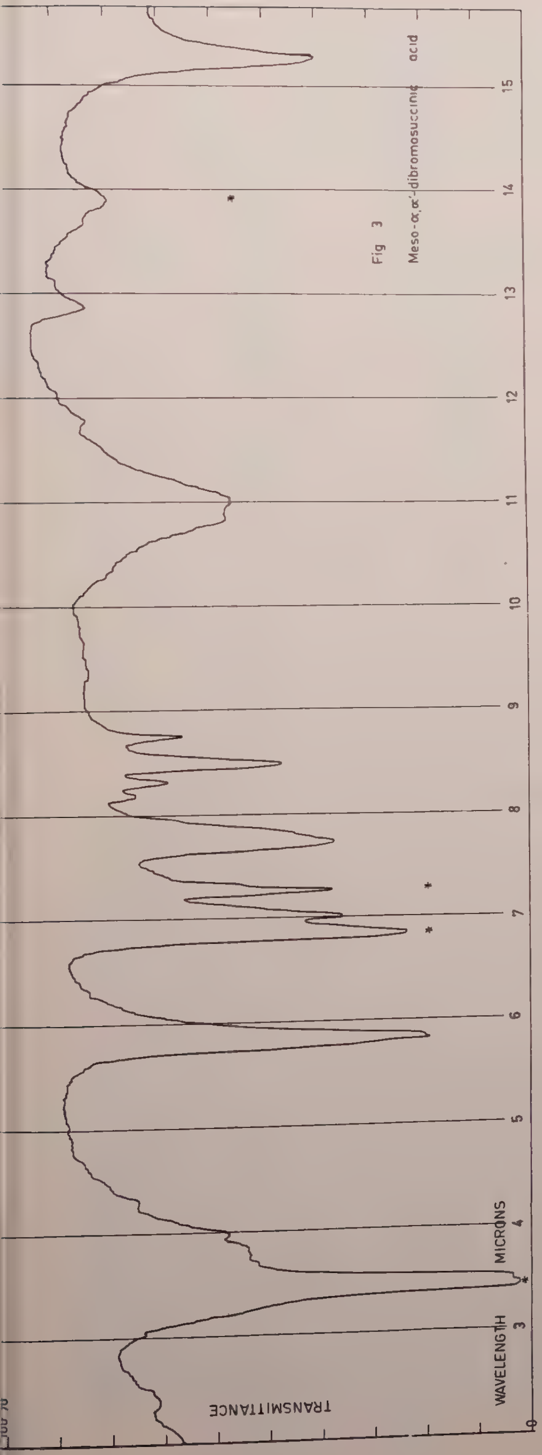
Fig 3
Meso-α,α'-dibromosuccinic acid

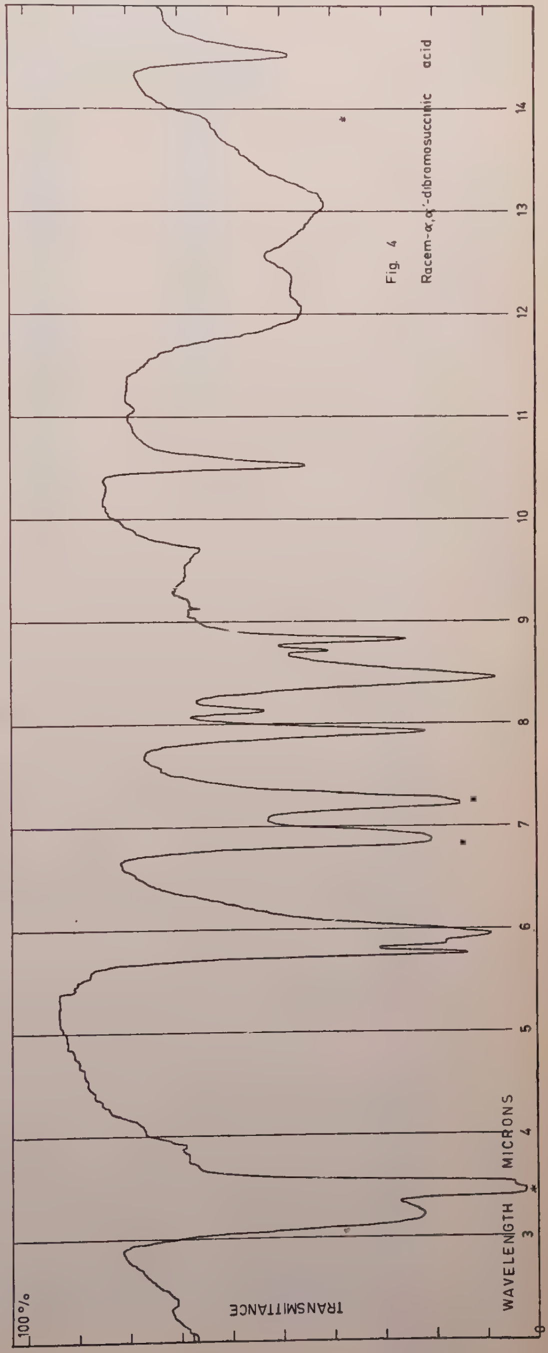
Fig. 4
Racem-α,α'-dibromosuccinic acid

Table 1. The infrared absorption bands of α,α′-dichlorosuccinic acids.

Meso form		Racemic form	
Wavelength in μ	Wavenumber in cm⁻¹	Wavelength in μ	Wavenumber in cm⁻¹
3.42	2924	3.42	2924
3.51	2850	3.51	2850
3.72	2688	3.73	2681
3.83	2611	3.91	2558
3.92	2551	4.25	2353
4.22	2367	5.70	1754
5.84	1712	5.80	1724
6.85	1460	6.86	1458
7.04	1421	7.08	1413
7.27	1376	7.26	1377
7.70	1299	7.68	1302
8.14	1226	7.83	1277
8.37	1195	7.96	1256
8.47	1181	8.05	1242
10.80	926	8.28	1208
12.39	807	9.59	1043
14.43	693	10.18	982
16.2	617	11.25	889
17.5	571	11.76	850
23.25	430	13.64	733
		13.98	715
		15.20	658
		18.0	555
		20.6	485
		21.75	460

shows a single well-defined top at 7.70 μ which frequency is usually assigned to the carbon-oxygen stretching of the carboxylic group (4). On the other hand there is no such peak in the spectrum of the racemic form which instead has a set of bands the assignments of which are difficult. The broad band at 10.80 μ in the meso form commonly ascribed to out of plane bendings of OH (5) has in the racemic isomer shifted to 11.25 μ. The exact wavelengths for the absorption bands can be seen from Table 1.

When comparing the infrared absorption curves for the diastereomers of α,α′-dibromosuccinic acid it can be seen from Figs. 3 and 4 that the splitting of the carbonyl stretching frequency has become even more pronounced as compared with that of analogous chloro- and methylsubstituted succinic acid derivatives. The meso form has its absorption peak at 5.84 μ, whereas the racemic form shows one well-defined top at 5.76 μ and a second at 5.94 μ with a clear shoulder at 5.85 μ. The usual 7.70 μ band mentioned above for the meso isomer of α,α′-dichlorosuccinic acid is also found here. The racemic form shows no absorption peak at this wavelength. A sharp band at 7.95 μ is, on the other hand, probably connected with this stretching. The OH bending is found for the meso form as a broad absorption maximum at 11.0 μ. The picture of the racemic isomer is rather complicated, as the curve shows two broad maxima at 12 μ and 13.1 μ respectively, the assignment of which is difficult. The spectrum of the racemic form shows an anomalous band at 3.25 μ not found for

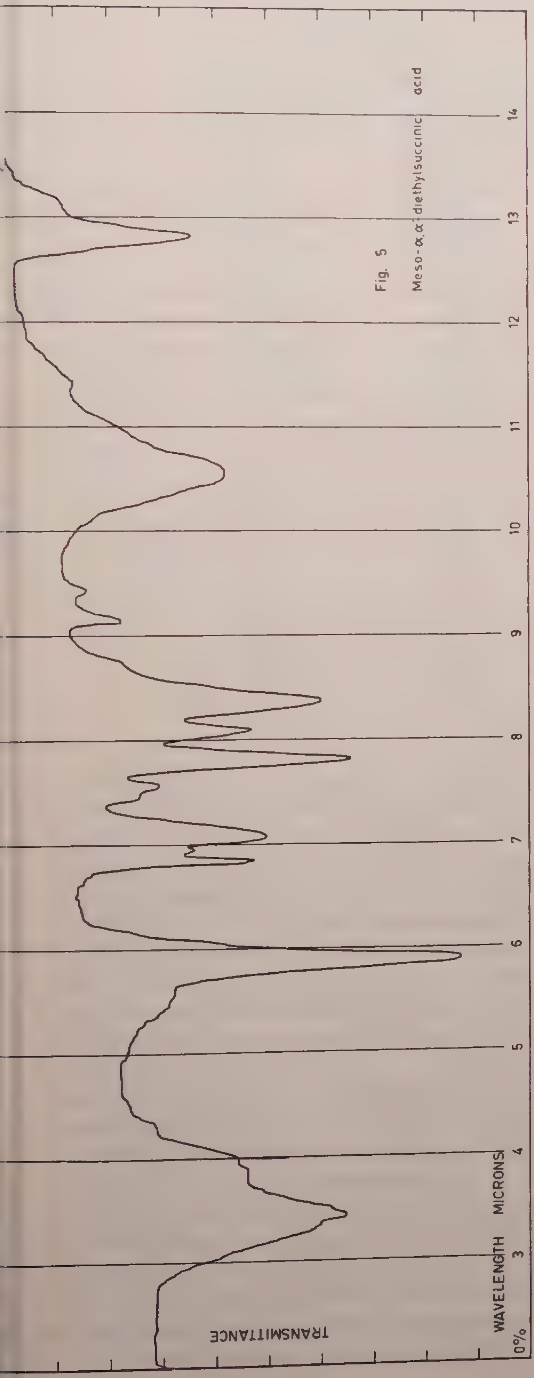

Fig. 5

Meso-α,α'-diethylsuccinic acid

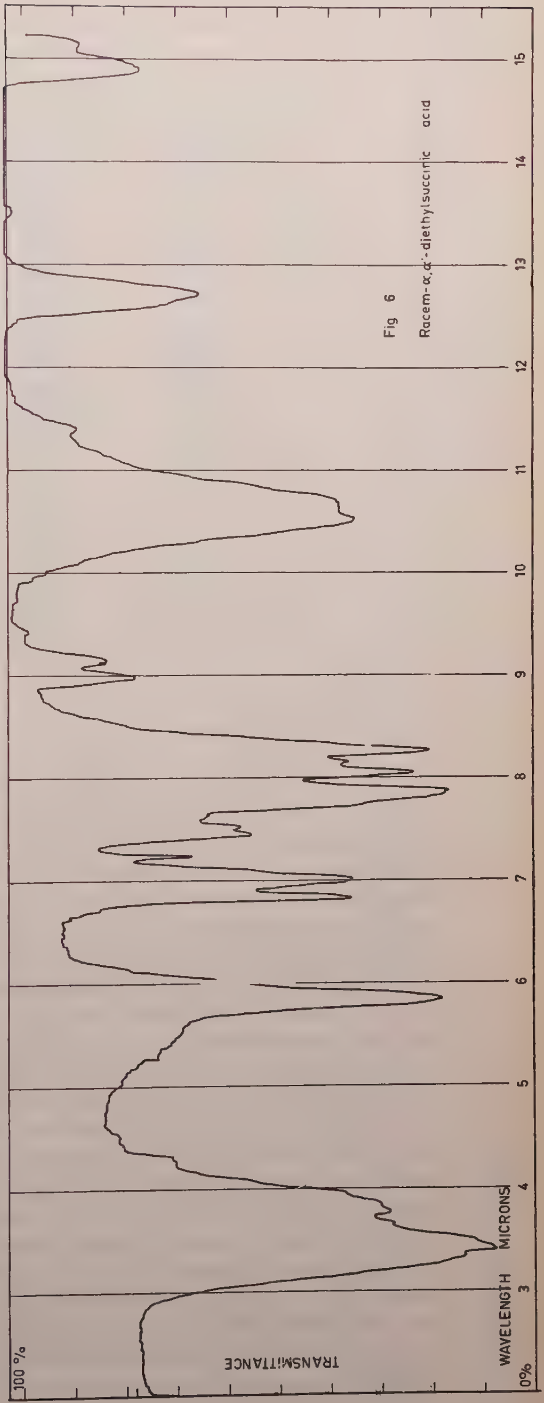

Fig 6

Racem-α,α'-diethylsuccinic acid

Table 2. The infrared absorption bands of α,α′-dibromosuccinic acids.

Meso form		Racemic form	
Wavelength in μ	Wavenumber in cm^{-1}	Wavelength in μ	Wavenumber in cm^{-1}
3.45	2898	3.25	3077
3.51	2850	3.45	2898
3.95	2532	3.51	2850
4.25	2353	3.90	2564
5.84	1712	4.10	2440
6.85	1460	5.76	1736
7.01	1427	5.85	1709
7.26	1377	5.94	1684
7.75	1290	6.87	1457
8.18	1223	7.24	1381
8.31	1203	7.93	1261
8.48	1179	8.13	1230
8.75	1143	8.44	1185
10.8	926	8.71	1148
11.0	909	8.83	1133
12.85	778	9.7	1031
13.90	719	10.76	929
15.30	653	12.0	833
17.2	581	12.3	813
18.4	543	13.1	763
		14.52	689
		15.60	641
		17.45	573
		19.2	521

any of the other substances. The wavelengths of the absorption bands for the two diastereomers are given in Table 2.

The last pair of diastereomers derived from succinic acid to be discussed in this investigation is the meso and racemic form of α,α′-diethylsuccinic acid. Their infrared absorption spectra can be seen in Figs. 5 and 6. The exact wavelengths are further reported in Table 3. In contrast to the diastereomers examined above the two forms show very similar spectra and only small shifts in the absorption frequencies can be observed. The most remarkable feature is that the absorption curve for the racemic form does not show a splitting of the carbonyl band as found for the other racemic isomers investigated. The small shifts observed can probably be ascribed to slight differences in the crystal packing.

The behaviour of the diastereomers of α,α′-dimethylglutaric acid concerning infrared absorption has already been discussed by the present authors (2). As previously mentioned the treatment of the α,α′-dibromo derivatives from the same point of view will be given later. In the present investigation, however, the infrared absorption spectra of the meso and racemic form of α,α′-diethylglutaric acid are reported, as the differences between the curves are similar to those observed for the succinic acid series. The spectra in question are given in Figs. 7 and 8. The meso form shows a sharp single band at 5.84 μ, whereas the racemic isomer shows one carbonyl absorption peak at 5.76 μ with a shoulder at 5.85 μ and a second band that must also be ascribed to carbonyl frequency at 6.10 μ. Even the rest of the two spectra show

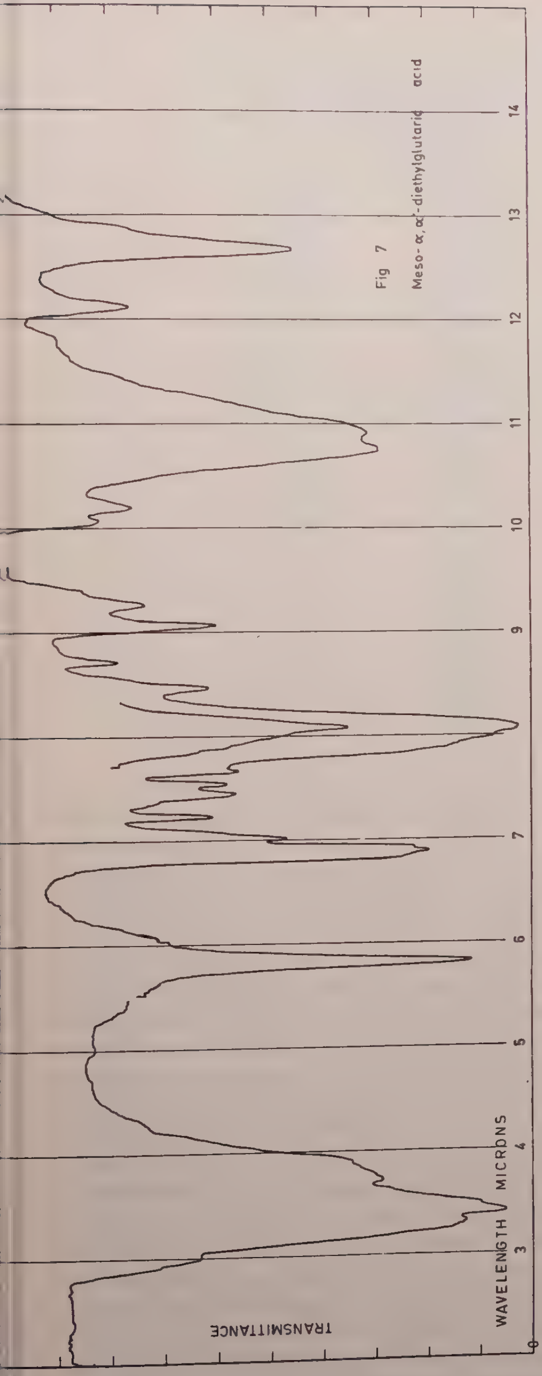

Fig 7 Meso-α, α'-diethylglutaric acid

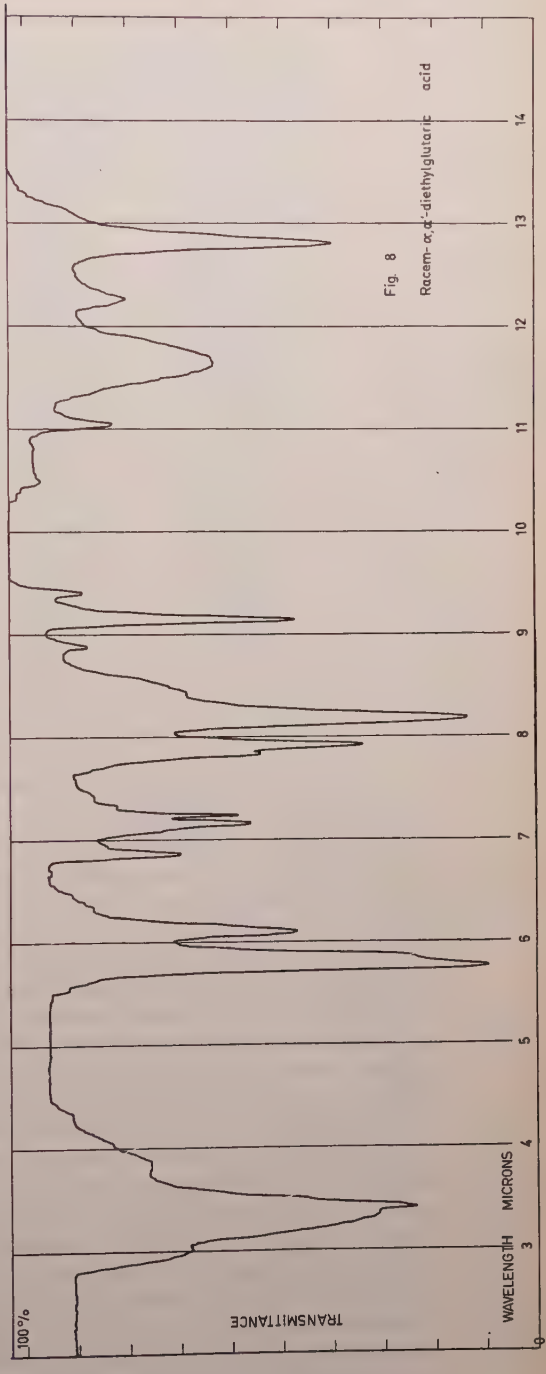

Fig. 8 Racem-α, α'-diethylglutaric acid

Table 3. The infrared absorption bands of α,α′-diethylsuccinic acids.

Meso form		Racemic form	
Wavelength in μ	Wavenumber in cm^{-1}	Wavelength in μ	Wavenumber in cm^{-1}
3.42	2924	3.42	2924
3.85	2597	3.75	2666
4.00	2500	3.84	2604
4.25	2353	4.25	2354
5.89	1698	5.84	1712
6.85	1460	6.84	1462
6.95	1439	7.03	1422
7.07	1414	7.24	1381
7.45	1342	7.44	1344
7.55	1325	7.53	1328
7.80	1282	7.85	1274
8.09	1236	8.05	1242
8.36	1196	8.15	1227
9.14	1094	8.26	1211
9.44	1059	8.97	1115
10.55	948	9.14	1094
12.82	780	10.52	951
14.75	678	10.6	943
16.0	625	11.40	877
17.5	571	12.70	787
21.0	476	14.90	671
		15.10	662
		15.95	627
		17.0	588

marked differences. The region about 8 μ may be especially noticed as the spectrum of the meso form has a top at 8.06 μ and that of the racemic acid a double band at 7.93 μ and 8.17 μ. These peaks are possibly connected with the stretching of the carboxylic groups. A thorough report of the wavelengths for the absorption maxima is given in Table 4.

From the adipic acid series the two diastereomers of α,α′-dibromoadipic acid have been investigated. As the main absorption bands here do not exhibit significant shifts the spectra are omitted and the wavelengths only given for the sodium chloride prism region in Table 5. The behaviour of the analogous α,α′-dimethyladipic acids is quite similar (2). The explanation given there is valid also for the bromo substituted acids.

For the interpretation of the material given we have not taken into consideration the changes of absorption maxima in the finger print region even if they are distinct enough. First of all it is difficult to assign any of these bands to a certain group or atom and furthermore most of the shifts may be caused by small changes in the packing of the crystal lattice. The attempts to correlate any frequency of that kind to special steric configurations can easily lead to contradictions as is obvious from works on *threo* and *erythro* isomers of substituted 1,3-propane diols and β-phenylserines (6 and 7). We have instead chosen to study the frequencies connected to the carboxylic group, as these bands can be readily detected and have been relatively well investigated, so that the shifts usually can be interpreted. As the most dominat-

Table 4. The infrared absorption bands of α,α′-diethylglutaric acids.

Meso form		Racemic form	
Wavelength in μ	Wavenumber in cm^{-1}	Wavelength in μ	Wavenumber in cm^{-1}
3.00	3333	3.00	3333
3.30	3030	3.32	3012
3.42	2924	3.42	2924
3.51	2850	3.50	2849
3.74	2677	3.80	2631
4.25	2353	4.25	2353
5.84	1712	5.76	1736
6.90	1449	5.85	1709
6.93	1443	6.10	1639
7.03	1422	6.85	1460
7.23	1383	7.15	1396
7.45	1342	7.23	1383
7.55	1324	7.83	1277
7.66	1305	7.93	1261
8.06	1241	8.17	1224
8.45	1183	8.86	1129
8.70	1149	9.15	1093
9.05	1105	9.40	1064
9.25	1081	10.50	952
10.05	995	11.05	905
10.20	980	11.65	858
10.75	930	12.25	816
10.90	917	12.80	781
12.11	826	15.65	639
12.67	789	16.60	602
15.90	629	17.85	560
17.95	557	19.35	517
19.75	506		

ing change in the spectra of a pair of diasteromers we have considered the splitting of the carbonyl stretching frequency for the racemic isomer into double peaks.

It must be mentioned here that the infrared absorption curve for unsubstituted succinic acid according to FLETT (8) shows one strong band at 1700 ± 5 cm^{-1} (5.88 μ ± 0.02 μ) and a weak at 1780 cm^{-1} (5.62 μ). DUNCANSON (9), on the contrary, reports two bands at 1705 cm^{-1} (5.86 μ) and 1720 cm^{-1} (5.81 μ). Our own studies on a sample of high purity shows a strong band at 1695 cm^{-1} (5.90 μ) with a slight shoulder at 1725 cm^{-1} (5.80 μ) together with a very weak band at 1785 cm^{-1} (5.60 μ). The weak 1785 cm^{-1} (5.60 μ) frequency is probably an overtone band, but it is difficult to find an explanation for the occurrence of the slight shoulder at 1725 cm^{-1} (5.80 μ). The assignment to symmetrical and antisymmetrical vibrations involving carbonyl stretching is unlikely as X-ray work of MORRISON and ROBERTSON (10) gives evidence for the existence of a center of symmetry in the molecule. It therefore seems likely that the appearance of the above mentioned shoulder is connected with the extremely tight-packed crystal lattice. For the monosubstituted succinic acids DUNCANSON (9) reports single absorption maxima at 1701 cm^{-1} (5.88 μ) for the methyl derivative and 1723 cm^{-1} (5.80 μ) for the chlorosuccinic acid. In these racemic compounds the

Table 5. The infrared absorption bands of α,α′-dibromoadipic acids.

b = broad; vs = very strong; s = strong; m = medium; w = weak; sh = shoulder; e = emulsion peak.

Meso form			Racemic form		
Wavelength in μ	Wavenumber in cm^{-1}	Character of the band	Wavelength in μ	Wavenumber in cm^{-1}	Character of the band
3.42	2924	e	3.42	2924	e
3.50	2849	e	3.50	2849	e
3.78	2645	w	3.78	2645	w
3.92	2551	w	3.93	2545	w
4.25	2353	sh	4.25	2353	sh
5.85	1709	vs	5.85	1709	vs
6.85	1460	e	6.85	1460	e
6.93	1443	s	7.00	1428	s
7.00	1428	s	7.27	1375	e
7.27	1375	e	7.75	1290	s
7.70	1299	s	8.00	1250	w
7.80	1285	s	8.10	1235	w
8.05	1242	m	8.30	1205	m
8.24	1214	sh	8.55	1169	w
8.33	1200	w	8.85	1130	w
8.44	1185	m	9.30	1075	w
8.80	1136	w	9.75	1026	w
9.63	1038	m	10.85	922	b
10.75	930	sh	11.10	901	sh
11.0	909	b	12.10	826	m
12.37	808	m	12.40	806	w
13.5	741	w	13.9	719	e
13.9	719	e	14.34	697	m
14.40	694	m			

monosubstitution yields an unsymmetrical structure, where the heavy substituent probably causes a change in the structure as compared with the planar structure of the unsubstituted acid thus weakening the coupling between the vibrations of the two carbonyl groups. This must result in the appearance of a single top in the region in question.

The splitting of the carbonyl stretching frequency into double peaks for *racem* α,α′-dimethyl-, α,α′-dichloro- and α,α′-dibromosuccinic acid can be explained by different assumptions. Firstly, such a splitting of the carbonyl band should be expected for a substance, where the crystal lattice contains two carboxylic groups different with respect to the strength of the hydrogen bonding, e.g. as in formula I.

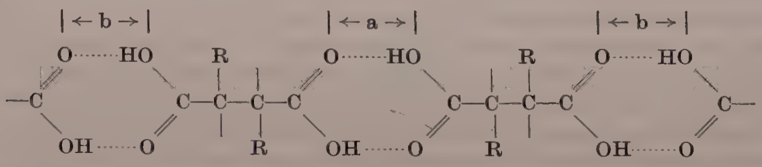

b > a

I

We are of course aware that there is no particular support for such an assumption for the acids under question except the proposal of LECOMTE (11) that optical antipodes tend to form racemic pairs that ought to be considered as units from the infrared point of view. Such an explanation is, however, in our case opposed by the fact that the spectra of the meso isomers in general are less complicated than those of the racemic forms. Further, if the LECOMTE hypothesis was correct the pairing tendency ought to be more pronounced for the monosubstituted acids, where the unsymmetrical structure should favour unequal carboxylic groups. Finally, this effect should be observed for the higher homologues in our investigation series, which is not the case.

The most probable explanation of the behaviour of the carbonyl bands is that coupling occurs between the stretching vibrations of the different carbonyl groups in the same acid molecule. A consideration of molecular models has shown that the heavy substituents in question cause rigid structures in the case of racemic forms, where the carbonyl groups are situated in the same plane. Thus as a result of the asymmetrical configuration both the symmetrical and unsymmetrical carbonyl vibration frequencies can be observed. For the meso isomers on the other hand there are two possible explanations for the existence of a single absorption top. Firstly, owing to the steric influence of the adjacent substituents the carboxylic groups can be forced to positions in different planes thus making a coupling as above completely impossible. Secondly, if the molecule contains a center of symmetry, only one absorption maximum is obtained, irrespective of an eventual total planar structure, as one of the vibrations then is infrared inactive. This interpretation seems the most likely to the authors in view of the intramolecular compensated structure of meso configurations. An explanation of this kind for the differences observed is also in agreement with experimental data for higher homologues, where the significant differences diminish with the length of the carbon chain. Even the differences in the effect of different substituents seem in this way to be easily explained as the effect increases in the order methyl < chlorine < bromine.

An unexpected exception to the general behaviour of the carbonyl groups in infrared absorption has already been pointed out for the diastereomers of α,α'-diethylsuccinic acid. When considering molecular models it seems obvious, however, that both the isomers are of such a configuration that coupling between the carbonyl stretching vibrations is impossible. This is due to the predominant character of the two ethyl groups when substituted at adjacent carbon atoms.

The observed strong effects of different spatial distribution on infrared absorption spectra for the succinic acid series can hardly be expected to appear for the higher homologues as one or more methylene groups are inserted between the two centers of asymmetry. However, the general conclusions drawn seem to be valid even for the glutaric acid derivatives, but the effects are less pronounced. They are under normal conditions first obvious for the diastereomers of α,α'-diethylglutaric acid. This result at first seems contradictory as compared with the behaviour of the succinic acid series but is in the following readily explained in accordance with the general interpretation presented.

In the succinic acid series the picture of the infrared absorption of the diethyl derivative differs from those of other acids investigated as the large ethyl groups exhibit a predominant influence on the conformation of the molecule. In the case of glutaric acid the additional methylene group has largely eliminated this effect and as the substituent can in contrary to the smaller methyl group cause a rigid structure with allowed mechanical coupling between the stretching vibrations of the carbonyl groups, the changes in infrared absorption will thus follow the general lines pointed out in the above discussion. It is further expected from the above that no marked differences should occur for the two inactive isomers of α,α′-dibromoadipic acid in the frequency region considered by us as significant.

It is very important to point out that the regular changes of infrared spectra for these acids cannot be expected to be valid for the racemic and meso character in general outside a limited and well-defined series. Considering e.g. dicarboxylic acid derivatives of cyclic systems it must be remembered that an effect on infrared absorption of the nature discussed above cannot *a priori* be regarded as characteristic for the racemic forms, as these often correspond to trans configurations. If a split of the carbonyl band really appears, it is more likely to be expected for the meso form as in the cis configurations the possibility of coupling between carbonyl vibrations seems more favoured.

This is fully illustrated by the behaviour of *cis*-(*meso*)- and *trans*-(*racem*)-1,2-dithiane-3,6-dicarboxylic acid on infrared analysis. The curves are presented by SCHOTTE in a paper on spectrochemical studies of sulphur compounds (12). The most striking feature of the absorption spectra is the splitting of the carbonyl band for the meso form into double peaks. The trans isomer shows a single well-defined top. Similar behaviour for another cyclic dicarboxylic acid is reported by FREDGA and SIKSTRÖM in a paper dealing with caronic acid (13). The infrared curve for *meso*-(*cis*)-caronic acid shows in general a more complicated character than that of the trans form, but the assignment for most of the absorption peaks cannot be done with sufficient accuracy. It is, however, possible to study the carbonyl absorption frequencies for the two isomers without any interference. The racemic form shows a single top at 5.90 μ, whereas the meso acid has a symmetrical double peak at the wavelengths 5.77 μ and 5.90 μ respectively. It seems important to underline this effect, as the conformation of the steric isomers of caronic acid is well established. Thus the conclusions drawn here possess a high degree of validity for further discussions. We consider coupling between the vibrations of the carbonyl groups of the *cis* form possible owing to the rigidity of the three-membered ring system. For the trans configuration, however, the coupling seems rather unlikely, but if it occurs, we should nevertheless expect a single absorption peak at the carbonyl frequency. One of the vibrations is, then, infrared inactive owing to the more symmetrical positions of the carboxylic groups even if the molecule has no center of symmetry. This explanation is in good agreement with infrared data.

In attempts to extend the investigation to other specific frequencies the disturbing influence of the neighbouring bands as mentioned above made it impossible to establish the shifts with sufficient accuracy, e.g. for the carbon–bromo and carbon–chloro stretching vibrations in the halogeno substituted acids examined. On the contrary, it was possible to determine the behaviour of the carbon–sulphur band for dithiodilactic acid (disulphide-di-α-propionic acid). Figs. 9 and 10 show the infrared spectra between 11 and 24 μ of the meso and racemic forms, and the exact wavelengths are given in Table 6. The interpretation of the spectra for this pair of isomers is simple because of the extreme simplicity of the absorption curve for the racemic form. It shows in the region 12 to 24 μ only two strong bands at 15.10 μ and 20.5 μ respectively that can be ascribed to the stretchings of C–S and S–S. From the more complicated spectrum of the meso form it can be seen that the carbon–sulphur band has split to double peaks at 14.82 μ and 15.10 μ. Dissolved in N,N-dimethyl-

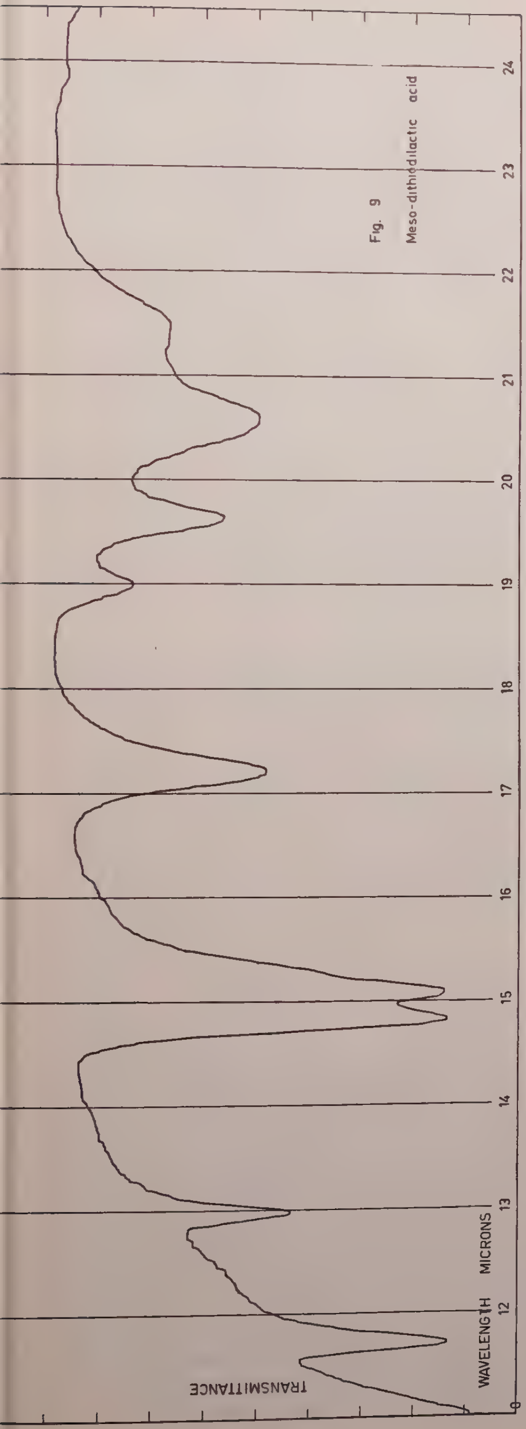

Fig. 9 Meso-dithiodilactic acid

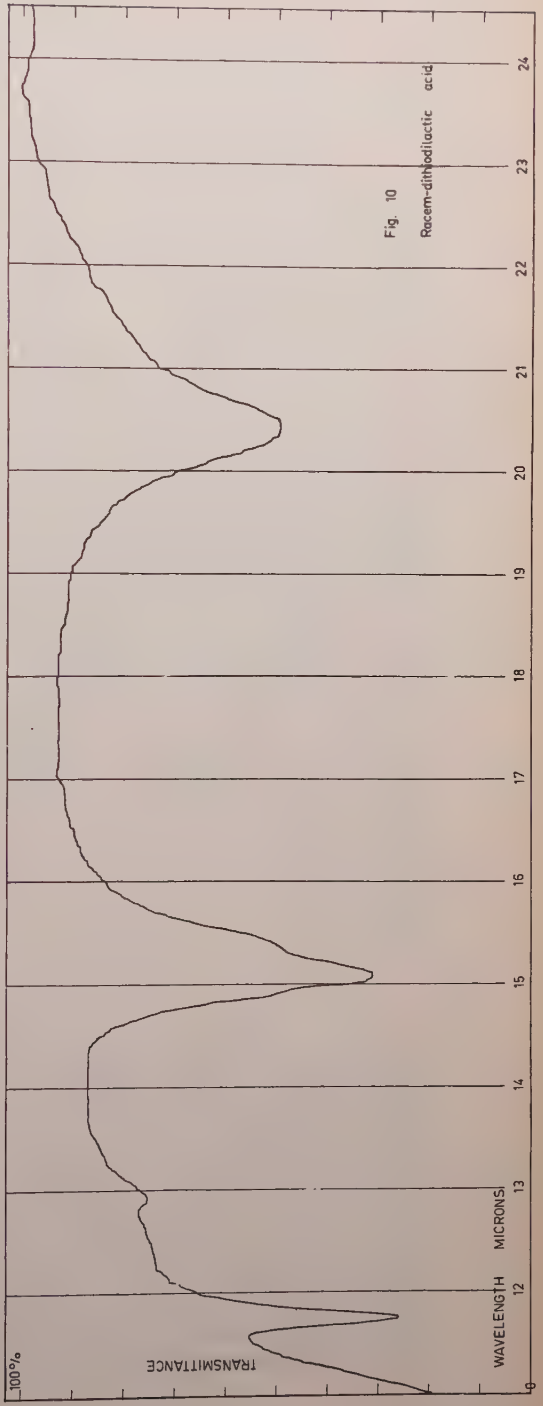

Fig. 10 Racem-dithiodilactic acid

Table 6. The infrared absorption bands of dithiodilactic acids.

Meso form		Racemic form	
Wavelength in μ	Wavenumber in cm^{-1}	Wavelength in μ	Wavenumber in cm^{-1}
11.7	855	11.75	851
12.98	770	15.10	662
14.82	675	20.5	488
15.10	662		
17.20	581		
19.00	526		
19.65	509		
20.6	485		
21.5	465		

formamide, however, both the forms show identical spectra in this region with a band at 14.85 μ. This result shows that even other stretching vibrations than those related to carboxylic groups can be the base of a study similar to ours, but it must be borne in mind that the absorption curves given here are far more simple than those of sulphur compounds in general.

All our studies on the infrared absorption of diastereomers show that the regular changes observed can be used for the establishment of stereochemical relationships within limits obvious from the discussion. The changes should, however, be of the same clear character as the splitting found in this investigation, for it must always be borne in mind that simple shifts in the same stretching frequency for the diastereomers can be readily explained by different packing in the crystal lattice. When such clear effects are obtained conclusions can easily be drawn, and it is very interesting to note the significant difference between the behaviour of linear and cyclic compounds, a difference which is well understood from the structural point of view. It can thus at last be established that a distinct and strong connection exists between the spatial distribution of substituents in diastereomers and their infrared absorption spectra.

Experimental

A Perkin Elmer model 21 spectrophotometer equipped with sodium chloride prism was used for the infrared absorption measurements in the region 2–15 μ. A potassium bromide prism was inserted for the region 15–25 μ. The halogeno substituted compounds were examined as Nujol mulls and the other acids as solid pressed potassium bromide plates according to the method described by Schiedt and Reinwein (14). The diastereomers of α,α′-dibromoadipic acid were only investigated in the sodium chloride region and the two isomers of dithiodilactic acid were recorded for the interval 11–24 μ. All the other acids were examined in the whole wavelength region mentioned. The bands due to the absorption of Nujol ifself in Figs. 1–4 are marked with an asterisk. The calibration of the absorption curves, linear in wavelength, is exact up to ± 0.01 μ in the sodium chloride region and to ± 0.04 μ in that of the potassium bromide prism.

The dicarboxylic acids investigated

Meso-α,α′-dichlorosuccinic acid.—M.p. 218° (d.). The substance was prepared by addition of chlorine to sodium maleinate in a saturated aqueous solution of sodium chloride (15 and 16). *Anal.* Subst., 52.91 mg: 7.77 ml of 0.0734 *N* NaOH. Equ. wt. Calc. 93.5; Found 92.7.

Racem-α,α′-dichlorosuccinic acid.—M.p. 173°–175°. The acid investigated was obtained by treatment of maleic anhydride with a slight excess of chlorine in carbon tetrachloride solution. The reaction was catalysed by light (17 and 18). *Anal.* Subst., 53.35 mg: 7.82 ml of 0.0734 *N* NaOH. Equ. wt. Calc. 93.5; Found 93.0.

Meso-α,α′-dibromosuccinic acid.—M.p. 259°–260° (preheated apparatus) (19 and 20). *Anal.* Subst., 86.62 mg: 8.56 ml of 0.0734 *N* NaOH. Equ. wt. Calc. 138.0; Found 137.9.

Racem-α,α′-dibromosuccinic acid.—M.p. 170° (19 and 21.) *Anal.* Subst., 80.80 mg: 8.00 ml of 0.0734 *N* NaOH. Equ. wt. Calc. 138.0; Found 137.7.

Meso-α,α′-diethylsuccinic acid.—M.p. 194°–195°. The substance was obtained in the following manner. The sodium salt of ethyl ethylmalonate was prepared in toluene and reacted with ethyl α-bromo-*n*-butyrate. The reaction product was fractionated in vacuo and then hydrolyzed under reflux in excess of concentrated hydrochloric acid. Partial decarboxylation occurred already during the hydrolysis but was completed by heating at 155°–165° until the evolution of carbon dioxide ceased. The resulting mixture of the diastereomers of α,α′-diethylsuccinic acid was dissolved in hot water. The high-melting isomer, which is ascribed the meso configuration, separated on cooling and was recrystallized twice from water. (Cf. 22 and 23.) *Anal.* Subst., 49.07 mg: 7.74 ml of 0.0734 *N* NaOH. Equ. wt. Calc. 87.1; Found 86.4.

Racem-α,α′-diethylsuccinic acid.—M.p. 131°–133°. The mother liquor from above (after separation of the meso isomer) was evaporated to dryness and the residue extracted repeatedly with ether. The ether solution was dried and the residue after removal of the solvent treated under reflux with excess of acetyl chloride. The trans anhydride formed was fractionated in vacuo. Hydrolysis of the anhydride in water yielded *racem*-α,α′-diethylsuccinic acid. The product was eventually recrystallized twice from water. (Cf. 22 and 23.) *Anal.* Subst., 50.90 mg: 7.99 ml of 0.0734 *N* NaOH. Equ. wt. Calc. 87.1; Found 86.8.

Meso-α,α′-diethylglutaric acid.—M.p. 118°–120° (24). *Anal.* Subst., 49.33 mg: 7.18 ml of 0.0734 *N* NaOH. Equ. wt. Calc. 94.1; Found 93.7.

Racem-α,α′-diethylglutaric acid.—M.p. 91°–93° (24). *Anal.* Subst., 54.25 mg: 7.90 ml of 0.0734 *N* NaOH. Equ. wt. Calc. 94.1; Found 93.6.

Meso-α,α′-dibromoadipic acid.—M.p. 192°–193° (25). *Anal.* Subst., 87.84 mg: 7.90 ml of 0.0734 *N* NaOH. Equ. wt. Calc. 152.0; Found 151.5.

Racem-α,α′-dibromoadipic acid.—M.p. 141°–143° (25). *Anal.* Subst., 77.45 mg: 6.93 ml of 0.0734 *N* NaOH. Equ. wt. Calc. 152.0; Found 152.3.

Meso-α,α′-dithiodilactic acid.—M.p. 118° (26). *Anal.* Subst., 61.25 mg: 7.99 ml of 0.0734 *N* NaOH. Equ. wt. Calc. 105.1; Found 104.5.

Racem-α,α′-dithiodilactic acid.—M.p. 148°–149° (26). *Anal.* Subst., 59.85 mg: 7.84 ml of 0.0734 *N* NaOH. Equ. wt. Calc. 105.1; Found 104.1.

Summary

The infrared absorption curves of the diastereomers of α,α′-dichloro-, α,α′-dibromo- and α,α′-diethylsuccinic acid, α,α′-diethylglutaric acid, α,α′-dibromoadipic acid and dithiodilactic acid have been investigated.

The differences observed have been discussed from the structural and sterical point of view.

Certain regularities have been pointed out in the differences between the spectra of meso and racemic forms of succinic and glutaric acid derivatives.

An interpretation of the effects observed on IR spectra is offered.

The discussion has been extended to include cyclic structures.

The importance and possibilities of applying infrared methods to stereochemical problems is pointed out.

ACKNOWLEDGEMENTS

The authors wish to express their sincere gratitude to Professor ARNE FREDGA and Professor ARNE TISELIUS for stimulating interest. Some of the substances were kindly placed at our disposal by Professor FREDGA, who also suggested to us the detailed examination of the infrared absorption spectra of *cis-* and *trans*-caronic acid.

Thanks are also due to Mr. STIG BERGWALL for valuable help with the infrared work.

This investigation is a part of a research program, which is financially supported by grants from the *Royal Swedish Academy of Sciences, The State Council of Technical Research, The Rockefeller Foundation* and the *Swedish National Science Research Council.*

Laboratory of Organic Chemistry, Chemical Institute and Institute of Biochemistry, University of Uppsala, March 1955.

REFERENCES

1. A. ROSENBERG and L. SCHOTTE, Acta Chem. Scand. *8*, 867 (1954).
2. L. SCHOTTE and A. ROSENBERG, Arkiv Kemi *7* (1954) nr 51.
3. A. ROSENBERG and L. SCHOTTE, Arkiv Kemi *8* (1955) nr 16.
4. L. J. BELLAMY, The Infra-red Spectra of Complex Molecules. London 1954.
5. D. HADZI and N. SHEPPARD, Proc. Roy. Soc. (London) *216*, 247 (1953).
6. R. A. CUTLER, C. M. MARTINI, and F. C. NACHOD, J. Am. Pharm. Assoc. *43*, 697 (1954).
7. W. A. BOLHOFER, J. Am. Chem. Soc. *76*, 1322 (1954).
8. M. ST. C. FLETT, J. Chem. Soc. *1951*, 962.
9. L. A. DUNCANSON, J. Chem. Soc. *1952*, 1753.
10. J. D. MORRISON and J. M. ROBERTSON, J. Chem. Soc. *1949*, 980.
11. J. LECOMTE, Contribution à l'étude de la structure moleculaire, p. 137. Maison Desoer, Liège 1947–1948.
12. L. SCHOTTE, Arkiv Kemi, In press.
13. A. FREDGA and Å. SIKSTRÖM, Arkiv Kemi, In press.
14. U. SCHIEDT and H. REINWEIN, Z. Naturforsch *7 b*, 270 (1952).
15. E. M. TERRY and L. EICHELBERGER, J. Am. Chem. Soc. *47*, 1067 (1925).
16. R. KUHN and T. WAGNER-JAUREGG, Ber. *61*, 501 (1928).
17. A. MICHAEL and G. TISSOT, J. prakt. Chem. [2] *46*, 393 (1892).
18. B. HOLMBERG, Svensk Kem. Tid. *24*, 105 (1912).
19. B. HOLMBERG, J. prakt. Chem. [2] *84*, 148 (1911).
20. Org. Syntheses *18*, 17 (1938).
21. A. MICHAEL, J. prakt. Chem. [2] *52*, 293 (1895).
22. P. E. VERKADE and H. HARTMAN, Rec. trav. chim. *52*, 953 (1933).
23. E. BERNER and R. LEONARDSEN, Ann. *538*, 26 (1939).
24. E. BERNER and L. H. LANDMARK, Acta Chem. Scand. *7*, 1347 (1953).
25. B. HOLMBERG and E. MÜLLER, Ber. *58*, 1601 (1925).
26. A. FREDGA, Arkiv Kemi, Mineral., Geol. *12 A* (1937) nr 13.

Tryckt den 14 november 1955

Uppsala 1955. Almqvist & Wiksells Boktryckeri AB

ARKIV FÖR KEMI Band 8 nr 55

Communicated 13 April 1955 by ARNE FREDGA and GUNNAR HÄGG

Resolution and configuration of 3-thenylsuccinic acid

By SALO GRONOWITZ and SVEN LARSSON

With 12 figures in the text

In order to obtain a better understanding of the aromatic character of thiophene, especially of the differences between 2- and 3-substituted derivatives, one of us (S. G.) has studied metalation (1) and electrophilic aromatic substitution (2) of certain 3-substituted thiophenes and the difference in conjugation of some 2- and 3-substituted thiophenes (2). As the rotatory power of an optically active compound is to a high degree dependent upon the electronic configuration of the groups attached to the asymmetric centre, a study of the optical rotatory power, besides its importance for the theory of optical activity, should give, as FREDGA (3) has pointed out, some information about the aromatic character of these substances. From these points of view, FREDGA (3) and PETTERSON (4) have studied the optical activity of 2-substituted thiophenes. FREDGA (5) has also found that optically active thiophene derivatives are very useful for the steric correlation of aromatic and aliphatic compounds.

3-Thenylsuccinic acid (6) could be resolved by strychnine and (+)-α-phenylethylamine. As both methods give the same maximum activity it is justifiable to assume that the preparations having a m.p. 159.0° represent the optically pure antipodes.

The method of quasi-racemates (7) which has successfully been applied by FREDGA and collaborators to a great number of sterical problems was used for determining the configurational relationships between 3-thenylsuccinic acid (3-T), 2-thenylsuccinic acid (2-T) and benzylsuccinic acid (B). The existence of the quasi-racemate is usually demonstrated by means of melting point diagrams. Such diagrams may be obtained by the method of RHEINBOLDT (8) or more rapidly by the microscopical methods of KOFLER (9). As MATELL (11) has pointed out, it is possible to detect a molecular compound in a few minutes by the contact method (10). It must of course then be shown that the molecular compound is in the ratio 1:1. It is, however, also possible to demonstrate the existence of the quasi-racemate by means of X-ray powder photographs (12).

The conditions for the formation of quasi-racemates have been systematically investigated by MATELL (11). It should be noted that contrary to LETTRÉ (13) even components in which the structural differences exceed the limits of isomorphic exchangeability may form a quasi-racemic compound. FREDGA (14) has found several cases where the components with opposite configuration form a quasi-racemate and the components of the same configuration did not give solid solutions.

In such a case it may be rather difficult and complicated to demonstrate the existence of a quasi-racemate by X-ray powder photographs [c. f. PETTERSON (12)].

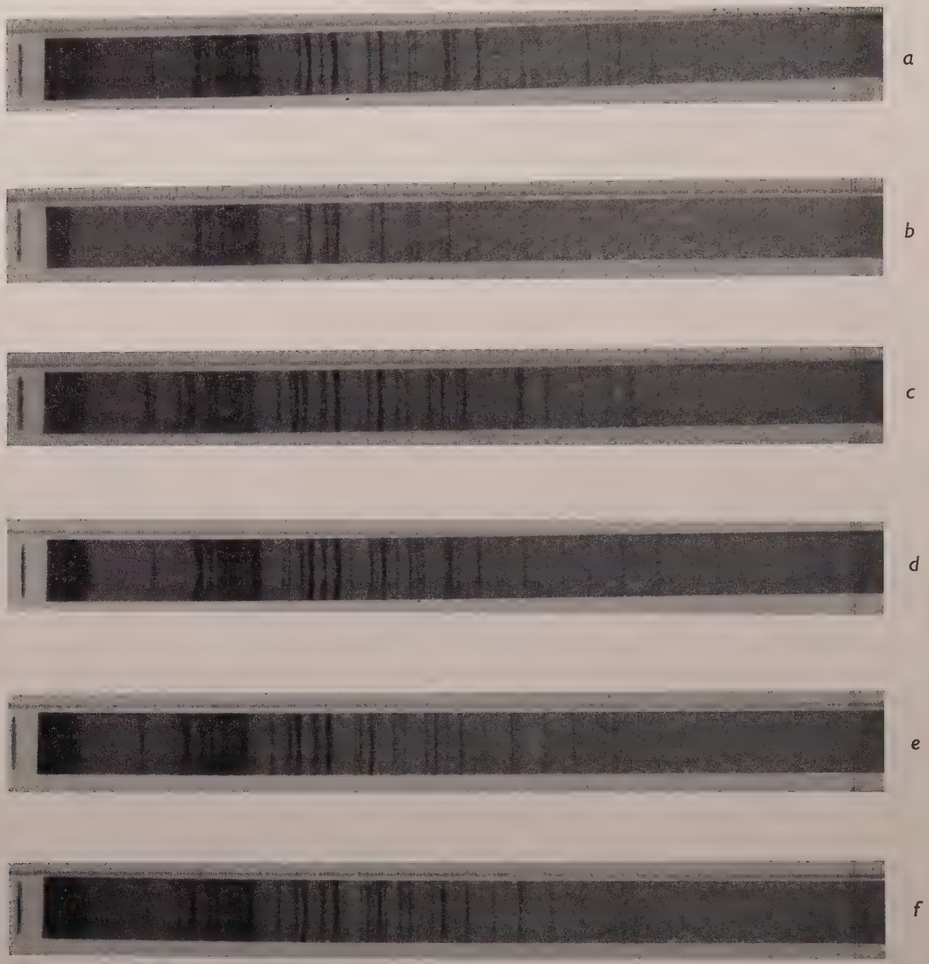

Fig. 1. *a*, (+)-2-Thenylsuccinic acid. *b*, (+)-3-Thenylsuccinic acid. *c*, (+)-Benzylsuccinic acid. *d*, Equimolar amounts of (+)-2-Thenylsuccinic acid and (+)-3-Thenylsuccinic acid. *e*, Equimolar amounts of (+)-3-Thenylsuccinic acid and (+)-Benzylsuccinic acid. *f*, Equimolar amounts of (+)-2-Thenylsuccinic acid and (+)-Benzylsuccinic acid.

The mixture of the components with the same configuration would then give a powder photograph which would be composite of that of the two components. The quasi-racemate obtained would have a powder photograph fundamentally different from those of the components and perhaps also from that of the two racemic modifications, whose photographs need not be the same. If, however, and this is usually the case, the structural differences do not exceed the limits of isomorphic exchangeability, the existence of the quasi-racemate may be easily and elegantly demonstrated by X-ray powder photographs.

This is often the case in the thiophene series where the tendency to form solid solutions occurs to a very great extent between 2- and 3-substituted thiophenes

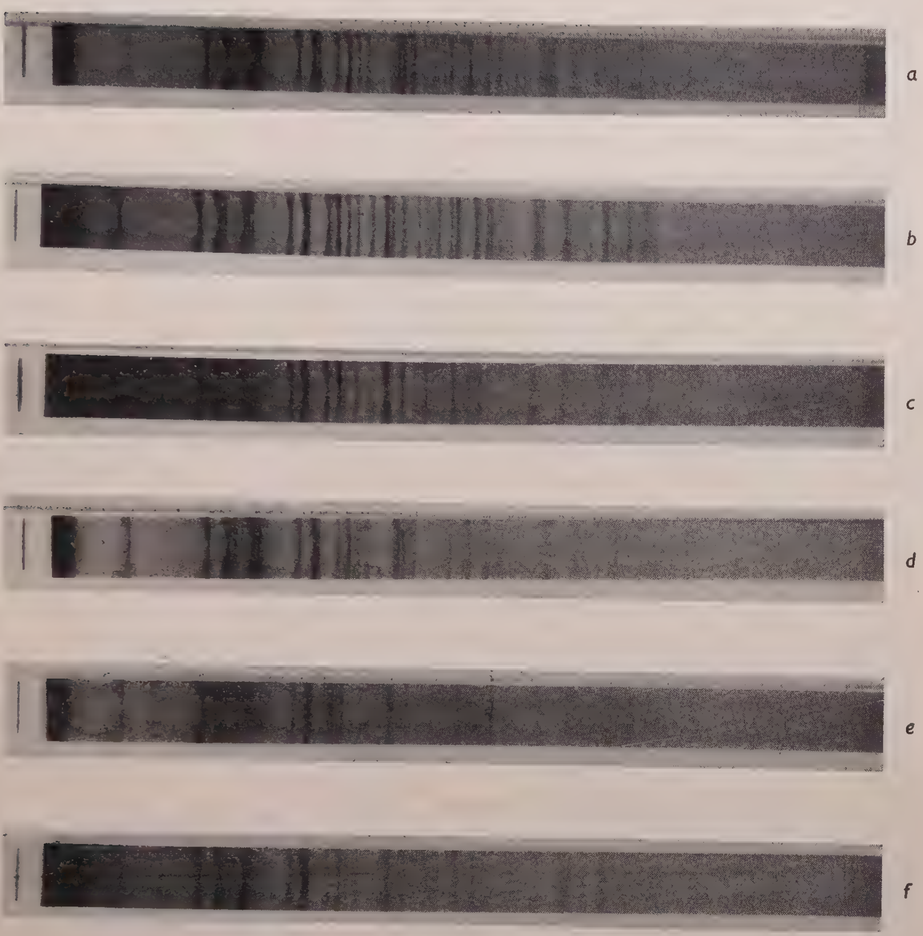

Fig. 2. *a*, *rac*-2-Thenylsuccinic acid. *b*, *rac*-3-Thenylsuccinic acid. *c*, *rac*-Benzylsuccinic acid. *d*, Equimolar amounts of (−)-2-Thenylsuccinic acid and (+)-3-Thenylsuccinic acid. *e*, Equimolar amounts of (−)-Benzylsuccinic acid and (+)-3-Thenylsuccinic acid. *f*, Equimolar amounts of (−)-2-Thenylsuccinic acid and (+)-Benzylsuccinic acid.

(6, 15) and also the phenyl group often seems to be exchangeable for a 2-thienyl (12) or 3-thienyl group (6) without exceeding the limits of isomorphic exchangeability.

It has been shown by one of us (6) that racemic 2-T and racemic 3-T give powder photographs with the same line distribution, differing from that of B only in the spacing of the lines. A similar series has now been obtained for the optically active acids (Fig. 1), which is quite different from that of the racemic series, thus demonstrating the true racemate character of the racemic acids. Equimolar mixtures of the optically active acids with the same mode of rotation gave powder photographs with a line distribution so similar to that of the components that isomorphism is indicated (Fig. 1). Equimolar mixtures of the optically active acids with opposite mode of rotation gave photographs with a line distribution very similar to that of

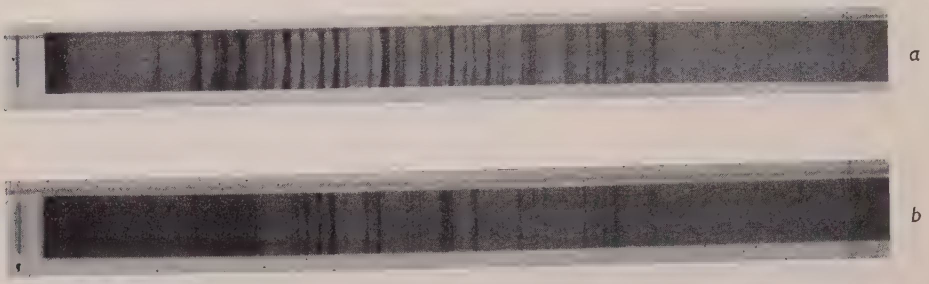

Fig. 3. *a*, "Unmelted" form of (+)-2-Thenylsuccinic acid. *b*, "Melted" form of *rac*-3-thenylsuccinic acid.

the racemic acids (Fig. 2). This clearly shows the existence of the quasi-racemates between (+)-3-T and (−)-2-T, (+)-3-T and (−)-B and between (+)-2-T and (−)-B, *and their crystallographical similarity with the racemic modifications.* The existence of the quasi-racemate in the last-mentioned case has previously been shown by FREDGA and PALM (3). The case now investigated is, however, very favourable as the dif-

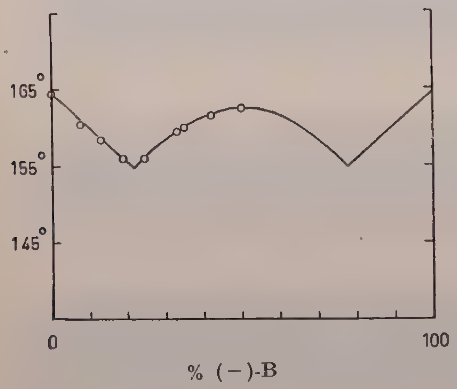

Fig. 4. (+)- and (−)-Benzylsuccinic acid.

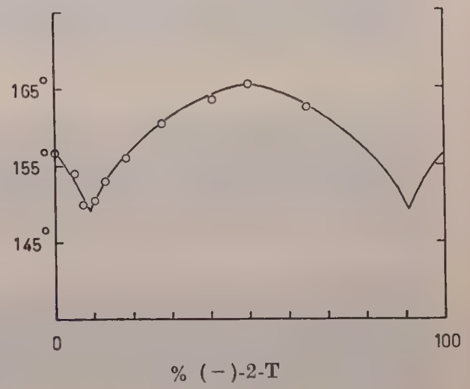

Fig. 5. (+)- and (−)-2-Thenylsuccinic acid.

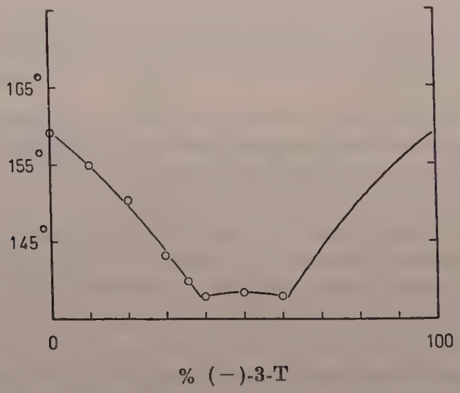

Fig. 6. (+)- and (−)-3-Thenylsuccinic acid.

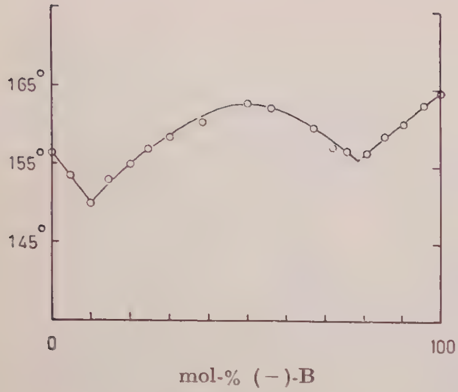

Fig. 7. (+)-2-Thenylsuccinic acid and (−)-Benzylsuccinic acid.

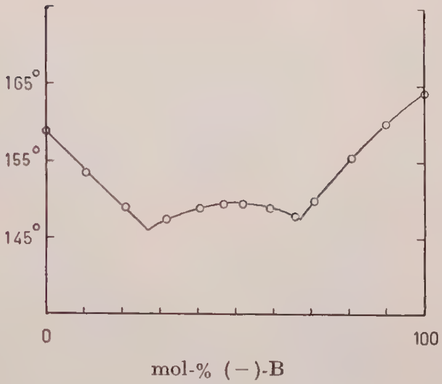

Fig. 8. (+)-3-Thenylsuccinic acid and (−)-Benzylsuccinic acid.

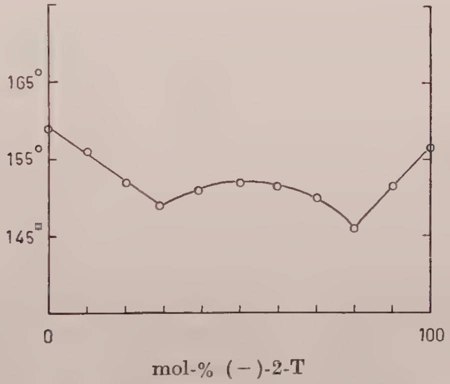

Fig. 9. (+)-3-Thenylsuccinic acid and (−)-2-Thenylsuccinic acid.

ference in structure and space requirement between 2- and 3-substituted thiophenes must be very small. The X-ray powder photographs of the quasi-racemates in the system 3-T–B (Fig. 2*e*) and 2-T–B (Fig. 2*f*) are very similar to the powder photograph of *rac*-B (Fig. 2*c*). This is to be expected as the phenyl group is larger than the thienyl group. The greater space requirements of the benzylsuccinic acid component in the quasi-racemate thus has a dominating influence on the crystal lattice.

Polymorphism, which often complicates the thermal analysis of the systems and makes the detection of the quasi-racemate more difficult, may easily be detected by X-ray powder photographs. It was thus found that optically active 2-T and racemic 3-T are at least dimorphic (Fig. 3).

The X-ray method is of course most useful when a thermal analysis is impossible on account of the instability of the components at higher temperature.

It should, however, be noted that the tendency for the formation of racemates and quasi-racemates, which may roughly be measured by the difference in melting point of the racemic compound and the eutectics, cannot be determined by the X-ray method.

Table 1.

Solvent	$[M]_D^{25}$ of acid		
	(−)-B	(−)-3-T	(−)-2-T
Water	−79.1°	−51.6°	−50.3°
Water (neutr.)	−71.8°	−43.1°	−46.9°
Acetone	−60.4°	−42.8°	−31.7°
Ethyl acetate	−56.2°	−42.2°	−26.3°
Alcohol	−43.5°	−32.1°	−16.3°
Ether	−38.1°	−29.8°	−15.0°
Acetic acid	−40.6°	−20.1°	−2.7°

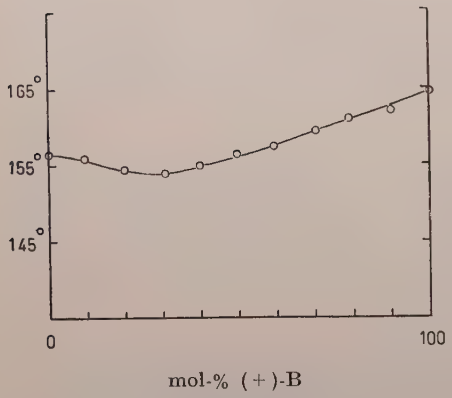

Fig. 10. (+)-2-Thenylsuccinic acid and (+)-Benzylsuccinic acid.

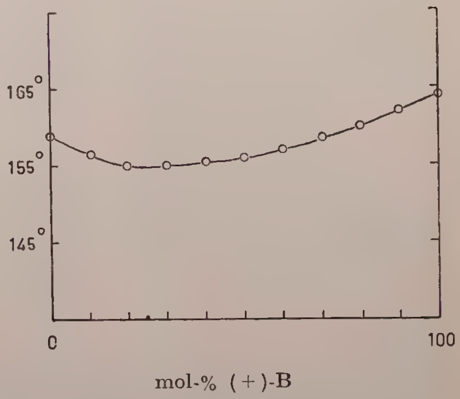

Fig. 11. (+)-3-Thenylsuccinic acid and (+)-Benzylsuccinic acid.

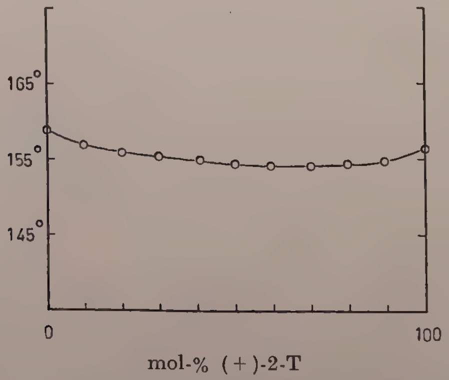

Fig. 12. (+)-3-Thenylsuccinic acid and (+)-2-Thenylsuccinic acid.

The melting point diagrams are in complete agreement with the results obtained from the X-ray powder photographs. The results are collected in Figs. 6, 8, 9, 11, 12 and Tables 2–6. For comparison the melting point diagrams for the system 2-T–B obtained by FREDGA are shown in Figs. 4, 5, 7, 10. They show that 3-T has a considerably smaller tendency to form a racemate than 2-T and B (Figs. 4–6).

FREDGA has pointed out the remarkable parallelism of the rotatory power of (−)-2-T and (−)-B in different solvents (3). In this respect (−)-3-T seems to be even more like (−)-B than (−)-2-T (Table 1). The rotatory power of 3-T lies between that of 2-T and B.

From the results obtained it can be concluded that 3-thenylsuccinic acid, 2-thenylsuccinic acid and benzylsuccinic acid with the same mode of rotation also have the same configuration. FREDGA (5) has connected 2-thenylsuccinic acid to the glyceraldehyde system by desulphurisation of this acid with Raney-nickel and found that (−)-2-thenylsuccinic acid is represented by stereo-formula I. Consequently, (−)-3-thenylsuccinic acid has the corresponding formula II.

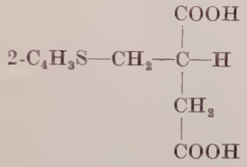

$$\begin{array}{r@{}c@{}l} & \mathrm{COOH} & \\ & | & \\ 2\text{-}\mathrm{C_4H_3S{-}CH_2{-}} & \mathrm{C} & \mathrm{{-}H} \\ & | & \\ & \mathrm{CH_2} & \\ & | & \\ & \mathrm{COOH} & \end{array}$$

I

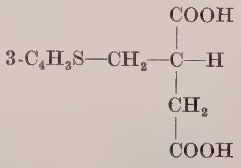

$$\begin{array}{r@{}c@{}l} & \mathrm{COOH} & \\ & | & \\ 3\text{-}\mathrm{C_4H_3S{-}CH_2{-}} & \mathrm{C} & \mathrm{{-}H} \\ & | & \\ & \mathrm{CH_2} & \\ & | & \\ & \mathrm{COOH} & \end{array}$$

II

Experimental

Preliminary tests on resolution.—0.0025 moles of optically inactive acid and 0.005 moles of the base were dissolved in 25 ml of dilute ethanol. The solutions were allowed to stand and some water gradually added until crystals were formed. In some cases the salts were too soluble to precipitate even when a large excess of water was added. Experiments with (+)-α-phenylethylamine and (+)-benzedrine were made in ethyl acetate. The results are given below.

Base	$[\alpha]_D^{25}$ of acid in acetone
Strychnine	+14.7°
Brucine	+3.5°
Quinine	±0°
Cinchonine	s
Cinchonidine	±0°
Chinidine	s
(+)-α-Phenylethylamine	−9.4°
(+)-Benzedrine	+5.7°

Optical resolution of 3-thenylsuccinic acid.—24.65 g (0.115 moles) of 3-thenylsuccinic acid and 76.8 g (0.230 moles) of strychnine were dissolved in 3300 ml of 33 % ethanol and the solution left in a refrigerator for 24 hours. The precipitate was filtered off, washed with cold dilute ethanol, and dried. About 0.3 g of the salt was

Table 2.

(+)-3-Thenylsuccinic acid
(−)-3-Thenylsuccinic acid

Mol-% (−)-3-T	m.p.
0.0	159.0°
10.1	155.0°
20.2	150.5°
29.8	143.5°
35.4	140.0°
40.0	138.0°
49.9	138.5°
59.8	138.0°

Table 3.

(+)-3-Thenylsuccinic acid
(−)-2-Thenylsuccinic acid

Mol-% (−)-2-T	m.p.
0.0	159.0°
10.3	156.0°
20.3	152.0°
29.0	149.0°
33.0	149.5°
39.2	151.0°
50.0	152.0°
59.7	151.5°
70.2	150.0°
75.2	148.5°
80.1	146.0°
90.4	151.5°
100.0	156.5°

Table 4.

(+)-3-Thenylsuccinic acid
(+)-2-Thenylsuccinic acid

Mol-% (+)-2-T	m.p.
0.0	159.0°
9.8	157.0°
20.0	156.0°
29.8	155.5°
40.8	155.0°
50.0	154.5°
59.6	154.1°
70.0	154.3°
79.6	154.5°
89.4	155.0°
100.0	156.5°

Table 5.

(+)-3-Thenylsuccinic acid
(−)-Benzylsuccinic acid

Mol-% (−)-B	m.p.
0.0	159.0°
10.3	153.5°
21.0	149.0°
31.8	147.5°
40.7	149.0°
46.9	149.5°
51.9	149.5°
59.1	149.0°
65.8	148.0°
70.9	150.0°
80.7	155.5°
89.7	160.0°
100.0	164.0°

set apart, the acid isolated and the optical activity measured in acetone. The remaining salt was recrystallised from dilute ethanol and the process repeated until the optical activity of the acid remained constant. The course of the resolution is seen below.

Crystallisation	1.	2.	3.	4.	5.
g salt	52.0	39.0	27.0	21.0	17.2
ml 33 % ethanol	3400	3200	1800	900	800
$[\alpha]_D^{25}$ of acid	+13.9°	+16.8°	+18.0°	+17.9°	+17.9°

Table 6.

(+)-3-Thenylsuccinic acid
(+)-Benzylsuccinic acid

Mol-% (+)-B	m.p.
0.0	159.0°
10.5	156.5°
19.9	155.0°
30.0	155.0°
40.2	155.5°
50.1	156.0°
60.0	157.0°
70.3	158.5°
79.8	160.0°
89.8	162.0°
100.0	164.0°

The strychnine salt obtained in the course of resolution, which crystallised in heavy plates, was not further examined.

The mother liquor from the first crystallisation with strychnine was evaporated at room temperature and 39.0 g salt was obtained. This salt yielded 8.76 g acid, having $[\alpha]_D^{25} = -14.1°$. This acid was dissolved in 450 ml of hot ethyl acetate and 9.92 g of (+)-α-phenylethylamine was added. The salt was deposited almost instantly and was filtered off when the solution had cooled. The progress of the resolution is seen below.

Crystallisation	1.	2.	3.
g, salt	17.8	14.5	11.6
ml ethyl acetate	450	450	450
$[\alpha]_D^{25}$ of acid	$-16.3°$	$-18.0°$	$-18.0°$

The phenylethylamine salt (which crystallised in fine needles) obtained in the course of the resolution was not further examined.

(+)-*3-Thenylsuccinic acid.*—The strychnine salt (17.2 g) was decomposed with 2 *N* sodium hydroxide and the strychnine extracted four times with chloroform. The aqueous phase was acidified with hydrochloric acid and the active acid extracted six times with ether. The ether was evaporated at room temperature and the acid recrystallised three times from water and decolourised with charcoal. The yield of pure acid was 3.0 g and the m.p. 159.0°. The acid crystallised in rectangular plates.

0.07489 g acid: 9.57 ml 0.07336 *N* NaOH.
$C_9H_{10}O_4S$ (214.2). Equiv. wt. calc. 107.1, found 106.7.
0.2102 g acid made up to 10.00 ml with acetone:
$2\ \alpha_D^{25} = +0.84°$, $[\alpha]_D^{25} = +20.0°$, $[M]_D^{25} = +42.8°$.

(−)-*3-Thenylsuccinic acid.*—11.6 g of the (+)-α-phenylethylamine salt was decomposed with 2 *N* sulphuric acid and the active acid extracted six times with ether. The ether was evaporated and the acid decolourised and recrystallised in the same way as the antipode which it resembles in appearance and properties. The yield was 4.8 g having m.p. 159.0°.

0.07056 g acid: 8.97 ml 0.07325 *N* NaOH.
$C_9H_{10}O_4S$ (214.2). Equiv. wt. calc. 107.1, found 107.4.

Weighed amounts of acid were made up to 10.00 ml with different solvents and the optical activity measured. The results are given below.

Solvent	mg of acid	$2\,\alpha_D^{25}$	$[\alpha]_D^{25}$	$[M]_D^{25}$
Water	41.43	−0.20°	−24.1°	−51.6°
Water (neutr.)	84.55	−0.34°	−20.1°	−43.1°
Acetone	182.5	−0.73°	−20.0°	−42.8°
Ethyl acetate	180.5	−0.71°	−19.7°	−42.2°
Ethanol	176.5	−0.53°	−15.0°	−32.1°
Ether	180.3	−0.50°	−13.9°	−29.8°
Acetic acid	175.4	−0.33°	−9.4°	−20.1°

Melting point diagrams.—Weighed amounts of the components (total weight 10 mg) were dissolved in a few drops of acetone. The solvent was evaporated at room temperature and the residue carefully powdered and dried in a desiccator. Before the melting points were determined in a hot stage microscope, the mixtures were instantaneously melted on a Kofler "Heizbank".

The optically active 3-T does not seem to be perfectly stable at its melting point and appears to be racemised to the extent of two to three per cent when heated for some minutes at this temperature. As the melting in the preparations is instantaneous, the eventual racemisation is much smaller than 2 % and does not affect the determination of the melting point diagram. The reproducibility of the m.p. was better than 0.5°. The racemates and quasi-racemates were also detected in the contact preparations (10).

X-ray powder photographs.—X-ray powder photographs were taken in a focusing camera of the GUINIER (16) type with CuK_α radiation (45 kV, 25 mA). Time of exposure three hours. The preparations were obtained in the same manner as described for the melting point diagrams. Powder photographs were taken on the powdered mixtures obtained by dissolving in acetone and evaporating the solvent and also on preparations which were instantaneously melted together and then allowed to crystallise rapidly. The powder photographs of the "melted" and "unmelted" preparations were identical except in the case of (+)-2-T and racemic 3-T, indicating that these compounds are at least dimorphic. In the case of (+)-2-T it was the "melted" form which belonged to the series obtained for the optically active acids (Fig. 1). In the case of racemic 3-T it was the unmelted form which belonged to the series of racemates and quasi-racemates (Fig. 2).

The authors whish to express their thanks to Professor ARNE FREDGA for valuable discussions and for the antipodes of benzylsuccinic acid and 2-thenylsuccinic acid which he kindly placed at our disposal. We are also indebted to fil. kand. SIXTEN ABRAHAMSSON, for taking the X-ray powder photographs and for his expert advice in connection with them. A grant from "O. E. Nycanders Forskningsfond" is gratefully acknowledged.

Summary

3-Thenylsuccinic acid has been resolved into its antipodes. Its steric relationship to 2-thenylsuccinic acid and benzylsuccinic acid has been established by the quasi-racemate method and through them it has been connected to the glyceraldehyde system. The usefulness of X-ray powder photographs for the detection of quasi-racemates has been discussed. The crystallographical similarity between the racemates and quasi-racemates of these acids has been demonstrated.

Department of Organic Chemistry, Chemical Institute, University of Uppsala, March 1955.

REFERENCES

1. Gronowitz, S., Arkiv Kemi *7*, 361 (1954).
2. Gronowitz, S. and Rosenberg, A., Arkiv Kemi *8*, 23 (1955).
3. Fredga, A. and Palm, O., Arkiv Kemi, Mineral. Geol. *26 A*, no. 26 (1949).
4. Petterson, K., Arkiv Kemi *7*, 339 (1954).
5. Fredga, A., Arkiv Kemi *6*, 277 (1953).
6. Gronowitz, S., Arkiv Kemi *6*, 283 (1953).
7. Fredga, A., "The Svedberg 1884 30/8 1944." Uppsala 1944, p. 261.
8. Rheinboldt, H., J. prakt. Chem. [2] *111*, 242 (1925).
9. Kofler, L. and A., Mikromethoden zur Kennzeichnung organischer Stoffe und Stoffgemische. Innsbruck 1948.
10. —— ibid. p. 215.
11. Matell, M., Arkiv Kemi *5*, 17 (1953).
12. Petterson, K., Arkiv Kemi *7*, 347 (1954).
13. Lettré, H., Z. angew. Chem. *50*, 581 (1937).
14. Fredga, A. Arkiv Kemi, Miner. Geol. *12 B*, no. 22 (1936).
    —— ibid. *14 B*, no. 15 (1940).
    —— ibid. *14 B*, no. 27 (1941).
15. Hartough, H. D., Thiophene and Its Derivatives. New York, 1952.
16. Guinier, A., Ann. Phys. [11], *12*, 161 (1939).

Tryckt den 14 december 1955

Uppsala 1955. Almqvist & Wiksells Boktryckeri AB

ARKIV FÖR KEMI Band 8 nr 56

Communicated 27 April 1955 by ARNE FREDGA and GUNNAR HÄGG

Spectrochemical studies on disulphides

I. An investigation of some linear and cyclic carboxylic substituted disulphides with special reference to the 1,2-dithiolane system

By LENNART SCHOTTE

With 14 figures in the text

As has previously been pointed out by the present author (1, 2) an investigation of cyclic disulphides and related compounds is in progress at this institute with particular reference to the glutaric and pimelic acid series. Special attention has been paid to the study of 1,2-dithiolane derivatives and already long before the discovery of lipoic acid inspired added interest in sulphur-containing rings, FREDGA (3) had underlined the importance of a thorough knowledge about analogous compounds. It is easily understood that the 1,2-dithiolane ring system has become a matter of current interest since the discovery that 6-thioctic (α-lipoic) acid (I) is an active coenzyme in the oxidative decarboxylation of pyruvic acid (4, also for further references). The assumption of CALVIN *et al.* (4) that the disulphide acid itself is involved in the conversion of the electromagnetic energy of the quanta into chemical bond energy has furthermore emphasized the necessity of extended knowledge about this special ring system which in fact has been rather incompletely examined.

One way of approaching this problem is to find a method to correlate significant properties of different types of disulphides to each other and obtain a common basis from which conclusions can be drawn. Spectrometric measurements may afford such a convenient method and in the present investigation it has been applied mainly to the study of carboxylic substituted disulphides. The work includes determination of the ultraviolet and infrared absorption spectra. The results within the ultraviolet absorption region will be discussed separately at first, as available data in the literature allow a comparison to other systems of dialkyl disulphides in general. The applications of infrared research to organic sulphur compounds have hitherto been rather few, and so this paper has in view not only a comparative study of the homologues in question but also a contribution to the extension of the material available for qualitative deductions concerning bonds involving sulphur.

Ultraviolet absorption measurements mainly on aliphatic dialkyl disulphides have previously been reported by e.g. KOCH (5) and BAER & CARMACK (6) including theoretical interpretations of the effects observed. For aliphatic dialkyl disulphides an absorption maximum is generally found near 250 mμ, as exhibited by dimethyl (7), diethyl (8), di-*n*-propyl (4), di-*iso*-amyl (5) and di-*n*-hexadecyl disulphide (6).

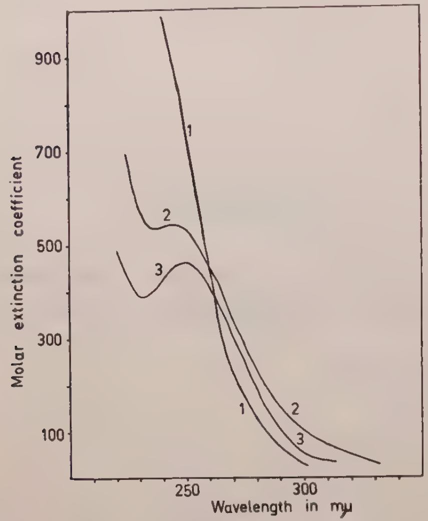

Fig. 1.

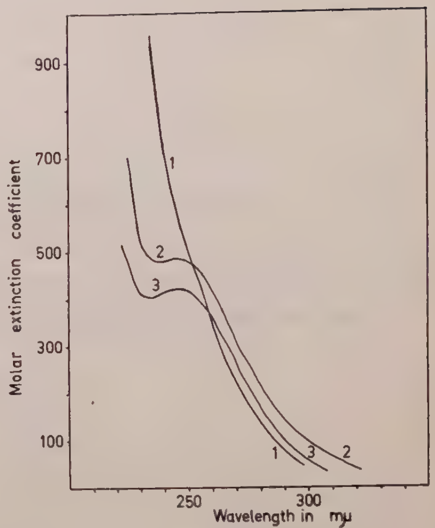

Fig. 2.

Fig. 1. UV absorption spectra of: (1) dithio-diglycolic acid; (2) β,β'-dithio-di-propionic acid; (3) γ,γ'-dithio-di-*n*-butyric acid. Solvent: alcohol.

Fig. 2. UV absorption spectra in aqueous solution of the di-Na salts of: (1) dithio-diglycolic acid; (2) β,β'-dithio-di-propionic acid; (3) γ,γ'-dithio-di-*n*-butyric acid.

The same type of selective absorption is also shown by dicyclohexyl disulphide (5) and cystine (9 and 10). Most of the discussion presented by KOCH on the absorption spectra and structure of organic sulphur compounds is given in terms of the commonly accepted hypothesis that the excited state resulting from high-intensity absorption of light contains a significant proportion of polar structures in the resonance hybrid. Anomalous behaviour is found for di-*tert.*-butyl disulphide, where the absorption spectrum does not contain the 250 mμ peak but only endabsorption. Absorption spectra of the five- and six-membered saturated cyclic disulphides have been recorded by CALVIN and co-workers (4) together with that of 4,8-thioctic acid, representing the seven-membered ring system. A displacement of the absorption top to longer wavelengths is observed when the size of the disulphide ring diminishes. The absorption peak for 4,8-thioctic acid corresponds rather well to that of a linear disulphide.

The influence of substituents in the disulphide molecule on ultraviolet spectra is clearly illustrated by the present investigation. In Fig. 1 the absorption curves are shown for dithio-di-glycolic acid (II), β,β'-dithio-di-propionic acid (III) and γ,γ'-dithio-di-*n*-butyric acid (IV) respectively in alcoholic solution. The characteristic disulphide peak is recognized for the propionic acid derivative at 245 mμ and for γ,γ'-dithio-di-*n*-butyric acid at 249 mμ. The spectrum of the glycolic acid derivative, however, shows only continuous absorption in the wavelength region under question. The significant difference in absorption behaviour is obvious. In general the disulphide absorption peaks are broad and characterized by rather weak intensities. On comparison with the absorption curve of di-*n*-propyl disulphide it is seen that the top for γ,γ'-dithio-di-*n*-butyric acid has exhibited a hypsochromic shift of only one mμ and the absorption is of about the same intensity. Thus, the introduction of the

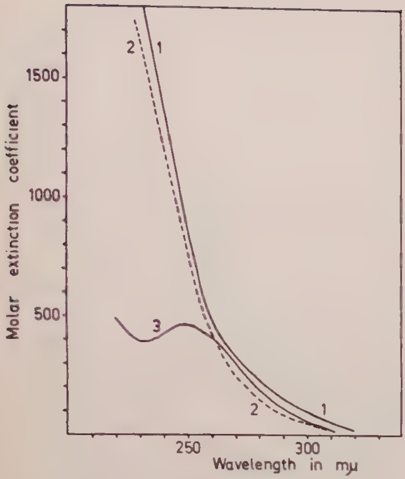

Fig. 3.

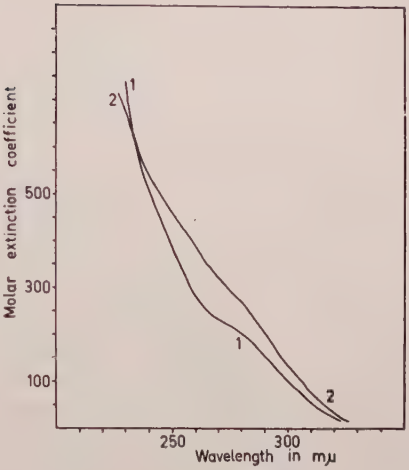

Fig. 4.

Fig. 3. UV absorption spectra in alcohol of: (1) *racem*-dithiodilactic acid; (2) *meso*-dithiodilactic acid (dashed curve); (3) γ,γ'-dithio-di-*n*-butyric acid.

Fig. 4. UV absorption spectra in alcohol of: (1) *racem*-1,2-dithiane-3,6-dicarboxylic acid; (2) *meso*-1,2-dithiane-3,6-dicarboxylic acid.

carboxylic groups into the γ-positions of the sulphur atoms has only a very slight effect on the general picture of ultraviolet absorption. When the heavy substituent, on the other hand, is situated in the α-position to the disulphide group, the type of absorption is quite different. It can be seen from Fig. 2 that the di-sodium salts of the above-mentioned acids in aqueous solution show ultraviolet absorption curves which are similar to those of the free acids. The intensities are throughout somewhat higher for the salts and the peak for the butyric acid derivative has shifted to 245 mμ but the general character of absorption is quite the same in both cases. Another example of the substituent influence on ultraviolet absorption is demonstrated in Fig. 3, where the spectra of *racem* and *meso*-dithiodilactic acid (disulphide-di-α-propionic acid) (V) in alcoholic solution are given; it is obvious that only endabsorption occurs. It is further interesting to notice the nearly identical course of the curves for the two diastereomers. For comparison the spectrum of γ,γ'-dithio-di-*n*-butyric acid is recorded again. The change in molar extinction coefficient for linear dialkyl disulphides seems to be such that the intensity of the absorption maxima slightly decreases with increasing number of the atoms in the chain.

If we now consider derivatives of some saturated cyclic disulphides the same substituent influence is expected. Remembering the form of the ultraviolet absorption curve of 1,2-dithiane (cyclotetramethylene disulphide) (λ max = 286 mμ) this is clearly demonstrated in Fig. 4, where *racem* (*trans*)- and *meso* (*cis*)-1,2-dithiane 3,6-dicarboxylic acid (VI) are recorded. The course of the absorption curves is of the same character as already found for the diastereomers of dithiodilactic acid, but the intensity of absorption is lower and the differences between the spectra of the two isomers more pronounced. The racemic form shows a shoulder in the region of about 280 mμ but for the rest only endabsorption in conformity to the steric isomer. The absorption curves for the di-sodium salts in aqueous solution are given in Fig. 5,

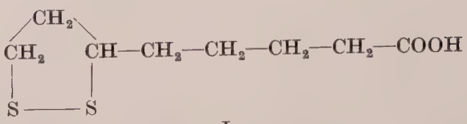

I

$\mathrm{HOOC{-}CH_2{-}S{-}S{-}CH_2{-}COOH}$

II

$\mathrm{HOOC{-}CH_2{-}CH_2{-}S{-}S{-}CH_2{-}CH_2{-}COOH}$

III

$\mathrm{HOOC{-}CH_2{-}CH_2{-}CH_2{-}S{-}S{-}CH_2{-}CH_2{-}CH_2{-}COOH}$

IV

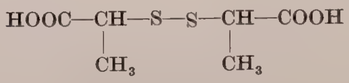

$$\mathrm{HOOC{-}\underset{\displaystyle CH_3}{\underset{|}{CH}}{-}S{-}S{-}\underset{\displaystyle CH_3}{\underset{|}{CH}}{-}COOH}$$

V

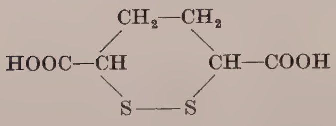

VI

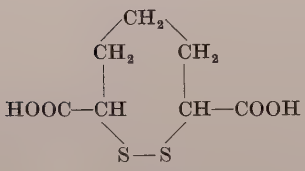

VII

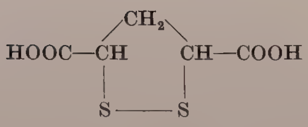

VIII

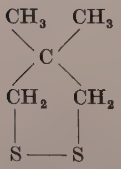

IX

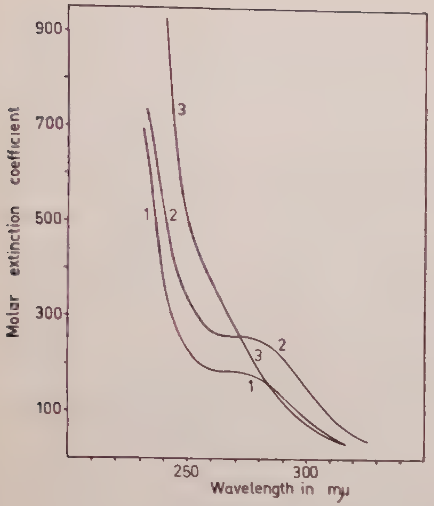

Fig. 5.

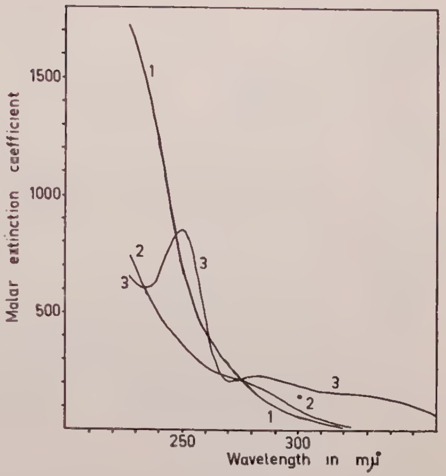

Fig. 6.

Fig. 5. UV absorption spectra in aqueous solution of the di-Na salts of: (1) *racem*-1,2-dithiane-3,6-dicarboxylic acid; (2) *meso*-1,2-dithiane-3,6-dicarboxylic acid; (3) 1,2-dithiacycloheptane-3,7-dicarboxylic acid.

Fig. 6. UV absorption spectra in alcohol of: (1) 1,2-dithiacycloheptane-3,7-dicarboxylic acid; (2) *racem*-1,2-dithiane-3,6-dicarboxylic acid; (3) *racem*-1,2-dithiolane-3,5-dicarboxylic acid.

where clearly marked changes in the region 260 to 280 mμ is observed as compared with the spectra of the free acids. The curves have an inflexion in that wavelength interval. In view of the result for the linear disulphides above the effect of the salt formation is remarkable and especially defined for the meso isomer. The same kind of ultraviolet absorption as observed for the dithiane-dicarboxylic acid is found for the only as yet available form of 1,2-dithiacycloheptane-3,7-dicarboxylic acid (VII), surely of meso-configuration, when examined in alcoholic solution. This is obvious from Fig. 6, where its absorption curve is given together with those of *racem*-1,2-dithiane-3,6-dicarboxylic acid as a comparison and *racem*-1,2-dithiolane-3,5-dicarboxylic acid (VIII). From this picture of the behaviour of cyclic disulphide dicarboxylic acids with different ring size to ultraviolet absorption the special character of the 1,2-dithiolane derivative is obvious. Its absorption curve as measured in alcoholic solution has a peak at 250 mμ, whereas the unsubstituted five-membered cyclic disulphide has a maximum at 330 mμ. Recently an absorption peak at 280 mμ for 1,2-dithiolane-3-carboxylic acid has been reported by Claeson (11). The shift 330 → 280 → 250 mμ is surely significant and might well reflect the importance of substitution at the α-positions.

An extended study of the 1,2-dithiolane system has for the dicarboxylic acid derivative shown that the free acid and its dimethyl ester (prepared from the acid in reaction with diazomethane) have in alcoholic solution their absorption peaks at 250 mμ and 252 mμ respectively. A small shift to longer wavelengths is exhibited by the acid in its undissociated state as examined in 0.1 molar sulphuric acid, whereas the course of the absorption in general is analogous to the spectra already discussed. This can be seen in Fig. 7, where the curve for the di-sodium salt in aqueous solution

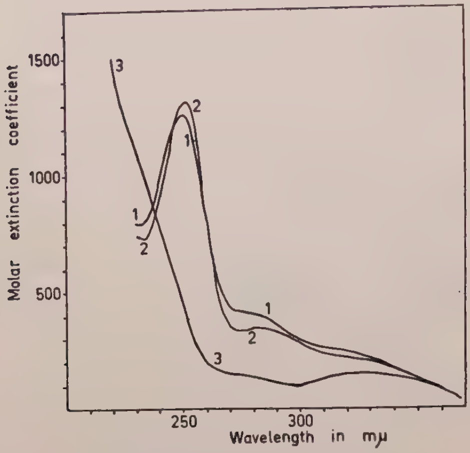

Fig. 7.

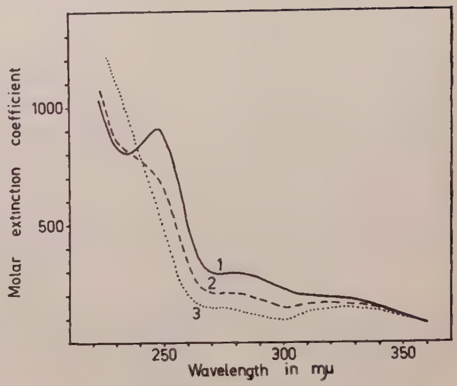

Fig. 8.

Fig. 7. UV absorption spectra of: (1) *racem*-1,2-dithiolane-3,5-dicarboxylic acid in 0.1 *M* sulphuric acid; (2) *racem*-dimethyl 1,2-dithiolane-3,5-dicarboxylate in alcohol; (3) di-Na salt of *racem*-1,2-dithiolane-3,5-dicarboxylic acid in aqueous solution.

Fig. 8. UV absorption spectra in aqueous solution of: (1) *racem*-1,2-dithiolane-3,5-dicarboxylic acid; (2) mono-Na salt of (1) (dashed curve); (3) di-Na salt of (1) (dotted curve).

is also reproduced. Here the interesting feature is observed that the absorption peak characteristic for the acid and ester disappears and the absorption extends into the visible with a weak maximum developed in the region about 330 mμ. The gradual change of the spectrum character upon neutralization of the 1,2-dithiolane-3,5-dicarboxylic acid in aqueous solution is demonstrated in Fig. 8, where the general course of the absorption curve is compared for the acid, its mono-sodium salt and the di-sodium salt. At first sight it appears that a change in selective ultraviolet absorption with the solvent is indicated by the fact that the peak for the acid in aqueous solution is found at 248 mμ, at 250 mμ using alcoholic solution and finally at 251 mμ in dilute sulphuric acid (0.1 *M*). This shift may be supposed to correlate with the changing degree of dissociation of the acid. The ultraviolet absorption is composed of two curves, one for the dissociated and one for the undissociated state of the acid, and as the intensity of the absorption for the salt increases rapidly in the wavelength region under discussion, a shift as reported above must follow. It is further interesting to observe the appearance of an entirely new absorption type for the compound upon neutralization with sodium bicarbonate. For the mono salt the curve passes through a point of inflexion in the wavelength region, where the acid has its maximum. A more marked tendency of absorption at higher wavelengths is also observed, for the mono salt around 280 mμ and for the fully neutralized molecule at 330 mμ. It must further be pointed out that the characteristic spectrum picture for 1,2-dithiolane-3,5-dicarboxylic acid is obtained again for the acidified solution. The effect observed is thus caused by the salt formation itself and not by an eventual reaction of the disulphide group in the dilute weakly alkaline solution. It must be noted here that the di-sodium salt of *racem*-dithiodilactic acid shows the same ultraviolet absorption behaviour as the free acid in conformity to the other linear disulphides investigated.

These results on the influence of substitution in the α-positions of 1,2-dithiolane on the ultraviolet absorption have lead to a comparative study of some 4-substituted derivatives from the same point of view. Preliminary results on e.g. 4,4-dimethyl-1,2-dithiolane (IX) (12) have shown the same specific absorption frequency as found for the unsubstituted ring system. The detailed data will soon be published. The results of Calvin (4) about the close similarity of the absorption spectra for the unsubstituted cyclic disulphides and the related thioctic acid derivatives seem to show the absence of an absorption effect of an alkyl substituent in one of the α-positions in contrast to the behaviour of substituents like carboxylic groups. From the considerations above it is clear that in this respect the carboxylic group in the ω-position of the alkyl group of 6-thioctic acid is of no importance. A more complete investigation of the effect of different substituents is in progress at this institute (11).

For an interpretation of the general effects observed on ultraviolet absorption spectra by different disulphide structures a consideration of the steric arrangement of the bonds around the S–S group is important. Quantum-mechanical calculations have for the analogous peroxide bond, as in hydrogen peroxide (13), shown that there exists an azimuthal angle of about 100°. As it seemed very reasonable to assume a similar behaviour for the disulphide group with an azimuthal angle close to 90° and a restricted rotation about the S–S– single bond, Affleck and Dougherty (14) made the suggestion that these characteristics were responsible for the relative reactivities observed for the series of unsubstituted saturated cyclic disulphides. Careful spectroscopic studies on dimethyl disulphide (15) and diethyl disulphide (16) have later confirmed these structural considerations, and by analogy with structurally related molecules the dihedral angle of the two S–S–C planes has been found to be about 90°. An angle of 93° is reported for 2,3,4-trithia-*n*-pentane (17), and Pauling (18) states for the ordinary S_8 molecule an azimuthal angle of 102°.

Available physical data for the dialkyl disulphides thus seem to indicate a stabilized non-planar skew configuration of the two valencies attached to the sulphur–sulphur bond. It then seems natural to assume that the absorption in the 250 mμ region for the linear disulphides is in some way connected with the electronic structure of this energetically preferred configuration, and there is surely a certain hybridization of the non-bonding *s* and *p* electrons, which correlates to the azimuthal angle. A change in the electronic configurations around the disulphide groups, e.g. by an expansion of the sulphur valence shell, causes an alteration of the hybridization and the valence angles of interest which must be clearly noticeable in the selective ultraviolet absorption. An inductive effect of the substituents might thus be responsible for the effects observed, but as groups with different modes of inductive electronic effects exhibit influences of the same kind, it seems more probable that the shifts or complete changes are instead due to steric effects. Koch (5) proposes such an explanation for the anomalous behaviour of di-*tert.* butyl disulphide compared to dicyclohexyl disulphide which shows quite normal spectral properties. The two large *tert.* butyl groups should exert spatial influence on each other if bonded in the usual disulphide configuration, and so the molecule is forced to a different structure with a changed electron distribution. It seems to the author that this hypothesis of Koch is further strengthened by the results of this investigation concerning the effect of carboxylic group substituents in α-positions to the disulphide bond. Such a heavy substituent must exert a dominating influence on the configuration of the system –C–S–S–C–, and the azimuthal angle is changed as compared with that of dialkyl disulphides in general. From this follows the appearance of quite a different ultraviolet absorption picture in the wavelength region under discussion. The effect is clearly illustrated by the fact that β,β'-dithio-di-propionic acid and cystine shows a normal absorption, as the carboxylic acid substituents in the β-positions can have no mentionable influence. The behaviour of γ,γ'-dithio-di-*n*-butyric acid also lends support to this interpretation. The observation that the salts show the same type of ultraviolet absorption as the free acids seems consistent with the theory about steric effects. A study of the corresponding diselenides would possibly be valuable for further conclusions.

From the foregoing general discussion about the theoretically deduced characteristic properties of a disulphide link it is well understood that the five- and six-membered cyclic unsubstituted systems must be ascribed a special character. The required deviation from the value of the normal azimuthal angle is assumed to involve rigid structures, at least for the five-membered ring (14), and the spectral behaviour of the compounds is interpreted in terms of attributed ring strain (4). The obvious influence of substituents like the carboxylic group in the α-positions to the S–S bond on the ultraviolet absorption spectra is found also for the cyclic systems as is clear from the material presented. For the linear disulphides the analogous effect could be explained entirely in terms of steric considerations even if inductive effects are not quite excluded, but for the cyclic derivatives it must be remembered that although a substitution may cause a change in the angle between the two S–C bonds the rigidity of the systems do not allow large deviations. Studies of molecular models show for the seven-membered cyclic disulphide that a skew configuration as stated above is possible and the spectral behaviour can then simply be correlated to linear compounds. The general absorption type of the seven-membered dicarboxylic acid is thus in complete accordance with the already reported observations. From the absorption curves presented it is further evident that the general effect observed is also valid for the 1,2-dithiane compounds. The extended study of the 1,2-dithiolane system and the fact that the acid really shows a selective absorption peak in the wavelength region under consideration allows an approach to the nature of the substituent influence. The hypsochromic shift as compared with the absorption peak for 1,2-dithiolane and 1,2-dithiolane-3-carboxylic acid respectively is surely caused by changed valency angles for the S–C bonds and it is likely that even small differences would give rise to marked effects on the ultraviolet absorption because of the rigidity of the nearly planar ring conformation. The changes are associated with the absorption through changing hybridization of the non-bonding *s* and *p* electrons. However, the effects observed cannot be explained only by an assumption about purely steric influence of the substituents in the 1,2-dithiolane system. For in such a case it seems difficult to account for the completely changed appearance of the ultraviolet absorption for the di-sodium salt. The different spectral behaviour is not due to any possible influence of hydrogen bonding in the case of the free acid, as the same absorption peak is found for the dimethyl ester. There are several exemples known where a change of pH in the solution to be examined causes a clear shift of the absorption frequency, but in general one structure is then appreciably stabilized by some kind of conjugation. Cystine also changes its ultraviolet absorption spectrum with the acidity of the solution, which is possibly understood simply by the fact that cystine is an α-amino acid. For the observations on *racem*-1,2-dithiolane-3,5-dicarboxylic acid, on the other hand, it seems reasonable to interpret the changes as caused by different electronic interaction between the disulphide group and the substituents. The free carboxylic acid group exhibits an effect on the electronic

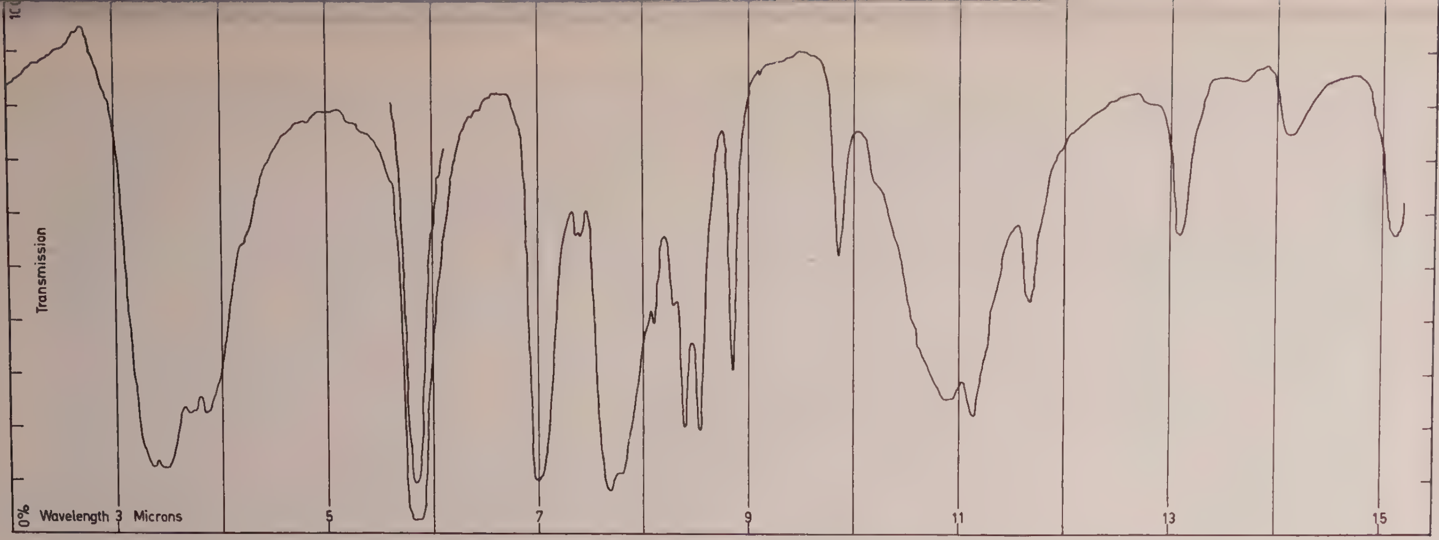

Fig. 9. IR absorption curve of *racem*-1,2-dithiane-3,6-dicarboxylic acid (NaCl prism region).

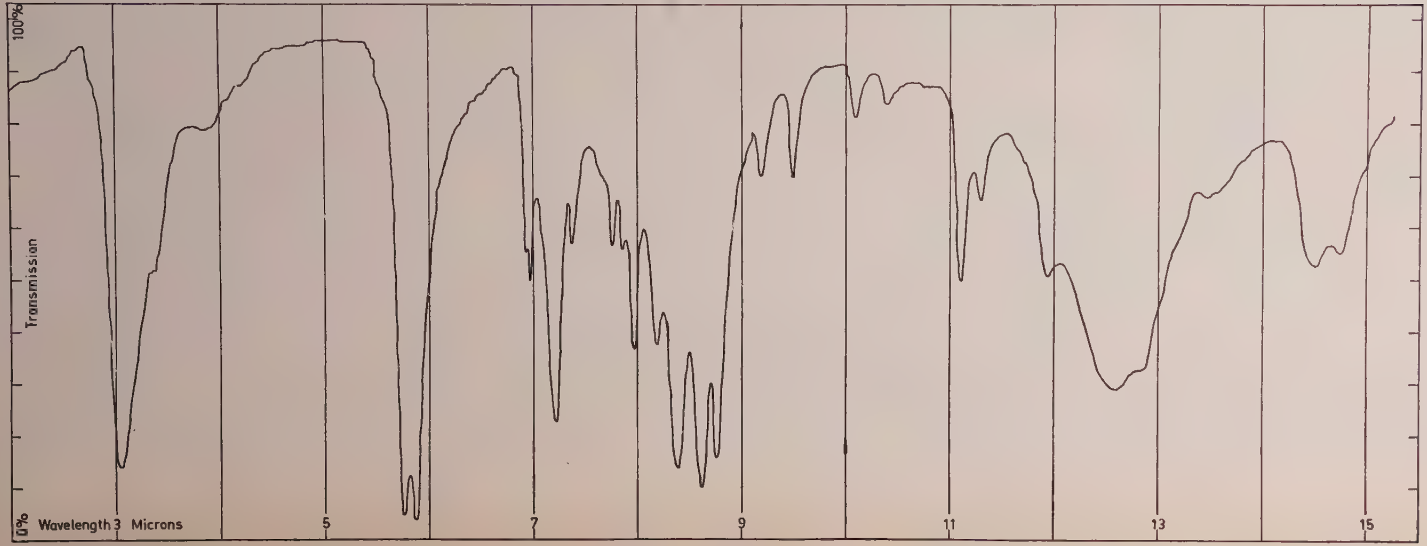

conditions of the disulphide bond which is characterized by a hypsochromic shift of 80 mμ in the spectra as compared to the unsubstituted system. The observed absorption peak at 250 mμ must correspond to another special quantum-mechanically possible hybridization and has of course nothing to do with the linear disulphide absorption frequency as far as what concerns the configuration of the S–S bond and its azimuthal angle. As was pointed out in the above description of the absorption curves examined, the di-sodium salt of the acid was found to give a weak absorption maximum in the region about 330 mμ, i.e. where 1,2-dithiolane has its absorption peak. This behaviour seems to suggest that due to the internal conjugation of the carboxylate anion the molecule as a whole or better the geometrical arrangement around the disulphide group resembles that of the unsubstituted ring system. The same type of effect although not so marked exists also for the dithiane derivatives as seen from Figs. 4 and 5.

The spectrochemical studies on the carboxylic substituted linear and cyclic disulphides have also been extended to infrared absorption. Most of the substances discussed above have thus been examined in both the sodium chloride prism region (2–15 μ) and the potassium bromide prism wavelength interval (15–25 μ). A study of the carbon–sulphur and sulphur–sulphur bond is perhaps best achieved using Raman spectroscopy but infrared absorption spectra recorded for the region of the potassium bromide prism are also of importance. Due to what was said in the beginning of this paper about infrared work on sulphur compounds, however, some curves representing the region of higher frequencies are reported also. Fig. 9 and 10 show the infrared absorption curves for *trans*-(*racem*)- and *cis*-(*meso*)-1,2-dithiane-3,6-dicarboxylic acid in the wavelength interval 2–15 μ. The most characteristic feature of the spectra is the splitting of the carbonyl stretching frequency for the meso form into double peaks at 5.75 μ and 5.87 μ respectively. The trans isomer shows a single well-defined top at 5.84 μ. A discussion of this effect from a more general theoretical point of view is given by SCHOTTE and ROSENBERG (19). The spectrum of the meso form is more complicated than that of the trans acid. In Figure 11 the infrared absorption curves are recorded for the two diastereomers in the wavelength region 11 to 24 μ. From available data in the literature the carbon–sulphur stretching frequency has been assigned to 600–700 cm^{-1} (16.7–14.3 μ) and that of the sulphur–sulphur bond to 430–490 cm^{-1} (23.2–20.4 μ). An interpretation of the absorption bands in Fig. 11 as regards these groups cannot be made definitely for both the diastereomers, but the curve of the racemic form allows conclusions to be drawn. The absorption band at 15.10 μ must be ascribed to the stretching vibration of the C–S linkage. For the disulphide group the absorption peak is found at 20.70 μ. If we now consider the spectrum of the meso form it is obvious that the frequency for the stretching vibration of the S–S– bond has shifted to 19.45 μ. There are a few other peaks in the neighbourhood but they are probably due to structural vibrations. For the carbon–sulphur absorption band, on the other hand, the assignment is uncertain. One interpretation implies the assumption that the band has split into two peaks at 14.50 μ and 14.72 μ. Such an effect is found for the diastereomers of dithiodilactic acid, where the assignment was possible due to the extreme simplicity of the absorption curves (19). However, the strong peak at 16.15 μ involves uncertainty and can possibly be connected with the vibrations of the carbon–sulphur linkage. In this respect the explanation must be left open. It can be concluded, nevertheless, that marked differences occur. The shift of the S–S absorption band for the meso form to 19.45 μ is unexpectedly great. The exact wavelengths are given in Table 1.

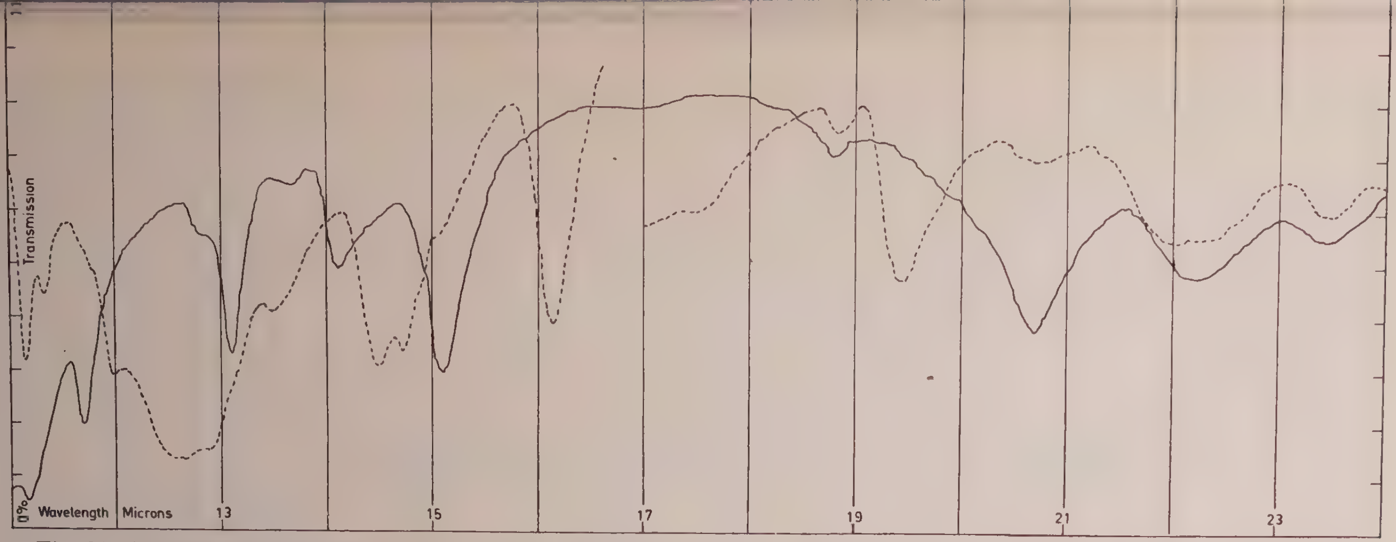

Fig. 11. IR absorption spectra in the KBr prism region for *racem-* and *meso*-1,2-dithiane-3,6-dicarboxylic acid. The dotted curve represents the meso form.

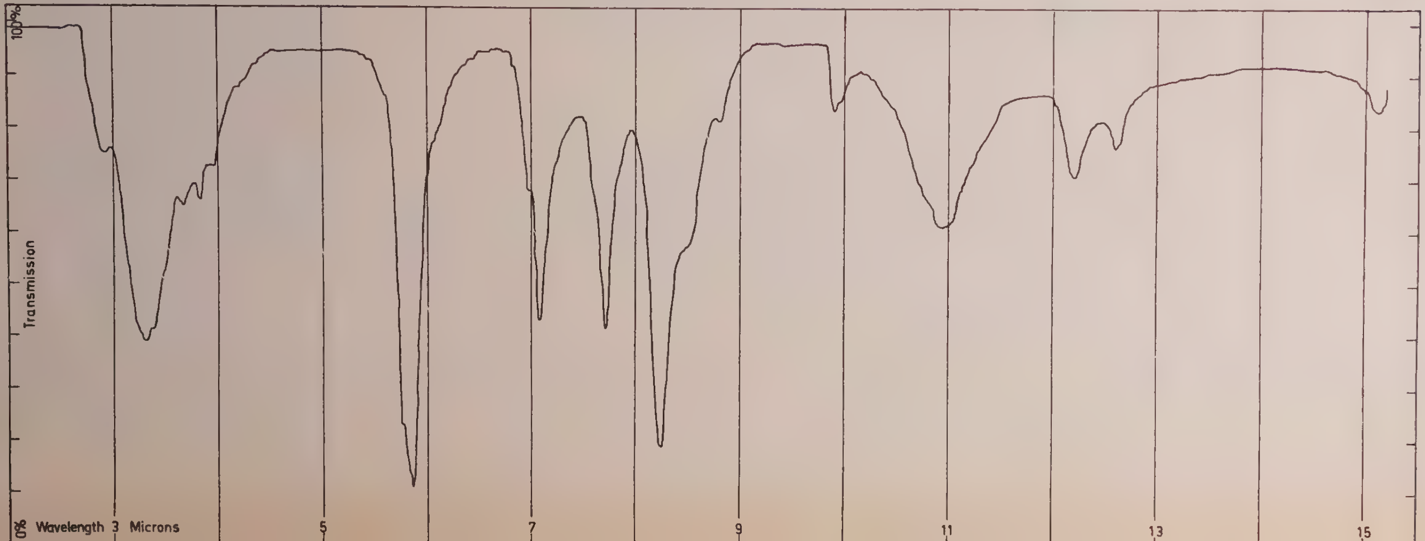

Table 1. The infrared absorption bands of *racem*- and *meso*-1,2-dithiane-3,6-dicarboxylic acid.

Racemic form		Meso form	
Wavelength in μ	Wavenumber in cm⁻¹	Wavelength in μ	Wavenumber in cm⁻¹
3.35	2985	3.05	3279
3.46	2890	3.35	2985
3.70	2703	3.85	2597
3.85	2597	5.75	1739
5.84	1712	5.87	1704
7.00	1429	6.92	1445
7.36	1359	6.96	1437
7.40	1351	7.22	1385
7.69	1300	7.37	1357
7.85	1274	7.75	1290
8.10	1235	7.85	1274
8.28	1208	7.97	1255
8.40	1190	8.18	1222
8.54	1171	8.39	1192
8.85	1130	8.62	1160
9.85	1015	8.75	1143
10.9	917	9.18	1089
11.14	898	9.50	1053
11.68	856	10.10	990
13.11	763	10.40	962
14.12	708	11.11	900
15.10	662	11.30	885
18.8	532	11.97	835
20.70	483	12.6	794
22.22	450	12.85	778
23.45	426	13.50	741
		14.50	690
		14.72	679
		15.00	667
		16.15	619
		18.84	531
		19.45	514
		20.7	483
		22.1	452
		23.5	426

The infrared absorption of *racem*-1,2-dithiolane-3,5-dicarboxylic acid is shown in Figs. 12 and 13. From the absorption bands in the sodium chloride region (Fig. 12) it is obvious that the acid shows a rather simple spectrum with well-defined peaks. The carbonyl stretching frequency is found to be quite normal (5.86 μ) like that of OH-bending which gives a broad maximum at about 11 μ. The absorption frequencies for the bonds involving sulphur can be studied in Fig. 13, where the carbon–sulphur stretching vibration is recognized at 15.06 μ. The absorption peak of the S–S linkage is found at an unexpectedly high frequency 539 cm⁻¹ (18.57 μ), thus indicating the special character of the five-membered ring. The simplicity of the curve allows interpretations to be given, but of course the objection might be made that the disulphide band could have exhibited a shift out of the wavelength region investigated. This

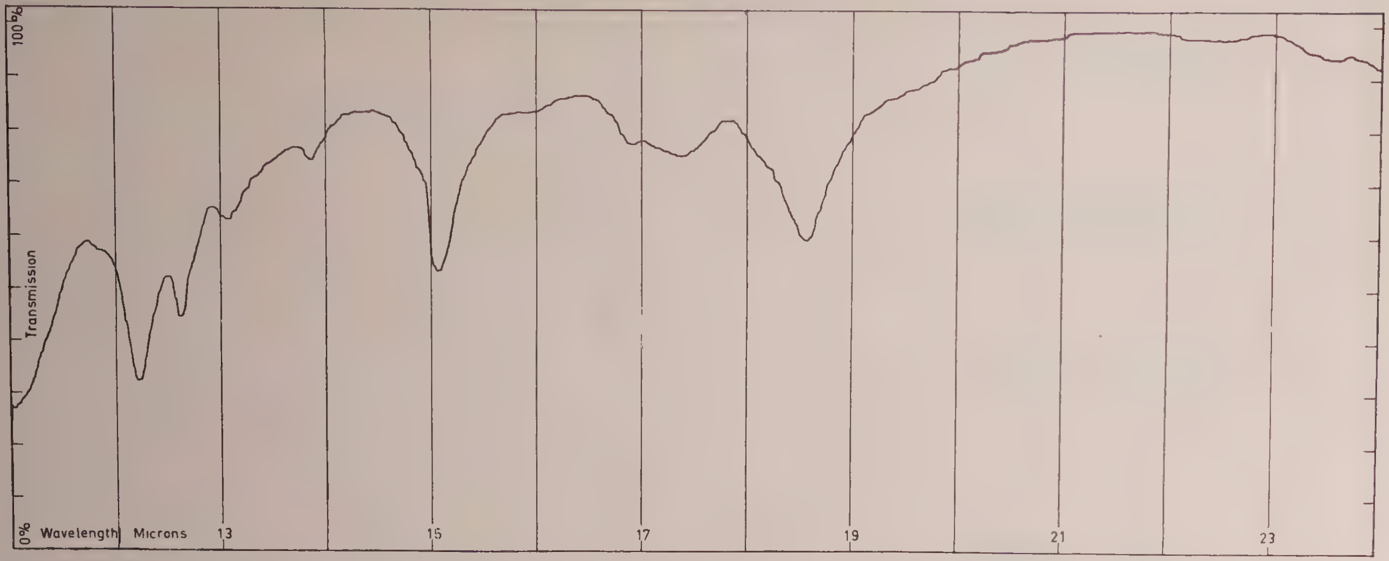

Fig. 13. IR absorption curve of *racem*-1,2-dithiolane-3,5-dicarboxylic acid (KBr prism region).

Table 2. The infrared absorption bands of *racem*-1,2-dithiolane-3,5-dicarboxylic acid.

Wavelength in μ	Wavenumber in cm^{-1}	Wavelength in μ	Wavenumber in cm^{-1}
2.92	3425	8.5	1176
3.30	3030	8.80	1136
3.35	2985	9.90	1010
3.67	2725	10.95	913
3.84	2604	12.22	818
3.90	2564	12.62	792
5.75	1739	13.05	766
5.86	1706	13.85	722
6.95	1439	15.06	664
7.07	1414	16.9	592
7.70	1299	17.4	575
8.24	1214	18.57	539

seems on the whole very unlikely to the author and furthermore an analogous absorption peak (at 18.37 μ) has been found by Claeson (20) for 1,2-dithiolane-3-carboxylic acid. It must thus be concluded that under special conditions the sulphur–sulphur bond gives selective infrared absorption at appreciably higher frequencies than previously reported in the literature for linear compounds. The wavelengths of the infrared absorption bands of the five-membered cyclic disulphide acid are reported in Table 2.

The infrared absorption curves of 1,2-dithiacycloheptane-3,7-dicarboxylic acid and γ,γ'-dithio-di-*n*-butyric acid have also been examined. The wavelengths are given in Tables 3 and 4 respectively. The seven-membered cyclic disulphide acid has been studied in both the sodium chloride and potassium bromide prism region. The spectrum is rather complicated. This is also true for the part involving the C–S and S–S stretching vibration frequencies and makes an assignment of bands to the linkages quite impossible. This character of the curve is of course due to the structural vibrations which are more pronounced with increasing number of methylene groups in the ring or the chain. The complicated nature of the infrared spectrum for γ,γ'-dithio-di-*n*-butyric acid in the region 12–24 μ can also be interpreted in this way. Here only the wavelengths of the absorption bands will be given (Table 4) and no attempt is made to draw any conclusions as the uncertainty in assignment is too great.

The infrared work presented here has given additional information as regards the absorption bands of the C–S and S–S bonds in compounds of different structures. Even if an interpretation of the spectra is in some cases impossible this investigation has nevertheless shown that reliable conclusions are possible for the dicarboxylic acid derivatives of the five- and six-membered cyclic disulphides. It is of most interest to discuss the sulphur–sulphur linkage and note the appreciable shift of its vibration frequency for the dithiolane derivative. In view of the result for the two diastereomers of dithiodilactic acid and the data available in the literature the absorbtion peak is obtained at an unexpectedly high frequency, which indicates marked changes in the force constant of the S–S linkage involved. This probably has something to do with the nearly planar structure. The frequencies observed for the dithiodilactic acids correspond well to the generally accepted ones and the same is found for *racem*-1,2-dithiane-3,6-dicarboxylic acid. The slight deviation of the dithiane

Table 3. The infrared absorption bands of 1,2-dithiacycloheptane-3,7-dicarboxylic acid.

b = broad; vs = very strong; s = strong; m = medium; w = weak; sh = shoulder.

Wavelength in μ	Wavenumber in cm⁻¹	Character of the band	Wavelength in μ	Wavenumber in cm⁻¹	Character of the band
3.30	3030	sh	8.50	1176	s
3.41	2933	s	9.30	1075	w
3.70	2703	w	9.87	1013	m
3.77	2653	w	10.6	943	s b
3.86	2591	m	11.35	881	w
5.87	1704	vs	12.22	818	m
6.88	1453	s	13.66	732	m
6.97	1435	s	14.40	694	s
7.05	1418	s	15.05	664	s
7.40	1351	m	16.60	602	m
7.59	1318	s	18.75	533	m
7.77	1287	s	19.45	514	m
7.88	1269	m	21.35	468	m
8.03	1245	m	23.02	434	m
8.24	1214	m			

Table 4. The infrared absorption bands of γ,γ'-dithio-di-n-butyric acid in the potassium bromide prism region. For abbreviations see Table 3.

Wawelength in μ	Wavenumber in cm⁻¹	Character of the band
12.05	830	w
12.91	775	s
13.49	741	s
13.95	717	m
14.82	675	vs
15.23	657	s
15.76	635	w
17.45	573	m b
19.45	514	s
20.47	489	m
21.25	471	m
22.21	450	s

derivatives from the common behaviour of disulphides is indicated in the spectrum of the meso form. The shift is of the same kind as that mentioned above for the five-membered ring system, but the effect is less pronounced. According to **Sheppard** (21) the rather low intensity of the S–S valence stretching modes is due to the fact that the symmetrical vibration of the linkage involves little change in dipole moment. It is, however, also stated that the close similarity between the C–S stretching frequencies of analogous sulphides and disulphides means that the force constants of these bonds vary in the same manner with the nature of the substituent alkyl group.

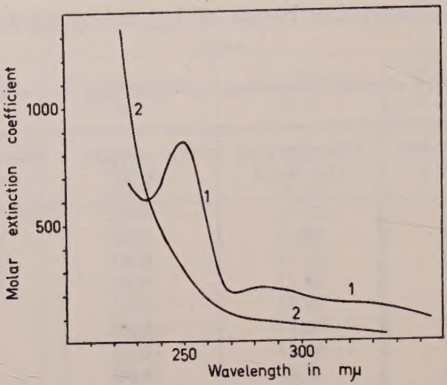

Fig. 14. UV absorption spectra in alcohol of *racem*-1,2-dithiolane-3,5-dicarboxylic acid: (1) before, and (2) after photolysis (30 min. exposure).

Such an effect is questionable for cyclic systems, but it is very valuable for the clear understanding of the spectral behaviour of some compounds. The question therefore arises if the anomalous ultraviolet absorption of di-*tert.* butyl disulphide could not in some way be correlated to the results of SHEPPARD that the C–S stretching frequency for *tert.* alkyl sulphides is appreciably lower than that of similar compounds with *primary* alkyl groups. These differences are interpreted in terms of changes in the force constants of the linkages. TROTTER and THOMPSON (22) have also observed these variations in the C–S stretching frequency for thiols, sulphides and disulphides.

From the spectrochemical studies presented it can be concluded that special properties must be ascribed to the 1,2-dithiolane derivatives. The differences as compared with linear disulphides are surely due to the energetically unfavourable geometrical arrangements around the sulphur–sulphur bond in the rigid structure and should be reflected in a higher reactivity or better, a lower stability of the molecules. *Racem*-1,2-dithiolane-3,5-dicarboxylic acid is found to be unchanged after keeping in alcoholic solution for several days at room temperature. As could be expected, however, a marked effect has been observed upon photolysis. With sufficiently long exposure the characteristic ultraviolet absorption peak at 250 mμ in alcoholic solution disappears completely and only continuous absorption occurs in the wavelength region. Fig. 14 shows the absorption curves of the acid in alcohol as solvent before and after a photolysis experiment.

Because of the continuous type of absorption for the other cyclic disulphide acids investigated the relative reactivities in this respect cannot be easily compared. The investigation has in view only to present data for a comparison to the exhaustive results of CALVIN and co-workers (4) on the unsubstituted 1,2-dithiolane. The dithiolane derivative has been photolyzed at room temperature in alcohol, water and 0.1 *M* sulphuric acid as solvents. The effect was of the same character involving the fission of the S–S linkage in the cyclic disulphide. Due to the symmetrical structure it seems reasonable to assume a homolytic fission of the bond into a diradical which immediately reacts in some way, e.g. with the solvent. When alcohol was used as solvent the solution remained clear after photolysis. A turbid solution is obtained in aqueous and sulphuric acid medium and a small amount of hydrogen sulphide is liberated.

Finally it should be pointed out that a comparison of disulphides to corresponding peroxides surely is of importance. Attention may be drawn to the fact that di-*tert.* butyl peroxide shows chemical properties quite different from those of alkyl peroxides in general.

Experimental

For the ultraviolet absorption determinations a Beckman model DU quartz spectrophotometer was used. Alcohol, water and 0.1 *M* sulphuric acid were used as solvents. The curves were recorded at least twice.

A Perkin Elmer model 21 spectrophotometer equipped with sodium chloride prism was used for the infrared absorption measurements in the region 2–15 μ. A potassium bromide prism was inserted for the region 15–25 μ. The substances have been examined as solid pressed potassium bromide plates according to the method described by SCHIEDT and REINWEIN (23). The calibration of the absorption curves, linear in wavelength, is exact up to ± 0.02 μ in the sodium chloride region and to ± 0.04 μ in that of the potassium bromide prism.

The photolysis has been performed with a Hanovia low pressure mercury lamp. The solutions were kept in quarz absorption cells at a distance from the lamp of about 5 cm during 30 minutes. The power of the ultraviolet radiation source is 5 watt, and it gives at total absorption about 0.3×10^{18} quanta per sec. and ml. Most of the radiation (95 %) is obtained at 2537 Å.

The acids investigated

Dithio-diglycolic acid.—M.p. 106°–107°. The acid was recrystallized twice from a mixture of ethyl acetate and benzene (24). *Anal.* Subst., 54.71 mg: 8.15 ml of 0.0733 *N* NaOH. Equ. wt. Calc. 91.1; Found 91.6.

β,β′-Dithio-di-propionic acid.—M.p. 152°–153°. The acid was recrystallized once from ethyl acetate and three times from water (25). *Anal.* Subst., 60.70 mg: 7.85 ml of 0.0733 *N* NaOH. Equ. wt. Calc. 105.1; Found 105.5.

γ,γ′-Dithio-di-n-butyric acid.—M.p. 109°–111°. The substance was recrystallized twice from water (26). *Anal.* Subst., 70.19 mg: 8.00 ml of 0.0733 *N* NaOH. Equ. wt. Calc. 119.2; Found 119.7.

Racem-dithiodilactic acid.—M.p. 148°–149° (27). *Anal.* Subst., 59.85 mg: 7.84 ml of 0.0734 *N* NaOH. Equ. wt. Calc. 105.1; Found 104.1.

Meso-dithiodilactic acid.—M.p. 118° (27). *Anal.* Subst., 61.25 mg: 7.99 ml of 0.0734 *N* NaOH. Equ. wt. Calc. 105.1; Found 104.5.

Racem-1,2-dithiane-3,6-dicarboxylic acid.—M.p. *c.* 275° (d) (3). *Anal.* Subst., 60.61 mg: 7.94 ml of 0.0734 *N* NaOH. Equ. wt. Calc. 104.1; Found 104.0.

Meso-1,2-dithiane-3,6-dicarboxylic acid.—M.p. 198° (3). *Anal.* Subst., 63.05 mg: 8.30 ml of 0.0734 *N* NaOH. Equ. wt. Calc. 104.1; Found 103.5.

Racem-1,2-dithiolane-3,5-dicarboxylic acid.—M.p. 197°–199° (preheated apparatus) (1). *Anal.* Subst., 31.63 mg: 9.73 ml of 0.0334 *N* NaOH. Equ. wt. Calc. 97.1; Found 97.3.

1,2-Dithiacycloheptane-3,7-dicarboxylic acid.—M.p. 193°–194° (preheated apparatus) (2). *Anal.* Subst., 24.99 mg: 6.71 ml of 0.0334 *N* NaOH. Equ. wt. Calc. 111.1; Found 111.5.

Summary

The ultraviolet and infrared absorption curves of some linear and cyclic saturated carboxylic substituted disulphides have been investigated.

Special attention has been paid to the study of 1,2-dithiolane-3,5-dicarboxylic acid representing the interesting five-membered disulphide ring.

The clear influence of substituents such as carboxylic groups on the ultraviolet absorption is pointed out and theoretically discussed in terms of changed geometrical arrangements around the disulphide linkage. The considerations involve steric and inductive effects.

ACKNOWLEDGEMENTS

The author wishes to express his gratitude to Professor Arne Fredga for valuable discussions and for the kindness to put some of the substances at his disposal. The author also wishes to thank Dr. Andreas Rosenberg for expert advice about the infrared work.

My sincere thanks are further due to Dr. Ingrid Claesson at the Institute of Physical Chemistry for the loan of a mercury lamp for photolysis and for data pertaining to its use.

Finally I am indebted to Mr. Stig Bergwall and Mr. Sixten Johansson for some help with the experimental work.

A grant from the *Swedish Natural Science Research Council* is gratefully acknowledged.

Laboratory of Organic Chemistry, Chemical Institute, University of Uppsala, April 1955.

REFERENCES

1. L. Schotte, Acta Chem. Scand. *8*, 130 (1954).
2. L. Schotte, Acta Chem. Scand. *8*, 131 (1954).
3. A. Fredga, Arkiv Kemi, Mineral. Geol. *12 A* (1938) nr. 27.
4. J. A. Barltrop, P. M. Hayes, and M. Calvin, J. Am. Chem. Soc. *76*, 4348 (1954).
5. H. P. Koch, J. Chem. Soc. *1949*, 394.
6. J. E. Baer and M. Carmack, J. Am. Chem. Soc. *71*, 1215 (1949).
7. H. J. Backer and H. Kloosterziel, Rec. trav. chim. *73*, 136 (1954).
8. H. Ley and B. Arends, Z. physik. Chem. *B 15*, 311 (1932).
9. G. A. Anslow and M. L. Foster, J. Biol. Chem. *97*, 37 (1932).
10. G. A. Anslow and E. R. Lyman, J. Optical Soc. Am. *31*, 114 (1941).
11. G. Claeson, Acta Chem. Scand., *9*, 178 (1955).
12. H. J. Backer and N. Evenhuis, Rec. trav. chim. *56*, 129 (1937).
13. W. G. Penney and G. B. B. M. Sutherland, Trans. Faraday Soc. *30*, 898 (1934).
14. J. G. Affleck and G. Dougherty, J. Org. Chem. *15*, 865 (1950).
15. D. W. Scott *et al.* J. Am. Chem. Soc. *72*, 2424 (1950).
16. D. W. Scott *et al.* J. Am. Chem. Soc. *74*, 2478 (1952).
17. J. Donohue, J. Am. Chem. Soc. *72*, 2701 (1950).
18. L. Pauling, Proc. Nat. Acad. Sci. U.S. *35*, 495 (1949).
19. L. Schotte and A. Rosenberg, Arkiv Kemi, in press.
20. G. Claeson, Private communication.
21. N. Sheppard, Trans. Faraday Soc. *46*, 429 (1950).
22. I. F. Trotter and H. W. Thompson, J. Chem. Soc. *1946*, 481.
23. U. Schiedt and H. Reinwein, Z. Naturforsch. *7 b*, 270 (1952).
24. B. Holmberg, Z. anorg. Chem. *56*, 385 (1907).
25. E. Biilman, Ann. *339*, 365 (1905).
26. B. Holmberg and E. Schjånberg, Arkiv Kemi, Mineral., Geol. *14 A* (1940) nr. 7.
27. A. Fredga, Arkiv Kemi, Mineral., Geol. *12 A* (1937) nr. 13.

Tryckt den 10 november 1955

Uppsala 1955. Almqvist & Wiksells Boktryckeri AB